

**Ongoing Face Recognition
Vendor Test (FRVT)**
Part 1: Verification

Patrick Grother
Mei Ngan
Kayee Hanaoka
Joyce C. Yang
Austin Hom

*Information Access Division
Information Technology Laboratory*

This publication is available free of charge from:
<https://www.nist.gov/programs-projects/face-recognition-vendor-test-frvt-ongoing>

2023/04/20



ACKNOWLEDGMENTS

The authors are grateful for the long-standing support and collaboration of the the Department of Homeland Security's Science & Technology Directorate (S&T) and the Office of Biometric Identity Management (OBIM).

Additionally, the authors are grateful to staff in the NIST Biometrics Research Laboratory for infrastructure supporting rapid evaluation of algorithms.

DISCLAIMER

Specific hardware and software products identified in this report were used in order to perform the evaluations described in this document. In no case does identification of any commercial product, trade name, or vendor, imply recommendation or endorsement by the National Institute of Standards and Technology, nor does it imply that the products and equipment identified are necessarily the best available for the purpose.

INSTITUTIONAL REVIEW BOARD

The National Institute of Standards and Technology's Research Protections Office reviewed the protocol for this project and determined it is not human subjects research as defined in Department of Commerce Regulations, 15 CFR 27, also known as the Common Rule for the Protection of Human Subjects (45 CFR 46, Subpart A).

FRVT STATUS

This report is a draft NIST Interagency Report, and is open for comment. It is the thirty sixth edition of the report since the first was published in June 2017. Prior editions of this report are maintained on the FRVT [website](#), and may contain useful information about older algorithms and datasets no longer used in FRVT.

FRVT remains open: All [four tracks](#) of the FRVT are open to new algorithm submissions.

2023-04-20 changes since 2023-04-04:

- ▷ We have added results for first algorithms from one developers: IDENTITY.
- ▷ We have added results for new algorithms from three returning developers: Metsakuur, Autentika Digital Indonesia, and Verigram.
- ▷ FRVT will re-open 2023-05-01.
- ▷ We have retired results for 3 algorithms per our policy to only list results for two algorithms per developer. Results for retired algorithms appear in prior versions of this report in the [archive](#).

2023-04-04 changes since 2023-03-09:

- ▷ We have added results for first algorithms from six developers: Aratek Biometrics City and County of Honolulu, FOO, Intelligent Control Technology NCS, and Swsam Solutions.
- ▷ We have added results for new algorithms from nine returning developers: Cubox, Glory, InsightFace AI, Maxis Biometrics, Mukh Technologies, Turkcell Technology, Samsung S1, Via Technologies, and Vision Intelligence Center of Meituan
- ▷ We have retired results for 7 algorithms per our policy to only list results for two algorithms per developer. Results for retired algorithms appear in prior versions of this report in the [archive](#).

2023-03-09 changes since 2023-02-01:

- ▷ We have added results for first algorithms from eight developers: Biometric LLC ([biometric.vision](#)) KZ, Candour Biometrics, Fast Enterprises, KakaoBank, Mitek Systems, Nominder, Private Identity, and UNICC-Solution Architecture Section.
- ▷ We have added results for new algorithms from 22 returning developers: AFR Engine, Biocube Matrics, CMC Institute of Science and Technology, Cloudwalk - Moontime Smart Technology, Cyberlink Corp, Beijing DeepSense Technologies, First Credit Bureau Kazakhstan, Enface, Hangzhuo Allu Network Information Technology, Herta Security, IMDS Software, Inspur (Beijing) Electronic Information Industry Co, Intellivision, MicroFocus, Neurotechnology, Pangiam, NSENSE Corp, STCON LLC, Touchless ID, University of Surrey-CVSSP, Vision-Box, and YooniK.
- ▷ We have retired results for 14 algorithms per our policy to only list results for two algorithms per developer. Results for retired algorithms appear in prior versions of this report in the [archive](#).
- ▷ We have introduced new set of non-frontal portrait to border comparisons. The new images are described in section [2.3](#) and their use in section [3.2](#).

2023-02-01 changes since 2022-12-15:

- ▷ We have added results for first algorithms from four developers: CU-Face, Korea ID, Onfido, and TrueID-VNG.
- ▷ We have added results for new algorithms from 21 returning developers: Alchera, Armatura, Cogent-Thales, Dermalog, Didi ChuXing Global Face, Gorilla, Hyperverge, Innovatrics, Intel Research, Intel-liViX, Intema-LGL, Kasikorn Labs, Paravision, Rank One Computing, Sensetime Group, Suprema AI, Tech5, Unissey, U. Coimbra Visteam, Vixvizon (Imagus), and Yuan High-Tech Development.
- ▷ We have retired results for 20 algorithms per our policy to only list results for two algorithms per developer. Results for retired algorithms appear in prior versions of this report in the [archive](#).
- ▷ We have introduced new set of non-frontal portrait to border comparisons. The new images are described in section [2.3](#) and their use in section [3.2](#).

2022-12-15 changes since 2022-11-06:

- ▷ We have added results for first algorithms from four developers: Maxis Biometrics, PT Autentika Digital Indonesia, PT Qlue Performa Indonesia, and STCON.
- ▷ We have added results for new algorithms from 14 returning developers: Adera Global, Aiseemu Technology, Chunghwa Telecom, chtface, FRP, Griaule, Line Corporation, Maxvision Technology, Mukh Technologies, Papilon Savunma, Qnap Security, Realnetworks, Securif AI, SQISoft, and Veridium.
- ▷ We have retired results for 10 algorithms per our policy to only list results for two algorithms per developer. Results for retired algorithms appear in prior versions of this report in the [archive](#).

2022-11-06 changes since 2022-09-26:

- ▷ We have added results for first algorithms from six developers: AFR Engine, CMC Institute of Science and Technology, Saga Densan Center, Turkcell Technology, UXLabs, and Wise AI SDN BHD.
- ▷ We have added results for new algorithms from 14 returning developers: Coretech Knowledge, Cloudwalk - Moontime, Cloudmatrix, Deepglint, Guangzhou Pixel Solutions, Hangzhou Allu Network Information Technology, NEO Systems, One More Security, Palit Microsystems, Panasonic R+D Center Singapore, Samsung S1, Seventh Sense Artificial Intelligence, Touchless ID, and Veridas Digital Authentication Solutions S.L.
- ▷ We have retired results for 10 algorithms per our policy to only list results for two algorithms per developer. Results for retired algorithms appear in prior versions of this report in the [archive](#).

2022-09-26 changes since 2022-08-30:

- ▷ We have added results for first algorithms from three developers: Codeline, First Credit Bureau Kazakhstan, and InfoCert.
- ▷ We have added results for new algorithms from 14 returning developers: Advancegroup, Armatura LLC, Beijing Hisign Technology, Cybercore, Cyberlink Corp, Herta Security, ICM Airport Technics, InsightFace AI, Metsakuur, NSENSE Corp, Samsung-SDS, Videmo Intelligent Videoanalyse, Vietnam Posts and Telecommunications Group, and Vision Intelligence Center of Meituan.
- ▷ We have retired results for 11 algorithms per our policy to only list results for two algorithms per developer. Results for retired algorithms appear in prior versions of this report in the [archive](#).

2022-08-30 changes since 2022-07-29:

- ▷ We have added results for first algorithms from two developers: Aximetria, Intellibrain Technological Projects
- ▷ We have added results for new algorithms from twelve returning developers: Alchera Inc, Dermalog, Idemia, Incode Technologies Inc, Intellivision, Kasikorn Labs, Megvii/Face++, Techsign, TuringTech.vip, Universidade de Coimbra, Verijelais, Vixvizon
- ▷ We have retired results for six algorithms per our policy to only list results for two algorithms per developer. Results for retired algorithms appear in prior versions of this report in the [archive](#).

2022-07-29 changes since 2022-06-27:

- ▷ We have added results for first algorithms from seven developers: FRP LLC (Hawaii), IMDS Software, Inspur (Beijing) Electronic Information Industry, Intema - LGL Group, PAPAGO, Qaz Biometric Systems, and VIDA-Digital Identity
- ▷ We have added results for new algorithms from nine returning developers: Cyberextruder, Glory, Maxvision Technology, Rank One Computing, Securif AI, Suprema AI, Suprema ID, Toshiba, and Yuan High-Tech Development.
- ▷ We have retired results for nine algorithms per our policy to only list results for two algorithms per developer. Results for retired algorithms appear in prior versions of this report in the [archive](#).

2022-07-29 changes since 2022-06-27:

- ▷ We have added results for first algorithms from seven developers: FRP LLC (Hawaii), IMDS Software, Inspur (Beijing) Electronic Information Industry, Intema - LGL Group, PAPAGO, Qaz Biometric Systems, and VIDA-Digital Identity
- ▷ We have added results for new algorithms from nine returning developers: Cyberextruder, Glory, Maxvision Technology, Rank One Computing, Securif AI, Suprema AI, Suprema ID, Toshiba, and Yuan High-Tech Development.
- ▷ We have retired results for nine algorithms per our policy to only list results for two algorithms per developer. Results for retired algorithms appear in prior versions of this report in the [archive](#).

2022-06-27 changes since 2022-06-03:

- ▷ We have added results for first algorithms from two developers: Krungthai Bank, and Smartbiometrik.
- ▷ We have added results for new algorithms from thirteen returning developers: Aiseemu, Corsight, Digidata, Griaule, Guangzhou Pixel Solutions, Hangzhuo AI Network Information Technology, Neurotechnology, Real Networks, Samsung S1, Sensetime Group, Smart Engines, Verihubs Inteligensia, and VinBigData.
- ▷ We have retired results for eight algorithms per our policy to only list results for two algorithms per developer. Results for retired algorithms appear in prior versions of this report in the [archive](#).

2022-06-03 changes since 2022-05-05:

- ▷ We have added results for first algorithms from seven developers: Jaak IT, Metsakuur, Palit Microsystems, Smarvist Teknoloji, and Touchless ID.

- ▷ We have added results for new algorithms from sixteen returning developers: Cyberlink, FaceOnLive, Kakao Enterprise, Line Corporation (Line Clova), Multi-Modality Intelligence, NEO Systems, and Unissey
- ▷ We have retired results for four algorithms per our policy to only list results for two algorithms per developer. Results for retired algorithms appear in prior versions of this report in the [archive](#).
- ▷ We have moved the results for the twenty human-difficult pairs used in the May 2018 paper *Face recognition accuracy of forensic examiners, superrecognizers, and face recognition algorithms* by Phillips et al. [1]. to the algorithm-specific report cards (example: [PDF](#)).
- ▷ Likewise, we have added figures showing impostor distribution shifts across demographics to the report card.

2022-05-05 changes since 2022-03-18:

- ▷ We have added results for first algorithms from seven developers: Accurascan, DICIO, FacePhi, Pangiam, University of Surrey-CVSSP, and Veridium.
- ▷ We have added results for new algorithms from sixteen returning developers: ACI Software, Canon Inc, Cloudwalk - Moontime Smart Technology, Cybercore,

2022-05-05 changes since 2022-03-18:

- ▷ We have added results for first algorithms from seven developers: Accurascan, DICIO, FacePhi, Pangiam, University of Surrey-CVSSP, and Veridium.
- ▷ We have added results for new algorithms from sixteen returning developers: ACI Software, Canon Inc, Cloudwalk - Moontime Smart Technology, Cybercore, Cyberextruder, Gemalto Cogent, HyperVerge Inc, KuKe3D Technology, Megvii/Face++, Mobbeel Solutions, Panasonic R+D Center Singapore, Qnap Security, Samsung-SDS, Vietnam Posts and Telecommunications Group, Viettel Group, and Vision Intelligence Center of Meituan.
- ▷ We have retired results for 12 algorithms per our policy to only list results for two algorithms per developer. Results for retired algorithms appear in prior versions of this report in the [archive](#).

2022-03-18 changes since 2022-02-23:

- ▷ We have added support for the detection of multiple people in a single image (see Section 1.2). Specifically the API allows an algorithm to extract features from one or more faces it detects in an image. NIST scores such cases as a correct match when any detected face matches the reference photo, and as a false positive when either face matches a non-mated reference photo. The expected effect of doing this will be to improve reported false non-match rates, and to minimally elevate false match rates. This technique was only applied to images of type "border" and "kiosk".
- ▷ We have added results for first algorithms from four developers: IntelliVIX, Kasikorn Labs, Lebentech Biometrics, and Wicket.
- ▷ We have added results for new algorithms from 10 returning developers: Chunghwa Telecom, Cloudmatrix, Beijing DeepSense Technologies, FarBar Inc, Imagus Technology Pty, Intellivision, Maxvision Technology, NHN Corp, Seventh Sense Artificial Intelligence, and Verigram.
- ▷ We have retired results for 4 algorithms per our policy to only list results for two algorithms per developer. Results for retired algorithms appear in prior versions of this report in the [archive](#).

2022-02-23 changes since 2022-01-24:

- ▷ We have added results for first algorithms from four developers: AFIS and Biometrics Consulting, Digi-data, Graymatics, Hangzhuo Allu Network Information Technology, KnowUTech LLC, Sukshi Technology Innovation, T4iSB, and TuringTech.vip
- ▷ We have added results for new algorithms from 18 returning developers: Cognitec Systems GmbH, GeoVision Inc, Glory, Herta Security, Intel Research Group, InsightFace AI, Kakao Enterprise, N-Tech Lab, Omnidarde Ltd, Papilon Savunma, Paravision, Realnetworks Inc, Reveal Media Ltd, Shenzhen Inst Adv Integrated Tech CAS, Suprema AI Inc, Toshiba, Universidade de Coimbra, and Yuan High-Tech Development
- ▷ We have retired results for 14 algorithms per our policy to only list results for two algorithms per developer. Results for retired algorithms appear in prior versions of this report in the [archive](#).

2022-01-24 changes since 2022-01-20:

- ▷ We have added results for new algorithms from one returning developer: Vocord.

2022-01-20 changes since 2021-12-18:

- ▷ We have added results for first algorithms from four developers: Armatura, Beyne.AI, One More Security, and VinBigData
- ▷ We have added results for new algorithms from 19 returning developers: AuthenMetric, BOE Technology Group, Cybercore, Cyberlink, Dahua Technology, FaceTag Co, Innovatrics, Megvii, Mobbeel Solutions, Neurotechnology, Oz Forensics, Rank One Computing, Regula Forensics, Samsung S1, Securif AI, Sensetime Group, TigerIT Americas, Videmo Intelligent Videoanalyse, and YooniK.
- ▷ We have retired results for 14 algorithms per our policy to only list results for two algorithms per developer. Results for retired algorithms appear in prior versions of this report in the [archive](#).

: **2021-12-16 changes since 2021-11-22:**

- ▷ We have added results for first algorithms from five developers: Alfabet, Cloudmatrix, Euronovate SA, FaceOnLive Inc, and Mobicin Technology.
- ▷ We have added results for new algorithms from ten returning developers: ACI Software, ITMO University, NEO Systems, Guangzhou Pixel Solutions, Panasonic R+D Center Singapore, Qnap Security, Scanovate, Tevian, Unissey, and Vietnam Posts and Telecommunications Group.
- ▷ We have retired results for eight algorithms per our policy to only list results for two algorithms per developer. Results for retired algorithms appear in prior versions of this report in the [archive](#).
- ▷ We have revamped the figure showing performance on 20 pairs of open-source images. It now color-codes false negatives and positives against a default threshold value.

2021-11-22 changes since 2021-10-28:

- ▷ We have added results to the [website](#) for kiosk-collected images where the design and geometry configuration mean that many images have considerable downward pitch angle. In some images, the face is partially cropped. Some images have other background faces.
- ▷ We have stopped using child exploitation images in FRVT, as we lost access to the imagery. All results for that set have been removed from the [website](#), and will be removed from future PDF reports.
- ▷ We have added results for first algorithms from seven new developers: CUDO Communication, Daon, KuKe3D Technology, Mantra Softech India, Maxvision Technology, Multi-Modality Intelligence, and Samsung-SDS.
- ▷ We have added results for new algorithms from seven returning developers: Acer Incorporated, Cloudwalk-Moontime Smart Technology, Gorilla Technology, ID3 Technology, Incode Technologies, NSENSE Corp., and SQIsoft.
- ▷ We have retired results for six algorithms per our policy to only list results for two algorithms per developer. Results for retired algorithms appear in prior versions of this report in the [archive](#).

2021-10-28 changes since 2021-09-08:

- ▷ We have substantially revised the algorithm-specific report cards that are linked from the [FRVT results page](#). (Example: [HTML](#)).
- ▷ We have added results for first algorithms from eight new developers: Beijing Mendaxia Technology, Beijing Hisign Technology, Biocube Matrics, Clearview AI, Reveal Media, Toppan ID Gate, Verigram, and Viettel High Technology.
- ▷ We have added results for new algorithms from thirty returning developers: 20Face, 3divi, Canon Inc Chunghwa Telecom, Corsight, Decatur Industries, Deepglint, Dermalog, FaceTag, Fiberhome Telecommunication Technologies, GeoVision, ICM Airport Technics, Imagus Technology, InsightFace AI, Kakao Enterprise, Kookmin University, Line Corporation, N-Tech Lab, NotionTag Technologies, Realnetworks, Suprema ID, Taiwan-Certificate Authority, Toshiba, Tripleize, Trueface.ai, Veridas Digital Authentication, Visidon, VisionLabs, YooniK, and Yuan High-Tech Development.
- ▷ We have retired results for twenty algorithms per our policy to only list results for two algorithms per developer. Results for retired algorithms appear in prior versions of this report in the [archive](#).

2021-09-08 changes since 2021-08-02:

- ▷ We have added results for first algorithms from seven new developers: Griaule, SQIsoft, Qnap Security, Techsign, Smart Engines, Verihubs, and Wuhan Tianyu Information Industry.
- ▷ We have added results for new algorithms from sixteen returning developers: ADVANCE.AI, AuthenMetric, CloudSmart Consulting, Code Everest Pvt, Cognitec Systems, Thales Gemalto Cogent, Intel Research Group, Omnidarde, Oz Forensics, Rank One Computing, Samsung S1 Corp, Securif AI, Tevian, TigerIT Americas, Universidade de Coimbra, and Vigilant Solutions
- ▷ We have retired results for eleven algorithms per our policy to only list results for two algorithms per developer. Results for retired algorithms appear in prior versions of this report in the [archive](#).

2021-08-02 changes since 2021-06-25:

- ▷ We have added results for first algorithms from eight new developers: Bee the Data, Closeli Inc, Coretech Knowledge Inc, Deepsense (France), ioNetworks Inc, Kakao Pay Corp, Seventh Sense Artificial Intelligence, and SK Telecom.

- ▷ We have added results for new algorithms from fifteen returning developers: Alchera Inc, Adera Global PTE, Aware, Bresee Technology, Cyberlink Corp, Expasoft LLC, Fujitsu Research and Development Center, Gorilla Technology, Idemia, Neurotechnology, NEO Systems, NHN Corp, Paravision, Panasonic R+D Center Singapore, and Shenzhen University-Macau University of Science and Technology.
- ▷ We have retired results for twelve algorithms per our policy to only list results for two algorithms per developer. Results for retired algorithms appear in prior versions of this report in the [archive](#).

2021-06-25 changes since 2021-05-21:

- ▷ We have added results for first algorithms from six new developers: Alice Biometrics, BOE Technology Group, Fincore, Neosecu, Sodec App, and Yuntu Data and Technology.
- ▷ We have added results for new algorithms from seven returning developers: Incode Technologies, HyperVerge, Mobbeel Solutions, Guangzhou Pixel Solutions, Remark Holdings, Sensetime, and Vietnam Posts and Telecommunications Group.
- ▷ We have retired results for four algorithms per our policy to only list results for two algorithms per developer. Results for retired algorithms appear in prior versions of this report in the [archive](#).

2021-05-21 changes since 2021-04-26:

- ▷ We have added results for first algorithms from five new developers: Ekin Smart City Technologies, Suprema ID, Tripleize, Taiwan-Certificate Authority, and Vision Intelligence Center of Meituan.
- ▷ We have added results for new algorithms from eight returning developers: ID3 Technology, Imagus Technology, Momentum Digital, N-Tech Lab, NSENSE, Shanghai Jiao Tong University, Vision-Box, and Yuan High-Tech Development
- ▷ We have retired results for seven algorithms per our policy to only list results for two algorithms per developer. Results for retired algorithms appear in prior versions of this report in the [archive](#).

2021-04-26 changes since 2021-04-16:

- ▷ We have added results for first algorithms from three new developers: Quantasoft, Rendip, and NEO Systems.
- ▷ We have added results for new algorithms from four returning developers: 3Divi, Realnetworks, Veridas Digital Authentication Solutions, and Universidade de Coimbra.
- ▷ We have retired results for three algorithms per our policy to only list results for two algorithms per developer. Results for retired algorithms appear in prior versions of this report in the [archive](#).

2021-04-16 changes since 2021-03-19:

- ▷ We have added results for first algorithms from six new developers: 20Face, Beijing DeepSense Technologies, BitCenter UK, Enface, FaceTag, InsightFace AI, Line Corporation, Lema Labs, Nanjing Kiwi Network Technology, Omnidarde, Regula Forensics, and Suprema.
- ▷ We have added results for new algorithms from ten returning developers: CloudSmart Consulting, Dermalog, GeoVision, Neurotechnology, Panasonic R+D Center Singapore, Samsung S1, Securif AI, Trueface.ai, Vigilant Solutions, and Visidon.

- ▷ We have retired results for ten algorithms per our policy to only list results for two algorithms per developer. Results for retired algorithms appear in prior versions of this report in the [archive](#).

2021-03-19 changes since 2021-03-05:

- ▷ We have added results for first algorithms from six new developers: Ajou University, AuthenMetric, Code Everest, Corsight, Papilon Savunma, and NHN Corp
- ▷ We have added results for new algorithms from seven returning developers: Alchera, Deepglint, Fiber-home Telecommunication Technologies, Kakao Enterprise, Kookmin University, Megvii/Face++, and NotionTag Technologies.
- ▷ We have updated many of the hyperlinked HTML report-cards to include seven figures on demographic dependence. Figures of this kind first appeared, and are documented in, the December 2019 document, [NIST Interagency Report 8280](#) on demographic differentials in face recognition. The figures quantify false negative dependence on demographics using “visa-border” comparisons, and false positive dependence using comparisons of “application” photos that uniformly of quality and similar to visa photos.

2021-03-05 changes since 2021-01-19:

- ▷ We have added results for first algorithms from three new developers: IVA Cognitive, Mobbeel, and MoreDian Technology.
- ▷ We have added results for new algorithms from returning developers: Ability Enterprise - Andro Video, ACI Software, Adera Global, AnyVision, BioID Technologies, China Electronics Import-Export, Cognitec Systems, Fujitsu Research and Development Center, Glory, Guangzhou Pixel Solutions, Hengrui AI Technology, Incode Technologies, Intel Research, iQIYI, Mobai, Oz Forensics, Paravision, VisionLabs, and Xforward AI Technology.
- ▷ We have added a new “resources” tab to the main [webpage](#). It includes sortable columns for data related to speed, model size, storage, and memory consumption.
- ▷ We have retired results for 13 algorithms per our policy to only list results for two algorithms per developer. Results for retired algorithms appear in prior versions of this report in the [archive](#).

2021-01-19 changes since 2020-12-18:

- ▷ This report adds results for first algorithms from four developers: Herta Security, Irax AI, Shenzhen University-Macau University of Science and Technology, and Vietnam Posts and Telecommunications Group. See Table 8 for more information.
- ▷ The report also includes results for thirteen developers who have previously submitted algorithms: Bresee Technology, Canon (previously Canon Information Technology (Beijing)), Cyberlink, CSA IntelliCloud Technology, Dahua Technology, ID3 Technology, Imagus Technology (Vixvization), Moontime Smart Technology, N-Tech Lab, Thales Cogent, Veridas Digital Authentication Solutions, Vocord, and Yuan High-Tech Development.
- ▷ We have retired results for ten algorithms per our policy to only list results for two algorithms per developer. Results for retired algorithms appear in prior versions of this report in the [archive](#).

2020-12-18 changes since 2020-10-09:

- ▷ This report adds results for first algorithms from ten developers: BitCenter UK, CloudSmart Consulting, Cubox, Institute of Computing Technology, Naver Corp, Minivision, NSENSE Corp, Viettel Group, Visage Technologies, and Xiamen University. See Table 8 for more information.
- ▷ The report also includes results for eighteen developers who have previously submitted algorithms: ADVANCE.AI, Awidit Systems, Chosun University, Dermalog, GeoVision, ICM Airport Technics, Idemia, Institute of Information Technologies, Kakao Enterprise, Neurotechnology, Panasonic R+D Center Singapore, Rank One Computing, Sensetime Group, Shanghai Jiao Tong University, TigerIT Americas LLC, Vigilant Solutions, Winsense, and YooniK
- ▷ We have retired results for twelve algorithms per our policy to only list results for two algorithms per developer. Results for retired algorithms appear in prior versions of this report in the [archive](#).

Changes since September 18, 2020:

- ▷ This report adds results for first algorithms from five developers: Aigen, Cortica, Kookmin University, Securif AI and Vinai.
- ▷ The report also includes results for three developers who have previously submitted algorithms: Fujitsu Laboratories, Hengrui AI, and X-Forward AI.
- ▷ In the per-algorithm report-cards linked from tables and the main webpage, we have added a chart to showing reduction in error rates over the course of FRVT i.e. from 2017 onwards for all algorithms supplied by that developer. Similarly we have added a chart showing error rate reductions for our test of protective face mask verification.
- ▷ We plan to continue evaluating algorithms on various mask datasets. We hold that algorithms should be capable of detecting masks and verifying identity of all combinations of masked and unmasked faces. We have accordingly increased the amount of time allowed to extract those features from 1.0 to 1.5 seconds.

Changes since August 25, 2020:

- ▷ This report adds results for first algorithms from eight new developers. Akurat Satu Indonesia, Cybercore, Decatur Industries, Innef Labs, Satellite Innovation/Eocortex, Expasoft, and Mobai.
- ▷ The report includes results for seven developers who have previously submitted algorithms: 3Divi, BioID Technologies, Incode Technologies, Innovatrics, iSAP Solution, Synology, and Tevian.
- ▷ We have retired results for five algorithms per our policy to only list results for two algorithms per developer. Results for retired algorithms appear in prior versions of this report in the [archive](#).

Changes since July 27, 2020:

- ▷ We have introduced per-algorithm report sheets. These are HTML documents linked from the accuracy tables in this report (i.e. Table 32) and on the FRVT 1:1 [homepage](#). The sheets contain interactive graphics allowing, for example, mouseover exploration of FNMR(T) and FMR(T). Some of their content had previously appeared in this document.
- ▷ This report adds results for algorithms from six new developers. ACI Software, Bresee Technology, Fiberhome Telecommunication Technologies, Imageware Systems, Oz Forensics, and Pensees.
- ▷ The report includes results for thirteen developers who have previously submitted algorithms: Canon Information Technology (Beijing), Cyberlink, Dahua Technology, Gorilla Technology, ID3 Technology, Intel Research Group, iQIYI Inc, Momentum Digital, Netbridge Technology, Tech5 SA, Shenzhen AiMall Tech, Vigilant Solutions, and VisionLabs.

- ▷ We have retired results for nine algorithms per our policy to only list results for two algorithms per developer. Results for retired algorithms appear in prior versions of this report in the [archive](#).

Changes since May 18, 2020:

- ▷ The report is the first FRVT update since the pandemic closed it from March to June 2020.
- ▷ This report includes results for algorithms from nine new developers: GeoVision Inc, Su Zhou NaZhi-TianDi Intelligent Technology, YooniK, AYF Technology, PXL Vision AG, Yuan High-Tech Development, Beihang University-ERCACAT, ICM Airport Technics, and Staqu Technologies
- ▷ This report includes results for algorithms from 15 returning developers Acer Incorporated, Antheus Technologia, Chosun University, Chunghwa Telecom, Idemia, Moontime Smart Technology, Neurotechnology, Guangzhou Pixel Solutions, Panasonic R+D Center Singapore, Rank One Computing, Scanovate, Shanghai Universiy - Shanghai Film Academy, Synesis, Trueface.ai, and Veridas Digital Authentication Solutions
- ▷ We have retired results for ten algorithms per our policy to only list results for two algorithms per developer. Results for retired algorithms appear in prior versions of this report in the [archive](#).
- ▷ We separated timing and other resource consumption from the main participation table. The new Table [20](#) includes template generation durations for four kinds of images, not just mugshots.
- ▷ We have published a separate report, [NIST Interagency Report 8311](#) on accuracy of pre-pandemic algorithms on subjects wearing face masks. We plan to track improvements in accuracy on masked images going forward. In particular, we invite submission of algorithms that can detect whether a person is wearing a mask, extract features from the full face or the exposed periocular region, and do appropriate comparison. We do not intend to evaluate algorithms that assume 100% of images will be of masked individuals.

Changes since March 25, 2020:

- ▷ The report is a maintenance release - it does not add any new algorithms, and FRVT has been closed to new algorithms since mid March 2020.
- ▷ We modified the primary accuracy summary, Table [32](#), as follows:
 - ▷▷ For visa images, the column for FNMR at FMR = 0.0001 has been removed. The visa images are so highly controlled that the error rates for the most accurate algorithms are dominated by false rejection of very young children and by the presence of a few noisy greyscale images. For now, two visa columns remain: FNMR at $FMR = 10^{-6}$ and, for matched covariates, FNMR at $FMR = 10^{-4}$.
 - ▷▷ We have inserted a new column labelled "BORDER" giving accuracy for comparison of moderately poor webcam border-crossing photos that exhibit pose variations, poor compression, and low contrast due to strong background illumination. The accuracies are the worst from all cooperative image datasets used in FRVT.
- ▷ Accordingly, we updated the failure-to-template rates in Table [41](#).
- ▷ We withdrew a figure showing how false matches are concentrated in certain visa images used in cross-comparison, because it didn't attempt to include demographic information.

Changes since February 27, 2020:

- ▷ The report adds results algorithms from two new developers: Beijing Alleyes Technology, and the Chinese University of Hong Kong. Results for newly submitted algorithms from two other developers will appear in the next report.
- ▷ The report adds results for algorithms from thirteen returning developers: ASUSTek Computer, Aware, Cyberlink Corp, Gorilla Technology, Innovative Technology, Kakao Enterprise, Lomonosov Moscow State University, Panasonic R+D Center Singapore, Shenzhen AiMall Technology, Shenzhen Intellifusion Technologies, Synology, Tech5 SA, and Via Technologies.
- ▷ Per policy to only list results for two algorithms per developer, we have dropped results for algorithms from Aware, Cyberlink, Gorilla Technology, Kakao Enterprise, Lomonosov Moscow State University, Panasonic R+D Center Singapore, and Tech5 SA.

Changes since January 20, 2020:

- ▷ The report adds results for five new developers: Ability Enterprise (Andro Video), Chosun University, Fujitsu Research and Development Center, University of Coimbra, and Xforward AI Technology.
- ▷ The report adds results for algorithms from six returning developers: AlphaSSTG, Incode Technologies, Kneron, Shanghai Jiao Tong University, Vocord, and X-Laboratory.
- ▷ We have corrected template comparison timing numbers for algorithms submitted September 2019 to January 2020. The values reported previously were slower due to a software bug.
- ▷ We have dropped results for algorithms from Vocord and Incode per policy to only list results for two algorithms per developer.
- ▷ The [FRVT 1:1 homepage](#) has been updated with latest accuracy results.
- ▷ The [FRVT 1:N homepage](#) now includes an update to the September 2019 NIST Interagency Report 8271. The new report adds results for one-to-many search algorithms submitted to NIST from June 2019 to January 2020.

Changes since January 6, 2020:

- ▷ Section 2 has been updated to better describe the Visa and Border images. The caption for Table 32 has been updated to better relate the accuracy values to particular image comparisons.
- ▷ The report adds results for five new developers: Acer, Advance.AI, Expasoft, Netbridge Technology, and Videmo Intelligent Videoanalyse.
- ▷ The report adds results for algorithms from 7 returning developers: China Electronics Import-Export Corp, Intel Research Group, ITMO University, Neurotechnology, N-Tech Lab, Rokid, and VisionLabs.
- ▷ We have dropped results from this edition of the report per policy to only list results for two algorithms per developer: N-Tech Lab, Neurotechnology, ITMO, Visionlabs, and CEIEC.
- ▷ The [FRVT homepage](#) has been updated with latest accuracy results.

Changes since November 11, 2019:

- ▷ Table 20 has been updated to include runtime memory usage. This is the first time such a quantity has been reported. The value is the peak size of the resident set size logged during enrollment of single images.
- ▷ We have migrated summary results table to a new platform that supports sortable tables:
<https://pages.nist.gov/frvt/html/frvt11.html>

- ▷ The report adds results for four new developers: Antheus Technologia, BioID Technologies SA, Canon Information Tech. (Beijing), Samsung S1 (listed in the tables as S1), and Taiwan AI Labs.
- ▷ The report adds results for algorithms from 13 returning developers: Anke Investments, Chunghwa Telecom, Deepglint, Institute of Information Technologies, iQIYI, Kneron, Ping An Technology, Paravision, KanKan Ai, Rokid Corporation, Shanghai Universiy - Shanghai Film Academy, Veridas Digital Authentication Solutions, and Videometrics Technology.
- ▷ We have dropped results from this edition of the report per policy to only list results for two algorithms per developer: remarkai-000, veridas-001, sensetime-001, iit-000, anke-003, and everai-002. Results for these are available in prior editions of this report linked from the FRVT page.
- ▷ We issued [NIST Interagency Report 8280: FRVT Part 3: Demographics](#) on 2019-12-19. It includes results for many of the algorithms covered by this report.

Changes since October 16, 2019:

- ▷ The report adds results for ten new developers: Ai-Union Technology, ASUSTek Computer, DiDi ChuXing Technology, Innovative Technology, Luxand, MVision, Pyramid Cyber Security + Forensic, Scanovate, Shenzhen AiMall Tech, and TUPU Technology.
- ▷ The report adds results for 12 returning developers: CTBC Bank Glory Gorilla Technology Guangzhou Pixel Solutions Imagus Technology Incode Technologies Lomonosov Moscow State University Rank One Computing Samtech InfoNet Shanghai Ulucu Electronics Technology Synesis, and Winsense.
- ▷ We have dropped results from this edition of the report per policy to only list results for two algorithms per developer: glory-000, gorilla-002, incode-003, rankone-006, and synesis-004.
- ▷ Results for five recently submitted algorithms will appear in the next report.

Changes since September 11, 2019:

- ▷ The report adds results for five new participants: Awidit Systems (Awiros), Momemtum Digital (Sertis), Trueface AI, Shanghai Jiao Tong University, and X-Laboratory.
- ▷ The reports adds results for five new algorithms from returning developers: Cyberlink, Hengrui AI Technology, Idemia, Panasonic R+D Singapore, and Tevian. This causes three algorithm, to be de-listed from the report per policy to list results for two algorithms per developer.

Changes since July 31 2019:

- ▷ The HTML table on the [FRVT 1:1 homepage](#) has been updated to include a column for cross-domain Visa-Border verification. Results for this new dataset appeared in the July 29 report under the name "CrossEV" - these are now renamed "Visa-Border".
- ▷ The [FRVT 1:1 homepage](#) lists algorithms according to lowest mean rank accuracy:

$$\begin{aligned} & \text{Rank(FNMR}_{\text{VISA}}\text{ at FMR = 0.000001}) + \\ & \text{Rank(FNMR}_{\text{VISA-BORDER}}\text{ at FMR = 0.000001}) + \\ & \text{Rank(FNMR}_{\text{MUGSHOT}}\text{ at FMR = 0.00001 after 14 years}) + \\ & \text{Rank(FNMR}_{\text{WILD}}\text{ at FMR = 0.00001}) \end{aligned}$$

This ordering rewards high accuracy across all datasets.
- ▷ The main results in Table 32 is now in landscape format to accomodate extra columns for the Visa-Border set, and mugshot comparisons after at least 12 years.
- ▷ The report adds results for nine new participants: Alpha SSTG, Intel Research, ULSee, Chungwa Telecon, iSAP Solution, Rokid, Shenzhen EI Networks, CSA Intellicloud, Shenzhen Intellifusion Technologies.

- ▷ The report adds results for six new algorithms from returning developers: Innovatrics, Dahua Technology, Tech5 SA, Intellivision, Nodeflux and Imperial College, London. One algorithm, from Imperial has been retired, per policy to list results for two algorithms per developer.
- ▷ The cross-country false match rate heatmaps have been replotted to reveal more structure by listing countries by region instead of alphabetically.
- ▷ The next version of this report will be posted around October 18, 2019.

Changes since July 3 2019:

- ▷ The HTML table on the [FRVT 1:1 homepage](#) has been updated to list the 20 most accurate developers rather than algorithms, choosing the most accurate algorithm from each developer based on visa and mugshot results. Also, the algorithms are ordered in terms of lowest mean rank across mugshot, visa and wild datasets, rewarding broad accuracy over a good result on one particular dataset.
- ▷ This report includes results for a new dataset - see the column labelled "visa-border" in Table 5. It compares a new set of high quality visa-like portraits with a set webcam border-crossing photos that exhibit moderately poor pose variations and background illumination. The two new sets are described in sections [2.2](#) and [2.4](#). The comparisons are "cross-domain" in that the algorithm must compare "visa" and "wild" images. Results for other algorithms will be added in future reports as they become available.
- ▷ This report adds results for algorithms from 9 developers submitted in early July 2019. These are from 3DiVi, Camvi, EverAI-Paravision, Facesoft, Farbar (F8), Institute of Information Technologies, Shanghai U. Film Academy, Via Technologies, and Ulucu Electronics Tech. Six of these are new participants.
- ▷ Several other algorithms have been submitted and are being evaluated. Results will be released in the next report, scheduled for September 5. That report will include results for new datasets.
- ▷ Older algorithms from Everai, Camvi and 3DiVi, have been retired, per the policy to list only two algorithms per developer.

Changes since June 20 2019:

- ▷ This report adds results for algorithms from 18 developers submitted in early June 2019. These are from CTBC Bank, Deep Glint, Thales Cogent, Ever AI Paravision, Gorilla Technology, Imagus, Incode, Kneron, N-Tech Lab, Neurotechnology, Notiontag Technologies, Star Hybrid, Videonetics, Vigilant Solutions, Winsense, Anke Investments, CEIEC, and DSK. Nine of these are new participants.
- ▷ Several other algorithms have been submitted and are being evaluated. Results will be released in the next report, scheduled for August 1.
- ▷ Older algorithms from Everai, Thales Cogent, Gorilla Technology, Incode, Neurotechnology, N-Tech Lab and Vigilant Solutions have been retired, per the policy to list only two algorithms per developer.

Changes since April 2019:

- ▷ This report adds results for nine algorithms from nine developers submitted in early June 2019. These are from Tencent Deepsea, Hengrui, Kedacom, Moontime, Guangzhou Pixel, Rank One Computing, Synesis, Sensetime and Vocord.
- ▷ Another 23 algorithms have been submitted and are being evaluated. Results will be released in the next report, scheduled for July 3.
- ▷ Older algorithms for Rank One, Synesis, and Vocord have been retired, per the policy to list only two algorithms per developer.

Changes since February 2019:

- ▷ This report adds results for 49 algorithms from 42 developers submitted in early March 2019.

- ▷ This report omits results for algorithms that we retired. We retired for three reasons: 1. The developer submitted a new algorithm, and we only list two. 2. The algorithm needs a GPU, and we no longer allow GPU-based algorithms. 3. Inoperable algorithms.
- ▷ Previous results for retired algorithms are available in older editions of this report linked [here](#).
- ▷ The mugshot database used from February 2017 to January 2019 has been replaced with an extract of the mugshot database documented in NIST Interagency Report 8238, November 2018. The new mugshot set is described in section [2.5](#) and is adopted because:
 - ▷▷ It has much better identity label integrity, so that false non-match rates are substantially lower than those reported in FRVT 1:1 reports to date - see Figure [121](#).
 - ▷▷ It includes images collected over a 17 year period such that ageing can be much better characterized - - see Figure [329](#).
- ▷ Using the new mugshot database, Figure [329](#) shows accuracy for four demographic groups identified in the biographic metadata that accompanies the data: black females, black males, white females and white males.
- ▷ The report added a figure (now moved to web) with results for the twenty human-difficult pairs used in the May 2018 paper *Face recognition accuracy of forensic examiners, superrecognizers, and face recognition algorithms* by Phillips et al. [[1](#)].
- ▷ The report uses an update to the wild image database that corrects some ground truth labels.
- ▷ Some results for the child exploitation database are not complete. They are typically updated less frequently than for other image sets.

Contents

ACKNOWLEDGMENTS	1
DISCLAIMER	1
INSTITUTIONAL REVIEW BOARD	1
1 METRICS	59
1.1 CORE ACCURACY	59
1.2 MULTI-TEMPLATE SCORING METHODOLOGY	59
2 DATASETS	60
2.1 VISA IMAGES	60
2.2 APPLICATION IMAGES	60
2.3 APPLICATION IMAGES WITH HEAD YAW	60
2.4 BORDER CROSSING IMAGES	61
2.5 MUGSHOT IMAGES	61
2.6 KIOSK IMAGES	61
2.7 WILD IMAGES	62
3 RESULTS	62
3.1 TEST GOALS	62
3.2 TEST DESIGN	63
3.3 FAILURE TO ENROLL	66
3.4 RECOGNITION ACCURACY	76
3.5 GENUINE DISTRIBUTION STABILITY	330
3.5.1 EFFECT OF BIRTH PLACE ON THE GENUINE DISTRIBUTION	330
3.5.2 EFFECT OF AGEING	373
3.5.3 EFFECT OF AGE ON GENUINE SUBJECTS	405
3.6 IMPOSTOR DISTRIBUTION STABILITY	449
3.6.1 EFFECT OF BIRTH PLACE ON THE IMPOSTOR DISTRIBUTION	449
3.6.2 EFFECT OF AGE ON IMPOSTORS	452

List of Tables

1 PARTICIPANT INFORMATION	25
2 PARTICIPANT INFORMATION	26
3 PARTICIPANT INFORMATION	27
4 PARTICIPANT INFORMATION	28
5 PARTICIPANT INFORMATION	29
6 PARTICIPANT INFORMATION	30
7 PARTICIPANT INFORMATION	31
8 PARTICIPANT INFORMATION	32
9 ALGORITHM SUMMARY	33
10 ALGORITHM SUMMARY	34
11 ALGORITHM SUMMARY	35
12 ALGORITHM SUMMARY	36
13 ALGORITHM SUMMARY	37
14 ALGORITHM SUMMARY	38
15 ALGORITHM SUMMARY	39
16 ALGORITHM SUMMARY	40
17 ALGORITHM SUMMARY	41
18 ALGORITHM SUMMARY	42

19	ALGORITHM SUMMARY	43
20	ALGORITHM SUMMARY	44
21	FALSE NON-MATCH RATE	45
22	FALSE NON-MATCH RATE	46
23	FALSE NON-MATCH RATE	47
24	FALSE NON-MATCH RATE	48
25	FALSE NON-MATCH RATE	49
26	FALSE NON-MATCH RATE	50
27	FALSE NON-MATCH RATE	51
28	FALSE NON-MATCH RATE	52
29	FALSE NON-MATCH RATE	53
30	FALSE NON-MATCH RATE	54
31	FALSE NON-MATCH RATE	55
32	FALSE NON-MATCH RATE	56
33	FAILURE TO ENROL RATES	67
34	FAILURE TO ENROL RATES	68
35	FAILURE TO ENROL RATES	69
36	FAILURE TO ENROL RATES	70
37	FAILURE TO ENROL RATES	71
38	FAILURE TO ENROL RATES	72
39	FAILURE TO ENROL RATES	73
40	FAILURE TO ENROL RATES	74
41	FAILURE TO ENROL RATES	75

List of Figures

1	PERFORMANCE SUMMARY: FNMR VS. TEMPLATE SIZE TRADEOFF	57
2	PERFORMANCE SUMMARY: FNMR VS. TEMPLATE TIME TRADEOFF	58
3	EXAMPLE IMAGES	62
(A)	VISA	62
(B)	MUGSHOT	62
(C)	WILD	62
(D)	BORDER	62
4	PERFORMANCE ON 20 HUMAN-DIFFICULT PAIRS	77
5	PERFORMANCE ON 20 HUMAN-DIFFICULT PAIRS	78
6	PERFORMANCE ON 20 HUMAN-DIFFICULT PAIRS	79
7	PERFORMANCE ON 20 HUMAN-DIFFICULT PAIRS	80
8	PERFORMANCE ON 20 HUMAN-DIFFICULT PAIRS	81
9	PERFORMANCE ON 20 HUMAN-DIFFICULT PAIRS	82
10	PERFORMANCE ON 20 HUMAN-DIFFICULT PAIRS	83
11	PERFORMANCE ON 20 HUMAN-DIFFICULT PAIRS	84
12	PERFORMANCE ON 20 HUMAN-DIFFICULT PAIRS	85
13	PERFORMANCE ON 20 HUMAN-DIFFICULT PAIRS	86
14	PERFORMANCE ON 20 HUMAN-DIFFICULT PAIRS	87
15	PERFORMANCE ON 20 HUMAN-DIFFICULT PAIRS	88
16	PERFORMANCE ON 20 HUMAN-DIFFICULT PAIRS	89
17	PERFORMANCE ON 20 HUMAN-DIFFICULT PAIRS	90
18	PERFORMANCE ON 20 HUMAN-DIFFICULT PAIRS	91
19	PERFORMANCE ON 20 HUMAN-DIFFICULT PAIRS	92
20	PERFORMANCE ON 20 HUMAN-DIFFICULT PAIRS	93
21	PERFORMANCE ON 20 HUMAN-DIFFICULT PAIRS	94
22	PERFORMANCE ON 20 HUMAN-DIFFICULT PAIRS	95
23	PERFORMANCE ON 20 HUMAN-DIFFICULT PAIRS	96
24	PERFORMANCE ON 20 HUMAN-DIFFICULT PAIRS	97
25	PERFORMANCE ON 20 HUMAN-DIFFICULT PAIRS	98

26	PERFORMANCE ON 20 HUMAN-DIFFICULT PAIRS	99
27	PERFORMANCE ON 20 HUMAN-DIFFICULT PAIRS	100
28	PERFORMANCE ON 20 HUMAN-DIFFICULT PAIRS	101
29	PERFORMANCE ON 20 HUMAN-DIFFICULT PAIRS	102
30	PERFORMANCE ON 20 HUMAN-DIFFICULT PAIRS	103
31	PERFORMANCE ON 20 HUMAN-DIFFICULT PAIRS	104
32	PERFORMANCE ON 20 HUMAN-DIFFICULT PAIRS	105
33	PERFORMANCE ON 20 HUMAN-DIFFICULT PAIRS	106
34	PERFORMANCE ON 20 HUMAN-DIFFICULT PAIRS	107
35	PERFORMANCE ON 20 HUMAN-DIFFICULT PAIRS	108
36	PERFORMANCE ON 20 HUMAN-DIFFICULT PAIRS	109
37	PERFORMANCE ON 20 HUMAN-DIFFICULT PAIRS	110
38	PERFORMANCE ON 20 HUMAN-DIFFICULT PAIRS	111
39	PERFORMANCE ON 20 HUMAN-DIFFICULT PAIRS	112
40	PERFORMANCE ON 20 HUMAN-DIFFICULT PAIRS	113
41	PERFORMANCE ON 20 HUMAN-DIFFICULT PAIRS	114
42	PERFORMANCE ON 20 HUMAN-DIFFICULT PAIRS	115
43	PERFORMANCE ON 20 HUMAN-DIFFICULT PAIRS	116
44	PERFORMANCE ON 20 HUMAN-DIFFICULT PAIRS	117
45	PERFORMANCE ON 20 HUMAN-DIFFICULT PAIRS	118
46	ERROR TRADEOFF CHARACTERISTIC: VISA IMAGES	119
47	ERROR TRADEOFF CHARACTERISTIC: VISA IMAGES	120
48	ERROR TRADEOFF CHARACTERISTIC: VISA IMAGES	121
49	ERROR TRADEOFF CHARACTERISTIC: VISA IMAGES	122
50	ERROR TRADEOFF CHARACTERISTIC: VISA IMAGES	123
51	ERROR TRADEOFF CHARACTERISTIC: VISA IMAGES	124
52	ERROR TRADEOFF CHARACTERISTIC: VISA IMAGES	125
53	ERROR TRADEOFF CHARACTERISTIC: VISA IMAGES	126
54	ERROR TRADEOFF CHARACTERISTIC: VISA IMAGES	127
55	ERROR TRADEOFF CHARACTERISTIC: VISA IMAGES	128
56	ERROR TRADEOFF CHARACTERISTIC: VISA IMAGES	129
57	ERROR TRADEOFF CHARACTERISTIC: VISA IMAGES	130
58	ERROR TRADEOFF CHARACTERISTIC: VISA IMAGES	131
59	ERROR TRADEOFF CHARACTERISTIC: VISA IMAGES	132
60	ERROR TRADEOFF CHARACTERISTIC: VISA IMAGES	133
61	ERROR TRADEOFF CHARACTERISTIC: VISA IMAGES	134
62	ERROR TRADEOFF CHARACTERISTIC: VISA IMAGES	135
63	ERROR TRADEOFF CHARACTERISTIC: VISA IMAGES	136
64	ERROR TRADEOFF CHARACTERISTIC: VISA IMAGES	137
65	ERROR TRADEOFF CHARACTERISTIC: VISA IMAGES	138
66	ERROR TRADEOFF CHARACTERISTIC: VISA IMAGES	139
67	ERROR TRADEOFF CHARACTERISTIC: VISA IMAGES	140
68	ERROR TRADEOFF CHARACTERISTIC: VISA IMAGES	141
69	ERROR TRADEOFF CHARACTERISTIC: VISA IMAGES	142
70	ERROR TRADEOFF CHARACTERISTIC: VISA IMAGES	143
71	ERROR TRADEOFF CHARACTERISTIC: VISA IMAGES	144
72	ERROR TRADEOFF CHARACTERISTIC: VISA IMAGES	145
73	ERROR TRADEOFF CHARACTERISTIC: VISA IMAGES	146
74	ERROR TRADEOFF CHARACTERISTIC: VISA IMAGES	147
75	ERROR TRADEOFF CHARACTERISTIC: VISA IMAGES	148
76	ERROR TRADEOFF CHARACTERISTIC: VISA IMAGES	149
77	ERROR TRADEOFF CHARACTERISTIC: VISA IMAGES	150
78	ERROR TRADEOFF CHARACTERISTIC: VISA IMAGES	151
79	ERROR TRADEOFF CHARACTERISTIC: VISA IMAGES	152
80	ERROR TRADEOFF CHARACTERISTIC: VISA IMAGES	153
81	ERROR TRADEOFF CHARACTERISTIC: VISA IMAGES	154

82	ERROR TRADEOFF CHARACTERISTIC: VISA IMAGES	155
83	ERROR TRADEOFF CHARACTERISTIC: VISA IMAGES	156
84	ERROR TRADEOFF CHARACTERISTIC: VISA IMAGES	157
85	ERROR TRADEOFF CHARACTERISTIC: VISA IMAGES	158
86	ERROR TRADEOFF CHARACTERISTIC: VISA IMAGES	159
87	ERROR TRADEOFF CHARACTERISTIC: VISA IMAGES	160
88	ERROR TRADEOFF CHARACTERISTIC: VISA IMAGES	161
89	ERROR TRADEOFF CHARACTERISTIC: VISA IMAGES	162
90	ERROR TRADEOFF CHARACTERISTIC: VISA IMAGES	163
91	ERROR TRADEOFF CHARACTERISTIC: VISA IMAGES	164
92	ERROR TRADEOFF CHARACTERISTIC: VISA IMAGES	165
93	ERROR TRADEOFF CHARACTERISTIC: VISA IMAGES	166
94	ERROR TRADEOFF CHARACTERISTIC: VISA IMAGES	167
95	ERROR TRADEOFF CHARACTERISTIC: VISA IMAGES	168
96	ERROR TRADEOFF CHARACTERISTIC: VISA IMAGES	169
97	ERROR TRADEOFF CHARACTERISTIC: MUGSHOT IMAGES	170
98	ERROR TRADEOFF CHARACTERISTIC: MUGSHOT IMAGES	171
99	ERROR TRADEOFF CHARACTERISTIC: MUGSHOT IMAGES	172
100	ERROR TRADEOFF CHARACTERISTIC: MUGSHOT IMAGES	173
101	ERROR TRADEOFF CHARACTERISTIC: MUGSHOT IMAGES	174
102	ERROR TRADEOFF CHARACTERISTIC: MUGSHOT IMAGES	175
103	ERROR TRADEOFF CHARACTERISTIC: MUGSHOT IMAGES	176
104	ERROR TRADEOFF CHARACTERISTIC: MUGSHOT IMAGES	177
105	ERROR TRADEOFF CHARACTERISTIC: MUGSHOT IMAGES	178
106	ERROR TRADEOFF CHARACTERISTIC: MUGSHOT IMAGES	179
107	ERROR TRADEOFF CHARACTERISTIC: MUGSHOT IMAGES	180
108	ERROR TRADEOFF CHARACTERISTIC: MUGSHOT IMAGES	181
109	ERROR TRADEOFF CHARACTERISTIC: MUGSHOT IMAGES	182
110	ERROR TRADEOFF CHARACTERISTIC: MUGSHOT IMAGES	183
111	ERROR TRADEOFF CHARACTERISTIC: MUGSHOT IMAGES	184
112	ERROR TRADEOFF CHARACTERISTIC: MUGSHOT IMAGES	185
113	ERROR TRADEOFF CHARACTERISTIC: MUGSHOT IMAGES	186
114	ERROR TRADEOFF CHARACTERISTIC: MUGSHOT IMAGES	187
115	ERROR TRADEOFF CHARACTERISTIC: MUGSHOT IMAGES	188
116	ERROR TRADEOFF CHARACTERISTIC: MUGSHOT IMAGES	189
117	ERROR TRADEOFF CHARACTERISTIC: MUGSHOT IMAGES	190
118	ERROR TRADEOFF CHARACTERISTIC: MUGSHOT IMAGES	191
119	ERROR TRADEOFF CHARACTERISTIC: MUGSHOT IMAGES	192
120	ERROR TRADEOFF CHARACTERISTIC: MUGSHOT IMAGES	193
121	ERROR TRADEOFF CHARACTERISTIC: MUGSHOT IMAGES	194
122	ERROR TRADEOFF CHARACTERISTIC: WILD IMAGES	195
123	ERROR TRADEOFF CHARACTERISTIC: WILD IMAGES	196
124	ERROR TRADEOFF CHARACTERISTIC: WILD IMAGES	197
125	ERROR TRADEOFF CHARACTERISTIC: WILD IMAGES	198
126	ERROR TRADEOFF CHARACTERISTIC: WILD IMAGES	199
127	ERROR TRADEOFF CHARACTERISTIC: WILD IMAGES	200
128	ERROR TRADEOFF CHARACTERISTIC: WILD IMAGES	201
129	ERROR TRADEOFF CHARACTERISTIC: WILD IMAGES	202
130	ERROR TRADEOFF CHARACTERISTIC: WILD IMAGES	203
131	ERROR TRADEOFF CHARACTERISTIC: WILD IMAGES	204
132	ERROR TRADEOFF CHARACTERISTIC: WILD IMAGES	205
133	ERROR TRADEOFF CHARACTERISTIC: WILD IMAGES	206
134	ERROR TRADEOFF CHARACTERISTIC: WILD IMAGES	207
135	ERROR TRADEOFF CHARACTERISTIC: WILD IMAGES	208
136	ERROR TRADEOFF CHARACTERISTIC: WILD IMAGES	209
137	ERROR TRADEOFF CHARACTERISTIC: WILD IMAGES	210
138	ERROR TRADEOFF CHARACTERISTIC: WILD IMAGES	211

139	ERROR TRADEOFF CHARACTERISTIC: WILD IMAGES	212
140	ERROR TRADEOFF CHARACTERISTIC: WILD IMAGES	213
141	ERROR TRADEOFF CHARACTERISTIC: WILD IMAGES	214
142	ERROR TRADEOFF CHARACTERISTIC: WILD IMAGES	215
143	FALSE MATCH RATES WITHIN AND ACROSS DEMOGRAPHIC GROUPS	216
144	FALSE MATCH RATES WITHIN AND ACROSS DEMOGRAPHIC GROUPS	217
145	FALSE MATCH RATES WITHIN AND ACROSS DEMOGRAPHIC GROUPS	218
146	FALSE MATCH RATES WITHIN AND ACROSS DEMOGRAPHIC GROUPS	219
147	FALSE MATCH RATES WITHIN AND ACROSS DEMOGRAPHIC GROUPS	220
148	FALSE MATCH RATES WITHIN AND ACROSS DEMOGRAPHIC GROUPS	221
149	FALSE MATCH RATES WITHIN AND ACROSS DEMOGRAPHIC GROUPS	222
150	FALSE MATCH RATES WITHIN AND ACROSS DEMOGRAPHIC GROUPS	223
151	FALSE MATCH RATES WITHIN AND ACROSS DEMOGRAPHIC GROUPS	224
152	FALSE MATCH RATES WITHIN AND ACROSS DEMOGRAPHIC GROUPS	225
153	FALSE MATCH RATES WITHIN AND ACROSS DEMOGRAPHIC GROUPS	226
154	FALSE MATCH RATES WITHIN AND ACROSS DEMOGRAPHIC GROUPS	227
155	FALSE MATCH RATES WITHIN AND ACROSS DEMOGRAPHIC GROUPS	228
156	FALSE MATCH RATES WITHIN AND ACROSS DEMOGRAPHIC GROUPS	229
157	FALSE MATCH RATES WITHIN AND ACROSS DEMOGRAPHIC GROUPS	230
158	FALSE MATCH RATES WITHIN AND ACROSS DEMOGRAPHIC GROUPS	231
159	FALSE MATCH RATES WITHIN AND ACROSS DEMOGRAPHIC GROUPS	232
160	FALSE MATCH RATES WITHIN AND ACROSS DEMOGRAPHIC GROUPS	233
161	FALSE MATCH RATES WITHIN AND ACROSS DEMOGRAPHIC GROUPS	234
162	FALSE MATCH RATES WITHIN AND ACROSS DEMOGRAPHIC GROUPS	235
163	FALSE MATCH RATES WITHIN AND ACROSS DEMOGRAPHIC GROUPS	236
164	FALSE MATCH RATES WITHIN AND ACROSS DEMOGRAPHIC GROUPS	237
165	SEX AND RACE EFFECTS: MUGSHOT IMAGES	238
166	SEX AND RACE EFFECTS: MUGSHOT IMAGES	239
167	SEX AND RACE EFFECTS: MUGSHOT IMAGES	240
168	SEX AND RACE EFFECTS: MUGSHOT IMAGES	241
169	SEX AND RACE EFFECTS: MUGSHOT IMAGES	242
170	SEX AND RACE EFFECTS: MUGSHOT IMAGES	243
171	SEX AND RACE EFFECTS: MUGSHOT IMAGES	244
172	SEX AND RACE EFFECTS: MUGSHOT IMAGES	245
173	SEX AND RACE EFFECTS: MUGSHOT IMAGES	246
174	SEX AND RACE EFFECTS: MUGSHOT IMAGES	247
175	SEX AND RACE EFFECTS: MUGSHOT IMAGES	248
176	SEX AND RACE EFFECTS: MUGSHOT IMAGES	249
177	SEX AND RACE EFFECTS: MUGSHOT IMAGES	250
178	SEX AND RACE EFFECTS: MUGSHOT IMAGES	251
179	SEX AND RACE EFFECTS: MUGSHOT IMAGES	252
180	SEX AND RACE EFFECTS: MUGSHOT IMAGES	253
181	SEX AND RACE EFFECTS: MUGSHOT IMAGES	254
182	SEX AND RACE EFFECTS: MUGSHOT IMAGES	255
183	SEX AND RACE EFFECTS: MUGSHOT IMAGES	256
184	SEX AND RACE EFFECTS: MUGSHOT IMAGES	257
185	SEX AND RACE EFFECTS: MUGSHOT IMAGES	258
186	SEX AND RACE EFFECTS: MUGSHOT IMAGES	259
187	SEX AND RACE EFFECTS: MUGSHOT IMAGES	260
188	SEX AND RACE EFFECTS: MUGSHOT IMAGES	261
189	SEX AND RACE EFFECTS: MUGSHOT IMAGES	262
190	SEX EFFECTS: VISA IMAGES	263
191	SEX EFFECTS: VISA IMAGES	264
192	SEX EFFECTS: VISA IMAGES	265
193	SEX EFFECTS: VISA IMAGES	266
194	SEX EFFECTS: VISA IMAGES	267
195	SEX EFFECTS: VISA IMAGES	268

196	SEX EFFECTS: VISA IMAGES	269
197	SEX EFFECTS: VISA IMAGES	270
198	SEX EFFECTS: VISA IMAGES	271
199	SEX EFFECTS: VISA IMAGES	272
200	SEX EFFECTS: VISA IMAGES	273
201	SEX EFFECTS: VISA IMAGES	274
202	SEX EFFECTS: VISA IMAGES	275
203	SEX EFFECTS: VISA IMAGES	276
204	SEX EFFECTS: VISA IMAGES	277
205	SEX EFFECTS: VISA IMAGES	278
206	SEX EFFECTS: VISA IMAGES	279
207	SEX EFFECTS: VISA IMAGES	280
208	SEX EFFECTS: VISA IMAGES	281
209	SEX EFFECTS: VISA IMAGES	282
210	SEX EFFECTS: VISA IMAGES	283
211	SEX EFFECTS: VISA IMAGES	284
212	SEX EFFECTS: VISA IMAGES	285
213	SEX EFFECTS: VISA IMAGES	286
214	SEX EFFECTS: VISA IMAGES	287
215	SEX EFFECTS: VISA IMAGES	288
216	SEX EFFECTS: VISA IMAGES	289
217	SEX EFFECTS: VISA IMAGES	290
218	SEX EFFECTS: VISA IMAGES	291
219	SEX EFFECTS: VISA IMAGES	292
220	SEX EFFECTS: VISA IMAGES	293
221	SEX EFFECTS: VISA IMAGES	294
222	SEX EFFECTS: VISA IMAGES	295
223	SEX EFFECTS: VISA IMAGES	296
224	SEX EFFECTS: VISA IMAGES	297
225	SEX EFFECTS: VISA IMAGES	298
226	SEX EFFECTS: VISA IMAGES	299
227	SEX EFFECTS: VISA IMAGES	300
228	SEX EFFECTS: VISA IMAGES	301
229	SEX EFFECTS: VISA IMAGES	302
230	SEX EFFECTS: VISA IMAGES	303
231	FALSE MATCH RATE CALIBRATION: MUGSHOT IMAGES	304
232	FALSE MATCH RATE CALIBRATION: MUGSHOT IMAGES	305
233	FALSE MATCH RATE CALIBRATION: MUGSHOT IMAGES	306
234	FALSE MATCH RATE CALIBRATION: MUGSHOT IMAGES	307
235	FALSE MATCH RATE CALIBRATION: MUGSHOT IMAGES	308
236	FALSE MATCH RATE CALIBRATION: MUGSHOT IMAGES	309
237	FALSE MATCH RATE CALIBRATION: MUGSHOT IMAGES	310
238	FALSE MATCH RATE CALIBRATION: MUGSHOT IMAGES	311
239	FALSE MATCH RATE CALIBRATION: MUGSHOT IMAGES	312
240	FALSE MATCH RATE CALIBRATION: MUGSHOT IMAGES	313
241	FALSE MATCH RATE CALIBRATION: MUGSHOT IMAGES	314
242	FALSE MATCH RATE CALIBRATION: MUGSHOT IMAGES	315
243	FALSE MATCH RATE CALIBRATION: MUGSHOT IMAGES	316
244	FALSE MATCH RATE CALIBRATION: MUGSHOT IMAGES	317
245	FALSE MATCH RATE CALIBRATION: MUGSHOT IMAGES	318
246	FALSE MATCH RATE CALIBRATION: MUGSHOT IMAGES	319
247	FALSE MATCH RATE CALIBRATION: MUGSHOT IMAGES	320
248	FALSE MATCH RATE CALIBRATION: MUGSHOT IMAGES	321
249	FALSE MATCH RATE CALIBRATION: MUGSHOT IMAGES	322
250	FALSE MATCH RATE CALIBRATION: MUGSHOT IMAGES	323
251	FALSE MATCH RATE CALIBRATION: MUGSHOT IMAGES	324
252	FALSE MATCH RATE CALIBRATION: MUGSHOT IMAGES	325

253	FALSE MATCH RATE CALIBRATION: MUGSHOT IMAGES	326
254	FALSE MATCH RATE CALIBRATION: MUGSHOT IMAGES	327
255	FALSE MATCH RATE CALIBRATION: MUGSHOT IMAGES	328
256	FALSE MATCH RATE CALIBRATION: VISA IMAGES	329
257	EFFECT OF COUNTRY OF BIRTH ON FNMR	331
258	EFFECT OF COUNTRY OF BIRTH ON FNMR	332
259	EFFECT OF COUNTRY OF BIRTH ON FNMR	333
260	EFFECT OF COUNTRY OF BIRTH ON FNMR	334
261	EFFECT OF COUNTRY OF BIRTH ON FNMR	335
262	EFFECT OF COUNTRY OF BIRTH ON FNMR	336
263	EFFECT OF COUNTRY OF BIRTH ON FNMR	337
264	EFFECT OF COUNTRY OF BIRTH ON FNMR	338
265	EFFECT OF COUNTRY OF BIRTH ON FNMR	339
266	EFFECT OF COUNTRY OF BIRTH ON FNMR	340
267	EFFECT OF COUNTRY OF BIRTH ON FNMR	341
268	EFFECT OF COUNTRY OF BIRTH ON FNMR	342
269	EFFECT OF COUNTRY OF BIRTH ON FNMR	343
270	EFFECT OF COUNTRY OF BIRTH ON FNMR	344
271	EFFECT OF COUNTRY OF BIRTH ON FNMR	345
272	EFFECT OF COUNTRY OF BIRTH ON FNMR	346
273	EFFECT OF COUNTRY OF BIRTH ON FNMR	347
274	EFFECT OF COUNTRY OF BIRTH ON FNMR	348
275	EFFECT OF COUNTRY OF BIRTH ON FNMR	349
276	EFFECT OF COUNTRY OF BIRTH ON FNMR	350
277	EFFECT OF COUNTRY OF BIRTH ON FNMR	351
278	EFFECT OF COUNTRY OF BIRTH ON FNMR	352
279	EFFECT OF COUNTRY OF BIRTH ON FNMR	353
280	EFFECT OF COUNTRY OF BIRTH ON FNMR	354
281	EFFECT OF COUNTRY OF BIRTH ON FNMR	355
282	EFFECT OF COUNTRY OF BIRTH ON FNMR	356
283	EFFECT OF COUNTRY OF BIRTH ON FNMR	357
284	EFFECT OF COUNTRY OF BIRTH ON FNMR	358
285	EFFECT OF COUNTRY OF BIRTH ON FNMR	359
286	EFFECT OF COUNTRY OF BIRTH ON FNMR	360
287	EFFECT OF COUNTRY OF BIRTH ON FNMR	361
288	EFFECT OF COUNTRY OF BIRTH ON FNMR	362
289	EFFECT OF COUNTRY OF BIRTH ON FNMR	363
290	EFFECT OF COUNTRY OF BIRTH ON FNMR	364
291	EFFECT OF COUNTRY OF BIRTH ON FNMR	365
292	EFFECT OF COUNTRY OF BIRTH ON FNMR	366
293	EFFECT OF COUNTRY OF BIRTH ON FNMR	367
294	EFFECT OF COUNTRY OF BIRTH ON FNMR	368
295	EFFECT OF COUNTRY OF BIRTH ON FNMR	369
296	EFFECT OF COUNTRY OF BIRTH ON FNMR	370
297	EFFECT OF COUNTRY OF BIRTH ON FNMR	371
298	EFFECT OF COUNTRY OF BIRTH ON FNMR	372
299	ERROR TRADEOFF CHARACTERISTIC: MUGSHOT IMAGES	374
300	ERROR TRADEOFF CHARACTERISTIC: MUGSHOT IMAGES	375
301	ERROR TRADEOFF CHARACTERISTIC: MUGSHOT IMAGES	376
302	ERROR TRADEOFF CHARACTERISTIC: MUGSHOT IMAGES	377
303	ERROR TRADEOFF CHARACTERISTIC: MUGSHOT IMAGES	378
304	ERROR TRADEOFF CHARACTERISTIC: MUGSHOT IMAGES	379
305	ERROR TRADEOFF CHARACTERISTIC: MUGSHOT IMAGES	380
306	ERROR TRADEOFF CHARACTERISTIC: MUGSHOT IMAGES	381
307	ERROR TRADEOFF CHARACTERISTIC: MUGSHOT IMAGES	382
308	ERROR TRADEOFF CHARACTERISTIC: MUGSHOT IMAGES	383
309	ERROR TRADEOFF CHARACTERISTIC: MUGSHOT IMAGES	384

310	ERROR TRADEOFF CHARACTERISTIC: MUGSHOT IMAGES	385
311	ERROR TRADEOFF CHARACTERISTIC: MUGSHOT IMAGES	386
312	ERROR TRADEOFF CHARACTERISTIC: MUGSHOT IMAGES	387
313	ERROR TRADEOFF CHARACTERISTIC: MUGSHOT IMAGES	388
314	ERROR TRADEOFF CHARACTERISTIC: MUGSHOT IMAGES	389
315	ERROR TRADEOFF CHARACTERISTIC: MUGSHOT IMAGES	390
316	ERROR TRADEOFF CHARACTERISTIC: MUGSHOT IMAGES	391
317	ERROR TRADEOFF CHARACTERISTIC: MUGSHOT IMAGES	392
318	ERROR TRADEOFF CHARACTERISTIC: MUGSHOT IMAGES	393
319	ERROR TRADEOFF CHARACTERISTIC: MUGSHOT IMAGES	394
320	ERROR TRADEOFF CHARACTERISTIC: MUGSHOT IMAGES	395
321	ERROR TRADEOFF CHARACTERISTIC: MUGSHOT IMAGES	396
322	ERROR TRADEOFF CHARACTERISTIC: MUGSHOT IMAGES	397
323	ERROR TRADEOFF CHARACTERISTIC: MUGSHOT IMAGES	398
324	ERROR TRADEOFF CHARACTERISTIC: MUGSHOT IMAGES	399
325	ERROR TRADEOFF CHARACTERISTIC: MUGSHOT IMAGES	400
326	ERROR TRADEOFF CHARACTERISTIC: MUGSHOT IMAGES	401
327	ERROR TRADEOFF CHARACTERISTIC: MUGSHOT IMAGES	402
328	ERROR TRADEOFF CHARACTERISTIC: MUGSHOT IMAGES	403
329	ERROR TRADEOFF CHARACTERISTIC: MUGSHOT IMAGES	404
330	EFFECT OF SUBJECT AGE ON FNMR	406
331	EFFECT OF SUBJECT AGE ON FNMR	407
332	EFFECT OF SUBJECT AGE ON FNMR	408
333	EFFECT OF SUBJECT AGE ON FNMR	409
334	EFFECT OF SUBJECT AGE ON FNMR	410
335	EFFECT OF SUBJECT AGE ON FNMR	411
336	EFFECT OF SUBJECT AGE ON FNMR	412
337	EFFECT OF SUBJECT AGE ON FNMR	413
338	EFFECT OF SUBJECT AGE ON FNMR	414
339	EFFECT OF SUBJECT AGE ON FNMR	415
340	EFFECT OF SUBJECT AGE ON FNMR	416
341	EFFECT OF SUBJECT AGE ON FNMR	417
342	EFFECT OF SUBJECT AGE ON FNMR	418
343	EFFECT OF SUBJECT AGE ON FNMR	419
344	EFFECT OF SUBJECT AGE ON FNMR	420
345	EFFECT OF SUBJECT AGE ON FNMR	421
346	EFFECT OF SUBJECT AGE ON FNMR	422
347	EFFECT OF SUBJECT AGE ON FNMR	423
348	EFFECT OF SUBJECT AGE ON FNMR	424
349	EFFECT OF SUBJECT AGE ON FNMR	425
350	EFFECT OF SUBJECT AGE ON FNMR	426
351	EFFECT OF SUBJECT AGE ON FNMR	427
352	EFFECT OF SUBJECT AGE ON FNMR	428
353	EFFECT OF SUBJECT AGE ON FNMR	429
354	EFFECT OF SUBJECT AGE ON FNMR	430
355	EFFECT OF SUBJECT AGE ON FNMR	431
356	EFFECT OF SUBJECT AGE ON FNMR	432
357	EFFECT OF SUBJECT AGE ON FNMR	433
358	EFFECT OF SUBJECT AGE ON FNMR	434
359	EFFECT OF SUBJECT AGE ON FNMR	435
360	EFFECT OF SUBJECT AGE ON FNMR	436
361	EFFECT OF SUBJECT AGE ON FNMR	437
362	EFFECT OF SUBJECT AGE ON FNMR	438

363	EFFECT OF SUBJECT AGE ON FNMR	439
364	EFFECT OF SUBJECT AGE ON FNMR	440
365	EFFECT OF SUBJECT AGE ON FNMR	441
366	EFFECT OF SUBJECT AGE ON FNMR	442
367	EFFECT OF SUBJECT AGE ON FNMR	443
368	EFFECT OF SUBJECT AGE ON FNMR	444
369	EFFECT OF SUBJECT AGE ON FNMR	445
370	EFFECT OF SUBJECT AGE ON FNMR	446
371	EFFECT OF SUBJECT AGE ON FNMR	447
372	IMPOSTOR COUNTS FOR CROSS COUNTRY FMR CALCULATIONS	451

	Location	Developer Name	Short Name	Seq. Num.	Validation Date
1	NL	20Face	20face-000	000	2021-04-12
2	NL	20Face	20face-001	001	2021-09-29
3	US	3Divi	3divi-006	006	2021-04-14
4	US	3Divi	3divi-007	007	2021-09-27
5	TH	ACI Software	acisw-007	007	2021-11-15
6	TH	ACI Software	acisw-008	008	2022-03-22
7	US	AFIS and Biometrics Consulting	afisbiometrics-000	000	2022-01-27
8	US	AFR Engine	afrengine-000	000	2022-09-29
9	US	AFR Engine	afrengine-001	001	2023-01-26
10	TW	ASUSTek Computer Inc	asusaics-000	000	2019-10-24
11	TW	ASUSTek Computer Inc	asusaics-001	001	2020-02-25
12	CN	AYF Technology	ayftech-001	001	2020-07-06
13	TW	Ability Enterprise - Andro Video	androvideo-000	000	2021-01-25
14	IN	Accurascan	accurascan-001	001	2023-0-15
15	TW	Acer Incorporated	acer-001	001	2020-06-30
16	TW	Acer Incorporated	acer-002	002	2021-11-10
17	SG	Adera Global PTE	adera-003	003	2021-07-12
18	SG	Adera Global PTE	adera-004	004	2022-11-14
19	SG	Advancegroup	advance-003	003	2021-08-05
20	SG	Advancegroup	advance-004	004	2022-09-06
21	TH	Ai First	aifirst-001	001	2019-11-21
22	TW	AiUnion Technology	aiunionface-000	000	2019-10-22
23	TH	Aigen	aigen-001	001	2020-10-06
24	TH	Aigen	aigen-002	002	2021-03-15
25	CN	Aiseemu Technology	aiseemu-001	001	2022-06-16
26	CN	Aiseemu Technology	aiseemu-002	002	2022-11-18
27	KR	Ajou University	ajou-001	001	2021-03-08
28	ID	Akurat Satu Indonesia	ptakuratsatu-000	000	2020-09-11
29	KR	Alchera Inc	alchera-004	004	2022-08-12
30	KR	Alchera Inc	alchera-005	005	2023-01-04
31	ID	Alfabeta	alfabeta-001	001	2021-12-02
32	ES	Alice Biometrics	alice-000	000	2021-06-15
33	RU	Alivia / Innovation Sys	isystems-001	001	2018-06-12
34	RU	Alivia / Innovation Sys	isystems-002	002	2018-10-18
35	IN	AllGoVision	allgovision-000	000	2019-03-01
36	CN	AlphaSSTG	alphaface-001	001	2019-09-03
37	CN	AlphaSSTG	alphaface-002	002	2020-02-20
38	GB	Amplified Group	amplifiedgroup-001	001	2019-03-01
39	CN	Anke Investments	anke-004	004	2019-06-27
40	CN	Anke Investments	anke-005	005	2019-11-21
41	BR	Antheus Technologia	antheus-000	000	2019-12-05
42	BR	Antheus Technologia	antheus-001	001	2020-06-25
43	GB	AnyVision	anyvision-004	004	2018-06-15
44	GB	AnyVision	anyvision-005	005	2021-02-03
45	CN	Aratek Biometrics Co Ltd	aratek-001	001	2023-03-27
46	US	Armatura LLC	armatura-001	001	2022-01-04
47	US	Armatura LLC	armatura-003	003	2023-01-13
48	CN	AuthenMetric	authenmetric-003	003	2021-08-09
49	CN	AuthenMetric	authenmetric-004	004	2022-01-03
50	US	Aware	aware-005	005	2020-02-27
51	US	Aware	aware-006	006	2021-07-03
52	IN	Awidit Systems	awiros-001	001	2019-09-23
53	IN	Awidit Systems	awiros-002	002	2020-10-28
54	CH	Aximetria	aximetria-001	001	2022-08-10
55	JP	Ayonix	ayonix-000	000	2017-06-22
56	CN	BOE Technology Group	boetech-001	001	2021-06-22
57	CN	BOE Technology Group	boetech-002	002	2021-12-21
58	ES	Bee the Data	beethedata-000	000	2021-07-26
59	CN	Beihang University-ERCACAT	ercacat-001	001	2020-07-06
60	CN	Beijing Alleyes Technology	alleyes-000	000	2020-03-09
61	CN	Beijing DeepSense Technologies	deepsense-001	001	2022-03-11
62	CN	Beijing DeepSense Technologies	deepsense-002	002	2023-02-22
63	CN	Beijing Hisign Technology	hisign-001	001	2021-09-24
64	CN	Beijing Hisign Technology	hisign-002	002	2022-09-09
65	CN	Beijing Mendaxia Technology	mendaxiatech-000	000	2021-09-15
66	CN	Beijing Vion Technology Inc	vion-000	000	2018-10-19
67	KZ	Beyne.AI	beyneai-000	000	2022-01-03
68	CH	BioID Technologies SA	bioidechswiss-001	001	2020-08-28
69	CH	BioID Technologies SA	bioidechswiss-002	002	2021-02-17
70	IN	Biocube Matrics	biocube-001	001	2021-09-08

Table 1: Summary of participant information included in this report.

	Location	Developer Name	Short Name	Seq. Num.	Validation Date
71	IN	Biocube Matrics	biocube-002	002	2023-02-09
72	KZ	Biometric LLC	biometric-vision-000	000	2023-01-25
73	UK	BitCenter UK	farfaces-001	001	2021-04-09
74	CN	Bitmain	bm-001	001	2018-10-17
75	CN	Bresee Technology	bresee-001	001	2020-12-30
76	CN	Bresee Technology	bresee-002	002	2021-06-30
77	VN	CMC Institute of Science and Technology	cist-001	001	2022-10-20
78	VN	CMC Institute of Science and Technology	cist-002	002	2023-02-09
79	CN	CSA IntelliCloud Technology	intellicloudai-001	001	2019-08-13
80	CN	CSA IntelliCloud Technology	intellicloudai-002	002	2020-12-17
81	TW	CTBC Bank	ctbcbank-000	000	2019-06-28
82	TW	CTBC Bank	ctbcbank-001	001	2019-10-28
83	KR	CUDO Communication	cudocommunication-001	001	2021-10-20
84	US	Camvi Technologies	camvi-002	002	2018-10-19
85	US	Camvi Technologies	camvi-004	004	2019-07-12
86	FI	Candour Biometrics	candour-001	001	2023-02-10
87	JP	Canon Inc	canon-003	003	2021-09-15
88	JP	Canon Inc	canon-004	004	2022-04-25
89	CN	China Electronics Import-Export Corp	ceiec-003	003	2020-01-06
90	CN	China Electronics Import-Export Corp	ceiec-004	004	2021-01-18
91	CN	China University of Petroleum	upc-001	001	2019-06-05
92	CN	Chinese University of Hong Kong	cuhkee-001	001	2020-03-18
93	KR	Chosun University	chosun-001	001	2020-07-01
94	KR	Chosun University	chosun-002	002	2020-11-25
95	TW	Chunghwa Telecom	chtface-005	005	2022-03-09
96	TW	Chunghwa Telecom	chtface-006	006	2022-11-03
97	US	City and County of Honolulu	cchonolulu-000	000	2023-03-27
98	US	Clearview AI Inc	clearviewai-000	000	2021-09-22
99	CN	Closeli Inc	closeli-001	001	2021-07-15
100	US	CloudSmart Consulting LLC	csc-002	002	2021-03-24
101	US	CloudSmart Consulting LLC	csc-003	003	2021-08-26
102	TW	Cloudmatrix	cloudmatrix-001	001	2022-02-16
103	TW	Cloudmatrix	cloudmatrix-002	002	2022-10-17
104	CN	Cloudwalk - Hengrui AI Technology	cloudwalk-hr-003	003	2020-09-25
105	CN	Cloudwalk - Hengrui AI Technology	cloudwalk-hr-004	004	2021-02-10
106	CN	Cloudwalk - Moontime Smart Technology	cloudwalk-mt-006	006	2022-10-20
107	CN	Cloudwalk - Moontime Smart Technology	cloudwalk-mt-007	007	2023-02-21
108	IN	Code Everest Pvt	facex-001	001	2021-03-08
109	IN	Code Everest Pvt	facex-002	002	2021-08-24
110	KR	Codeline	codeline-000	000	2022-09-13
111	DE	Cognitec Systems GmbH	cognitec-003	003	2021-07-30
112	DE	Cognitec Systems GmbH	cognitec-004	004	2022-02-10
113	TW	Coretech Knowledge Inc	coretech-000	000	2021-07-12
114	TW	Coretech Knowledge Inc	coretech-001	001	2022-09-29
115	IL	Corsight	corsight-002	002	2021-09-01
116	IL	Corsight	corsight-003	003	2022-06-09
117	IL	Cortica	cor-001	001	2020-09-24
118	TW	Cu-Face	cu-face-002	002	2023-01-05
119	KR	Cubox	cubox-002	002	2021-08-24
120	KR	Cubox	cubox-003	003	2023-03-07
121	JP	Cybercore	cybercore-002	002	2022-04-25
122	JP	Cybercore	cybercore-003	003	2022-08-31
123	US	Cyberextruder	cyberextruder-003	003	2022-03-16
124	US	Cyberextruder	cyberextruder-004	004	2022-07-20
125	TW	Cyberlink Corp	cyberlink-010	010	2022-09-16
126	TW	Cyberlink Corp	cyberlink-011	011	2023-01-30
127	MX	DÍCIO	dicio-001	001	2022-03-22
128	CN	DSK	dsk-000	000	2019-06-28
129	CN	Dahua Technology	dahua-006	006	2020-12-30
130	CN	Dahua Technology	dahua-007	007	2021-12-20
131	IE	Daon	daon-000	000	2021-11-03
132	US	Decatur Industries Inc	decatur-000	000	2020-08-18
133	US	Decatur Industries Inc	decatur-001	001	2021-09-27
134	CN	Deepglint	deepglint-004	004	2021-09-17
135	CN	Deepglint	deepglint-005	005	2022-10-17
136	FR	Deepsense	dps-000	000	2021-07-16
137	DE	Dermalog	dermalog-010	010	2022-07-25
138	DE	Dermalog	dermalog-011	011	2022-12-12
139	CN	DiDi ChuXing Technology	didiglobaface-001	001	2019-10-23
140	CN	DiDi ChuXing Technology	didiglobaface-002	002	2023-01-09

Table 2: Summary of participant information included in this report.

	Location	Developer Name	Short Name	Seq. Num.	Validation Date
141	IN	Digidata	digidata-000	000	2022-01-27
142	IN	Digidata	digidata-001	001	2022-06-10
143	GB	Digital Barriers	digitalbarriers-002	002	2019-03-01
144	TR	Ekin Smart City Technologies	ekin-002	002	2021-05-04
145	AE	Enface	enface-001	001	2021-12-17
146	AE	Enface	enface-002	002	2023-02-27
147	CH	Euronovate SA	euronovate-001	001	2021-11-15
148	RU	Expasoft LLC	expasoft-001	001	2020-09-03
149	RU	Expasoft LLC	expasoft-002	002	2021-07-26
150	LB	FOO	foomobi-001	001	2023-03-13
151	US	FRP LLC	frpkauai-001	001	2022-07-18
152	US	FRP LLC	frpkauai-002	002	2022-11-21
153	DE	FaceOnLive Inc	faceonlive-001	001	2021-11-23
154	DE	FaceOnLive Inc	faceonlive-002	002	2022-04-11
155	ES	FacePhi	facephi-000	000	2022-04-06
156	GB	FaceSoft	facesoft-000	000	2019-07-10
157	KR	FaceTag Co	facetag-000	000	2021-03-22
158	KR	FaceTag Co	facetag-002	002	2022-01-06
159	TW	FarBar Inc	f8-001	001	2019-07-11
160	TW	FarBar Inc	f8-002	002	2022-03-02
161	US	Fast Enterprises	fastenterprises-000	000	2023-03-01
162	CN	Fiberhome Telecommunication Technologies	fiberhome-nanjing-003	003	2021-03-12
163	CN	Fiberhome Telecommunication Technologies	fiberhome-nanjing-004	004	2021-09-14
164	UK	Fincore Ltd	fincore-000	000	2021-06-07
165	KZ	First Credit Bureau Kazakhstan	firstcreditkz-001	001	2022-08-22
166	KZ	First Credit Bureau Kazakhstan	firstcreditkz-002	002	2023-02-21
167	CN	Fujitsu Research and Development Center	fujitsulab-002	002	2021-02-24
168	CN	Fujitsu Research and Development Center	fujitsulab-003	003	2021-07-12
169	US	Gemalto Cogent	cogent-007	007	2022-04-11
170	US	Gemalto Cogent	cogent-008	008	2023-01-03
171	TW	GeoVision Inc	geo-002	002	2021-04-01
172	TW	GeoVision Inc	geo-004	004	2022-02-10
173	JP	Glory	glory-005	005	2022-07-08
174	JP	Glory	glory-006	006	2023-03-23
175	TW	Gorilla Technology	gorilla-008	008	2021-11-08
176	TW	Gorilla Technology	gorilla-009	009	2022-12-14
177	US	Graymatics	graymatics-001	001	2022-01-13
178	US	Griaule	griaule-001	001	2022-05-31
179	US	Griaule	griaule-002	002	2022-12-02
180	CN	Guangzhou Pixel Solutions	pixelall-008	008	2022-06-16
181	CN	Guangzhou Pixel Solutions	pixelall-009	009	2022-10-26
182	CN	Hangzhou Allu Network Information Technology	hzailu-003	003	2022-10-11
183	CN	Hangzhou Allu Network Information Technology	hzailu-004	004	2023-02-27
184	ES	Herta Security	hertasecurity-002	002	2022-09-02
185	ES	Herta Security	hertasecurity-003	003	2023-01-27
186	CN	Hikvision Research Institute	hik-001	001	2019-03-01
187	IN	HyperVerge Inc	hyperverge-003	003	2022-04-11
188	IN	HyperVerge Inc	hyperverge-004	004	2022-12-14
189	AU	ICM Airport Technics	icm-003	003	2021-09-06
190	AU	ICM Airport Technics	icm-004	004	2022-09-07
191	FR	ID3 Technology	id3-006	006	2020-12-17
192	FR	ID3 Technology	id3-008	008	2021-11-10
193	UK	IDENTY	identity-000	000	2023-04-04
194	CA	IMDS Software	imds-software-001	001	2022-07-06
195	CA	IMDS Software	imds-software-002	002	2023-02-10
196	RU	ITMO University	itmo-007	007	2020-01-06
197	RU	ITMO University	itmo-008	008	2021-11-19
198	RU	IVA Cognitive	ivacognitive-001	001	2021-01-29
199	FR	Idemia	idemia-008	008	2021-07-07
200	FR	Idemia	idemia-009	009	2022-07-27
201	US	Imageware Systems	iws-000	000	2020-08-12
202	GB	Imperial College London	imperial-000	000	2019-03-01
203	GB	Imperial College London	imperial-002	002	2019-08-28
204	US	Incode Technologies Inc	incode-010	010	2021-10-22
205	US	Incode Technologies Inc	incode-011	011	2022-08-10
206	IT	InfoCert	infocert-001	001	2022-09-08
207	IN	Innef Labs	inneflabs-000	000	2020-09-04
208	GB	Innovative Technology	innovativetechnologyltd-001	001	2019-10-22
209	GB	Innovative Technology	innovativetechnologyltd-002	002	2020-02-26
210	SK	Innovatrics	innovatrics-008	008	2021-12-15

Table 3: Summary of participant information included in this report.

	Location	Developer Name	Short Name	Seq. Num.	Validation Date
211	SK	Innovatrics	innovatrics-009	009	2022-01-19
212	CN	InsightFace AI	insightface-003	003	2022-08-23
213	CN	InsightFace AI	insightface-004	004	2023-03-31
214	CN	Inspur (Beijing) Electronic Information Industry Co	inspur-000	000	2022-07-19
215	CN	Inspur (Beijing) Electronic Information Industry Co	inspur-001	001	2023-02-24
216	CN	Institute of Computing Technology	icthtc-000	000	2020-11-29
217	RU	Institute of Information Technologies	iit-002	002	2019-12-04
218	RU	Institute of Information Technologies	iit-003	003	2020-12-01
219	IS	Intel Research Group	intelresearch-005	005	2022-02-13
220	IS	Intel Research Group	intelresearch-006	006	2022-12-19
221	KR	IntelliVIX	intellivix-002	002	2022-07-14
222	KR	IntelliVIX	intellivix-003	003	2022-12-12
223	AE	Intellibrain Technological Projects	g42-intellibrain-001	001	2022-07-27
224	CN	Intelligent Control Technology Co Ltd - IGearx	igearx-face-000	000	2023-03-28
225	US	Intellivision	intellivision-004	004	2022-07-28
226	US	Intellivision	intellivision-005	005	2023-02-06
227	LU	Intema-LGL Group	intema-000	000	2022-07-15
228	LU	Intema-LGL Group	intema-001	001	2023-01-11
229	US	IrexAI	irex-000	000	2020-12-17
230	IL	Is It You	isityou-000	000	2017-06-26
231	MX	Jaak IT	jaakit-001	001	2022-05-20
232	KR	Kakao Enterprise	kakao-007	007	2022-01-12
233	KR	Kakao Enterprise	kakao-008	008	2022-05-12
234	KR	Kakao Pay Corp	kakaopay-001	001	2021-07-06
235	KR	KakaoBank	kakaobank-000	000	2023-02-27
236	TH	Kasikorn Labs	kasikornlabs-000	000	2022-03-02
237	TH	Kasikorn Labs	kasikornlabs-002	002	2022-12-13
238	SG	Kedacom International Pte	kedacom-000	000	2019-06-03
239	US	Kneron Inc	kneron-003	003	2019-07-01
240	US	Kneron Inc	kneron-005	005	2020-02-21
241	US	KnowUTech LLC	knowutech-000	000	2022-02-13
242	KR	Kookmin University	kookmin-002	002	2021-03-05
243	KR	Korea Identification Inc	koreaid-001	001	2022-12-12
244	TH	Krungthai	krungthai-002	002	2022-06-21
245	CN	KuKe3D Technology	kuke3d-001	001	2021-10-28
246	CN	KuKe3D Technology	kuke3d-002	002	2022-04-14
247	MX	Lebentech Biometrics	lebentech-000	000	2022-02-16
248	IN	Lema Labs	lemalabs-001	001	2021-04-13
249	JP	Line Corporation	lineclova-002	002	2022-05-18
250	JP	Line Corporation	lineclova-003	003	2022-11-28
251	RU	Lomonosov Moscow State University	intsysmsu-001	001	2019-10-22
252	RU	Lomonosov Moscow State University	intsysmsu-002	002	2020-03-12
253	IN	Lookman Electroplast Industries	lookman-002	002	2018-06-13
254	IN	Lookman Electroplast Industries	lookman-004	004	2019-06-03
255	US	Luxand Inc	luxand-000	000	2019-11-07
256	RU	MVision	mvision-001	001	2019-11-12
257	IN	Mantra Softtech India	mantra-000	000	2021-10-28
258	CN	Maxvision Technology	maxvision-002	002	2022-07-12
259	CN	Maxvision Technology	maxvision-003	003	2022-11-14
260	CN	Megvii/Face++	megvii-005	005	2022-03-28
261	CN	Megvii/Face++	megvii-006	006	2022-08-08
262	KR	Metsakuur	metsakuurcompany-002	002	2022-09-14
263	KR	Metsakuur	metsakuurcompany-003	003	2023-04-04
264	CN	Miaxis Biometrics	miaxis-001	001	2022-11-15
265	CN	Miaxis Biometrics	miaxis-002	002	2023-03-22
266	GB	MicroFocus	microfocus-002	002	2018-10-17
267	GB	MicroFocus	microfocus-003	003	2023-02-23
268	CN	Minivision	minivision-000	000	2020-10-28
269	UK	Mitek Systems	mitek-000	000	2023-01-27
270	NO	Mobai	mobai-000	000	2020-08-26
271	NO	Mobai	mobai-001	001	2021-02-17
272	ES	Mobbel Solutions	mobbl-001	001	2021-06-16
273	ES	Mobbel Solutions	mobbl-003	003	2022-04-19
274	KR	Mobipin Technology	mobipintech-000	000	2021-11-23
275	TH	Momentum Digital	sertis-000	000	2019-10-07
276	TH	Momentum Digital	sertis-002	002	2021-05-13
277	CN	MoreDian Technology	moreedian-000	000	2021-02-24
278	US	Mukh Technologies	mukh-002	002	2022-11-01
279	US	Mukh Technologies	mukh-003	003	2023-03-15
280	CN	Multi-Modality Intelligence	multimodality-000	000	2021-10-19

Table 4: Summary of participant information included in this report.

	Location	Developer Name	Short Name	Seq. Num.	Validation Date
281	CN	Multi-Modality Intelligence	multimodality-001	001	2022-05-16
282	RU	N-Tech Lab	ntechlab-011	011	2021-09-13
283	RU	N-Tech Lab	ntechlab-012	012	2022-01-20
284	SG	NCS Pte Ltd	ncssg-001	001	2023-03-24
285	CA	NEO Systems	neosystems-004	004	2022-05-02
286	KR	NHN Corp	nhn-002	002	2021-07-15
287	KR	NHN Corp	nhn-003	003	2022-02-22
288	KR	NSENSE Corp	nsensecorp-004	004	2022-09-08
289	KR	NSENSE Corp	nsensecorp-005	005	2023-02-08
290	CN	Nanjing Kiwi Network Technology	kiwitech-000	000	2021-03-19
291	KR	Neosecu Co	openface-001	001	2021-06-15
292	TW	Netbridge Technology Incoporation	netbridgetech-001	001	2020-01-08
293	TW	Netbridge Technology Incoporation	netbridgetech-002	002	2020-08-11
294	LT	Neurotechnology	neurotechnology-015	015	2022-06-07
295	LT	Neurotechnology	neurotechnology-016	016	2023-02-01
296	ID	Nodeflux	nodeflux-002	002	2019-08-13
297	LT	Nominder	nominder-000	000	2023-02-06
298	IN	NotionTag Technologies Private Limited	notiontag-001	001	2021-03-04
299	IN	NotionTag Technologies Private Limited	notiontag-002	002	2021-09-17
300	US	Omnigarde Ltd	omnigarde-001	001	2021-08-23
301	US	Omnigarde Ltd	omnigarde-002	002	2022-01-19
302	KR	One More Security	omface-000	000	2021-12-15
303	KR	One More Security	omface-001	001	2022-10-21
304	UK	Onfido	onfido-000	000	2022-12-13
305	RU	Oz Forensics LLC	oz-003	003	2021-08-09
306	RU	Oz Forensics LLC	oz-004	004	2021-12-13
307	TW	PAPAGO Inc	papago-001	001	2022-07-19
308	ID	PT Autentika Digital Indonesia	autentika-000	000	2022-12-05
309	ID	PT Autentika Digital Indonesia	autentika-001	001	2023-04-05
310	ID	PT Qlue Performa Indonesia	qluevision-001	001	2022-11-15
311	CH	PXL Vision AG	pxl-001	001	2020-06-30
312	TW	Palit Microsystems	palit-000	000	2022-05-16
313	TW	Palit Microsystems	palit-001	001	2022-09-26
314	SG	Panasonic R+D Center Singapore	psl-010	010	2022-04-19
315	SG	Panasonic R+D Center Singapore	psl-011	011	2022-10-06
316	US	Pangiam	pangiam-000	000	2022-04-04
317	US	Pangiam	pangiam-001	001	2023-02-21
318	TR	Papilon Savunma	papsav1923-002	002	2022-01-20
319	TR	Papilon Savunma	papsav1923-003	003	2022-11-25
320	US	Paravision (EverAI)	paravision-010	010	2022-02-02
321	US	Paravision (EverAI)	paravision-011	011	2022-12-12
322	SG	Pensees Pte	pensees-001	001	2020-08-17
323	US	Private Identity LLC	privid-001	001	2023-02-06
324	IN	Pyramid Cyber Security + Forensic (P)	pyramid-000	000	2019-11-04
325	KZ	Qaz Biometric Systems	qazbs-000	000	2022-06-22
326	TW	Qnap Security	qnap-002	002	2022-04-15
327	TW	Qnap Security	qnap-003	003	2022-12-09
328	CZ	Quantasoft	quantasoft-003	003	2021-04-19
329	US	Rank One Computing	rankone-013	013	2022-07-09
330	US	Rank One Computing	rankone-014	014	2022-12-21
331	US	Realnetworks Inc	realnetworks-007	007	2022-06-14
332	US	Realnetworks Inc	realnetworks-008	008	2022-11-10
333	US	Regula Forensics	regula-000	000	2021-04-13
334	US	Regula Forensics	regula-001	001	2021-12-14
335	CN	Remark Holdings	remarkai-001	001	2019-03-01
336	CN	Remark Holdings	remarkai-003	003	2021-06-22
337	SG	Rendip	rendip-000	000	2021-04-19
338	UK	Reveal Media Ltd	revealmedia-005	005	2021-09-24
339	UK	Reveal Media Ltd	revealmedia-006	006	2022-01-26
340	CN	Rokid Corporation	rokid-000	000	2019-08-01
341	CN	Rokid Corporation	rokid-001	001	2019-12-13
342	KR	SK Telecom	sktelecom-000	000	2021-07-09
343	KR	SQISoft	sqisoft-002	002	2021-11-03
344	KR	SQISoft	sqisoft-003	003	2022-10-26
345	SA	STCON LLC	stcon-000	000	2022-11-02
346	SA	STCON LLC	stcon-001	001	2023-03-03
347	DE	Saffe	saffe-001	001	2018-10-19
348	DE	Saffe	saffe-002	002	2019-03-01
349	JP	Saga Densan Center Co Ltd	sdc-000	000	2022-10-18
350	KR	Samsung S1 Corp	s1-005	005	2022-06-17

Table 5: Summary of participant information included in this report.

	Location	Developer Name	Short Name	Seq. Num.	Validation Date
351	KR	Samsung S1 Corp	s1-007	007	2023-03-20
352	KR	Samsung-SDS	samsungsds-001	001	2022-04-18
353	KR	Samsung-SDS	samsungsds-002	002	2022-09-16
354	IN	Samtech InfoNet Limited	samtech-001	001	2019-10-15
355	RU	Satellite Innovation/Eocortex	eocortex-000	000	2020-08-26
356	IL	Scanovate	scanovate-002	002	2020-06-26
357	IL	Scanovate	scanovate-003	003	2021-11-15
358	RO	Securif AI	securifai-005	005	2022-05-16
359	RO	Securif AI	securifai-006	006	2022-11-14
360	CN	Sensetime Group	sensetime-007	007	2022-06-17
361	CN	Sensetime Group	sensetime-008	008	2023-01-04
362	SG	Seventh Sense Artificial Intelligence	seventhsense-001	001	2022-03-04
363	SG	Seventh Sense Artificial Intelligence	seventhsense-002	002	2022-10-17
364	US	Shaman Software	shaman-000	000	2017-12-05
365	US	Shaman Software	shaman-001	001	2018-01-13
366	CN	Shanghai Jiao Tong University	sjtu-003	003	2020-11-02
367	CN	Shanghai Jiao Tong University	sjtu-004	004	2021-05-13
368	CN	Shanghai Ulucu Electronics Technology	uluface-002	002	2019-07-10
369	CN	Shanghai Ulucu Electronics Technology	uluface-003	003	2019-11-12
370	CN	Shanghai University - Shanghai Film Academy	shu-002	002	2019-12-10
371	CN	Shanghai University - Shanghai Film Academy	shu-003	003	2020-06-24
372	CN	Shanghai Yitu Technology	yitu-003	003	2019-03-01
373	CN	Shenzhen AiMall Tech	aimall-002	002	2020-03-12
374	CN	Shenzhen AiMall Tech	aimall-003	003	2020-08-12
375	CN	Shenzhen EI Networks	einetworks-000	000	2019-08-13
376	CN	Shenzhen Inst Adv Integrated Tech CAS	siat-002	002	2018-06-13
377	CN	Shenzhen Inst Adv Integrated Tech CAS	siat-005	005	2022-02-08
378	CN	Shenzhen Intellifusion Technologies	intellifusion-001	001	2019-08-22
379	CN	Shenzhen Intellifusion Technologies	intellifusion-002	002	2020-03-18
380	CN	Shenzhen University-Macau University of Science and Technology	sztu-000	000	2020-12-17
381	CN	Shenzhen University-Macau University of Science and Technology	sztu-001	001	2021-07-13
382	RU	Smart Engines	smartengines-000	000	2021-08-25
383	RU	Smart Engines	smartengines-001	001	2022-05-31
384	ES	Smartbiometrik	smartbiometrik-001	001	2022-05-16
385	TR	Smarvist Teknoloji	smartvist-000	000	2022-05-10
386	DE	Smilart	smilart-002	002	2018-02-06
387	DE	Smilart	smilart-003	003	2019-03-01
388	TR	Sodec App Inc	sodec-000	000	2021-06-02
389	IN	Staqua Technologies	staqua-000	000	2020-07-15
390	CN	Star Hybrid Limited	starhybrid-001	001	2019-06-19
391	CN	Su Zhou NaZhiTianDi intelligent technology	nazhiai-000	000	2020-06-25
392	IN	Sukshi Technology Innovation	sukshi-000	000	2022-02-13
393	KR	Suprema AI Inc	suprema-003	003	2022-07-20
394	KR	Suprema AI Inc	suprema-004	004	2023-01-09
395	KR	Suprema ID Inc	supremaid-001	001	2021-05-04
396	KR	Suprema ID Inc	supremaid-002	002	2022-06-24
397	UK	Swsam Solutions	swsam-001	001	2023-03-13
398	RU	Synesis	synesis-006	006	2019-10-10
399	RU	Synesis	synesis-007	007	2020-06-24
400	TW	Synology Inc	synology-000	000	2019-10-23
401	TW	Synology Inc	synology-002	002	2020-08-20
402	BR	T4ISB	t4isb-000	000	2022-01-28
403	CN	TUPU Technology	tuputech-000	000	2019-10-11
404	TW	Taiwan AI Labs	ailabs-001	001	2019-12-18
405	TW	Taiwan-Certificate Authority Incorporation	twface-000	000	2021-05-14
406	TW	Taiwan-Certificate Authority Incorporation	twface-001	001	2021-09-14
407	CH	Tech5 SA	tech5-005	005	2020-07-24
408	CH	Tech5 SA	tech5-007	007	2022-12-30
409	TR	Techsign	techsign-000	000	2021-08-25
410	TR	Techsign	techsign-001	001	2022-07-01
411	CN	Tencent Deepsea Lab	deepsea-001	001	2019-06-03
412	RU	Tevian	tevian-007	007	2021-08-06
413	RU	Tevian	tevian-008	008	2021-12-06
414	US	TigerIT Americas LLC	tiger-005	005	2021-07-29
415	US	TigerIT Americas LLC	tiger-006	006	2021-12-13
416	RU	Tinkoff Bank	tinkoff-001	001	2021-05-13
417	CN	Tong Yi Transportation Technology	tongyi-005	005	2019-06-12
418	TW	Toppan ID Gate	toppanidgate-000	000	2021-09-28
419	JP	Toshiba	toshiba-004	004	2021-09-27
420	JP	Toshiba	toshiba-006	006	2022-06-29

Table 6: Summary of participant information included in this report.

	Location	Developer Name	Short Name	Seq. Num.	Validation Date
421	ES	Touchless ID	touchlessid-001	001	2022-09-21
422	ES	Touchless ID	touchlessid-002	002	2023-01-23
423	JP	Tripleize	aize-001	001	2021-04-23
424	JP	Tripleize	aize-002	002	2021-10-08
425	VN	TrueID-VNG	trueidvng-001	001	2023-01-05
426	US	Trueface.ai	trueface-002	002	2021-03-29
427	US	Trueface.ai	trueface-003	003	2021-09-30
428	CN	TuringTech.vip	turingtechvip-001	001	2022-02-03
429	CN	TuringTech.vip	turingtechvip-002	002	2022-07-27
430	TR	Turkcell Technology	turkcell-000	000	2022-10-11
431	TR	Turkcell Technology	turkcell-001	001	2023-03-15
432	CN	ULSee Inc	ulsee-001	001	2019-07-31
433	UN	UNICC-Solution Architecture Section	unicc-001	001	2023-02-17
434	TW	UXLabs	uxlabs-001	001	2022-09-19
435	FR	Unissey	unissey-002	002	2022-04-29
436	FR	Unissey	unissey-003	003	2022-12-19
437	PT	Universidade de Coimbra	visteam-004	004	2022-08-01
438	PT	Universidade de Coimbra	visteam-005	005	2023-01-04
439	UK	University of Surrey-CVSSP	surrey-cvssp-001	001	2022-09-22
440	UK	University of Surrey-CVSSP	surrey-cvssp-002	002	2023-02-16
441	US	VCognition	vcog-002	002	2017-06-12
442	ES	Veridas Digital Authentication Solutions S.L.	veridas-007	007	2021-09-02
443	ES	Veridas Digital Authentication Solutions S.L.	veridas-008	008	2022-10-17
444	UK	Veridium	veridium-000	000	2022-03-28
445	UK	Veridium	veridium-001	001	2022-11-03
446	KZ	Verigram	verigram-001	001	2022-03-09
447	KZ	Verigram	verigram-002	002	2023-04-03
448	ID	Verihubs	verihubs-inteligensia-000	000	2021-07-27
449	ID	Verihubs	verihubs-inteligensia-001	001	2022-06-16
450	ID	Verijelas	verijelas-000	000	2022-08-01
451	TW	Via Technologies Inc	via-001	001	2020-01-08
452	TW	Via Technologies Inc	via-004	004	2023-02-23
453	DE	Videmo Intelligent Videoanalyse	videmo-001	001	2021-12-22
454	DE	Videmo Intelligent Videoanalyse	videmo-002	002	2022-08-31
455	IN	Videonetics Technology Pvt	videonetics-001	001	2019-06-19
456	IN	Videonetics Technology Pvt	videonetics-002	002	2019-11-21
457	VN	Vietnam Posts and Telecommunications Group	vnpt-004	004	2022-04-15
458	VN	Vietnam Posts and Telecommunications Group	vnpt-005	005	2022-08-24
459	VN	Viettel Group	vts-000	000	2020-11-04
460	VN	Viettel Group	vts-001	001	2022-04-20
461	VN	Viettel High Technology	viettelhightech-000	000	2021-08-04
462	US	Vigilant Solutions	vigilantsolutions-010	010	2021-04-07
463	US	Vigilant Solutions	vigilantsolutions-011	011	2021-08-07
464	VN	VinAI Research VietNam	vinai-000	000	2020-09-24
465	VN	VinBigData	vinbigdata-001	001	2022-01-06
466	VN	VinBigData	vinbigdata-002	002	2022-06-07
467	SE	Visage Technologies	visage-000	000	2020-12-09
468	FI	Visidon	vd-002	002	2021-04-12
469	FI	Visidon	vd-003	003	2021-10-12
470	CN	Vision Intelligence Center of Meituan	meituan-002	002	2022-09-14
471	CN	Vision Intelligence Center of Meituan	meituan-003	003	2023-03-06
472	PT	Vision-Box	visionbox-002	002	2021-04-29
473	PT	Vision-Box	visionbox-003	003	2023-02-01
474	RU	VisionLabs	visionlabs-010	010	2021-01-25
475	RU	VisionLabs	visionlabs-011	011	2021-10-13
476	AU	Vixvizon	vixvizion-006	006	2022-08-11
477	AU	Vixvizon	vixvizion-007	007	2023-01-17
478	RU	Vocard	vocard-009	009	2020-12-28
479	RU	Vocard	vocard-010	010	2021-12-20
480	US	Wicket	wicket-000	000	2022-02-14
481	CN	Winsense	winsense-001	001	2019-10-16
482	CN	Winsense	winsense-002	002	2020-11-20
483	MY	Wise AI SDN BHD	wiseai-001	001	2022-10-25
484	CN	Wuhan Tianyu Information Industry	wuhantianyu-001	001	2021-08-05
485	CN	X-Laboratory	x-laboratory-000	000	2019-09-03
486	CN	X-Laboratory	x-laboratory-001	001	2020-01-21
487	CN	Xforward AI Technology	xforwardai-001	001	2020-09-25
488	CN	Xforward AI Technology	xforwardai-002	002	2021-02-10
489	CN	Xiamen Meiya Pico Information	meiya-001	001	2019-03-01
490	CN	Xiamen University	xm-000	000	2020-10-19

Table 7: Summary of participant information included in this report.

	Location	Developer Name	Short Name	Seq. Num.	Validation Date
491	PT	YooniK	yoonik-003	003	2022-01-06
492	PT	YooniK	yoonik-004	004	2023-02-10
493	TW	Yuan High-Tech Development	yuan-005	005	2022-06-22
494	TW	Yuan High-Tech Development	yuan-006	006	2022-12-14
495	CN	Yuntu Data and Technology	ytu-000	000	2021-06-16
496	CN	Zhuhai Yisheng Electronics Technology	yisheng-004	004	2018-06-12
497	CN	iQIYI Inc	iqface-000	000	2019-06-04
498	CN	iQIYI Inc	iqface-003	003	2021-02-23
499	TW	iSAP Solution Corporation	isap-001	001	2019-08-07
500	TW	iSAP Solution Corporation	isap-002	002	2020-09-01
501	TW	ioNetworks Inc	ionetworks-000	000	2021-07-20

Table 8: Summary of participant information included in this report.

	ALGORITHM	CONFIG	LIBRARY	TEMPLATE								COMPARISON ⁴		
				NAME	DATA	DATA	MEMORY	SIZE	GENERATION TIME (ms) ⁴				TIME (ns) ⁵	
									(KB) ¹	(KB) ²	(MB) ³	(B)	MUGSHOT	480x720
1	20face-000	117155	324083	²²² 905	¹⁸³ 2048 ± 0	⁴⁴ 232 ± 1	³² 223 ± 1	²⁸ 226 ± 4	²³ 222 ± 1	¹⁷ 224 ± 1	⁴⁶⁸ 44880 ± 134	⁴⁶⁷ 44462 ± 163		
2	20face-001	226824	324119	³⁹² 1940	⁴⁵⁸ 4096 ± 0	⁵⁶ 279 ± 2	⁴⁰ 266 ± 1	³² 266 ± 1	³⁰ 267 ± 1	²⁴ 267 ± 0	³⁶⁷ 5553 ± 54	³⁶⁴ 5541 ± 65		
3	3divi-006	273866	52656	⁹⁶ 472	²⁹⁷ 2048 ± 0	²¹⁷ 654 ± 1	¹⁸¹ 651 ± 0	¹⁶³ 660 ± 1	¹⁴⁷ 678 ± 2	¹⁴⁸ 759 ± 13	¹¹⁶ 775 ± 19	¹¹⁴ 770 ± 22		
4	3divi-007	483115	24723	³⁰⁹ 1285	¹⁸⁵ 2048 ± 0	¹⁹³ 615 ± 1	¹⁶⁸ 616 ± 1	¹⁴⁹ 623 ± 1	¹³³ 644 ± 1	¹³⁵ 727 ± 5	¹⁰⁴ 707 ± 31	¹⁰⁴ 712 ± 25		
5	accurascan-001	14057	24437	²³⁵ 944	⁴⁶ 512 ± 0	³⁹ 204 ± 27	³⁰ 215 ± 17	²⁶ 220 ± 16	²⁸ 237 ± 18	³¹ 339 ± 19	⁴²⁸ 15634 ± 54	⁴²⁷ 15647 ± 77		
6	acer-001	36650	66086	⁷⁹ 417	²³ 512 ± 0	³⁷ 199 ± 0	³⁵ 237 ± 28	²⁹ 229 ± 26	²⁹ 242 ± 37	²² 259 ± 21	²⁷⁰ 2453 ± 44	²⁷¹ 2461 ± 62		
7	acer-002	43922	624858	³⁹ 187	²⁴⁰ 2048 ± 0	³² 184 ± 0	²⁴ 184 ± 0	¹⁸ 185 ± 0	¹⁵ 185 ± 0	¹³ 186 ± 0	³¹⁵ 3370 ± 47	³¹⁵ 3350 ± 54		
8	acisw-007	267619	36111	⁵⁴ 286	³⁰⁰ 2048 ± 0	⁶¹ 283 ± 0	⁵² 293 ± 3	⁶⁷ 414 ± 0	⁵⁷ 404 ± 0	⁵⁷ 484 ± 1	¹⁷⁴ 1316 ± 22	¹⁷⁴ 1297 ± 23		
9	acisw-008	171703	39359	²⁶⁹ 1101	¹²² 2048 ± 0	¹⁰² 400 ± 1	⁷⁰ 362 ± 28	⁵³ 369 ± 9	³⁶ 300 ± 2	³⁰ 336 ± 5	¹⁷⁵ 1327 ± 19	¹⁷⁷ 1337 ± 32		
10	ader-a-003	0	749778	²²⁸ 917	⁴⁸² 5120 ± 0	⁴⁶² 1381 ± 12	⁴³³ 1385 ± 1	⁴³¹ 1394 ± 1	⁴⁰⁴ 1401 ± 1	³⁵² 1469 ± 1	²⁵³ 2148 ± 34	²⁵² 2130 ± 32		
11	ader-a-004	0	959123	³⁷⁴ 1748	⁴⁸⁴ 6144 ± 0	⁴²⁷ 1246 ± 1	³⁸⁰ 1204 ± 1	³⁷³ 1230 ± 2	³³⁵ 1207 ± 2	²⁸² 1254 ± 1	²²⁵ 1840 ± 34	²²⁴ 1828 ± 31		
12	advance-003	258867	78699	¹¹⁰ 518	¹⁸⁶ 2048 ± 0	¹⁸² 586 ± 0	¹⁵⁶ 584 ± 0	¹³⁴ 583 ± 0	¹¹¹ 588 ± 0	⁹¹ 591 ± 1	²²⁴ 1813 ± 17	²²⁰ 1788 ± 26		
13	advance-004	803133	954494	¹⁵⁰ 679	¹⁷⁶ 2048 ± 0	³⁸⁴ 1099 ± 20	³⁵⁶ 1107 ± 15	³³⁵ 1093 ± 21	²⁹⁷ 1103 ± 21	²⁵² 1138 ± 21	²³⁸ 1935 ± 35	²⁴⁰ 1936 ± 32		
14	afisbiometrics-000	545886	32882	²⁶⁶ 1088	⁴⁷ 512 ± 0	⁴¹⁷ 1219 ± 1	³⁶⁰ 1135 ± 1	³⁴⁵ 1137 ± 2	³⁰⁹ 1137 ± 1	²⁵⁴ 1147 ± 1	¹⁸¹ 1400 ± 29	¹⁷⁸ 1357 ± 32		
15	afrengine-000	151875	382842	³⁸ 177	⁴⁴⁴ 4096 ± 0	¹⁶ 107 ± 0	¹³ 112 ± 0	³⁶ 284 ± 2	¹⁵⁶ 697 ± 2	⁴³⁸ 3299 ± 17	⁴⁷⁷ 54329 ± 140	⁴⁷⁶ 56195 ± 256		
16	afrengine-001	410712	391289	²⁴⁸ 1015	⁴⁶⁰ 4096 ± 0	³⁴⁶ 970 ± 0	³¹⁰ 982 ± 1	²⁸¹ 979 ± 2	²⁵⁸ 996 ± 0	²⁰² 990 ± 4	⁴⁷⁶ 54240 ± 169	⁴⁷⁵ 56125 ± 179		
17	aifirst-001	224157	808777	⁹⁷ 485	³⁴⁷ 2048 ± 0	¹⁸⁴ 587 ± 2	¹⁴⁹ 568 ± 2	¹³⁵ 584 ± 3	¹¹⁸ 601 ± 6	¹⁴³ 755 ± 5	¹⁵⁸ 1099 ± 14	¹⁶⁰ 1087 ± 45		
18	aigen-001	256958	595227	²⁸¹ 1136	¹⁴⁹ 2048 ± 0	⁴⁸³ 1448 ± 9	⁴⁵⁷ 1451 ± 8	⁴⁶⁷ 1759 ± 6	⁴⁶² 2594 ± 4	⁴⁵⁰ 5691 ± 44	³³⁴ 3772 ± 57	³³³ 3736 ± 56		
19	aigen-002	205300	1316138	²¹⁵ 874	²⁷⁸ 2048 ± 0	¹⁸³ 586 ± 24	¹⁵⁸ 582 ± 4	²⁵¹ 920 ± 4	⁴⁴⁷ 1758 ± 5	⁴⁴⁹ 5427 ± 17	³³⁰ 3678 ± 44	³²⁹ 3646 ± 48		
20	ailabs-001	1054663	338989	²⁹⁸ 1252	³²¹ 2048 ± 0	²²¹ 664 ± 4	²²⁶ 774 ± 50	³⁵⁰ 1145 ± 12	⁴⁵³ 1972 ± 74	⁴⁴⁶ 5205 ± 272	⁴⁹³ 104034 ± 661	⁴⁹³ 103415 ± 7722		
21	aimall-002	370156	25210	³⁴⁸ 1576	¹⁰⁸ 2048 ± 0	²⁶⁴ 776 ± 4	²⁸⁷ 927 ± 27	²⁶⁰ 940 ± 21	²⁴² 955 ± 34	²⁰⁶ 1003 ± 75	⁴⁸⁹ 72811 ± 7399	⁴⁸⁷ 71216 ± 6286		
22	aimall-003	504324	171935	³⁸⁸ 1913	⁸⁷ 1024 ± 0	²¹⁹ 662 ± 1	²¹⁵ 740 ± 51	¹⁹⁶ 752 ± 62	¹⁷² 741 ± 46	¹⁵⁶ 807 ± 47	⁴⁶¹ 34565 ± 93	⁴⁶² 34598 ± 118		
23	aiseemu-001	0	1005354	⁴³⁴ 2697	⁴⁴⁸ 4096 ± 0	³⁶² 1001 ± 1	³²⁶ 1017 ± 0	³⁰² 1014 ± 5	²⁷² 1022 ± 2	²²⁸ 1059 ± 4	³⁵⁴ 4864 ± 25	³⁵⁴ 4855 ± 32		
24	aiseemu-002	0	1216980	⁴⁵⁶ 3446	⁴⁵⁴ 4096 ± 0	⁴⁴³ 1298 ± 5	⁴¹² 1303 ± 4	⁴⁰² 1313 ± 2	³⁷⁸ 1329 ± 0	³¹⁴ 1348 ± 2	³⁵⁷ 4917 ± 37	³⁵⁵ 4916 ± 37		
25	aiunionface-000	241642	840295	⁷⁵ 402	¹⁸⁴ 2048 ± 0	²⁰⁹ 637 ± 13	²²⁰ 754 ± 41	³⁰³ 1025 ± 28	³²³ 1179 ± 29	³⁸⁸ 1639 ± 47	¹⁵³ 1072 ± 19	¹⁵⁸ 1080 ± 47		
26	aize-001	268456	168970	³³⁴ 1436	²²⁵ 2048 ± 0	¹¹⁷ 437 ± 10	⁹⁷ 440 ± 8	¹²² 542 ± 17	¹⁷⁵ 756 ± 27	³⁸² 1583 ± 53	²⁴⁰ 1937 ± 22	²³⁴ 1919 ± 23		
27	aize-002	257106	182517	¹²⁹ 586	²⁷⁹ 2048 ± 0	¹³¹ 467 ± 1	¹¹² 479 ± 1	¹⁹⁸ 756 ± 1	⁴³¹ 1477 ± 1	⁴⁴³ 4617 ± 41	⁶⁷ 597 ± 16	⁷⁰ 598 ± 14		
28	ajou-001	363257	31734	⁸⁷ 442	¹⁹⁵ 2048 ± 0	¹⁵⁷ 530 ± 0	¹³⁷ 536 ± 0	¹¹⁷ 535 ± 0	¹⁰¹ 549 ± 0	⁸⁸ 577 ± 0	⁶⁴ 597 ± 19	⁶⁹ 596 ± 13		
29	alchera-004	1001019	388616	³⁰⁴ 1270	³⁴⁵ 2048 ± 0	³⁵⁶ 975 ± 0	²⁹⁶ 955 ± 0	²⁷¹ 960 ± 0	²⁵⁴ 989 ± 0	²⁵⁵ 1152 ± 1	³²⁴ 3529 ± 54	³²⁵ 3530 ± 63		
30	alchera-005	1001019	388616	³⁰² 1268	²¹⁵ 2048 ± 0	³⁴⁵ 969 ± 1	³¹³ 987 ± 3	²⁸⁷ 985 ± 3	²⁶⁰ 998 ± 0	²⁶² 1162 ± 2	³²² 3481 ± 59	³²⁰ 3422 ± 57		
31	alfabeta-001	128232	21780	⁸ 73	³⁰ 512 ± 0	⁵¹ 271 ± 0	⁴⁵ 276 ± 0	⁸⁴ 459 ± 2	²¹⁵ 886 ± 2	⁴²² 2547 ± 9	⁴⁵ 470 ± 25	⁴⁷ 458 ± 20		
32	alice-000	1741293	19355	³⁷⁰ 1732	⁴⁵¹ 4096 ± 0	³³⁶ 950 ± 2	²⁸⁹ 933 ± 1	²⁶⁴ 949 ± 1	²⁷⁰ 1011 ± 3	²⁸⁶ 1264 ± 8	⁴²⁵ 14975 ± 201	⁴²⁴ 14890 ± 229		
33	alleyes-000	507636	997090	²¹¹ 857	¹⁵² 2048 ± 0	²⁶⁸ 784 ± 1	³⁰² 970 ± 61	²⁷⁷ 974 ± 62	²³⁷ 943 ± 69	²²² 1057 ± 23	¹⁷³ 1298 ± 34	¹⁷⁵ 1303 ± 51		
34	allgogradion-000	172509	155862	¹²² 561	²⁸² 2048 ± 0	⁹⁷ 384 ± 8	⁸⁰ 395 ± 17	⁶⁵ 413 ± 14	⁷⁴ 471 ± 14	¹²⁸ 710 ± 21	⁴⁵² 29903 ± 406	⁴⁵² 29735 ± 194		
35	alphaface-001	259849	81636	¹¹³ 527	³³⁹ 2048 ± 0	¹⁹³ 612 ± 1	¹⁶⁵ 613 ± 3	¹⁴⁵ 612 ± 1	¹²⁴ 619 ± 1	¹⁰⁹ 640 ± 2	¹⁴² 1008 ± 10	¹⁴³ 1002 ± 19		
36	alphaface-002	768995	70692	³³³ 1434	²⁵³ 2048 ± 0	²⁰⁴ 628 ± 2	²¹⁷ 746 ± 19	¹⁹⁵ 751 ± 18	¹⁸¹ 779 ± 22	¹⁶⁰ 828 ± 40	¹³³ 945 ± 25	¹³⁴ 935 ± 17		
37	amplifiedgroup-001	0	47053	¹² 81	⁷⁰ 866 ± 2	¹³ 93 ± 0	-	-	-	-	⁴⁸⁰ 57803 ± 4210	⁴⁷⁷ 56365 ± 1196		
38	androvideo-000	174847	585063	⁷⁶ 403	³³¹ 2048 ± 0	⁵⁴ 277 ± 0	⁴⁹ 285 ± 0	⁴¹ 314 ± 0	⁴⁷ 372 ± 1	¹⁰⁰ 620 ± 0	²⁹⁰ 2860 ± 28	²⁸⁹ 2847 ± 22		
39	anke-004	349388	410776	¹⁶¹ 706	³⁷⁶ 2056 ± 0	²⁰² 625 ± 1	¹⁷² 627 ± 2	¹⁵⁶ 635 ± 3	¹³⁸ 653 ± 2	²⁰⁰ 982 ± 8	⁸⁷ 633 ± 22	⁸⁸ 632 ± 34		
40	anke-005	328553	429160	²⁷⁸ 1134	³⁸² 2056 ± 0	¹⁸⁵ 590 ± 2	¹⁶⁰ 594 ± 5	¹⁴² 601 ± 3	¹³¹ 638 ± 4	¹⁵⁹ 821 ± 24	⁹⁹ 685 ± 19	¹⁰¹ 687 ± 26		
41	antheus-000	119453	41994	²⁰ 116	⁵⁵ 520 ± 0	¹⁷ 109 ± 1	²⁶ 187 ± 1	²¹ 189 ± 1	¹⁶ 195 ± 1	¹⁹ 236 ± 2	³⁸⁵ 6901 ± 268	³⁸⁴ 6936 ± 103		
42	antheus-001	119453	41962	²¹ 118	⁵⁸ 520 ± 0	²⁰ 120 ± 1	³⁹ 265 ± 13	⁸⁹ 468 ± 22	³⁴⁰ 1223 ± 27	⁴²⁴ 2660 ± 87	³⁸¹ 6218 ± 47	³⁷⁹ 6216 ± 45		
43	anyvision-004	401001	630797	²⁷⁰ 1102	⁷³ 1024 ± 0	⁸³ 355 ± 1	-	-	-	-	²³⁴ 1891 ± 51	²²⁵ 1829 ± 85		
44	anyvision-005	190979	116595	²³⁷ 963	⁸⁰ 1024 ± 0	³⁵⁶ 985 ± 1	³¹⁹ 997 ± 1	²⁹⁹ 1004 ± 1	²⁵⁷ 995 ± 1	²⁰⁴ 995 ± 1	¹⁰⁹ 733 ± 14	¹⁰⁹ 733 ± 16		

Table 9: Summary of algorithms and properties included in this report. The red superscripts give ranking for the quantity in that column.

Notes

- 1 The configuration size does not capture static data included in libraries.
- 2 The library size is the combined total of all files provided in the submission lib folder. These libraries e.g. OpenCV may or may not be installed on any end user's platform natively and would not need to be installed with the algorithm. Some developers put neural network models in their libraries.
- 3 The memory usage is the peak resident set size reported by the ps system call during template generation.
- 4 The median template creation times are measured on Intel®Xeon®CPU E5-2630 v4 @ 2.20GHz processors.
- 5 The comparison durations, in nanoseconds, are estimated using std::chrono::high_resolution_clock which on the machine in (2) counts 1ns clock ticks. Precision is somewhat worse than that however. The ± value is the median absolute deviation times 1.48 for Normal consistency.

ALGORITHM	CONFIG	LIBRARY	TEMPLATE								COMPARISON ⁴										
			NAME	DATA	DATA	MEMORY	SIZE	GENERATION TIME (ms) ⁴				TIME (ns) ⁵									
								(KB) ¹	(KB) ²	(MB) ³	(B)	MUGSHOT	480x720	960x1440	1600x2400	3000x4500	GENUINE	IMPOSTOR			
45	aratek-001	254521	15993	408	2169	210	2048 ± 0	47	251 ± 1	44	275 ± 0	31	252 ± 0	31	278 ± 0	26	286 ± 0	217	1776 ± 20	214	1744 ± 38
46	armatura-001	0	374608	284	1151	325	2048 ± 0	235	688 ± 1	197	689 ± 1	177	693 ± 1	160	708 ± 3	144	756 ± 13	21	270 ± 17	25	268 ± 11
47	armatura-003	0	836082	349	1577	485	6144 ± 0	371	1028 ± 1	332	1032 ± 1	305	1027 ± 0	275	1036 ± 1	214	1041 ± 3	475	51850 ± 56	474	51835 ± 48
48	asusaics-000	257418	245320	136	605	246	2048 ± 0	142	484 ± 13	129	506 ± 21	224	850 ± 26	449	1789 ± 61	451	6305 ± 188	365	5455 ± 78	363	5422 ± 112
49	asusaics-001	257418	245330	133	595	449	4096 ± 0	294	842 ± 17	324	1008 ± 20	423	1377 ± 28	461	2423 ± 90	455	7284 ± 277	395	8618 ± 42	394	8638 ± 136
50	autentika-000	266093	3200425	393	1942	167	2048 ± 0	168	553 ± 1	162	605 ± 1	144	609 ± 2	120	608 ± 1	99	618 ± 2	490	72833 ± 577	488	71829 ± 541
51	autentika-001	0	3198534	357	1660	335	2048 ± 0	233	683 ± 2	278	912 ± 4	247	908 ± 3	228	919 ± 3	176	893 ± 4	487	71804 ± 600	486	70747 ± 582
52	authenmetric-003	293599	39492	241	982	134	2048 ± 0	360	992 ± 1	323	1006 ± 1	298	1003 ± 2	264	1002 ± 1	213	1036 ± 1	215	1757 ± 19	215	1755 ± 19
53	authenmetric-004	381165	39492	292	1214	298	2048 ± 0	319	910 ± 1	277	909 ± 1	248	915 ± 1	229	921 ± 2	192	950 ± 1	210	1724 ± 14	209	1691 ± 29
54	aware-005	300017	26320	301	1265	105	1572 ± 0	313	886 ± 23	333	1038 ± 21	341	1121 ± 22	381	1337 ± 58	412	2195 ± 144	190	1475 ± 63	187	1427 ± 115
55	aware-006	298543	14124	233	943	15	352 ± 0	400	1148 ± 3	365	1146 ± 2	364	1190 ± 2	364	1306 ± 20	398	1754 ± 84	279	2598 ± 42	279	2559 ± 60
56	awiros-001	15499	87480	14	88	29	512 ± 0	14	97 ± 6	11	98 ± 4	13	138 ± 6	24	225 ± 7	84	556 ± 8	155	1079 ± 44	153	1050 ± 45
57	awiros-002	289016	203723	123	562	326	2048 ± 0	137	479 ± 0	125	500 ± 0	116	534 ± 0	123	618 ± 0	189	946 ± 1	241	1966 ± 31	242	1957 ± 25
58	aximetria-001	408902	487912	149	674	211	2048 ± 0	366	1013 ± 1	327	1023 ± 21	307	1029 ± 5	261	999 ± 2	236	1091 ± 5	347	4401 ± 94	345	4490 ± 80
59	ayftech-001	195423	43580	168	731	24	512 ± 0	108	408 ± 23	110	476 ± 52	217	814 ± 108	451	1827 ± 384	448	5412 ± 1029	78	615 ± 16	128	885 ± 44
60	ayonix-000	58505	5252	6	69	92	1036 ± 0	2	18 ± 2	-	-	-	-	-	-	-	81	621 ± 23	84	620 ± 26	
61	beethedata-000	227849	1087592	121	555	323	2048 ± 0	128	465 ± 0	108	467 ± 0	90	468 ± 0	73	467 ± 0	54	467 ± 0	249	2121 ± 34	250	2110 ± 38
62	beyneai-000	256958	591433	276	1124	192	2048 ± 0	121	451 ± 8	99	449 ± 1	200	767 ± 7	444	1603 ± 25	444	4669 ± 124	331	3730 ± 57	330	3668 ± 54
63	biocube-001	25030	6192987	91	458	429	4096 ± 0	59	282 ± 22	51	292 ± 24	114	521 ± 57	148	684 ± 59	292	1282 ± 68	442	21787 ± 96	441	21812 ± 109
64	biocube-002	69898	10651580	92	459	450	4096 ± 0	288	826 ± 4	244	838 ± 4	357	1175 ± 4	465	2933 ± 1074	457	9144 ± 1090	444	23074 ± 94	443	23036 ± 99
65	bioditechswiss-001	1178769	120811	335	1455	38	512 ± 0	343	966 ± 4	400	1270 ± 270	394	1294 ± 96	408	1409 ± 157	402	1793 ± 79	280	2610 ± 25	280	2624 ± 32
66	bioditechswiss-002	744786	114842	246	993	37	512 ± 0	324	917 ± 2	288	930 ± 2	265	952 ± 2	238	947 ± 3	223	1058 ± 11	256	2177 ± 29	257	2170 ± 31
67	biometric-vision-000	445487	72132	223	906	112	2048 ± 0	291	836 ± 3	243	831 ± 3	228	869 ± 5	241	955 ± 8	322	1370 ± 19	421	14437 ± 161	419	14325 ± 167
68	bm-001	287734	38076	28	148	1	64 ± 0	118	444 ± 88	-	-	-	-	-	-	-	233	1887 ± 31	232	1877 ± 26	
69	boetech-001	261376	88710	325	1384	177	2048 ± 0	52	271 ± 1	41	268 ± 1	33	273 ± 0	33	286 ± 1	28	318 ± 1	485	68519 ± 1921	484	67648 ± 822
70	boetech-002	294347	88710	340	1489	257	2048 ± 0	70	305 ± 4	55	296 ± 1	38	302 ± 1	37	313 ± 1	33	348 ± 2	486	68921 ± 2137	485	69473 ± 2104
71	bresee-001	287880	23227	293	1214	232	2048 ± 0	419	1223 ± 3	384	1216 ± 1	408	1331 ± 1	342	1227 ± 1	320	1360 ± 1	464	37240 ± 655	464	37167 ± 584
72	bresee-002	313627	30902	396	1956	208	2048 ± 0	255	743 ± 4	363	1143 ± 2	351	1146 ± 2	311	1148 ± 2	268	1176 ± 2	218	1778 ± 22	218	1775 ± 23
73	camvi-002	236278	225285	170	737	72	1024 ± 0	227	677 ± 7	213	726 ± 36	229	869 ± 28	305	1129 ± 43	430	2785 ± 113	76	612 ± 26	78	603 ± 20
74	camvi-004	280733	615819	229	919	234	2048 ± 0	258	759 ± 10	253	861 ± 17	288	986 ± 34	358	1279 ± 51	431	2891 ± 158	134	948 ± 40	135	963 ± 31
75	candour-001	150086	97632	214	866	343	2048 ± 0	472	1400 ± 1	440	1396 ± 1	437	1408 ± 1	407	1407 ± 1	351	1464 ± 1	406	10725 ± 133	405	10712 ± 127
76	canon-003	2550850	101378	484	5472	487	6180 ± 0	430	1263 ± 3	397	1263 ± 1	391	1283 ± 1	373	1320 ± 1	359	1482 ± 2	351	4783 ± 17	348	4780 ± 19
77	canon-004	2399160	114188	486	5956	488	6200 ± 0	334	948 ± 4	297	955 ± 3	270	959 ± 3	248	977 ± 3	229	1064 ± 2	390	7172 ± 63	388	7169 ± 51
78	cchonolulu-000	727461	37284	78	416	35	512 ± 0	22	123 ± 13	16	126 ± 10	12	129 ± 10	11	134 ± 10	16	223 ± 10	211	1726 ± 35	210	1697 ± 35
79	ceiec-003	260371	88707	83	430	173	2048 ± 0	279	817 ± 4	268	883 ± 57	240	897 ± 60	222	899 ± 72	188	944 ± 72	263	2256 ± 38	263	2241 ± 54
80	ceiec-004	263476	67011	77	408	289	2048 ± 0	368	1024 ± 1	330	1027 ± 1	306	1027 ± 1	274	1030 ± 1	220	1055 ± 1	227	1844 ± 26	226	1836 ± 20
81	chosun-001	765615	707	100	491	309	2048 ± 0	267	783 ± 2	239	826 ± 4	466	1662 ± 13	468	3679 ± 67	464	11694 ± 243	139	998 ± 25	150	1035 ± 11
82	chosun-002	234001	31875	88	450	178	2048 ± 0	46	248 ± 3	42	273 ± 3	461	1495 ± 14	469	7920 ± 90	465	80302 ± 1349	82	623 ± 17	89	634 ± 13
83	chtface-005	408364	311100	329	1412	146	2048 ± 0	74	322 ± 0	58	316 ± 1	43	325 ± 2	39	324 ± 1	45	411 ± 2	235	1907 ± 19	233	1898 ± 23
84	chtface-006	733645	610439	417	2417	265	2048 ± 0	155	522 ± 1	130	514 ± 1	118	536 ± 2	104	561 ± 1	123	693 ± 2	246	2034 ± 41	247	2049 ± 29
85	cist-001	0	300551	126	583	133	2048 ± 0	347	972 ± 0	305	977 ± 1	283	981 ± 0	251	983 ± 0	226	1061 ± 0	297	2947 ± 20	297	2940 ± 22
86	cist-002	0	1186073	368	1729	416	3200 ± 0	351	976 ± 0	316	992 ± 0	329	1085 ± 1	359	1279 ± 0	411	2101 ± 1	380	6165 ± 22	378	6207 ± 38
87	clearviewai-000	342491	211852	440	2750	193	2048 ± 0	473	1402 ± 1	442	1403 ± 1	439	1412 ± 1	412	1420 ± 1	335	1418 ± 1	197	1592 ± 37	195	1561 ± 37
88	closeli-001	420342	9851	182	773	418	4096 ± 0	293	839 ± 1	246	843 ± 1	221	841 ± 1	202	845 ± 1	169	865 ± 1	364	5404 ± 17	362	5400 ± 25

Notes

1 The configuration size does not capture static data included in libraries.

2 The library size is the combined total of all files provided in the submission lib folder. These libraries e.g. OpenCV may or may not be installed on any end user's platform natively and would not need to be installed with the algorithm. Some developers put neural network models in their libraries.

3 The memory usage is the peak resident set size reported by the ps system call during template generation.

4 The median template creation times are measured on Intel®Xeon®CPU E5-2630 v4 @ 2.20GHz processors.

5 The comparison durations, in nanoseconds, are estimated using std::chrono::high_resolution_clock which on the machine in (2) counts 1ns clock ticks. Precision is somewhat worse than that however. The ± value is the median absolute deviation times 1.48 for Normal consistency.

	ALGORITHM	CONFIG	LIBRARY	TEMPLATE								COMPARISON ⁴									
				NAME	DATA	DATA	MEMORY	SIZE	GENERATION TIME (ms) ⁴				TIME (ns) ⁵								
									(KB) ¹	(KB) ²	(MB) ³	(B)	MUGSHOT	480x720	960x1440	1600x2400	3000x4500	GENUINE	IMPOSTOR		
89	cloudmatrix-001	10390	542121	46	249	231	2048 ± 0	19	114 ± 1	14	117 ± 0	11	118 ± 0	10	123 ± 1	11	169 ± 1	472	50263 ± 212	471	50243 ± 237
90	cloudmatrix-002	256635	693318	253	1030	137	2048 ± 0	100	395 ± 1	82	398 ± 1	61	399 ± 1	55	402 ± 1	49	437 ± 20	471	49578 ± 120	470	49602 ± 180
91	cloudwalk-hr-003	383739	144263	244	984	395	2057 ± 0	190	606 ± 0	157	588 ± 0	138	594 ± 0	122	612 ± 1	-	387	6982 ± 80	385	6972 ± 84	
92	cloudwalk-hr-004	502916	520169	328	1394	348	2049 ± 0	307	873 ± 1	262	877 ± 1	234	876 ± 1	213	879 ± 1	181	902 ± 3	410	11652 ± 127	409	11608 ± 123
93	cloudwalk-mt-006	563322	480071	444	2836	259	2048 ± 0	465	1385 ± 0	436	1392 ± 1	432	1398 ± 1	403	1397 ± 4	346	1444 ± 2	313	3364 ± 96	313	3324 ± 83
94	cloudwalk-mt-007	563322	480071	443	2827	322	2048 ± 0	461	1379 ± 2	449	1425 ± 7	443	1427 ± 6	411	1417 ± 2	345	1443 ± 7	301	3000 ± 68	299	2971 ± 74
95	codeline-000	361659	138388	290	1188	273	2048 ± 0	485	1453 ± 0	460	1456 ± 2	452	1456 ± 0	424	1457 ± 0	360	1483 ± 1	254	2171 ± 69	259	2194 ± 84
96	cogent-007	621565	72316	387	1884	65	550 ± 0	452	1329 ± 2	423	1333 ± 5	412	1337 ± 4	385	1353 ± 5	329	1390 ± 4	34	355 ± 8	37	367 ± 14
97	cogent-008	856817	73587	410	2173	66	550 ± 0	477	1412 ± 1	448	1419 ± 2	442	1426 ± 3	418	1437 ± 3	357	1476 ± 1	41	436 ± 14	44	441 ± 23
98	cognitec-003	471458	62502	198	817	358	2052 ± 0	89	366 ± 9	85	403 ± 9	63	408 ± 9	61	424 ± 9	64	509 ± 13	319	3417 ± 51	321	3433 ± 53
99	cognitec-004	705645	62678	128	585	356	2052 ± 0	126	463 ± 9	121	497 ± 9	106	504 ± 10	91	521 ± 10	10	631 ± 12	305	3028 ± 197	306	3059 ± 238
100	cor-001	1194948	11240	297	1249	398	2060 ± 0	244	699 ± 3	255	863 ± 76	227	865 ± 80	209	872 ± 89	193	952 ± 39	496	270145 ± 2259	496	282686 ± 11788
101	coretech-000	186423	43964	74	393	19	512 ± 0	189	602 ± 15	182	659 ± 12	347	1139 ± 24	312	1149 ± 25	263	1165 ± 23	29	333 ± 14	30	321 ± 13
102	coretech-001	235361	305490	344	1524	254	2048 ± 0	236	688 ± 7	201	695 ± 7	230	870 ± 17	212	879 ± 15	173	877 ± 15	83	625 ± 25	93	641 ± 25
103	corsight-002	1474921	32093	402	2061	404	2080 ± 0	440	1290 ± 1	407	1287 ± 1	399	1290 ± 1	369	1307 ± 2	329	1388 ± 4	447	24953 ± 637	445	24263 ± 578
104	corsight-003	1413063	32198	355	1637	403	2080 ± 0	412	1202 ± 2	378	1190 ± 5	369	1199 ± 3	343	1236 ± 3	451	28754 ± 434	451	28787 ± 446		
105	csc-002	0	519768	323	1376	62	544 ± 0	134	473 ± 0	120	494 ± 0	95	481 ± 1	81	490 ± 1	67	514 ± 5	38	367 ± 11	371	371 ± 10
106	csc-003	0	400435	353	1609	61	544 ± 0	148	499 ± 0	123	500 ± 1	104	502 ± 0	88	508 ± 1	77	535 ± 4	40	393 ± 8	40	397 ± 7
107	ctcbcbank-000	257208	599238	125	570	209	2048 ± 0	173	568 ± 43	163	606 ± 38	176	690 ± 53	161	711 ± 50	161	831 ± 51	329	3551 ± 87	351	4805 ± 209
108	ctcbcbank-001	275511	599238	134	603	294	2048 ± 0	214	652 ± 35	227	781 ± 30	231	875 ± 43	221	898 ± 51	211	1030 ± 47	336	3926 ± 45	334	3924 ± 56
109	cu-face-002	812008	38655	169	735	426	4096 ± 0	378	1054 ± 1	341	1059 ± 0	322	1060 ± 0	284	1063 ± 1	231	1070 ± 0	479	57287 ± 1750	479	57027 ± 945
110	cubox-002	542254	90975	398	1964	288	2048 ± 0	326	921 ± 1	282	921 ± 1	253	922 ± 1	233	933 ± 1	205	1003 ± 1	244	2008 ± 72	244	1969 ± 57
111	cubox-003	1694397	209684	397	1964	203	2048 ± 0	403	1179 ± 0	377	1189 ± 0	368	1198 ± 0	336	1208 ± 0	287	1264 ± 1	266	2289 ± 112	266	2297 ± 68
112	cudocommunication-001	385258	341277	263	1077	168	2048 ± 0	328	925 ± 1	284	923 ± 1	257	928 ± 1	232	932 ± 0	195	964 ± 1	275	2534 ± 20	277	2537 ± 20
113	cuhkee-001	787853	74917	425	2515	357	2052 ± 0	353	977 ± 31	-	-	-	-	-	-	-	281	2719 ± 60	286	2783 ± 56	
114	cybercore-002	166096	7374	428	2564	117	2048 ± 0	144	489 ± 1	124	500 ± 4	103	500 ± 1	86	499 ± 2	75	528 ± 1	415	12389 ± 123	414	12352 ± 112
115	cybercore-003	289176	7969	474	4310	452	4096 ± 0	295	844 ± 2	252	855 ± 4	226	864 ± 4	208	862 ± 4	174	878 ± 2	372	5737 ± 31	372	5737 ± 31
116	cyberextruder-003	253300	12354	85	437	17	512 ± 0	99	390 ± 1	77	388 ± 1	59	393 ± 1	53	399 ± 1	48	435 ± 1	12	198 ± 4	13	189 ± 8
117	cyberextruder-004	169301	12354	66	349	3	128 ± 0	40	206 ± 0	29	208 ± 0	24	209 ± 0	25	229 ± 0	21	249 ± 1	6	145 ± 14	7	155 ± 14
118	cyberlink-010	1590818	102180	460	3672	495	8260 ± 0	431	1265 ± 2	412	1314 ± 5	399	1294 ± 2	355	1273 ± 2	301	1305 ± 2	46	476 ± 23	48	472 ± 14
119	cyberlink-011	1397496	102171	450	3014	489	6212 ± 0	411	1196 ± 3	379	1193 ± 2	367	1195 ± 3	338	1215 ± 6	279	1231 ± 5	333	3768 ± 75	332	3735 ± 57
120	dahua-006	831641	119261	479	5068	295	2048 ± 0	470	1398 ± 2	441	1397 ± 1	436	1404 ± 1	405	1402 ± 1	332	1402 ± 1	19	249 ± 13	21	250 ± 11
121	dahua-007	1578737	119418	491	7237	419	4096 ± 0	469	1393 ± 2	432	1373 ± 1	425	1378 ± 1	393	1378 ± 1	325	1379 ± 2	37	367 ± 102	42	434 ± 108
122	daon-000	280726	2307	400	2013	399	2065 ± 0	170	562 ± 3	154	581 ± 5	202	791 ± 9	199	838 ± 15	219	1055 ± 32	429	16052 ± 88	428	16041 ± 85
123	decatur-000	350495	171271	224	907	467	4100 ± 0	367	1024 ± 2	-	-	-	-	-	-	-	409	11439 ± 80	408	11418 ± 112	
124	decatur-001	342866	253734	341	1507	362	2052 ± 0	386	1103 ± 2	342	1064 ± 2	325	1063 ± 2	286	1067 ± 2	232	1084 ± 2	74	610 ± 19	73	602 ± 8
125	deepglint-004	1073382	261571	451	3084	130	2048 ± 0	489	1470 ± 1	464	1474 ± 1	458	1485 ± 1	429	1474 ± 1	364	1492 ± 2	377	5961 ± 34	376	5955 ± 29
126	deepglint-005	960326	213877	448	2947	202	2048 ± 0	476	1408 ± 1	451	1431 ± 2	441	1424 ± 3	414	1424 ± 3	347	1446 ± 2	384	6765 ± 38	382	6765 ± 40
127	deepsea-001	147497	336250	68	358	78	1024 ± 0	205	630 ± 7	219	752 ± 37	194	746 ± 30	167	727 ± 32	158	820 ± 32	182	1401 ± 37	189	1467 ± 50
128	deeepsense-001	73173	1288355	481	5314	18	512 ± 0	398	1142 ± 2	367	1164 ± 3	363	1183 ± 3	332	1201 ± 3	308	1323 ± 2	268	2356 ± 42	268	2354 ± 42
129	deeepsense-002	73173	1266131	480	5280	71	896 ± 0	455	1350 ± 1	411	1299 ± 8	405	1324 ± 0	383	1348 ± 0	355	1474 ± 4	323	3505 ± 32	324	3515 ± 40
130	dermalog-010	0	525908	250	1023	31	512 ± 0	208	635 ± 0	179	640 ± 1	157	639 ± 4	135	647 ± 3	122	691 ± 5	43	444 ± 13	34	341 ± 26
131	dermalog-011	0	278395	163	715	2	128 ± 0	80	343 ± 0	64	345 ± 0	47	347 ± 0	42	351 ± 0	37	363 ± 0	24	299 ± 19	23	253 ± 14
132	dicio-001	61751	119517	17	77	56	520 ± 0	162	538 ± 0	148	563 ± 10	249	915 ± 3	450	1800 ± 7	447	5286 ± 30	285	2818 ± 20	287	2807 ± 31

Notes

- 1 The configuration size does not capture static data included in libraries.
- 2 The library size is the combined total of all files provided in the submission lib folder. These libraries e.g. OpenCV may or may not be installed on any end user's platform natively and would not need to be installed with the algorithm. Some developers put neural network models in their libraries.
- 3 The memory usage is the peak resident set size reported by the ps system call during template generation.
- 4 The median template creation times are measured on Intel®Xeon®CPU E5-2630 v4 @ 2.20GHz processors.
- 5 The comparison durations, in nanoseconds, are estimated using std::chrono::high_resolution_clock which on the machine in (2) counts 1ns clock ticks. Precision is somewhat worse than that however. The ± value is the median absolute deviation times 1.48 for Normal consistency.

Table 11: Summary of algorithms and properties included in this report. The red superscripts give ranking for the quantity in that column.

ALGORITHM		CONFIG	LIBRARY	TEMPLATE								COMPARISON ⁴									
NAME		DATA	DATA	MEMORY	SIZE	GENERATION TIME (ms) ⁴				TIME (ns) ⁵											
		(KB) ¹	(KB) ²	(MB) ³	(B)	MUGSHOT	480x720	960x1440	1600x2400	3000x4500	GENUINE	IMPOSTOR									
133	didiglobalface-001	259849	70680	112	527	124	2048 ± 0	191	612 ± 1	175	633 ± 3	153	634 ± 3	136	650 ± 15	114	666 ± 4	135	973 ± 20	137	988 ± 20
134	didiglobalface-002	260054	161508	200	826	271	2048 ± 0	200	622 ± 1	176	633 ± 1	160	642 ± 2	140	659 ± 4	134	726 ± 15	57	560 ± 10	61	567 ± 13
135	digidata-000	133370	30249	49	257	208	2048 ± 0	88	361 ± 0	68	360 ± 0	51	361 ± 0	44	363 ± 0	39	380 ± 0	248	2084 ± 37	246	2039 ± 42
136	digidata-001	254564	33036	69	367	129	2048 ± 0	169	559 ± 1	146	561 ± 1	128	562 ± 1	105	564 ± 1	95	602 ± 1	405	10308 ± 102	404	10301 ± 121
137	digitalbarriers-002	83002	598577	39	1930	374	2056 ± 0	41	209 ± 11	36	250 ± 19	64	411 ± 37	188	808 ± 72	413	2236 ± 123	417	13409 ± 228	416	13267 ± 206
138	dps-000	0	2211812	257	1058	430	4096 ± 0	301	868 ± 2	271	893 ± 6	448	1445 ± 9	464	2910 ± 38	458	9345 ± 17	189	1473 ± 37	190	1479 ± 37
139	dsk-000	11967	782905	48	252	43	512 ± 0	68	304 ± 47	59	317 ± 33	297	1001 ± 96	463	2660 ± 170	462	10451 ± 832	389	7152 ± 115	386	7134 ± 111
140	einetworks-000	372608	219883	217	880	380	2056 ± 0	212	645 ± 3	-	-	-	-	-	-	355	4876 ± 66	357	5156 ± 77		
141	ekin-002	51434	278	23	139	410	3072 ± 0	408	1186 ± 13	374	1180 ± 12	360	1181 ± 11	330	1191 ± 11	274	1207 ± 8	344	4294 ± 80	366	5569 ± 112
142	enface-001	370710	173609	148	670	79	1024 ± 0	166	550 ± 4	145	555 ± 3	166	668 ± 7	249	981 ± 15	419	2416 ± 59	383	6734 ± 68	383	6766 ± 69
143	enface-002	858356	98741	492	7578	84	1024 ± 0	369	1026 ± 1	336	1038 ± 3	319	1057 ± 7	301	1123 ± 4	312	1338 ± 8	194	1529 ± 23	193	1530 ± 35
144	eocortex-000	255937	59432	44	224	109	2048 ± 0	69	305 ± 22	63	341 ± 25	78	440 ± 47	70	464 ± 45	65	513 ± 44	132	923 ± 11	133	918 ± 11
145	ercacat-001	811623	58012	442	2816	367	2052 ± 0	377	1052 ± 3	-	-	-	-	-	-	277	2551 ± 62	274	2501 ± 81		
146	euronovate-001	0	1774966	315	1308	96	1177 ± 0	372	1034 ± 2	368	1165 ± 3	354	1160 ± 3	321	1177 ± 3	266	1172 ± 2	492	81294 ± 591	492	81631 ± 931
147	expasoft-001	39057	983064	25	142	330	2048 ± 0	9	70 ± 0	74	± 0	77	± 0	673	± 0	74	± 0	205	1660 ± 35	206	1676 ± 48
148	expasoft-002	38760	59825	34	168	229	2048 ± 0	54	34 ± 0	34	34 ± 0	34	34 ± 0	234	34 ± 0	234	34 ± 0	397	8870 ± 78	396	8838 ± 77
149	f8-001	272977	19668	305	1276	196	2048 ± 0	285	822 ± 39	-	-	-	-	-	-	427	15262 ± 139	426	15277 ± 212		
150	f8-002	28278	215616	13	83	127	2048 ± 0	69	39 ± 0	41	± 0	675	± 0	19	197 ± 1	126	702 ± 1	424	14765 ± 131	423	14790 ± 133
151	faceonlive-001	0	71529	57	302	378	2056 ± 0	29	179 ± 0	21	179 ± 0	22	190 ± 0	21	217 ± 0	32	343 ± 1	151	1064 ± 37	149	1033 ± 35
152	faceonlive-002	155220	141019	247	995	175	2048 ± 0	266	783 ± 1	232	797 ± 2	204	794 ± 2	189	809 ± 3	180	901 ± 2	418	13798 ± 197	417	13743 ± 127
153	facephf-000	148904	5219	495	11481	150	2048 ± 0	303	871 ± 2	264	881 ± 3	236	880 ± 4	218	888 ± 4	191	949 ± 12	342	4067 ± 53	340	4047 ± 53
154	facesoft-000	370120	10612	188	796	333	2048 ± 0	225	675 ± 18	185	669 ± 3	172	686 ± 3	145	675 ± 5	118	687 ± 2	262	2239 ± 28	265	2277 ± 96
155	facetag-000	1232331	4022	238	965	69	684 ± 0	82	355 ± 17	71	369 ± 8	291	989 ± 33	460	2408 ± 91	456	7930 ± 316	488	72003 ± 625	489	71912 ± 612
156	facetag-002	819806	4021	163	726	116	2048 ± 0	163	544 ± 1	141	544 ± 0	121	542 ± 0	100	545 ± 0	82	554 ± 0	212	1730 ± 25	211	1733 ± 25
157	facex-001	305074	930372	447	2931	293	2048 ± 0	112	422 ± 4	95	434 ± 4	113	520 ± 7	171	737 ± 13	391	1670 ± 27	230	1871 ± 23	228	1846 ± 29
158	facex-002	305074	928334	452	3095	285	2048 ± 0	113	426 ± 5	93	429 ± 4	111	516 ± 8	169	730 ± 12	397	1738 ± 36	86	631 ± 25	82	614 ± 19
159	farfaces-001	346494	44581	50	261	36	512 ± 0	404	1179 ± 1	375	1180 ± 1	359	1180 ± 0	327	1185 ± 1	275	1209 ± 2	125	855 ± 25	124	860 ± 31
160	fastenterprises-000	273365	235899	251	1026	244	2048 ± 0	220	662 ± 1	186	671 ± 0	165	664 ± 0	144	673 ± 3	119	688 ± 5	335	3806 ± 96	460	32064 ± 185
161	fiberhome-nanjing-003	352895	1482309	207	845	324	2048 ± 0	395	1136 ± 7	359	1134 ± 4	344	1132 ± 3	310	1139 ± 3	257	1154 ± 5	157	1097 ± 38	159	1083 ± 42
162	fiberhome-nanjing-004	443779	1482313	256	1048	463	4096 ± 0	449	1321 ± 5	413	1304 ± 3	401	1307 ± 2	368	1308 ± 3	310	1326 ± 5	171	1276 ± 40	172	1265 ± 38
163	fincore-000	256615	19409	117	535	207	2048 ± 0	152	508 ± 3	128	505 ± 0	107	508 ± 1	90	513 ± 2	76	535 ± 1	216	1765 ± 31	216	1763 ± 22
164	firstcreditkz-001	553811	24803	272	1112	302	2048 ± 0	275	808 ± 0	318	997 ± 0	324	1061 ± 1	320	1174 ± 1	401	1774 ± 54	129	904 ± 20	130	903 ± 23
165	firstcreditkz-002	977538	24879	394	1954	113	2048 ± 0	432	1265 ± 1	402	1275 ± 4	399	1299 ± 7	382	1341 ± 17	370	1515 ± 40	114	761 ± 28	115	774 ± 32
166	foomobi-001	0	219961	41	191	125	2048 ± 0	84	357 ± 0	76	388 ± 2	346	1138 ± 1	466	2974 ± 10	460	10101 ± 10	470	47409 ± 453	469	47413 ± 421
167	frpkauai-001	507771	24807	262	1076	217	2048 ± 0	237	689 ± 1	199	691 ± 0	180	697 ± 2	163	714 ± 6	149	775 ± 31	112	752 ± 29	113	764 ± 23
168	frpkauai-002	519141	24803	273	1112	299	2048 ± 0	314	799 ± 0	315	1046 ± 1	316	1163 ± 2	400	1769 ± 4	130	907 ± 20	129	886 ± 28		
169	fujitsulab-002	0	1088887	354	1613	473	4104 ± 0	423	1237 ± 2	387	1222 ± 2	374	1236 ± 1	346	1251 ± 2	311	1327 ± 2	286	2836 ± 25	288	2809 ± 44
170	fujitsulab-003	662263	318209	490	6907	471	4104 ± 0	337	951 ± 20	290	941 ± 19	266	952 ± 19	246	971 ± 20	216	1045 ± 21	289	2855 ± 16	290	2849 ± 19
171	g42-intellibrain-001	1031335	235521	500	25628	10	269 ± 0	352	976 ± 6	304	975 ± 1	296	997 ± 2	288	1068 ± 3	321	1362 ± 8	375	5878 ± 96	375	5865 ± 71
172	geo-002	369903	98667	249	1018	266	2048 ± 0	269	791 ± 1	230	793 ± 0	203	794 ± 0	183	795 ± 1	153	803 ± 1	318	3407 ± 45	319	3422 ± 65
173	geo-004	168980	107714	307	1280	284	2048 ± 0	433	1268 ± 1	404	1279 ± 1	387	1274 ± 0	350	1259 ± 1	297	1296 ± 1	146	1023 ± 20	147	1028 ± 22
174	glory-005	0	999999	420	2428	477	4182 ± 0	247	703 ± 1	229	789 ± 0	276	972 ± 1	456	2200 ± 25	459	9679 ± 22	361	5224 ± 93	359	5176 ± 81
175	glory-006	0	1004784	419	2427	476	4182 ± 0	248	704 ± 1	225	774 ± 0	274	968 ± 2	458	2286 ± 18	461	10381 ± 151	374	5853 ± 77	374	5819 ± 74
176	gorilla-008	450175	707000	377	1789	496	8338 ± 0	188	595 ± 1	158	590 ± 0	141	600 ± 1	127	621 ± 2	131	720 ± 9	349	4530 ± 44	346	4524 ± 38

Notes
 1 The configuration size does not capture static data included in libraries.
 2 The library size is the combined total of all files provided in the submission lib folder. These libraries e.g. OpenCV may or may not be installed on any end user's platform natively and would not need to be installed with the algorithm. Some developers put neural network models in their libraries.
 3 The memory usage is the peak resident set size reported by the ps system call during template generation.
 4 The median template creation times are measured on Intel®Xeon®CPU E5-2630 v4 @ 2.20GHz processors.
 5 The comparison durations, in nanoseconds, are estimated using std::chrono::high_resolution_clock which on the machine in (2) counts 1ns clock ticks. Precision is somewhat worse than that however. The ± value is the median absolute deviation times 1.48 for Normal consistency.

	ALGORITHM	CONFIG	LIBRARY	TEMPLATE								COMPARISON ⁴									
				NAME		DATA	DATA	MEMORY	SIZE	GENERATION TIME (ms) ⁴				TIME (ns) ⁵							
				(KB) ¹	(KB) ²	(MB) ³	(B)	MUGSHOT	480x720	960x1440	1600x2400	3000x4500	GENUINE	IMPOSTOR							
177	gorilla-009	329584	297395	317	1312	478	4242 ± 0	316	899 ± 2	283	922 ± 1	243	901 ± 3	230	924 ± 4	212	1032 ± 12	267	2294 ± 74	267	2301 ± 66
178	graymatics-001	13095	70406	22	127	461	4096 ± 0	34	191 ± 1	27	203 ± 1	137	592 ± 5	446	1698 ± 9	454	7150 ± 34	466	39874 ± 309	465	39762 ± 295
179	griaule-001	0	412061	303	1269	368	2052 ± 0	401	1164 ± 1	352	1096 ± 5	337	1099 ± 4	308	1136 ± 2	368	1509 ± 2	339	3948 ± 23	337	3957 ± 32
180	griaule-002	0	1320474	381	1815	352	2052 ± 0	286	822 ± 1	285	924 ± 4	246	907 ± 1	278	1038 ± 21	341	1430 ± 9	340	4005 ± 32	339	4012 ± 31
181	hertasecurity-002	0	944582	288	1177	32	512 ± 0	141	484 ± 7	111	478 ± 3	94	480 ± 3	85	495 ± 3	72	520 ± 3	269	2289 ± 40	264	2267 ± 48
182	hertasecurity-003	0	944583	289	1177	34	512 ± 0	147	495 ± 7	113	480 ± 3	99	486 ± 3	82	491 ± 3	73	520 ± 4	391	7619 ± 65	390	7597 ± 94
183	hik-001	667866	9290	488	6597	100	1408 ± 0	213	651 ± 0	184	667 ± 8	168	677 ± 16	149	686 ± 13	138	737 ± 12	48	488 ± 19	49	477 ± 22
184	hisign-001	732412	167488	346	1553	401	2080 ± 0	449	1306 ± 1	417	1320 ± 1	404	1315 ± 1	371	1312 ± 1	309	1325 ± 1	13	201 ± 10	11	185 ± 13
185	hisign-002	1014906	102652	406	2123	402	2080 ± 0	272	797 ± 0	233	800 ± 5	206	800 ± 0	185	801 ± 0	154	803 ± 1	18	232 ± 11	19	207 ± 11
186	hyperverge-003	1167779	282156	439	2748	85	1024 ± 0	493	1477 ± 2	466	1503 ± 3	463	1520 ± 3	439	1525 ± 4	379	1565 ± 3	59	566 ± 11	59	561 ± 8
187	hyperverge-004	4924393	282156	466	3907	204	2048 ± 0	490	1471 ± 2	452	1434 ± 1	449	1446 ± 6	420	1445 ± 3	363	1491 ± 3	138	996 ± 10	141	1000 ± 19
188	hzailu-003	1923030	222185	477	4817	415	3080 ± 0	467	1389 ± 5	422	1331 ± 7	409	1334 ± 2	384	1349 ± 6	338	1424 ± 8	191	1483 ± 35	188	1464 ± 31
189	hzailu-004	1938475	275639	449	2963	412	3080 ± 0	500	1495 ± 8	462	1490 ± 6	460	1493 ± 8	436	1502 ± 8	381	1583 ± 17	177	1361 ± 32	184	1419 ± 44
190	icm-003	1513988	940	102	500	286	2048 ± 0	229	681 ± 6	188	672 ± 4	186	714 ± 11	198	837 ± 41	326	1381 ± 131	446	24351 ± 161	444	24227 ± 146
191	icm-004	2012129	1089	255	1040	156	2048 ± 0	111	419 ± 6	86	407 ± 6	82	454 ± 15	119	603 ± 51	373	1527 ± 235	423	14730 ± 154	422	14521 ± 152
192	icthtc-000	172459	1471004	379	1805	346	2048 ± 0	79	338 ± 11	62	338 ± 9	74	437 ± 16	158	705 ± 24	395	1719 ± 44	363	5284 ± 63	361	5290 ± 54
193	id3-006	210116	7706	242	982	57	520 ± 0	232	683 ± 0	347	1088 ± 1	365	1192 ± 1	337	1209 ± 1	288	1270 ± 1	366	5547 ± 34	365	5563 ± 34
194	id3-008	242416	8151	260	1068	9	264 ± 0	281	819 ± 0	382	1209 ± 2	398	1297 ± 2	379	1329 ± 1	343	1433 ± 1	370	5658 ± 44	370	5624 ± 40
195	idemzia-008	374017	69922	291	1194	14	348 ± 0	123	457 ± 1	106	461 ± 0	87	466 ± 1	77	476 ± 2	66	513 ± 10	308	3080 ± 41	304	3046 ± 56
196	idemzia-009	1066728	70572	435	2702	68	636 ± 0	413	1207 ± 1	385	1218 ± 1	372	1222 ± 2	339	1222 ± 3	290	1280 ± 10	371	5664 ± 84	368	5597 ± 90
197	identity-000	271397	14217	95	469	170	2048 ± 0	238	689 ± 0	204	702 ± 0	185	712 ± 3	176	757 ± 0	198	970 ± 1	93	655 ± 25	92	637 ± 23
198	igearx-face-000	665623	298245	219	885	126	2048 ± 0	300	860 ± 1	251	855 ± 4	222	844 ± 0	214	881 ± 0	185	924 ± 3	201	1628 ± 45	204	1657 ± 41
199	iit-002	259579	52070	167	731	214	2048 ± 0	153	514 ± 1	133	531 ± 2	125	547 ± 1	109	583 ± 1	136	733 ± 2	145	1023 ± 7	144	1011 ± 66
200	iit-003	261288	53791	199	817	197	2048 ± 0	138	482 ± 0	118	493 ± 0	108	509 ± 0	97	541 ± 0	112	661 ± 0	28	324 ± 17	31	326 ± 8
201	imds-software-001	373399	352623	180	772	270	2048 ± 0	129	465 ± 1	298	958 ± 6	343	1131 ± 5	307	1134 ± 2	245	1119 ± 10	412	11885 ± 120	410	11779 ± 174
202	imds-software-002	373632	352627	202	828	336	2048 ± 0	133	469 ± 1	295	954 ± 2	336	1094 ± 5	285	1064 ± 4	256	1153 ± 4	407	11100 ± 155	406	11090 ± 145
203	imperial-000	370120	10623	189	796	227	2048 ± 0	224	669 ± 1	190	675 ± 3	171	683 ± 17	146	676 ± 2	120	689 ± 2	250	2130 ± 32	248	2052 ± 100
204	imperial-002	472327	16134	382	1826	191	2048 ± 0	174	569 ± 1	153	581 ± 15	131	575 ± 5	108	576 ± 2	90	588 ± 3	264	2278 ± 90	253	2131 ± 44
205	incode-010	627808	21014	431	2628	194	2048 ± 0	405	1180 ± 2	371	1178 ± 1	361	1182 ± 1	324	1184 ± 1	277	1221 ± 1	160	1164 ± 32	166	1144 ± 32
206	incode-011	477280	21781	363	1708	110	2048 ± 0	304	872 ± 0	261	875 ± 0	237	881 ± 1	220	892 ± 1	186	939 ± 0	161	1117 ± 31	162	1109 ± 37
207	infocert-001	1204340	38972	339	1483	327	2048 ± 0	308	874 ± 1	269	891 ± 1	316	1050 ± 5	428	1473 ± 2	436	3174 ± 8	359	5055 ± 108	356	5008 ± 100
208	innefublas-000	370588	162172	86	439	128	2048 ± 0	363	1006 ± 3	328	1025 ± 3	308	1030 ± 4	279	1041 ± 2	250	1135 ± 3	373	5782 ± 41	373	5741 ± 45
209	innovativetechnologyltd-001	177232	335757	63	341	132	2048 ± 0	116	433 ± 7	98	446 ± 8	77	439 ± 4	65	452 ± 4	59	485 ± 7	232	1877 ± 42	237	1924 ± 97
210	innovativetechnologyltd-002	173939	372324	226	912	276	2048 ± 0	218	661 ± 2	214	726 ± 4	282	981 ± 27	259	997 ± 40	147	766 ± 3	220	1841 ± 50	230	1857 ± 59
211	innovatrics-008	307323	59842	331	1424	60	538 ± 0	265	778 ± 6	222	767 ± 3	201	770 ± 3	187	803 ± 3	166	853 ± 10	303	3021 ± 66	282	2673 ± 88
212	innovatrics-009	624485	105187	389	1917	474	4136 ± 0	391	1116 ± 1	355	1107 ± 5	339	1104 ± 5	299	1110 ± 5	253	1146 ± 6	358	5051 ± 54	347	4733 ± 102
213	insightface-003	1016917	26668	342	1515	182	2048 ± 0	381	1073 ± 0	348	1092 ± 2	328	1070 ± 1	293	1082 ± 1	238	1101 ± 1	65	597 ± 16	65	595 ± 17
214	insightface-004	928816	26668	356	1641	155	2048 ± 0	442	1298 ± 1	427	1356 ± 2	403	1313 ± 1	370	1311 ± 0	316	1349 ± 1	58	565 ± 7	58	559 ± 5
215	inspur-000	364844	91926	193	808	433	4096 ± 0	458	1367 ± 1	421	1331 ± 2	418	1368 ± 2	427	1465 ± 1	406	1861 ± 3	402	9831 ± 37	400	9860 ± 40
216	inspur-001	364862	91934	203	832	187	2048 ± 0	464	1385 ± 1	429	1361 ± 4	434	1401 ± 2	435	1495 ± 1	407	1891 ± 1	369	5641 ± 42	369	5622 ± 40
217	intelliecloudai-001	220831	868246	145	655	272	2048 ± 0	132	468 ± 2	103	456 ± 1	86	466 ± 3	84	492 ± 1	102	632 ± 2	149	1056 ± 4	154	1051 ± 72
218	intelliecloudai-002	259047	58559	458	3584	465	4100 ± 0	296	847 ± 1	247	847 ± 2	223	849 ± 1	204	853 ± 1	175	878 ± 4	121	822 ± 28	120	818 ± 23
219	intellifusion-001	271872	289387	176	762	118	2048 ± 0	259	764 ± 38	224	774 ± 39	208	797 ± 42	186	803 ± 34	155	805 ± 33	160	1112 ± 28	163	1128 ± 41
220	intellifusion-002	762731	385841	232	941	443	4096 ± 0	335	950 ± 2	353	1096 ± 42	331	1088 ± 33	318	1168 ± 31	264	1171 ± 10	209	1713 ± 57	205	1665 ± 87

Notes

- 1 The configuration size does not capture static data included in libraries.
- 2 The library size is the combined total of all files provided in the submission lib folder. These libraries e.g. OpenCV may or may not be installed on any end user's platform natively and would not need to be installed with the algorithm. Some developers put neural network models in their libraries.
- 3 The memory usage is the peak resident set size reported by the ps system call during template generation.
- 4 The median template creation times are measured on Intel®Xeon®CPU E5-2630 v4 @ 2.20GHz processors.
- 5 The comparison durations, in nanoseconds, are estimated using std::chrono::high_resolution_clock which on the machine in (2) counts 1ns clock ticks. Precision is somewhat worse than that however. The ± value is the median absolute deviation times 1.48 for Normal consistency.

Table 13: Summary of algorithms and properties included in this report. The red superscripts give ranking for the quantity in that column.

	ALGORITHM	CONFIG	LIBRARY	TEMPLATE								COMPARISON ⁴									
				NAME	DATA	DATA	MEMORY	SIZE	GENERATION TIME (ms) ⁴				TIME (ns) ⁵								
									(KB) ¹	(KB) ²	(MB) ³	(B)	MUGSHOT	480x720	960x1440	1600x2400	3000x4500	GENUINE	IMPOSTOR		
221	intellivision-004	117727	131310	109	515	375	2056 ± 0	76	330 ± 0	61	330 ± 0	46	347 ± 0	48	382 ± 0	68	514 ± 0	408	11197 ± 63	407	11165 ± 72
222	intellivision-005	372608	257259	153	686	381	2056 ± 0	198	618 ± 0	170	623 ± 0	154	634 ± 0	139	659 ± 0	148	771 ± 0	438	19244 ± 68	436	19270 ± 77
223	intellivix-002	361566	116162	287	1172	121	2048 ± 0	339	956 ± 0	294	947 ± 6	279	976 ± 0	253	984 ± 4	234	1089 ± 1	454	30096 ± 128	455	31287 ± 140
224	intellivix-003	234409	116167	313	1299	154	2048 ± 0	318	908 ± 0	279	916 ± 1	259	930 ± 0	244	961 ± 1	249	1129 ± 3	454	30025 ± 137	454	31190 ± 131
225	intelresearch-005	398137	85290	285	1158	320	2048 ± 0	451	1328 ± 1	424	1334 ± 2	413	1344 ± 2	386	1356 ± 2	336	1423 ± 4	348	4524 ± 87	344	4461 ± 74
226	intelresearch-006	445223	101126	252	1028	252	2048 ± 0	325	918 ± 1	265	881 ± 0	239	892 ± 0	226	913 ± 1	207	1008 ± 3	379	6137 ± 410	377	6024 ± 109
227	intema-000	1532392	19488	268	1097	49	513 ± 0	365	1010 ± 0	320	1001 ± 4	294	994 ± 0	256	993 ± 5	221	1056 ± 1	131	910 ± 29	132	906 ± 32
228	intema-001	1122562	19536	336	1460	51	513 ± 0	406	1354 ± 1	416	1318 ± 5	411	1336 ± 4	377	1328 ± 2	323	1375 ± 0	130	977 ± 31	136	980 ± 31
229	intsysmsu-001	384409	172480	186	789	237	2048 ± 0	194	614 ± 2	167	615 ± 2	161	642 ± 2	173	750 ± 3	261	1159 ± 4	80	621 ± 8	80	611 ± 31
230	intsysmsu-002	765921	172298	185	786	82	1024 ± 0	187	593 ± 1	231	793 ± 2	215	827 ± 1	210	875 ± 104	296	1293 ± 3	53	549 ± 25	56	548 ± 29
231	ionetworks-000	287609	51236	67	351	281	2048 ± 0	115	430 ± 0	96	435 ± 0	73	433 ± 0	63	432 ± 0	51	444 ± 0	386	6913 ± 102	387	7150 ± 160
232	iqface-000	268819	596337	160	704	480	4750 ± 32	161	538 ± 26	119	494 ± 2	123	543 ± 3	170	734 ± 4	330	1393 ± 4	500	636433 ± 38446	500	632654 ± 85615
233	iqface-003	370803	963398	197	817	481	4763 ± 37	156	529 ± 1	134	532 ± 2	140	599 ± 8	203	850 ± 2	392	1694 ± 2	499	575924 ± 2601	499	576653 ± 2051
234	irex-000	741899	47419	404	2086	414	3080 ± 0	298	852 ± 2	249	850 ± 1	232	874 ± 2	236	939 ± 1	280	1249 ± 5	18	201 ± 11	18	208 ± 8
235	isap-001	99049	204201	1	18	439	4096 ± 0	1	0 ± 0	-	-	-	-	-	-	44	459 ± 17	46	456 ± 11		
236	isap-002	256765	49931	55	288	138	2048 ± 0	262	769 ± 3	329	1027 ± 2	235	877 ± 2	179	761 ± 1	182	912 ± 2	306	3045 ± 94	300	2973 ± 66
237	isityou-000	48010	36621	17	110	497	19200 ± 0	18	113 ± 5	-	-	-	-	-	-	495	237517 ± 1318	495	237374 ± 1279		
238	isystems-001	274621	639268	267	1091	310	2048 ± 0	62	291 ± 9	-	-	-	-	-	-	53	557 ± 16	60	564 ± 22		
239	isystems-002	358984	803389	351	1595	283	2048 ± 0	287	822 ± 8	-	-	-	-	-	-	111	749 ± 31	87	632 ± 28		
240	itmo-007	415979	245376	413	2199	180	2048 ± 0	254	741 ± 2	-	-	-	-	-	-	276	2551 ± 50	276	2529 ± 80		
241	itmo-008	726866	318238	324	1377	436	4096 ± 0	380	1060 ± 1	339	1058 ± 1	320	1059 ± 1	290	1072 ± 4	240	1104 ± 1	327	3578 ± 25	328	3580 ± 28
242	ivacognitive-001	256958	62791	236	947	277	2048 ± 0	441	1292 ± 3	408	1289 ± 4	393	1292 ± 4	363	1292 ± 3	306	1321 ± 4	343	4228 ± 41	341	4226 ± 41
243	iws-000	30875	3063	10	77	33	512 ± 0	53	277 ± 5	48	283 ± 1	101	494 ± 3	252	984 ± 3	432	2987 ± 39	140	999 ± 40	139	992 ± 22
244	jaakit-001	99024	24754	47	251	45	512 ± 0	10	76 ± 0	87	77 ± 0	89	79 ± 0	781	80 ± 0	93	90 ± 0	271	2466 ± 57	272	2465 ± 66
245	kakao-007	526993	129545	469	3953	334	2048 ± 0	338	952 ± 1	299	961 ± 1	269	958 ± 1	245	962 ± 1	197	968 ± 1	148	1056 ± 16	152	1047 ± 28
246	kakao-008	734583	104820	463	3876	151	2048 ± 0	394	1135 ± 3	366	1148 ± 3	352	1150 ± 3	314	1156 ± 1	267	1175 ± 1	110	736 ± 23	107	727 ± 22
247	kakaobank-000	570796	98479	429	2566	422	4096 ± 0	421	1234 ± 1	394	1254 ± 7	379	1248 ± 3	397	1389 ± 3	404	1843 ± 11	352	4790 ± 35	350	4803 ± 35
248	kakaopay-001	397864	179869	152	684	453	4096 ± 0	119	448 ± 0	140	542 ± 0	120	542 ± 0	98	542 ± 0	80	553 ± 0	88	633 ± 22	86	630 ± 22
249	kasikornlabs-000	256471	61000	156	693	224	2048 ± 0	317	908 ± 36	263	878 ± 22	275	969 ± 39	325	1184 ± 54	417	2382 ± 145	456	31669 ± 188	456	31714 ± 182
250	kasikornlabs-002	256431	61063	175	757	306	2048 ± 0	323	917 ± 35	276	907 ± 13	272	963 ± 13	374	1320 ± 45	423	2629 ± 178	455	31025 ± 180	453	31054 ± 186
251	kedacom-000	245292	37401	499	23574	13	292 ± 0	150	506 ± 3	144	547 ± 10	147	614 ± 9	112	588 ± 10	113	665 ± 24	96	684 ± 14	99	682 ± 16
252	kiwitech-000	369711	21375	194	808	145	2048 ± 0	186	591 ± 0	159	594 ± 0	139	595 ± 1	117	596 ± 0	96	609 ± 0	214	1755 ± 20	212	1734 ± 16
253	kneron-003	58366	1747	40	188	219	2048 ± 0	57	281 ± 3	47	280 ± 1	42	315 ± 13	46	365 ± 7	278	1224 ± 30	362	5237 ± 63	360	5274 ± 99
254	kneron-005	375374	13633	90	457	165	2048 ± 0	154	518 ± 2	132	522 ± 4	127	556 ± 5	177	757 ± 19	399	1760 ± 25	237	1922 ± 11	238	1926 ± 20
255	knowutech-000	808045	32886	314	1303	101	1536 ± 0	478	1419 ± 2	431	1372 ± 1	424	1377 ± 1	394	1382 ± 2	327	1386 ± 2	332	3743 ± 31	331	3693 ± 38
256	kookmin-002	371771	30734	201	827	221	2048 ± 0	374	1038 ± 2	338	1047 ± 1	313	1045 ± 1	283	1061 ± 1	243	1116 ± 1	91	638 ± 19	91	636 ± 20
257	koreaid-001	256261	20152	380	1811	169	2048 ± 0	96	384 ± 2	78	390 ± 1	80	444 ± 2	102	556 ± 6	151	795 ± 5	90	636 ± 11	90	636 ± 10
258	krungthai-002	2360957	15033	286	1171	212	2048 ± 0	71	308 ± 0	57	314 ± 5	39	309 ± 0	38	319 ± 0	36	362 ± 0	302	3014 ± 20	301	2980 ± 22
259	kuke3d-001	403462	68786	115	530	462	4096 ± 0	278	814 ± 2	235	811 ± 2	210	814 ± 2	190	814 ± 1	164	834 ± 1	382	6412 ± 57	381	6413 ± 51
260	kuke3d-002	270544	1227855	195	809	159	2048 ± 0	149	504 ± 3	127	504 ± 1	109	511 ± 1	93	523 ± 2	89	585 ± 1	296	2943 ± 22	298	2966 ± 38
261	lebentech-000	0	10360	18	110	28	512 ± 0	3	22 ± 0	122	22 ± 0	122	22 ± 0	123	23 ± 0	123	23 ± 0	119	801 ± 42	121	825 ± 51
262	lemalabs-001	748400	198794	438	2738	256	2048 ± 0	276	810 ± 0	236	812 ± 0	209	813 ± 0	192	819 ± 0	165	844 ± 1	413	11930 ± 35	412	11913 ± 37
263	lineclova-002	475779	406756	320	1353	274	2048 ± 0	438	1284 ± 1	403	1275 ± 2	388	1275 ± 1	356	1273 ± 2	291	1281 ± 2	284	2765 ± 10	284	2767 ± 31
264	lineclova-003	585149	410482	367	1726	239	2048 ± 0	481	1444 ± 1	454	1438 ± 1	444	1439 ± 2	419	1440 ± 1	348	1446 ± 2	292	2890 ± 23	294	2899 ± 29

Notes

- The configuration size does not capture static data included in libraries.
- The library size is the combined total of all files provided in the submission lib folder. These libraries e.g. OpenCV may or may not be installed on any end user's platform natively and would not need to be installed with the algorithm. Some developers put neural network models in their libraries.
- The memory usage is the peak resident set size reported by the ps system call during template generation.
- The median template creation times are measured on Intel®Xeon®CPU E5-2630 v4 @ 2.20GHz processors.
- The comparison durations, in nanoseconds, are estimated using std::chrono::high_resolution_clock which on the machine in (2) counts 1ns clock ticks. Precision is somewhat worse than that however. The ± value is the median absolute deviation times 1.48 for Normal consistency.

Table 14: Summary of algorithms and properties included in this report. The red superscripts give ranking for the quantity in that column.

	ALGORITHM	CONFIG	LIBRARY	TEMPLATE								COMPARISON ⁴								
				NAME	DATA	DATA	MEMORY	SIZE	GENERATION TIME (ms) ⁴				TIME (ns) ⁵							
									(KB) ¹	(KB) ²	(MB) ³	(B)	MUGSHOT	480x720	960x1440	1600x2400	3000x4500	GENUINE	IMPOSTOR	
265	lookman-002	138200	25410	497	16518	64	548 ± 0	27	173 ± 1	-	-	-	-	75	610 ± 19	81	612 ± 22			
266	lookman-004	244775	37401	498	23548	63	548 ± 0	151	507 ± 5	142	545 ± 12	146	613 ± 12	115	590 ± 11	110	656 ± 16	126	871 ± 29	
267	luxand-000	0	57908	322	1366	93	1040 ± 0	107	407 ± 23	94	433 ± 11	79	444 ± 14	71	464 ± 14	85	562 ± 25	122	828 ± 28	
268	mantra-000	471458	62566	173	749	353	2052 ± 0	109	413 ± 18	117	487 ± 19	102	494 ± 18	89	511 ± 18	93	598 ± 19	310	3151 ± 51	
269	maxvision-002	171894	60623	386	1863	113	2048 ± 0	20	172 ± 0	20	171 ± 0	17	172 ± 0	14	174 ± 0	15	221 ± 0	107	725 ± 5	
270	maxvision-003	234062	61252	415	2292	157	2048 ± 0	135	474 ± 0	109	468 ± 0	92	471 ± 0	76	475 ± 0	71	519 ± 0	273	2467 ± 28	
271	megvii-005	1378009	44038	471	4036	351	2049 ± 0	448	1319 ± 5	393	1247 ± 6	375	1240 ± 2	345	1245 ± 2	298	1298 ± 3	459	32025 ± 121	
272	megvii-006	1554938	44038	475	4354	349	2049 ± 0	439	1287 ± 3	406	1286 ± 0	429	1393 ± 5	372	1319 ± 1	319	1360 ± 1	458	31845 ± 100	
273	meituau-002	686114	244091	411	2191	435	4096 ± 0	376	1052 ± 0	345	1086 ± 1	326	1064 ± 2	282	1060 ± 5	228	1063 ± 1	150	1064 ± 10	
274	meituau-003	860010	244091	441	2763	422	4096 ± 0	498	1487 ± 1	468	1518 ± 0	455	1469 ± 6	432	1478 ± 0	354	1471 ± 7	159	1112 ± 16	
275	meiya-001	280055	264913	105	507	350	2049 ± 0	201	622 ± 12	-	-	-	-	-	-	394	8356 ± 615	393	8134 ± 97	
276	mendaxiatech-000	1941475	45484	455	3195	464	4097 ± 0	425	1243 ± 2	395	1255 ± 1	421	1373 ± 2	443	1598 ± 3	425	2689 ± 8	469	46906 ± 275	
277	metsakuurcompany-002	0	957558	243	983	384	2056 ± 0	354	980 ± 1	306	978 ± 1	278	976 ± 2	267	1005 ± 1	239	1103 ± 2	396	8766 ± 326	
278	metsakuurcompany-003	0	957562	239	969	394	2056 ± 0	342	965 ± 2	303	970 ± 5	321	1060 ± 12	266	1005 ± 6	246	1121 ± 1	393	8234 ± 145	
279	miaxis-001	0	215019	59	322	26	512 ± 0	55	279 ± 0	46	278 ± 0	34	278 ± 1	32	285 ± 0	27	297 ± 0	127	872 ± 14	
280	miaxis-002	0	216484	60	324	20	512 ± 0	63	292 ± 0	50	290 ± 1	37	297 ± 0	35	298 ± 0	34	359 ± 1	152	1065 ± 48	
281	microfocus-002	96288	27362	37	176	5	256 ± 0	49	259 ± 18	-	-	-	-	-	-	31	337 ± 34	20	230 ± 25	
282	microfocus-003	169603	27689	104	507	4	256 ± 0	145	490 ± 19	131	517 ± 30	197	752 ± 55	303	1126 ± 121	426	2713 ± 345	3	117 ± 5	
283	minivision-000	836697	16597	470	4013	445	4096 ± 0	373	1035 ± 1	334	1033 ± 2	309	1035 ± 1	277	1037 ± 1	224	1059 ± 2	272	2466 ± 26	
284	mitek-000	105584	44643	53	277	75	1024 ± 0	48	256 ± 21	38	265 ± 10	54	375 ± 24	99	545 ± 42	237	1098 ± 124	287	2846 ± 88	
285	mobai-000	365451	80573	184	786	486	6144 ± 0	260	766 ± 8	256	869 ± 6	370	1205 ± 31	452	1867 ± 45	441	3549 ± 190	430	16458 ± 333	
286	mobai-001	265297	60164	116	534	291	2048 ± 0	192	612 ± 3	166	614 ± 3	174	687 ± 9	216	886 ± 31	393	1707 ± 103	178	1386 ± 25	
287	mobbl-001	231160	58706	43	223	123	2048 ± 0	31	183 ± 32	25	184 ± 25	50	354 ± 76	194	823 ± 396	429	2781 ± 1166	411	11832 ± 109	
288	mobbl-003	172248	60960	52	270	250	2048 ± 0	223	664 ± 6	183	661 ± 5	164	663 ± 5	142	665 ± 6	121	691 ± 5	416	12506 ± 111	
289	mobipintech-000	370514	303291	276	1130	141	2048 ± 0	426	1245 ± 1	388	1234 ± 1	384	1264 ± 1	388	1360 ± 1	394	1707 ± 1	422	14506 ± 214	
290	moredian-000	525259	21374	231	932	344	2048 ± 0	242	694 ± 0	202	698 ± 0	181	699 ± 0	157	700 ± 0	130	713 ± 1	221	1803 ± 11	
291	mukh-002	693809	454936	271	1109	307	2048 ± 0	344	968 ± 1	281	921 ± 12	268	957 ± 2	240	954 ± 6	194	953 ± 5	77	612 ± 13	
292	mukh-003	556405	180996	385	1850	328	2048 ± 0	501	1896 ± 3	470	1948 ± 1	469	2003 ± 0	454	1981 ± 0	409	2016 ± 0	66	597 ± 13	
293	multimodality-000	0	503924	330	1417	189	2048 ± 0	110	416 ± 0	91	420 ± 0	70	423 ± 0	62	427 ± 0	53	463 ± 0	124	848 ± 25	
294	multimodality-001	185719	545045	326	1388	420	4096 ± 0	410	1190 ± 2	369	1169 ± 2	355	1165 ± 2	317	1167 ± 2	269	1177 ± 2	185	1424 ± 35	
295	mvision-001	227502	149531	164	723	21	512 ± 0	240	691 ± 21	205	702 ± 19	179	697 ± 24	159	708 ± 29	129	710 ± 27	162	1123 ± 40	
296	nazhai-000	547484	16141	436	2716	317	2048 ± 0	231	683 ± 3	196	687 ± 2	218	835 ± 27	201	840 ± 31	163	834 ± 34	261	2230 ± 34	
297	ncsg-001	148743	490151	171	737	269	2048 ± 0	330	936 ± 2	293	946 ± 3	263	944 ± 2	235	938 ± 5	199	972 ± 2	328	3579 ± 50	
298	neosystems-004	243546	352623	114	529	131	2048 ± 0	75	324 ± 0	209	711 ± 3	216	827 ± 7	205	854 ± 2	183	916 ± 2	420	14437 ± 176	
299	netbridgetech-001	133108	205875	106	508	457	4096 ± 0	12	85 ± 1	10	83 ± 0	984	± 0	9	92 ± 0	9	113 ± 4	398	9280 ± 74	
300	netbridgetech-002	257687	49931	56	299	243	2048 ± 0	292	838 ± 6	245	838 ± 2	220	839 ± 1	200	839 ± 3	167	859 ± 3	293	2893 ± 65	
301	neurotechnology-015	474782	86045	427	2564	53	515 ± 0	370	1028 ± 3	333	1033 ± 3	317	1055 ± 4	294	1097 ± 4	300	1304 ± 18	4	130 ± 2	
302	neurotechnology-016	661450	89972	472	4066	52	515 ± 0	453	1339 ± 3	425	1351 ± 2	419	1369 ± 4	398	1390 ± 4	367	1508 ± 21	9	179 ± 20	
303	nhn-002	363471	817674	147	667	431	4096 ± 0	397	1141 ± 3	361	1138 ± 2	348	1141 ± 2	313	1151 ± 6	273	1203 ± 2	478	56608 ± 579	
304	nhn-003	933665	432730	337	1464	428	4096 ± 0	420	1229 ± 2	396	1261 ± 1	383	1263 ± 3	360	1279 ± 2	324	1375 ± 3	473	50560 ± 105	
305	nodeflux-002	774668	690213	94	466	230	2048 ± 0	249	708 ± 4	208	709 ± 4	187	716 ± 5	165	716 ± 7	137	736 ± 3	321	3475 ± 62	
306	nominder-000	547519	102693	366	1720	6	258 ± 0	245	701 ± 0	203	701 ± 2	189	721 ± 2	166	720 ± 3	152	796 ± 1	27	314 ± 5	
307	notiontag-001	92753	427967	124	566	67	584 ± 0	329	929 ± 35	349	1092 ± 39	470	3709 ± 81	470	10233 ± 180	-	467	43636 ± 286	466	43724 ± 330
308	notiontag-002	271987	967207	445	2840	407	2120 ± 0	122	453 ± 2	101	453 ± 3	82	453 ± 3	66	458 ± 2	55	471 ± 3	440	20278 ± 194	

Notes

- 1 The configuration size does not capture static data included in libraries.
- 2 The library size is the combined total of all files provided in the submission lib folder. These libraries e.g. OpenCV may or may not be installed on any end user's platform natively and would not need to be installed with the algorithm. Some developers put neural network models in their libraries.
- 3 The memory usage is the peak resident set size reported by the ps system call during template generation.
- 4 The median template creation times are measured on Intel®Xeon®CPU E5-2630 v4 @ 2.20GHz processors.
- 5 The comparison durations, in nanoseconds, are estimated using std::chrono::high_resolution_clock which on the machine in (2) counts 1ns clock ticks. Precision is somewhat worse than that however. The ± value is the median absolute deviation times 1.48 for Normal consistency.

Table 15: Summary of algorithms and properties included in this report. The red superscripts give ranking for the quantity in that column.

	ALGORITHM	CONFIG	LIBRARY	TEMPLATE							COMPARISON ⁴										
				NAME	DATA	DATA	MEMORY	SIZE	GENERATION TIME (ms) ⁴			TIME (ns) ⁵									
									(KB) ¹	(KB) ²	(MB) ³	(B)	MUGSHOT	480x720	960x1440	1600x2400	3000x4500	GENUINE	IMPOSTOR		
309	nsensecorp-004	513276	139178	358	1663	235	2048 ± 0	480	1433 ± 0	455	1445 ± 7	451	1450 ± 3	434	1487 ± 5	-	269	2388 ± 42	269	2385 ± 63	
310	nsensecorp-005	411845	138437	295	1237	260	2048 ± 0	486	1455 ± 0	459	1453 ± 0	450	1449 ± 0	423	1457 ± 2	362	1490 ± 4	251	2131 ± 51	256	2165 ± 66
311	ntechlab-011	786933	209458	489	6867	97	1280 ± 0	399	1148 ± 2	362	1142 ± 1	353	1159 ± 1	326	1185 ± 1	295	1290 ± 3	8	179 ± 11	10	173 ± 11
312	ntechlab-012	570796	212350	483	5451	409	2560 ± 0	447	1309 ± 1	420	1323 ± 1	407	1331 ± 1	389	1360 ± 1	350	1460 ± 3	17	211 ± 8	18	211 ± 7
313	omface-000	45945	844976	30	150	74	1024 ± 0	33	185 ± 1	28	206 ± 2	23	203 ± 1	17	195 ± 1	14	193 ± 1	47	481 ± 42	45	456 ± 20
314	omface-001	146370	1799745	27	145	77	1024 ± 0	35	194 ± 2	31	222 ± 2	29	209 ± 0	20	216 ± 1	18	233 ± 1	433	18369 ± 19	432	18366 ± 32
315	omnigarde-001	200523	32882	93	464	27	512 ± 0	331	941 ± 0	267	883 ± 1	238	886 ± 1	219	891 ± 1	178	898 ± 0	183	1405 ± 31	180	1379 ± 26
316	omnigarde-002	368860	32882	174	757	76	1024 ± 0	444	1303 ± 1	392	1246 ± 1	380	1249 ± 1	347	1253 ± 1	285	1261 ± 1	283	2727 ± 34	283	2686 ± 32
317	onfido-000	273478	959781	225	908	188	2048 ± 0	124	459 ± 17	100	451 ± 15	81	451 ± 14	69	462 ± 15	63	505 ± 18	200	1617 ± 50	201	1637 ± 53
318	openface-001	0	40111	16	100	340	2048 ± 0	23	148 ± 1	17	154 ± 0	52	365 ± 3	59	409 ± 9	98	616 ± 31	73	608 ± 14	77	604 ± 13
319	oz-003	484147	519652	496	11949	372	2053 ± 0	459	1375 ± 12	434	1388 ± 3	468	1773 ± 16	455	2039 ± 6	437	3209 ± 5	491	73905 ± 456	491	73892 ± 444
320	oz-004	373982	1075452	493	8071	373	2053 ± 0	290	832 ± 7	257	871 ± 6	241	899 ± 10	292	1078 ± 12	385	1608 ± 10	482	61654 ± 418	481	61749 ± 450
321	palit-000	428754	144958	321	1355	455	4096 ± 0	176	570 ± 1	151	578 ± 1	132	576 ± 3	110	583 ± 1	97	614 ± 1	260	2227 ± 16	262	2226 ± 16
322	palit-001	173886	145564	127	583	318	2048 ± 0	42	227 ± 0	33	224 ± 1	27	224 ± 1	20	229 ± 3	23	262 ± 2	163	1150 ± 16	164	1135 ± 23
323	pangiam-000	464252	24512	468	3919	172	2048 ± 0	203	627 ± 5	169	618 ± 4	148	615 ± 3	126	620 ± 3	108	639 ± 3	2	118 ± 7	2	113 ± 7
324	pangiam-001	1015455	37259	347	1554	119	2048 ± 0	348	972 ± 1	309	982 ± 3	284	981 ± 2	256	990 ± 7	218	1052 ± 2	6	136 ± 11	5	139 ± 13
325	papago-001	669274	52817	416	2341	161	2048 ± 0	434	1272 ± 6	410	1296 ± 7	397	1295 ± 6	361	1281 ± 3	426	15236 ± 169	425	15184 ± 142		
326	papsav1923-002	491185	24727	280	1136	364	2052 ± 0	270	792 ± 1	307	978 ± 1	311	1042 ± 1	315	1158 ± 1	389	1641 ± 19	167	1209 ± 29	169	1206 ± 38
327	papsav1923-003	515576	24803	274	1112	218	2048 ± 0	271	797 ± 0	312	987 ± 1	312	1043 ± 1	322	1178 ± 1	403	1809 ± 7	128	903 ± 26	131	905 ± 34
328	paravision-010	688291	205854	407	2150	470	4100 ± 0	207	634 ± 0	178	635 ± 0	155	635 ± 0	128	635 ± 0	105	635 ± 1	196	1577 ± 35	197	1571 ± 32
329	paravision-011	781138	95589	418	2420	469	4100 ± 0	297	852 ± 0	258	871 ± 1	225	858 ± 1	206	854 ± 0	172	873 ± 1	199	1608 ± 35	199	1625 ± 32
330	pensees-001	1619431	408932	390	1922	493	8200 ± 0	388	1108 ± 3	456	1448 ± 17	445	1439 ± 10	426	1464 ± 5	377	1546 ± 9	311	3151 ± 34	310	3143 ± 25
331	pixelall-008	0	992249	373	1741	491	8192 ± 0	491	1471 ± 3	444	1405 ± 4	438	1409 ± 4	410	1413 ± 3	340	1426 ± 4	220	1799 ± 50	223	1807 ± 48
332	pixelall-009	0	1009114	369	1731	492	8192 ± 0	497	1484 ± 3	439	1395 ± 3	433	1400 ± 4	399	1391 ± 3	342	1433 ± 3	228	1848 ± 13	227	1842 ± 19
333	privid-001	0	76008	26	143	499	30720 ± 0	120	450 ± 0	102	454 ± 0	88	467 ± 1	75	472 ± 1	62	504 ± 1	431	17041 ± 74	430	17053 ± 100
334	psl-010	411027	591157	482	5361	475	4168 ± 0	474	1403 ± 9	438	1393 ± 3	428	1392 ± 3	401	1395 ± 3	331	1396 ± 3	33	354 ± 53	32	329 ± 29
335	psl-011	814579	606050	478	4984	494	8248 ± 0	450	1324 ± 2	419	1323 ± 8	406	1326 ± 8	375	1324 ± 8	307	1322 ± 4	207	1680 ± 37	208	1688 ± 40
336	ptakuratsatu-000	0	585434	319	1347	59	538 ± 0	309	875 ± 3	254	863 ± 48	258	928 ± 9	243	958 ± 17	230	1066 ± 26	376	5900 ± 103	371	5687 ± 167
337	pxl-001	110116	78231	33	168	16	512 ± 0	15	101 ± 5	12	104 ± 5	20	189 ± 12	58	408 ± 27	353	1470 ± 144	368	5598 ± 45	367	5590 ± 68
338	pyramid-000	372608	219883	190	804	388	2056 ± 0	179	583 ± 2	-	-	-	-	-	-	388	7147 ± 59	389	7586 ± 425		
339	qazbs-000	362015	805258	210	856	158	2048 ± 0	446	1307 ± 1	391	1243 ± 0	378	1248 ± 9	348	1253 ± 1	289	1270 ± 0	360	5181 ± 62	358	5167 ± 93
340	qluevision-001	173605	205230	73	376	490	8192 ± 0	43	229 ± 1	34	230 ± 1	30	231 ± 1	27	233 ± 1	20	239 ± 1	316	3374 ± 38	310	3365 ± 41
341	qnap-002	346963	33284	158	700	171	2048 ± 0	283	821 ± 1	238	824 ± 1	214	824 ± 1	197	826 ± 1	162	832 ± 1	22	293 ± 13	26	287 ± 17
342	qnap-003	245476	61427	179	770	206	2048 ± 0	98	387 ± 0	79	393 ± 0	60	393 ± 0	52	393 ± 1	43	400 ± 2	95	683 ± 20	94	651 ± 17
343	quantasoft-003	370518	211354	258	1058	315	2048 ± 0	206	632 ± 2	177	634 ± 0	151	632 ± 0	128	631 ± 1	103	634 ± 0	14	201 ± 7	14	203 ± 8
344	rankone-013	0	228729	29	149	8	261 ± 0	239	690 ± 5	187	672 ± 1	184	712 ± 1	182	780 ± 1	244	1118 ± 3	35	356 ± 23	28	304 ± 23
345	rankone-014	0	243130	31	163	7	261 ± 0	240	701 ± 1	207	705 ± 0	191	732 ± 1	184	800 ± 1	242	1113 ± 1	26	306 ± 16	22	251 ± 13
346	realnetworks-007	570797	101527	453	3137	390	2056 ± 0	454	1348 ± 2	428	1358 ± 11	417	1363 ± 10	395	1386 ± 9	371	1517 ± 6	56	559 ± 31	54	539 ± 35
347	realnetworks-008	73346	75421	71	369	387	2056 ± 0	66	296 ± 3	53	294 ± 3	49	353 ± 4	43	361 ± 5	58	485 ± 5	52	539 ± 31	55	543 ± 29
348	regula-000	262444	29384	138	610	222	2048 ± 0	409	1187 ± 1	358	1126 ± 1	342	1129 ± 0	306	1132 ± 1	260	1159 ± 1	50	491 ± 16	51	500 ± 22
349	regula-001	256075	25980	240	976	114	2048 ± 0	437	1284 ± 1	386	1220 ± 1	371	1222 ± 1	341	1226 ± 1	283	1255 ± 1	36	361 ± 10	35	342 ± 25
350	remarkai-001	241857	868314	166	730	355	2052 ± 0	289	831 ± 6	248	849 ± 18	318	1055 ± 25	331	1198 ± 34	372	1519 ± 38	169	1229 ± 20	119	805 ± 56
351	remarkai-003	280516	58559	465	3896	468	4100 ± 0	357	986 ± 1	317	993 ± 1	292	992 ± 1	262	999 ± 3	208	1019 ± 2	118	787 ± 20	116	793 ± 22
352	rendip-000	0	437653	151	682	247	2048 ± 0	127	464 ± 2	104	458 ± 0	93	473 ± 0	78	483 ± 1	83	556 ± 4	60	576 ± 13	62	573 ± 11

Notes

- 1 The configuration size does not capture static data included in libraries.
- 2 The library size is the combined total of all files provided in the submission lib folder. These libraries e.g. OpenCV may or may not be installed on any end user's platform natively and would not need to be installed with the algorithm. Some developers put neural network models in their libraries.
- 3 The memory usage is the peak resident set size reported by the ps system call during template generation.
- 4 The median template creation times are measured on Intel®Xeon®CPU E5-2630 v4 @ 2.20GHz processors.
- 5 The comparison durations, in nanoseconds, are estimated using std::chrono::high_resolution_clock which on the machine in (2) counts 1ns clock ticks. Precision is somewhat worse than that however. The ± value is the median absolute deviation times 1.48 for Normal consistency.

	ALGORITHM	CONFIG	LIBRARY	TEMPLATE								COMPARISON ⁴									
				NAME	DATA		MEMORY	SIZE	GENERATION TIME (ms) ⁴				TIME (ns) ⁵								
					(KB) ¹	(KB) ²	(MB) ³	(B)	MUGSHOT	480x720	960x1440	1600x2400	3000x4500	GENUINE	IMPOSTOR						
353	revealmedia-005	293933	202465	178	763	466	4100 ± 0	114	428 ± 0	92	428 ± 0	72	430 ± 0	64	433 ± 0	50	442 ± 0	245	2023 ± 38	245	2009 ± 26
354	revealmedia-006	293933	200912	172	741	359	2052 ± 0	94	381 ± 0	73	381 ± 0	56	382 ± 0	49	384 ± 0	41	394 ± 0	84	626 ± 35	72	600 ± 2
355	rokid-000	258612	396624	294	1218	386	2056 ± 0	164	546 ± 3	139	542 ± 2	124	545 ± 1	92	522 ± 3	86	563 ± 4	320	3457 ± 62	323	3463 ± 77
356	rokid-001	641223	413733	261	1071	397	2060 ± 0	320	911 ± 2	273	901 ± 5	242	899 ± 2	223	900 ± 3	179	901 ± 3	313	3345 ± 50	314	3346 ± 149
357	s1-005	482369	95685	282	1137	318	2048 ± 0	361	1001 ± 0	322	1002 ± 0	300	1004 ± 0	268	1008 ± 0	210	1029 ± 2	85	626 ± 74	64	589 ± 14
358	s1-007	482385	59657	279	1135	241	2048 ± 0	358	988 ± 1	300	965 ± 0	273	966 ± 0	247	972 ± 0	203	991 ± 0	92	648 ± 26	96	658 ± 25
359	saffe-001	85973	62488	35	168	98	1280 ± 0	58	281 ± 1	-	-	-	-	-	-	170	1274 ± 19	173	1277 ± 26		
360	saffe-002	260622	28285	209	855	174	2048 ± 0	280	817 ± 11	234	805 ± 15	208	809 ± 19	191	815 ± 29	157	813 ± 23	105	717 ± 7	105	714 ± 29
361	samsungsds-001	1189592	147444	464	3893	456	4096 ± 0	396	1140 ± 3	364	1145 ± 4	414	1344 ± 5	391	1366 ± 5	369	1514 ± 7	474	51559 ± 773	473	51721 ± 1003
362	samsungsds-002	1040732	147475	421	2431	393	2056 ± 0	393	1118 ± 1	370	1175 ± 12	420	1372 ± 6	376	1324 ± 2	361	1489 ± 4	462	35803 ± 266	463	36181 ± 674
363	samtech-001	288082	219883	135	605	389	2056 ± 0	64	294 ± 3	-	-	-	-	-	-	392	7694 ± 59	391	7678 ± 91		
364	scanovate-002	256986	457227	208	850	329	2048 ± 0	243	696 ± 32	210	713 ± 33	193	738 ± 28	180	779 ± 32	265	1172 ± 53	304	3021 ± 38	308	3120 ± 163
365	scanovate-003	135585	89469	192	808	120	2048 ± 0	180	585 ± 1	164	613 ± 12	136	591 ± 1	121	610 ± 2	117	684 ± 1	295	2926 ± 22	295	2925 ± 20
366	sdc-000	256814	481583	183	786	200	2048 ± 0	321	913 ± 14	275	906 ± 9	349	1142 ± 19	448	1774 ± 45	445	4719 ± 222	460	32645 ± 93	461	32653 ± 112
367	securifai-005	252532	81777	111	525	166	2048 ± 0	460	1377 ± 2	426	1355 ± 1	416	1353 ± 0	387	1357 ± 0	318	1356 ± 0	231	1873 ± 25	229	1847 ± 35
368	securifai-006	452474	81856	181	773	432	4096 ± 0	382	1090 ± 2	346	1086 ± 3	334	1093 ± 1	298	1104 ± 10	235	1090 ± 2	317	3376 ± 42	317	3399 ± 40
369	sensetime-007	765353	37533	485	5699	89	1028 ± 0	466	1386 ± 41	418	1323 ± 2	415	1347 ± 2	390	1366 ± 2	384	1593 ± 8	187	1460 ± 29	186	1425 ± 26
370	sensetime-008	1176483	60067	487	5976	88	1028 ± 0	495	1479 ± 31	453	1436 ± 4	457	1482 ± 4	438	1525 ± 5	390	1669 ± 2	172	1283 ± 51	170	1240 ± 47
371	sertis-000	265572	68770	81	427	160	2048 ± 0	257	754 ± 0	221	759 ± 0	199	764 ± 0	178	760 ± 0	146	763 ± 0	192	1497 ± 29	198	1582 ± 38
372	sertis-002	460790	68929	327	1391	142	2048 ± 0	407	1181 ± 1	372	1178 ± 0	362	1183 ± 0	329	1187 ± 0	276	1221 ± 0	156	1086 ± 32	156	1076 ± 31
373	seventhsense-001	369850	3183365	196	811	363	2052 ± 0	429	1255 ± 2	409	1294 ± 15	389	1277 ± 3	357	1275 ± 2	293	1288 ± 3	239	1936 ± 26	241	1943 ± 34
374	seventhsense-002	452197	1567903	234	944	360	2052 ± 0	428	1252 ± 1	401	1271 ± 1	385	1269 ± 1	354	1272 ± 1	294	1290 ± 1	252	2131 ± 45	251	2123 ± 45
375	shaman-000	0	120033	103	507	438	4096 ± 0	215	653 ± 16	-	-	-	-	-	-	39	380 ± 25	39	379 ± 31		
376	shaman-001	0	174446	108	511	447	4096 ± 0	65	294 ± 2	-	-	-	-	-	-	89	635 ± 19	43	441 ± 25		
377	shu-002	731250	148309	220	890	425	4096 ± 0	256	751 ± 2	223	769 ± 4	254	922 ± 4	417	1431 ± 9	440	3489 ± 47	501	2930763 ± 47355	501	2929759 ± 39149
378	shu-003	428774	146940	107	511	153	2048 ± 0	282	820 ± 6	240	828 ± 3	261	941 ± 9	367	1308 ± 15	433	3045 ± 44	274	2506 ± 26	275	2512 ± 38
379	siat-002	486842	7738	422	2434	369	2052 ± 0	177	579 ± 0	-	-	-	-	-	-	115	769 ± 13	111	750 ± 13		
380	siat-005	380936	16935	312	1298	303	2048 ± 0	104	403 ± 0	84	400 ± 0	62	401 ± 0	56	403 ± 1	47	422 ± 7	61	577 ± 13	63	580 ± 17
381	sjtu-003	480795	148243	119	538	148	2048 ± 0	284	821 ± 2	237	820 ± 2	255	923 ± 3	333	1201 ± 3	416	2373 ± 9	195	1560 ± 20	194	1560 ± 14
382	sjtu-004	1953267	241108	437	2727	479	4608 ± 0	422	1236 ± 2	381	1209 ± 2	396	1294 ± 4	441	1554 ± 5	428	2738 ± 8	307	3057 ± 14	307	3070 ± 20
383	sktelecom-000	527132	298496	316	1311	102	1536 ± 0	390	1110 ± 1	357	1113 ± 1	340	1114 ± 1	300	1120 ± 1	258	1155 ± 1	450	26583 ± 128	448	26508 ± 126
384	smartbiometrik-001	30875	92620	7	71	41	512 ± 0	199	620 ± 7	171	625 ± 7	159	640 ± 4	168	728 ± 6	217	1047 ± 8	102	703 ± 31	103	710 ± 40
385	smartengines-000	1711	3025	4	50	11	288 ± 0	25	168 ± 7	22	180 ± 1	19	188 ± 3	22	217 ± 3	25	275 ± 1	11	197 ± 5	8	167 ± 11
386	smartengines-001	7095	4601	346	12	288	2048 ± 0	78	333 ± 89	87	408 ± 1	69	423 ± 1	67	460 ± 2	79	553 ± 5	7	153 ± 11	6	143 ± 13
387	smartvist-000	5959	134084	32	165	25	512 ± 0	8	59 ± 0	6	56 ± 0	5	56 ± 0	6	58 ± 0	6	90 ± 1	186	1435 ± 31	185	1422 ± 48
388	smilart-002	111826	87805	51	263	86	1024 ± 0	28	176 ± 16	-	-	-	-	-	-	434	18784 ± 136	434	18795 ± 151		
389	smilart-003	67339	91670	42	192	22	512 ± 0	30	180 ± 12	23	181 ± 10	40	313 ± 22	141	665 ± 49	414	2299 ± 196	179	1395 ± 74	146	1027 ± 66
390	sodec-000	836592	13142	454	3186	427	4096 ± 0	375	1041 ± 2	331	1032 ± 1	310	1035 ± 1	276	1037 ± 2	227	1061 ± 2	219	1794 ± 37	217	1775 ± 23
391	sqisoft-002	278039	386291	146	666	391	2056 ± 0	130	466 ± 8	107	466 ± 2	91	468 ± 11	68	461 ± 6	56	472 ± 4	113	758 ± 11	112	760 ± 23
392	sqisoft-003	362737	607964	191	805	383	2056 ± 0	210	638 ± 2	189	674 ± 7	188	718 ± 17	143	665 ± 6	132	720 ± 6	123	844 ± 11	123	844 ± 23
393	stauq-000	879661	624676	259	1064	424	4096 ± 0	277	813 ± 25	-	-	-	-	-	-	299	2979 ± 31	303	3007 ± 75		
394	starhybrid-001	100509	289356	206	845	338	2048 ± 0	86	358 ± 82	67	355 ± 49	55	379 ± 58	54	401 ± 79	40	393 ± 67	154	1075 ± 51	157	1078 ± 53
395	stcon-000	408095	49619	277	1131	81	1024 ± 0	197	617 ± 1	174	632 ± 4	152	634 ± 1	134	645 ± 2	116	676 ± 6	42	437 ± 10	41	434 ± 11
396	stcon-001	322871	64463	218	884	83	1024 ± 0	355	980 ± 1	315	991 ± 1	295	995 ± 5	265	1003 ± 6	215	1042 ± 4	30	336 ± 14	33	334 ± 14

Notes

- 1 The configuration size does not capture static data included in libraries.
- 2 The library size is the combined total of all files provided in the submission lib folder. These libraries e.g. OpenCV may or may not be installed on any end user's platform natively and would not need to be installed with the algorithm. Some developers put neural network models in their libraries.
- 3 The memory usage is the peak resident set size reported by the ps system call during template generation.
- 4 The median template creation times are measured on Intel®Xeon®CPU E5-2630 v4 @ 2.20GHz processors.
- 5 The comparison durations, in nanoseconds, are estimated using std::chrono::high_resolution_clock which on the machine in (2) counts 1ns clock ticks. Precision is somewhat worse than that however. The ± value is the median absolute deviation times 1.48 for Normal consistency.

Table 17: Summary of algorithms and properties included in this report. The red superscripts give ranking for the quantity in that column.

	ALGORITHM	CONFIG	LIBRARY	TEMPLATE								COMPARISON ⁴								
				NAME	DATA	DATA	MEMORY	SIZE	GENERATION TIME (ms) ⁴				TIME (ns) ⁵							
									(KB) ¹	(KB) ²	(MB) ³	(B)	MUGSHOT	480x720	960x1440	1600x2400	3000x4500	GENUINE	IMPOSTOR	
397	sukshi-000	94035	688738	72372	500	32768 ± 0	106	407 ± 11	88	413 ± 8	105	504 ± 8	150	689 ± 11	380	1574 ± 28	401	9817 ± 50	399	9787 ± 62
398	suprema-003	498231	116054	2961239	268	2048 ± 0	484	1448 ± 1	447	1417 ± 4	440	1418 ± 3	413	1421 ± 4	349	1451 ± 5	257	2201 ± 10	260	2198 ± 13
399	suprema-004	1430475	116085	4142272	434	4096 ± 0	494	1478 ± 2	462	1472 ± 2	456	1469 ± 1	430	1476 ± 1	369	1496 ± 1	312	3201 ± 14	312	3202 ± 22
400	supremaid-001	258193	23479	120541	163	2048 ± 0	130	479 ± 1	114	481 ± 0	96	481 ± 0	80	490 ± 0	74	522 ± 0	103	704 ± 19	95	652 ± 19
401	supremaid-002	256273	23899	62335	144	2048 ± 0	140	483 ± 0	129	501 ± 0	100	488 ± 0	87	503 ± 0	87	565 ± 0	243	1990 ± 19	236	1923 ± 29
402	surrey-cvssp-001	900280	76392	3621707	213	2048 ± 0	418	1221 ± 1	389	1238 ± 2	376	1240 ± 0	344	1243 ± 0	284	1257 ± 0	436	18970 ± 161	435	18999 ± 176
403	surrey-cvssp-002	903493	87776	3651717	342	2048 ± 0	414	1213 ± 1	383	1211 ± 1	390	1279 ± 0	362	1282 ± 0	299	1300 ± 0	403	9906 ± 120	401	9911 ± 167
404	swsam-001	265887	95072	3781801	179	2048 ± 0	379	1058 ± 34	344	1079 ± 31	332	1091 ± 35	291	1076 ± 9	241	1109 ± 45	294	2902 ± 31	293	2892 ± 32
405	synesis-006	731941	21817	3381472	472	4104 ± 0	163	549 ± 1	143	546 ± 1	126	552 ± 1	103	558 ± 2	107	639 ± 28	101	697 ± 32	102	688 ± 31
406	synesis-007	1442961	24145	4232443	413	3080 ± 0	415	1215 ± 5	399	1268 ± 30	400	1306 ± 67	369	1311 ± 58	337	1423 ± 52	97	684 ± 32	100	686 ± 25
407	synology-000	221021	25809	89453	136	2048 ± 0	105	407 ± 14	89	415 ± 14	178	694 ± 31	402	1396 ± 58	442	4568 ± 211	439	19720 ± 203	437	19767 ± 379
408	synology-002	256713	25943	99488	238	2048 ± 0	314	886 ± 4	270	892 ± 3	252	920 ± 2	263	1000 ± 5	304	1317 ± 12	188	1466 ± 32	191	1496 ± 45
409	sztu-000	338637	15871	3101298	280	2048 ± 0	159	531 ± 0	139	532 ± 0	113	533 ± 0	99	537 ± 0	78	548 ± 0	62	585 ± 11	66	592 ± 13
410	sztu-001	338650	15871	3111298	313	2048 ± 0	160	535 ± 0	138	537 ± 0	119	538 ± 0	96	540 ± 0	81	553 ± 0	69	599 ± 10	71	598 ± 10
411	t4isb-000	234227	115237	64343	162	2048 ± 0	364	1006 ± 5	321	1001 ± 1	301	1006 ± 1	269	1009 ± 1	209	1022 ± 2	329	3586 ± 34	326	3534 ± 34
412	tech5-005	1178769	120517	3321426	40	512 ± 0	435	1272 ± 109	337	1038 ± 63	314	1046 ± 39	302	1124 ± 38	317	1351 ± 44	278	2573 ± 37	278	2545 ± 32
413	tech5-007	0	340324	4332643	39	512 ± 0	457	1360 ± 0	430	1366 ± 0	422	1376 ± 0	392	1373 ± 0	344	1438 ± 6	51	538 ± 19	52	516 ± 22
414	techsign-000	0	1101622	3951955	248	2048 ± 0	90	366 ± 1	83	398 ± 1	356	1172 ± 3	467	3065 ± 18	463	10460 ± 65	350	4758 ± 112	349	4789 ± 93
415	techsign-001	0	586983	3721741	220	2048 ± 0	263	772 ± 35	228	788 ± 23	207	802 ± 42	239	949 ± 10	334	1409 ± 26	63	592 ± 11	67	592 ± 13
416	tevian-007	779934	19523	3641714	90	1032 ± 0	178	583 ± 1	152	579 ± 0	133	580 ± 0	113	588 ± 1	106	636 ± 0	356	4894 ± 65	353	4841 ± 83
417	tevian-008	847177	19519	4573490	91	1032 ± 0	312	884 ± 2	274	903 ± 1	244	903 ± 1	229	911 ± 1	190	946 ± 1	353	4828 ± 40	352	4811 ± 41
418	tiger-005	342866	253734	3451531	365	2052 ± 0	383	1097 ± 2	343	1065 ± 2	327	1066 ± 2	287	1067 ± 3	233	1088 ± 3	79	620 ± 19	83	615 ± 16
419	tiger-006	421186	394688	162707	366	2052 ± 0	468	1392 ± 16	446	1411 ± 10	446	1444 ± 10	440	1531 ± 11	405	1848 ± 10	223	1810 ± 20	222	1801 ± 13
420	tinkoff-001	274660	389272	132592	341	2048 ± 0	402	1176 ± 3	373	1179 ± 3	358	1178 ± 3	319	1169 ± 2	272	1203 ± 3	346	4361 ± 74	343	4364 ± 75
421	tongyi-005	1140701	138919	4052121	406	2089 ± 0	24	165 ± 1	-	-	-	-	-	-	-	435	18924 ± 65	438	2018 ± 103	
422	toppanigate-000	671181	711850	3761786	421	4096 ± 0	322	915 ± 1	280	916 ± 1	250	916 ± 1	227	917 ± 1	184	917 ± 1	448	25262 ± 84	446	25264 ± 97
423	toshiba-004	599297	27880	3521595	379	2056 ± 0	482	1447 ± 3	458	1453 ± 2	453	1457 ± 9	422	1457 ± 3	358	1479 ± 4	143	1020 ± 25	140	998 ± 32
424	toshiba-006	599566	44078	3501588	377	2056 ± 0	496	1481 ± 16	467	1515 ± 7	462	1506 ± 6	437	1521 ± 2	376	1546 ± 30	144	1022 ± 17	145	1022 ± 23
425	touchlessid-001	255274	14355	118537	308	2048 ± 0	81	344 ± 1	63	347 ± 1	66	414 ± 3	116	595 ± 10	396	1732 ± 61	222	1806 ± 35	221	1800 ± 35
426	touchlessid-002	255586	14284	70367	190	2048 ± 0	92	371 ± 1	72	375 ± 1	79	438 ± 3	132	640 ± 10	378	1548 ± 57	236	1915 ± 41	231	1871 ± 38
427	trueface-002	253947	123116	98486	107	2000 ± 0	87	360 ± 0	69	361 ± 0	71	423 ± 0	114	590 ± 1	-	10	192 ± 14	12	186 ± 19	
428	trueface-003	346530	24308	4673915	290	2048 ± 0	387	1107 ± 22	192	677 ± 3	192	732 ± 7	224	905 ± 5	-	-	103	111 ± 11	1	112 ± 29
429	trueidvng-001	766071	37721	3591692	483	6144 ± 0	349	975 ± 1	311	985 ± 1	290	989 ± 1	271	1016 ± 1	248	1128 ± 2	463	37129 ± 216	490	72067 ± 305
430	tuputech-000	11476	17185	233	255	2048 ± 0	21	122 ± 4	15	120 ± 1	14	142 ± 2	18	196 ± 5	44	411 ± 14	448	23893 ± 406	44	25279 ± 406
431	turingtechvip-001	399874	54535	140617	140	2048 ± 0	463	1384 ± 4	435	1391 ± 1	430	1393 ± 1	409	1411 ± 1	356	1476 ± 2	213	1733 ± 19	213	1734 ± 20
432	turingtechvip-002	167556	140995	216876	312	2048 ± 0	499	1493 ± 2	414	1306 ± 1	426	1382 ± 1	380	1337 ± 1	339	1426 ± 3	419	13819 ± 103	418	13807 ± 137
433	turkcell-000	271083	133553	143637	301	2048 ± 0	389	1110 ± 1	350	1094 ± 0	338	1103 ± 0	304	1126 ± 1	270	1201 ± 1	291	2866 ± 23	292	2873 ± 40
434	turkcell-001	287616	133870	144654	311	2048 ± 0	230	682 ± 0	209	695 ± 0	173	688 ± 1	152	692 ± 0	125	702 ± 0	345	4342 ± 71	342	4310 ± 72
435	twface-000	661735	11782	4302610	111	2048 ± 0	302	871 ± 1	259	873 ± 2	231	873 ± 2	21	876 ± 2	177	898 ± 1	193	1504 ± 29	192	1510 ± 34
436	twface-001	671511	11782	4462855	332	2048 ± 0	327	923 ± 1	286	925 ± 2	256	926 ± 1	23	929 ± 2	187	940 ± 2	180	1400 ± 32	182	1402 ± 37
437	ulsee-001	370519	57261	-	139	2048 ± 0	216	654 ± 2	-	-	-	-	-	-	-	378	6065 ± 94	380	6228 ± 77	
438	uluface-002	0	480761	2651088	228	2048 ± 0	306	873 ± 42	250	855 ± 9	280	978 ± 24	352	1271 ± 40	415	2333 ± 68	437	19207 ± 114	433	18501 ± 274
439	uluface-003	97357	529422	3001264	411	3072 ± 0	341	965 ± 11	301	968 ± 10	330	1087 ± 20	396	1387 ± 36	421	2469 ± 86	449	26057 ± 195	450	26865 ± 566
440	unicc-001	24840	5123261	3841850	199	2048 ± 0	72	316 ± 4	66	349 ± 4	219	838 ± 14	296	1102 ± 11	303	1312 ± 15	298	2950 ± 29	296	2929 ± 26

Notes

- 1 The configuration size does not capture static data included in libraries.
- 2 The library size is the combined total of all files provided in the submission lib folder. These libraries e.g. OpenCV may or may not be installed on any end user's platform natively and would not need to be installed with the algorithm. Some developers put neural network models in their libraries.
- 3 The memory usage is the peak resident set size reported by the ps system call during template generation.
- 4 The median template creation times are measured on Intel®Xeon®CPU E5-2630 v4 @ 2.20GHz processors.
- 5 The comparison durations, in nanoseconds, are estimated using std::chrono::high_resolution_clock which on the machine in (2) counts 1ns clock ticks. Precision is somewhat worse than that however. The ± value is the median absolute deviation times 1.48 for Normal consistency.

Table 18: Summary of algorithms and properties included in this report. The red superscripts give ranking for the quantity in that column.

	ALGORITHM	CONFIG	LIBRARY	TEMPLATE								COMPARISON ⁴								
				NAME	DATA	DATA	MEMORY	SIZE	GENERATION TIME (ms) ⁴				TIME (ns) ⁵							
									(KB) ¹	(KB) ²	(MB) ³	(B)	MUGSHOT	480x720	960x1440	1600x2400	3000x4500	GENUINE	IMPOSTOR	
441	unissey-002	0	1443765	177	763	441	4096 ± 0	253	736 ± 1	218	752 ± 1	293	994 ± 1	415	1426 ± 1	439	3331 ± 2	414	12308 ± 91	413 12302 ± 137
442	unissey-003	0	814526	142	618	446	4096 ± 0	250	718 ± 1	216	744 ± 0	267	956 ± 1	406	1403 ± 1	434	3055 ± 2	198	1594 ± 20	196 1570 ± 44
443	upc-001	0	89914	264	1077	94	1052 ± 0	167	551 ± 15	206	703 ± 56	190	724 ± 51	174	751 ± 49	168	863 ± 33	309	3114 ± 44	311 3165 ± 97
444	uxlabs-001	291127	39378	159	700	459	4096 ± 0	101	395 ± 0	73	387 ± 0	58	388 ± 0	50	390 ± 0	42	396 ± 0	229	1863 ± 31	233 1921 ± 45
445	vcog-002	3229434	118946	459	3666	501	61504 ± 5	85	357 ± 25	-	-	-	-	-	-	-	497	296154 ± 3077	497 296436 ± 4183	
446	vd-002	254498	34389	155	688	54	516 ± 0	234	684 ± 5	193	679 ± 4	167	676 ± 5	153	693 ± 5	142	754 ± 5	26	300 ± 14	29 319 ± 32
447	vd-003	254505	44051	157	696	361	2052 ± 0	241	691 ± 5	198	690 ± 5	170	683 ± 4	151	691 ± 5	133	722 ± 5	141	1003 ± 11	142 1001 ± 7
448	veridas-007	355105	891492	426	2527	143	2048 ± 0	305	872 ± 9	260	875 ± 8	382	1261 ± 18	457	2238 ± 38	452	6374 ± 147	94	655 ± 16	97 660 ± 19
449	veridas-008	1100495	1190915	494	8932	147	2048 ± 0	333	944 ± 12	292	945 ± 11	410	1334 ± 27	459	2382 ± 48	453	6959 ± 172	106	723 ± 14	108 731 ± 16
450	veridium-000	0	47198	1598	498	29399	± 2045	11	79 ± 0	9	80 ± 0	10	89 ± 0	8	90 ± 0	8	111 ± 0	484	64880 ± 171	483 64697 ± 247
451	veridium-001	0	40561	24	142	408	2489 ± 0	74	44 ± 0	545	40 ± 0	448	40 ± 0	450	40 ± 0	472	40 ± 0	483	63417 ± 1061	482 63225 ± 2133
452	verigram-001	282155	11773	432	2638	251	2048 ± 0	222	664 ± 2	191	675 ± 2	217	833 ± 4	334	1202 ± 7	427	2733 ± 32	206	1664 ± 60	202 1648 ± 56
453	verigram-002	1588249	20691	401	2051	437	4096 ± 0	488	1464 ± 3	445	1406 ± 0	459	1486 ± 1	416	1431 ± 0	383	1586 ± 5	498	453119 ± 13595	498 452140 ± 9654
454	verihubs-inteligensia-000	209562	51877	82	427	164	2048 ± 0	172	567 ± 0	469	1558 ± 8	465	1560 ± 8	442	1568 ± 8	386	1621 ± 8	443	22351 ± 91	442 22371 ± 81
455	verihubs-inteligensia-001	216524	51916	84	437	258	2048 ± 0	171	564 ± 0	147	562 ± 0	129	566 ± 1	106	566 ± 0	94	600 ± 0	441	21770 ± 84	440 21735 ± 102
456	verijelas-000	254540	10322	371	1736	135	2048 ± 0	73	321 ± 0	60	325 ± 1	4329	0 ± 0	41	335 ± 5	35	360 ± 0	404	10267 ± 143	403 10218 ± 109
457	via-001	370255	11151	360	1697	304	2048 ± 0	340	964 ± 3	325	1011 ± 3	304	1026 ± 4	280	1045 ± 3	251	1137 ± 28	137	983 ± 31	138 989 ± 40
458	via-004	530941	93634	318	1321	223	2048 ± 0	91	368 ± 0	81	397 ± 1	48	352 ± 1	43	364 ± 2	60	490 ± 1	20	255 ± 7	24 255 ± 8
459	videmo-001	212051	95063	58	304	319	2048 ± 0	38	199 ± 0	18	164 ± 0	15	164 ± 0	12	164 ± 0	10	165 ± 0	23	296 ± 17	27 288 ± 16
460	videmo-002	212053	32963	61	332	198	2048 ± 0	36	199 ± 0	19	169 ± 0	16	169 ± 0	13	170 ± 0	12	170 ± 0	16	209 ± 7	17 208 ± 8
461	videonetics-001	30875	5963	5	61	42	512 ± 0	50	262 ± 3	43	273 ± 1	76	439 ± 3	193	820 ± 3	418	2393 ± 43	164	1153 ± 38	165 1142 ± 65
462	videonetics-002	121981	6289	19	115	370	2052 ± 0	60	282 ± 5	54	295 ± 1	110	513 ± 4	273	1029 ± 3	435	3151 ± 46	168	1219 ± 57	171 1262 ± 56
463	viettelhightech-000	259471	215557	80	419	226	2048 ± 0	125	461 ± 1	108	461 ± 2	82	461 ± 1	72	467 ± 2	61	494 ± 0	68	599 ± 11	65 591 ± 13
464	vigilantsolutions-010	348798	49973	205	840	104	1548 ± 0	196	615 ± 0	173	631 ± 0	150	632 ± 0	130	636 ± 0	111	659 ± 0	49	490 ± 13	50 488 ± 11
465	vigilantsolutions-011	255661	49973	131	591	103	1548 ± 0	103	402 ± 0	90	418 ± 0	68	418 ± 0	60	422 ± 0	52	445 ± 0	32	339 ± 20	36 366 ± 37
466	vinai-000	402391	866522	254	1032	263	2048 ± 0	385	1099 ± 1	351	1095 ± 1	333	1093 ± 1	295	1099 ± 1	247	1126 ± 1	300	2996 ± 20	302 2993 ± 26
467	vinbigdata-001	271405	44746	130	589	181	2048 ± 0	471	1400 ± 5	437	1393 ± 2	427	1391 ± 2	400	1393 ± 1	333	1404 ± 1	176	1351 ± 50	176 1310 ± 38
468	vinbigdata-002	256322	138864	137	606	249	2048 ± 0	175	569 ± 2	150	572 ± 1	130	571 ± 1	107	572 ± 1	92	596 ± 1	255	2175 ± 44	255 2160 ± 53
469	vion-000	228219	7533	101	498	354	2052 ± 0	77	333 ± 1	-	-	-	-	-	-	-	465	39839 ± 3561	449 26830 ± 2241	
470	visage-000	49218	70150	9	73	45	512 ± 0	42	27 ± 0	227	± 0	231	± 0	38	38 ± 0	3	63 ± 0	259	2220 ± 14	261 2218 ± 14
471	visionbox-002	259063	135281	139	612	396	2059 ± 0	139	482 ± 1	116	482 ± 0	97	484 ± 1	83	492 ± 1	70	517 ± 3	242	1969 ± 44	239 1931 ± 42
472	visionbox-003	259542	156891	299	1260	400	2068 ± 0	228	678 ± 2	194	682 ± 1	169	682 ± 2	154	695 ± 2	140	739 ± 5	204	1643 ± 56	203 1649 ± 66
473	visionlabs-010	1067280	19357	221	902	48	513 ± 0	251	730 ± 0	211	717 ± 1	182	709 ± 0	162	713 ± 1	139	739 ± 0	70	600 ± 41	85 626 ± 35
474	visionlabs-011	1067280	19353	212	862	50	513 ± 0	252	731 ± 1	212	717 ± 1	183	710 ± 1	164	714 ± 1	141	741 ± 1	54	556 ± 26	57 559 ± 25
475	visteam-004	61594	35369	36	168	201	2048 ± 0	67	303 ± 5	50	313 ± 6	35	278 ± 4	34	288 ± 4	38	377 ± 7	338	3936 ± 72	336 3938 ± 79
476	visteam-005	288140	35427	65	348	233	2048 ± 0	392	1117 ± 6	354	1106 ± 6	323	1060 ± 4	289	1071 ± 4	259	1156 ± 8	337	3932 ± 97	335 3932 ± 71
477	vixvizon-006	594053	396294	227	914	296	2048 ± 0	310	876 ± 9	241	828 ± 3	213	817 ± 1	196	825 ± 2	171	871 ± 1	71	600 ± 23	78 611 ± 25
478	vixvizon-007	594053	470119	308	1282	292	2048 ± 0	313	885 ± 35	242	828 ± 1	212	816 ± 1	195	825 ± 1	170	870 ± 1	72	600 ± 28	74 602 ± 34
479	vnpt-004	370110	240841	245	988	262	2048 ± 0	424	1238 ± 1	390	1241 ± 1	377	1242 ± 2	366	1307 ± 2	366	1505 ± 2	341	4047 ± 48	338 4008 ± 108
480	vnpt-005	560630	240888	283	1141	267	2048 ± 0	475	1403 ± 0	443	1404 ± 6	435	1403 ± 6	421	1456 ± 0	387	1630 ± 10	326	3562 ± 23	327 3554 ± 29
481	vocord-009	1380132	201560	473	4162	106	1920 ± 0	492	1472 ± 2	463	1472 ± 1	464	1549 ± 1	445	1667 ± 2	410	2064 ± 2	247	2052 ± 50	249 2056 ± 39
482	vocord-010	902552	206873	462	3858	95	1088 ± 0	487	1459 ± 2	461	1459 ± 1	454	1463 ± 2	433	1484 ± 1	374	1535 ± 3	282	2724 ± 31	281 2653 ± 45
483	vts-000	256589	169760	361	1704	261	2048 ± 0	143	486 ± 1	113	481 ± 0	98	484 ± 0	79	485 ± 1	69	517 ± 0	494	124209 ± 352	494 123652 ± 358
484	vts-001	293000	475743	141	618	264	2048 ± 0	226	676 ± 1	193	683 ± 6	173	687 ± 3	155	695 ± 2	127	709 ± 2	400	9620 ± 44	398 9618 ± 54

Notes

- The configuration size does not capture static data included in libraries.
- The library size is the combined total of all files provided in the submission lib folder. These libraries e.g. OpenCV may or may not be installed on any end user's platform natively and would not need to be installed with the algorithm. Some developers put neural network models in their libraries.
- The memory usage is the peak resident set size reported by the ps system call during template generation.
- The median template creation times are measured on Intel®Xeon®CPU E5-2630 v4 @ 2.20GHz processors.
- The comparison durations, in nanoseconds, are estimated using std::chrono::high_resolution_clock which on the machine in (2) counts 1ns clock ticks. Precision is somewhat worse than that however. The ± value is the median absolute deviation times 1.48 for Normal consistency.

Table 19: Summary of algorithms and properties included in this report. The red superscripts give ranking for the quantity in that column.

	ALGORITHM	CONFIG	LIBRARY	TEMPLATE								COMPARISON ⁴	
	NAME	DATA	DATA	MEMORY	SIZE		GENERATION TIME (ms) ⁴					TIME (ns) ⁵	
		(KB) ¹	(KB) ²	(MB) ³	(B)	MUGSHOT	480x720	960x1440	1600x2400	3000x4500		GENUINE	IMPOSTOR
485	wicket-000	826392	641802	⁴⁰³ 2071	³⁰⁵ 2048 ± 0	⁴⁷⁹ 1419 ± 2	⁴⁵⁰ 1429 ± 3	⁴⁴⁷ 1444 ± 4	⁴²⁵ 1460 ± 3	³⁷⁵ 1537 ± 6	⁴⁸¹ 60976 ± 232	⁴⁸⁰ 61096 ± 323	
486	winsense-001	264428	32035	²³⁰ 922	⁹⁹ 1280 ± 0	²⁶¹ 766 ± 7	³⁴⁰ 1058 ± 47	²⁸⁵ 983 ± 97	²⁸¹ 1053 ± 119	³⁰⁵ 1320 ± 84	²⁰² 1631 ± 28	²⁴³ 1964 ± 171	
487	winsense-002	281379	25780	³⁷⁵ 1781	²³⁶ 2048 ± 0	¹⁴⁶ 494 ± 2	¹²² 498 ± 1	¹¹² 519 ± 1	⁹⁴ 537 ± 1	¹⁰⁴ 634 ± 1	²⁰⁸ 1683 ± 8	²⁰⁷ 1685 ± 7	
488	wiseai-001	189467	60781	⁴⁵ 245	²¹⁶ 2048 ± 0	⁴⁵ 240 ± 0	³⁷ 251 ± 0	⁴⁴ 328 ± 1	⁴⁰ 327 ± 0	²⁹ 332 ± 0	²⁸⁸ 2850 ± 29	²⁹¹ 2852 ± 31	
489	wuhantianyu-001	465118	66457	²¹³ 866	²⁸⁷ 2048 ± 0	²¹¹ 642 ± 1	¹⁸⁰ 642 ± 1	¹⁶² 644 ± 0	¹³⁷ 652 ± 0	¹²⁴ 697 ± 0	³⁹⁹ 9502 ± 151	⁴⁰² 9920 ± 253	
490	x-laboratory-000	520020	197310	³⁴³ 1524	³⁹² 2056 ± 0	²⁷⁴ 808 ± 7	²⁷² 897 ± 113	²⁴⁵ 907 ± 103	²¹⁷ 886 ± 103	¹¹⁵ 673 ± 39	¹⁰⁸ 725 ± 19	¹¹⁰ 749 ± 34	
491	x-laboratory-001	625140	398792	³⁸³ 1844	³⁸⁰ 2056 ± 0	¹⁸¹ 586 ± 2	¹⁶¹ 596 ± 5	¹⁴³ 603 ± 6	¹²⁵ 620 ± 7	¹⁵⁰ 793 ± 14	¹²⁰ 813 ± 28	¹²⁵ 872 ± 32	
492	xforwardai-001	340100	51163	⁴⁰⁹ 2173	²⁴² 2048 ± 0	⁴⁰⁶ 1180 ± 2	³⁷⁶ 1182 ± 1	³⁶⁶ 1194 ± 1	³²⁸ 1186 ± 2	²⁷¹ 1203 ± 1	¹¹⁷ 779 ± 17	¹¹⁷ 797 ± 13	
493	xforwardai-002	707715	51163	³⁹⁹ 1989	⁴⁴² 2096 ± 0	³³² 944 ± 1	²⁹¹ 942 ± 1	²⁶² 943 ± 4	²³⁴ 935 ± 1	¹⁹⁶ 967 ± 1	¹⁸⁴ 1406 ± 8	¹⁸³ 1405 ± 13	
494	xm-000	578041	148920	¹⁵⁴ 688	³⁷¹ 2052 ± 0	³¹¹ 878 ± 2	²⁶⁶ 882 ± 1	²⁸⁹ 988 ± 2	³⁴⁹ 1258 ± 3	⁴²⁰ 2434 ± 7	²⁰³ 1634 ± 17	²⁰⁰ 1632 ± 20	
495	yisheng-004	486351	38653	³⁰⁶ 1279	⁴¹⁷ 3704 ± 0	⁹³ 378 ± 12	-	-	-	-	¹⁰⁰ 693 ± 137	⁵³ 526 ± 34	
496	yitu-003	1525719	1388919	⁴⁶¹ 3737	⁴⁰⁵ 2082 ± 0	²⁹⁹ 860 ± 0	-	-	-	-	⁴³² 18305 ± 71	⁴³¹ 18286 ± 62	
497	yoonik-003	346691	265415	⁴¹² 2196	³¹⁴ 2048 ± 0	³⁵⁹ 991 ± 3	³⁰⁸ 980 ± 1	²⁸⁶ 984 ± 4	²⁵⁰ 982 ± 1	²⁰¹ 983 ± 1	⁹⁸ 684 ± 45	⁹⁸ 678 ± 41	
498	yoonik-004	469597	88673	¹⁸⁷ 791	³³⁷ 2048 ± 0	⁴¹⁶ 1219 ± 1	⁴⁰⁵ 1284 ± 1	³⁸¹ 1255 ± 1	³⁵¹ 1266 ± 0	²⁸¹ 1251 ± 1	¹⁴⁷ 1039 ± 42	¹⁴⁸ 1030 ± 40	
499	ytu-000	1477360	44032	⁴²⁴ 2484	²⁷⁵ 2048 ± 0	¹⁵⁸ 530 ± 0	¹³⁶ 533 ± 0	¹⁵⁸ 640 ± 0	²⁰⁷ 861 ± 2	⁴⁰⁸ 1949 ± 8	⁴⁵⁷ 31797 ± 131	⁴⁵⁷ 31794 ± 133	
500	yuan-005	258312	145564	²⁰⁴ 839	²⁴⁵ 2048 ± 0	⁹⁵ 381 ± 0	⁷⁴ 386 ± 0	⁵⁷ 387 ± 2	⁵¹ 390 ± 4	⁴⁶ 421 ± 3	¹⁶⁵ 1156 ± 8	¹⁶⁸ 1196 ± 26	
501	yuan-006	1622733	145572	⁴⁷⁶ 4365	⁴⁴⁰ 4096 ± 0	⁴³⁶ 1280 ± 2	³⁹⁸ 1268 ± 1	³⁸⁶ 1273 ± 0	³⁵³ 1272 ± 2	³⁰² 1306 ± 3	²⁵⁸ 2202 ± 19	²⁵⁸ 2190 ± 20	

Notes

- 1 The configuration size does not capture static data included in libraries.
- 2 The library size is the combined total of all files provided in the submission lib folder. These libraries e.g. OpenCV may or may not be installed on any end user's platform natively and would not need to be installed with the algorithm. Some developers put neural network models in their libraries.
- 3 The memory usage is the peak resident set size reported by the ps system call during template generation.
- 4 The median template creation times are measured on Intel®Xeon®CPU E5-2630 v4 @ 2.20GHz processors.
- 5 The comparison durations, in nanoseconds, are estimated using std::chrono::high_resolution_clock which on the machine in (2) counts 1ns clock ticks. Precision is somewhat worse than that however. The ± value is the median absolute deviation times 1.48 for Normal consistency.

Table 20: Summary of algorithms and properties included in this report. The red superscripts give ranking for the quantity in that column.

	Algorithm	FALSE NON-MATCH RATE (FNMR)										LESS CONSTRAINED, NON-COOP.					
		CONSTRAINED, COOPERATIVE								WILD							
		Name	VISAMC	VISA	MUGSHOT	MUGSHOT12+YRS	VISABORDER	BORDER	BORDER	1E-05							
	FMR	0.0001	1E-06	1E-05	1E-05	1E-06	1E-06	1E-06	1E-05	0.0001							
1	20face-000	0.1268	439	0.1828	436	0.1748	441	0.2768	441	0.1765	422	0.1864	306	0.0927	343	0.0405	308
2	20face-001	0.0521	414	0.0732	415	0.1414	439	0.2549	440	0.0769	396	0.1354	298	0.0419	299	0.0295	196
3	3divi-006	0.0064	219	0.0094	217	0.0047	201	0.0066	204	0.0091	214	0.0191	166	0.0113	170	0.0289	165
4	3divi-007	0.0024	76	0.0038	81	0.0028	83	0.0034	81	0.0046	121	0.0101	97	0.0082	118	0.0300	211
5	accurascan-001	0.3670	465	0.4777	463	0.5313	463	0.6155	460	0.5583	451	0.6120	364	0.2569	373	0.0816	392
6	acer-001	0.0294	393	0.0504	395	0.0240	385	0.0463	388	0.0436	375	0.0622	264	0.0360	292	0.0307	226
7	acer-002	0.0169	359	0.0262	362	0.0103	323	0.0167	330	0.0182	310	0.0281	205	0.0159	220	0.0297	202
8	acisw-007	0.4276	469	0.5493	471	0.8425	486	0.9185	486	0.8424	466	0.9976	448	0.9930	468	0.4963	468
9	acisw-008	0.0100	292	0.0147	289	0.0094	317	0.0126	287	0.1740	421	0.6651	372	0.4545	406	0.0925	397
10	ader-a-003	0.0043	153	0.0059	149	0.0036	149	0.0043	127	0.0076	186	0.0151	133	0.0128	190	0.0989	398
11	ader-a-004	0.0014	25	0.0022	27	0.0035	144	0.0050	153	0.0023	12	0.0212	177	0.0058	63	0.0278	48
12	advance-003	0.0060	212	0.0087	205	0.0052	218	0.0067	206	0.0389	367	0.4914	351	0.1291	350	0.0508	343
13	advance-004	0.0083	267	0.0101	235	0.0037	155	0.0054	166	0.0051	135	0.3555	339	0.1088	348	0.1635	420
14	afisbiometrics-000	0.0051	172	0.0073	175	0.0030	106	0.0050	154	0.0044	115	0.0077	58	0.0057	60	0.0282	109
15	afrengine-000	0.6244	490	0.7336	489	0.8318	485	0.9083	484	0.8122	462	0.9980	450	0.9895	466	0.6480	476
16	afrengine-001	0.0071	235	0.0129	271	0.0094	319	0.0201	347	0.0097	231	0.9737	425	0.8179	437	0.0282	95
17	aifirst-001	0.0119	321	0.0170	309	0.0084	296	0.0127	292	0.0131	269	0.0212	176	0.0138	197	0.0432	324
18	aigen-001	0.0124	326	0.0219	342	0.0143	357	0.0217	353	0.0236	335	0.8960	407	0.3255	388	0.0681	371
19	aigen-002	0.0192	371	0.0343	375	0.0256	386	0.0402	382	0.0389	366	0.9196	410	0.3876	398	0.1096	403
20	ailabs-001	0.0158	355	0.0276	366	0.0192	373	0.0317	372	0.0352	361	0.0608	261	0.0434	302	0.0338	274
21	aimall-002	0.0119	319	0.0167	307	0.0224	381	0.0411	383	0.0233	333	0.0373	236	0.0235	266	0.0327	261
22	aimall-003	0.0033	111	0.0041	92	0.0033	135	0.0035	93	0.0056	149	0.0109	104	0.0087	130	0.0312	236
23	aiseemu-001	0.0021	58	0.0029	51	0.0027	69	0.0033	75	0.0038	90	0.0339	224	0.0057	61	0.0282	99
24	aiseemu-002	0.0023	71	0.0032	59	0.0026	56	0.0027	35	0.0036	84	0.0439	243	0.0057	57	0.0280	84
25	aiunionface-000	0.0104	297	0.0154	298	0.0082	293	0.0122	282	0.0141	276	0.0243	189	0.0169	224	0.0306	223
26	aize-001	0.0223	379	0.0344	376	0.0199	374	0.0313	371	0.0367	363	0.0522	255	0.0359	291	0.0446	331
27	aize-002	0.0210	377	0.0327	371	0.0280	391	0.0489	393	0.0504	382	0.0692	269	0.0434	301	0.0854	393
28	ajou-001	0.0093	281	0.0147	288	0.0071	270	0.0126	288	0.0173	307	0.0274	200	0.0186	241	0.0348	280
29	alchera-004	0.0035	126	0.0052	134	0.0028	92	0.0039	110	0.0029	43	0.0075	55	0.0044	23	0.0304	218
30	alchera-005	0.0027	87	0.0040	86	0.0026	51	0.0030	55	0.0025	20	0.0055	26	0.0040	17	0.0306	225
31	alfabeta-001	0.4867	476	0.5831	474	0.6855	472	0.8156	474	0.8253	465	0.7765	388	0.6416	421	0.3427	454
32	alice-000	0.0119	322	0.0192	328	0.0106	328	0.0170	331	0.0167	298	0.0265	197	0.0150	214	0.0288	153
33	alleyes-000	0.0058	201	0.0090	212	0.0055	230	0.0087	250	0.0068	172	0.0105	103	0.0076	105	0.0282	108
34	allgovision-000	0.0346	402	0.0527	399	0.0232	382	0.0339	373	0.0372	365	0.0620	263	0.0443	305	0.0607	359
35	alphaface-001	0.0065	220	0.0097	228	0.0039	166	0.0063	199	0.0083	200	-	-	-	-	0.0280	85
36	alphaface-002	0.0052	177	0.0075	181	0.0030	99	0.0044	133	1.0000	492	0.0115	110	0.0084	124	0.0279	71
37	amplifiedgroup-001	0.5034	478	0.5848	475	0.6973	475	0.8316	475	0.7807	459	0.7724	385	0.6354	418	0.4250	462
38	androvideo-000	0.0243	383	0.0438	389	0.0239	384	0.0365	379	0.0483	380	0.1870	307	0.0635	326	0.1163	405
39	anke-004	0.0080	259	0.0154	297	0.0073	272	0.0112	274	0.0102	241	0.0178	159	0.0118	178	0.0288	157
40	anke-005	0.0070	228	0.0109	249	0.0059	241	0.0094	258	0.0105	243	0.0142	125	0.0102	149	0.0289	164
41	antheus-000	0.2564	453	0.3776	456	0.7240	476	0.8699	479	0.8899	473	0.9872	433	0.9483	453	0.7668	481
42	antheus-001	0.1311	440	0.2306	441	0.5113	461	0.6797	464	0.8748	472	0.9908	438	0.9649	461	0.7586	480
43	anyvision-004	0.0267	386	0.0385	385	0.0258	387	0.0487	392	0.0234	334	0.0301	211	0.0191	244	0.0470	336
44	anyvision-005	0.0023	72	0.0037	80	0.0027	80	0.0035	89	0.0049	131	0.0084	74	0.0069	88	0.0285	128

Table 21: FNMR is the proportion of mated comparisons below a threshold set to achieve the FMR given in the header on the fourth row. FMR is the proportion of impostor comparisons at or above that threshold. The light grey values give rank over all algorithms in that column. The pink columns use only same-sex impostors; others are selected regardless of demographics. The exception, in the green column, uses "matched-covariates" i.e. impostors of the same sex, age group, and country of birth. The second pink column includes effects of extended ageing. Missing entries for border, visa, mugshot and wild images generally mean the algorithm did not run to completion. The VISA columns compare images described in section 2.1. The MUGSHOT columns compare images described in section 2.5. The VISA-BORDER column compare images described in section 2.2 with those of section 2.4. The BORDER column compares images described in section 2.4. The WILD columns compare images described in section 2.7.

Algorithm	FALSE NON-MATCH RATE (FNMR)												LESS CONSTRAINED, NON-COOP.			
	CONSTRAINED, COOPERATIVE								WILD							
	Name	VISAMC	VISA	MUGSHOT	MUGSHOT12+YRS	VISABORDER	BORDER	BORDER	1E-06	1E-05	0.0001					
FMR	0.0001	1E-06	1E-05	1E-05	1E-06	1E-06	1E-06	1E-06								
45 aratek-001	0.0033	119	0.0045	112	0.0028	87	0.0031	68	0.0043	111	0.0092	86	0.0069	90	0.0317	249
46 armatura-001	0.0033	112	0.0042	99	0.0031	110	0.0037	102	0.0056	148	0.0110	105	0.0092	135	0.0815	390
47 armatura-003	0.0020	53	0.0029	49	0.0026	62	0.0028	41	0.0025	23	0.0049	14	0.0043	21	0.0292	185
48 asusaics-000	0.0125	330	0.0209	337	0.0085	298	0.0134	300	0.0143	280	0.7189	375	0.0285	278	0.0295	195
49 asusaics-001	0.0125	331	0.0210	338	0.0085	300	0.0134	301	0.0143	281	0.7437	379	0.0289	280	0.0295	192
50 autentika-000	0.1415	442	0.1916	437	0.4130	454	0.5521	455	0.4217	446	0.9998	465	0.9954	472	0.3183	452
51 autentika-001	0.0444	409	0.0688	411	0.0987	431	0.1531	430	0.1547	417	1.0000	474	0.9997	481	0.1413	410
52 authenmetric-003	0.0036	134	0.0053	137	0.0039	172	0.0051	155	0.0095	225	0.9930	443	0.5932	416	0.0290	168
53 authenmetric-004	0.0027	90	0.0042	98	0.0033	130	0.0036	99	0.0083	203	0.9879	434	0.4058	400	0.0290	173
54 aware-005	0.0457	411	0.0643	408	0.0603	421	0.1094	425	0.0613	390	0.1075	290	0.0491	310	0.0314	242
55 aware-006	0.0487	412	0.0819	419	0.0529	415	0.1090	423	0.1011	408	0.1058	287	0.0502	313	0.0317	250
56 awiroos-001	0.4044	467	0.4622	462	0.5530	464	0.6518	461	0.2008	426	0.1994	310	0.1386	355	0.5584	471
57 awiroos-002	0.1990	447	0.2561	443	0.3319	449	0.4411	449	0.3821	443	0.9938	444	0.2634	377	0.0997	399
58 aximetria-001	0.0111	309	0.0186	322	0.0110	334	0.0148	318	0.0170	302	0.3928	342	0.2090	369	0.0409	313
59 ayftech-001	0.0946	433	0.1941	438	0.2438	444	0.3625	444	0.1558	418	0.1589	301	0.0936	344	0.0785	382
60 ayonix-000	0.4351	471	0.4872	464	0.6150	469	0.7510	469	0.6557	455	0.6361	367	0.4981	408	0.3635	457
61 beethedata-000	0.0127	334	0.0195	329	0.0092	310	0.0157	324	0.0171	304	0.0306	212	0.0204	254	0.0285	131
62 beyneai-000	0.0071	236	0.0107	246	0.0104	326	0.0131	298	0.0170	303	0.9837	428	0.6171	417	0.0597	358
63 biocube-001	0.5596	485	0.6834	484	0.7700	482	0.8712	480	0.8446	467	0.9661	423	0.7922	434	0.2377	437
64 biocube-002	0.0612	421	0.0856	420	0.2330	442	0.2972	442	0.2365	431	0.9327	416	0.6947	423	0.4818	467
65 bioidtechswiss-001	0.0054	184	0.0072	172	0.0069	263	0.0124	285	0.0060	156	0.0094	88	0.0065	79	0.0313	240
66 bioidtechswiss-002	0.0049	164	0.0067	163	0.0064	252	0.0116	277	0.0067	171	0.0117	112	0.0086	127	0.0279	59
67 biometric-vision-000	0.0023	70	0.0036	75	0.0028	88	0.0034	85	0.0028	41	0.3109	333	0.1504	358	0.0279	63
68 bm-001	0.7431	495	0.9494	497	0.9586	491	0.9843	490	0.9049	475	0.9021	409	0.8395	441	0.9935	491
69 boetech-001	0.0662	425	0.0802	418	0.0493	413	0.0791	412	0.0682	393	0.1074	289	0.0758	334	0.1719	422
70 boetech-002	0.0535	417	0.0565	403	0.0114	341	0.0136	303	0.0403	369	0.0650	265	0.0606	324	0.1697	421
71 bresee-001	0.0085	269	0.0143	283	0.0086	303	0.0153	321	0.0108	247	0.0168	150	0.0115	175	0.0355	291
72 bresee-002	0.0079	257	0.0101	234	0.0065	255	0.0079	233	0.0129	265	0.0263	196	0.0224	263	0.0327	262
73 camvi-002	0.0125	329	0.0221	343	0.0089	307	0.0145	316	0.0142	277	0.2650	326	0.0166	223	0.0288	151
74 camvi-004	0.0171	363	0.0316	370	0.0042	184	0.0049	151	0.0097	233	0.6636	371	0.0141	202	0.0284	117
75 candour-001	0.1048	436	0.3189	448	0.0130	353	0.0182	335	0.3879	444	0.9216	411	0.7071	427	0.8096	485
76 canon-003	0.0041	148	0.0059	148	0.0030	98	0.0040	113	0.0040	97	0.0073	53	0.0059	68	0.0274	24
77 canon-004	0.0052	176	0.0091	215	0.0033	134	0.0058	180	0.0037	86	0.0770	274	0.0494	311	0.0267	2
78 cchonolulu-000	0.7910	498	0.8611	494	0.9824	492	-	0.9940	486	0.9861	429	0.9534	454	0.6647	477	
79 ceiec-003	0.0071	237	0.0107	245	0.0061	248	0.0079	236	0.0160	290	0.0316	213	0.0260	274	0.0308	232
80 ceiec-004	0.0038	139	0.0051	126	0.0045	196	0.0053	161	0.0062	164	0.3939	343	0.0104	155	0.0325	258
81 chosun-001	0.0525	415	0.0936	422	0.0742	427	0.1263	429	0.0978	407	1.0000	482	0.9354	450	0.4446	464
82 chosun-002	0.0390	404	0.0646	409	0.0339	403	0.0576	403	0.0455	379	0.6904	374	0.1746	364	0.0696	373
83 chiface-005	0.0033	108	0.0049	121	0.0029	94	0.0041	118	0.0044	114	0.0317	214	0.0066	82	0.0306	224
84 chiface-006	0.0029	94	0.0043	100	0.0026	66	0.0034	86	0.0040	98	0.2701	327	0.0065	78	0.0305	222
85 cist-001	0.0046	158	0.0065	160	0.0042	185	0.0063	198	0.9675	484	0.9997	463	0.9994	477	0.0407	310
86 cist-002	0.0073	244	0.0096	225	0.0085	301	0.0090	253	0.9990	488	0.9997	462	0.9996	480	0.1458	411
87 clearviewai-000	0.0010	9	0.0019	18	0.0024	24	0.0028	43	0.0030	48	0.0058	31	0.0050	35	0.0271	5
88 closeli-001	0.0136	336	0.0163	301	0.0039	170	0.0054	165	0.0072	179	1.0000	475	0.0094	139	0.0318	251

Table 22: FNMR is the proportion of mated comparisons below a threshold set to achieve the FMR given in the header on the fourth row. FMR is the proportion of impostor comparisons at or above that threshold. The light grey values give rank over all algorithms in that column. The pink columns use only same-sex impostors; others are selected regardless of demographics. The exception, in the green column, uses “matched-covariates” i.e. impostors of the same sex, age group, and country of birth. The second pink column includes effects of extended ageing. Missing entries for border, visa, mugshot and wild images generally mean the algorithm did not run to completion. The VISA columns compare images described in section 2.1. The MUGSHOT columns compare images described in section 2.5. The VISA-BORDER column compare images described in section 2.2 with those of section 2.4. The BORDER column compares images described in section 2.4. The WILD columns compare images described in section 2.7.

Algorithm	FALSE NON-MATCH RATE (FNMR)										LESS CONSTRAINED, NON-COOP.						
	CONSTRAINED, COOPERATIVE								WILD								
	Name	VISAMC	VISA	MUGSHOT	MUGSHOT12+YRS	VISABORDER	BORDER	BORDER	1E-05								
FMR	0.0001	1E-06	1E-05	1E-05	1E-06	1E-06	1E-06	1E-05	0.0001								
89	cloudmatrix-001	0.0668	426	0.1141	426	0.0539	416	0.0905	417	0.3509	440	0.9819	427	0.9010	446	0.0636	363
90	cloudmatrix-002	0.0075	249	0.0113	255	0.0084	297	0.0120	279	0.9248	479	0.9997	461	0.9985	476	0.0358	292
91	cloudwalk-hr-003	0.0026	85	0.0041	88	0.0040	177	0.0058	179	0.0060	161	0.9992	456	0.0094	137	0.7206	479
92	cloudwalk-hr-004	0.0009	6	0.0018	14	0.0034	138	0.0028	49	0.0052	137	0.9992	457	0.0093	136	0.1625	419
93	cloudwalk-mt-006	0.0006	1	0.0006	1	0.0023	12	0.0019	1	0.0016	2	0.0032	2	0.0030	3	0.0290	170
94	cloudwalk-mt-007	0.0006	3	0.0007	2	0.0023	15	0.0019	2	0.0016	1	0.0032	1	0.0030	2	0.0295	193
95	codeline-000	0.0057	195	0.0079	193	0.0037	152	0.0053	164	0.2721	433	1.0000	476	0.9763	463	0.0273	14
96	cogent-007	0.0022	64	0.0038	83	0.0028	89	0.0031	62	0.0040	99	0.0082	67	0.0067	83	0.0438	329
97	cogent-008	0.0015	33	0.0027	44	0.0023	16	0.0025	23	0.0033	66	0.0063	39	0.0055	53	0.0281	89
98	cognitec-003	0.0038	138	0.0052	132	0.0054	228	0.0057	176	0.0225	328	0.0416	242	0.0388	295	0.0348	281
99	cognitec-004	0.0036	127	0.0053	136	0.0053	221	0.0056	172	0.0098	234	0.0202	174	0.0154	216	0.0352	289
100	cor-001	0.0075	248	0.0113	253	0.0055	232	0.0084	242	0.0091	216	0.0148	131	0.0092	134	0.0277	46
101	coretech-000	0.7699	497	1.0000	502	1.0000	500	-		1.0000	494	1.0000	489	1.0000	494	1.0000	499
102	coretech-001	0.0052	174	0.0067	165	0.0083	295	0.0092	255	0.0346	360	0.1363	299	0.0252	270	0.0793	385
103	corsight-002	0.0053	178	0.0068	167	0.0030	103	0.0041	119	0.0039	94	0.0079	61	0.0054	51	0.0276	40
104	corsight-003	0.0026	86	0.0040	87	0.0028	84	0.0045	137	0.0035	82	0.0059	33	0.0046	27	0.0279	65
105	csc-002	0.0099	291	0.0132	272	0.0077	278	0.0142	313	0.0126	264	0.0195	167	0.0146	208	0.1779	425
106	csc-003	0.0053	179	0.0065	159	0.0037	153	0.0047	142	0.0074	181	0.0124	117	0.0112	169	0.1773	424
107	ctbcbank-000	0.0168	357	0.0250	356	0.0146	359	0.0224	355	0.0211	325	0.8964	408	0.3779	397	1.0000	500
108	ctbcbank-001	0.0155	351	0.0235	351	0.0148	364	0.0243	361	0.0207	321	0.9279	413	0.3469	391	1.0000	502
109	cu-face-002	0.0105	302	0.0116	257	0.0650	423	0.0568	400	0.0271	348	0.0139	124	0.0076	104	0.3984	460
110	cubox-002	0.0034	123	0.0041	91	0.0025	40	0.0025	26	0.0033	65	0.0064	41	0.0058	64	0.0480	340
111	cubox-003	0.0021	55	0.0028	48	0.0024	38	0.0026	30	0.0025	22	0.0046	8	0.0037	10	0.0314	243
112	cudocommunication-001	0.4777	473	1.0000	500	0.4373	456	0.5360	452	1.0000	499	1.0000	497	1.0000	501	1.0000	496
113	cuhkee-001	0.0036	133	0.0045	110	0.0031	116	0.0046	139	0.0051	136	0.0095	91	0.0079	109	0.1492	414
114	cybercore-002	0.0092	279	0.0119	260	0.0049	207	0.0072	213	0.9105	477	1.0000	481	1.0000	486	0.5484	470
115	cybercore-003	0.0155	352	0.0164	303	0.0032	125	0.0033	80	0.0024	13	0.9719	424	0.8213	439	0.0705	376
116	cyberextruder-003	0.0109	306	0.0169	308	0.0071	268	0.0112	275	0.0165	296	0.0410	241	0.0272	277	0.0302	216
117	cyberextruder-004	0.0118	317	0.0181	318	0.0081	290	0.0133	299	0.0191	316	0.0329	217	0.0268	275	0.0679	370
118	cyberlink-010	0.0011	14	0.0019	19	0.0041	179	0.0041	115	0.0039	92	0.1829	305	0.0054	52	0.0280	77
119	cyberlink-011	0.0010	7	0.0017	11	0.0035	142	0.0034	82	0.0045	116	0.0080	62	0.0070	94	0.0283	115
120	dahua-006	0.0027	88	0.0039	84	0.0031	113	0.0039	111	0.0039	93	0.0067	48	0.0058	62	0.0280	74
121	dahua-007	0.0017	37	0.0023	29	0.0026	60	0.0032	69	0.0033	61	0.0060	34	0.0054	50	0.0278	51
122	daon-000	0.0095	286	0.0117	259	0.0068	260	0.0077	228	0.0092	220	0.0174	156	0.0137	196	0.0331	266
123	decatur-000	0.0714	427	0.1115	425	0.0608	422	0.1106	426	0.0866	401	1.0000	479	0.0714	332	0.0658	366
124	decatur-001	0.0424	407	0.0711	413	0.0237	383	0.0458	386	0.0447	377	1.0000	471	0.9969	474	0.0280	82
125	deepglint-004	0.0025	82	0.0034	67	0.0039	171	0.0061	194	0.0050	132	0.0091	84	0.0082	117	0.0285	136
126	deepglint-005	0.0052	175	0.0059	151	0.0030	100	0.0031	63	0.0033	69	0.7620	384	0.1535	359	0.0320	255
127	deepsea-001	0.0136	338	0.0215	340	0.0142	356	0.0214	352	0.0163	294	0.0250	192	0.0192	245	0.0347	279
128	deepsense-001	0.0013	24	0.0019	16	0.0024	31	0.0025	24	0.0027	35	0.0115	111	0.0053	44	0.0285	130
129	deepsense-002	0.0010	8	0.0016	10	0.0024	19	0.0023	13	0.0026	25	0.0052	19	0.0043	22	0.0284	127
130	dermalog-010	0.0030	99	0.0041	89	0.0034	139	0.0037	104	0.0075	182	0.5181	356	0.2530	372	0.0275	26
131	dermalog-011	0.0045	156	0.0062	155	0.0035	143	0.0059	186	0.0057	152	0.2242	316	0.0407	297	0.0276	33
132	dicio-001	0.5486	484	0.6442	479	0.7516	478	0.8607	476	0.8678	471	0.8268	399	0.7034	426	0.3605	456

Table 23: FNMR is the proportion of mated comparisons below a threshold set to achieve the FMR given in the header on the fourth row. FMR is the proportion of impostor comparisons at or above that threshold. The light grey values give rank over all algorithms in that column. The pink columns use only same-sex impostors; others are selected regardless of demographics. The exception, in the green column, uses “matched-covariates” i.e. impostors of the same sex, age group, and country of birth. The second pink column includes effects of extended ageing. Missing entries for border, visa, mugshot and wild images generally mean the algorithm did not run to completion. The VISA columns compare images described in section 2.1. The MUGSHOT columns compare images described in section 2.5. The VISA-BORDER column compare images described in section 2.2 with those of section 2.4. The BORDER column compares images described in section 2.4. The WILD columns compare images described in section 2.7.

Algorithm	FALSE NON-MATCH RATE (FNMR)										LESS CONSTRAINED, NON-COOP.	
	CONSTRAINED, COOPERATIVE											
	Name	VISAMC	VISA	MUGSHOT	MUGSHOT12+YRS	VISABORDER	BORDER	BORDER	WILD			
FMR	0.0001	1E-06	1E-05	1E-05	1E-06	1E-06	1E-06	1E-05	0.0001			
133 didiglobalface-001	0.0055	187	0.0092	216	0.0030	102	0.0045	136	0.0088	209	0.0119	
134 didiglobalface-002	0.0033	117	0.0051	129	0.0026	61	0.0034	88	0.0033	64	0.0085	
135 digidata-000	0.0967	434	0.1410	431	0.2596	445	0.3462	443	0.0293	351	0.0363	
136 digidata-001	0.0224	380	0.0352	378	0.0330	400	0.0570	402	0.0109	249	0.0481	
137 digitalbarriers-002	0.3360	462	0.3690	454	0.0877	430	0.1557	431	0.0971	406	0.0951	
138 dps-000	0.0115	314	0.0176	315	0.0149	366	0.0185	340	0.0173	306	0.0275	
139 dsk-000	0.1526	444	0.2169	440	0.3787	451	0.5426	454	0.3115	436	0.3089	
140 einetworks-000	0.0099	290	0.0180	317	0.0088	306	0.0140	308	0.0130	266	0.0225	
141 ekin-002	0.1168	438	0.2042	439	0.1530	440	0.2524	439	0.1777	423	0.2773	
142 enface-001	0.0072	241	0.0107	244	0.0071	265	0.0138	305	0.0068	173	0.0515	
143 enface-002	0.0033	115	0.0052	135	0.0038	162	0.0073	217	0.0026	30	0.9998	
144 eocortex-000	0.3485	463	0.6943	485	0.1122	432	0.1574	432	0.2155	429	0.2257	
145 ercacat-001	0.0036	131	0.0044	107	0.0033	129	0.0047	143	0.0106	244	0.0202	
146 euronovate-001	0.2786	456	0.3608	453	0.4489	458	0.6105	459	0.5010	450	0.5392	
147 expasoft-001	0.0328	399	0.0488	392	0.0211	379	0.0342	375	0.0629	392	0.6483	
148 expasoft-002	0.0170	360	0.0274	364	0.0787	429	0.0768	411	0.1629	419	0.9996	
149 f8-001	0.0249	384	0.0336	373	0.0178	371	0.0232	357	0.0303	353	0.0615	
150 f8-002	0.0340	401	0.0591	406	0.0213	380	0.0374	380	0.0452	378	0.0760	
151 faceonlive-001	0.0269	388	0.0359	381	0.0387	406	0.0721	409	0.0246	341	0.0349	
152 faceonlive-002	0.0121	323	0.0135	275	0.0033	131	0.0041	117	0.0037	87	0.9427	
153 facephi-000	0.0044	154	0.0059	147	0.0047	198	0.0057	177	0.0088	210	1.0000	
154 facesoft-000	0.0085	268	0.0112	251	0.0064	253	0.0107	270	0.0091	215	0.0171	
155 facetag-000	0.2836	457	0.4081	459	0.2933	447	0.4303	448	0.3448	438	0.6312	
156 facetag-002	0.0098	288	0.0147	287	0.0064	254	0.0110	272	0.0116	258	0.0190	
157 facex-001	1.0000	501	1.0000	503	1.0000	496	-	1.0000	498	1.0000	491	
158 facex-002	0.0803	430	0.1404	430	0.1283	435	0.1979	436	0.1440	415	0.1952	
159 farfaces-001	0.4890	477	0.5860	476	0.5650	465	0.7268	467	0.8015	461	0.7511	
160 fastenterprises-000	0.0093	282	0.0151	295	0.0098	320	0.0140	309	0.0209	322	0.2991	
161 fiberhome-nanjing-003	0.0090	272	0.0139	280	0.0082	292	0.0144	314	0.0110	250	0.0174	
162 fiberhome-nanjing-004	0.0037	136	0.0056	145	0.0031	111	0.0043	126	0.0043	113	0.0083	
163 fincore-000	0.0309	397	0.0502	394	0.0281	392	0.0510	396	0.0521	385	0.0815	
164 firstcreditkz-001	0.0024	80	0.0034	64	0.0024	36	0.0024	19	0.0034	70	1.0000	
165 firstcreditkz-002	0.0018	45	0.0026	38	0.0024	28	0.0024	17	0.0029	47	0.0056	
166 foomobi-001	0.4827	475	0.5795	472	0.6823	471	0.8132	472	0.8217	463	1.0000	
167 frpkauai-001	0.0023	74	0.0035	74	0.0026	49	0.0030	59	0.0040	101	0.0080	
168 frpkauai-002	0.0024	81	0.0035	70	0.0024	34	0.0024	18	0.0033	68	0.0065	
169 fujitsulab-002	0.0091	277	0.0124	266	0.0105	327	0.0156	322	0.0169	301	0.0345	
170 fujitsulab-003	0.0045	157	0.0065	161	0.0057	236	0.0083	239	0.0080	191	0.0154	
171 g42-intelibrain-001	0.0006	2	0.0009	3	0.0037	151	0.0044	129	0.0030	52	0.0059	
172 geo-002	0.0171	362	0.0187	324	0.0035	141	0.0051	157	0.0064	165	0.0117	
173 geo-004	0.0030	98	0.0041	93	0.0025	45	0.0030	54	0.0035	81	0.0065	
174 glory-005	0.0056	190	0.0076	182	0.0054	229	0.0072	214	0.0075	183	0.9237	
175 glory-006	0.0050	166	0.0068	166	0.0051	216	0.0070	210	0.0069	174	0.7869	
176 gorilla-008	0.0058	200	0.0091	213	0.0049	206	0.0079	235	0.0079	190	0.0126	

Table 24: FNMR is the proportion of mated comparisons below a threshold set to achieve the FMR given in the header on the fourth row. FMR is the proportion of impostor comparisons at or above that threshold. The light grey values give rank over all algorithms in that column. The pink columns use only same-sex impostors; others are selected regardless of demographics. The exception, in the green column, uses “matched-covariates” i.e. impostors of the same sex, age group, and country of birth. The second pink column includes effects of extended ageing. Missing entries for border, visa, mugshot and wild images generally mean the algorithm did not run to completion. The VISA columns compare images described in section 2.1. The MUGSHOT columns compare images described in section 2.5. The VISA-BORDER column compare images described in section 2.2 with those of section 2.4. The BORDER column compares images described in section 2.4. The WILD columns compare images described in section 2.7.

	Algorithm	FALSE NON-MATCH RATE (FNMR)								LESS CONSTRAINED, NON-COOP.							
		CONSTRAINED, COOPERATIVE															
		Name	VISAMC	VISA	MUGSHOT	MUGSHOT12+YRS	VISA BORDER	BORDER	BORDER								
	FMR	0.0001	1E-06	1E-05	1E-05	1E-05	1E-06	1E-06	1E-05	0.0001							
177	gorilla-009	0.0049	165	0.0072	170	0.0038	158	0.0056	173	0.0065	168	0.0104	98	0.0070	92	0.0278	54
178	graymatics-001	0.1039	435	0.1620	435	0.1344	437	0.1917	435	0.1648	420	0.5160	354	0.2689	378	0.3057	450
179	griaule-001	0.0057	194	0.0078	189	0.0045	195	0.0065	202	0.0070	175	0.7515	381	0.5106	411	0.0277	45
180	griaule-002	0.0021	60	0.0032	58	0.0025	48	0.0027	36	0.0034	76	0.0996	286	0.0201	253	0.0279	68
181	hertasecurity-002	0.0206	375	0.0315	369	0.0060	244	0.0078	231	0.0253	343	0.0696	271	0.0457	306	0.0523	346
182	hertasecurity-003	0.0079	258	0.0104	240	0.0060	245	0.0078	229	0.0255	344	0.0732	272	0.0460	307	0.0382	302
183	hik-001	0.0096	287	0.0125	267	0.0093	315	0.0164	328	0.0108	248	0.0937	280	0.0127	189	0.0271	6
184	hisign-001	0.0036	130	0.0050	124	0.0034	136	0.0046	138	0.0079	189	0.0153	137	0.0133	193	0.0286	143
185	hisign-002	0.0029	95	0.0044	104	0.0027	76	0.0032	74	0.0028	40	0.0409	240	0.0132	192	0.0286	139
186	hyperverge-003	0.0019	51	0.0030	53	0.0025	41	0.0029	52	0.0027	32	0.0049	16	0.0042	19	0.0280	83
187	hyperverge-004	0.0072	243	0.0116	258	0.0040	175	0.0071	211	0.0058	155	0.0080	63	0.0057	58	0.0279	62
188	hzailu-003	0.0178	366	0.0291	368	0.0031	118	0.0042	124	0.0035	78	0.0061	38	0.0052	41	0.0524	347
189	hzailu-004	0.0175	365	0.0197	332	0.0031	119	0.0042	122	0.0034	74	0.0060	35	0.0051	37	0.0528	350
190	icm-003	0.0138	340	0.0222	345	0.0149	365	0.0282	368	0.0227	329	0.0384	237	0.0257	271	0.0333	268
191	icm-004	0.0079	255	0.0120	261	0.0074	274	0.0107	269	0.0091	217	0.0281	206	0.0128	191	0.0315	244
192	ichthc-000	0.0260	385	0.0396	386	0.0207	378	0.0339	374	0.0291	350	0.0474	249	0.0346	288	0.0459	334
193	id3-006	0.0072	242	0.0103	237	0.0049	208	0.0074	220	0.0095	224	0.0165	148	0.0119	182	0.9938	492
194	id3-008	0.0039	141	0.0055	142	0.0032	123	0.0042	121	0.0081	196	0.0155	139	0.0134	194	0.8856	486
195	idemia-008	0.0023	73	0.0032	61	0.0023	17	0.0028	38	0.0034	77	0.0067	47	0.0056	56	0.0290	172
196	idemia-009	0.0022	67	0.0030	55	0.0022	7	0.0023	15	0.0023	11	0.0046	9	0.0039	12	0.0285	129
197	identy-000	0.0073	245	0.0095	221	0.0050	210	0.0067	205	0.0071	178	0.8257	398	0.4310	402	0.2662	447
198	igearx-face-000	0.0091	275	0.0146	286	0.0163	369	0.0362	378	0.0399	368	0.6436	368	0.3305	389	0.0282	100
199	iit-002	0.0111	311	0.0177	316	0.0085	299	0.0140	307	0.0193	317	0.0332	220	0.0260	273	0.1373	409
200	iit-003	0.0082	265	0.0151	294	0.0053	223	0.0084	243	0.0122	261	0.0199	171	0.0137	195	0.0407	311
201	imds-software-001	0.0126	332	0.0228	346	0.0130	352	0.0221	354	0.0231	331	0.0469	248	0.0199	252	0.0365	295
202	imds-software-002	0.0048	161	0.0072	173	0.0036	148	0.0052	160	0.0047	124	0.9981	451	0.0078	107	0.0274	23
203	imperial-000	0.0067	223	0.0108	248	0.0080	287	0.0134	302	0.0087	207	0.0581	257	0.0102	150	0.0281	91
204	imperial-002	0.0058	202	0.0081	196	0.0055	231	0.0085	246	0.0083	201	0.0157	140	0.0103	151	0.0273	17
205	incode-010	0.0041	147	0.0063	156	0.0028	90	0.0043	125	0.0047	126	0.0077	59	0.0061	74	0.0296	201
206	incode-011	0.0032	105	0.0044	106	0.0026	64	0.0034	84	0.0032	57	0.0359	229	0.0140	200	0.0295	197
207	infocert-001	0.0105	301	0.0172	310	0.0078	281	0.0125	286	0.0159	288	0.1573	300	0.0565	320	0.0307	228
208	innefulabs-000	0.0122	325	0.0199	333	0.0112	339	0.0197	345	0.0222	327	0.0372	235	0.0271	276	0.0348	282
209	innovativetechnologyltd-001	0.0578	420	0.0938	423	0.0501	414	0.0981	418	0.0592	389	0.0779	275	0.0422	300	0.0449	333
210	innovativetechnologyltd-002	0.0451	410	0.0716	414	0.0541	417	0.1009	420	0.0506	383	0.0682	267	0.0371	293	0.0804	388
211	innovatrics-008	0.0047	160	0.0064	158	0.0038	163	0.0052	159	0.0053	139	0.0088	81	0.0069	91	0.0287	144
212	innovatrics-009	0.0022	62	0.0031	57	0.0028	82	0.0032	72	0.0034	72	0.1165	294	0.0326	283	0.0279	61
213	insightface-003	0.0015	32	0.0021	24	0.0045	194	0.0034	87	0.1298	409	1.0000	493	0.9407	452	0.0277	43
214	insightface-004	0.0015	29	0.0023	30	0.0052	220	0.0036	98	0.1403	413	0.9923	442	0.9128	447	0.0279	67
215	inspur-000	0.0060	210	0.0078	187	0.7415	477	0.9093	485	0.2838	435	0.9996	459	0.9976	475	0.0283	113
216	inspur-001	0.0035	125	0.0049	122	0.0025	42	0.0030	57	0.0029	46	0.9951	445	0.9592	457	0.0274	19
217	intellicloudai-001	0.0142	343	0.0234	350	0.0092	312	0.0145	315	0.0162	292	0.0371	234	0.0171	226	0.0409	314
218	intellicloudai-002	0.0059	207	0.0085	203	0.0060	246	0.0069	209	0.0108	246	0.2477	324	0.0171	225	0.0303	217
219	intellifusion-001	0.0072	239	0.0094	220	0.0056	235	0.0085	247	0.0111	253	0.0212	178	0.0143	204	0.0289	162
220	intellifusion-002	0.0059	206	0.0077	183	0.0040	176	0.0074	219	0.0085	205	0.5352	357	0.0104	156	0.0305	221

Table 25: FNMR is the proportion of mated comparisons below a threshold set to achieve the FMR given in the header on the fourth row. FMR is the proportion of impostor comparisons at or above that threshold. The light grey values give rank over all algorithms in that column. The pink columns use only same-sex impostors; others are selected regardless of demographics. The exception, in the green column, uses “matched-covariates” i.e. impostors of the same sex, age group, and country of birth. The second pink column includes effects of extended ageing. Missing entries for border, visa, mugshot and wild images generally mean the algorithm did not run to completion. The VISA columns compare images described in section 2.1. The MUGSHOT columns compare images described in section 2.5. The VISA-BORDER column compare images described in section 2.2 with those of section 2.4. The BORDER column compares images described in section 2.4. The WILD columns compare images described in section 2.7.

	Algorithm	FALSE NON-MATCH RATE (FNMR)															
		CONSTRAINED, COOPERATIVE								LESS CONSTRAINED, NON-COOP.							
		Name	VISAMC	VISA	MUGSHOT	MUGSHOT12+YRS	VISABORDER	BORDER	BORDER	WILD							
	FMR	0.0001	1E-06	1E-05	1E-05	1E-05	1E-06	1E-06	1E-05	0.0001							
221	intellivision-004	0.0271	390	0.0559	402	0.0294	398	0.0503	395	0.0327	357	0.0461	246	0.0293	281	0.0645	365
222	intellivision-005	0.0105	303	0.0182	320	0.0093	316	0.0141	310	0.0146	284	0.0252	193	0.0172	227	0.0300	209
223	intellivix-002	0.0062	213	0.0085	204	0.0039	168	0.0056	171	0.0060	159	0.3464	336	0.0857	339	0.0289	163
224	intellivix-003	0.0075	250	0.0125	268	0.0052	219	0.0091	254	0.0066	169	0.0297	209	0.0096	142	0.0286	141
225	intelresearch-005	0.0016	34	0.0023	31	0.0028	81	0.0034	83	0.0042	109	0.0084	71	0.0066	81	0.0290	171
226	intelresearch-006	0.0010	10	0.0015	7	0.0026	68	0.0028	46	0.0032	59	0.8123	394	0.4742	407	0.0291	178
227	intema-000	0.0012	21	0.0017	13	0.0023	8	0.0022	10	0.0022	9	0.0172	153	0.0061	73	0.0279	66
228	intema-001	0.0010	11	0.0014	5	0.0021	3	0.0020	6	0.0019	6	0.0037	5	0.0030	4	0.0282	103
229	intsysmsu-001	0.9543	500	0.9888	499	0.9923	493	-		0.9977	487	0.9955	446	0.9892	465	0.7871	483
230	intsysmsu-002	0.0130	335	0.0254	358	0.0137	354	0.0267	366	0.0160	289	0.0267	199	0.0145	207	0.0289	166
231	ionetworks-000	0.0060	211	0.0087	208	0.0044	188	0.0058	182	0.0080	195	0.0144	129	0.0112	167	0.0319	253
232	iqface-000	0.0091	278	0.0143	281	0.0075	276	0.0110	273	0.0171	305	0.2234	315	0.0359	290	0.0381	301
233	iqface-003	0.0058	204	0.0079	192	0.0051	215	0.0058	183	0.0104	242	0.0200	172	0.0193	246	0.0402	305
234	irex-000	0.0052	173	0.0099	232	0.0056	234	0.0083	240	0.0137	274	0.0163	146	0.0078	106	0.0285	132
235	isap-001	0.5092	479	0.6588	481	0.6899	474	0.7978	471	0.7200	456	0.7253	376	0.5373	413	0.1931	427
236	isap-002	0.0114	313	0.0186	323	0.0087	304	0.0151	320	0.0156	287	0.5134	353	0.0333	284	0.0354	290
237	isityou-000	0.5682	486	0.7033	487	1.0000	498	-		1.0000	501	1.0000	495	1.0000	503	1.0000	497
238	isystems-001	0.0149	348	0.0245	354	0.0138	355	0.0210	350	0.0209	324	0.0332	219	0.0223	262	0.0524	349
239	isystems-002	0.0118	316	0.0182	319	0.0111	336	0.0162	326	0.0166	297	0.0284	208	0.0195	248	0.0516	344
240	itmo-007	0.0080	260	0.0125	269	0.0107	329	0.0185	338	0.0167	299	0.0222	182	0.0144	206	0.0300	210
241	itmo-008	0.0090	274	0.0150	291	0.0058	238	0.0059	188	0.0187	313	0.0355	228	0.0339	285	0.1498	415
242	ivacognitive-001	0.0189	369	0.0351	377	0.0123	348	0.0235	358	0.0198	319	0.0274	201	0.0155	217	0.0296	199
243	iws-000	0.4824	474	0.5801	473	0.6859	473	0.8155	473	0.8251	464	0.7756	387	0.6400	420	0.3251	453
244	jaakit-001	0.5830	487	0.7146	488	0.8173	484	0.8893	482	0.8950	474	0.8387	402	0.7091	428	0.5849	474
245	kakao-007	0.0019	50	0.0028	47	0.0024	23	0.0026	27	0.0033	63	0.0061	36	0.0053	45	0.0427	321
246	kakao-008	0.0011	15	0.0018	15	0.0023	9	0.0023	12	0.0021	8	0.0041	6	0.0035	7	0.0427	322
247	kakaobank-000	0.0041	149	0.0058	146	0.0041	180	0.0058	185	0.0060	160	0.9988	454	0.3243	387	0.0280	79
248	kakaopay-001	0.0152	350	0.0252	357	0.0145	358	0.0270	367	0.0232	332	0.0344	225	0.0194	247	0.0416	317
249	kasikornlabs-000	0.0112	312	0.0184	321	0.0086	302	0.0137	304	0.0130	268	0.0225	183	0.0148	212	0.0674	368
250	kasikornlabs-002	0.0069	227	0.0091	214	0.0048	202	0.0063	197	0.0076	185	0.0144	128	0.0110	165	0.0670	367
251	kedacom-000	0.0055	185	0.0081	197	0.0111	338	0.0120	280	0.0415	371	0.0966	284	0.0686	329	0.2511	441
252	kiwitech-000	0.0076	251	0.0105	241	0.0081	291	0.0128	294	0.0096	227	0.0163	145	0.0101	148	0.0279	70
253	kneron-003	0.0542	419	0.0902	421	0.0346	404	0.0562	399	0.0919	404	0.1251	297	0.0973	345	0.3053	449
254	kneron-005	0.0157	353	0.0259	360	0.0126	351	0.0212	351	0.0406	370	0.0693	270	0.0542	318	0.0471	337
255	knowutech-000	0.0039	142	0.0055	141	0.0028	93	0.0042	120	0.0042	107	0.0077	57	0.0059	70	0.0271	7
256	kookmin-002	0.0054	183	0.0077	186	0.0043	186	0.0065	201	0.0123	262	0.7591	383	0.0198	251	0.0285	134
257	koreaid-001	0.0031	104	0.0045	109	0.0026	59	0.0032	70	0.0043	112	0.0083	68	0.0068	87	0.0318	252
258	krungthai-002	0.0105	300	0.0161	299	0.0091	309	0.0141	311	0.7350	457	0.9889	436	0.9605	458	0.0620	360
259	kuke3d-001	0.0058	198	0.0104	239	0.0083	294	0.0093	257	0.0270	347	0.9901	437	0.8341	440	0.0404	306
260	kuke3d-002	0.0077	253	0.0135	276	0.0069	262	0.0098	265	0.0111	252	1.0000	483	1.0000	489	0.0316	247
261	lebentech-000	0.5940	488	0.7032	486	0.8854	487	0.9511	487	0.9089	476	0.9970	447	0.9861	464	0.6250	475
262	lemalabs-001	0.0111	310	0.0175	313	0.0088	305	0.0142	312	0.0143	278	0.0228	185	0.0140	199	0.0281	86
263	lineclova-002	0.0021	57	0.0035	68	0.0025	39	0.0027	33	0.0041	103	0.0086	77	0.0072	96	0.0279	57
264	lineclova-003	0.0018	46	0.0030	54	0.0028	91	0.0031	64	0.0041	104	0.0083	69	0.0075	103	0.0333	269

Table 26: FNMR is the proportion of mated comparisons below a threshold set to achieve the FMR given in the header on the fourth row. FMR is the proportion of impostor comparisons at or above that threshold. The light grey values give rank over all algorithms in that column. The pink columns use only same-sex impostors; others are selected regardless of demographics. The exception, in the green column, uses “matched-covariates” i.e. impostors of the same sex, age group, and country of birth. The second pink column includes effects of extended ageing. Missing entries for border, visa, mugshot and wild images generally mean the algorithm did not run to completion. The VISA columns compare images described in section 2.1. The MUGSHOT columns compare images described in section 2.5. The VISA-BORDER column compare images described in section 2.2 with those of section 2.4. The BORDER column compares images described in section 2.4. The WILD columns compare images described in section 2.7.

	Algorithm	FALSE NON-MATCH RATE (FNMR)										LESS CONSTRAINED, NON-COOP.					
		CONSTRAINED, COOPERATIVE								WILD							
		Name	VISAMC	VISA	MUGSHOT	MUGSHOT12+YRS	VISABORDER	BORDER	BORDER								
		FMR	0.0001	1E-06	1E-05	1E-05	1E-06	1E-06	1E-05		0.0001						
265	lookman-002	0.0297	395	0.0547	401	0.0339	402	0.0562	398	0.0614	391	0.0960	283	0.0790	335	0.2640	445
266	lookman-004	0.0074	247	0.0099	230	0.0124	350	0.0149	319	0.0430	374	0.0866	278	0.0694	330	0.2516	442
267	luxand-000	0.2056	448	0.2814	445	0.4053	453	0.5365	453	0.3497	439	0.3743	340	0.2605	375	0.2222	435
268	mantra-000	0.0037	135	0.0052	133	0.0054	226	0.0056	174	0.0097	232	0.0181	160	0.0151	215	0.0350	284
269	maxvision-002	0.0070	232	0.0107	243	0.0061	247	0.0093	256	0.0080	192	0.5726	360	0.2943	383	0.0372	297
270	maxvision-003	0.0056	189	0.0083	201	0.0038	164	0.0060	189	0.0061	162	0.2614	325	0.0650	327	0.0376	299
271	megvii-005	0.0010	12	0.0015	6	0.0026	57	0.0031	67	0.0019	5	0.0500	252	0.0057	59	0.0292	183
272	megvii-006	0.0011	13	0.0016	8	0.0026	65	0.0033	79	0.0025	19	0.0050	17	0.0048	31	0.0296	200
273	meituuan-002	0.0017	40	0.0025	34	0.0024	27	0.0023	11	0.0024	18	0.0067	49	0.0044	24	0.0312	239
274	meituuan-003	0.0017	41	0.0021	23	0.0024	25	0.0023	16	0.0024	16	0.0084	72	0.0046	26	0.0316	246
275	meiya-001	0.0171	361	0.0275	365	0.0159	368	0.0261	365	0.0311	354	0.2250	318	0.0245	268	0.0363	294
276	mendaxiatech-000	0.0027	89	0.0036	76	0.0029	95	0.0036	100	0.0031	55	0.0057	30	0.0051	38	0.0275	30
277	metsakuurcompany-002	0.0048	162	0.0071	169	0.0030	105	0.0043	128	0.0032	60	0.2059	313	0.0665	328	0.0408	312
278	metsakuurcompany-003	0.0034	122	0.0051	127	0.0026	58	0.0036	94	0.0028	38	0.2418	322	0.1001	347	0.0406	309
279	miaxis-001	0.0068	225	0.0099	231	0.0059	242	0.0097	264	0.0096	229	0.0231	187	0.0109	164	0.0298	205
280	miaxis-002	0.0745	429	0.0774	417	0.3215	448	0.4000	447	0.1485	416	0.2087	314	0.2058	368	0.3512	455
281	microfocus-002	0.3605	464	0.5057	467	0.5783	467	0.7223	466	0.5909	452	0.5963	362	0.4160	401	0.1582	417
282	microfocus-003	0.0416	405	0.0607	407	0.0652	424	0.1025	421	0.0793	397	0.2248	317	0.0923	342	0.0709	377
283	minivision-000	0.0033	113	0.0048	118	0.0038	161	0.0049	147	0.0055	144	0.0094	90	0.0079	111	0.0273	13
284	mitek-000	0.6882	493	0.8192	493	0.9568	490	-		0.9545	483	0.9437	419	0.8494	443	0.5836	473
285	mobai-000	0.0360	403	0.0439	390	0.0372	405	0.0700	407	0.0367	364	0.0939	281	0.0795	336	0.2640	446
286	mobai-001	0.0199	374	0.0219	341	0.0047	199	0.0061	191	0.0093	222	0.0174	155	0.0138	198	0.1045	400
287	mobbl-001	0.3208	458	0.4375	460	0.5680	466	0.7193	465	0.6282	453	0.5783	361	0.3984	399	0.1866	426
288	mobbl-003	0.0087	270	0.0134	274	0.0062	249	0.0087	249	0.0099	235	0.0197	168	0.0122	187	0.0312	237
289	mobilpinotech-000	0.0090	273	0.0149	290	0.0039	174	0.0057	175	0.0115	257	0.0465	247	0.0182	236	0.0315	245
290	moreedian-000	0.3874	466	0.4912	465	0.9988	494	-		0.9990	489	0.9999	468	0.9998	483	0.4788	465
291	mukh-002	0.0269	389	0.0357	380	0.0435	411	0.0799	413	0.0143	279	0.0213	179	0.0122	186	0.0345	276
292	mukh-003	0.0077	254	0.0113	252	0.0111	337	0.0224	356	0.0061	163	0.7813	389	0.4504	405	0.0284	123
293	multimodality-000	0.0034	120	0.0047	116	0.0036	150	0.0044	132	0.0077	187	0.9976	449	0.4456	404	0.0287	145
294	multimodality-001	0.0029	96	0.0042	96	0.0031	109	0.0035	90	0.0038	88	0.0071	50	0.0059	69	0.0281	90
295	mvision-001	0.0191	370	0.0233	348	0.0204	376	0.0356	377	0.0198	320	0.0337	222	0.0242	267	0.0431	323
296	nazhiae-000	0.0040	146	0.0059	152	0.0036	145	0.0048	145	0.0057	151	0.0125	118	0.0083	121	0.0275	31
297	ncssg-001	0.0207	376	0.1540	433	0.0045	193	0.0067	207	0.0056	150	0.1180	295	0.0301	282	0.0559	355
298	neosystems-004	0.0279	392	0.0495	393	0.0289	394	0.0585	405	0.0439	376	0.9621	421	0.1296	351	0.0333	270
299	netbridgegetech-001	0.4749	472	0.6599	482	0.4438	457	0.5676	456	0.4491	448	1.0000	473	0.9541	455	0.1098	404
300	netbridgegetech-002	0.0101	294	0.0166	306	0.0077	279	0.0127	291	0.0133	270	0.8215	396	0.0523	316	0.0351	286
301	neurotechnology-015	0.0022	65	0.0036	79	0.0024	22	0.0028	45	0.0030	49	0.0052	20	0.0041	18	0.0276	37
302	neurotechnology-016	0.0022	66	0.0032	60	0.0023	14	0.0027	34	0.0027	31	0.0049	15	0.0039	14	0.0276	34
303	nhn-002	0.0068	226	0.0096	222	0.0057	237	0.0087	251	0.0136	273	0.0253	195	0.0186	242	0.0302	214
304	nhn-003	0.0033	110	0.0048	119	0.0027	73	0.0038	106	0.0036	85	0.0198	169	0.0071	95	0.0285	137
305	nodeflux-002	0.0186	368	0.0340	374	0.0261	388	0.0451	385	0.0548	386	1.0000	480	1.0000	487	0.0299	207
306	nominder-000	0.0025	84	0.0036	77	0.0029	97	0.0033	78	0.0026	28	0.9919	441	0.8877	445	0.0276	39
307	notiontag-001	0.6846	492	0.8006	492	0.3955	452	0.5247	451	0.8669	469	0.8313	401	0.6362	419	0.2221	434
308	notiontag-002	0.0066	222	0.0089	209	0.0045	192	0.0061	192	0.0077	188	0.0137	123	0.0104	154	0.0299	206

Table 27: FNMR is the proportion of mated comparisons below a threshold set to achieve the FMR given in the header on the fourth row. FMR is the proportion of impostor comparisons at or above that threshold. The light grey values give rank over all algorithms in that column. The pink columns use only same-sex impostors; others are selected regardless of demographics. The exception, in the green column, uses “matched-covariates” i.e. impostors of the same sex, age group, and country of birth. The second pink column includes effects of extended ageing. Missing entries for border, visa, mugshot and wild images generally mean the algorithm did not run to completion. The VISA columns compare images described in section 2.1. The MUGSHOT columns compare images described in section 2.5. The VISA-BORDER column compare images described in section 2.2 with those of section 2.4. The BORDER column compares images described in section 2.4. The WILD columns compare images described in section 2.7.

	Algorithm	FALSE NON-MATCH RATE (FNMR)										LESS CONSTRAINED, NON-COOP.					
		CONSTRAINED, COOPERATIVE								WILD							
		Name	VISAMC	VISA	MUGSHOT	MUGSHOT12+YRS	VISABORDER	BORDER	BORDER								
	FMR	0.0001	1E-06	1E-05	1E-05	1E-05	1E-06	1E-06	1E-05		0.0001						
309	nsensecorp-004	0.1370	441	0.1397	429	0.0066	257	0.0094	259	1.0000	500	1.0000	496	1.0000	502	0.0805	389
310	nsensecorp-005	0.0055	188	0.0080	194	0.0039	169	0.0058	184	0.2723	434	0.9999	467	0.9949	469	0.0271	8
311	ntechlab-011	0.0012	17	0.0019	17	0.0024	29	0.0028	50	0.0029	45	0.0055	24	0.0047	29	0.0288	154
312	ntechlab-012	0.0011	16	0.0016	9	0.0023	18	0.0030	56	0.0026	26	0.0050	18	0.0043	20	0.0280	81
313	omface-000	0.2573	454	0.3835	457	0.3590	450	0.4903	450	0.3956	445	0.5003	352	0.2595	374	0.2400	438
314	omface-001	0.0137	339	0.0212	339	0.0114	343	0.0187	341	0.0174	308	1.0000	498	0.0214	259	0.0789	384
315	omnigarde-001	0.0168	358	0.0260	361	0.0203	375	0.0402	381	0.0243	339	0.0327	216	0.0177	230	0.0288	152
316	omnigarde-002	0.0033	116	0.0046	114	0.0027	79	0.0039	108	0.0041	105	0.0076	56	0.0059	72	0.0278	55
317	onfido-000	0.1472	443	0.2881	446	0.0335	401	0.0731	410	0.0515	384	0.9915	440	0.9579	456	0.0731	380
318	openface-001	0.1804	445	0.2921	447	0.2878	446	0.3906	446	0.2054	428	0.2338	321	0.1549	360	0.2445	439
319	oz-003	0.0095	285	0.0143	282	0.0054	227	0.0077	227	0.0096	228	0.0175	157	0.0118	179	0.0288	158
320	oz-004	0.0033	118	0.0049	123	0.0038	165	0.0055	168	0.0081	197	0.0163	147	0.0142	203	0.0329	264
321	palit-000	0.0062	215	0.0084	202	0.0039	167	0.0055	167	0.0055	146	0.4610	349	0.2468	371	0.0280	80
322	palit-001	0.0050	167	0.0068	168	0.0032	126	0.0047	144	0.0045	118	0.0110	106	0.0058	67	0.0287	147
323	pangiam-000	0.0031	101	0.0043	102	0.0026	52	0.0030	61	0.0038	89	0.0071	52	0.0061	77	0.0424	320
324	pangiam-001	0.0031	103	0.0044	103	0.0029	96	0.0040	114	0.0028	39	0.0362	231	0.0056	55	0.0437	328
325	papago-001	0.0067	224	0.0096	226	0.0051	217	0.0077	226	0.0071	176	0.0126	119	0.0086	128	0.0816	391
326	papsav1923-002	0.0021	61	0.0034	66	0.0026	53	0.0030	60	0.0048	127	0.0093	87	0.0086	126	0.0312	238
327	papsav1923-003	0.0025	83	0.0035	73	0.0024	37	0.0025	21	0.0034	71	0.0066	45	0.0058	66	0.0281	94
328	paravision-010	0.0012	20	0.0021	21	0.0022	6	0.0021	8	0.0027	34	0.0055	25	0.0050	36	0.0288	159
329	paravision-011	0.0008	4	0.0020	20	0.0021	4	0.0020	5	0.0026	27	0.0053	21	0.0049	34	0.0289	167
330	pensees-001	0.0087	271	0.0133	273	0.0071	267	0.0122	284	0.0145	282	0.0252	194	0.0195	249	0.0283	112
331	pixelall-008	0.0015	27	0.0023	32	0.0034	140	0.0049	146	0.0031	54	0.0057	29	0.0052	40	0.0278	49
332	pixelall-009	0.0018	44	0.0025	36	0.0024	33	0.0026	28	0.0031	56	0.3475	337	0.0053	46	0.0276	35
333	privid-001	0.3350	461	0.5013	466	0.4327	455	0.5880	457	0.9790	485	1.0000	478	0.9998	482	0.2043	430
334	psl-010	0.0017	43	0.0035	72	0.0023	10	0.0025	20	0.0035	80	0.0104	99	0.0052	43	0.0282	97
335	psl-011	0.0013	23	0.0026	41	0.0021	1	0.0021	7	0.0024	14	0.0047	10	0.0035	8	0.0285	133
336	ptakuratsatu-000	0.0060	208	0.0089	211	0.0070	264	0.0104	268	0.0096	230	0.0152	135	0.0100	145	0.0284	118
337	pxl-001	0.0488	413	0.0752	416	0.0586	420	0.1087	422	0.0946	405	0.1065	288	0.0625	325	0.1088	402
338	pyramid-000	0.0136	337	0.0233	349	0.0117	345	0.0192	343	0.0185	312	0.0322	215	0.0206	255	0.0304	220
339	qazbs-000	0.0058	196	0.0083	200	0.0046	197	0.0072	212	0.0130	267	0.0244	190	0.0196	250	0.0297	204
340	qluevision-001	0.0223	378	0.0419	388	0.0205	377	0.0343	376	0.0327	358	0.8762	405	0.7413	431	0.0460	335
341	qnap-002	0.0122	324	0.0191	327	0.0075	277	0.0095	262	0.0146	283	0.0281	207	0.0184	238	0.0352	288
342	qnap-003	0.0637	423	0.0657	410	0.0058	239	0.0078	230	0.0082	199	0.9985	453	0.9658	462	0.0287	146
343	quantasoft-003	0.0081	263	0.0113	254	0.0056	233	0.0076	223	0.0091	218	0.0161	144	0.0107	161	0.0414	316
344	rankone-013	0.0028	91	0.0041	90	0.0026	54	0.0033	76	0.0028	42	0.0055	27	0.0040	16	0.0291	177
345	rankone-014	0.0016	36	0.0021	22	0.0024	20	0.0027	32	0.0022	10	0.0047	11	0.0035	6	0.0293	186
346	realnetworks-007	0.0031	102	0.0051	128	0.0028	86	0.0035	91	0.0048	128	0.0091	83	0.0074	101	0.0279	58
347	realnetworks-008	0.0022	69	0.0039	85	0.0038	157	0.0045	134	0.0055	142	0.0100	96	0.0080	115	0.0292	182
348	regula-000	0.0184	367	0.0376	384	0.0103	324	0.0185	337	0.0120	259	0.9983	452	0.0231	264	0.0273	16
349	regula-001	0.0072	240	0.0107	247	0.0102	322	0.0179	334	0.0123	263	0.0333	221	0.0174	228	0.0295	191
350	remarkai-001	0.0144	344	0.0256	359	0.0102	321	0.0159	325	0.0162	293	0.0582	258	0.0185	240	0.0308	231
351	remarkai-003	0.0047	159	0.0063	157	0.0033	133	0.0049	149	0.0054	140	0.0100	95	0.0072	98	0.0275	32
352	rendip-000	0.0055	186	0.0077	185	0.0048	204	0.0060	190	0.0080	193	0.0142	127	0.0110	166	0.0433	325

Table 28: FNMR is the proportion of mated comparisons below a threshold set to achieve the FMR given in the header on the fourth row. FMR is the proportion of impostor comparisons at or above that threshold. The light grey values give rank over all algorithms in that column. The pink columns use only same-sex impostors; others are selected regardless of demographics. The exception, in the green column, uses “matched-covariates” i.e. impostors of the same sex, age group, and country of birth. The second pink column includes effects of extended ageing. Missing entries for border, visa, mugshot and wild images generally mean the algorithm did not run to completion. The VISA columns compare images described in section 2.1. The MUGSHOT columns compare images described in section 2.5. The VISA-BORDER column compare images described in section 2.2 with those of section 2.4. The BORDER column compares images described in section 2.4. The WILD columns compare images described in section 2.7.

Algorithm	Name	FALSE NON-MATCH RATE (FNMR)										LESS CONSTRAINED, NON-COOP.					
		CONSTRAINED, COOPERATIVE								WILD							
		VISAMC	VISA	MUGSHOT	MUGSHOT12+YRS	VISABORDER	BORDER	BORDER	1E-06	1E-05	0.0001						
FMR		0.0001	1E-06	1E-05	1E-05	1E-06	1E-06	1E-06		1E-05							
353	revealmedia-005	0.0050	170	0.0074	179	0.0050	211	0.0068	208	0.0075	184	0.0124	116	0.0104	157	0.3960	459
354	revealmedia-006	0.0040	145	0.0067	164	0.0041	182	0.0056	170	0.0056	147	0.0085	76	0.0068	85	0.0278	53
355	rokid-000	0.0093	283	0.0145	284	0.0073	273	0.0102	267	0.0164	295	0.0280	204	0.0214	258	0.0857	394
356	rokid-001	0.0105	299	0.0162	300	0.0094	318	0.0163	327	0.0181	309	0.0276	203	0.0165	222	0.0325	259
357	s1-005	0.0024	78	0.0036	78	0.0025	47	0.0029	53	0.0026	29	0.0048	13	0.0038	11	0.0359	293
358	s1-007	0.0023	75	0.0056	144	0.0024	21	0.0028	39	0.0025	21	0.0048	12	0.0039	13	0.0366	296
359	saffe-001	0.4339	470	0.5261	469	0.7539	480	0.8736	481	0.7977	460	0.9810	426	0.7435	432	0.3887	458
360	saffe-002	0.0119	320	0.0206	334	0.0107	332	0.0177	332	0.0244	340	0.9998	464	0.2785	379	0.0308	230
361	samsungsds-001	0.0015	30	0.0026	40	0.0023	13	0.0023	14	0.0024	15	0.1660	302	0.0536	317	0.0282	96
362	samsungsds-002	0.0017	42	0.0027	42	0.0023	11	0.0022	9	0.0021	7	0.0043	7	0.0036	9	0.0283	110
363	samtech-001	0.0197	372	0.0365	382	0.0146	362	0.0241	360	0.0238	338	0.0394	238	0.0251	269	0.0337	271
364	scanovate-002	0.0175	364	0.0355	379	0.0146	360	0.0286	369	0.0269	346	0.0301	210	0.0178	232	0.0301	213
365	scanovate-003	0.0054	181	0.0080	195	0.0054	224	0.0072	216	0.0312	355	0.0599	259	0.0568	321	0.0283	111
366	sdc-000	0.0303	396	0.0526	398	0.0572	419	0.1094	424	0.0867	402	0.6230	365	0.3682	395	0.1201	407
367	securifai-005	0.0125	328	0.0190	325	0.0080	288	0.0126	289	0.0134	271	0.9861	430	0.9205	448	0.0329	263
368	securifai-006	0.0140	342	0.0196	330	0.0067	259	0.0102	266	0.0113	255	0.9888	435	0.9239	449	0.0346	278
369	sensetime-007	0.0012	18	0.0022	25	0.0021	5	0.0020	4	0.0018	3	0.0034	3	0.0029	1	0.0280	75
370	sensetime-008	0.0008	5	0.0014	4	0.0021	2	0.0020	3	0.0018	4	0.0036	4	0.0033	5	0.0284	125
371	sertis-000	0.0118	318	0.0208	336	0.0080	284	0.0127	290	0.0110	251	0.0176	158	0.0114	172	0.0285	135
372	sertis-002	0.0049	163	0.0061	153	0.0039	173	0.0061	195	0.0055	143	0.0099	94	0.0070	93	0.0281	88
373	seventhsense-001	0.0034	124	0.0047	117	0.0025	46	0.0031	66	0.0029	44	0.0338	223	0.0109	163	0.0279	60
374	seventhsense-002	0.0036	132	0.0050	125	0.0028	85	0.0036	95	0.0035	79	0.0811	276	0.0183	237	0.0278	52
375	shaman-000	0.9297	499	0.9774	498	0.9990	495	-	-	0.9999	490	1.0000	477	0.9999	485	0.9575	489
376	shaman-001	0.3346	460	0.4616	461	0.2368	443	0.3723	445	0.3574	441	0.3527	338	0.2304	370	0.1498	416
377	shu-002	-	-	0.0079	191	0.0146	361	0.0308	370	1.0000	491	0.0183	161	0.0115	174	0.0284	119
378	shu-003	0.0028	92	0.0041	94	0.0050	209	0.0088	252	0.0081	198	0.0133	122	0.0094	138	0.0283	116
379	siat-002	0.0091	276	0.0126	270	0.0109	333	0.0190	342	0.0276	349	0.0516	254	0.0464	309	0.0520	345
380	siat-005	0.0021	59	0.0038	82	0.0059	240	0.0049	150	0.0742	394	0.9623	422	0.6801	422	0.0279	64
381	sjtu-003	0.0017	39	0.0033	62	0.0030	104	0.0037	103	0.0058	153	0.0104	100	0.0081	116	0.0284	126
382	sjtu-004	0.0014	26	0.0025	35	0.0027	70	0.0028	51	0.0046	119	0.0086	79	0.0073	99	0.0272	9
383	sktelecom-000	0.0038	140	0.0054	139	0.0031	108	0.0051	156	0.0042	106	0.3418	334	0.0061	76	0.0293	188
384	smartbiometrik-001	0.5485	483	0.6442	478	0.7550	481	0.8611	478	0.8677	470	0.8270	400	0.7030	425	0.3144	451
385	smartengines-000	0.6240	489	0.7562	490	0.9552	489	0.9784	489	0.9515	482	0.9288	415	0.8200	438	0.8037	484
386	smartengines-001	0.6434	491	0.7666	491	0.9446	488	0.9750	488	0.9387	481	0.9556	420	0.8647	444	0.7748	482
387	smartvist-000	0.0912	431	0.1587	434	0.1163	434	0.1841	433	0.1397	412	0.9372	417	0.7107	429	0.0779	381
388	smilart-002	0.2440	450	0.3532	452	-	-	-	3785	442	0.4145	346	0.2611	376	-	-	-
389	smilart-003	0.6944	494	0.8836	495	0.0695	426	0.1193	428	0.0894	403	0.1221	296	0.0737	333	0.1190	406
390	sodec-000	0.0033	114	0.0044	108	0.0040	178	0.0053	163	0.0054	141	0.0096	92	0.0080	112	0.0274	21
391	sqisoft-002	0.0082	266	0.0124	264	0.0051	214	0.0086	248	0.0102	240	0.0183	162	0.0122	185	0.0287	148
392	sqisoft-003	0.0041	151	0.0055	140	0.0026	50	0.0032	73	0.0039	95	1.0000	499	1.0000	500	0.0295	194
393	stauq-000	0.0139	341	0.0208	335	0.0104	325	0.0145	317	0.0156	286	0.8063	393	0.1408	356	0.0332	267
394	starhybrid-001	0.0108	304	0.0138	278	0.0081	289	0.0113	276	0.0152	285	0.0265	198	0.0189	243	0.0350	285
395	stcon-000	0.0040	144	0.0056	143	0.0031	114	0.0047	141	0.0048	129	0.9863	431	0.3562	393	0.0300	212
396	stcon-001	0.0040	143	0.0053	138	0.0030	107	0.0045	135	0.0047	123	0.8632	404	0.1788	365	0.0297	203

Table 29: FNMR is the proportion of mated comparisons below a threshold set to achieve the FMR given in the header on the fourth row. FMR is the proportion of impostor comparisons at or above that threshold. The light grey values give rank over all algorithms in that column. The pink columns use only same-sex impostors; others are selected regardless of demographics. The exception, in the green column, uses "matched-covariates" i.e. impostors of the same sex, age group, and country of birth. The second pink column includes effects of extended ageing. Missing entries for border, visa, mugshot and wild images generally mean the algorithm did not run to completion. The VISA columns compare images described in section 2.1. The MUGSHOT columns compare images described in section 2.5. The VISA-BORDER column compare images described in section 2.2 with those of section 2.4. The BORDER column compares images described in section 2.4. The WILD columns compare images described in section 2.7.

Algorithm	FALSE NON-MATCH RATE (FNMR)															
	CONSTRAINED, COOPERATIVE															
	Name	VISAMC	VISA	MUGSHOT	MUGSHOT12+YRS	VISABORDER	BORDER	BORDER	WILD							
FMR	0.0001	1E-06	1E-05	1E-05	1E-06	1E-06	1E-06	1E-05	0.0001							
397 <i>sukshi-000</i>	0.5409	481	0.6612	483	0.4556	459	0.6567	462	0.9296	480	0.8898	406	0.7384	430	0.6892	478
398 <i>suprema-003</i>	0.0028	93	0.0041	95	0.0034	137	0.0039	109	0.0030	51	0.3095	332	0.0580	323	0.0284	120
399 <i>suprema-004</i>	0.0024	77	0.0035	69	0.0032	122	0.0036	96	0.0028	36	0.0053	22	0.0045	25	0.0281	87
400 <i>supremaid-001</i>	0.0053	180	0.0073	176	0.0045	191	0.0066	203	0.0099	237	0.0186	163	0.0148	211	0.0352	287
401 <i>supremaid-002</i>	0.0063	217	0.0094	219	0.0044	187	0.0062	196	0.0072	180	0.0229	186	0.0095	141	0.0345	277
402 <i>surrey-cvssp-001</i>	1.0000	503	1.0000	501	0.0077	280	0.0079	234	0.0266	345	0.3822	341	0.0551	319	1.0000	495
403 <i>surrey-cvssp-002</i>	0.0019	48	0.0028	45	0.0027	75	0.0028	42	0.0024	17	0.5978	363	0.1206	349	0.0710	378
404 <i>swsam-001</i>	0.0268	387	0.0476	391	0.0271	390	0.0460	387	0.0584	388	0.7745	386	0.5013	409	0.0538	351
405 <i>synesis-006</i>	0.0070	233	0.0096	223	0.0107	330	0.0166	329	-	-	0.0128	121	0.0089	131	0.0292	181
406 <i>synesis-007</i>	0.0050	168	0.0073	178	0.0062	251	0.0076	222	-	-	0.0105	101	0.0080	113	0.0288	150
407 <i>synology-000</i>	0.0149	347	0.0238	352	0.0148	363	0.0261	363	0.0221	326	0.0331	218	0.0209	256	0.0330	265
408 <i>synology-002</i>	0.0104	298	0.0153	296	0.0107	331	0.0184	336	0.0189	315	0.2032	311	0.0180	233	0.0312	235
409 <i>sztu-000</i>	0.0092	280	0.0139	279	0.0091	308	0.0201	348	0.0136	272	0.0685	268	0.0118	181	0.0270	4
410 <i>sztu-001</i>	0.0031	100	0.0043	101	0.0025	43	0.0028	48	0.0051	133	0.0113	107	0.0089	132	0.0275	25
411 <i>t4isb-000</i>	0.0058	197	0.0087	207	0.0041	183	0.0064	200	0.0083	202	0.0157	141	0.0103	152	0.0282	104
412 <i>tech5-005</i>	0.0054	182	0.0072	171	0.0069	261	0.0122	283	0.0060	157	0.0094	89	0.0066	80	0.0349	283
413 <i>tech5-007</i>	0.0020	52	0.0029	50	0.0024	26	0.0028	40	0.0034	75	0.8622	403	0.5335	412	0.0280	72
414 <i>techsign-000</i>	0.0325	398	0.0511	396	0.0435	410	0.0710	408	0.0746	395	0.1104	291	0.0841	337	0.0639	364
415 <i>techsign-001</i>	0.0110	307	0.0196	331	0.0067	258	0.0120	281	0.0087	208	0.2475	323	0.0883	341	0.0299	208
416 <i>tevian-007</i>	0.0019	49	0.0027	43	0.0032	124	0.0041	116	0.0045	117	0.0086	78	0.0078	108	0.0310	234
417 <i>tevian-008</i>	0.0012	19	0.0017	12	0.0033	127	0.0042	123	0.0042	108	0.0081	65	0.0068	86	0.0290	169
418 <i>tiger-005</i>	0.0624	422	0.2450	442	0.0292	396	0.0556	397	0.0430	373	1.0000	470	0.9964	473	0.0278	50
419 <i>tiger-006</i>	0.0066	221	0.0101	236	0.0050	213	0.0075	221	0.0089	212	0.0158	142	0.0117	177	0.0290	176
420 <i>tinkoff-001</i>	0.0145	345	0.0244	353	0.0318	399	0.0636	406	0.0236	336	1.0000	485	0.0339	286	0.0563	356
421 <i>tongyi-005</i>	0.0073	246	0.0146	285	0.0187	372	0.0421	384	0.0161	291	0.0215	180	0.0149	213	0.0399	304
422 <i>toppanidgate-000</i>	0.0021	54	0.0033	63	0.0026	55	0.0028	44	0.0039	96	0.0075	54	0.0068	84	0.0376	300
423 <i>toshiba-004</i>	0.0030	97	0.0042	97	0.0025	44	0.0027	37	0.0034	73	0.0063	40	0.0053	49	0.0278	47
424 <i>toshiba-006</i>	0.0022	68	0.0035	71	0.0024	32	0.0025	25	0.0027	33	0.7425	378	0.3070	385	0.0275	28
425 <i>touchlessid-001</i>	0.0076	252	0.0104	238	0.0680	425	0.0842	415	0.1358	410	1.0000	472	0.9995	478	0.0499	341
426 <i>touchlessid-002</i>	0.0070	229	0.0096	227	0.0407	408	0.0469	389	0.4234	447	0.9991	455	0.9953	471	0.0436	327
427 <i>trueface-002</i>	0.0060	209	0.0096	224	0.0048	203	0.0061	193	0.0112	254	0.0198	170	0.0155	218	0.0793	386
428 <i>trueface-003</i>	0.0070	231	0.0094	218	0.0053	222	0.0081	237	0.0122	260	0.0217	181	0.0159	221	0.0785	383
429 <i>trueidvng-001</i>	0.0063	216	0.0077	184	0.0033	132	0.0044	130	0.0046	120	0.0086	80	0.0069	89	0.0628	361
430 <i>tuputech-000</i>	0.3218	459	0.3696	455	-	-	-	0.3237	437	0.4304	347	0.2973	384	0.9415	487	
431 <i>turingtechvip-001</i>	0.0330	400	0.0540	400	0.0458	412	0.1007	419	0.4715	449	0.9286	414	0.8448	442	0.4035	461
432 <i>turingtechvip-002</i>	0.0126	333	0.0163	302	0.0092	313	0.0118	278	0.2264	430	1.0000	494	0.9925	467	0.2144	432
433 <i>turkcell-000</i>	0.1134	437	0.1288	428	0.0770	428	0.1112	427	0.2570	432	1.0000	469	0.9999	484	0.9556	488
434 <i>turkcell-001</i>	0.0043	152	0.0066	162	0.0037	156	0.0055	169	0.0043	110	0.0440	244	0.0082	119	0.0274	20
435 <i>twface-000</i>	0.0051	171	0.0072	174	0.0041	181	0.0058	178	0.0071	177	0.0153	136	0.0100	144	0.0276	36
436 <i>twface-001</i>	0.0036	128	0.0051	130	0.0031	115	0.0038	105	0.0049	130	0.0091	85	0.0075	102	0.0277	41
437 <i>ulsee-001</i>	0.0151	349	0.0246	355	0.0113	340	0.0185	339	0.0187	314	0.6766	373	0.0181	235	0.0316	248
438 <i>ultinous-000</i>	0.2343	449	0.3484	451	-	-	-	-	-	-	-	-	-	-	-	
439 <i>ultinous-001</i>	0.2485	451	0.4003	458	-	-	-	-	-	-	-	-	-	-	-	
440 <i>uluface-002</i>	0.0081	261	0.0123	263	0.0071	266	0.0095	263	0.0107	245	1.0000	487	0.0140	201	0.0444	330

Table 30: FNMR is the proportion of mated comparisons below a threshold set to achieve the FMR given in the header on the fourth row. FMR is the proportion of impostor comparisons at or above that threshold. The light grey values give rank over all algorithms in that column. The pink columns use only same-sex impostors; others are selected regardless of demographics. The exception, in the green column, uses “matched-covariates” i.e. impostors of the same sex, age group, and country of birth. The second pink column includes effects of extended ageing. Missing entries for border, visa, mugshot and wild images generally mean the algorithm did not run to completion. The VISA columns compare images described in section 2.1. The MUGSHOT columns compare images described in section 2.5. The VISA-BORDER column compare images described in section 2.2 with those of section 2.4. The BORDER column compares images described in section 2.4. The WILD columns compare images described in section 2.7.

FRVT - FACE RECOGNITION VENDOR TEST - VERIFICATION

Algorithm	Name	FALSE NON-MATCH RATE (FNMR)								LESS CONSTRAINED, NON-COOP.							
		CONSTRAINED, COOPERATIVE						WILD									
		VISAMC	VISA	MUGSHOT	MUGSHOT12+YRS	VISABORDER	BORDER	BORDER	1E-06	1E-05							
FMR		0.0001	1E-06	1E-05	1E-05	1E-06			0.0001								
441	uluface-003	0.0100	293	0.0150	292	0.0079	282	0.0128	293	-	0.0635	362					
442	unicc-001	0.5101	480	0.6167	477	0.6577	470	0.7894	470	0.9208	478	0.9866	432	0.9386	451	0.1754	423
443	unissey-002	0.0094	284	0.0151	293	0.0079	283	0.0110	271	0.0114	256	0.4424	348	0.1914	366	0.0420	319
444	unissey-003	0.0057	191	0.0082	198	0.0047	200	0.0082	238	0.0067	170	0.5179	355	0.2863	382	0.0288	155
445	upc-001	0.0234	381	0.0519	397	0.0291	395	0.0490	394	0.0294	352	0.2316	320	0.0389	296	0.0314	241
446	uxlabs-001	0.0534	416	0.0570	404	0.0118	346	0.0131	297	0.0237	337	0.0399	239	0.0288	279	0.0876	395
447	vcog-002	0.7522	496	0.9033	496	-	-	-	-	-	-	-	-	-	-	-	-
448	vd-002	0.0429	408	0.0704	412	0.0569	418	0.0844	416	0.0801	398	0.0937	279	0.0577	322	0.0556	354
449	vd-003	0.0199	373	0.0222	344	0.0115	344	0.0130	296	0.0138	275	0.0239	188	0.0177	231	0.0389	303
450	veridas-007	0.0063	218	0.0083	199	0.0044	189	0.0058	181	0.0080	194	0.0152	134	0.0120	184	0.0284	121
451	veridas-008	0.0032	107	0.0045	111	0.0030	101	0.0033	77	0.0085	206	0.0206	175	0.0143	205	0.0288	156
452	veridium-000	0.0726	428	0.1248	427	0.5226	462	0.6652	463	0.6425	454	0.8150	395	0.7989	436	0.4988	469
453	veridium-001	0.0274	391	0.0368	383	0.0292	397	0.0475	390	0.0488	381	0.0673	266	0.0463	308	0.0800	387
454	verigram-001	0.0032	106	0.0044	105	0.0027	71	0.0032	71	0.0030	50	0.9995	458	0.9953	470	0.0276	38
455	verigram-002	0.0079	256	0.0089	210	0.0038	159	0.0040	112	0.0060	158	0.0113	108	0.0107	159	0.1481	413
456	verihubs-inteligensia-000	0.0070	230	0.0098	229	0.0048	205	0.0076	225	0.0092	219	0.0160	143	0.0117	176	0.0283	114
457	verihubs-inteligensia-001	0.0071	234	0.0114	256	0.0050	212	0.0076	224	0.0096	226	0.0165	149	0.0114	173	0.0282	101
458	verijelas-000	0.2488	452	0.3431	450	0.4861	460	0.6004	458	0.0811	399	0.1148	292	0.0440	303	0.0524	348
459	via-001	0.0149	346	0.0229	347	0.0114	342	0.0177	333	0.0183	311	0.4056	345	0.0176	229	0.0373	298
460	via-004	0.0099	289	0.0135	277	0.0031	117	0.0044	131	0.0055	145	0.4009	344	0.0080	114	0.0416	318
461	videmo-001	0.0295	394	0.0417	387	0.0164	370	0.0261	364	0.0355	362	0.0603	260	0.0442	304	0.1473	412
462	videmo-002	0.0158	354	0.0288	367	0.0149	367	0.0249	362	0.0230	330	0.3429	335	0.1468	357	0.0294	190
463	videonetics-001	0.5483	482	0.6446	480	0.7517	479	0.8607	477	0.8664	468	0.8255	397	0.6956	424	0.2986	448
464	videonetics-002	0.4274	468	0.5329	470	0.6081	468	0.7438	468	0.7775	458	0.7297	377	0.5756	414	0.1976	429
465	viettelhightech-000	0.0117	315	0.0166	305	0.0110	335	0.0198	346	0.0167	300	0.0249	191	0.0158	219	0.0409	315
466	vigilantsolutions-010	0.0109	305	0.0164	304	0.0074	275	0.0095	261	0.0209	323	0.0365	233	0.0233	265	0.0277	42
467	vigilantsolutions-011	0.0124	327	0.0176	314	0.0073	271	0.0095	260	0.0196	318	0.0360	230	0.0221	261	0.0274	18
468	vinai-000	0.0081	262	0.0124	265	0.0045	190	0.0072	215	0.0089	211	0.1814	304	0.0112	168	0.0274	22
469	vinbigdata-001	0.2576	455	0.2763	444	0.1404	438	0.1988	437	0.1407	414	0.1150	293	0.0703	331	0.9767	490
470	vinbigdata-002	0.0102	295	0.0175	312	0.0071	269	0.0084	244	0.0090	213	0.8017	392	0.3134	386	0.0304	219
471	vion-000	0.0419	406	0.0590	405	0.0422	409	0.0478	391	0.0581	387	0.0968	285	0.0847	338	0.2479	440
472	visage-000	0.0933	432	0.1441	432	0.1316	436	0.2416	438	0.1395	411	0.1920	308	0.1001	346	0.0500	342
473	visionbox-002	0.0058	199	0.0079	190	0.0060	243	0.0074	218	0.0084	204	0.0149	132	0.0113	171	0.0447	332
474	visionbox-003	0.0057	193	0.0075	180	0.0062	250	0.0083	241	0.0100	238	0.9915	439	0.9625	459	0.0478	339
475	visionlabs-010	0.0017	38	0.0024	33	0.0026	63	0.0030	58	0.0033	67	0.0061	37	0.0052	42	0.0282	107
476	visionlabs-011	0.0012	22	0.0022	26	0.0024	35	0.0026	29	0.0028	37	0.0053	23	0.0046	28	0.0280	78
477	visteam-004	0.0541	418	0.5202	468	0.0406	407	0.0827	414	0.1879	424	0.1795	303	0.0347	289	0.0289	161
478	visteam-005	0.0235	382	0.0333	372	0.0265	389	0.0583	404	0.0341	359	0.0524	256	0.0259	272	0.0292	180
479	vixvizion-006	0.0082	264	0.0122	262	0.0093	314	0.0194	344	0.0099	236	0.0169	151	0.0108	162	0.0268	3
480	vixvizion-007	0.0110	308	0.0191	326	0.0080	286	0.0157	323	0.0101	239	0.0190	164	0.0118	180	0.0273	15
481	vnpt-004	0.0058	203	0.0078	188	0.0037	154	0.0053	162	0.0051	134	0.4640	350	0.1384	354	0.0275	29
482	vnpt-005	0.0036	129	0.0052	131	0.0027	72	0.0031	65	0.0036	83	0.0066	46	0.0056	54	0.0286	140
483	vocord-009	0.0022	63	0.0029	52	0.0036	146	0.0046	140	0.0052	138	0.0098	93	0.0086	129	0.0284	124
484	vocord-010	0.0024	79	0.0031	56	0.0036	147	0.0049	152	0.0025	24	0.0065	42	0.0040	15	0.0280	76

Table 31: FNMR is the proportion of mated comparisons below a threshold set to achieve the FMR given in the header on the fourth row. FMR is the proportion of impostor comparisons at or above that threshold. The light grey values give rank over all algorithms in that column. The pink columns use only same-sex impostors; others are selected regardless of demographics. The exception, in the green column, uses “matched-covariates” i.e. impostors of the same sex, age group, and country of birth. The second pink column includes effects of extended ageing. Missing entries for border, visa, mugshot and wild images generally mean the algorithm did not run to completion. The VISA columns compare images described in section 2.1. The MUGSHOT columns compare images described in section 2.5. The VISA-BORDER column compare images described in section 2.2 with those of section 2.4. The BORDER column compares images described in section 2.4. The WILD columns compare images described in section 2.7.

	Algorithm	FALSE NON-MATCH RATE (FNMR)															
		CONSTRAINED, COOPERATIVE								LESS CONSTRAINED, NON-COOP.							
		Name	VISAMC	VISA	MUGSHOT	MUGSHOT12+YRS	VISABORDER	BORDER	BORDER	WILD							
		FMR	0.0001	1E-06	1E-05	1E-05	1E-06	1E-06	1E-05	0.0001							
485	vts-000	0.0103	296	0.0174	311	0.0080	285	0.0129	295	0.0250	342	0.0450	245	0.0372	294	0.0596	357
486	vts-001	0.0033	109	0.0048	120	0.0027	74	0.0036	97	0.0032	58	0.6519	370	0.3563	394	0.0338	273
487	wicket-000	0.0018	47	0.0028	46	0.0024	30	0.0027	31	0.0031	53	0.7968	391	0.4340	403	0.0323	256
488	winsense-001	0.0062	214	0.0099	233	0.0092	311	0.0210	349	0.0093	221	0.0144	130	0.0098	143	0.0320	254
489	winsense-002	0.0050	169	0.0073	177	0.0038	160	0.0059	187	0.0064	166	0.0118	114	0.0084	123	0.0307	227
490	wiseai-001	0.0658	424	0.0964	424	0.7743	483	0.8956	483	0.1967	425	0.7526	382	0.3419	390	0.5780	472
491	wuhantianyu-001	0.0163	356	0.0262	363	0.0281	393	0.0569	401	0.0316	356	0.0486	251	0.0344	287	0.0324	257
492	x-laboratory-000	0.0071	238	0.0106	242	0.0123	349	0.0138	306	0.0419	372	0.5629	359	0.2852	381	0.0295	198
493	x-laboratory-001	0.0059	205	0.0110	250	0.0054	225	0.0078	232	0.0094	223	0.0142	126	0.0100	146	0.0294	189
494	xforwardai-001	0.0021	56	0.0034	65	0.0027	77	0.0028	47	0.0046	122	0.0088	82	0.0079	110	0.0281	93
495	xforwardai-002	0.0016	35	0.0023	28	0.0026	67	0.0025	22	0.0040	100	0.0081	66	0.0074	100	0.0282	98
496	xm-000	0.0015	28	0.0026	39	0.0031	112	0.0038	107	0.0058	154	0.0105	102	0.0082	120	0.0282	105
497	yisheng-004	0.1988	446	0.3329	449	0.1147	433	0.1849	434	0.2044	427	-	-	-	-	0.0908	396
498	yitu-003	0.0015	31	0.0026	37	0.0066	256	0.0085	245	0.0064	167	0.0114	109	0.0103	153	0.0325	260
499	yoonik-003	0.0034	121	0.0047	115	0.0032	121	0.0037	101	0.0816	400	0.2033	312	0.1601	361	0.0699	374
500	yoonik-004	0.0041	150	0.0059	150	0.0033	128	0.0052	158	0.0040	102	0.0071	51	0.0051	39	0.0290	174
501	ytu-000	0.0057	192	0.0087	206	0.0121	347	0.0238	359	0.0047	125	0.0078	60	0.0059	71	0.0286	142
502	yuan-005	0.0037	137	0.0046	113	0.0027	78	0.0035	92	0.0033	62	0.2706	328	0.0876	340	0.0288	160
503	yuan-006	0.0045	155	0.0062	154	0.0032	120	0.0049	148	0.0038	91	0.0084	73	0.0049	32	0.0273	12

Table 32: FNMR is the proportion of mated comparisons below a threshold set to achieve the FMR given in the header on the fourth row. FMR is the proportion of impostor comparisons at or above that threshold. The light grey values give rank over all algorithms in that column. The pink columns use only same-sex impostors; others are selected regardless of demographics. The exception, in the green column, uses “matched-covariates” i.e. impostors of the same sex, age group, and country of birth. The second pink column includes effects of extended ageing. Missing entries for border, visa, mugshot and wild images generally mean the algorithm did not run to completion. The VISA columns compare images described in section 2.1. The MUGSHOT columns compare images described in section 2.5. The VISA-BORDER column compare images described in section 2.2 with those of section 2.4. The BORDER column compares images described in section 2.4. The WILD columns compare images described in section 2.7.

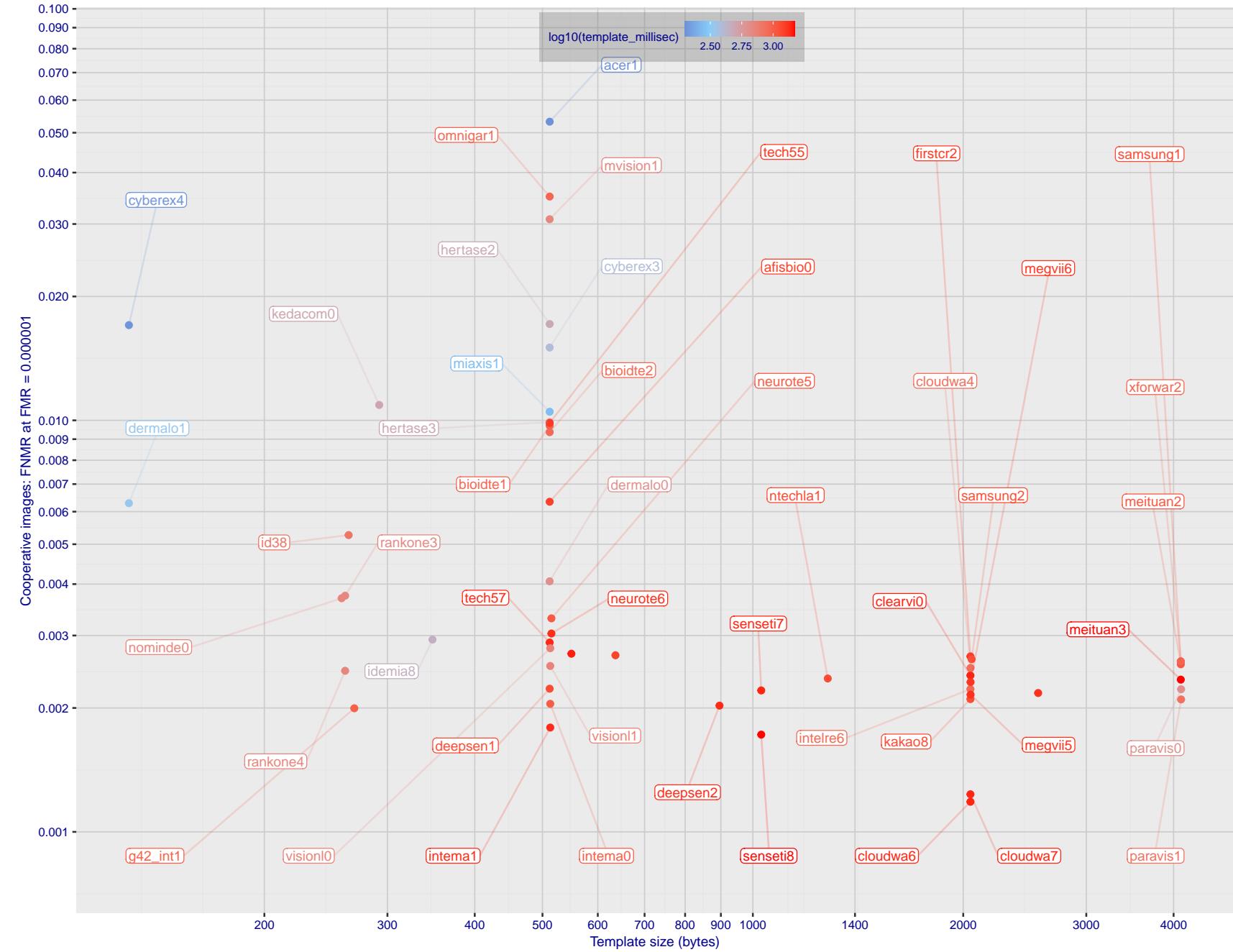


Figure 1: The points show false non-match rates (FNMR) versus the size of the encoded template. FNMR is the geometric mean of FNMR values for visa and mugshot images (from Figs. 96 and 121) at the false match rate (FMR) given in the y-axis label. The color of the points encodes template generation time - which spans at least one order of magnitude. Durations are measured on a single core of a c. 2016 Intel Xeon CPU E5-2630 v4 running at 2.20GHz. Algorithms with poor FNMR are omitted.

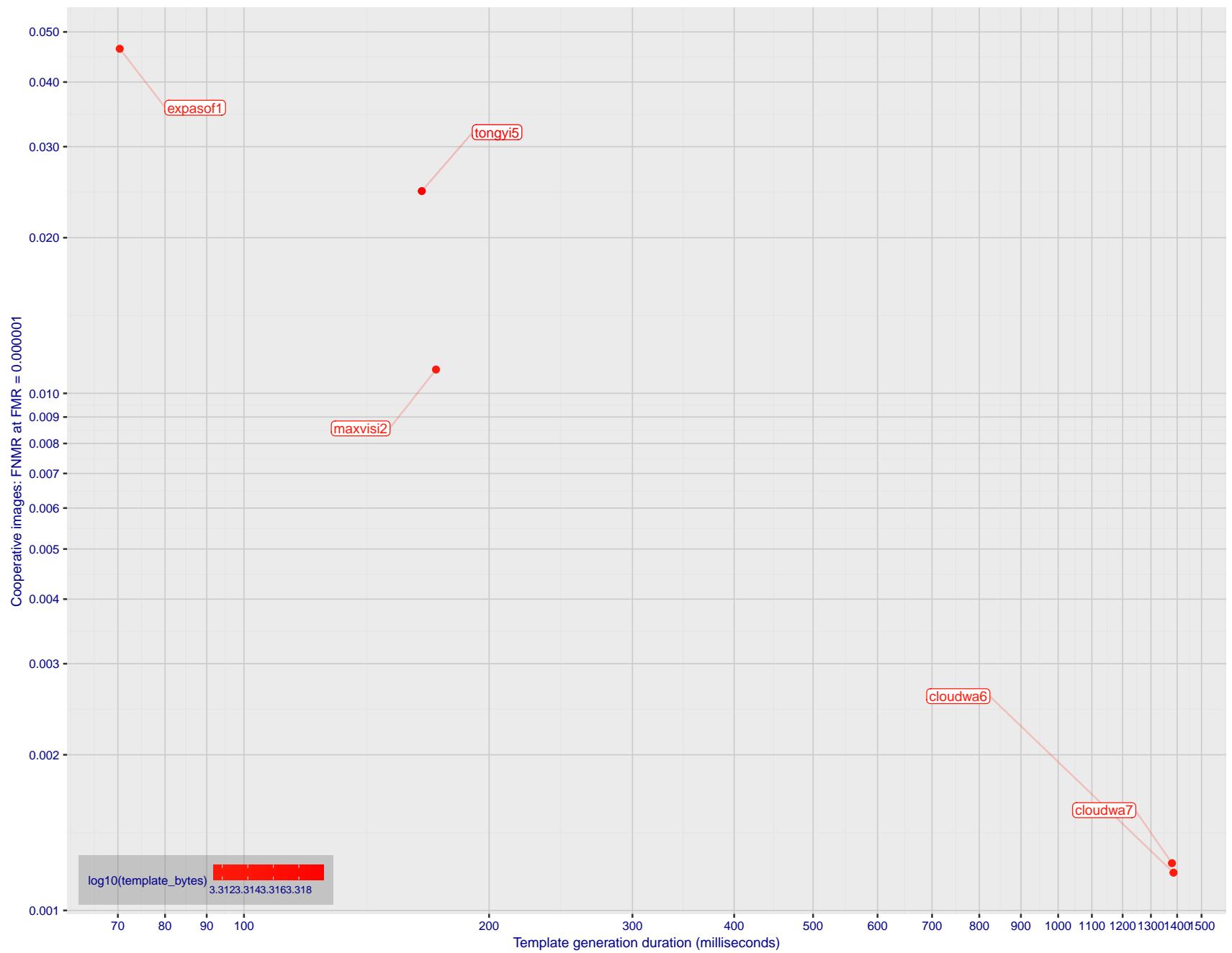


Figure 2: The points show false non-match rates (FNMR) versus the duration of the template generation operation. FNMR is the geometric mean of FNMR values for visa and mugshot images (from Figs. 96 and 121) at a false match rate (FMR) given in the y-axis label. Template generation time is a median estimated over 640 x 480 pixel portraits. It is measured on a single core of a c. 2016 Intel Xeon CPU E5-2630 v4 running at 2.20GHz. The color of the points encodes template size - which span two orders of magnitude. Algorithms with poor FNMR are omitted.

1 Metrics

1.1 Core accuracy

Given a vector of N genuine scores, u , the false non-match rate (FNMR) is computed as the proportion below some threshold, T:

$$\text{FNMR}(T) = 1 - \frac{1}{N} \sum_{i=1}^N H(u_i - T) \quad (1)$$

where $H(x)$ is the unit step function, and $H(0)$ taken to be 1.

Similarly, given a vector of N impostor scores, v , the false match rate (FMR) is computed as the proportion above T:

$$\text{FMR}(T) = \frac{1}{N} \sum_{i=1}^N H(v_i - T) \quad (2)$$

The threshold, T, can take on any value. We typically generate a set of thresholds from quantiles of the observed impostor scores, v , as follows. Given some interesting false match rate range, $[\text{FMR}_L, \text{FMR}_U]$, we form a vector of K thresholds corresponding to FMR measurements evenly spaced on a logarithmic scale

$$T_k = Q_v(1 - \text{FMR}_k) \quad (3)$$

where Q is the quantile function, and FMR_k comes from

$$\log_{10} \text{FMR}_k = \log_{10} \text{FMR}_L + \frac{k}{K} [\log_{10} \text{FMR}_U - \log_{10} \text{FMR}_L] \quad (4)$$

Error tradeoff characteristics are plots of FNMR(T) vs. FMR(T). These are plotted with $\text{FMR}_U \rightarrow 1$ and FMR_L as low as is sustained by the number of impostor comparisons, N. This is somewhat higher than the “rule of three” limit $3/N$ because samples are not independent, due to re-use of images.

1.2 Multi-template scoring methodology

There are some scenarios when one or more people exist and are detected in an image, and some of the proposed test images include $K > 1$ persons for some images and situations where the subject of interest may or may not be the foreground face (largest face in the image). The NIST FRVT 1:1 API supports this by allowing generation of multiple templates representing each person detected in an image. When this occurs, NIST will match all templates generated from the enrollment image with all templates generated from the verification image and use the **maximum** similarity score across all template comparisons. This scoring approach will be used in our calculation of FMR and FNMR (this applies to both genuine and imposter comparisons).

2 Datasets

2.1 Visa images

- ▷ The number of images is on the order of 10^5 .
- ▷ The number of subjects is on the order of 10^5 .
- ▷ The number of subjects with two images is on the order of 10^4 .
- ▷ The images have geometry in reasonable conformance with the ISO/IEC 19794-5 Full Frontal image type. Pose is generally excellent.
- ▷ The images are of size 252x300 pixels. The mean interocular distance (IOD) is 69 pixels.
- ▷ The images are of subjects from greater than 100 countries, with significant imbalance due to visa issuance patterns.
- ▷ The images are of subjects of all ages, including children, again with imbalance due to visa issuance demand.
- ▷ Many of the images are live capture. A substantial number of the images are photographs of paper photographs.
- ▷ When these images are input to the algorithm, they are labelled as being of type "ISO" - see Table 4 of the FRVT API.

2.2 Application images

- ▷ The number of images is on the order of 10^6 .
- ▷ The number of subjects is on the order of 10^6 .
- ▷ The number of subjects with two images is on the order of 10^6 .
- ▷ The images have geometry in good conformance with the ISO/IEC 19794-5 Full Frontal image type. Pose is generally excellent.
- ▷ The images are of size 300x300 pixels. The mean interocular distance (IOD) is 61 pixels.
- ▷ The images are of subjects from greater than 100 countries, with significant imbalance due to population and immigration patterns.
- ▷ The images are of subjects of adults.
- ▷ All of the images are live capture.
- ▷ When these images are input to the algorithm, they are labelled as being of type "ISO" - see Table 4 of the FRVT API.

2.3 Application images with head yaw

- ▷ The number of images is on the order of 10^5 .
- ▷ The number of subjects is on the order of 10^5 .
- ▷ The number of subjects with two images is on the order of 10^5 .
- ▷ The images have geometry in good conformance with the ISO/IEC 19794-5 Full Frontal image type *except* the yaw angle is between 25 and 85 degrees. Our pose estimates are approximate, with an angular error that increases with yaw. The angular estimates will be improved over time.
- ▷ The images are of size 300x300 pixels. The mean interocular distance (IOD), if frontal, would be about pixels, but reduces with cosine of yaw.
- ▷ The images are of subjects from greater than 100 countries, with significant imbalance due to population and immigration patterns.

- ▷ The images are of subjects of adults.
- ▷ All of the images are live capture.
- ▷ When these images are input to the algorithm, they are labelled as being of type "WILD" - see Table 4 of the FRVT API.

2.4 Border crossing images

- ▷ The number of images is on the order of 10^6 .
- ▷ The number of subjects is on the order of 10^6 .
- ▷ The number of subjects with two images is on the order of 10^6 .
- ▷ The images are taken with a camera oriented by an attendant toward a cooperating subject. This is done under time constraints so there are roll, pitch and yaw angle variations. Also background illumination is sometimes strong, so the face is under-exposed. There is some perspective distortion due to close range images. Some faces are partially cropped.
- ▷ The images have mean IOD of 38 pixels.
- ▷ The images are of subjects of adults and children aged 12 or above.
- ▷ The images are of subjects from greater than 100 countries, with significant imbalance due to population and immigration patterns.
- ▷ The images are all live capture.
- ▷ When these images are input to the algorithm, they are labelled as being of type "WILD" - see Table 4 of the FRVT API.

2.5 Mugshot images

- ▷ The number of images is on the order of 10^6 .
- ▷ The number of subjects is on the order of 10^6 .
- ▷ The number of subjects with two images is on the order of 10^6 .
- ▷ The images have geometry in reasonable conformance with the ISO/IEC 19794-5 Full Frontal image type.
- ▷ The images are of variable sizes. The median IOD is 105 pixels. The mean IOD is 113 pixels. The 1-st, 5-th, 10-th, 25-th, 75-th, 90-th and 99-th percentiles are 34, 58, 70, 87, 121, 161 and 297 pixels.
- ▷ The images are of subjects from the United States.
- ▷ The images are of adults.
- ▷ The images are all live capture.
- ▷ When these images are input to the algorithm, they are labelled as being of type "mugshot" - see Table 4 of the FRVT API.

2.6 Kiosk images

- ▷ The number of images is on the order of 10^6 .
- ▷ The number of subjects is on the order of 10^5 .
- ▷ The number of subjects with multiple images is the order of 10^5 .

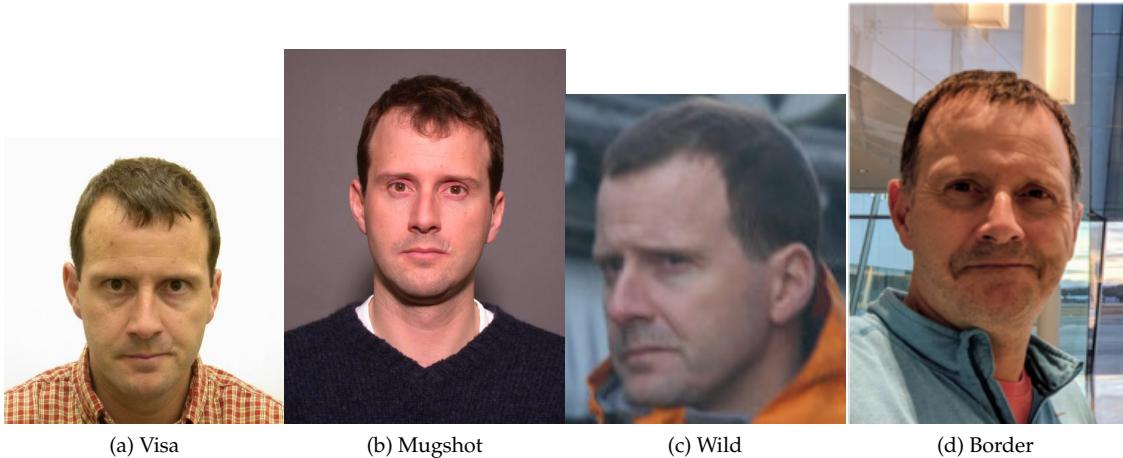


Figure 3: The figure gives simulated samples of image types used in this report.

- ▷ The images are taken at kiosk equipped with a camera intended to capture a centered face. However the images have specific quality defects arising from the camera triggering before the subject looks at it. These are downward pitch of the face relative to the optical axis; cropping of the forehead; and cropping of left or right part of the face. Partial cropping affects perhaps 10% of the images. Resolution does not vary widely.
 - ▷ The images are of adults.
 - ▷ The images have mean IOD of 44 pixels, with maximum below 75, and minimum when both eyes are present above 25 pixels.
 - ▷ All of the images are live capture, none are scanned.
 - ▷ When these images are input to the algorithm, they are labelled as being of type "WILD" - see Table 4 of the FRVT API.

2.7 Wild images

- ▷ The number of images is on the order of 10^5 .
 - ▷ The number of subjects is on the order of 10^4 .
 - ▷ The number of subjects with two images on the order of 10^4 .
 - ▷ The images include many photojournalism-style images. Images are given to the algorithm using a variable but generally tight crop of the head. Resolution varies very widely. The images are very unconstrained, with wide yaw and pitch pose variation. Faces can be occluded, including hair and hands.
 - ▷ The images are of adults.
 - ▷ All of the images are live capture, none are scanned.
 - ▷ When these images are input to the algorithm, they are labelled as being of type "WILD" - see Table 4 of the FRVT API.

3 Results

3.1 Test goals

- To state absolute accuracy for different kinds of images, including those with and without subject cooperation.

- ▷ To state comparative accuracy, across algorithms.

3.2 Test design

Method: For visa images:

- ▷ The comparisons are of visa photos against visa photos.
- ▷ The number of genuine comparisons is on the order of 10^4 .
- ▷ The number of impostor comparisons is on the order of 10^{10} .
- ▷ The comparisons are fully zero-effort, meaning impostors are paired without attention to sex, age or other covariates. However, later analysis is conducted on subsets.
- ▷ The number of persons is on the order of 10^5 .
- ▷ The number of images used to make a template is one.
- ▷ The number of templates used to make each comparison score is two corresponding to simple one-to-one verification.

Method: For mugshot images:

- ▷ The comparisons are of mugshot photos against mugshot photos.
- ▷ The number of genuine comparisons is on the order of 10^6 .
- ▷ The number of impostor comparisons is on the order of 10^8 .
- ▷ The impostors are paired by sex, but not by age or other covariates.
- ▷ The number of persons is on the order of 10^6 .
- ▷ The number of images used to make a template is one.
- ▷ The number of templates used to make each comparison score is two, corresponding to simple one-to-one verification.

Method: For visa-border comparisons:

- ▷ The comparisons are of visa-like frontals against border crossing webcam photos.
- ▷ The number of genuine comparisons is on the order of 10^6 .
- ▷ The number of impostor comparisons is on the order of 10^8 .
- ▷ The impostors are paired by sex, but not by age or other covariates.
- ▷ The number of persons is on the order of 10^6 .
- ▷ The number of images used to make a template is one.
- ▷ The number of templates used to make each comparison score is two, corresponding to simple one-to-one verification.

Method: For visa-border non-frontal yaw comparisons:

- ▷ The comparisons are of visa-like images with yaw 25 to 85 degrees against border crossing webcam photos.
- ▷ The number of genuine comparisons is on the order of 10^5 .
- ▷ The number of impostor comparisons is on the order of 10^8 .
- ▷ The impostors are paired by sex, but not by age or other covariates.

- ▷ The number of persons is on the order of 10^5 .
- ▷ The number of images used to make a template is one.
- ▷ The number of templates used to make each comparison score is two, corresponding to simple one-to-one verification.

Method: For kiosk-border comparisons:

- ▷ The comparisons are of visa-like frontals against kiosk-style photos.
- ▷ The number of genuine comparisons is on the order of 10^6 .
- ▷ The number of impostor comparisons is on the order of 10^8 .
- ▷ The impostors are paired by sex, but not by age or other covariates.
- ▷ The number of persons is on the order of 10^5 .
- ▷ The number of images used to make a template is one.
- ▷ The number of templates used to make each comparison score is two, corresponding to simple one-to-one verification.

Method: For border-border comparisons:

- ▷ The comparisons are of border crossing webcam photos.
- ▷ The number of genuine comparisons is on the order of 10^6 .
- ▷ The number of impostor comparisons is on the order of 10^8 .
- ▷ The impostors are paired by sex, but not by age or other covariates.
- ▷ The number of persons is on the order of 10^6 .
- ▷ The number of images used to make a template is one.
- ▷ The number of templates used to make each comparison score is two corresponding to simple one-to-one verification.

Method: For wild images:

- ▷ The comparisons are of wild photos against wild photos.
- ▷ The number of genuine comparisons is on the order of 10^6 .
- ▷ The number of impostor comparisons is on the order of 10^8 .
- ▷ The comparisons are fully zero-effort, meaning impostors are paired without attention to sex, age or other covariates.
- ▷ The number of persons is on the order of 10^4 .
- ▷ The number of images used to make a template is one.
- ▷ The number of templates used to make each comparison score is two corresponding to simple one-to-one verification.

Method: For child exploitation images:

- ▷ The comparisons are of unconstrained child exploitation photos against others of the same type.
- ▷ The number of genuine comparisons is on the order of 10^4 .
- ▷ The number of impostor comparisons is on the order of 10^7 .

- ▷ The comparisons are fully zero-effort, meaning impostors are paired without attention to sex, age or other covariates.
- ▷ The number of persons is on the order of 10^3 .
- ▷ The number of images used to make 1 template is 1.
- ▷ The number of templates used to make each comparison score is two corresponding to simple one-to-one verification.
- ▷ We produce two performance statements. First, is a DET as used for visa and mugshot images. The second is a cumulative match characteristic (CMC) summarizing a simulated one-to-many search process. This is done as follows.
 - We regard M enrollment templates as items in a gallery.
 - These M templates come from $M > N$ individuals, because multiple images of a subject are present in the gallery under separate identifiers.
 - We regard the verification templates as search templates.
 - For each search we compute the rank of the highest scoring mate.
 - This process should properly be conducted with a 1:N algorithm, such as those tested in NIST IR 8009. We use the 1:1 algorithms in a simulated 1:N mode here to a) better reflect what a child exploitation analyst does, and b) to show algorithm efficacy is better than that revealed in the verification DETs.

3.3 Failure to enroll

	Algorithm	Failure to Enrol Rate ¹											
		APPLICATION		BORDER		KIOSK	MUGSHOT	VISA	WILD				
Name	SEC. 2.2	SEC. 2.4	SEC. 2.6	SEC. 2.5	SEC. 2.1	SEC. 2.7							
1	20face-000	0.0000	280	0.0008	253	0.0217	194	0.0000	147	0.0004	291	0.0004	219
2	20face-001	0.0000	279	0.0008	254	0.0000	51	0.0000	148	0.0004	292	0.0004	218
3	3divi-006	0.0000	311	0.0007	221	0.0214	191	0.0001	267	0.0002	148	0.0005	278
4	3divi-007	0.0000	291	0.0007	220	0.0214	192	0.0001	269	0.0002	147	0.0005	279
5	accurascan-001	0.0001	444	0.0060	451	0.0838	318	0.0006	421	0.0022	481	0.0196	435
6	acer-001	0.0000	335	0.0011	312	-	446	0.0001	232	0.0004	313	0.0004	233
7	acer-002	0.0000	412	0.0008	246	0.0191	170	0.0003	365	0.0004	308	0.0011	335
8	acisw-007	0.0000	200	0.0000	111	0.0000	40	0.0000	61	0.0000	67	0.0000	78
9	acisw-008	0.0000	312	0.0009	277	0.0173	153	0.0004	389	0.0004	214	0.0007	309
10	adera-003	0.0000	394	0.0034	412	0.0403	278	0.0003	369	0.0005	411	0.0505	460
11	adera-004	0.0000	237	0.0008	243	0.0202	176	0.0003	376	0.0004	268	0.0003	174
12	advance-003	0.0000	384	0.0012	324	0.0247	214	0.0001	292	0.0004	362	0.0011	334
13	advance-004	0.0001	448	0.0010	303	0.0157	142	0.0008	439	0.0006	424	0.0222	439
14	afisbiometrics-000	0.0000	239	0.0008	235	0.0213	189	0.0000	145	0.0004	316	0.0003	204
15	afrengine-000	0.0000	245	0.0015	345	0.0254	225	0.0008	438	0.0004	247	0.0265	447
16	afrengine-001	0.0000	226	0.0007	230	0.0183	158	0.0005	403	0.0004	363	0.0004	235
17	afirst-001	0.0000	93	0.0000	47	-	368	0.0000	8	0.0000	121	0.0000	116
18	aigen-001	0.0000	158	0.0000	84	-	444	0.0000	91	0.0000	40	0.0000	51
19	aigen-002	0.0000	189	0.0000	101	0.0000	25	0.0000	83	0.0000	46	0.0000	68
20	ailabs-001	0.0000	231	0.0090	459	-	420	0.0007	431	0.0005	387	0.0016	348
21	aimall-002	0.0000	400	0.0043	432	-	482	0.0012	452	0.0005	404	0.0005	286
22	aimall-003	0.0000	377	0.0012	329	-	454	0.0004	381	0.0005	379	0.0004	246
23	aiseemu-001	0.0000	131	0.0000	69	0.0000	65	0.0000	110	0.0000	20	0.0000	104
24	aiseemu-002	0.0000	206	0.0000	112	0.0000	42	0.0000	63	0.0000	66	0.0000	77
25	aiunionface-000	0.0000	143	0.0000	73	-	492	0.0000	100	0.0000	31	0.0000	122
26	aize-001	0.0001	449	0.0040	425	0.0652	297	0.0026	475	0.0022	480	0.0058	393
27	aize-002	0.0000	5	0.0014	341	0.0230	207	0.0005	414	0.0004	295	0.0071	399
28	ajou-001	0.0000	332	0.0020	371	-	458	0.0001	272	0.0004	366	0.0045	383
29	alchera-004	0.0000	283	0.0009	275	0.0228	203	0.0001	302	0.0004	238	0.0003	192
30	alchera-005	0.0000	266	0.0009	274	0.0228	202	0.0001	300	0.0004	249	0.0003	188
31	alfabeta-001	0.0005	473	0.0650	495	0.2142	331	0.0024	471	0.0018	474	0.1071	483
32	alice-000	0.0000	48	0.0006	189	0.0133	123	0.0000	165	0.0004	234	0.0004	244
33	alleyes-000	0.0000	217	0.0010	292	-	402	0.0002	314	0.0004	336	0.0004	256
34	allgovision-000	0.0007	478	0.0062	452	-	339	0.0026	474	0.0052	491	0.0131	419
35	alphaface-001	0.0000	267	0.0012	318	-	385	0.0000	218	0.0004	342	0.0004	221
36	alphaface-002	0.0000	274	0.0012	319	-	366	0.0000	217	0.0004	343	0.0004	224
37	amplifiedgroup-001	0.0114	494	0.1023	497	-	413	0.0189	496	0.0279	499	0.1390	491
38	androvideo-000	0.0000	8	0.0000	5	-	397	0.0000	58	0.0000	70	0.0002	134
39	anke-004	0.0000	254	0.0011	308	-	355	0.0001	282	0.0004	349	0.0006	301
40	anke-005	0.0000	264	0.0012	322	-	379	0.0001	295	0.0004	359	0.0007	307
41	antheus-000	0.0000	60	0.0000	33	-	340	0.0000	27	0.0000	103	0.0242	442
42	antheus-001	0.0000	149	0.0000	77	-	490	0.0000	104	0.0000	26	0.0242	443
43	anyvision-004	0.0000	385	0.0017	357	-	434	0.0001	296	0.0004	298	0.0080	402
44	anyvision-005	0.0000	248	0.0013	331	-	405	0.0000	183	0.0004	233	0.0004	248
45	aratek-001	0.0000	114	0.0000	62	0.0000	47	0.0000	113	0.0000	16	0.0000	99
46	armatura-001	0.0000	401	0.0021	378	0.0257	228	0.0005	408	0.0005	391	0.0357	456
47	armatura-003	0.0000	253	0.0012	325	0.0333	256	0.0004	385	0.0004	287	0.0008	318
48	asusaics-000	0.0000	88	0.0000	45	-	375	0.0000	3	0.0000	125	0.0000	23
49	asusaics-001	0.0000	191	0.0000	106	-	462	0.0000	74	0.0000	55	0.0000	72
50	autentika-000	0.0000	28	0.0000	16	0.0000	20	0.0000	45	0.0000	85	0.0000	43
51	autentika-001	0.0000	63	0.0000	31	0.0000	1	0.0000	25	0.0000	105	0.0000	11
52	authenmetric-003	0.0000	46	0.0000	26	0.0000	5	0.0000	34	0.0000	96	0.0000	1
53	authenmetric-004	0.0000	121	0.0000	64	0.0000	45	0.0000	117	0.0000	13	0.0000	101
54	aware-005	0.0000	340	0.0020	368	-	400	0.0001	311	0.0004	348	0.0011	329
55	aware-006	0.0000	268	0.0009	271	0.0249	217	0.0000	187	0.0004	306	0.0006	297
56	awiros-001	0.0039	482	0.0369	486	-	371	0.0386	497	0.0872	503	0.3415	497
57	awiros-002	0.0000	413	0.0038	422	-	404	0.0007	429	0.0012	464	0.0208	436
58	aximetria-001	0.0000	357	0.0010	304	0.0217	195	0.0001	313	0.0004	293	0.0024	360

Table 33: FTE is the proportion of failed template generation attempts. Failures can occur because the software throws an exception, or because the software electively refuses to process the input image. This would typically occur if a face is not detected. FTE is measured as the number of function calls that give EITHER a non-zero error code OR that give a "small" template. This is defined as one whose size is less than 0.3 times the median template size for that algorithm. This second rule is needed because some algorithms incorrectly fail to return a non-zero error code when template generation fails.

A hyphen "-" indicates the dataset was not produced.¹ The effects of FTE are included in the accuracy results of this report by regarding any template comparison involving a failed template to produce a low similarity score. Thus higher FTE results in higher FNMR and lower FMR.

	Algorithm	Failure to Enrol Rate ¹											
		APPLICATION	BORDER	KIOSK	MUGSHOT	VISA	WILD	SEC. 2.2	SEC. 2.4	SEC. 2.6	SEC. 2.5	SEC. 2.1	SEC. 2.7
59	ayftech-001	0.0002	464	0.0046	436	-	501	0.0043	485	0.0011	446	0.0091	407
60	ayonix-000	0.0053	485	0.0341	483	-	496	0.0113	494	0.0137	496	0.1194	487
61	beethedata-000	0.0005	471	0.0042	430	0.0366	264	0.0002	327	0.0010	441	0.0006	290
62	beyneai-000	0.0000	209	0.0000	113	0.0000	37	0.0000	64	0.0000	64	0.0000	86
63	biocube-001	0.0006	475	0.0391	487	0.1207	323	0.0015	458	0.0020	477	0.0253	446
64	biocube-002	0.0000	230	0.0046	439	0.0721	312	0.0008	437	0.0012	459	0.0486	458
65	bioditechswiss-001	0.0000	307	0.0007	216	-	439	0.0000	175	0.0004	325	0.0025	362
66	bioditechswiss-002	0.0000	319	0.0007	219	-	432	0.0000	178	0.0004	320	0.0005	288
67	biometric-vision-000	0.0000	220	0.0005	172	0.0107	110	0.0002	355	0.0004	257	0.0004	273
68	bm-001	0.0000	147	0.0000	74	-	495	0.0000	132	0.0000	29	0.0000	110
69	boetech-001	0.0087	490	0.0272	477	0.2117	328	0.0032	480	0.0160	498	0.0946	478
70	boetech-002	0.0087	491	0.0272	478	0.2117	329	0.0032	481	0.0160	497	0.0946	479
71	bresee-001	0.0000	240	0.0010	298	-	418	0.0002	328	0.0003	181	0.0003	149
72	bresee-002	0.0000	387	0.0020	374	0.0219	197	0.0008	432	0.0004	275	0.0031	371
73	camvi-002	0.0000	4	0.0000	1	-	403	0.0000	55	0.0000	74	0.0000	30
74	camvi-004	0.0000	47	0.0000	125	-	353	0.0000	35	0.0000	95	0.0000	6
75	candour-001	0.0000	124	0.0000	66	0.0000	44	0.0000	116	0.0000	12	0.0000	100
76	canon-003	0.0000	317	0.0008	238	0.0234	212	0.0000	209	0.0004	310	0.0003	197
77	canon-004	0.0000	272	0.0008	236	0.0234	211	0.0000	208	0.0004	319	0.0003	195
78	cchonolulu-000	0.0054	486	0.0395	489	0.2802	336	0.0036	483	0.0012	458	0.0867	473
79	ceiec-003	0.0000	175	0.0013	339	-	429	0.0001	244	0.0004	326	0.0004	216
80	ceiec-004	0.0000	23	0.0008	251	-	392	0.0000	182	0.0004	242	0.0004	257
81	chosun-001	0.0000	171	0.0000	92	-	435	0.0000	97	0.0000	32	0.0000	54
82	chosun-002	0.0000	75	0.0000	38	-	383	0.0000	15	0.0000	114	0.0000	13
83	chtface-005	0.0000	201	0.0017	354	0.0320	247	0.0000	195	0.0004	335	0.0020	358
84	chtface-006	0.0000	55	0.0017	353	0.0320	246	0.0000	194	0.0004	341	0.0020	357
85	cist-001	0.0000	78	0.0005	183	0.0087	101	0.0000	17	0.0000	112	0.0000	20
86	cist-002	0.0000	31	0.0048	441	0.0128	120	0.0000	46	0.0000	84	0.0000	42
87	clearviewai-000	0.0000	246	0.0003	143	0.0081	96	0.0000	198	0.0003	164	0.0003	150
88	closeli-001	0.0000	159	0.0000	85	0.0000	36	0.0000	90	0.0000	39	0.0001	131
89	cloudmatrix-001	0.0000	345	0.0028	391	0.0225	200	0.0001	237	0.0004	227	0.0004	240
90	cloudmatrix-002	0.0000	356	0.0028	392	0.0225	201	0.0001	241	0.0004	222	0.0004	241
91	cloudwalk-hr-003	0.0000	258	0.0008	255	-	351	0.0001	251	0.0004	235	0.0113	414
92	cloudwalk-hr-004	0.0000	297	0.0011	315	-	498	0.0004	383	0.0003	201	0.0129	418
93	cloudwalk-mt-006	0.0000	270	0.0006	193	0.0158	143	0.0002	339	0.0004	351	0.0004	222
94	cloudwalk-mt-007	0.0000	301	0.0006	194	0.0158	144	0.0002	340	0.0004	345	0.0004	228
95	codeline-000	0.0000	70	0.0000	37	0.0000	11	0.0000	14	0.0000	115	0.0000	15
96	cogent-007	0.0000	388	0.0000	122	0.0000	67	0.0000	184	0.0000	136	0.0001	128
97	cogent-008	0.0000	184	0.0010	305	0.0304	243	0.0000	203	0.0004	216	0.0003	166
98	cognitec-003	0.0001	438	0.0194	472	0.0820	317	0.0003	374	0.0005	389	0.0039	377
99	cognitec-004	0.0001	439	0.0037	421	0.0580	290	0.0003	375	0.0005	388	0.0035	372
100	cor-001	0.0000	249	0.0006	197	-	358	0.0002	356	0.0004	303	0.0004	271
101	coretech-000	0.0000	188	0.0000	99	0.0000	26	0.0000	84	0.0000	48	0.0000	69
102	coretech-001	0.0000	433	0.0033	409	0.0677	302	0.0005	412	0.0011	453	0.0027	366
103	corsight-002	0.0000	282	0.0005	186	0.0152	136	0.0001	285	0.0004	277	0.0003	198
104	corsight-003	0.0000	286	0.0006	205	0.0175	154	0.0001	278	0.0004	290	0.0003	208
105	csc-002	0.0015	480	0.0033	406	-	378	0.0006	423	0.0006	429	0.0968	480
106	csc-003	0.0015	481	0.0033	407	0.0445	283	0.0006	424	0.0006	428	0.0968	481
107	ctbcbank-000	0.0001	442	0.0051	444	-	461	0.0011	449	0.0019	475	0.0868	474
108	ctbcbank-001	0.0000	415	0.0036	420	-	445	0.0005	409	0.0010	440	0.0844	470
109	cu-face-002	0.0000	39	0.0000	19	0.0000	18	0.0000	39	0.0000	91	0.0000	50
110	cubox-002	0.0000	343	0.0006	201	0.0159	146	0.0002	357	0.0005	407	0.0016	347
111	cubox-003	0.0000	9	0.0010	302	0.0210	186	0.0002	324	0.0004	327	0.0005	277
112	cudocommunication-001	0.0000	1	0.0000	2	0.0000	16	0.0000	56	0.0000	73	0.0000	119
113	cuhkee-001	0.0000	320	0.0011	314	-	424	0.0000	146	0.0004	279	0.1278	489
114	cybercore-002	0.0000	396	0.0001	129	0.0014	72	0.0002	319	0.0002	144	0.0018	352
115	cybercore-003	0.0000	338	0.0003	146	0.0060	83	0.0005	413	0.0003	166	0.0192	434
116	cyberextruder-003	0.0000	399	0.0077	456	0.0887	319	0.0001	307	0.0006	422	0.0009	325

Table 34: FTE is the proportion of failed template generation attempts. Failures can occur because the software throws an exception, or because the software electively refuses to process the input image. This would typically occur if a face is not detected. FTE is measured as the number of function calls that give EITHER a non-zero error code OR that give a “small” template. This is defined as one whose size is less than 0.3 times the median template size for that algorithm. This second rule is needed because some algorithms incorrectly fail to return a non-zero error code when template generation fails.

A hyphen “-” indicates the dataset was not produced.¹ The effects of FTE are included in the accuracy results of this report by regarding any template comparison involving a failed template to produce a low similarity score. Thus higher FTE results in higher FNMR and lower FMR.

	Algorithm	Failure to Enrol Rate ¹							
		APPLICATION	BORDER	KIOSK	MUGSHOT	VISA	WILD	SEC. 2.1	SEC. 2.7
	Name	SEC. 2.2	SEC. 2.4	SEC. 2.6	SEC. 2.5	SEC. 2.1	SEC. 2.7	SEC. 2.1	SEC. 2.7
117	cyberextruder-004	0.0000	393	0.0097	460	0.1025	321	0.0001	299
118	cyberlink-010	0.0000	118	0.0004	165	0.0106	107	0.0000	141
119	cyberlink-011	0.0000	98	0.0004	164	0.0106	108	0.0000	142
120	dahua-006	0.0000	196	0.0000	120	-	460	0.0000	202
121	dahua-007	0.0000	105	0.0000	119	0.0000	69	0.0000	207
122	daon-000	0.0000	420	0.0028	395	0.0577	289	0.0014	456
123	decatur-000	0.0000	348	0.0020	367	-	377	0.0004	394
124	decatur-001	0.0000	275	0.0009	280	0.0194	171	0.0001	252
125	deepglint-004	0.0000	288	0.0005	169	0.0130	122	0.0002	354
126	deepglint-005	0.0000	370	0.0019	362	0.0438	282	0.0006	419
127	deepsea-001	0.0000	85	0.0000	46	-	374	0.0000	6
128	deepsense-001	0.0000	45	0.0006	207	0.0191	168	0.0000	164
129	deepsense-002	0.0000	203	0.0006	208	0.0191	169	0.0000	167
130	dermalog-010	0.0000	406	0.0031	403	0.0148	132	0.0006	416
131	dermalog-011	0.0000	430	0.0005	170	0.0116	114	0.0001	233
132	dicio-001	0.0005	474	0.0649	492	0.2136	330	0.0024	469
133	didiglobalface-001	0.0000	242	0.0012	317	-	416	0.0000	219
134	didiglobalface-002	0.0000	218	0.0012	316	0.0247	216	0.0000	220
135	digidata-000	0.0000	294	0.0023	383	0.0375	271	0.0004	400
136	digidata-001	0.0000	304	0.0023	384	0.0375	270	0.0004	399
137	digitalbarriers-002	0.0001	454	0.0045	434	-	468	0.0028	477
138	dps-000	0.0000	215	0.0000	114	0.0000	39	0.0000	66
139	dsk-000	0.0000	72	0.0000	36	-	380	0.0000	13
140	einetworks-000	0.0000	414	0.0017	355	-	363	0.0002	343
141	ekin-002	0.0000	56	0.0000	126	0.0004	70	0.0000	137
142	enface-001	0.0000	26	0.0012	327	0.0304	244	0.0000	170
143	enface-002	0.0000	324	0.0004	154	0.0084	100	0.0000	157
144	eocortex-000	0.0095	492	0.0602	491	-	409	0.0094	492
145	ercacat-001	0.0000	30	0.0005	177	-	417	0.0000	192
146	uronovate-001	0.0255	498	0.0102	462	0.0517	286	0.0021	465
147	expasoft-001	0.0000	42	0.0000	24	-	359	0.0000	32
148	expasoft-002	0.0000	101	0.0000	54	0.0000	55	0.0000	123
149	f8-001	0.0003	466	0.0059	449	-	411	0.0035	482
150	f8-002	0.0000	435	0.0150	469	0.0685	306	0.0005	402
151	faceonlive-001	0.0000	426	0.0029	400	0.0481	284	0.0013	454
152	faceonlive-002	0.0002	462	0.0009	283	0.0075	90	0.0008	435
153	facephi-000	0.0000	137	0.0004	150	0.0090	102	0.0001	284
154	facesoft-000	0.0000	102	0.0000	55	-	484	0.0000	124
155	facetag-000	0.0000	154	0.0000	82	0.0000	35	0.0000	88
156	facetag-002	0.0000	161	0.0000	90	0.0000	30	0.0000	96
157	facex-001	0.0001	460	0.0360	484	-	348	0.0047	487
158	facex-002	0.0001	461	0.0360	485	0.2663	334	0.0047	488
159	farfaces-001	0.0000	410	0.0007	218	0.0061	85	0.0003	371
160	fastenterprises-000	0.0000	329	0.0082	457	0.0169	151	0.0001	304
161	fiberhome-nanjing-003	0.0000	214	0.0004	158	-	452	0.0000	67
162	fiberhome-nanjing-004	0.0000	52	0.0004	157	-	346	0.0000	22
163	fincore-000	0.0000	251	0.0008	258	0.0185	162	0.0001	228
164	firstcreditkz-001	0.0000	367	0.0019	364	0.0321	249	0.0000	214
165	firstcreditkz-002	0.0000	236	0.0010	306	0.0232	210	0.0000	191
166	foomobi-001	0.0007	476	0.0000	70	0.0000	64	0.0020	464
167	frpkauai-001	0.0000	373	0.0024	387	0.0360	262	0.0001	240
168	frpkauai-002	0.0000	371	0.0019	365	0.0321	248	0.0000	213
169	fujitsulab-002	0.0000	138	0.0009	267	-	500	0.0001	293
170	fujitsulab-003	0.0000	32	0.0008	242	0.0166	150	0.0001	281
171	g42-intelbrain-001	0.0000	152	0.0000	79	0.0000	59	0.0000	106
172	geo-002	0.0000	318	0.0015	344	0.0332	254	0.0001	225
173	geo-004	0.0000	243	0.0005	185	0.0138	126	0.0001	266
174	glory-005	0.0000	349	0.0020	372	0.0345	257	0.0001	287

Table 35: FTE is the proportion of failed template generation attempts. Failures can occur because the software throws an exception, or because the software electively refuses to process the input image. This would typically occur if a face is not detected. FTE is measured as the number of function calls that give EITHER a non-zero error code OR that give a “small” template. This is defined as one whose size is less than 0.3 times the median template size for that algorithm. This second rule is needed because some algorithms incorrectly fail to return a non-zero error code when template generation fails.

A hyphen “-” indicates the dataset was not produced.¹ The effects of FTE are included in the accuracy results of this report by regarding any template comparison involving a failed template to produce a low similarity score. Thus higher FTE results in higher FNMR and lower FMR.

	Algorithm	Failure to Enrol Rate ¹											
		APPLICATION	BORDER	KIOSK	MUGSHOT	VISA	WILD	SEC. 2.2	SEC. 2.4	SEC. 2.6	SEC. 2.5	SEC. 2.1	SEC. 2.7
175	glory-006	0.0000	355	0.0020	373	0.0345	258	0.0001	289	0.0004	354	0.0167	426
176	gorilla-008	0.0000	247	0.0009	286	0.0259	229	0.0001	253	0.0004	329	0.0004	236
177	gorilla-009	0.0000	278	0.0010	295	0.0276	238	0.0001	234	0.0004	318	0.0004	223
178	graymatrics-001	0.0000	141	0.0010	287	0.0210	184	0.0001	306	0.0004	264	0.0006	299
179	griaule-001	0.0000	3	0.0012	328	0.0366	265	0.0000	161	0.0004	321	0.0005	282
180	griaule-002	0.0000	77	0.0007	223	0.0209	181	0.0000	211	0.0004	276	0.0004	214
181	hertasecurity-002	0.0000	199	0.0000	109	0.0000	41	0.0000	150	0.0000	132	0.0000	80
182	hertasecurity-003	0.0000	35	0.0000	17	0.0000	19	0.0000	139	0.0000	133	0.0000	45
183	hik-001	0.0000	139	0.0000	127	-	491	0.0000	101	0.0000	30	0.0000	111
184	hisign-001	0.0000	97	0.0000	51	0.0000	53	0.0000	119	0.0000	10	0.0000	92
185	hisign-002	0.0000	362	0.0006	202	0.0150	133	0.0001	290	0.0003	194	0.0005	285
186	hyperverge-003	0.0000	183	0.0008	240	0.0210	185	0.0002	358	0.0004	265	0.0004	260
187	hyperverge-004	0.0000	322	0.0008	256	0.0218	196	0.0002	346	0.0004	278	0.0004	245
188	hzailu-003	0.0000	309	0.0004	152	0.0081	98	0.0002	321	0.0003	189	0.0003	170
189	hzailu-004	0.0000	241	0.0004	151	0.0081	97	0.0002	320	0.0003	192	0.0003	169
190	icm-003	0.0000	51	0.0001	128	0.0023	73	0.0000	23	0.0000	129	0.0000	120
191	icm-004	0.0000	421	0.0033	411	0.0698	307	0.0006	422	0.0010	445	0.0026	365
192	icthtc-000	0.0001	458	0.0047	440	-	372	0.0028	478	0.0029	488	0.0086	404
193	id3-006	0.0000	368	0.0009	285	-	352	0.0004	388	0.0005	400	0.0008	319
194	id3-008	0.0000	115	0.0006	204	0.0184	160	0.0001	303	0.0004	212	0.0003	153
195	idemria-008	0.0000	119	0.0004	166	0.0078	94	0.0000	154	0.0003	187	0.0003	167
196	idemria-009	0.0000	210	0.0004	162	0.0077	92	0.0000	151	0.0003	190	0.0003	171
197	identity-000	0.0000	436	0.0020	375	0.0152	135	0.0012	451	0.0004	352	0.0835	468
198	igearx-face-000	0.0000	262	0.0006	190	0.0153	138	0.0004	386	0.0004	322	0.0003	201
199	iit-002	0.0000	418	0.0021	377	-	389	0.0009	444	0.0005	409	0.0443	457
200	iit-003	0.0000	233	0.0008	257	-	422	0.0000	181	0.0004	226	0.0069	397
201	imds-software-001	0.0000	128	0.0000	67	0.0000	63	0.0000	108	0.0000	22	0.0000	106
202	imds-software-002	0.0000	103	0.0000	56	0.0000	54	0.0000	122	0.0000	6	0.0000	88
203	imperial-000	0.0000	216	0.0000	115	-	451	0.0000	65	0.0000	63	0.0000	84
204	imperial-002	0.0000	54	0.0000	28	-	345	0.0000	21	0.0000	108	0.0000	8
205	incode-010	0.0000	359	0.0009	272	0.0255	226	0.0002	331	0.0004	252	0.0007	312
206	incode-011	0.0000	363	0.0009	273	0.0255	227	0.0002	330	0.0004	254	0.0007	313
207	infocert-001	0.0000	382	0.0059	450	0.0424	279	0.0001	256	0.0006	414	0.0018	353
208	innefulabs-000	0.0000	300	0.0024	386	-	493	0.0003	372	0.0005	396	0.0004	242
209	innovativetechnologyltd-001	0.0001	457	0.0050	443	-	483	0.0024	473	0.0025	484	0.0055	390
210	innovativetechnologyltd-002	0.0000	372	0.0046	435	-	486	0.0057	491	0.0005	397	0.0247	445
211	innovatrics-008	0.0000	250	0.0009	278	0.0204	177	0.0000	189	0.0004	210	0.0003	199
212	innovatrics-009	0.0000	67	0.0005	168	0.0142	129	0.0000	30	0.0000	134	0.0000	121
213	insightface-003	0.0000	213	0.0000	117	0.0000	38	0.0000	68	0.0000	60	0.0000	81
214	insightface-004	0.0000	113	0.0000	60	0.0000	50	0.0000	128	0.0000	2	0.0000	95
215	inspur-000	0.0000	90	0.0000	43	0.0000	7	0.0000	2	0.0000	126	0.0000	22
216	inspur-001	0.0000	109	0.0000	58	0.0000	49	0.0000	126	0.0000	4	0.0000	98
217	intelliloudai-001	0.0000	153	0.0000	83	-	436	0.0000	89	0.0000	41	0.0001	130
218	intelliloudai-002	0.0000	58	0.0008	247	-	350	0.0000	180	0.0004	220	0.0012	338
219	intellifusion-001	0.0000	314	0.0005	180	-	430	0.0001	249	0.0003	193	0.0005	283
220	intellifusion-002	0.0000	12	0.0000	124	-	395	0.0000	130	0.0000	83	0.0001	129
221	intellivision-004	0.0000	315	0.0011	309	0.0266	235	0.0002	360	0.0004	371	0.0179	431
222	intellivision-005	0.0001	452	0.0041	427	0.0528	288	0.0005	406	0.0007	433	0.0015	345
223	intellivix-002	0.0000	33	0.0009	284	0.0184	161	0.0000	37	0.0000	93	0.0000	46
224	intellivix-003	0.0000	24	0.0000	14	0.0000	21	0.0000	43	0.0000	87	0.0000	41
225	intelresearch-005	0.0000	234	0.0006	196	0.0144	130	0.0000	166	0.0004	246	0.0003	177
226	intelresearch-006	0.0000	11	0.0000	121	0.0004	71	0.0000	140	0.0004	244	0.0003	196
227	intema-000	0.0000	64	0.0005	173	0.0126	117	0.0000	200	0.0004	228	0.0003	165
228	intema-001	0.0000	285	0.0004	161	0.0106	109	0.0000	143	0.0003	199	0.0003	193
229	intsyssmu-001	0.0000	16	0.0010	296	-	386	0.0001	271	0.0004	301	0.0004	252
230	intsyssmu-002	0.0000	134	0.0010	297	-	497	0.0001	275	0.0004	296	0.0004	254
231	ionetworks-000	0.0000	110	0.0016	351	0.0387	274	0.0004	378	0.0005	386	0.0004	261
232	iqface-000	0.0000	38	0.0000	21	-	406	0.0000	40	0.0000	88	0.0000	47

Table 36: FTE is the proportion of failed template generation attempts. Failures can occur because the software throws an exception, or because the software electively refuses to process the input image. This would typically occur if a face is not detected. FTE is measured as the number of function calls that give EITHER a non-zero error code OR that give a “small” template. This is defined as one whose size is less than 0.3 times the median template size for that algorithm. This second rule is needed because some algorithms incorrectly fail to return a non-zero error code when template generation fails.

A hyphen “-” indicates the dataset was not produced.¹ The effects of FTE are included in the accuracy results of this report by regarding any template comparison involving a failed template to produce a low similarity score. Thus higher FTE results in higher FNMR and lower FMR.

	Algorithm	Failure to Enrol Rate ¹											
		APPLICATION	BORDER	KIOSK	MUGSHOT	VISA	WILD	SEC. 2.2	SEC. 2.4	SEC. 2.6	SEC. 2.5	SEC. 2.1	SEC. 2.7
233	iqface-003	0.0000	416	0.0076	455	-	459	0.0006	417	0.0005	412	0.0069	396
234	irex-000	0.0000	381	0.0009	282	-	347	0.0000	197	0.0005	381	0.0003	194
235	isap-001	0.0000	173	0.0000	95	-	428	0.0000	77	0.0000	52	0.0000	63
236	isap-002	0.0000	198	0.0000	110	-	455	0.0000	62	0.0000	68	0.0000	79
237	isityou-000	0.0068	489	0.0316	481	-	474	0.0023	468	0.0010	443	0.0663	465
238	isystems-001	0.0000	425	0.0035	417	-	487	0.0010	446	0.0007	432	0.0128	417
239	isystems-002	0.0000	424	0.0035	416	-	472	0.0010	447	0.0007	431	0.0128	416
240	itmo-007	0.0000	207	0.0009	266	-	457	0.0003	377	0.0000	65	0.0004	232
241	itmo-008	0.0000	59	0.0135	466	0.1239	324	0.0024	472	0.0000	107	0.0836	469
242	ivacognitive-001	0.0000	352	0.0011	311	-	370	0.0001	235	0.0004	360	0.0011	330
243	iws-000	0.0005	472	0.0650	494	-	471	0.0024	470	0.0012	460	0.0936	477
244	jaakit-001	0.0008	479	0.0858	496	0.2713	335	0.0042	484	0.0021	479	0.1062	482
245	kakao-007	0.0000	71	0.0007	209	0.0165	149	0.0001	263	0.0004	250	0.0097	410
246	kakao-008	0.0000	133	0.0009	269	0.0209	182	0.0001	264	0.0004	239	0.0097	411
247	kakaobank-000	0.0000	145	0.0000	76	0.0000	60	0.0000	103	0.0000	27	0.0000	109
248	kakaopay-001	0.0000	354	0.0013	337	0.0322	251	0.0001	246	0.0004	361	0.0078	401
249	kasikornlabs-000	0.0000	432	0.0035	415	0.0713	310	0.0004	395	0.0012	463	0.0270	449
250	kasikornlabs-002	0.0000	429	0.0033	408	0.0698	308	0.0004	391	0.0012	455	0.0269	448
251	kedacom-000	0.0000	212	0.0000	118	-	447	0.0000	69	0.0000	59	0.0000	82
252	kiwitech-000	0.0000	336	0.0009	265	-	448	0.0004	392	0.0005	385	0.0004	264
253	kneron-003	0.0239	496	0.0306	479	-	449	0.0044	486	0.0016	472	0.1823	493
254	kneron-005	0.0000	427	0.0226	473	-	364	0.0006	415	0.0005	395	0.0097	409
255	knowutech-000	0.0000	271	0.0008	239	0.0215	193	0.0000	185	0.0004	317	0.0003	202
256	koookmin-002	0.0000	190	0.0000	100	-	426	0.0000	82	0.0000	47	0.0000	67
257	koreaid-001	0.0000	181	0.0023	385	0.0371	268	0.0000	210	0.0005	378	0.0027	367
258	krungthai-002	0.0000	252	0.0005	175	0.0111	113	0.0002	344	0.0003	205	0.0005	274
259	kuke3d-001	0.0000	165	0.0000	86	0.0000	32	0.0000	93	0.0000	38	0.0000	58
260	kuke3d-002	0.0000	27	0.0000	15	0.0000	22	0.0000	44	0.0000	86	0.0000	40
261	lebentech-000	0.0042	483	0.0029	402	0.0252	223	0.0051	490	0.0066	493	0.0154	422
262	lemalabs-001	0.0000	150	0.0005	184	0.0141	127	0.0002	341	0.0004	224	0.0004	229
263	lineclova-002	0.0000	92	0.0007	210	0.0181	157	0.0000	9	0.0000	122	0.0000	115
264	lineclova-003	0.0000	407	0.0023	381	0.0700	309	0.0002	359	0.0005	380	0.0038	374
265	lookman-002	0.0000	18	0.0000	11	-	388	0.0000	51	0.0000	78	0.0000	39
266	lookman-004	0.0000	178	0.0000	97	-	431	0.0000	80	0.0000	50	0.0000	61
267	luxand-000	0.0000	164	0.0000	88	-	433	0.0000	95	0.0000	36	0.0000	60
268	mantra-000	0.0001	440	0.0041	429	0.0680	305	0.0003	370	0.0004	370	0.0037	373
269	maxvision-002	0.0000	235	0.0009	261	0.0229	205	0.0002	317	0.0004	283	0.0004	270
270	maxvision-003	0.0000	261	0.0009	262	0.0229	204	0.0002	316	0.0004	288	0.0004	267
271	megvii-005	0.0000	238	0.0010	289	0.0206	179	0.0002	350	0.0004	339	0.0011	331
272	megvii-006	0.0000	330	0.0010	291	0.0206	180	0.0002	351	0.0004	334	0.0011	332
273	meituuan-002	0.0000	298	0.0013	335	0.0251	221	0.0001	277	0.0004	307	0.0020	356
274	meituuan-003	0.0000	321	0.0013	336	0.0251	220	0.0001	276	0.0004	309	0.0020	355
275	meiya-001	0.0000	422	0.0028	396	-	401	0.0004	397	0.0010	444	0.0025	361
276	mendaxiatech-000	0.0000	259	0.0010	290	0.0206	178	0.0002	352	0.0004	340	0.0011	333
277	metsakuurcompany-002	0.0000	19	0.0000	10	0.0000	14	0.0000	50	0.0000	79	0.0000	38
278	metsakuurcompany-003	0.0000	96	0.0000	52	0.0000	52	0.0000	120	0.0000	11	0.0000	93
279	miaxis-001	0.0000	316	0.0013	332	0.0262	232	0.0001	305	0.0003	165	0.0003	205
280	miaxis-002	0.0448	500	0.1162	498	0.2565	333	0.2128	498	0.0347	501	0.2158	494
281	microfocus-002	0.0001	456	0.0053	447	-	488	0.0008	436	0.0016	471	0.0220	438
282	microfocus-003	0.0001	451	0.0049	442	0.0819	316	0.0007	430	0.0015	470	0.0163	424
283	minivision-000	0.0000	195	0.0000	104	-	466	0.0000	71	0.0000	57	0.0000	73
284	mitek-000	0.0000	380	0.0029	399	0.0521	287	0.0002	342	0.0003	177	0.0026	363
285	mobai-000	0.0000	391	0.0114	464	-	440	0.0003	373	0.0012	462	0.1242	488
286	mobai-001	0.0000	350	0.0040	424	-	373	0.0001	283	0.0012	461	0.0523	462
287	mobbl-001	0.0000	417	0.0052	445	0.0678	303	0.0002	325	0.0005	403	0.0181	432
288	mobbl-003	0.0000	428	0.0029	401	0.0633	296	0.0002	347	0.0009	439	0.0026	364
289	mobipintech-000	0.0000	151	0.0000	80	0.0000	58	0.0000	107	0.0000	24	0.0000	112
290	moreedian-000	0.0000	287	0.0009	264	-	478	0.0004	393	0.0005	384	0.0004	266

Table 37: FTE is the proportion of failed template generation attempts. Failures can occur because the software throws an exception, or because the software electively refuses to process the input image. This would typically occur if a face is not detected. FTE is measured as the number of function calls that give EITHER a non-zero error code OR that give a “small” template. This is defined as one whose size is less than 0.3 times the median template size for that algorithm. This second rule is needed because some algorithms incorrectly fail to return a non-zero error code when template generation fails.

A hyphen “-” indicates the dataset was not produced.¹ The effects of FTE are included in the accuracy results of this report by regarding any template comparison involving a failed template to produce a low similarity score. Thus higher FTE results in higher FNMR and lower FMR.

	Algorithm	Failure to Enrol Rate ¹							
		APPLICATION		BORDER		KIOSK	MUGSHOT	VISA	WILD
Name	SEC. 2.2	SEC. 2.4	SEC. 2.6	SEC. 2.5	SEC. 2.1	SEC. 2.7			
291	mukh-002	0.0000	179	0.0022	380	0.0513	285	0.0002	322
292	mukh-003	0.0000	326	0.0003	138	0.0060	84	0.0001	312
293	multimodality-000	0.0000	125	0.0000	63	0.0000	46	0.0000	115
294	multimodality-001	0.0000	69	0.0009	260	0.0259	230	0.0000	29
295	mvision-001	0.0000	111	0.0000	57	-	476	0.0000	125
296	nazhiai-000	0.0000	127	0.0000	68	-	502	0.0000	109
297	ncssg-001	0.0000	176	0.0000	93	0.0000	28	0.0000	76
298	neosystems-004	0.0000	49	0.0000	27	0.0000	3	0.0000	36
299	netbridgetech-001	0.0000	10	0.0000	7	-	393	0.0000	47
300	netbridgetech-002	0.0000	57	0.0000	30	-	349	0.0000	24
301	neurotechnology-015	0.0000	170	0.0004	153	0.0082	99	0.0000	98
302	neurotechnology-016	0.0000	117	0.0003	141	0.0069	88	0.0000	114
303	nhn-002	0.0000	126	0.0004	167	0.0091	103	0.0000	179
304	nhn-003	0.0000	369	0.0000	29	0.0000	2	0.0001	310
305	nodeflux-002	0.0000	303	0.0261	476	-	489	0.0008	434
306	nominder-000	0.0000	219	0.0003	134	0.0053	79	0.0000	172
307	notiontag-001	0.0000	129	0.0000	71	-	503	0.0027	476
308	notiontag-002	0.0000	14	0.0000	8	0.0000	15	0.0000	48
309	nsensecorp-004	0.0406	499	0.0035	414	0.0181	156	0.0016	460
310	nsensecorp-005	0.0000	182	0.0000	98	0.0000	23	0.0000	81
311	ntechlab-011	0.0000	123	0.0003	136	0.0057	81	0.0000	206
312	ntechlab-012	0.0000	86	0.0003	135	0.0057	80	0.0000	199
313	omface-000	0.0000	41	0.0000	25	0.0000	4	0.0000	33
314	omface-001	0.0000	155	0.0000	123	0.0000	68	0.0000	86
315	omnigarde-001	0.0000	302	0.0008	233	0.0213	188	0.0000	176
316	omnigarde-002	0.0000	325	0.0008	234	0.0213	187	0.0000	173
317	onfido-000	0.0000	423	0.0040	423	0.0804	315	0.0004	380
318	openface-001	0.0000	397	0.0104	463	0.0668	298	0.0004	387
319	oz-003	0.0000	81	0.0002	131	0.0042	76	0.0000	136
320	oz-004	0.0000	403	0.0003	140	0.0041	75	0.0000	144
321	palit-000	0.0000	225	0.0005	176	0.0134	124	0.0002	333
322	palit-001	0.0000	263	0.0007	232	0.0201	175	0.0002	332
323	pangiam-000	0.0000	66	0.0021	379	0.0364	263	0.0001	224
324	pangiam-001	0.0000	40	0.0005	182	0.0128	119	0.0002	362
325	papago-001	0.0000	360	0.0008	241	0.0159	147	0.0002	361
326	papsav1923-002	0.0000	224	0.0018	361	0.0268	236	0.0000	193
327	papsav1923-003	0.0000	376	0.0019	366	0.0321	250	0.0000	216
328	paravision-010	0.0000	144	0.0010	294	0.0201	174	0.0001	260
329	paravision-011	0.0000	50	0.0010	293	0.0201	173	0.0001	257
330	pensees-001	0.0000	265	0.0000	35	-	381	0.0000	12
331	pixelall-008	0.0000	84	0.0008	249	0.0247	215	0.0000	1
332	pixelall-009	0.0000	136	0.0000	72	0.0000	62	0.0000	112
333	privid-001	0.0001	459	0.0176	471	0.0598	293	0.0021	466
334	psl-010	0.0000	299	0.0004	156	0.0095	104	0.0000	134
335	psl-011	0.0000	281	0.0003	137	0.0063	87	0.0000	135
336	ptakuratsatu-000	0.0000	290	0.0007	229	-	475	0.0001	226
337	pxl-001	0.0000	437	0.0044	433	-	427	0.0005	407
338	pyramid-000	0.0001	453	0.0041	428	-	410	0.0005	405
339	qazbs-000	0.0000	177	0.0009	270	0.0265	234	0.0000	163
340	qluevision-001	0.0000	383	0.0008	245	0.0153	137	0.0008	433
341	qnap-002	0.0000	419	0.0033	405	0.0761	313	0.0004	382
342	qnap-003	0.0000	204	0.0016	349	0.0402	277	0.0000	212
343	quantasoft-003	0.0000	390	0.0015	347	0.0355	260	0.0005	404
344	rankone-013	0.0000	160	0.0005	174	0.0126	118	0.0000	158
345	rankone-014	0.0000	174	0.0005	171	0.0129	121	0.0000	156
346	realnetworks-007	0.0000	244	0.0013	338	0.0425	280	0.0000	138
347	realnetworks-008	0.0000	295	0.0002	133	0.0045	77	0.0000	133
348	regula-000	0.0000	197	0.0000	107	0.0000	43	0.0000	75
								0.0000	54
								0.0000	76

Table 38: FTE is the proportion of failed template generation attempts. Failures can occur because the software throws an exception, or because the software electively refuses to process the input image. This would typically occur if a face is not detected. FTE is measured as the number of function calls that give EITHER a non-zero error code OR that give a "small" template. This is defined as one whose size is less than 0.3 times the median template size for that algorithm. This second rule is needed because some algorithms incorrectly fail to return a non-zero error code when template generation fails.

A hyphen "-" indicates the dataset was not produced.¹ The effects of FTE are included in the accuracy results of this report by regarding any template comparison involving a failed template to produce a low similarity score. Thus higher FTE results in higher FNMR and lower FMR.

	Algorithm Name	Failure to Enrol Rate ¹							
		APPLICATION		BORDER		KIOSK	MUGSHOT	VISA	WILD
		SEC. 2.2	SEC. 2.4	SEC. 2.6	SEC. 2.5	SEC. 2.1	SEC. 2.7		
349	regula-001	0.0000	73	0.0000	39	0.0000	12	0.0000	16
350	remarkai-001	0.0000	62	0.0000	32	-	341	0.0000	26
351	remarkai-003	0.0000	313	0.0007	217	0.0187	163	0.0000	196
352	rendip-000	0.0000	365	0.0016	350	0.0293	239	0.0002	329
353	revealmedia-005	0.0000	379	0.0007	224	0.0189	165	0.0009	443
354	revealmedia-006	0.0000	83	0.0009	279	0.0238	213	0.0001	279
355	rokid-000	0.0000	99	0.0072	453	-	481	0.0001	265
356	rokid-001	0.0000	17	0.0013	334	-	387	0.0000	52
357	s1-005	0.0000	116	0.0004	159	0.0120	116	0.0001	242
358	s1-007	0.0000	20	0.0006	192	0.0110	112	0.0001	239
359	saffe-001	0.0000	37	0.0000	20	-	407	0.0000	42
360	saffe-002	0.0000	192	0.0000	105	-	463	0.0000	73
361	samsungsds-001	0.0000	29	0.0005	179	0.0146	131	0.0001	258
362	samsungsds-002	0.0000	208	0.0004	160	0.0119	115	0.0001	259
363	samtech-001	0.0001	450	0.0032	404	-	342	0.0004	390
364	scanovate-002	0.0000	339	0.0018	360	-	399	0.0000	221
365	scanovate-003	0.0000	358	0.0233	474	0.3371	338	0.0006	418
366	sdc-000	0.0000	434	0.0035	413	0.0678	304	0.0005	411
367	securifai-005	0.0000	76	0.0000	40	0.0000	9	0.0000	18
368	securifai-006	0.0000	167	0.0000	89	0.0000	31	0.0000	92
369	sensetime-007	0.0000	2	0.0004	155	0.0106	106	0.0000	177
370	sensetime-008	0.0000	163	0.0007	228	0.0250	218	0.0000	131
371	sertis-000	0.0000	25	0.0007	222	-	419	0.0000	222
372	sertis-002	0.0000	202	0.0007	213	0.0152	134	0.0000	215
373	seventhsense-001	0.0000	337	0.0006	206	0.0184	159	0.0001	229
374	seventhsense-002	0.0000	100	0.0003	149	0.0076	91	0.0000	223
375	shaman-000	0.0000	13	0.0000	9	-	396	0.0000	49
376	shaman-001	0.0000	205	0.0000	108	-	456	0.0000	60
377	shu-002	0.0000	347	0.0010	299	-	343	0.0005	401
378	shu-003	0.0000	106	0.0007	211	-	485	0.0001	231
379	siat-002	0.0000	229	0.0012	326	-	390	0.0000	190
380	siat-005	0.0000	95	0.0000	50	0.0000	66	0.0000	11
381	sjtu-003	0.0000	135	0.0005	187	-	499	0.0000	205
382	sjtu-004	0.0000	172	0.0000	94	0.0000	27	0.0000	78
383	sktelecom-000	0.0000	328	0.0008	250	0.0190	166	0.0000	201
384	smartbiometrik-001	0.0005	470	0.0649	493	0.2147	332	0.0017	461
385	smartengines-000	0.0066	488	0.0150	468	0.1656	326	0.0022	467
386	smartengines-001	0.0003	465	0.0073	454	0.0714	311	0.0007	427
387	smartvist-000	0.0000	162	0.0026	390	0.0357	261	0.0002	315
388	smilart-002	0.0000	431	0.0036	418	-	382	-	500
389	smilart-003	0.0003	467	0.0100	461	-	477	0.0014	455
390	sodec-000	0.0000	91	0.0000	49	0.0000	6	0.0000	10
391	sqisoft-002	0.0000	74	0.0003	145	0.0078	93	0.0000	155
392	sqisoft-003	0.0000	132	0.0003	147	0.0078	95	0.0000	159
393	staqu-000	0.0000	112	0.0000	61	-	480	0.0000	129
394	starhybrid-001	0.0001	455	0.0033	410	-	408	0.0009	442
395	stcon-000	0.0000	305	0.0017	359	0.0301	242	0.0000	174
396	stcon-001	0.0000	232	0.0017	358	0.0301	241	0.0000	171
397	sukshi-000	0.0000	87	0.0000	42	0.0000	8	0.0000	5
398	suprema-003	0.0000	277	0.0008	252	0.0231	208	0.0000	149
399	suprema-004	0.0000	306	0.0014	340	0.0299	240	0.0000	153
400	supremaid-001	0.0000	308	0.0020	370	0.0330	253	0.0001	274
401	supremaid-002	0.0000	223	0.0020	369	0.0330	252	0.0001	270
402	surrey-cvssp-001	0.0173	495	0.0007	214	0.0179	155	0.0011	450
403	surrey-cvssp-002	0.0000	408	0.0006	198	0.0156	140	0.0001	254
404	swsam-001	0.0000	82	0.0012	330	0.0263	233	0.0000	19
405	synesis-006	0.0000	140	0.0003	148	-	494	0.0000	204
406	synesis-007	0.0000	323	0.0013	333	-	425	0.0002	349

Table 39: FTE is the proportion of failed template generation attempts. Failures can occur because the software throws an exception, or because the software electively refuses to process the input image. This would typically occur if a face is not detected. FTE is measured as the number of function calls that give EITHER a non-zero error code OR that give a “small” template. This is defined as one whose size is less than 0.3 times the median template size for that algorithm. This second rule is needed because some algorithms incorrectly fail to return a non-zero error code when template generation fails.

A hyphen “-” indicates the dataset was not produced.¹ The effects of FTE are included in the accuracy results of this report by regarding any template comparison involving a failed template to produce a low similarity score. Thus higher FTE results in higher FNMR and lower FMR.

	Algorithm	Failure to Enrol Rate ¹									
		APPLICATION		BORDER		KIOSK		MUGSHOT		VISA	
Name	SEC. 2.2	SEC. 2.4	SEC. 2.6	SEC. 2.5	SEC. 2.1	SEC. 2.1	SEC. 2.7				
407	synology-000	0.0000	193	0.0000	103	-	467	0.0000	72	0.0000	58
408	synology-002	0.0000	68	0.0000	34	-	344	0.0000	28	0.0000	102
409	sztu-000	0.0000	157	0.0000	81	-	437	0.0000	87	0.0000	43
410	sztu-001	0.0000	146	0.0000	75	0.0000	61	0.0000	102	0.0000	28
411	t4isb-000	0.0000	166	0.0000	87	0.0000	33	0.0000	94	0.0000	37
412	tech5-005	0.0000	273	0.0007	231	-	365	0.0000	169	0.0004	332
413	tech5-007	0.0000	221	0.0014	342	0.0305	245	0.0000	162	0.0004	241
414	techsign-000	0.0007	477	0.0334	482	0.2093	327	0.0020	463	0.0011	449
415	techsign-001	0.0000	333	0.0008	259	0.0253	224	0.0002	336	0.0004	294
416	tevian-007	0.0000	227	0.0015	348	0.0429	281	0.0002	345	0.0004	314
417	tevian-008	0.0000	327	0.0006	191	0.0109	111	0.0000	168	0.0003	170
418	tiger-005	0.0000	289	0.0009	281	0.0194	172	0.0001	255	0.0004	263
419	tiger-006	0.0000	341	0.0011	313	0.0396	275	0.0001	301	0.0004	376
420	tinkoff-001	0.0000	353	0.0008	248	0.0171	152	0.0001	294	0.0004	262
421	tongyi-005	0.0000	44	0.0000	23	-	361	0.0000	31	0.0000	99
422	toppanidgate-000	0.0000	256	0.0008	244	0.0232	209	0.0004	379	0.0004	304
423	toshiba-004	0.0000	169	0.0000	91	0.0000	34	0.0000	99	0.0000	33
424	toshiba-006	0.0000	284	0.0004	163	0.0050	78	0.0001	297	0.0003	167
425	touchlessid-001	0.0000	130	0.0036	419	0.0923	320	0.0000	111	0.0000	19
426	touchlessid-002	0.0000	36	0.0043	431	0.1087	322	0.0000	41	0.0000	89
427	trueface-002	0.0000	346	0.0046	437	-	357	0.0003	363	0.0005	408
428	trueface-003	0.0000	364	0.0046	438	0.0397	276	0.0003	364	0.0005	405
429	trueidvng-001	0.0000	361	0.0020	376	0.0385	273	0.0002	338	0.0005	394
430	tuputech-000	0.0003	468	0.0116	465	-	354	-	502	0.0081	495
431	turingtechvip-001	0.0001	445	0.0007	225	0.0061	86	0.0007	426	0.0006	415
432	turingtechvip-002	0.0001	446	0.0017	356	0.0097	105	0.0007	425	0.0006	416
433	turkcell-000	0.0110	493	0.0234	475	0.0350	259	0.0103	493	0.0306	500
434	turkcell-001	0.0000	53	0.0002	132	0.0034	74	0.0001	262	0.0003	151
435	twface-000	0.0000	15	0.0000	12	0.0000	13	0.0000	53	0.0000	76
436	twface-001	0.0000	80	0.0000	41	0.0000	10	0.0000	20	0.0000	109
437	ulsee-001	0.0000	89	0.0000	44	-	376	0.0000	4	0.0000	124
438	ultinious-000	-	503	-	503	-	479	-	503	0.0003	174
439	ultinious-001	-	501	-	501	-	362	-	501	0.0003	176
440	uluface-002	0.0000	7	0.0000	4	-	398	0.0000	59	0.0000	71
441	uluface-003	0.0000	194	0.0001	130	-	464	0.0002	318	0.0002	145
442	unicc-001	0.0000	61	0.0012	321	0.0230	206	0.0004	396	0.0004	270
443	unissey-002	0.0000	107	0.0000	53	0.0000	56	0.0000	121	0.0000	9
444	unissey-003	0.0000	104	0.0008	237	0.0191	167	0.0001	261	0.0004	237
445	upc-001	0.0000	402	0.0003	142	-	473	0.0003	366	0.0003	188
446	uxlabs-001	0.0000	180	0.0000	96	0.0000	29	0.0000	79	0.0000	51
447	vcog-002	-	502	-	502	-	384	-	499	0.0019	476
448	vd-002	0.0000	94	0.0000	48	1.0000	367	0.0000	7	0.0000	120
449	vd-003	0.0001	447	0.0041	426	0.0676	301	0.0030	479	0.0029	489
450	veridas-007	0.0000	398	0.0026	389	0.0595	291	0.0001	286	0.0005	392
451	veridas-008	0.0000	395	0.0026	388	0.0595	292	0.0001	288	0.0005	390
452	veridium-000	0.0061	487	0.5956	499	0.2889	337	0.0050	489	0.0009	438
453	veridium-001	0.0001	443	0.0087	458	0.1615	325	0.0014	457	0.0006	413
454	verigram-001	0.0000	342	0.0003	144	0.0060	82	0.0002	348	0.0003	198
455	verigram-002	0.0000	411	0.0052	446	0.0378	272	0.0010	445	0.0006	425
456	verihubs-inteligensia-000	0.0000	228	0.0029	397	0.0669	300	0.0001	238	0.0004	328
457	verihubs-inteligensia-001	0.0000	257	0.0029	398	0.0669	299	0.0001	236	0.0004	331
458	verijelias-000	0.0000	269	0.0023	382	0.0375	269	0.0004	398	0.0006	420
459	via-001	0.0000	120	0.0000	65	-	470	0.0000	118	0.0000	14
460	via-004	0.0000	148	0.0000	78	0.0000	57	0.0000	105	0.0000	25
461	videmo-001	0.0000	392	0.0170	470	0.0332	255	0.0010	448	0.0011	454
462	videmo-002	0.0000	122	0.0006	203	0.0189	164	0.0001	268	0.0004	229
463	videonetics-001	0.0004	469	0.0309	480	-	412	0.0015	459	0.0010	442
464	videonetics-002	0.0000	366	0.0459	490	-	415	0.0006	420	0.0005	410

Table 40: FTE is the proportion of failed template generation attempts. Failures can occur because the software throws an exception, or because the software electively refuses to process the input image. This would typically occur if a face is not detected. FTE is measured as the number of function calls that give EITHER a non-zero error code OR that give a “small” template. This is defined as one whose size is less than 0.3 times the median template size for that algorithm. This second rule is needed because some algorithms incorrectly fail to return a non-zero error code when template generation fails.

A hyphen “-” indicates the dataset was not produced.¹ The effects of FTE are included in the accuracy results of this report by regarding any template comparison involving a failed template to produce a low similarity score. Thus higher FTE results in higher FNMR and lower FMR.

	Algorithm Name	Failure to Enrol Rate ¹											
		APPLICATION	BORDER	KIOSK	MUGSHOT	VISA	WILD	SEC. 2.1	SEC. 2.7				
		SEC. 2.2	SEC. 2.4	SEC. 2.6	SEC. 2.5			SEC. 2.1	SEC. 2.7				
465	viettelhightech-000	0.0000	405	0.0019	363	0.0368	266	0.0007	428	0.0005	406	0.0024	359
466	vigilantsolutions-010	0.0000	389	0.0028	394	0.0609	295	0.0001	245	0.0004	223	0.0005	281
467	vigilantsolutions-011	0.0000	386	0.0028	393	0.0609	294	0.0001	243	0.0004	225	0.0005	280
468	vinai-000	0.0000	211	0.0000	116	-	450	0.0000	70	0.0000	61	0.0000	83
469	vinbigdata-001	0.0000	6	0.0000	3	0.0000	17	0.0000	57	0.0000	72	0.0000	29
470	vinbigdata-002	0.0000	187	0.0015	346	0.0250	219	0.0000	186	0.0004	346	0.0012	337
471	vion-000	0.0050	484	0.0392	488	-	441	0.0130	495	0.0078	494	0.1389	490
472	visage-000	0.0000	409	0.0054	448	-	465	0.0009	441	0.0006	417	0.0064	395
473	visionbox-002	0.0000	168	0.0017	352	0.0270	237	0.0000	188	0.0004	369	0.0046	384
474	visionbox-003	0.0000	375	0.0010	288	0.0209	183	0.0001	273	0.0004	311	0.0008	316
475	visionlabs-010	0.0000	378	0.0009	268	-	421	0.0001	298	0.0004	302	0.0006	300
476	visionlabs-011	0.0000	21	0.0006	200	0.0156	141	0.0001	247	0.0004	232	0.0004	215
477	visteam-004	0.0000	296	0.0010	301	0.0225	199	0.0001	280	0.0004	251	0.0006	289
478	visteam-005	0.0000	222	0.0010	300	0.0224	198	0.0001	248	0.0004	256	0.0005	284
479	vixvizion-006	0.0000	108	0.0000	59	0.0000	48	0.0000	127	0.0000	3	0.0000	96
480	vixvizion-007	0.0000	186	0.0000	102	0.0000	24	0.0000	85	0.0000	45	0.0000	66
481	vnpt-004	0.0000	334	0.0006	195	0.0160	148	0.0002	326	0.0004	267	0.0003	180
482	vnpt-005	0.0000	65	0.0006	188	0.0154	139	0.0002	335	0.0004	260	0.0003	187
483	vocord-009	0.0000	276	0.0006	199	-	369	0.0001	308	0.0003	156	0.0003	156
484	vocord-010	0.0000	344	0.0005	181	0.0141	128	0.0002	337	0.0003	197	0.0004	238
485	vts-000	0.0000	374	0.0011	310	-	442	0.0001	309	0.0004	364	0.0013	340
486	vts-001	0.0000	185	0.0003	139	0.0073	89	0.0000	152	0.0003	152	0.0002	137
487	wicket-000	0.0000	260	0.0009	263	0.0260	231	0.0000	160	0.0004	269	0.0004	220
488	winsense-001	0.0000	22	0.0000	13	-	391	0.0000	54	0.0000	75	0.0000	36
489	winsense-002	0.0000	34	0.0000	18	-	414	0.0000	38	0.0000	92	0.0000	44
490	wiseai-001	0.0001	441	0.0137	467	0.0768	314	0.0018	462	0.0018	473	0.0624	464
491	wuhantianyu-001	0.0000	79	0.0007	215	0.0159	145	0.0001	227	0.0004	305	0.0002	138
492	x-laboratory-000	0.0247	497	0.0000	6	-	394	0.0005	410	0.0002	146	0.0000	35
493	x-laboratory-001	0.0000	310	0.0012	323	-	443	0.0001	291	0.0004	355	0.0007	306
494	xforwardai-001	0.0000	255	0.0007	226	-	356	0.0003	367	0.0004	350	0.0004	213
495	xforwardai-002	0.0000	331	0.0007	227	-	453	0.0003	368	0.0004	347	0.0004	217
496	xm-000	0.0000	156	0.0007	212	-	438	0.0001	230	0.0003	169	0.0004	263
497	yisheng-004	0.0002	463	-	500	-	423	0.0013	453	0.0006	423	0.0321	451
498	yitu-003	0.0000	43	0.0000	22	-	360	0.0009	440	0.0000	100	0.0000	3
499	yoonik-003	0.0000	351	0.0009	276	0.0214	190	0.0002	323	0.0004	324	0.0008	315
500	yoonik-004	0.0000	142	0.0012	320	0.0251	222	0.0001	250	0.0004	230	0.0004	255
501	ytu-000	0.0000	292	0.0010	307	-	469	0.0002	353	0.0004	344	0.0011	336
502	yuan-005	0.0000	293	0.0005	178	0.0134	125	0.0002	334	0.0004	240	0.0004	253
503	yuan-006	0.0000	404	0.0014	343	0.0369	267	0.0004	384	0.0005	401	0.0038	375

Table 41: FTE is the proportion of failed template generation attempts. Failures can occur because the software throws an exception, or because the software electively refuses to process the input image. This would typically occur if a face is not detected. FTE is measured as the number of function calls that give EITHER a non-zero error code OR that give a "small" template. This is defined as one whose size is less than 0.3 times the median template size for that algorithm. This second rule is needed because some algorithms incorrectly fail to return a non-zero error code when template generation fails.

A hyphen "-" indicates the dataset was not produced.¹ The effects of FTE are included in the accuracy results of this report by regarding any template comparison involving a failed template to produce a low similarity score. Thus higher FTE results in higher FNMR and lower FMR.

3.4 Recognition accuracy

Core algorithm accuracy is stated via:

▷ **Cooperative subjects**

- The summary table of Figure 32;
- The visa image DETs of Figure 96;
- The mugshot DETs of Figure 121;
- The mugshot ageing profiles of Figure 329;
- The human-difficult pairs of Figure 45

▷ **Non-cooperative subjects**

- The photojournalism DET of Figure 142

Figure 256 shows dependence of false match rate on algorithm score threshold. This allows a deployer to set a threshold to target a particular false match rate appropriate to the security objectives of the application.

Figure 255 likewise shows FMR(T) but for mugshots, and specially four subsets of the population.

Note that in both the mugshot and visa sets false match rates vary with the ethnicity, age, and sex, of the enrollee and impostor. For example figure 164 summarizes FMR for impostors paired from four groups black females, black males, white females, white males.

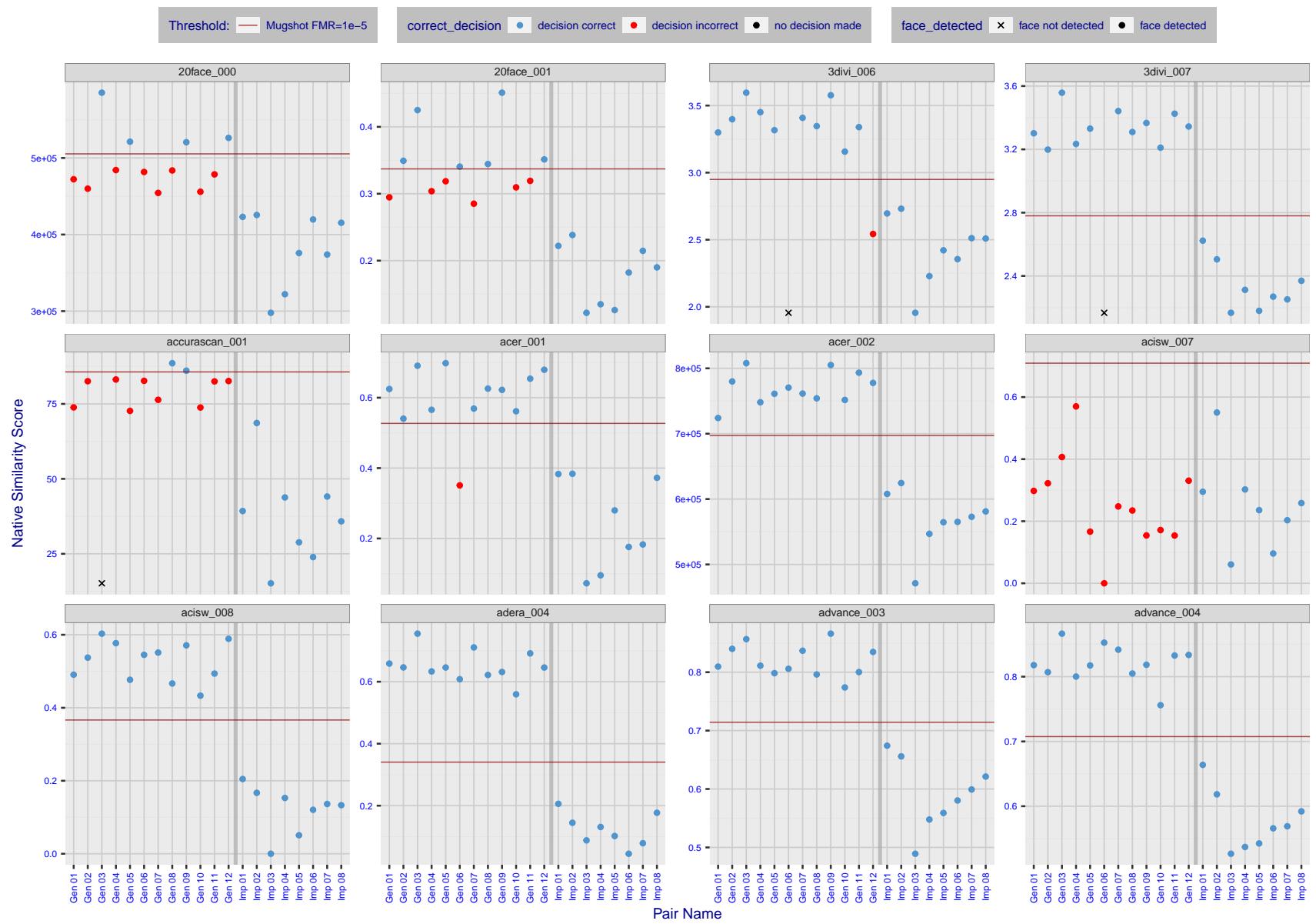


Figure 4: The figure shows algorithms' similarity scores for 12 genuine and 8 impostor image pairs used in a May 2018 paper by Phillips et al. ([1]). The threshold (red horizontal line) is a value calibrated to give $FMR = 0.0001$ on mugshot images. Points above the threshold correspond to pairs determined to be genuine, and points below the threshold correspond to pairs determined to be impostors. If the determined class (genuine or impostor) matches the real class, points will be blue; if not, red. An X represents face detection failure in either of the images in the pair. Note that the sample size ($n=20$) is small, and the figure may change substantially if larger or different sets are used. The images can be viewed on p. 13 of the Appendix, where Gen 01 corresponds to Same-Identity Pair 1, Gen 02 corresponds to Same-Identity Pair 2, and so on.

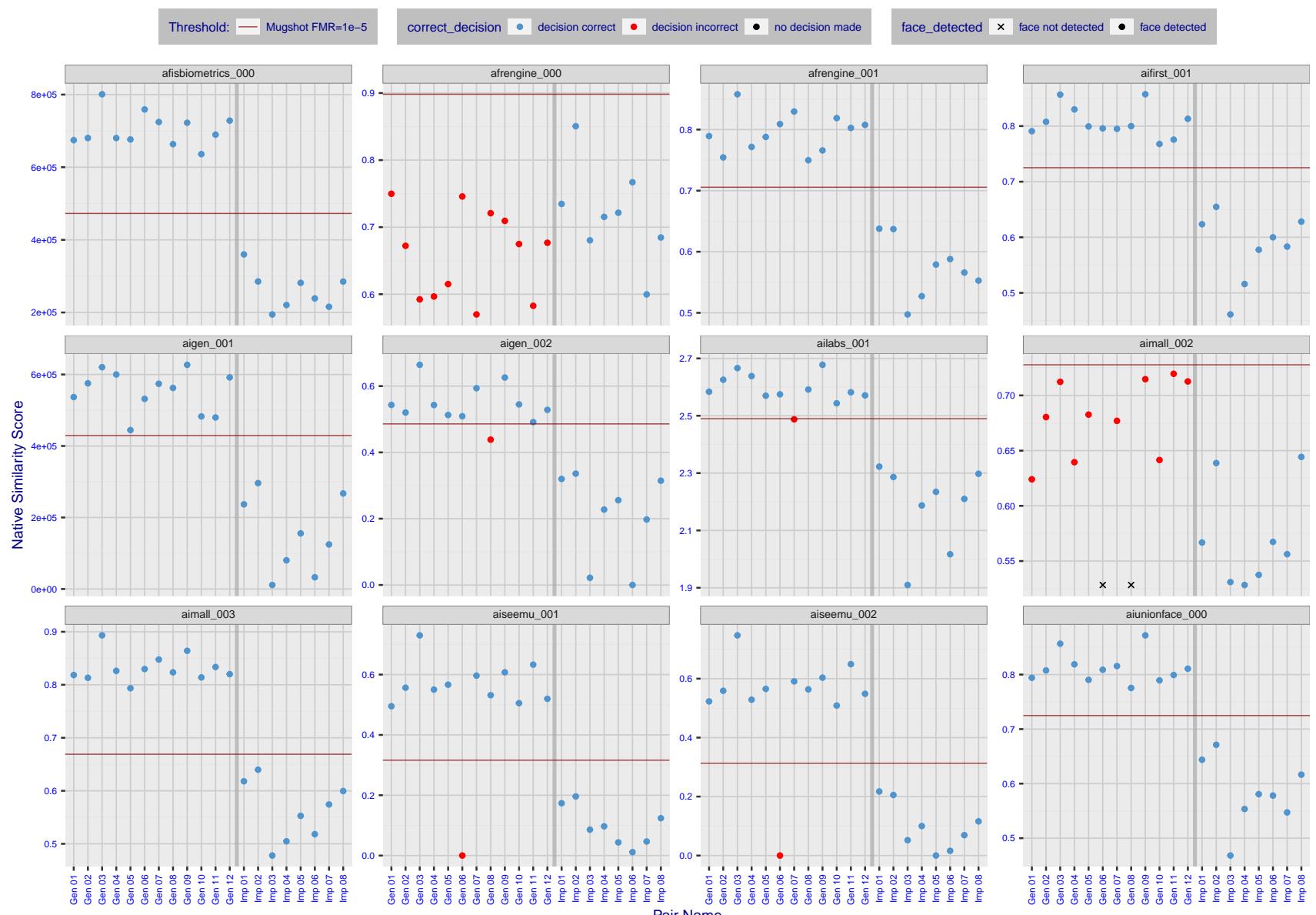


Figure 5: The figure shows algorithms' similarity scores for 12 genuine and 8 impostor image pairs used in a May 2018 paper by Phillips et al. ([1]). The threshold (red horizontal line) is a value calibrated to give $FMR = 0.0001$ on mugshot images. Points above the threshold correspond to pairs determined to be genuine, and points below the threshold correspond to pairs determined to be impostors. If the determined class (genuine or impostor) matches the real class, points will be blue; if not, red. An X represents face detection failure in either of the images in the pair. Note that the sample size ($n=20$) is small, and the figure may change substantially if larger or different sets are used. The images can be viewed on p. 13 of the Appendix, where Gen 01 corresponds to Same-Identity Pair 1, Gen 02 corresponds to Same-Identity Pair 2, and so on.

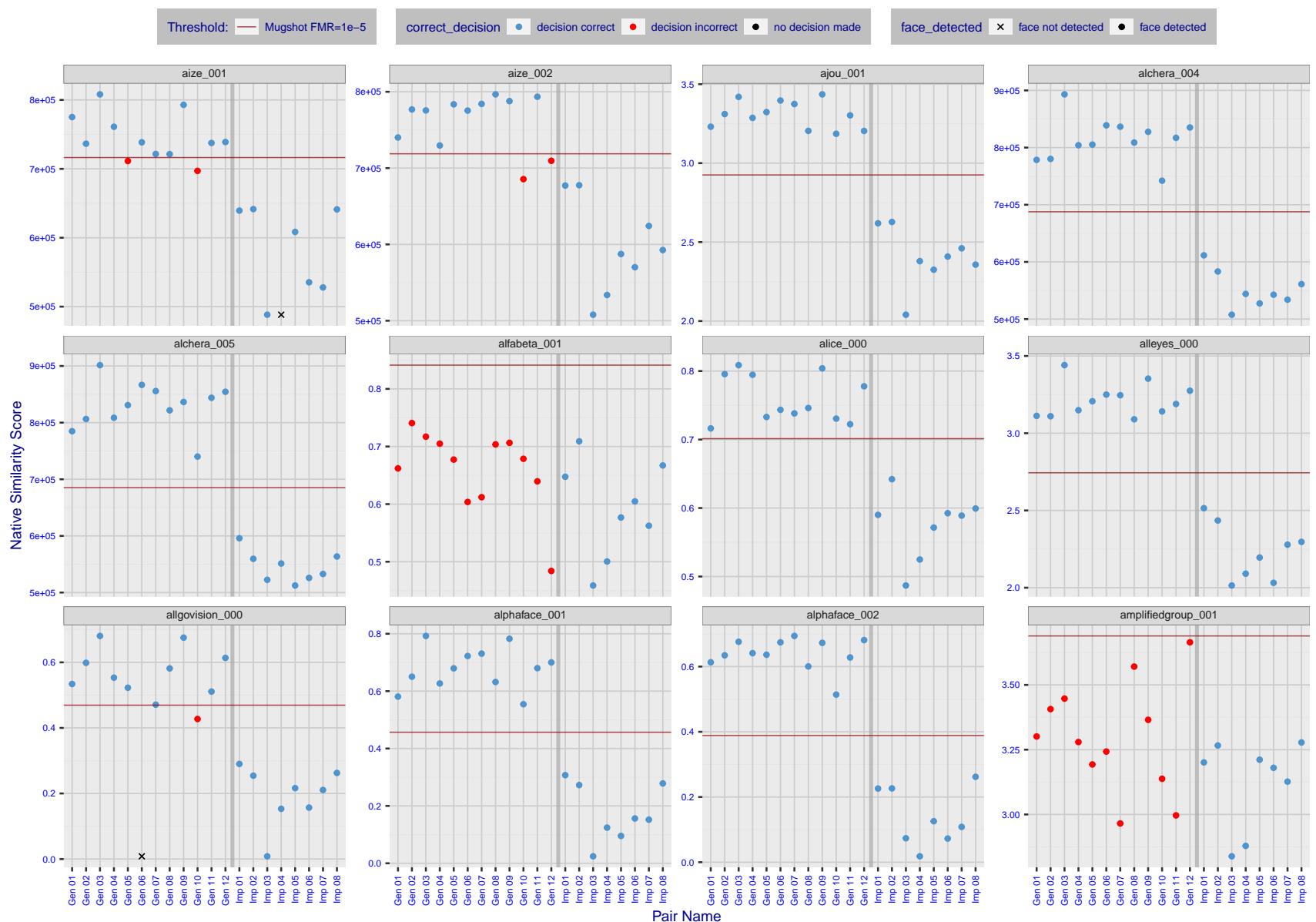


Figure 6: The figure shows algorithms' similarity scores for 12 genuine and 8 impostor image pairs used in a May 2018 paper by Phillips et al. ([1]). The threshold (red horizontal line) is a value calibrated to give $FMR = 0.0001$ on mugshot images. Points above the threshold correspond to pairs determined to be genuine, and points below the threshold correspond to pairs determined to be impostors. If the determined class (genuine or impostor) matches the real class, points will be blue; if not, red. An X represents face detection failure in either of the images in the pair. Note that the sample size ($n=20$) is small, and the figure may change substantially if larger or different sets are used. The images can be viewed on p. 13 of the Appendix, where Gen 01 corresponds to Same-Identity Pair 1, Gen 02 corresponds to Same-Identity Pair 2, and so on.

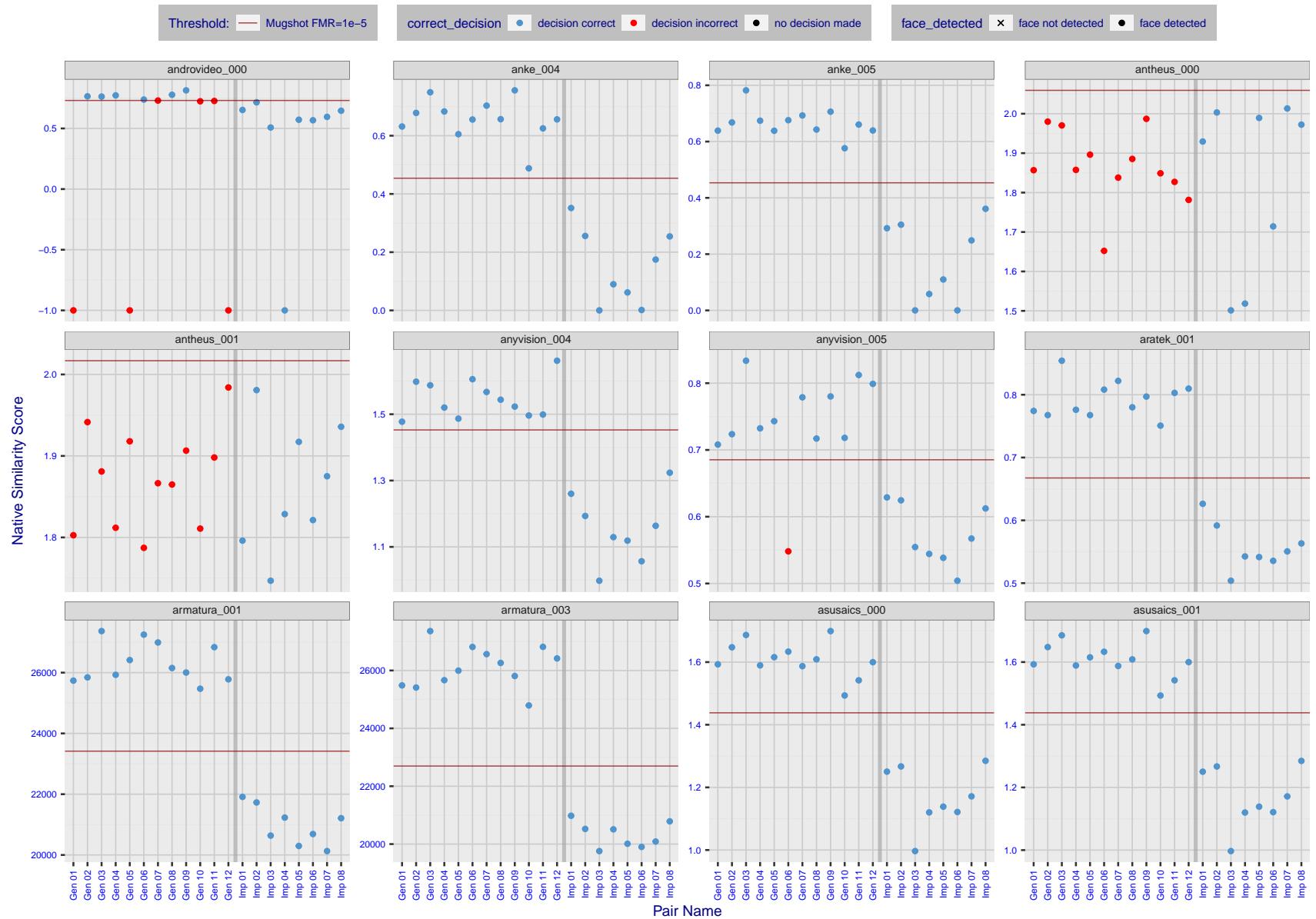


Figure 7: The figure shows algorithms' similarity scores for 12 genuine and 8 impostor image pairs used in a May 2018 paper by Phillips et al. ([1]). The threshold (red horizontal line) is a value calibrated to give $FMR = 0.0001$ on mugshot images. Points above the threshold correspond to pairs determined to be genuine, and points below the threshold correspond to pairs determined to be impostors. If the determined class (genuine or impostor) matches the real class, points will be blue; if not, red. An X represents face detection failure in either of the images in the pair. Note that the sample size ($n=20$) is small, and the figure may change substantially if larger or different sets are used. The images can be viewed on p. 13 of the Appendix, where Gen 01 corresponds to Same-Identity Pair 1, Gen 02 corresponds to Same-Identity Pair 2, and so on.

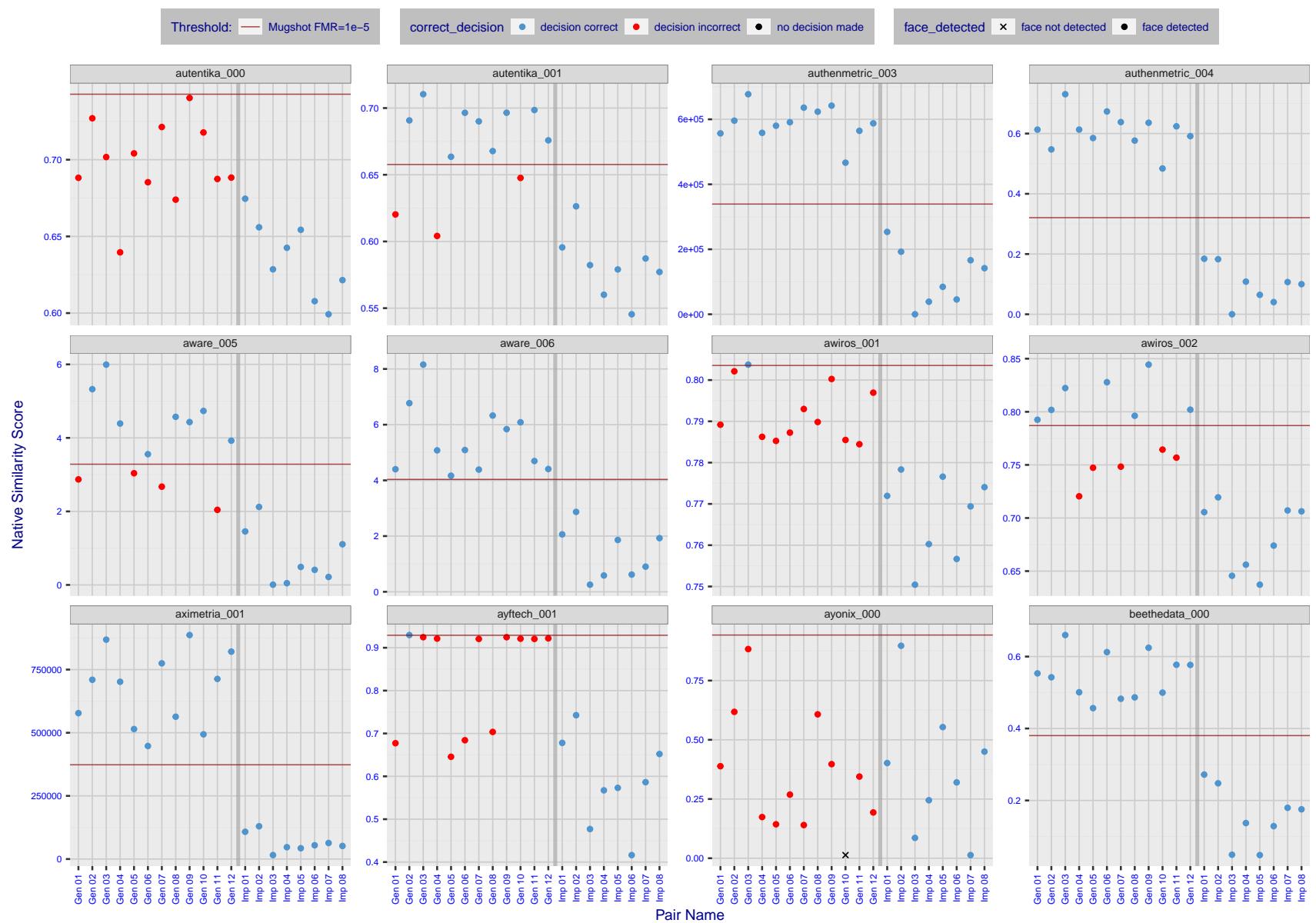


Figure 8: The figure shows algorithms' similarity scores for 12 genuine and 8 impostor image pairs used in a May 2018 paper by Phillips et al. ([1]). The threshold (red horizontal line) is a value calibrated to give $FMR = 0.0001$ on mugshot images. Points above the threshold correspond to pairs determined to be genuine, and points below the threshold correspond to pairs determined to be impostors. If the determined class (genuine or impostor) matches the real class, points will be blue; if not, red. An X represents face detection failure in either of the images in the pair. Note that the sample size ($n=20$) is small, and the figure may change substantially if larger or different sets are used. The images can be viewed on p. 13 of the Appendix, where Gen 01 corresponds to Same-Identity Pair 1, Gen 02 corresponds to Same-Identity Pair 2, and so on.

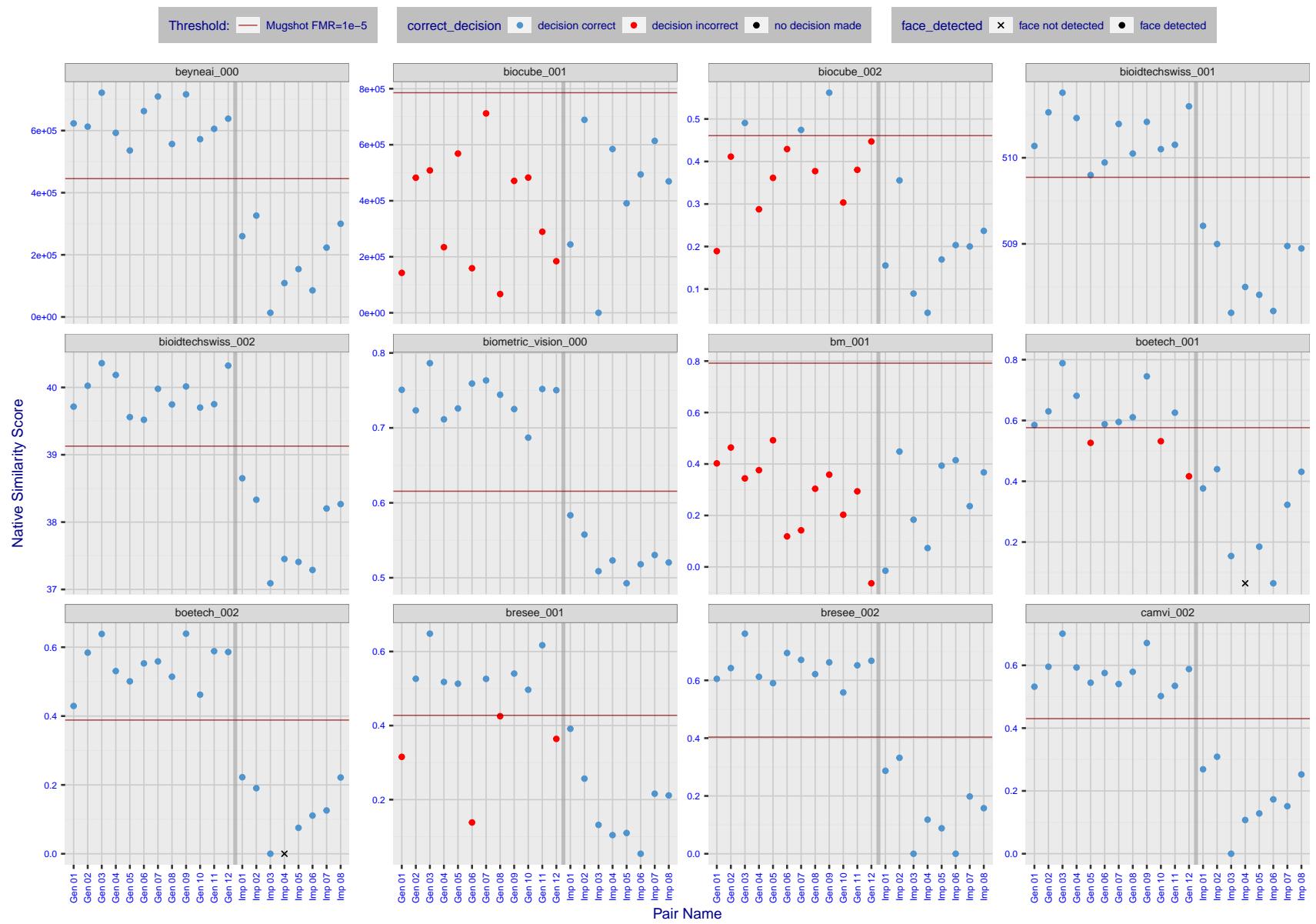


Figure 9: The figure shows algorithms' similarity scores for 12 genuine and 8 impostor image pairs used in a May 2018 paper by Phillips et al. ([1]). The threshold (red horizontal line) is a value calibrated to give $FMR = 0.0001$ on mugshot images. Points above the threshold correspond to pairs determined to be genuine, and points below the threshold correspond to pairs determined to be impostors. If the determined class (genuine or impostor) matches the real class, points will be blue; if not, red. An X represents face detection failure in either of the images in the pair. Note that the sample size ($n=20$) is small, and the figure may change substantially if larger or different sets are used. The images can be viewed on p. 13 of the Appendix, where Gen 01 corresponds to Same-Identity Pair 1, Gen 02 corresponds to Same-Identity Pair 2, and so on.

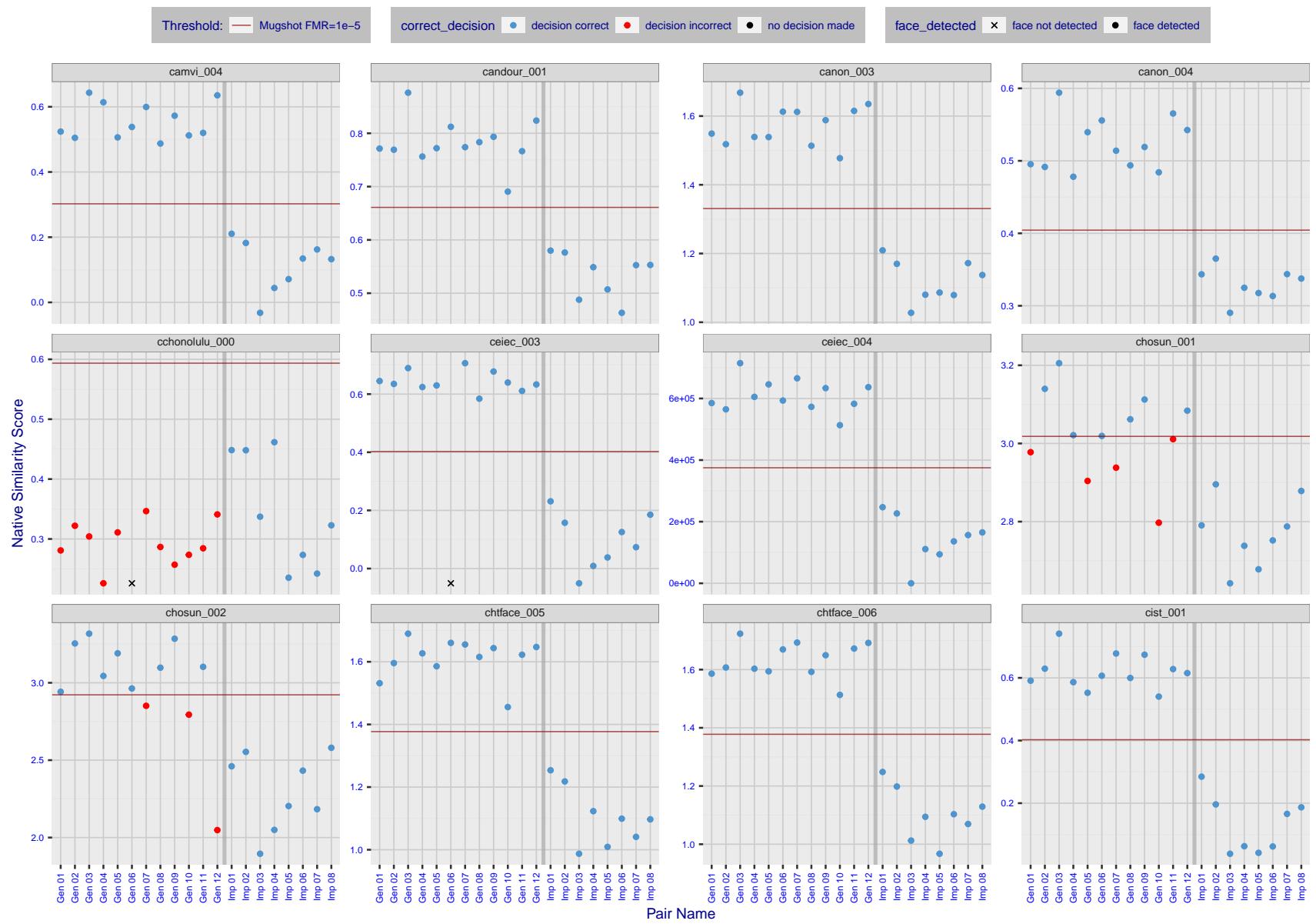


Figure 10: The figure shows algorithms' similarity scores for 12 genuine and 8 impostor image pairs used in a May 2018 paper by Phillips et al. ([1]). The threshold (red horizontal line) is a value calibrated to give $FMR = 0.0001$ on mugshot images. Points above the threshold correspond to pairs determined to be genuine, and points below the threshold correspond to pairs determined to be impostors. If the determined class (genuine or impostor) matches the real class, points will be blue; if not, red. An X represents face detection failure in either of the images in the pair. Note that the sample size ($n=20$) is small, and the figure may change substantially if larger or different sets are used. The images can be viewed on p. 13 of the Appendix, where Gen 01 corresponds to Same-Identity Pair 1, Gen 02 corresponds to Same-Identity Pair 2, and so on.

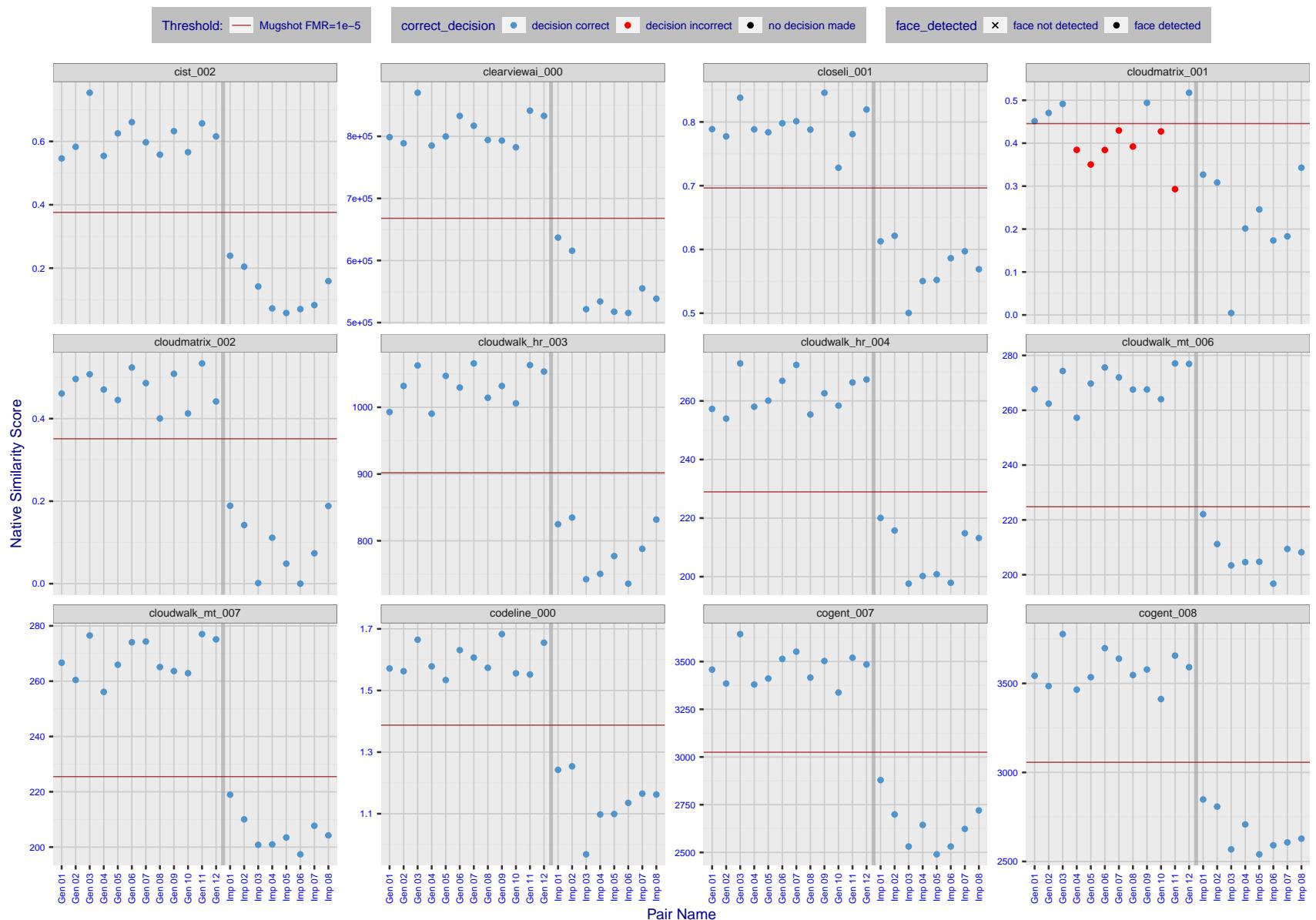


Figure 11: The figure shows algorithms' similarity scores for 12 genuine and 8 impostor image pairs used in a May 2018 paper by Phillips et al. ([1]). The threshold (red horizontal line) is a value calibrated to give $FMR = 0.0001$ on mugshot images. Points above the threshold correspond to pairs determined to be genuine, and points below the threshold correspond to pairs determined to be impostors. If the determined class (genuine or impostor) matches the real class, points will be blue; if not, red. An X represents face detection failure in either of the images in the pair. Note that the sample size ($n=20$) is small, and the figure may change substantially if larger or different sets are used. The images can be viewed on p. 13 of the Appendix, where Gen 01 corresponds to Same-Identity Pair 1, Gen 02 corresponds to Same-Identity Pair 2, and so on.

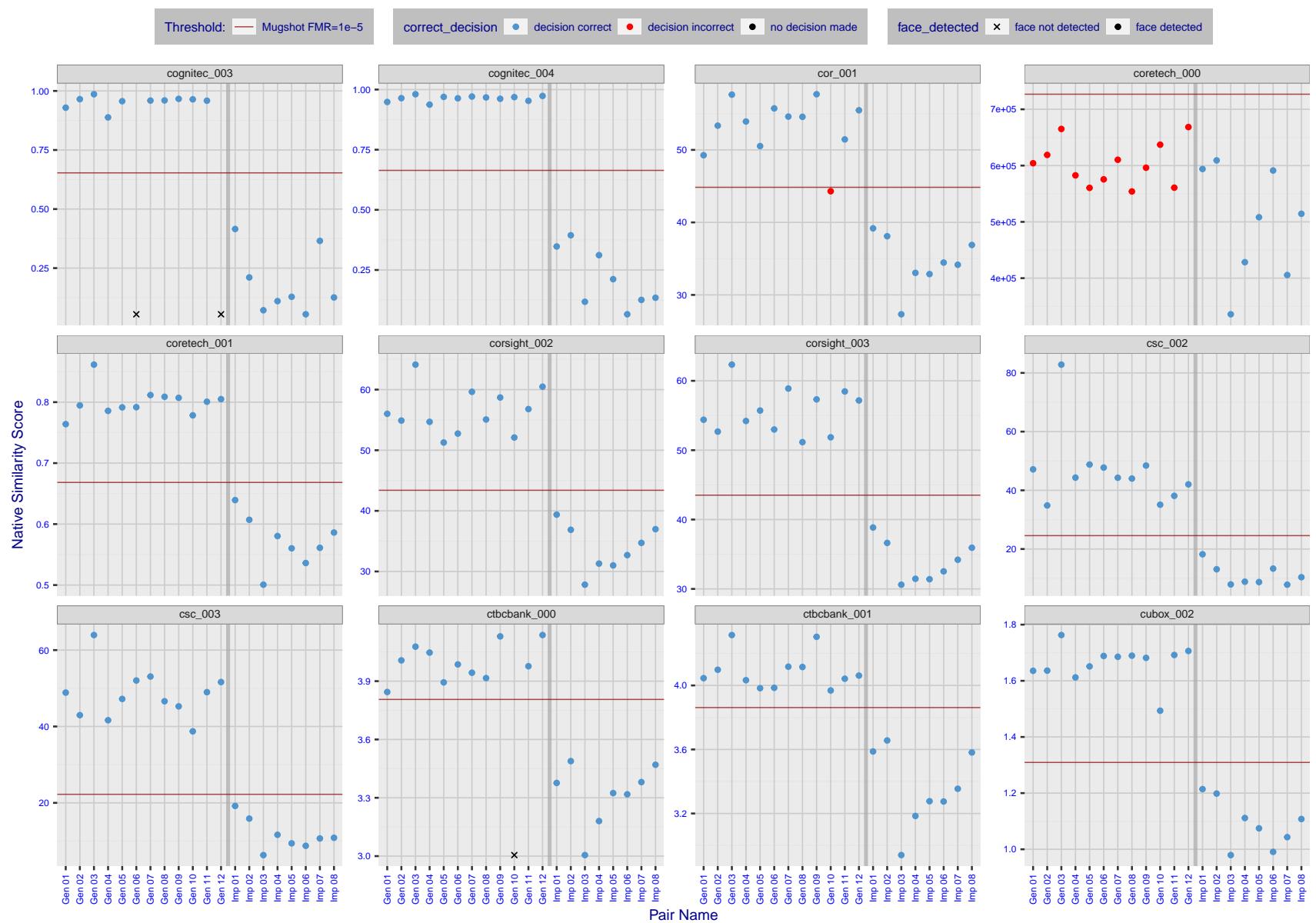


Figure 12: The figure shows algorithms' similarity scores for 12 genuine and 8 impostor image pairs used in a May 2018 paper by Phillips et al. ([1]). The threshold (red horizontal line) is a value calibrated to give $FMR = 0.0001$ on mugshot images. Points above the threshold correspond to pairs determined to be genuine, and points below the threshold correspond to pairs determined to be impostors. If the determined class (genuine or impostor) matches the real class, points will be blue; if not, red. An X represents face detection failure in either of the images in the pair. Note that the sample size ($n=20$) is small, and the figure may change substantially if larger or different sets are used. The images can be viewed on p. 13 of the Appendix, where Gen 01 corresponds to Same-Identity Pair 1, Gen 02 corresponds to Same-Identity Pair 2, and so on.

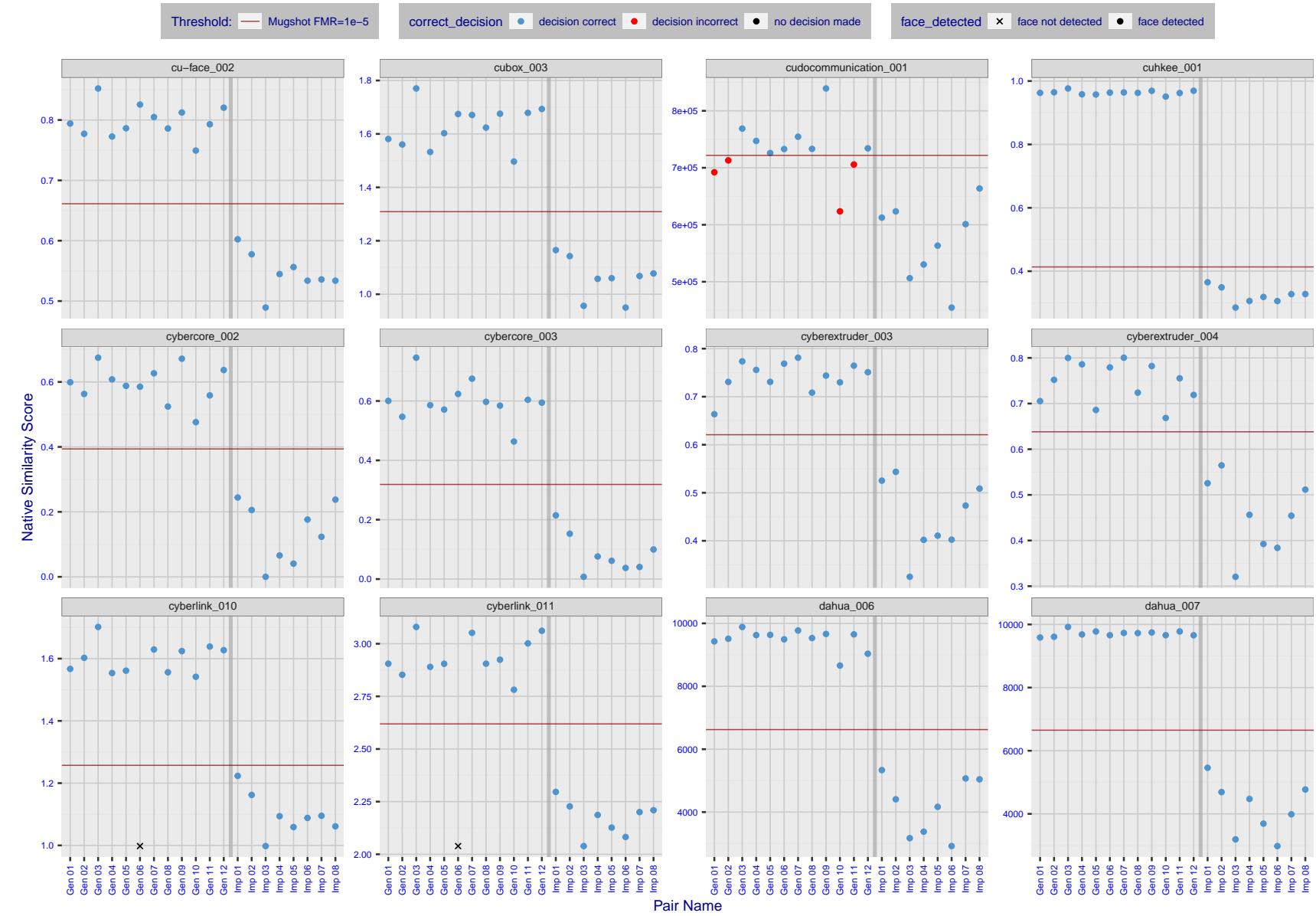


Figure 13: The figure shows algorithms' similarity scores for 12 genuine and 8 impostor image pairs used in a May 2018 paper by Phillips et al. ([1]). The threshold (red horizontal line) is a value calibrated to give $FMR = 0.0001$ on mugshot images. Points above the threshold correspond to pairs determined to be genuine, and points below the threshold correspond to pairs determined to be impostors. If the determined class (genuine or impostor) matches the real class, points will be blue; if not, red. An X represents face detection failure in either of the images in the pair. Note that the sample size ($n=20$) is small, and the figure may change substantially if larger or different sets are used. The images can be viewed on p. 13 of the Appendix, where Gen 01 corresponds to Same-Identity Pair 1, Gen 02 corresponds to Same-Identity Pair 2, and so on.

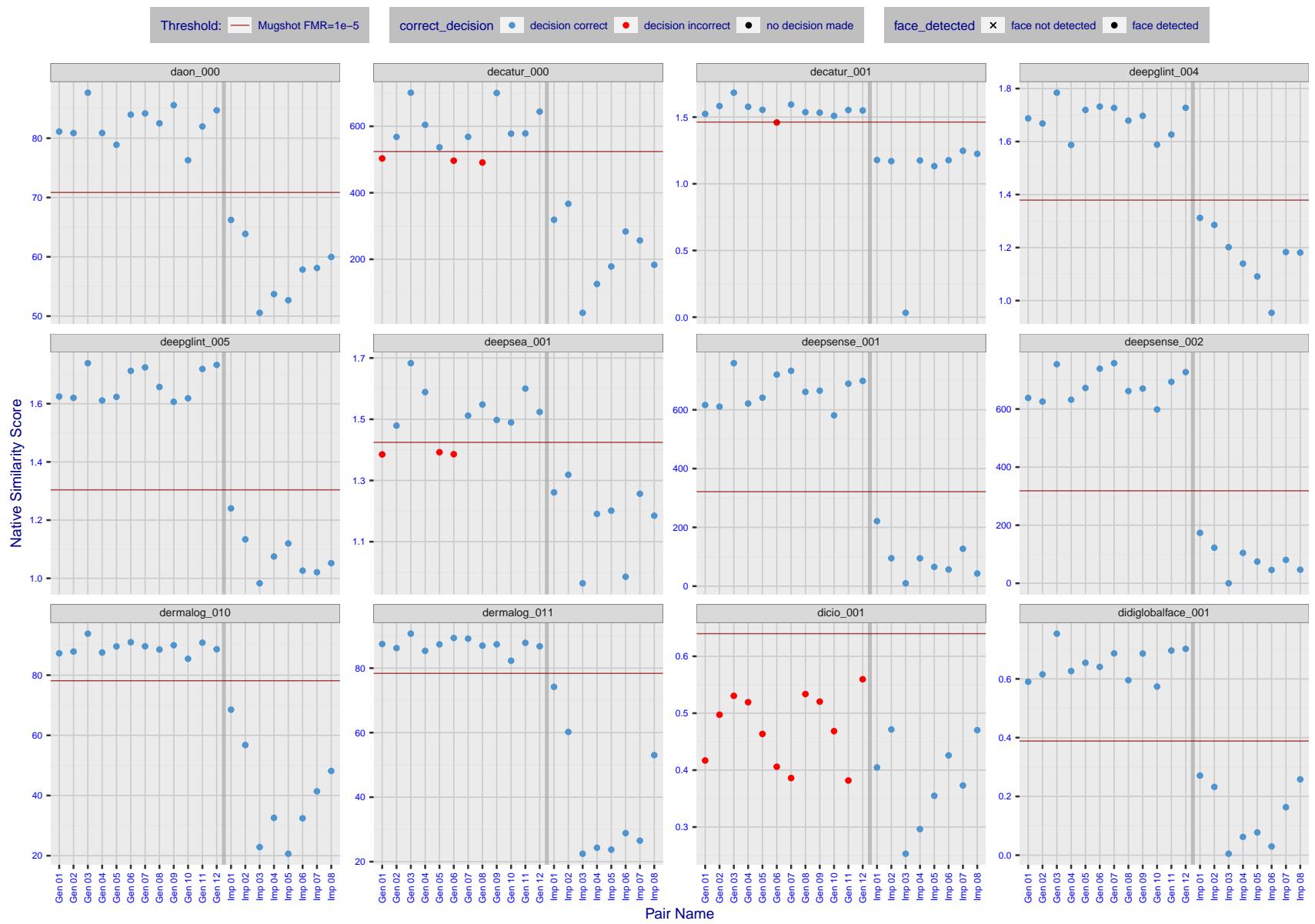


Figure 14: The figure shows algorithms' similarity scores for 12 genuine and 8 impostor image pairs used in a May 2018 paper by Phillips et al. ([1]). The threshold (red horizontal line) is a value calibrated to give $FMR = 0.0001$ on mugshot images. Points above the threshold correspond to pairs determined to be genuine, and points below the threshold correspond to pairs determined to be impostors. If the determined class (genuine or impostor) matches the real class, points will be blue; if not, red. An X represents face detection failure in either of the images in the pair. Note that the sample size ($n=20$) is small, and the figure may change substantially if larger or different sets are used. The images can be viewed on p. 13 of the Appendix, where Gen 01 corresponds to Same-Identity Pair 1, Gen 02 corresponds to Same-Identity Pair 2, and so on.

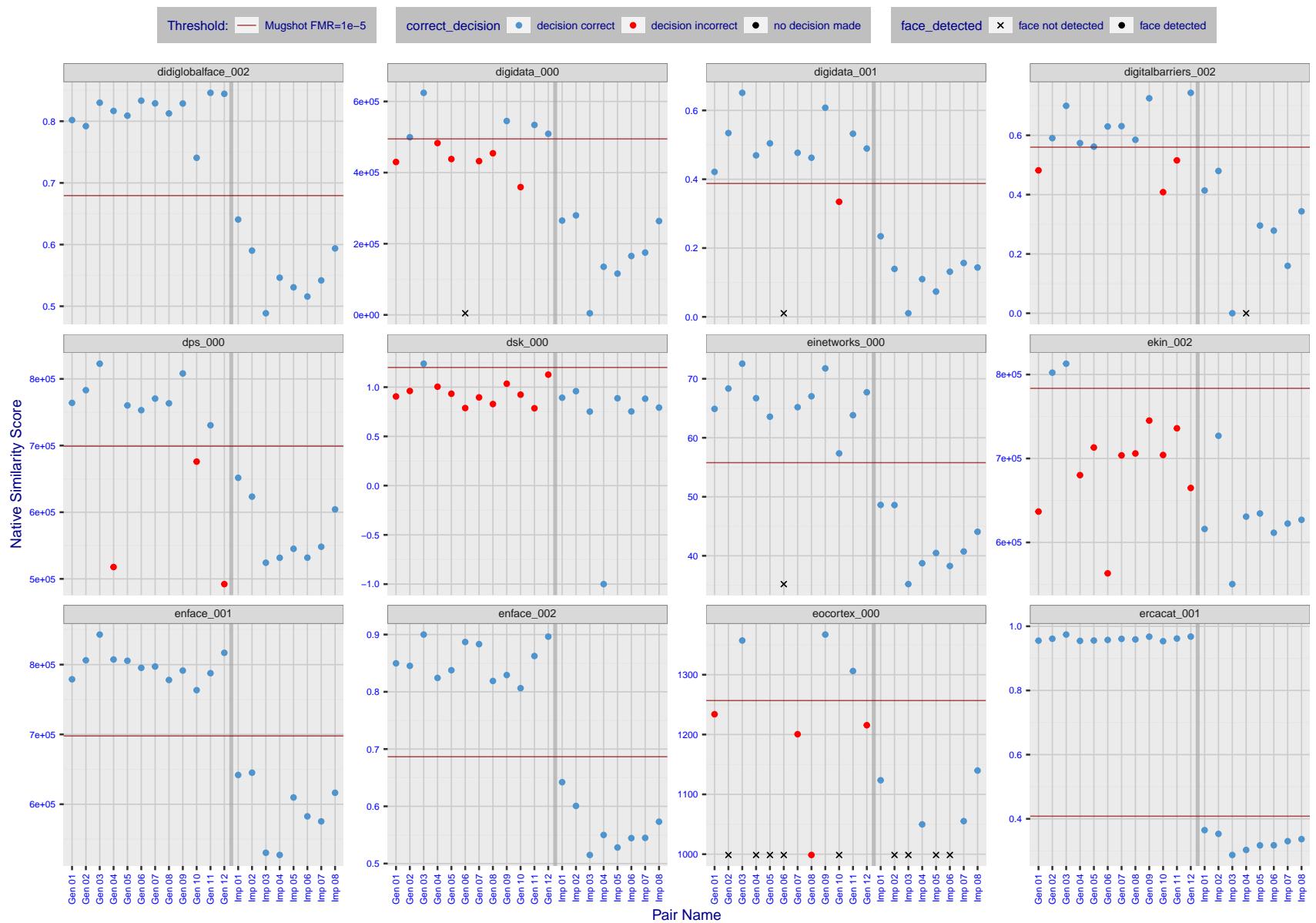


Figure 15: The figure shows algorithms' similarity scores for 12 genuine and 8 impostor image pairs used in a May 2018 paper by Phillips et al. ([1]). The threshold (red horizontal line) is a value calibrated to give $FMR = 0.0001$ on mugshot images. Points above the threshold correspond to pairs determined to be genuine, and points below the threshold correspond to pairs determined to be impostors. If the determined class (genuine or impostor) matches the real class, points will be blue; if not, red. An X represents face detection failure in either of the images in the pair. Note that the sample size ($n=20$) is small, and the figure may change substantially if larger or different sets are used. The images can be viewed on p. 13 of the Appendix, where Gen 01 corresponds to Same-Identity Pair 1, Gen 02 corresponds to Same-Identity Pair 2, and so on.

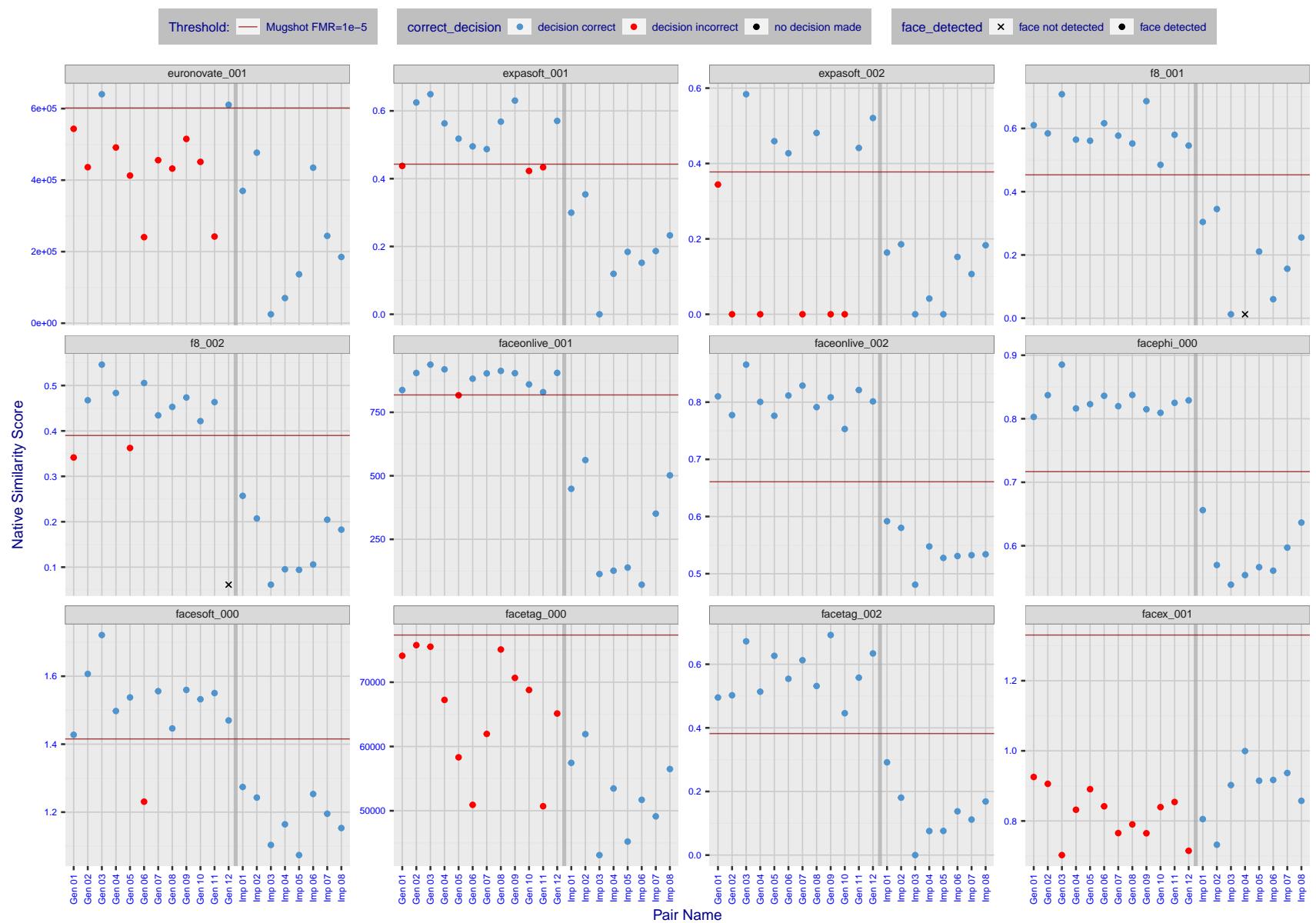


Figure 16: The figure shows algorithms' similarity scores for 12 genuine and 8 impostor image pairs used in a May 2018 paper by Phillips et al. ([1]). The threshold (red horizontal line) is a value calibrated to give $FMR = 0.0001$ on mugshot images. Points above the threshold correspond to pairs determined to be genuine, and points below the threshold correspond to pairs determined to be impostors. If the determined class (genuine or impostor) matches the real class, points will be blue; if not, red. An X represents face detection failure in either of the images in the pair. Note that the sample size ($n=20$) is small, and the figure may change substantially if larger or different sets are used. The images can be viewed on p. 13 of the Appendix, where Gen 01 corresponds to Same-Identity Pair 1, Gen 02 corresponds to Same-Identity Pair 2, and so on.

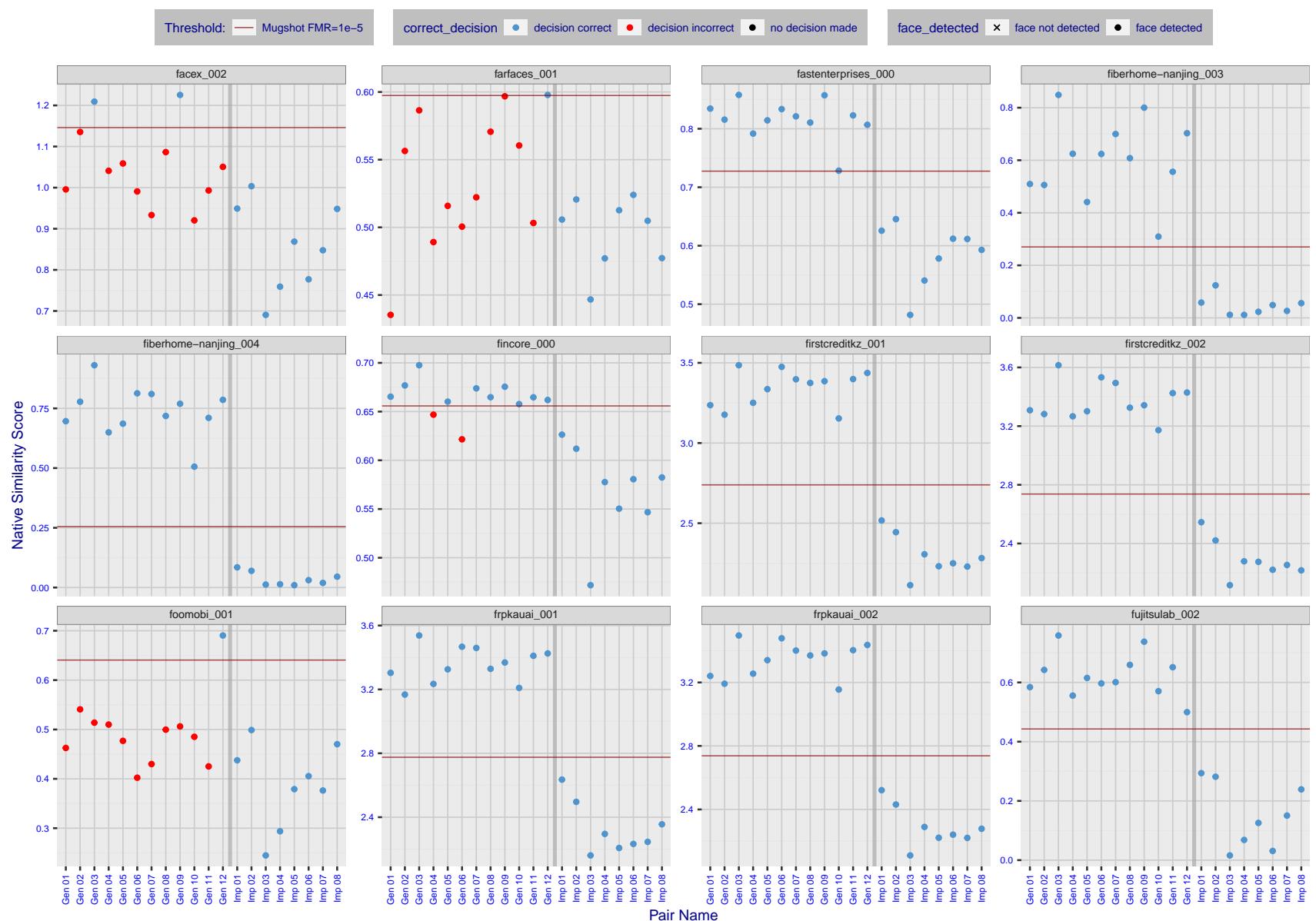


Figure 17: The figure shows algorithms' similarity scores for 12 genuine and 8 impostor image pairs used in a May 2018 paper by Phillips et al. ([1]). The threshold (red horizontal line) is a value calibrated to give $FMR = 0.0001$ on mugshot images. Points above the threshold correspond to pairs determined to be genuine, and points below the threshold correspond to pairs determined to be impostors. If the determined class (genuine or impostor) matches the real class, points will be blue; if not, red. An X represents face detection failure in either of the images in the pair. Note that the sample size ($n=20$) is small, and the figure may change substantially if larger or different sets are used. The images can be viewed on p. 13 of the Appendix, where Gen 01 corresponds to Same-Identity Pair 1, Gen 02 corresponds to Same-Identity Pair 2, and so on.

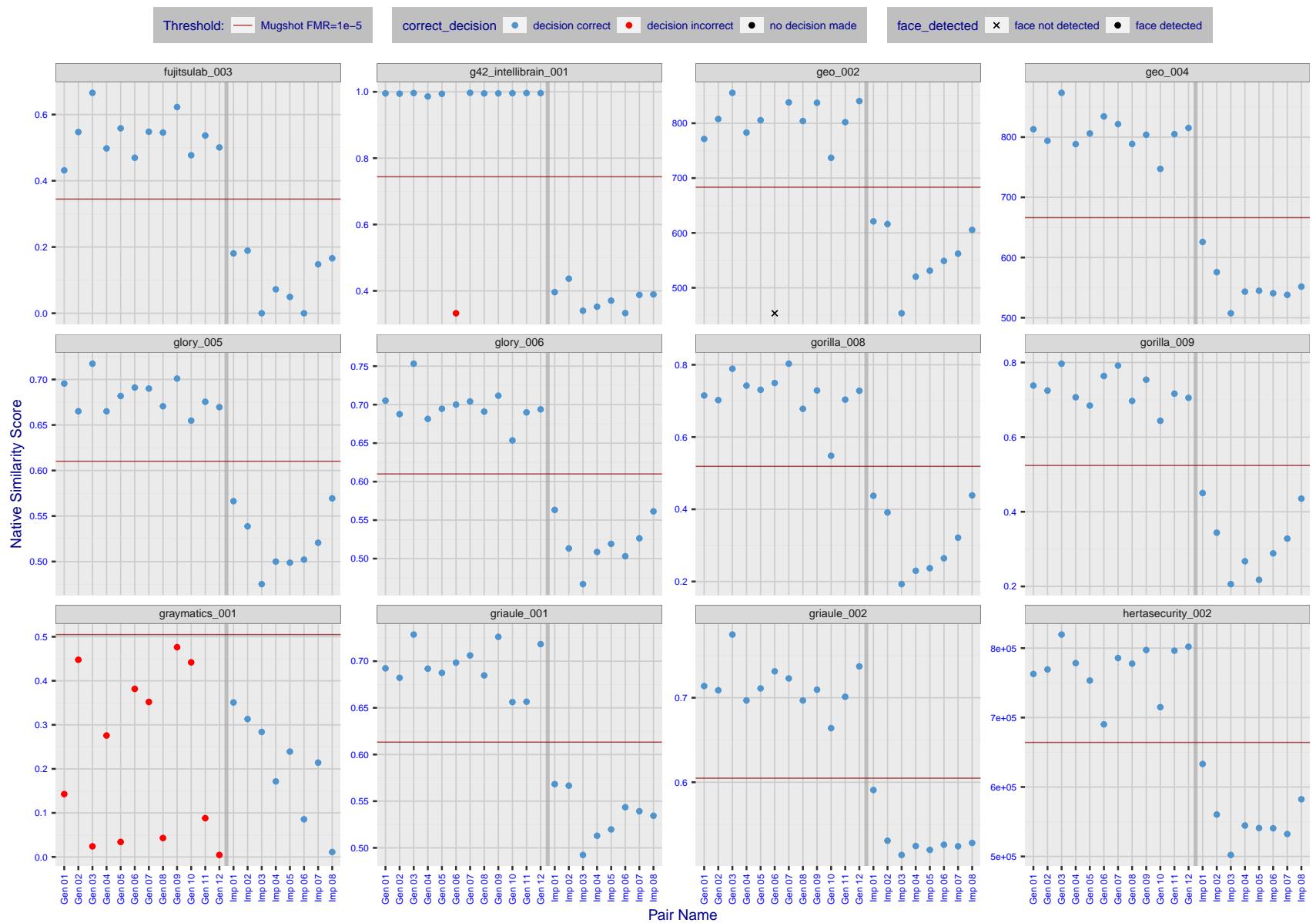


Figure 18: The figure shows algorithms' similarity scores for 12 genuine and 8 impostor image pairs used in a May 2018 paper by Phillips et al. ([1]). The threshold (red horizontal line) is a value calibrated to give $FMR = 0.0001$ on mugshot images. Points above the threshold correspond to pairs determined to be genuine, and points below the threshold correspond to pairs determined to be impostors. If the determined class (genuine or impostor) matches the real class, points will be blue; if not, red. An X represents face detection failure in either of the images in the pair. Note that the sample size ($n=20$) is small, and the figure may change substantially if larger or different sets are used. The images can be viewed on p. 13 of the Appendix, where Gen 01 corresponds to Same-Identity Pair 1, Gen 02 corresponds to Same-Identity Pair 2, and so on.

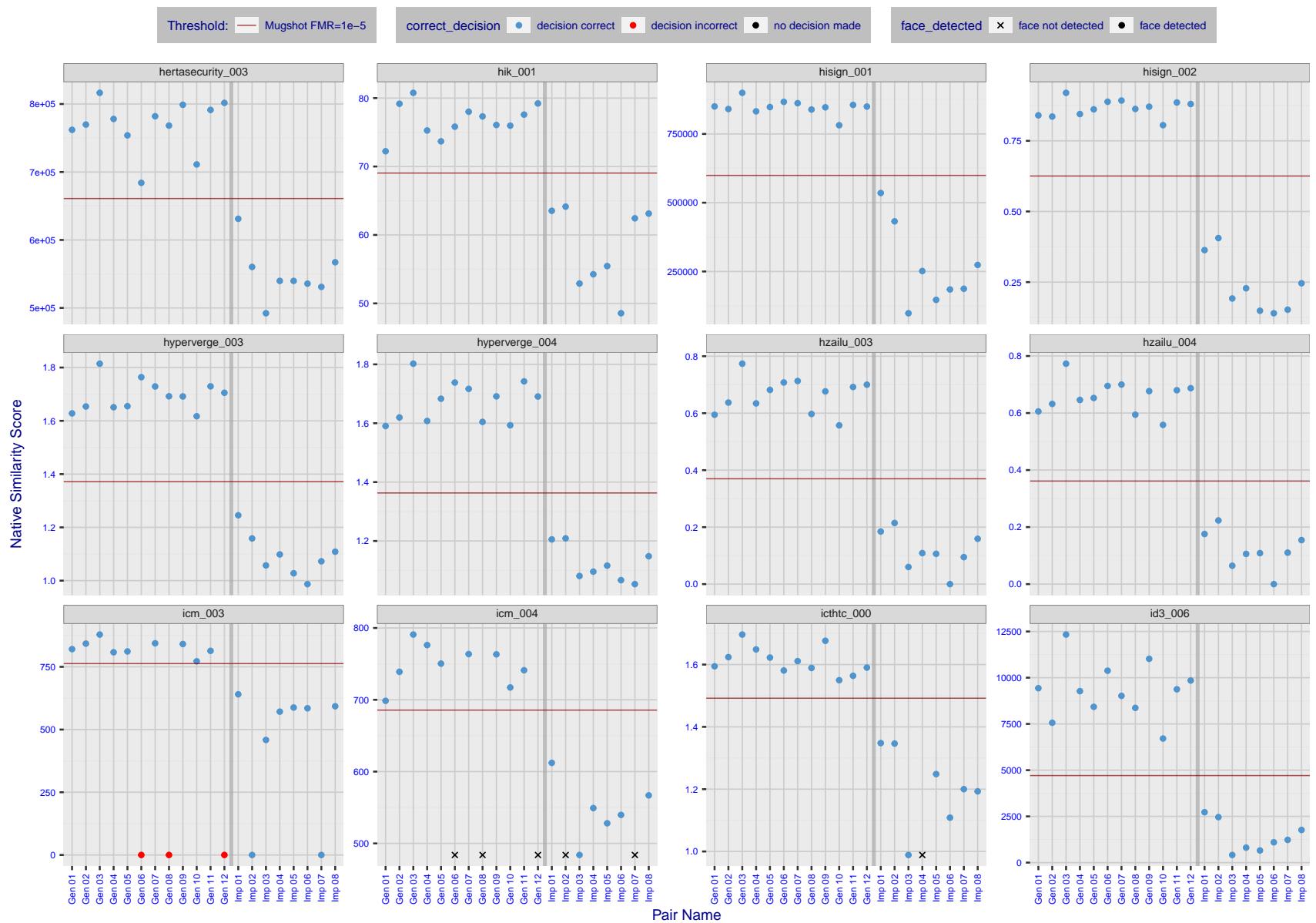


Figure 19: The figure shows algorithms' similarity scores for 12 genuine and 8 impostor image pairs used in a May 2018 paper by Phillips et al. ([1]). The threshold (red horizontal line) is a value calibrated to give $FMR = 0.0001$ on mugshot images. Points above the threshold correspond to pairs determined to be genuine, and points below the threshold correspond to pairs determined to be impostors. If the determined class (genuine or impostor) matches the real class, points will be blue; if not, red. An X represents face detection failure in either of the images in the pair. Note that the sample size ($n=20$) is small, and the figure may change substantially if larger or different sets are used. The images can be viewed on p. 13 of the Appendix, where Gen 01 corresponds to Same-Identity Pair 1, Gen 02 corresponds to Same-Identity Pair 2, and so on.

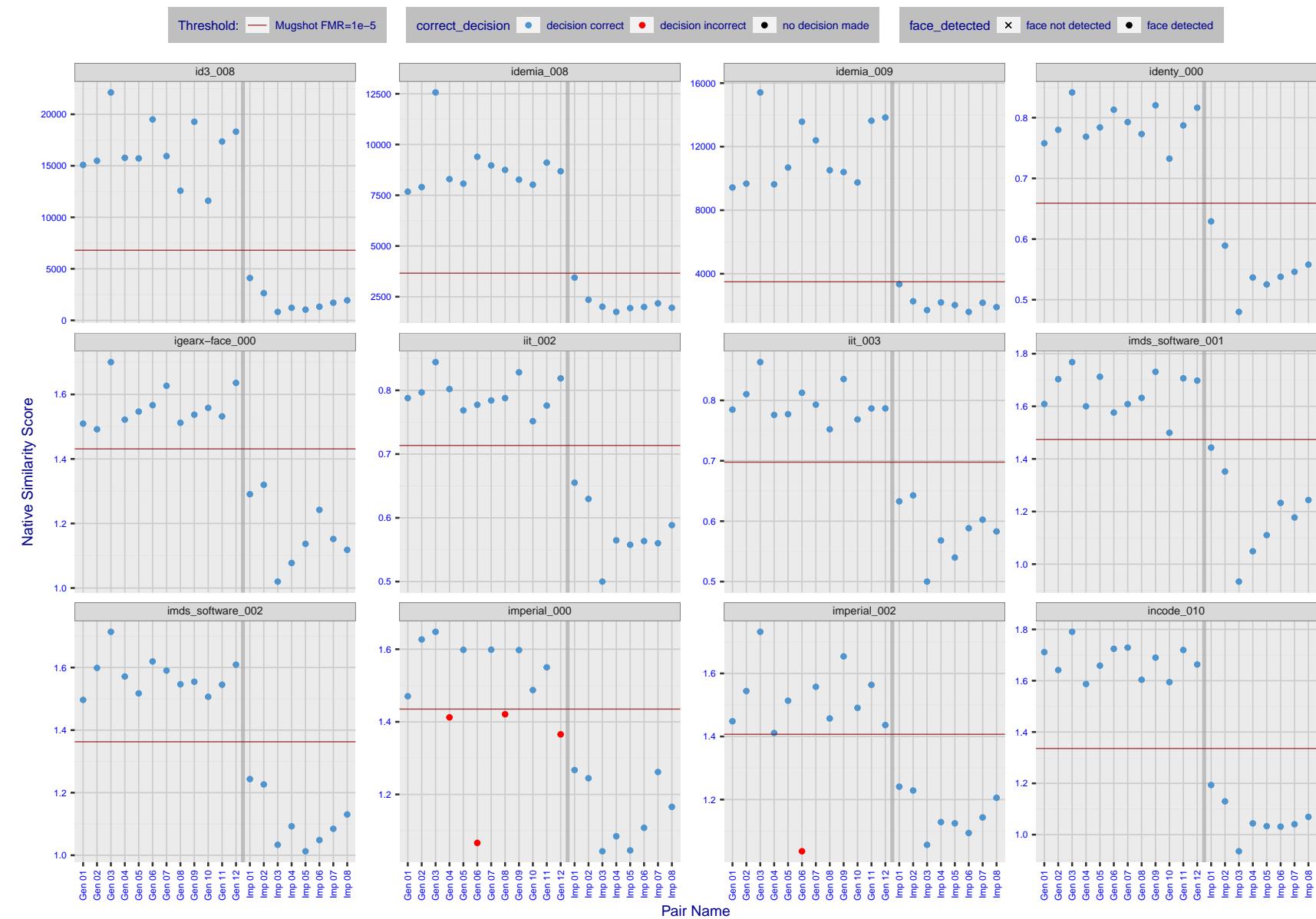


Figure 20: The figure shows algorithms' similarity scores for 12 genuine and 8 impostor image pairs used in a May 2018 paper by Phillips et al. ([1]). The threshold (red horizontal line) is a value calibrated to give $FMR = 0.0001$ on mugshot images. Points above the threshold correspond to pairs determined to be genuine, and points below the threshold correspond to pairs determined to be impostors. If the determined class (genuine or impostor) matches the real class, points will be blue; if not, red. An X represents face detection failure in either of the images in the pair. Note that the sample size ($n=20$) is small, and the figure may change substantially if larger or different sets are used. The images can be viewed on p. 13 of the Appendix, where Gen 01 corresponds to Same-Identity Pair 1, Gen 02 corresponds to Same-Identity Pair 2, and so on.

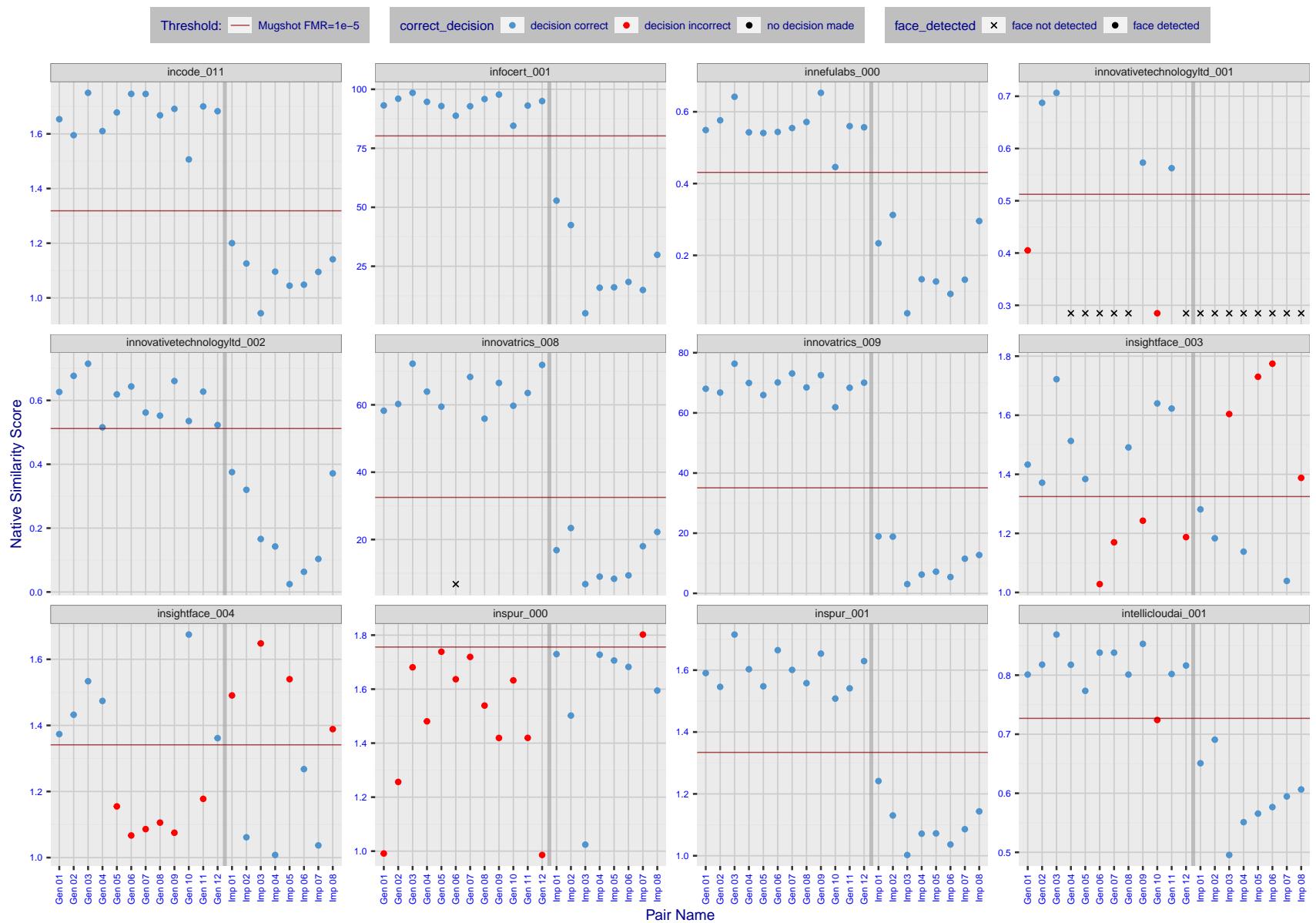


Figure 21: The figure shows algorithms' similarity scores for 12 genuine and 8 impostor image pairs used in a May 2018 paper by Phillips et al. ([1]). The threshold (red horizontal line) is a value calibrated to give $FMR = 0.0001$ on mugshot images. Points above the threshold correspond to pairs determined to be genuine, and points below the threshold correspond to pairs determined to be impostors. If the determined class (genuine or impostor) matches the real class, points will be blue; if not, red. An X represents face detection failure in either of the images in the pair. Note that the sample size ($n=20$) is small, and the figure may change substantially if larger or different sets are used. The images can be viewed on p. 13 of the Appendix, where Gen 01 corresponds to Same-Identity Pair 1, Gen 02 corresponds to Same-Identity Pair 2, and so on.

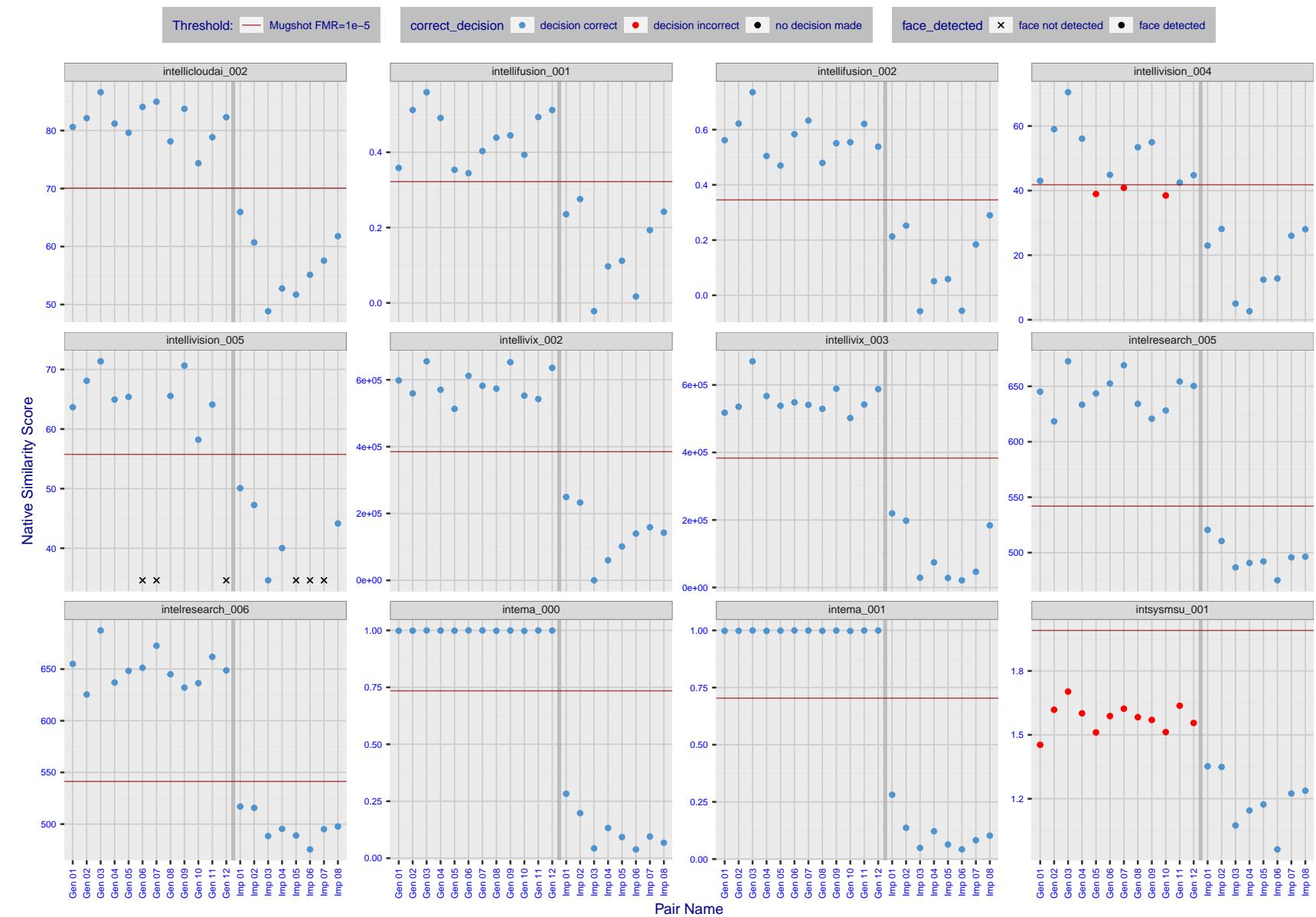


Figure 22: The figure shows algorithms' similarity scores for 12 genuine and 8 impostor image pairs used in a May 2018 paper by Phillips et al. ([1]). The threshold (red horizontal line) is a value calibrated to give $FMR = 0.0001$ on mugshot images. Points above the threshold correspond to pairs determined to be genuine, and points below the threshold correspond to pairs determined to be impostors. If the determined class (genuine or impostor) matches the real class, points will be blue; if not, red. An X represents face detection failure in either of the images in the pair. Note that the sample size ($n=20$) is small, and the figure may change substantially if larger or different sets are used. The images can be viewed on p. 13 of the Appendix, where Gen 01 corresponds to Same-Identity Pair 1, Gen 02 corresponds to Same-Identity Pair 2, and so on.

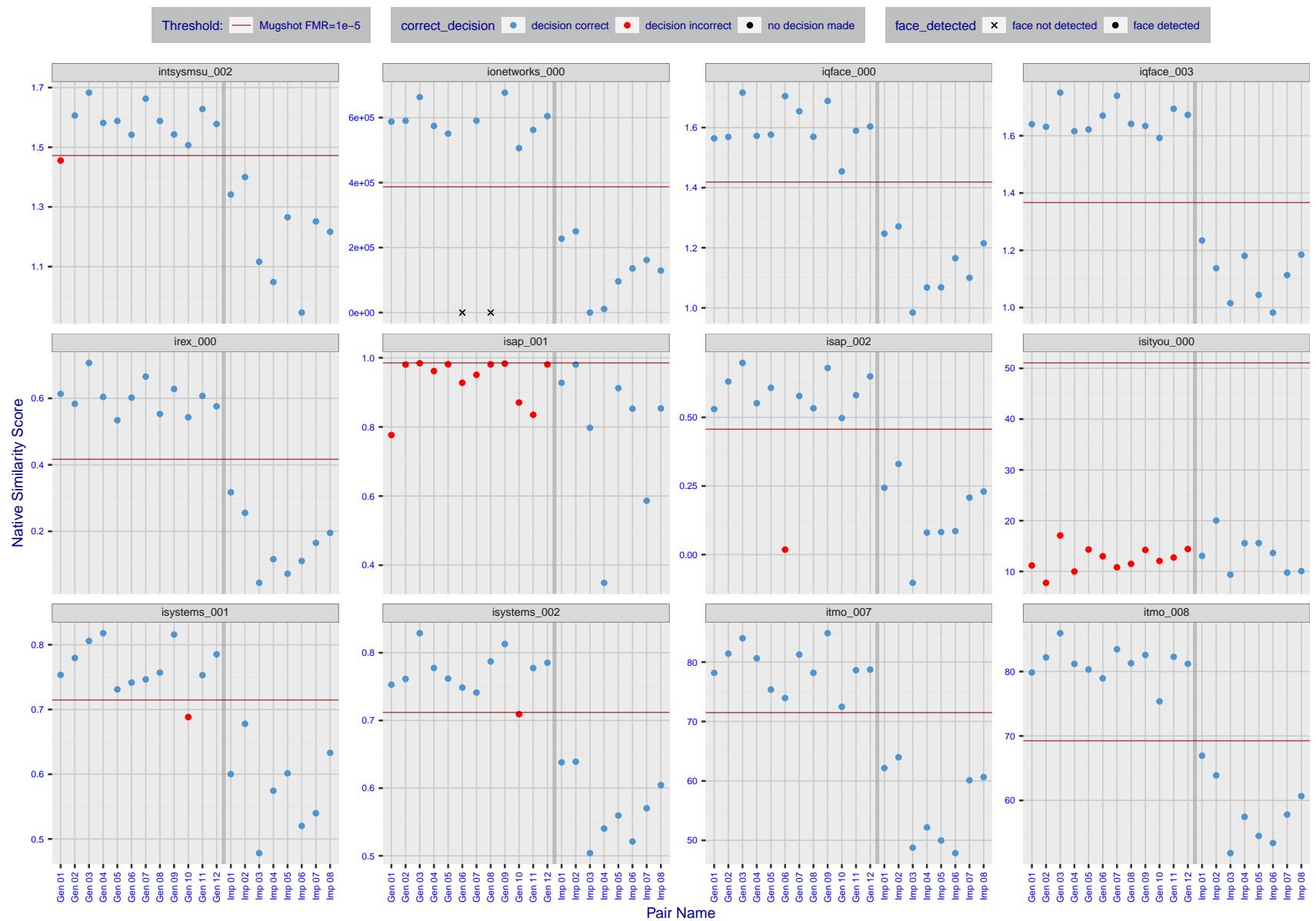


Figure 23: The figure shows algorithms' similarity scores for 12 genuine and 8 impostor image pairs used in a May 2018 paper by Phillips et al. ([1]). The threshold (red horizontal line) is a value calibrated to give $FMR = 0.0001$ on mugshot images. Points above the threshold correspond to pairs determined to be genuine, and points below the threshold correspond to pairs determined to be impostors. If the determined class (genuine or impostor) matches the real class, points will be blue; if not, red. An X represents face detection failure in either of the images in the pair. Note that the sample size ($n=20$) is small, and the figure may change substantially if larger or different sets are used. The images can be viewed on p. 13 of the Appendix, where Gen 01 corresponds to Same-Identity Pair 1, Gen 02 corresponds to Same-Identity Pair 2, and so on.

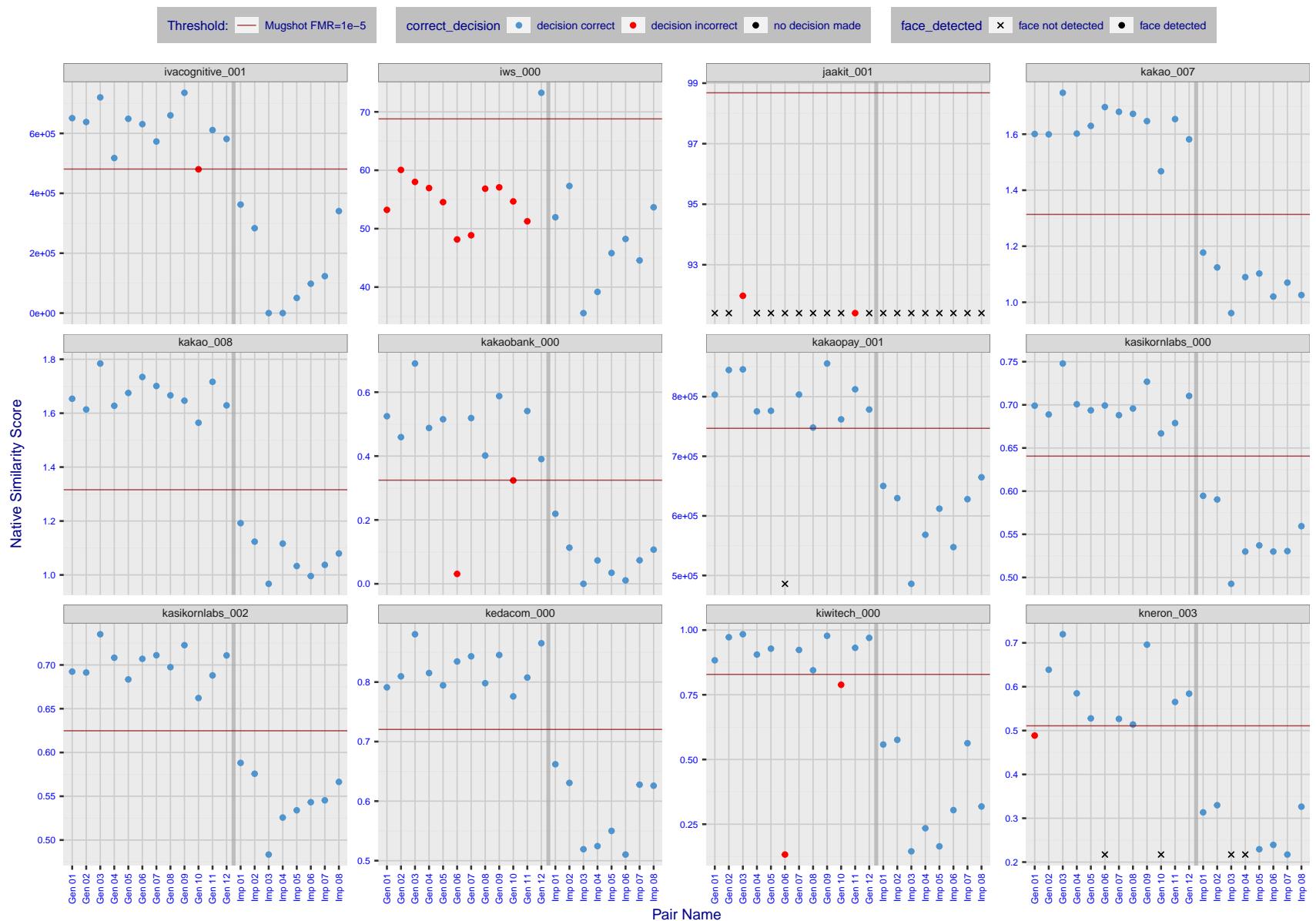


Figure 24: The figure shows algorithms' similarity scores for 12 genuine and 8 impostor image pairs used in a May 2018 paper by Phillips et al. ([1]). The threshold (red horizontal line) is a value calibrated to give $FMR = 0.0001$ on mugshot images. Points above the threshold correspond to pairs determined to be genuine, and points below the threshold correspond to pairs determined to be impostors. If the determined class (genuine or impostor) matches the real class, points will be blue; if not, red. An X represents face detection failure in either of the images in the pair. Note that the sample size ($n=20$) is small, and the figure may change substantially if larger or different sets are used. The images can be viewed on p. 13 of the Appendix, where Gen 01 corresponds to Same-Identity Pair 1, Gen 02 corresponds to Same-Identity Pair 2, and so on.

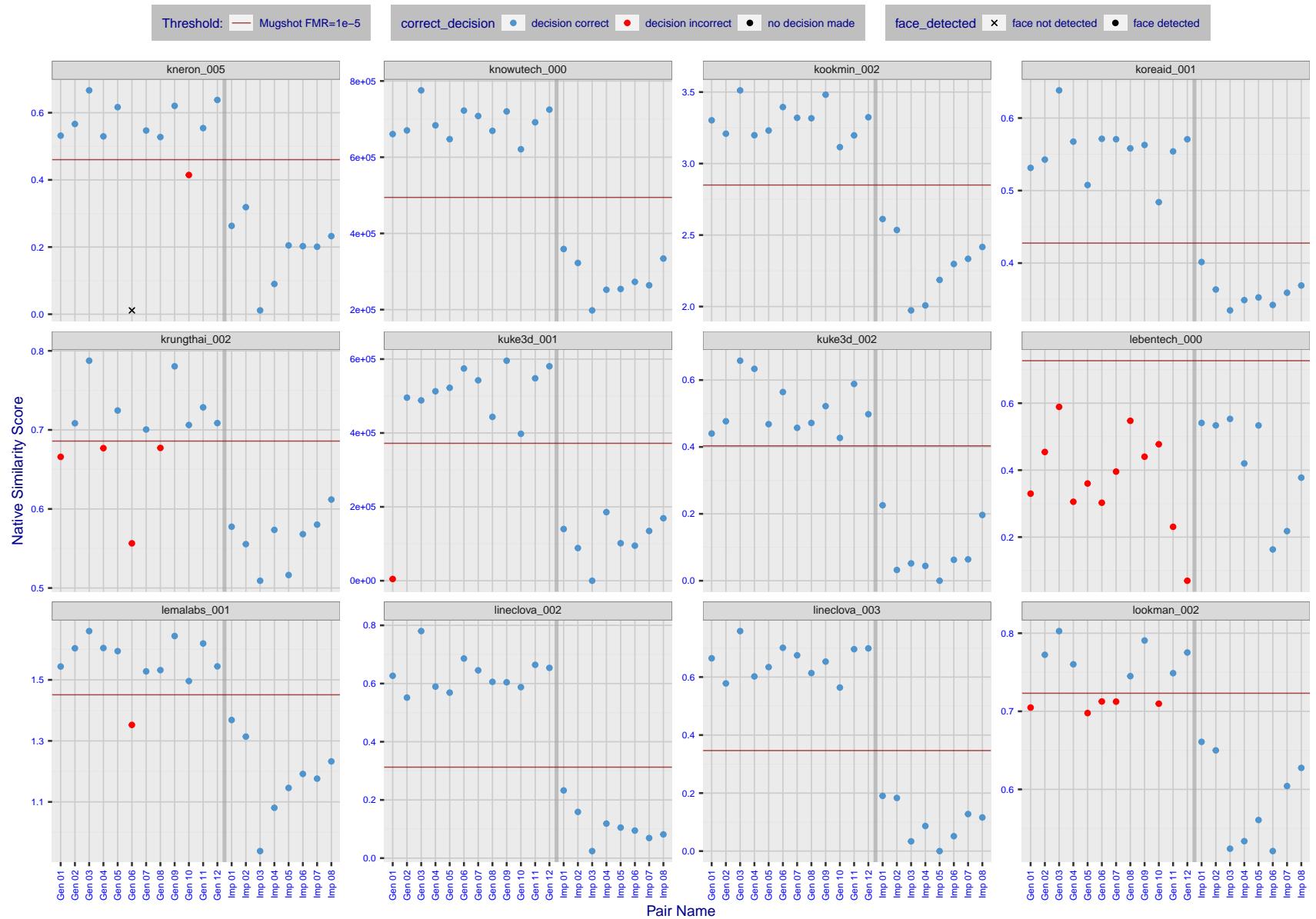


Figure 25: The figure shows algorithms' similarity scores for 12 genuine and 8 impostor image pairs used in a May 2018 paper by Phillips et al. ([1]). The threshold (red horizontal line) is a value calibrated to give $FMR = 0.0001$ on mugshot images. Points above the threshold correspond to pairs determined to be genuine, and points below the threshold correspond to pairs determined to be impostors. If the determined class (genuine or impostor) matches the real class, points will be blue; if not, red. An X represents face detection failure in either of the images in the pair. Note that the sample size ($n=20$) is small, and the figure may change substantially if larger or different sets are used. The images can be viewed on p. 13 of the Appendix, where Gen 01 corresponds to Same-Identity Pair 1, Gen 02 corresponds to Same-Identity Pair 2, and so on.

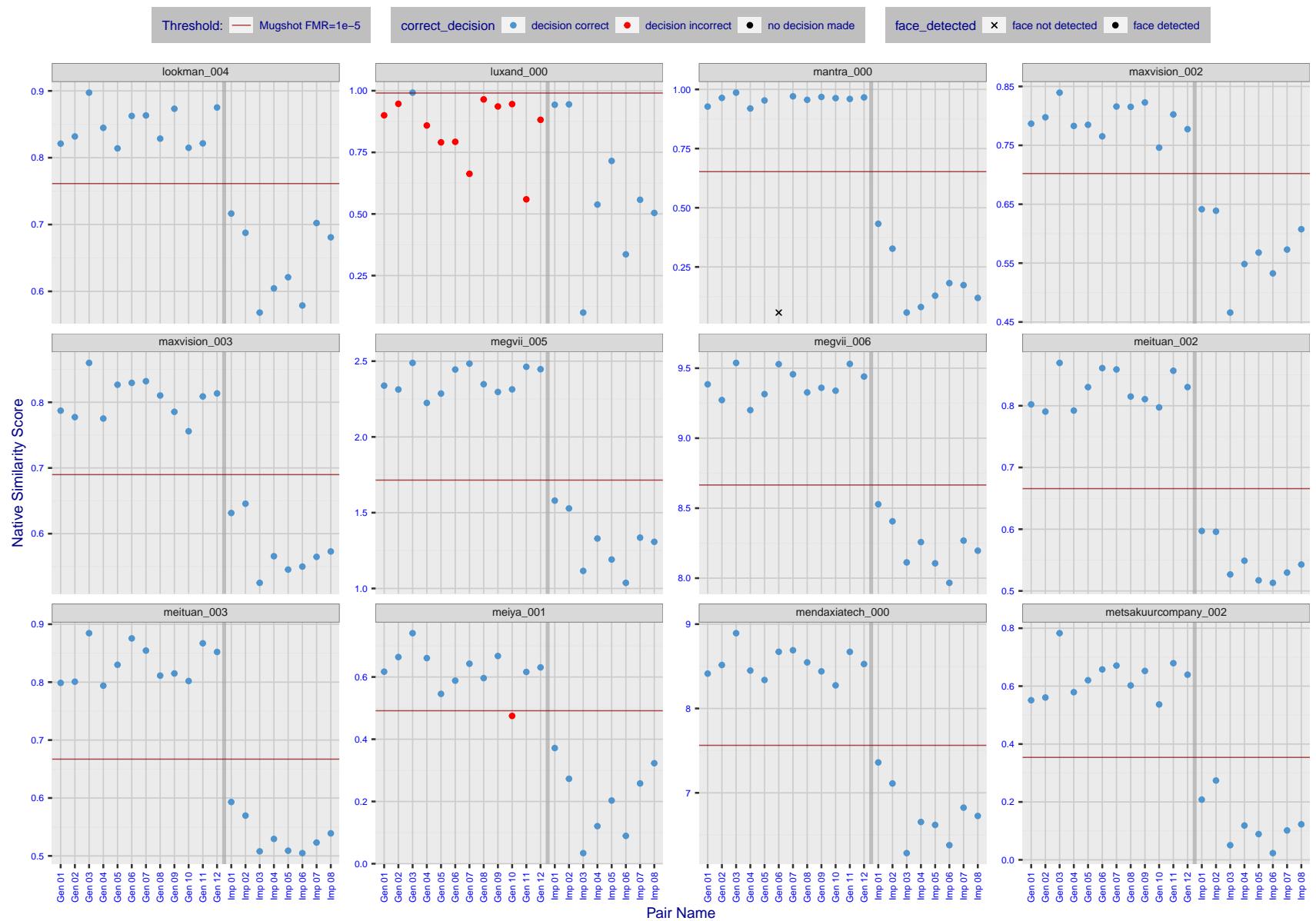


Figure 26: The figure shows algorithms' similarity scores for 12 genuine and 8 impostor image pairs used in a May 2018 paper by Phillips et al. ([1]). The threshold (red horizontal line) is a value calibrated to give $FMR = 0.0001$ on mugshot images. Points above the threshold correspond to pairs determined to be genuine, and points below the threshold correspond to pairs determined to be impostors. If the determined class (genuine or impostor) matches the real class, points will be blue; if not, red. An X represents face detection failure in either of the images in the pair. Note that the sample size ($n=20$) is small, and the figure may change substantially if larger or different sets are used. The images can be viewed on p. 13 of the Appendix, where Gen 01 corresponds to Same-Identity Pair 1, Gen 02 corresponds to Same-Identity Pair 2, and so on.

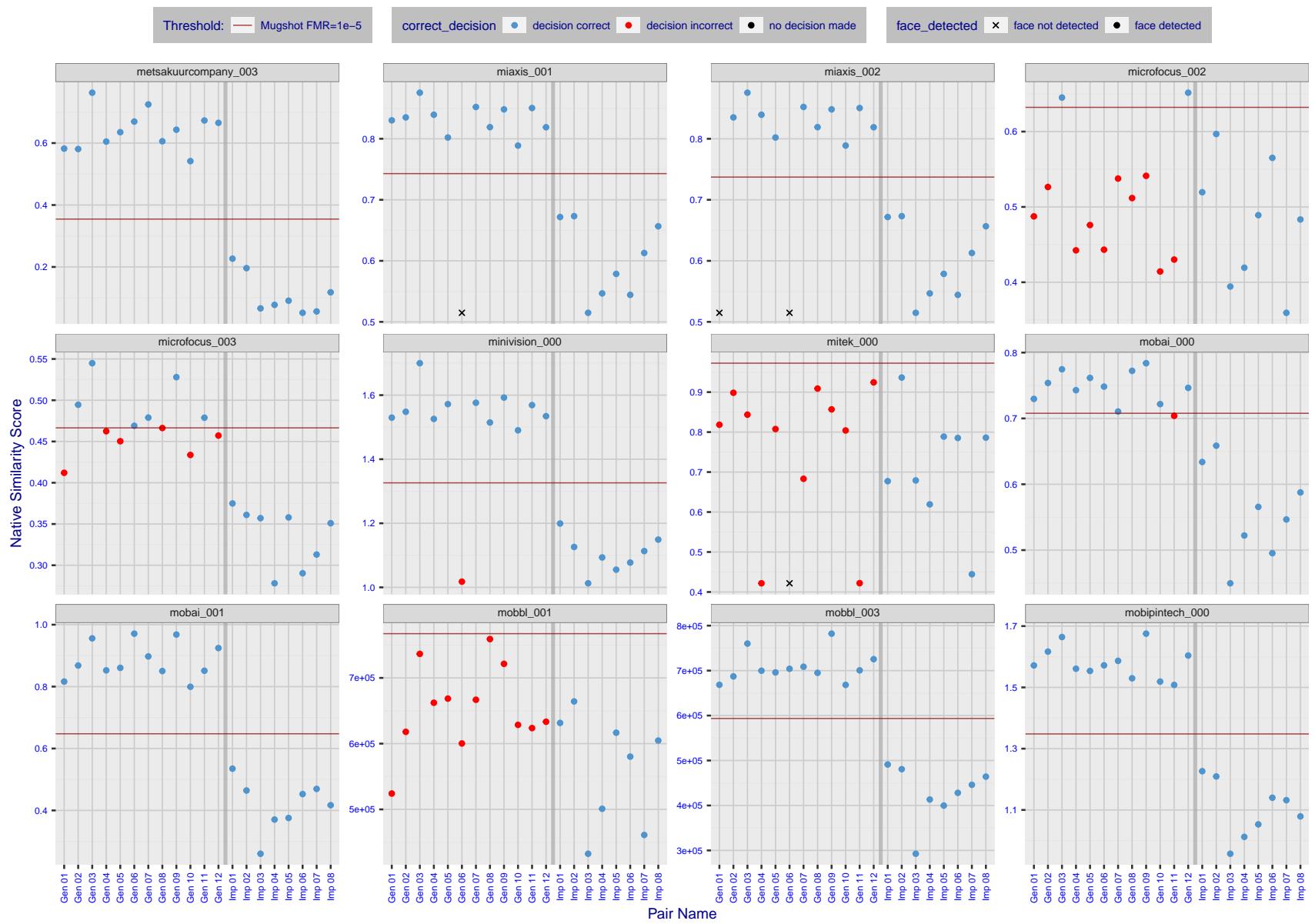


Figure 27: The figure shows algorithms' similarity scores for 12 genuine and 8 impostor image pairs used in a May 2018 paper by Phillips et al. ([1]). The threshold (red horizontal line) is a value calibrated to give $FMR = 0.0001$ on mugshot images. Points above the threshold correspond to pairs determined to be genuine, and points below the threshold correspond to pairs determined to be impostors. If the determined class (genuine or impostor) matches the real class, points will be blue; if not, red. An X represents face detection failure in either of the images in the pair. Note that the sample size ($n=20$) is small, and the figure may change substantially if larger or different sets are used. The images can be viewed on p. 13 of the Appendix, where Gen 01 corresponds to Same-Identity Pair 1, Gen 02 corresponds to Same-Identity Pair 2, and so on.

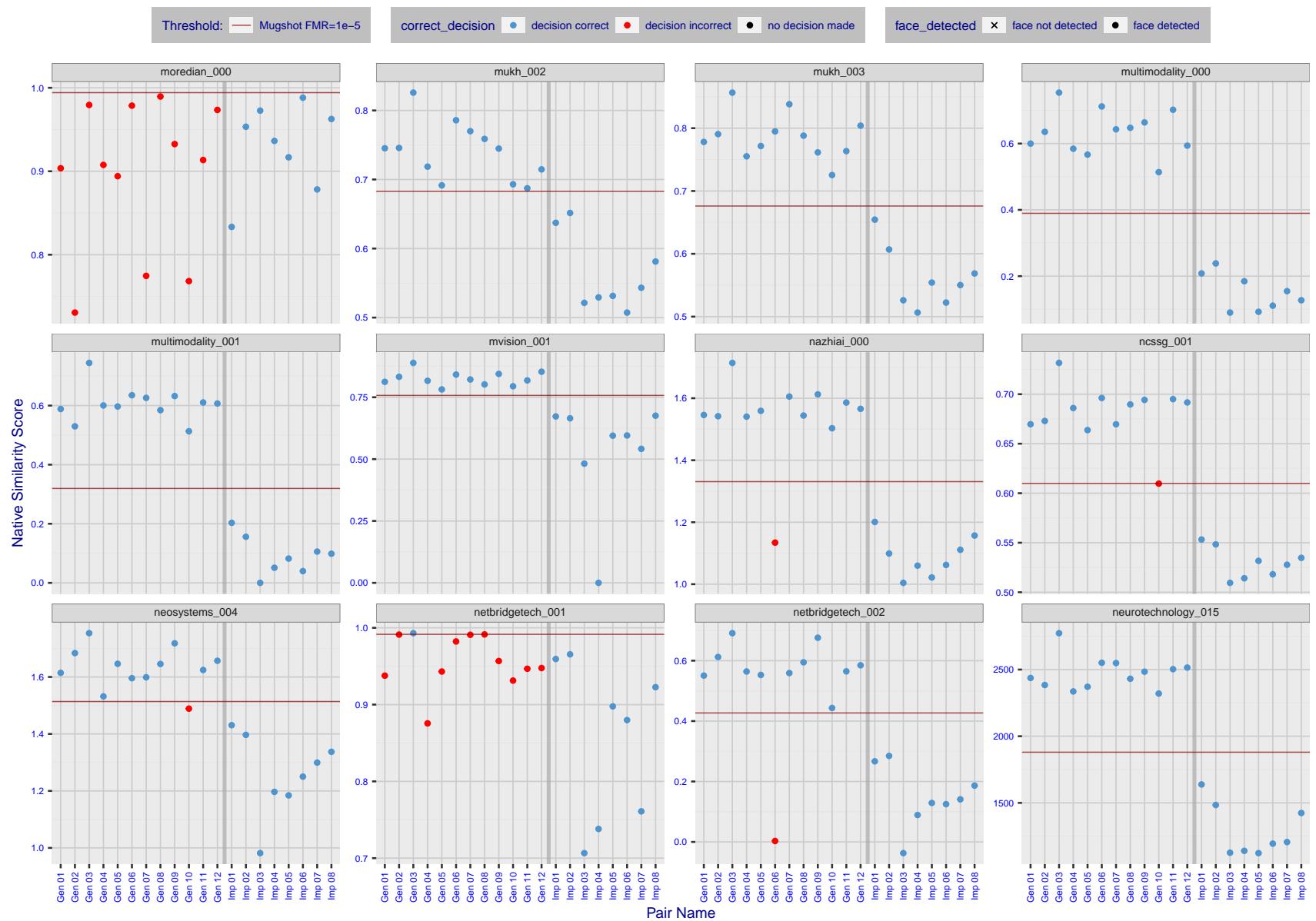


Figure 28: The figure shows algorithms' similarity scores for 12 genuine and 8 impostor image pairs used in a May 2018 paper by Phillips et al. ([1]). The threshold (red horizontal line) is a value calibrated to give $FMR = 0.0001$ on mugshot images. Points above the threshold correspond to pairs determined to be genuine, and points below the threshold correspond to pairs determined to be impostors. If the determined class (genuine or impostor) matches the real class, points will be blue; if not, red. An X represents face detection failure in either of the images in the pair. Note that the sample size ($n=20$) is small, and the figure may change substantially if larger or different sets are used. The images can be viewed on p. 13 of the Appendix, where Gen 01 corresponds to Same-Identity Pair 1, Gen 02 corresponds to Same-Identity Pair 2, and so on.

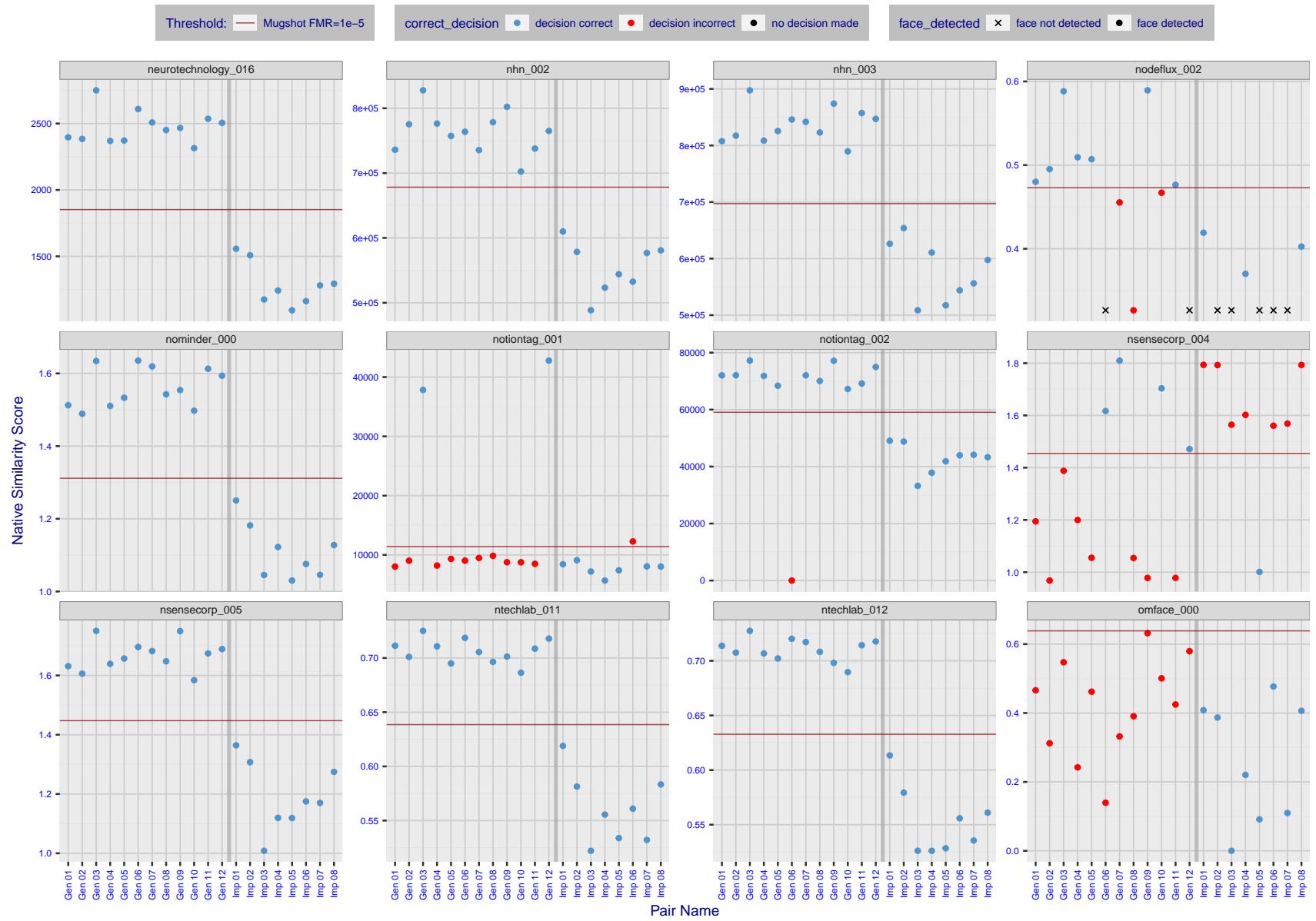


Figure 29: The figure shows algorithms' similarity scores for 12 genuine and 8 impostor image pairs used in a May 2018 paper by Phillips et al. ([1]). The threshold (red horizontal line) is a value calibrated to give $FMR = 0.0001$ on mugshot images. Points above the threshold correspond to pairs determined to be genuine, and points below the threshold correspond to pairs determined to be impostors. If the determined class (genuine or impostor) matches the real class, points will be blue; if not, red. An X represents face detection failure in either of the images in the pair. Note that the sample size ($n=20$) is small, and the figure may change substantially if larger or different sets are used. The images can be viewed on p. 13 of the Appendix, where Gen 01 corresponds to Same-Identity Pair 1, Gen 02 corresponds to Same-Identity Pair 2, and so on.

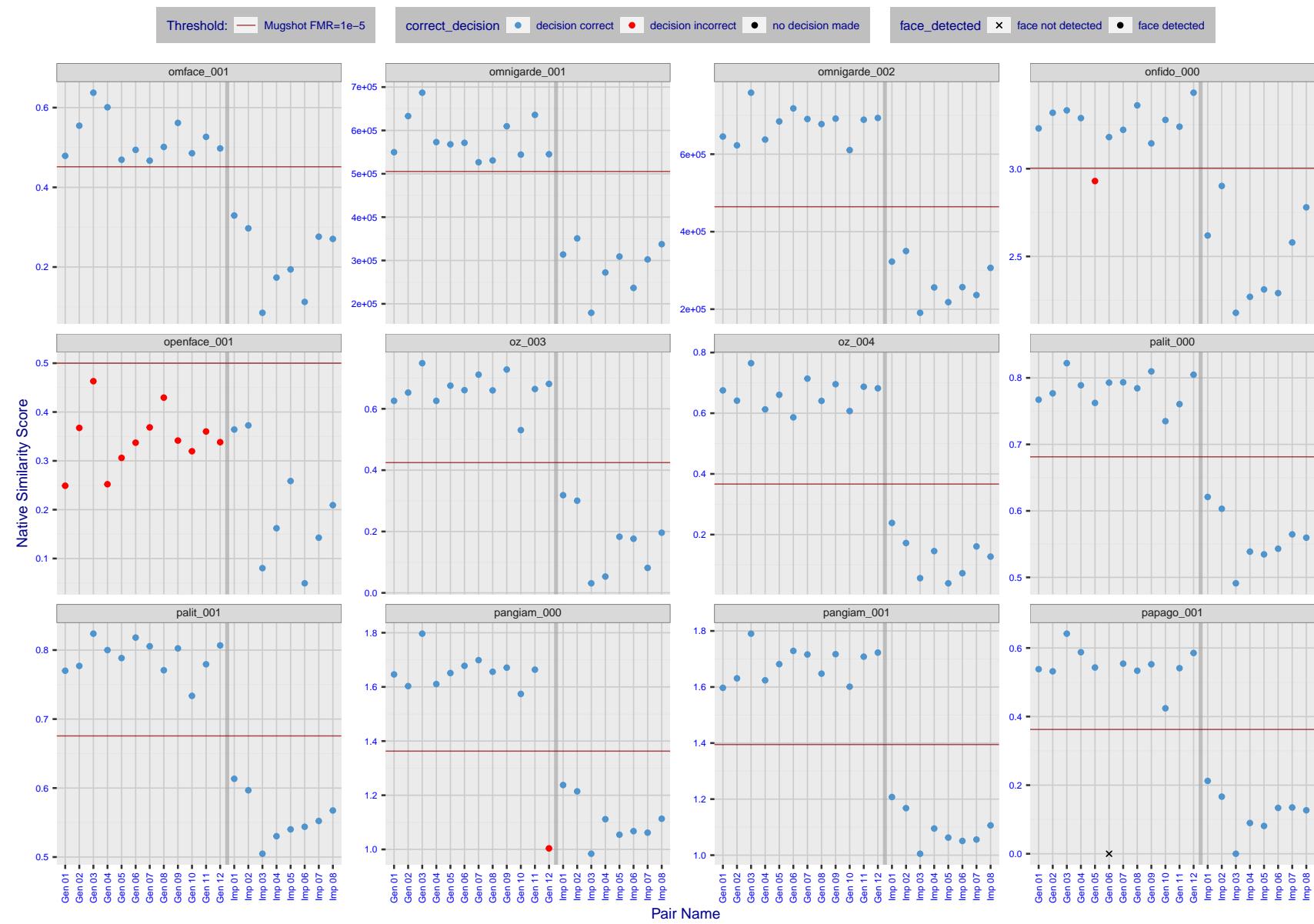


Figure 30: The figure shows algorithms' similarity scores for 12 genuine and 8 impostor image pairs used in a May 2018 paper by Phillips et al. ([1]). The threshold (red horizontal line) is a value calibrated to give $FMR = 0.0001$ on mugshot images. Points above the threshold correspond to pairs determined to be genuine, and points below the threshold correspond to pairs determined to be impostors. If the determined class (genuine or impostor) matches the real class, points will be blue; if not, red. An X represents face detection failure in either of the images in the pair. Note that the sample size ($n=20$) is small, and the figure may change substantially if larger or different sets are used. The images can be viewed on p. 13 of the Appendix, where Gen 01 corresponds to Same-Identity Pair 1, Gen 02 corresponds to Same-Identity Pair 2, and so on.

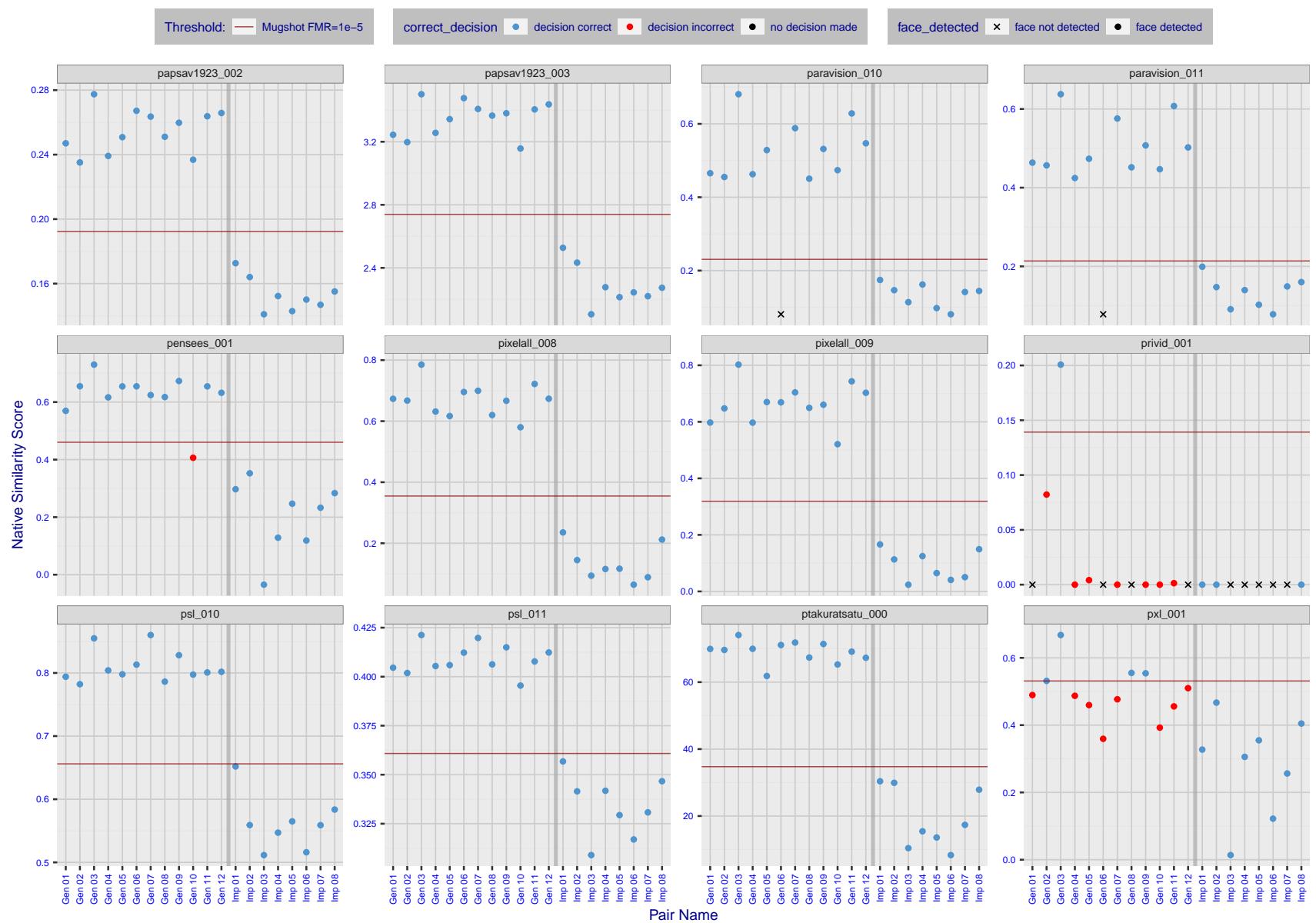


Figure 31: The figure shows algorithms' similarity scores for 12 genuine and 8 impostor image pairs used in a May 2018 paper by Phillips et al. ([1]). The threshold (red horizontal line) is a value calibrated to give $FMR = 0.0001$ on mugshot images. Points above the threshold correspond to pairs determined to be genuine, and points below the threshold correspond to pairs determined to be impostors. If the determined class (genuine or impostor) matches the real class, points will be blue; if not, red. An X represents face detection failure in either of the images in the pair. Note that the sample size ($n=20$) is small, and the figure may change substantially if larger or different sets are used. The images can be viewed on p. 13 of the Appendix, where Gen 01 corresponds to Same-Identity Pair 1, Gen 02 corresponds to Same-Identity Pair 2, and so on.

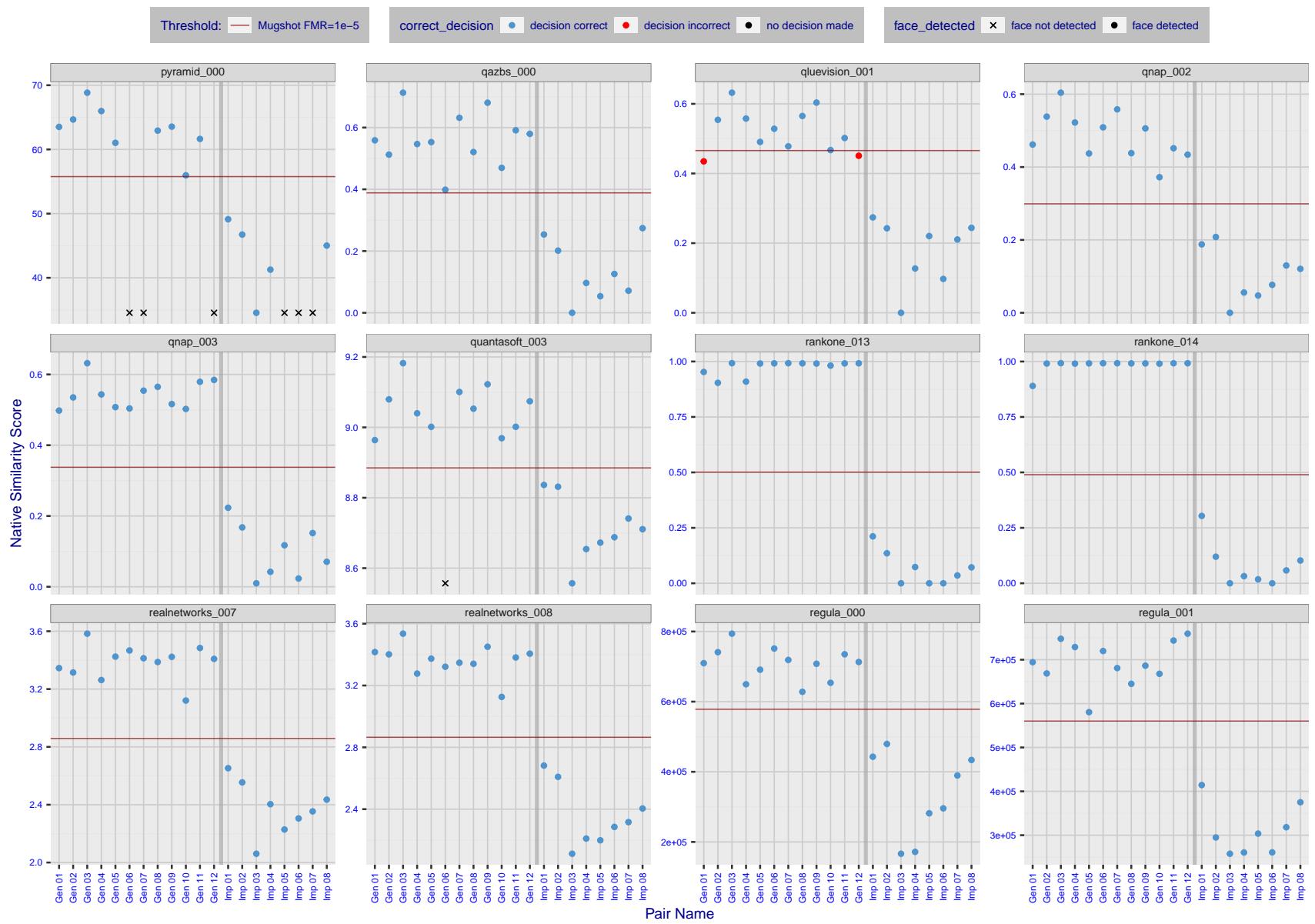


Figure 32: The figure shows algorithms' similarity scores for 12 genuine and 8 impostor image pairs used in a May 2018 paper by Phillips et al. ([1]). The threshold (red horizontal line) is a value calibrated to give $FMR = 0.0001$ on mugshot images. Points above the threshold correspond to pairs determined to be genuine, and points below the threshold correspond to pairs determined to be impostors. If the determined class (genuine or impostor) matches the real class, points will be blue; if not, red. An X represents face detection failure in either of the images in the pair. Note that the sample size ($n=20$) is small, and the figure may change substantially if larger or different sets are used. The images can be viewed on p. 13 of the Appendix, where Gen 01 corresponds to Same-Identity Pair 1, Gen 02 corresponds to Same-Identity Pair 2, and so on.

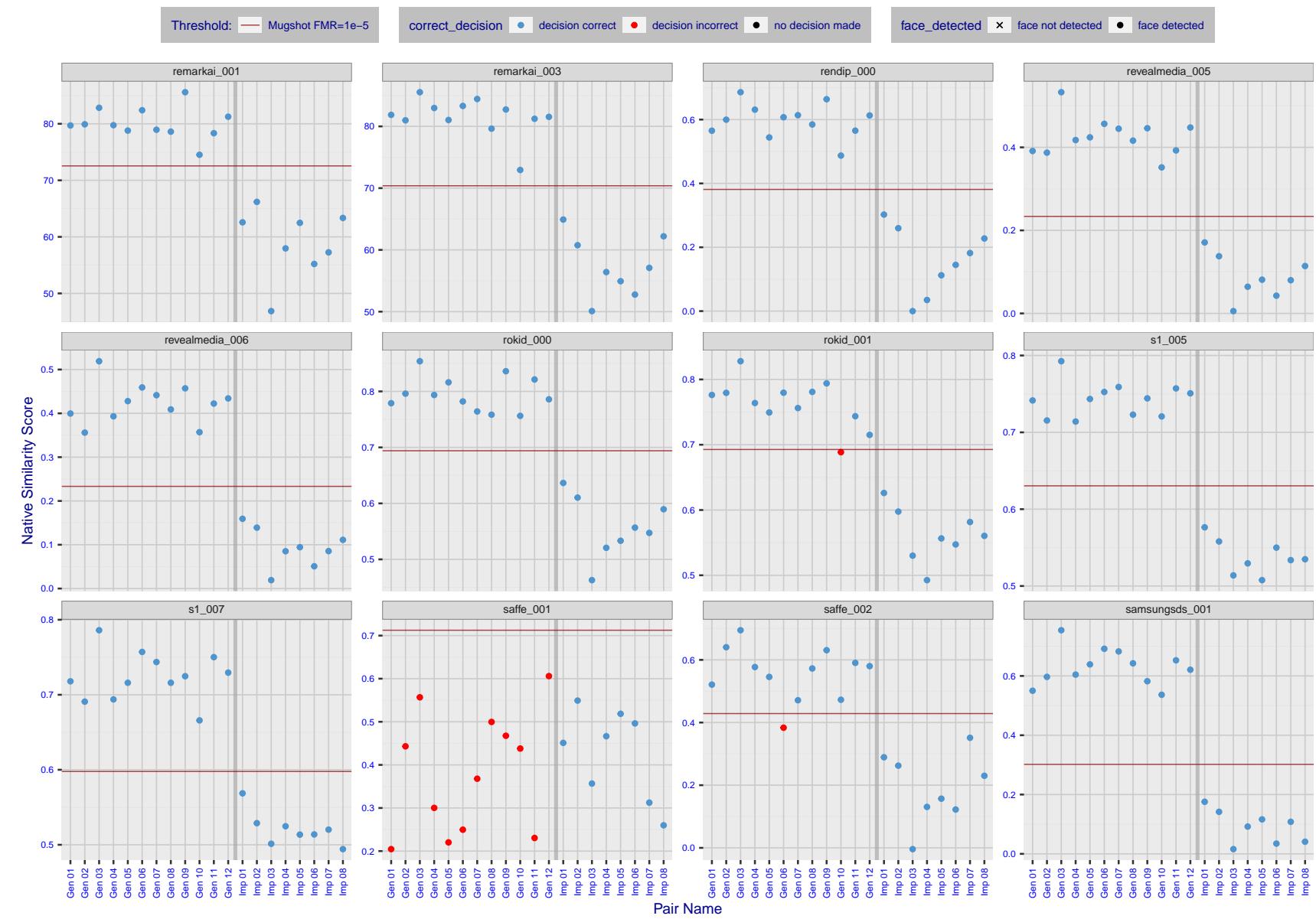


Figure 33: The figure shows algorithms' similarity scores for 12 genuine and 8 impostor image pairs used in a May 2018 paper by Phillips et al. ([1]). The threshold (red horizontal line) is a value calibrated to give $FMR = 0.0001$ on mugshot images. Points above the threshold correspond to pairs determined to be genuine, and points below the threshold correspond to pairs determined to be impostors. If the determined class (genuine or impostor) matches the real class, points will be blue; if not, red. An X represents face detection failure in either of the images in the pair. Note that the sample size ($n=20$) is small, and the figure may change substantially if larger or different sets are used. The images can be viewed on p. 13 of the Appendix, where Gen 01 corresponds to Same-Identity Pair 1, Gen 02 corresponds to Same-Identity Pair 2, and so on.

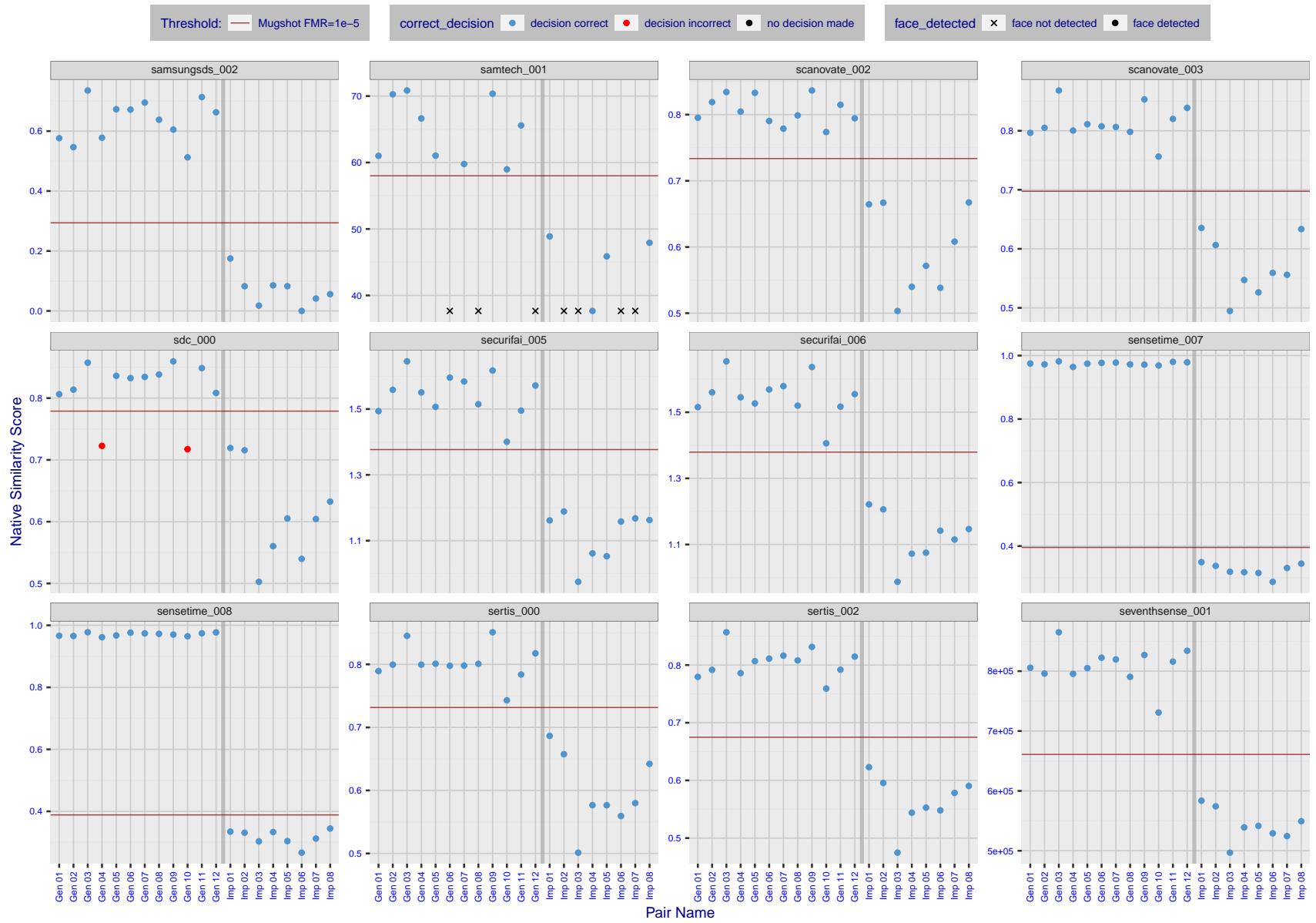


Figure 34: The figure shows algorithms' similarity scores for 12 genuine and 8 impostor image pairs used in a May 2018 paper by Phillips et al. ([1]). The threshold (red horizontal line) is a value calibrated to give $FMR = 0.0001$ on mugshot images. Points above the threshold correspond to pairs determined to be genuine, and points below the threshold correspond to pairs determined to be impostors. If the determined class (genuine or impostor) matches the real class, points will be blue; if not, red. An X represents face detection failure in either of the images in the pair. Note that the sample size ($n=20$) is small, and the figure may change substantially if larger or different sets are used. The images can be viewed on p. 13 of the Appendix, where Gen 01 corresponds to Same-Identity Pair 1, Gen 02 corresponds to Same-Identity Pair 2, and so on.

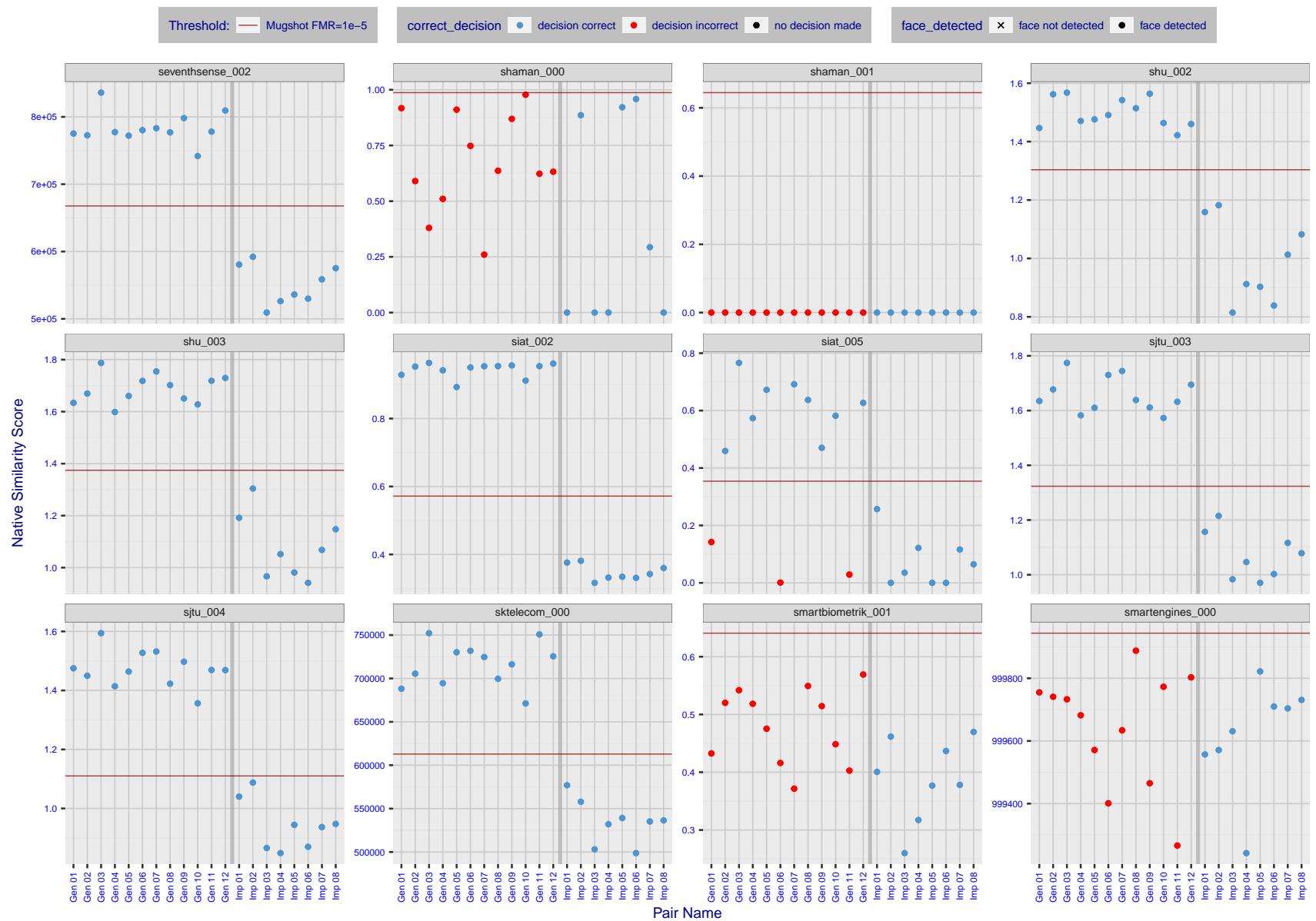


Figure 35: The figure shows algorithms' similarity scores for 12 genuine and 8 impostor image pairs used in a May 2018 paper by Phillips et al. ([1]). The threshold (red horizontal line) is a value calibrated to give $FMR = 0.0001$ on mugshot images. Points above the threshold correspond to pairs determined to be genuine, and points below the threshold correspond to pairs determined to be impostors. If the determined class (genuine or impostor) matches the real class, points will be blue; if not, red. An X represents face detection failure in either of the images in the pair. Note that the sample size ($n=20$) is small, and the figure may change substantially if larger or different sets are used. The images can be viewed on p. 13 of the Appendix, where Gen 01 corresponds to Same-Identity Pair 1, Gen 02 corresponds to Same-Identity Pair 2, and so on.

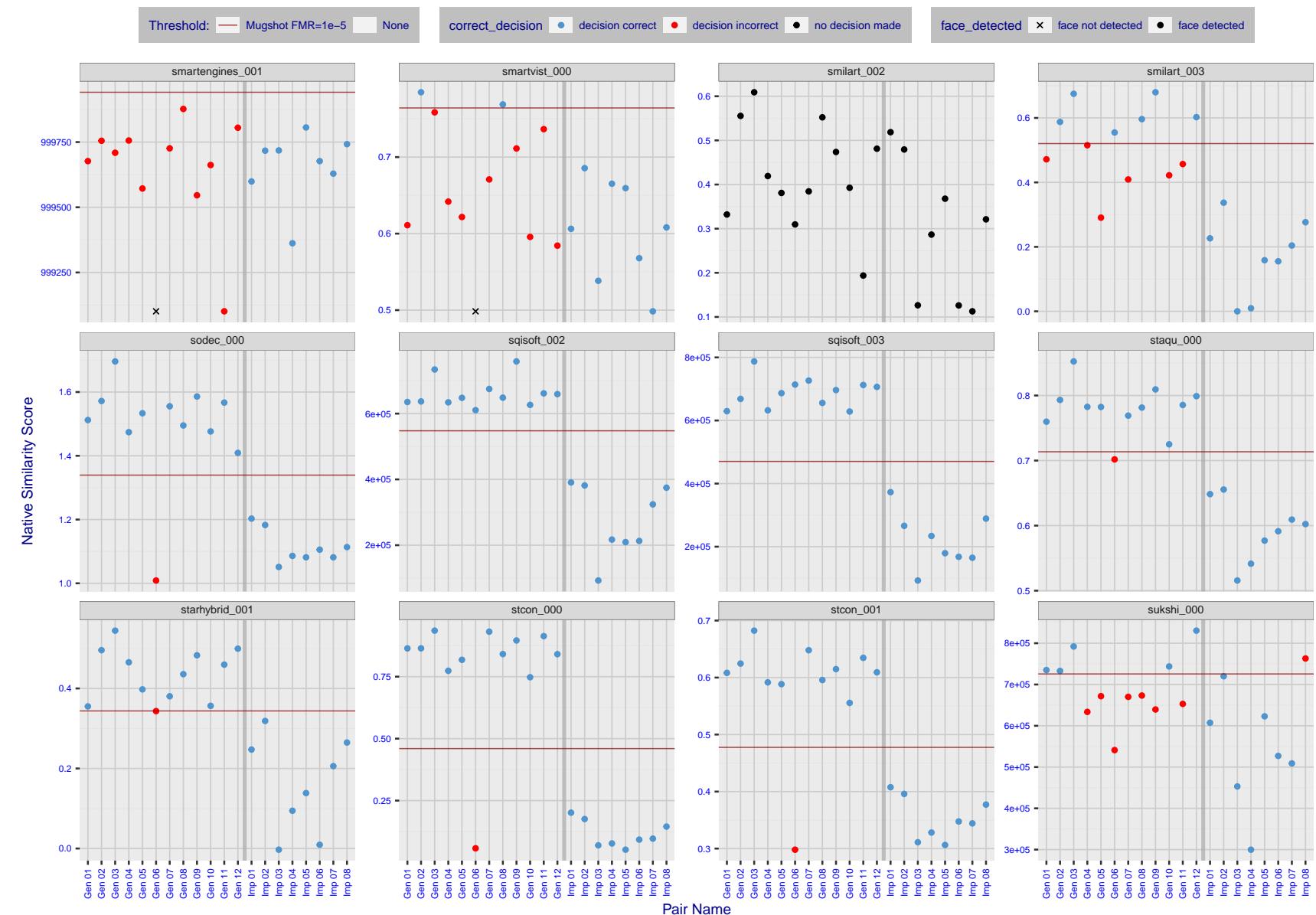


Figure 36: The figure shows algorithms' similarity scores for 12 genuine and 8 impostor image pairs used in a May 2018 paper by Phillips et al. ([1]). The threshold (red horizontal line) is a value calibrated to give $FMR = 0.0001$ on mugshot images. Points above the threshold correspond to pairs determined to be genuine, and points below the threshold correspond to pairs determined to be impostors. If the determined class (genuine or impostor) matches the real class, points will be blue; if not, red. An X represents face detection failure in either of the images in the pair. Note that the sample size ($n=20$) is small, and the figure may change substantially if larger or different sets are used. The images can be viewed on p. 13 of the Appendix, where Gen 01 corresponds to Same-Identity Pair 1, Gen 02 corresponds to Same-Identity Pair 2, and so on.

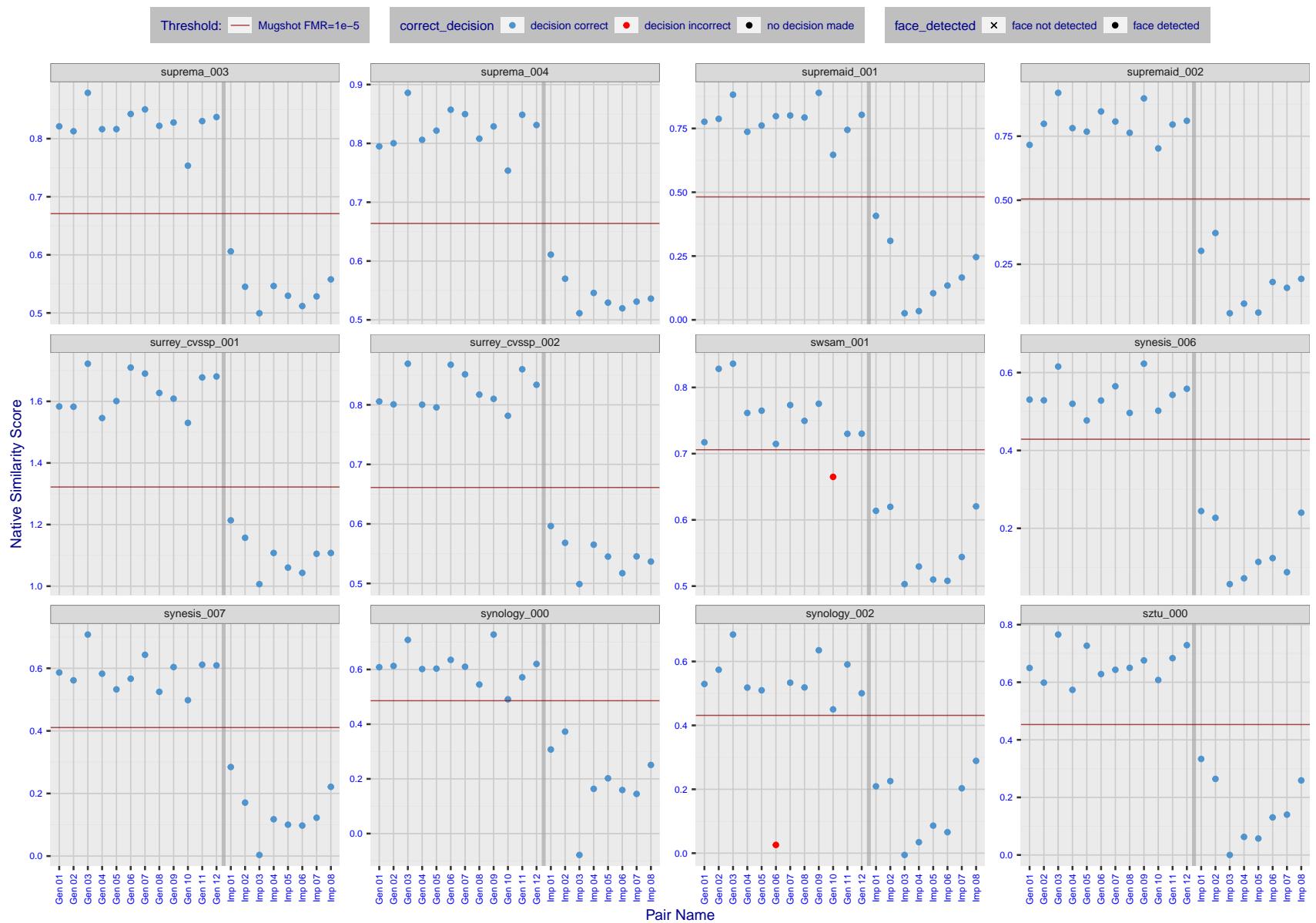


Figure 37: The figure shows algorithms' similarity scores for 12 genuine and 8 impostor image pairs used in a May 2018 paper by Phillips et al. ([1]). The threshold (red horizontal line) is a value calibrated to give $FMR = 0.0001$ on mugshot images. Points above the threshold correspond to pairs determined to be genuine, and points below the threshold correspond to pairs determined to be impostors. If the determined class (genuine or impostor) matches the real class, points will be blue; if not, red. An X represents face detection failure in either of the images in the pair. Note that the sample size ($n=20$) is small, and the figure may change substantially if larger or different sets are used. The images can be viewed on p. 13 of the Appendix, where Gen 01 corresponds to Same-Identity Pair 1, Gen 02 corresponds to Same-Identity Pair 2, and so on.

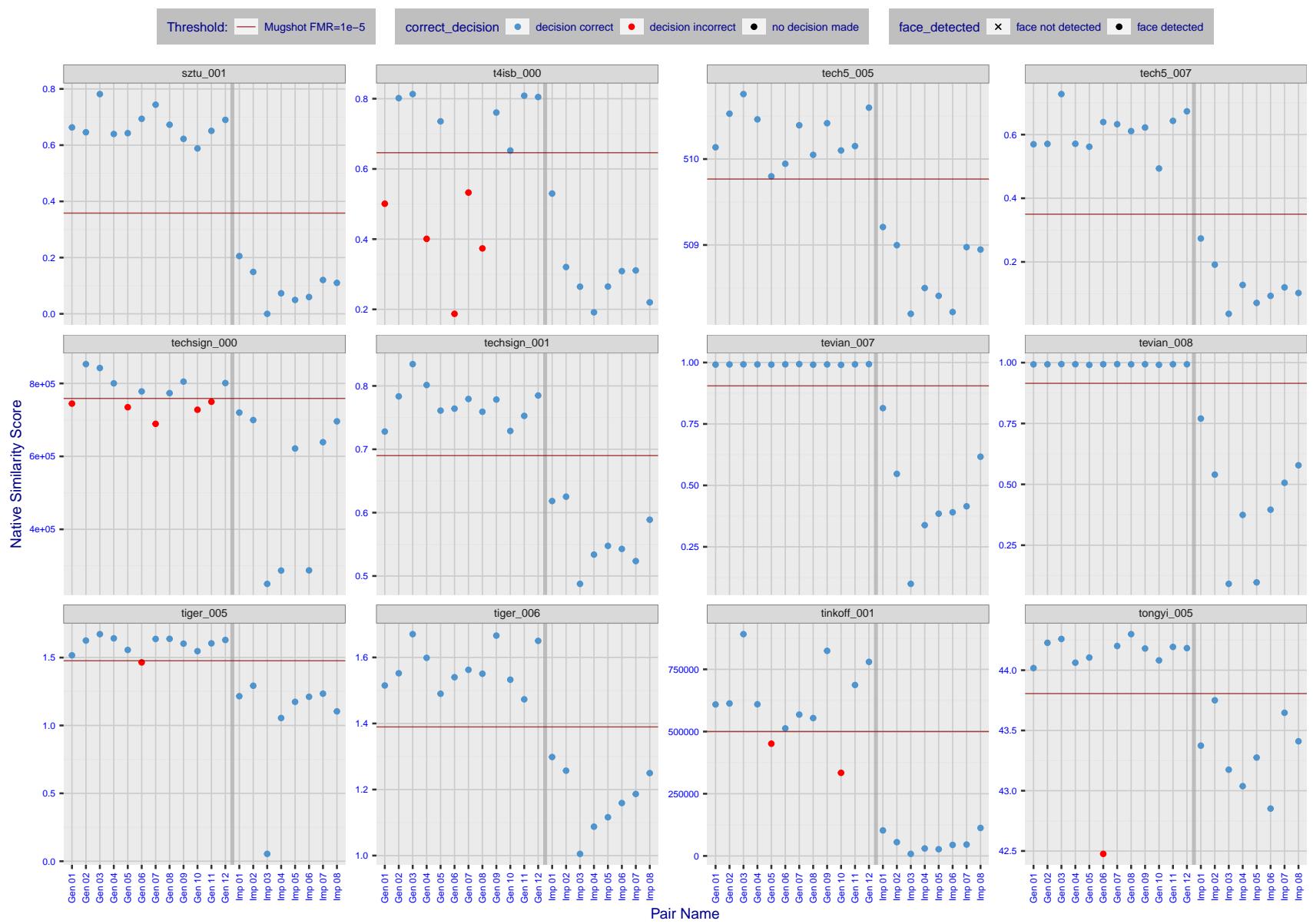


Figure 38: The figure shows algorithms' similarity scores for 12 genuine and 8 impostor image pairs used in a May 2018 paper by Phillips et al. ([1]). The threshold (red horizontal line) is a value calibrated to give $FMR = 0.0001$ on mugshot images. Points above the threshold correspond to pairs determined to be genuine, and points below the threshold correspond to pairs determined to be impostors. If the determined class (genuine or impostor) matches the real class, points will be blue; if not, red. An X represents face detection failure in either of the images in the pair. Note that the sample size ($n=20$) is small, and the figure may change substantially if larger or different sets are used. The images can be viewed on p. 13 of the Appendix, where Gen 01 corresponds to Same-Identity Pair 1, Gen 02 corresponds to Same-Identity Pair 2, and so on.

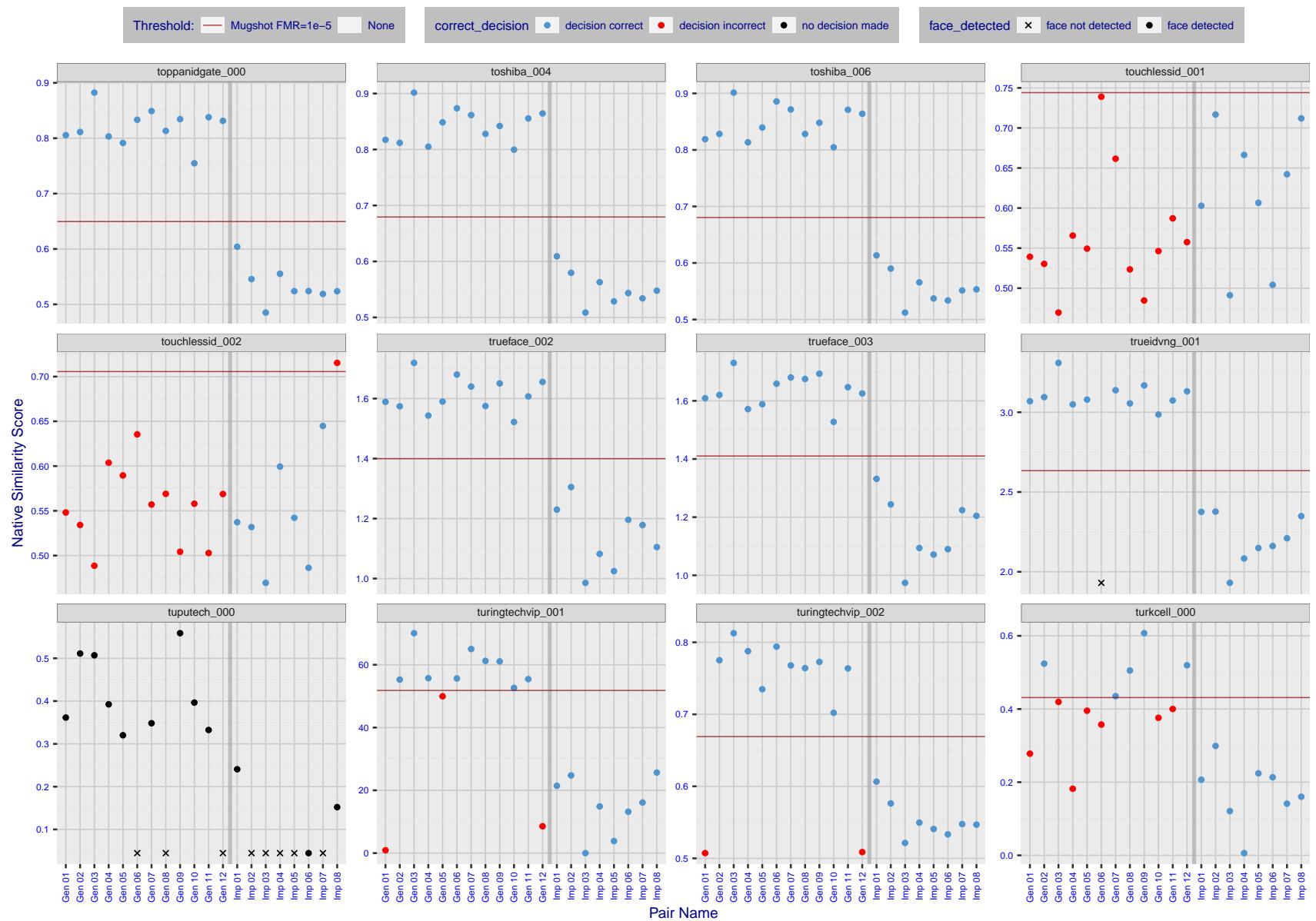


Figure 39: The figure shows algorithms' similarity scores for 12 genuine and 8 impostor image pairs used in a May 2018 paper by Phillips et al. ([1]). The threshold (red horizontal line) is a value calibrated to give $FMR = 0.0001$ on mugshot images. Points above the threshold correspond to pairs determined to be genuine, and points below the threshold correspond to pairs determined to be impostors. If the determined class (genuine or impostor) matches the real class, points will be blue; if not, red. An X represents face detection failure in either of the images in the pair. Note that the sample size ($n=20$) is small, and the figure may change substantially if larger or different sets are used. The images can be viewed on p. 13 of the Appendix, where Gen 01 corresponds to Same-Identity Pair 1, Gen 02 corresponds to Same-Identity Pair 2, and so on.

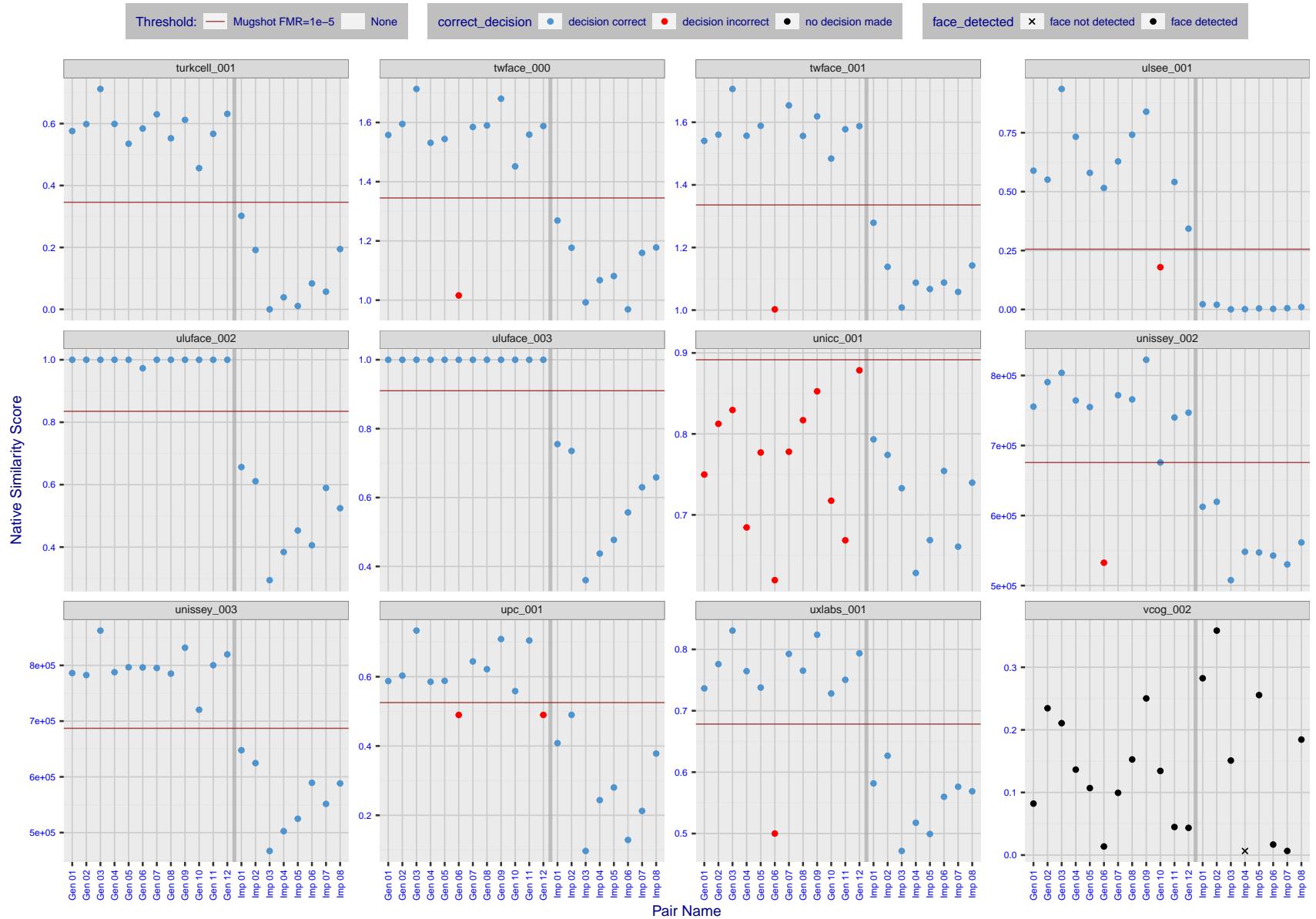


Figure 40: The figure shows algorithms' similarity scores for 12 genuine and 8 impostor image pairs used in a May 2018 paper by Phillips et al. ([1]). The threshold (red horizontal line) is a value calibrated to give $FMR = 0.0001$ on mugshot images. Points above the threshold correspond to pairs determined to be genuine, and points below the threshold correspond to pairs determined to be impostors. If the determined class (genuine or impostor) matches the real class, points will be blue; if not, red. An X represents face detection failure in either of the images in the pair. Note that the sample size ($n=20$) is small, and the figure may change substantially if larger or different sets are used. The images can be viewed on p. 13 of the Appendix, where Gen 01 corresponds to Same-Identity Pair 1, Gen 02 corresponds to Same-Identity Pair 2, and so on.

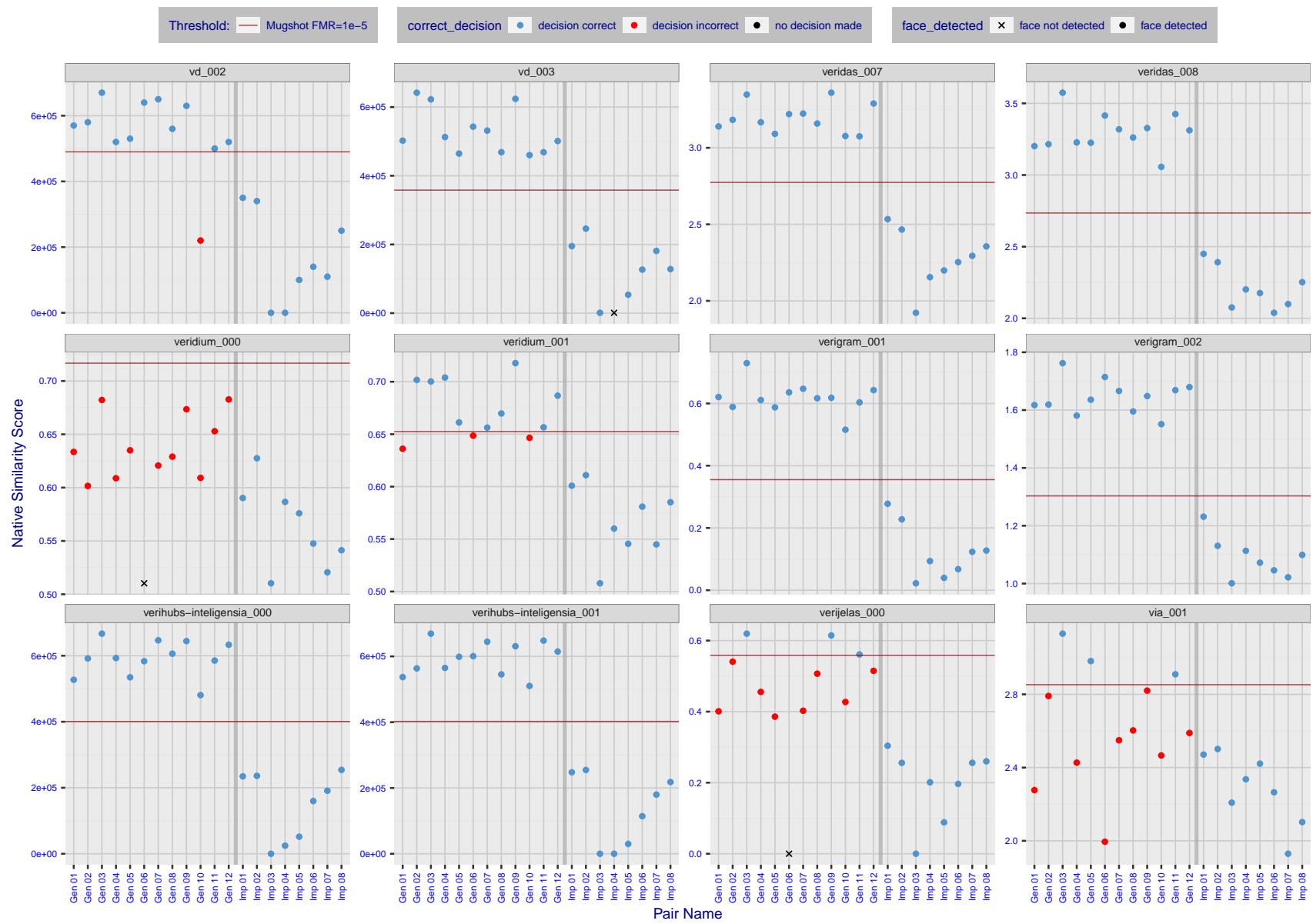


Figure 41: The figure shows algorithms' similarity scores for 12 genuine and 8 impostor image pairs used in a May 2018 paper by Phillips et al. ([1]). The threshold (red horizontal line) is a value calibrated to give $FMR = 0.0001$ on mugshot images. Points above the threshold correspond to pairs determined to be genuine, and points below the threshold correspond to pairs determined to be impostors. If the determined class (genuine or impostor) matches the real class, points will be blue; if not, red. An X represents face detection failure in either of the images in the pair. Note that the sample size ($n=20$) is small, and the figure may change substantially if larger or different sets are used. The images can be viewed on p. 13 of the Appendix, where Gen 01 corresponds to Same-Identity Pair 1, Gen 02 corresponds to Same-Identity Pair 2, and so on.

FNMR(T)
FMR(T)
"False non-match rate"
"False match rate"

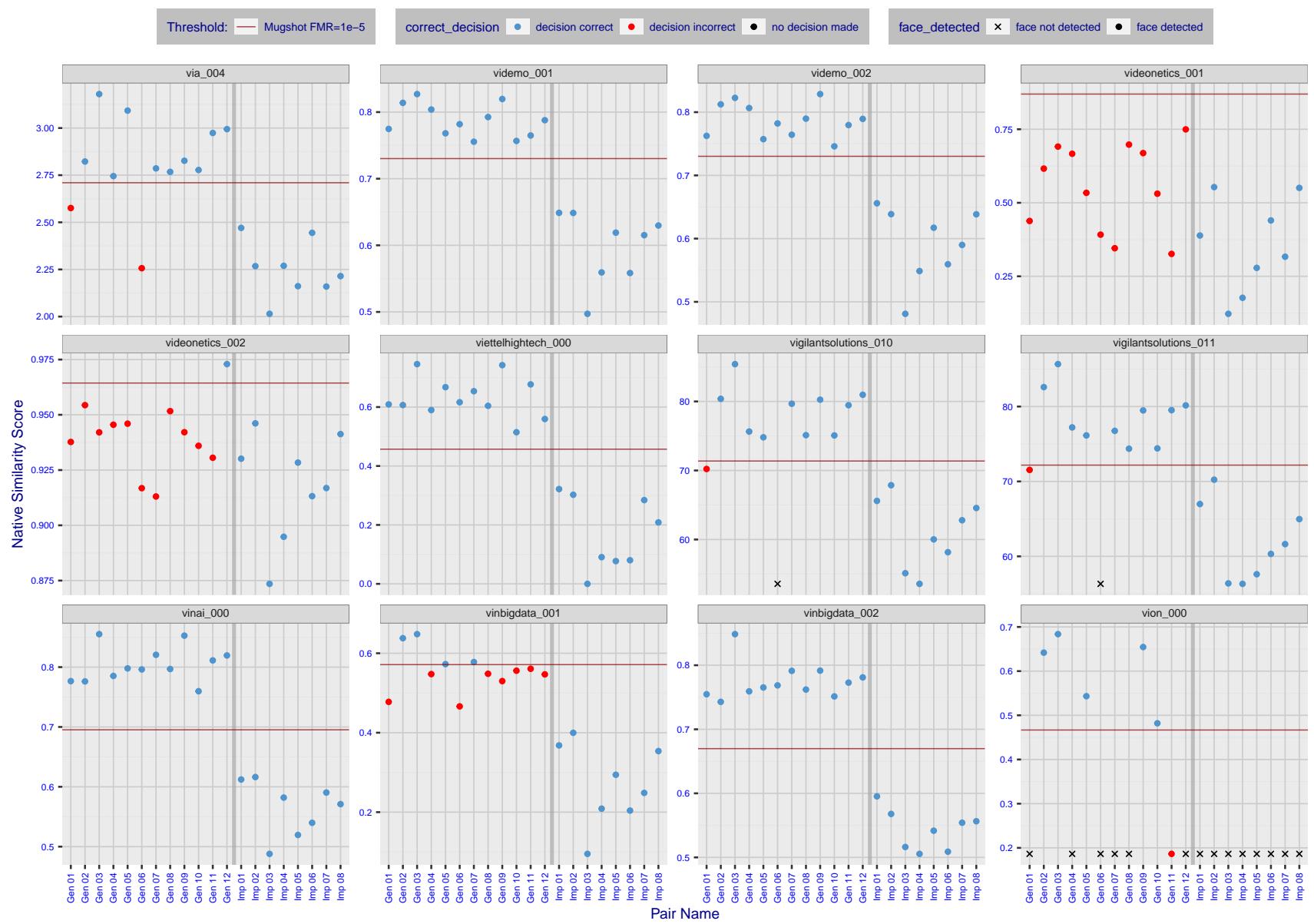


Figure 42: The figure shows algorithms' similarity scores for 12 genuine and 8 impostor image pairs used in a May 2018 paper by Phillips et al. ([1]). The threshold (red horizontal line) is a value calibrated to give $FMR = 0.0001$ on mugshot images. Points above the threshold correspond to pairs determined to be genuine, and points below the threshold correspond to pairs determined to be impostors. If the determined class (genuine or impostor) matches the real class, points will be blue; if not, red. An X represents face detection failure in either of the images in the pair. Note that the sample size ($n=20$) is small, and the figure may change substantially if larger or different sets are used. The images can be viewed on p. 13 of the Appendix, where Gen 01 corresponds to Same-Identity Pair 1, Gen 02 corresponds to Same-Identity Pair 2, and so on.

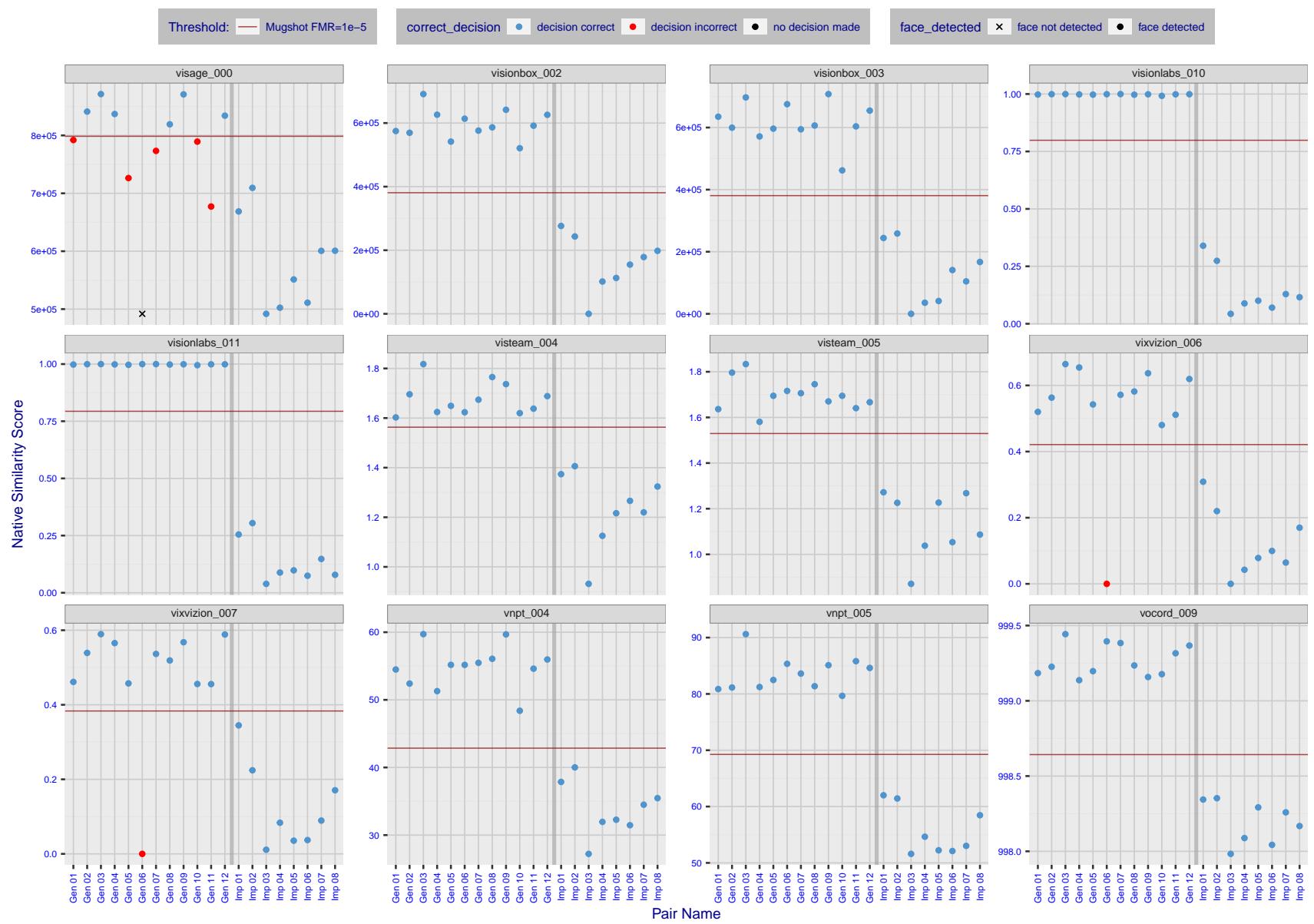


Figure 43: The figure shows algorithms' similarity scores for 12 genuine and 8 impostor image pairs used in a May 2018 paper by Phillips et al. ([1]). The threshold (red horizontal line) is a value calibrated to give $FMR = 0.0001$ on mugshot images. Points above the threshold correspond to pairs determined to be genuine, and points below the threshold correspond to pairs determined to be impostors. If the determined class (genuine or impostor) matches the real class, points will be blue; if not, red. An X represents face detection failure in either of the images in the pair. Note that the sample size ($n=20$) is small, and the figure may change substantially if larger or different sets are used. The images can be viewed on p. 13 of the Appendix, where Gen 01 corresponds to Same-Identity Pair 1, Gen 02 corresponds to Same-Identity Pair 2, and so on.

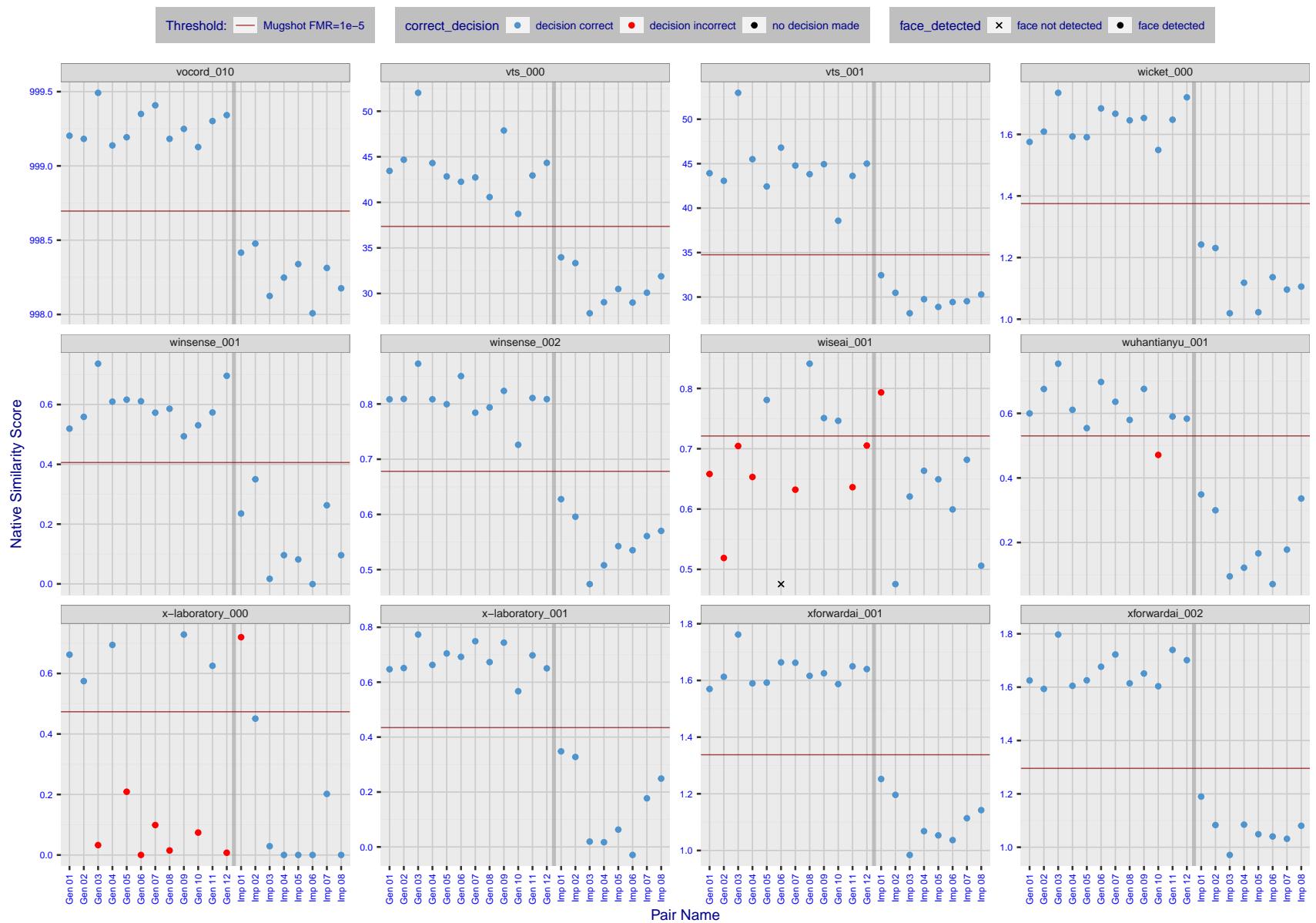


Figure 44: The figure shows algorithms' similarity scores for 12 genuine and 8 impostor image pairs used in a May 2018 paper by Phillips et al. ([1]). The threshold (red horizontal line) is a value calibrated to give $FMR = 0.0001$ on mugshot images. Points above the threshold correspond to pairs determined to be genuine, and points below the threshold correspond to pairs determined to be impostors. If the determined class (genuine or impostor) matches the real class, points will be blue; if not, red. An X represents face detection failure in either of the images in the pair. Note that the sample size ($n=20$) is small, and the figure may change substantially if larger or different sets are used. The images can be viewed on p. 13 of the Appendix, where Gen 01 corresponds to Same-Identity Pair 1, Gen 02 corresponds to Same-Identity Pair 2, and so on.

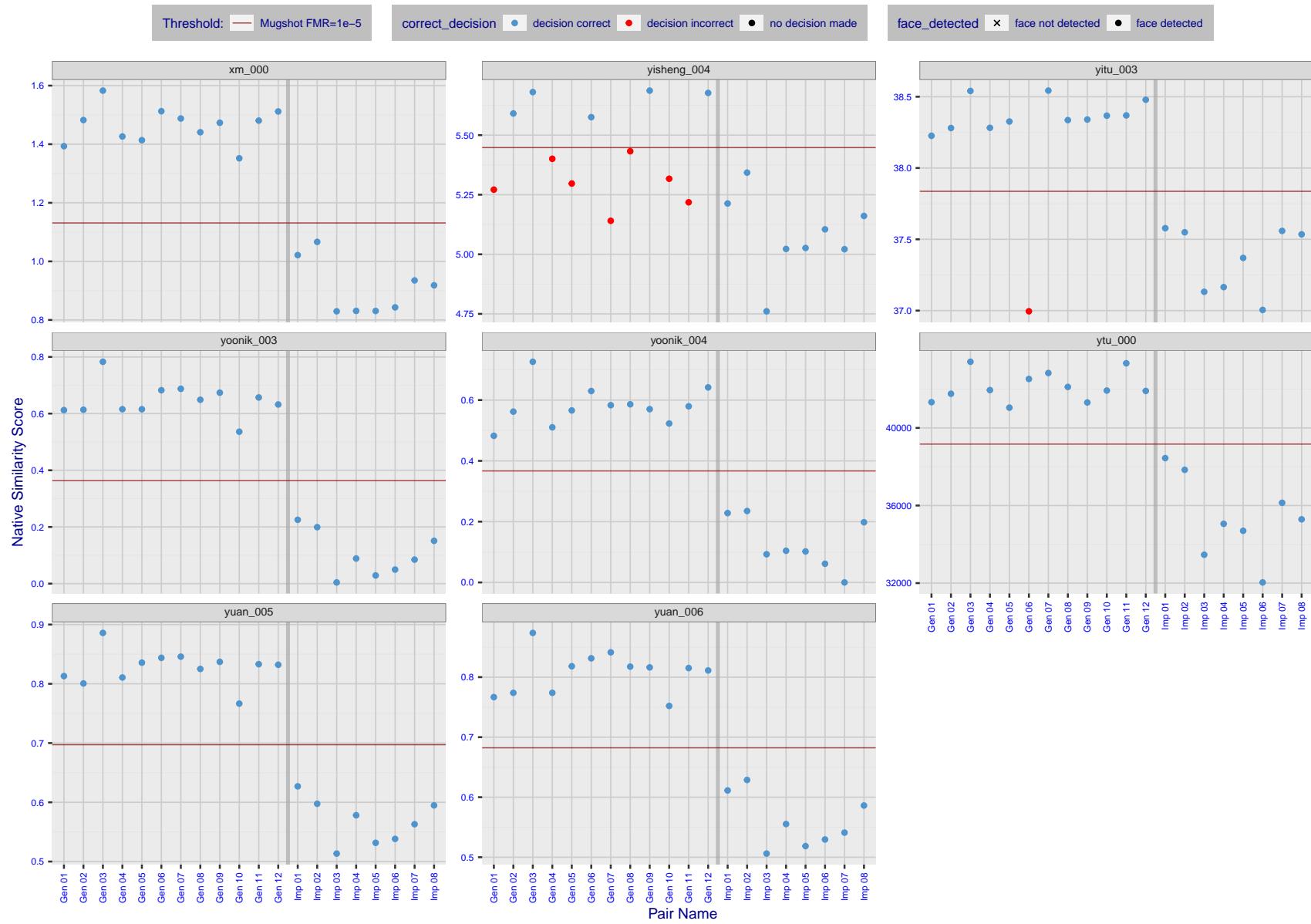


Figure 45: The figure shows algorithms' similarity scores for 12 genuine and 8 impostor image pairs used in a May 2018 paper by Phillips et al. ([1]). The threshold (red horizontal line) is a value calibrated to give $FMR = 0.0001$ on mugshot images. Points above the threshold correspond to pairs determined to be genuine, and points below the threshold correspond to pairs determined to be impostors. If the determined class (genuine or impostor) matches the real class, points will be blue; if not, red. An X represents face detection failure in either of the images in the pair. Note that the sample size ($n=20$) is small, and the figure may change substantially if larger or different sets are used. The images can be viewed on p. 13 of the Appendix, where Gen 01 corresponds to Same-Identity Pair 1, Gen 02 corresponds to Same-Identity Pair 2, and so on.

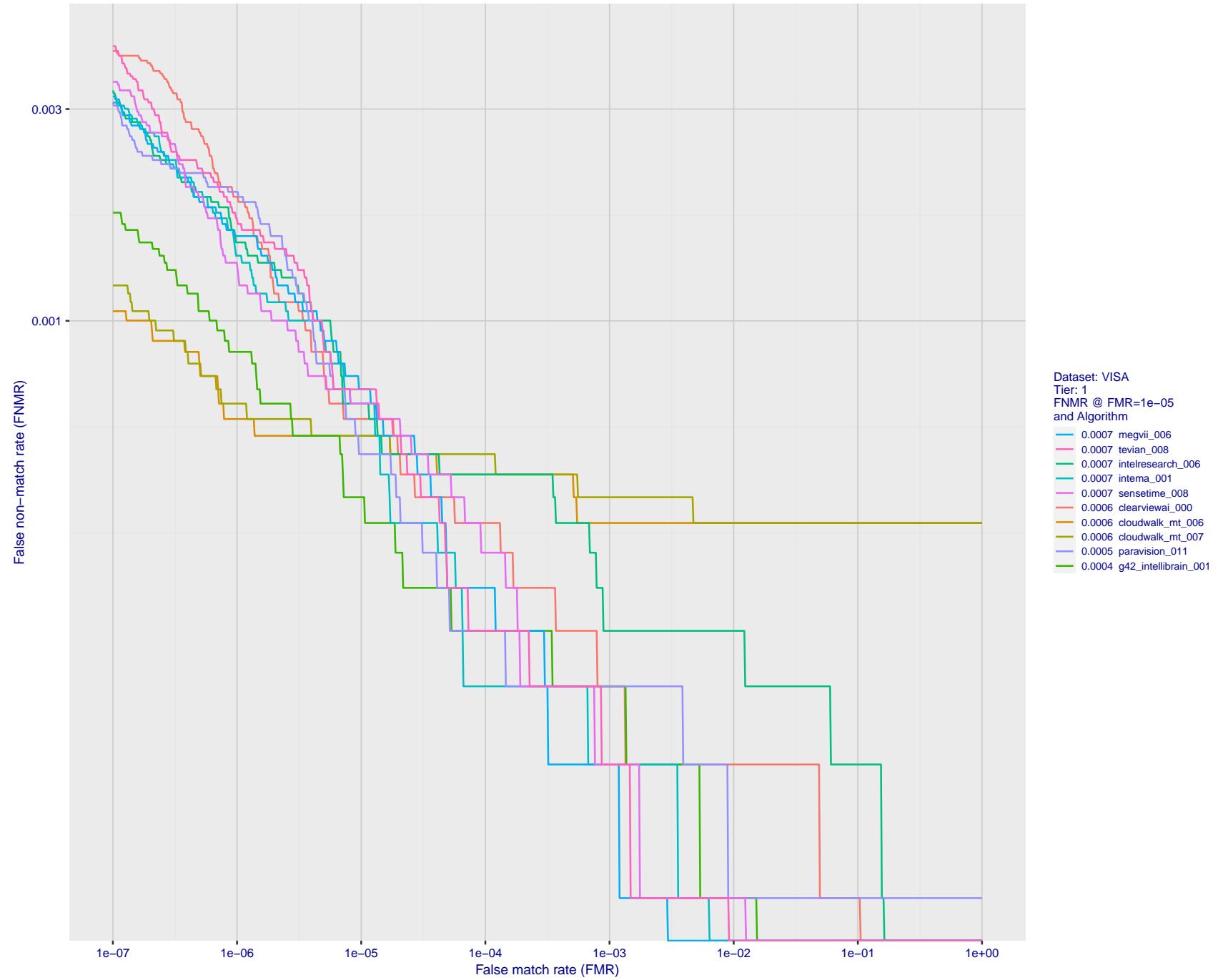


Figure 46: For the visa images, detection error tradeoff (DET) characteristics showing false non-match rate vs. false match rate plotted parametrically on threshold, T . The scales are logarithmic in order to show many decades of FMR.

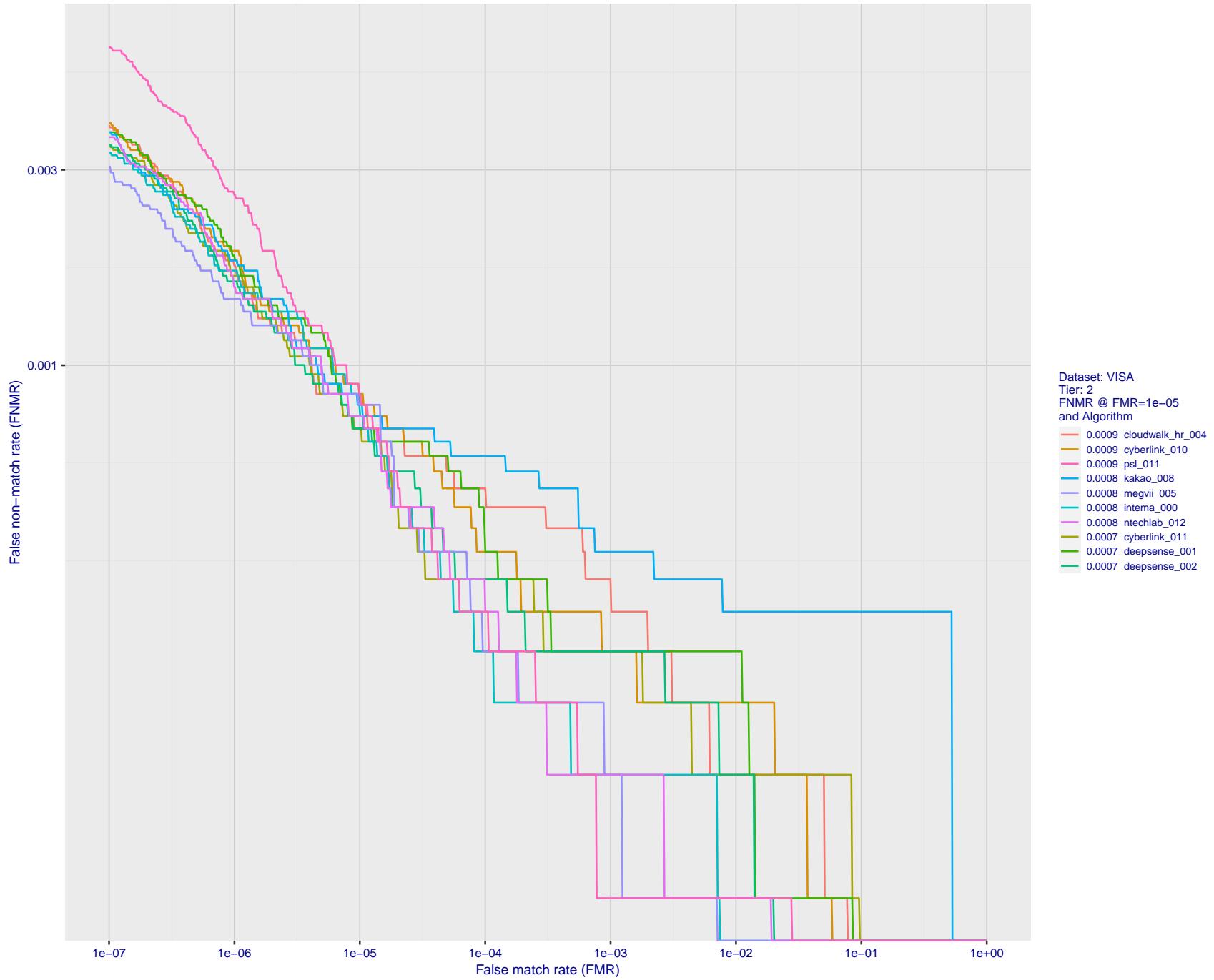


Figure 47: For the visa images, detection error tradeoff (DET) characteristics showing false non-match rate vs. false match rate plotted parametrically on threshold, T . The scales are logarithmic in order to show many decades of FMR.

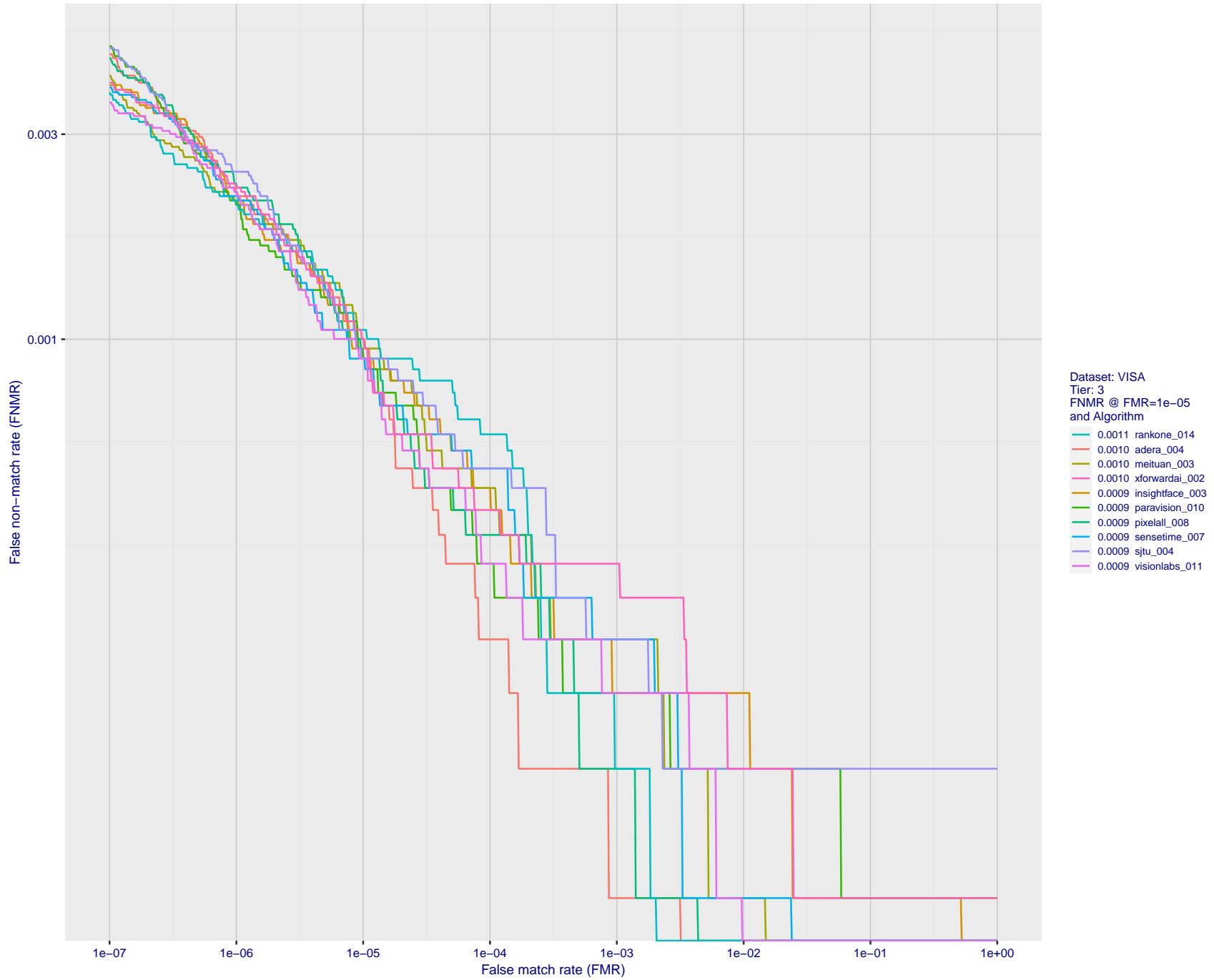


Figure 48: For the visa images, detection error tradeoff (DET) characteristics showing false non-match rate vs. false match rate plotted parametrically on threshold, T . The scales are logarithmic in order to show many decades of FMR.

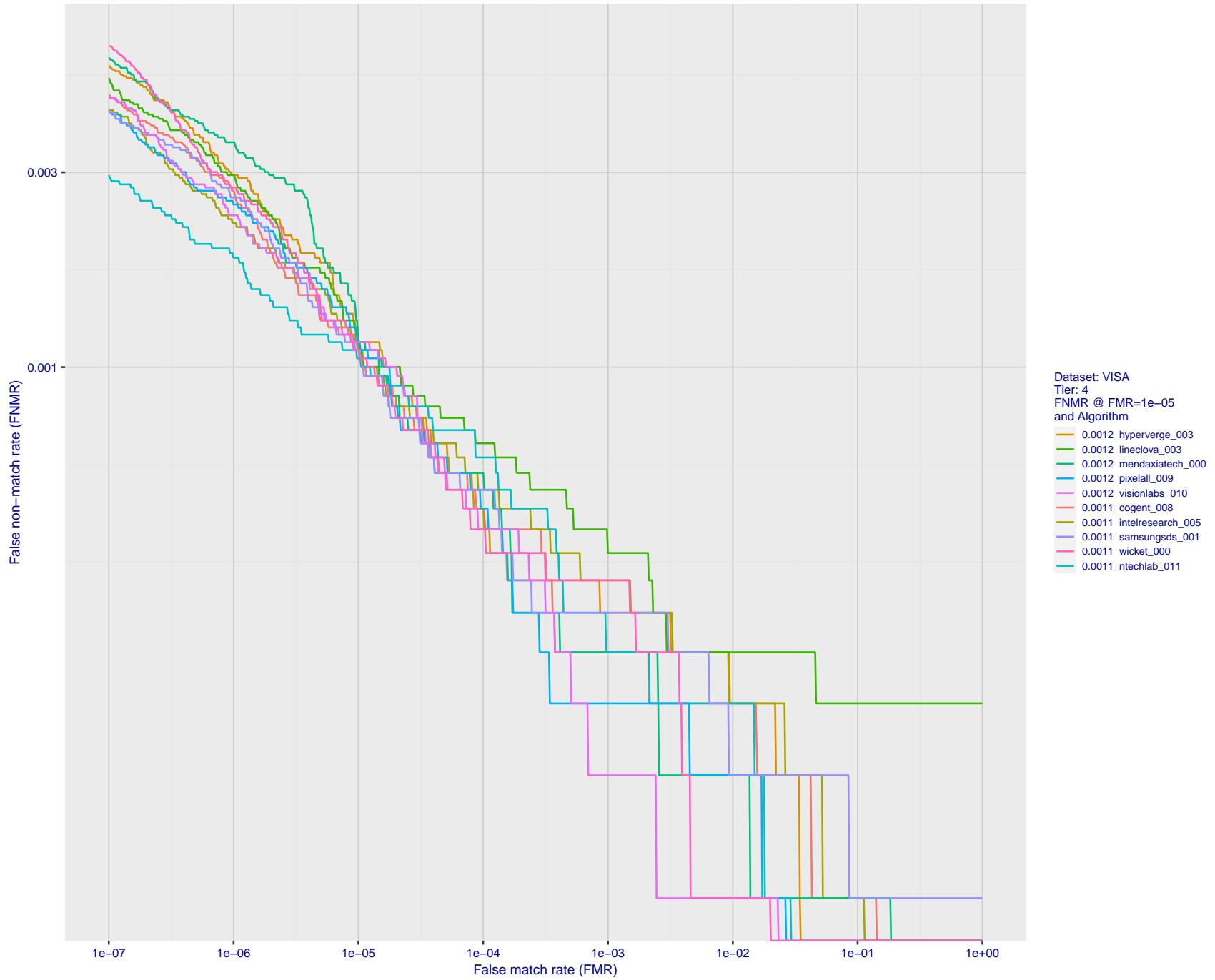


Figure 49: For the visa images, detection error tradeoff (DET) characteristics showing false non-match rate vs. false match rate plotted parametrically on threshold, T . The scales are logarithmic in order to show many decades of FMR.

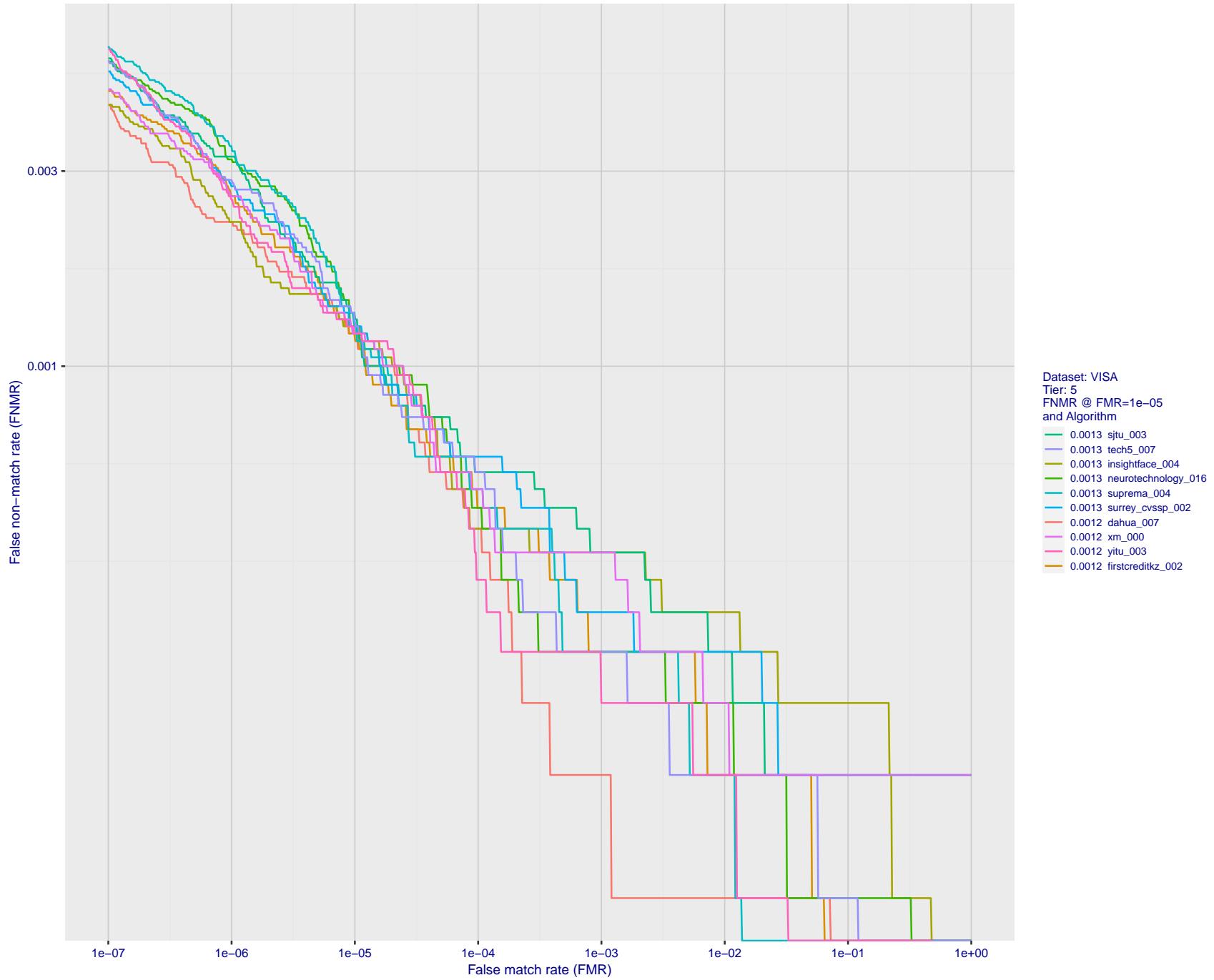


Figure 50: For the visa images, detection error tradeoff (DET) characteristics showing false non-match rate vs. false match rate plotted parametrically on threshold, T . The scales are logarithmic in order to show many decades of FMR.

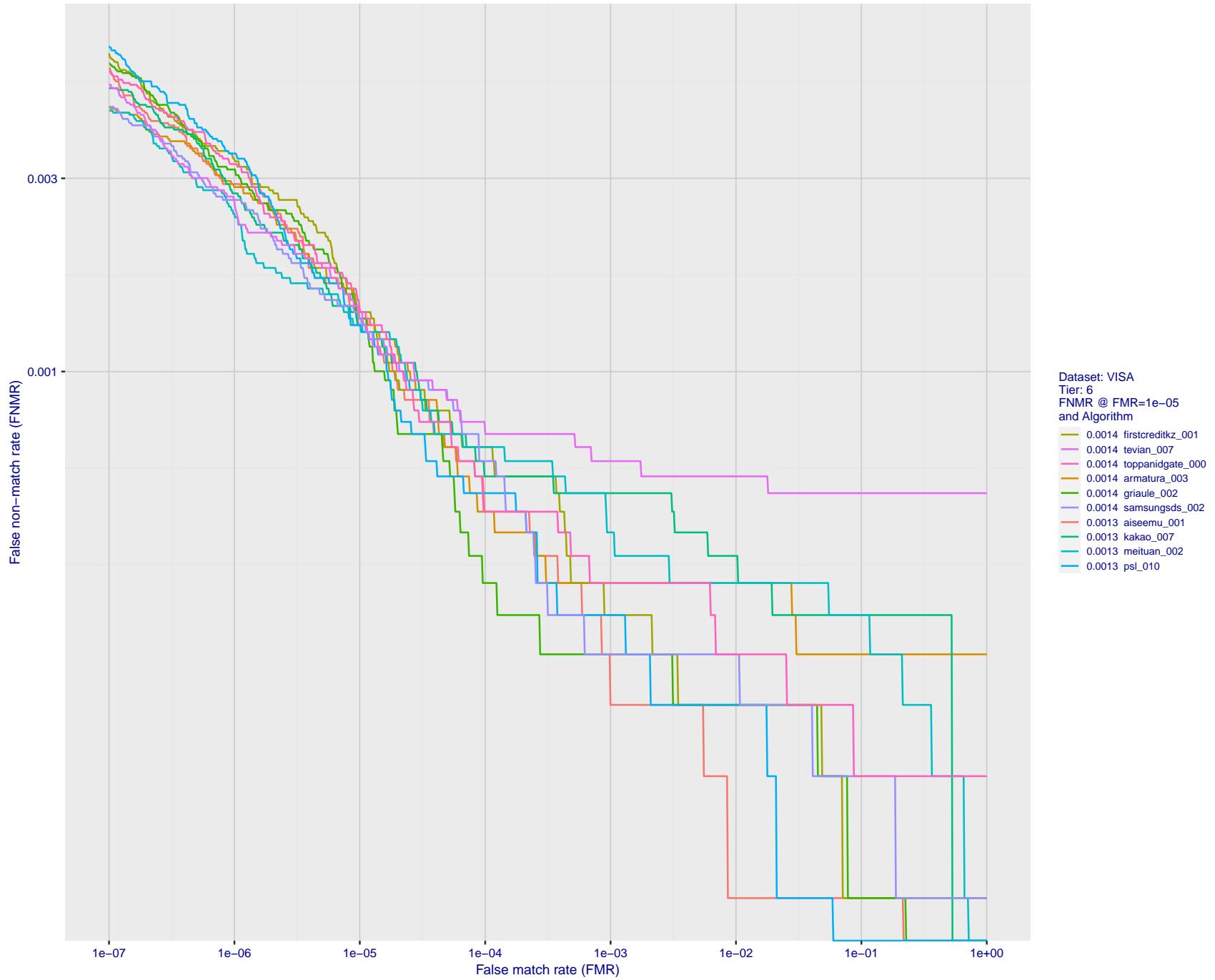


Figure 51: For the visa images, detection error tradeoff (DET) characteristics showing false non-match rate vs. false match rate plotted parametrically on threshold, T . The scales are logarithmic in order to show many decades of FMR.

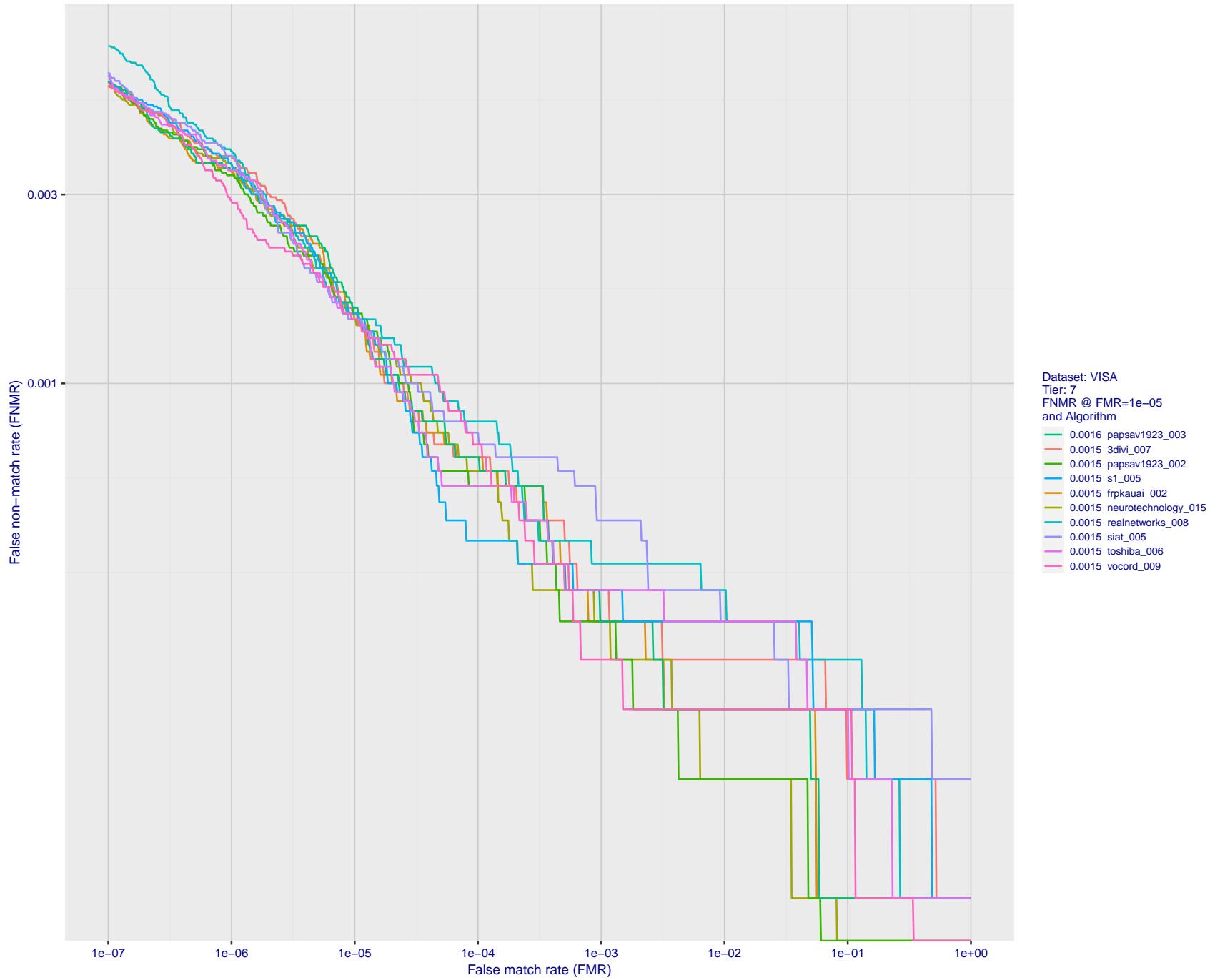


Figure 52: For the visa images, detection error tradeoff (DET) characteristics showing false non-match rate vs. false match rate plotted parametrically on threshold, T . The scales are logarithmic in order to show many decades of FMR.

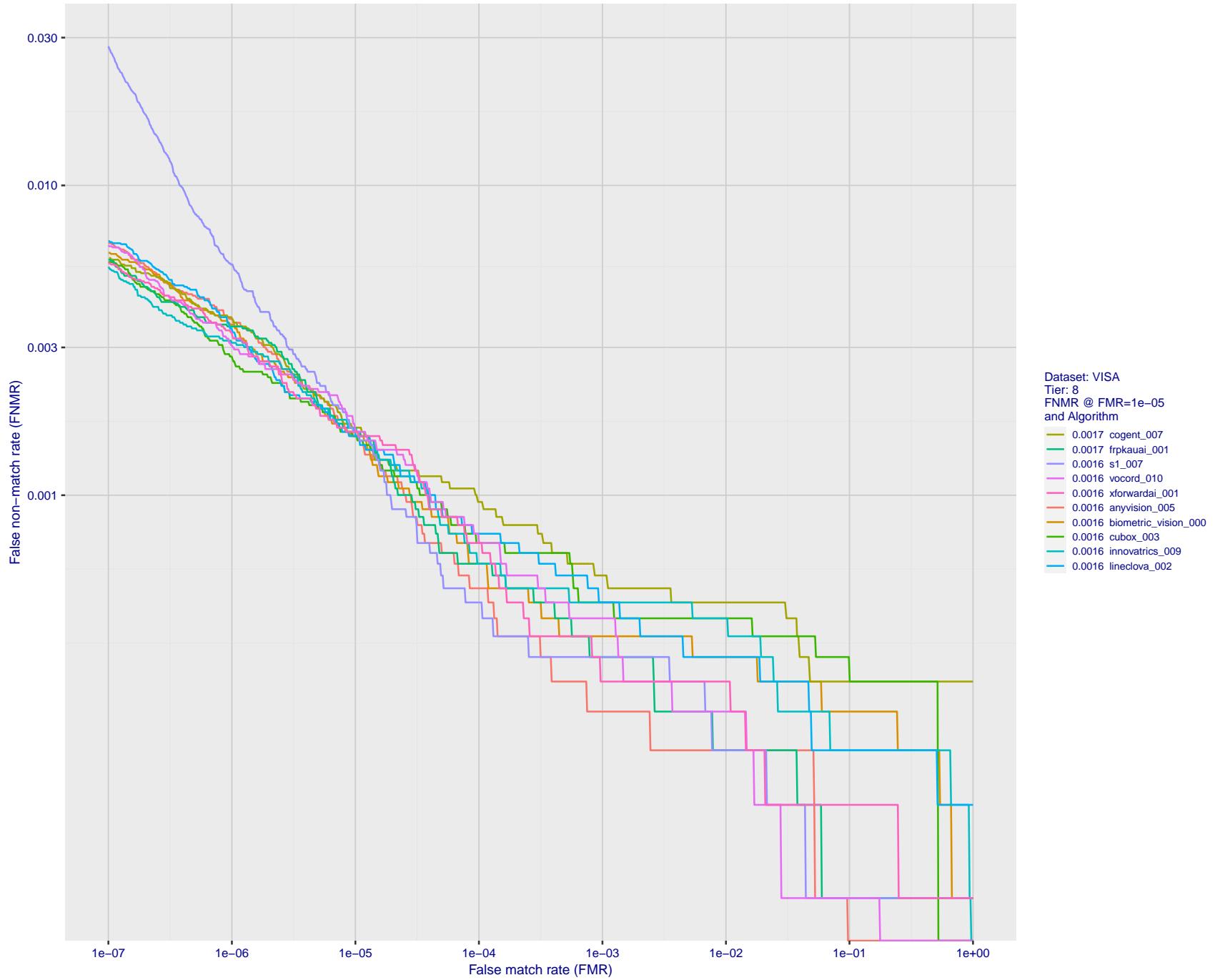


Figure 53: For the visa images, detection error tradeoff (DET) characteristics showing false non-match rate vs. false match rate plotted parametrically on threshold, T . The scales are logarithmic in order to show many decades of FMR.

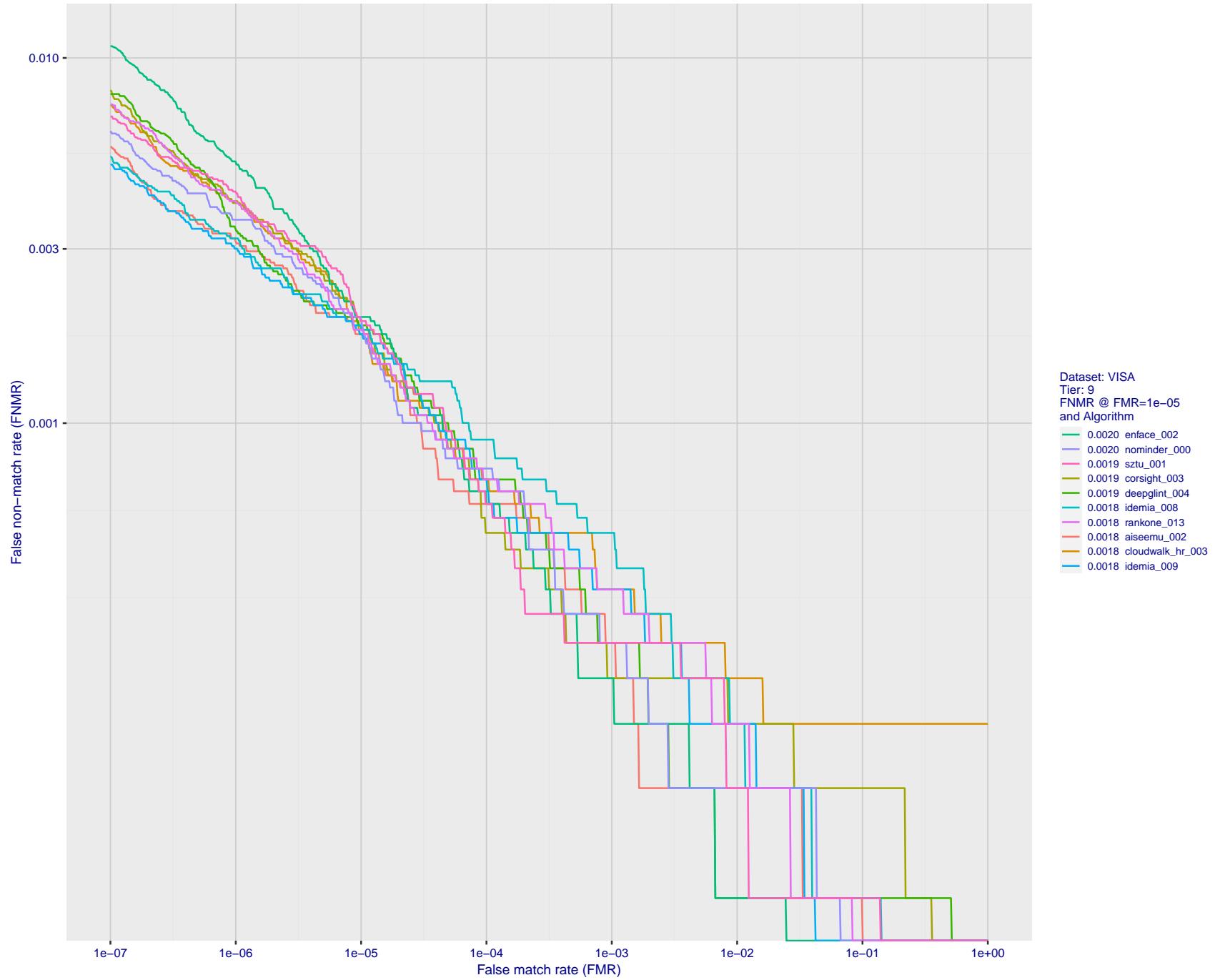


Figure 54: For the visa images, detection error tradeoff (DET) characteristics showing false non-match rate vs. false match rate plotted parametrically on threshold, T . The scales are logarithmic in order to show many decades of FMR.

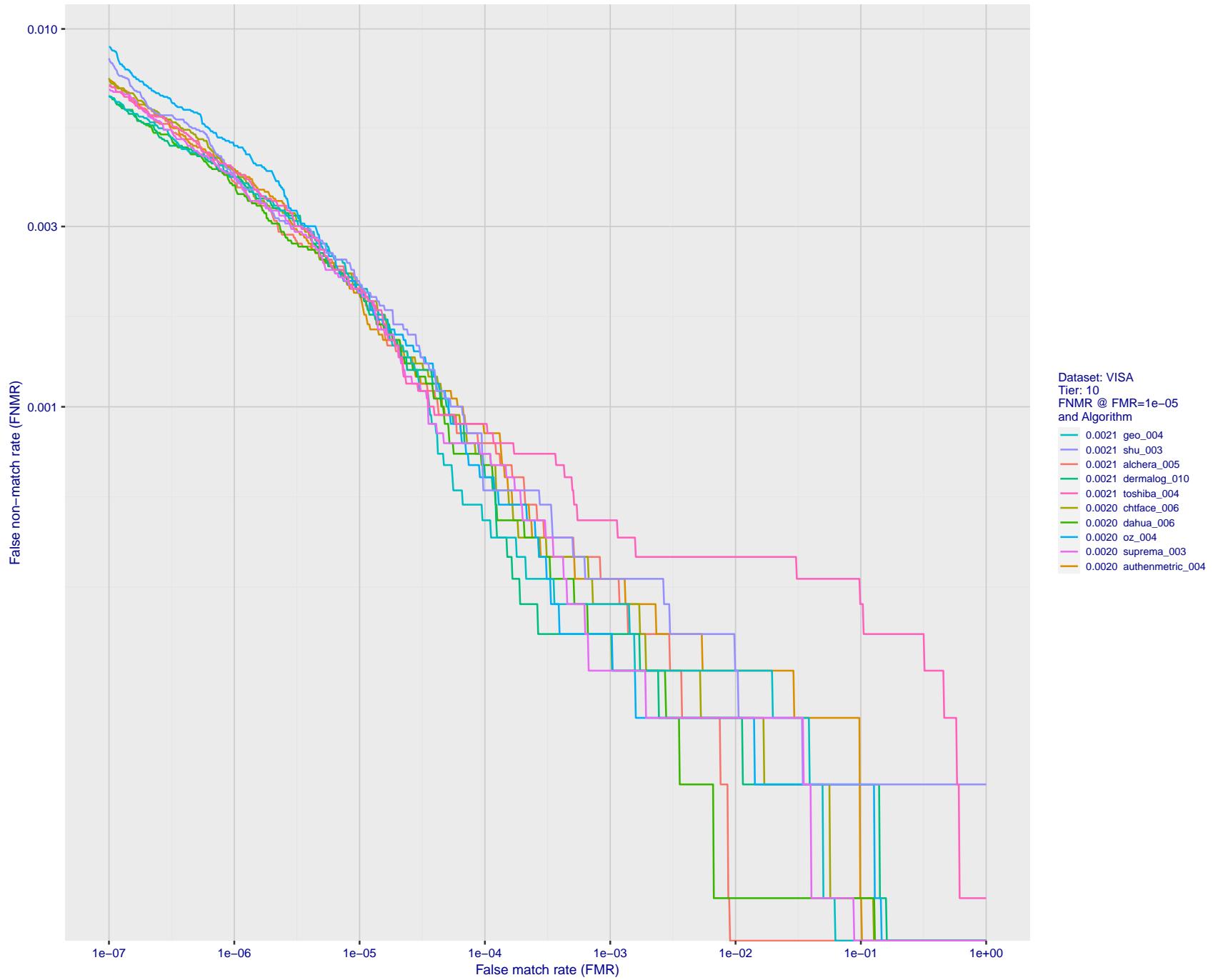


Figure 55: For the visa images, detection error tradeoff (DET) characteristics showing false non-match rate vs. false match rate plotted parametrically on threshold, T . The scales are logarithmic in order to show many decades of FMR.

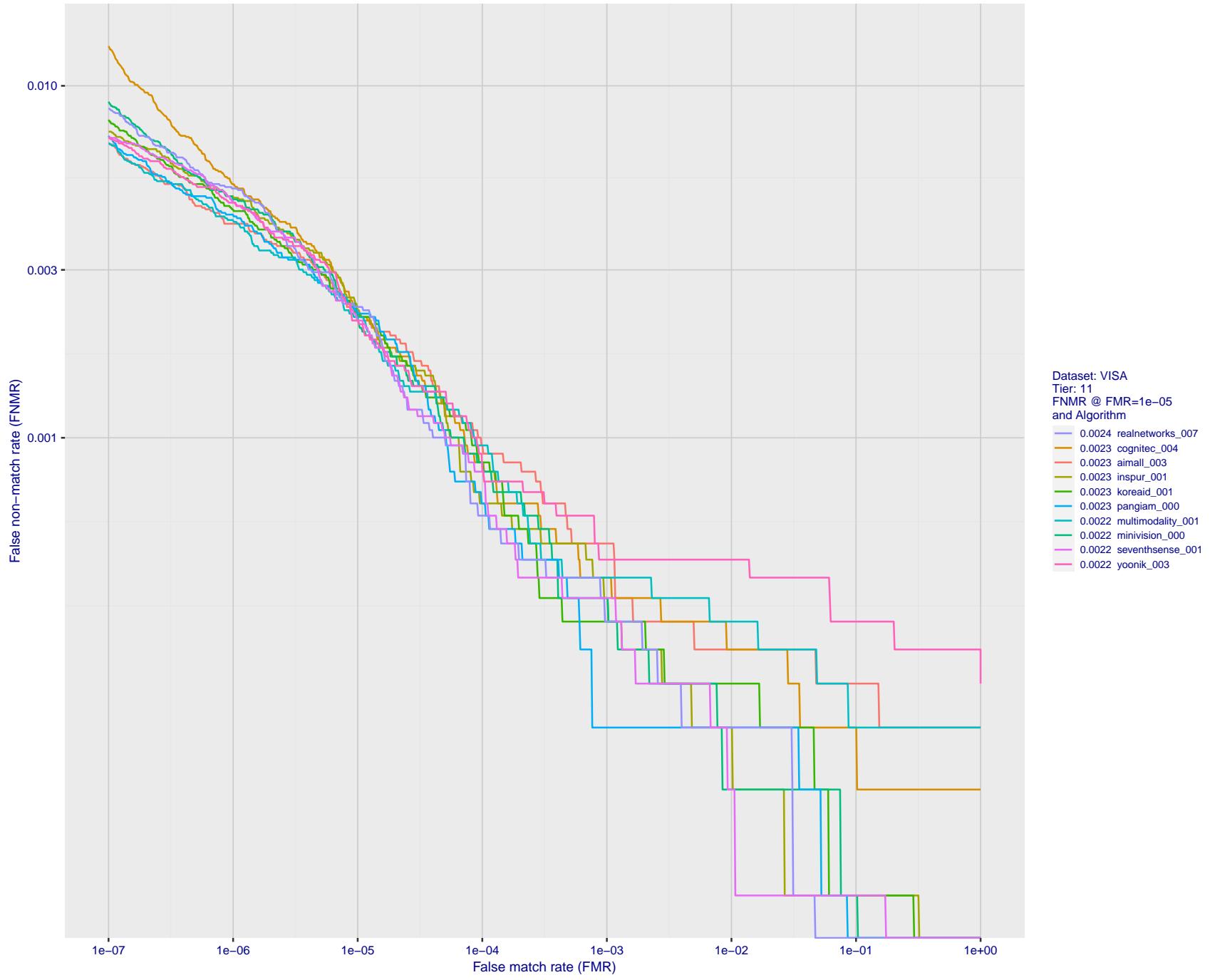


Figure 56: For the visa images, detection error tradeoff (DET) characteristics showing false non-match rate vs. false match rate plotted parametrically on threshold, T . The scales are logarithmic in order to show many decades of FMR.

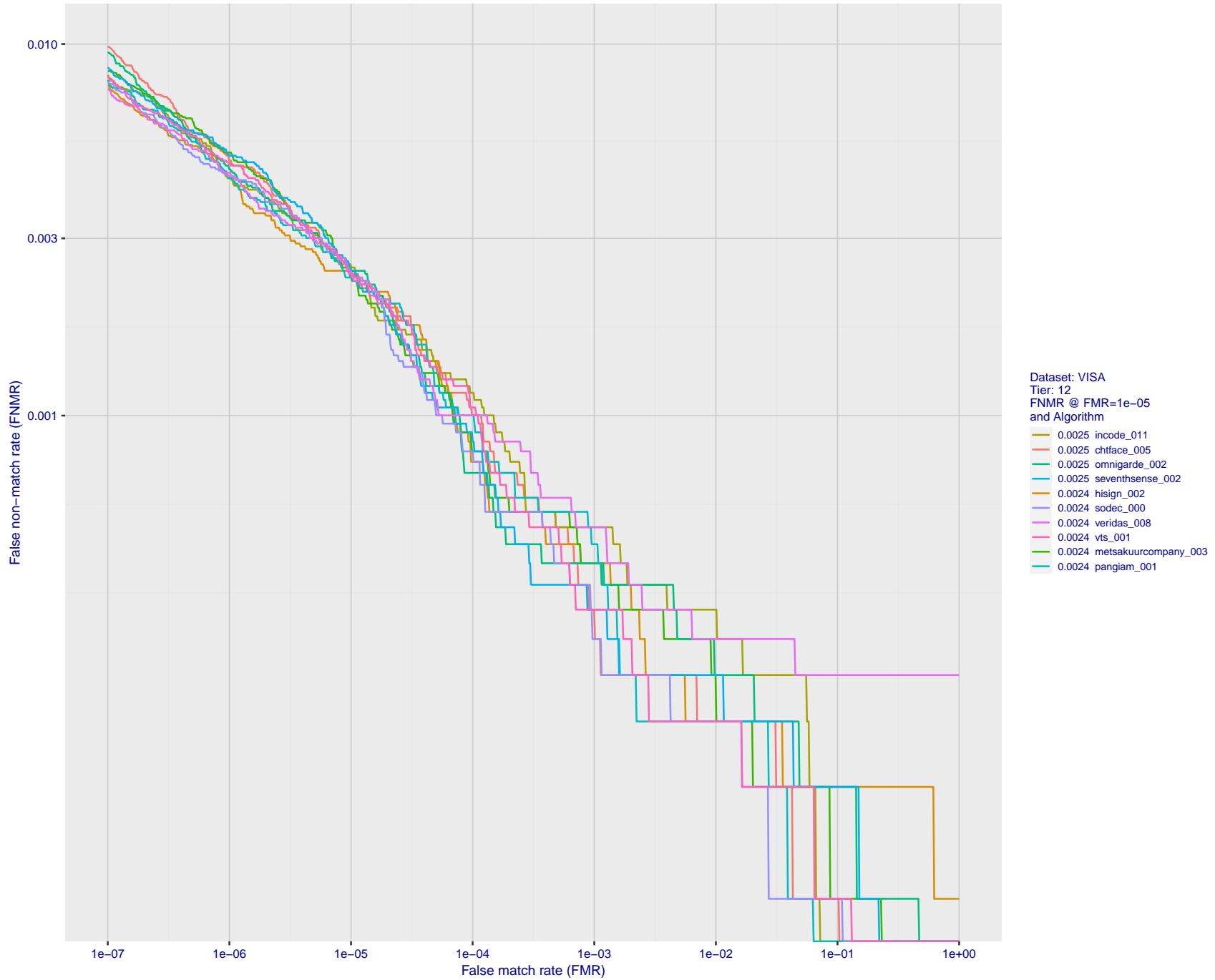


Figure 57: For the visa images, detection error tradeoff (DET) characteristics showing false non-match rate vs. false match rate plotted parametrically on threshold, T . The scales are logarithmic in order to show many decades of FMR.

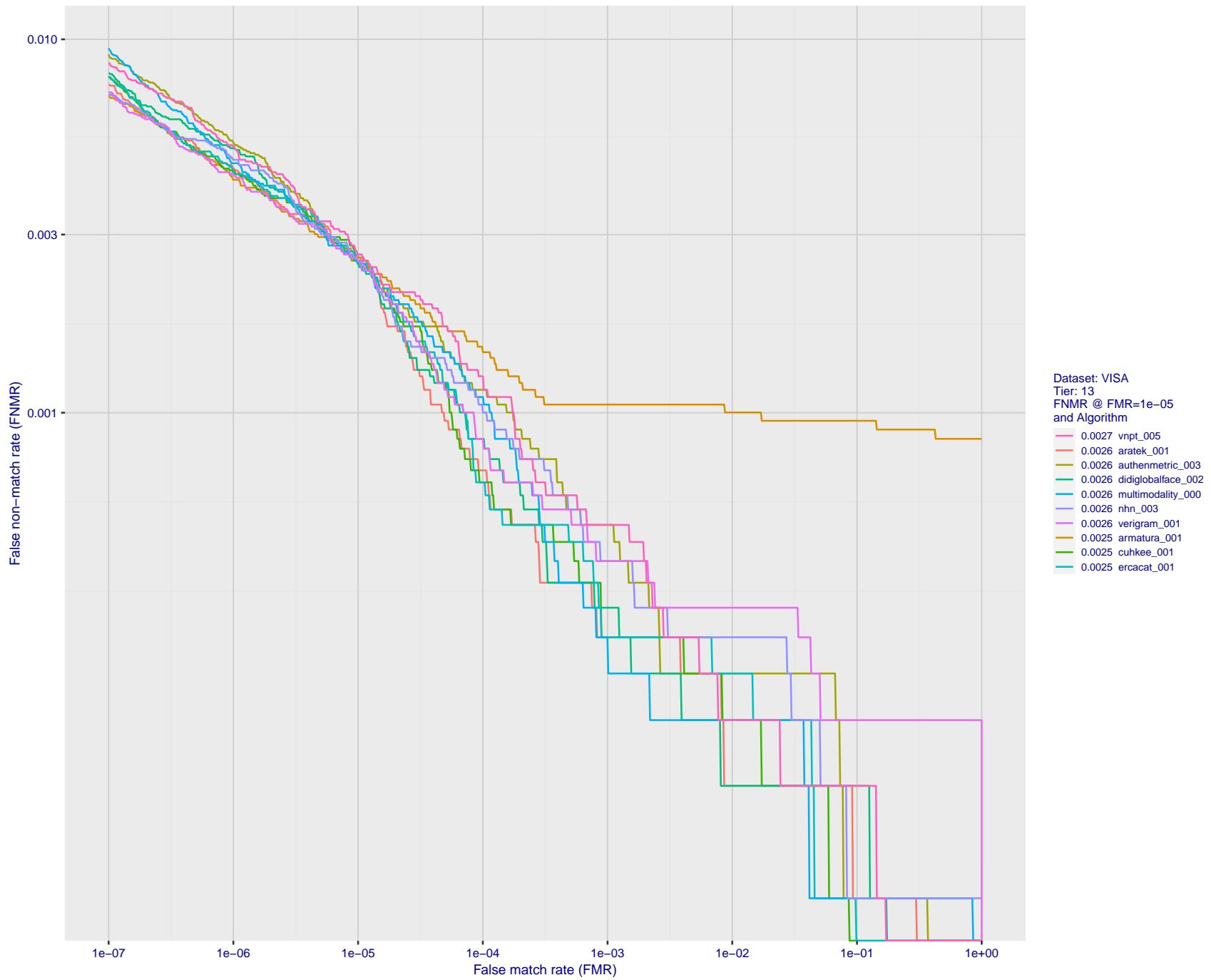


Figure 58: For the visa images, detection error tradeoff (DET) characteristics showing false non-match rate vs. false match rate plotted parametrically on threshold, T . The scales are logarithmic in order to show many decades of FMR.

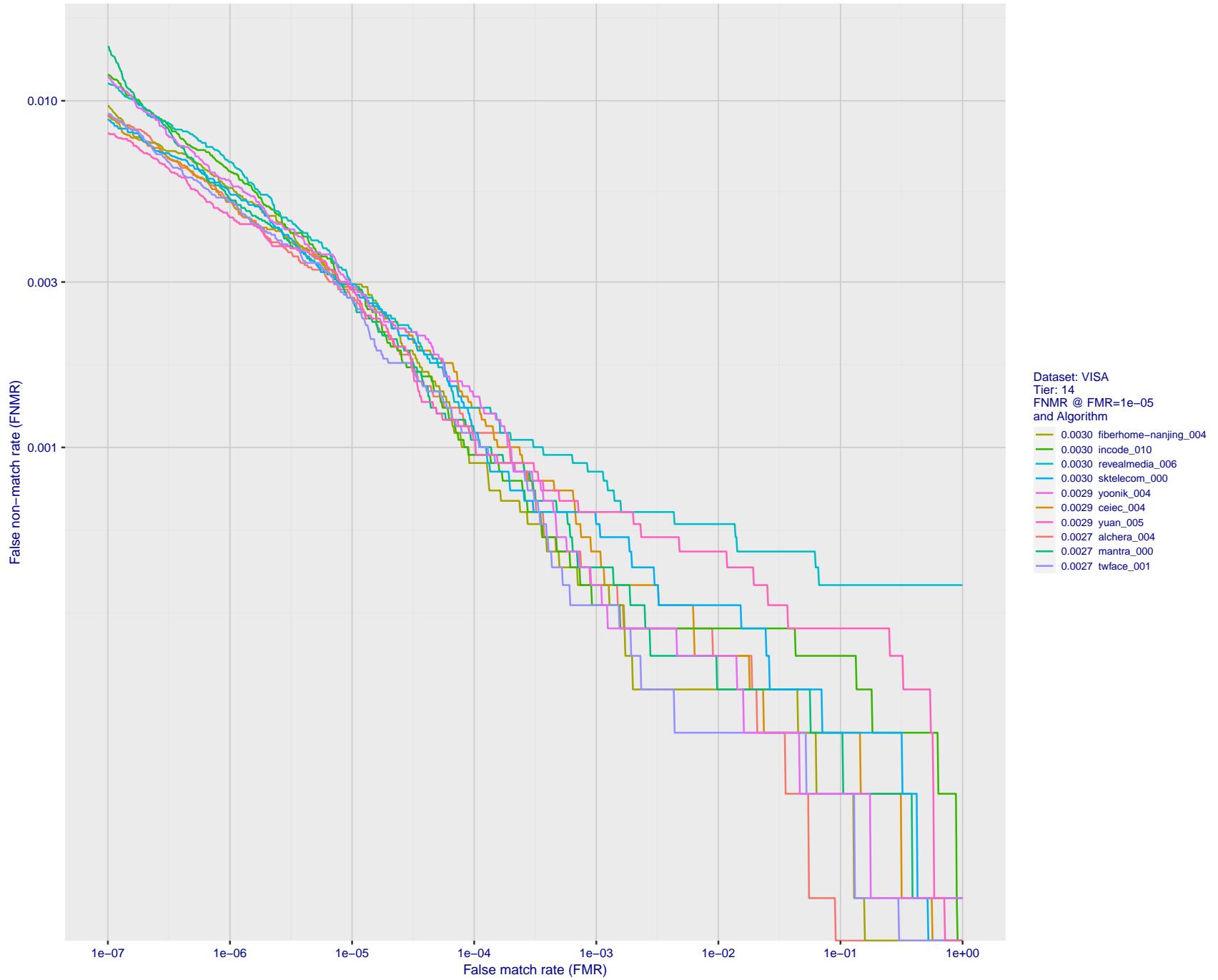


Figure 59: For the visa images, detection error tradeoff (DET) characteristics showing false non-match rate vs. false match rate plotted parametrically on threshold, T . The scales are logarithmic in order to show many decades of FMR.

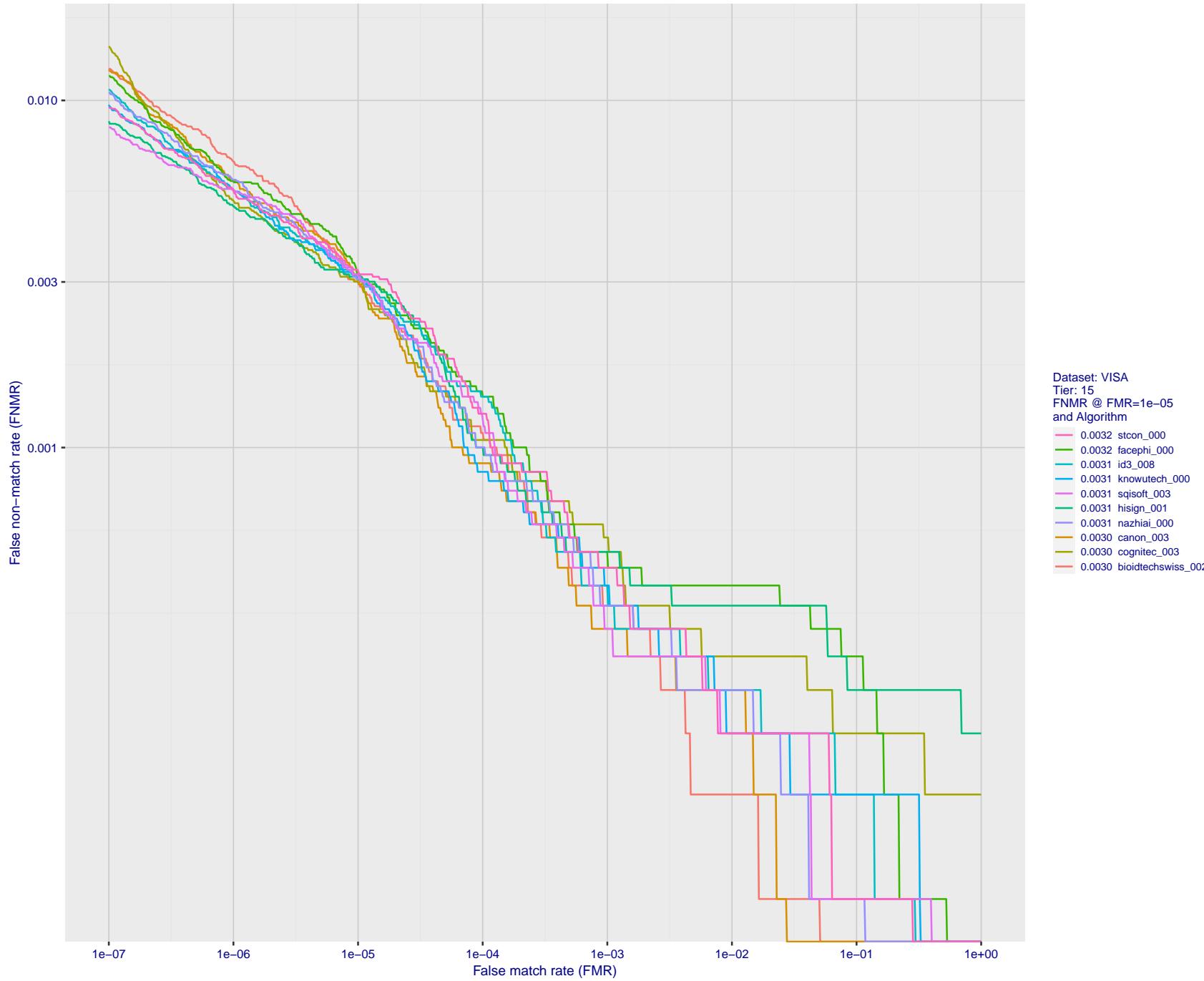


Figure 60: For the visa images, detection error tradeoff (DET) characteristics showing false non-match rate vs. false match rate plotted parametrically on threshold, T . The scales are logarithmic in order to show many decades of FMR.

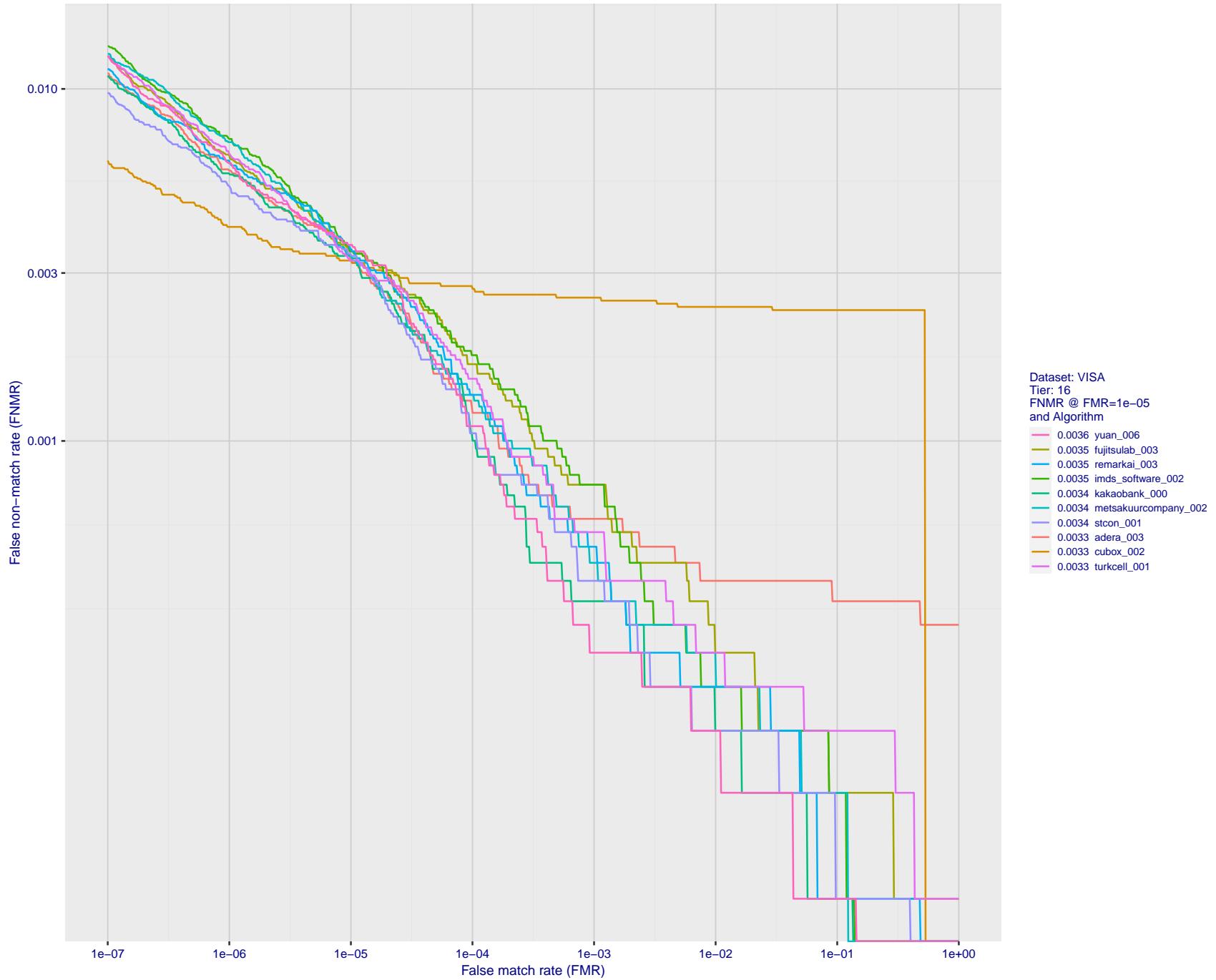


Figure 61: For the visa images, detection error tradeoff (DET) characteristics showing false non-match rate vs. false match rate plotted parametrically on threshold, T . The scales are logarithmic in order to show many decades of FMR.

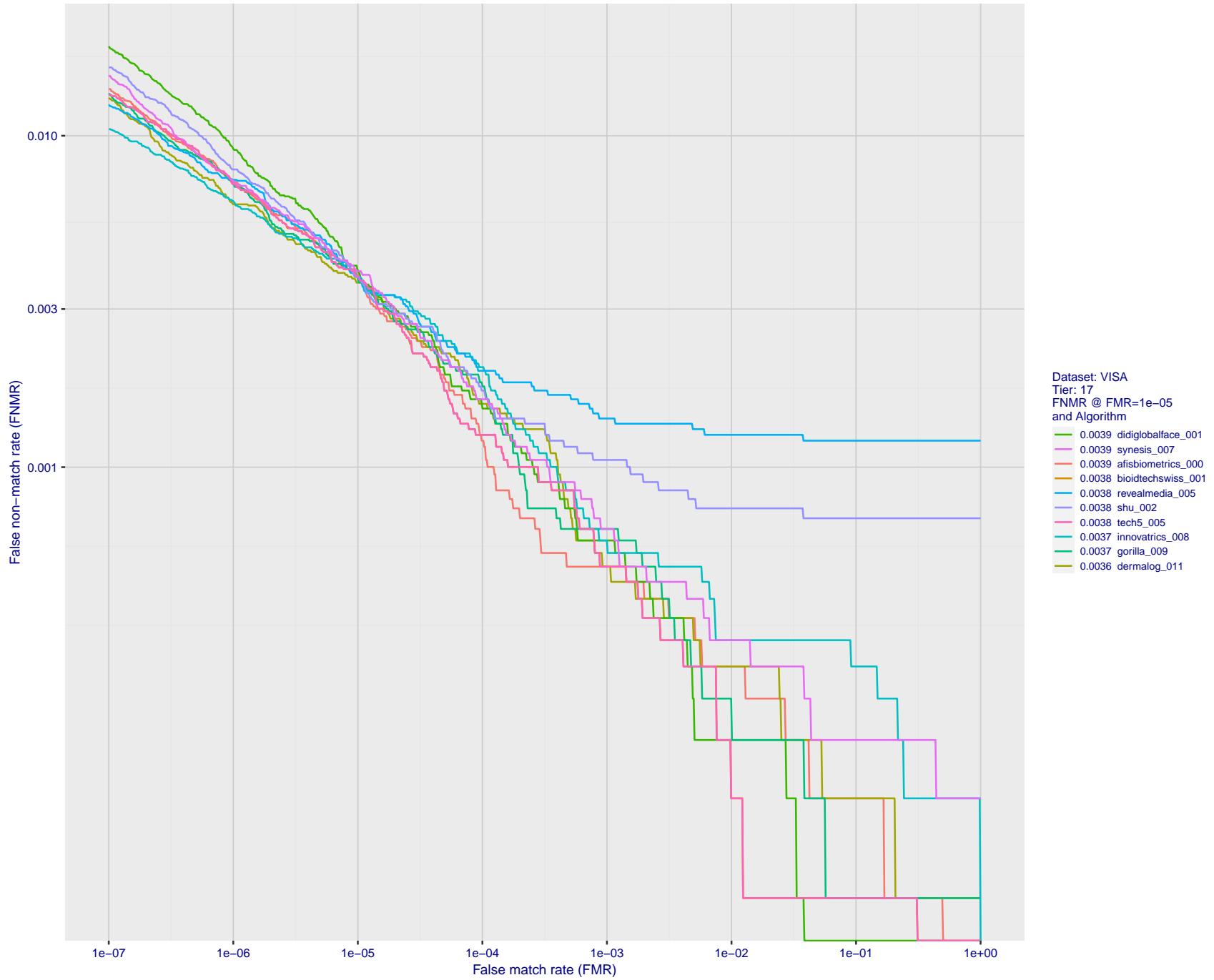


Figure 62: For the visa images, detection error tradeoff (DET) characteristics showing false non-match rate vs. false match rate plotted parametrically on threshold, T . The scales are logarithmic in order to show many decades of FMR.

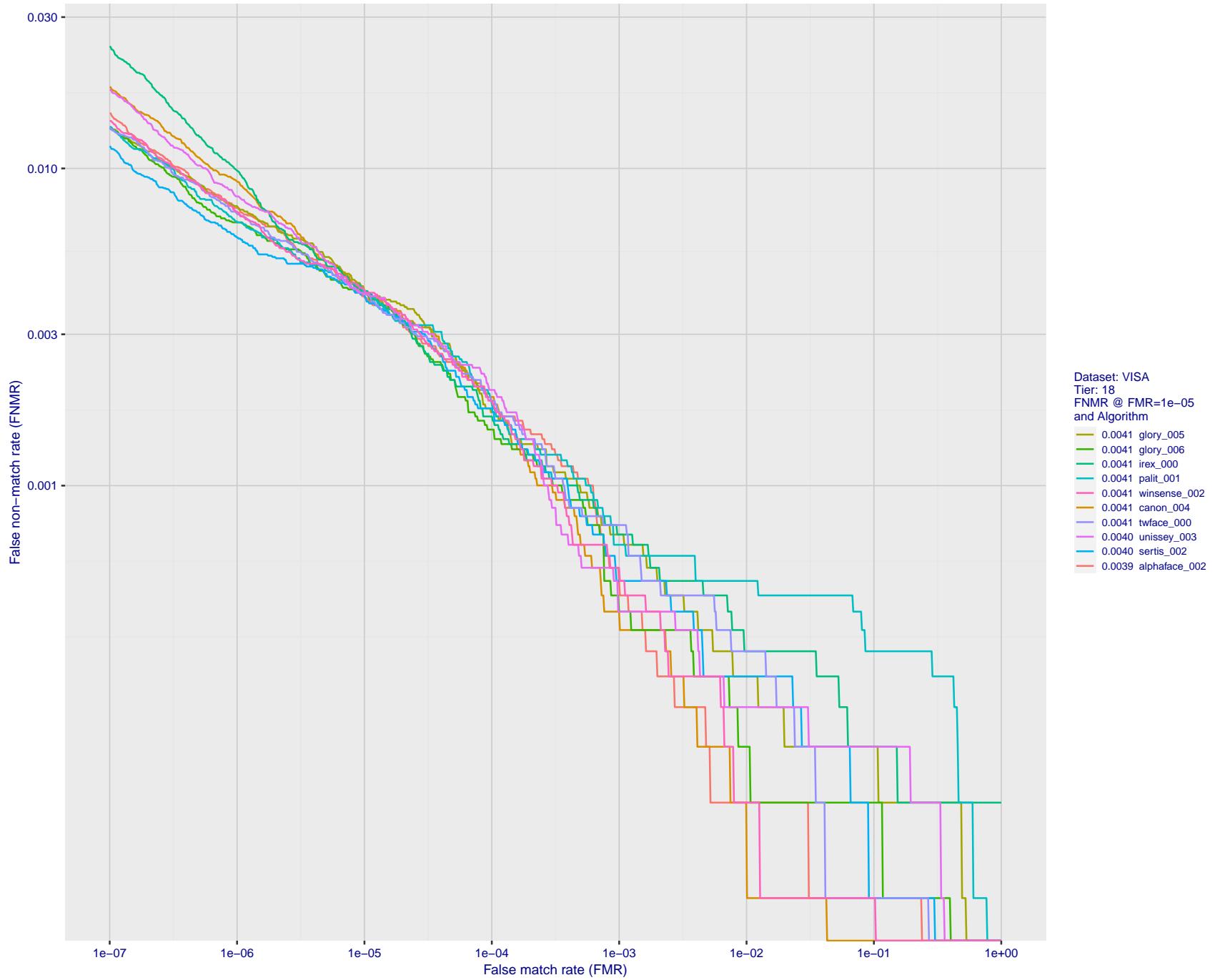


Figure 63: For the visa images, detection error tradeoff (DET) characteristics showing false non-match rate vs. false match rate plotted parametrically on threshold, T . The scales are logarithmic in order to show many decades of FMR.

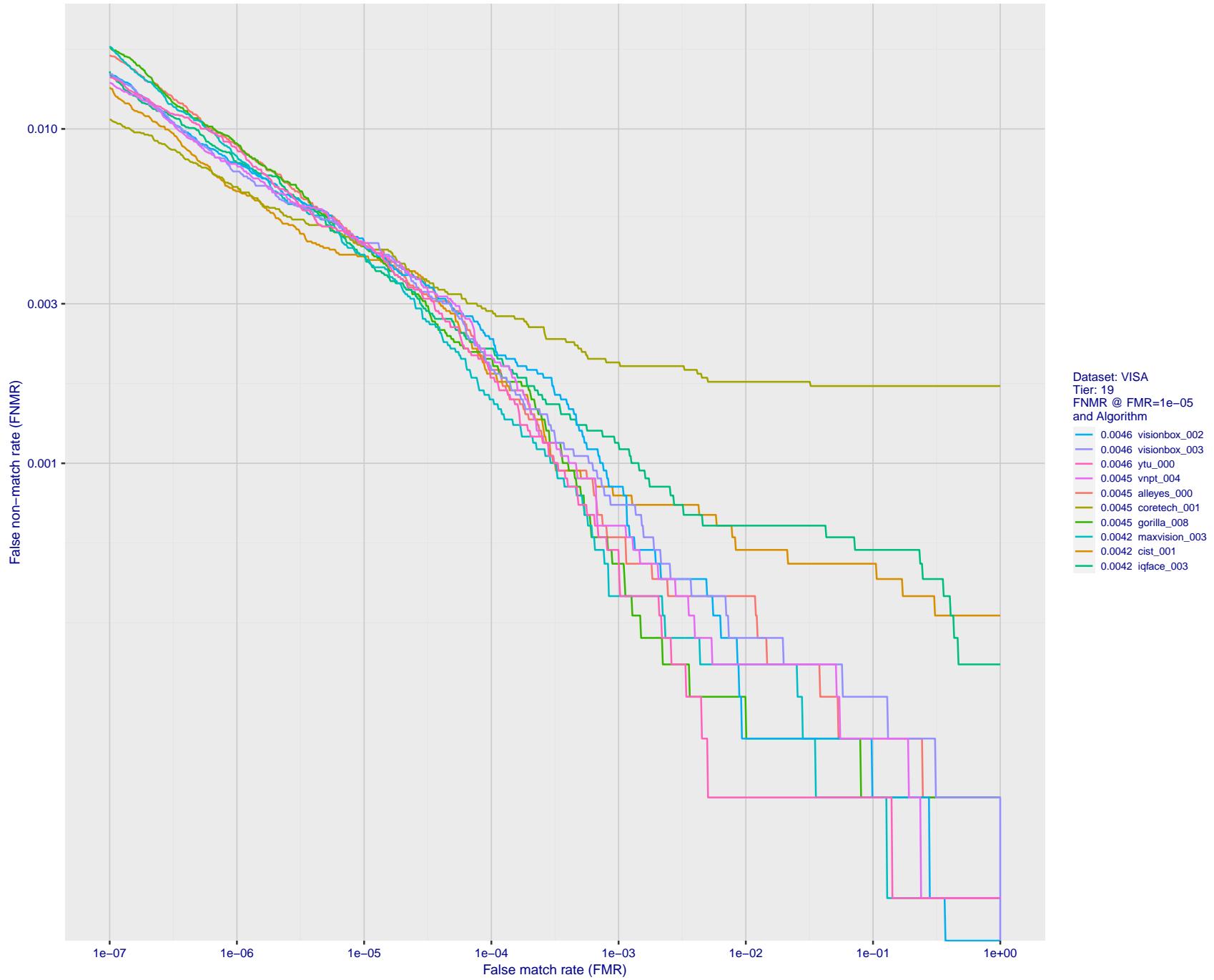


Figure 64: For the visa images, detection error tradeoff (DET) characteristics showing false non-match rate vs. false match rate plotted parametrically on threshold, T . The scales are logarithmic in order to show many decades of FMR.

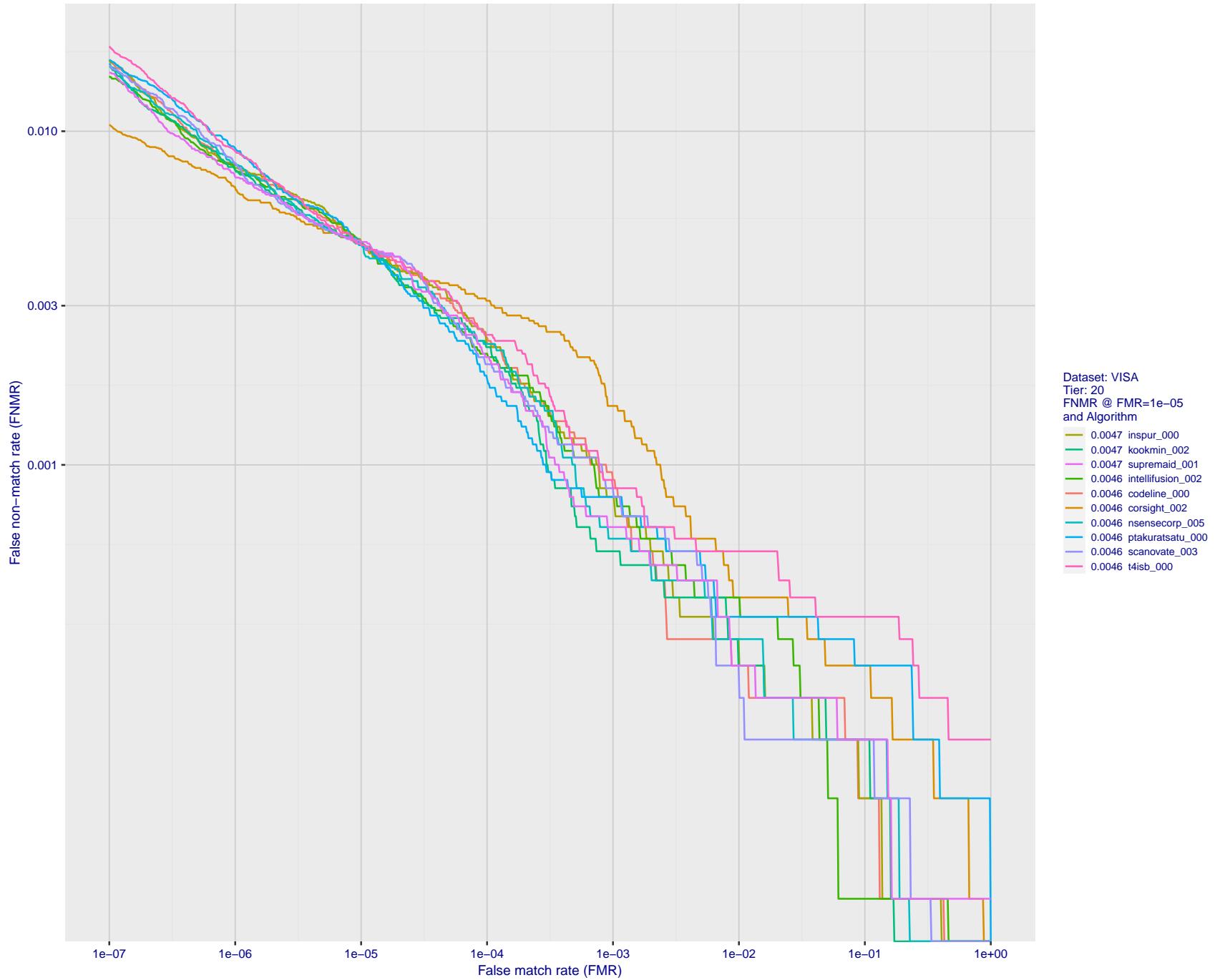


Figure 65: For the visa images, detection error tradeoff (DET) characteristics showing false non-match rate vs. false match rate plotted parametrically on threshold, T . The scales are logarithmic in order to show many decades of FMR.

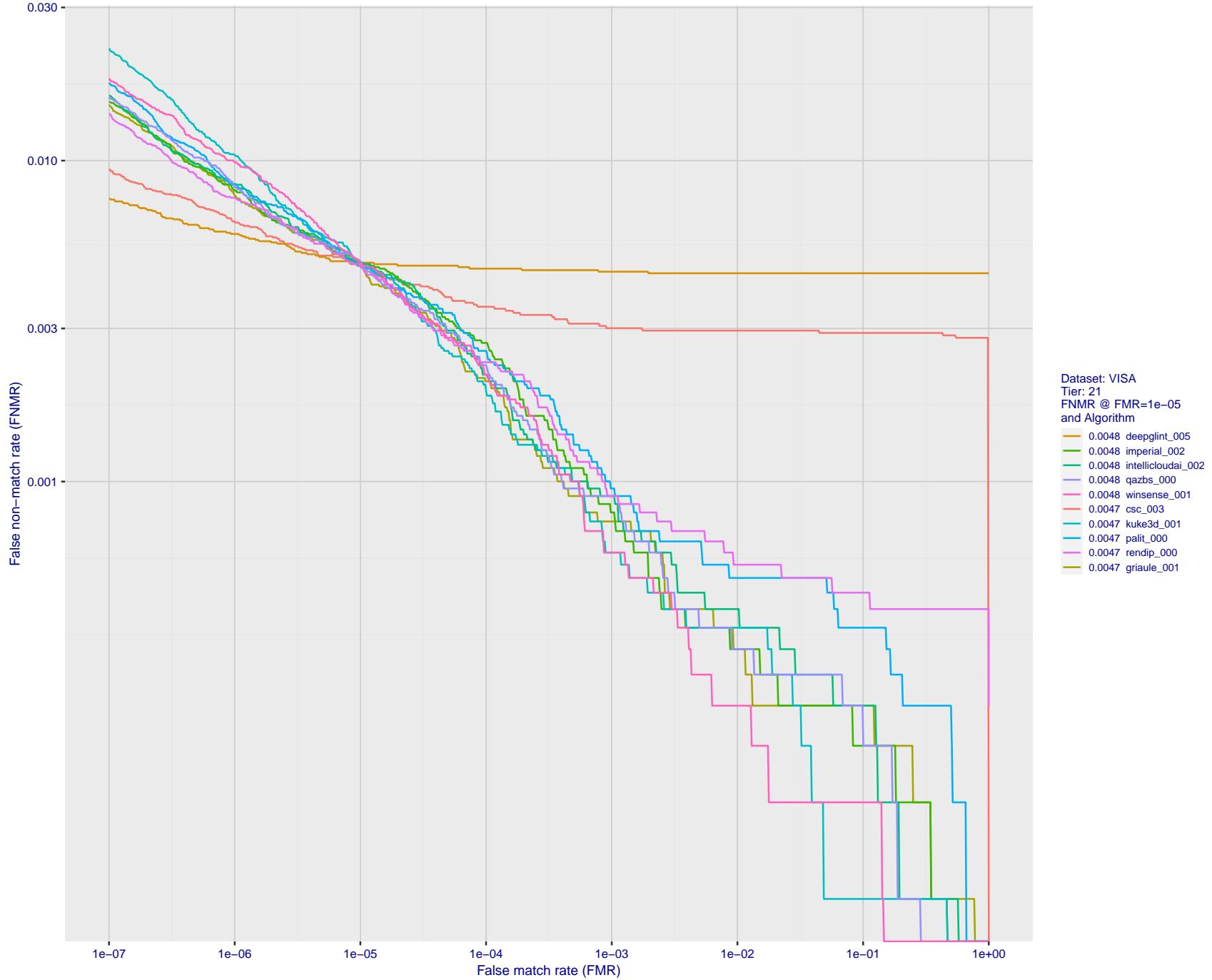


Figure 66: For the visa images, detection error tradeoff (DET) characteristics showing false non-match rate vs. false match rate plotted parametrically on threshold, T . The scales are logarithmic in order to show many decades of FMR.

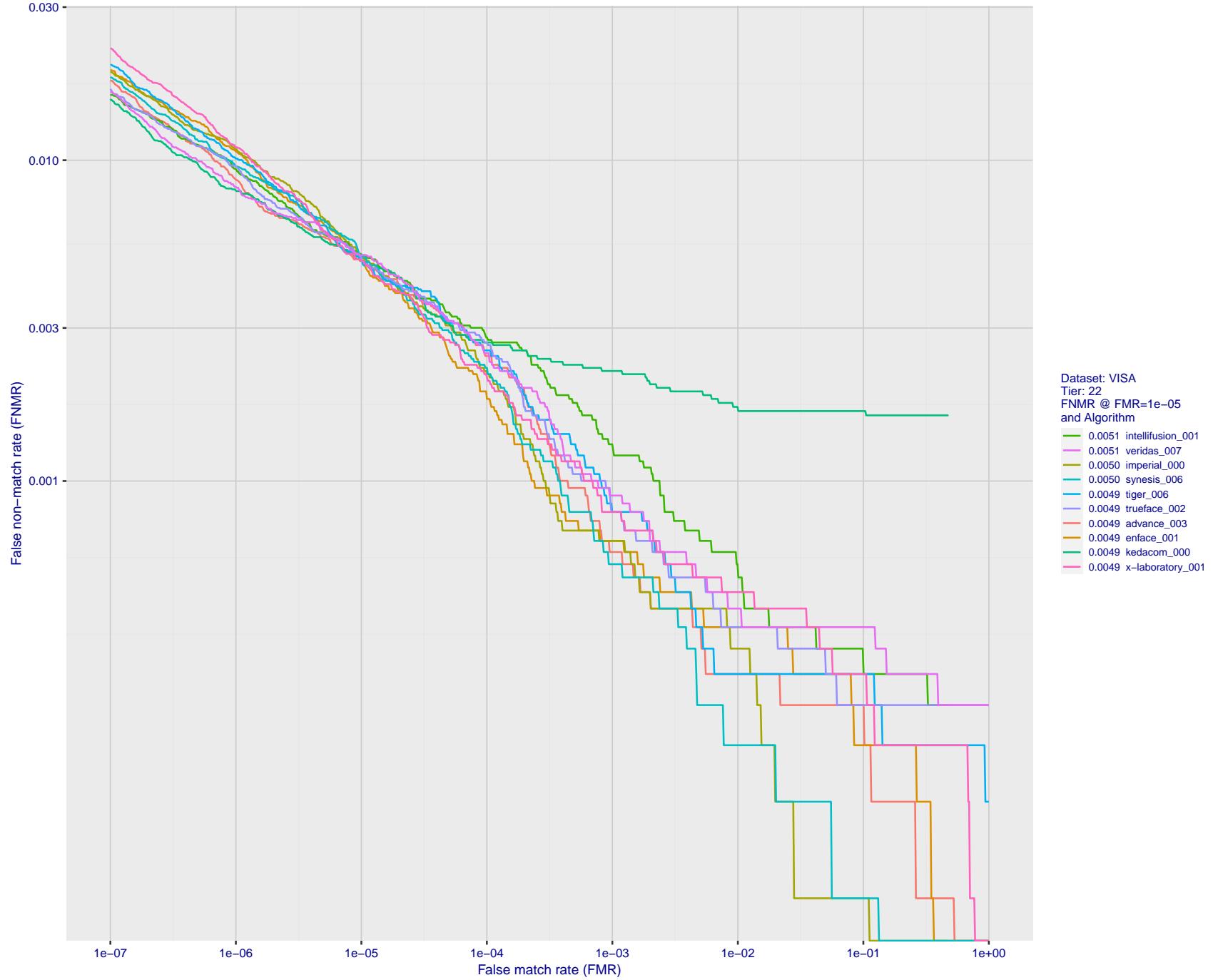


Figure 67: For the visa images, detection error tradeoff (DET) characteristics showing false non-match rate vs. false match rate plotted parametrically on threshold, T . The scales are logarithmic in order to show many decades of FMR.

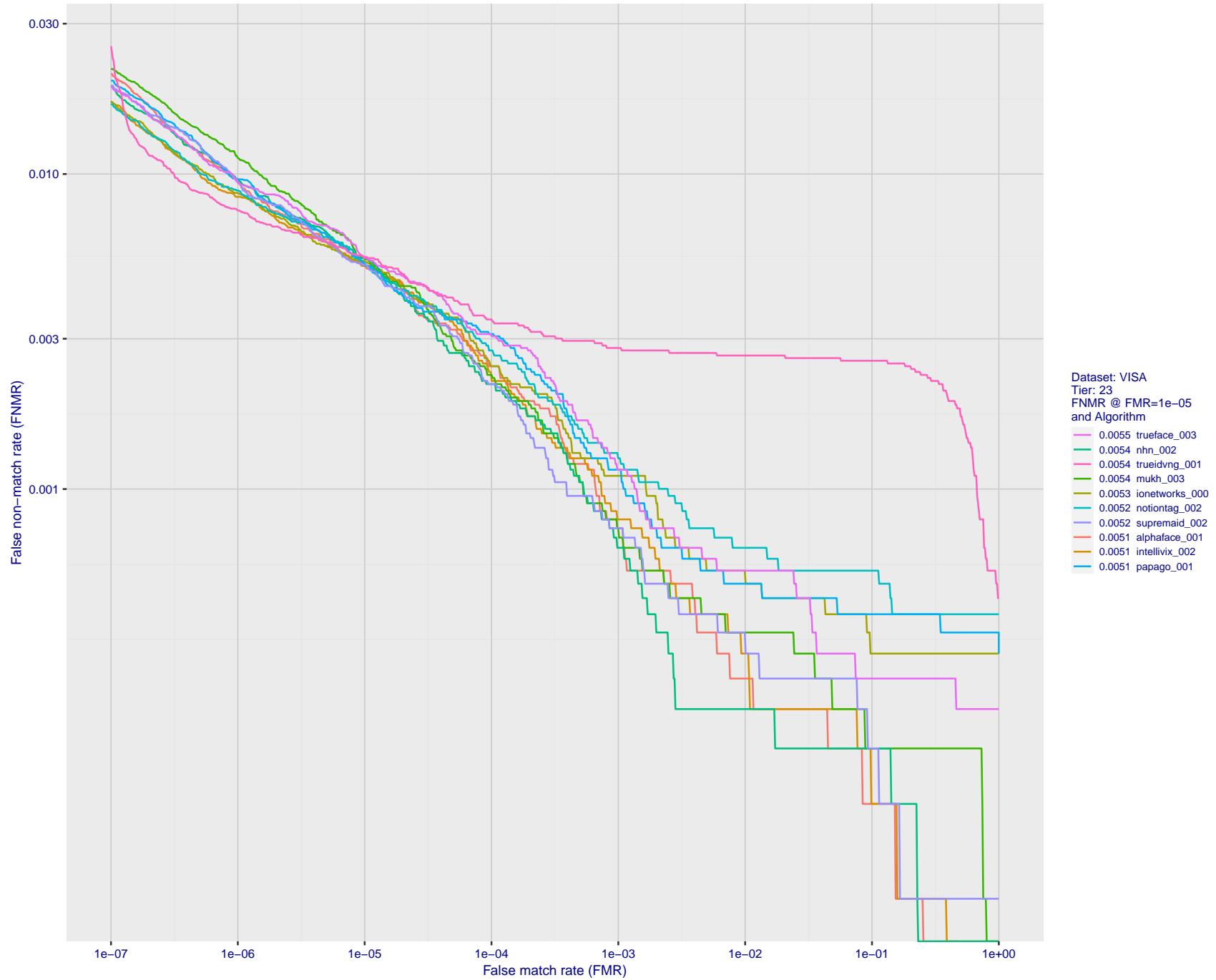


Figure 68: For the visa images, detection error tradeoff (DET) characteristics showing false non-match rate vs. false match rate plotted parametrically on threshold, T . The scales are logarithmic in order to show many decades of FMR.

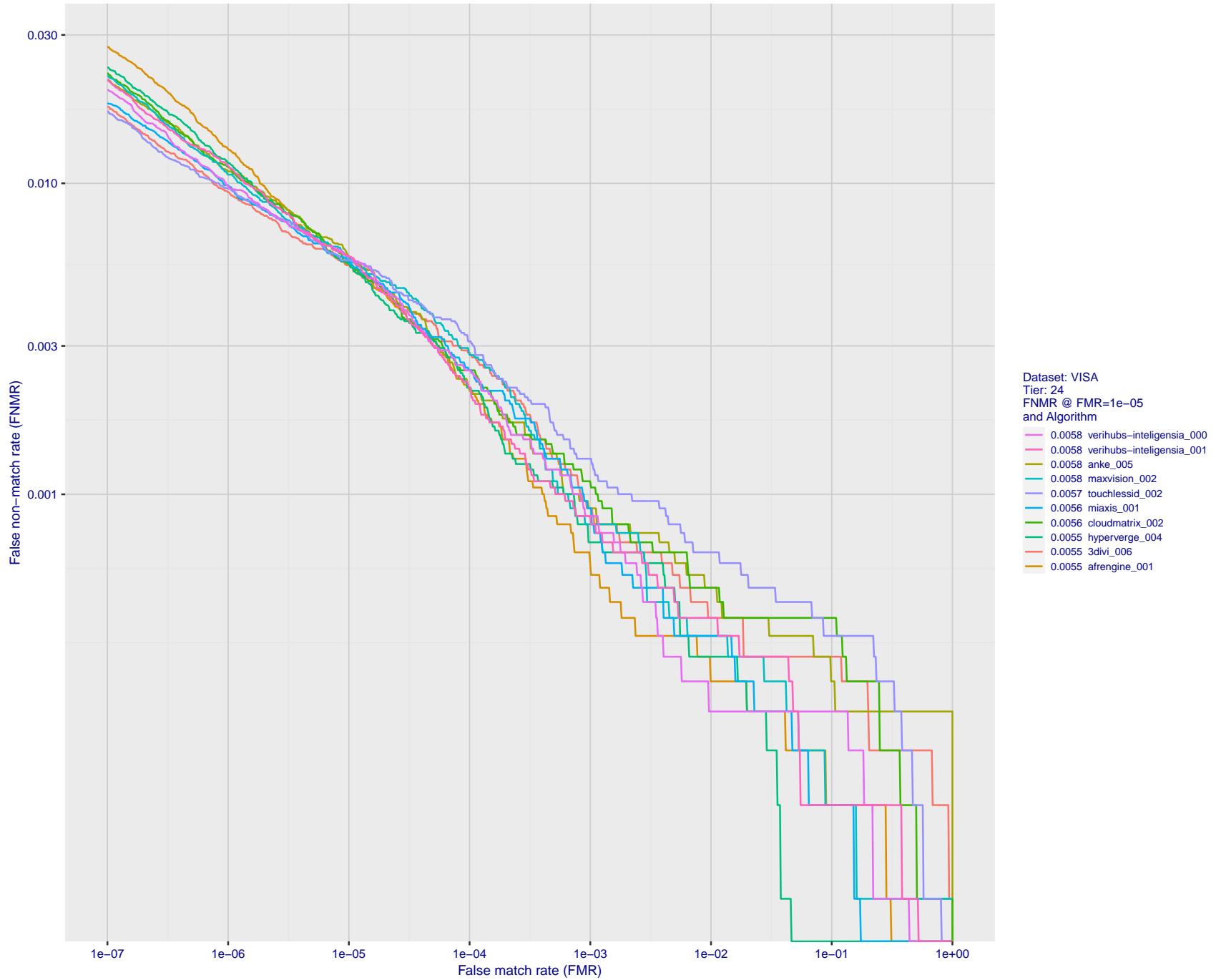


Figure 69: For the visa images, detection error tradeoff (DET) characteristics showing false non-match rate vs. false match rate plotted parametrically on threshold, T . The scales are logarithmic in order to show many decades of FMR.

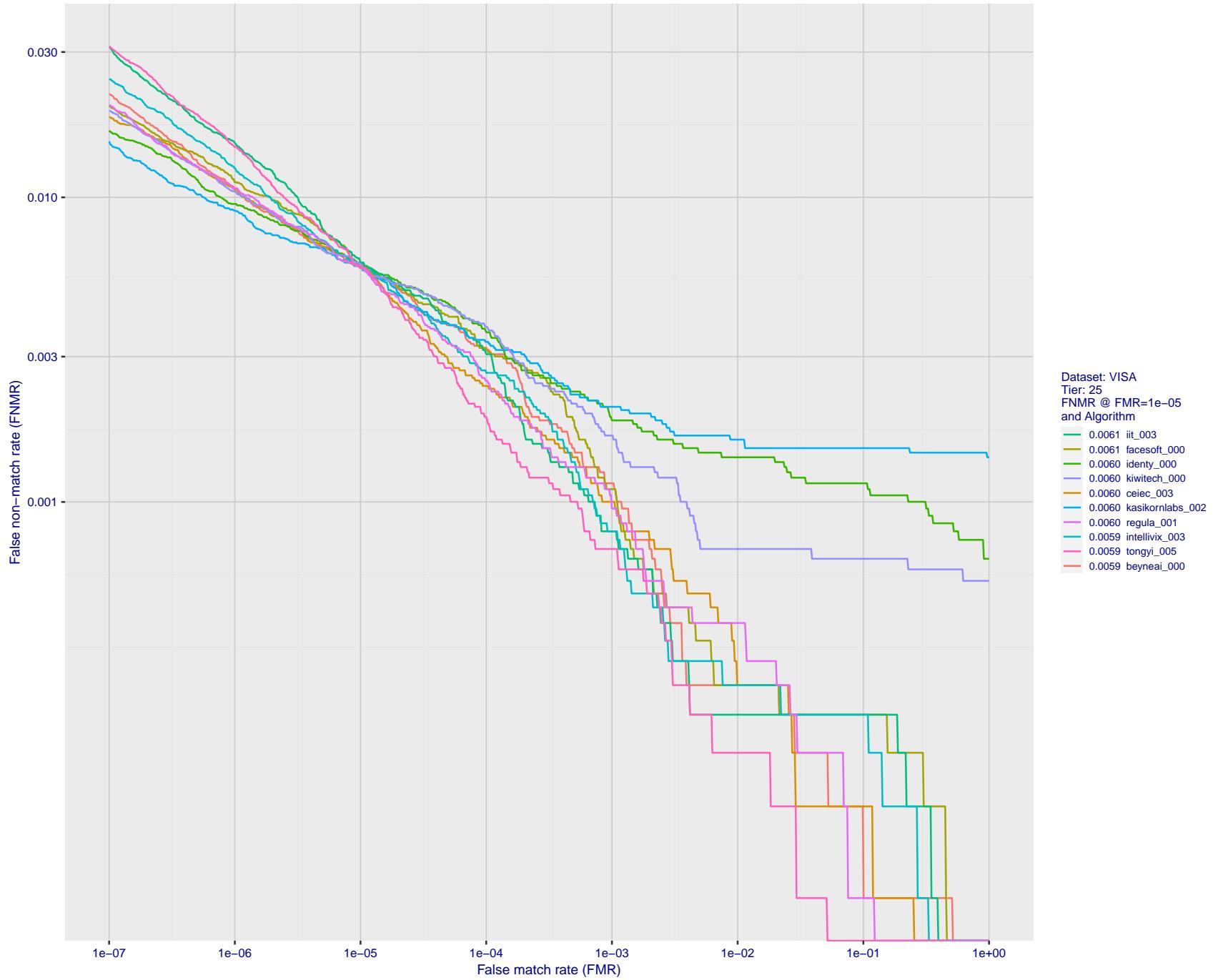


Figure 70: For the visa images, detection error tradeoff (DET) characteristics showing false non-match rate vs. false match rate plotted parametrically on threshold, T . The scales are logarithmic in order to show many decades of FMR.

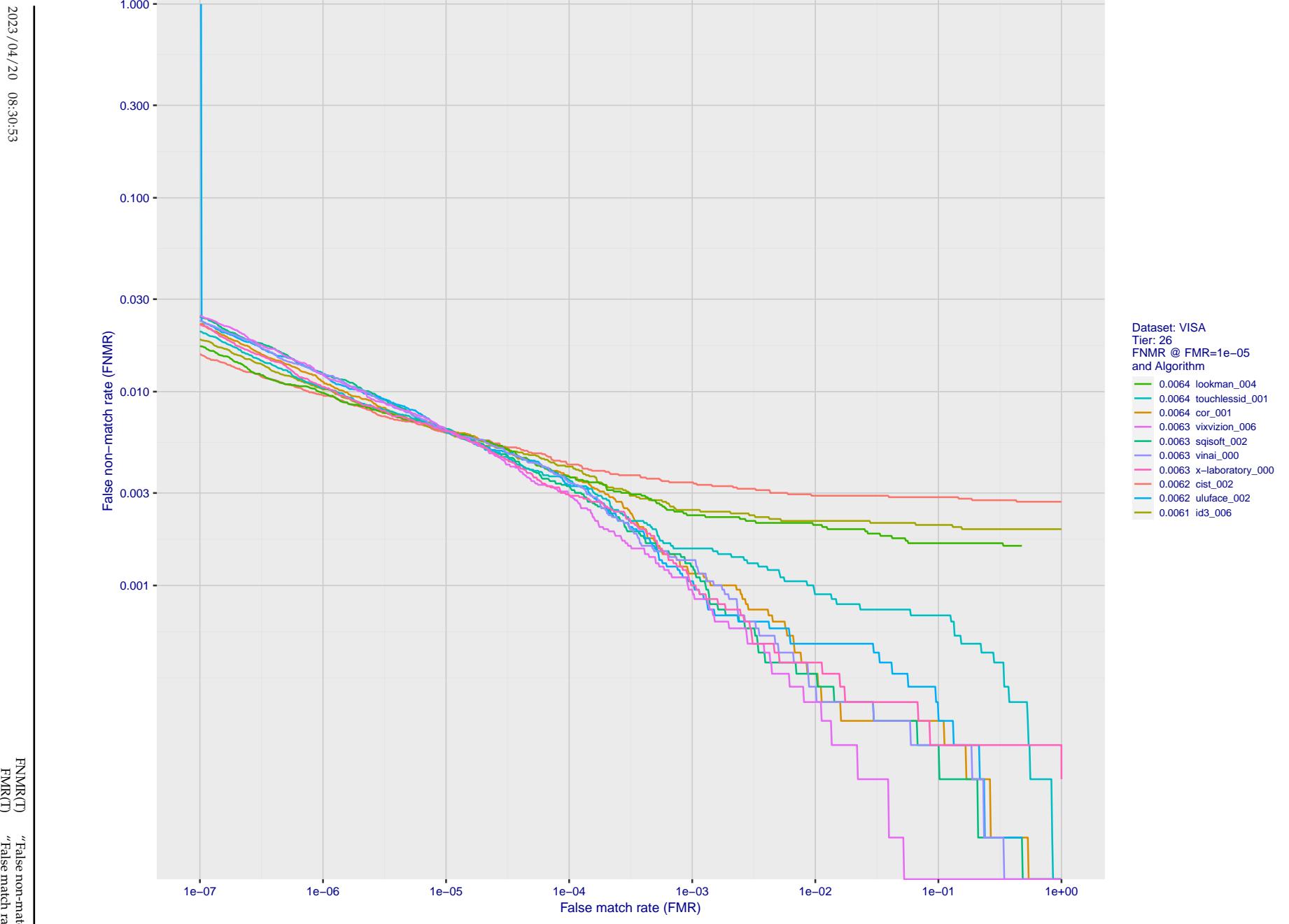


Figure 71: For the visa images, detection error tradeoff (DET) characteristics showing false non-match rate vs. false match rate plotted parametrically on threshold, T . The scales are logarithmic in order to show many decades of FMR.

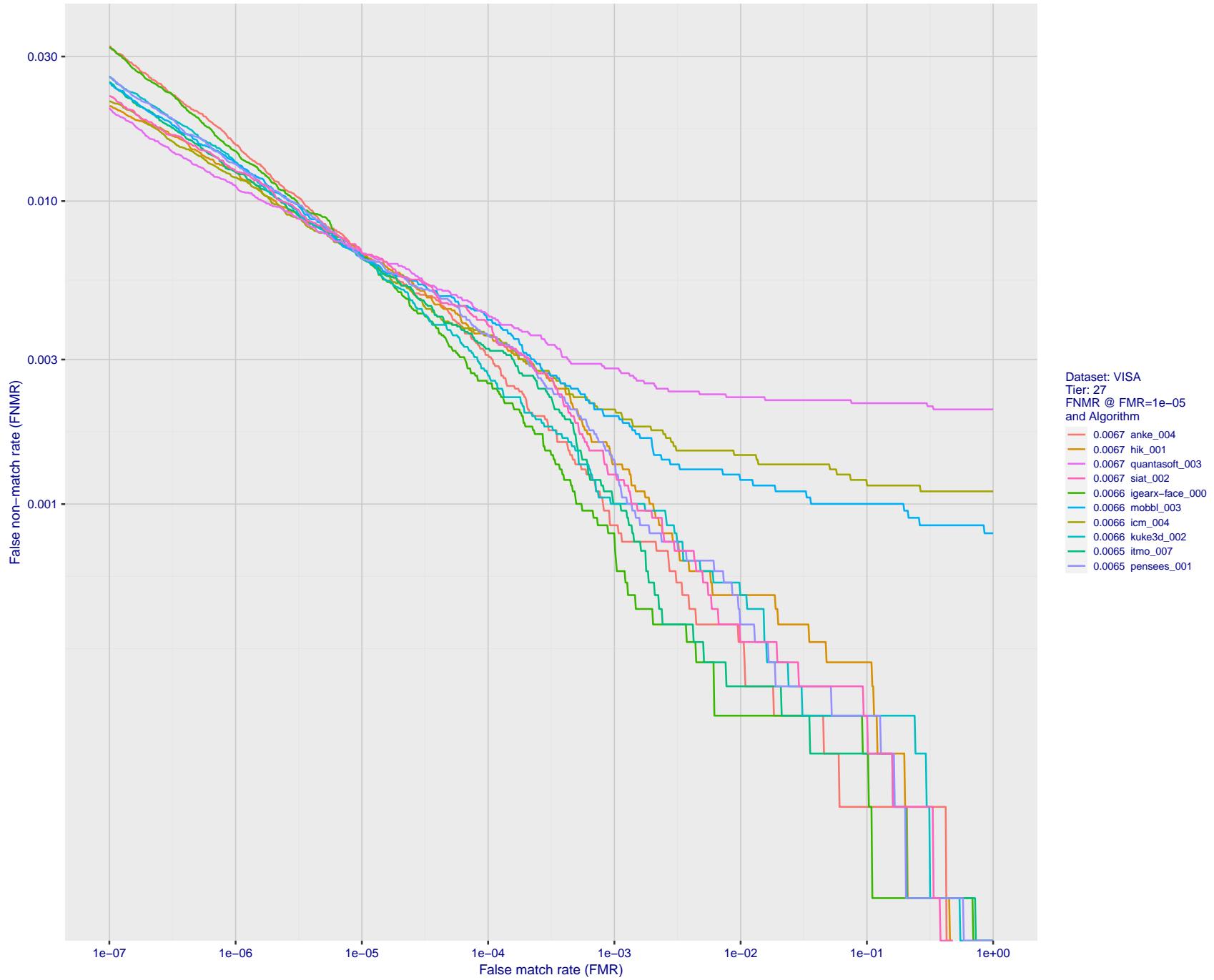


Figure 72: For the visa images, detection error tradeoff (DET) characteristics showing false non-match rate vs. false match rate plotted parametrically on threshold, T . The scales are logarithmic in order to show many decades of FMR.

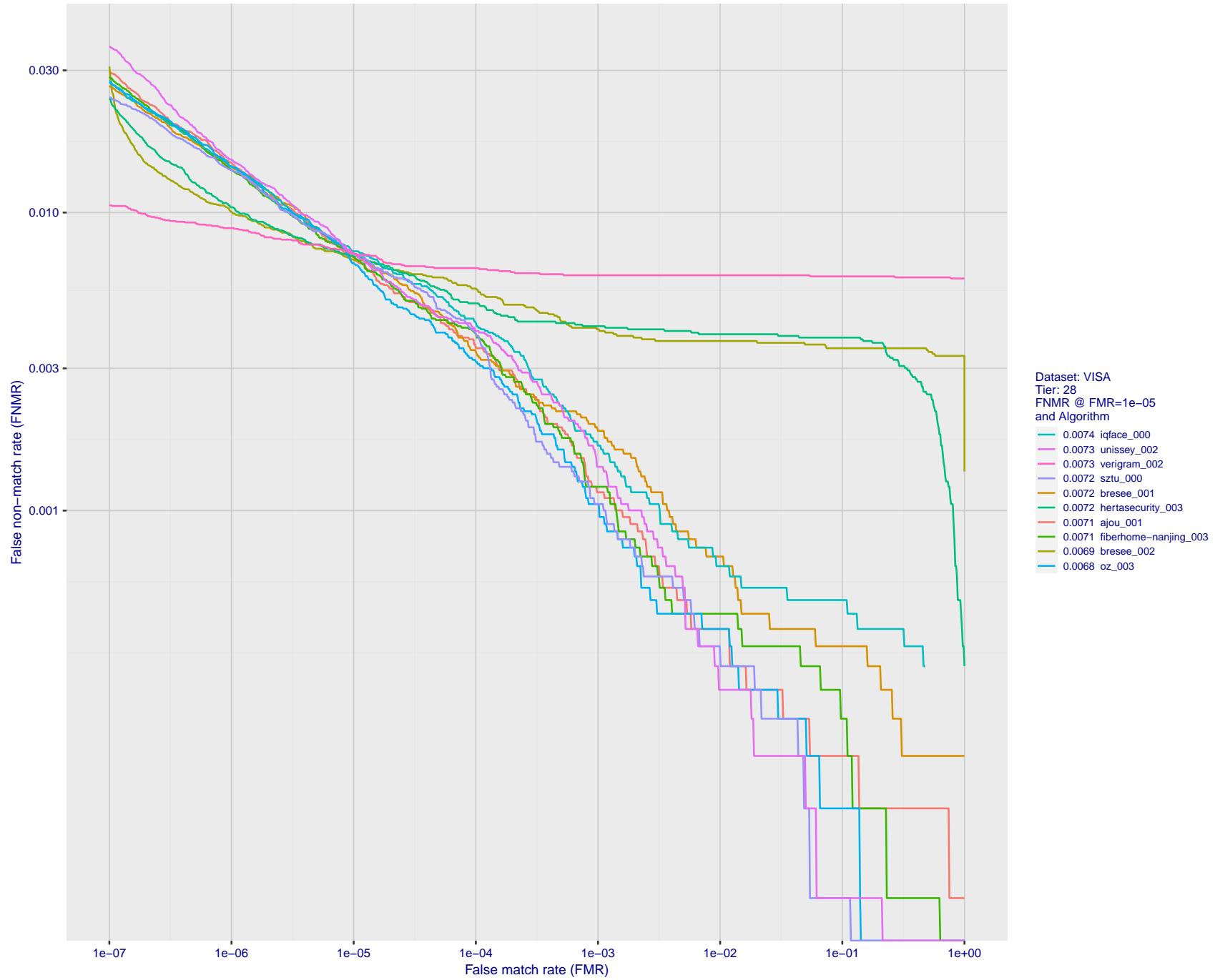


Figure 73: For the visa images, detection error tradeoff (DET) characteristics showing false non-match rate vs. false match rate plotted parametrically on threshold, T . The scales are logarithmic in order to show many decades of FMR.

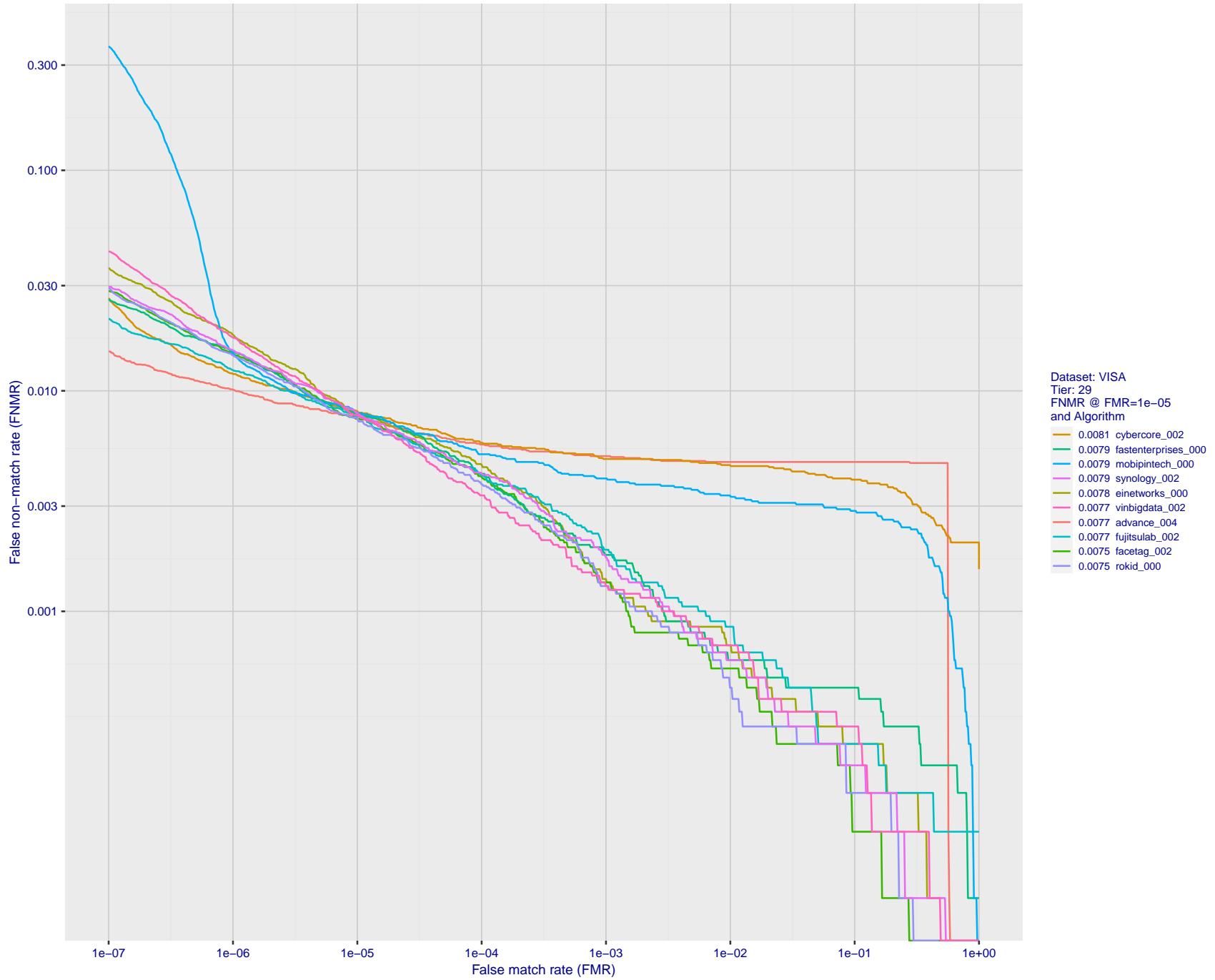


Figure 74: For the visa images, detection error tradeoff (DET) characteristics showing false non-match rate vs. false match rate plotted parametrically on threshold, T . The scales are logarithmic in order to show many decades of FMR.

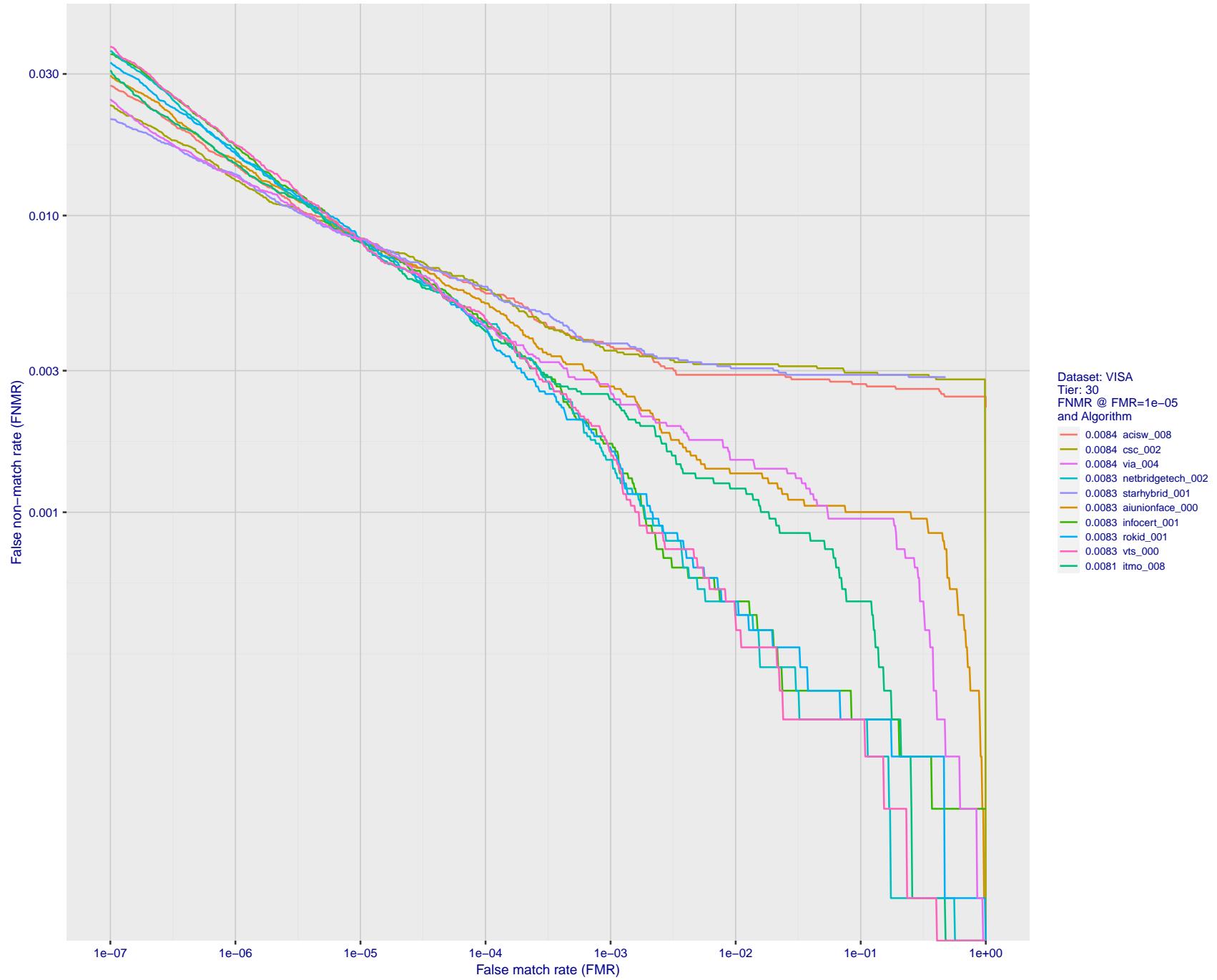


Figure 75: For the visa images, detection error tradeoff (DET) characteristics showing false non-match rate vs. false match rate plotted parametrically on threshold, T . The scales are logarithmic in order to show many decades of FMR.

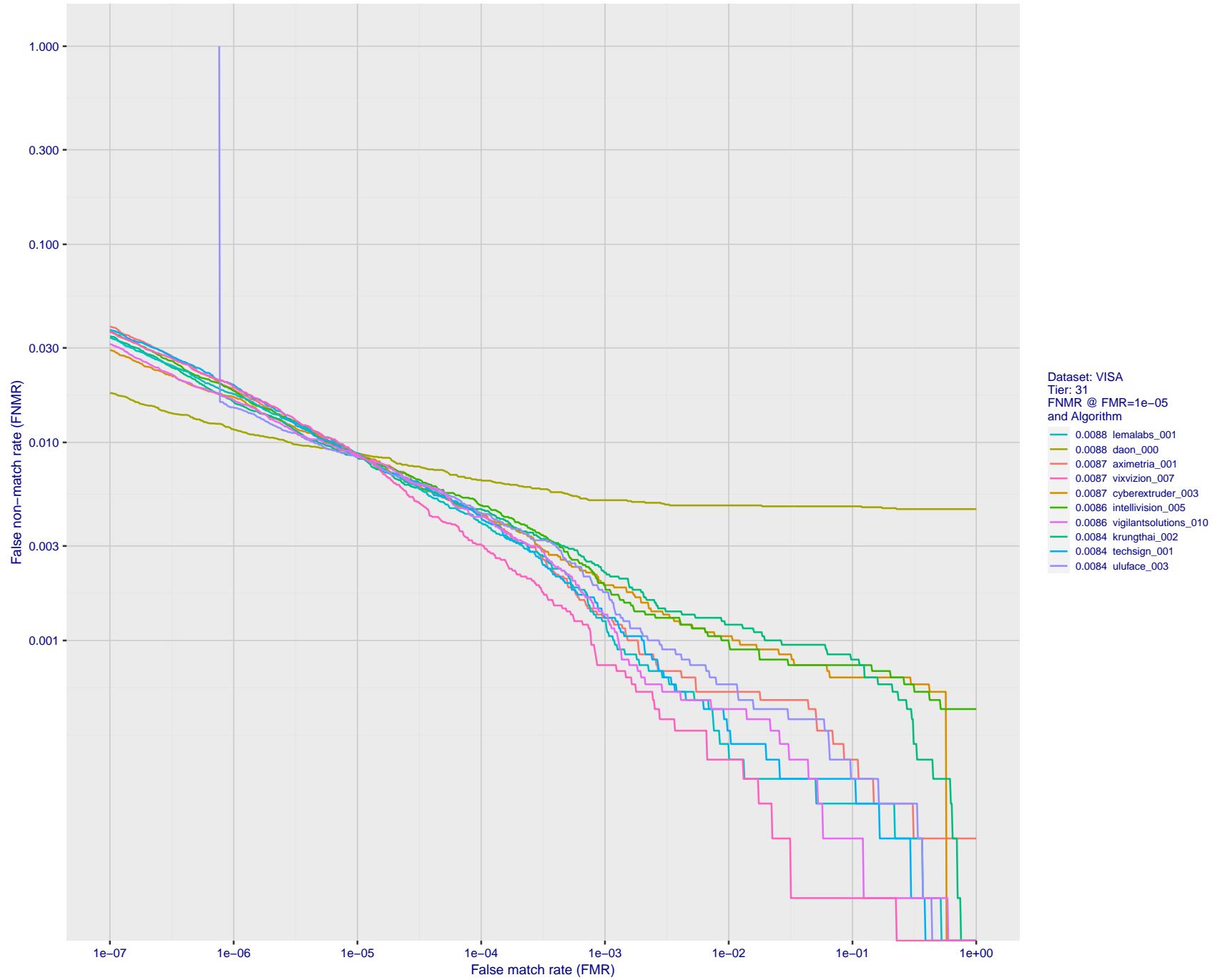


Figure 76: For the visa images, detection error tradeoff (DET) characteristics showing false non-match rate vs. false match rate plotted parametrically on threshold, T . The scales are logarithmic in order to show many decades of FMR.

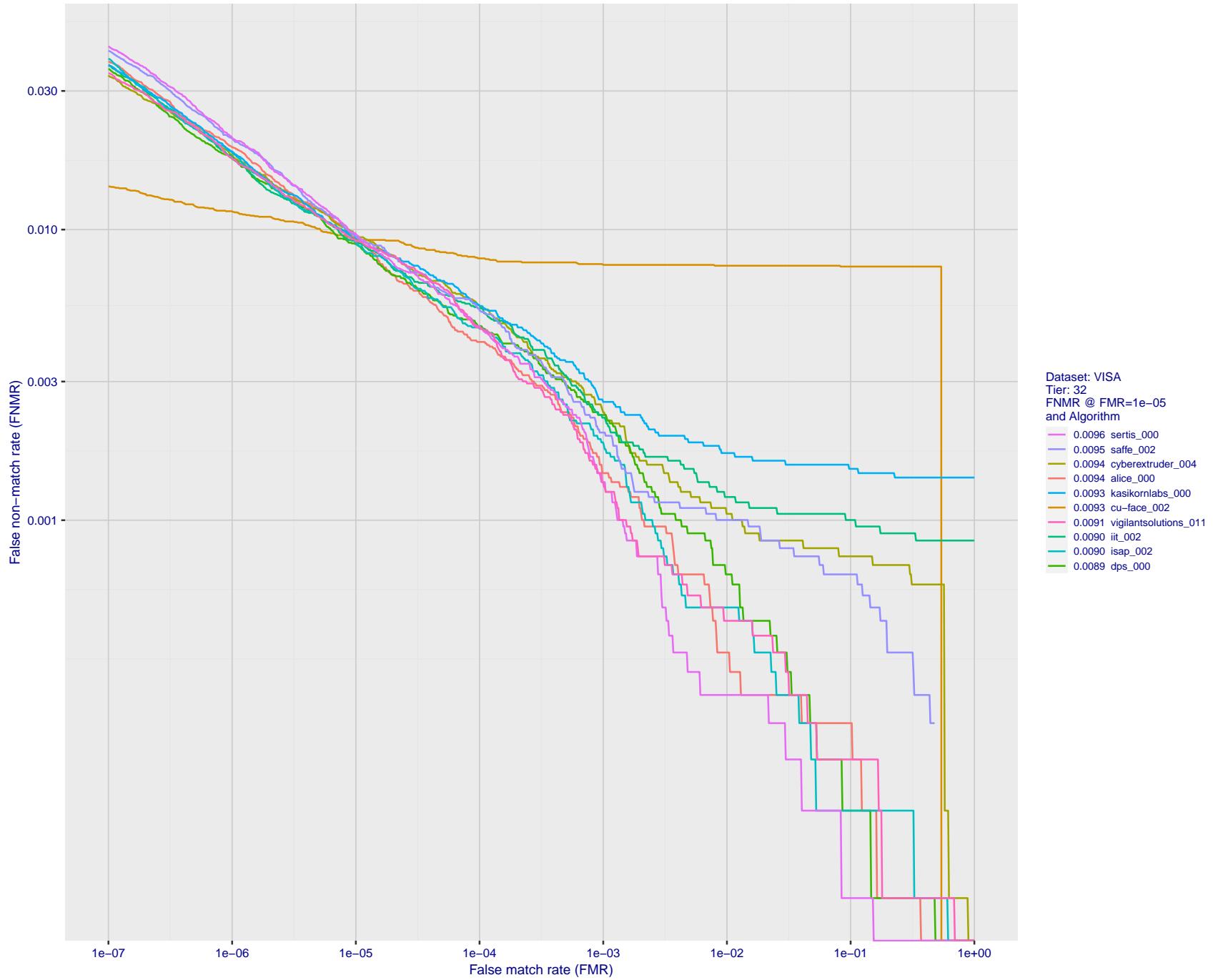


Figure 77: For the visa images, detection error tradeoff (DET) characteristics showing false non-match rate vs. false match rate plotted parametrically on threshold, T . The scales are logarithmic in order to show many decades of FMR.

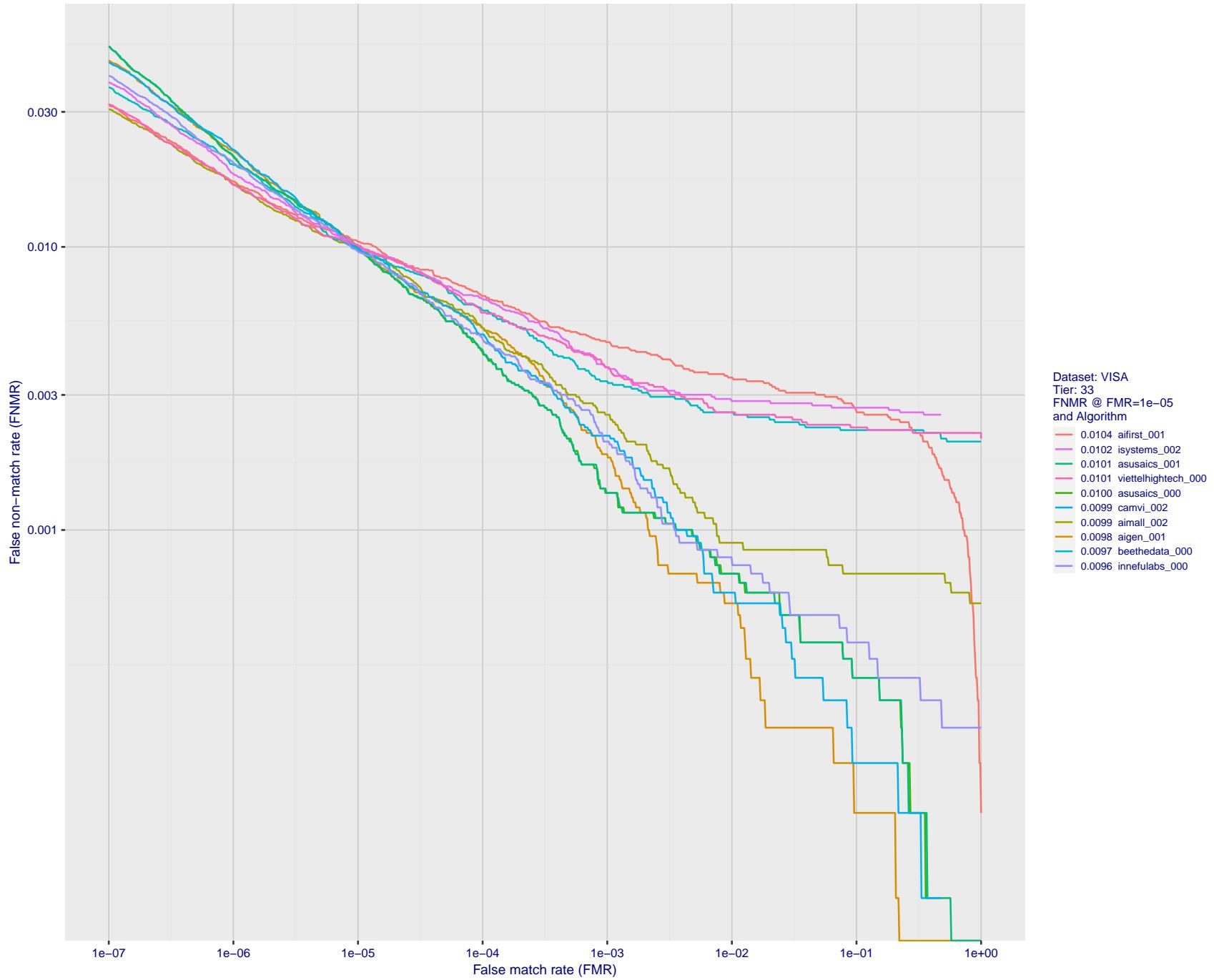


Figure 78: For the visa images, detection error tradeoff (DET) characteristics showing false non-match rate vs. false match rate plotted parametrically on threshold, T . The scales are logarithmic in order to show many decades of FMR.

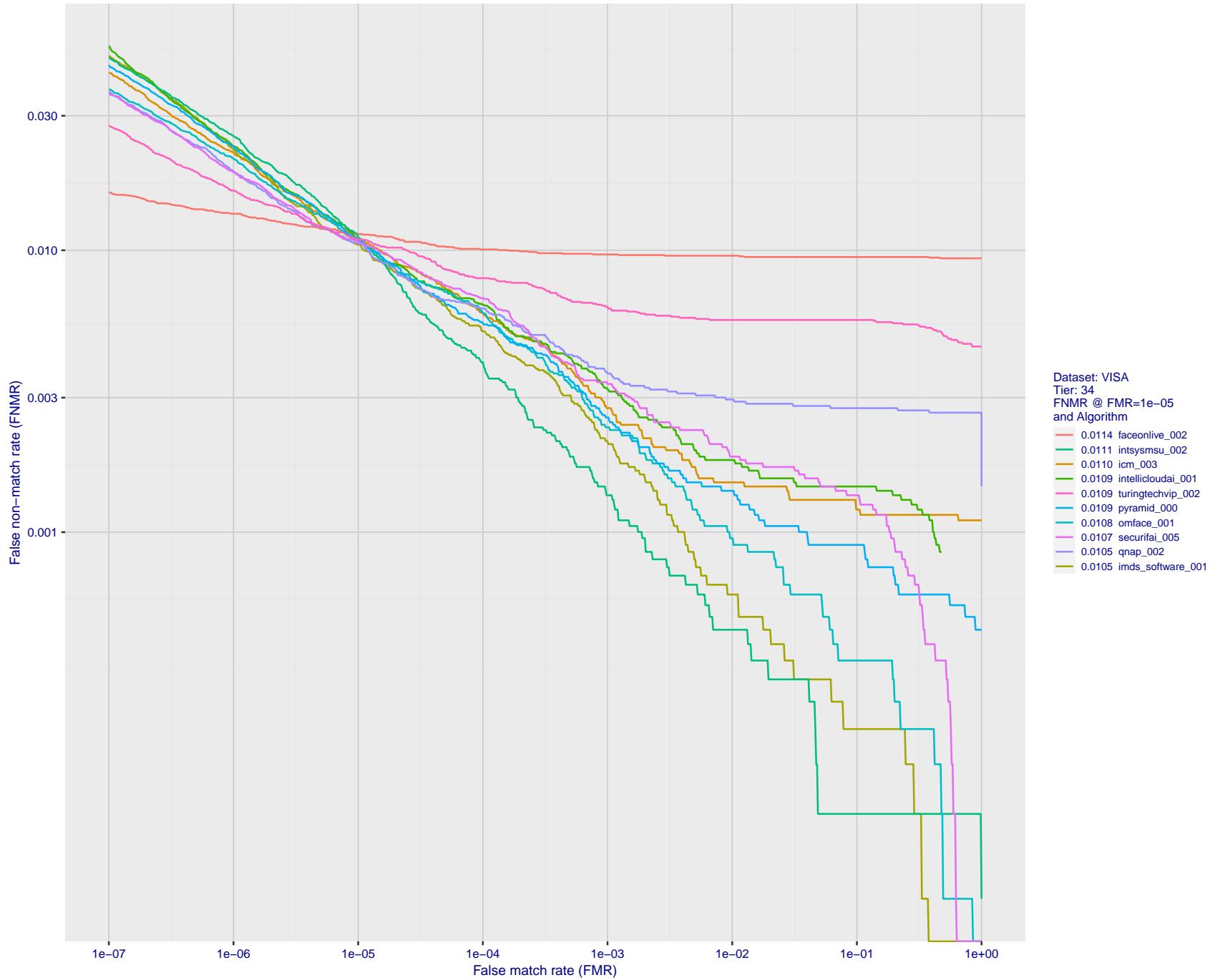


Figure 79: For the visa images, detection error tradeoff (DET) characteristics showing false non-match rate vs. false match rate plotted parametrically on threshold, T . The scales are logarithmic in order to show many decades of FMR.

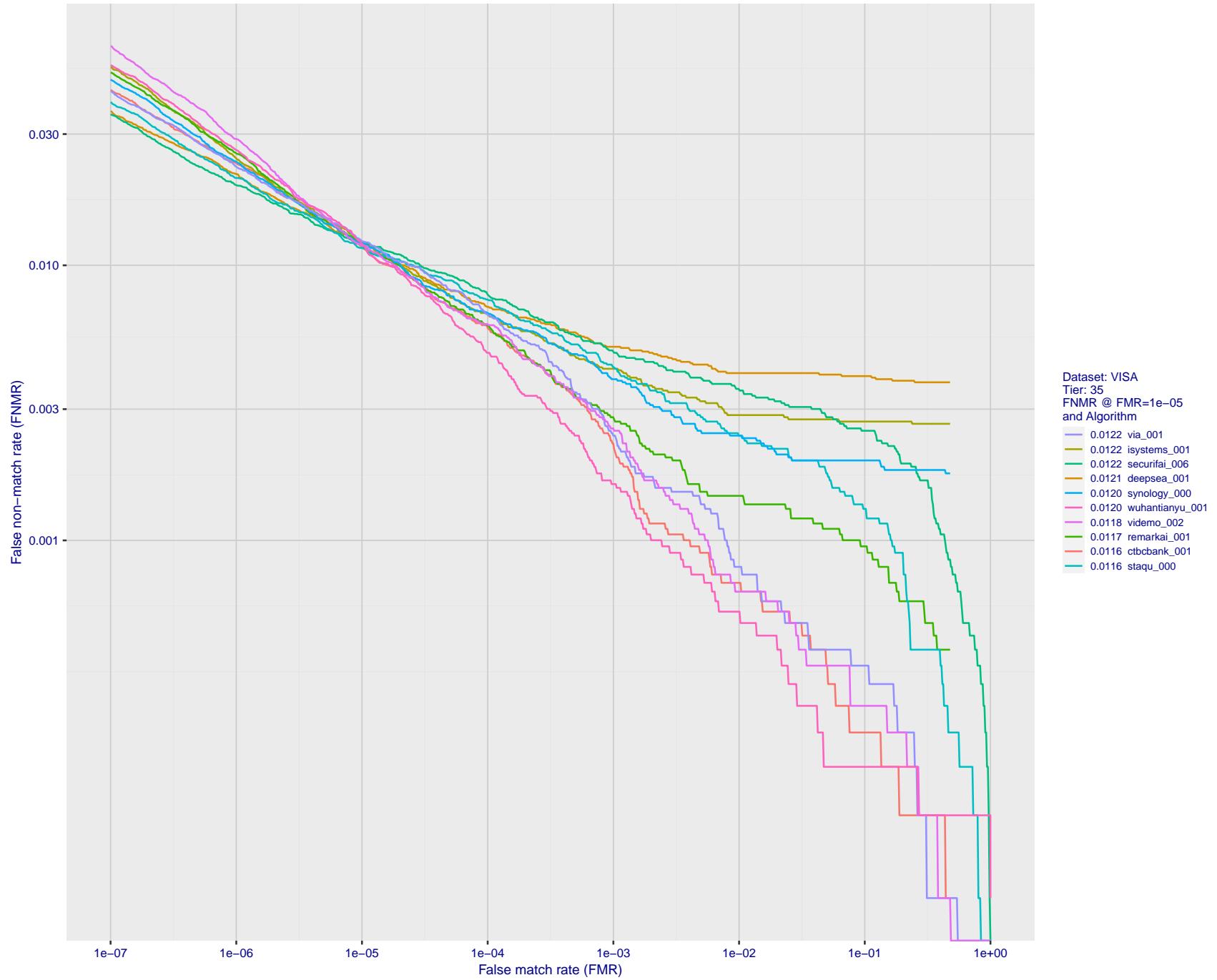


Figure 80: For the visa images, detection error tradeoff (DET) characteristics showing false non-match rate vs. false match rate plotted parametrically on threshold, T . The scales are logarithmic in order to show many decades of FMR.

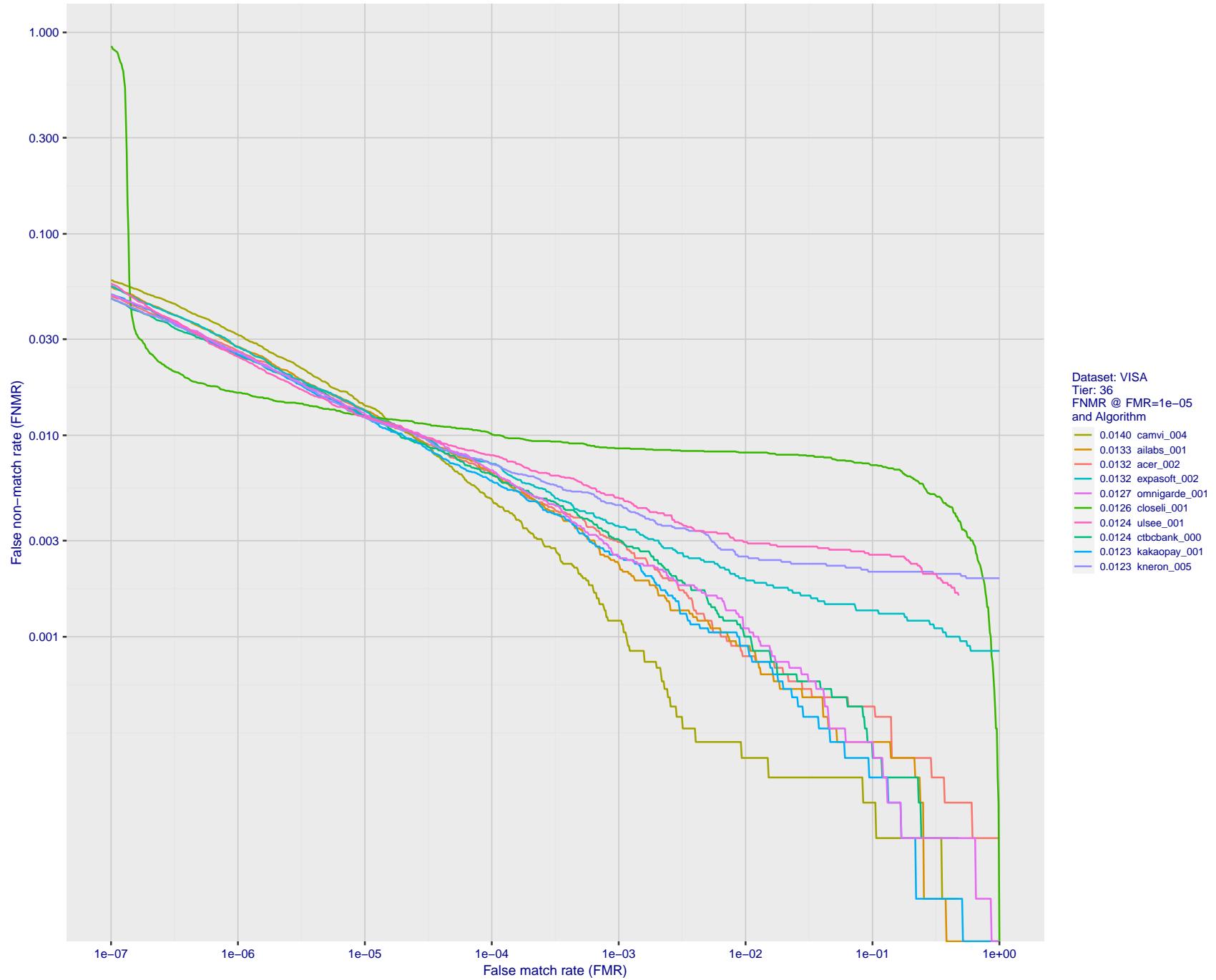


Figure 81: For the visa images, detection error tradeoff (DET) characteristics showing false non-match rate vs. false match rate plotted parametrically on threshold, T . The scales are logarithmic in order to show many decades of FMR.

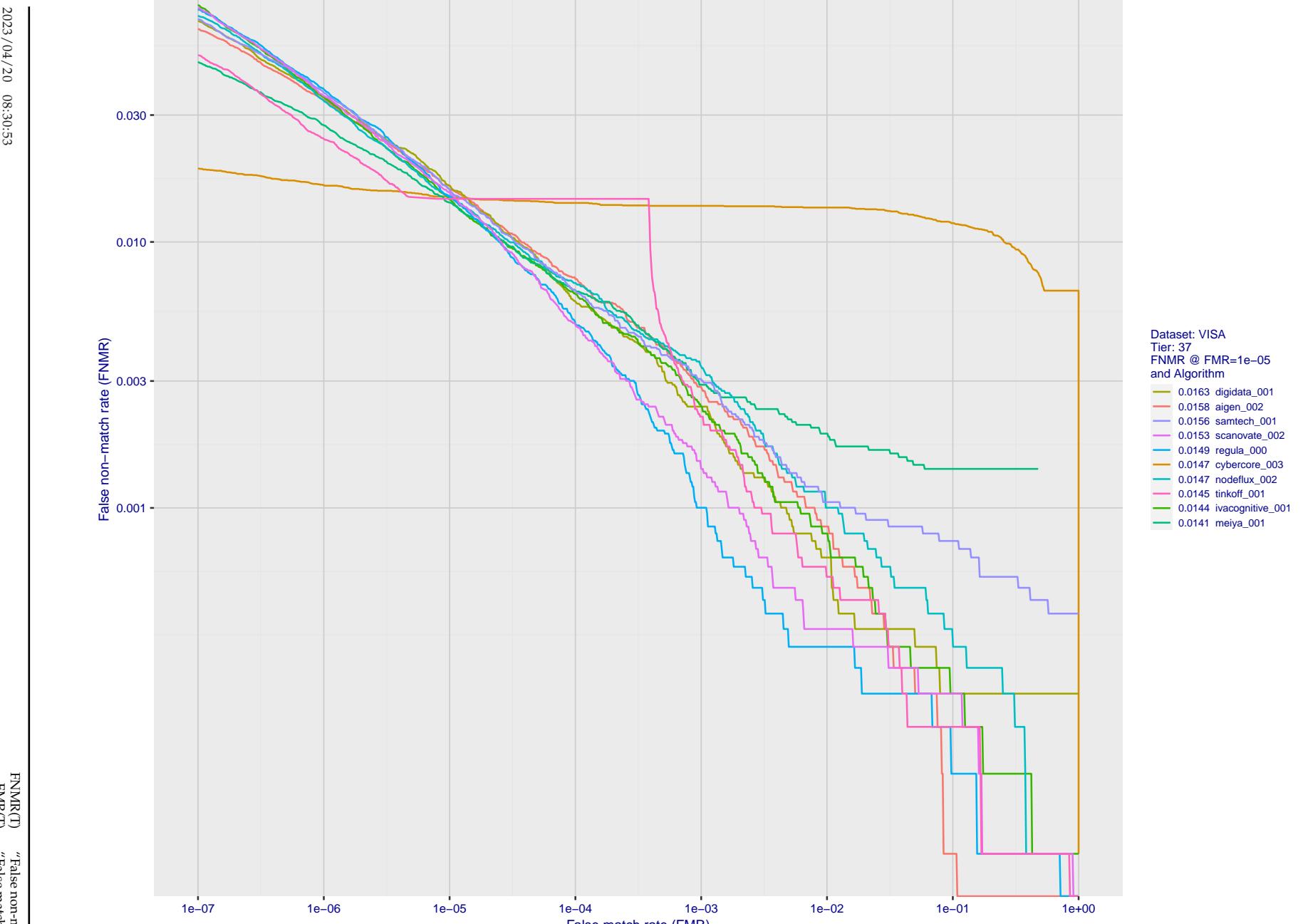


Figure 82: For the visa images, detection error tradeoff (DET) characteristics showing false non-match rate vs. false match rate plotted parametrically on threshold, T . The scales are logarithmic in order to show many decades of FMR.

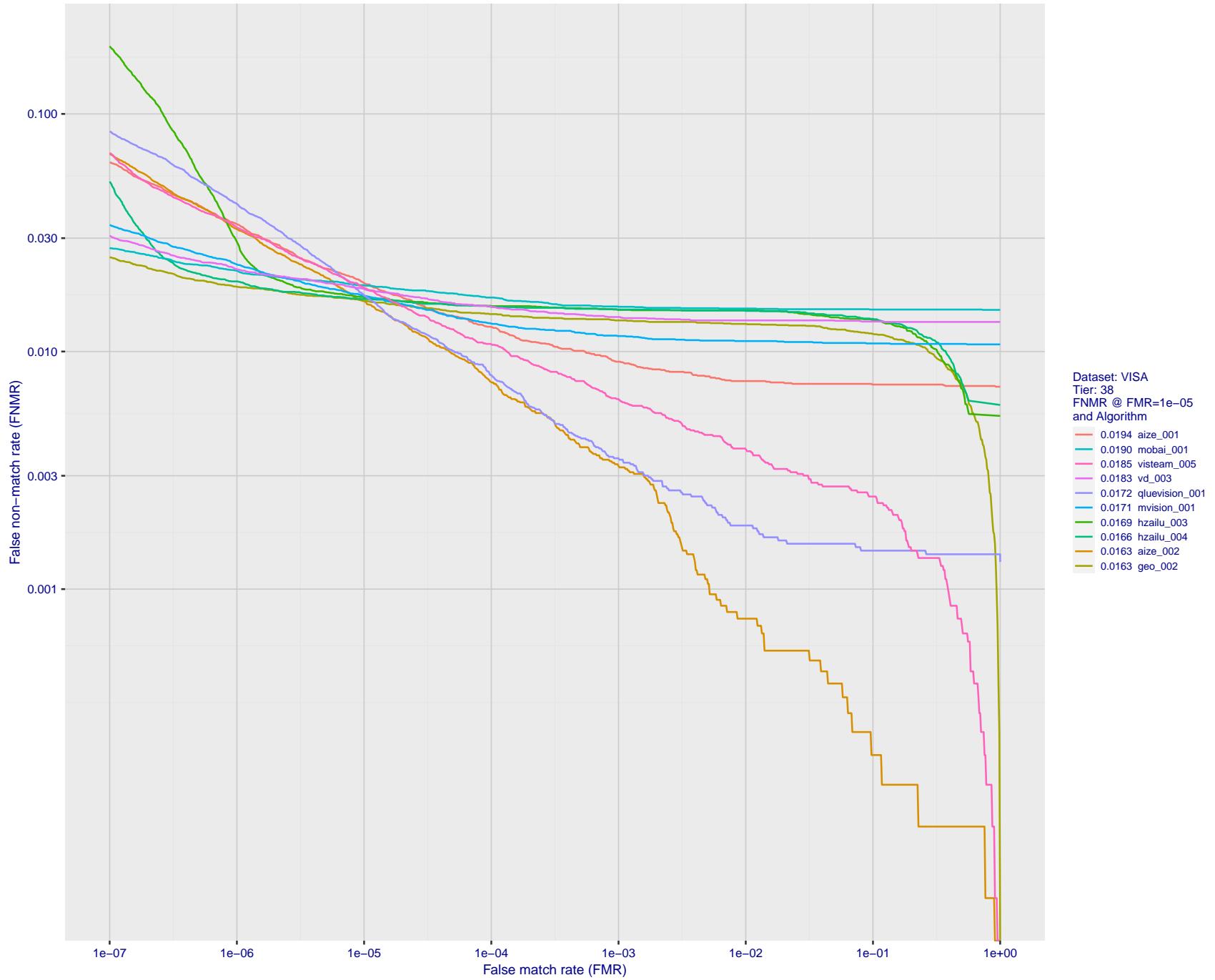


Figure 83: For the visa images, detection error tradeoff (DET) characteristics showing false non-match rate vs. false match rate plotted parametrically on threshold, T . The scales are logarithmic in order to show many decades of FMR.

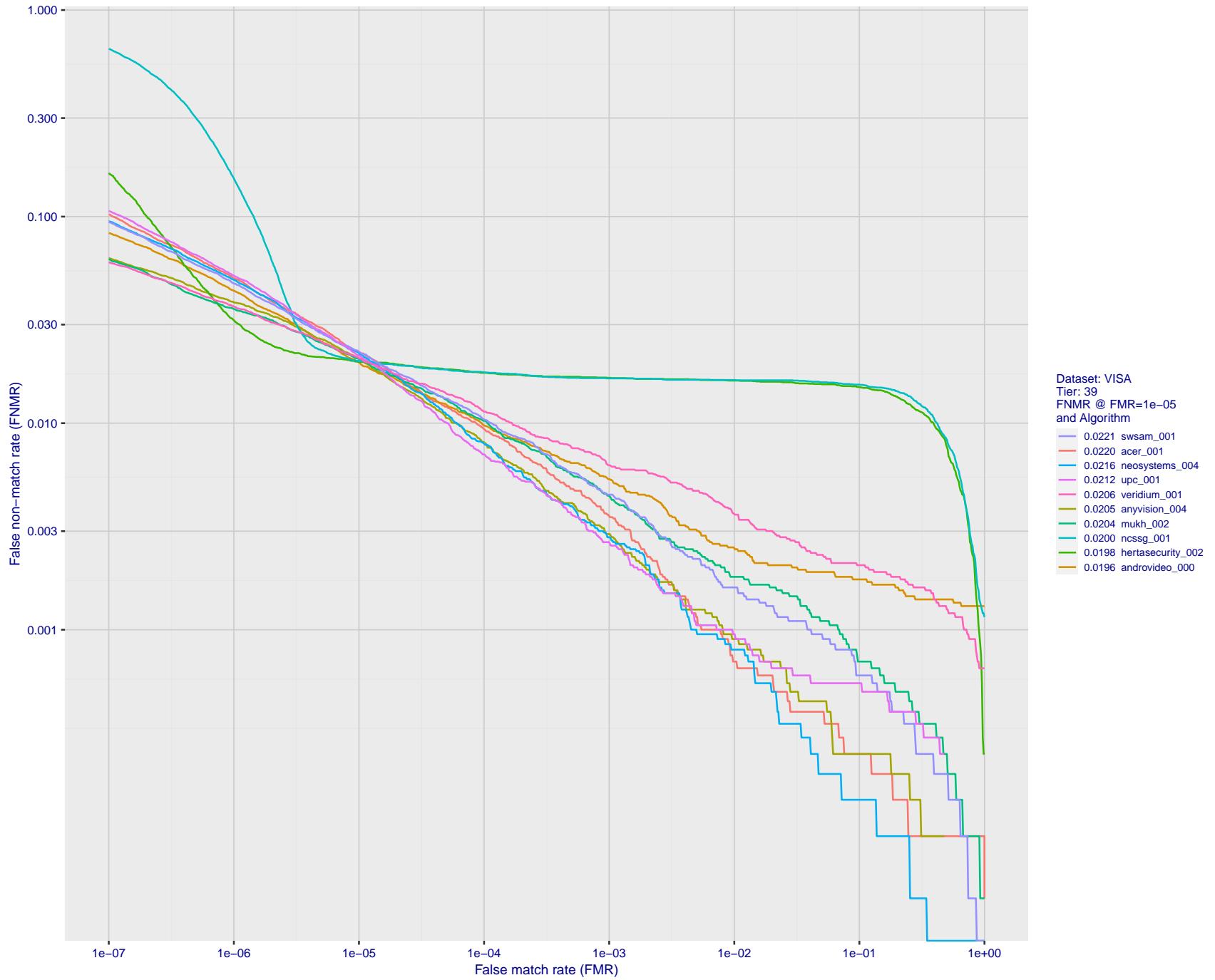


Figure 84: For the visa images, detection error tradeoff (DET) characteristics showing false non-match rate vs. false match rate plotted parametrically on threshold, T . The scales are logarithmic in order to show many decades of FMR.

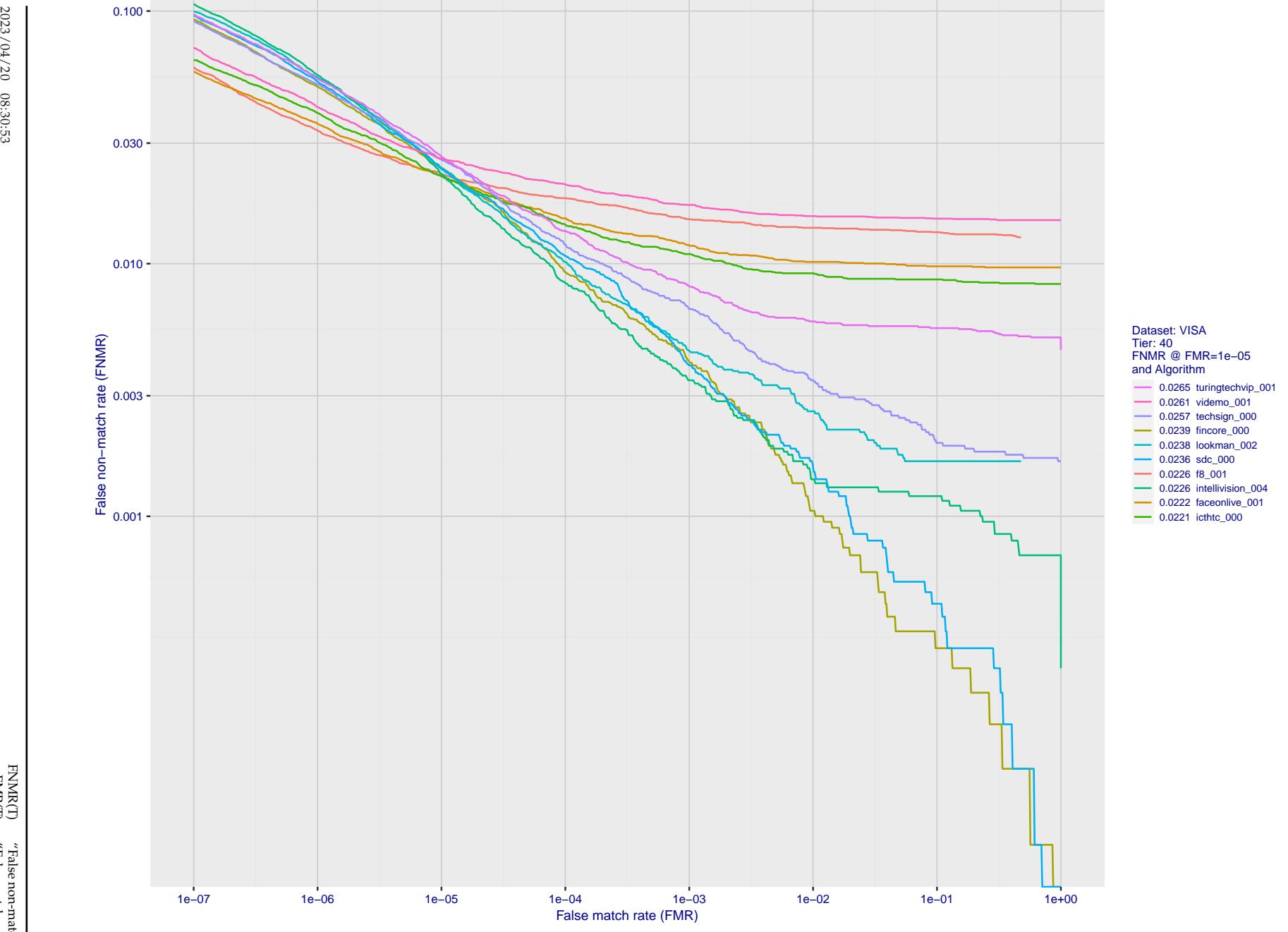


Figure 85: For the visa images, detection error tradeoff (DET) characteristics showing false non-match rate vs. false match rate plotted parametrically on threshold, T . The scales are logarithmic in order to show many decades of FMR.

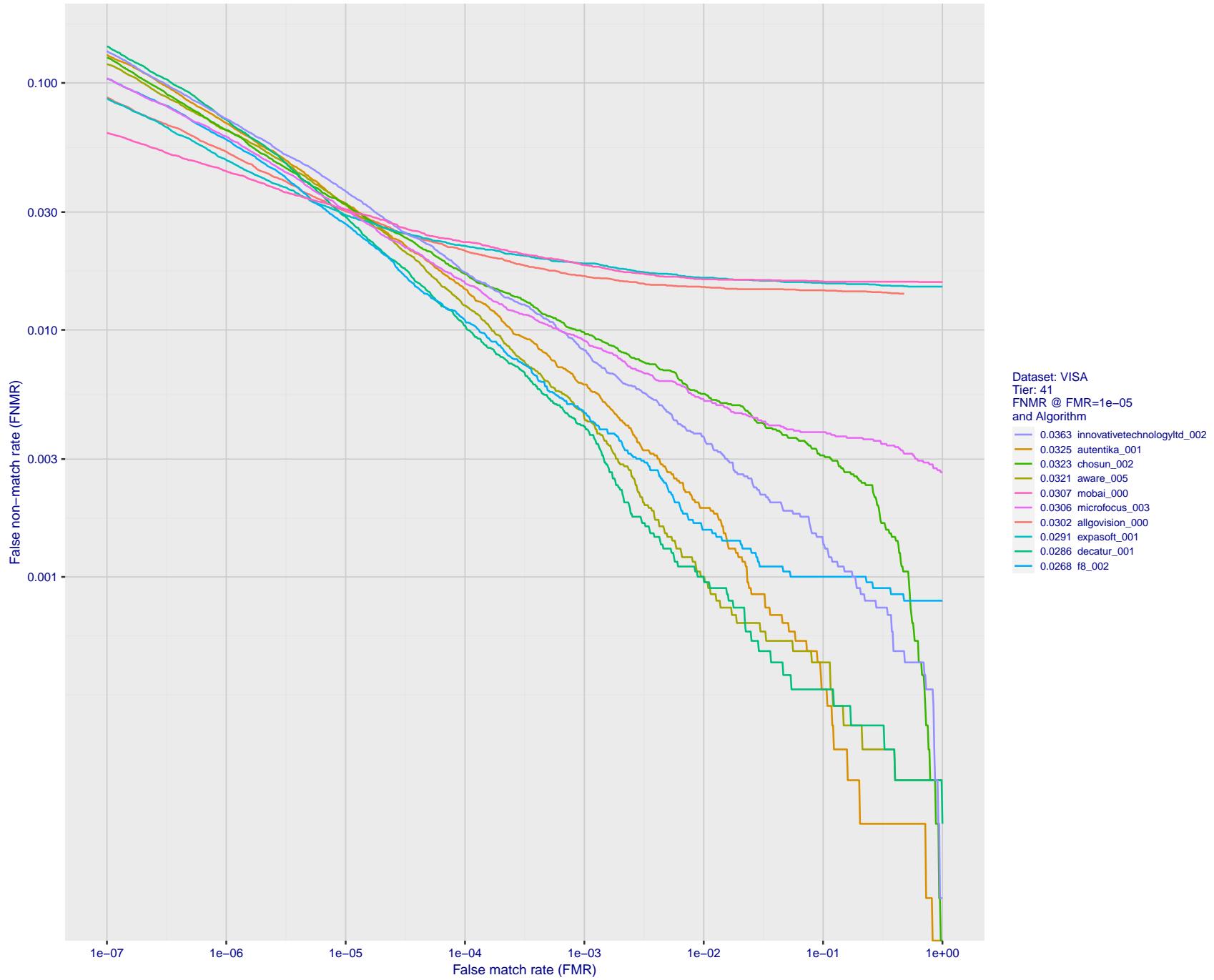


Figure 86: For the visa images, detection error tradeoff (DET) characteristics showing false non-match rate vs. false match rate plotted parametrically on threshold, T . The scales are logarithmic in order to show many decades of FMR.

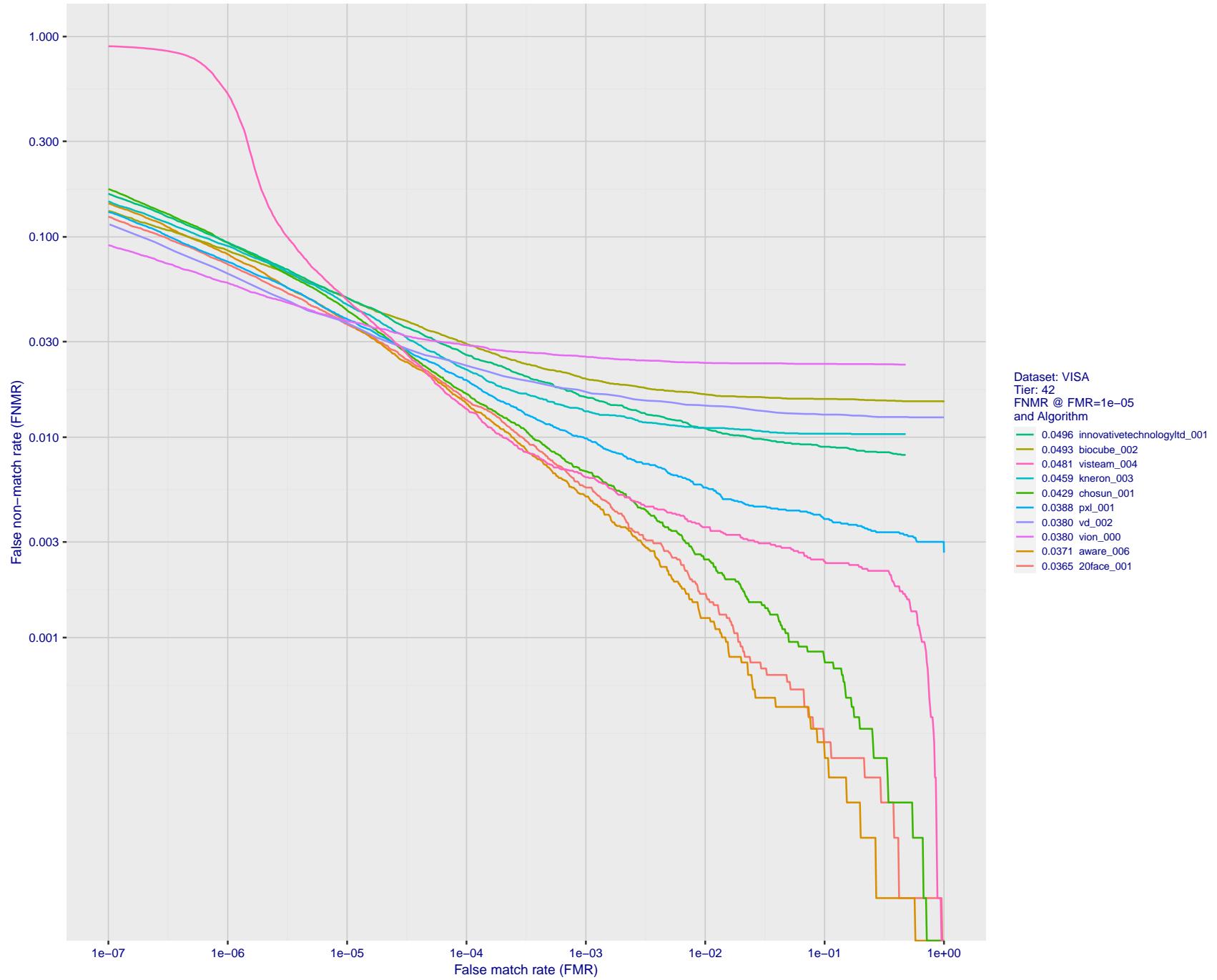


Figure 87: For the visa images, detection error tradeoff (DET) characteristics showing false non-match rate vs. false match rate plotted parametrically on threshold, T . The scales are logarithmic in order to show many decades of FMR.

2023/04/20 08:30:53

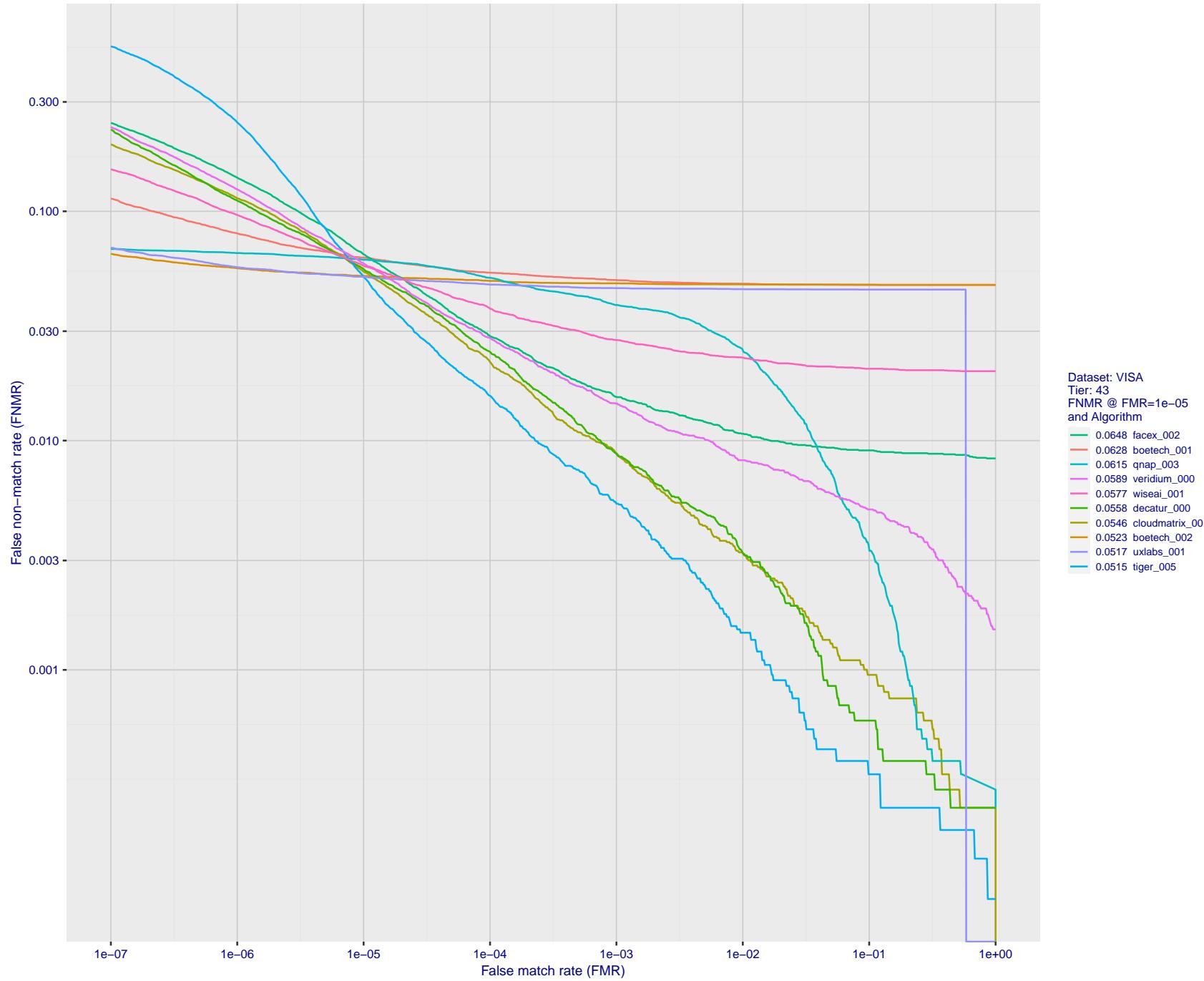


Figure 88: For the visa images, detection error tradeoff (DET) characteristics showing false non-match rate vs. false match rate plotted parametrically on threshold, T . The scales are logarithmic in order to show many decades of FMR.

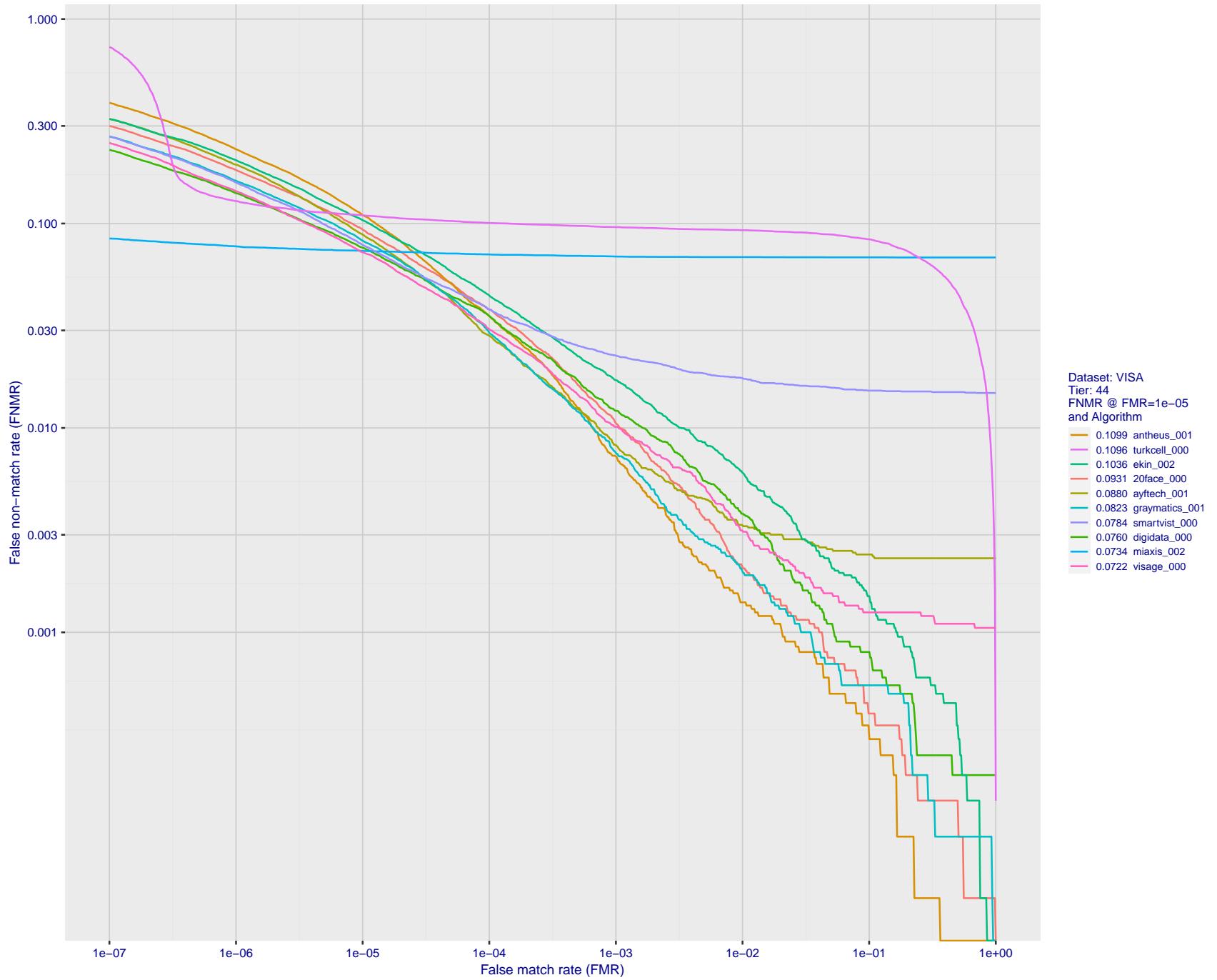


Figure 89: For the visa images, detection error tradeoff (DET) characteristics showing false non-match rate vs. false match rate plotted parametrically on threshold, T . The scales are logarithmic in order to show many decades of FMR.

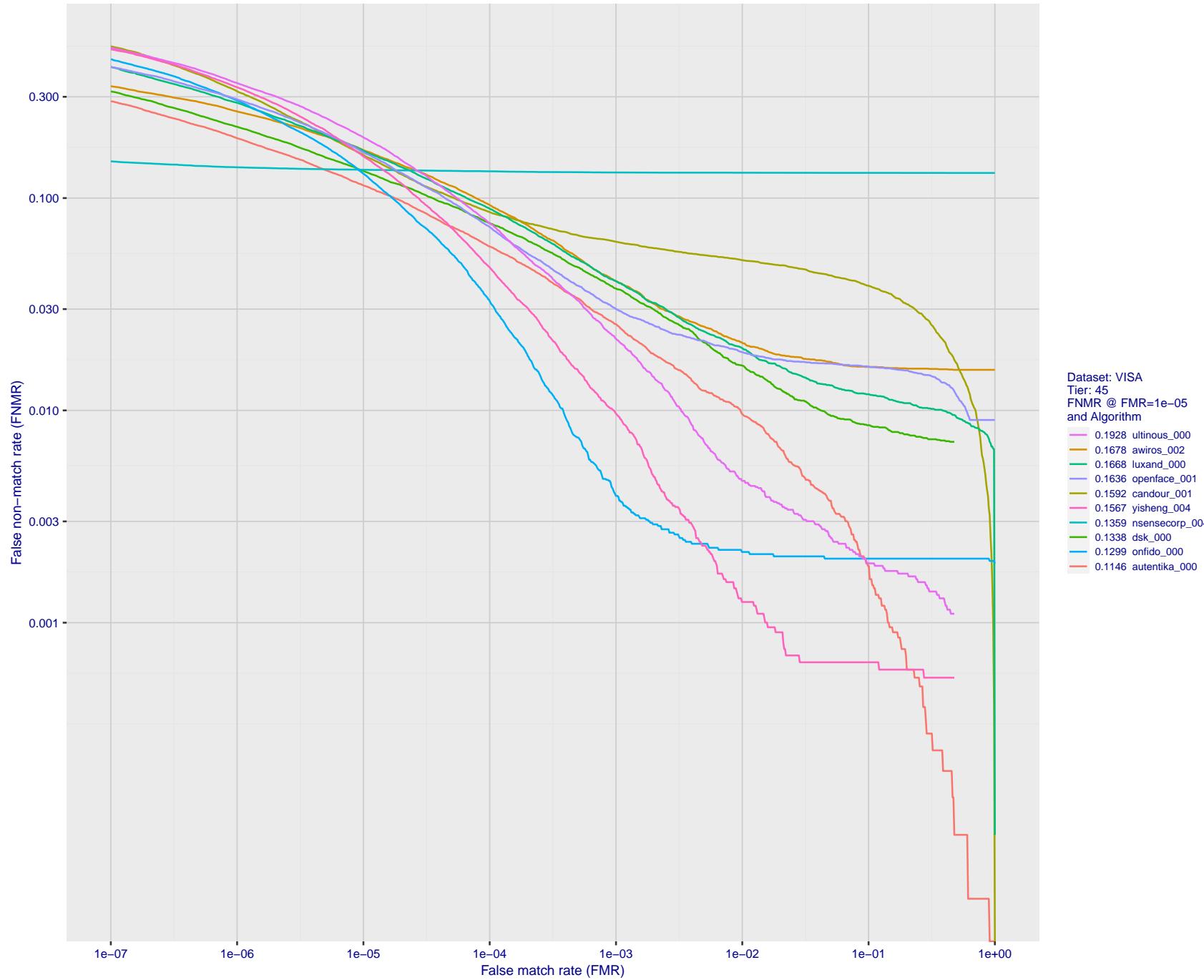


Figure 90: For the visa images, detection error tradeoff (DET) characteristics showing false non-match rate vs. false match rate plotted parametrically on threshold, T . The scales are logarithmic in order to show many decades of FMR.

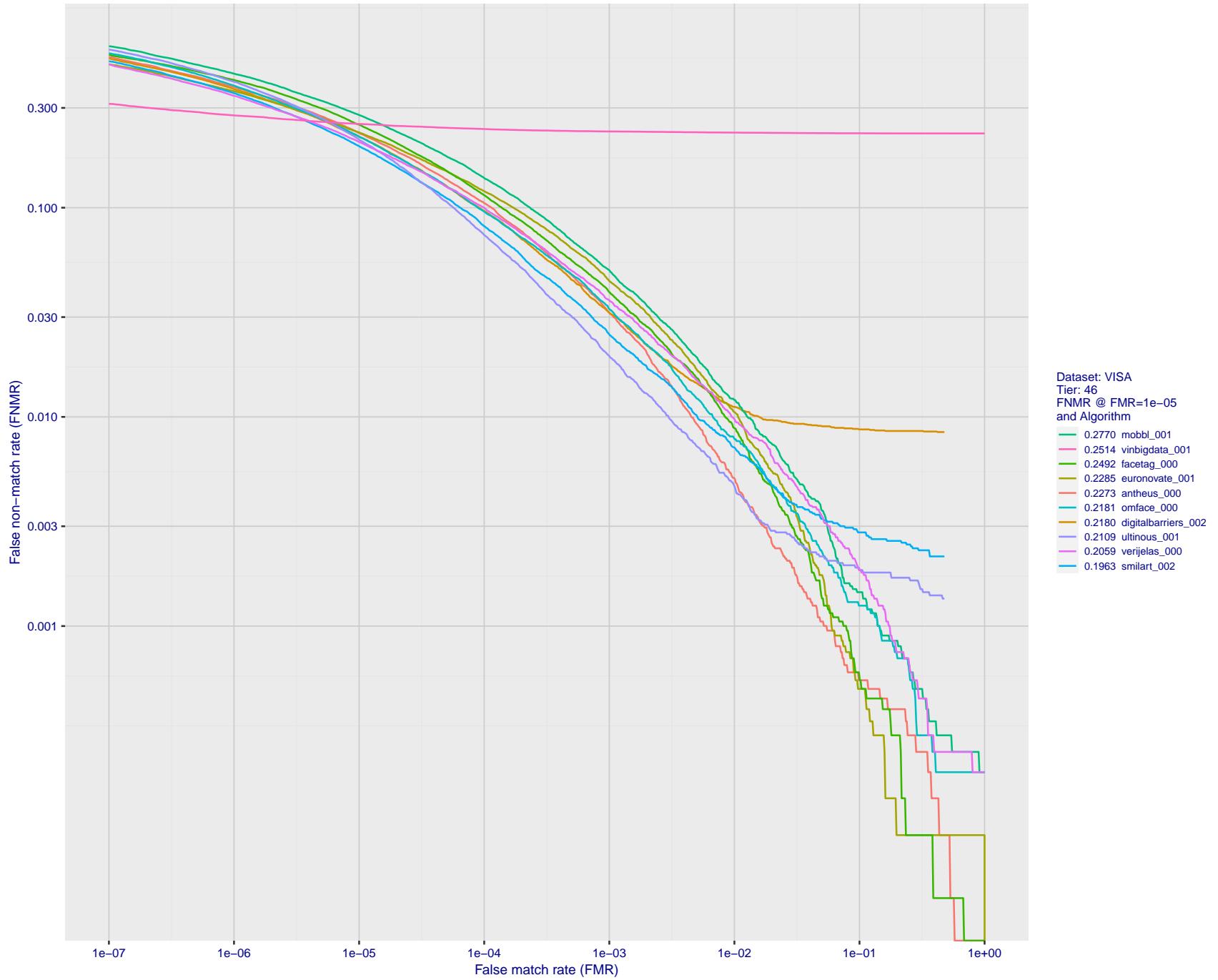


Figure 91: For the visa images, detection error tradeoff (DET) characteristics showing false non-match rate vs. false match rate plotted parametrically on threshold, T . The scales are logarithmic in order to show many decades of FMR.

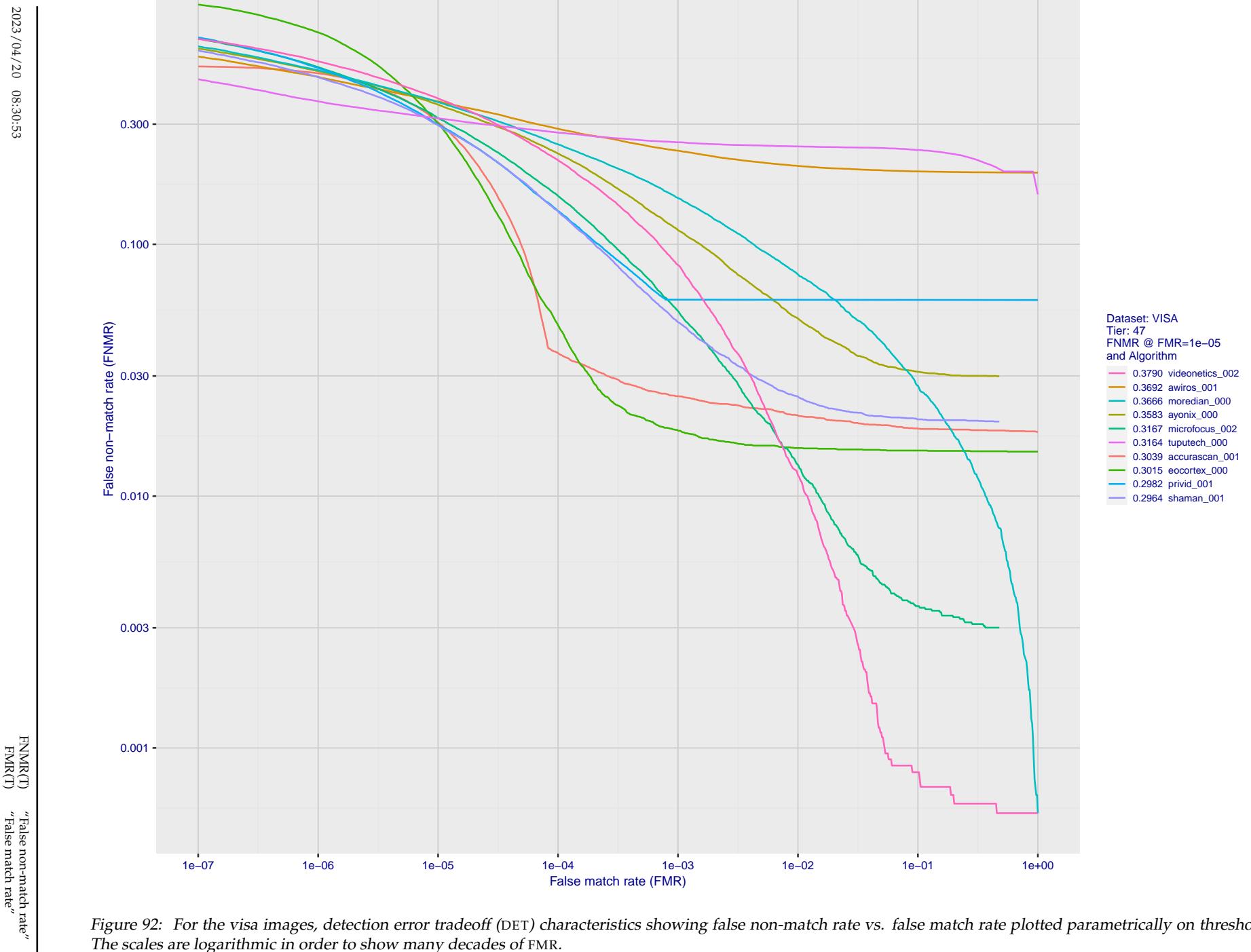


Figure 92: For the visa images, detection error tradeoff (DET) characteristics showing false non-match rate vs. false match rate plotted parametrically on threshold, T . The scales are logarithmic in order to show many decades of FMR.

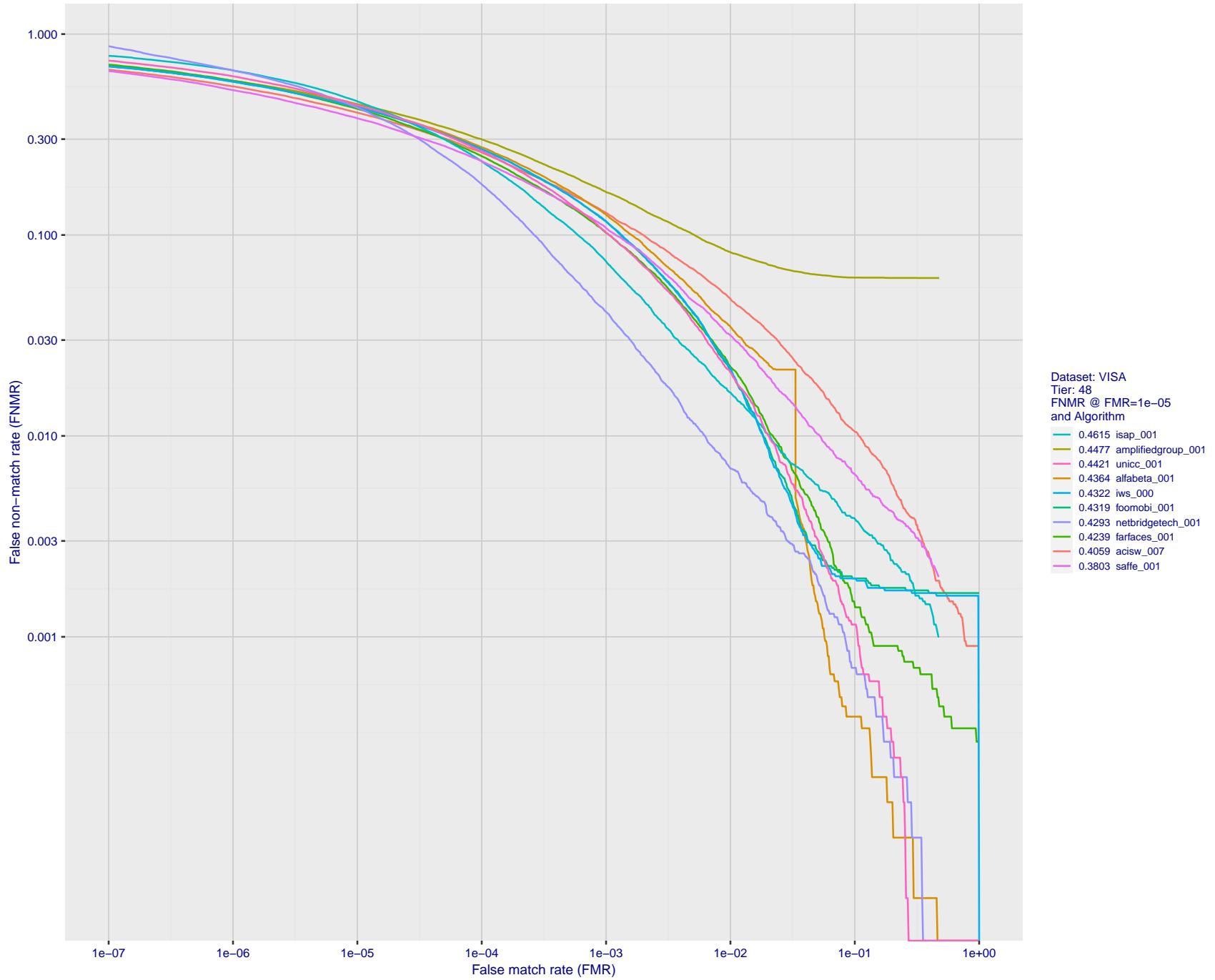


Figure 93: For the visa images, detection error tradeoff (DET) characteristics showing false non-match rate vs. false match rate plotted parametrically on threshold, T . The scales are logarithmic in order to show many decades of FMR.

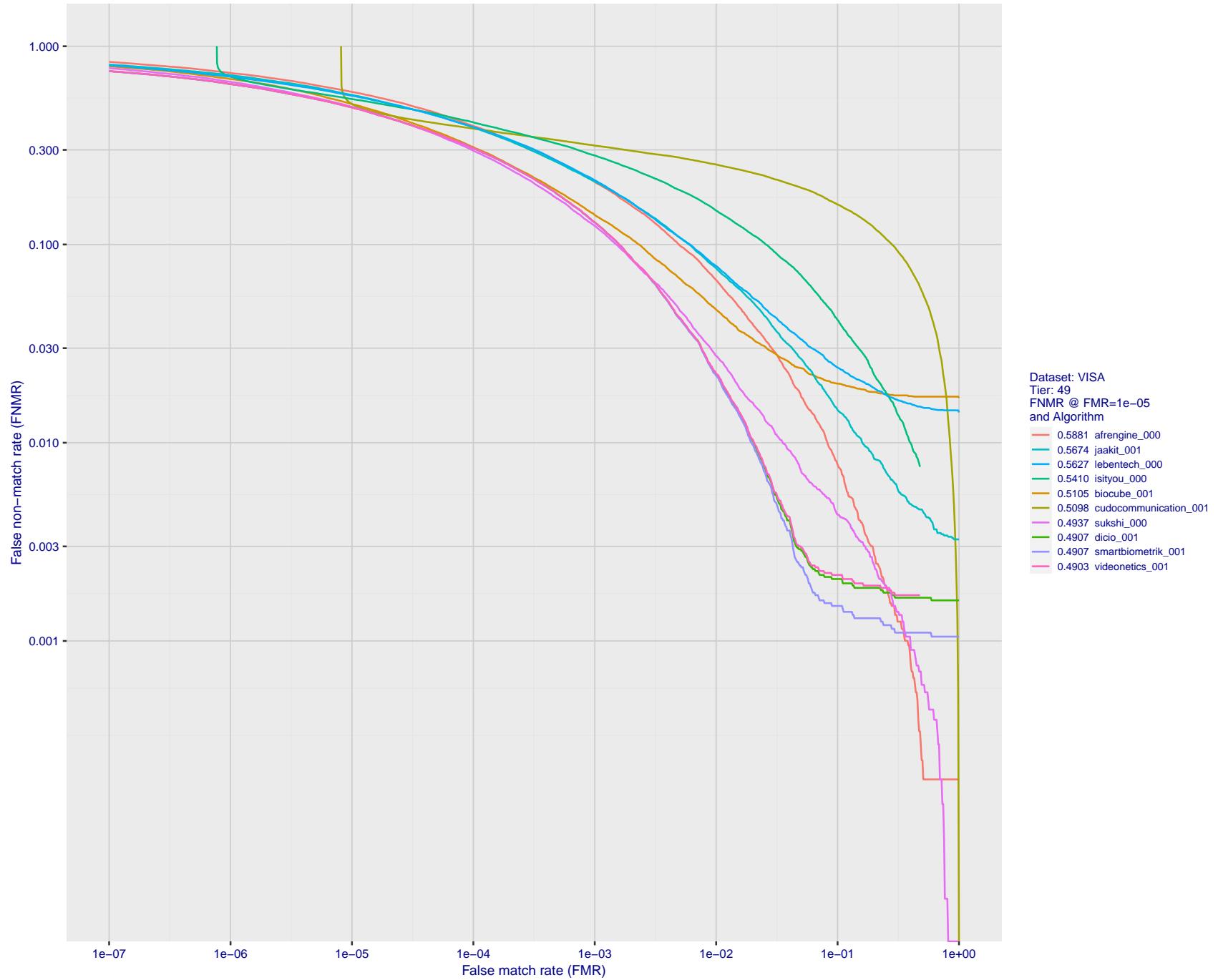


Figure 94: For the visa images, detection error tradeoff (DET) characteristics showing false non-match rate vs. false match rate plotted parametrically on threshold, T . The scales are logarithmic in order to show many decades of FMR.

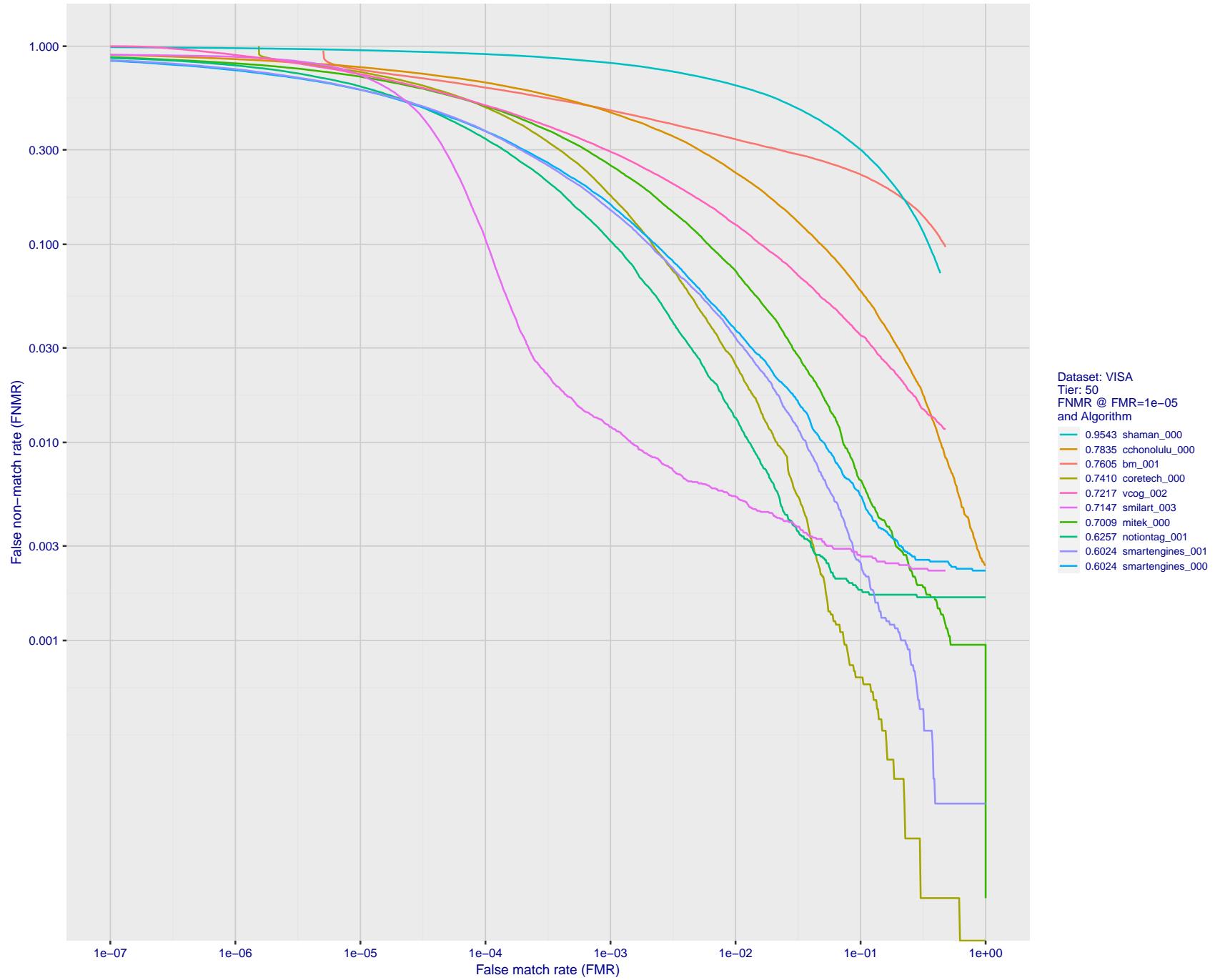


Figure 95: For the visa images, detection error tradeoff (DET) characteristics showing false non-match rate vs. false match rate plotted parametrically on threshold, T . The scales are logarithmic in order to show many decades of FMR.

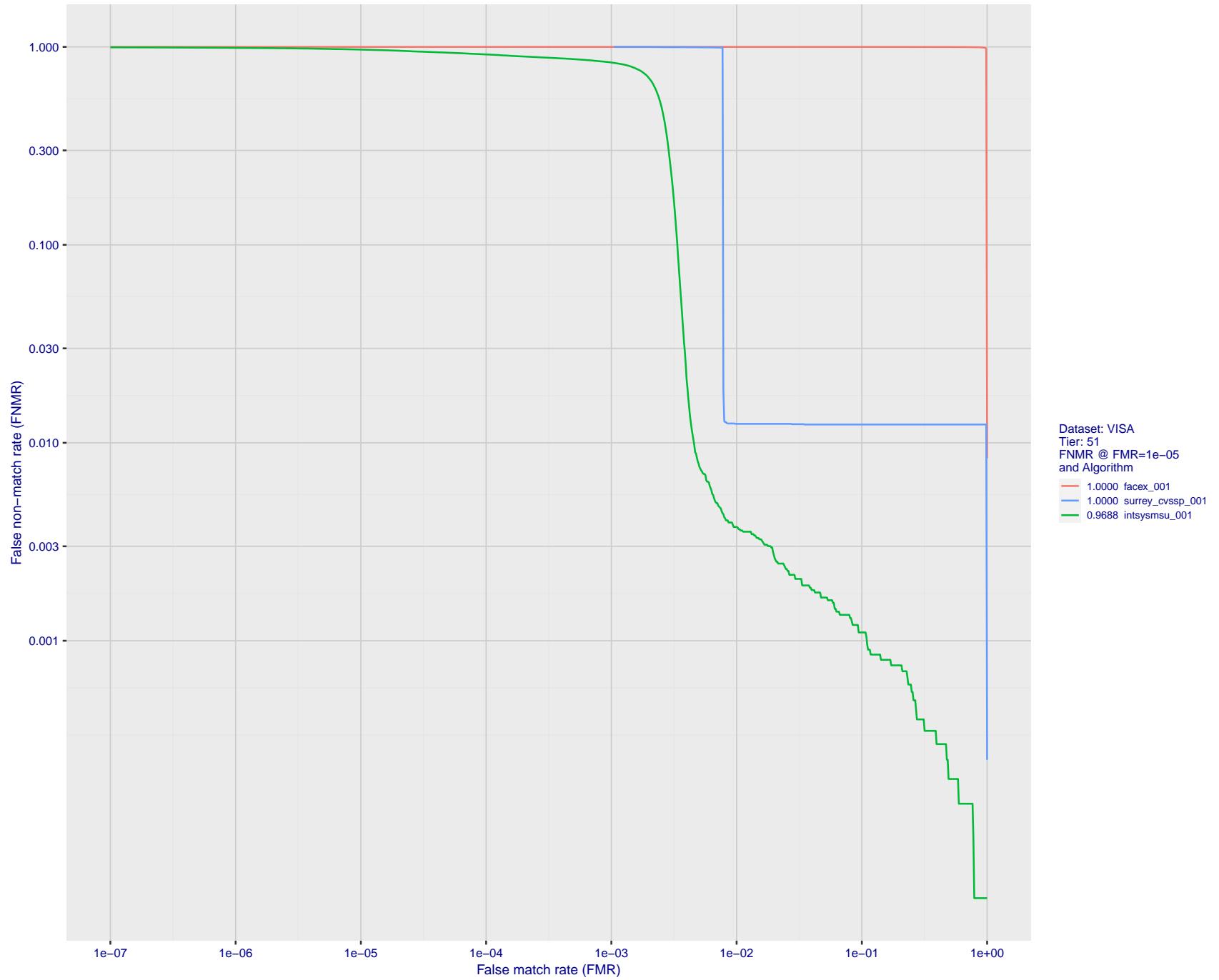


Figure 96: For the visa images, detection error tradeoff (DET) characteristics showing false non-match rate vs. false match rate plotted parametrically on threshold, T . The scales are logarithmic in order to show many decades of FMR.

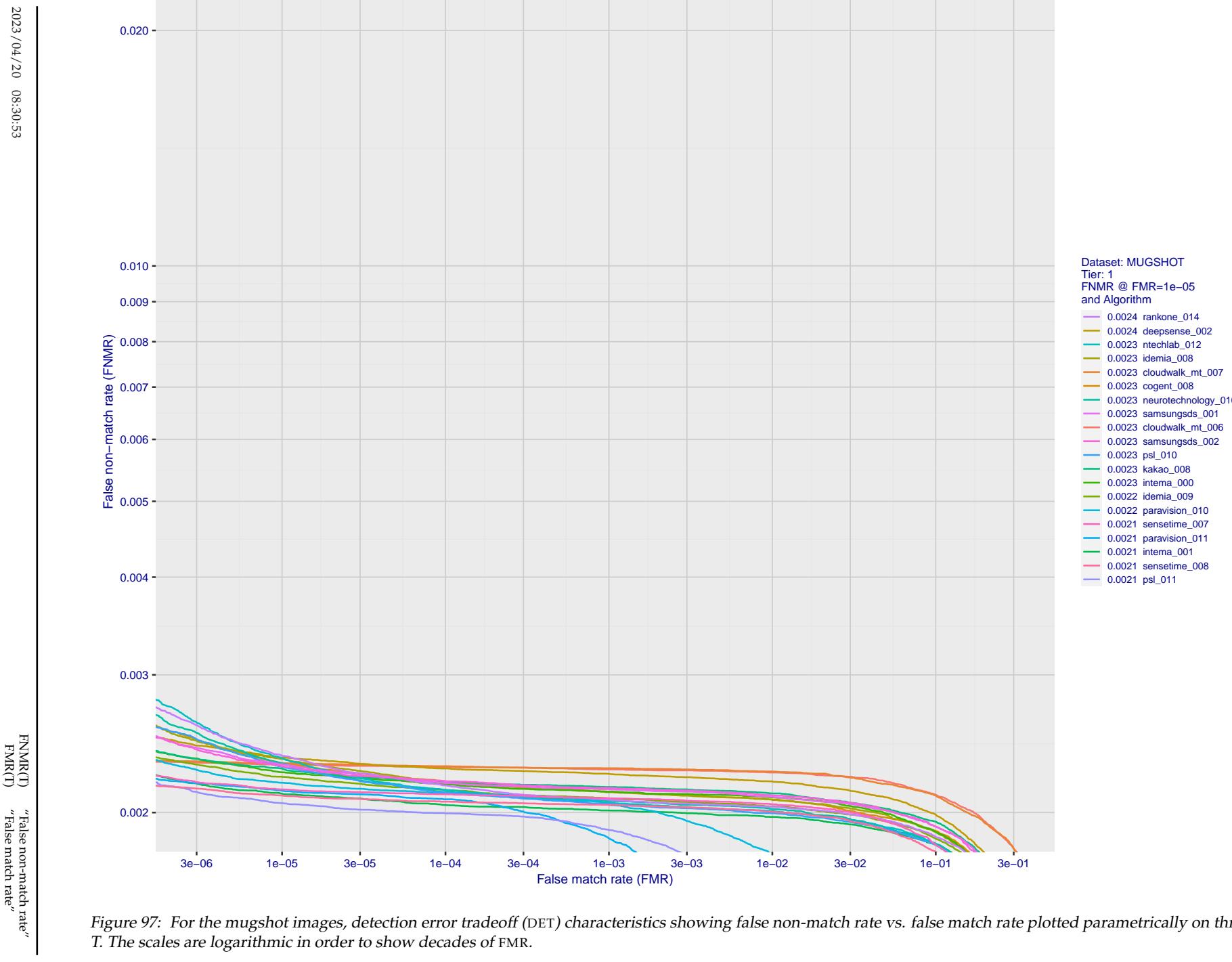
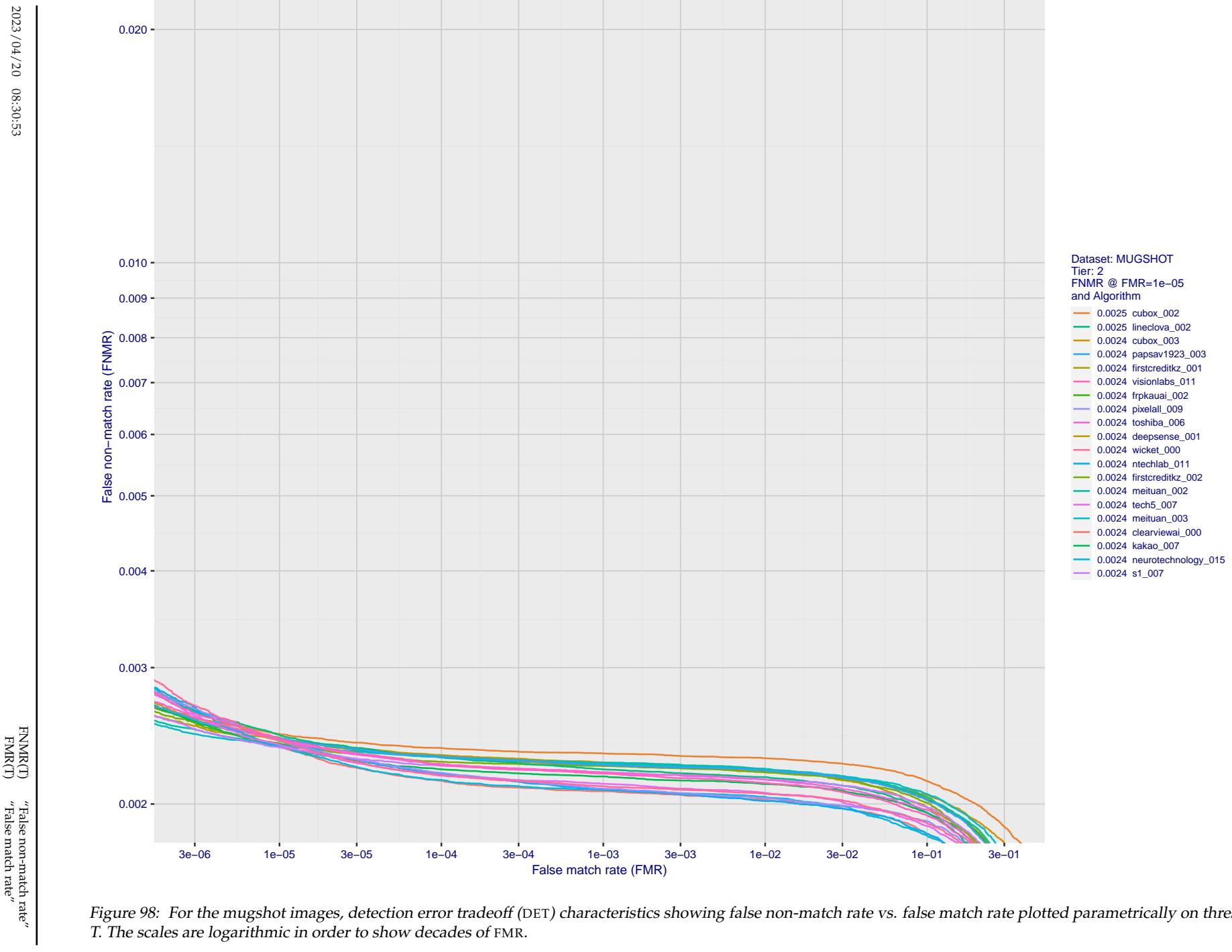


Figure 97: For the mugshot images, detection error tradeoff (DET) characteristics showing false non-match rate vs. false match rate plotted parametrically on threshold, T . The scales are logarithmic in order to show decades of FMR.



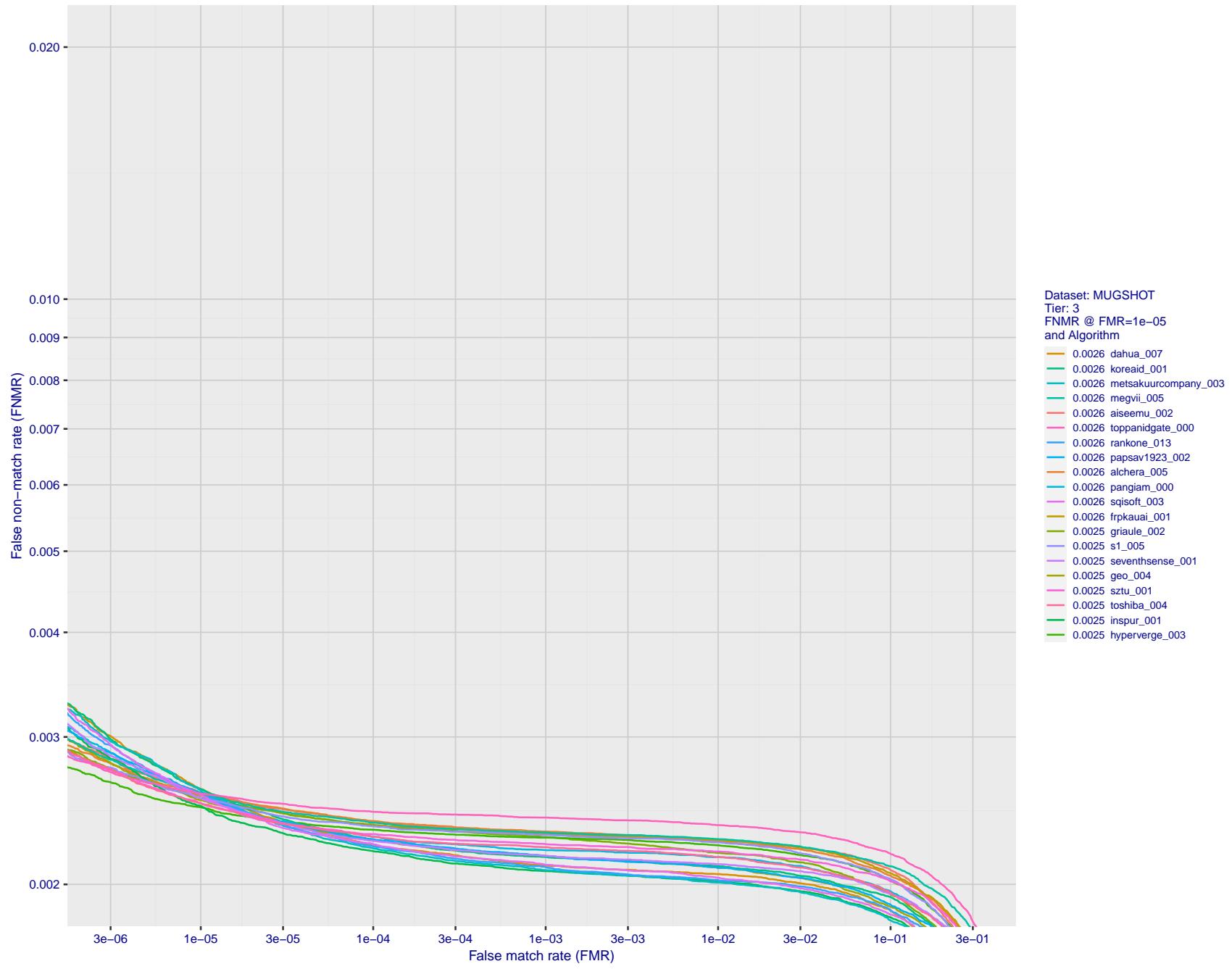
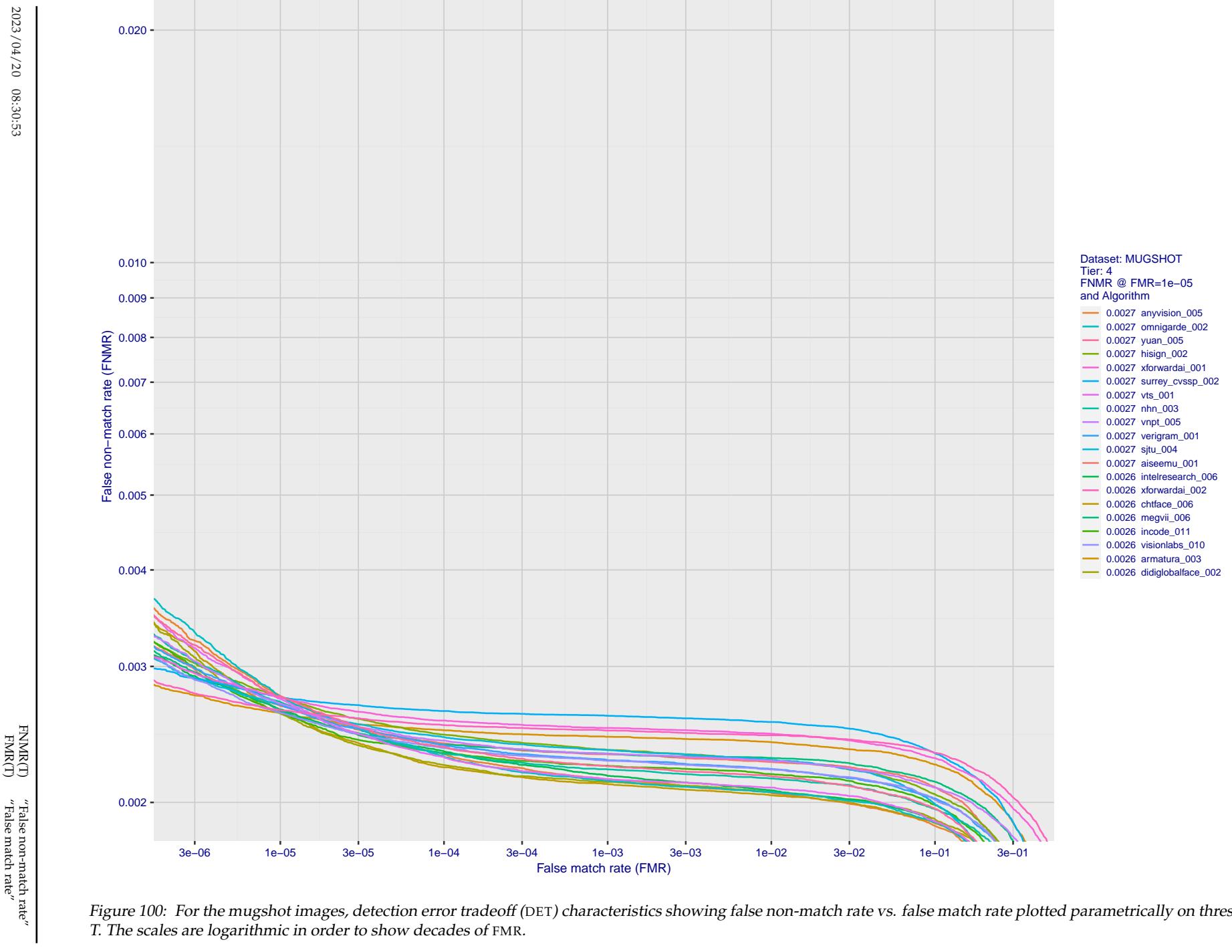


Figure 99: For the mugshot images, detection error tradeoff (DET) characteristics showing false non-match rate vs. false match rate plotted parametrically on threshold, T . The scales are logarithmic in order to show decades of FMR.



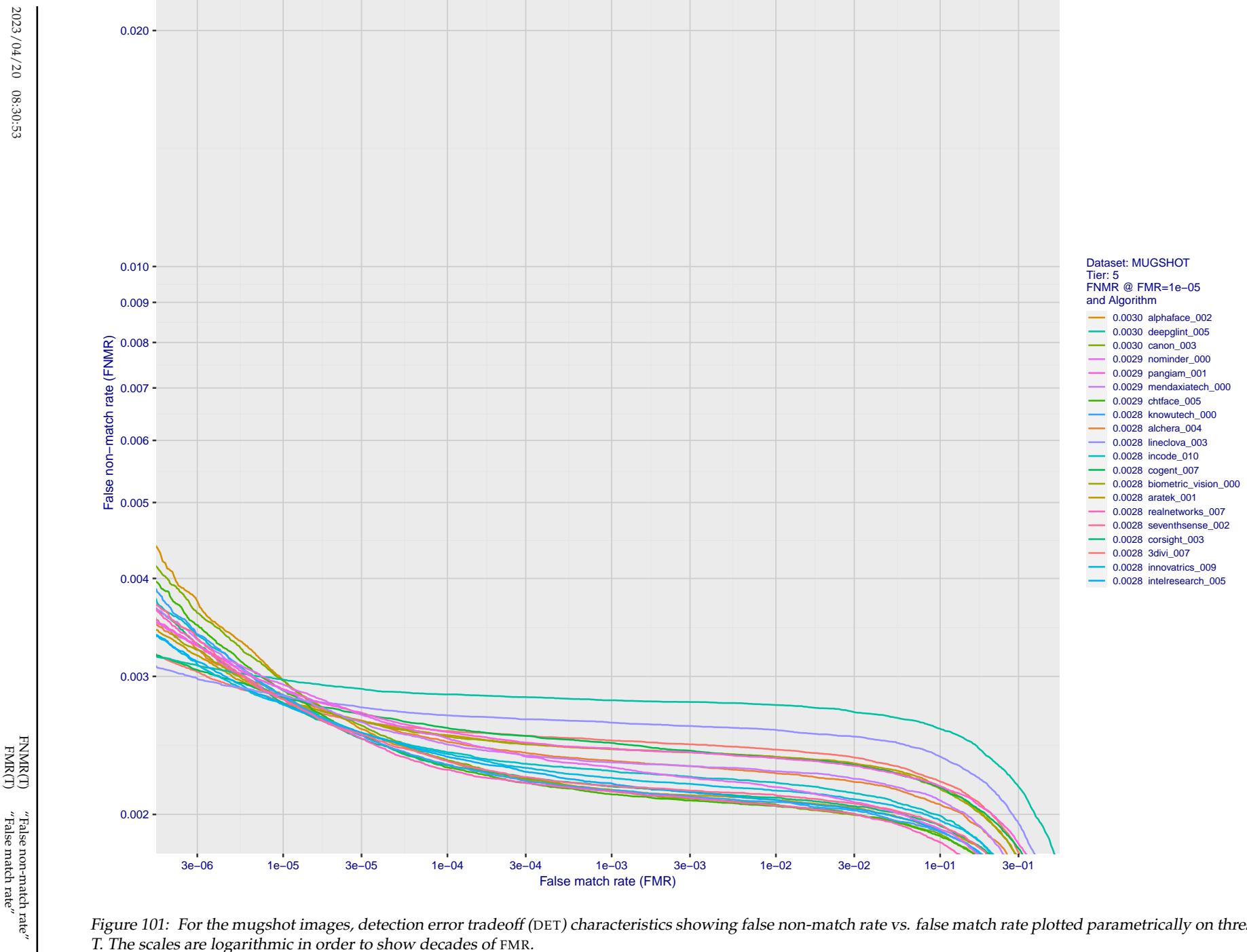


Figure 101: For the mugshot images, detection error tradeoff (DET) characteristics showing false non-match rate vs. false match rate plotted parametrically on threshold, T . The scales are logarithmic in order to show decades of FMR.

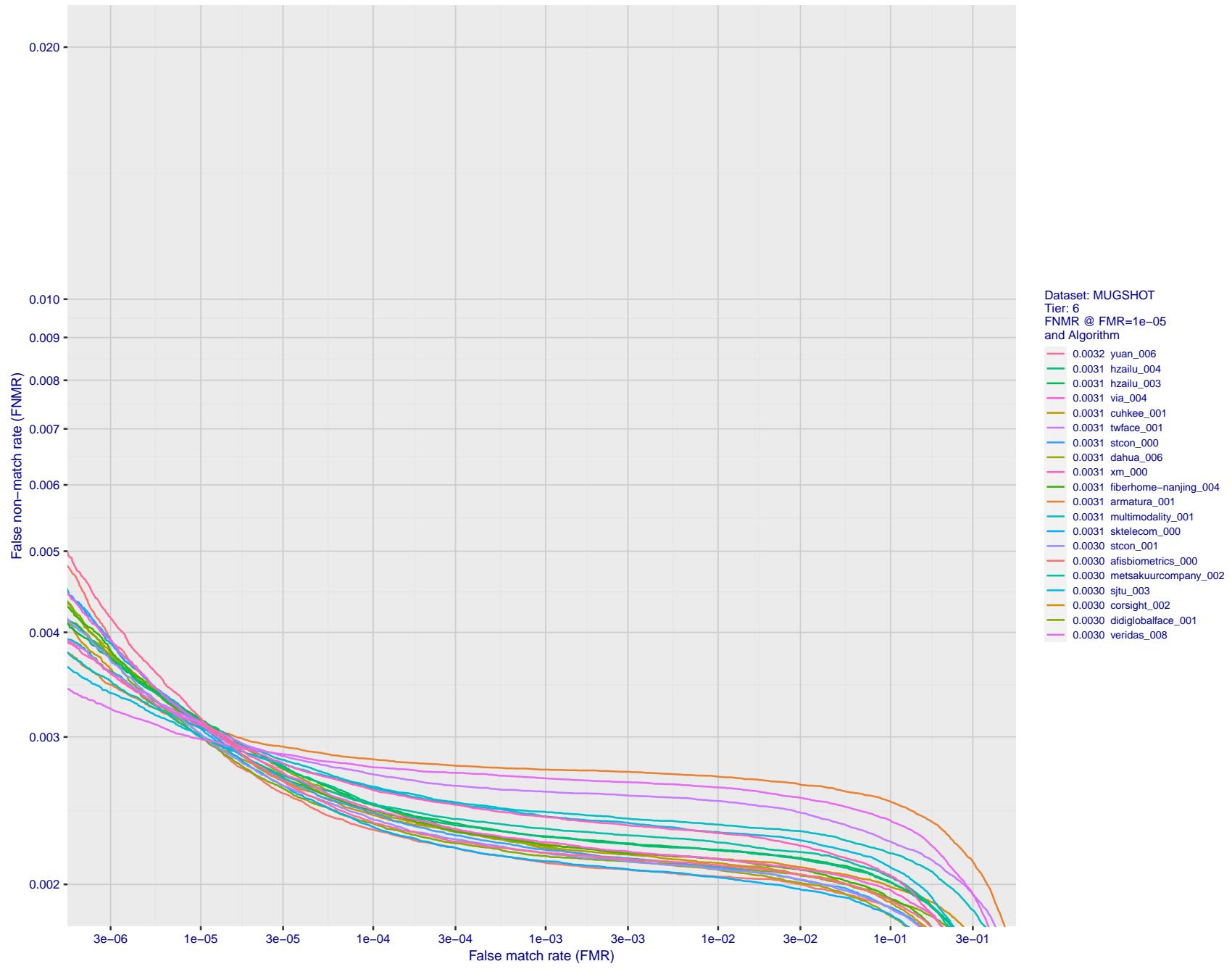


Figure 102: For the mugshot images, detection error tradeoff (DET) characteristics showing false non-match rate vs. false match rate plotted parametrically on threshold, T . The scales are logarithmic in order to show decades of FMR.

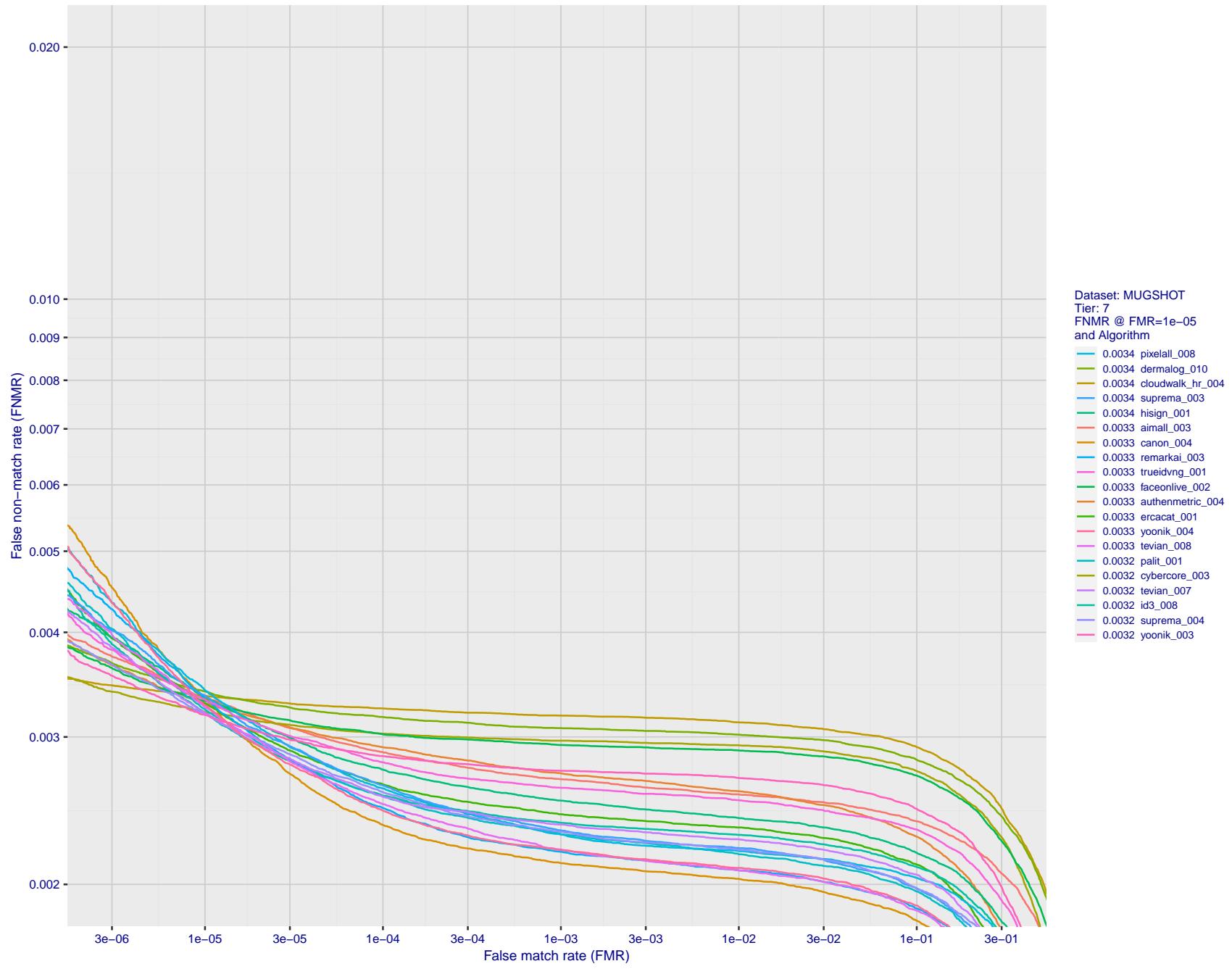


Figure 103: For the mugshot images, detection error tradeoff (DET) characteristics showing false non-match rate vs. false match rate plotted parametrically on threshold, T . The scales are logarithmic in order to show decades of FMR.

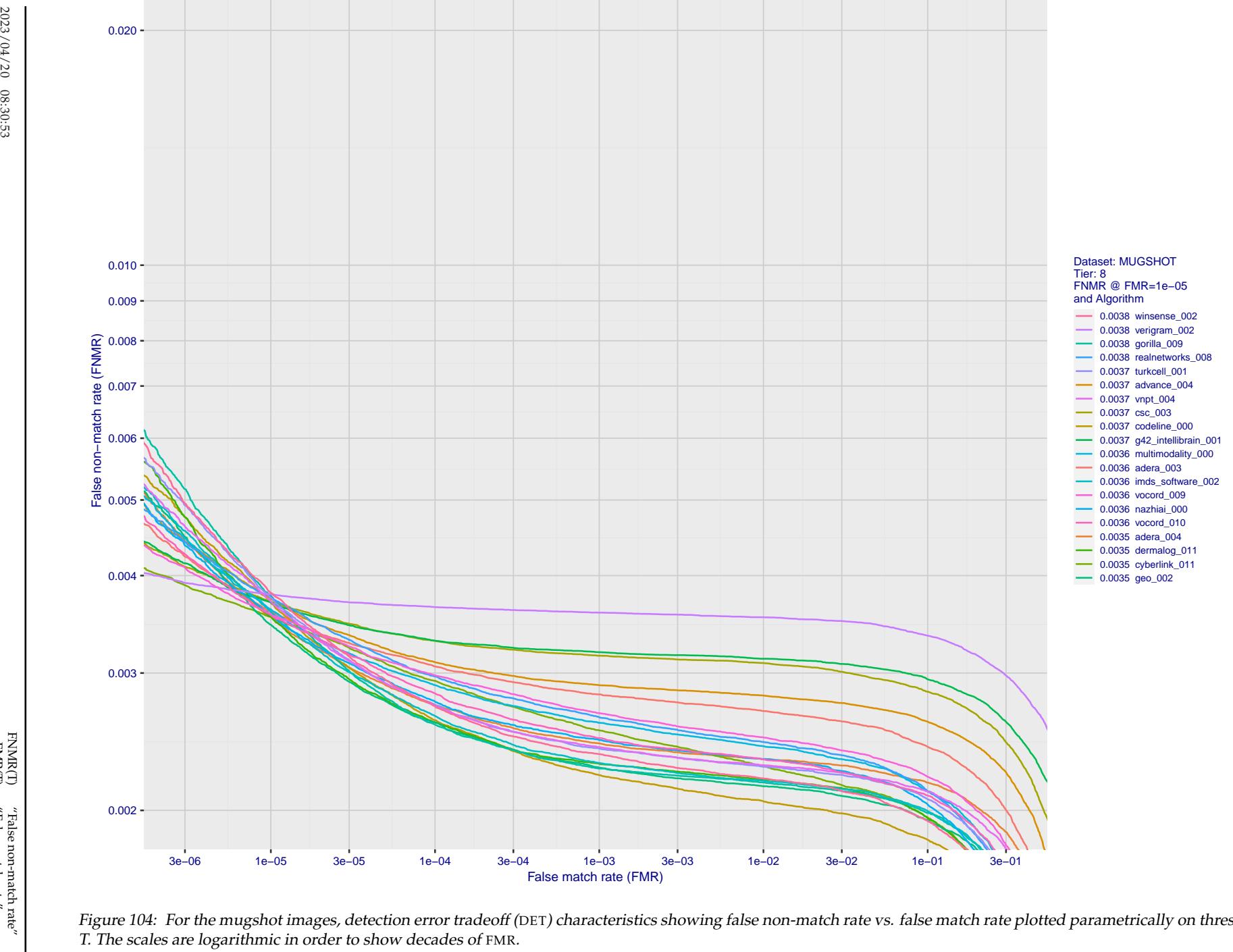


Figure 104: For the mugshot images, detection error tradeoff (DET) characteristics showing false non-match rate vs. false match rate plotted parametrically on threshold, T . The scales are logarithmic in order to show decades of FMR.

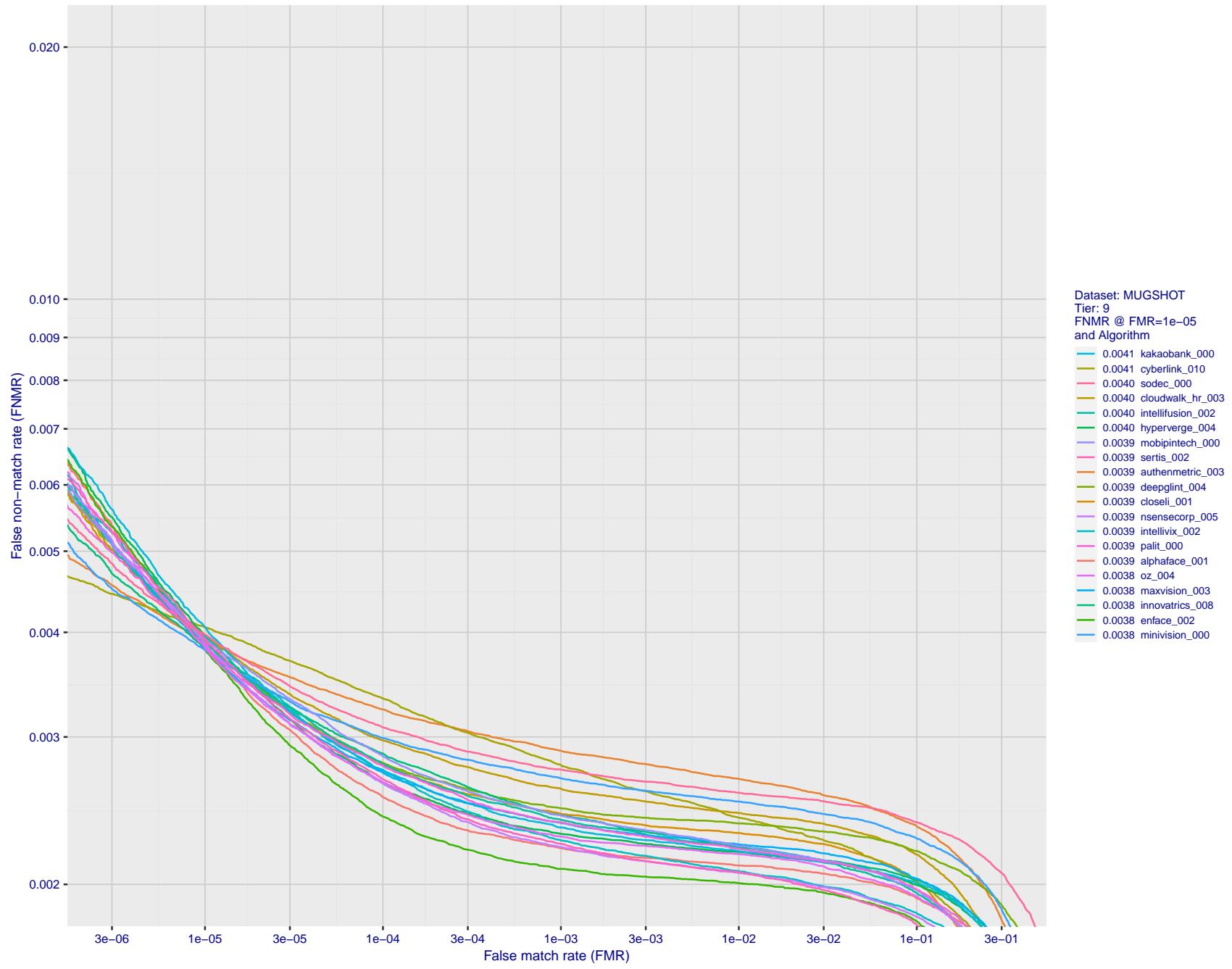


Figure 105: For the mugshot images, detection error tradeoff (DET) characteristics showing false non-match rate vs. false match rate plotted parametrically on threshold, T . The scales are logarithmic in order to show decades of FMR.

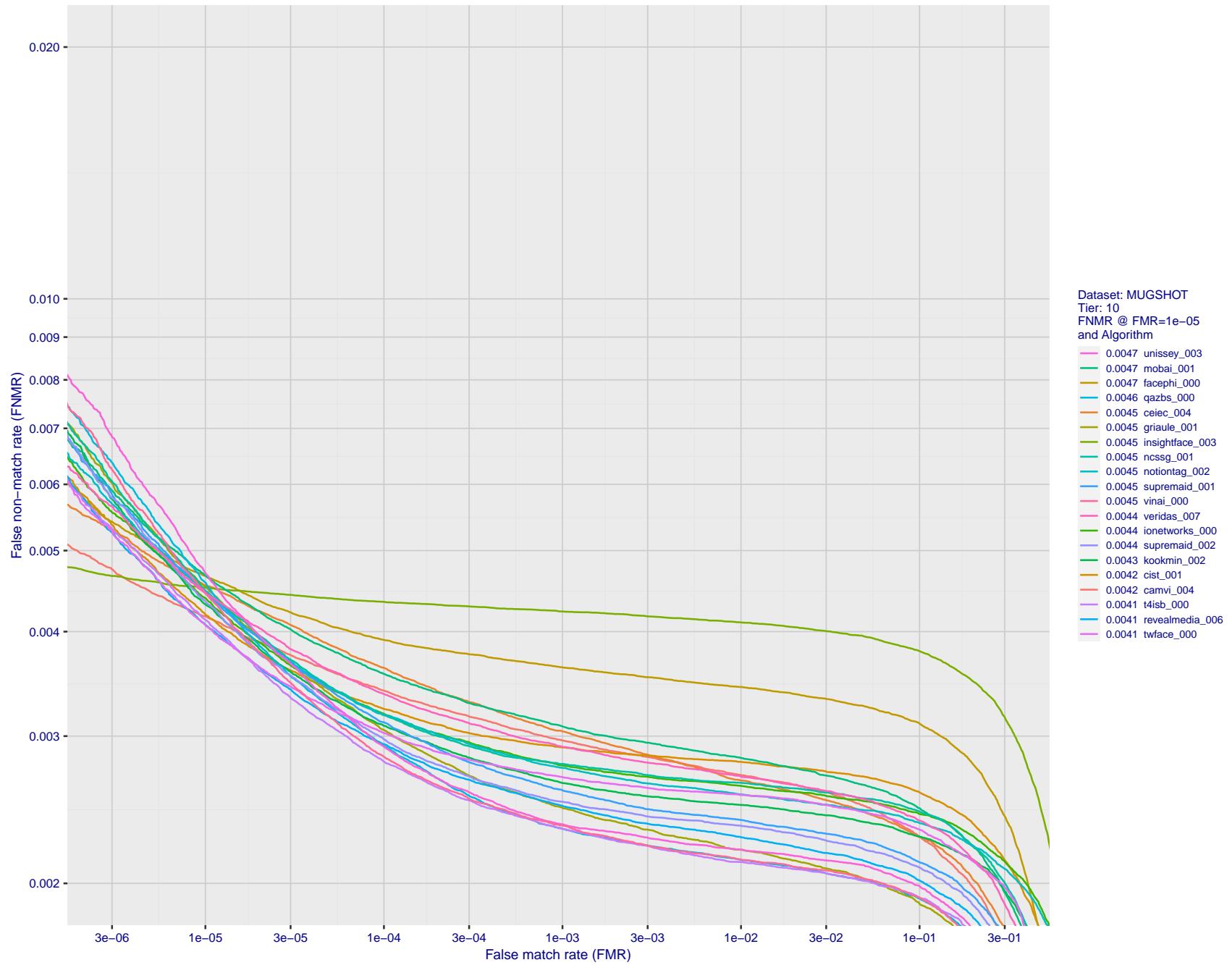


Figure 106: For the mugshot images, detection error tradeoff (DET) characteristics showing false non-match rate vs. false match rate plotted parametrically on threshold, T . The scales are logarithmic in order to show decades of FMR.

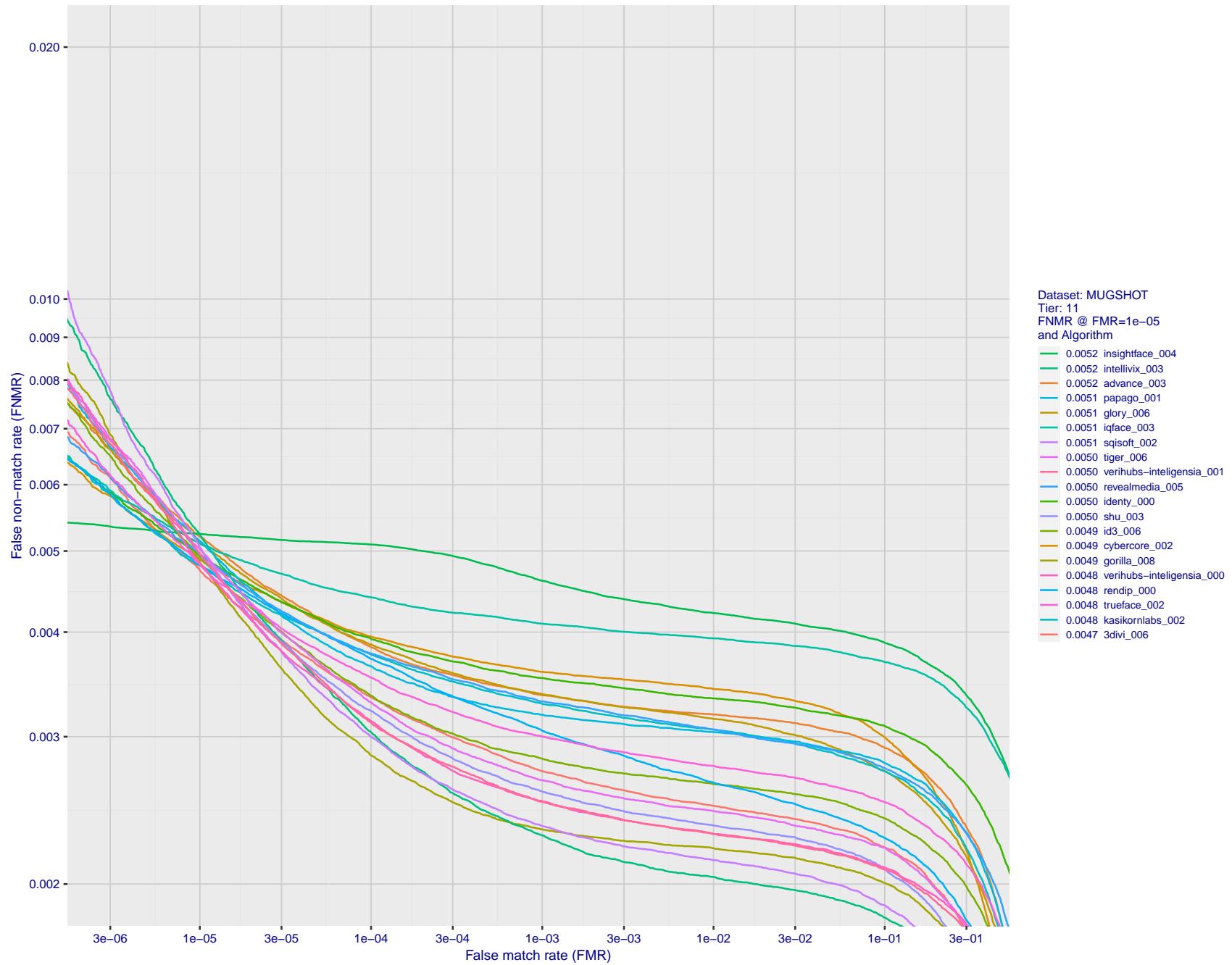


Figure 107: For the mugshot images, detection error tradeoff (DET) characteristics showing false non-match rate vs. false match rate plotted parametrically on threshold, T. The scales are logarithmic in order to show decades of FMR.

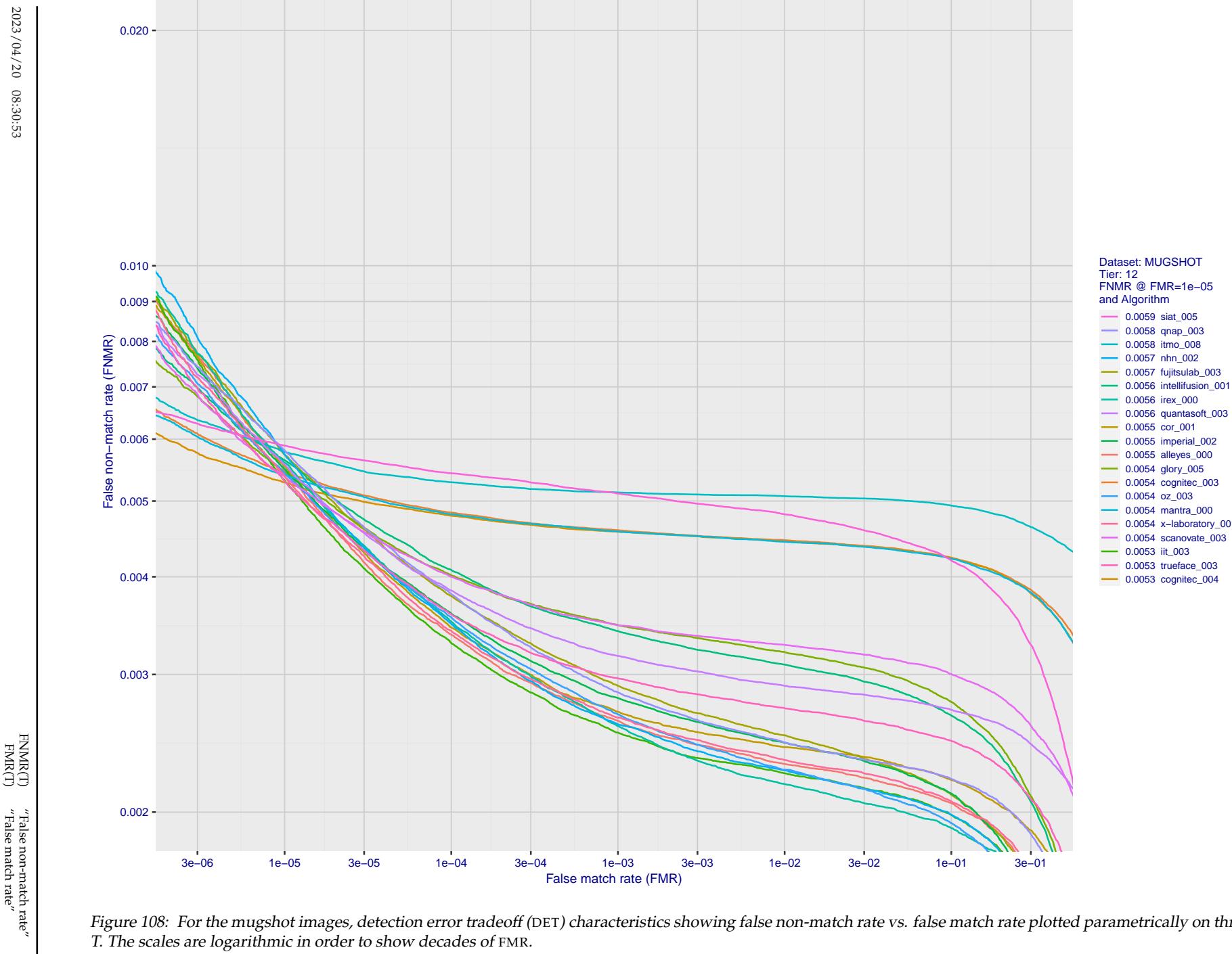


Figure 108: For the mugshot images, detection error tradeoff (DET) characteristics showing false non-match rate vs. false match rate plotted parametrically on threshold, T . The scales are logarithmic in order to show decades of FMR.

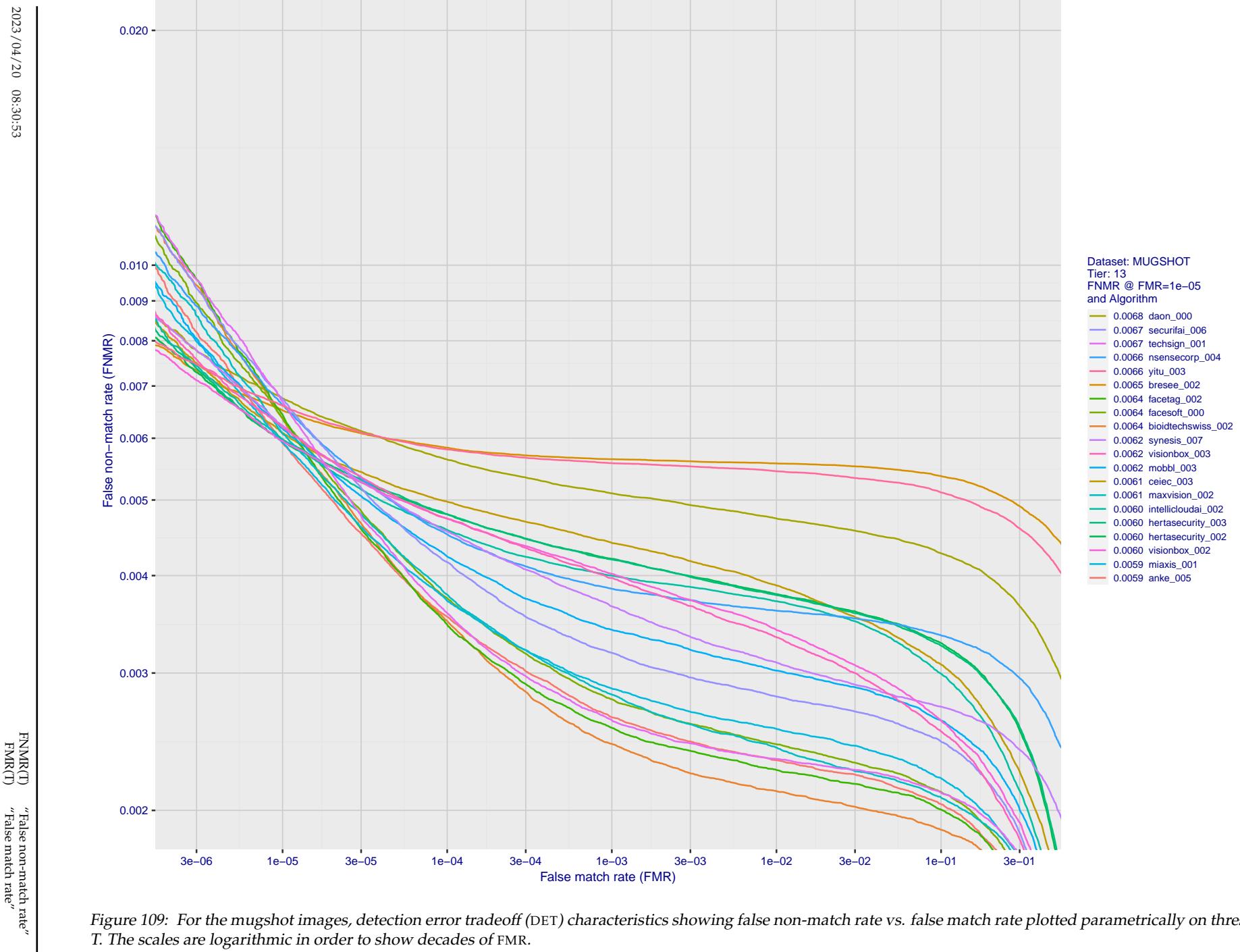


Figure 109: For the mugshot images, detection error tradeoff (DET) characteristics showing false non-match rate vs. false match rate plotted parametrically on threshold, T . The scales are logarithmic in order to show decades of FMR.

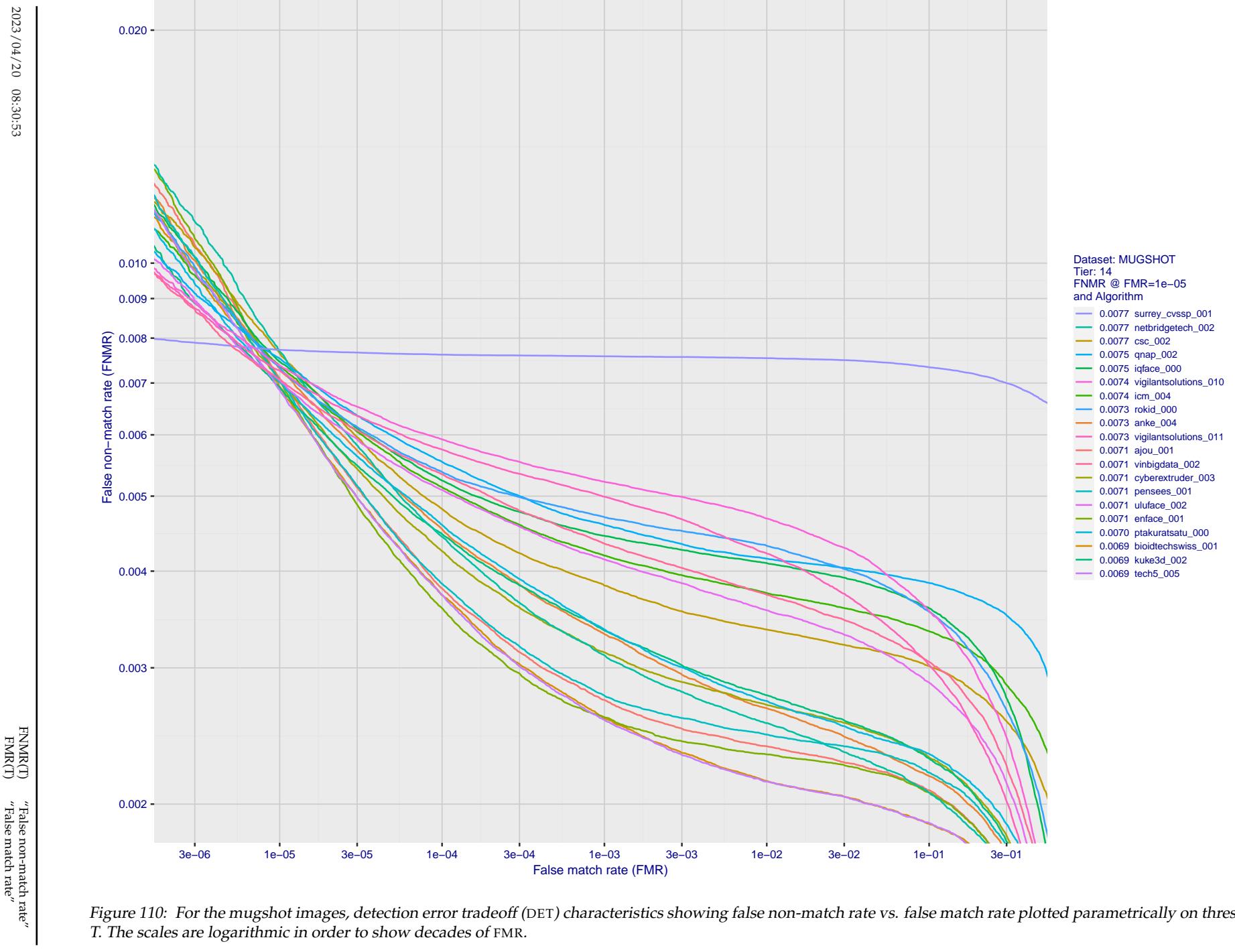


Figure 110: For the mugshot images, detection error tradeoff (DET) characteristics showing false non-match rate vs. false match rate plotted parametrically on threshold, T . The scales are logarithmic in order to show decades of FMR.

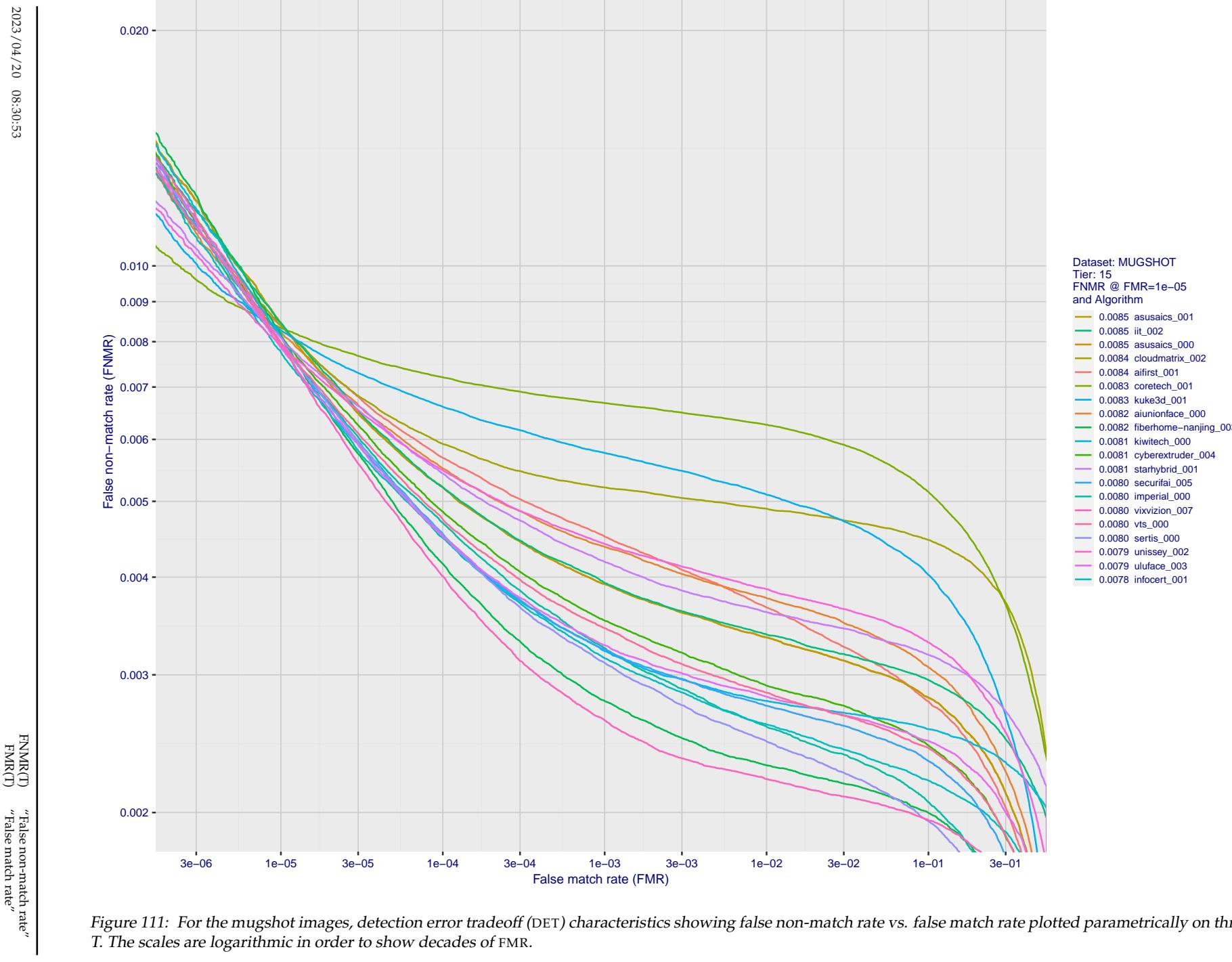


Figure 111: For the mugshot images, detection error tradeoff (DET) characteristics showing false non-match rate vs. false match rate plotted parametrically on threshold, T . The scales are logarithmic in order to show decades of FMR.

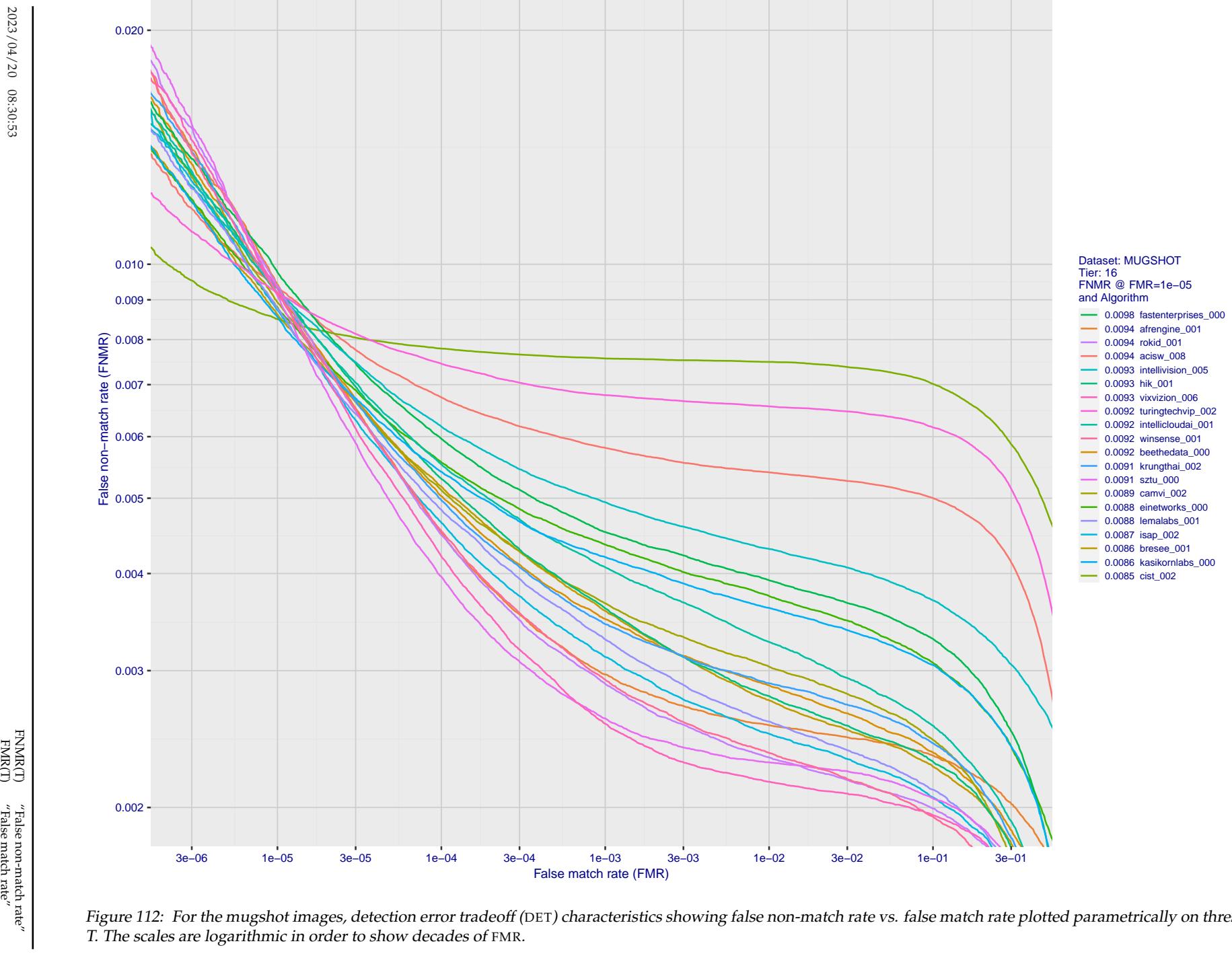


Figure 112: For the mugshot images, detection error tradeoff (DET) characteristics showing false non-match rate vs. false match rate plotted parametrically on threshold, T . The scales are logarithmic in order to show decades of FMR.

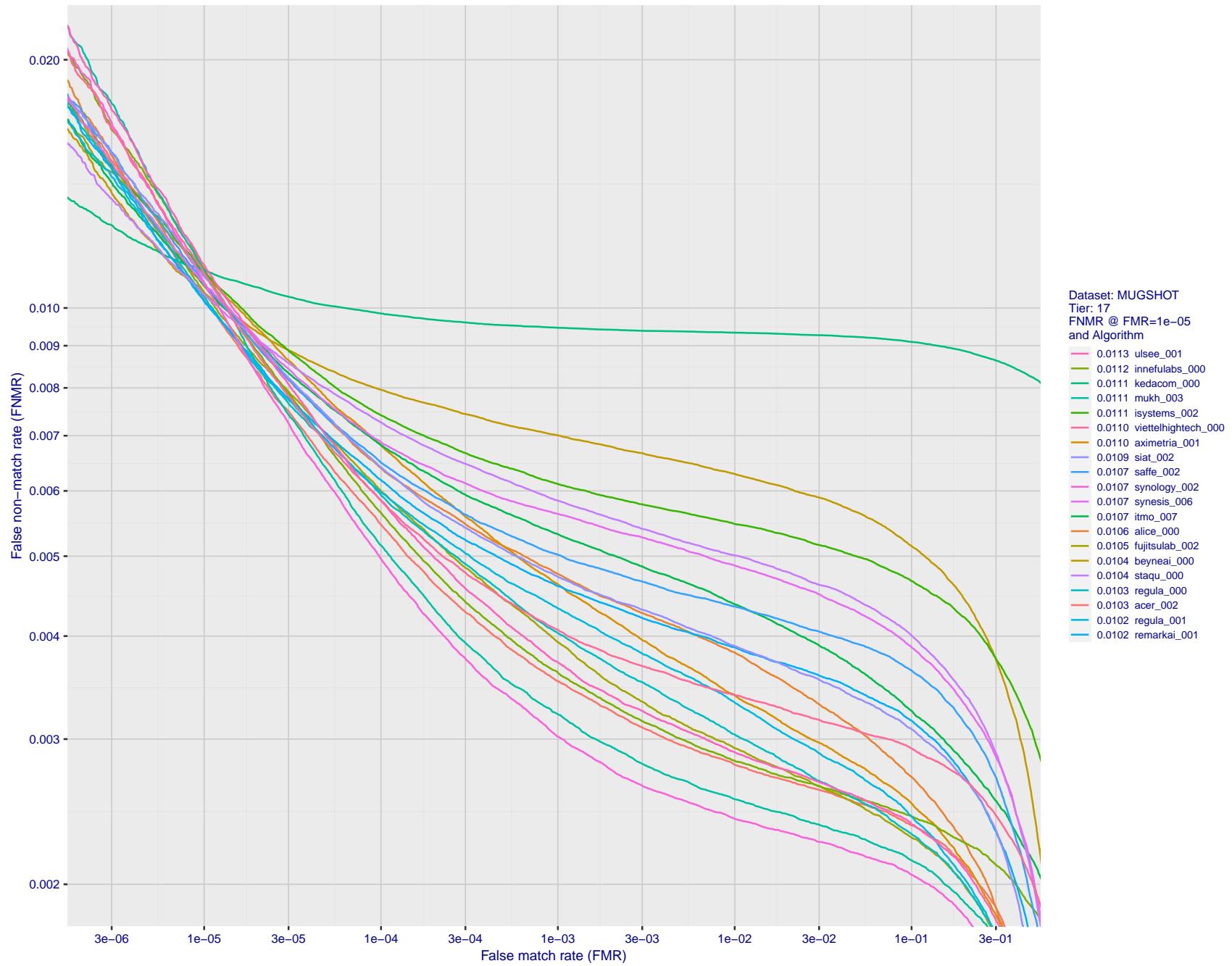


Figure 113: For the mugshot images, detection error tradeoff (DET) characteristics showing false non-match rate vs. false match rate plotted parametrically on threshold, T . The scales are logarithmic in order to show decades of FMR.

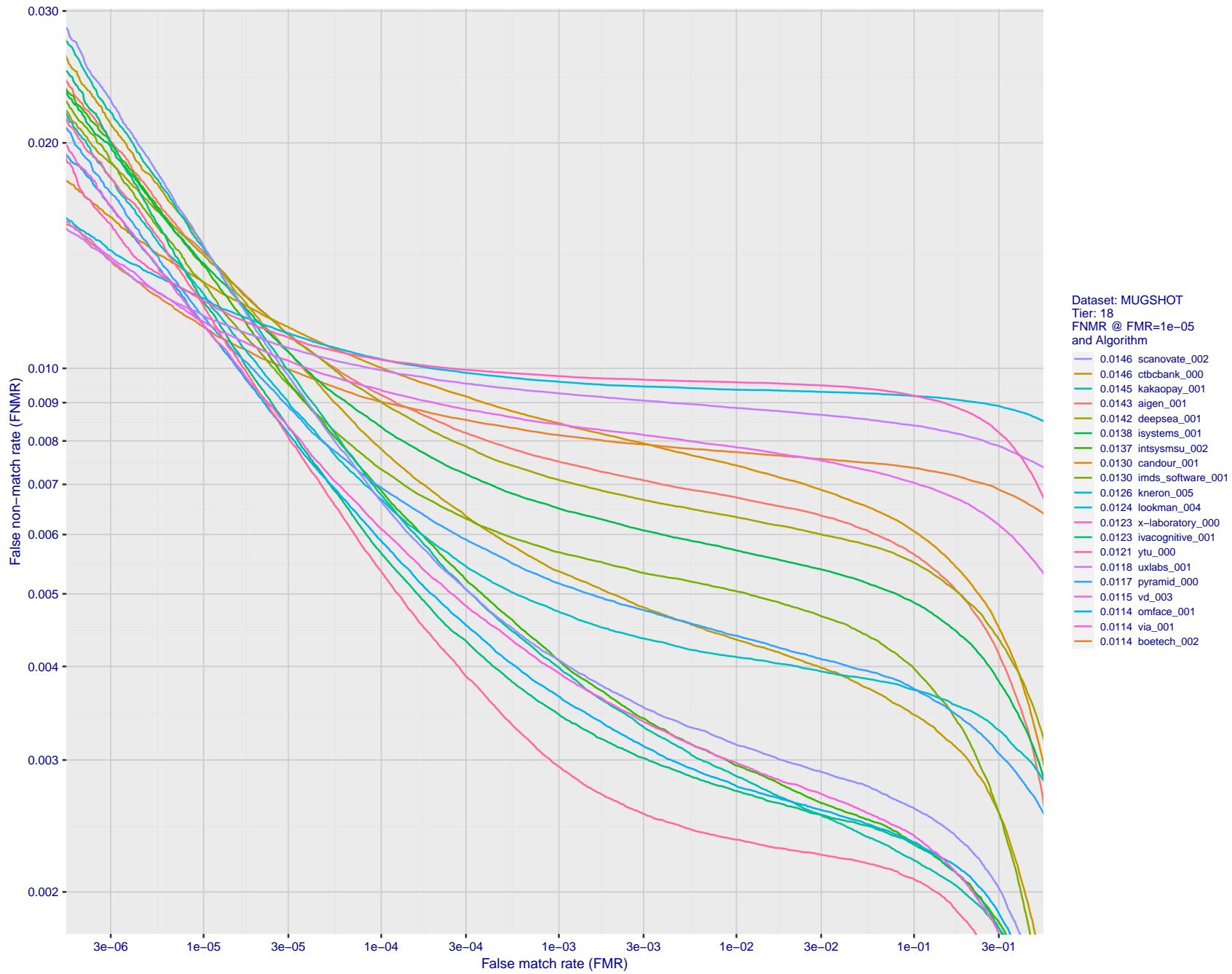


Figure 114: For the mugshot images, detection error tradeoff (DET) characteristics showing false non-match rate vs. false match rate plotted parametrically on threshold, T . The scales are logarithmic in order to show decades of FMR.

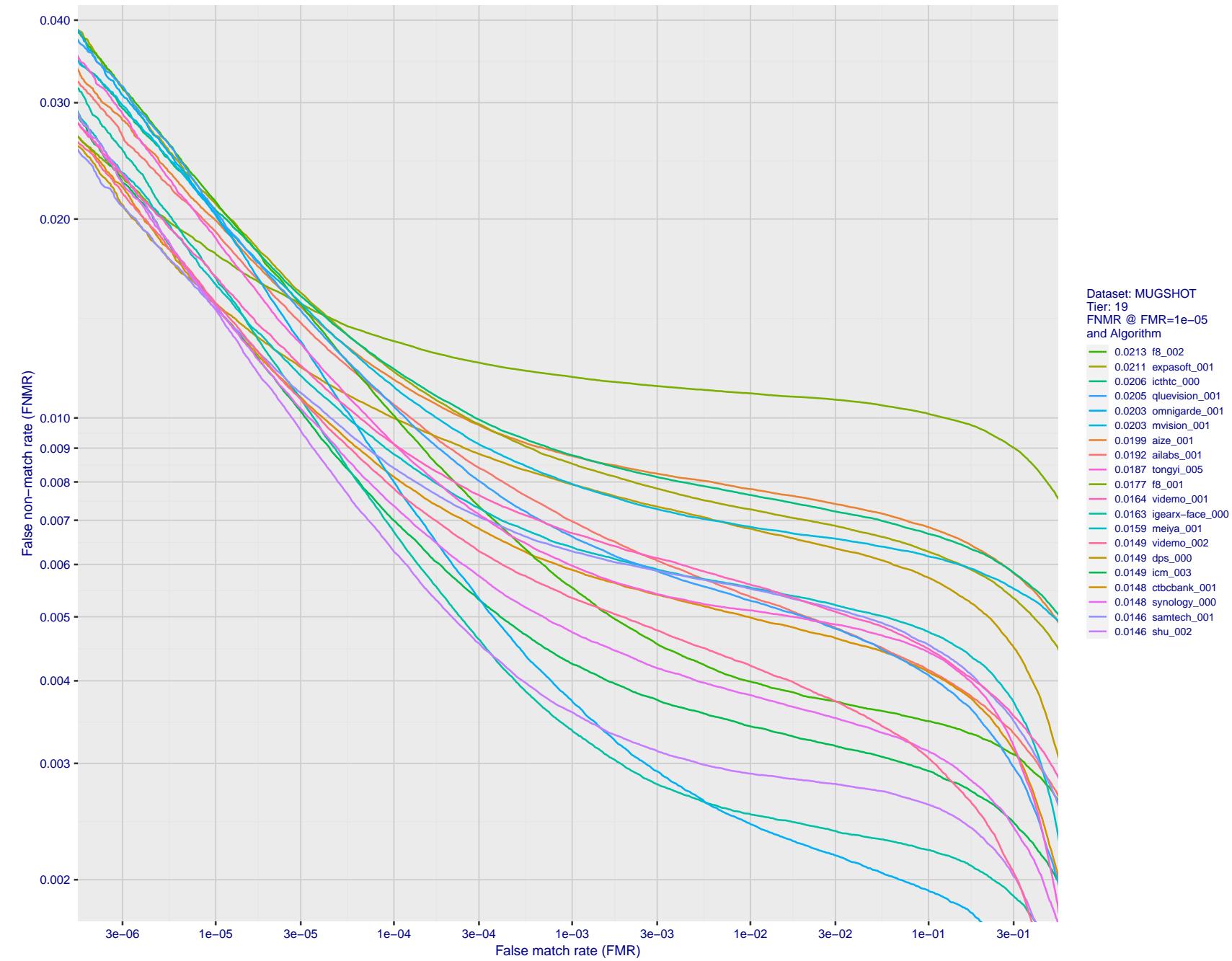


Figure 115: For the mugshot images, detection error tradeoff (DET) characteristics showing false non-match rate vs. false match rate plotted parametrically on threshold, T. The scales are logarithmic in order to show decades of FMR.

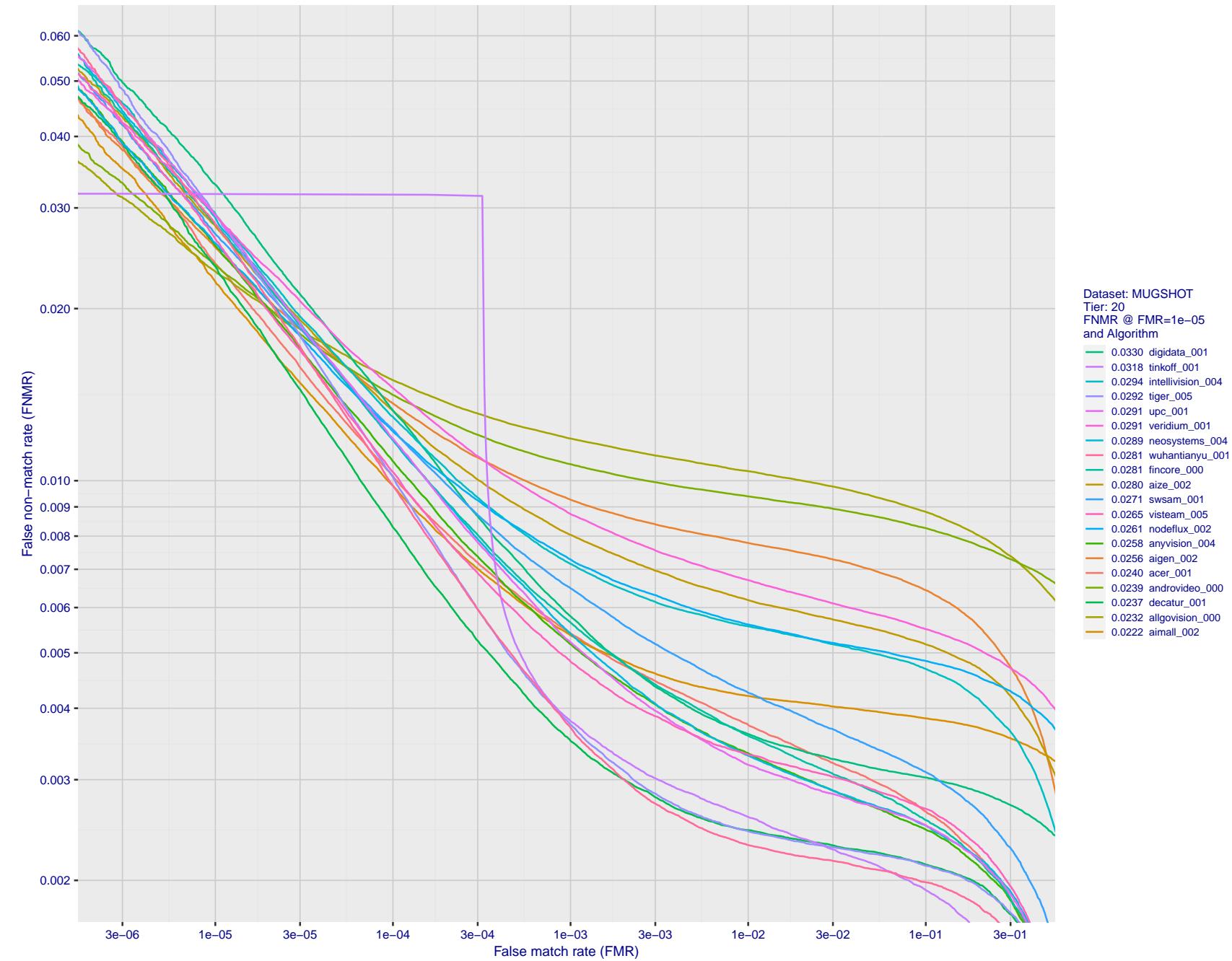


Figure 116: For the mugshot images, detection error tradeoff (DET) characteristics showing false non-match rate vs. false match rate plotted parametrically on threshold, T . The scales are logarithmic in order to show decades of FMR.

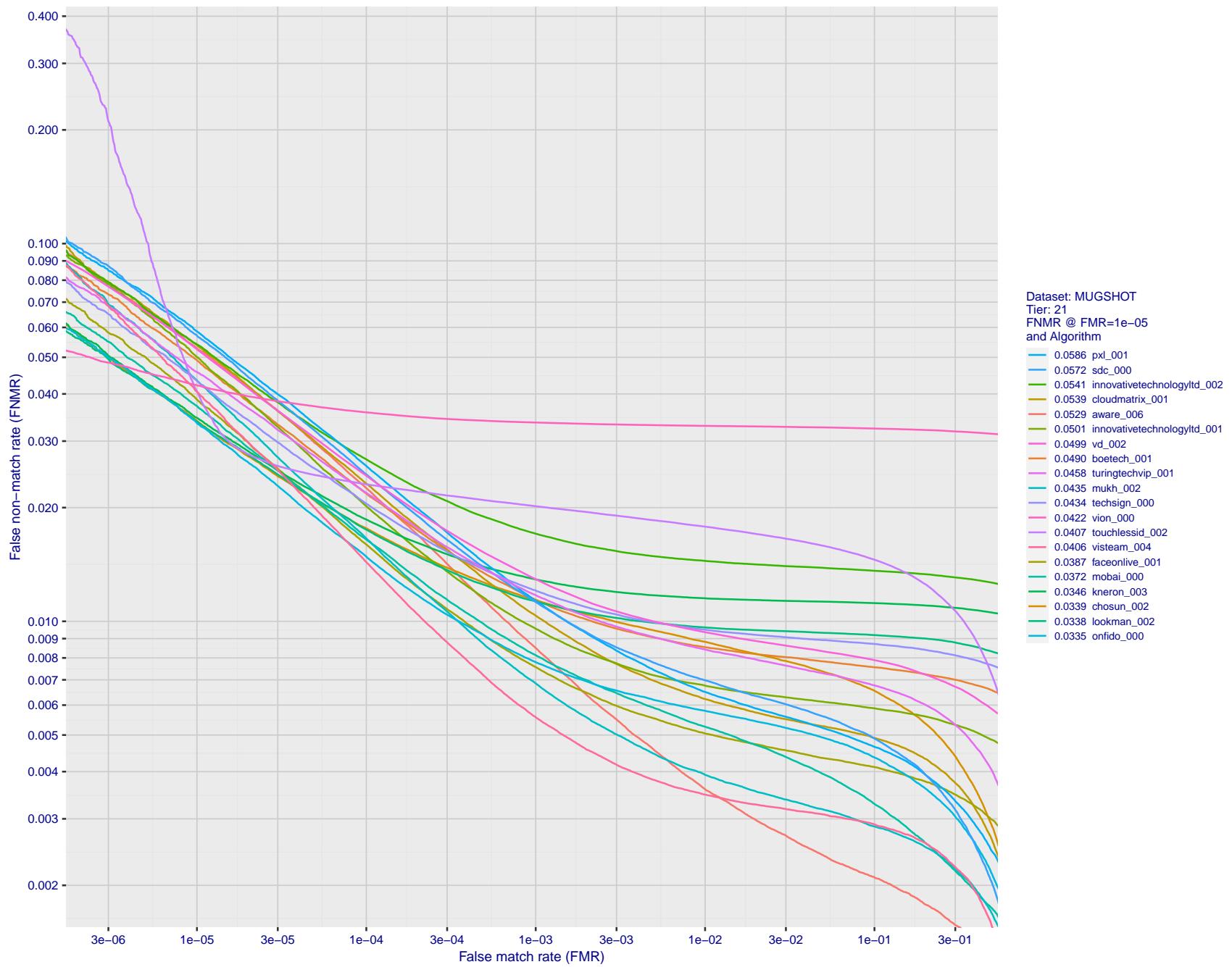


Figure 117: For the mugshot images, detection error tradeoff (DET) characteristics showing false non-match rate vs. false match rate plotted parametrically on threshold, T. The scales are logarithmic in order to show decades of FMR.

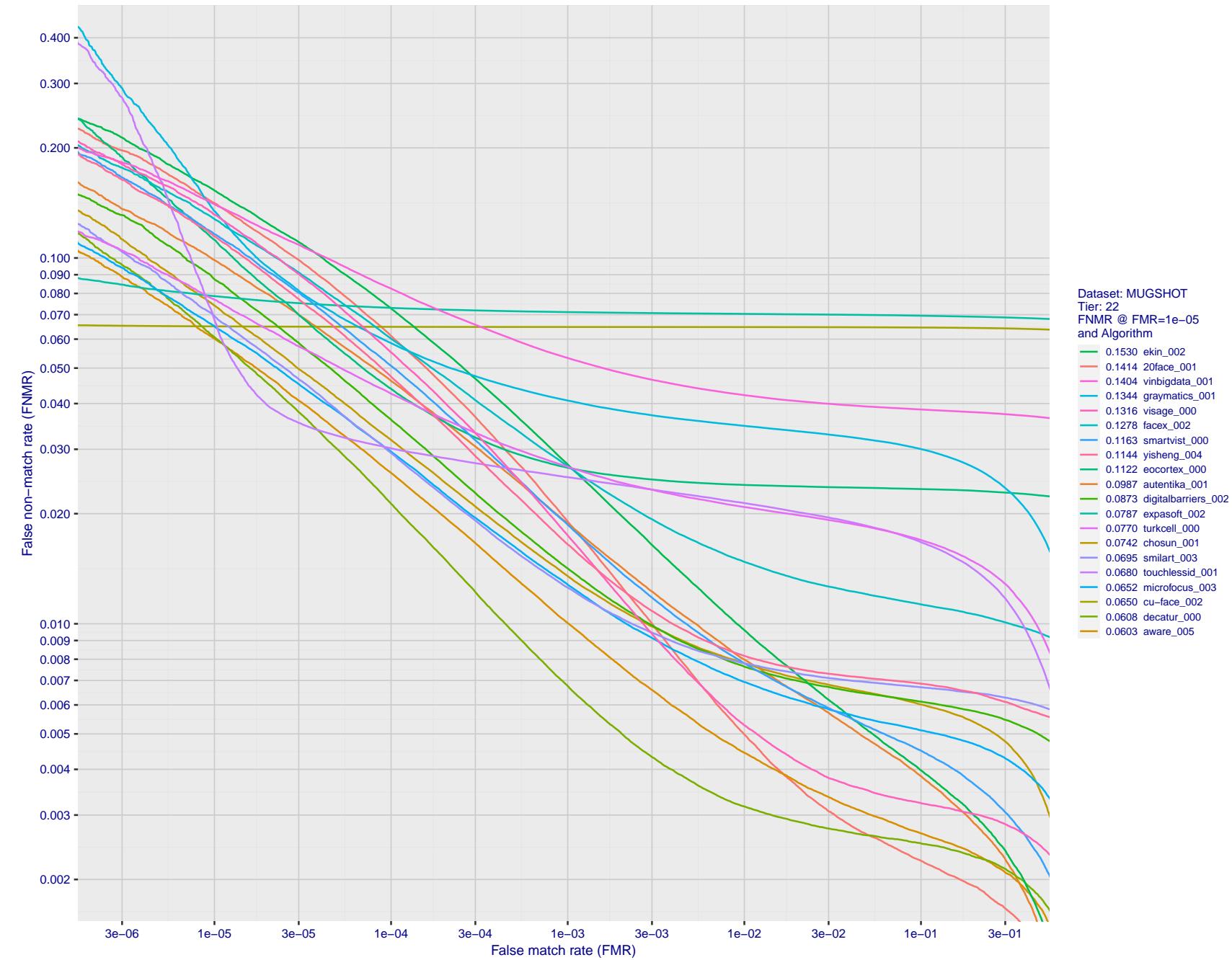


Figure 118: For the mugshot images, detection error tradeoff (DET) characteristics showing false non-match rate vs. false match rate plotted parametrically on threshold, T. The scales are logarithmic in order to show decades of FMR.

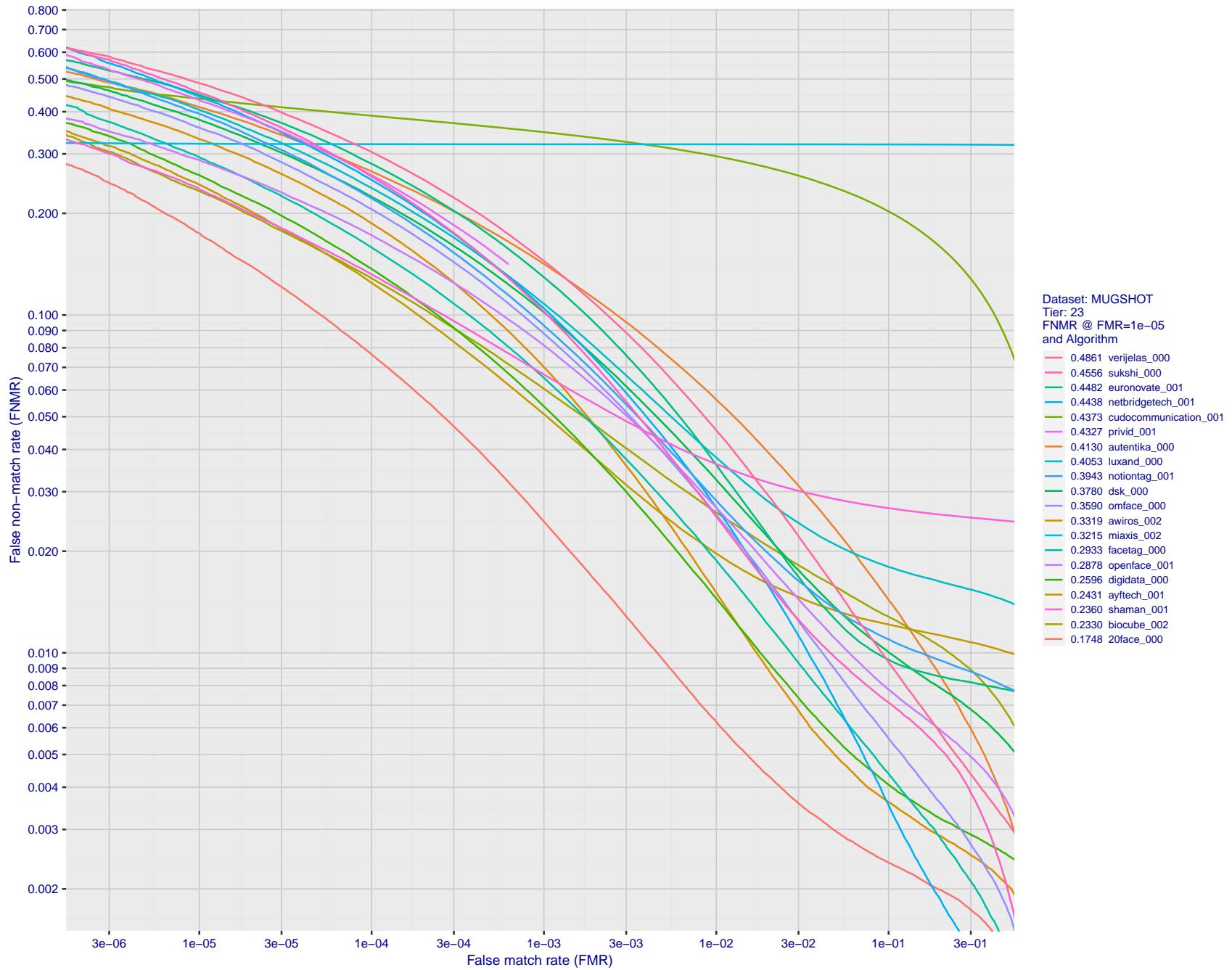


Figure 119: For the mugshot images, detection error tradeoff (DET) characteristics showing false non-match rate vs. false match rate plotted parametrically on threshold, T . The scales are logarithmic in order to show decades of FMR.

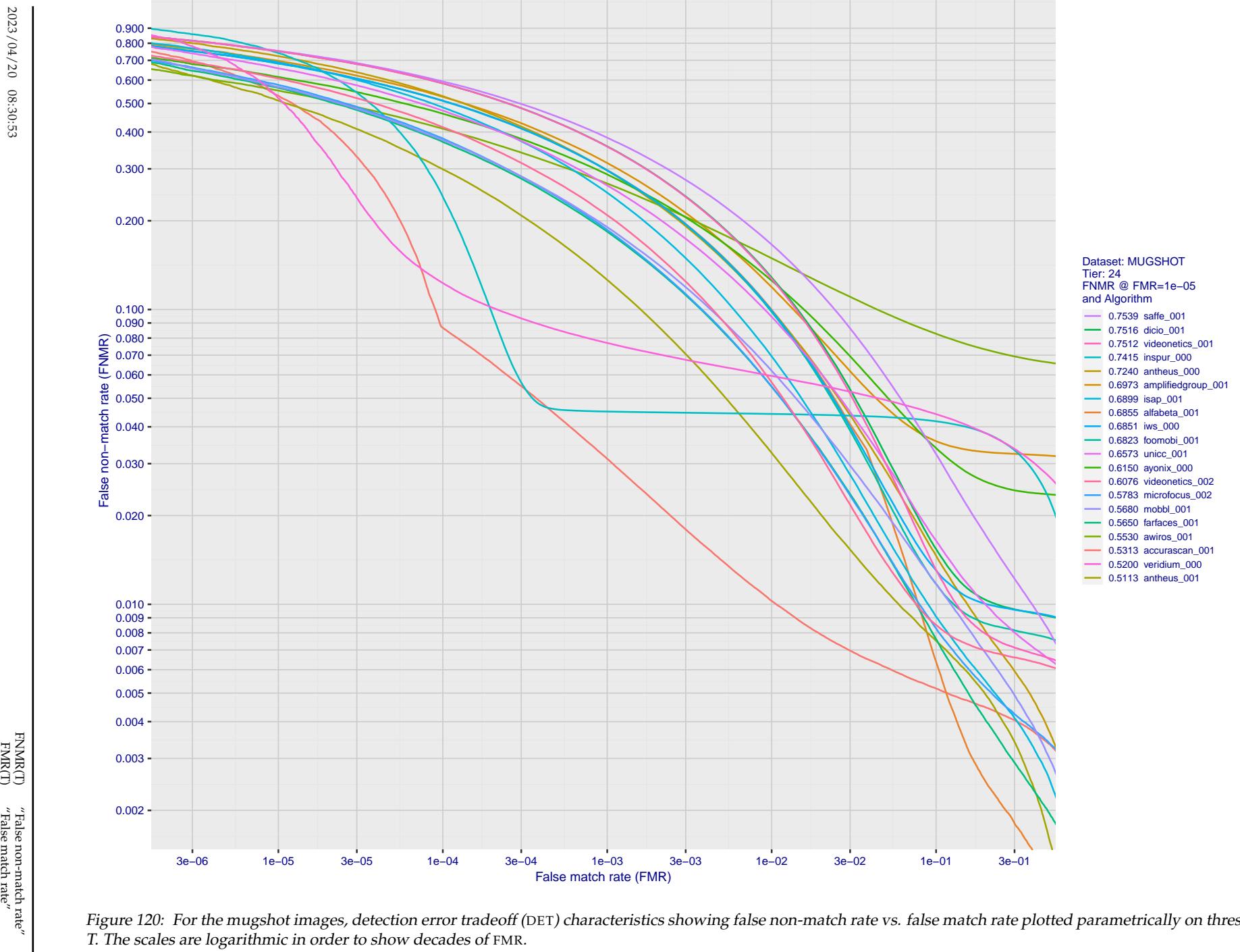


Figure 120: For the mugshot images, detection error tradeoff (DET) characteristics showing false non-match rate vs. false match rate plotted parametrically on threshold, T . The scales are logarithmic in order to show decades of FMR.

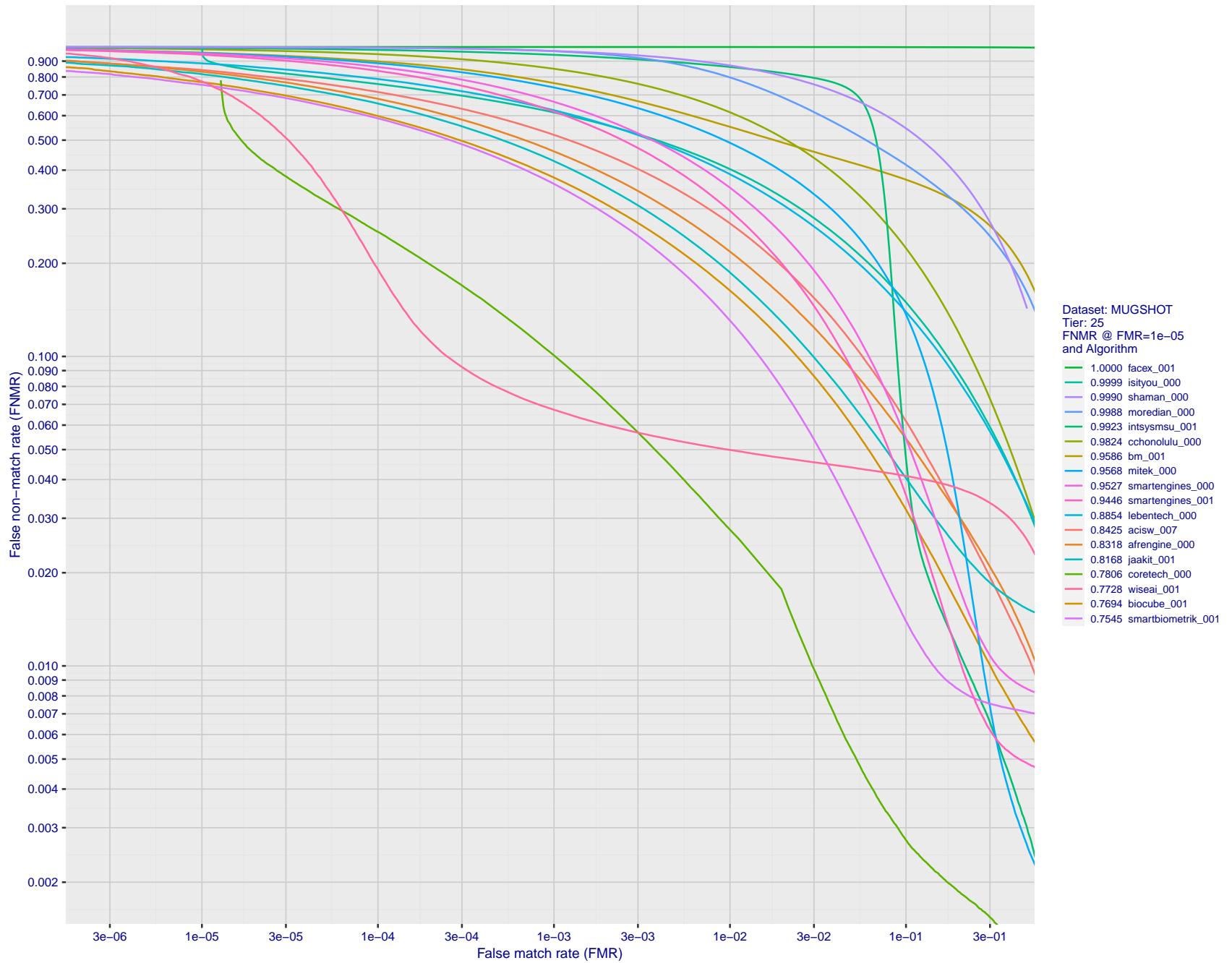


Figure 121: For the mugshot images, detection error tradeoff (DET) characteristics showing false non-match rate vs. false match rate plotted parametrically on threshold, T. The scales are logarithmic in order to show decades of FMR.

2023/04/20 08:30:53

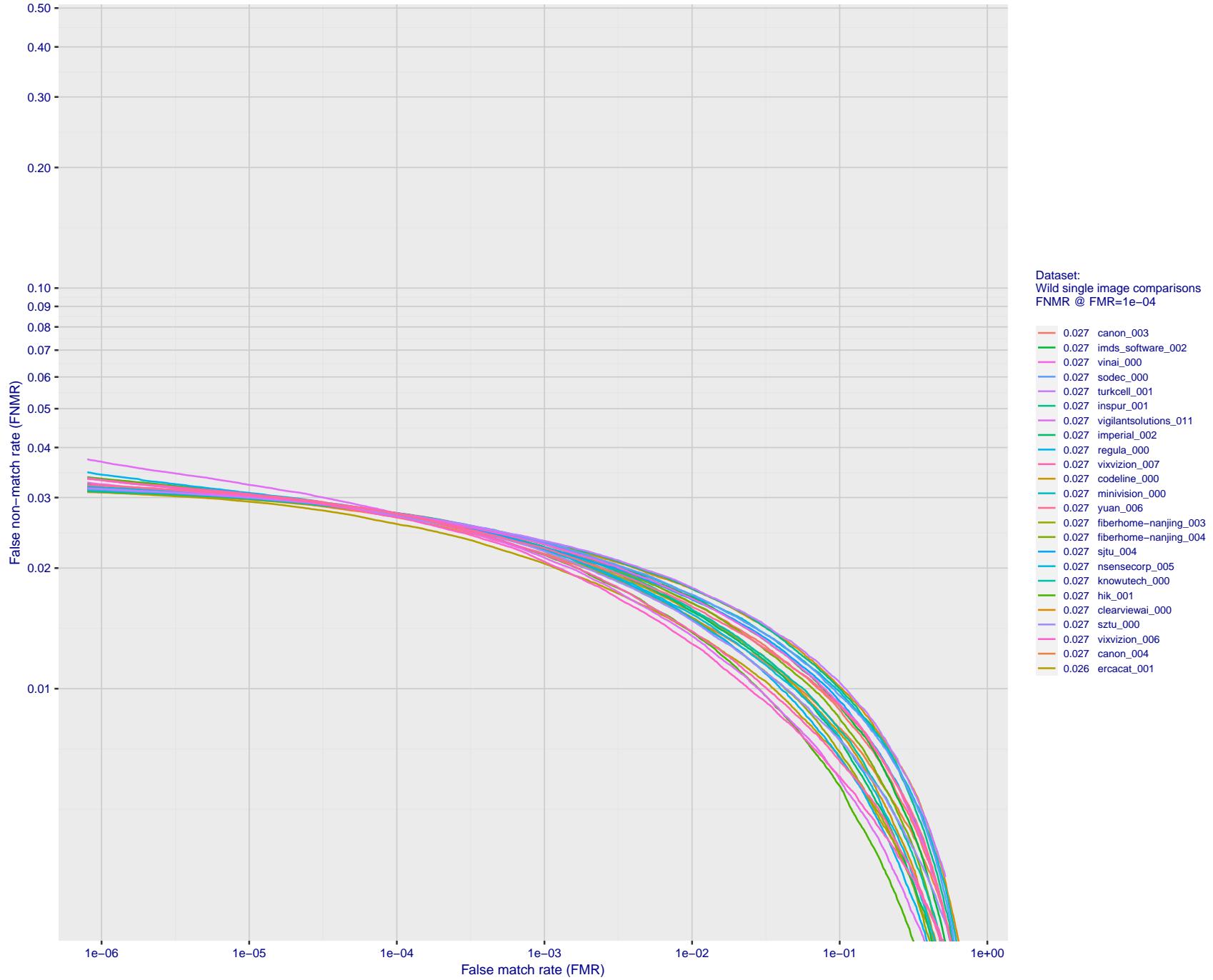


Figure 122: For the 2018 wild image comparisons, detection error tradeoff (DET) characteristics showing false non-match rate vs. false match rate plotted parametrically on threshold, T. The scales are logarithmic in order to show several decades of FMR.

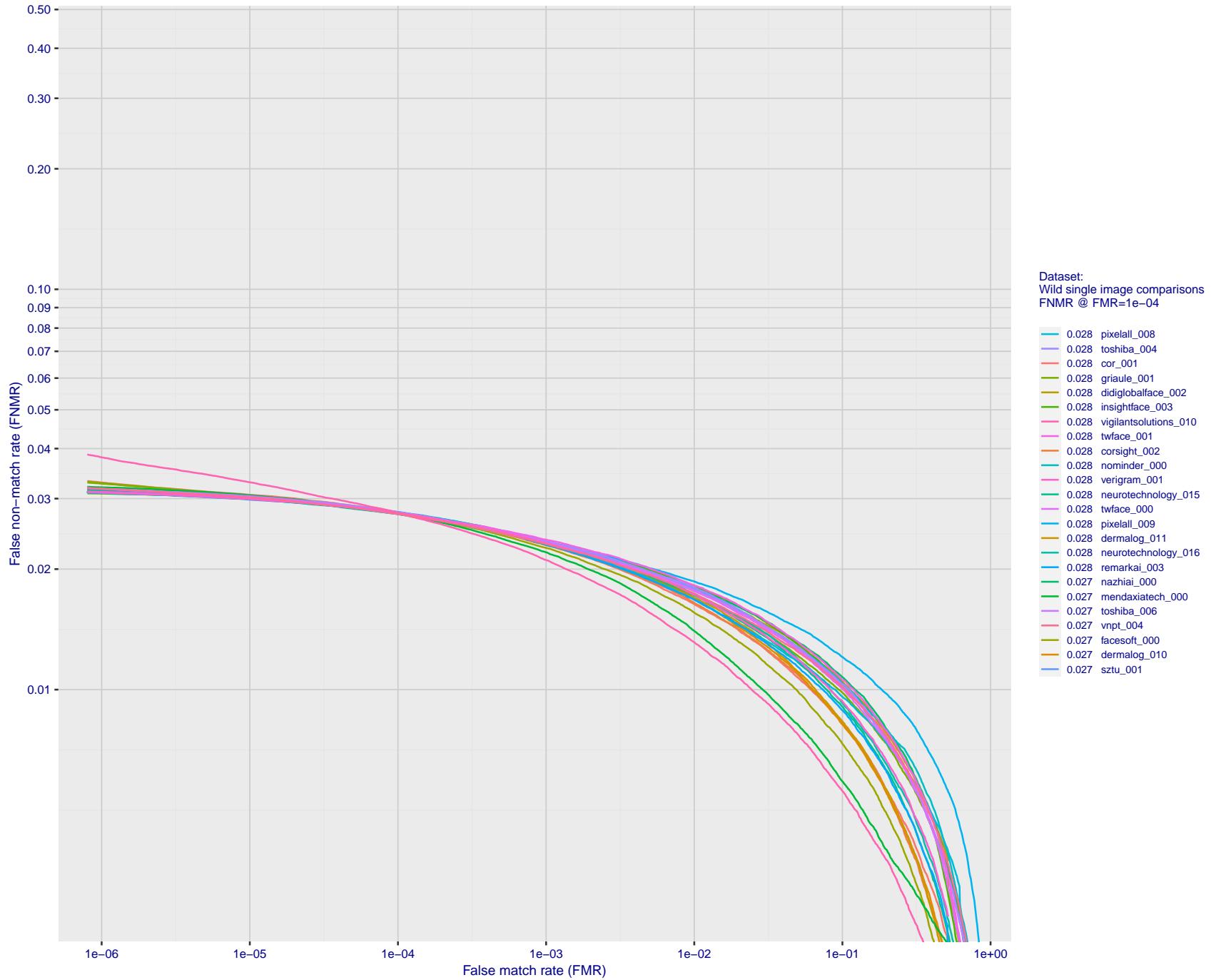


Figure 123: For the 2018 wild image comparisons, detection error tradeoff (DET) characteristics showing false non-match rate vs. false match rate plotted parametrically on threshold, T . The scales are logarithmic in order to show several decades of FMR.

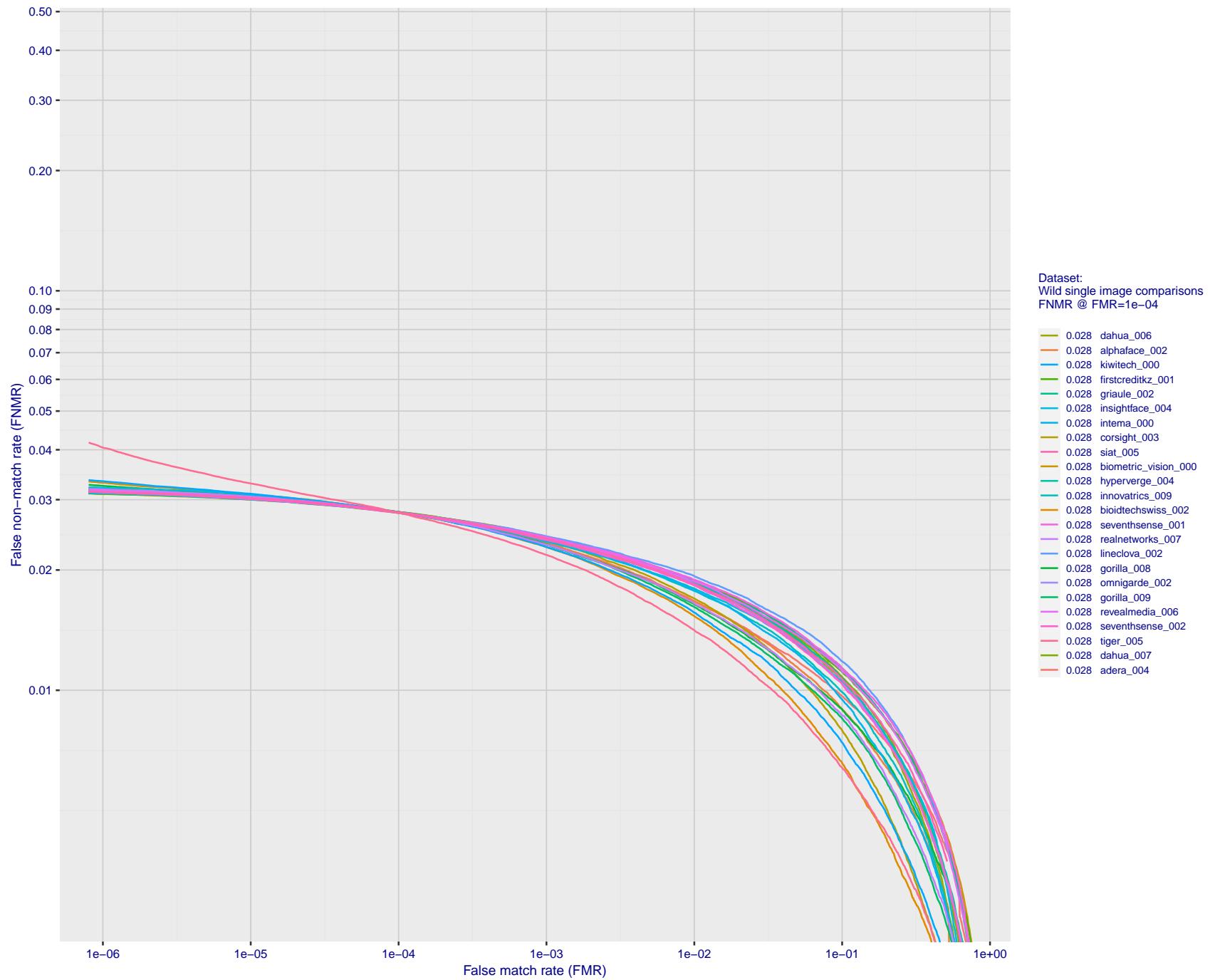


Figure 124: For the 2018 wild image comparisons, detection error tradeoff (DET) characteristics showing false non-match rate vs. false match rate plotted parametrically on threshold, T . The scales are logarithmic in order to show several decades of FMR.

2023/04/20 08:30:53

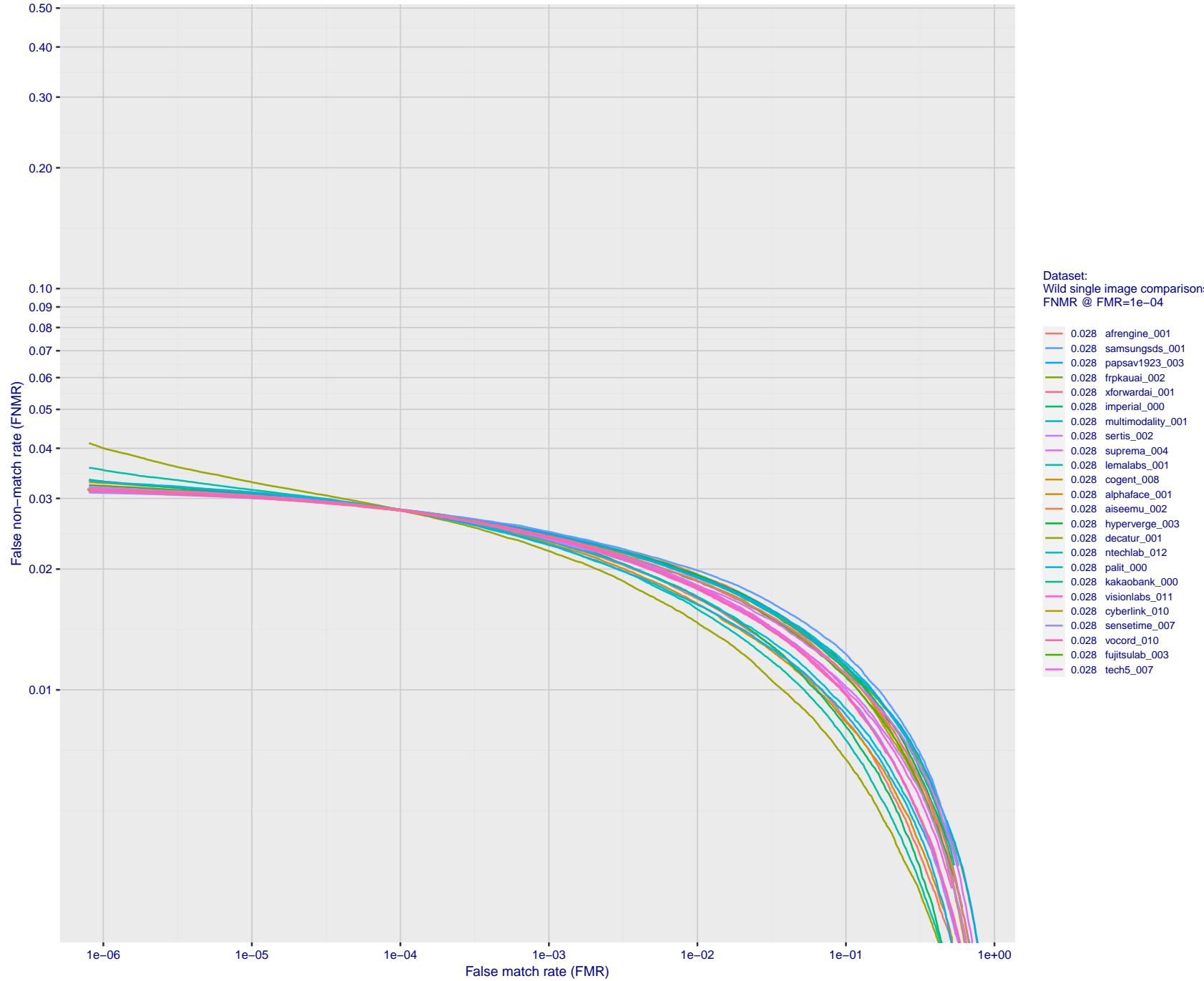


Figure 125: For the 2018 wild image comparisons, detection error tradeoff (DET) characteristics showing false non-match rate vs. false match rate plotted parametrically on threshold, T . The scales are logarithmic in order to show several decades of FMR.

2023/04/20 08:30:53

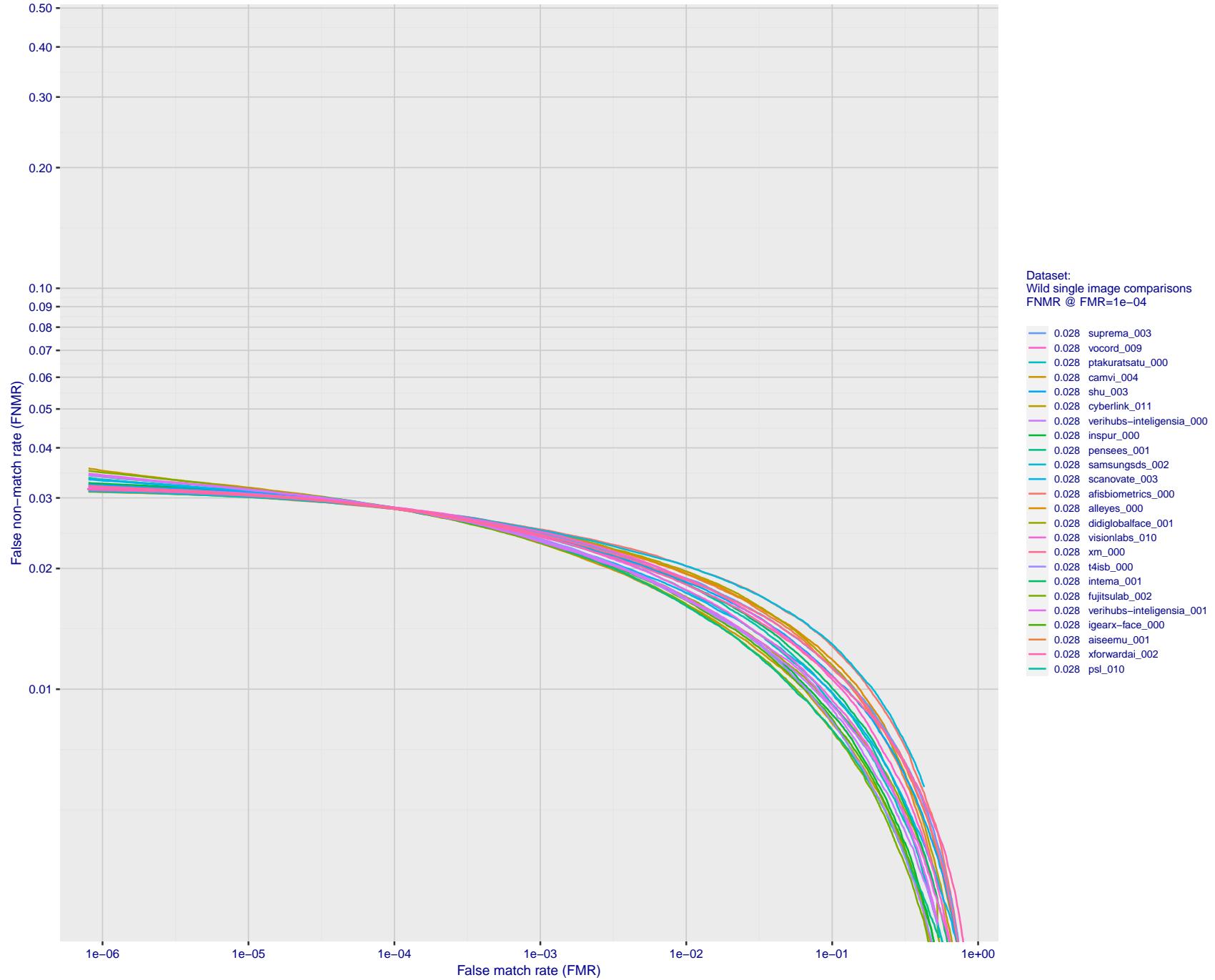


Figure 126: For the 2018 wild image comparisons, detection error tradeoff (DET) characteristics showing false non-match rate vs. false match rate plotted parametrically on threshold, T. The scales are logarithmic in order to show several decades of FMR.

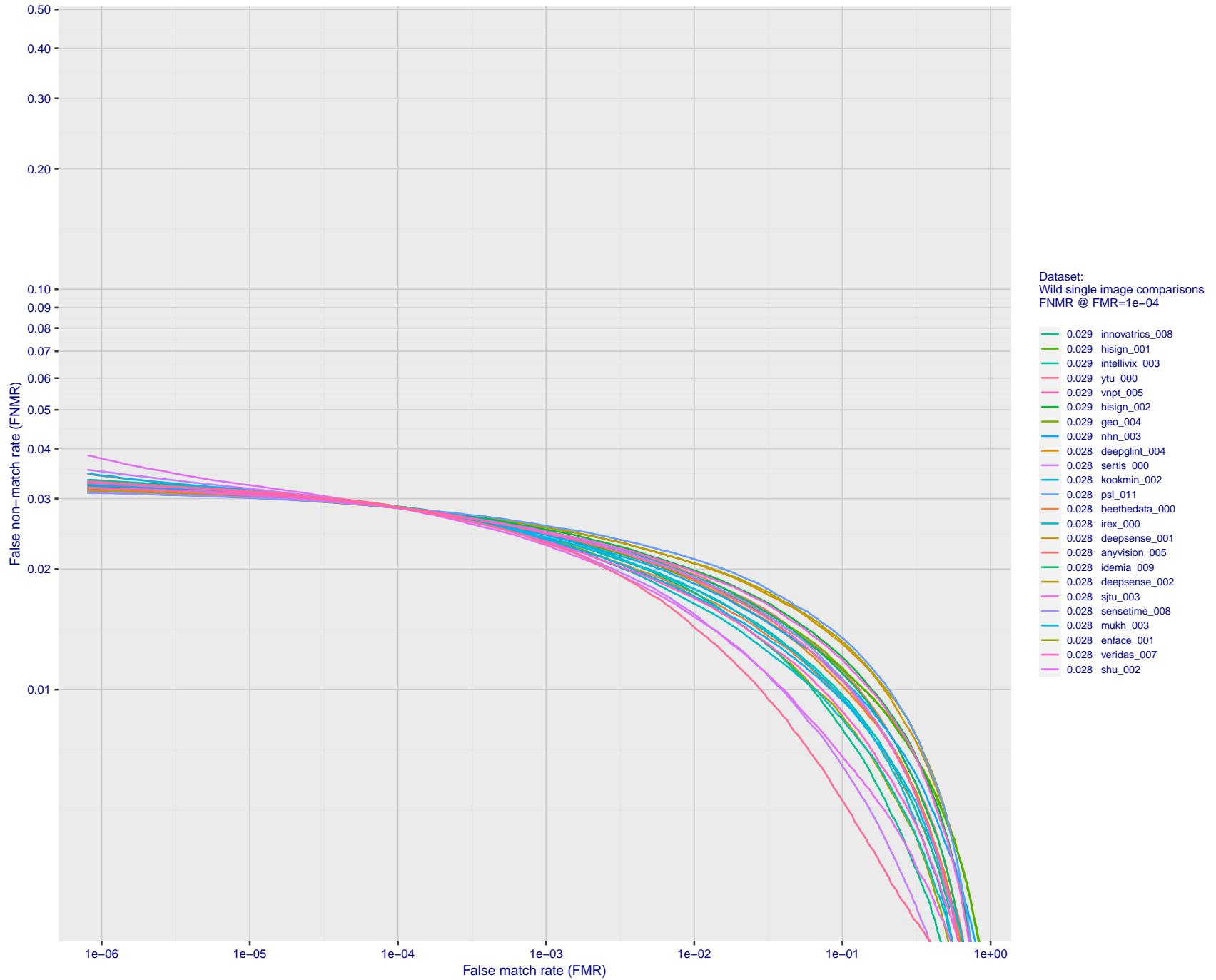


Figure 127: For the 2018 wild image comparisons, detection error tradeoff (DET) characteristics showing false non-match rate vs. false match rate plotted parametrically on threshold, T . The scales are logarithmic in order to show several decades of FMR.

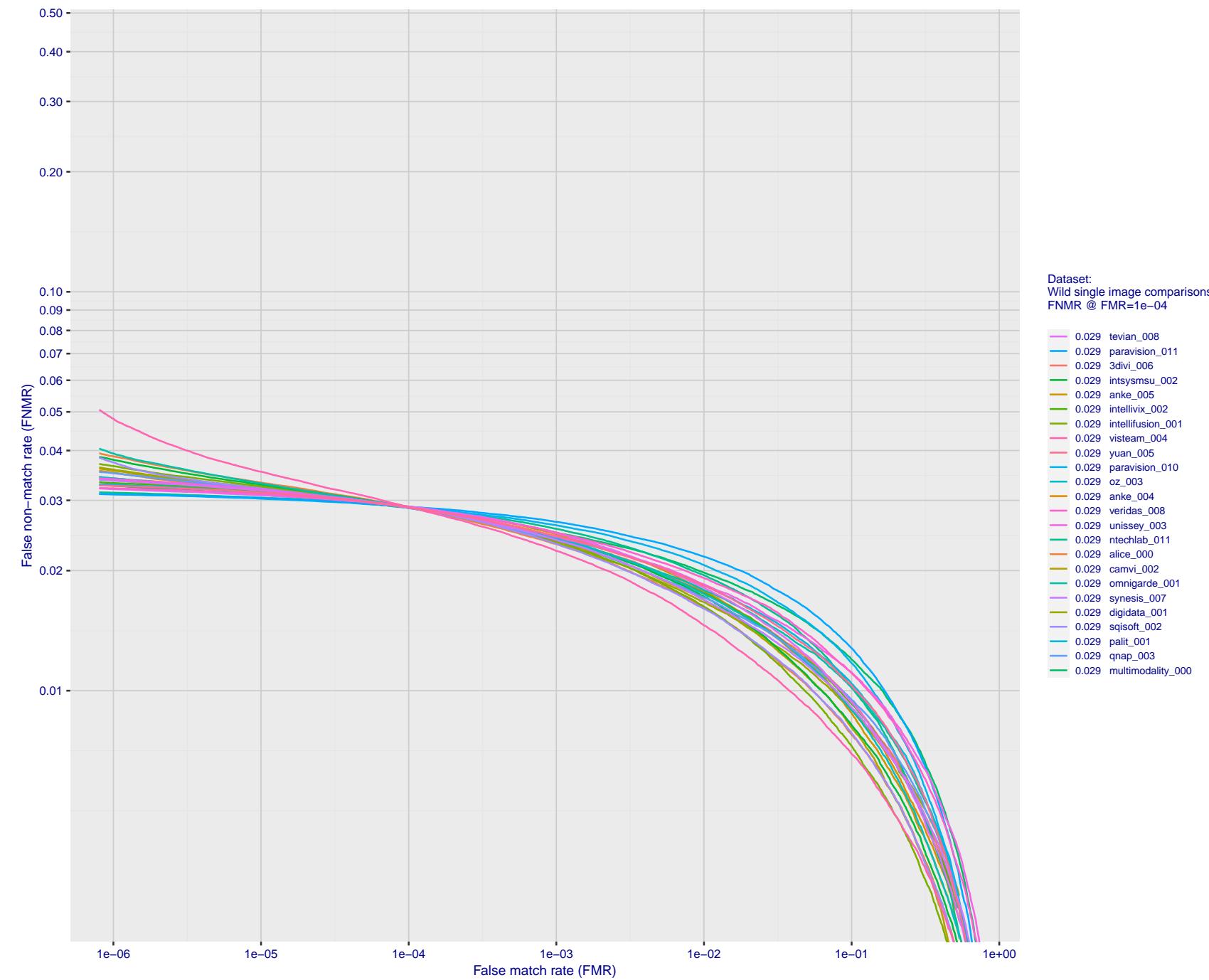


Figure 128: For the 2018 wild image comparisons, detection error tradeoff (DET) characteristics showing false non-match rate vs. false match rate plotted parametrically on threshold, T . The scales are logarithmic in order to show several decades of FMR.

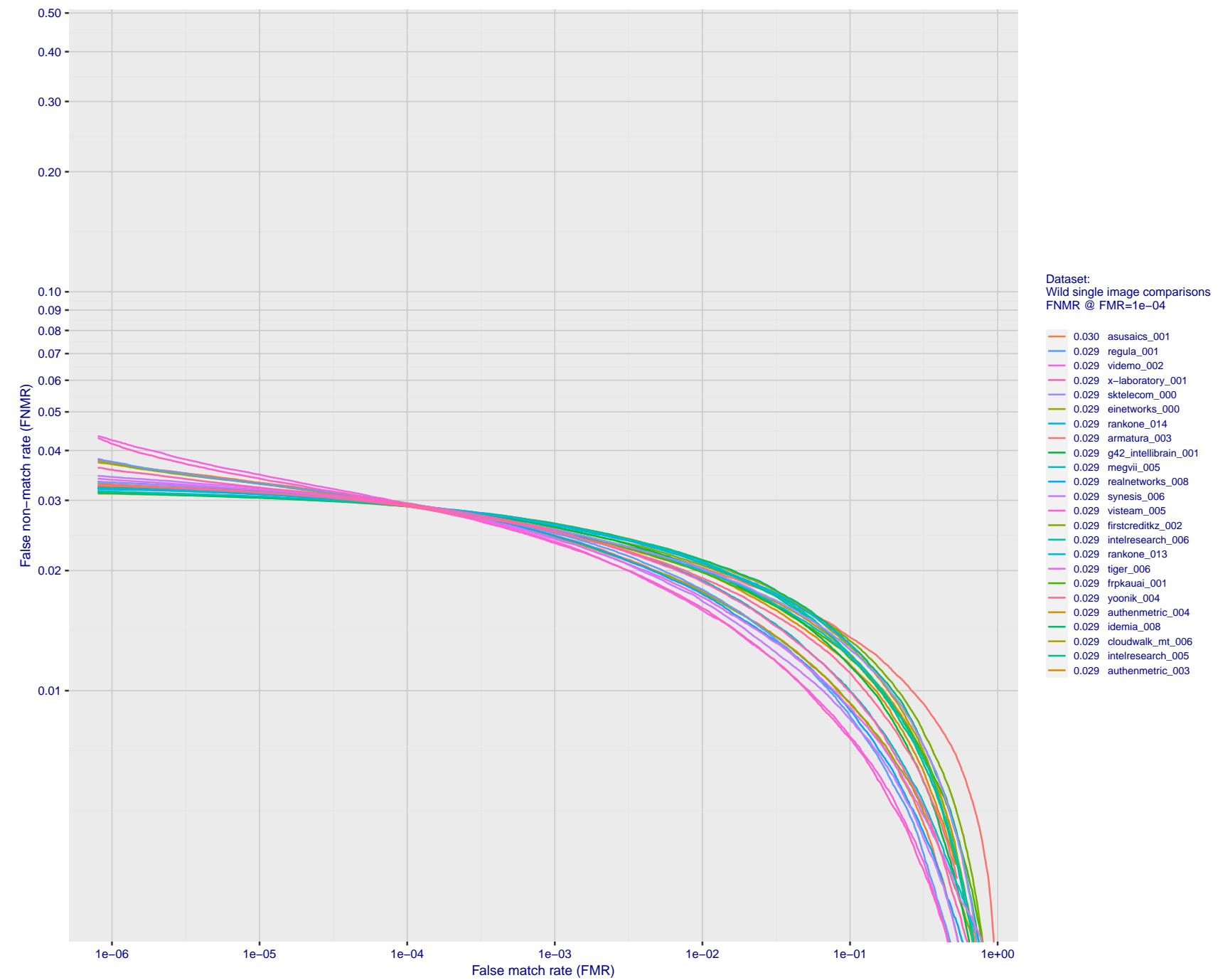


Figure 129: For the 2018 wild image comparisons, detection error tradeoff (DET) characteristics showing false non-match rate vs. false match rate plotted parametrically on threshold, T . The scales are logarithmic in order to show several decades of FMR.

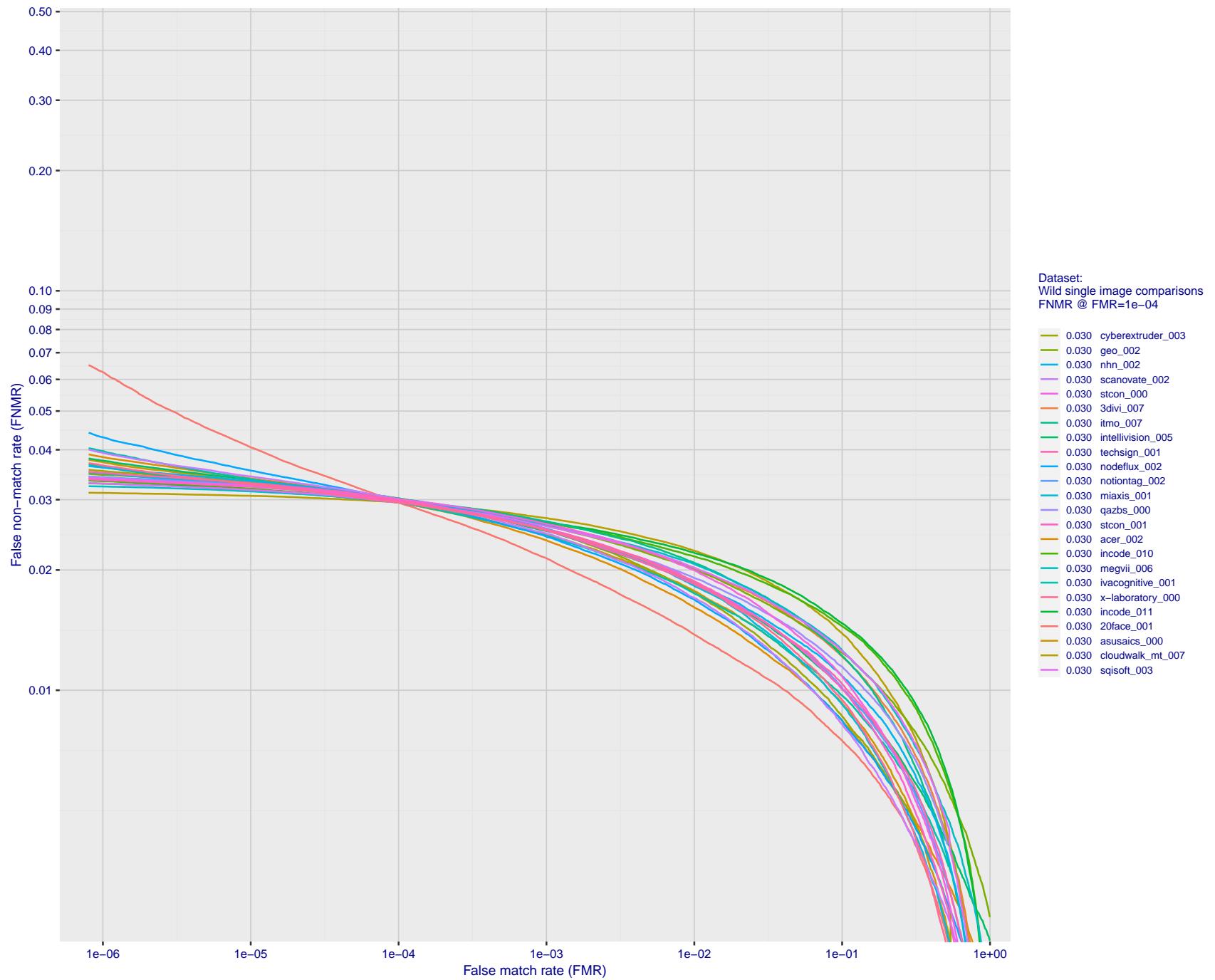


Figure 130: For the 2018 wild image comparisons, detection error tradeoff (DET) characteristics showing false non-match rate vs. false match rate plotted parametrically on threshold, T . The scales are logarithmic in order to show several decades of FMR.

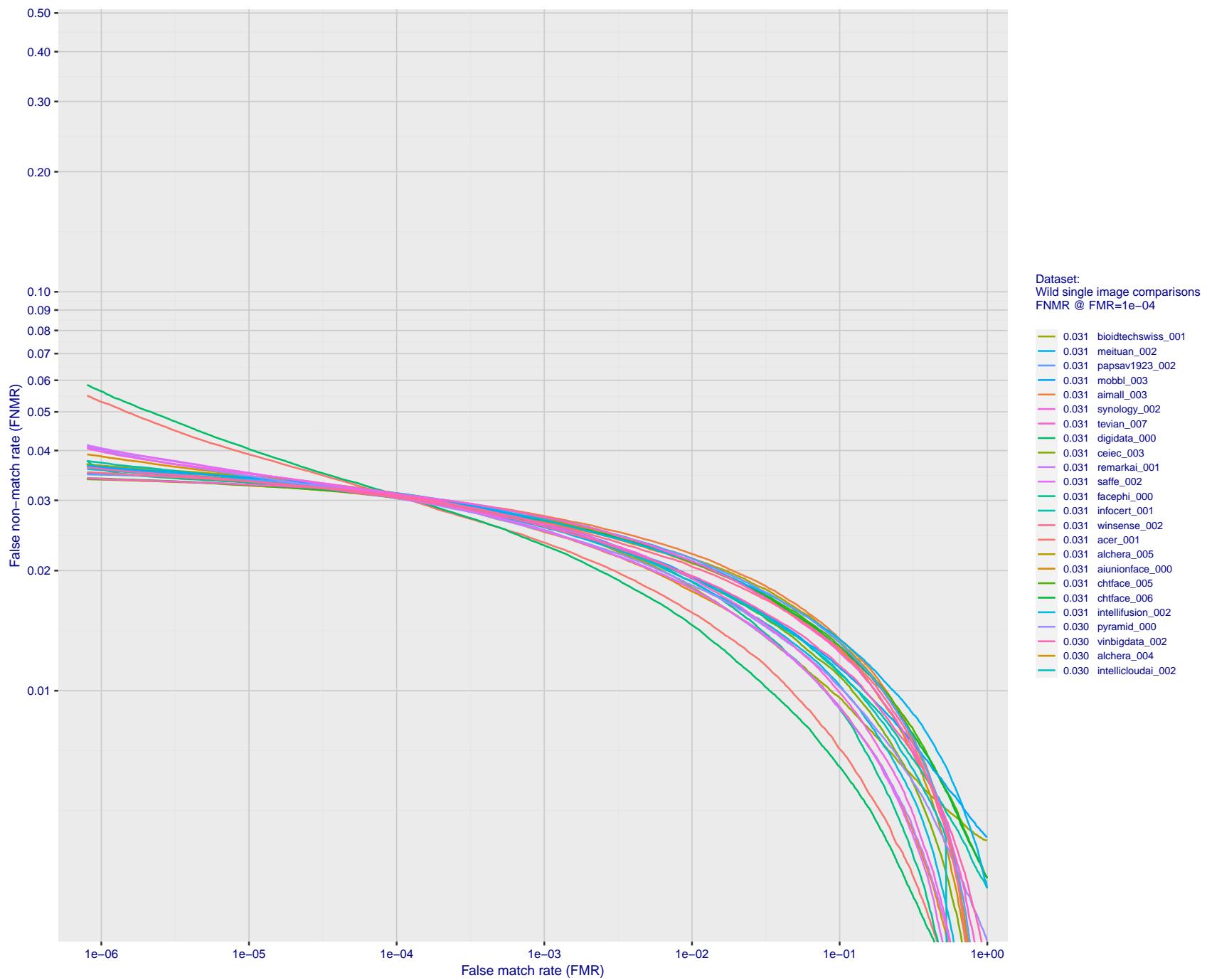


Figure 131: For the 2018 wild image comparisons, detection error tradeoff (DET) characteristics showing false non-match rate vs. false match rate plotted parametrically on threshold, T . The scales are logarithmic in order to show several decades of FMR.

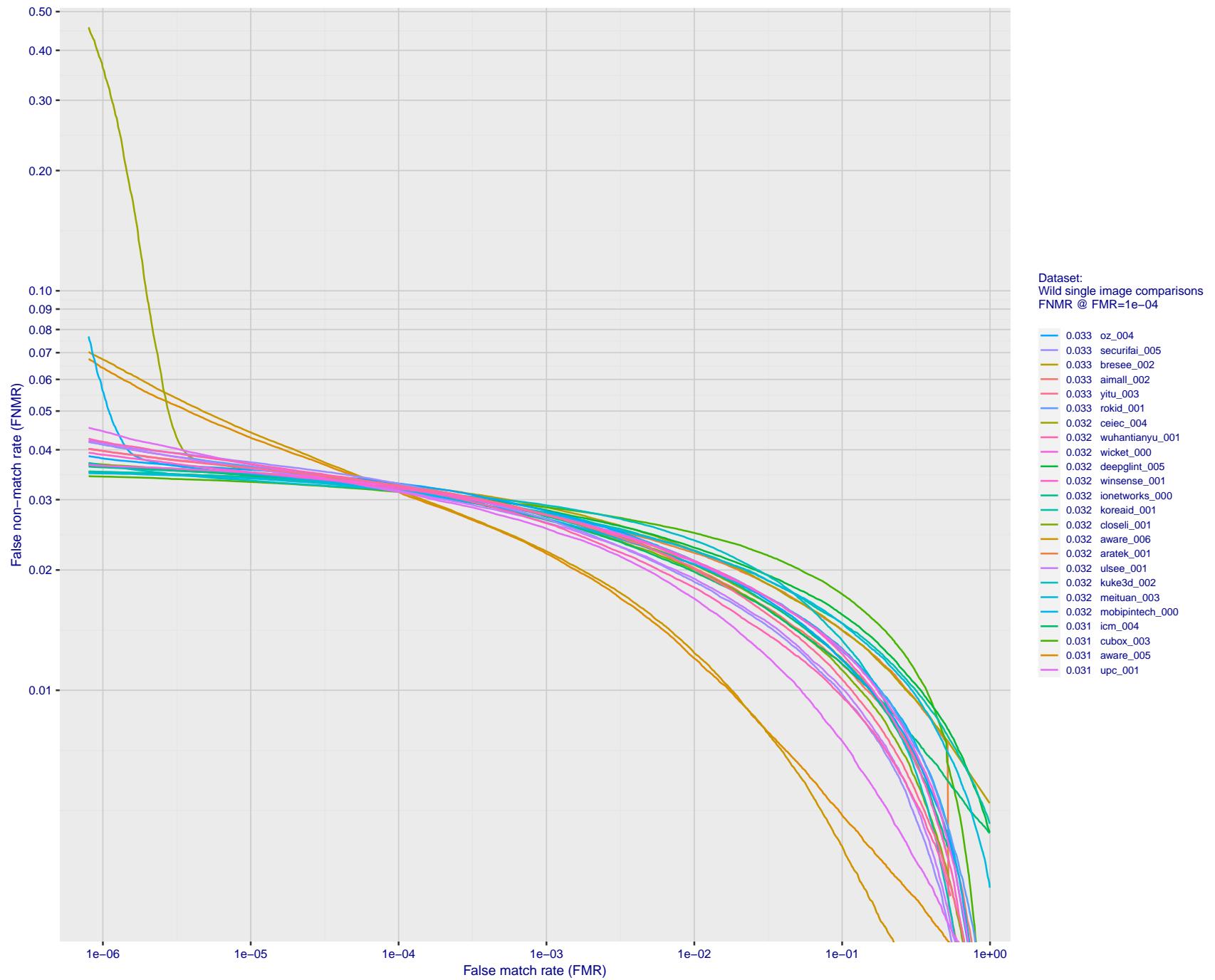


Figure 132: For the 2018 wild image comparisons, detection error tradeoff (DET) characteristics showing false non-match rate vs. false match rate plotted parametrically on threshold, T . The scales are logarithmic in order to show several decades of FMR.

2023/04/20 08:30:53

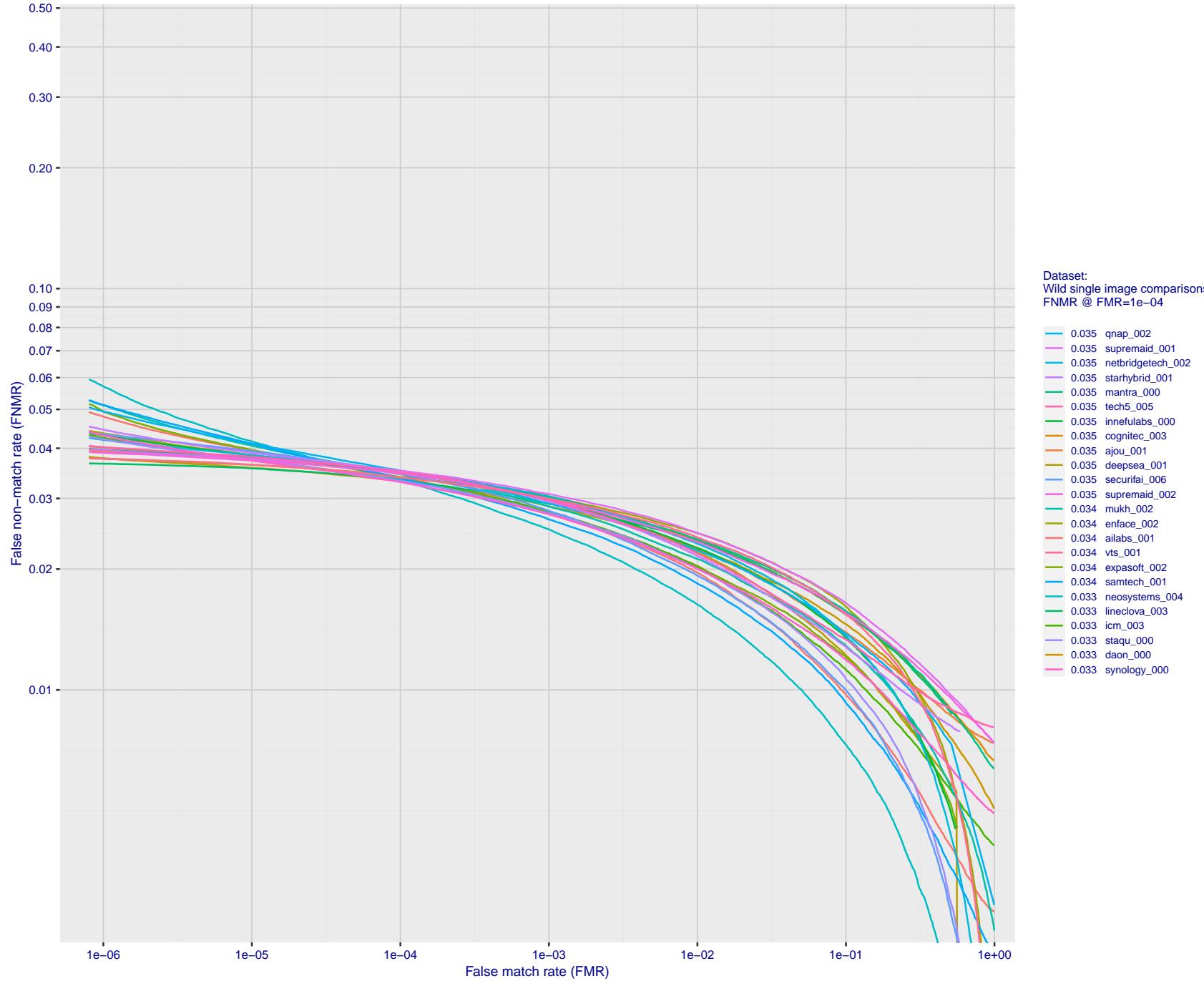


Figure 133: For the 2018 wild image comparisons, detection error tradeoff (DET) characteristics showing false non-match rate vs. false match rate plotted parametrically on threshold, T. The scales are logarithmic in order to show several decades of FMR.

2023/04/20 08:30:53

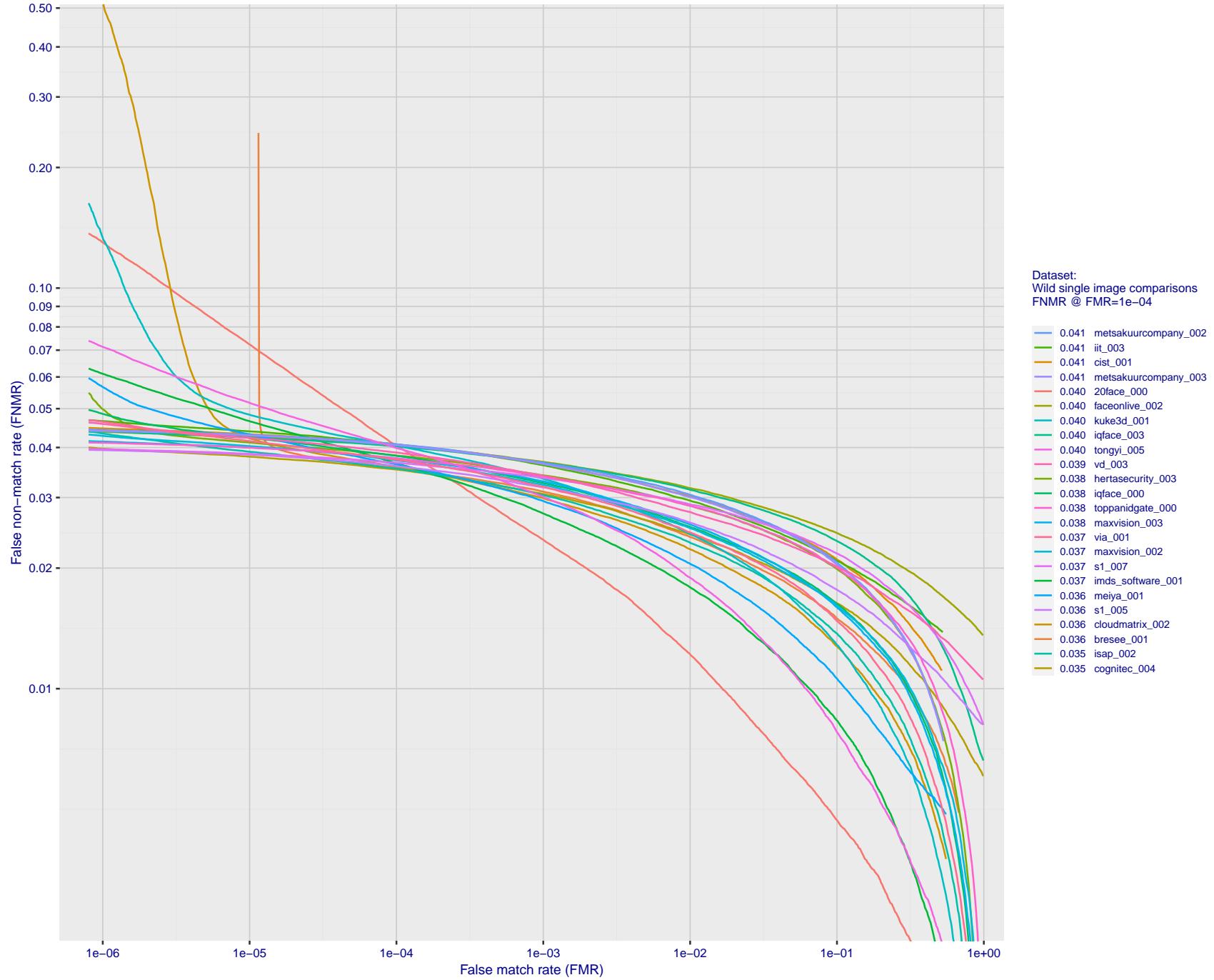


Figure 134: For the 2018 wild image comparisons, detection error tradeoff (DET) characteristics showing false non-match rate vs. false match rate plotted parametrically on threshold, T. The scales are logarithmic in order to show several decades of FMR.

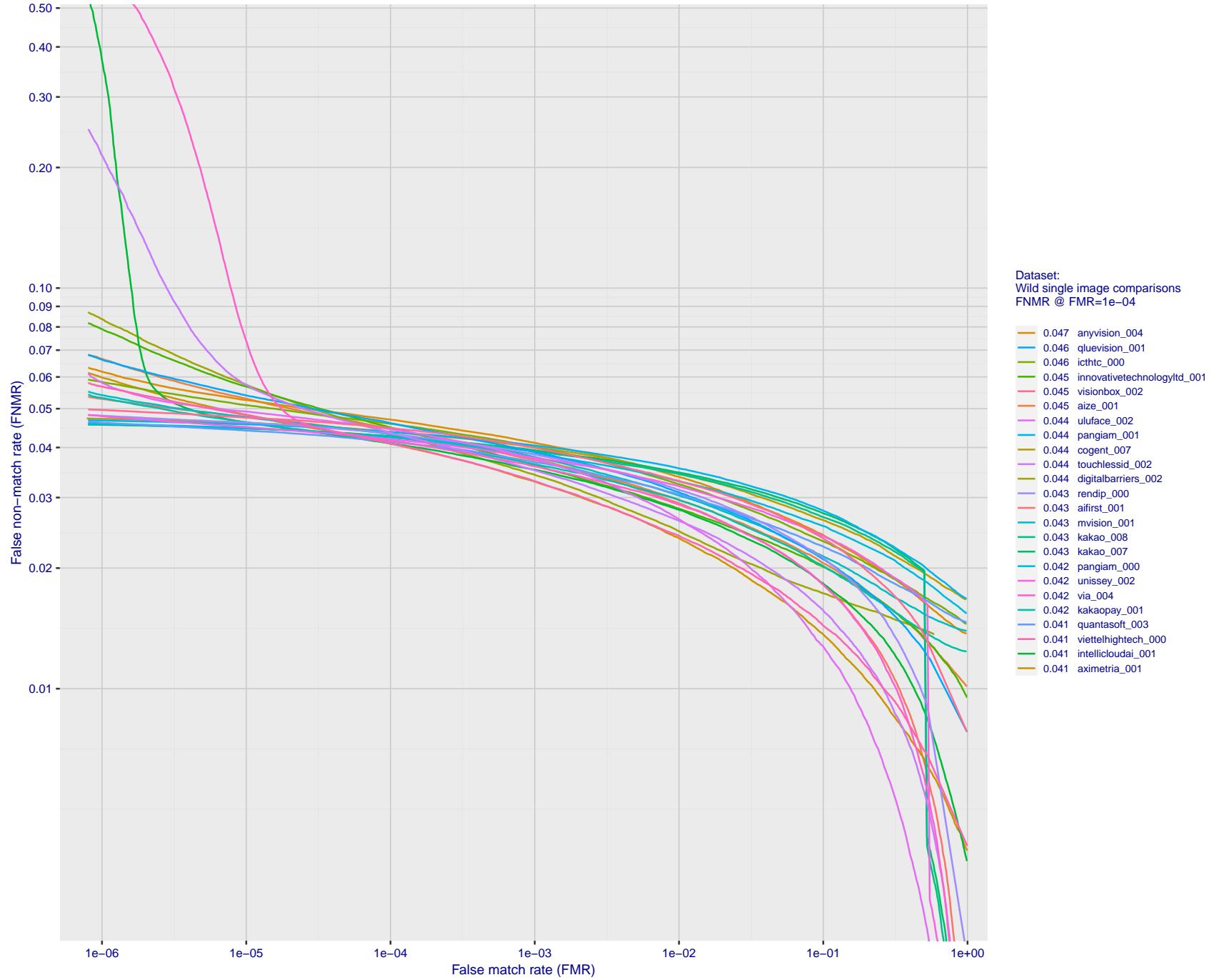


Figure 135: For the 2018 wild image comparisons, detection error tradeoff (DET) characteristics showing false non-match rate vs. false match rate plotted parametrically on threshold, T . The scales are logarithmic in order to show several decades of FMR.

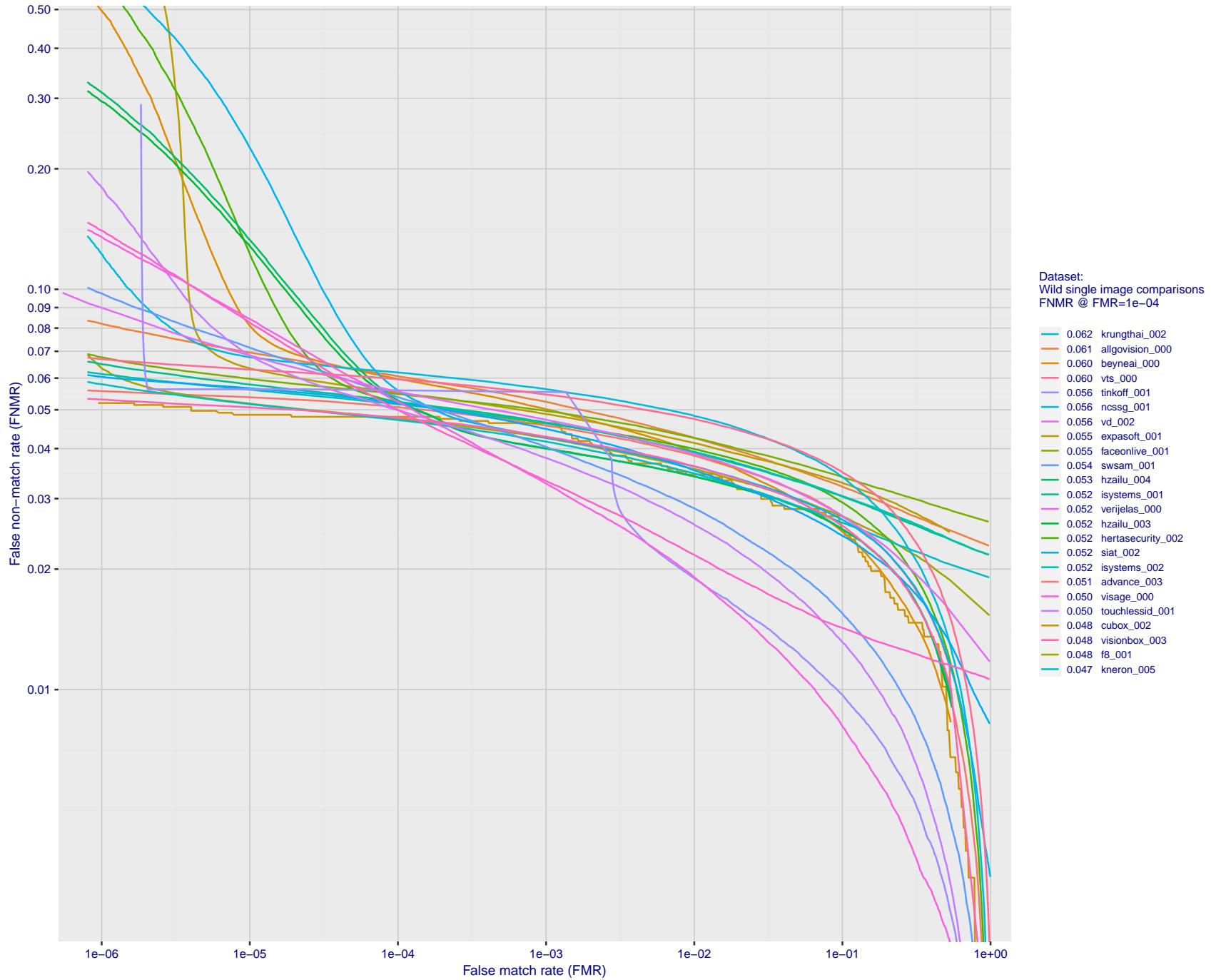


Figure 136: For the 2018 wild image comparisons, detection error tradeoff (DET) characteristics showing false non-match rate vs. false match rate plotted parametrically on threshold, T . The scales are logarithmic in order to show several decades of FMR.

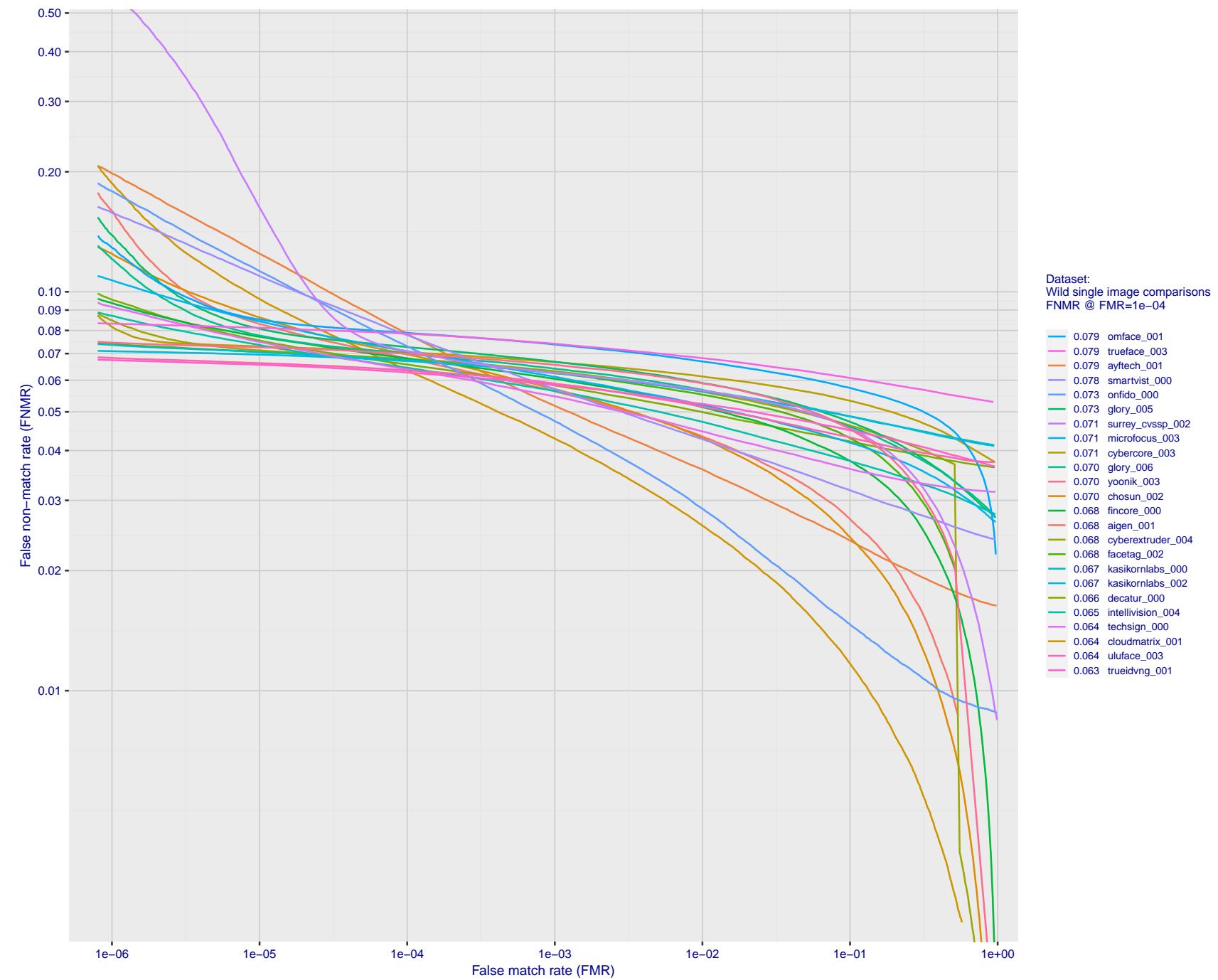


Figure 137: For the 2018 wild image comparisons, detection error tradeoff (DET) characteristics showing false non-match rate vs. false match rate plotted parametrically on threshold, T. The scales are logarithmic in order to show several decades of FMR.

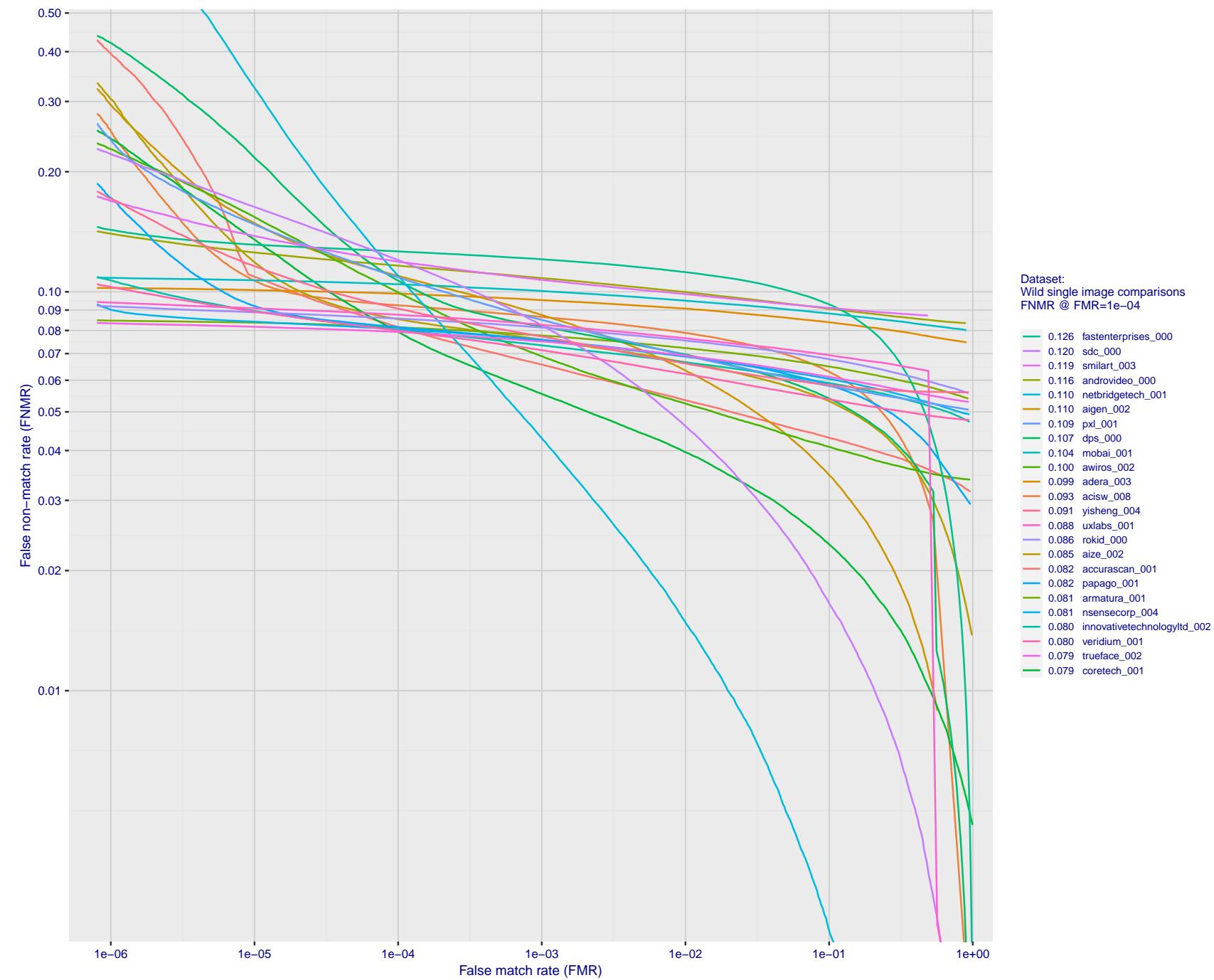


Figure 138: For the 2018 wild image comparisons, detection error tradeoff (DET) characteristics showing false non-match rate vs. false match rate plotted parametrically on threshold, T . The scales are logarithmic in order to show several decades of FMR.

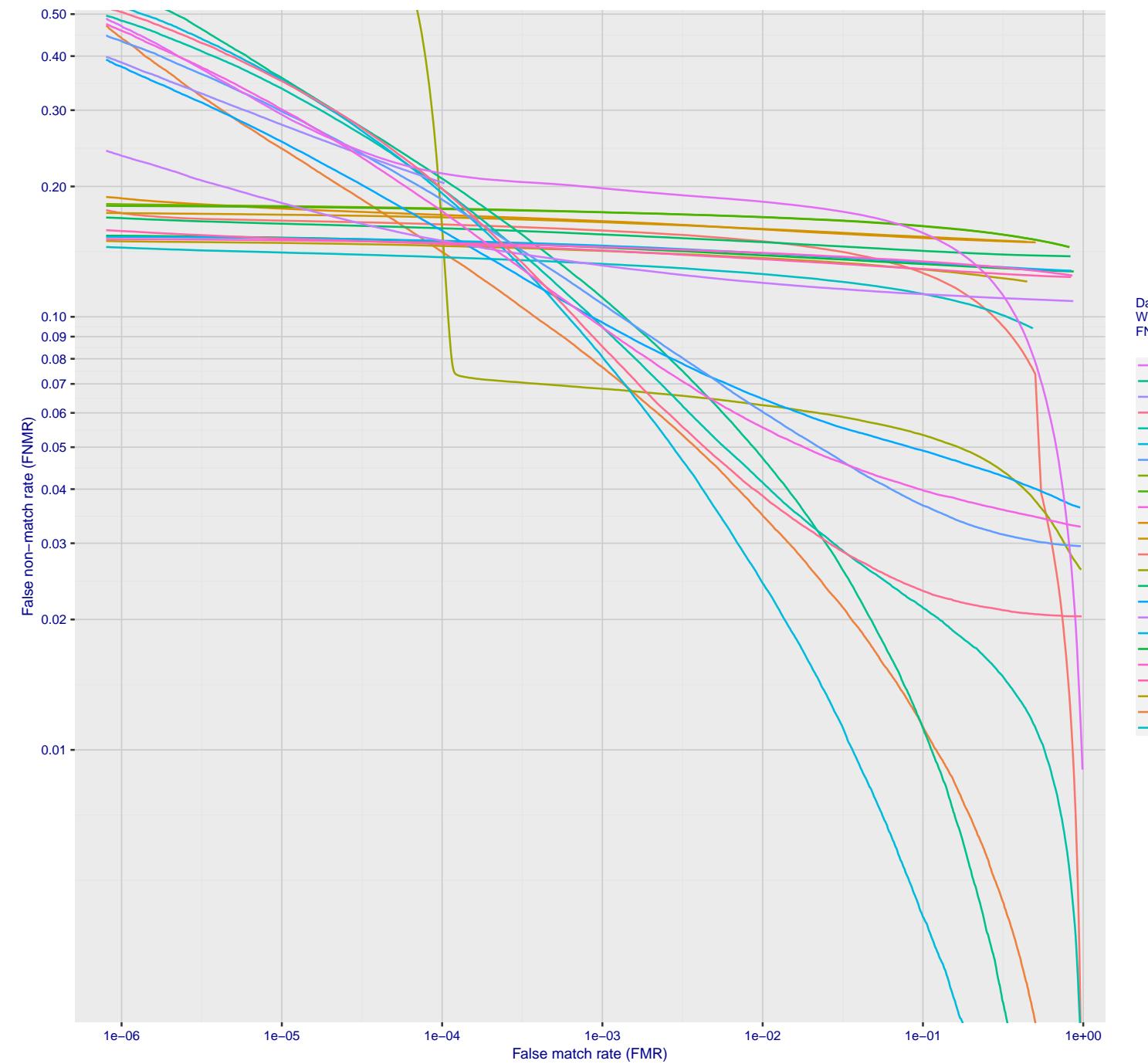


Figure 139: For the 2018 wild image comparisons, detection error tradeoff (DET) characteristics showing false non-match rate vs. false match rate plotted parametrically on threshold, T . The scales are logarithmic in order to show several decades of FMR.

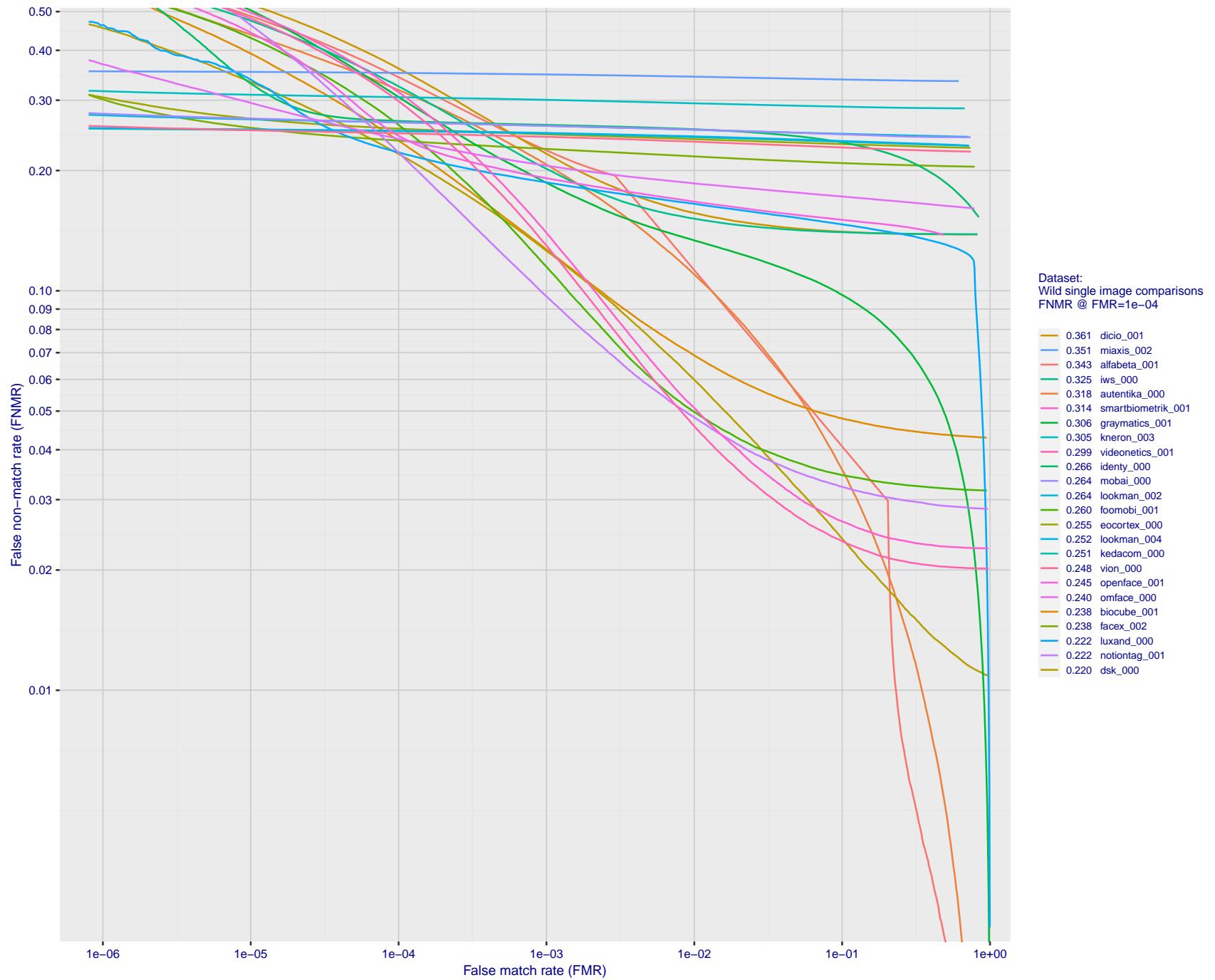


Figure 140: For the 2018 wild image comparisons, detection error tradeoff (DET) characteristics showing false non-match rate vs. false match rate plotted parametrically on threshold, T . The scales are logarithmic in order to show several decades of FMR.

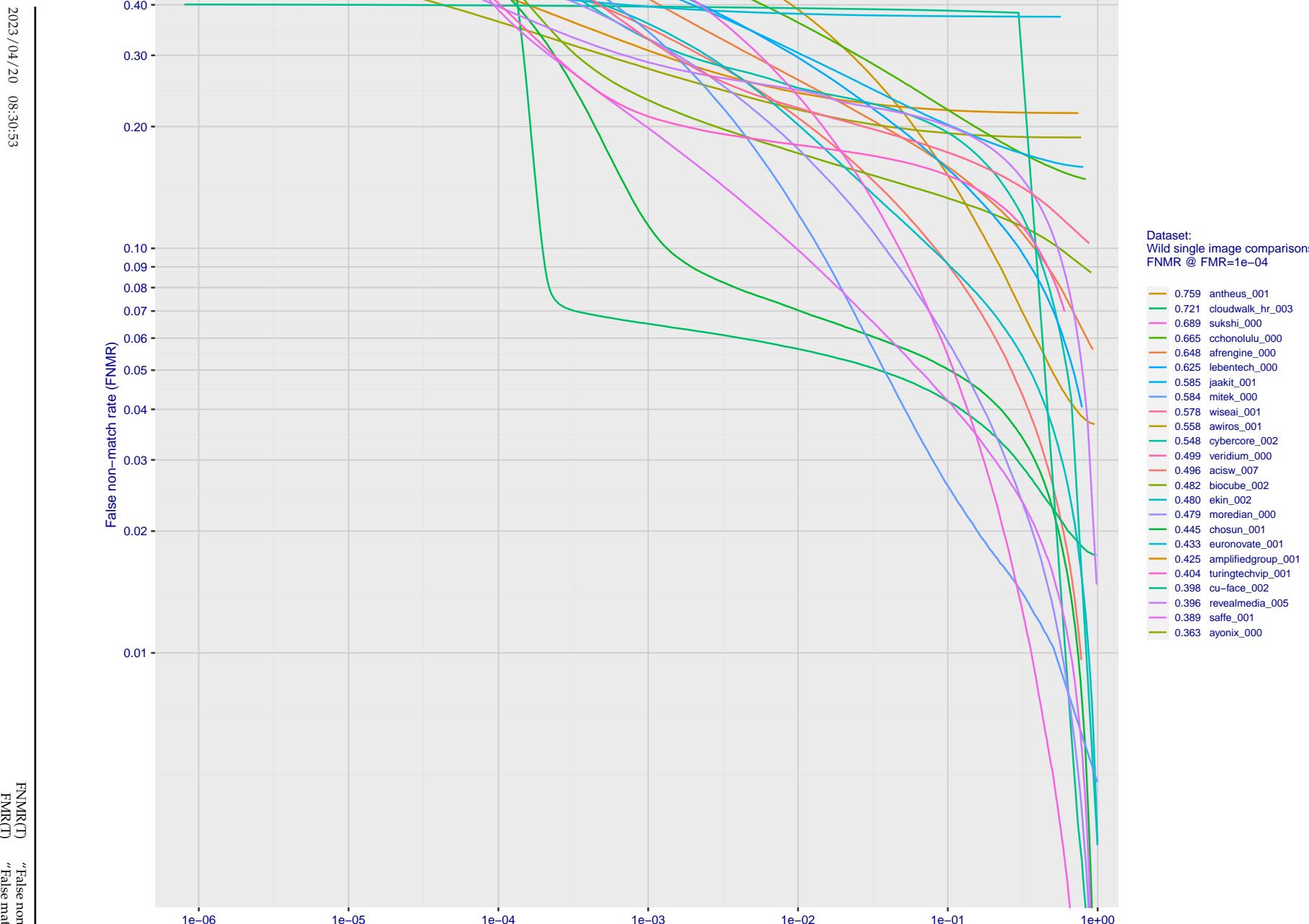


Figure 141: For the 2018 wild image comparisons, detection error tradeoff (DET) characteristics showing false non-match rate vs. false match rate plotted parametrically on threshold, T . The scales are logarithmic in order to show several decades of FMR.

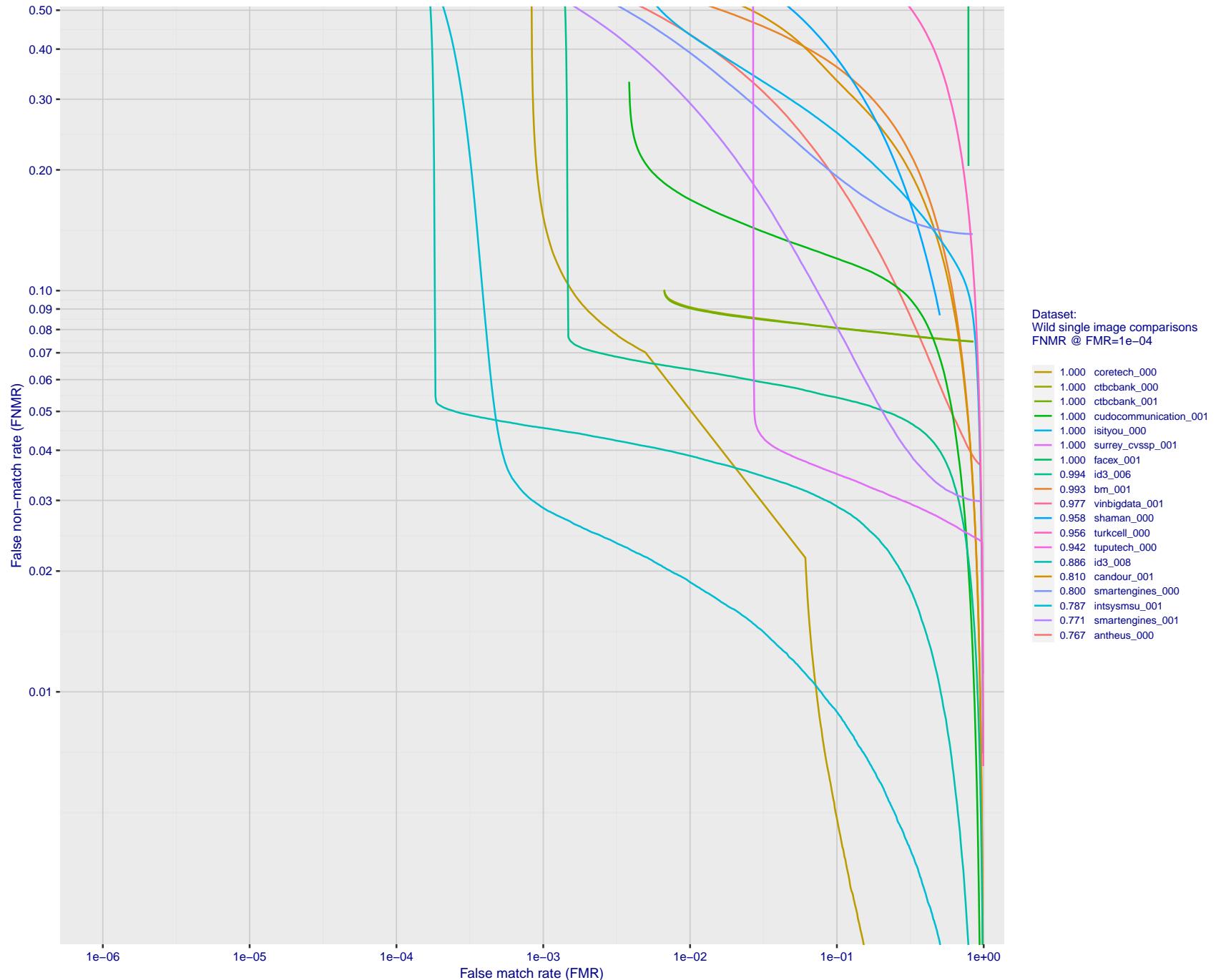


Figure 142: For the 2018 wild image comparisons, detection error tradeoff (DET) characteristics showing false non-match rate vs. false match rate plotted parametrically on threshold, T . The scales are logarithmic in order to show several decades of FMR.

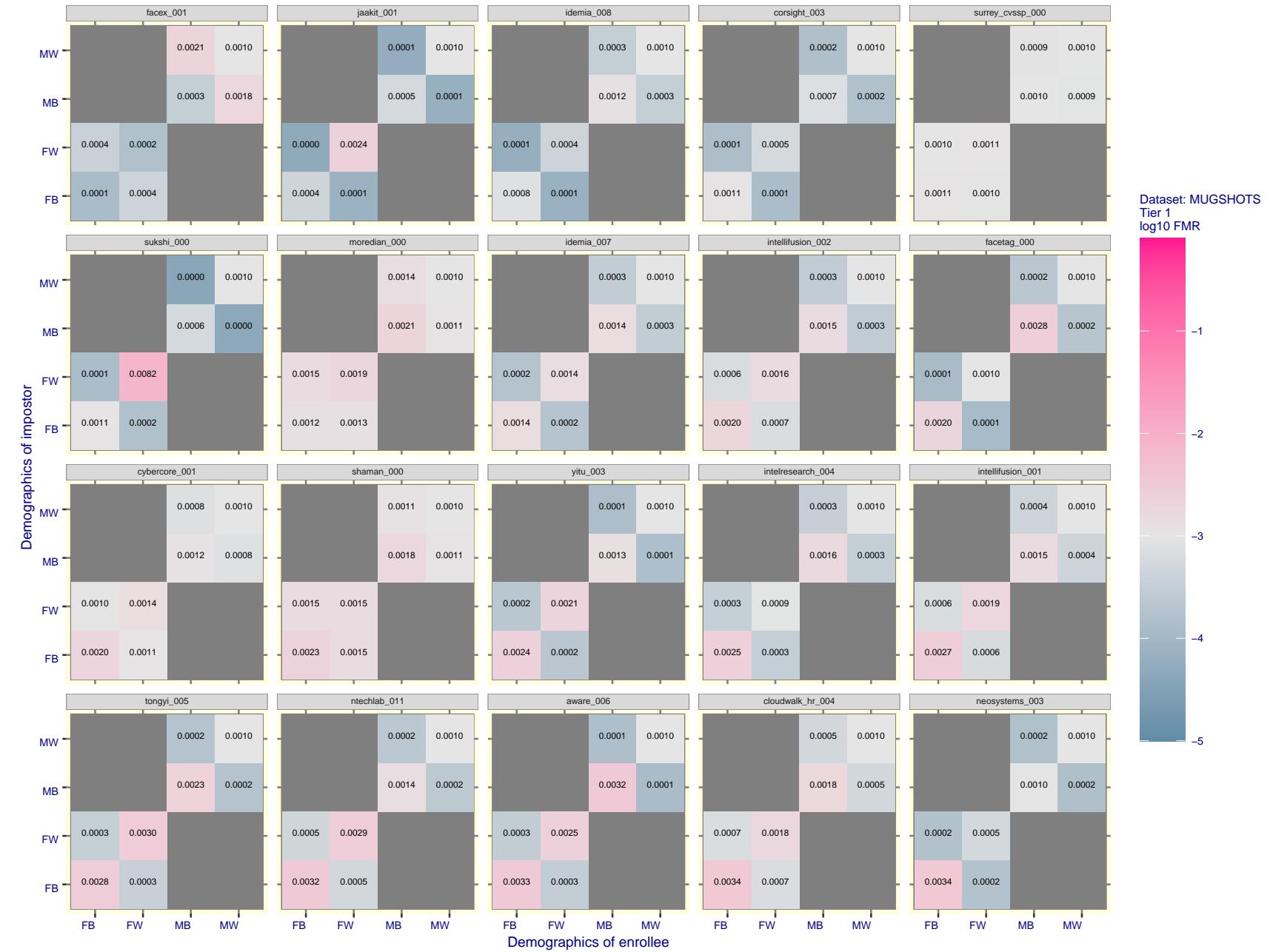


Figure 143: For the mugshot images, FMR for same-sex impostor pairs of images annotated with codes for black female, black male, white female, white male. The threshold is set for each algorithm to give FMR = 0.001 for white males which is the demographic that usually gives the lowest FMR. This means the top right box is the same color in all panels. The panels are sorted over multiple pages in order of FMR on black females, which is the demographic that usually gives the highest FMR.

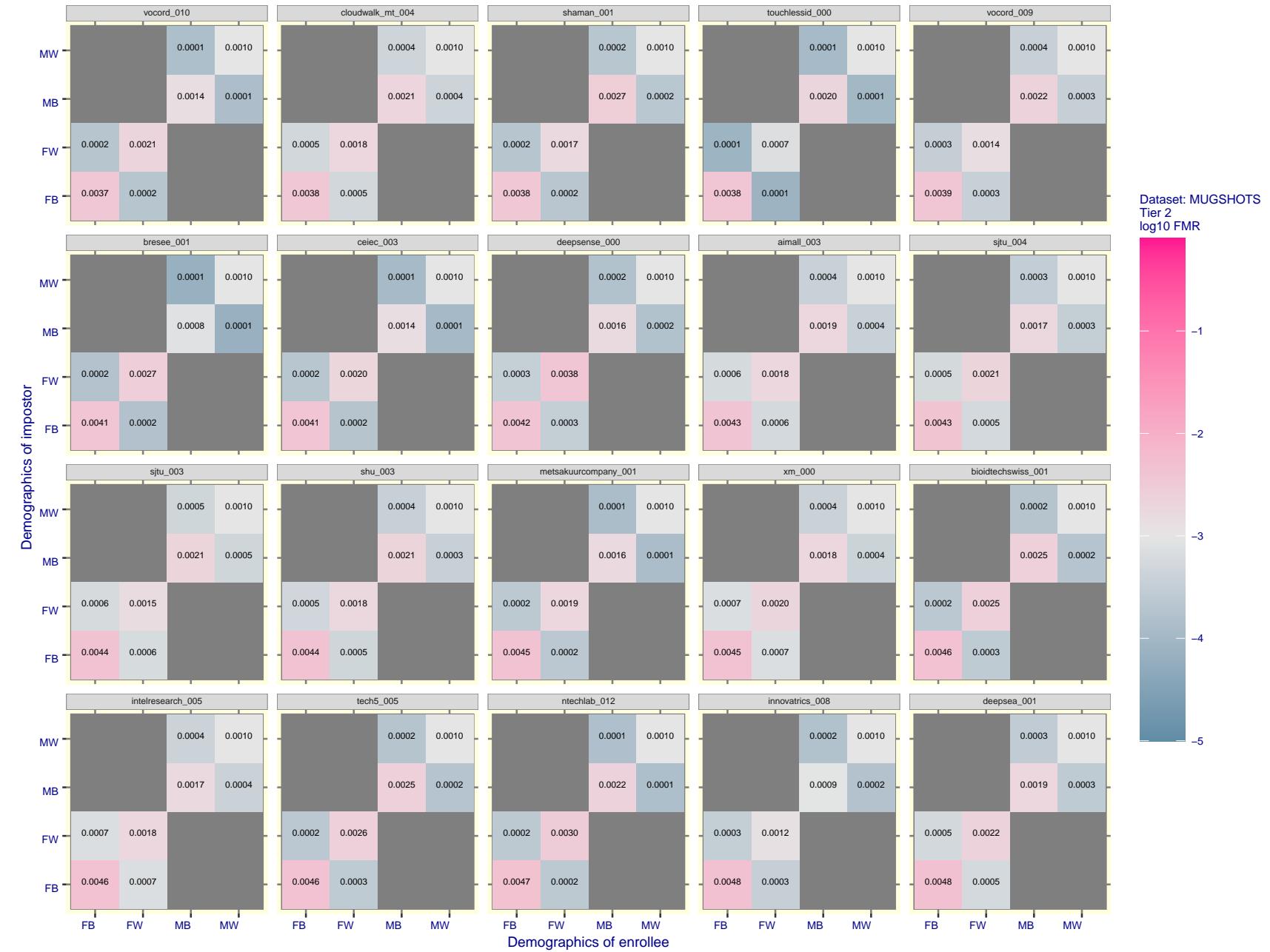


Figure 144: For the mugshot images, FMR for same-sex impostor pairs of images annotated with codes for black female, black male, white female, white male. The threshold is set for each algorithm to give FMR = 0.001 for white males which is the demographic that usually gives the lowest FMR. This means the top right box is the same color in all panels. The panels are sorted over multiple pages in order of FMR on black females, which is the demographic that usually gives the highest FMR.

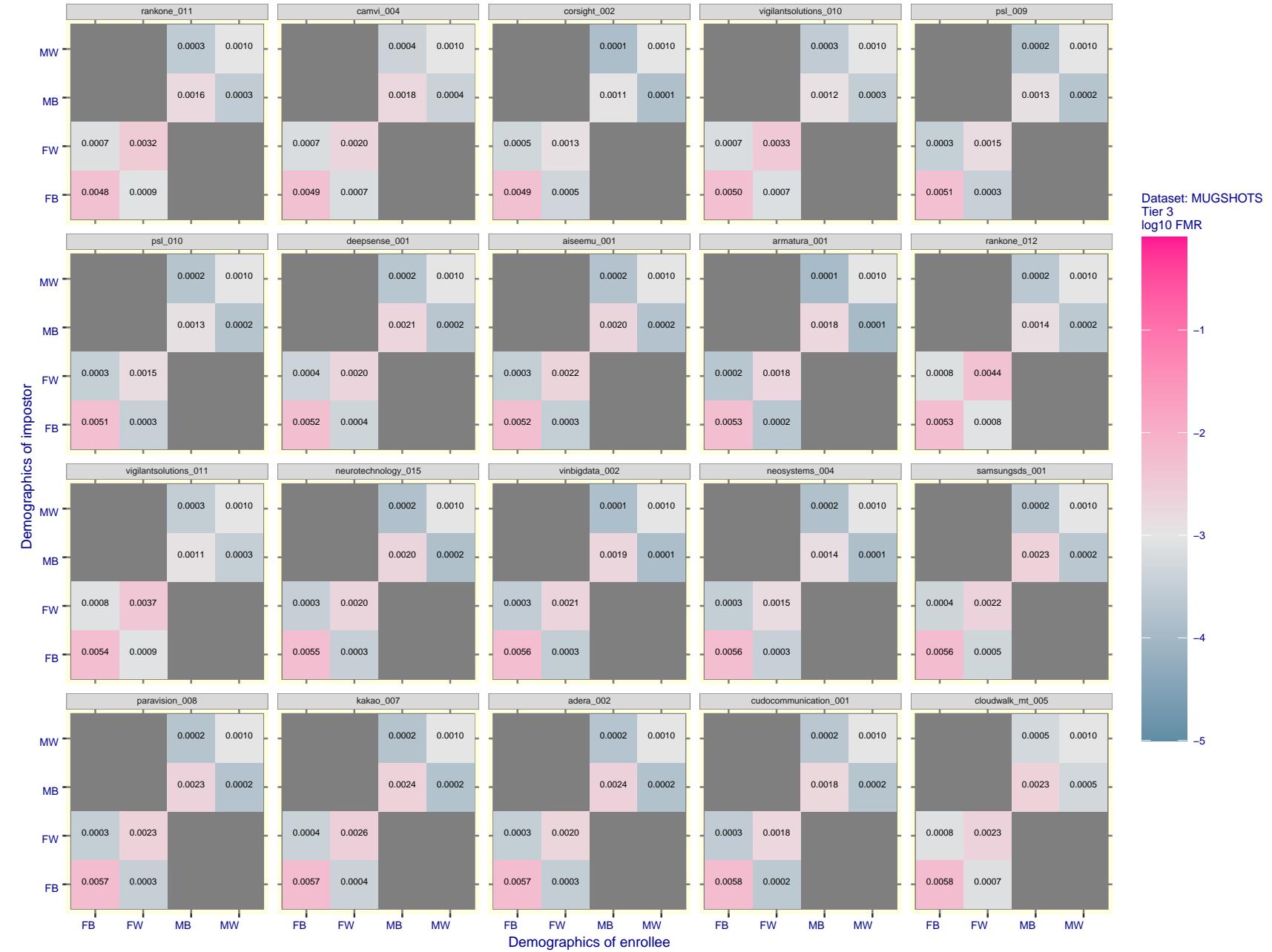


Figure 145: For the mugshot images, FMR for same-sex impostor pairs of images annotated with codes for black female, black male, white female, white male. The threshold is set for each algorithm to give FMR = 0.001 for white males which is the demographic that usually gives the lowest FMR. This means the top right box is the same color in all panels. The panels are sorted over multiple pages in order of FMR on black females, which is the demographic that usually gives the highest FMR.

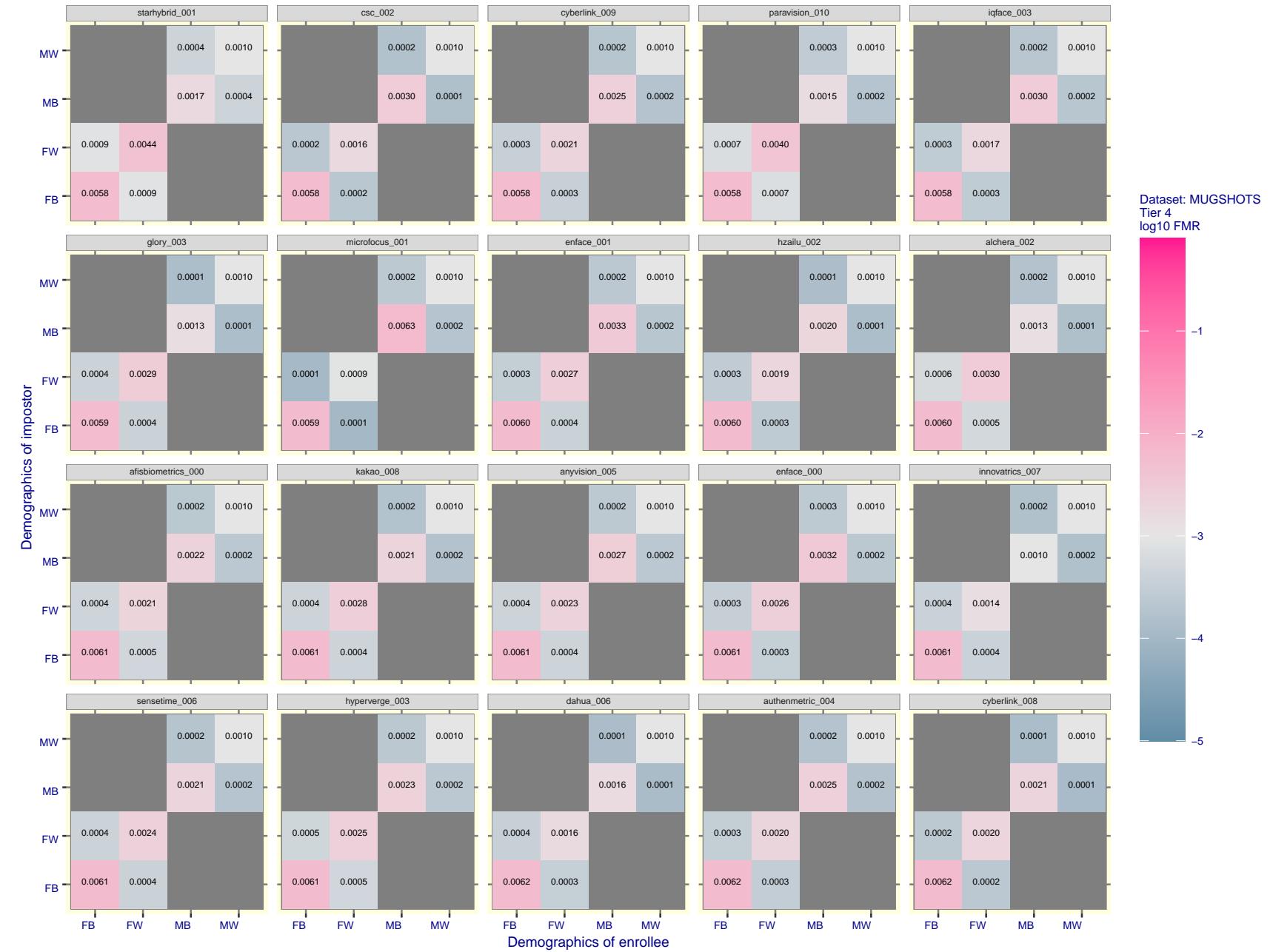


Figure 146: For the mugshot images, FMR for same-sex impostor pairs of images annotated with codes for black female, black male, white female, white male. The threshold is set for each algorithm to give FMR = 0.001 for white males which is the demographic that usually gives the lowest FMR. This means the top right box is the same color in all panels. The panels are sorted over multiple pages in order of FMR on black females, which is the demographic that usually gives the highest FMR.

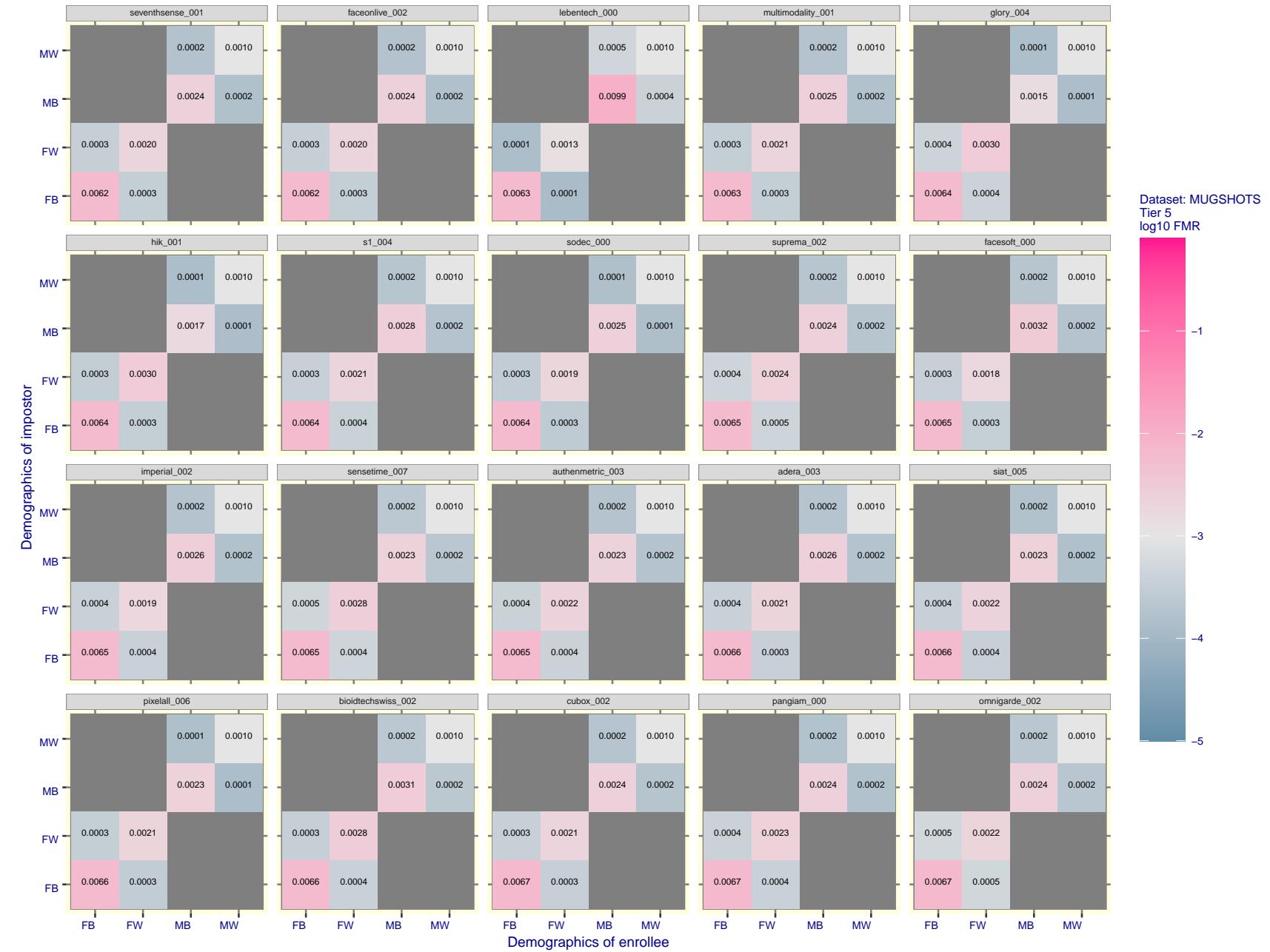


Figure 147: For the mugshot images, FMR for same-sex impostor pairs of images annotated with codes for black female, black male, white female, white male. The threshold is set for each algorithm to give $FMR = 0.001$ for white males which is the demographic that usually gives the lowest FMR. This means the top right box is the same color in all panels. The panels are sorted over multiple pages in order of FMR on black females, which is the demographic that usually gives the highest FMR.

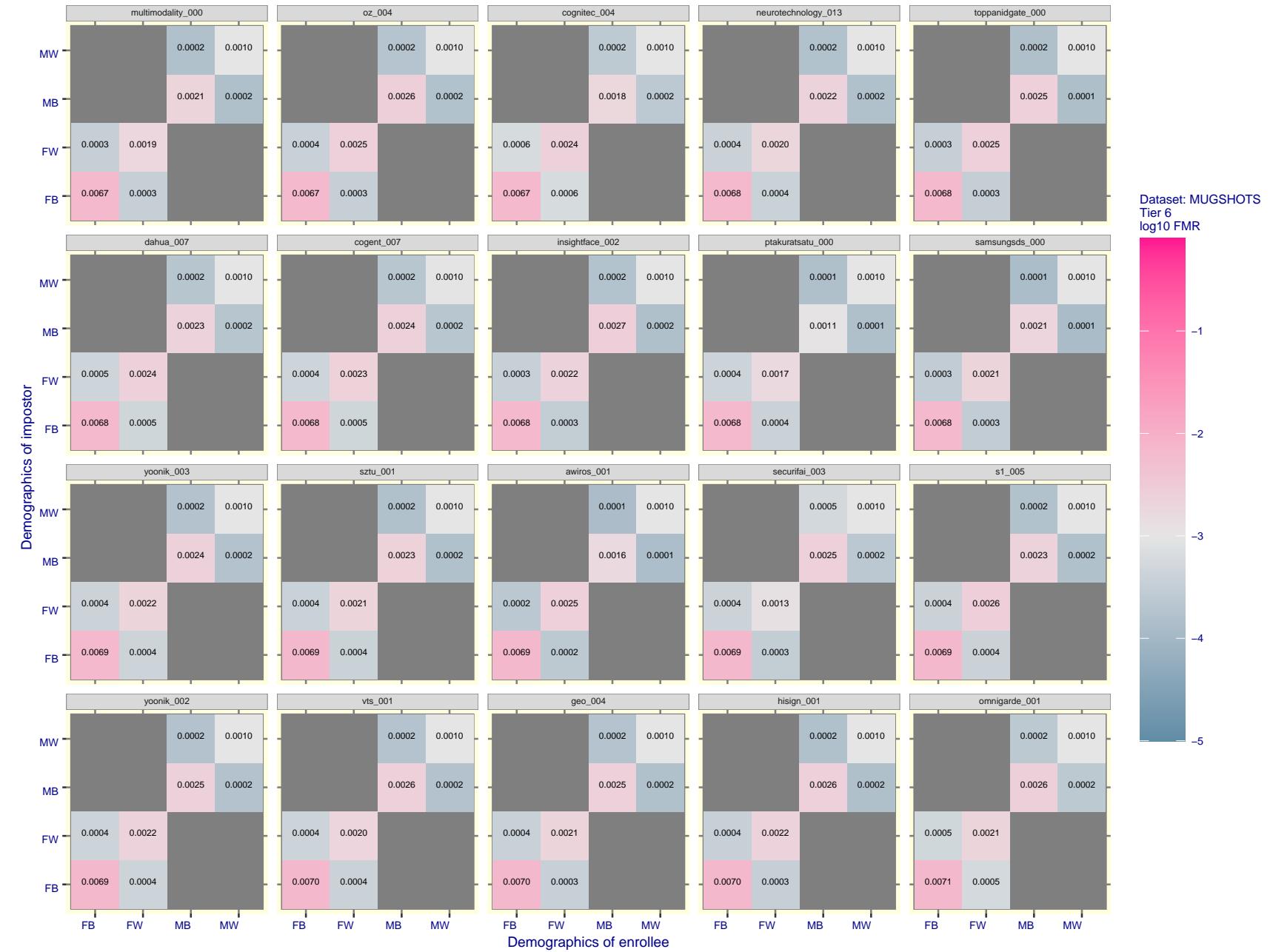


Figure 148: For the mugshot images, FMR for same-sex impostor pairs of images annotated with codes for black female, black male, white female, white male. The threshold is set for each algorithm to give $\text{FMR} = 0.001$ for white males which is the demographic that usually gives the lowest FMR. This means the top right box is the same color in all panels. The panels are sorted over multiple pages in order of FMR on black females, which is the demographic that usually gives the highest FMR.

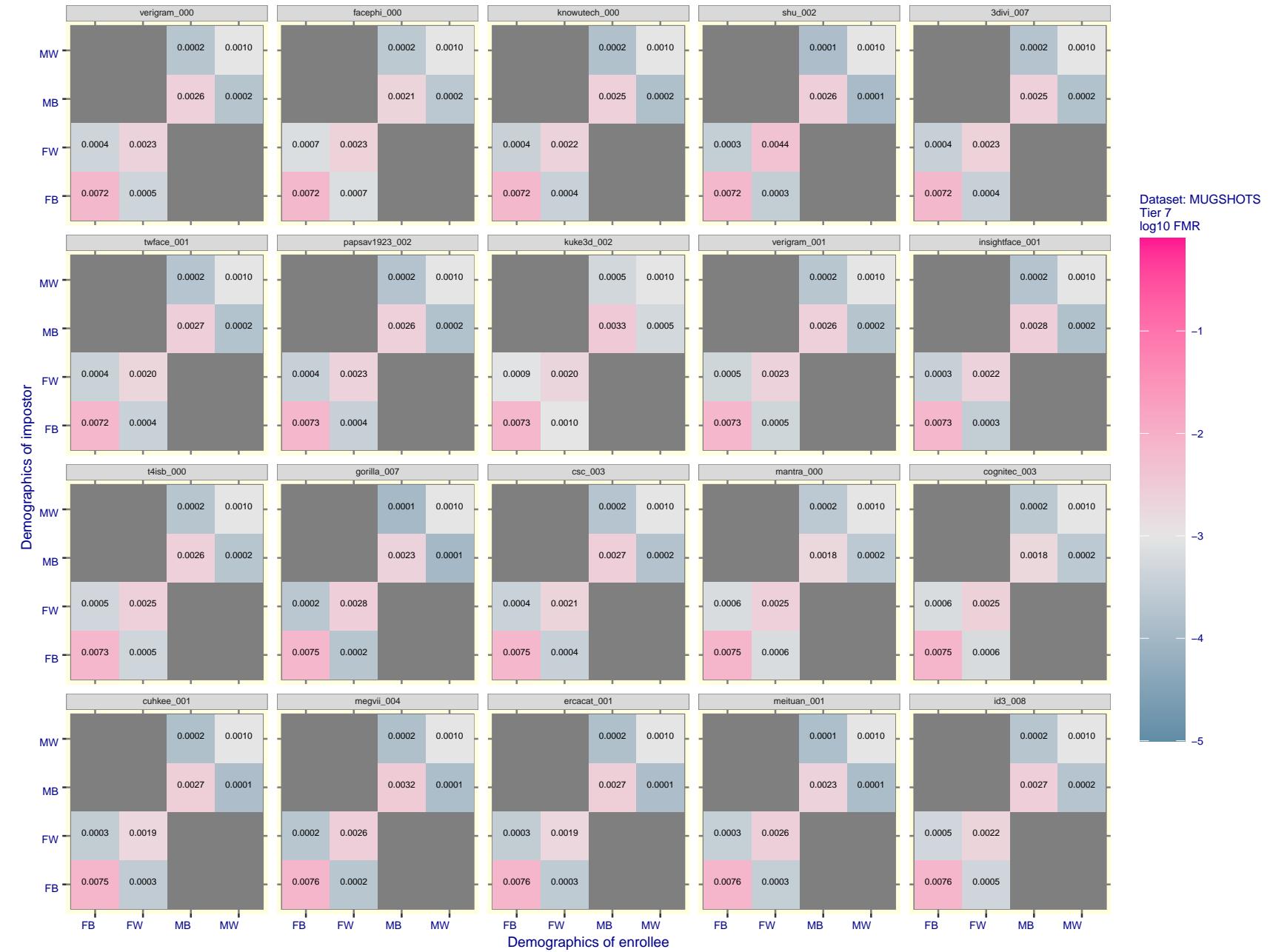


Figure 149: For the mugshot images, FMR for same-sex impostor pairs of images annotated with codes for black female, black male, white female, white male. The threshold is set for each algorithm to give FMR = 0.001 for white males which is the demographic that usually gives the lowest FMR. This means the top right box is the same color in all panels. The panels are sorted over multiple pages in order of FMR on black females, which is the demographic that usually gives the highest FMR.

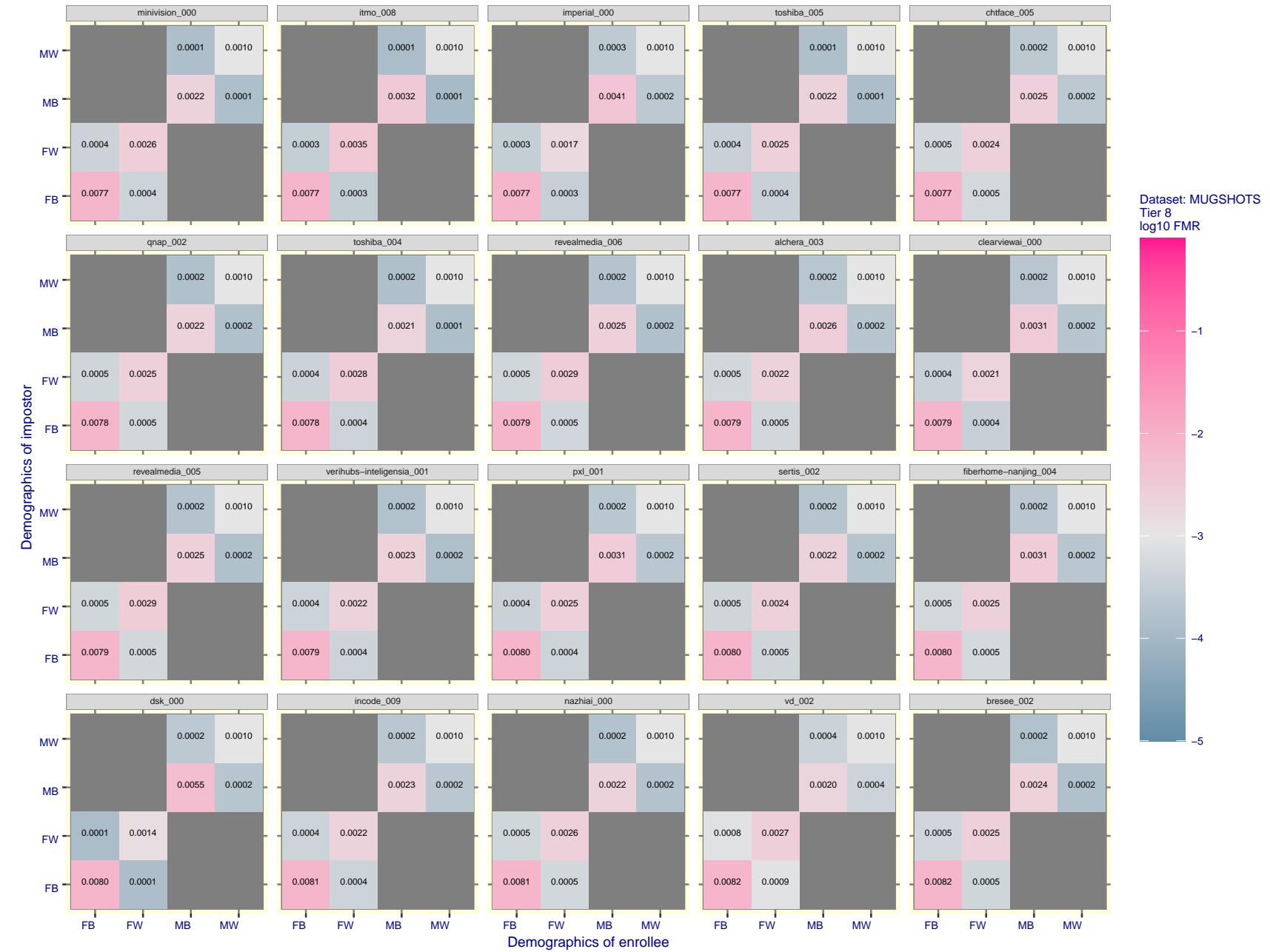


Figure 150: For the mugshot images, FMR for same-sex impostor pairs of images annotated with codes for black female, black male, white female, white male. The threshold is set for each algorithm to give $FMR = 0.001$ for white males which is the demographic that usually gives the lowest FMR. This means the top right box is the same color in all panels. The panels are sorted over multiple pages in order of FMR on black females, which is the demographic that usually gives the highest FMR.

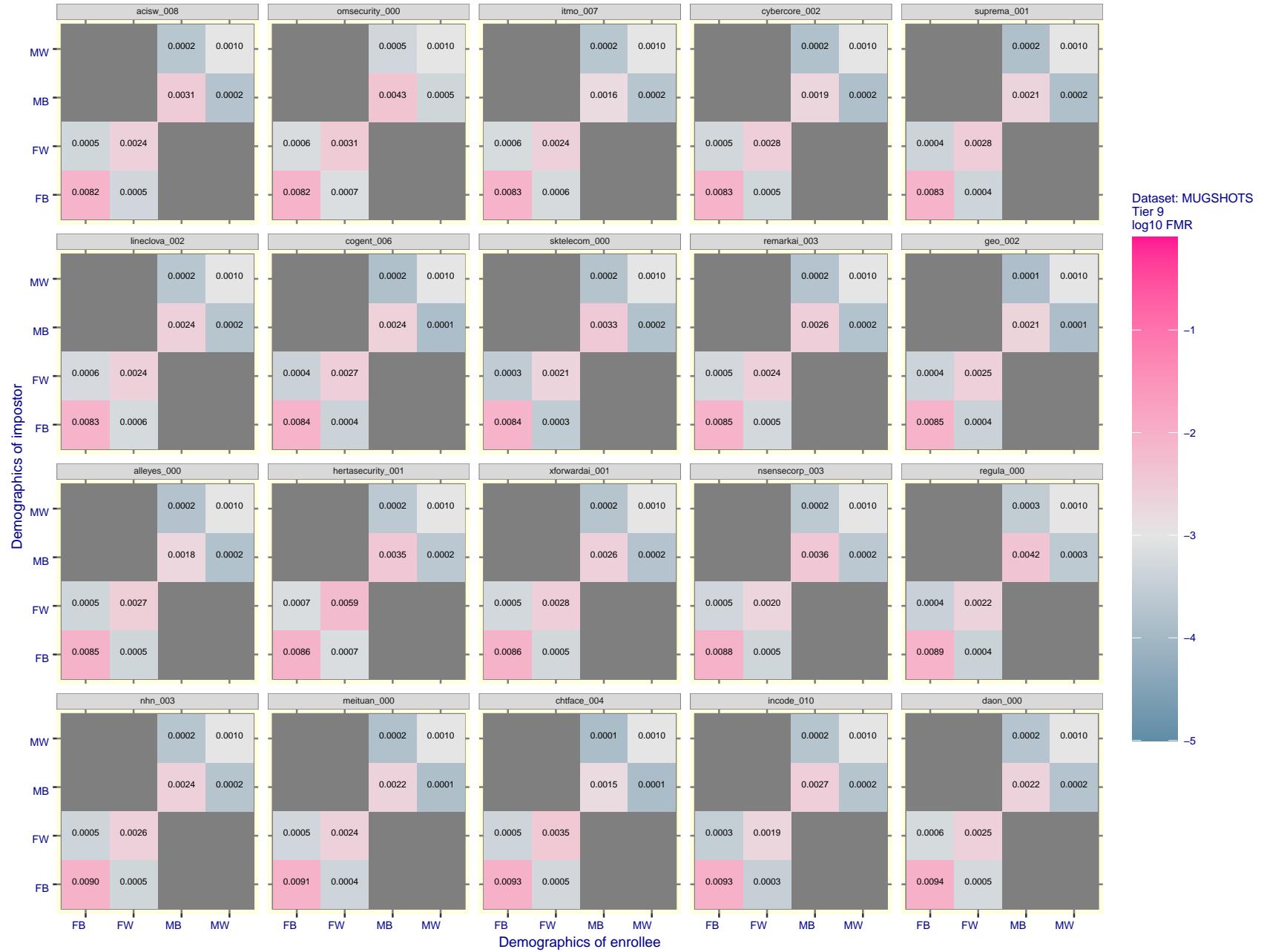


Figure 151: For the mugshot images, FMR for same-sex impostor pairs of images annotated with codes for black female, black male, white female, white male. The threshold is set for each algorithm to give $FMR = 0.001$ for white males which is the demographic that usually gives the lowest FMR. This means the top right box is the same color in all panels. The panels are sorted over multiple pages in order of FMR on black females, which is the demographic that usually gives the highest FMR.

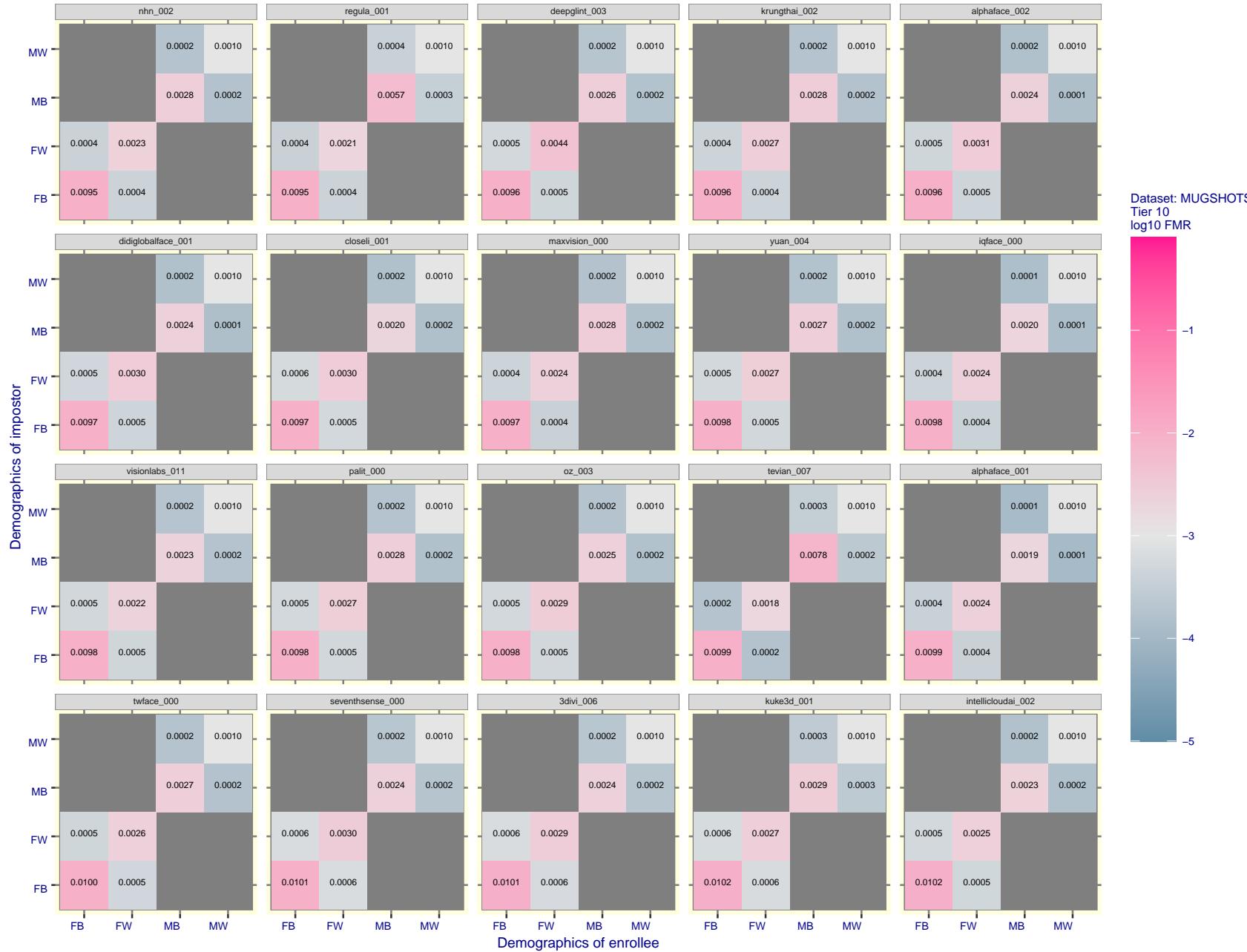


Figure 152: For the mugshot images, FMR for same-sex impostor pairs of images annotated with codes for black female, black male, white female, white male. The threshold is set for each algorithm to give $FMR = 0.001$ for white males which is the demographic that usually gives the lowest FMR. This means the top right box is the same color in all panels. The panels are sorted over multiple pages in order of FMR on black females, which is the demographic that usually gives the highest FMR.

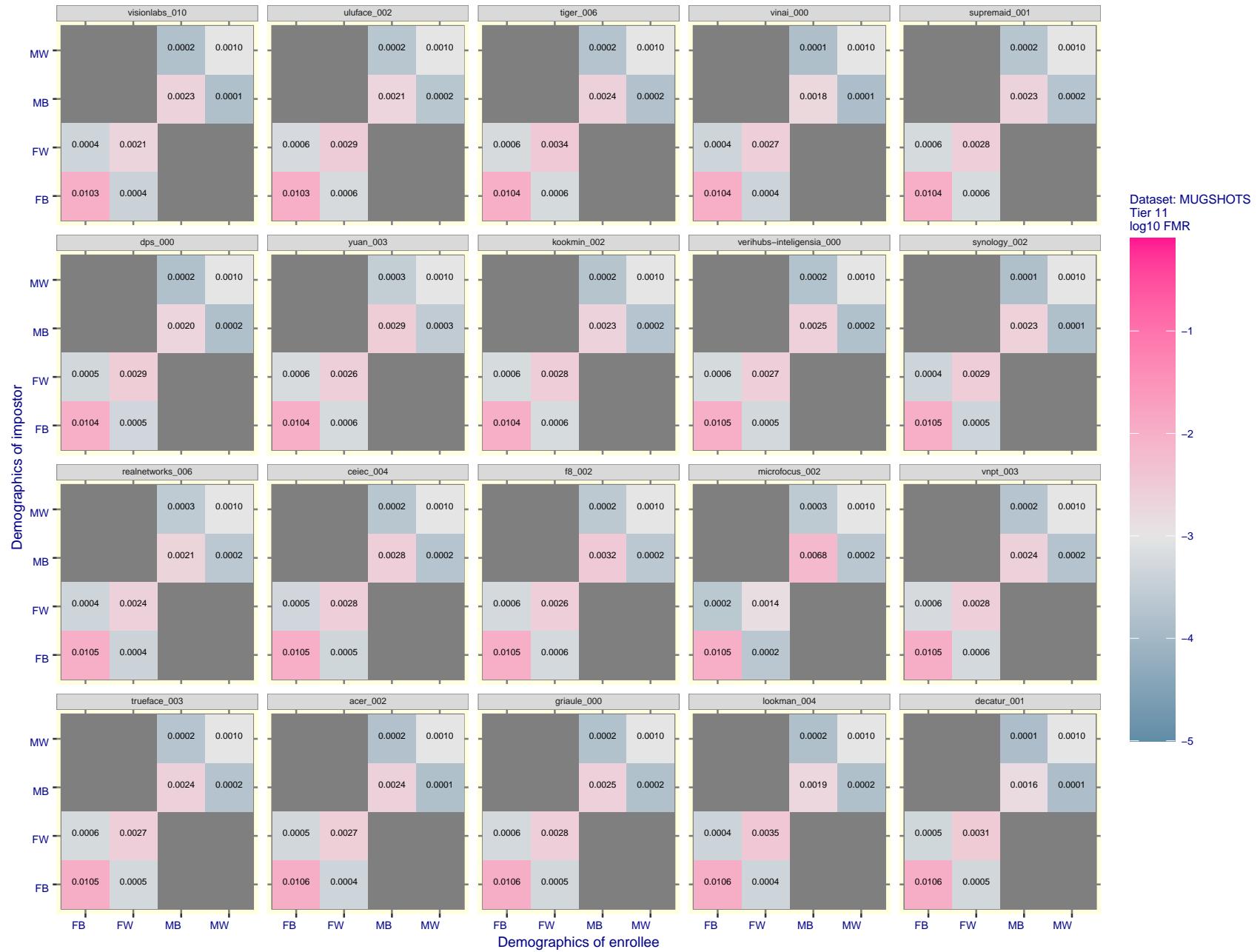


Figure 153: For the mugshot images, FMR for same-sex impostor pairs of images annotated with codes for black female, black male, white female, white male. The threshold is set for each algorithm to give $FMR = 0.001$ for white males which is the demographic that usually gives the lowest FMR. This means the top right box is the same color in all panels. The panels are sorted over multiple pages in order of FMR on black females, which is the demographic that usually gives the highest FMR.

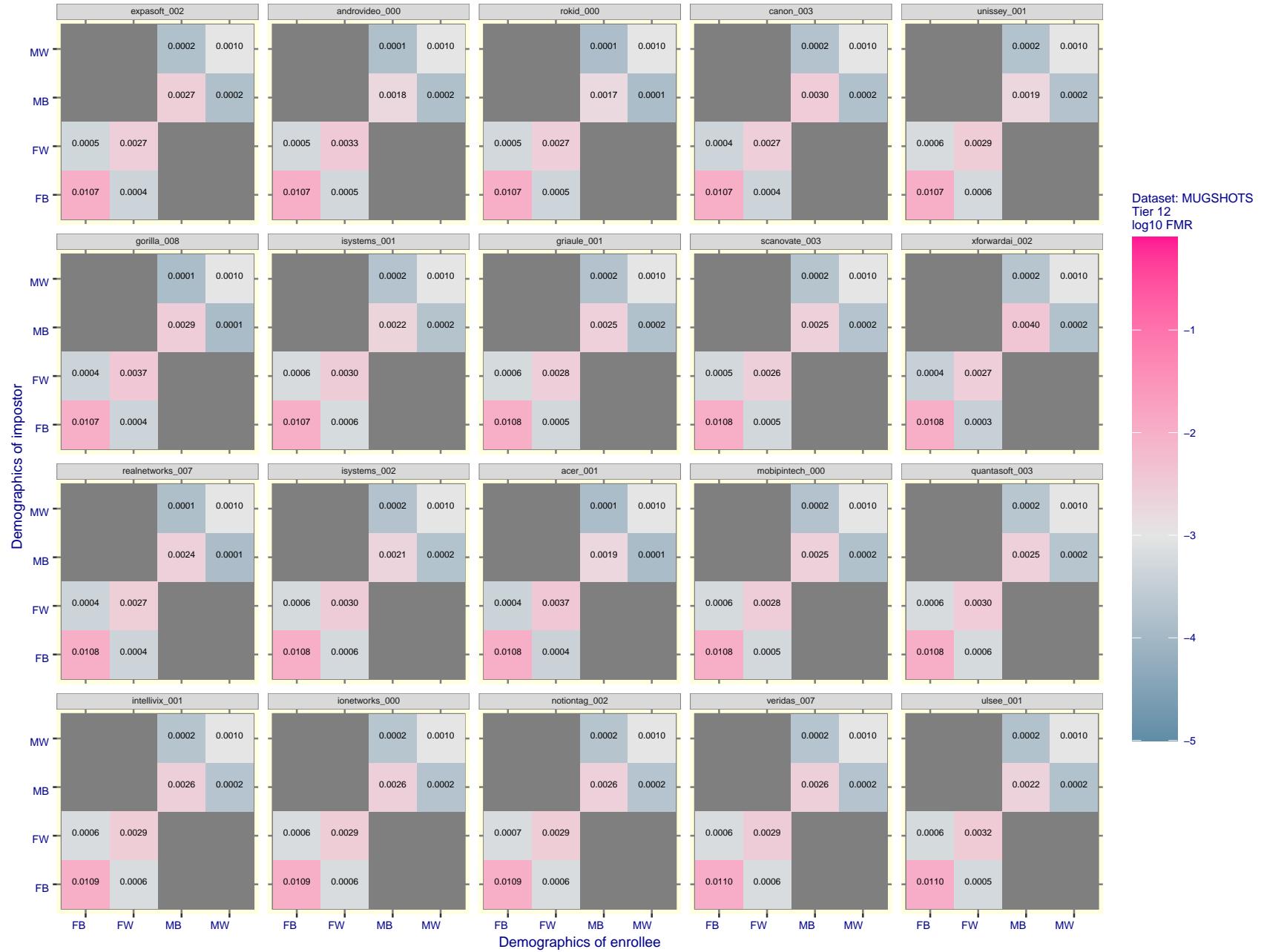


Figure 154: For the mugshot images, FMR for same-sex impostor pairs of images annotated with codes for black female, black male, white female, white male. The threshold is set for each algorithm to give $FMR = 0.001$ for white males which is the demographic that usually gives the lowest FMR. This means the top right box is the same color in all panels. The panels are sorted over multiple pages in order of FMR on black females, which is the demographic that usually gives the highest FMR.

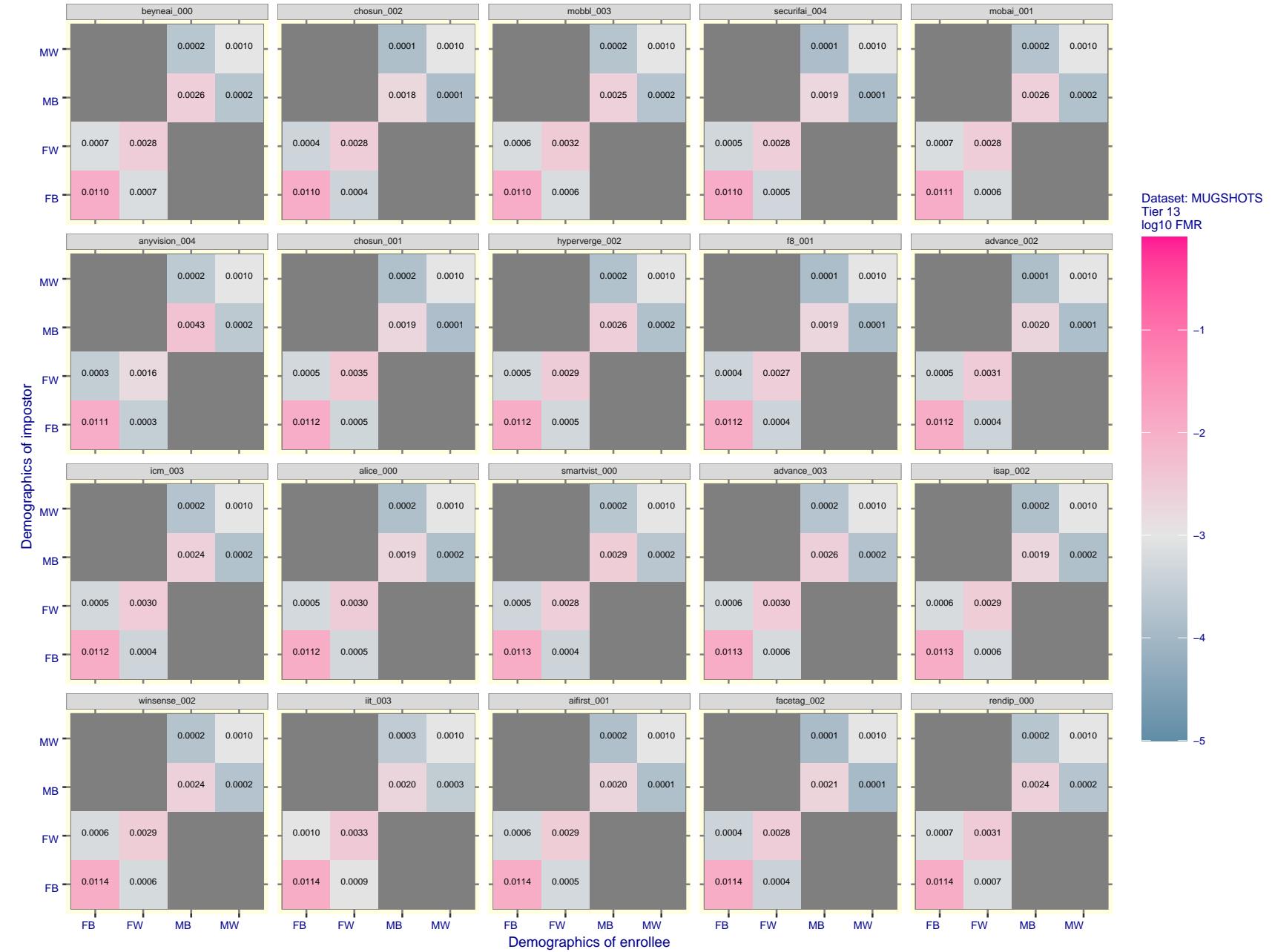


Figure 155: For the mugshot images, FMR for same-sex impostor pairs of images annotated with codes for black female, black male, white female, white male. The threshold is set for each algorithm to give $FMR = 0.001$ for white males which is the demographic that usually gives the lowest FMR. This means the top right box is the same color in all panels. The panels are sorted over multiple pages in order of FMR on black females, which is the demographic that usually gives the highest FMR.

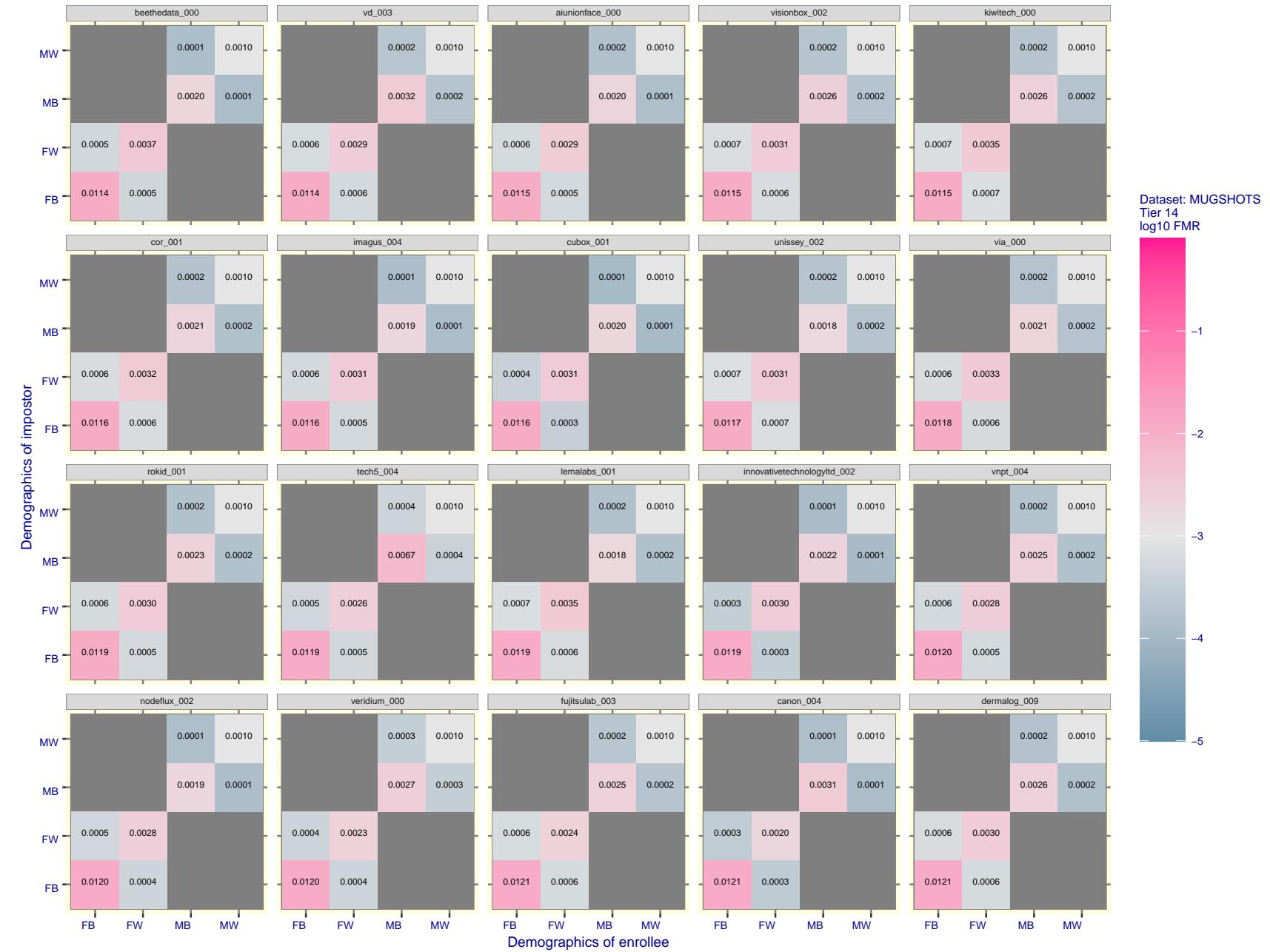


Figure 156: For the mugshot images, FMR for same-sex impostor pairs of images annotated with codes for black female, black male, white female, white male. The threshold is set for each algorithm to give FMR = 0.001 for white males which is the demographic that usually gives the lowest FMR. This means the top right box is the same color in all panels. The panels are sorted over multiple pages in order of FMR on black females, which is the demographic that usually gives the highest FMR.

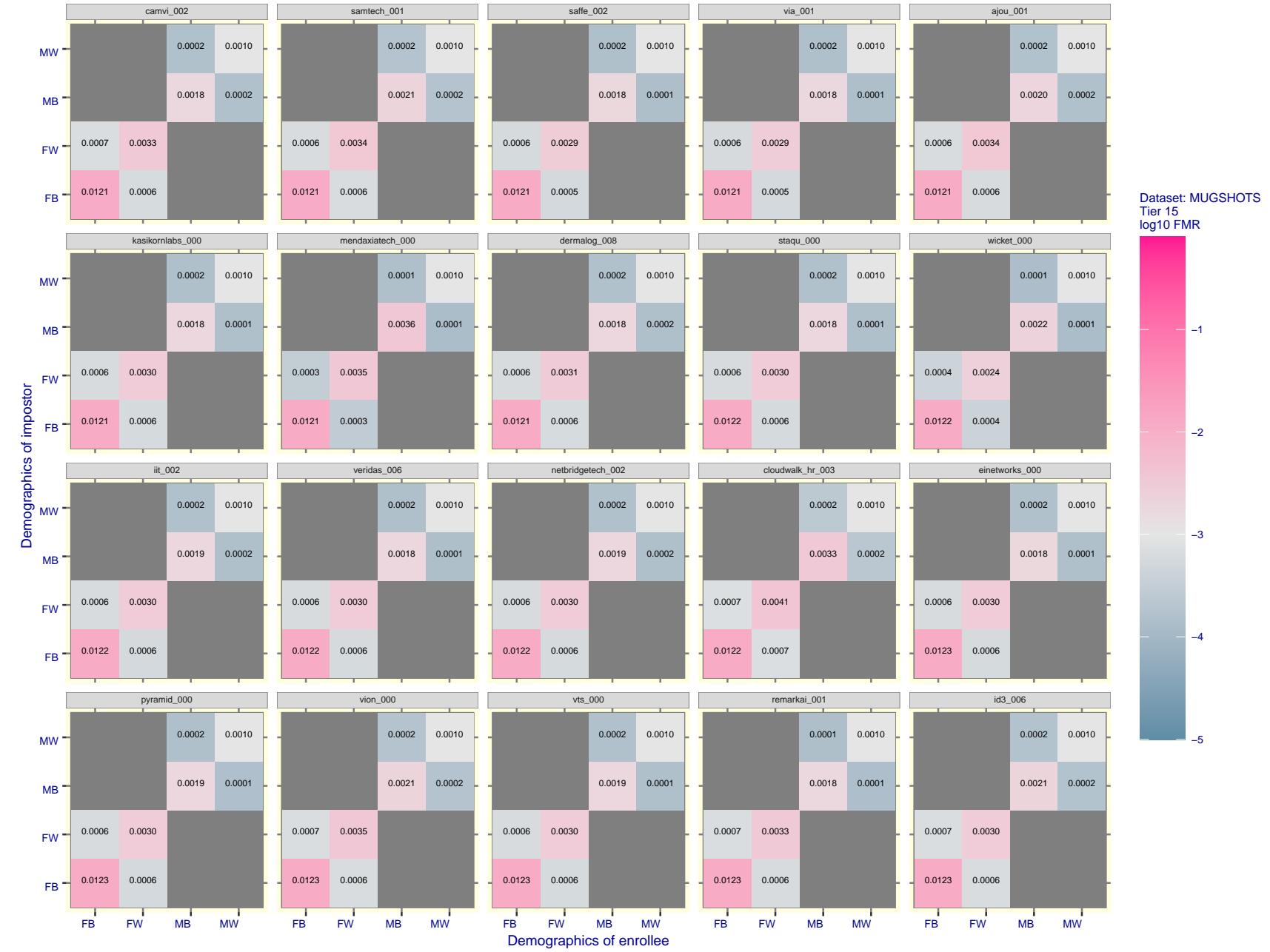


Figure 157: For the mugshot images, FMR for same-sex impostor pairs of images annotated with codes for black female, black male, white female, white male. The threshold is set for each algorithm to give FMR = 0.001 for white males which is the demographic that usually gives the lowest FMR. This means the top right box is the same color in all panels. The panels are sorted over multiple pages in order of FMR on black females, which is the demographic that usually gives the highest FMR.

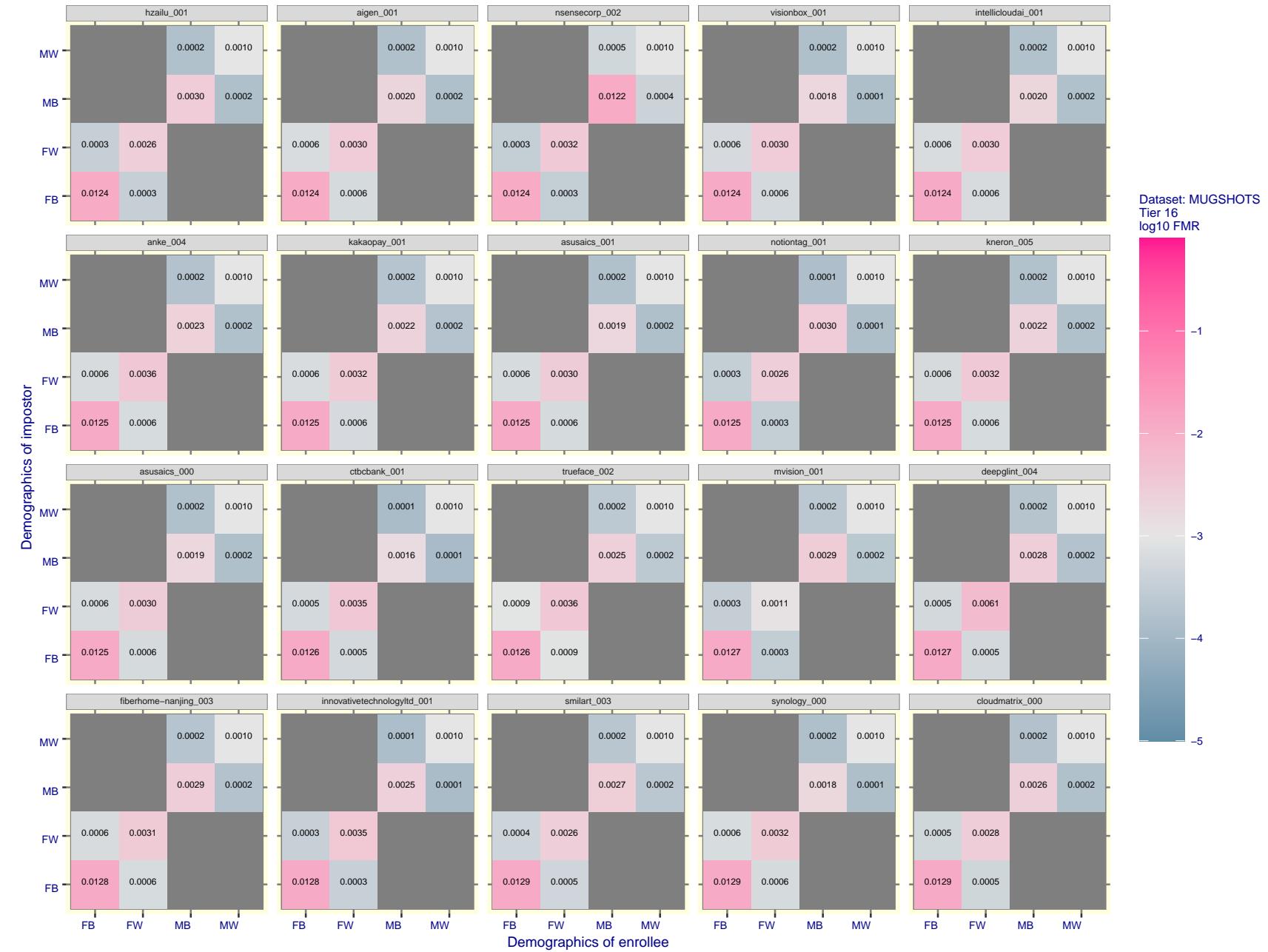


Figure 158: For the mugshot images, FMR for same-sex impostor pairs of images annotated with codes for black female, black male, white female, white male. The threshold is set for each algorithm to give FMR = 0.001 for white males which is the demographic that usually gives the lowest FMR. This means the top right box is the same color in all panels. The panels are sorted over multiple pages in order of FMR on black females, which is the demographic that usually gives the highest FMR.

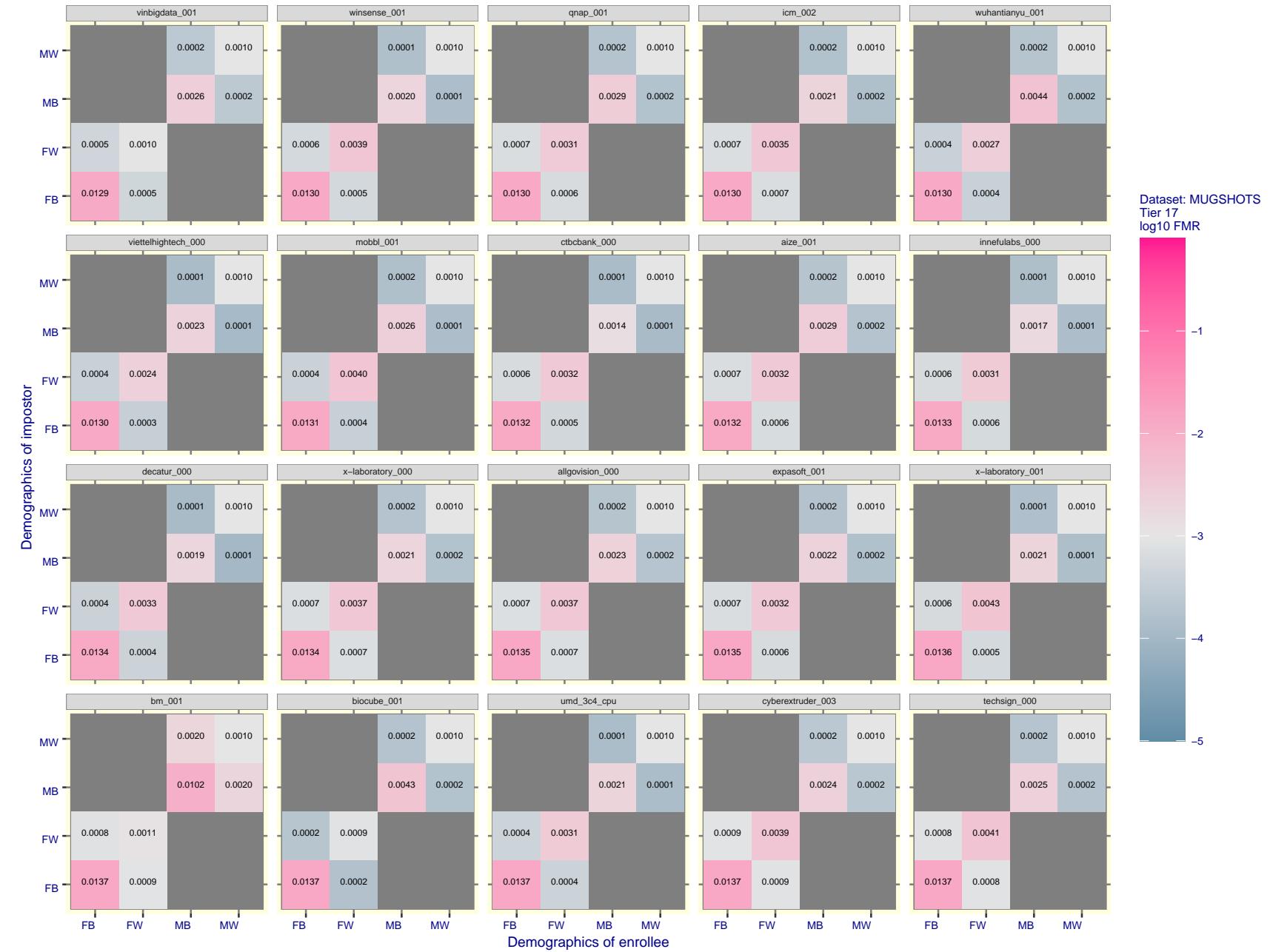


Figure 159: For the mugshot images, FMR for same-sex impostor pairs of images annotated with codes for black female, black male, white female, white male. The threshold is set for each algorithm to give $FMR = 0.001$ for white males which is the demographic that usually gives the lowest FMR. This means the top right box is the same color in all panels. The panels are sorted over multiple pages in order of FMR on black females, which is the demographic that usually gives the highest FMR.

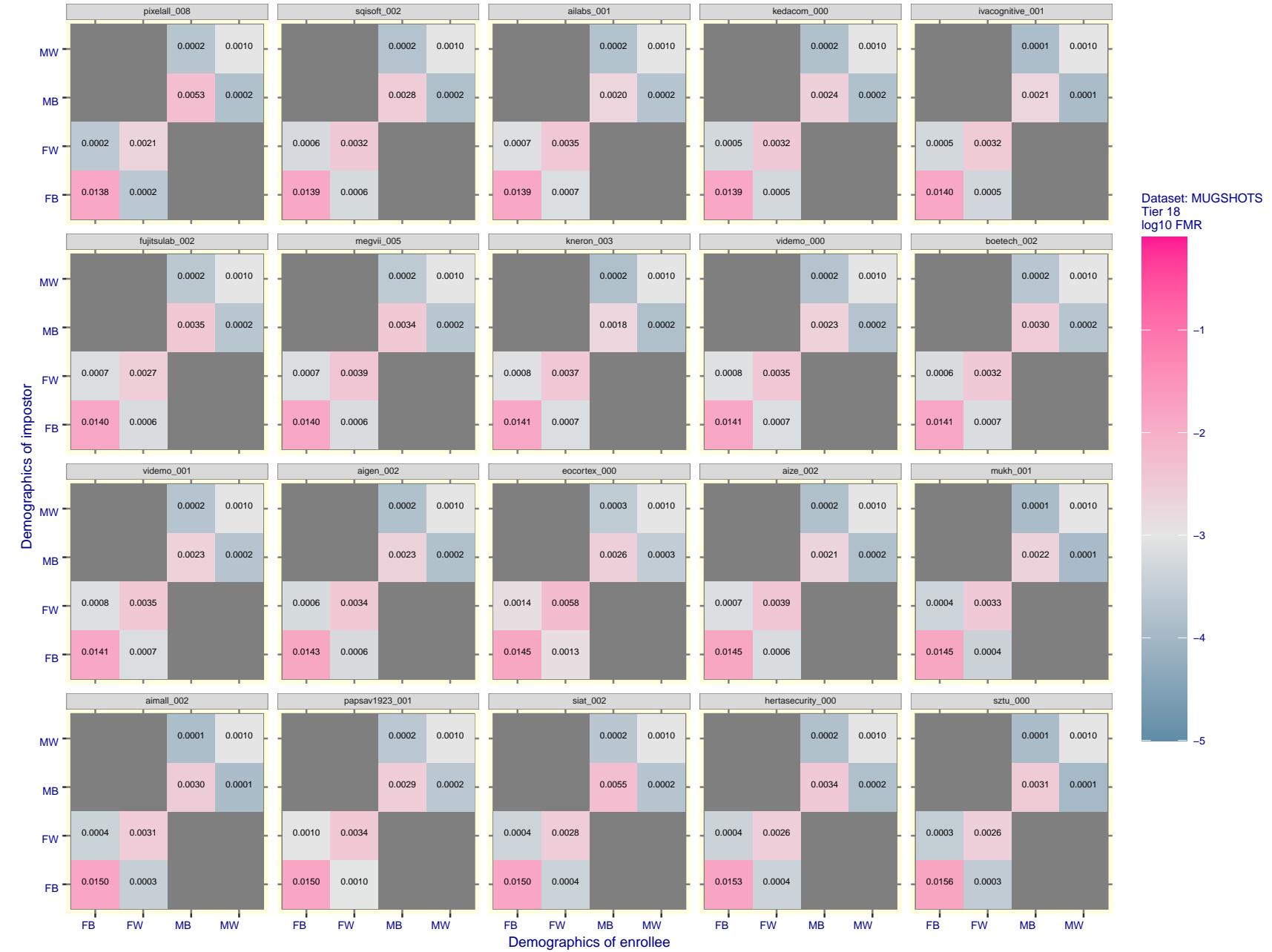


Figure 160: For the mugshot images, FMR for same-sex impostor pairs of images annotated with codes for black female, black male, white female, white male. The threshold is set for each algorithm to give FMR = 0.001 for white males which is the demographic that usually gives the lowest FMR. This means the top right box is the same color in all panels. The panels are sorted over multiple pages in order of FMR on black females, which is the demographic that usually gives the highest FMR.

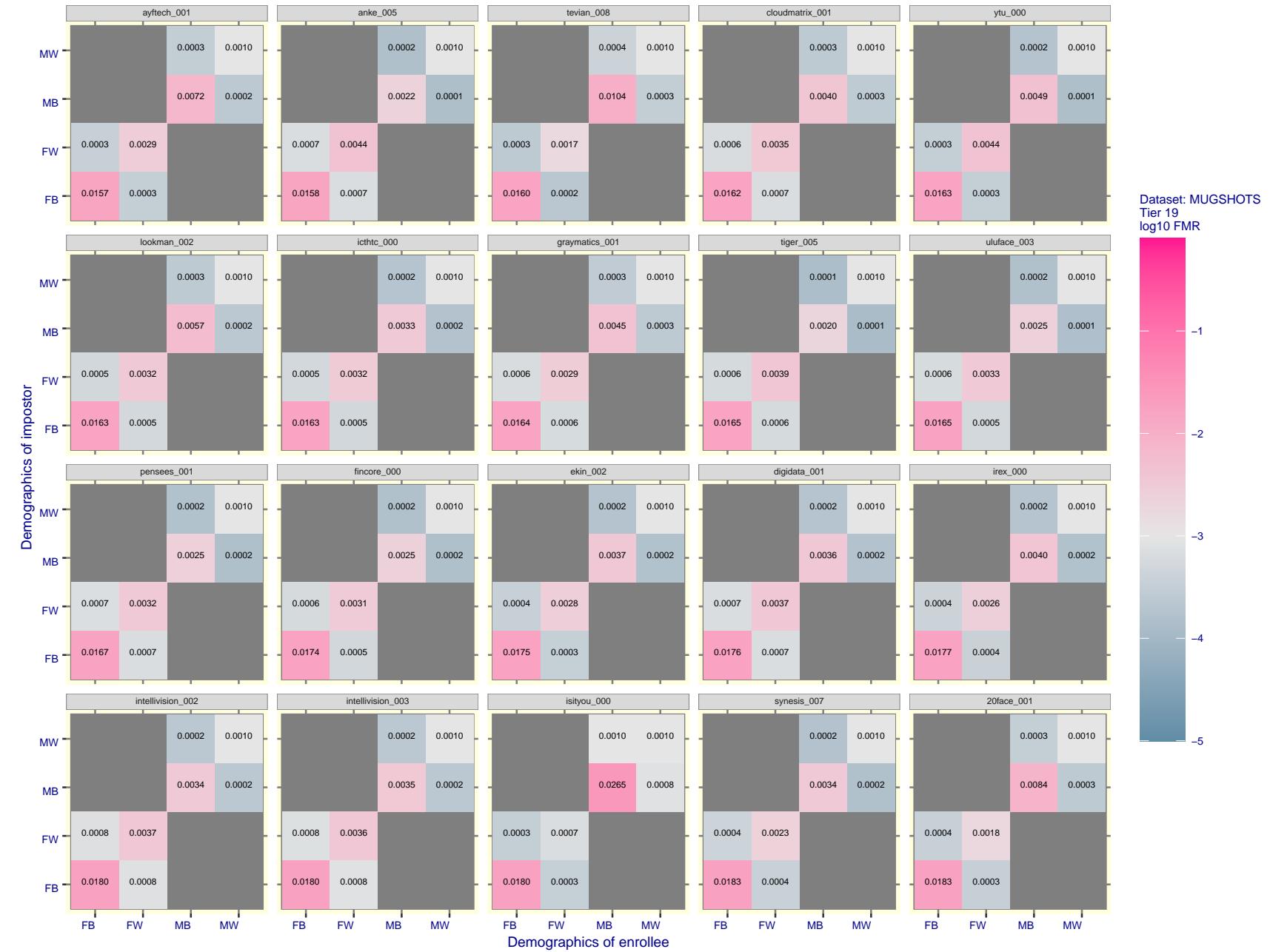


Figure 161: For the mugshot images, FMR for same-sex impostor pairs of images annotated with codes for black female, black male, white female, white male. The threshold is set for each algorithm to give FMR = 0.001 for white males which is the demographic that usually gives the lowest FMR. This means the top right box is the same color in all panels. The panels are sorted over multiple pages in order of FMR on black females, which is the demographic that usually gives the highest FMR.

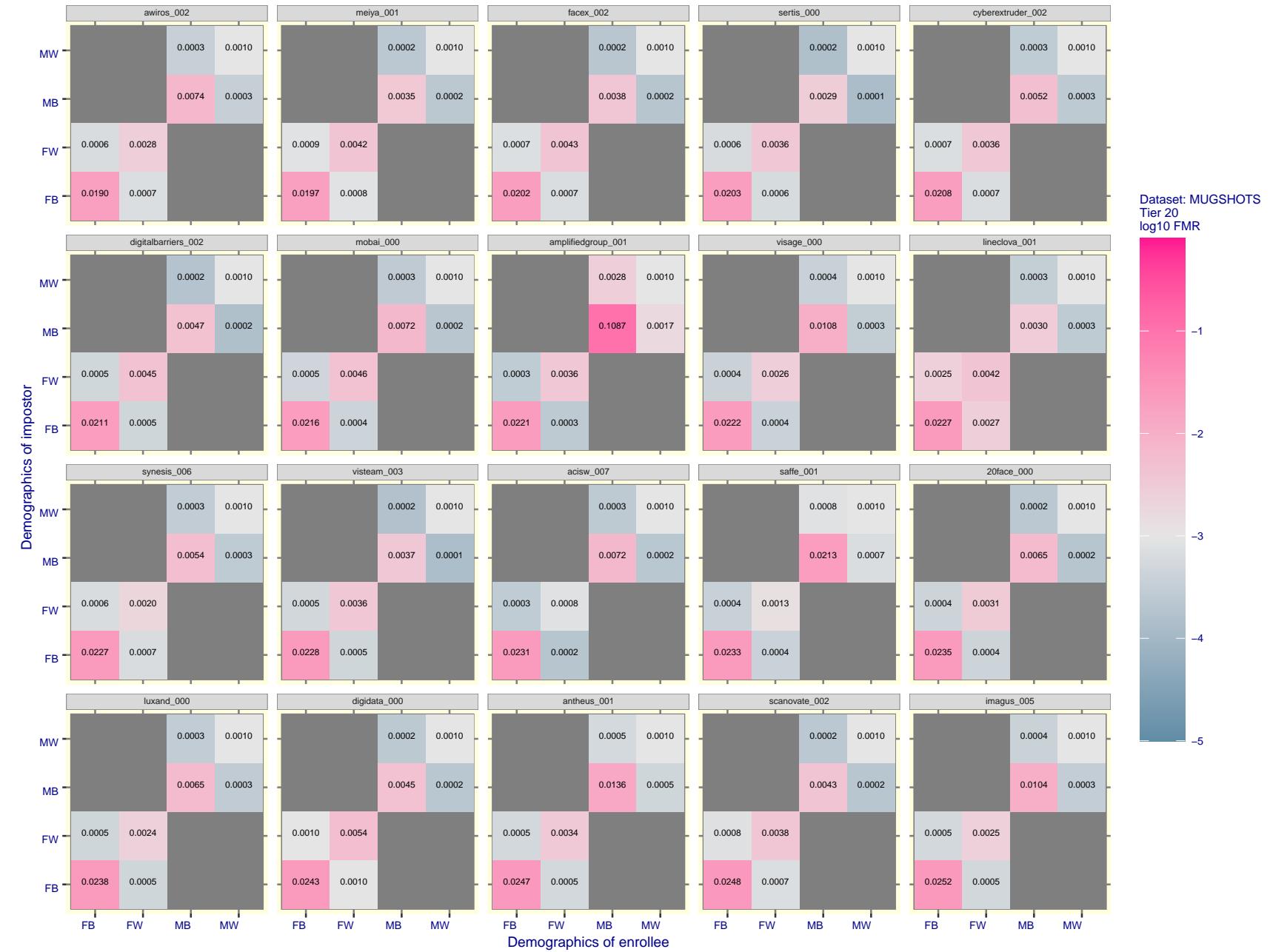


Figure 162: For the mugshot images, FMR for same-sex impostor pairs of images annotated with codes for black female, black male, white female, white male. The threshold is set for each algorithm to give $FMR = 0.001$ for white males which is the demographic that usually gives the lowest FMR. This means the top right box is the same color in all panels. The panels are sorted over multiple pages in order of FMR on black females, which is the demographic that usually gives the highest FMR.



Figure 163: For the mugshot images, FMR for same-sex impostor pairs of images annotated with codes for black female, black male, white female, white male. The threshold is set for each algorithm to give $FMR = 0.001$ for white males which is the demographic that usually gives the lowest FMR. This means the top right box is the same color in all panels. The panels are sorted over multiple pages in order of FMR on black females, which is the demographic that usually gives the highest FMR.

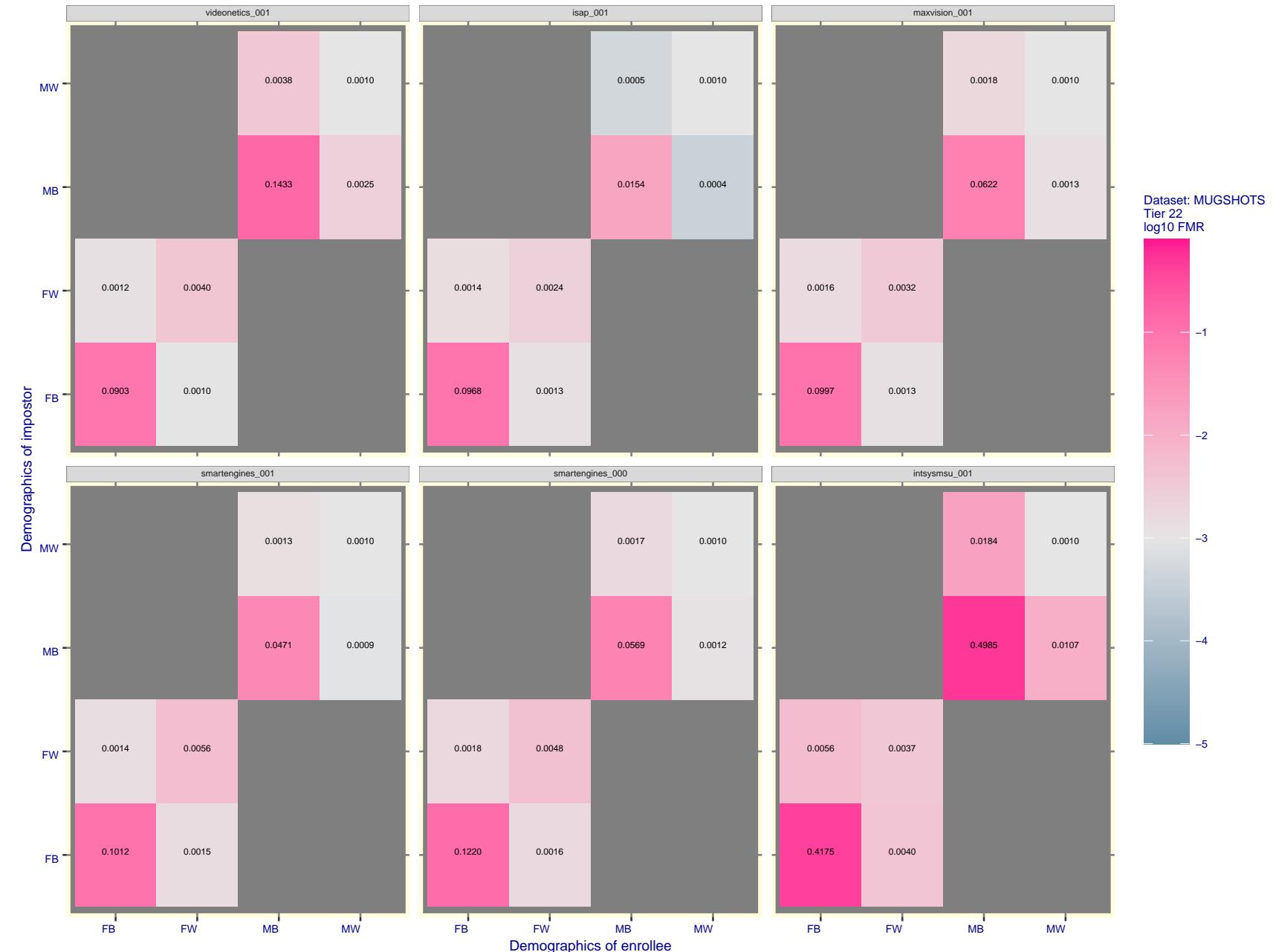


Figure 164: For the mugshot images, FMR for same-sex impostor pairs of images annotated with codes for black female, black male, white female, white male. The threshold is set for each algorithm to give $\text{FMR} = 0.001$ for white males which is the demographic that usually gives the lowest FMR. This means the top right box is the same color in all panels. The panels are sorted over multiple pages in order of FMR on black females, which is the demographic that usually gives the highest FMR.

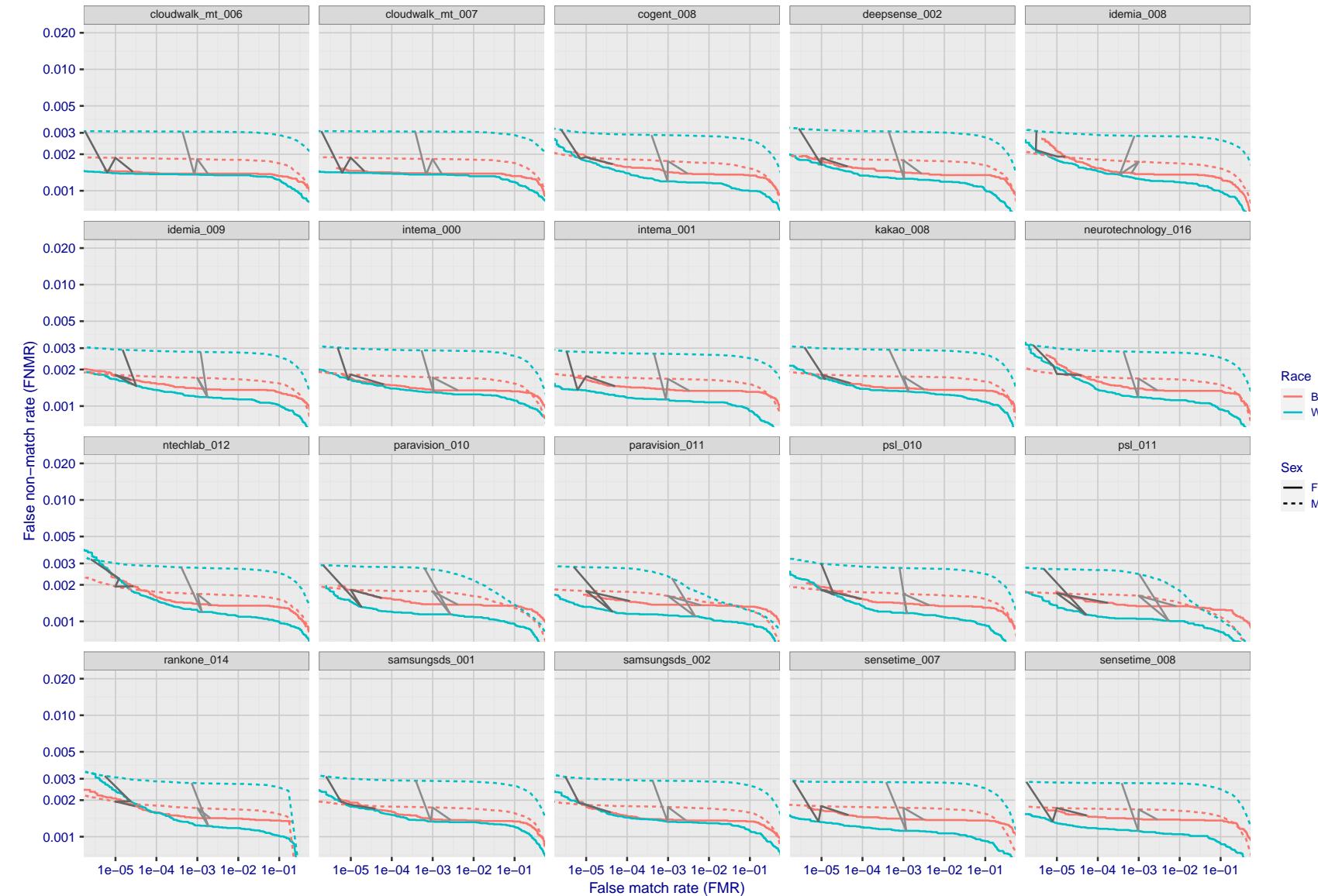


Figure 165: For the mugshot images, error tradeoff characteristics for white females, black females, black males and white males. The Z-shaped grey lines correspond to fixed thresholds, showing both FNMR and FMR vary at one T value. Note: Many of the plots will naively be read as saying women gives worse error rates than men because the solid traces lie above the dotted ones. However, this is misleading and incomplete: The grey lines show the traces reveal horizontal shifts. Thus for the cogent-003 algorithm FNMR for men is higher than for women at a fixed threshold but, at the same time, FMR is higher for women - see Figure 255. As access control systems almost always operate at a fixed threshold, the naive interpretation is incorrect.

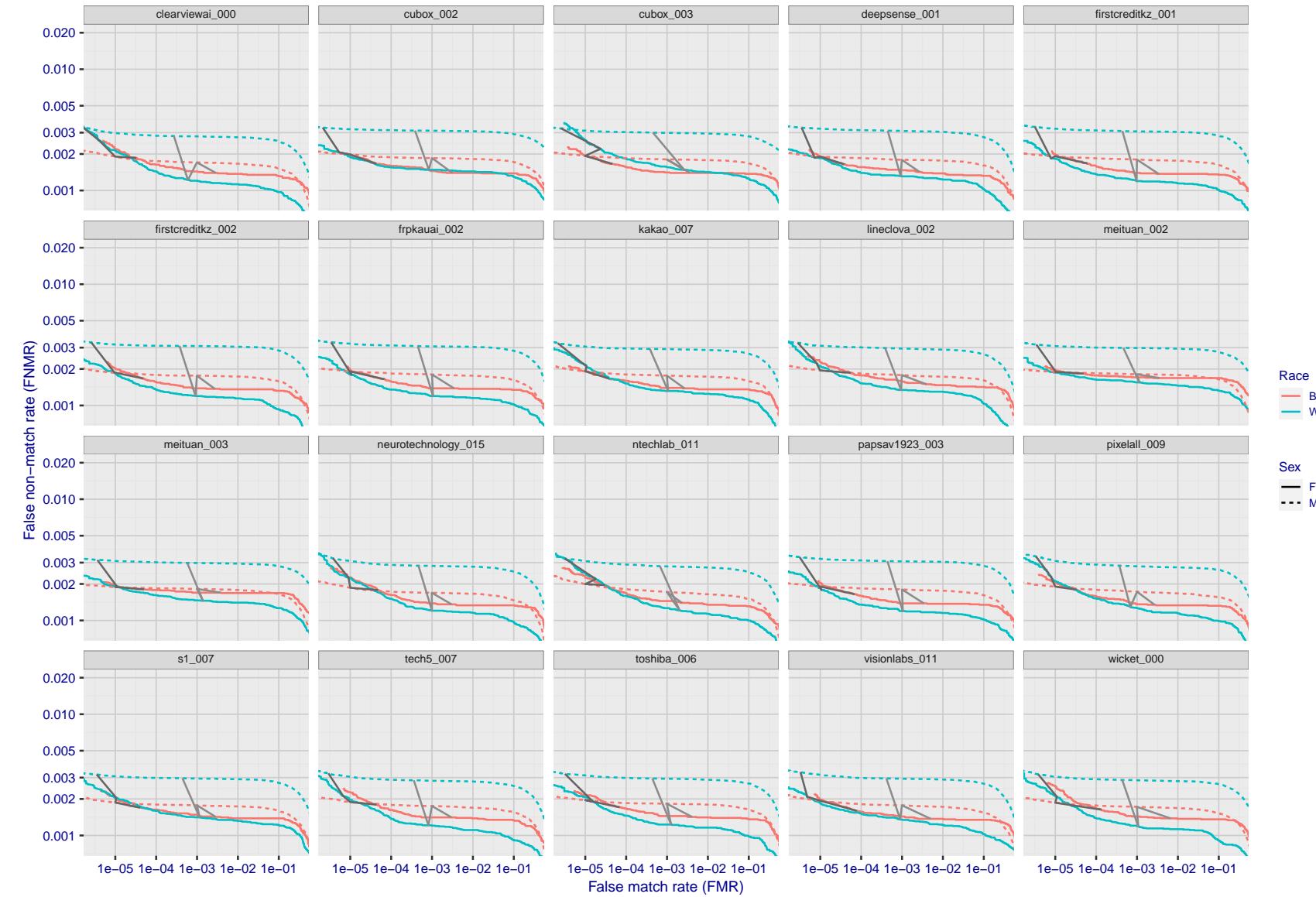


Figure 166: For the mugshot images, error tradeoff characteristics for white females, black females, black males and white males. The Z-shaped grey lines correspond to fixed thresholds, showing both FNMR and FMR vary at one T value. Note: Many of the plots will naively be read as saying women gives worse error rates than men because the solid traces lie above the dotted ones. However, this is misleading and incomplete: The grey lines show the traces reveal horizontal shifts. Thus for the cogent-003 algorithm FNMR for men is higher than for women at a fixed threshold but, at the same time, FMR is higher for women - see Figure 255. As access control systems almost always operate at a fixed threshold, the naive interpretation is incorrect.

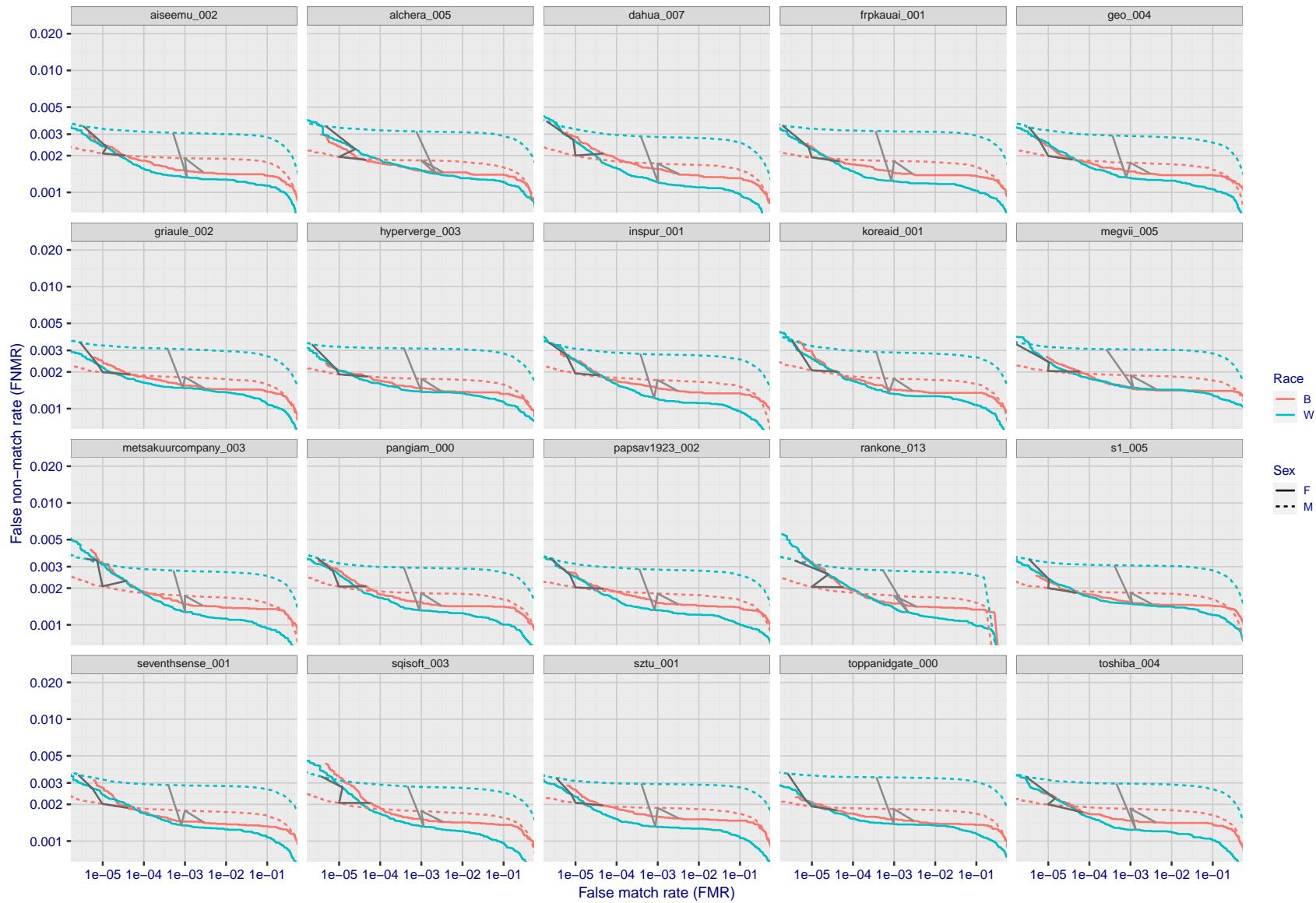


Figure 167: For the mugshot images, error tradeoff characteristics for white females, black females, black males and white males. The Z-shaped grey lines correspond to fixed thresholds, showing both FNMR and FMR vary at one T value. Note: Many of the plots will naively be read as saying women gives worse error rates than men because the solid traces lie above the dotted ones. However, this is misleading and incomplete: The grey lines show the traces reveal horizontal shifts. Thus for the cogent-003 algorithm FNMR for men is higher than for women at a fixed threshold but, at the same time, FMR is higher for women - see Figure 255. As access control systems almost always operate at a fixed threshold, the naive interpretation is incorrect.

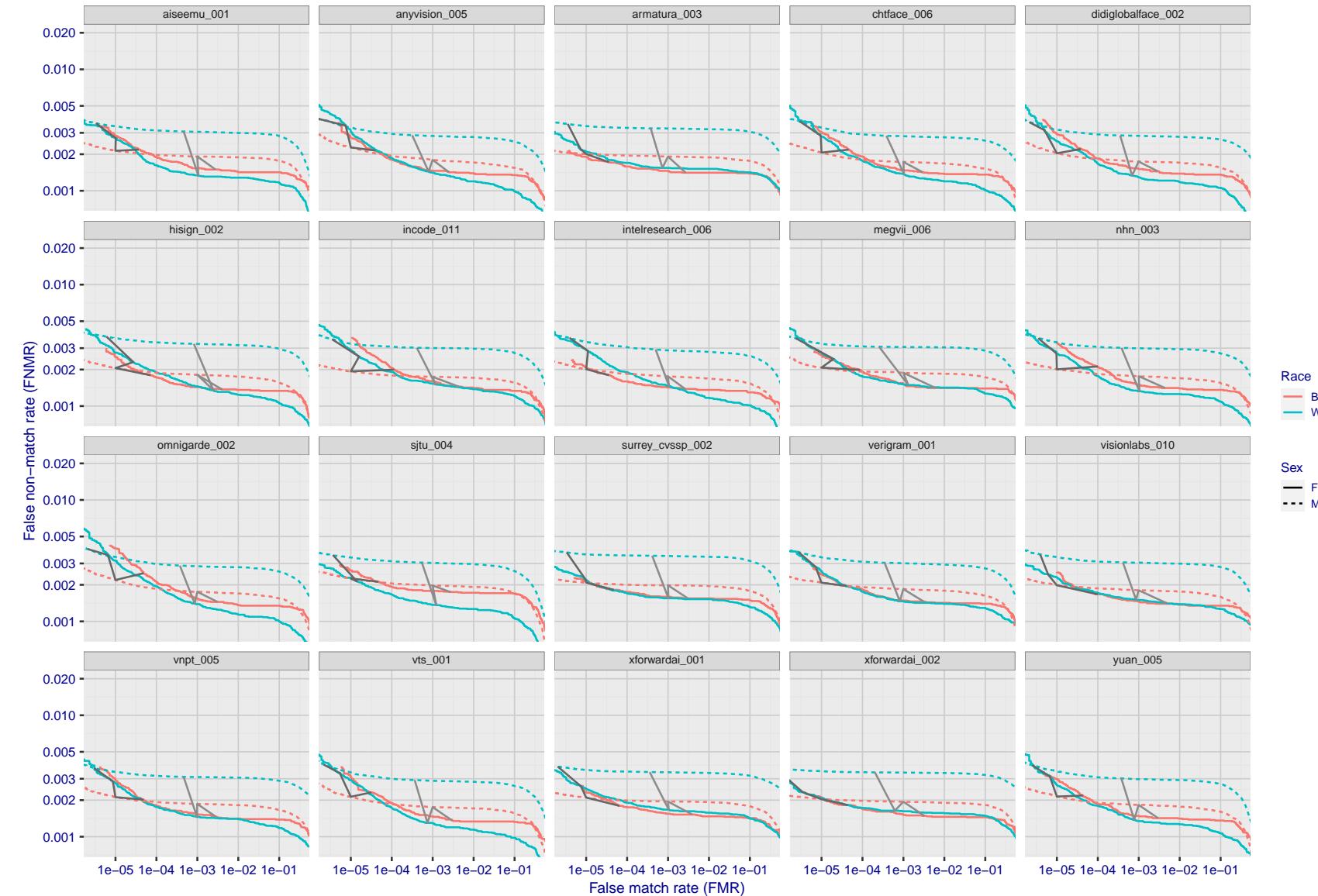


Figure 168: For the mugshot images, error tradeoff characteristics for white females, black females, black males and white males. The Z-shaped grey lines correspond to fixed thresholds, showing both FNMR and FMR vary at one T value. Note: Many of the plots will naively be read as saying women gives worse error rates than men because the solid traces lie above the dotted ones. However, this is misleading and incomplete: The grey lines show the traces reveal horizontal shifts. Thus for the cogent-003 algorithm FNMR for men is higher than for women at a fixed threshold but, at the same time, FMR is higher for women - see Figure 255. As access control systems almost always operate at a fixed threshold, the naive interpretation is incorrect.

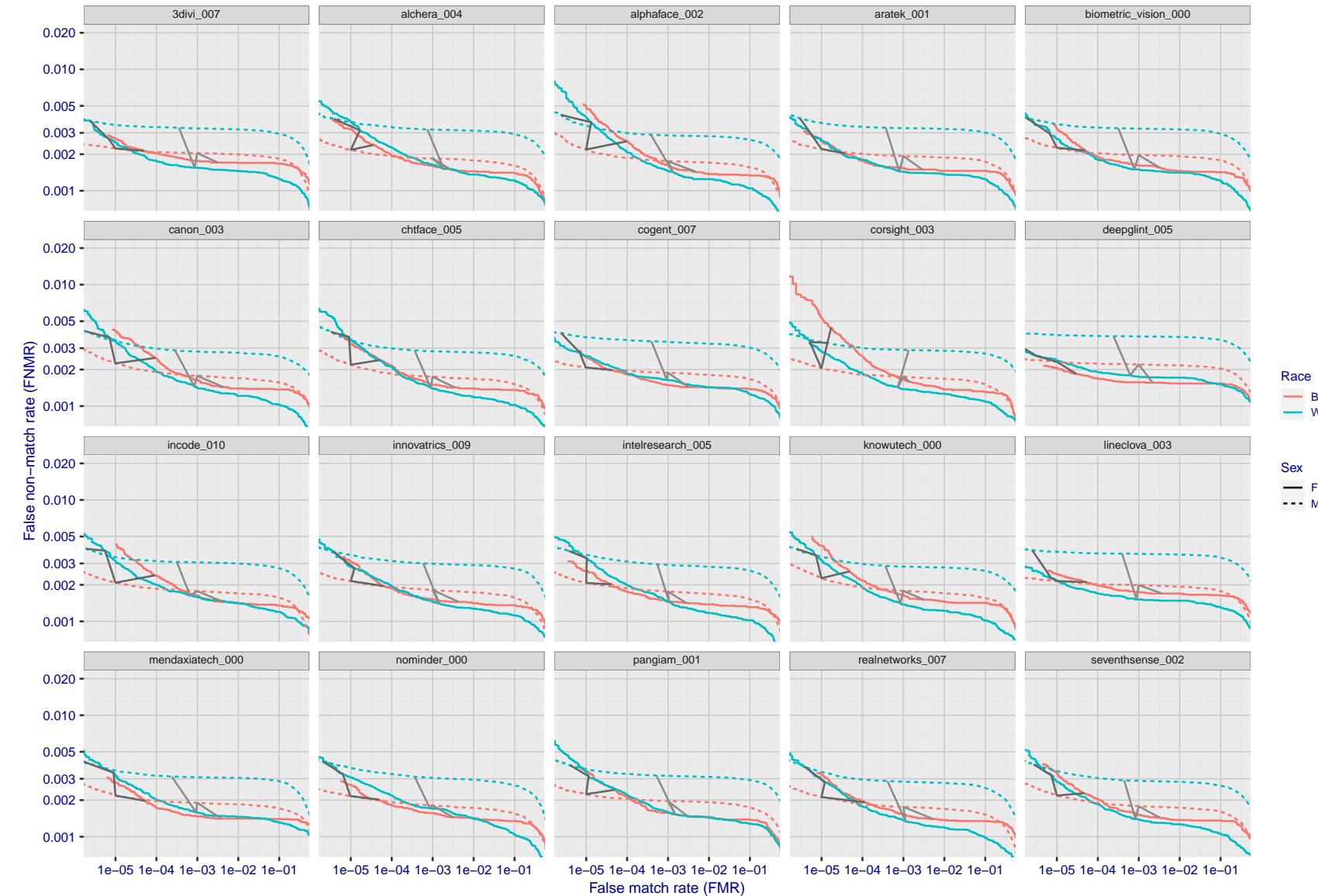


Figure 169: For the mugshot images, error tradeoff characteristics for white females, black females, black males and white males. The Z-shaped grey lines correspond to fixed thresholds, showing both FNMR and FMR vary at one T value. Note: Many of the plots will naively be read as saying women gives worse error rates than men because the solid traces lie above the dotted ones. However, this is misleading and incomplete: The grey lines show the traces reveal horizontal shifts. Thus for the cogent-003 algorithm FNMR for men is higher than for women at a fixed threshold but, at the same time, FMR is higher for women - see Figure 255. As access control systems almost always operate at a fixed threshold, the naive interpretation is incorrect.

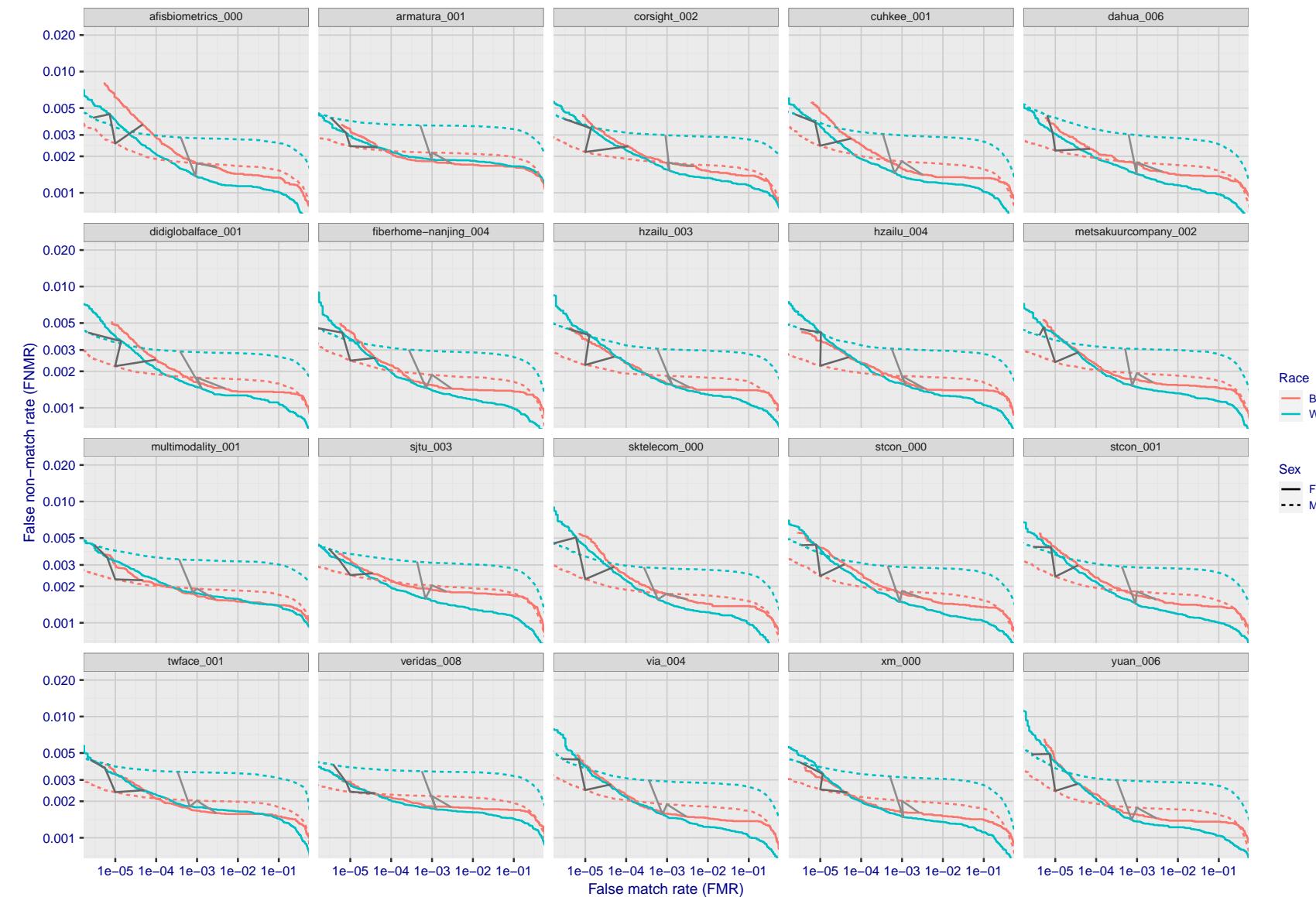


Figure 170: For the mugshot images, error tradeoff characteristics for white females, black females, black males and white males. The Z-shaped grey lines correspond to fixed thresholds, showing both FNMR and FMR vary at one T value. Note: Many of the plots will naively be read as saying women gives worse error rates than men because the solid traces lie above the dotted ones. However, this is misleading and incomplete: The grey lines show the traces reveal horizontal shifts. Thus for the cogent-003 algorithm FNMR for men is higher than for women at a fixed threshold but, at the same time, FMR is higher for women - see Figure 255. As access control systems almost always operate at a fixed threshold, the naive interpretation is incorrect.

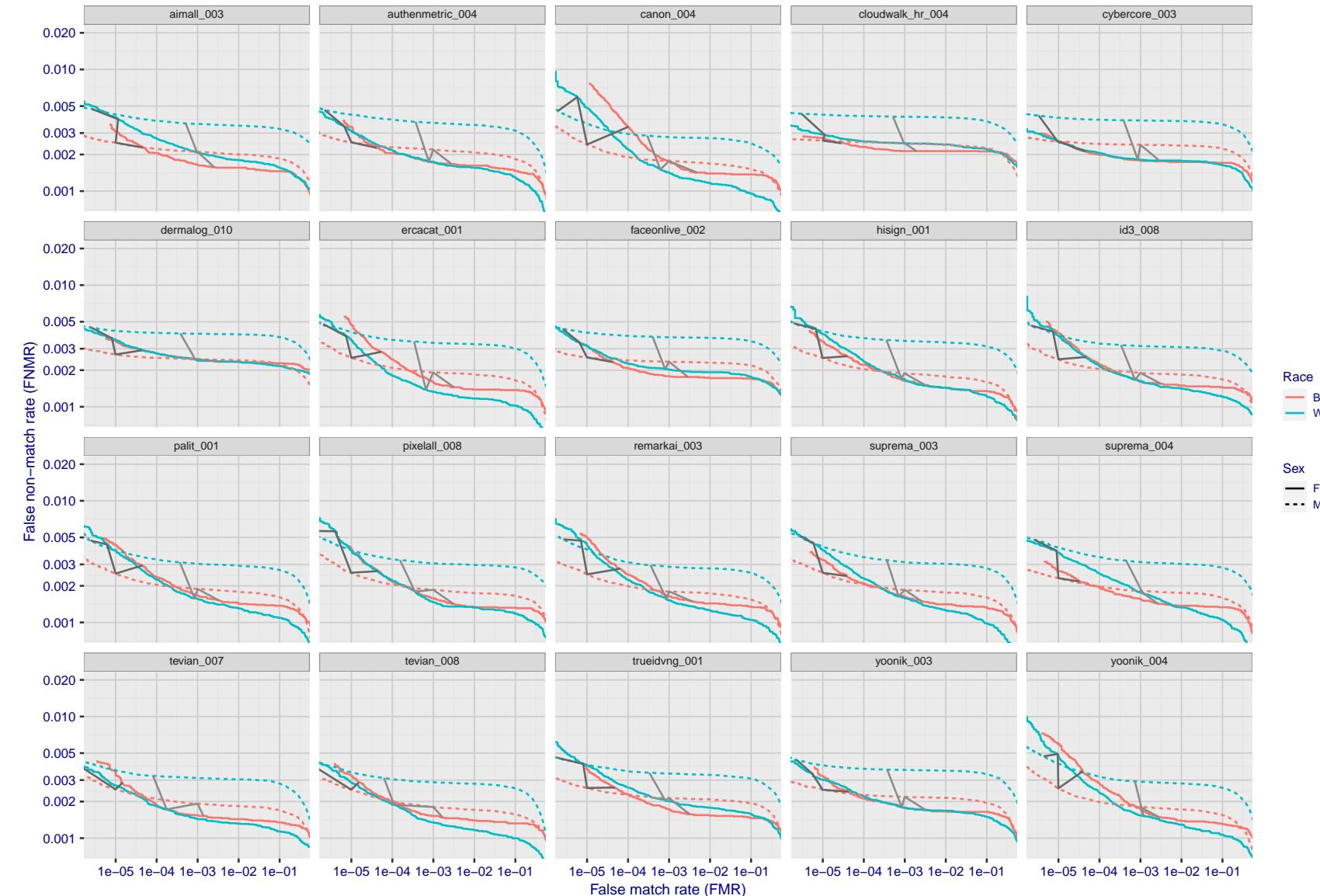


Figure 171: For the mugshot images, error tradeoff characteristics for white females, black females, black males and white males. The Z-shaped grey lines correspond to fixed thresholds, showing both FNMR and FMR vary at one T value. Note: Many of the plots will naively be read as saying women gives worse error rates than men because the solid traces lie above the dotted ones. However, this is misleading and incomplete: The grey lines show the traces reveal horizontal shifts. Thus for the cogent-003 algorithm FNMR for men is higher than for women at a fixed threshold but, at the same time, FMR is higher for women - see Figure 255. As access control systems almost always operate at a fixed threshold, the naive interpretation is incorrect.

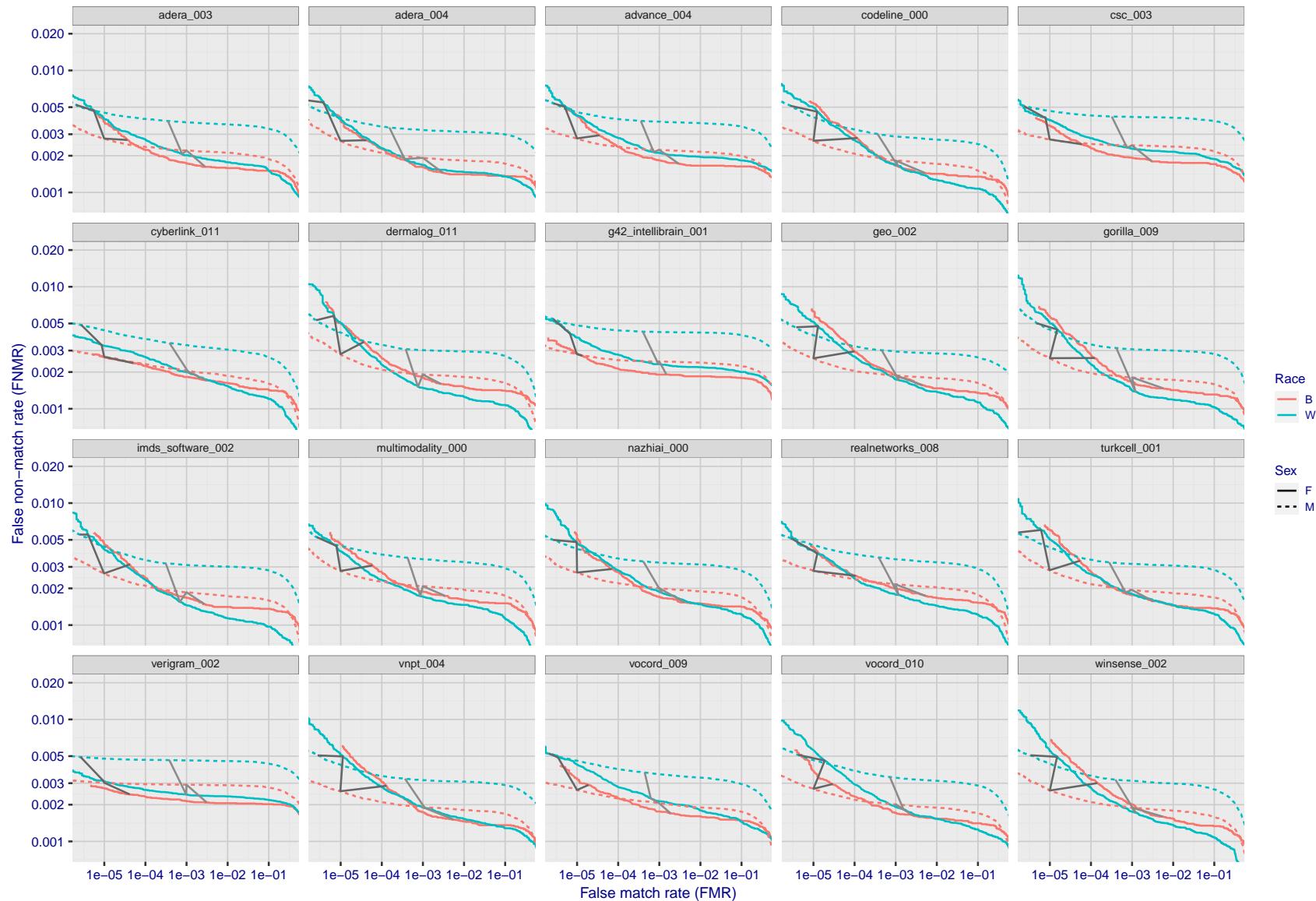


Figure 172: For the mugshot images, error tradeoff characteristics for white females, black females, black males and white males. The Z-shaped grey lines correspond to fixed thresholds, showing both FNMR and FMR vary at one T value. Note: Many of the plots will naively be read as saying women gives worse error rates than men because the solid traces lie above the dotted ones. However, this is misleading and incomplete: The grey lines show the traces reveal horizontal shifts. Thus for the cogent-003 algorithm FNMR for men is higher than for women at a fixed threshold but, at the same time, FMR is higher for women - see Figure 255. As access control systems almost always operate at a fixed threshold, the naive interpretation is incorrect.

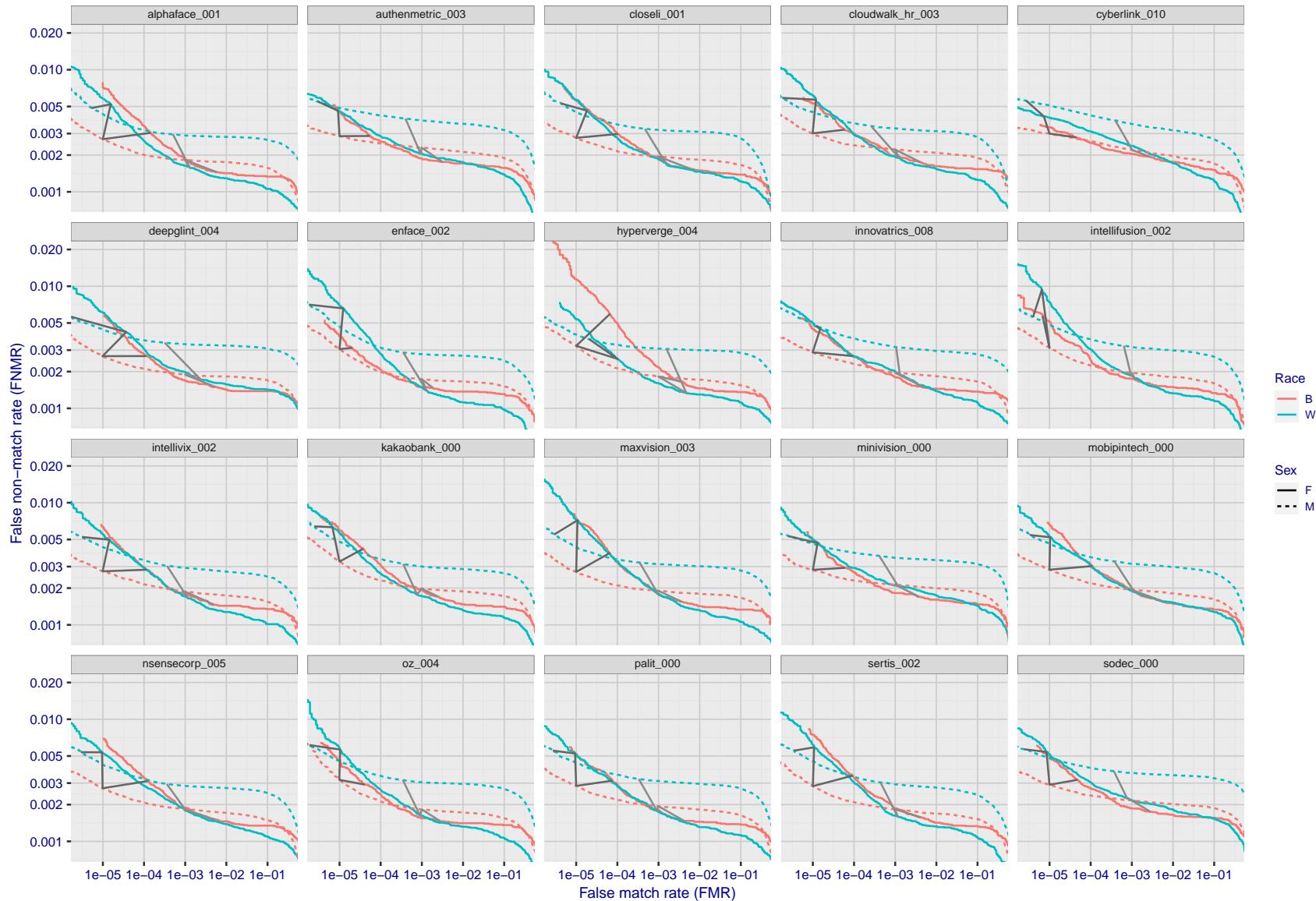


Figure 173: For the mugshot images, error tradeoff characteristics for white females, black females, black males and white males. The Z-shaped grey lines correspond to fixed thresholds, showing both FNMR and FMR vary at one T value. Note: Many of the plots will naively be read as saying women gives worse error rates than men because the solid traces lie above the dotted ones. However, this is misleading and incomplete: The grey lines show the traces reveal horizontal shifts. Thus for the cogent-003 algorithm FNMR for men is higher than for women at a fixed threshold but, at the same time, FMR is higher for women - see Figure 255. As access control systems almost always operate at a fixed threshold, the naive interpretation is incorrect.

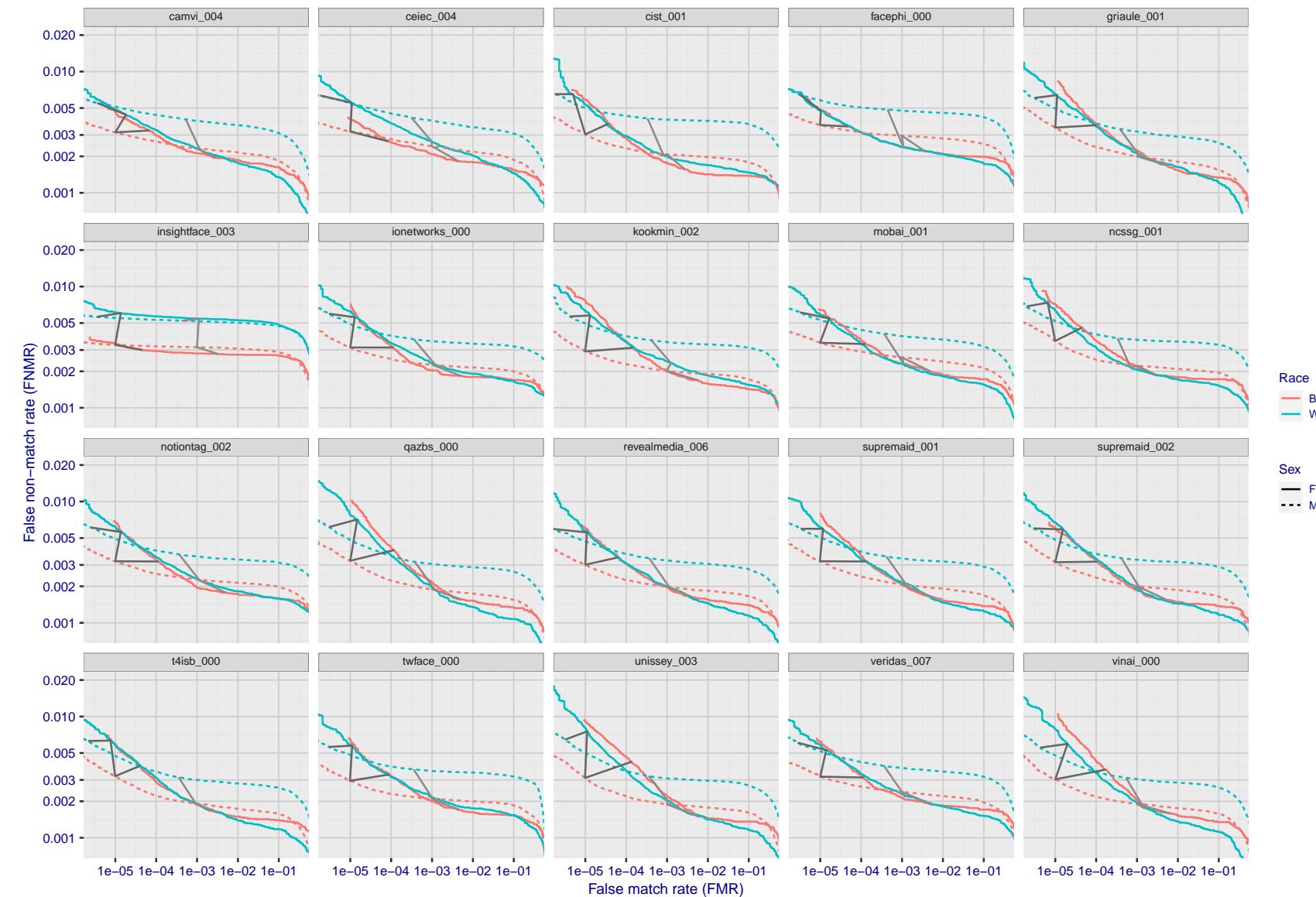


Figure 174: For the mugshot images, error tradeoff characteristics for white females, black females, black males and white males. The Z-shaped grey lines correspond to fixed thresholds, showing both FNMR and FMR vary at one T value. Note: Many of the plots will naively be read as saying women gives worse error rates than men because the solid traces lie above the dotted ones. However, this is misleading and incomplete: The grey lines show the traces reveal horizontal shifts. Thus for the cogent-003 algorithm FNMR for men is higher than for women at a fixed threshold but, at the same time, FMR is higher for women - see Figure 255. As access control systems almost always operate at a fixed threshold, the naive interpretation is incorrect.

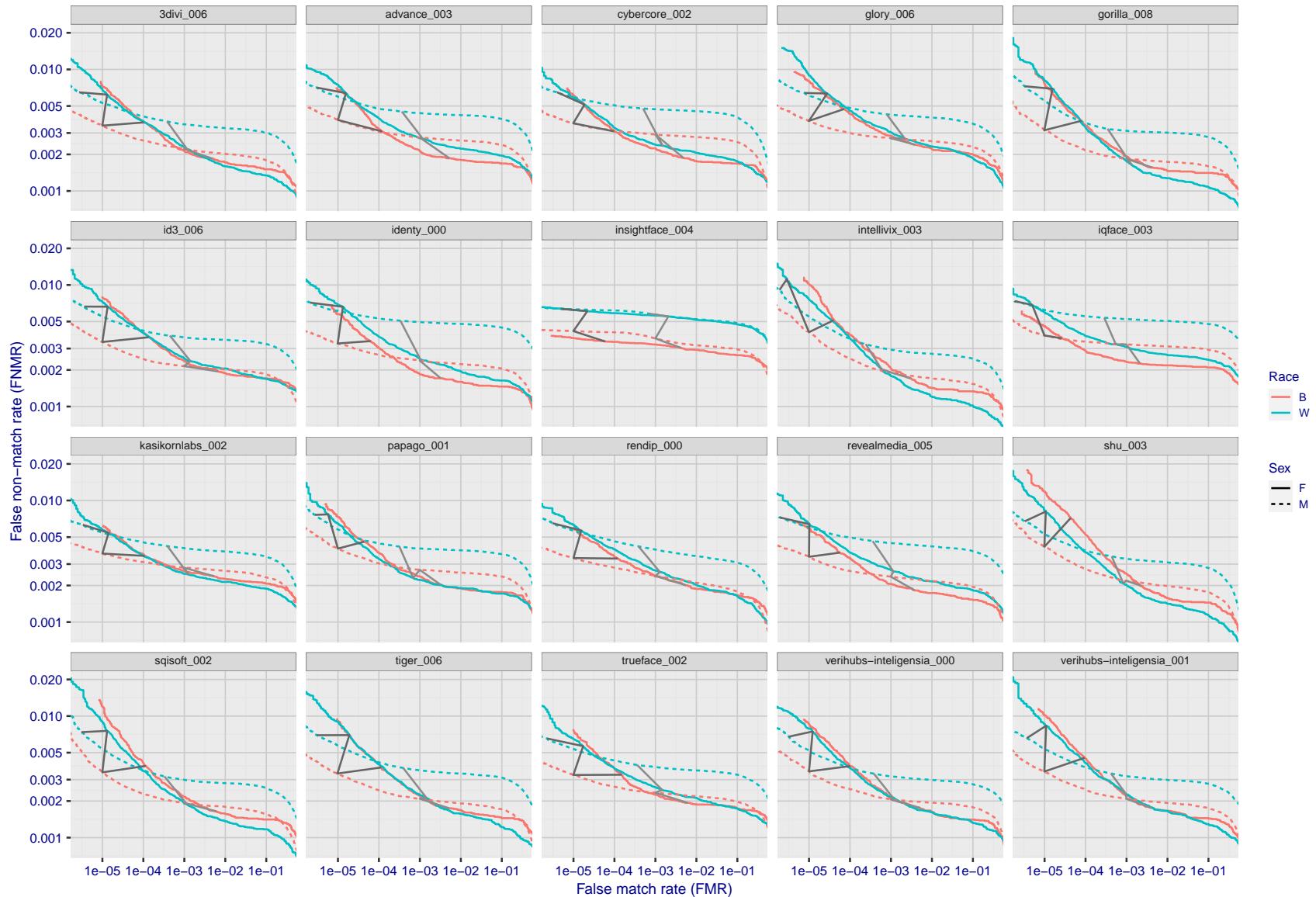


Figure 175: For the mugshot images, error tradeoff characteristics for white females, black females, black males and white males. The Z-shaped grey lines correspond to fixed thresholds, showing both FNMR and FMR vary at one T value. Note: Many of the plots will naively be read as saying women gives worse error rates than men because the solid traces lie above the dotted ones. However, this is misleading and incomplete: The grey lines show the traces reveal horizontal shifts. Thus for the cogent-003 algorithm FNMR for men is higher than for women at a fixed threshold but, at the same time, FMR is higher for women - see Figure 255. As access control systems almost always operate at a fixed threshold, the naive interpretation is incorrect.

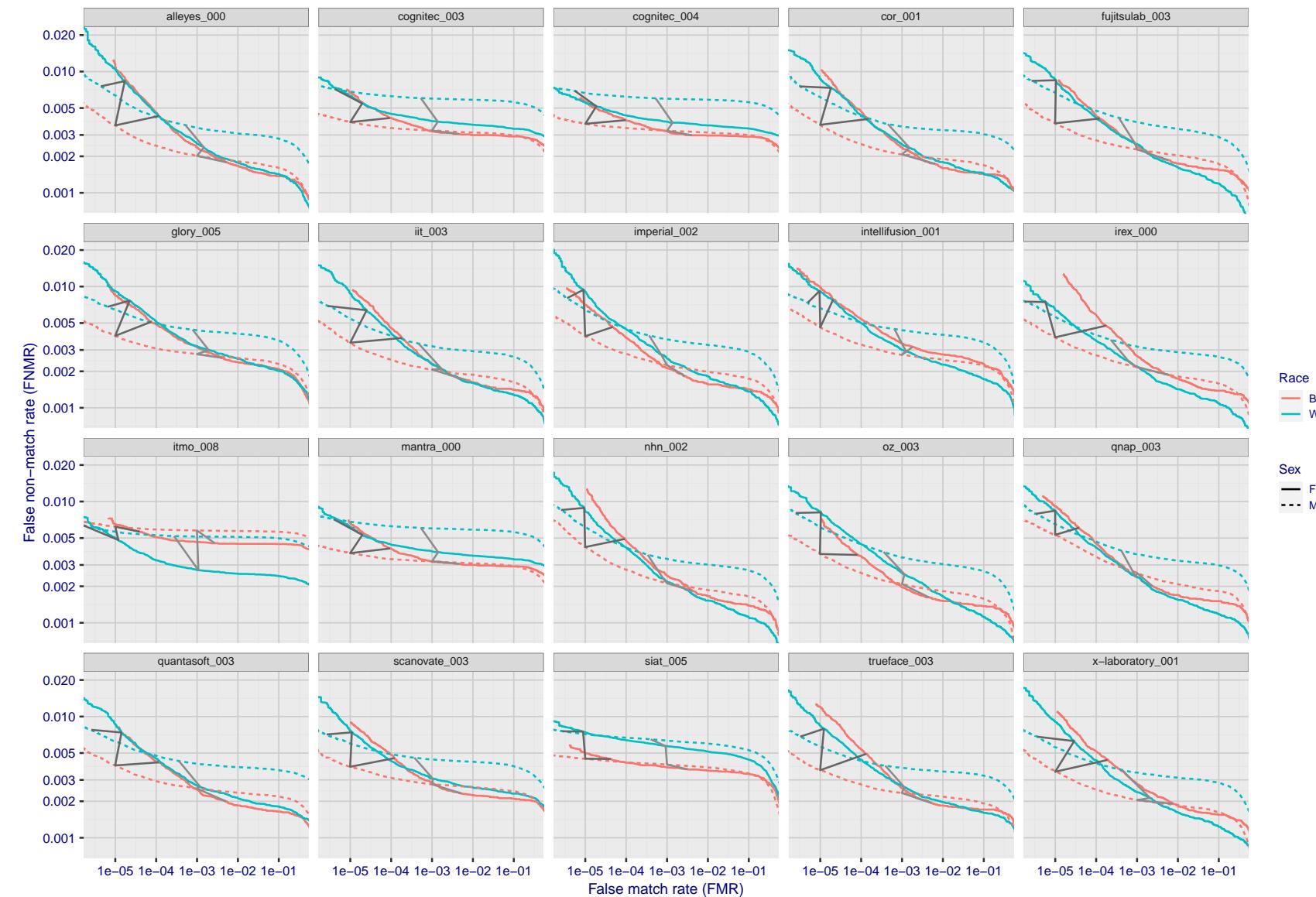


Figure 176: For the mugshot images, error tradeoff characteristics for white females, black females, black males and white males. The Z-shaped grey lines correspond to fixed thresholds, showing both FNMR and FMR vary at one T value. Note: Many of the plots will naively be read as saying women gives worse error rates than men because the solid traces lie above the dotted ones. However, this is misleading and incomplete: The grey lines show the traces reveal horizontal shifts. Thus for the cogent-003 algorithm FNMR for men is higher than for women at a fixed threshold but, at the same time, FMR is higher for women - see Figure 255. As access control systems almost always operate at a fixed threshold, the naive interpretation is incorrect.

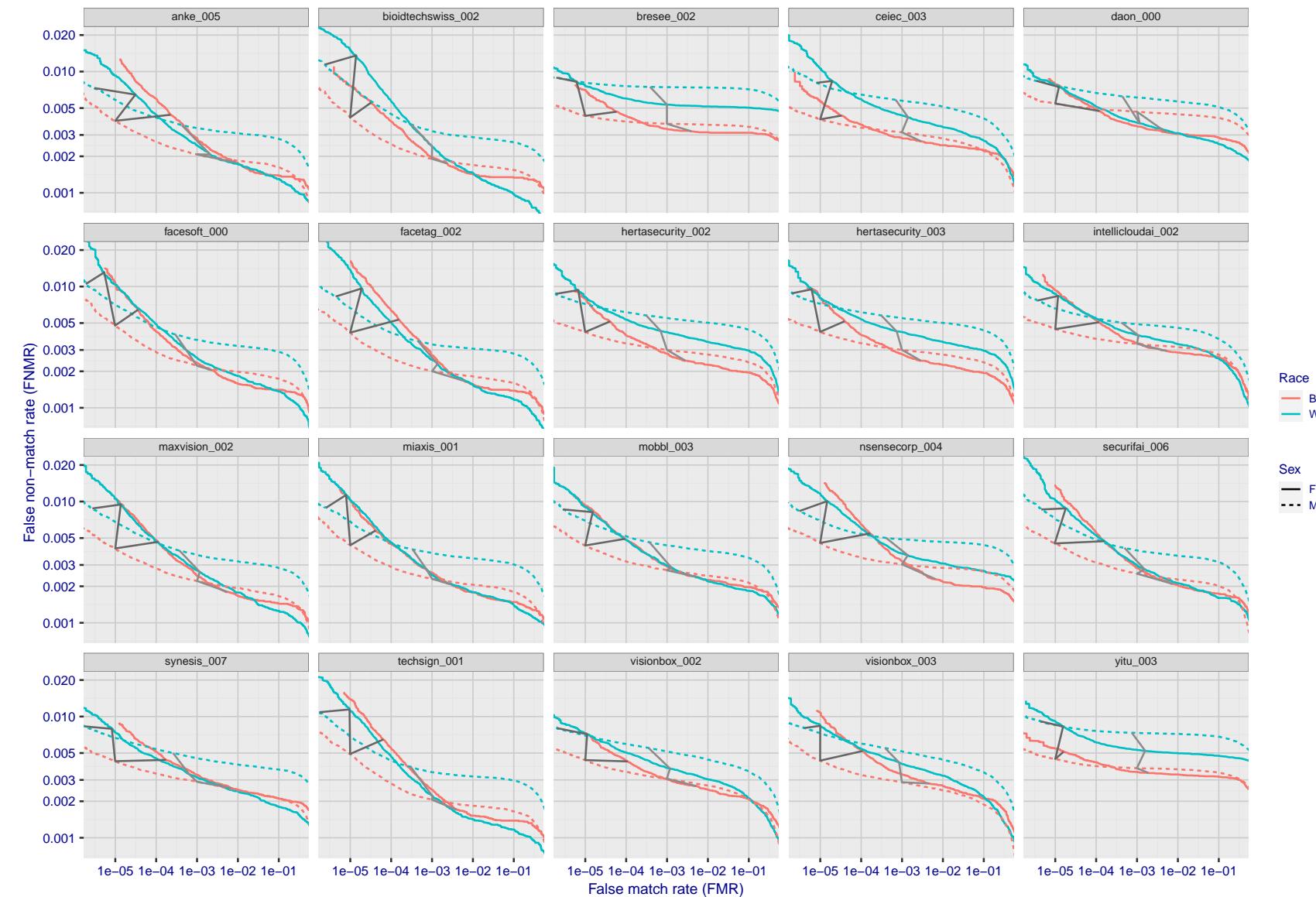


Figure 177: For the mugshot images, error tradeoff characteristics for white females, black females, black males and white males. The Z-shaped grey lines correspond to fixed thresholds, showing both FNMR and FMR vary at one T value. Note: Many of the plots will naively be read as saying women gives worse error rates than men because the solid traces lie above the dotted ones. However, this is misleading and incomplete: The grey lines show the traces reveal horizontal shifts. Thus for the cogent-003 algorithm FNMR for men is higher than for women at a fixed threshold but, at the same time, FMR is higher for women - see Figure 255. As access control systems almost always operate at a fixed threshold, the naive interpretation is incorrect.

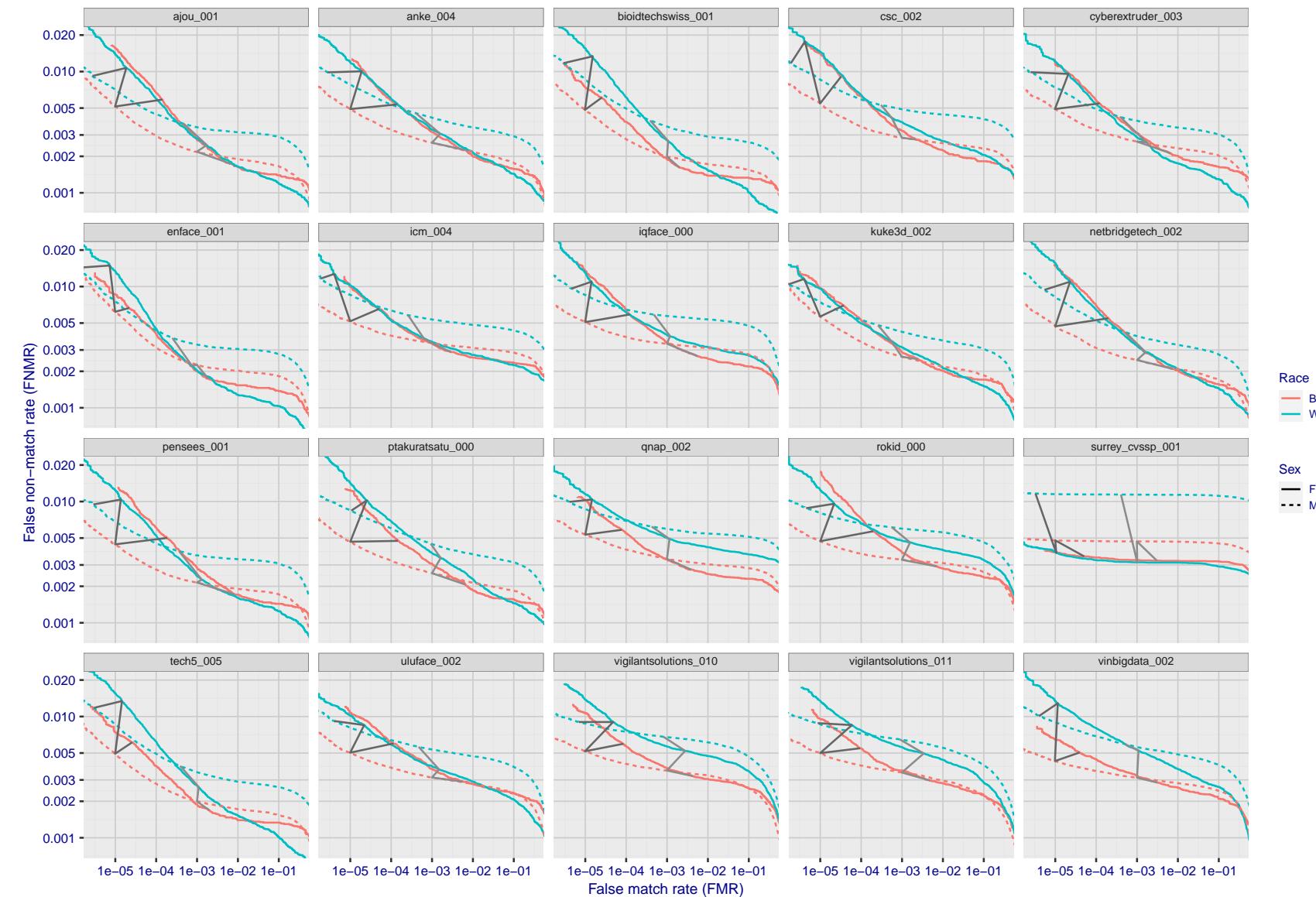


Figure 178: For the mugshot images, error tradeoff characteristics for white females, black females, black males and white males. The Z-shaped grey lines correspond to fixed thresholds, showing both FNMR and FMR vary at one T value. Note: Many of the plots will naively be read as saying women gives worse error rates than men because the solid traces lie above the dotted ones. However, this is misleading and incomplete: The grey lines show the traces reveal horizontal shifts. Thus for the cogent-003 algorithm FNMR for men is higher than for women at a fixed threshold but, at the same time, FMR is higher for women - see Figure 255. As access control systems almost always operate at a fixed threshold, the naive interpretation is incorrect.

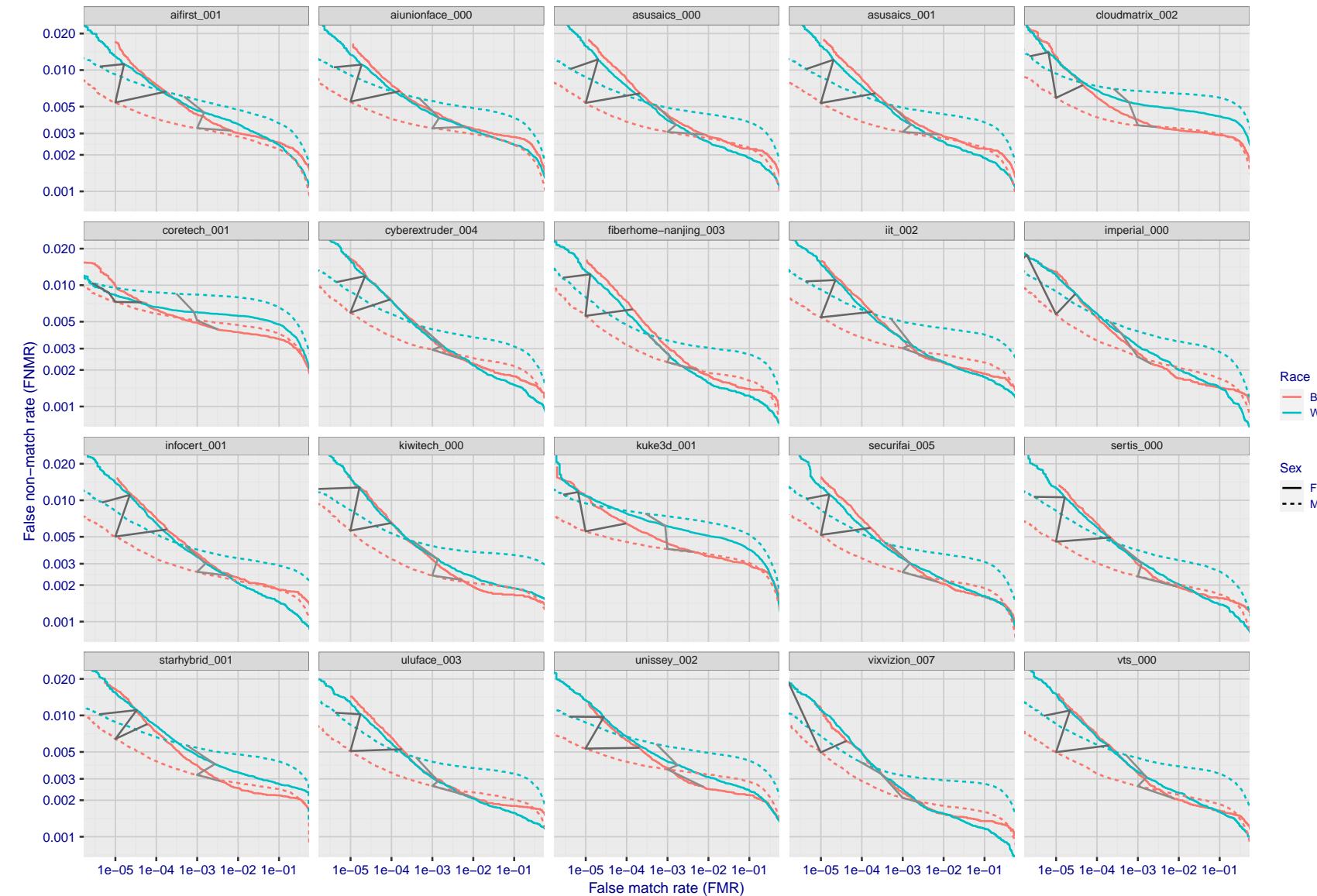


Figure 179: For the mugshot images, error tradeoff characteristics for white females, black females, black males and white males. The Z-shaped grey lines correspond to fixed thresholds, showing both FNMR and FMR vary at one T value. Note: Many of the plots will naively be read as saying women gives worse error rates than men because the solid traces lie above the dotted ones. However, this is misleading and incomplete: The grey lines show the traces reveal horizontal shifts. Thus for the cogent-003 algorithm FNMR for men is higher than for women at a fixed threshold but, at the same time, FMR is higher for women - see Figure 255. As access control systems almost always operate at a fixed threshold, the naive interpretation is incorrect.

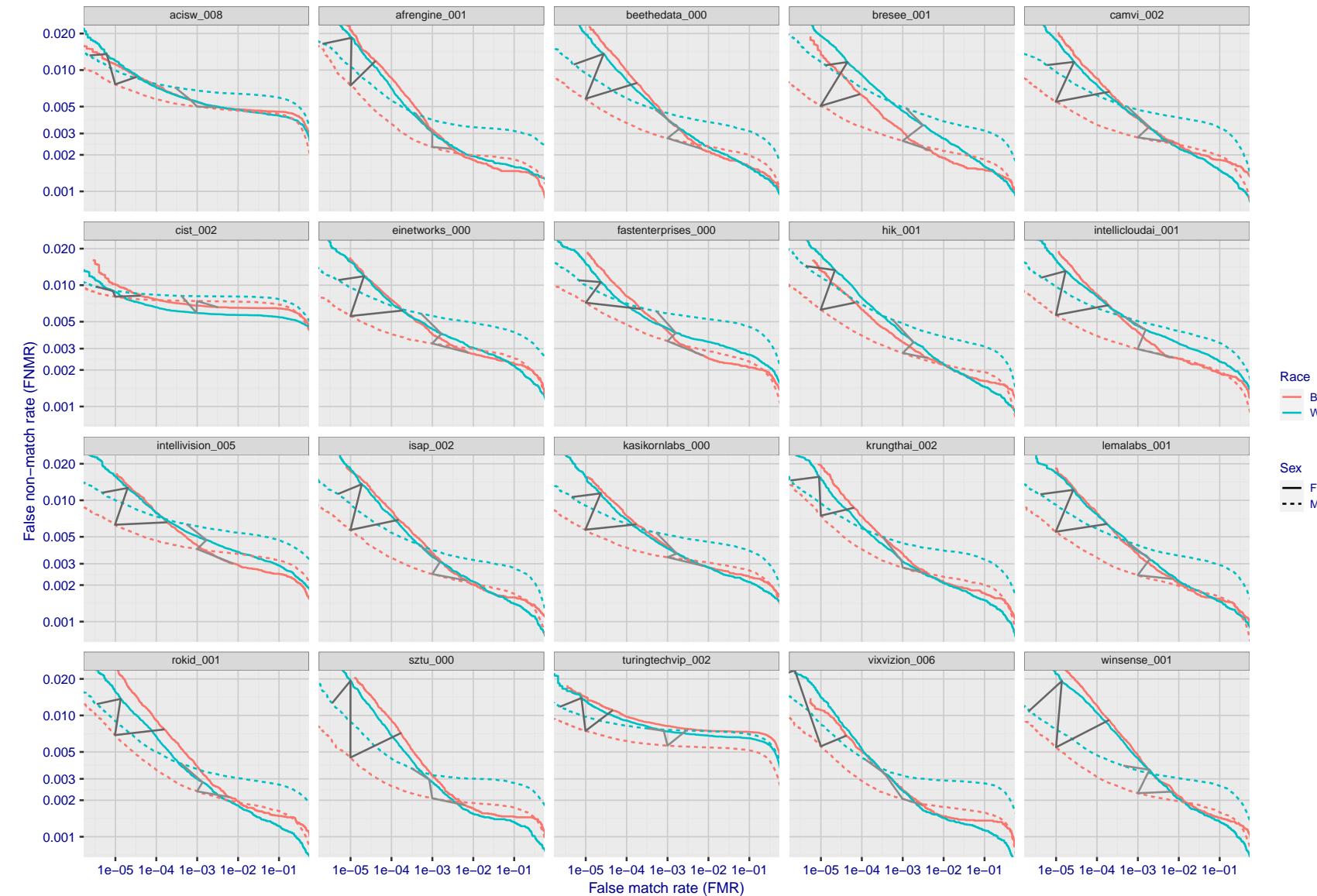


Figure 180: For the mugshot images, error tradeoff characteristics for white females, black females, black males and white males. The Z-shaped grey lines correspond to fixed thresholds, showing both FNMR and FMR vary at one T value. Note: Many of the plots will naively be read as saying women gives worse error rates than men because the solid traces lie above the dotted ones. However, this is misleading and incomplete: The grey lines show the traces reveal horizontal shifts. Thus for the cogent-003 algorithm FNMR for men is higher than for women at a fixed threshold but, at the same time, FMR is higher for women - see Figure 255. As access control systems almost always operate at a fixed threshold, the naive interpretation is incorrect.

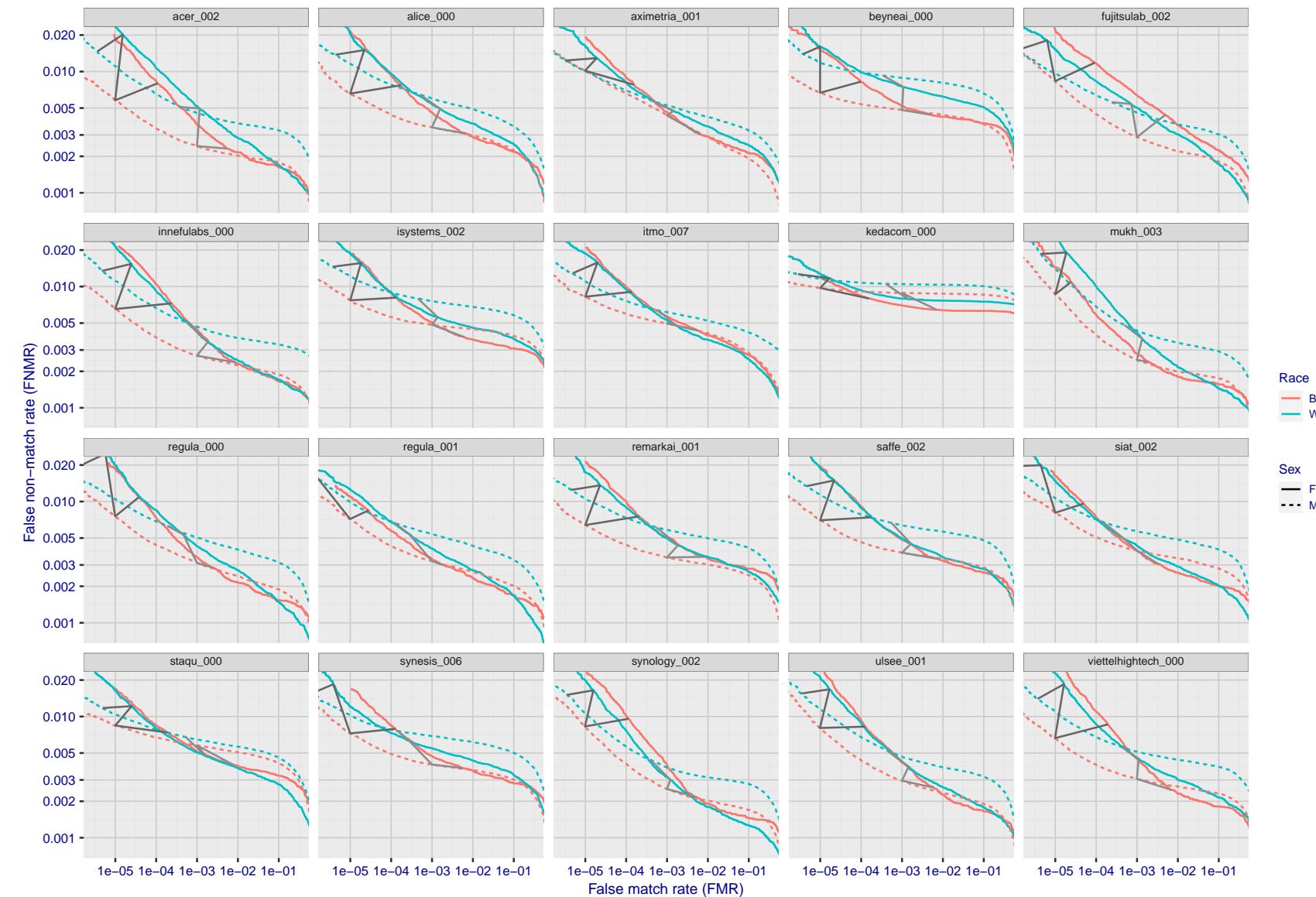


Figure 181: For the mugshot images, error tradeoff characteristics for white females, black females, black males and white males. The Z-shaped grey lines correspond to fixed thresholds, showing both FNMR and FMR vary at one T value. Note: Many of the plots will naively be read as saying women gives worse error rates than men because the solid traces lie above the dotted ones. However, this is misleading and incomplete: The grey lines show the traces reveal horizontal shifts. Thus for the cogent-003 algorithm FNMR for men is higher than for women at a fixed threshold but, at the same time, FMR is higher for women - see Figure 255. As access control systems almost always operate at a fixed threshold, the naive interpretation is incorrect.

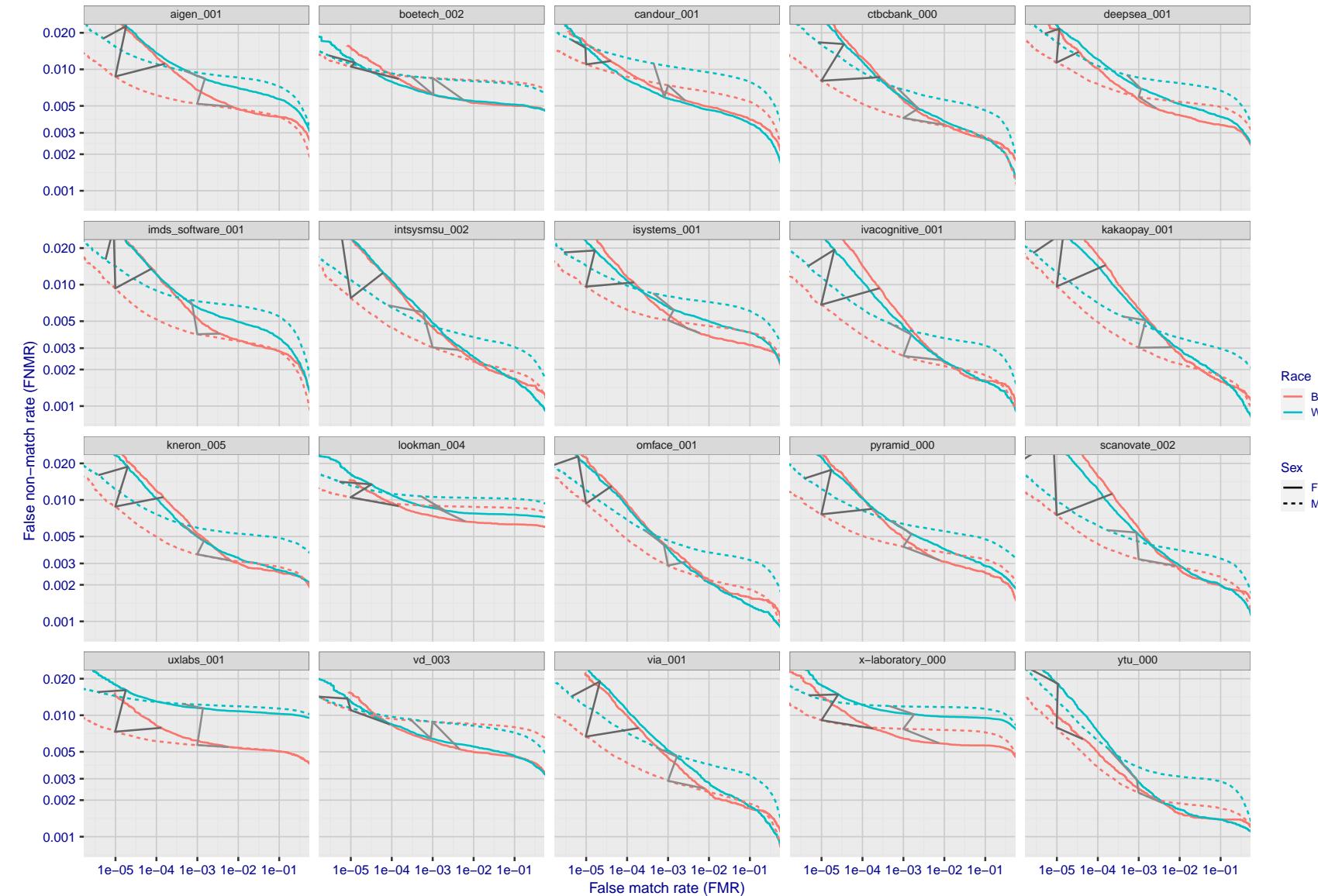


Figure 182: For the mugshot images, error tradeoff characteristics for white females, black females, black males and white males. The Z-shaped grey lines correspond to fixed thresholds, showing both FNMR and FMR vary at one T value. Note: Many of the plots will naively be read as saying women gives worse error rates than men because the solid traces lie above the dotted ones. However, this is misleading and incomplete: The grey lines show the traces reveal horizontal shifts. Thus for the cogent-003 algorithm FNMR for men is higher than for women at a fixed threshold but, at the same time, FMR is higher for women - see Figure 255. As access control systems almost always operate at a fixed threshold, the naive interpretation is incorrect.

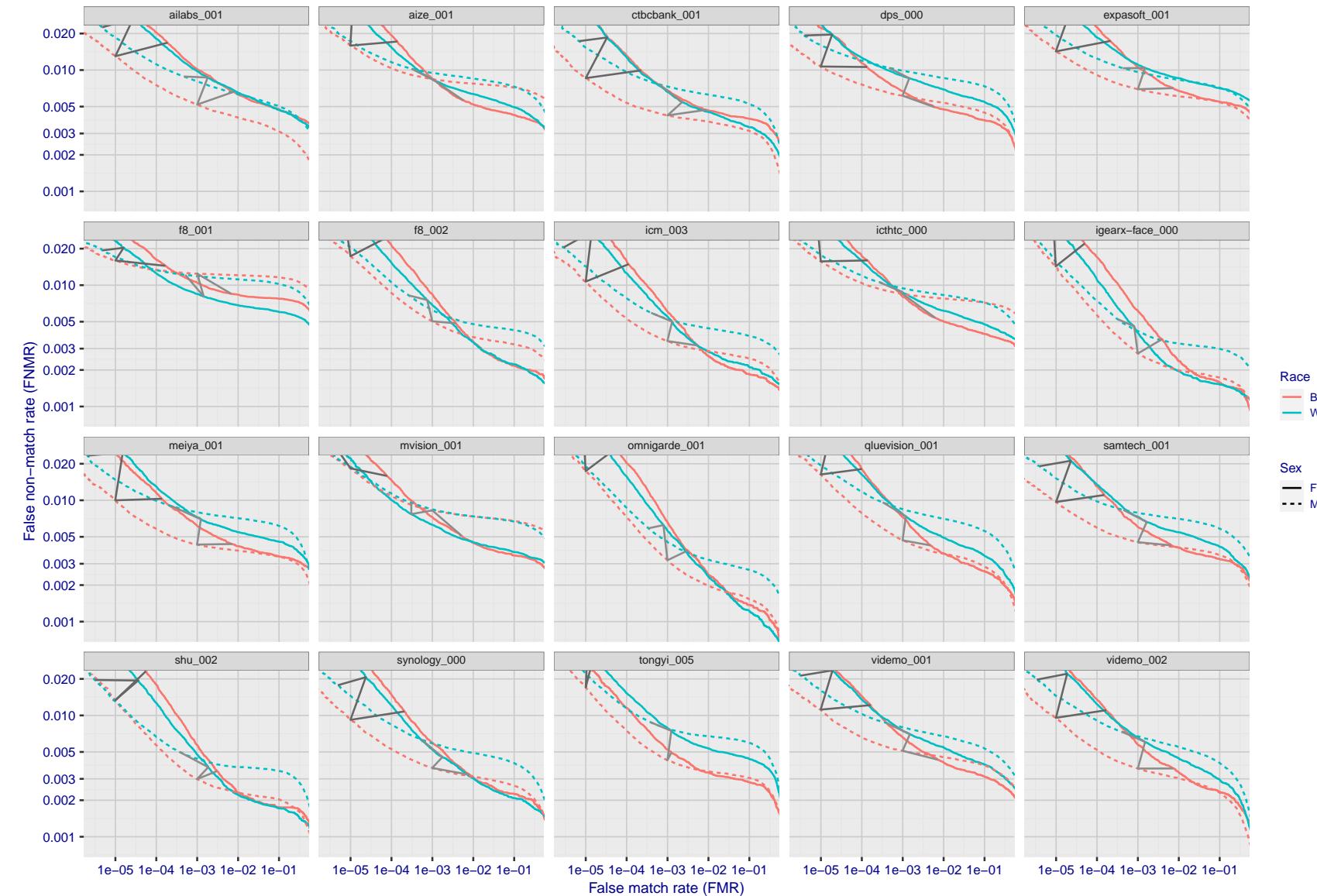


Figure 183: For the mugshot images, error tradeoff characteristics for white females, black females, black males and white males. The Z-shaped grey lines correspond to fixed thresholds, showing both FNMR and FMR vary at one T value. Note: Many of the plots will naively be read as saying women gives worse error rates than men because the solid traces lie above the dotted ones. However, this is misleading and incomplete: The grey lines show the traces reveal horizontal shifts. Thus for the cogent-003 algorithm FNMR for men is higher than for women at a fixed threshold but, at the same time, FMR is higher for women - see Figure 255. As access control systems almost always operate at a fixed threshold, the naive interpretation is incorrect.

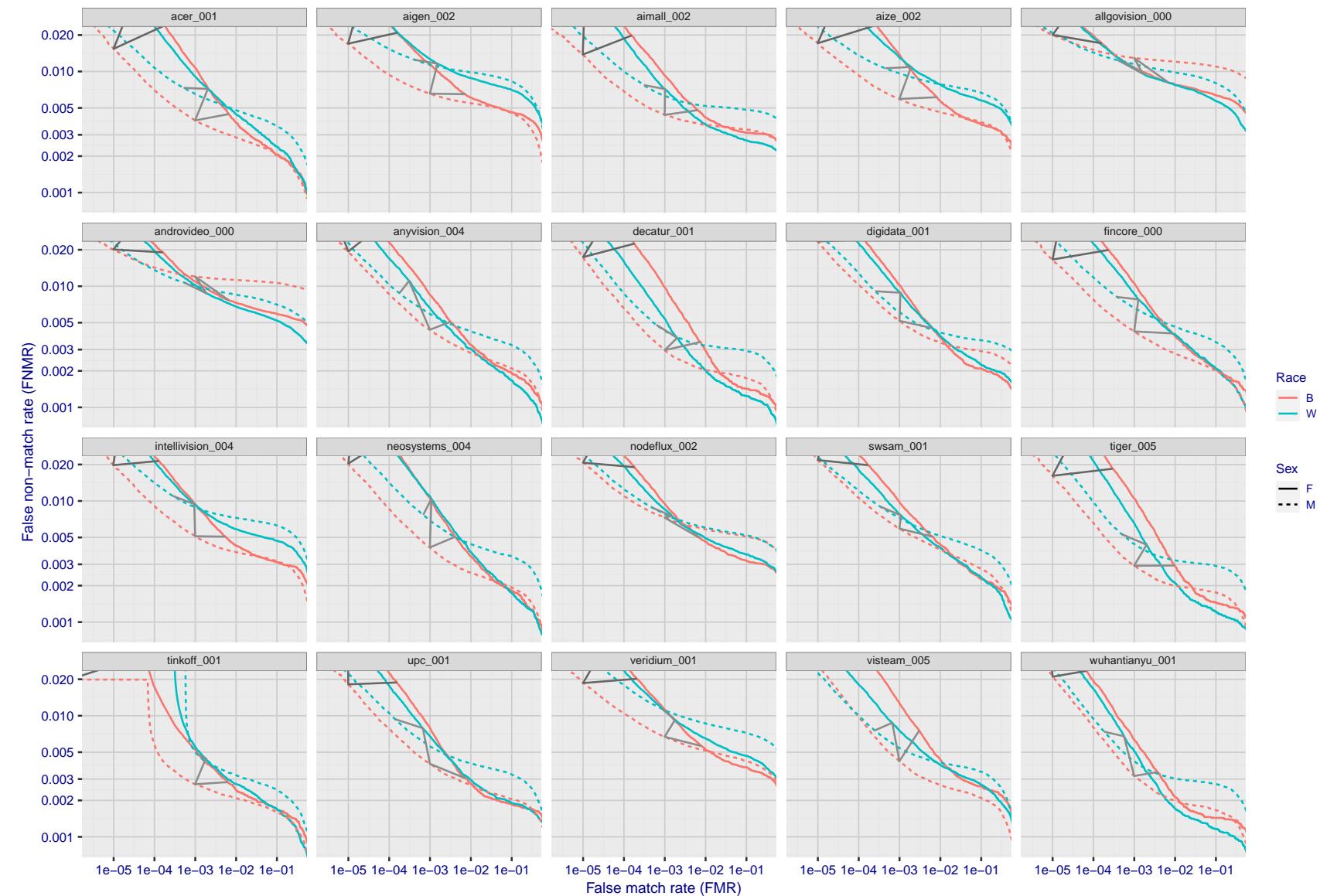


Figure 184: For the mugshot images, error tradeoff characteristics for white females, black females, black males and white males. The Z-shaped grey lines correspond to fixed thresholds, showing both FNMR and FMR vary at one T value. Note: Many of the plots will naively be read as saying women gives worse error rates than men because the solid traces lie above the dotted ones. However, this is misleading and incomplete: The grey lines show the traces reveal horizontal shifts. Thus for the cogent-003 algorithm FNMR for men is higher than for women at a fixed threshold but, at the same time, FMR is higher for women - see Figure 255. As access control systems almost always operate at a fixed threshold, the naive interpretation is incorrect.

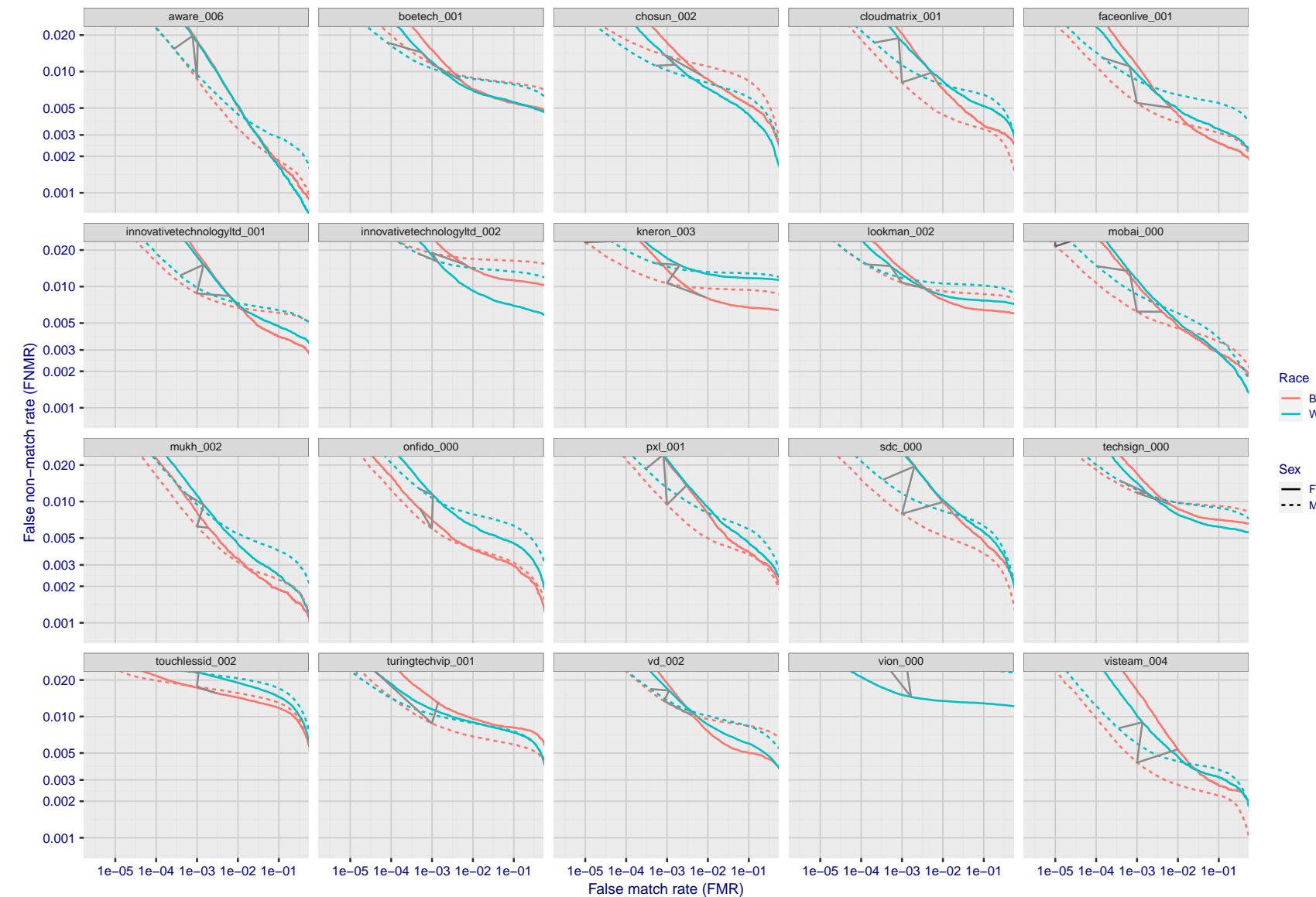


Figure 185: For the mugshot images, error tradeoff characteristics for white females, black females, black males and white males. The Z-shaped grey lines correspond to fixed thresholds, showing both FNMR and FMR vary at one T value. Note: Many of the plots will naively be read as saying women gives worse error rates than men because the solid traces lie above the dotted ones. However, this is misleading and incomplete: The grey lines show the traces reveal horizontal shifts. Thus for the cogent-003 algorithm FNMR for men is higher than for women at a fixed threshold but, at the same time, FMR is higher for women - see Figure 255. As access control systems almost always operate at a fixed threshold, the naive interpretation is incorrect.

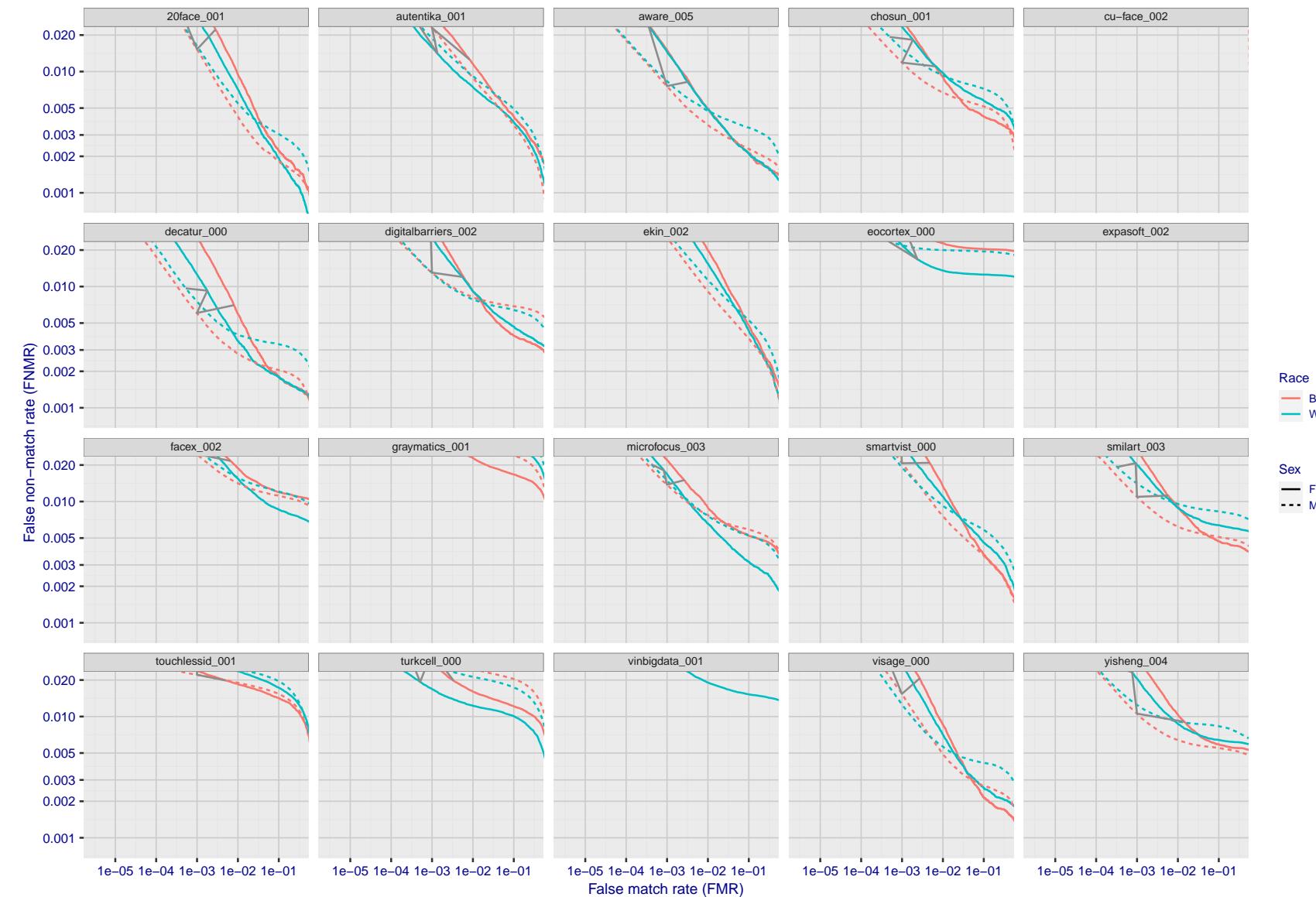


Figure 186: For the mugshot images, error tradeoff characteristics for white females, black females, black males and white males. The Z-shaped grey lines correspond to fixed thresholds, showing both FNMR and FMR vary at one T value. Note: Many of the plots will naively be read as saying women gives worse error rates than men because the solid traces lie above the dotted ones. However, this is misleading and incomplete: The grey lines show the traces reveal horizontal shifts. Thus for the cogent-003 algorithm FNMR for men is higher than for women at a fixed threshold but, at the same time, FMR is higher for women - see Figure 255. As access control systems almost always operate at a fixed threshold, the naive interpretation is incorrect.

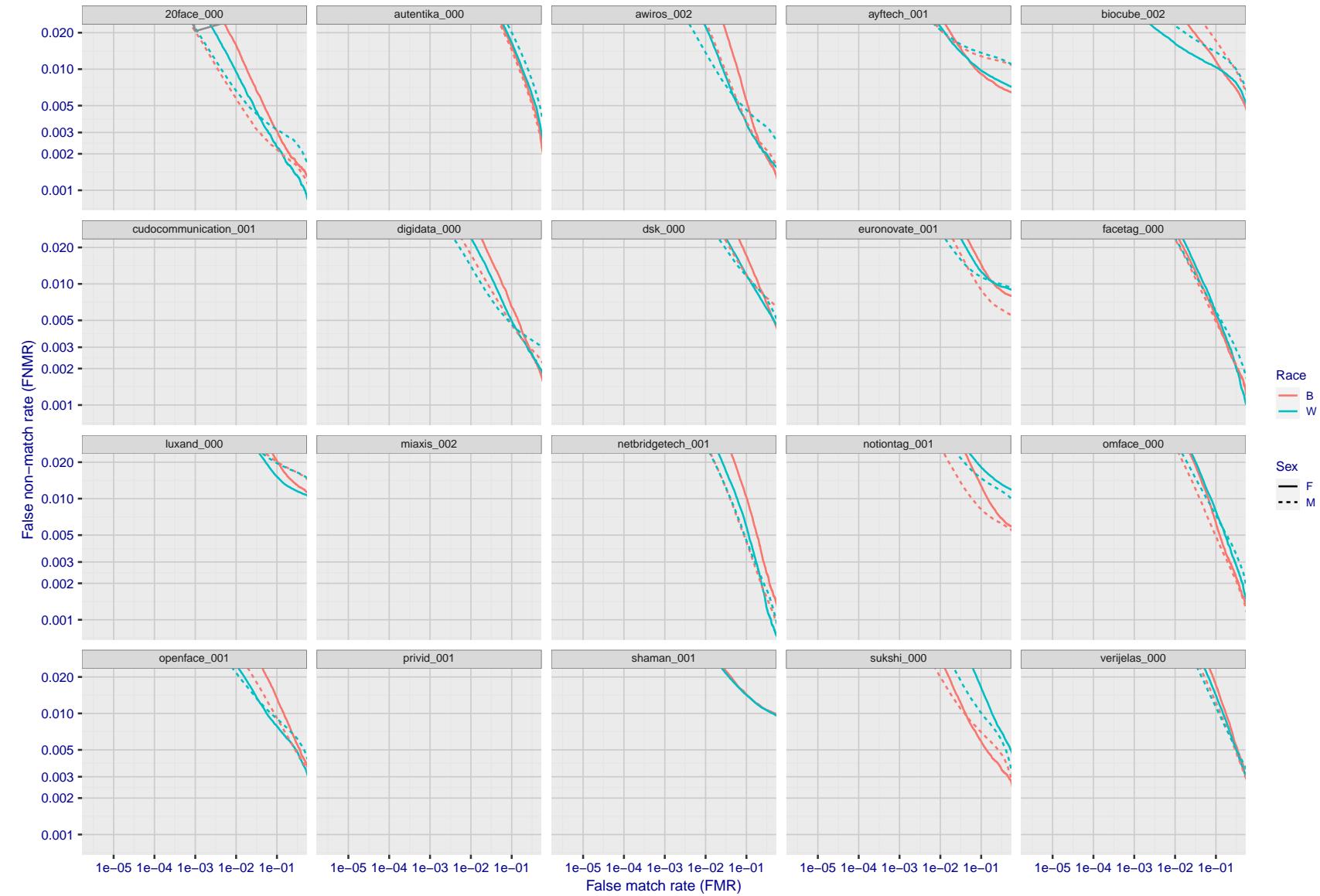


Figure 187: For the mugshot images, error tradeoff characteristics for white females, black females, black males and white males. The Z-shaped grey lines correspond to fixed thresholds, showing both FNMR and FMR vary at one T value. Note: Many of the plots will naively be read as saying women gives worse error rates than men because the solid traces lie above the dotted ones. However, this is misleading and incomplete: The grey lines show the traces reveal horizontal shifts. Thus for the cogent-003 algorithm FNMR for men is higher than for women at a fixed threshold but, at the same time, FMR is higher for women - see Figure 255. As access control systems almost always operate at a fixed threshold, the naive interpretation is incorrect.

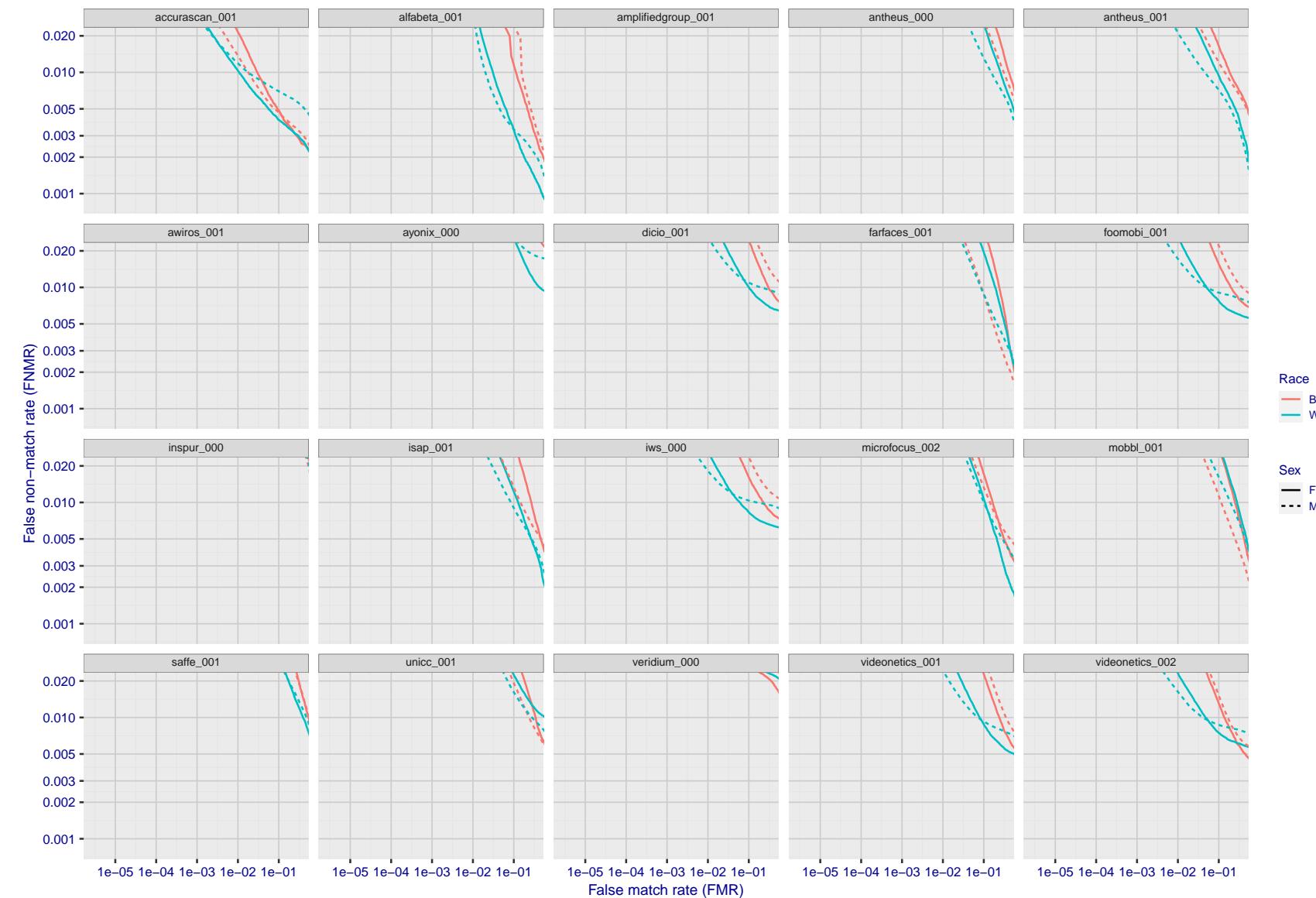


Figure 188: For the mugshot images, error tradeoff characteristics for white females, black females, black males and white males. The Z-shaped grey lines correspond to fixed thresholds, showing both FNMR and FMR vary at one T value. Note: Many of the plots will naively be read as saying women gives worse error rates than men because the solid traces lie above the dotted ones. However, this is misleading and incomplete: The grey lines show the traces reveal horizontal shifts. Thus for the cogent-003 algorithm FNMR for men is higher than for women at a fixed threshold but, at the same time, FMR is higher for women - see Figure 255. As access control systems almost always operate at a fixed threshold, the naive interpretation is incorrect.

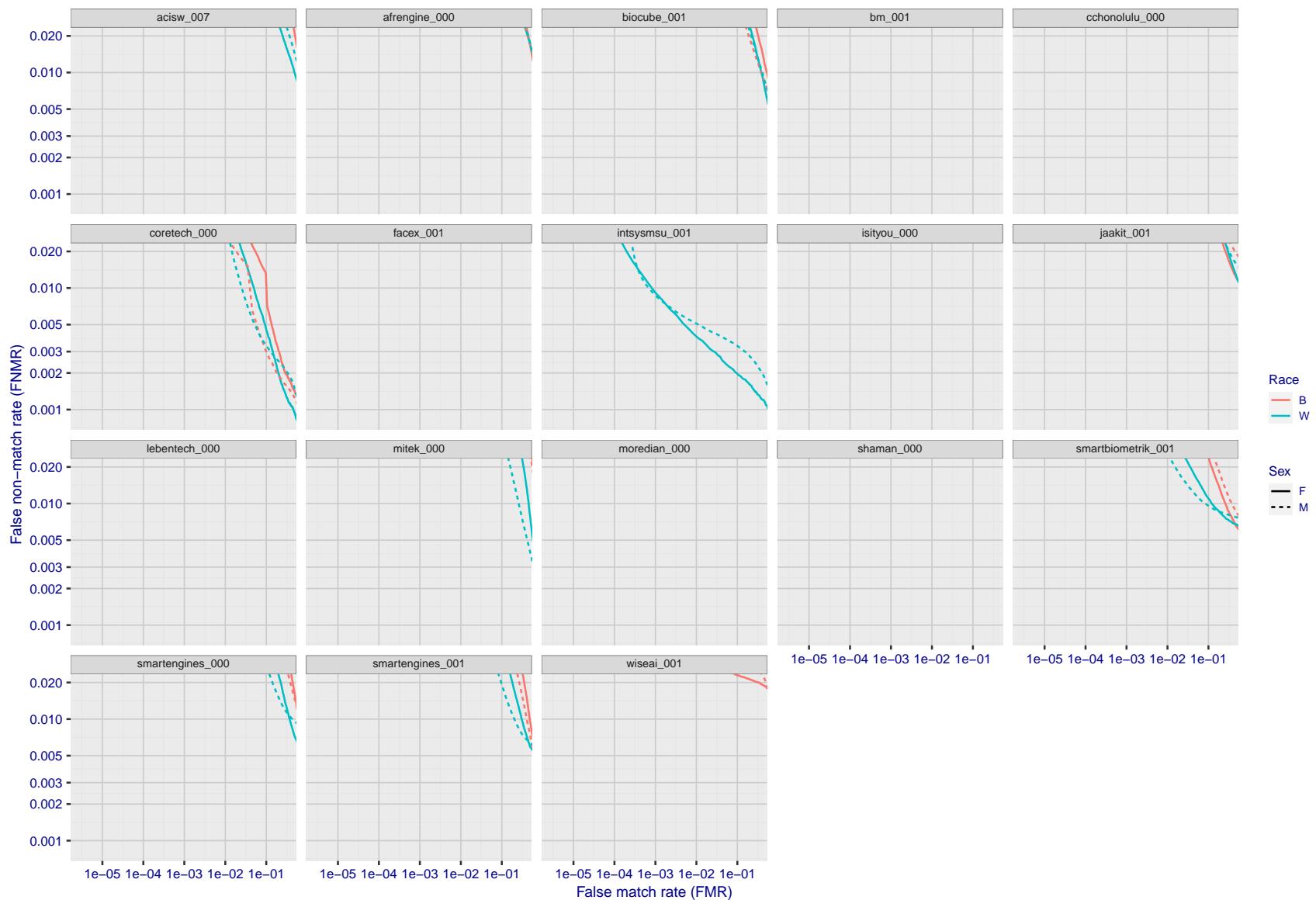


Figure 189: For the mugshot images, error tradeoff characteristics for white females, black females, black males and white males. The Z-shaped grey lines correspond to fixed thresholds, showing both FNMR and FMR vary at one T value. Note: Many of the plots will naively be read as saying women gives worse error rates than men because the solid traces lie above the dotted ones. However, this is misleading and incomplete: The grey lines show the traces reveal horizontal shifts. Thus for the cogent-003 algorithm FNMR for men is higher than for women at a fixed threshold but, at the same time, FMR is higher for women - see Figure 255. As access control systems almost always operate at a fixed threshold, the naive interpretation is incorrect.

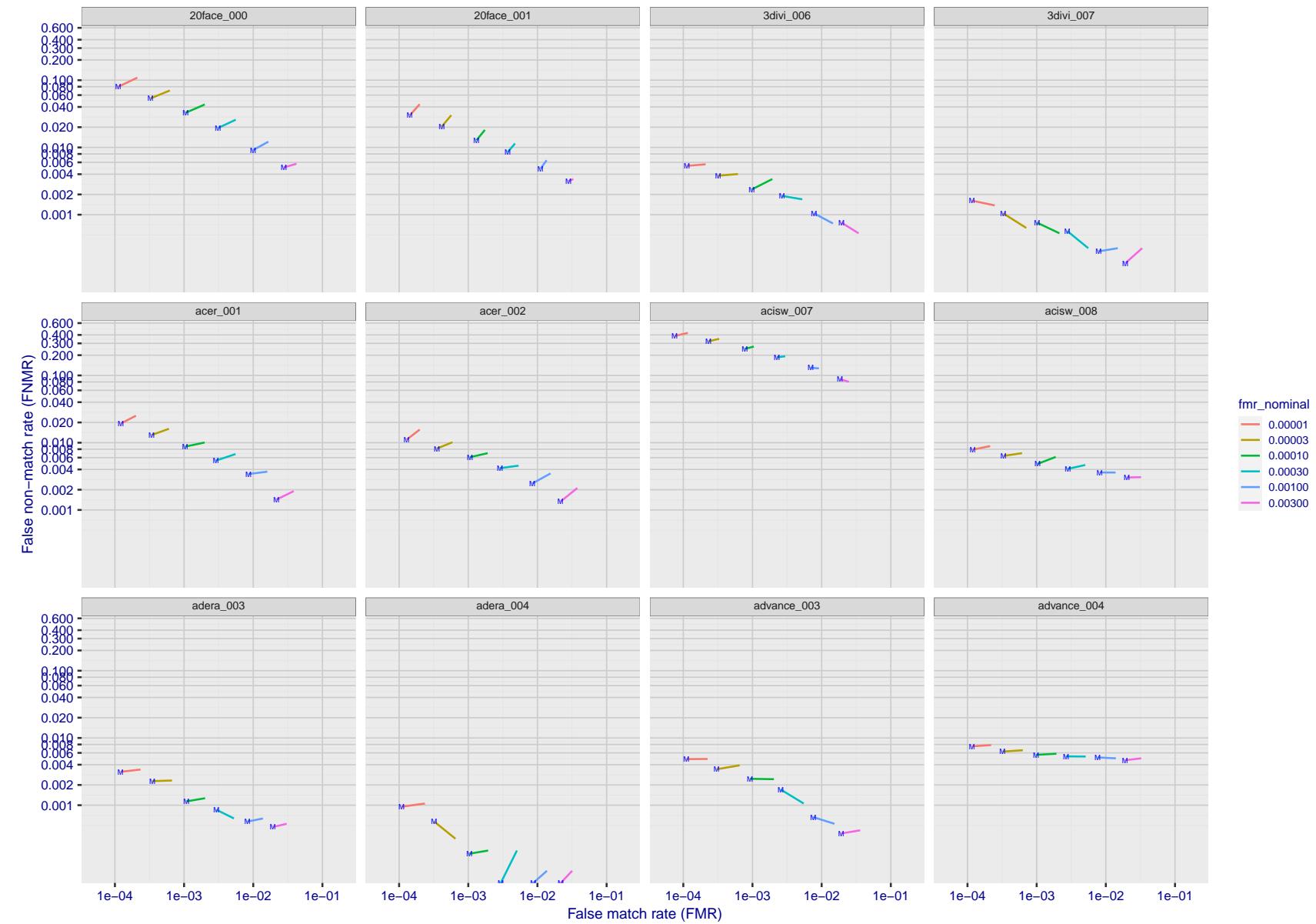


Figure 190: For the visa images, FNMR and FMR at six operating points along the DET characteristic. At each point a line is drawn between $(FMR, FNMR)_{MALE}$ and $(FMR, FNMR)_{FEMALE}$ showing how which sex has lower FMR and/or FNMR. The "M" label denotes male, the other end of the line corresponds to female. The six operating thresholds are selected to give the nominal false match rates given in the legend, and are computed over all impostor pairs regardless of age, sex, and place of birth. The plotted FMR values are broadly an order of magnitude larger than the nominal rates because FMR is computed over demographically-matched impostor pairs i.e individuals of the same sex, from the same geographic region (see section 3.6.1), and the same age group (see section 3.6.2).

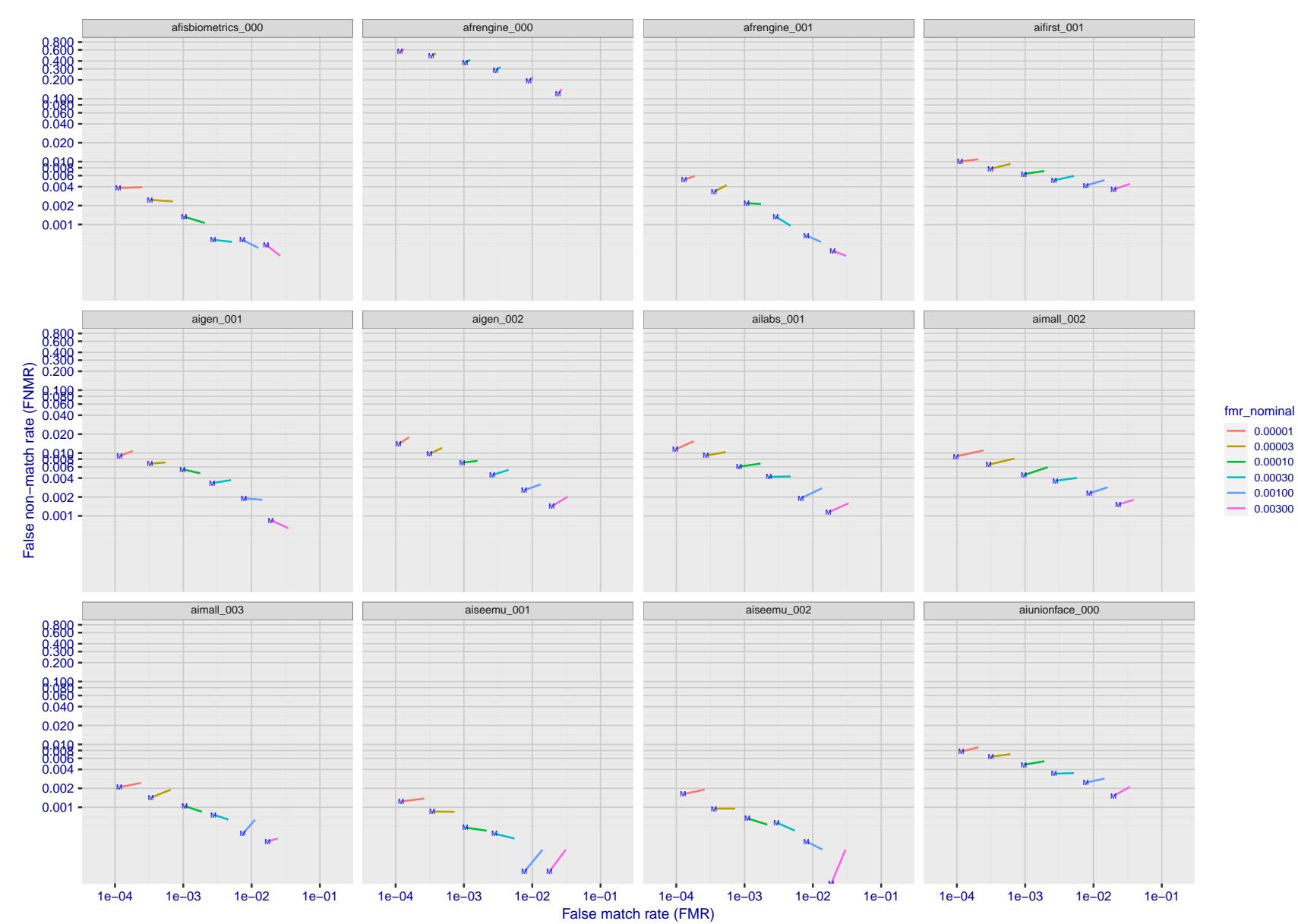


Figure 191: For the visa images, FNMR and FMR at six operating points along the DET characteristic. At each point a line is drawn between $(FMR, FNMR)_{MALE}$ and $(FMR, FNMR)_{FEMALE}$ showing how which sex has lower FMR and/or FNMR. The "M" label denotes male, the other end of the line corresponds to female. The six operating thresholds are selected to give the nominal false match rates given in the legend, and are computed over all impostor pairs regardless of age, sex, and place of birth. The plotted FMR values are broadly an order of magnitude larger than the nominal rates because FMR is computed over demographically-matched impostor pairs i.e individuals of the same sex, from the same geographic region (see section 3.6.1), and the same age group (see section 3.6.2).

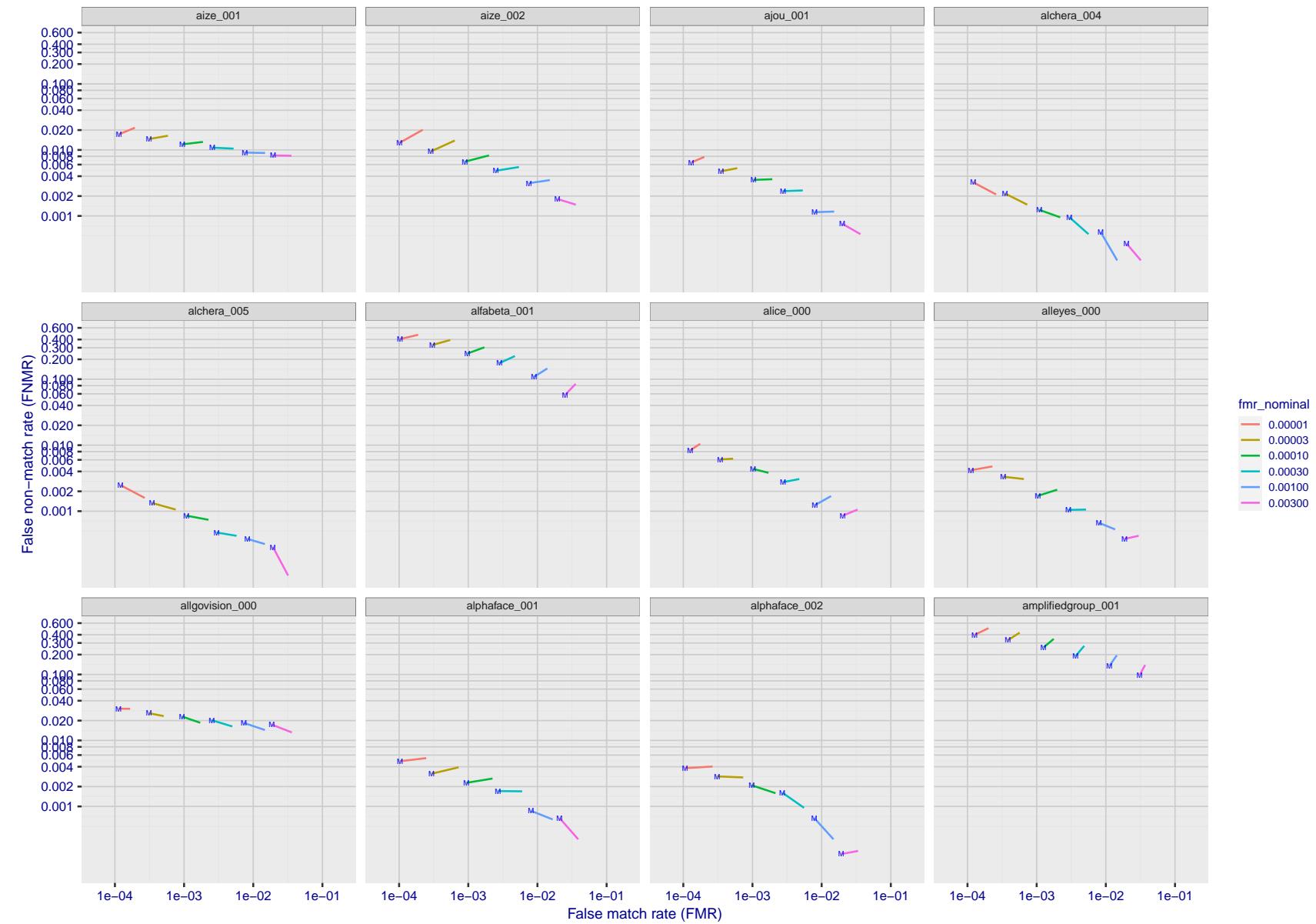


Figure 192: For the visa images, FNMR and FMR at six operating points along the DET characteristic. At each point a line is drawn between $(FMR, FNMR)_{MALE}$ and $(FMR, FNMR)_{FEMALE}$ showing how which sex has lower FMR and/or FNMR. The "M" label denotes male, the other end of the line corresponds to female. The six operating thresholds are selected to give the nominal false match rates given in the legend, and are computed over all impostor pairs regardless of age, sex, and place of birth. The plotted FMR values are broadly an order of magnitude larger than the nominal rates because FMR is computed over demographically-matched impostor pairs i.e individuals of the same sex, from the same geographic region (see section 3.6.1), and the same age group (see section 3.6.2).

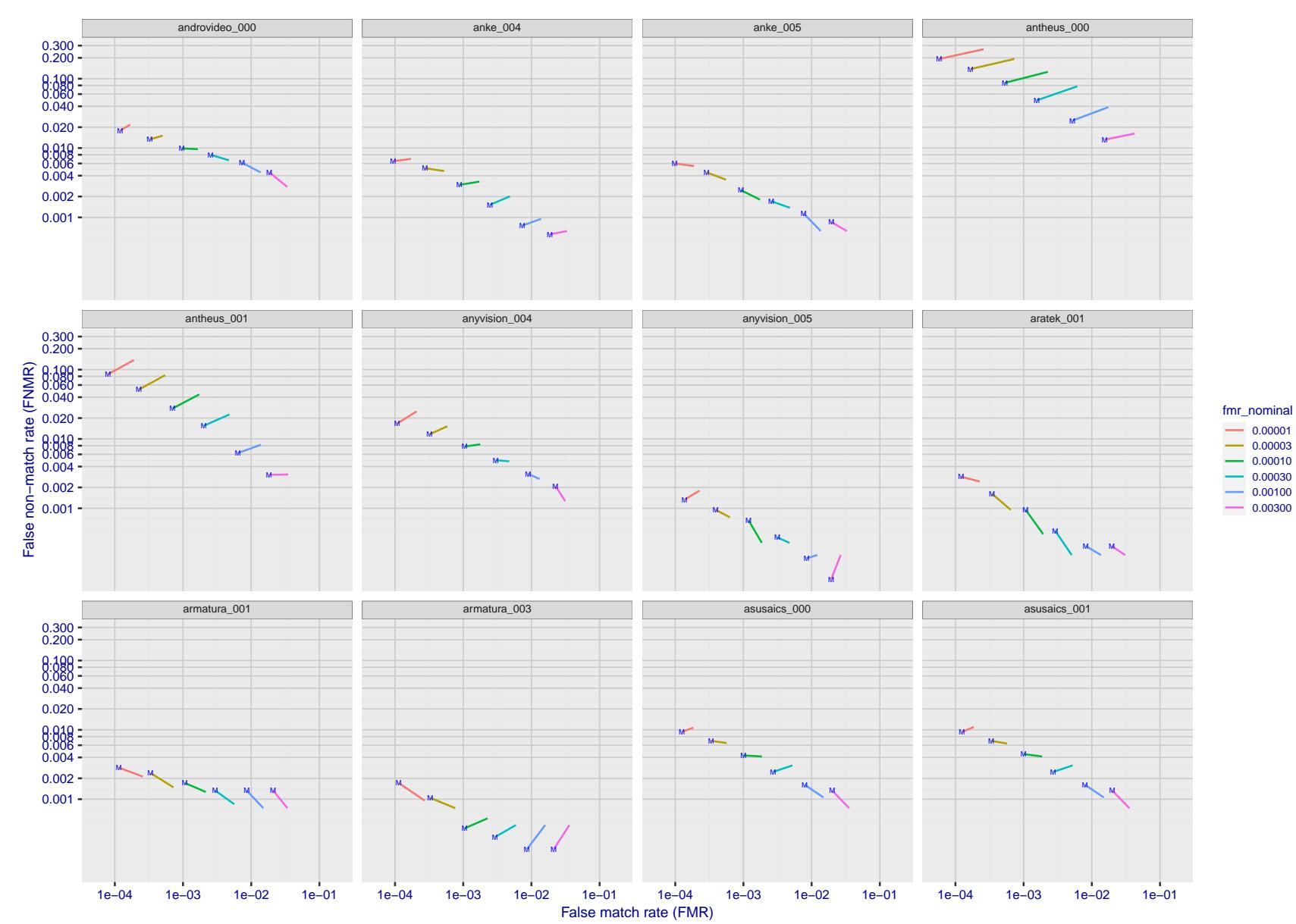


Figure 193: For the visa images, FNMR and FMR at six operating points along the DET characteristic. At each point a line is drawn between $(FMR, FNMR)_{MALE}$ and $(FMR, FNMR)_{FEMALE}$ showing how which sex has lower FMR and/or FNMR. The "M" label denotes male, the other end of the line corresponds to female. The six operating thresholds are selected to give the nominal false match rates given in the legend, and are computed over all impostor pairs regardless of age, sex, and place of birth. The plotted FMR values are broadly an order of magnitude larger than the nominal rates because FMR is computed over demographically-matched impostor pairs i.e individuals of the same sex, from the same geographic region (see section 3.6.1), and the same age group (see section 3.6.2).

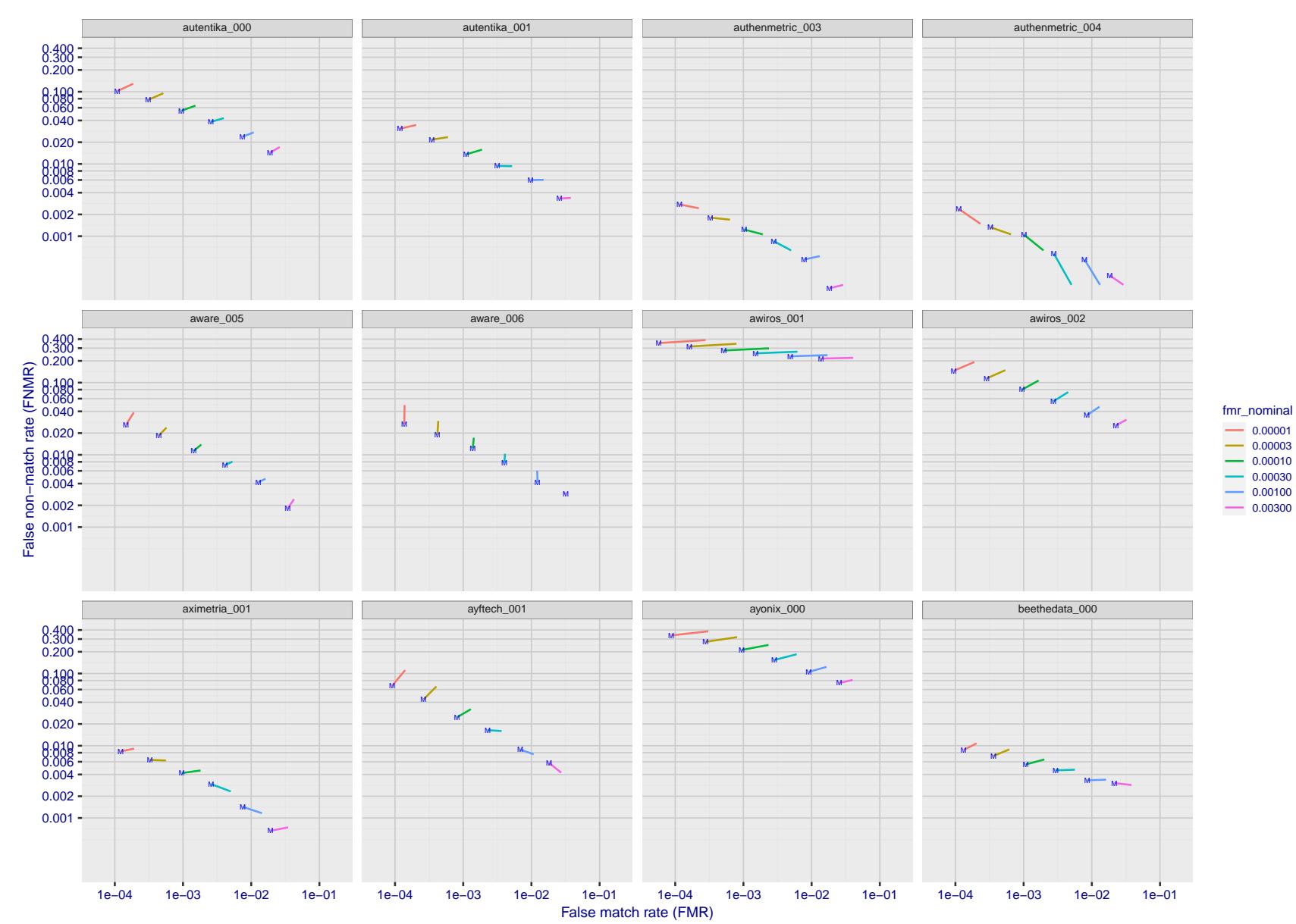


Figure 194: For the visa images, FNMR and FMR at six operating points along the DET characteristic. At each point a line is drawn between $(FMR, FNMR)_{MALE}$ and $(FMR, FNMR)_{FEMALE}$ showing how which sex has lower FMR and/or FNMR. The "M" label denotes male, the other end of the line corresponds to female. The six operating thresholds are selected to give the nominal false match rates given in the legend, and are computed over all impostor pairs regardless of age, sex, and place of birth. The plotted FMR values are broadly an order of magnitude larger than the nominal rates because FMR is computed over demographically-matched impostor pairs i.e individuals of the same sex, from the same geographic region (see section 3.6.1), and the same age group (see section 3.6.2).

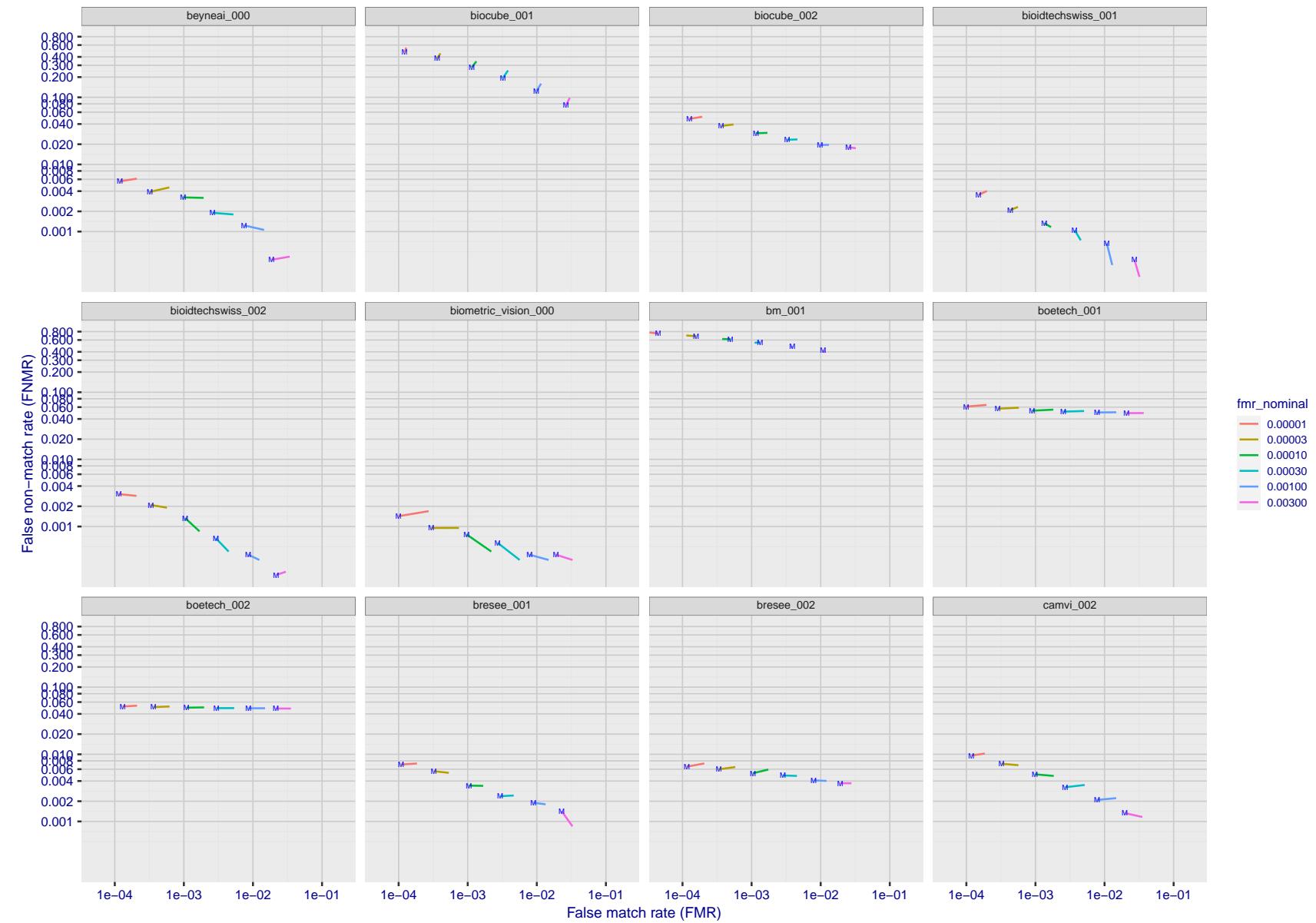


Figure 195: For the visa images, FNMR and FMR at six operating points along the DET characteristic. At each point a line is drawn between $(FMR, FNMR)_{MALE}$ and $(FMR, FNMR)_{FEMALE}$ showing how which sex has lower FMR and/or FNMR. The "M" label denotes male, the other end of the line corresponds to female. The six operating thresholds are selected to give the nominal false match rates given in the legend, and are computed over all impostor pairs regardless of age, sex, and place of birth. The plotted FMR values are broadly an order of magnitude larger than the nominal rates because FMR is computed over demographically-matched impostor pairs i.e individuals of the same sex, from the same geographic region (see section 3.6.1), and the same age group (see section 3.6.2).

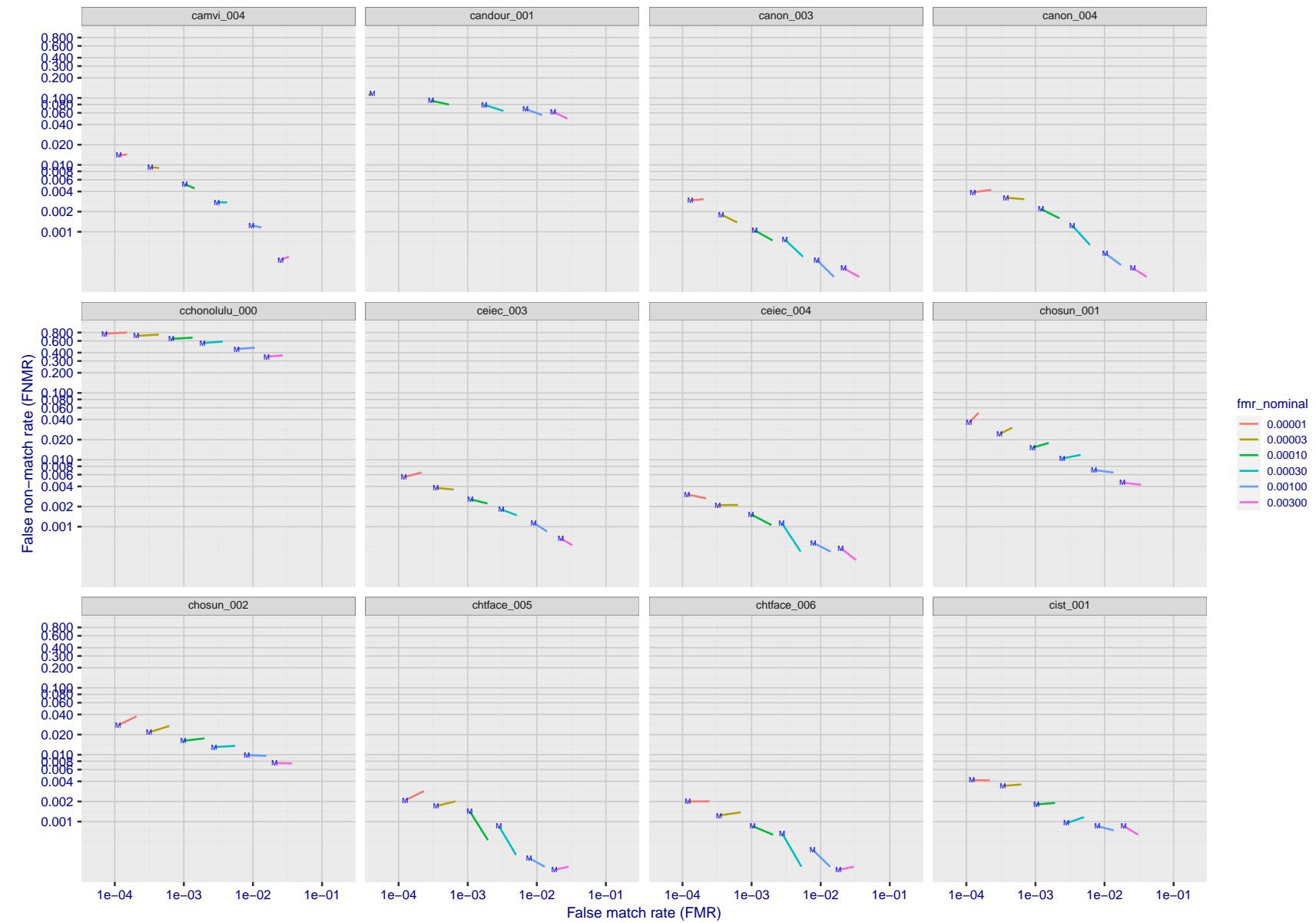


Figure 196: For the visa images, FNMR and FMR at six operating points along the DET characteristic. At each point a line is drawn between $(FMR, FNMR)_{MALE}$ and $(FMR, FNMR)_{FEMALE}$ showing how which sex has lower FMR and/or FNMR. The "M" label denotes male, the other end of the line corresponds to female. The six operating thresholds are selected to give the nominal false match rates given in the legend, and are computed over all impostor pairs regardless of age, sex, and place of birth. The plotted FMR values are broadly an order of magnitude larger than the nominal rates because FMR is computed over demographically-matched impostor pairs i.e individuals of the same sex, from the same geographic region (see section 3.6.1), and the same age group (see section 3.6.2).

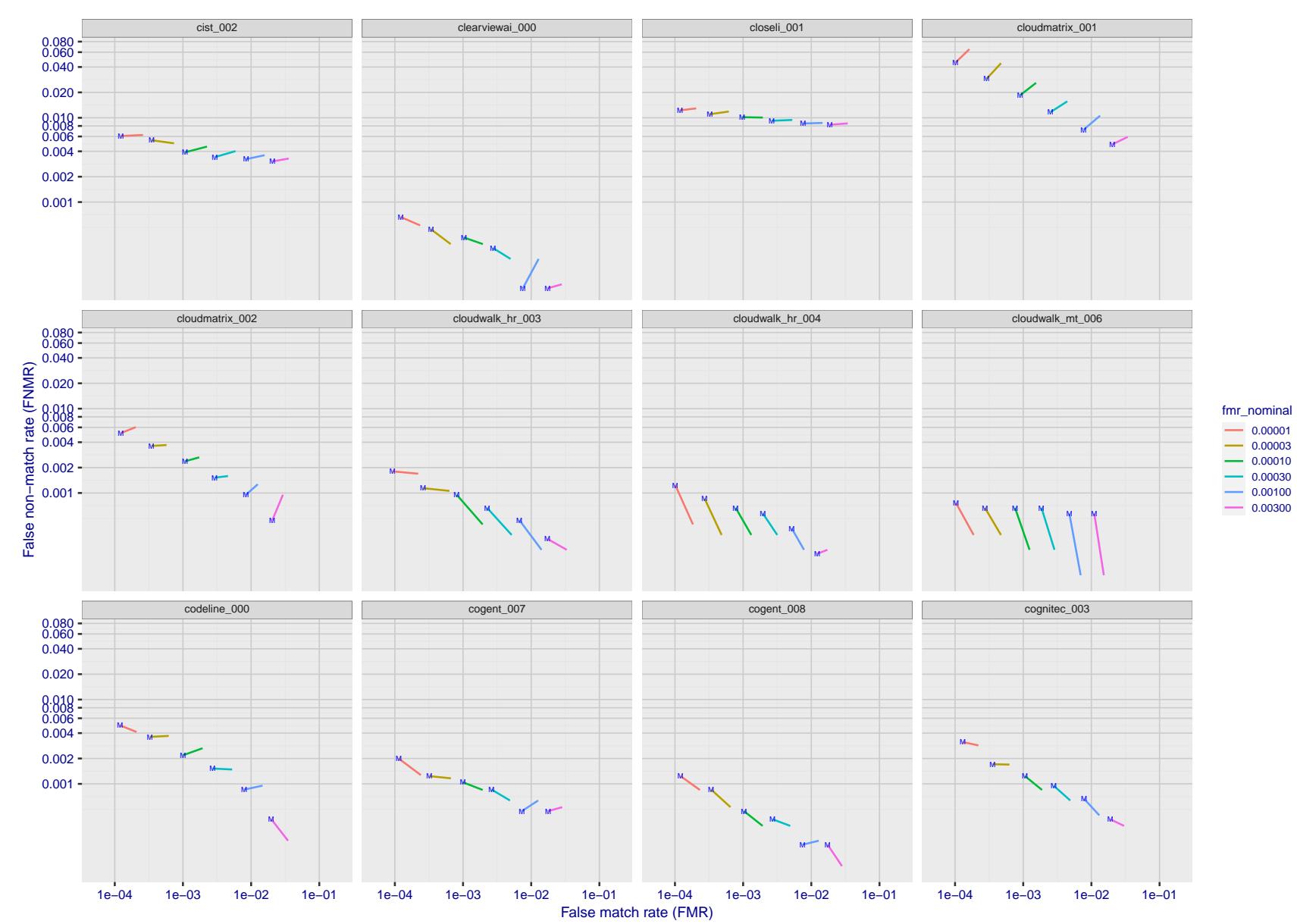


Figure 197: For the visa images, FNMR and FMR at six operating points along the DET characteristic. At each point a line is drawn between $(FMR, FNMR)_{MALE}$ and $(FMR, FNMR)_{FEMALE}$ showing how which sex has lower FMR and/or FNMR. The "M" label denotes male, the other end of the line corresponds to female. The six operating thresholds are selected to give the nominal false match rates given in the legend, and are computed over all impostor pairs regardless of age, sex, and place of birth. The plotted FMR values are broadly an order of magnitude larger than the nominal rates because FMR is computed over demographically-matched impostor pairs i.e individuals of the same sex, from the same geographic region (see section 3.6.1), and the same age group (see section 3.6.2).

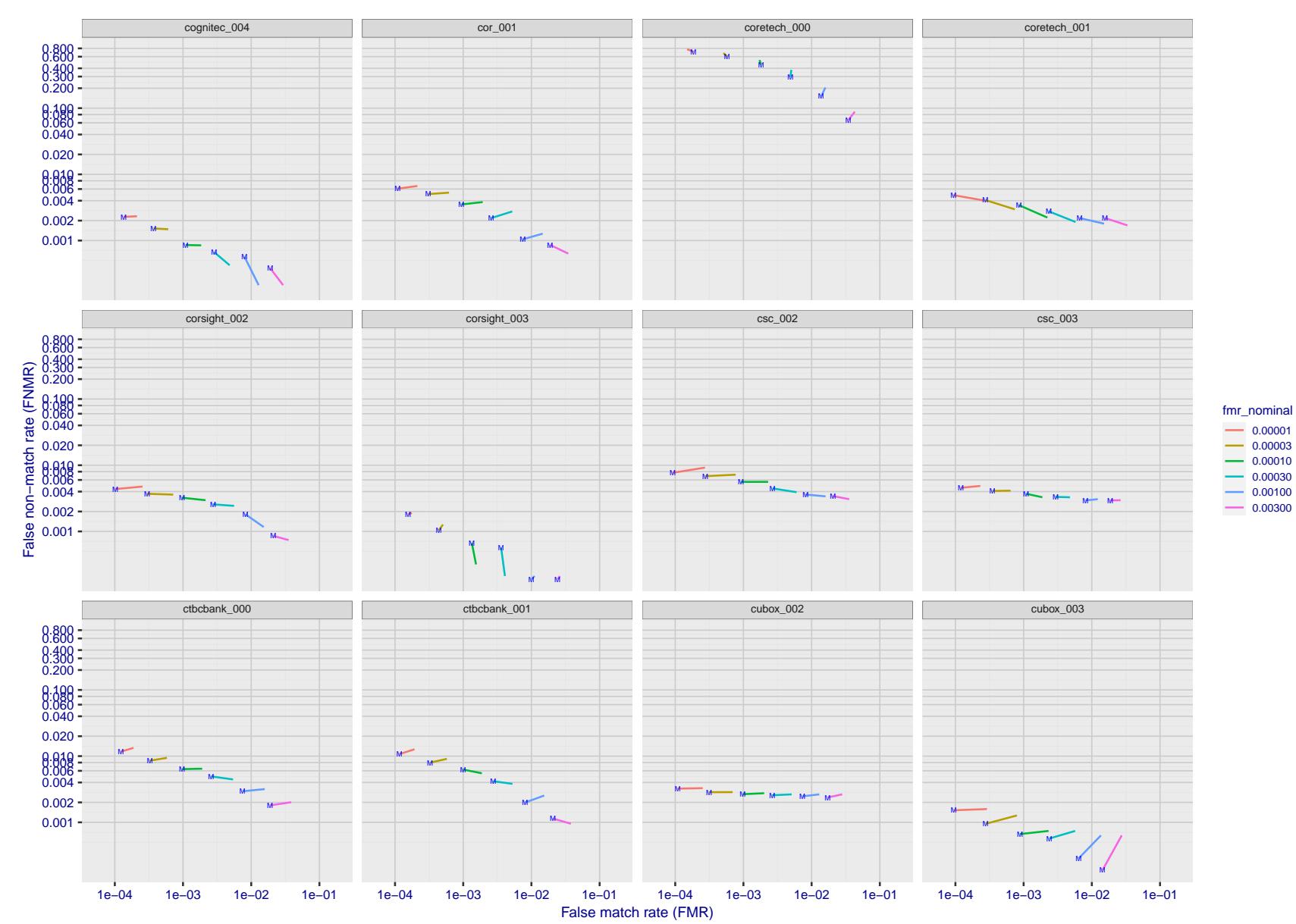


Figure 198: For the visa images, FNMR and FMR at six operating points along the DET characteristic. At each point a line is drawn between $(FMR, FNMR)_{MALE}$ and $(FMR, FNMR)_{FEMALE}$ showing how which sex has lower FMR and/or FNMR. The "M" label denotes male, the other end of the line corresponds to female. The six operating thresholds are selected to give the nominal false match rates given in the legend, and are computed over all impostor pairs regardless of age, sex, and place of birth. The plotted FMR values are broadly an order of magnitude larger than the nominal rates because FMR is computed over demographically-matched impostor pairs i.e individuals of the same sex, from the same geographic region (see section 3.6.1), and the same age group (see section 3.6.2).

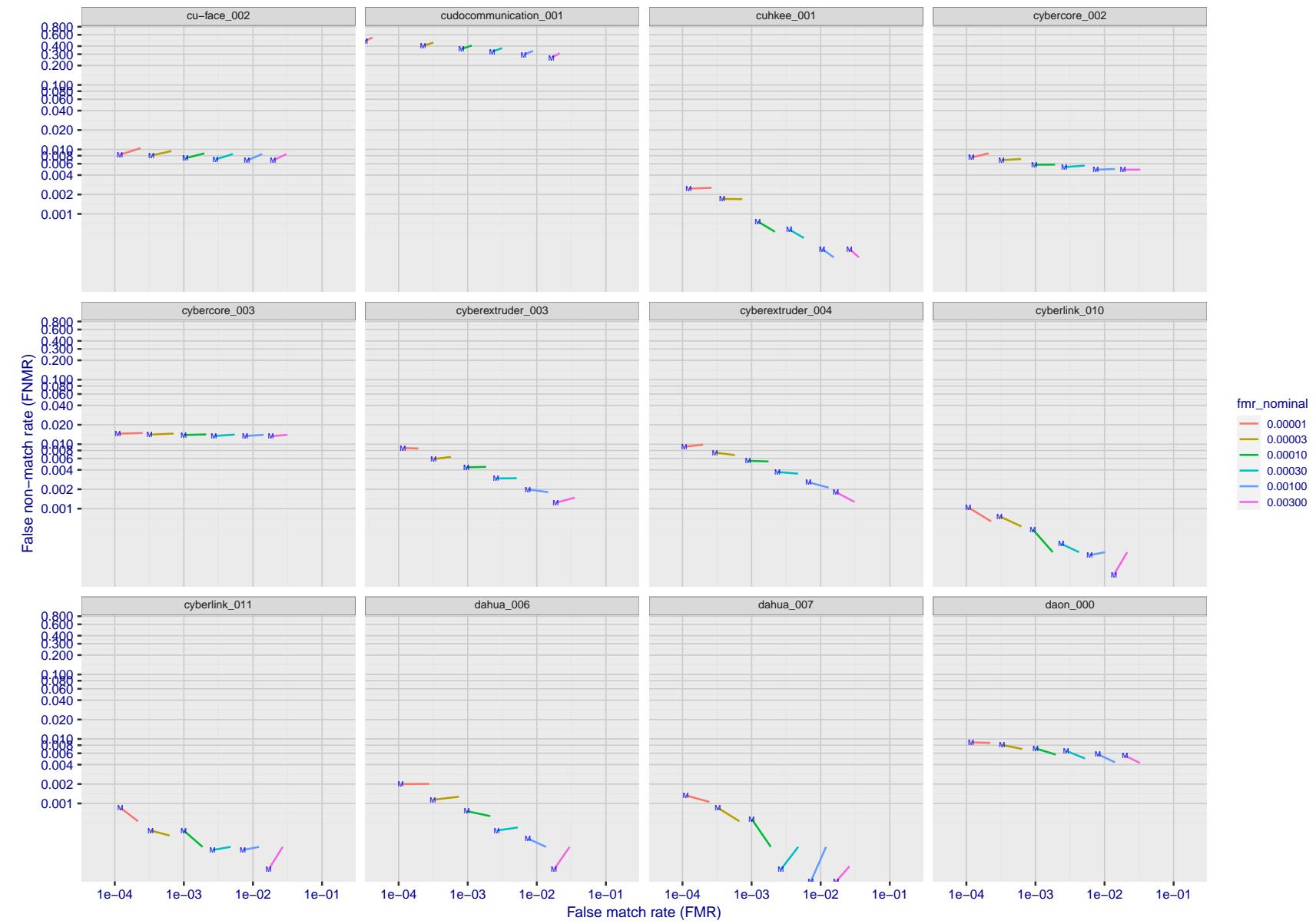


Figure 199: For the visa images, FNMR and FMR at six operating points along the DET characteristic. At each point a line is drawn between $(FMR, FNMR)_{MALE}$ and $(FMR, FNMR)_{FEMALE}$ showing how which sex has lower FMR and/or FNMR. The "M" label denotes male, the other end of the line corresponds to female. The six operating thresholds are selected to give the nominal false match rates given in the legend, and are computed over all impostor pairs regardless of age, sex, and place of birth. The plotted FMR values are broadly an order of magnitude larger than the nominal rates because FMR is computed over demographically-matched impostor pairs i.e individuals of the same sex, from the same geographic region (see section 3.6.1), and the same age group (see section 3.6.2).

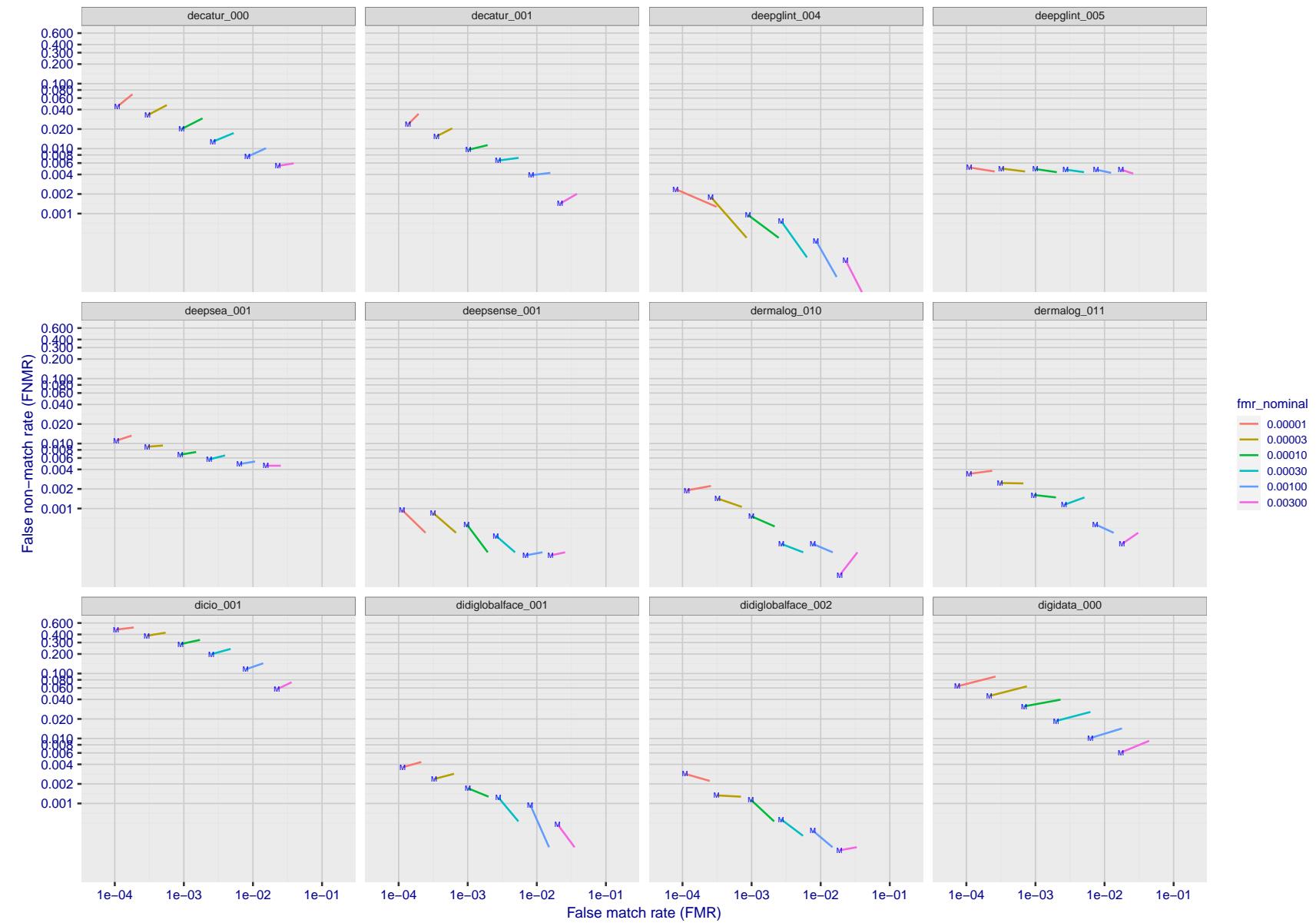


Figure 200: For the visa images, FNMR and FMR at six operating points along the DET characteristic. At each point a line is drawn between $(FMR, FNMR)_{MALE}$ and $(FMR, FNMR)_{FEMALE}$ showing how which sex has lower FMR and/or FNMR. The "M" label denotes male, the other end of the line corresponds to female. The six operating thresholds are selected to give the nominal false match rates given in the legend, and are computed over all impostor pairs regardless of age, sex, and place of birth. The plotted FMR values are broadly an order of magnitude larger than the nominal rates because FMR is computed over demographically-matched impostor pairs i.e individuals of the same sex, from the same geographic region (see section 3.6.1), and the same age group (see section 3.6.2).

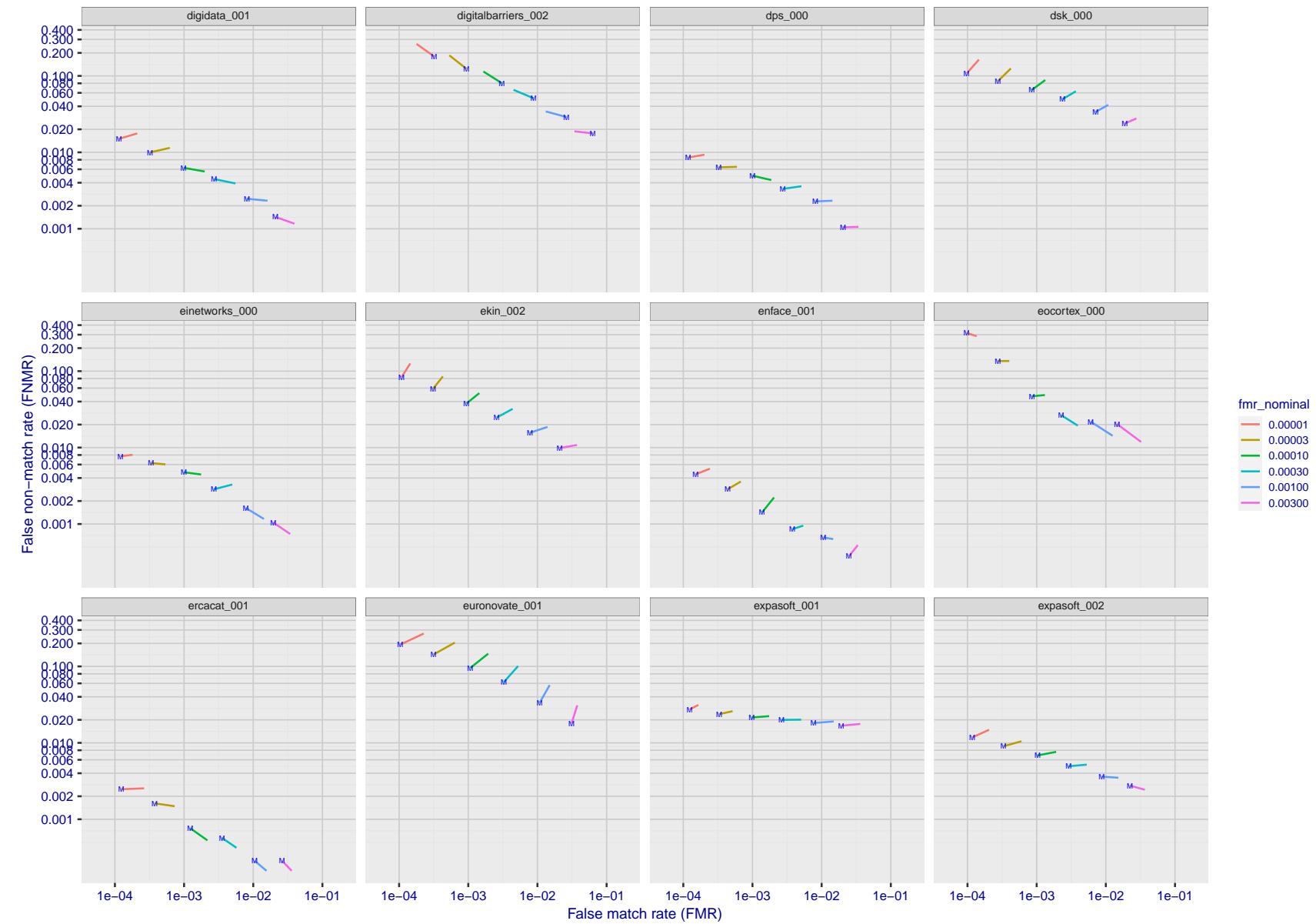


Figure 201: For the visa images, FNMR and FMR at six operating points along the DET characteristic. At each point a line is drawn between $(FMR, FNMR)_{MALE}$ and $(FMR, FNMR)_{FEMALE}$ showing how which sex has lower FMR and/or FNMR. The "M" label denotes male, the other end of the line corresponds to female. The six operating thresholds are selected to give the nominal false match rates given in the legend, and are computed over all impostor pairs regardless of age, sex, and place of birth. The plotted FMR values are broadly an order of magnitude larger than the nominal rates because FMR is computed over demographically-matched impostor pairs i.e individuals of the same sex, from the same geographic region (see section 3.6.1), and the same age group (see section 3.6.2).

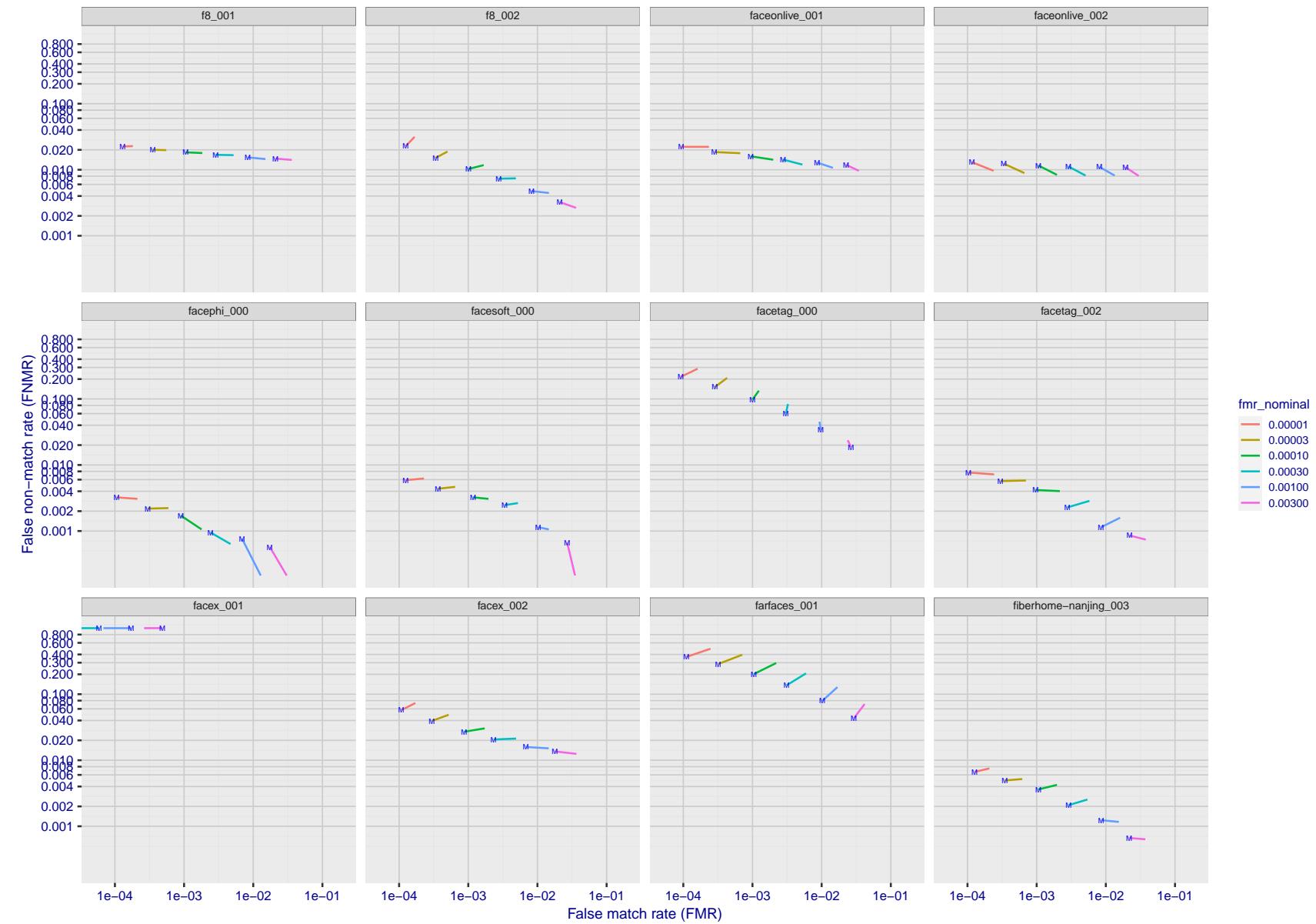


Figure 202: For the visa images, FNMR and FMR at six operating points along the DET characteristic. At each point a line is drawn between $(FMR, FNMR)_{MALE}$ and $(FMR, FNMR)_{FEMALE}$ showing how which sex has lower FMR and/or FNMR. The "M" label denotes male, the other end of the line corresponds to female. The six operating thresholds are selected to give the nominal false match rates given in the legend, and are computed over all impostor pairs regardless of age, sex, and place of birth. The plotted FMR values are broadly an order of magnitude larger than the nominal rates because FMR is computed over demographically-matched impostor pairs i.e individuals of the same sex, from the same geographic region (see section 3.6.1), and the same age group (see section 3.6.2).

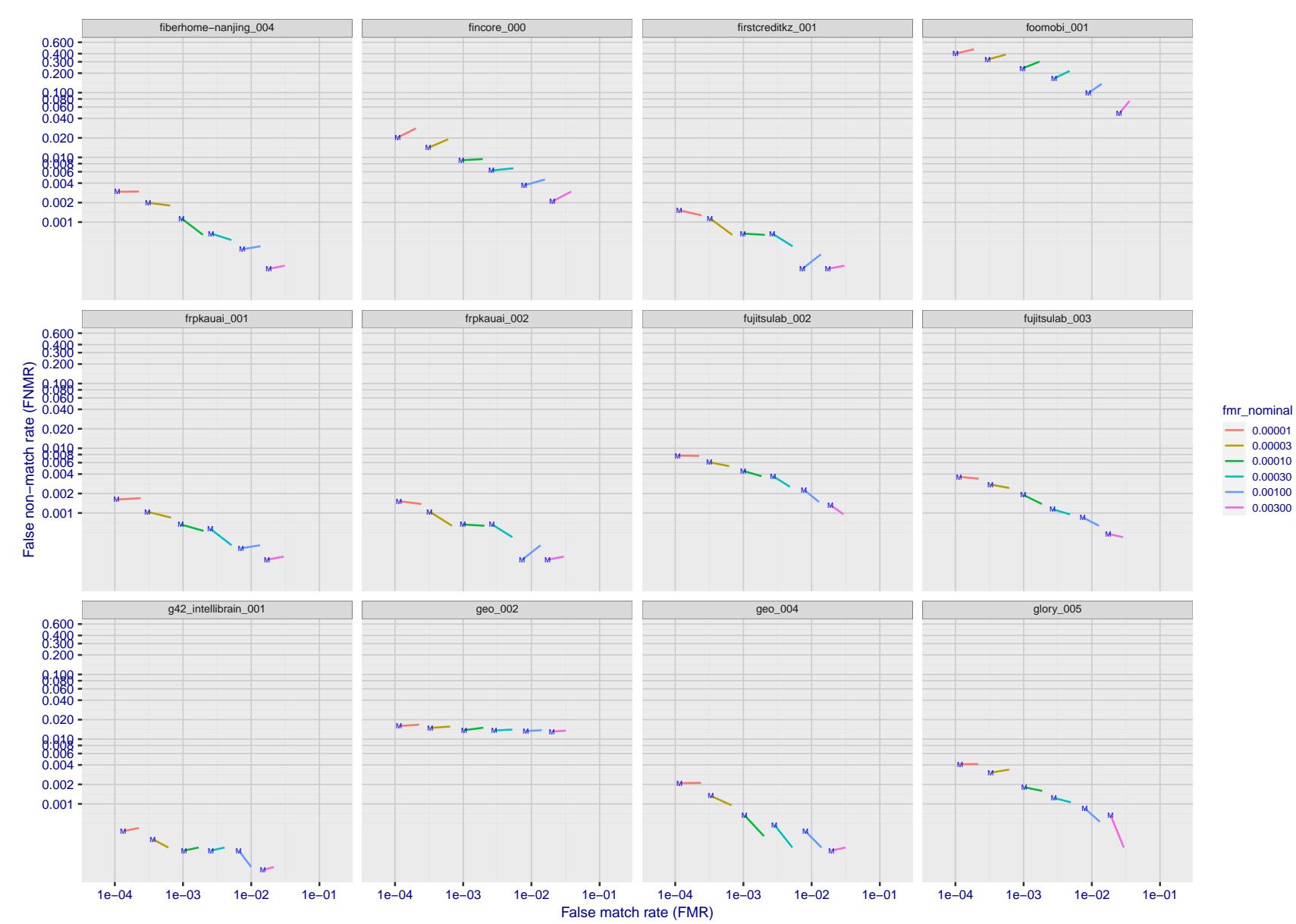


Figure 203: For the visa images, FNMR and FMR at six operating points along the DET characteristic. At each point a line is drawn between $(FMR, FNMR)_{MALE}$ and $(FMR, FNMR)_{FEMALE}$ showing how which sex has lower FMR and/or FNMR. The "M" label denotes male, the other end of the line corresponds to female. The six operating thresholds are selected to give the nominal false match rates given in the legend, and are computed over all impostor pairs regardless of age, sex, and place of birth. The plotted FMR values are broadly an order of magnitude larger than the nominal rates because FMR is computed over demographically-matched impostor pairs i.e individuals of the same sex, from the same geographic region (see section 3.6.1), and the same age group (see section 3.6.2).

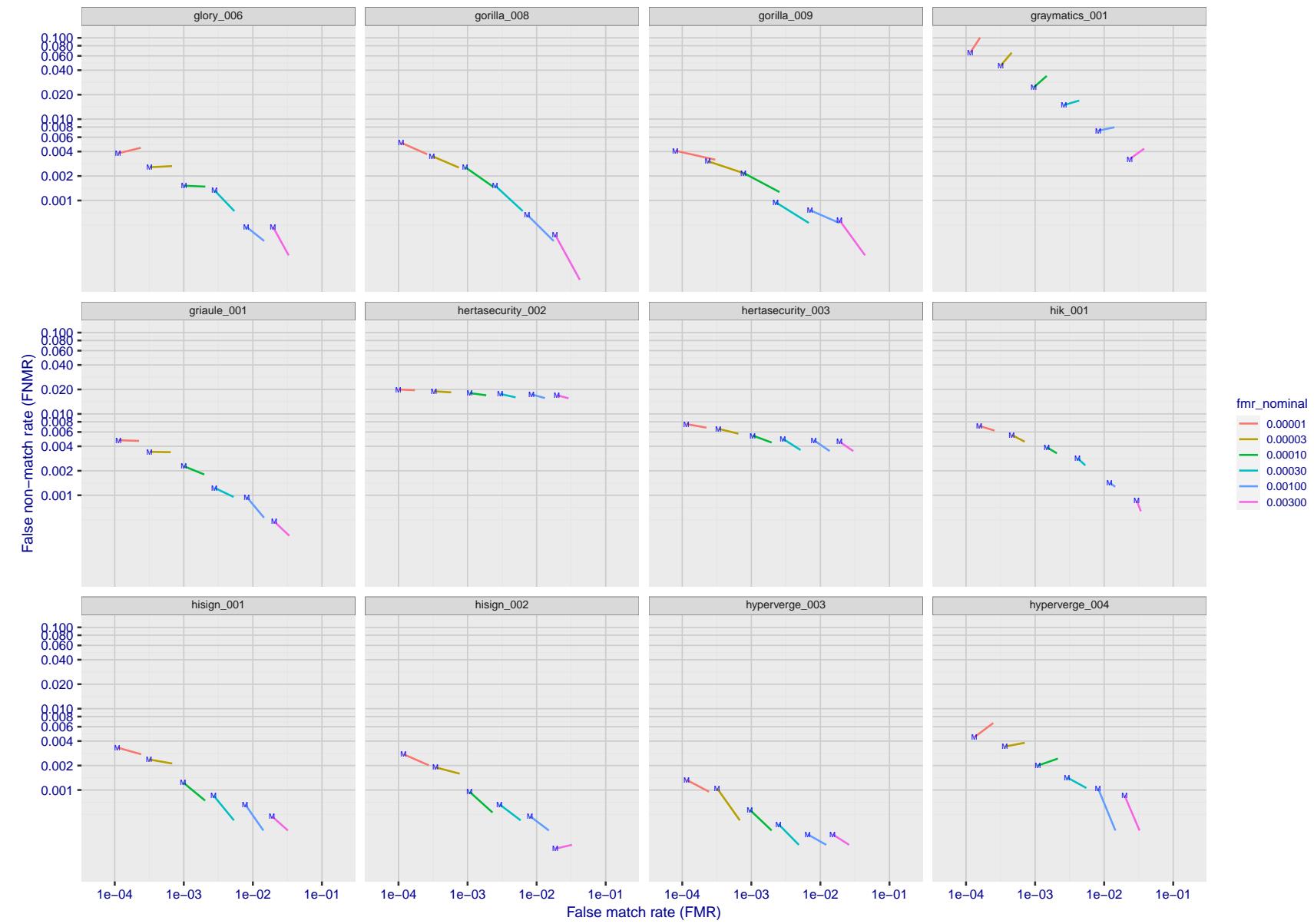


Figure 204: For the visa images, FNMR and FMR at six operating points along the DET characteristic. At each point a line is drawn between $(FMR, FNMR)_{MALE}$ and $(FMR, FNMR)_{FEMALE}$ showing how which sex has lower FMR and/or FNMR. The "M" label denotes male, the other end of the line corresponds to female. The six operating thresholds are selected to give the nominal false match rates given in the legend, and are computed over all impostor pairs regardless of age, sex, and place of birth. The plotted FMR values are broadly an order of magnitude larger than the nominal rates because FMR is computed over demographically-matched impostor pairs i.e individuals of the same sex, from the same geographic region (see section 3.6.1), and the same age group (see section 3.6.2).

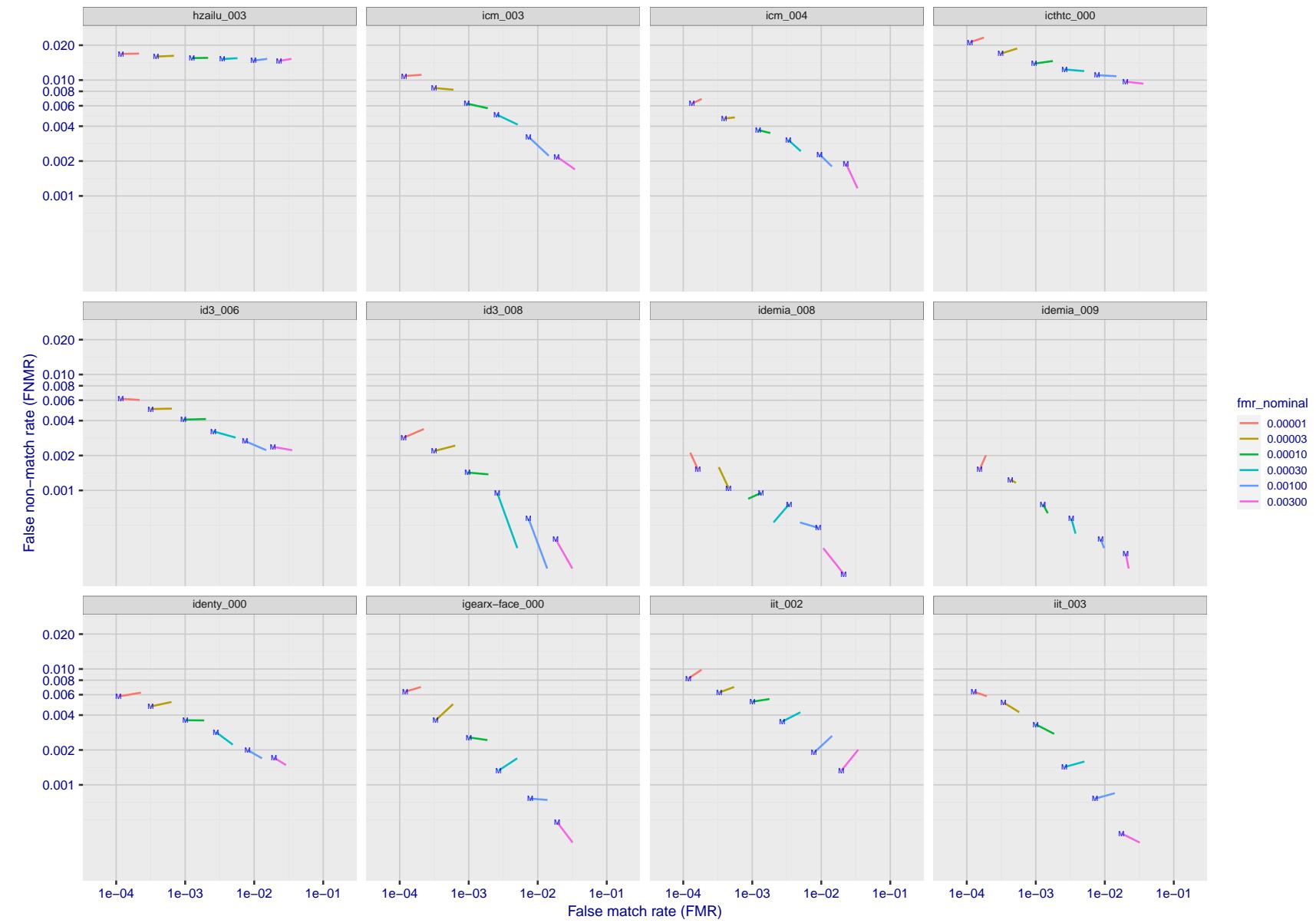


Figure 205: For the visa images, FNMR and FMR at six operating points along the DET characteristic. At each point a line is drawn between $(FMR, FNMR)_{MALE}$ and $(FMR, FNMR)_{FEMALE}$ showing how which sex has lower FMR and/or FNMR. The "M" label denotes male, the other end of the line corresponds to female. The six operating thresholds are selected to give the nominal false match rates given in the legend, and are computed over all impostor pairs regardless of age, sex, and place of birth. The plotted FMR values are broadly an order of magnitude larger than the nominal rates because FMR is computed over demographically-matched impostor pairs i.e individuals of the same sex, from the same geographic region (see section 3.6.1), and the same age group (see section 3.6.2).

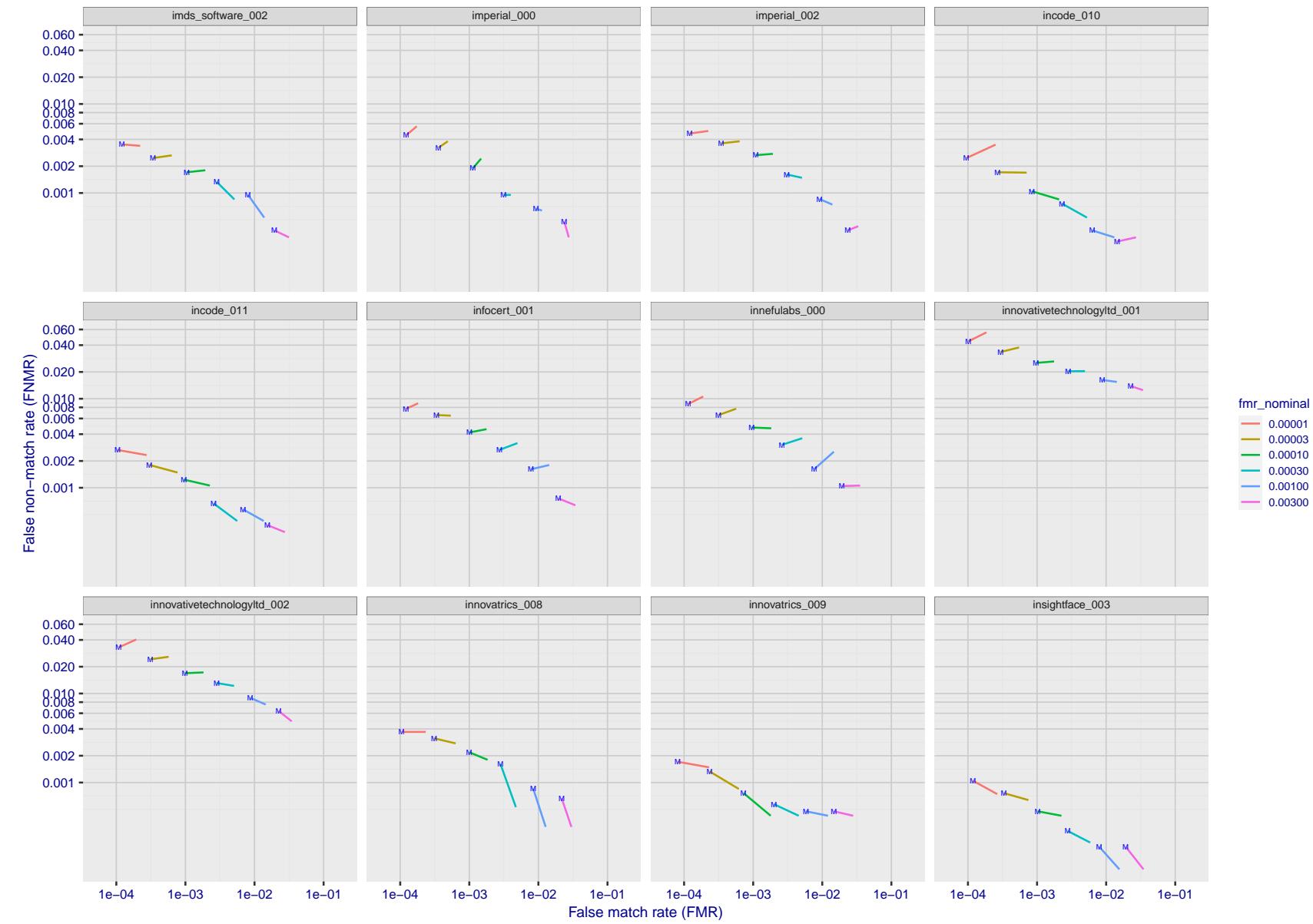


Figure 206: For the visa images, FNMR and FMR at six operating points along the DET characteristic. At each point a line is drawn between $(FMR, FNMR)_{MALE}$ and $(FMR, FNMR)_{FEMALE}$ showing how which sex has lower FMR and/or FNMR. The "M" label denotes male, the other end of the line corresponds to female. The six operating thresholds are selected to give the nominal false match rates given in the legend, and are computed over all impostor pairs regardless of age, sex, and place of birth. The plotted FMR values are broadly an order of magnitude larger than the nominal rates because FMR is computed over demographically-matched impostor pairs i.e individuals of the same sex, from the same geographic region (see section 3.6.1), and the same age group (see section 3.6.2).

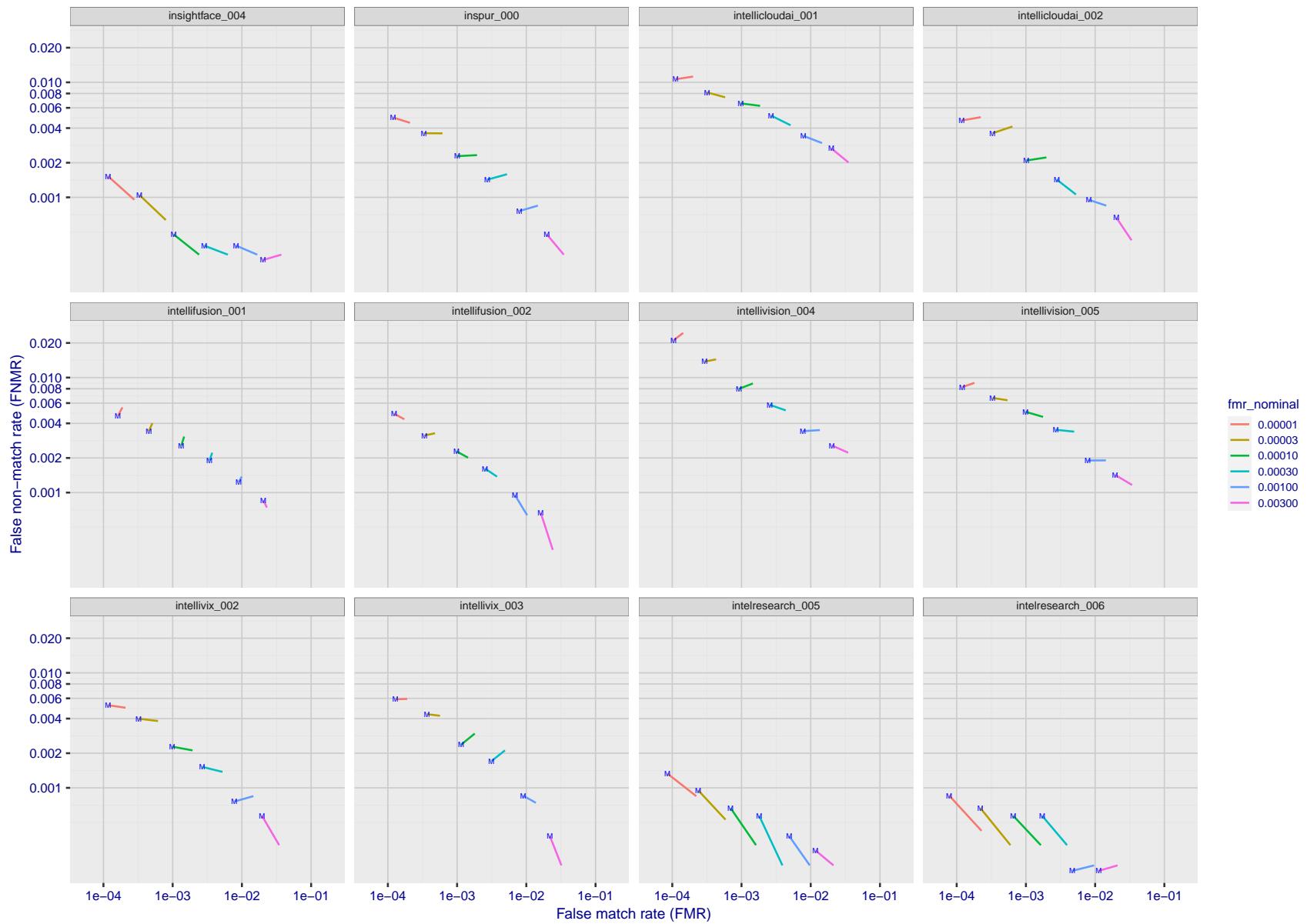


Figure 207: For the visa images, FNMR and FMR at six operating points along the DET characteristic. At each point a line is drawn between $(FMR, FNMR)_{MALE}$ and $(FMR, FNMR)_{FEMALE}$ showing how which sex has lower FMR and/or FNMR. The "M" label denotes male, the other end of the line corresponds to female. The six operating thresholds are selected to give the nominal false match rates given in the legend, and are computed over all impostor pairs regardless of age, sex, and place of birth. The plotted FMR values are broadly an order of magnitude larger than the nominal rates because FMR is computed over demographically-matched impostor pairs i.e individuals of the same sex, from the same geographic region (see section 3.6.1), and the same age group (see section 3.6.2).

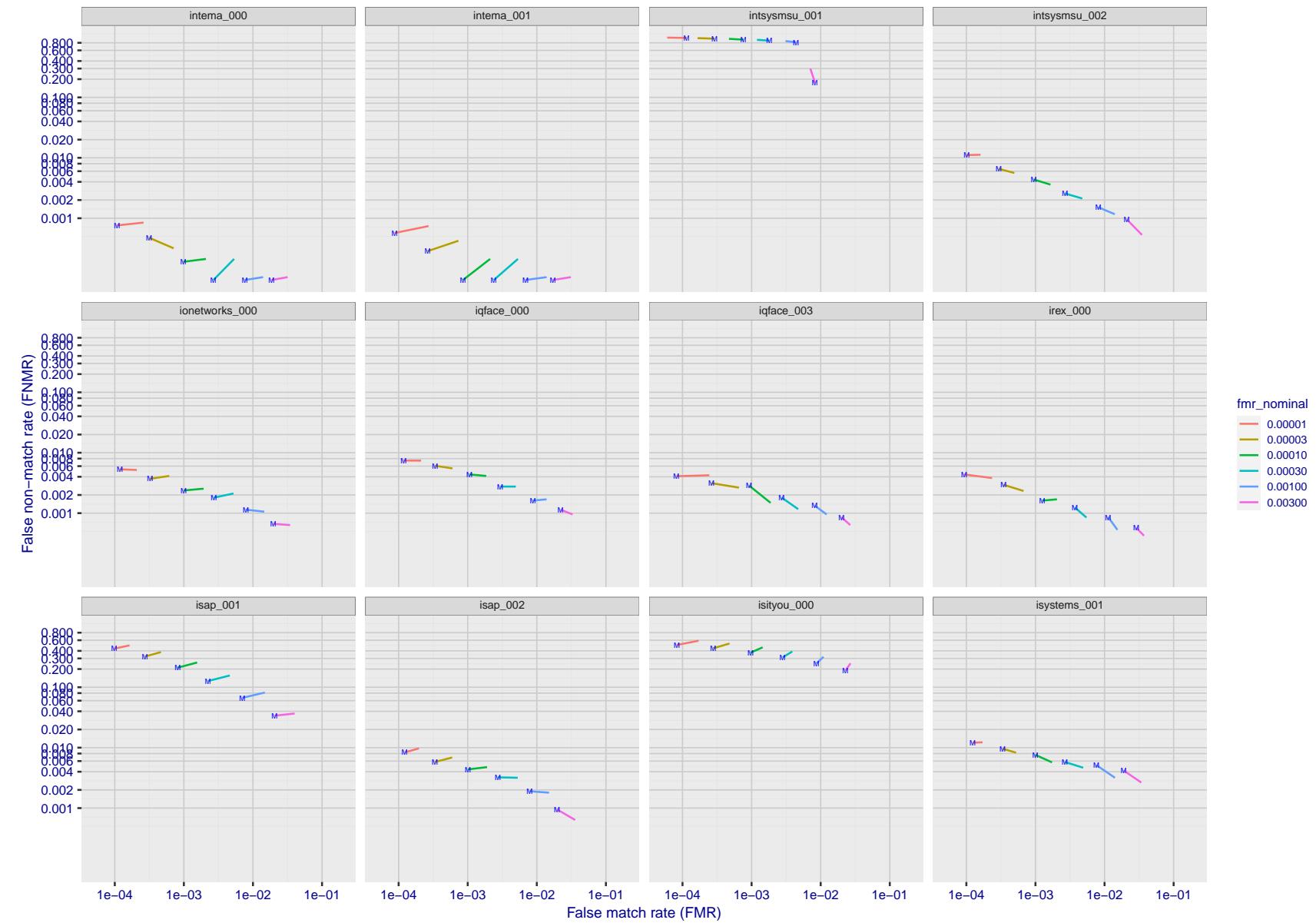


Figure 208: For the visa images, FNMR and FMR at six operating points along the DET characteristic. At each point a line is drawn between $(FMR, FNMR)_{MALE}$ and $(FMR, FNMR)_{FEMALE}$ showing how which sex has lower FMR and/or FNMR. The "M" label denotes male, the other end of the line corresponds to female. The six operating thresholds are selected to give the nominal false match rates given in the legend, and are computed over all impostor pairs regardless of age, sex, and place of birth. The plotted FMR values are broadly an order of magnitude larger than the nominal rates because FMR is computed over demographically-matched impostor pairs i.e individuals of the same sex, from the same geographic region (see section 3.6.1), and the same age group (see section 3.6.2).

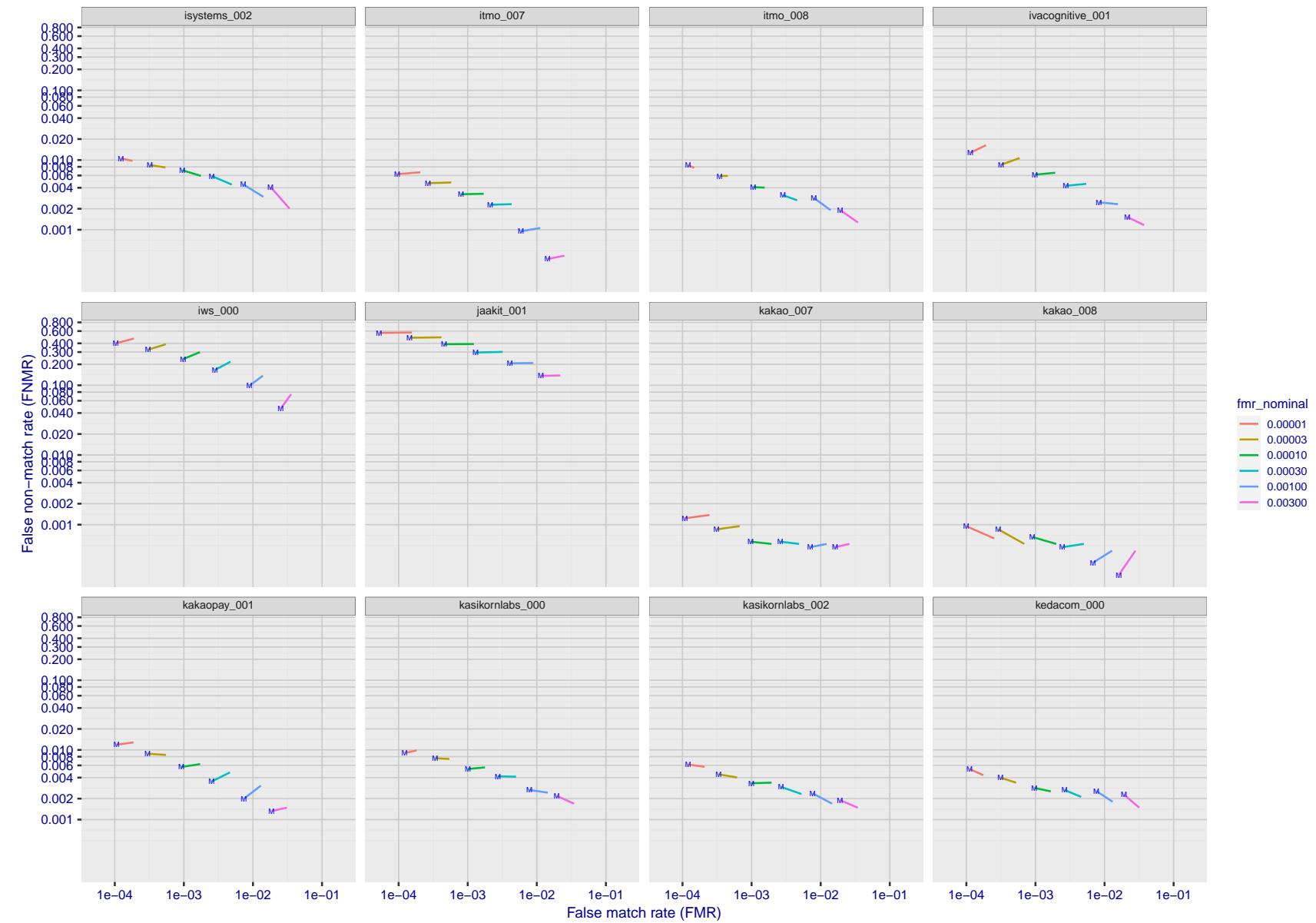


Figure 209: For the visa images, FNMR and FMR at six operating points along the DET characteristic. At each point a line is drawn between $(FMR, FNMR)_{MALE}$ and $(FMR, FNMR)_{FEMALE}$ showing how which sex has lower FMR and/or FNMR. The "M" label denotes male, the other end of the line corresponds to female. The six operating thresholds are selected to give the nominal false match rates given in the legend, and are computed over all impostor pairs regardless of age, sex, and place of birth. The plotted FMR values are broadly an order of magnitude larger than the nominal rates because FMR is computed over demographically-matched impostor pairs i.e individuals of the same sex, from the same geographic region (see section 3.6.1), and the same age group (see section 3.6.2).

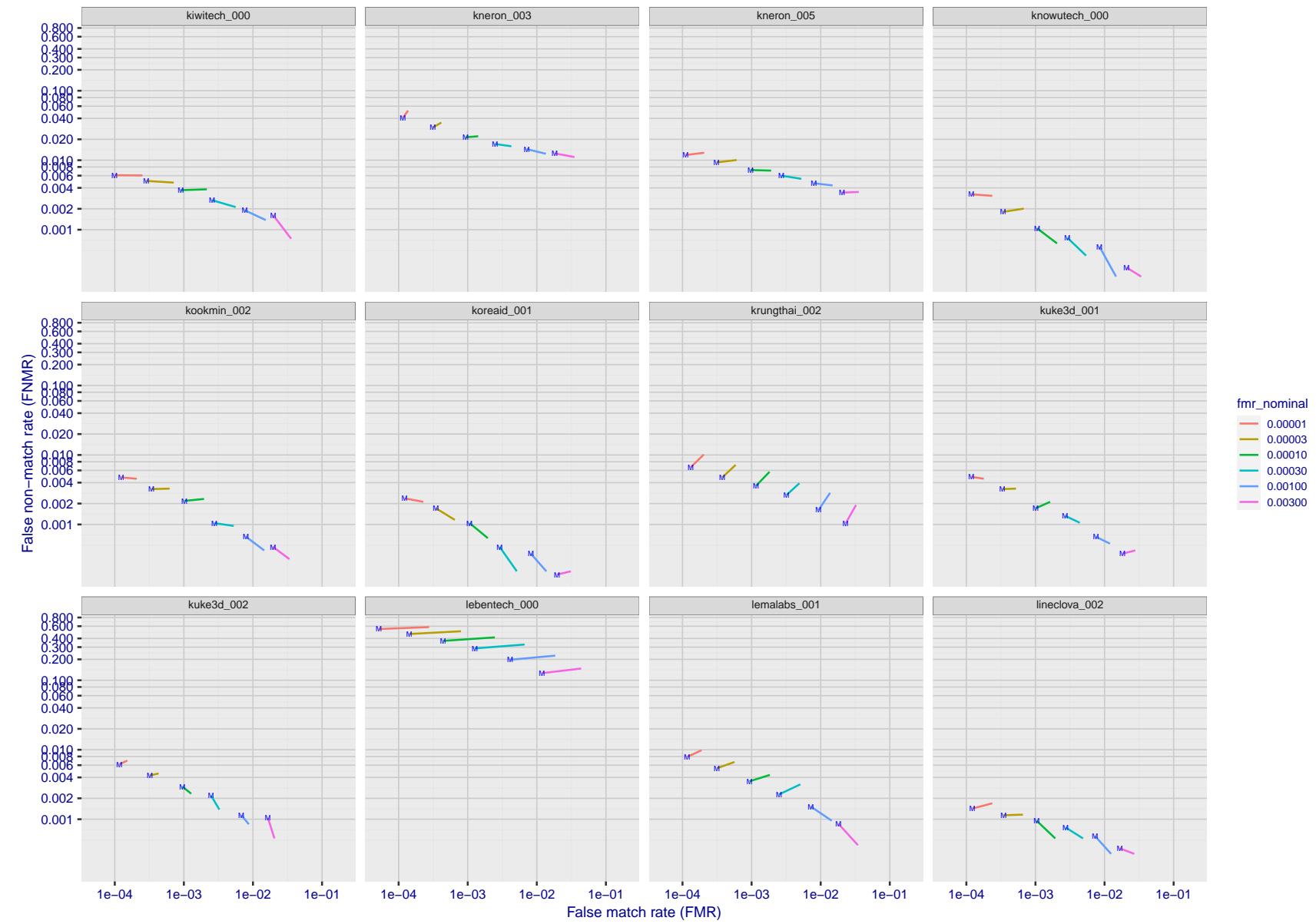


Figure 210: For the visa images, FNMR and FMR at six operating points along the DET characteristic. At each point a line is drawn between $(FMR, FNMR)_{MALE}$ and $(FMR, FNMR)_{FEMALE}$ showing how which sex has lower FMR and/or FNMR. The "M" label denotes male, the other end of the line corresponds to female. The six operating thresholds are selected to give the nominal false match rates given in the legend, and are computed over all impostor pairs regardless of age, sex, and place of birth. The plotted FMR values are broadly an order of magnitude larger than the nominal rates because FMR is computed over demographically-matched impostor pairs i.e individuals of the same sex, from the same geographic region (see section 3.6.1), and the same age group (see section 3.6.2).

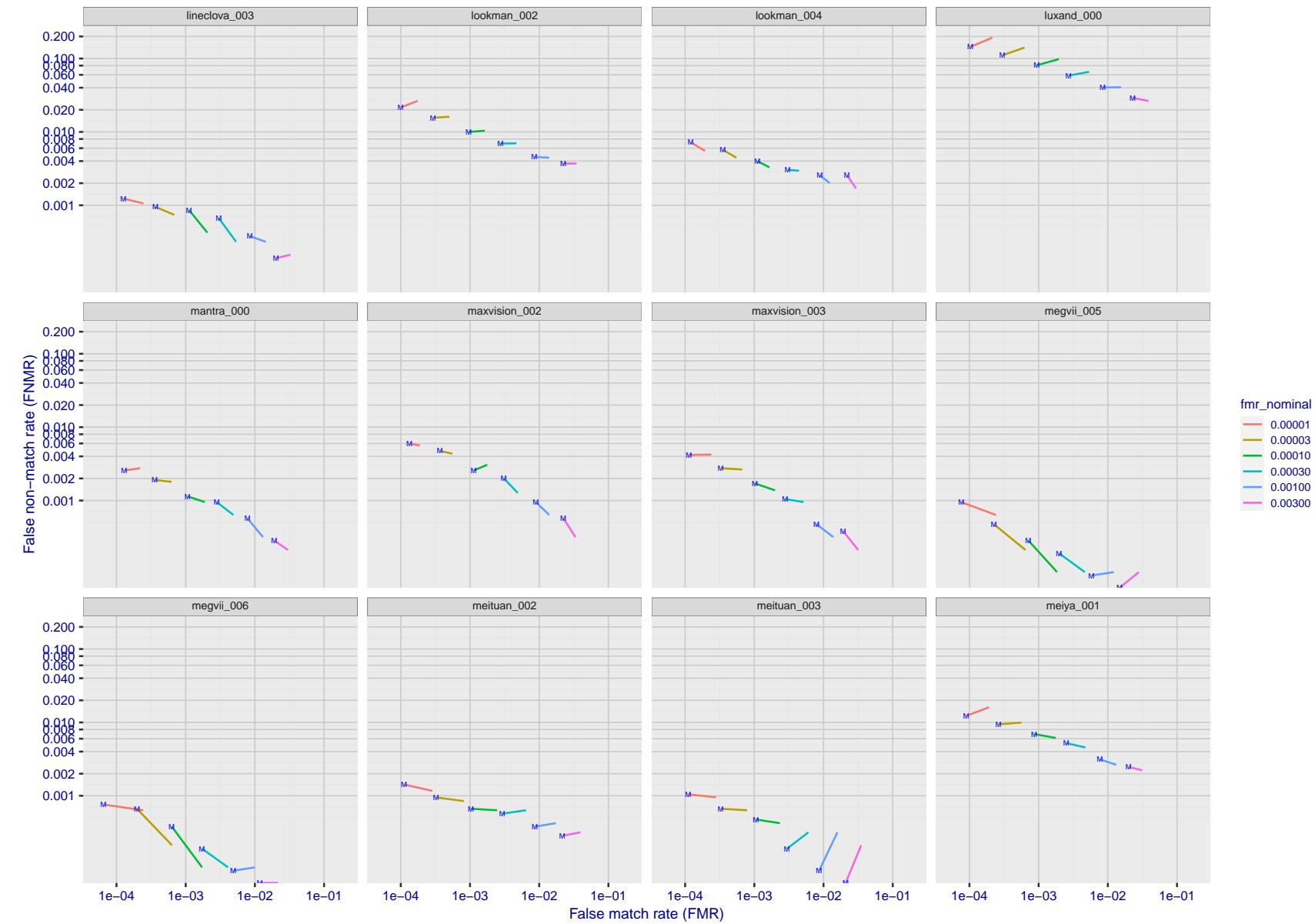


Figure 211: For the visa images, FNMR and FMR at six operating points along the DET characteristic. At each point a line is drawn between $(FMR, FNMR)_{MALE}$ and $(FMR, FNMR)_{FEMALE}$ showing how which sex has lower FMR and/or FNMR. The "M" label denotes male, the other end of the line corresponds to female. The six operating thresholds are selected to give the nominal false match rates given in the legend, and are computed over all impostor pairs regardless of age, sex, and place of birth. The plotted FMR values are broadly an order of magnitude larger than the nominal rates because FMR is computed over demographically-matched impostor pairs i.e individuals of the same sex, from the same geographic region (see section 3.6.1), and the same age group (see section 3.6.2).

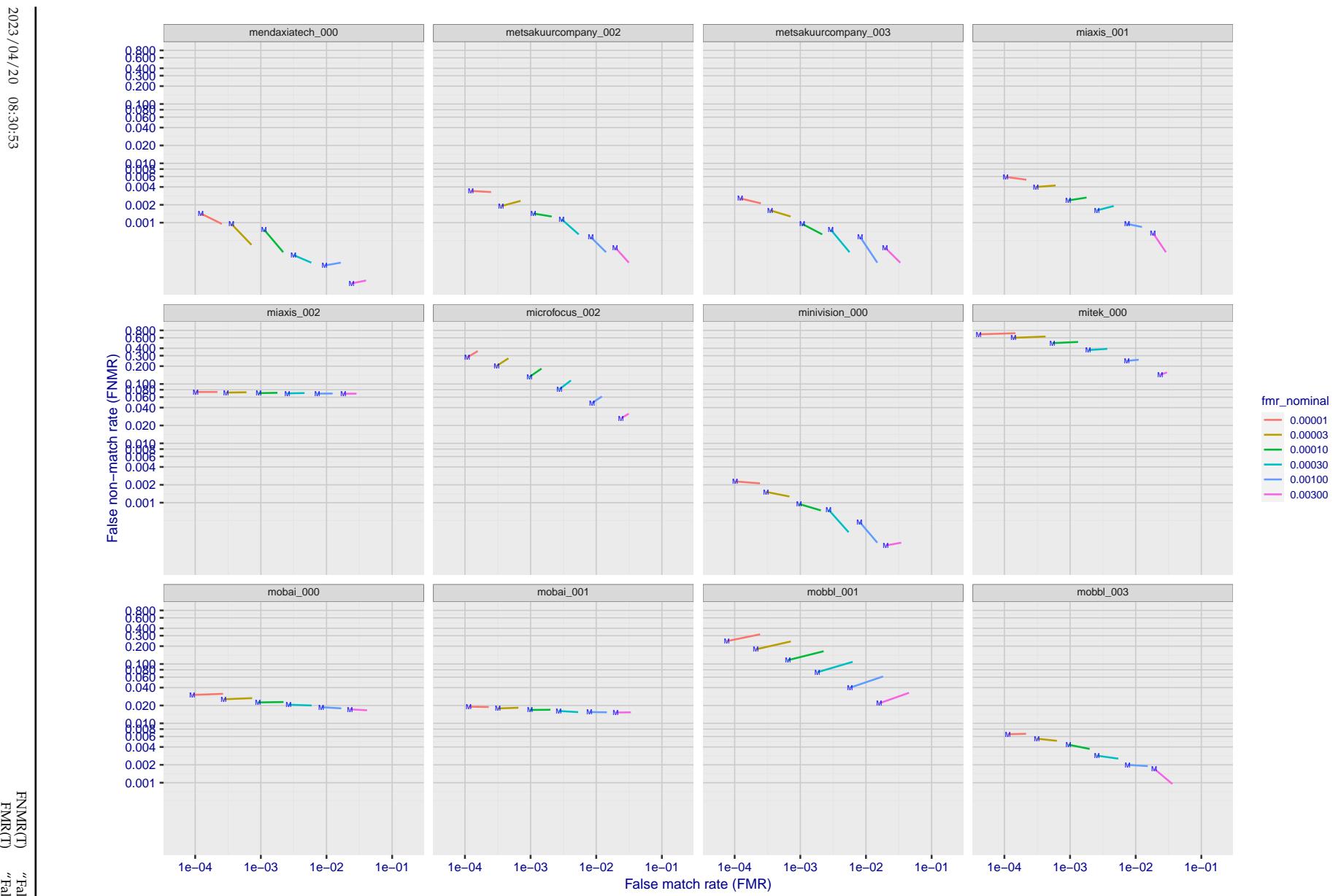


Figure 212: For the visa images, FNMR and FMR at six operating points along the DET characteristic. At each point a line is drawn between $(FMR, FNMR)_{MALE}$ and $(FMR, FNMR)_{FEMALE}$ showing how which sex has lower FMR and/or FNMR. The "M" label denotes male, the other end of the line corresponds to female. The six operating thresholds are selected to give the nominal false match rates given in the legend, and are computed over all impostor pairs regardless of age, sex, and place of birth. The plotted FMR values are broadly an order of magnitude larger than the nominal rates because FMR is computed over demographically-matched impostor pairs i.e individuals of the same sex, from the same geographic region (see section 3.6.1), and the same age group (see section 3.6.2).

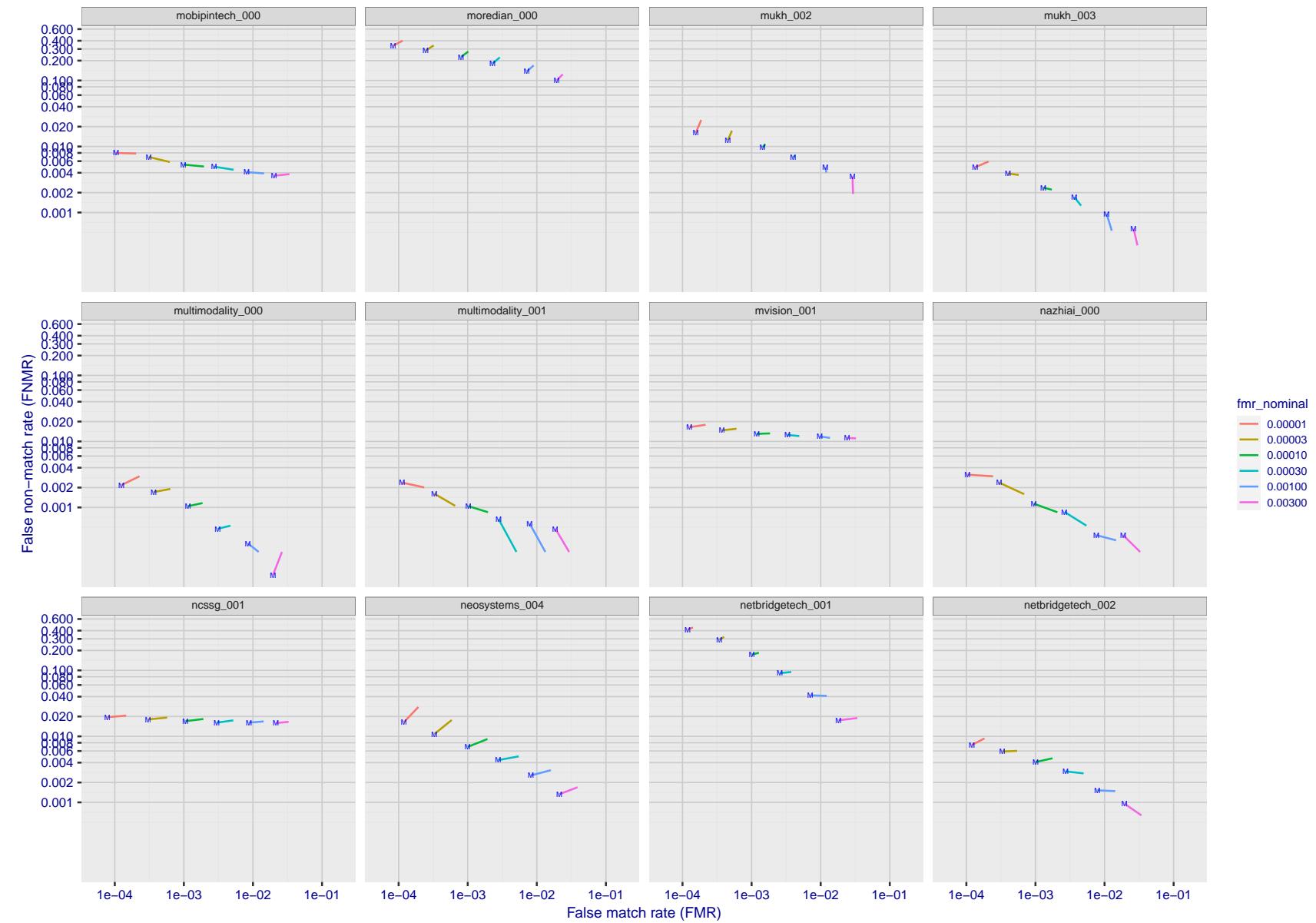


Figure 213: For the visa images, FNMR and FMR at six operating points along the DET characteristic. At each point a line is drawn between $(FMR, FNMR)_{MALE}$ and $(FMR, FNMR)_{FEMALE}$ showing how which sex has lower FMR and/or FNMR. The "M" label denotes male, the other end of the line corresponds to female. The six operating thresholds are selected to give the nominal false match rates given in the legend, and are computed over all impostor pairs regardless of age, sex, and place of birth. The plotted FMR values are broadly an order of magnitude larger than the nominal rates because FMR is computed over demographically-matched impostor pairs i.e individuals of the same sex, from the same geographic region (see section 3.6.1), and the same age group (see section 3.6.2).

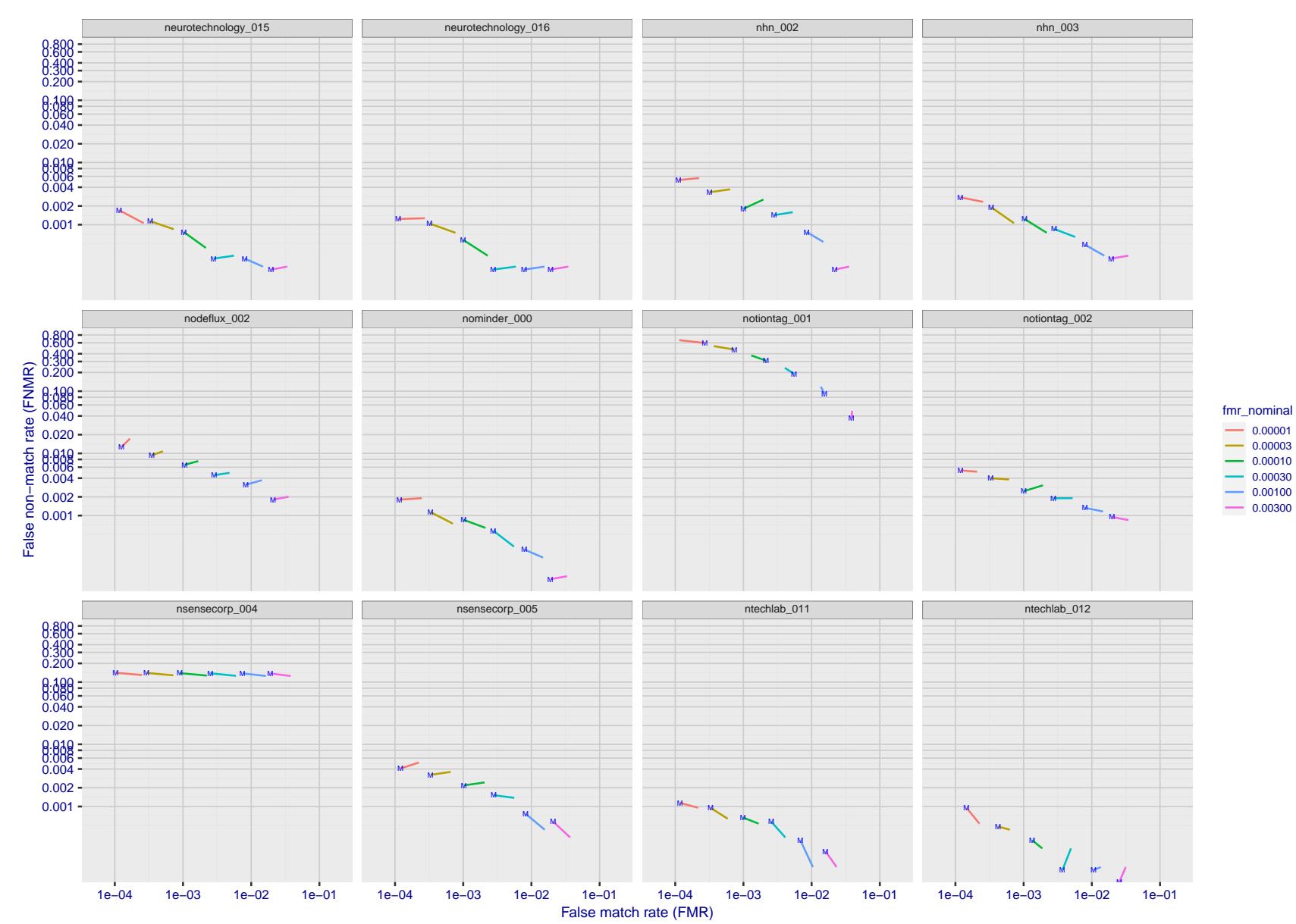


Figure 214: For the visa images, FNMR and FMR at six operating points along the DET characteristic. At each point a line is drawn between $(FMR, FNMR)_{MALE}$ and $(FMR, FNMR)_{FEMALE}$ showing how which sex has lower FMR and/or FNMR. The "M" label denotes male, the other end of the line corresponds to female. The six operating thresholds are selected to give the nominal false match rates given in the legend, and are computed over all impostor pairs regardless of age, sex, and place of birth. The plotted FMR values are broadly an order of magnitude larger than the nominal rates because FMR is computed over demographically-matched impostor pairs i.e individuals of the same sex, from the same geographic region (see section 3.6.1), and the same age group (see section 3.6.2).

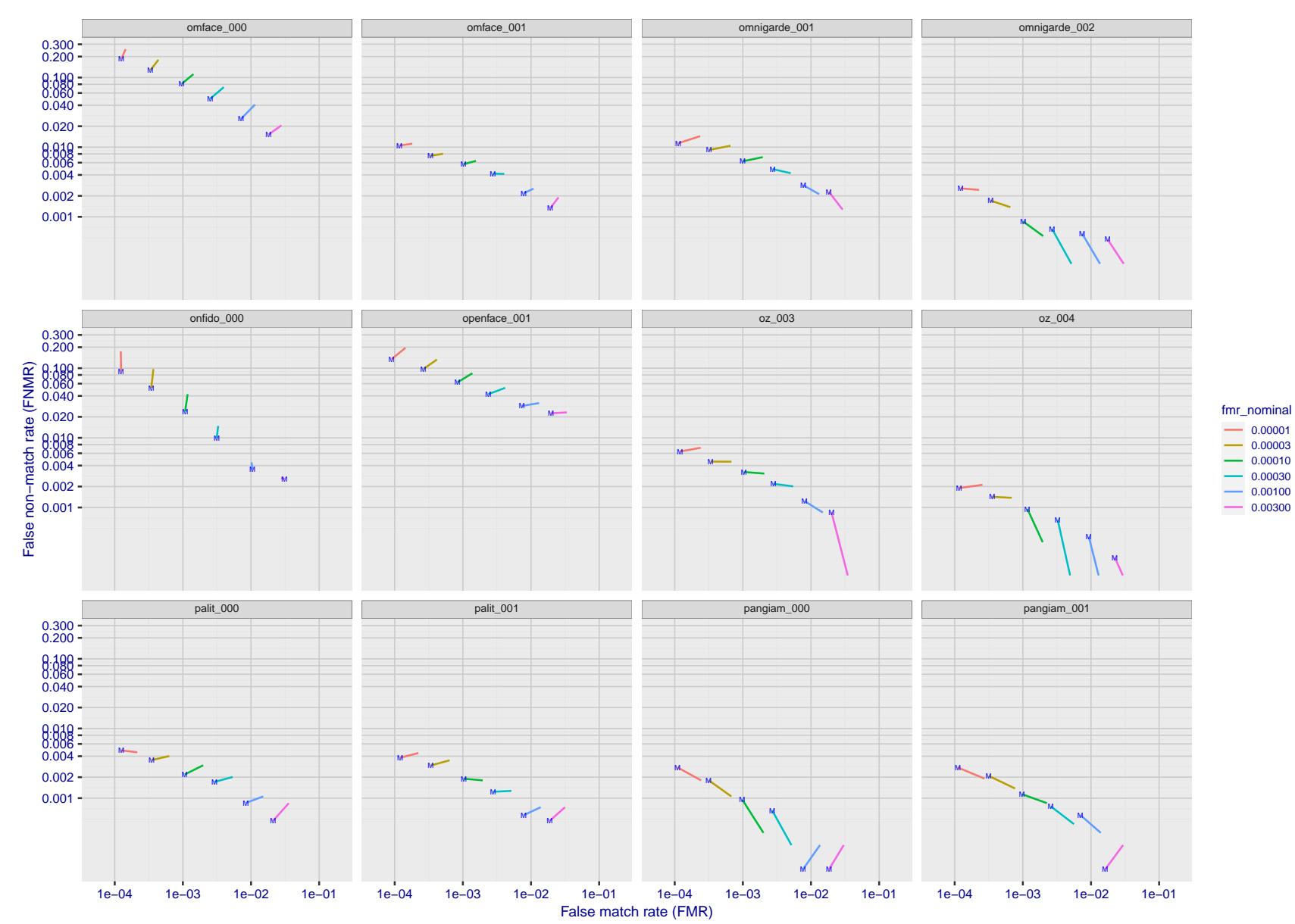


Figure 215: For the visa images, FNMR and FMR at six operating points along the DET characteristic. At each point a line is drawn between $(FMR, FNMR)_{MALE}$ and $(FMR, FNMR)_{FEMALE}$ showing how which sex has lower FMR and/or FNMR. The "M" label denotes male, the other end of the line corresponds to female. The six operating thresholds are selected to give the nominal false match rates given in the legend, and are computed over all impostor pairs regardless of age, sex, and place of birth. The plotted FMR values are broadly an order of magnitude larger than the nominal rates because FMR is computed over demographically-matched impostor pairs i.e individuals of the same sex, from the same geographic region (see section 3.6.1), and the same age group (see section 3.6.2).

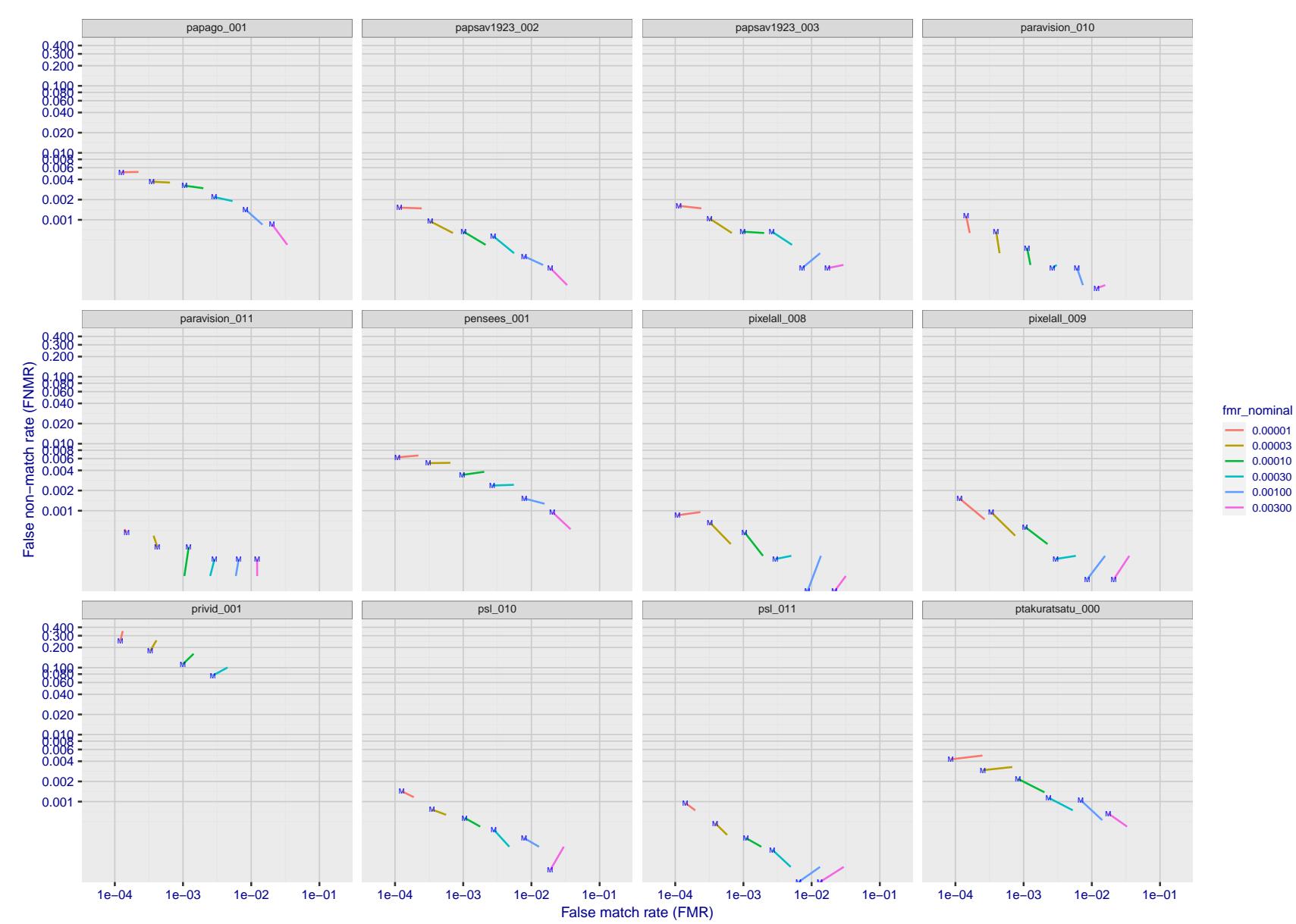


Figure 216: For the visa images, FNMR and FMR at six operating points along the DET characteristic. At each point a line is drawn between $(FMR, FNMR)_{MALE}$ and $(FMR, FNMR)_{FEMALE}$ showing how which sex has lower FMR and/or FNMR. The "M" label denotes male, the other end of the line corresponds to female. The six operating thresholds are selected to give the nominal false match rates given in the legend, and are computed over all impostor pairs regardless of age, sex, and place of birth. The plotted FMR values are broadly an order of magnitude larger than the nominal rates because FMR is computed over demographically-matched impostor pairs i.e individuals of the same sex, from the same geographic region (see section 3.6.1), and the same age group (see section 3.6.2).

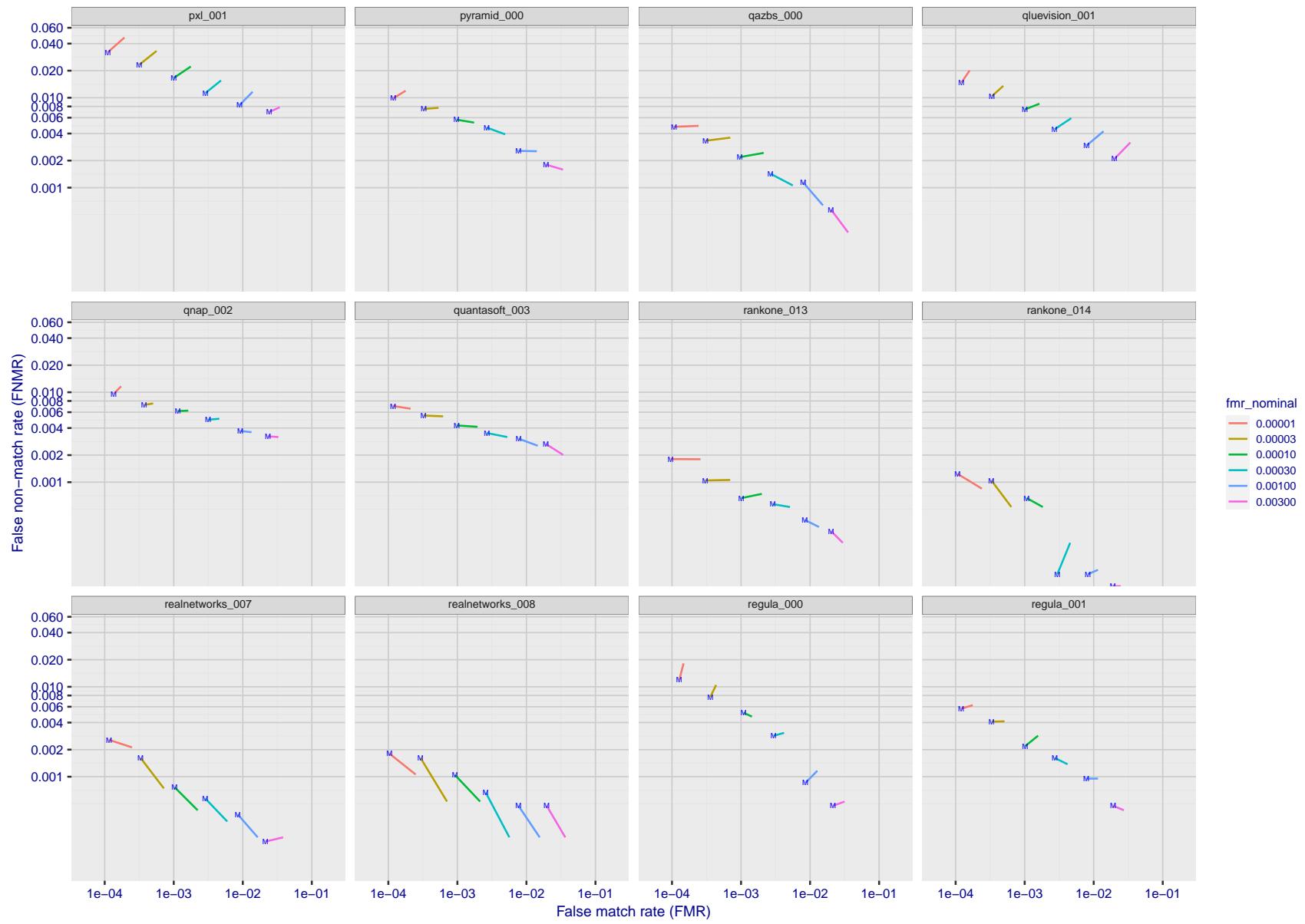


Figure 217: For the visa images, FNMR and FMR at six operating points along the DET characteristic. At each point a line is drawn between $(FMR, FNMR)_{MALE}$ and $(FMR, FNMR)_{FEMALE}$ showing how which sex has lower FMR and/or FNMR. The "M" label denotes male, the other end of the line corresponds to female. The six operating thresholds are selected to give the nominal false match rates given in the legend, and are computed over all impostor pairs regardless of age, sex, and place of birth. The plotted FMR values are broadly an order of magnitude larger than the nominal rates because FMR is computed over demographically-matched impostor pairs i.e individuals of the same sex, from the same geographic region (see section 3.6.1), and the same age group (see section 3.6.2).

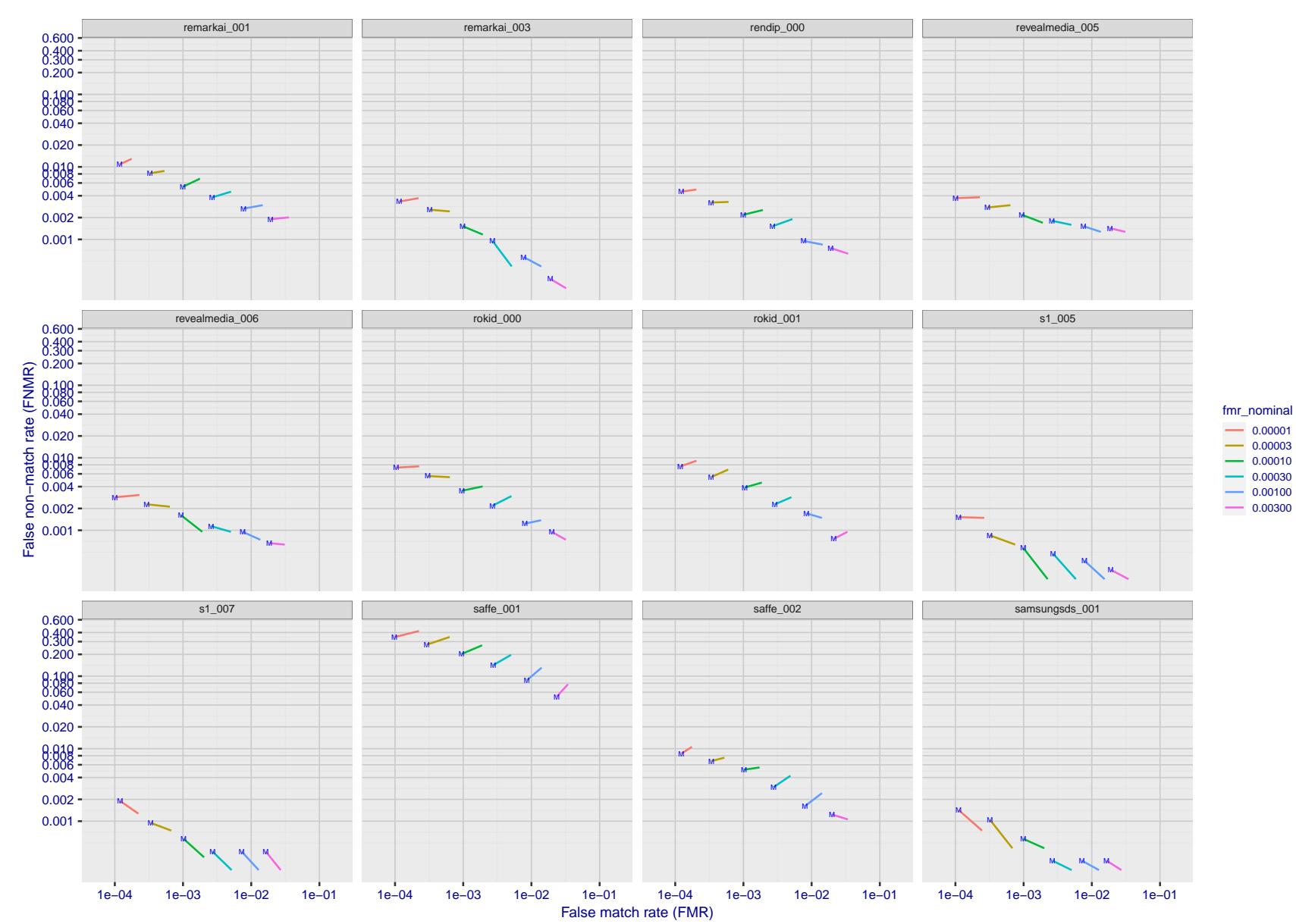


Figure 218: For the visa images, FNMR and FMR at six operating points along the DET characteristic. At each point a line is drawn between $(FMR, FNMR)_{MALE}$ and $(FMR, FNMR)_{FEMALE}$ showing how which sex has lower FMR and/or FNMR. The "M" label denotes male, the other end of the line corresponds to female. The six operating thresholds are selected to give the nominal false match rates given in the legend, and are computed over all impostor pairs regardless of age, sex, and place of birth. The plotted FMR values are broadly an order of magnitude larger than the nominal rates because FMR is computed over demographically-matched impostor pairs i.e individuals of the same sex, from the same geographic region (see section 3.6.1), and the same age group (see section 3.6.2).

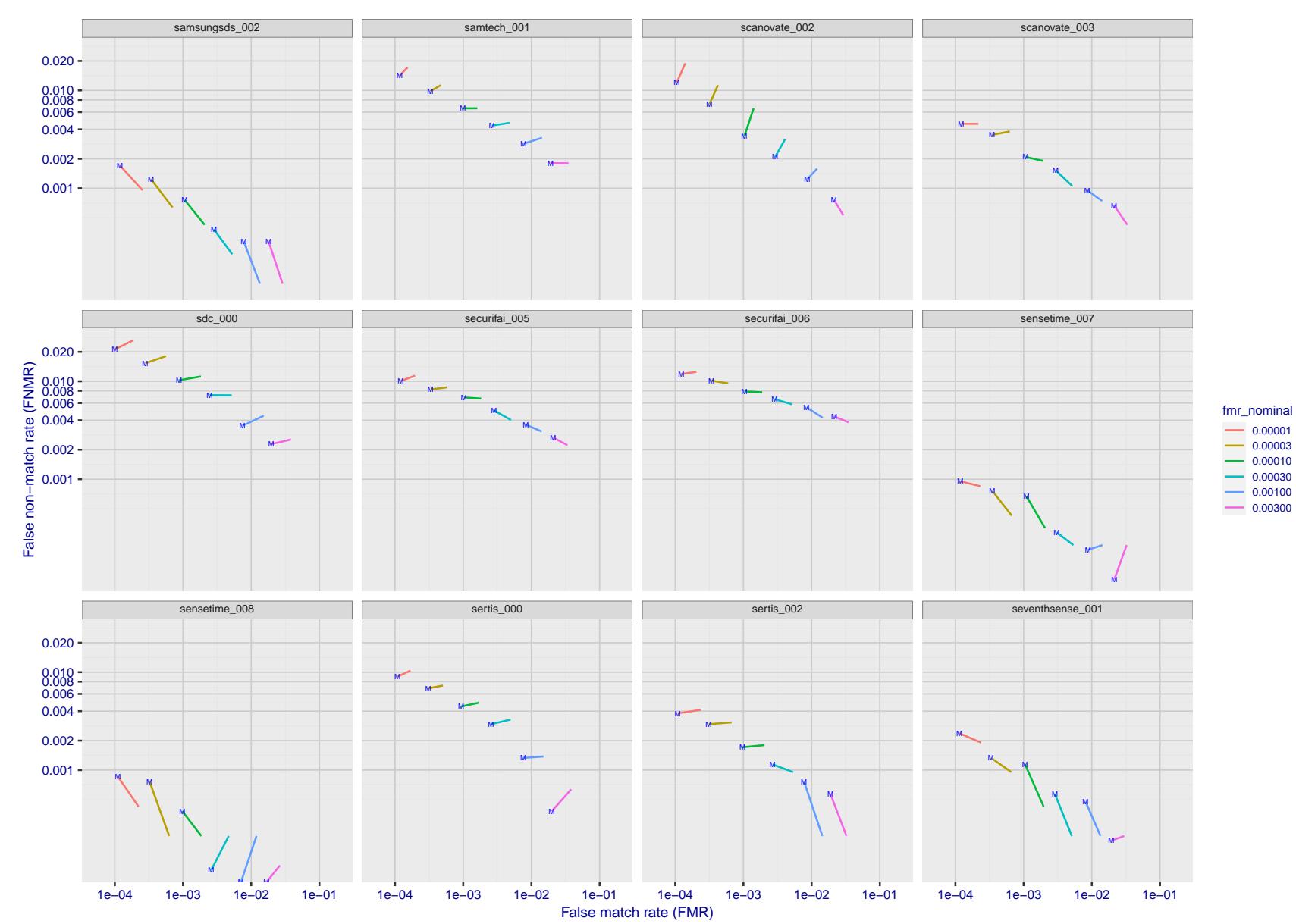


Figure 219: For the visa images, FNMR and FMR at six operating points along the DET characteristic. At each point a line is drawn between $(FMR, FNMR)_{MALE}$ and $(FMR, FNMR)_{FEMALE}$ showing how which sex has lower FMR and/or FNMR. The "M" label denotes male, the other end of the line corresponds to female. The six operating thresholds are selected to give the nominal false match rates given in the legend, and are computed over all impostor pairs regardless of age, sex, and place of birth. The plotted FMR values are broadly an order of magnitude larger than the nominal rates because FMR is computed over demographically-matched impostor pairs i.e individuals of the same sex, from the same geographic region (see section 3.6.1), and the same age group (see section 3.6.2).

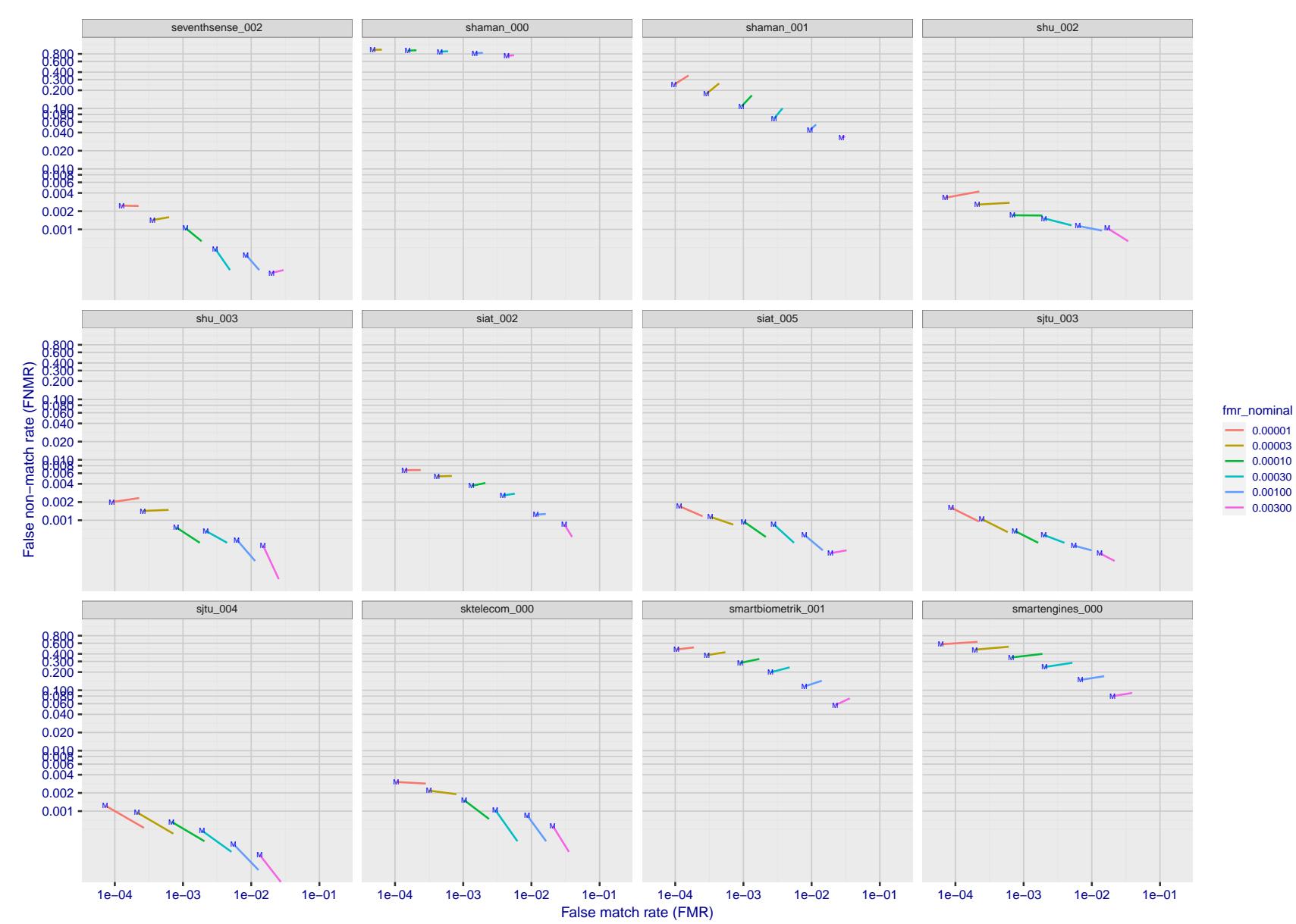


Figure 220: For the visa images, FNMR and FMR at six operating points along the DET characteristic. At each point a line is drawn between $(FMR, FNMR)_{MALE}$ and $(FMR, FNMR)_{FEMALE}$ showing how which sex has lower FMR and/or FNMR. The "M" label denotes male, the other end of the line corresponds to female. The six operating thresholds are selected to give the nominal false match rates given in the legend, and are computed over all impostor pairs regardless of age, sex, and place of birth. The plotted FMR values are broadly an order of magnitude larger than the nominal rates because FMR is computed over demographically-matched impostor pairs i.e individuals of the same sex, from the same geographic region (see section 3.6.1), and the same age group (see section 3.6.2).

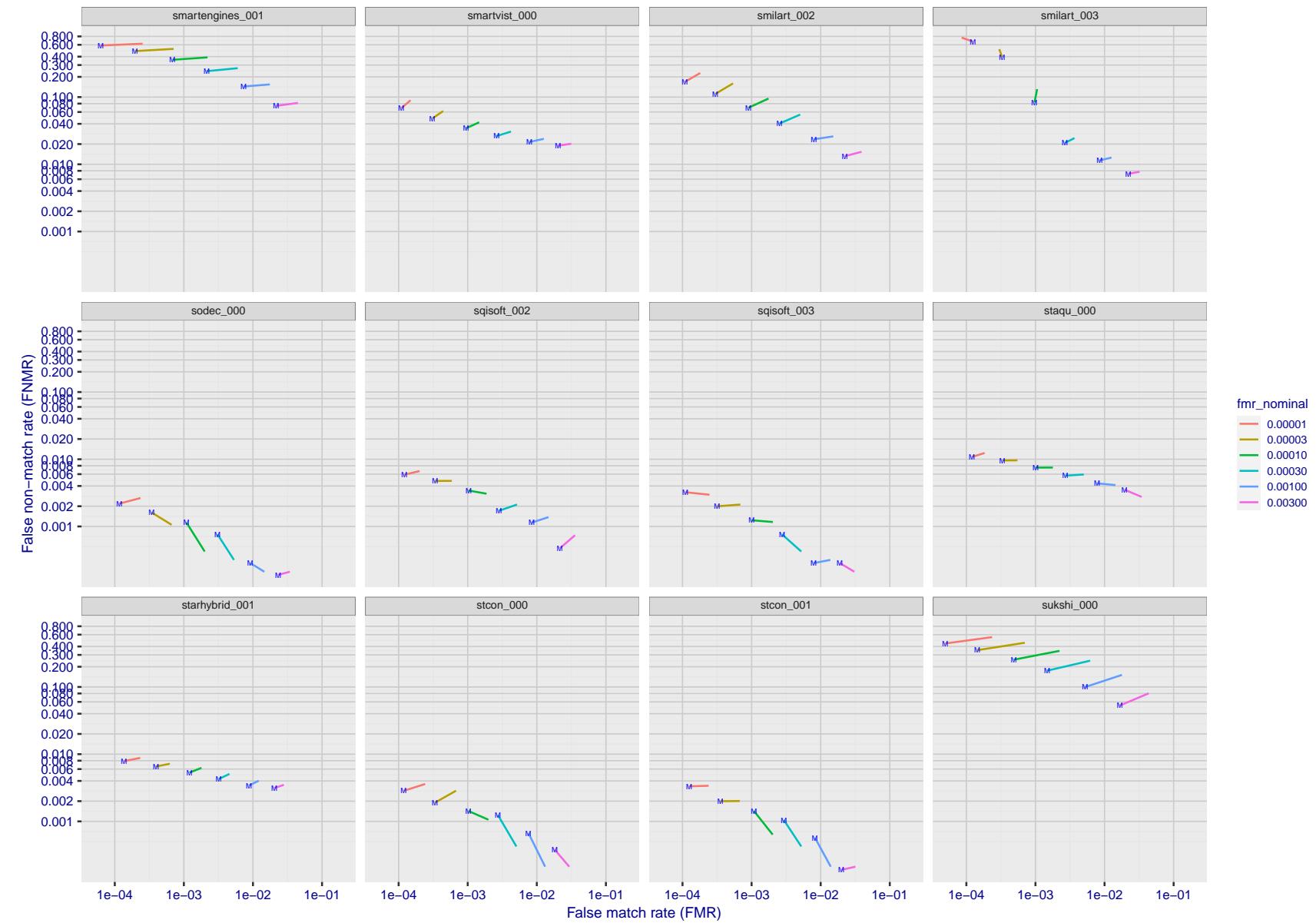


Figure 221: For the visa images, FNMR and FMR at six operating points along the DET characteristic. At each point a line is drawn between $(FMR, FNMR)_{MALE}$ and $(FMR, FNMR)_{FEMALE}$ showing how which sex has lower FMR and/or FNMR. The "M" label denotes male, the other end of the line corresponds to female. The six operating thresholds are selected to give the nominal false match rates given in the legend, and are computed over all impostor pairs regardless of age, sex, and place of birth. The plotted FMR values are broadly an order of magnitude larger than the nominal rates because FMR is computed over demographically-matched impostor pairs i.e individuals of the same sex, from the same geographic region (see section 3.6.1), and the same age group (see section 3.6.2).

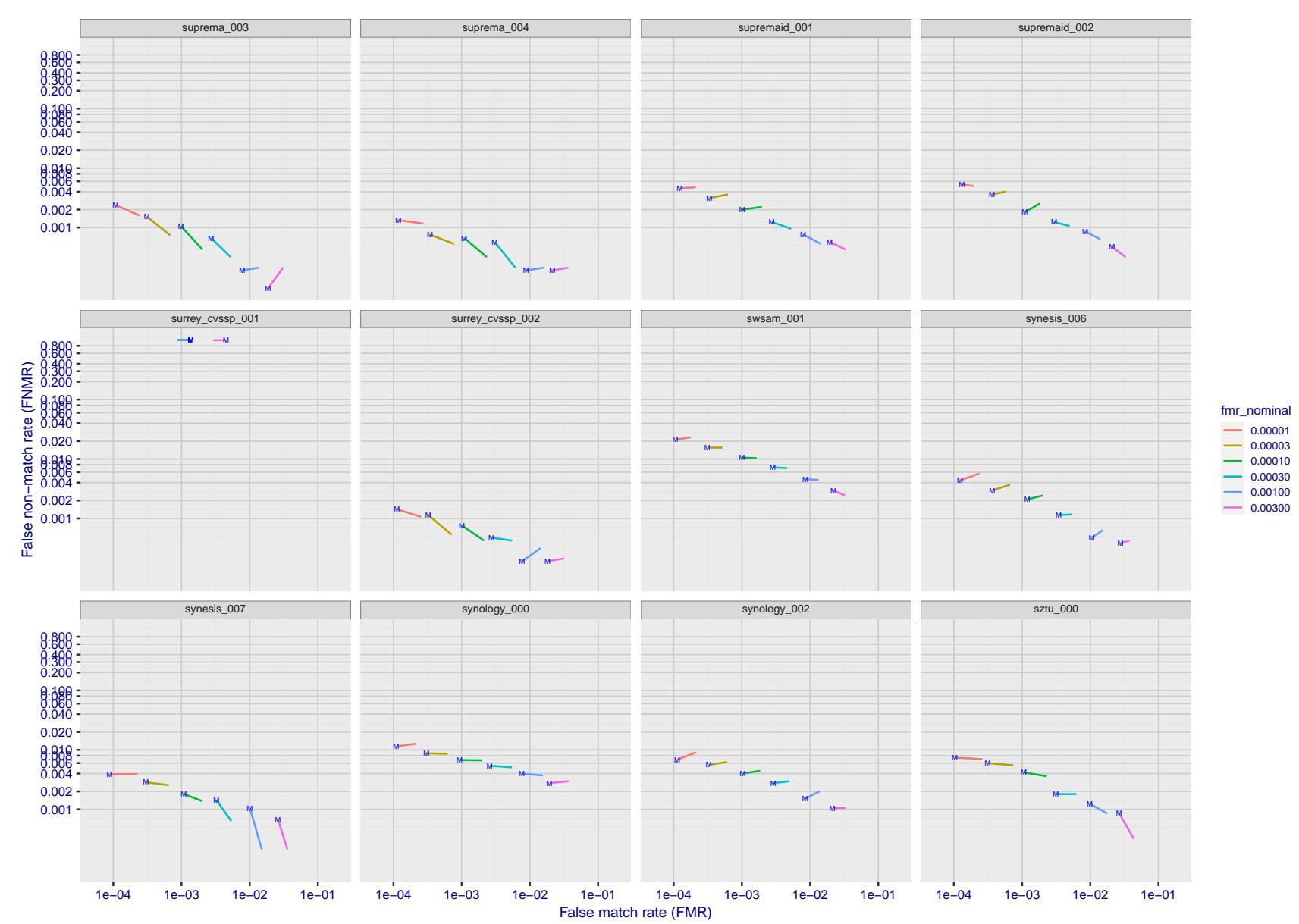


Figure 222: For the visa images, FNMR and FMR at six operating points along the DET characteristic. At each point a line is drawn between $(FMR, FNMR)_{MALE}$ and $(FMR, FNMR)_{FEMALE}$ showing how which sex has lower FMR and/or FNMR. The "M" label denotes male, the other end of the line corresponds to female. The six operating thresholds are selected to give the nominal false match rates given in the legend, and are computed over all impostor pairs regardless of age, sex, and place of birth. The plotted FMR values are broadly an order of magnitude larger than the nominal rates because FMR is computed over demographically-matched impostor pairs i.e individuals of the same sex, from the same geographic region (see section 3.6.1), and the same age group (see section 3.6.2).

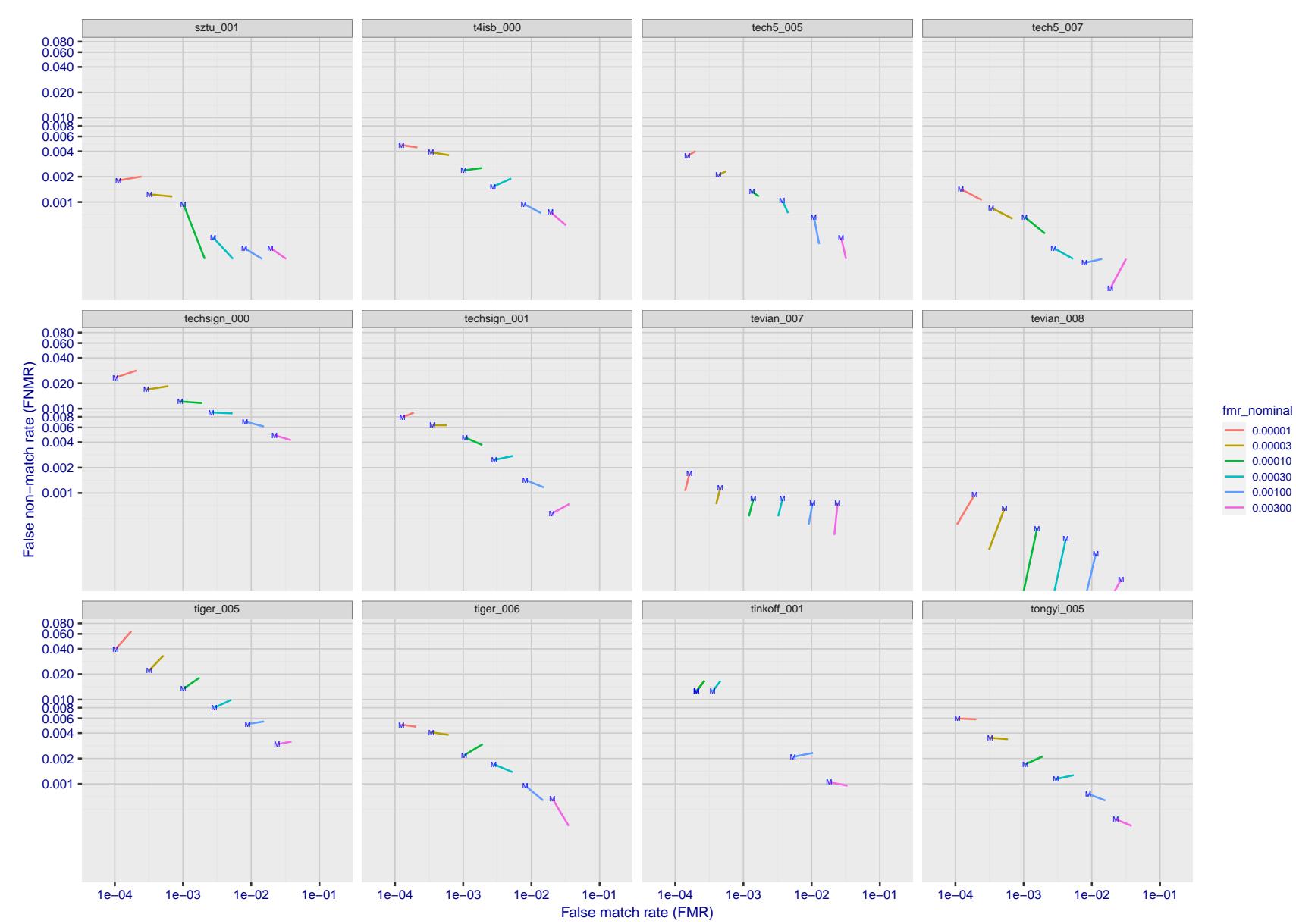


Figure 223: For the visa images, FNMR and FMR at six operating points along the DET characteristic. At each point a line is drawn between $(FMR, FNMR)_{MALE}$ and $(FMR, FNMR)_{FEMALE}$ showing how which sex has lower FMR and/or FNMR. The "M" label denotes male, the other end of the line corresponds to female. The six operating thresholds are selected to give the nominal false match rates given in the legend, and are computed over all impostor pairs regardless of age, sex, and place of birth. The plotted FMR values are broadly an order of magnitude larger than the nominal rates because FMR is computed over demographically-matched impostor pairs i.e individuals of the same sex, from the same geographic region (see section 3.6.1), and the same age group (see section 3.6.2).

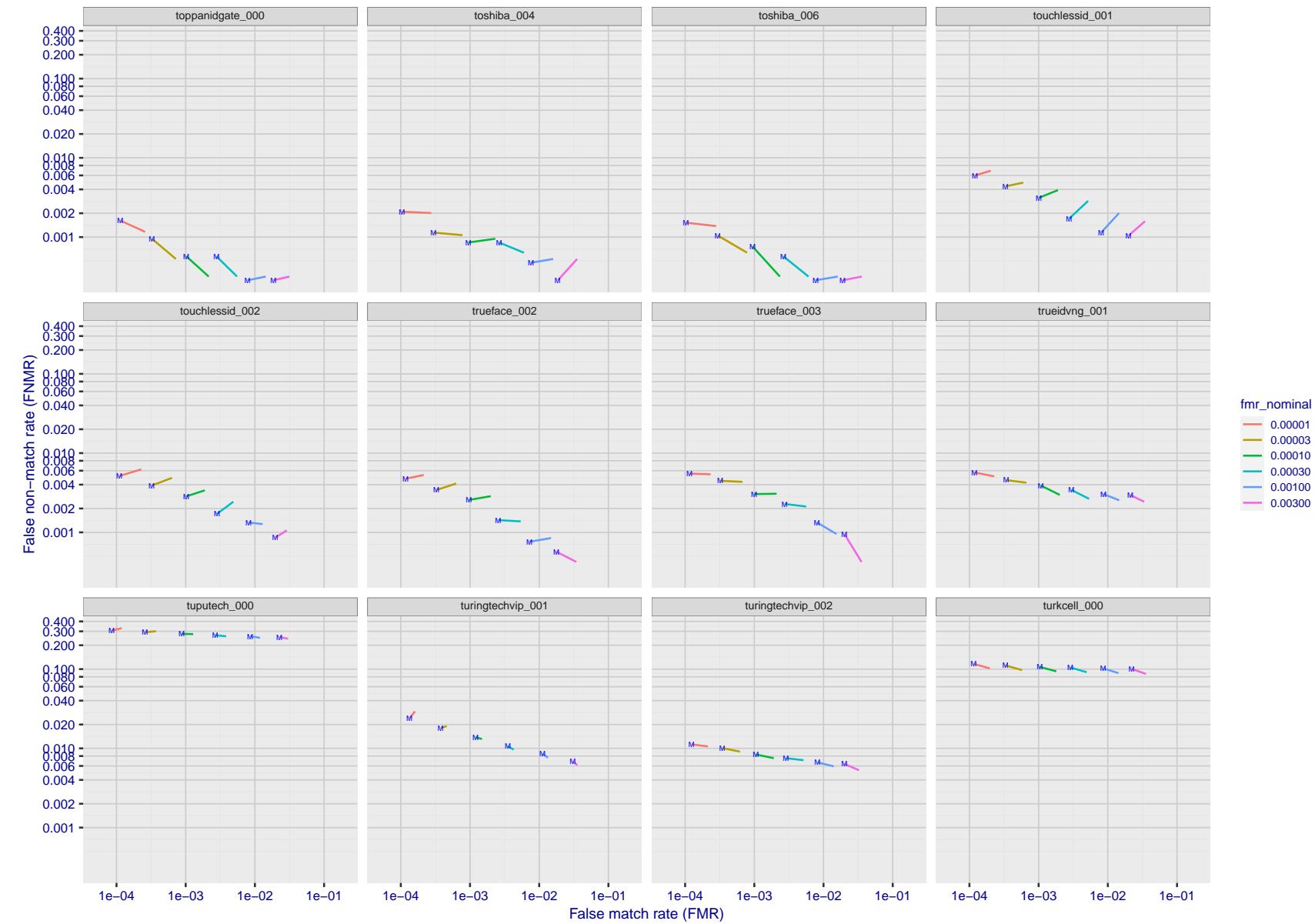


Figure 224: For the visa images, FNMR and FMR at six operating points along the DET characteristic. At each point a line is drawn between $(FMR, FNMR)_{MALE}$ and $(FMR, FNMR)_{FEMALE}$ showing how which sex has lower FMR and/or FNMR. The "M" label denotes male, the other end of the line corresponds to female. The six operating thresholds are selected to give the nominal false match rates given in the legend, and are computed over all impostor pairs regardless of age, sex, and place of birth. The plotted FMR values are broadly an order of magnitude larger than the nominal rates because FMR is computed over demographically-matched impostor pairs i.e individuals of the same sex, from the same geographic region (see section 3.6.1), and the same age group (see section 3.6.2).

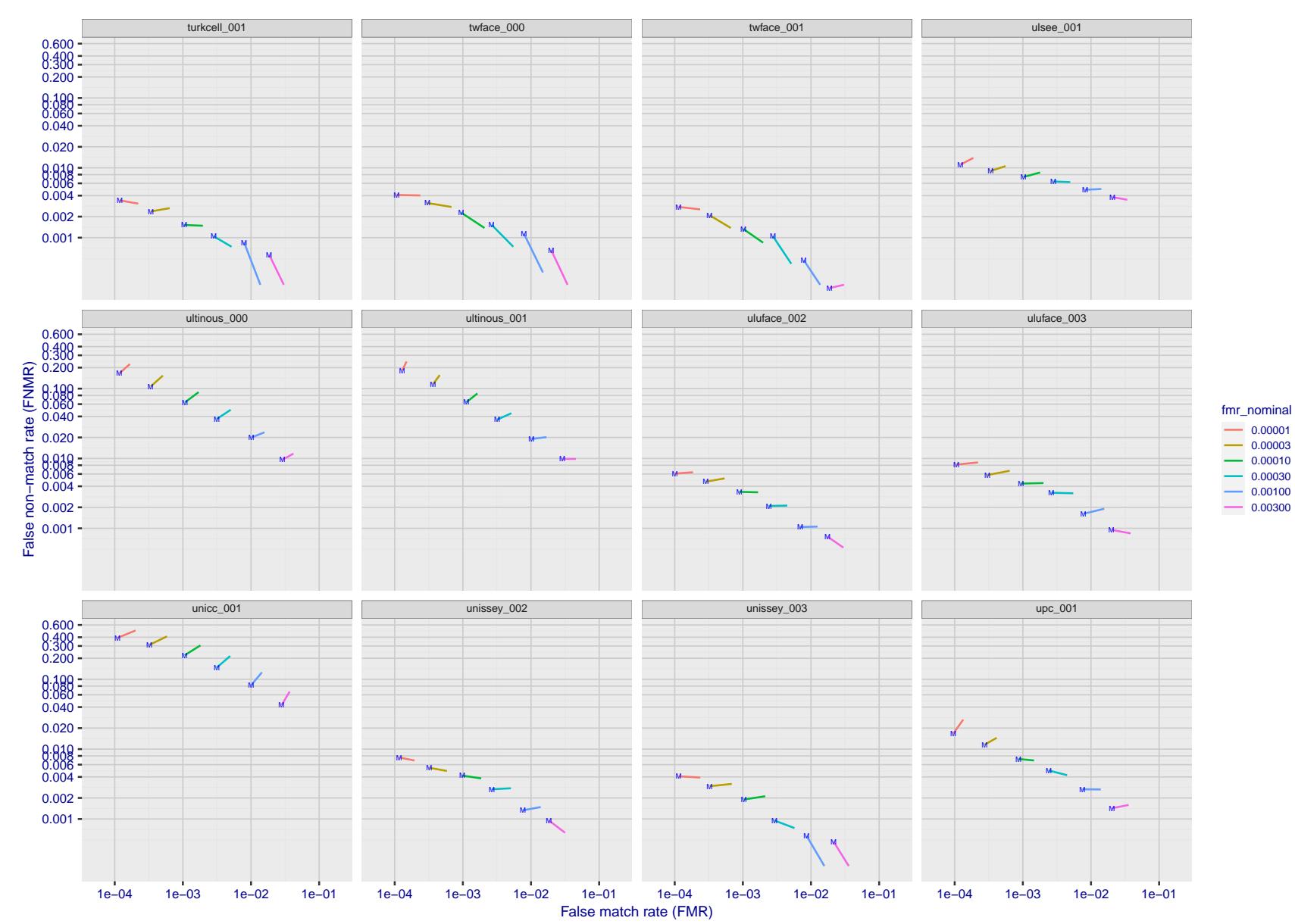


Figure 225: For the visa images, FNMR and FMR at six operating points along the DET characteristic. At each point a line is drawn between $(FMR, FNMR)_{MALE}$ and $(FMR, FNMR)_{FEMALE}$ showing how which sex has lower FMR and/or FNMR. The "M" label denotes male, the other end of the line corresponds to female. The six operating thresholds are selected to give the nominal false match rates given in the legend, and are computed over all impostor pairs regardless of age, sex, and place of birth. The plotted FMR values are broadly an order of magnitude larger than the nominal rates because FMR is computed over demographically-matched impostor pairs i.e individuals of the same sex, from the same geographic region (see section 3.6.1), and the same age group (see section 3.6.2).

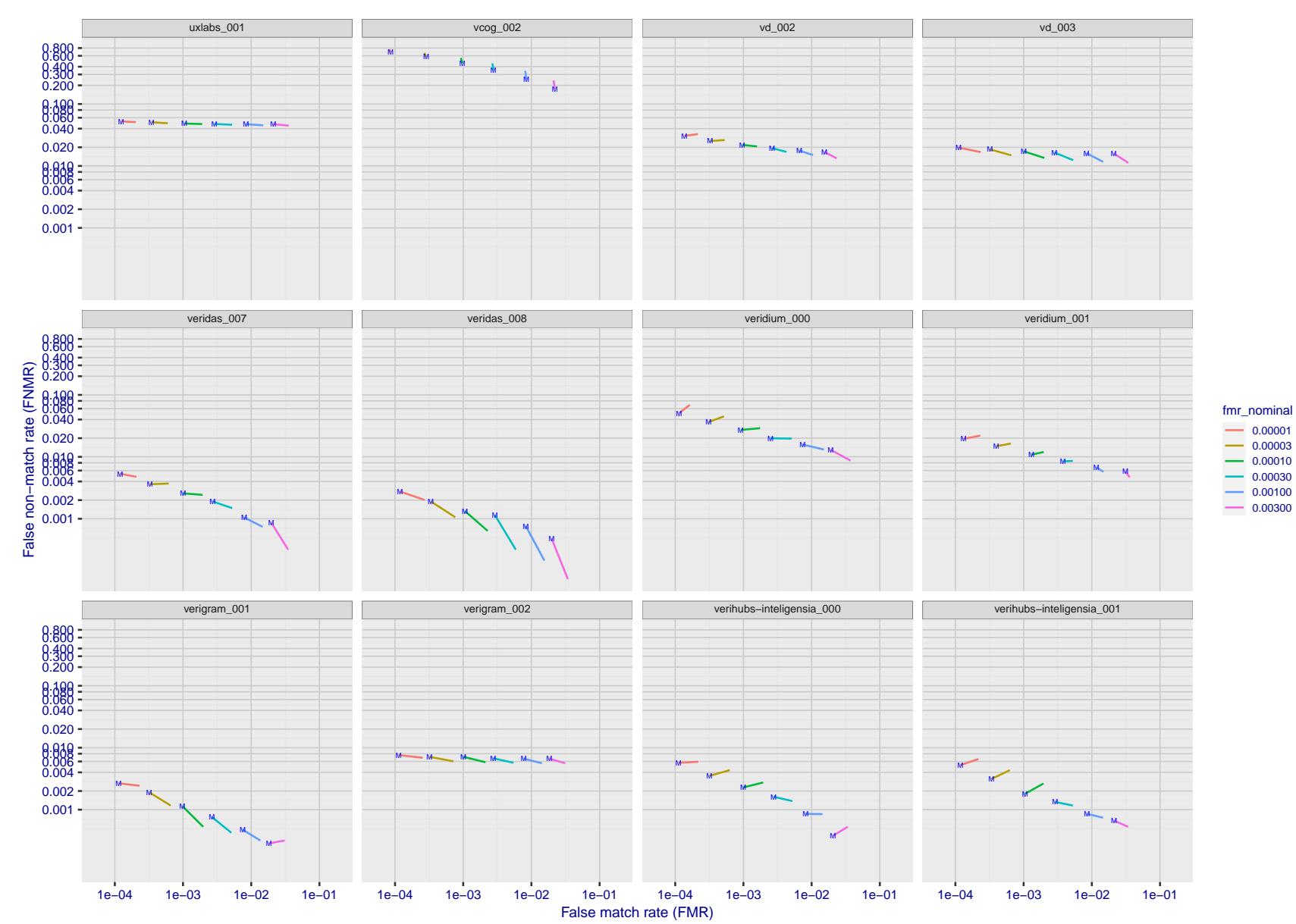


Figure 226: For the visa images, FNMR and FMR at six operating points along the DET characteristic. At each point a line is drawn between $(FMR, FNMR)_{MALE}$ and $(FMR, FNMR)_{FEMALE}$ showing how which sex has lower FMR and/or FNMR. The "M" label denotes male, the other end of the line corresponds to female. The six operating thresholds are selected to give the nominal false match rates given in the legend, and are computed over all impostor pairs regardless of age, sex, and place of birth. The plotted FMR values are broadly an order of magnitude larger than the nominal rates because FMR is computed over demographically-matched impostor pairs i.e individuals of the same sex, from the same geographic region (see section 3.6.1), and the same age group (see section 3.6.2).

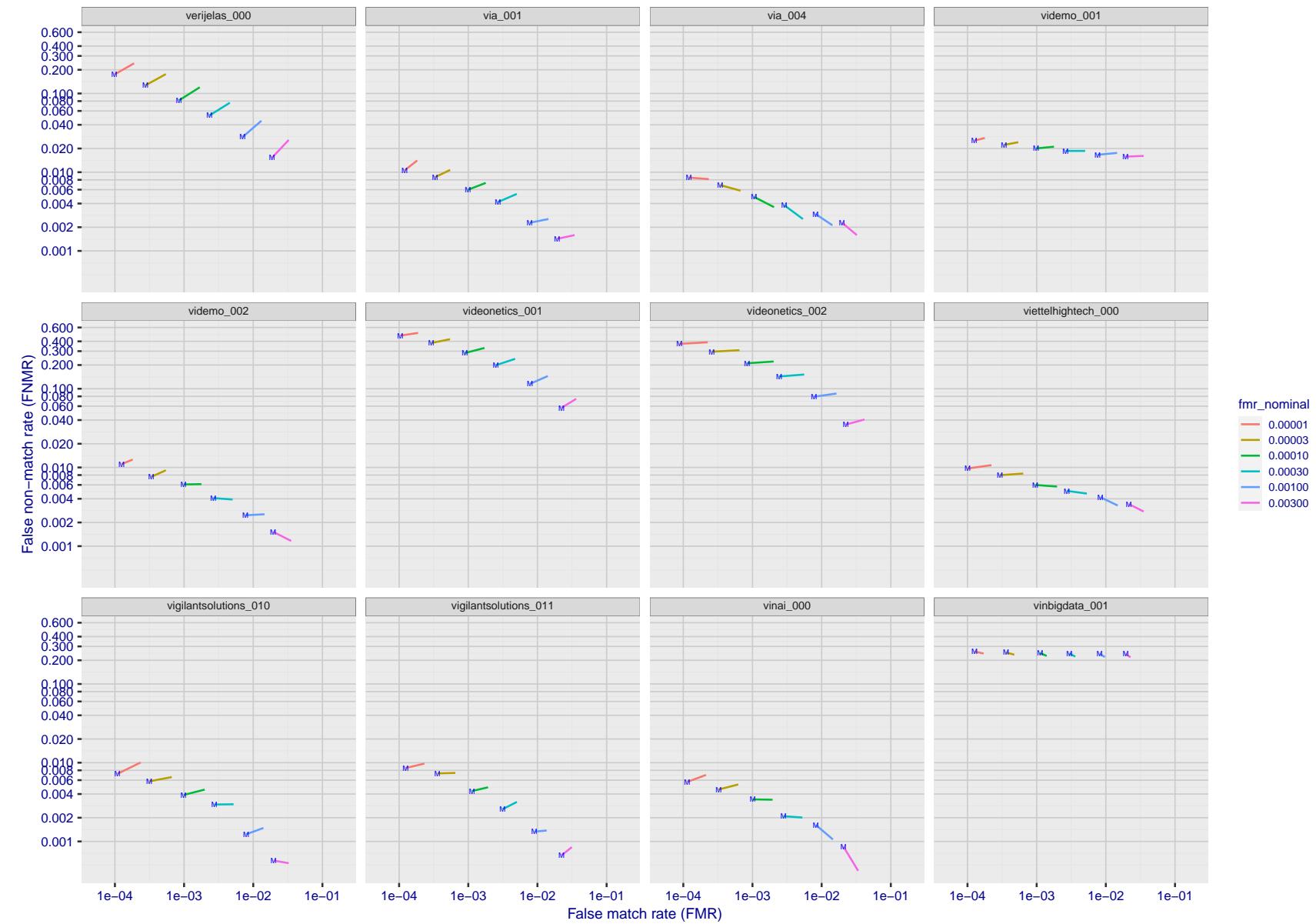


Figure 227: For the visa images, FNMR and FMR at six operating points along the DET characteristic. At each point a line is drawn between $(FMR, FNMR)_{MALE}$ and $(FMR, FNMR)_{FEMALE}$ showing how which sex has lower FMR and/or FNMR. The "M" label denotes male, the other end of the line corresponds to female. The six operating thresholds are selected to give the nominal false match rates given in the legend, and are computed over all impostor pairs regardless of age, sex, and place of birth. The plotted FMR values are broadly an order of magnitude larger than the nominal rates because FMR is computed over demographically-matched impostor pairs i.e individuals of the same sex, from the same geographic region (see section 3.6.1), and the same age group (see section 3.6.2).

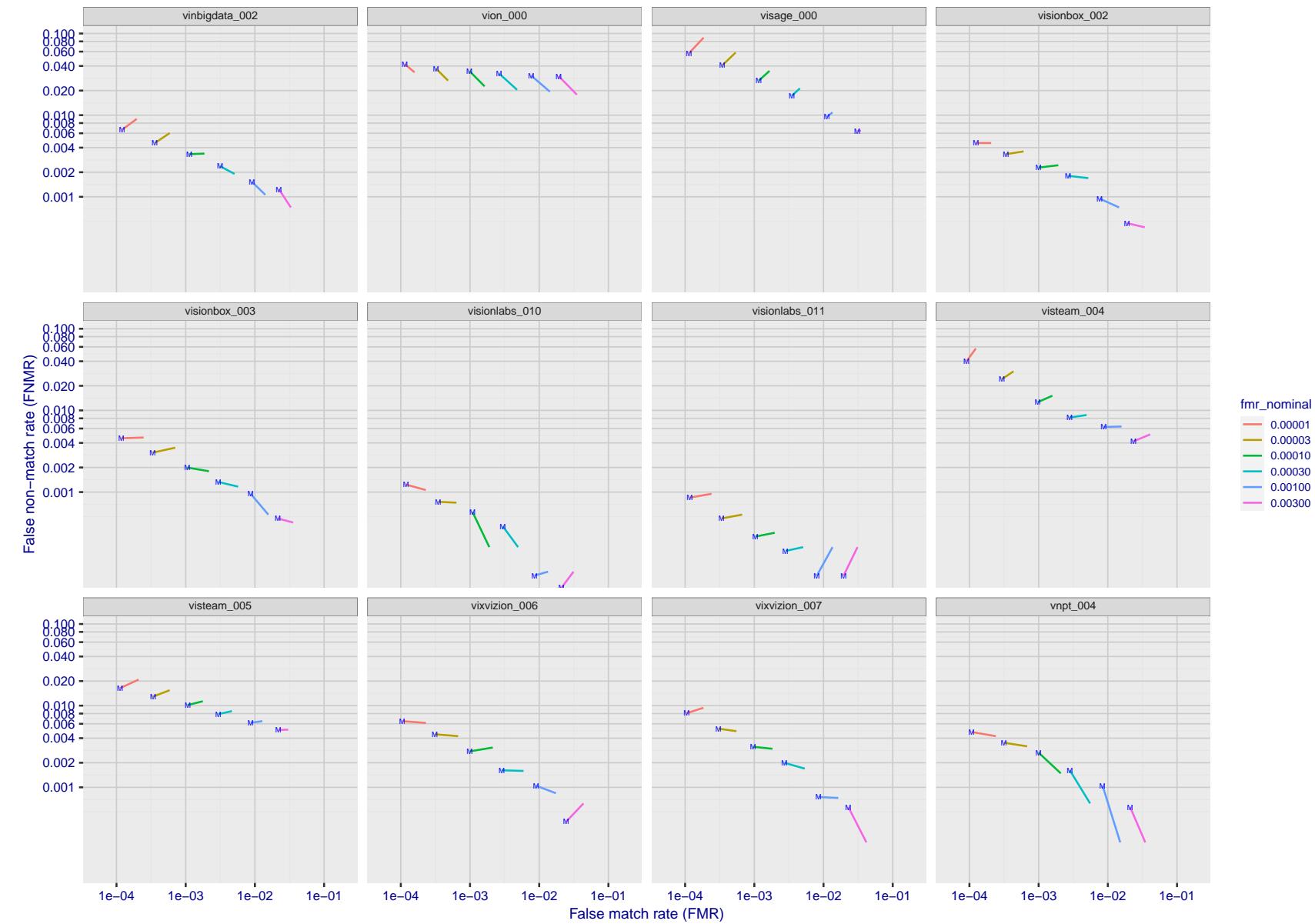


Figure 228: For the visa images, FNMR and FMR at six operating points along the DET characteristic. At each point a line is drawn between $(FMR, FNMR)_{MALE}$ and $(FMR, FNMR)_{FEMALE}$ showing how which sex has lower FMR and/or FNMR. The "M" label denotes male, the other end of the line corresponds to female. The six operating thresholds are selected to give the nominal false match rates given in the legend, and are computed over all impostor pairs regardless of age, sex, and place of birth. The plotted FMR values are broadly an order of magnitude larger than the nominal rates because FMR is computed over demographically-matched impostor pairs i.e individuals of the same sex, from the same geographic region (see section 3.6.1), and the same age group (see section 3.6.2).

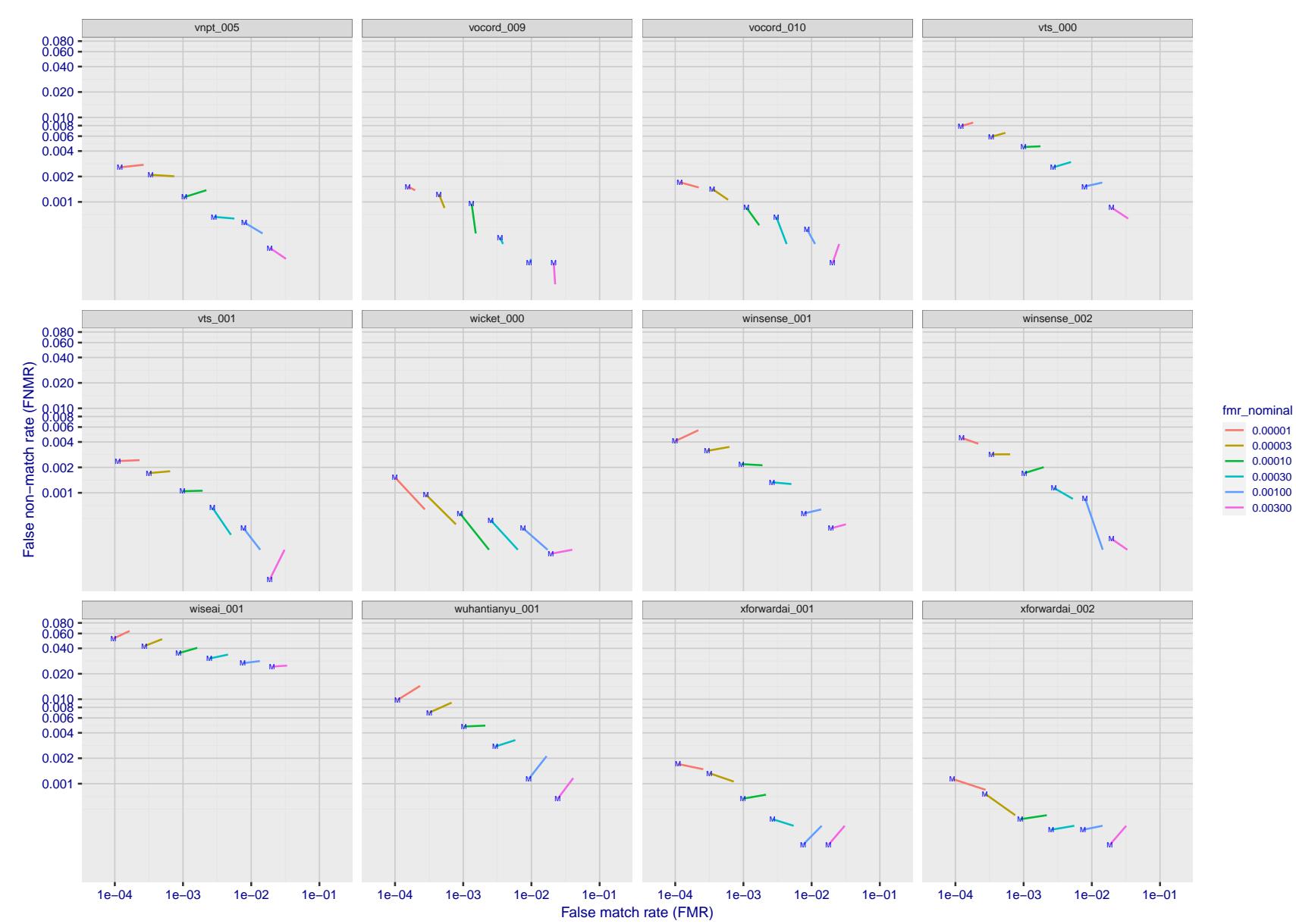


Figure 229: For the visa images, FNMR and FMR at six operating points along the DET characteristic. At each point a line is drawn between $(FMR, FNMR)_{MALE}$ and $(FMR, FNMR)_{FEMALE}$ showing how which sex has lower FMR and/or FNMR. The "M" label denotes male, the other end of the line corresponds to female. The six operating thresholds are selected to give the nominal false match rates given in the legend, and are computed over all impostor pairs regardless of age, sex, and place of birth. The plotted FMR values are broadly an order of magnitude larger than the nominal rates because FMR is computed over demographically-matched impostor pairs i.e individuals of the same sex, from the same geographic region (see section 3.6.1), and the same age group (see section 3.6.2).

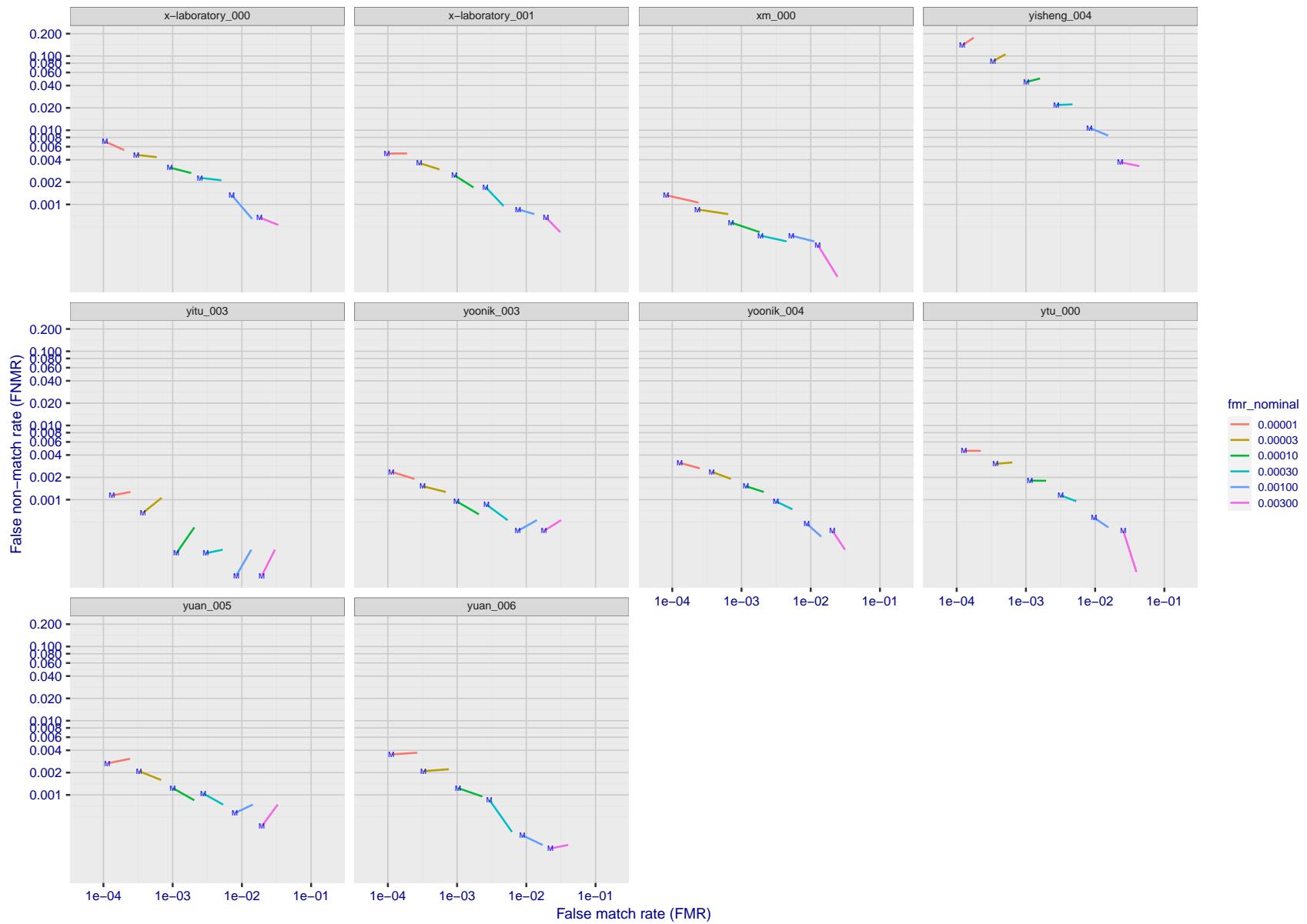


Figure 230: For the visa images, FNMR and FMR at six operating points along the DET characteristic. At each point a line is drawn between $(FMR, FNMR)_{MALE}$ and $(FMR, FNMR)_{FEMALE}$ showing how which sex has lower FMR and/or FNMR. The "M" label denotes male, the other end of the line corresponds to female. The six operating thresholds are selected to give the nominal false match rates given in the legend, and are computed over all impostor pairs regardless of age, sex, and place of birth. The plotted FMR values are broadly an order of magnitude larger than the nominal rates because FMR is computed over demographically-matched impostor pairs i.e individuals of the same sex, from the same geographic region (see section 3.6.1), and the same age group (see section 3.6.2).

2023/04/20 08:30:53

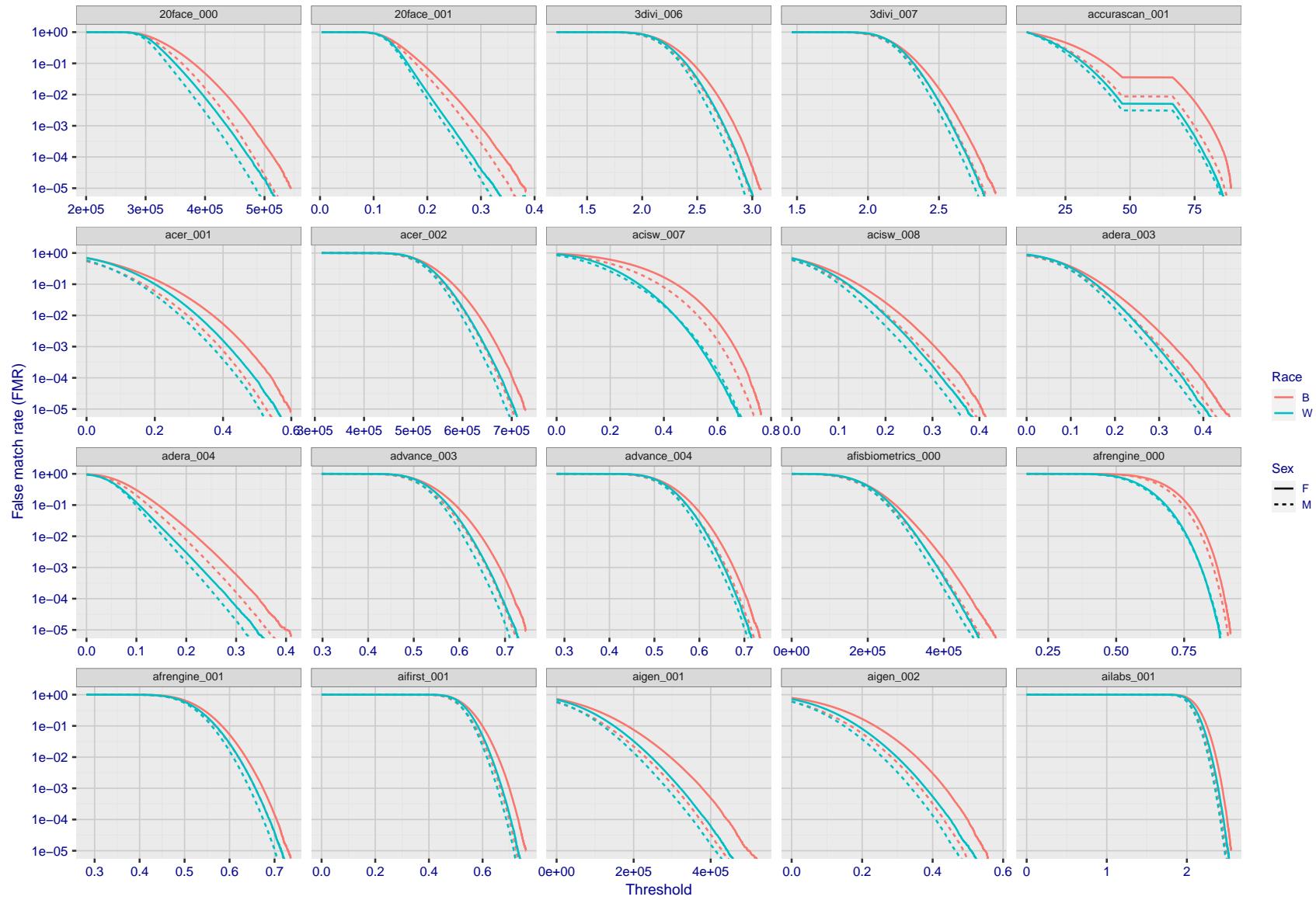


Figure 231: For the mugshot images, the false match calibration curves show false match rate vs. threshold. Separate curves appear for white females, black females, black males and white males.

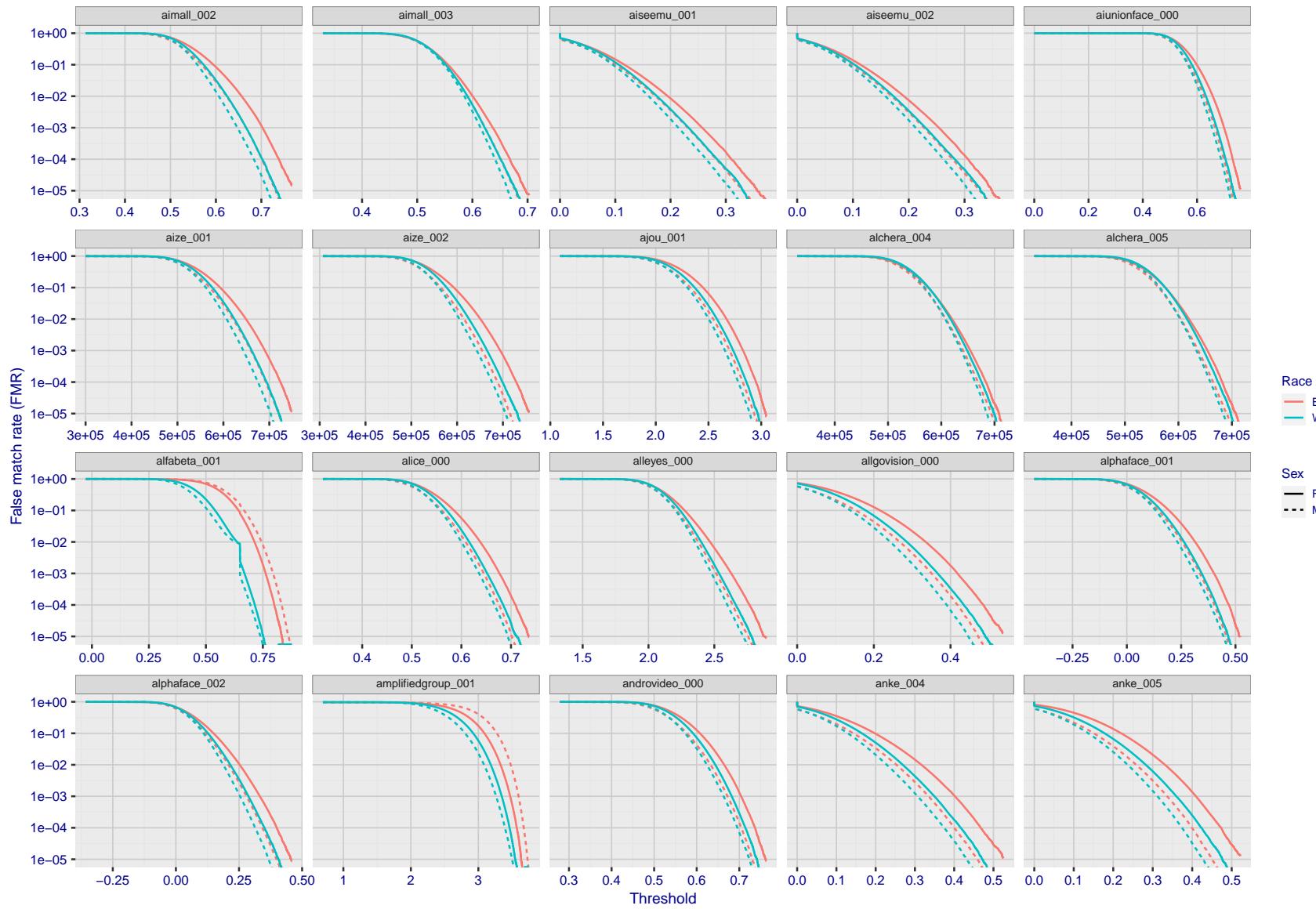


Figure 232: For the mugshot images, the false match calibration curves show false match rate vs. threshold. Separate curves appear for white females, black females, black males and white males.

2023/04/20 08:30:53

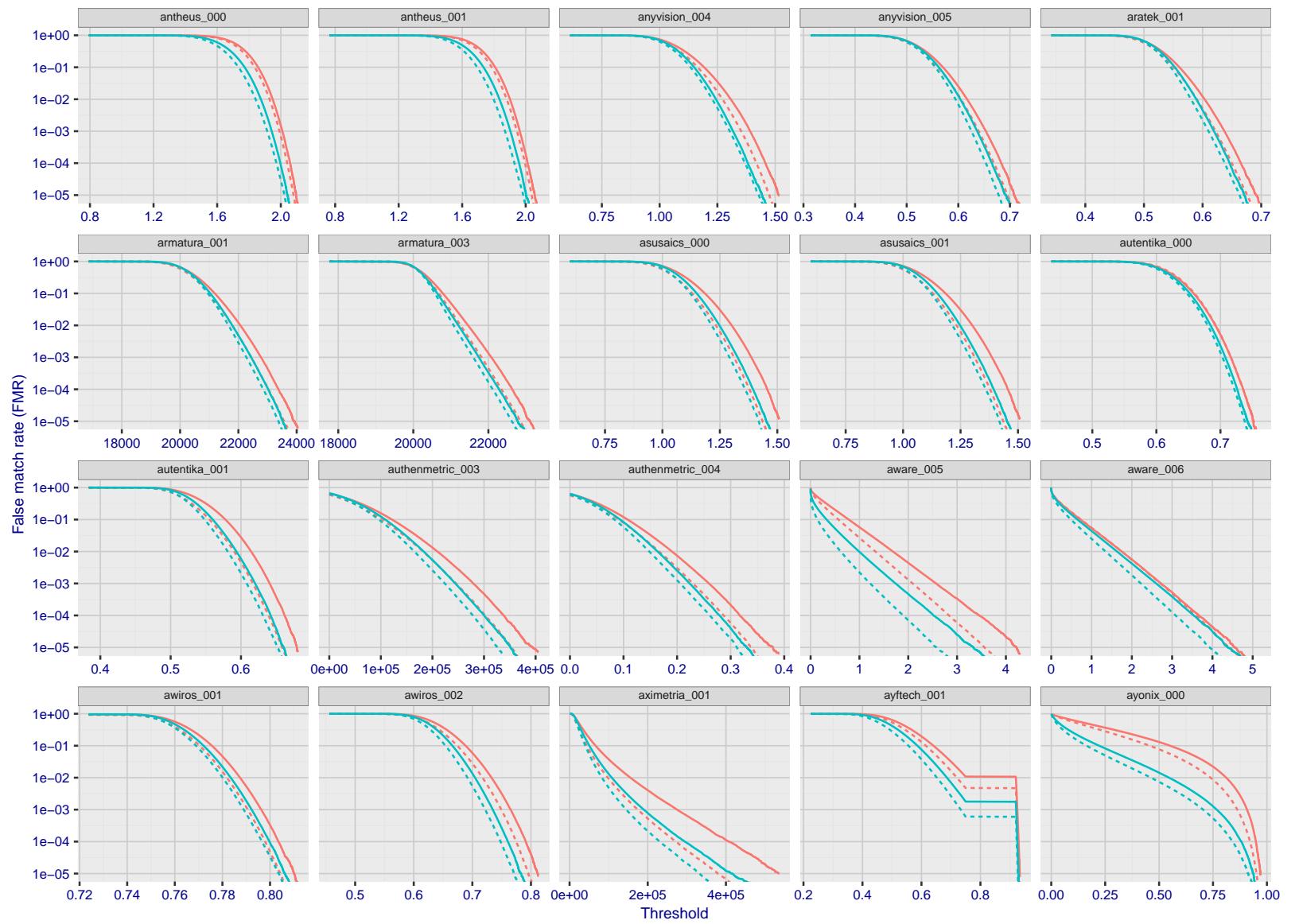


Figure 233: For the mugshot images, the false match calibration curves show false match rate vs. threshold. Separate curves appear for white females, black females, black males and white males.

2023/04/20 08:30:53

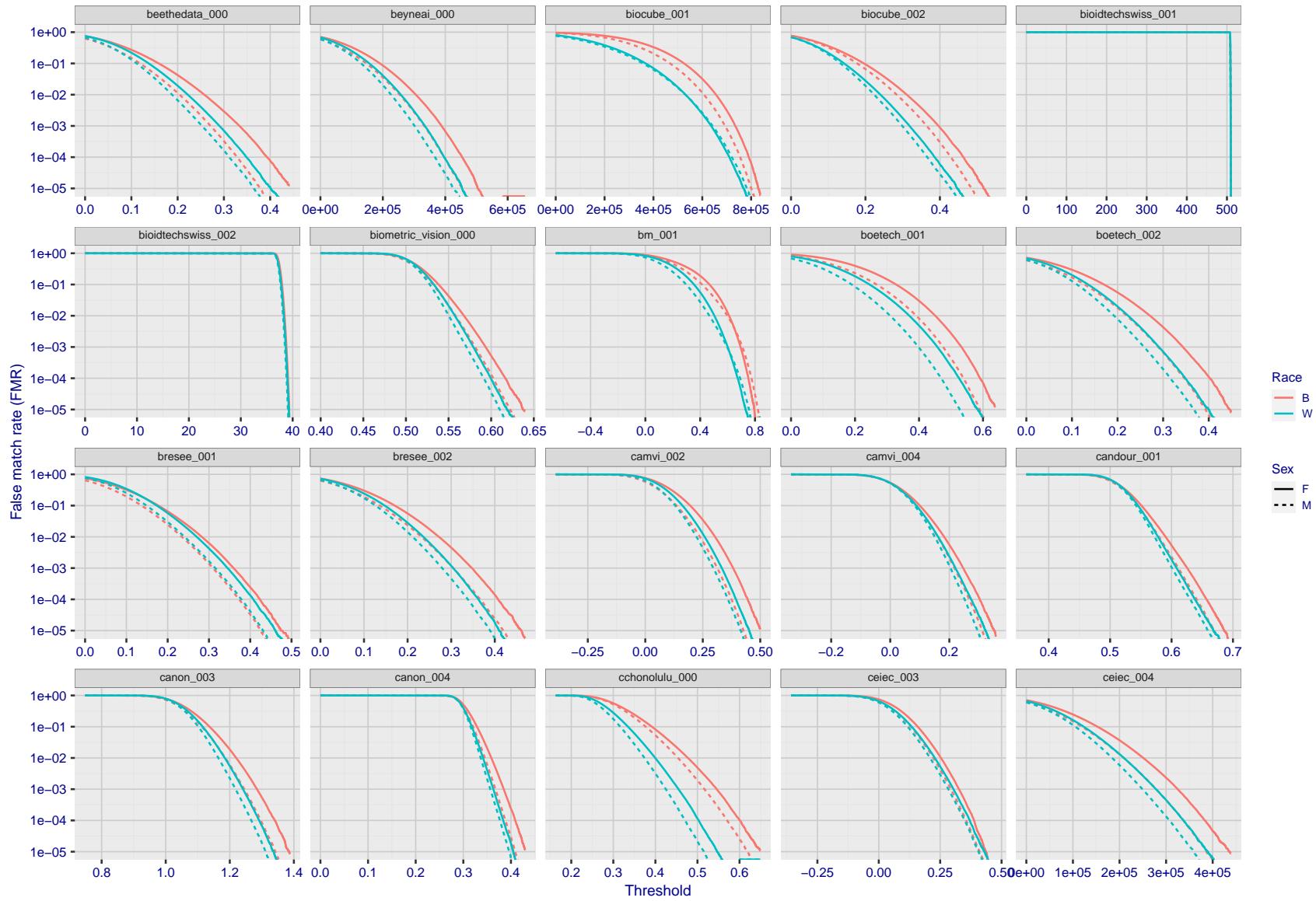


Figure 234: For the mugshot images, the false match calibration curves show false match rate vs. threshold. Separate curves appear for white females, black females, black males and white males.

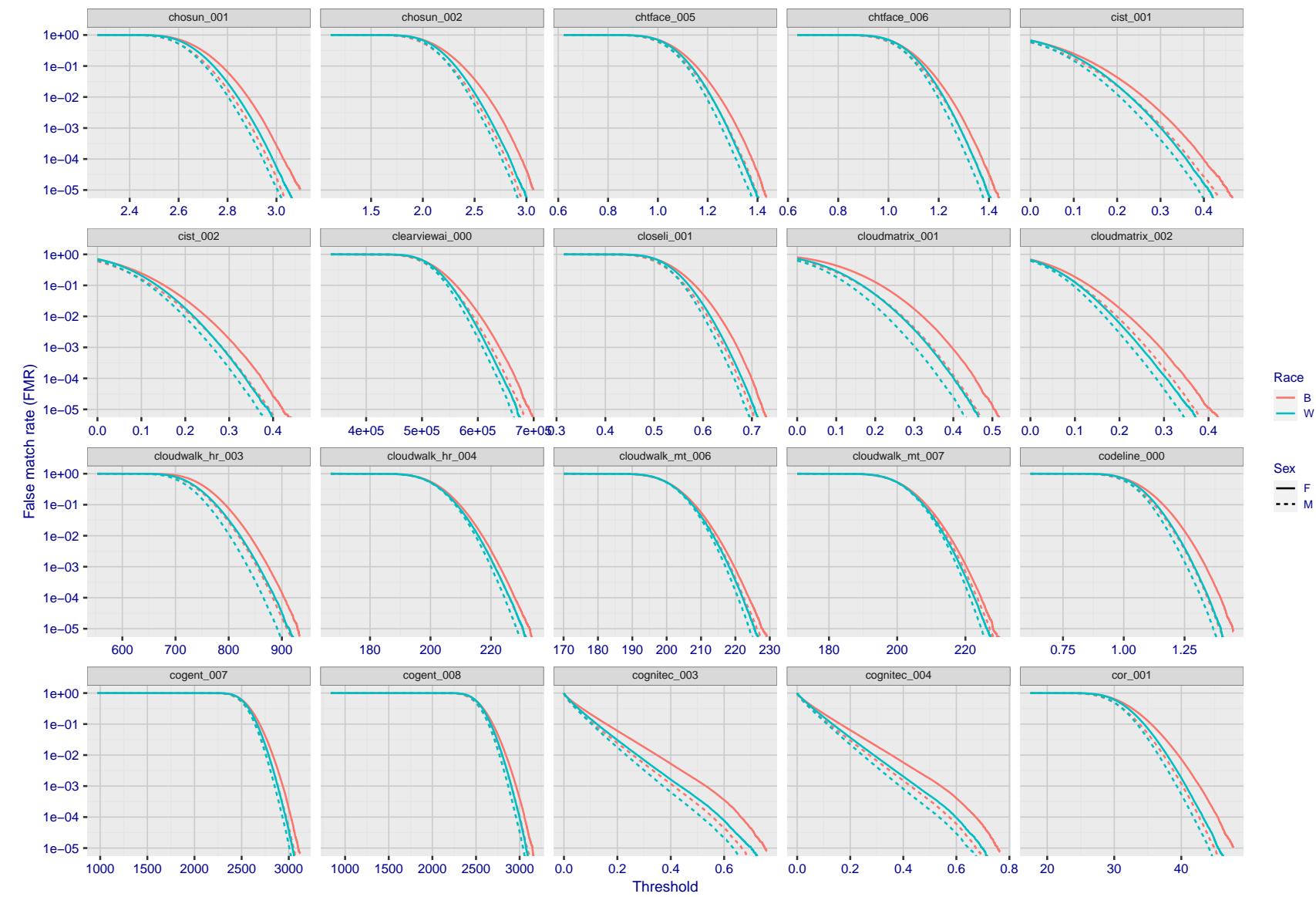


Figure 235: For the mugshot images, the false match calibration curves show false match rate vs. threshold. Separate curves appear for white females, black females, black males and white males.

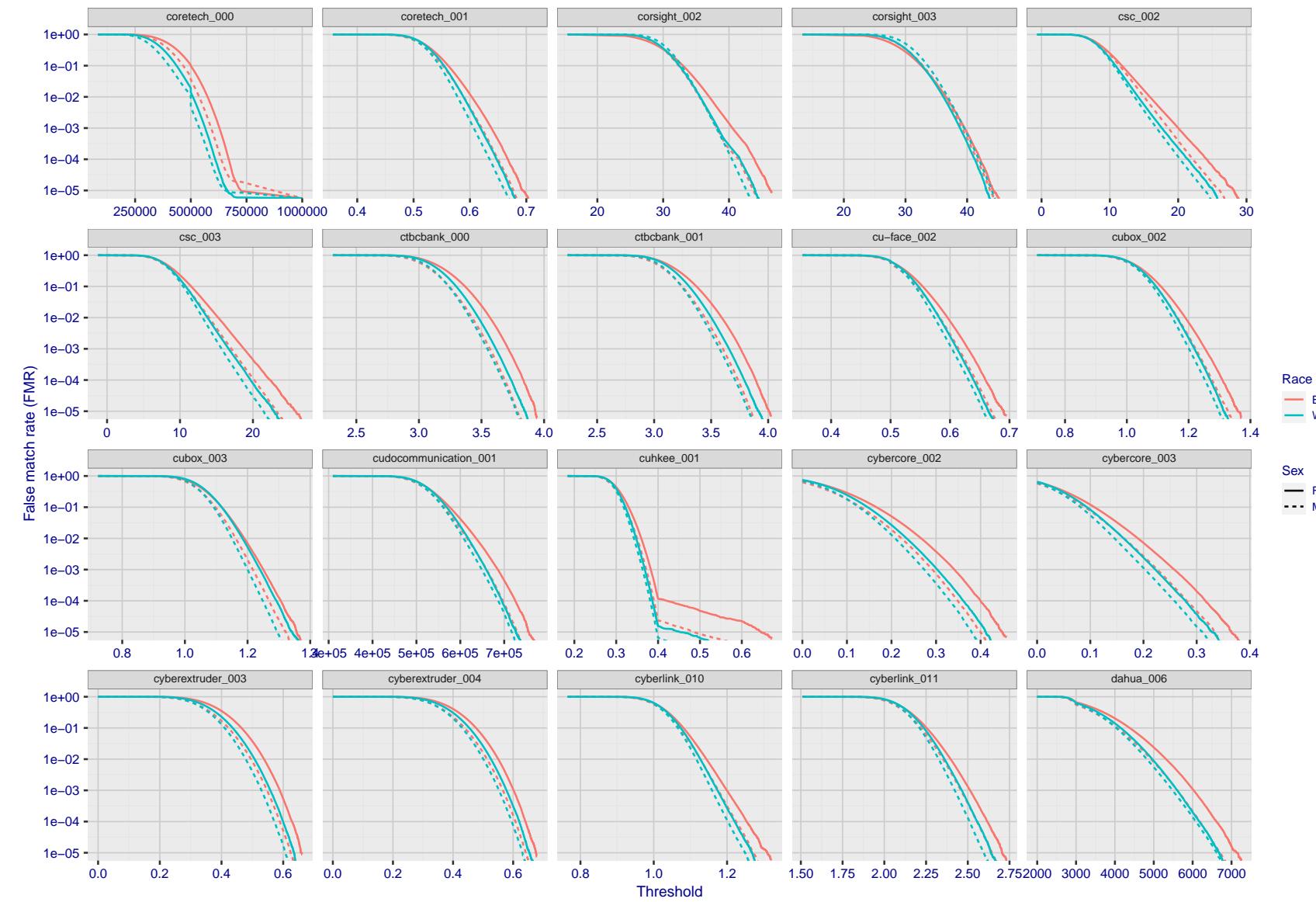


Figure 236: For the mugshot images, the false match calibration curves show false match rate vs. threshold. Separate curves appear for white females, black females, black males and white males.

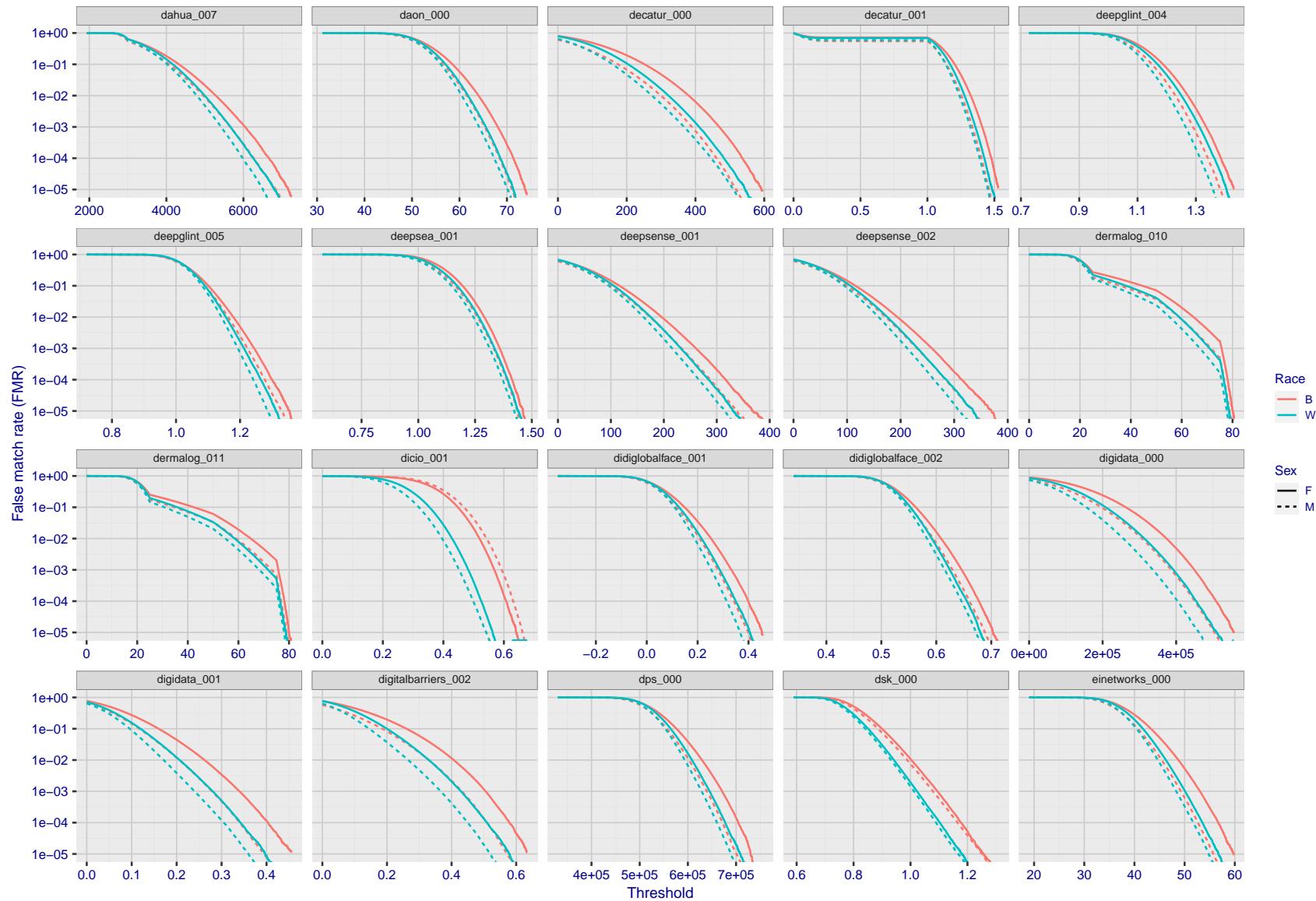


Figure 237: For the mugshot images, the false match calibration curves show false match rate vs. threshold. Separate curves appear for white females, black females, black males and white males.

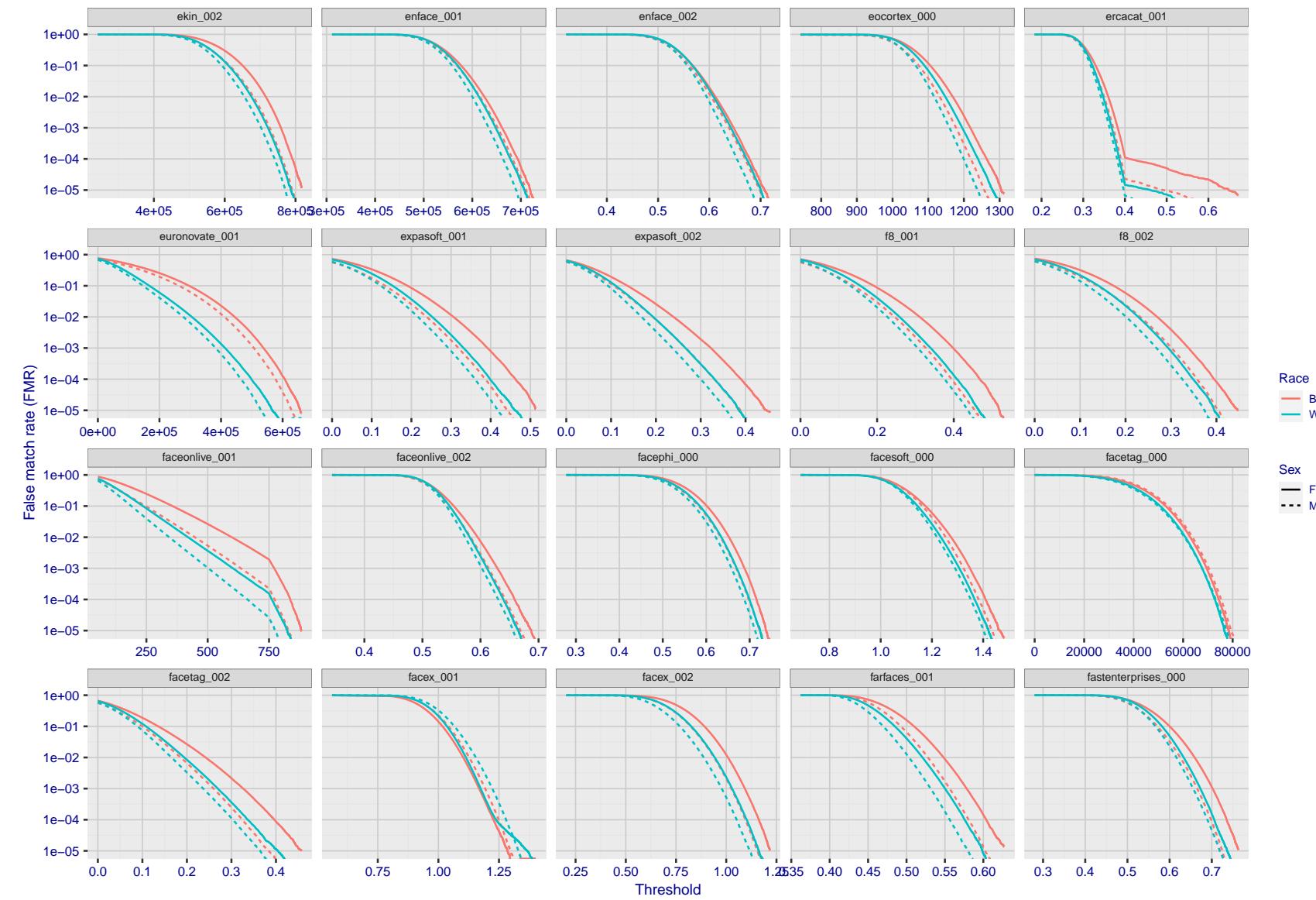


Figure 238: For the mugshot images, the false match calibration curves show false match rate vs. threshold. Separate curves appear for white females, black females, black males and white males.

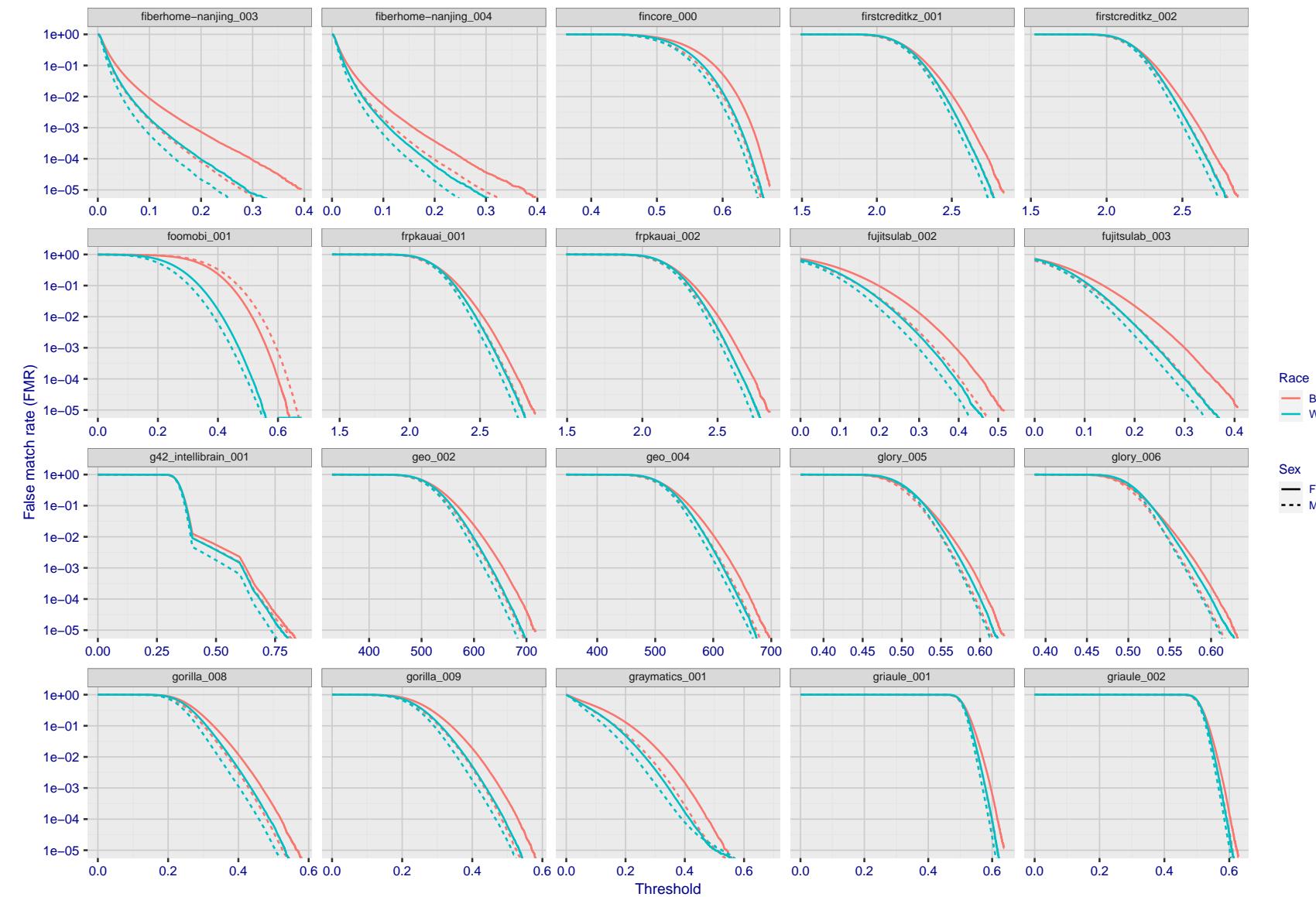


Figure 239: For the mugshot images, the false match calibration curves show false match rate vs. threshold. Separate curves appear for white females, black females, black males and white males.

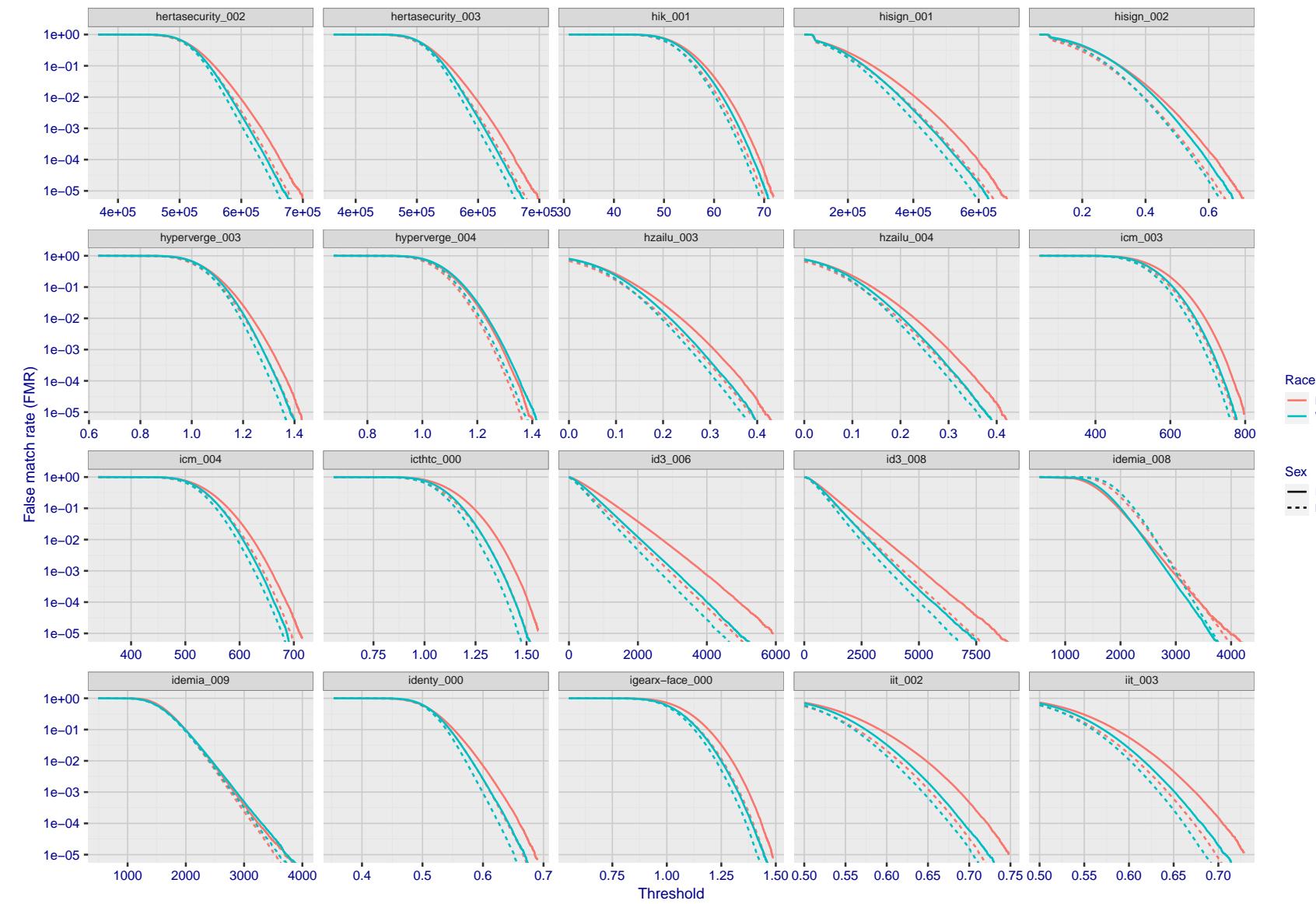


Figure 240: For the mugshot images, the false match calibration curves show false match rate vs. threshold. Separate curves appear for white females, black females, black males and white males.

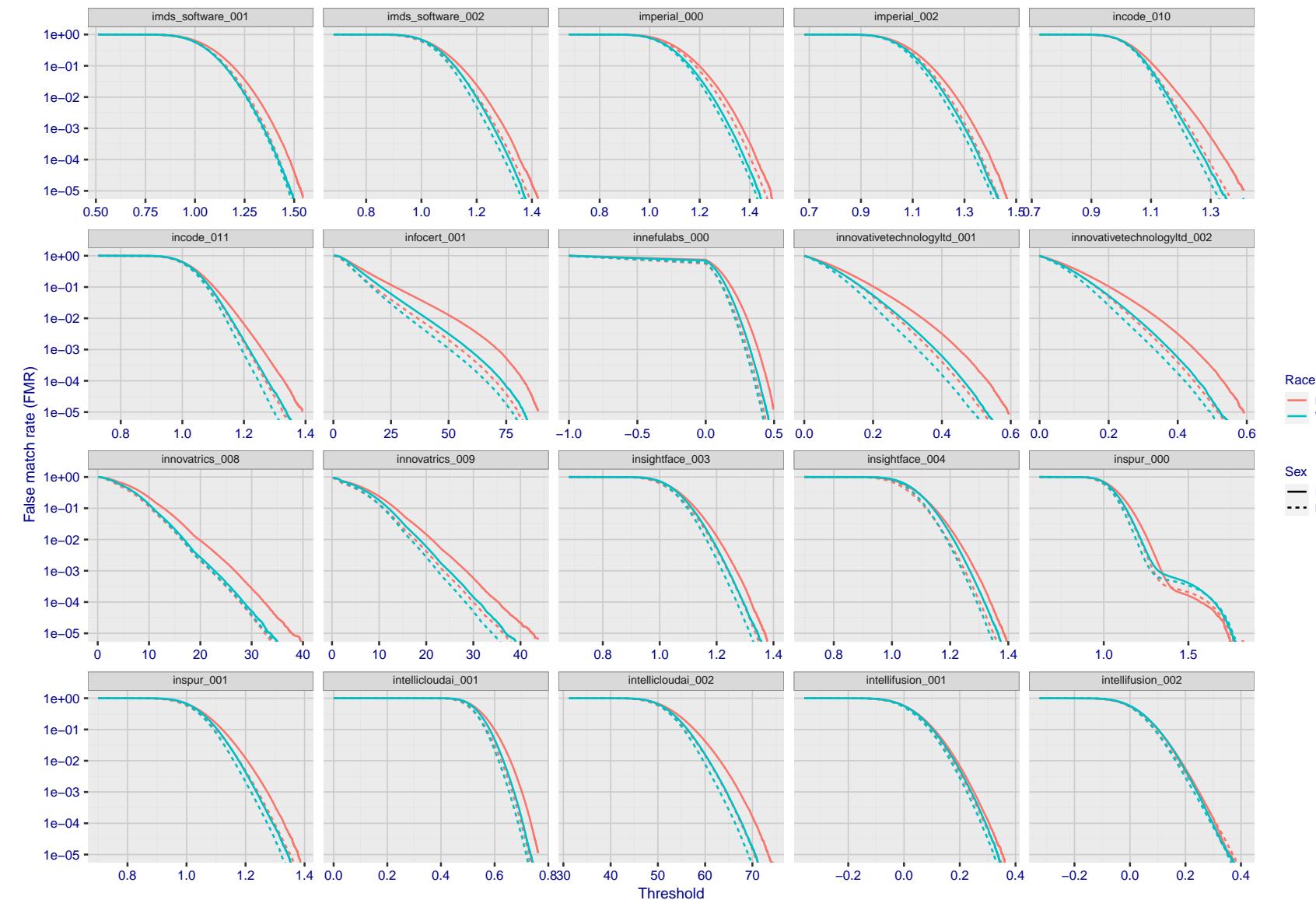


Figure 241: For the mugshot images, the false match calibration curves show false match rate vs. threshold. Separate curves appear for white females, black females, black males and white males.

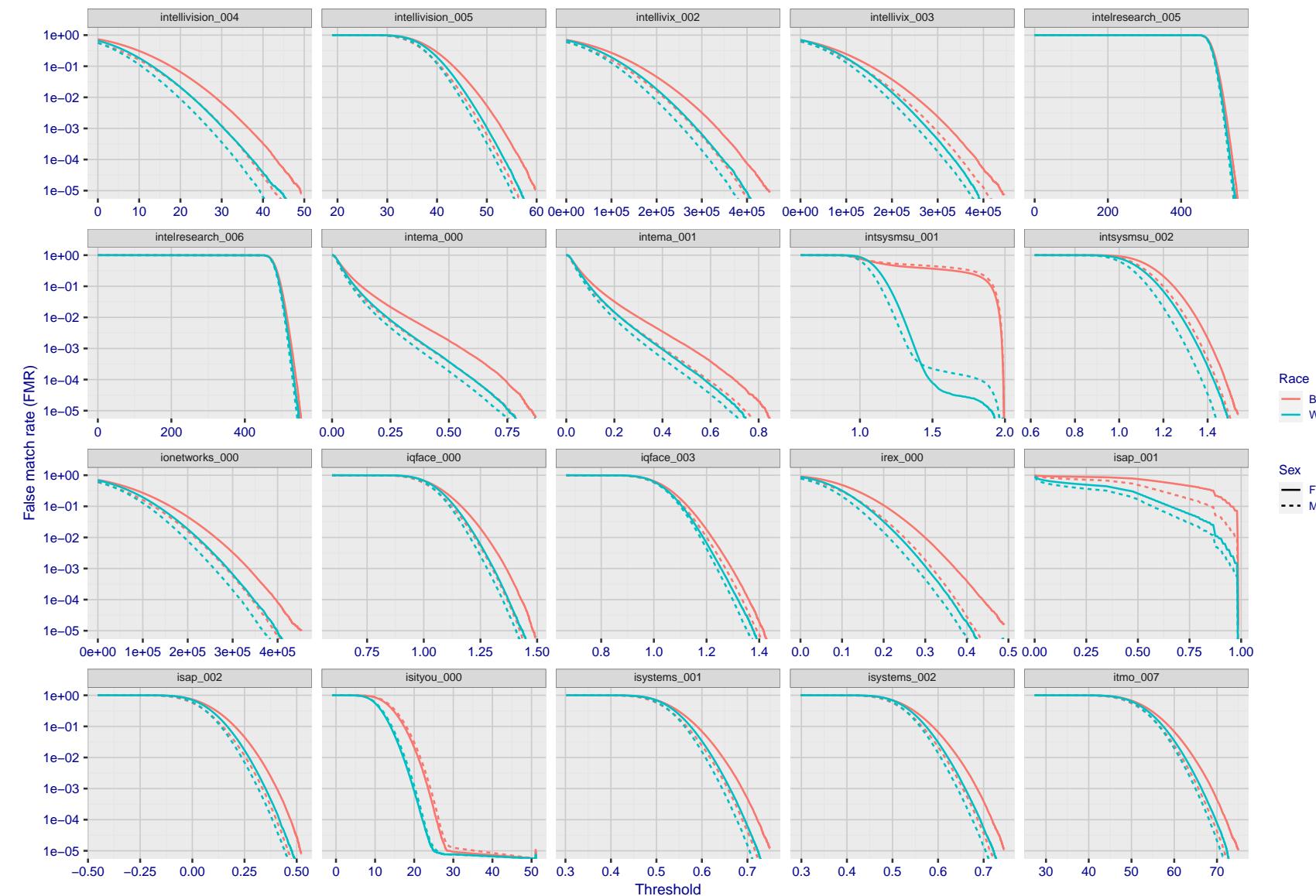


Figure 242: For the mugshot images, the false match calibration curves show false match rate vs. threshold. Separate curves appear for white females, black females, black males and white males.

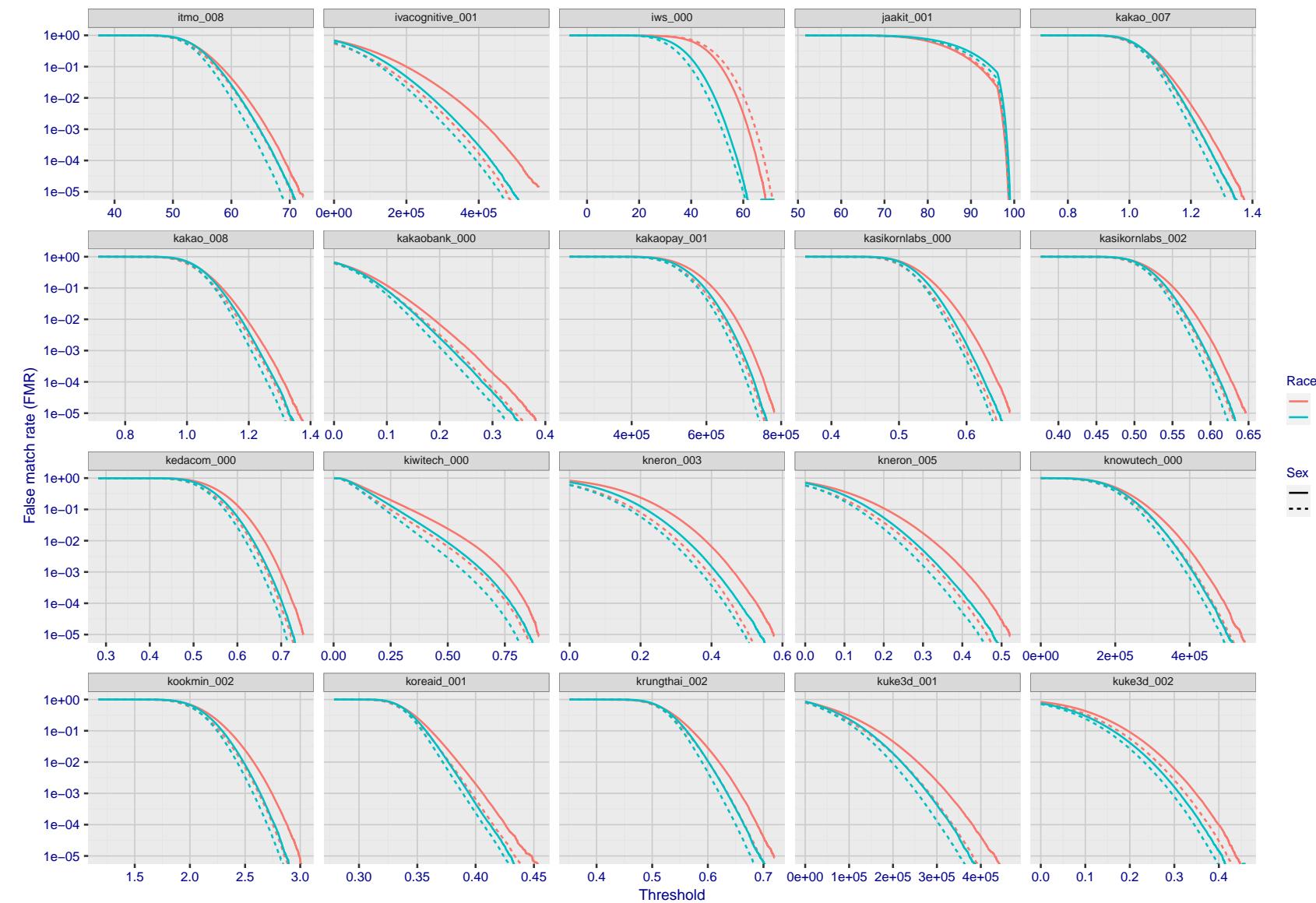


Figure 243: For the mugshot images, the false match calibration curves show false match rate vs. threshold. Separate curves appear for white females, black females, black males and white males.

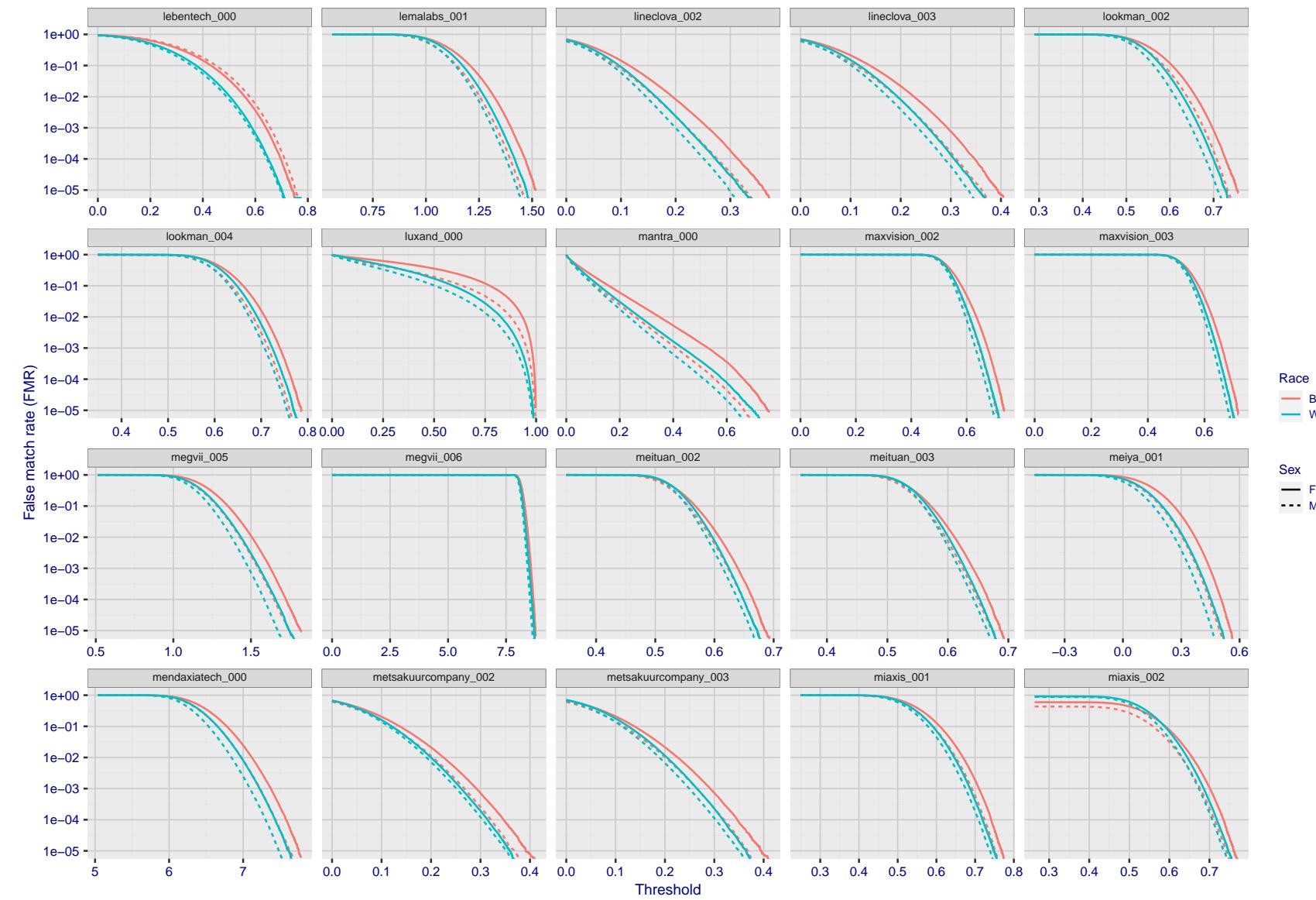


Figure 244: For the mugshot images, the false match calibration curves show false match rate vs. threshold. Separate curves appear for white females, black females, black males and white males.

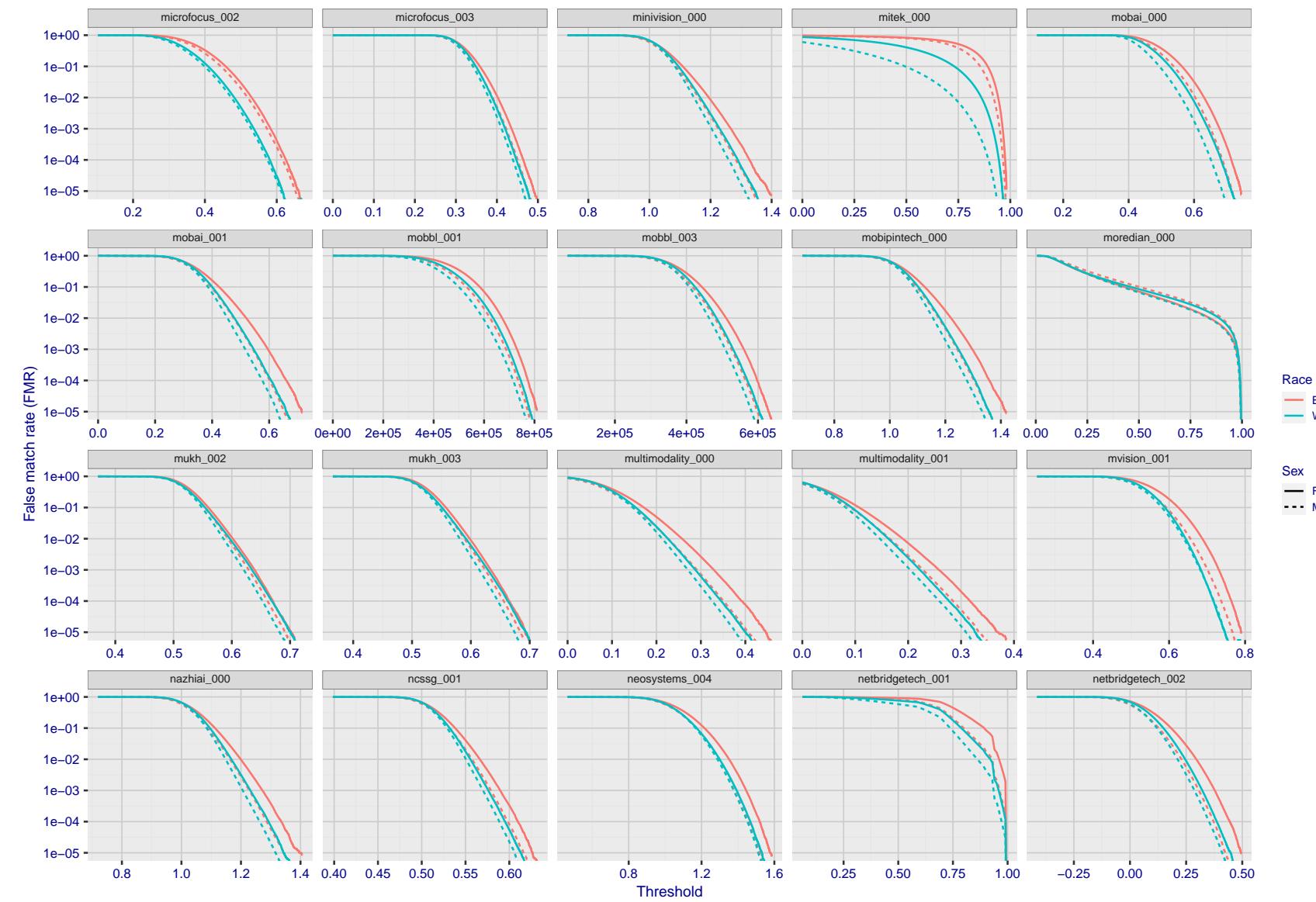


Figure 245: For the mugshot images, the false match calibration curves show false match rate vs. threshold. Separate curves appear for white females, black females, black males and white males.

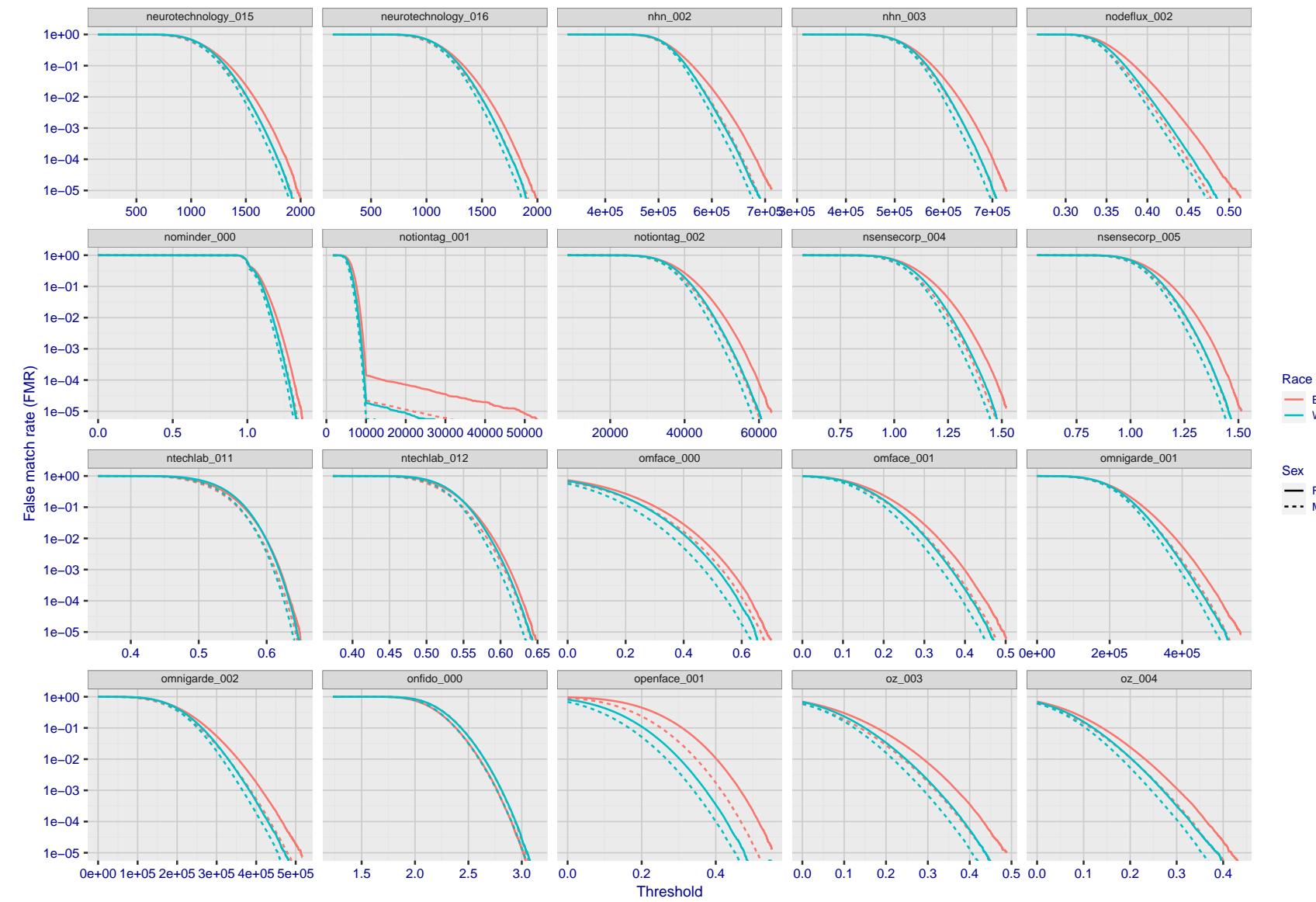


Figure 246: For the mugshot images, the false match calibration curves show false match rate vs. threshold. Separate curves appear for white females, black females, black males and white males.

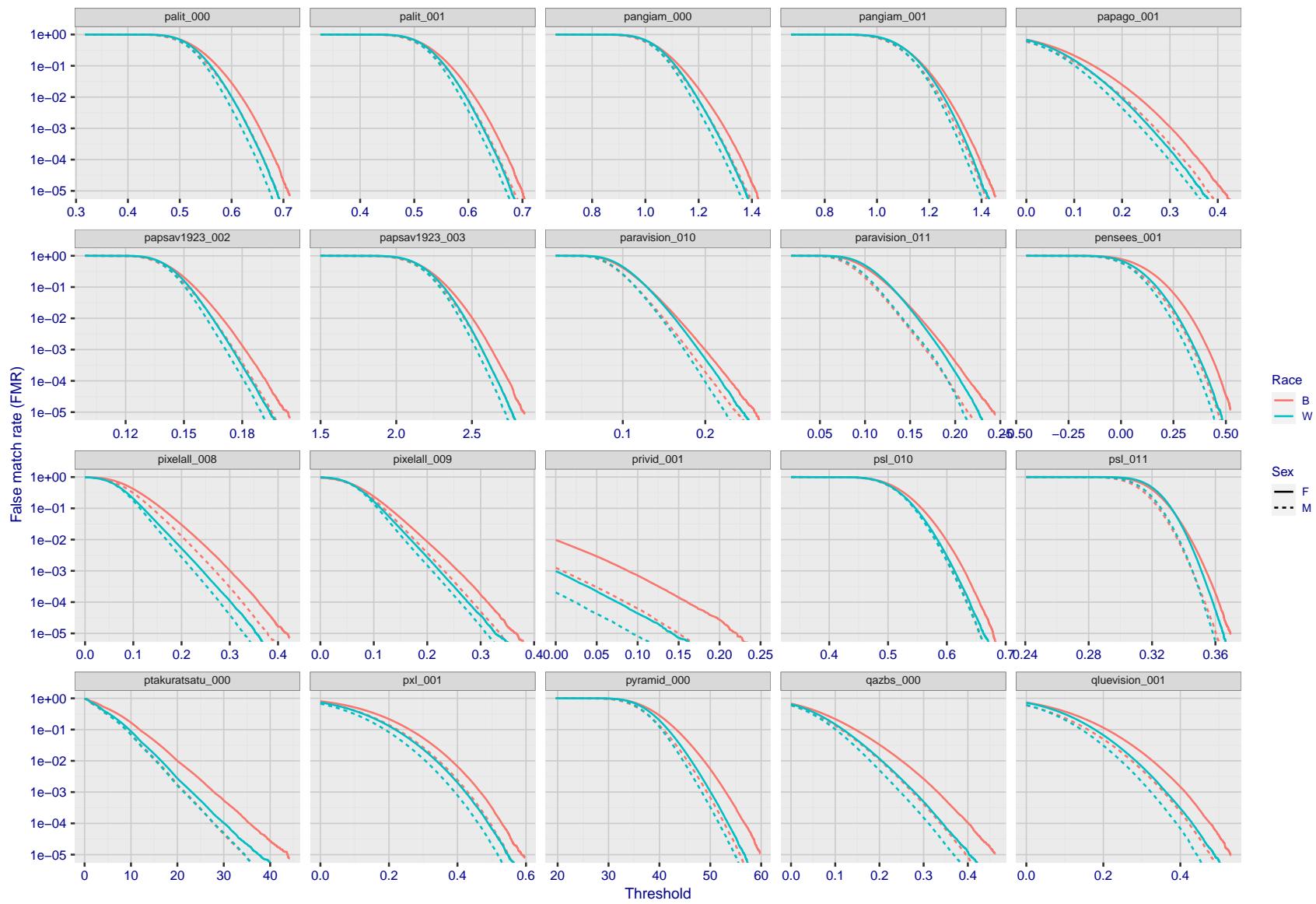


Figure 247: For the mugshot images, the false match calibration curves show false match rate vs. threshold. Separate curves appear for white females, black females, black males and white males.

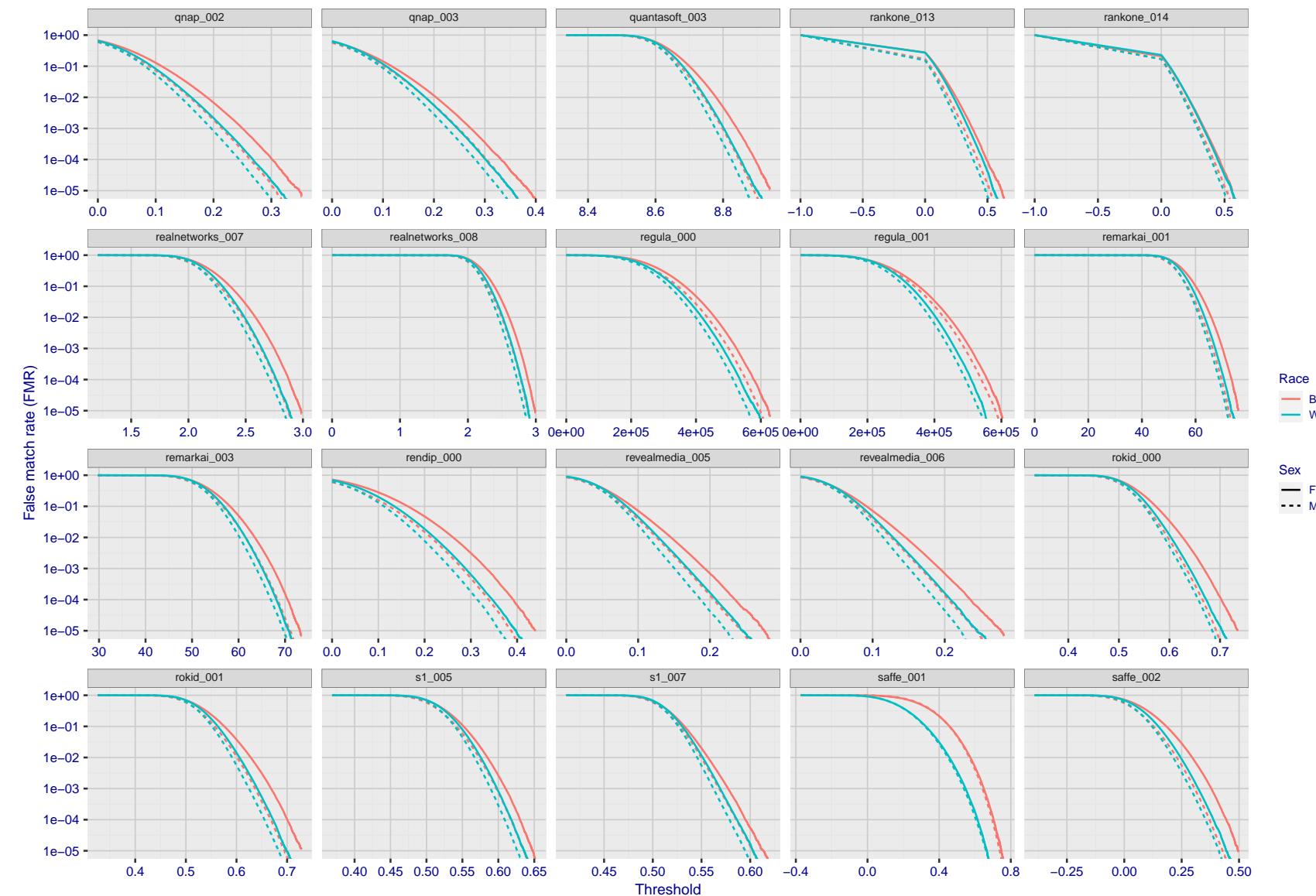


Figure 248: For the mugshot images, the false match calibration curves show false match rate vs. threshold. Separate curves appear for white females, black females, black males and white males.

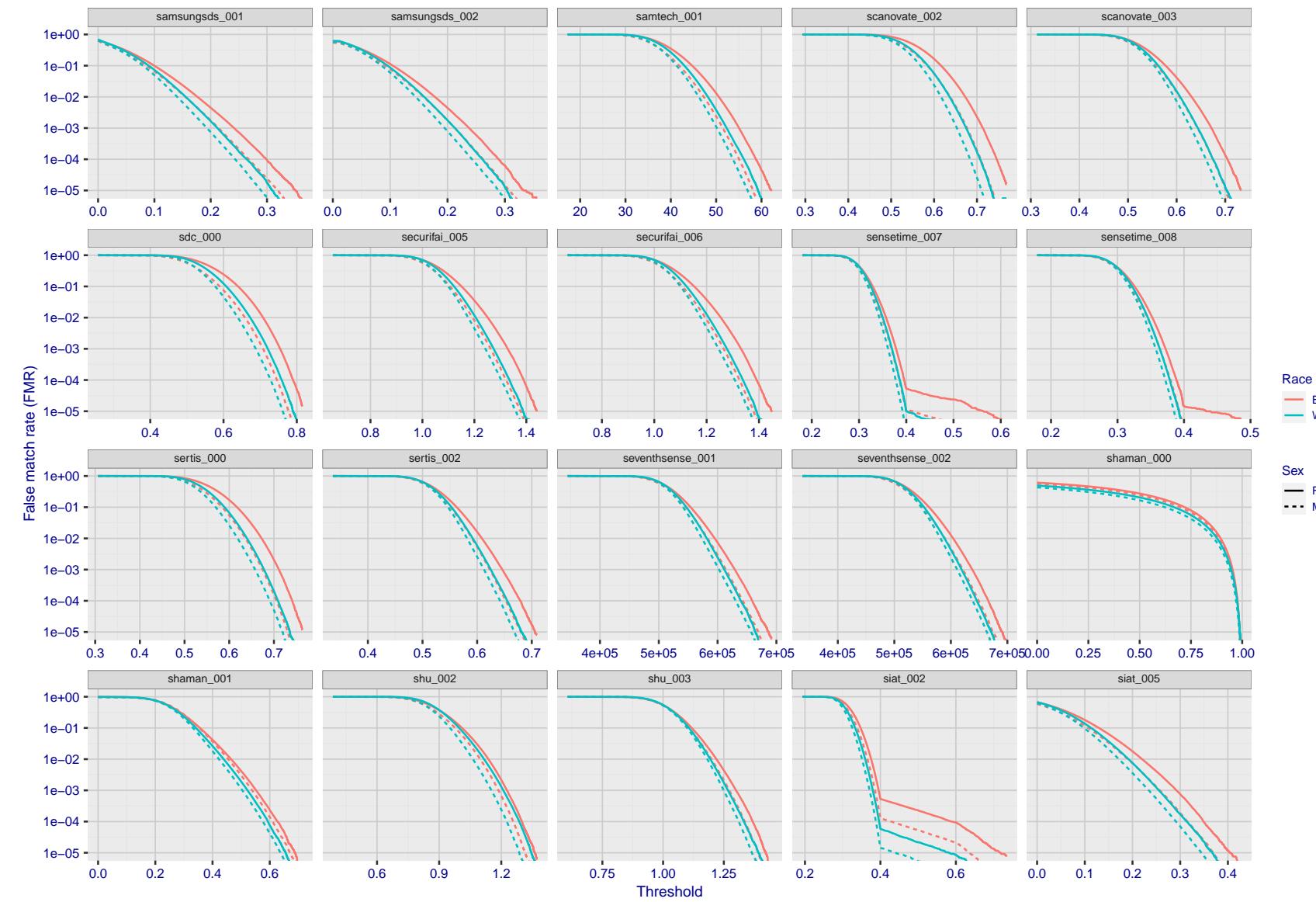


Figure 249: For the mugshot images, the false match calibration curves show false match rate vs. threshold. Separate curves appear for white females, black females, black males and white males.

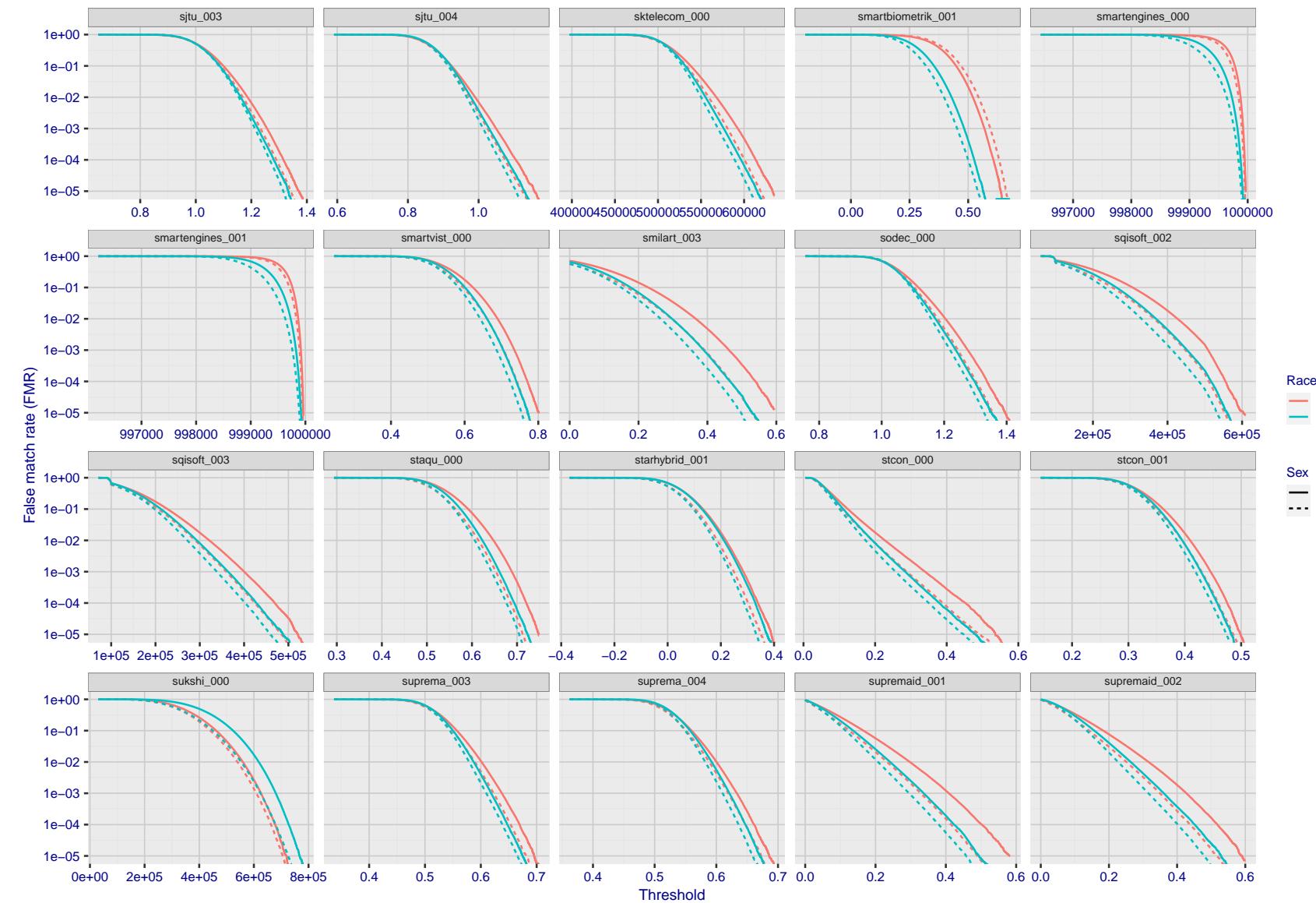


Figure 250: For the mugshot images, the false match calibration curves show false match rate vs. threshold. Separate curves appear for white females, black females, black males and white males.

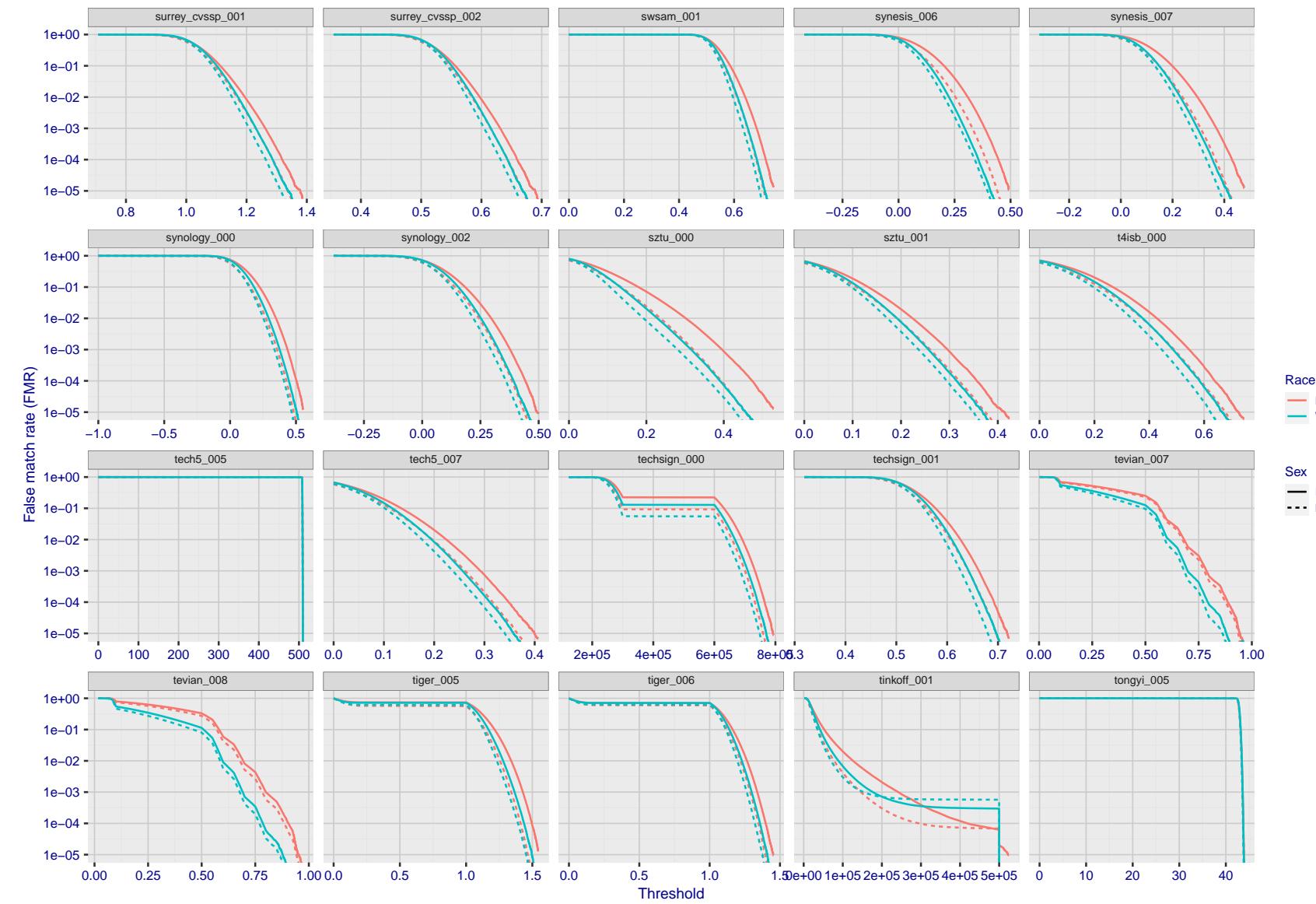


Figure 251: For the mugshot images, the false match calibration curves show false match rate vs. threshold. Separate curves appear for white females, black females, black males and white males.

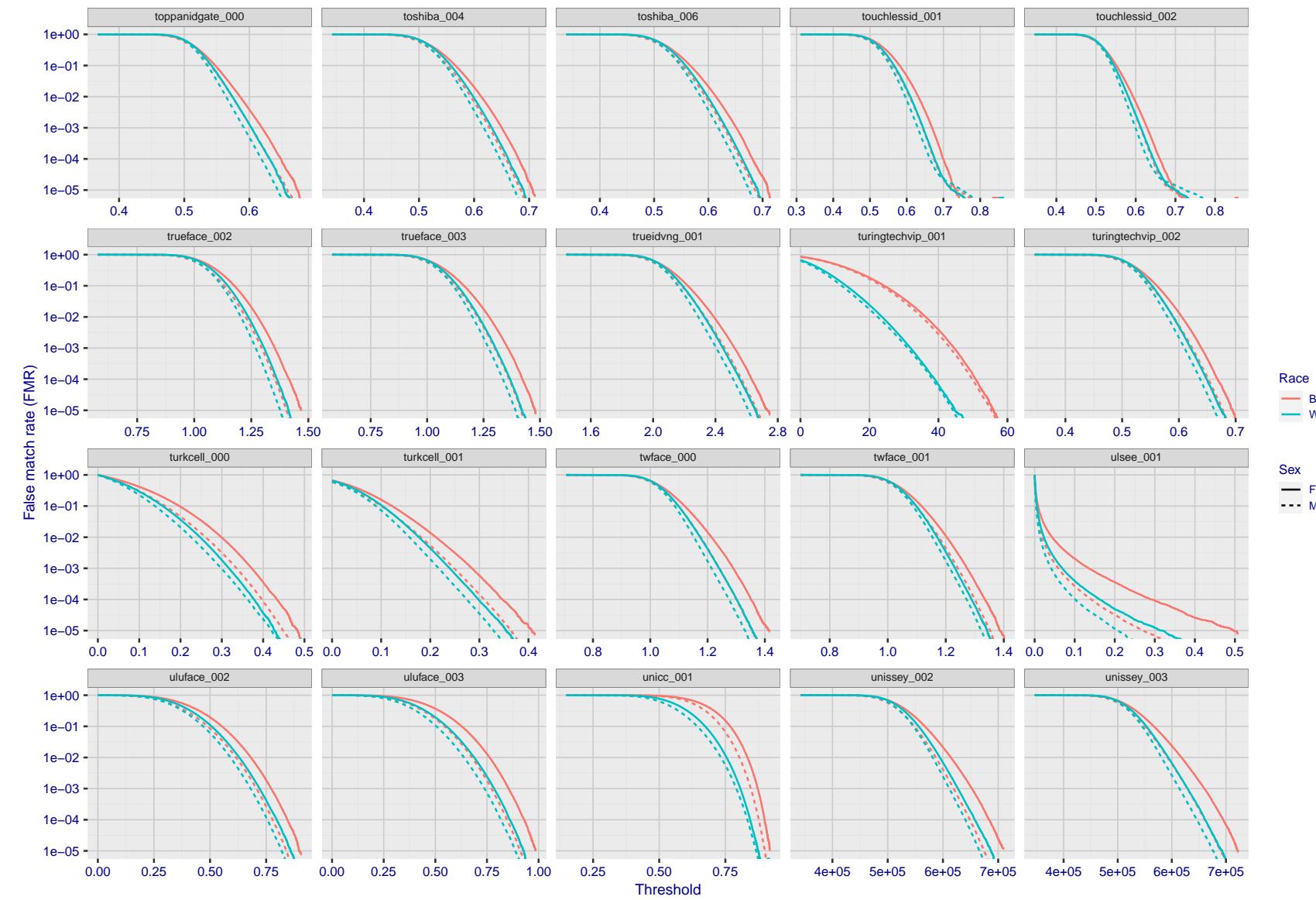


Figure 252: For the mugshot images, the false match calibration curves show false match rate vs. threshold. Separate curves appear for white females, black females, black males and white males.

2023/04/20 08:30:53

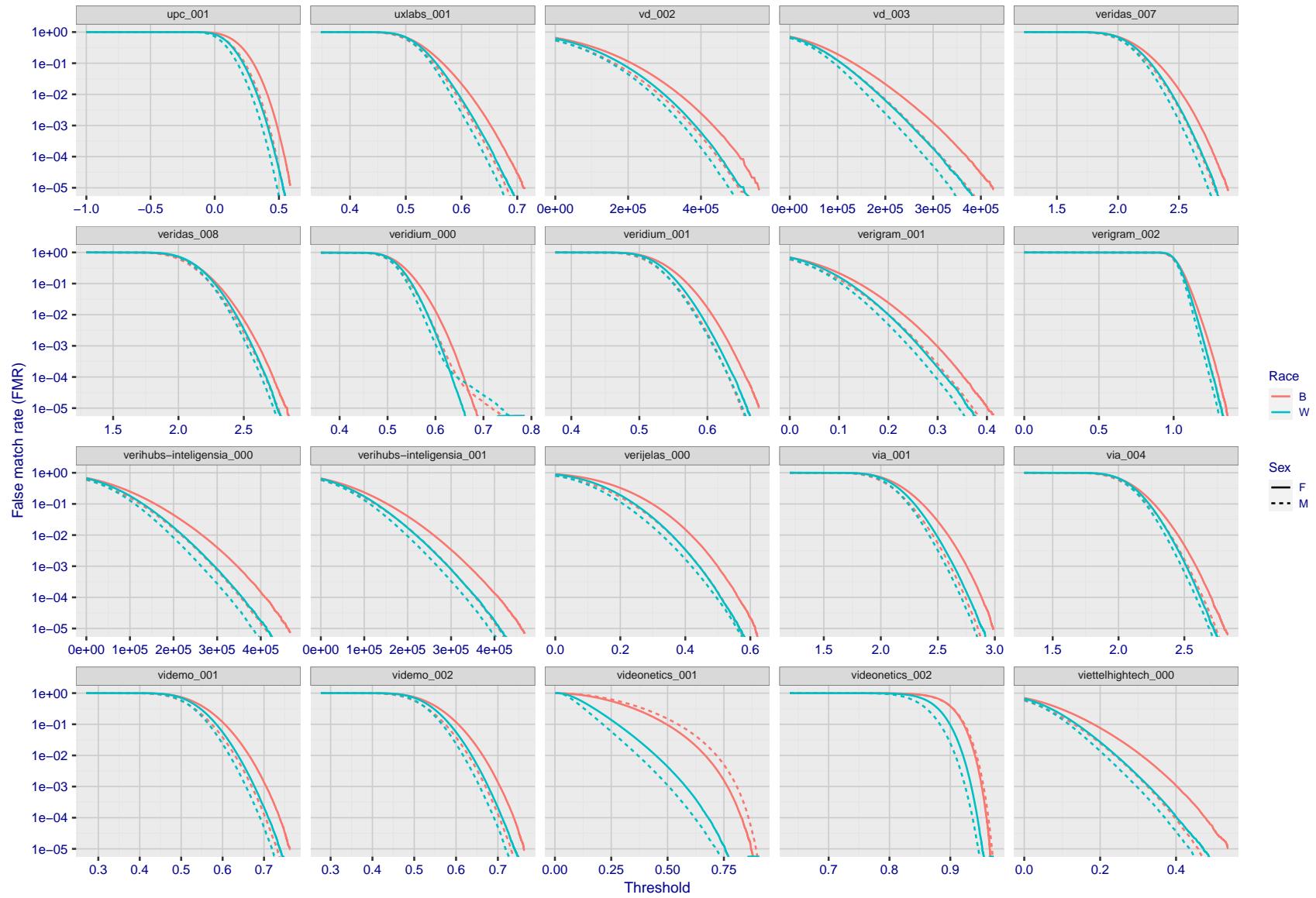


Figure 253: For the mugshot images, the false match calibration curves show false match rate vs. threshold. Separate curves appear for white females, black females, black males and white males.

FNMR(T)
"False non-match rate"
"False match rate"

2023/04/20 08:30:53

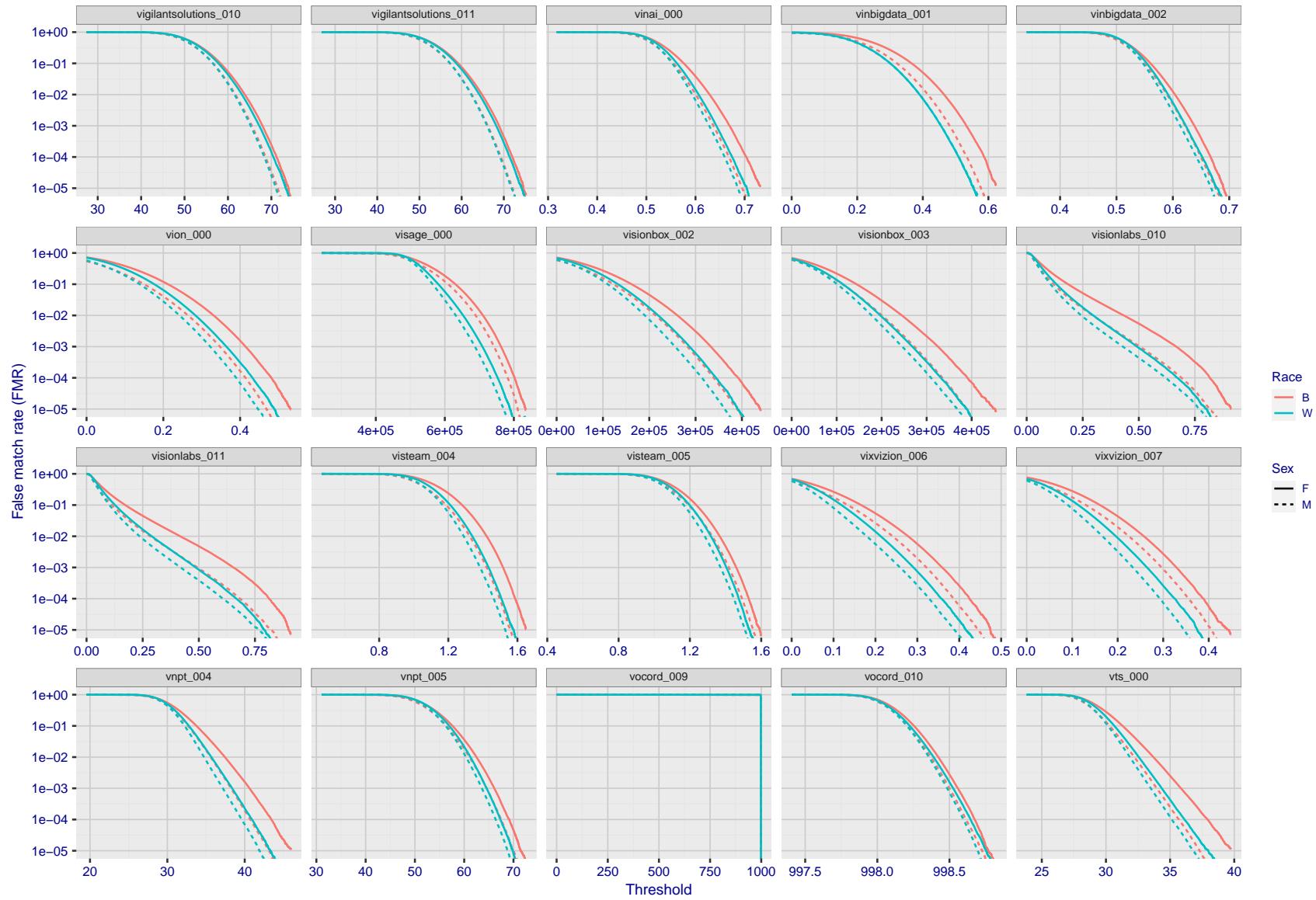
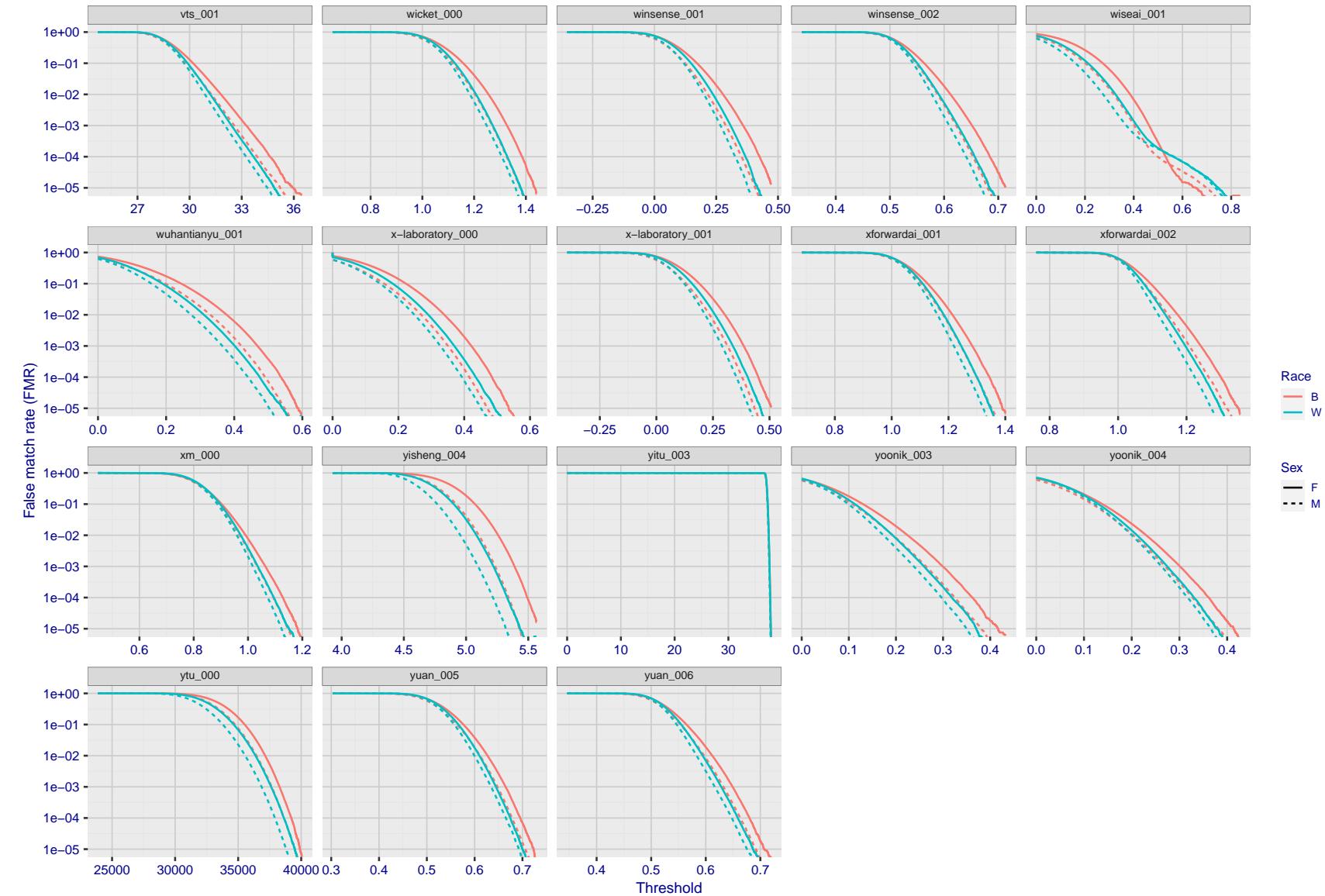


Figure 254: For the mugshot images, the false match calibration curves show false match rate vs. threshold. Separate curves appear for white females, black females, black males and white males.

FNMR(T)
"False non-match rate"

"False match rate"

Figure 255: For the mugshot images, the false match calibration curves show false match rate vs. threshold. Separate curves appear for white females, black females, black males and white males.

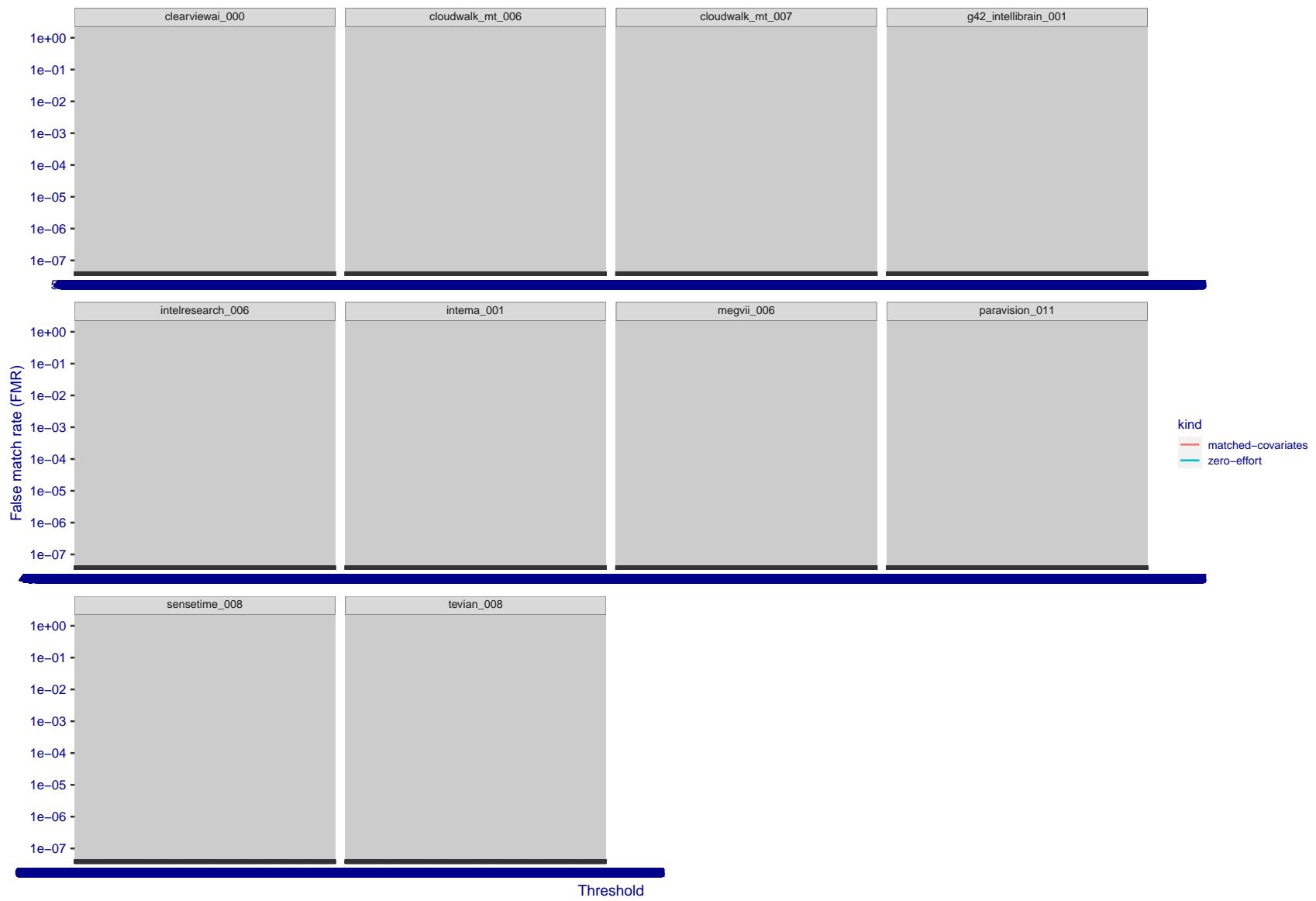


Figure 256: For the visa images, the false match calibration curves show FMR vs. threshold, T . The blue (lower) curves are for zero-effort impostors (i.e. comparing all images against all). The red (upper) curves are for persons of the same-sex, same-age, and same national-origin. This shows that FMR is underestimated (by a factor of 10 or more) by using a zero-effort impostor calculation to calibrate T . As shown later (sec. 3.6), FMR is higher for demographic-matched impostors.

3.5 Genuine distribution stability

3.5.1 Effect of birth place on the genuine distribution

Background: Both skin tone and bone structure vary geographically. Prior studies have reported variations in FNMR and FMR.

Goal: To measure false non-match rate (FNMR) variation with country of birth.

Methods: Thresholds are determined that give $FMR = \{0.001, 0.0001\}$ over the entire impostor set. Then FNMR is measured over 1000 bootstrap replications of the genuine scores. Only those countries with at least 140 individuals are included in the analysis.

Results: Figure 298 shows FNMR by country of birth for the two thresholds.

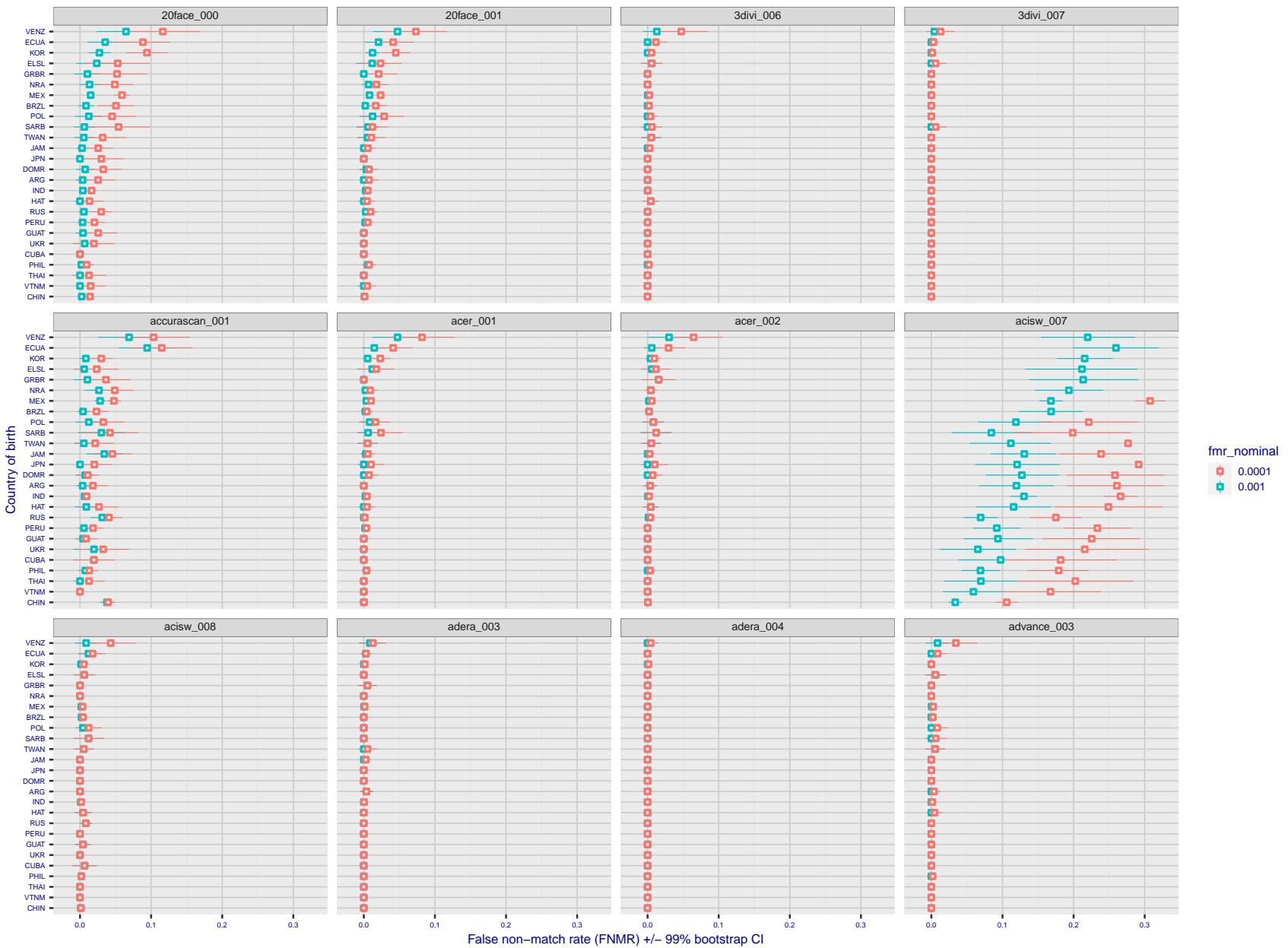


Figure 257: For the visa images, the dots show FNMR by country of birth for two globally set operating thresholds corresponding to $FMR = \{0.001, 0.0001\}$ computed over all on the order of 10^{10} impostor scores. The FMR in each bin will vary also - see subsequent impostor heatmaps in sec. 3.6.1. The figures shows an order of magnitude variation in FNMR across country of birth; these effects are likely due quality variations, then demographics like age and race. The error rates in some cases are zero, and in others the DET is flat so the error rates at the two thresholds are identical. The lines span 1% and 99% of bootstrap replicated FNMR estimates.

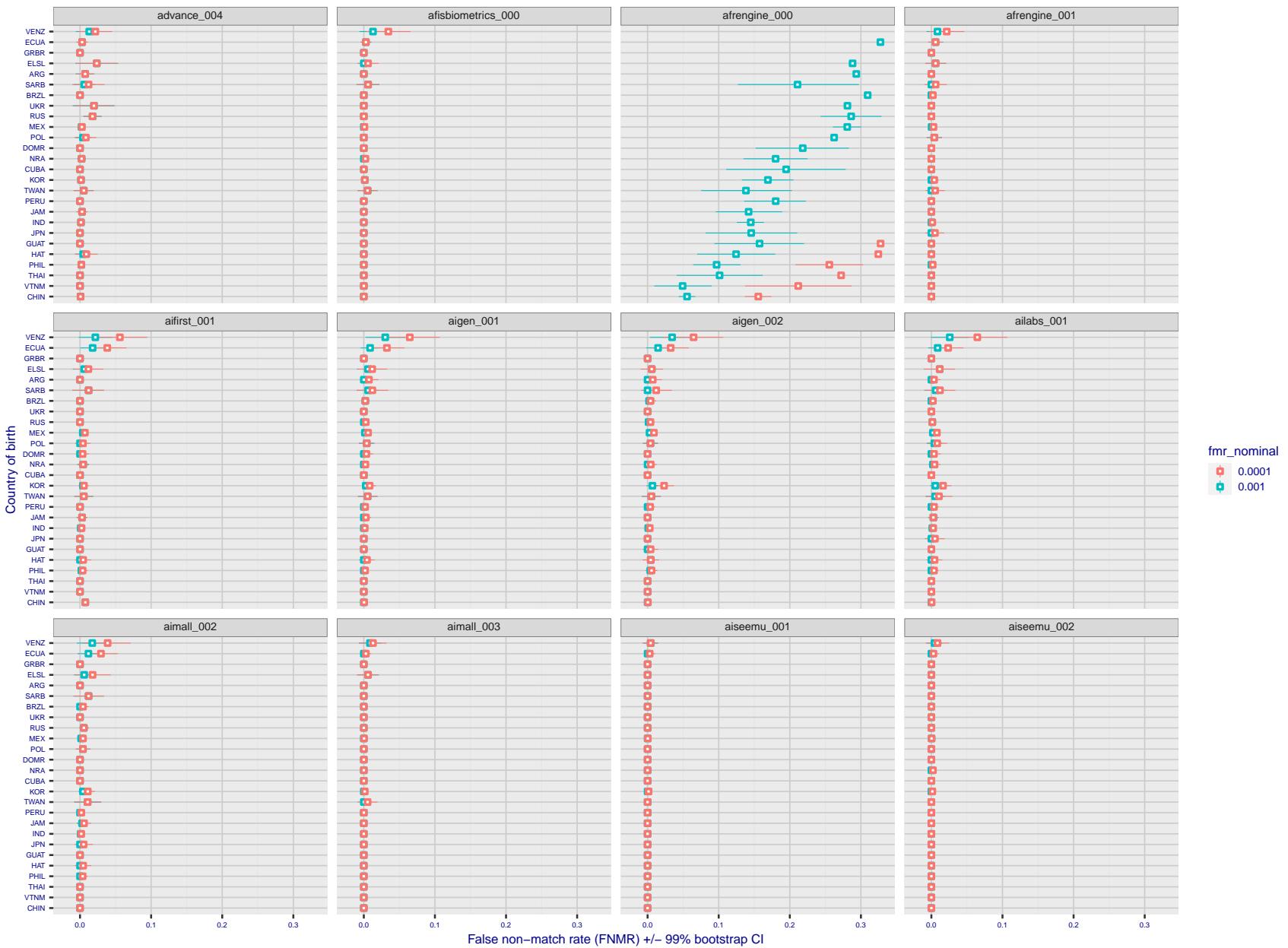


Figure 258: For the visa images, the dots show FNMR by country of birth for two globally set operating thresholds corresponding to $FMR = \{0.001, 0.0001\}$ computed over all on the order of 10^{10} impostor scores. The FMR in each bin will vary also - see subsequent impostor heatmaps in sec. 3.6.1. The figures shows an order of magnitude variation in FNMR across country of birth; these effects are likely due quality variations, then demographics like age and race. The error rates in some cases are zero, and in others the DET is flat so the error rates at the two thresholds are identical. The lines span 1% and 99% of bootstrap replicated FNMR estimates.

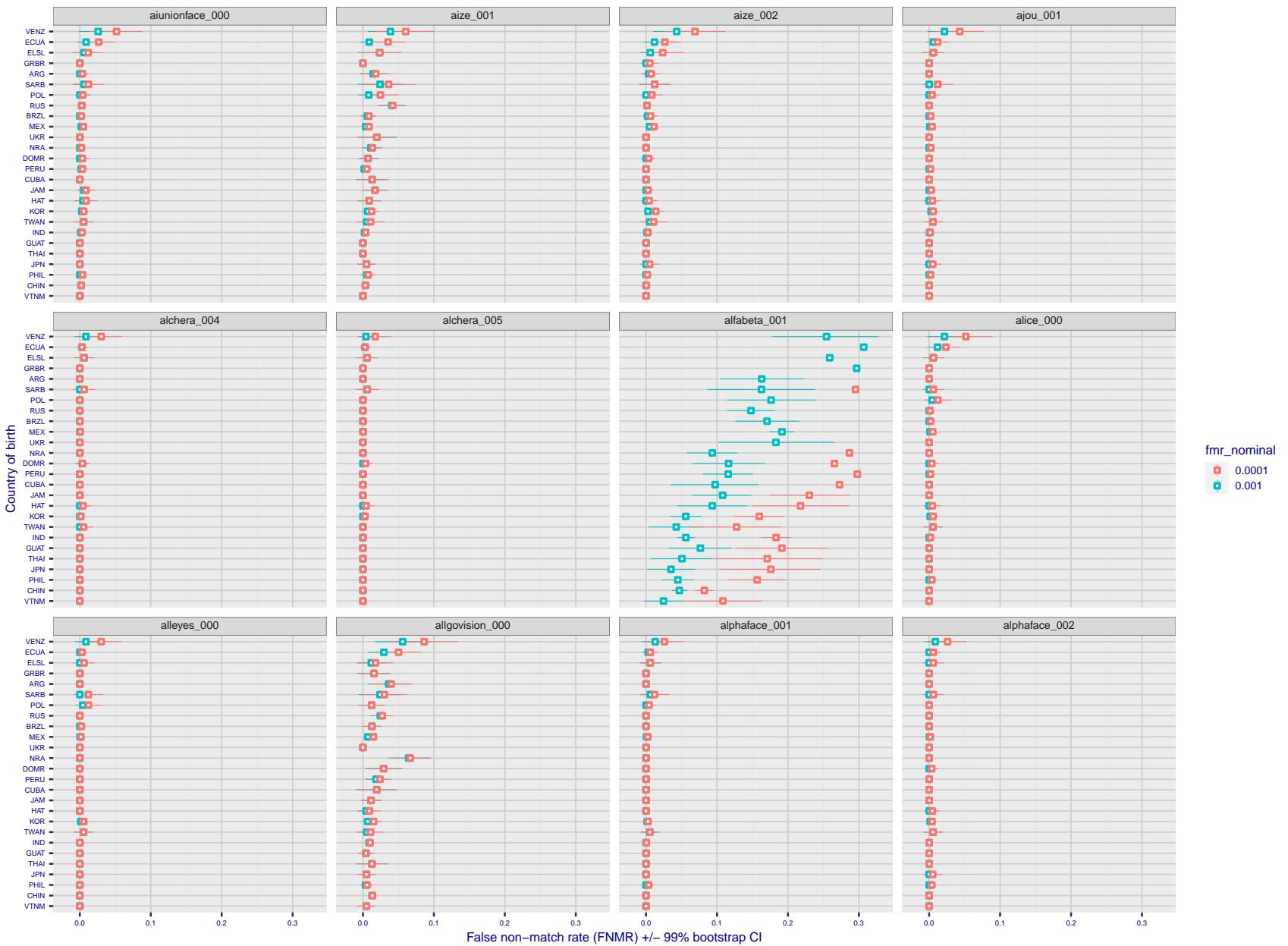


Figure 259: For the visa images, the dots show FNMR by country of birth for two globally set operating thresholds corresponding to $FMR = \{0.001, 0.0001\}$ computed over all on the order of 10^{10} impostor scores. The FMR in each bin will vary also - see subsequent impostor heatmaps in sec. 3.6.1. The figures shows an order of magnitude variation in FNMR across country of birth; these effects are likely due quality variations, then demographics like age and race. The error rates in some cases are zero, and in others the DET is flat so the error rates at the two thresholds are identical. The lines span 1% and 99% of bootstrap replicated FNMR estimates.

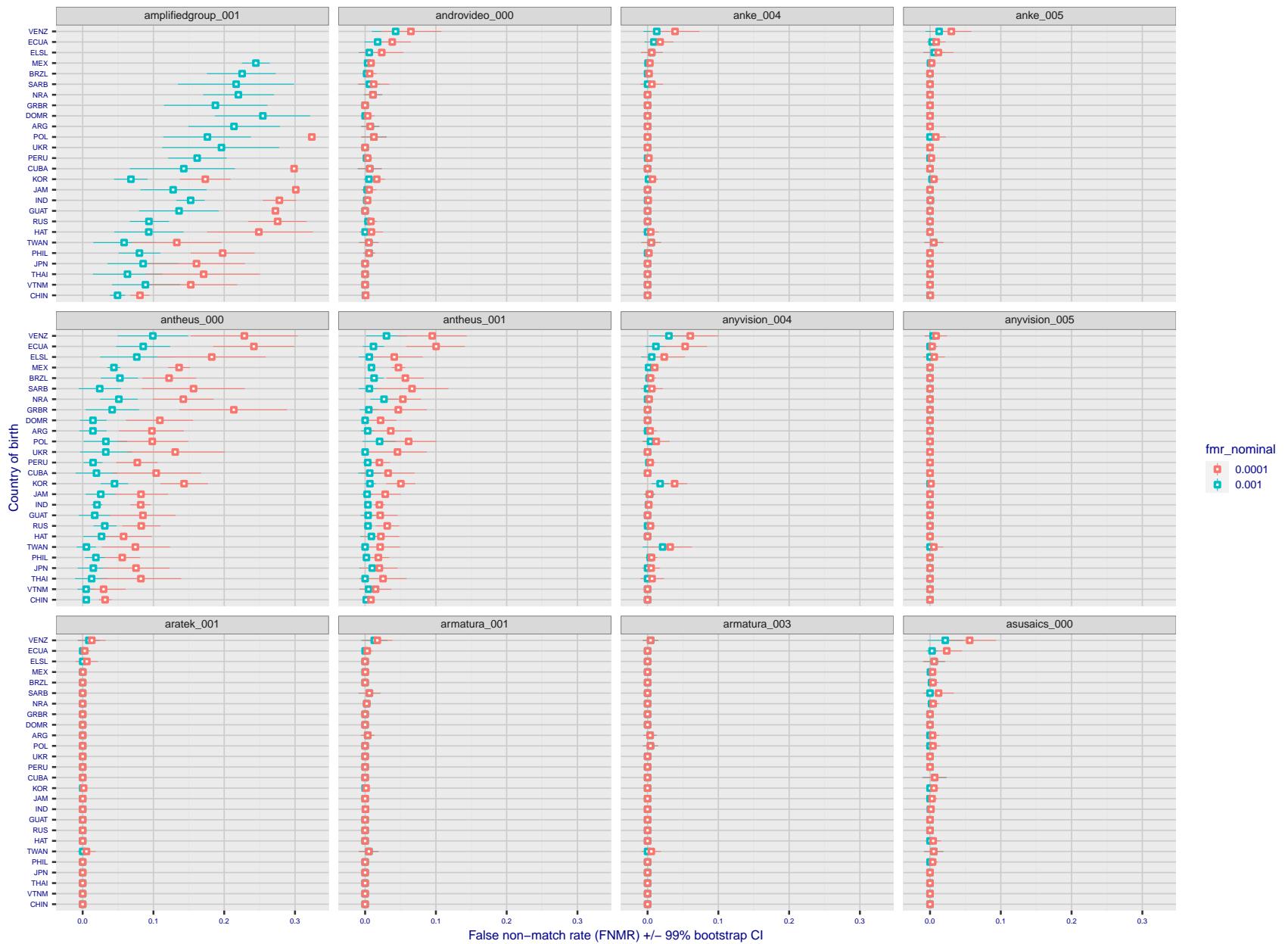


Figure 260: For the visa images, the dots show FNMR by country of birth for two globally set operating thresholds corresponding to $FMR = \{0.001, 0.0001\}$ computed over all on the order of 10^{10} impostor scores. The FMR in each bin will vary also - see subsequent impostor heatmaps in sec. 3.6.1. The figures shows an order of magnitude variation in FNMR across country of birth; these effects are likely due quality variations, then demographics like age and race. The error rates in some cases are zero, and in others the DET is flat so the error rates at the two thresholds are identical. The lines span 1% and 99% of bootstrap replicated FNMR estimates.

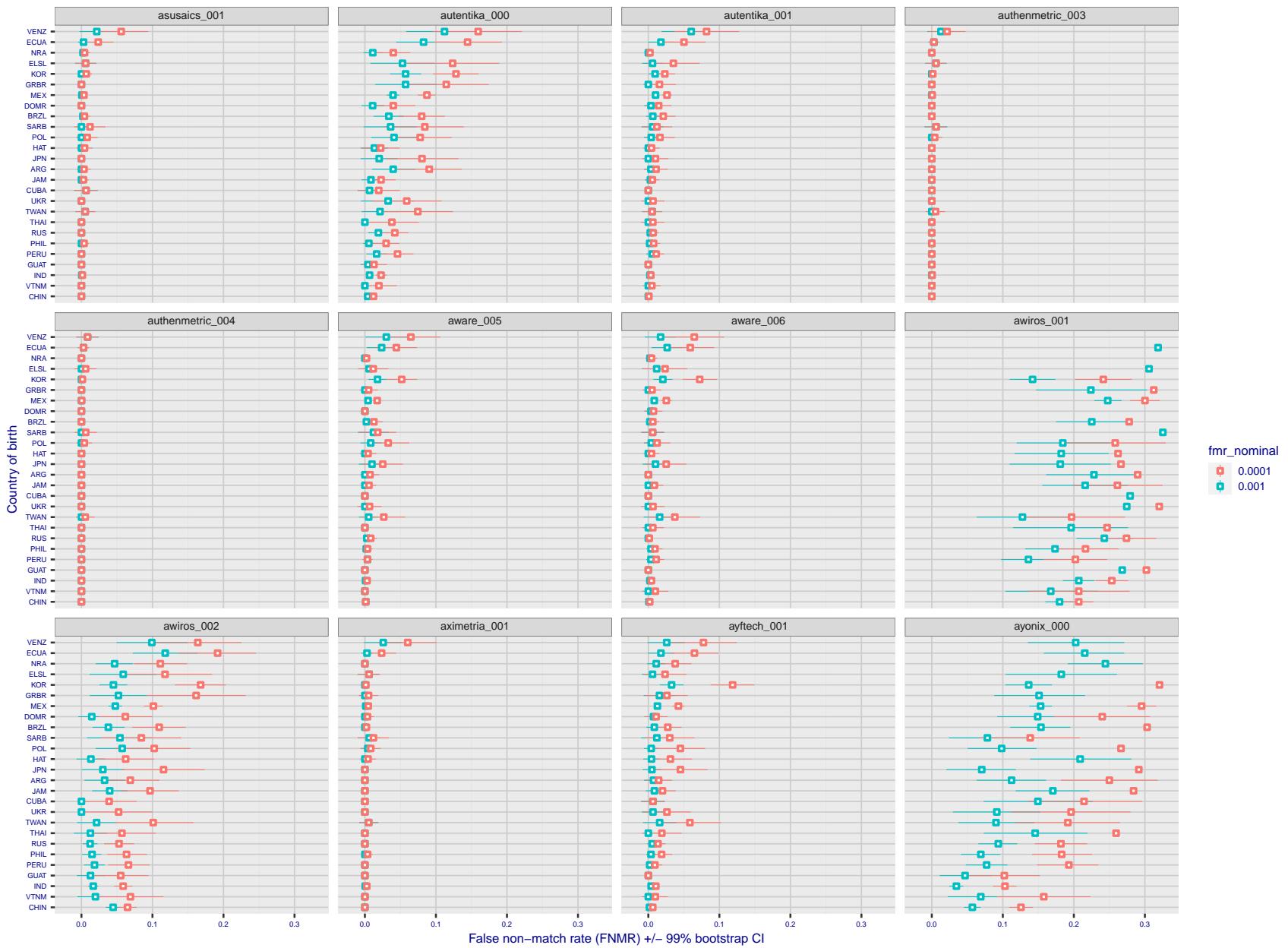


Figure 261: For the visa images, the dots show FNMR by country of birth for two globally set operating thresholds corresponding to $FMR = \{0.001, 0.0001\}$ computed over all on the order of 10^{10} impostor scores. The FMR in each bin will vary also - see subsequent impostor heatmaps in sec. 3.6.1. The figures shows an order of magnitude variation in FNMR across country of birth; these effects are likely due quality variations, then demographics like age and race. The error rates in some cases are zero, and in others the DET is flat so the error rates at the two thresholds are identical. The lines span 1% and 99% of bootstrap replicated FNMR estimates.

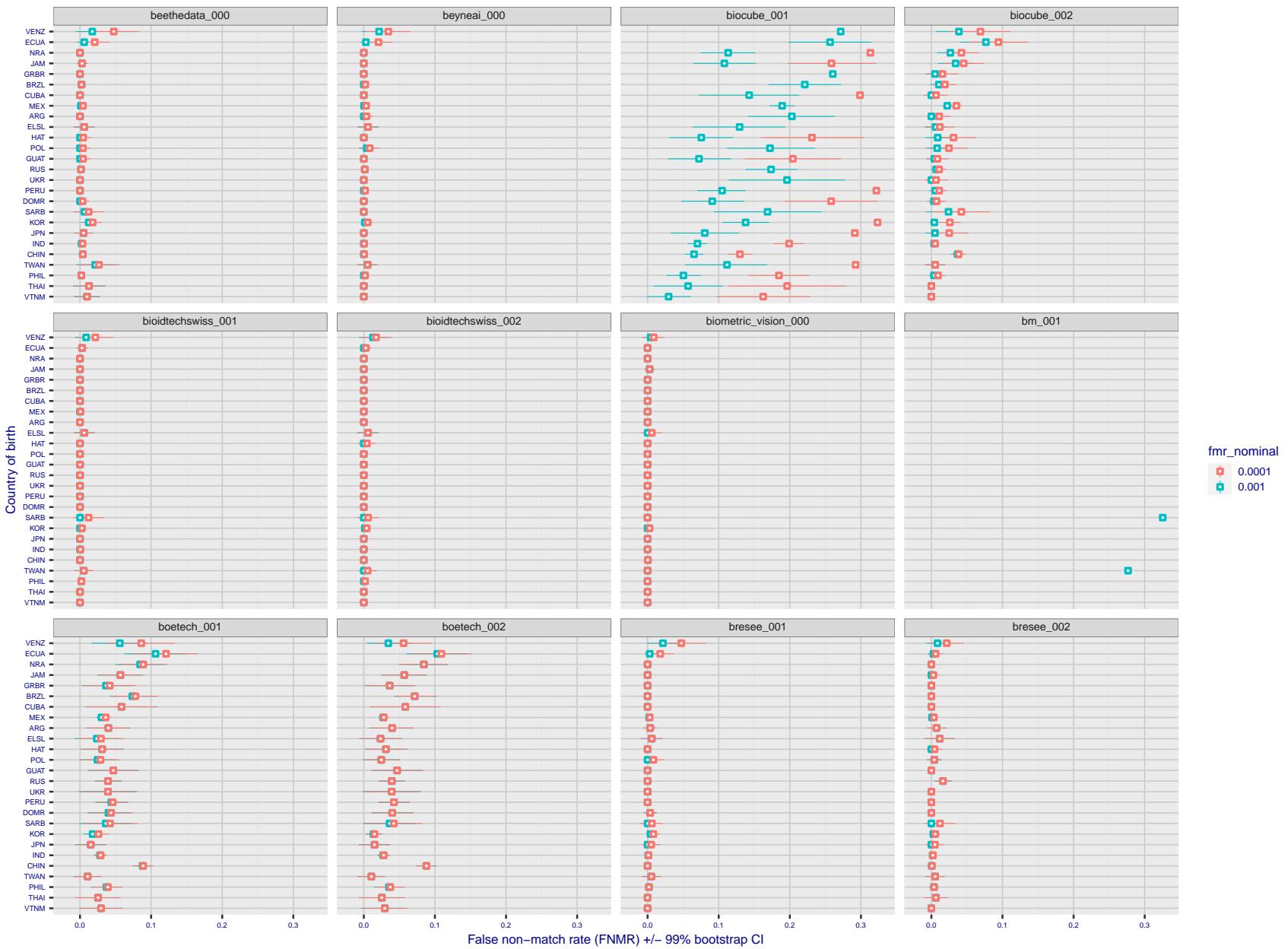


Figure 262: For the visa images, the dots show FNMR by country of birth for two globally set operating thresholds corresponding to $FMR = \{0.001, 0.0001\}$ computed over all on the order of 10^{10} impostor scores. The FMR in each bin will vary also - see subsequent impostor heatmaps in sec. 3.6.1. The figures shows an order of magnitude variation in FNMR across country of birth; these effects are likely due quality variations, then demographics like age and race. The error rates in some cases are zero, and in others the DET is flat so the error rates at the two thresholds are identical. The lines span 1% and 99% of bootstrap replicated FNMR estimates.

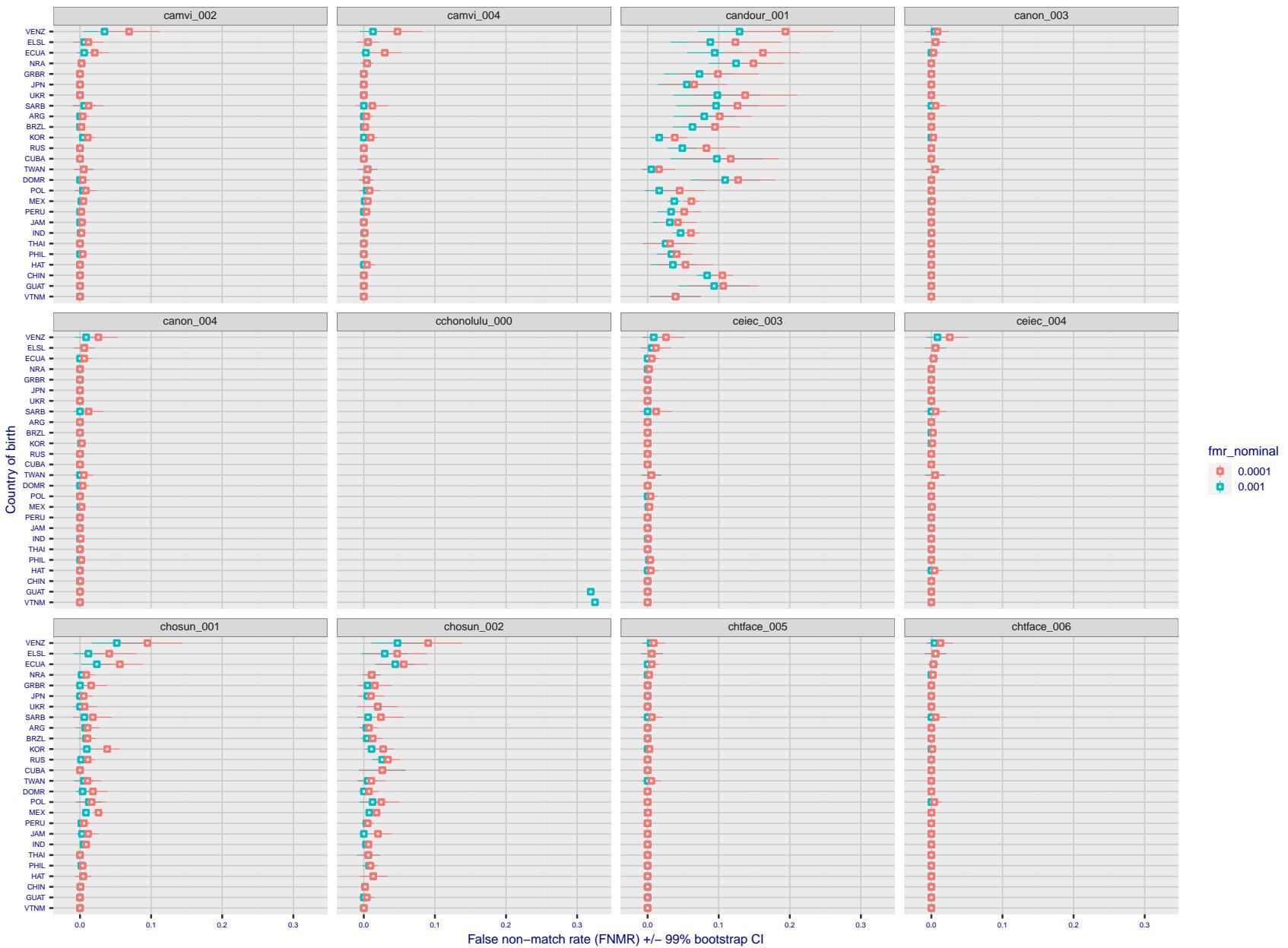


Figure 263: For the visa images, the dots show FNMR by country of birth for two globally set operating thresholds corresponding to $FMR = \{0.001, 0.0001\}$ computed over all on the order of 10^{10} impostor scores. The FMR in each bin will vary also - see subsequent impostor heatmaps in sec. 3.6.1. The figures shows an order of magnitude variation in FNMR across country of birth; these effects are likely due quality variations, then demographics like age and race. The error rates in some cases are zero, and in others the DET is flat so the error rates at the two thresholds are identical. The lines span 1% and 99% of bootstrap replicated FNMR estimates.

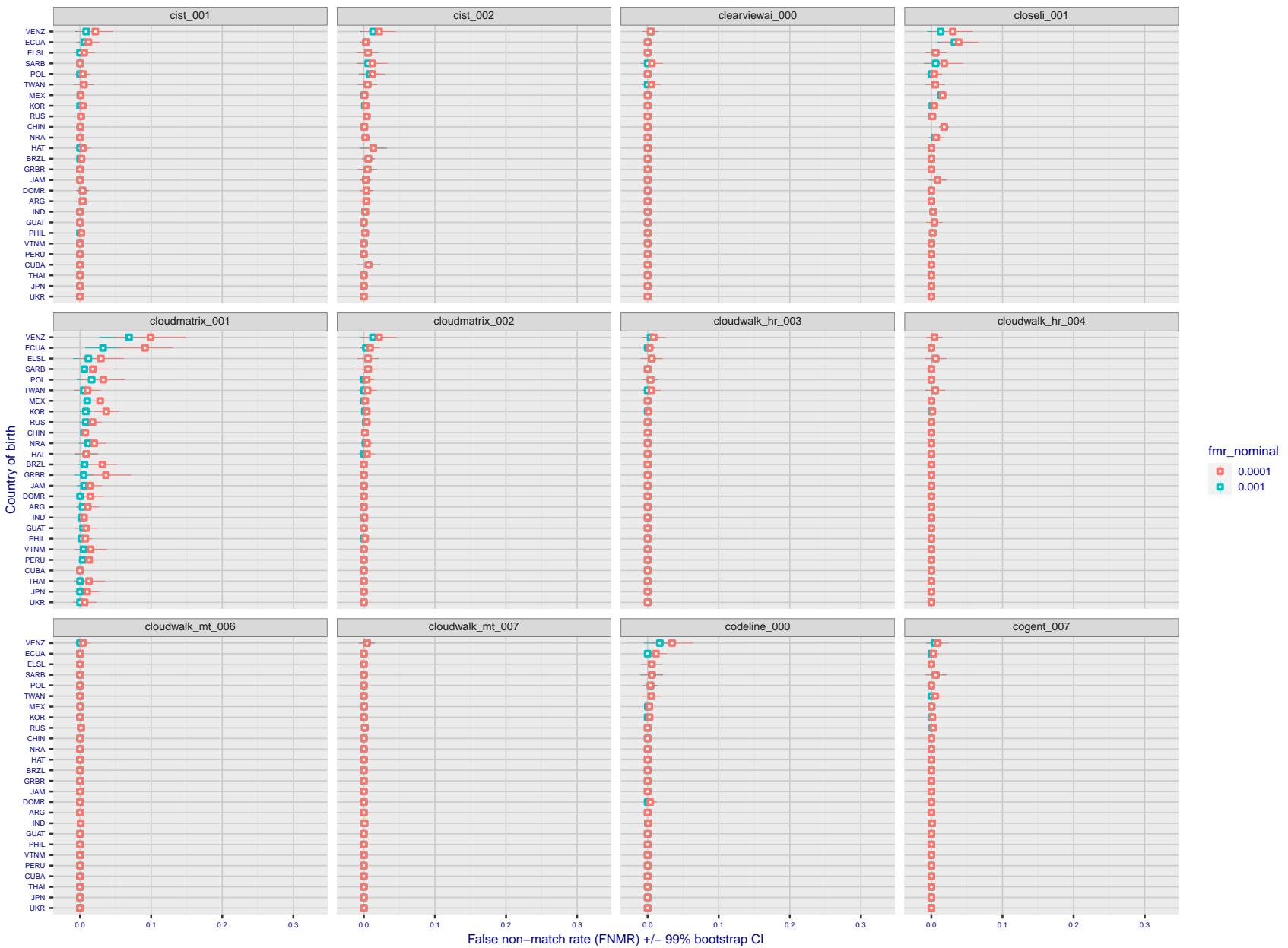


Figure 264: For the visa images, the dots show FNMR by country of birth for two globally set operating thresholds corresponding to $FMR = \{0.001, 0.0001\}$ computed over all on the order of 10^{10} impostor scores. The FMR in each bin will vary also - see subsequent impostor heatmaps in sec. 3.6.1. The figures shows an order of magnitude variation in FNMR across country of birth; these effects are likely due quality variations, then demographics like age and race. The error rates in some cases are zero, and in others the DET is flat so the error rates at the two thresholds are identical. The lines span 1% and 99% of bootstrap replicated FNMR estimates.

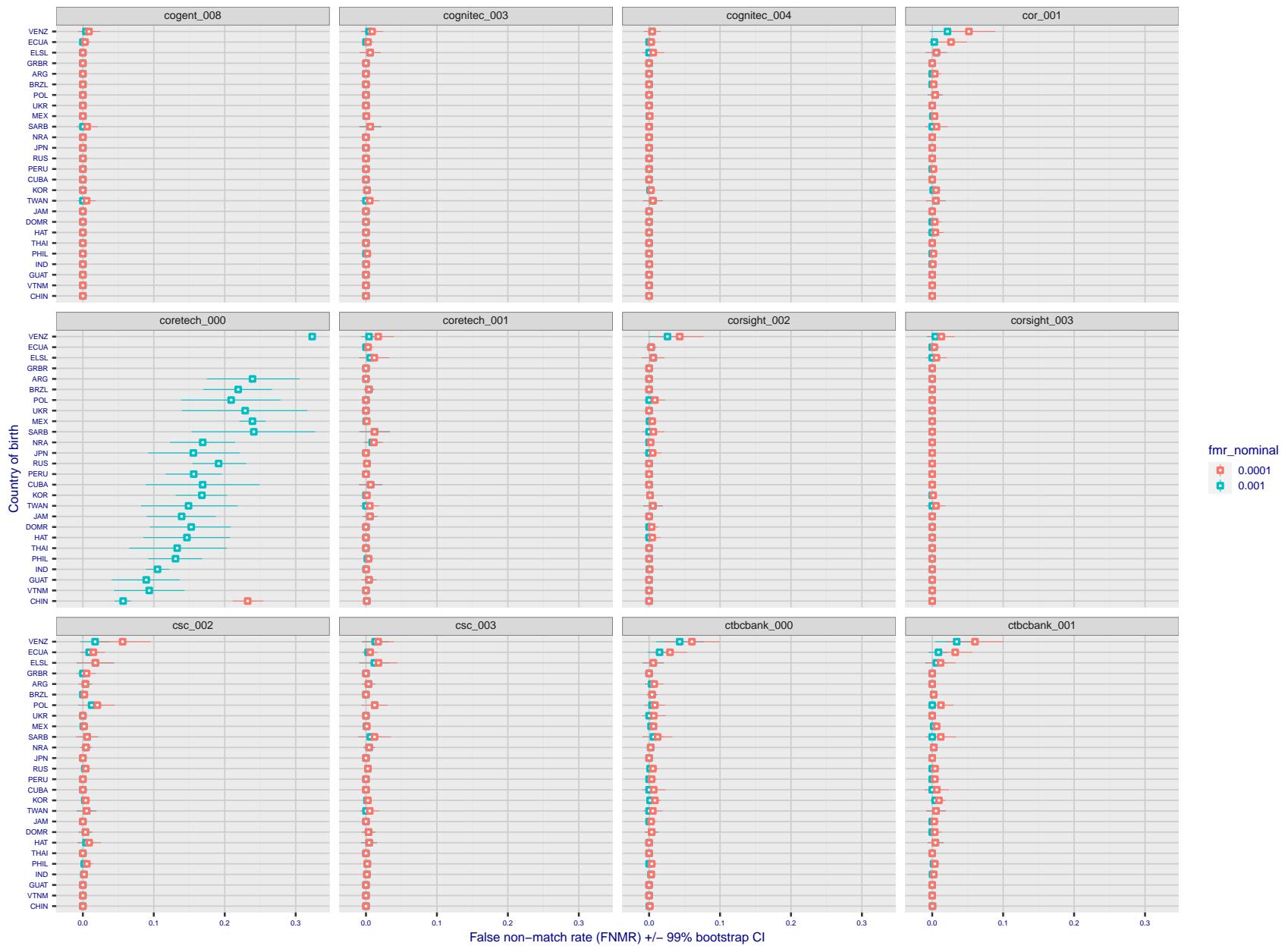


Figure 265: For the visa images, the dots show FNMR by country of birth for two globally set operating thresholds corresponding to $FMR = \{0.001, 0.0001\}$ computed over all on the order of 10^{10} impostor scores. The FMR in each bin will vary also - see subsequent impostor heatmaps in sec. 3.6.1. The figures shows an order of magnitude variation in FNMR across country of birth; these effects are likely due quality variations, then demographics like age and race. The error rates in some cases are zero, and in others the DET is flat so the error rates at the two thresholds are identical. The lines span 1% and 99% of bootstrap replicated FNMR estimates.

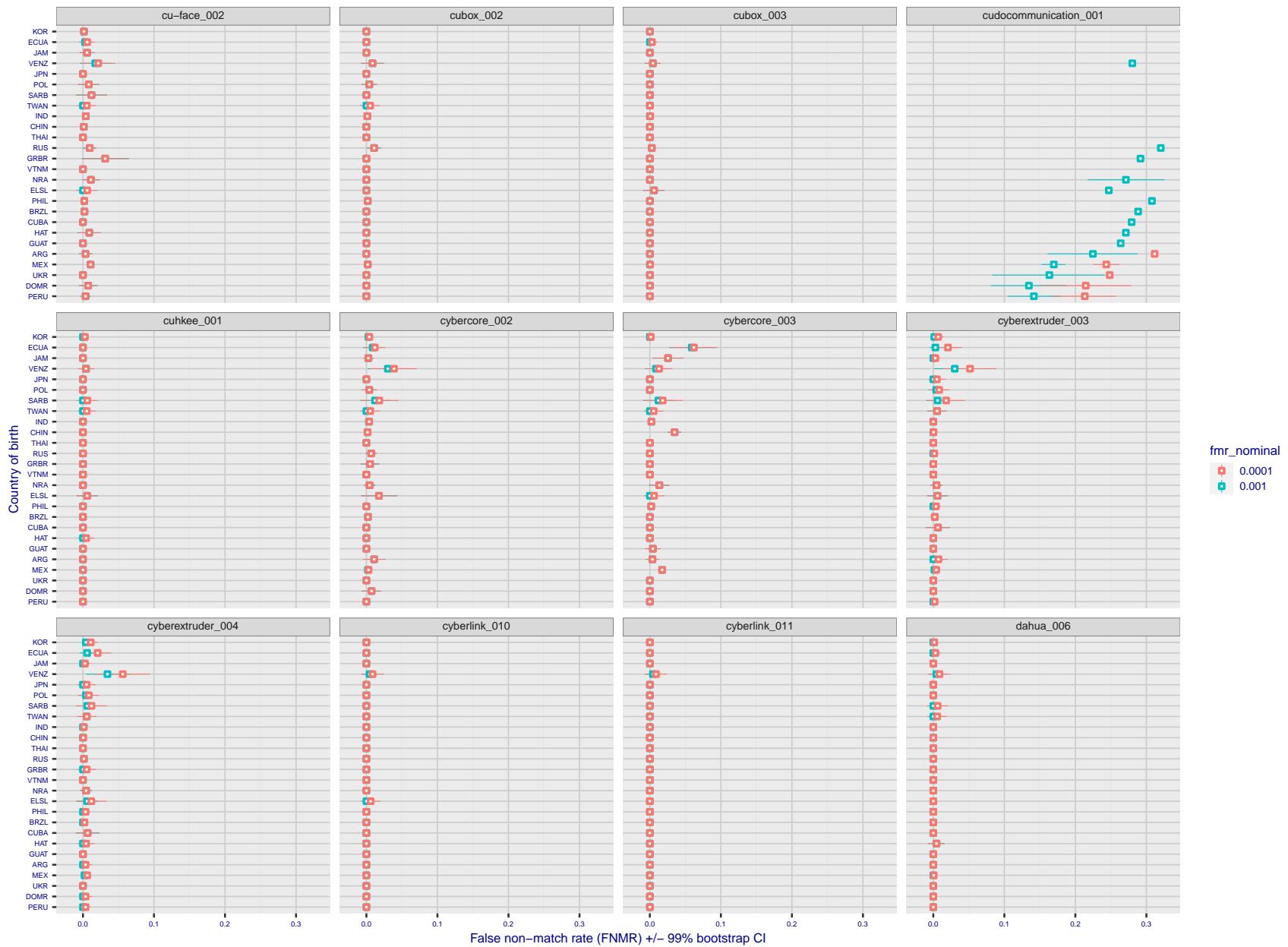


Figure 266: For the visa images, the dots show FNMR by country of birth for two globally set operating thresholds corresponding to $FMR = \{0.001, 0.0001\}$ computed over all on the order of 10^{10} impostor scores. The FMR in each bin will vary also - see subsequent impostor heatmaps in sec. 3.6.1. The figures shows an order of magnitude variation in FNMR across country of birth; these effects are likely due quality variations, then demographics like age and race. The error rates in some cases are zero, and in others the DET is flat so the error rates at the two thresholds are identical. The lines span 1% and 99% of bootstrap replicated FNMR estimates.

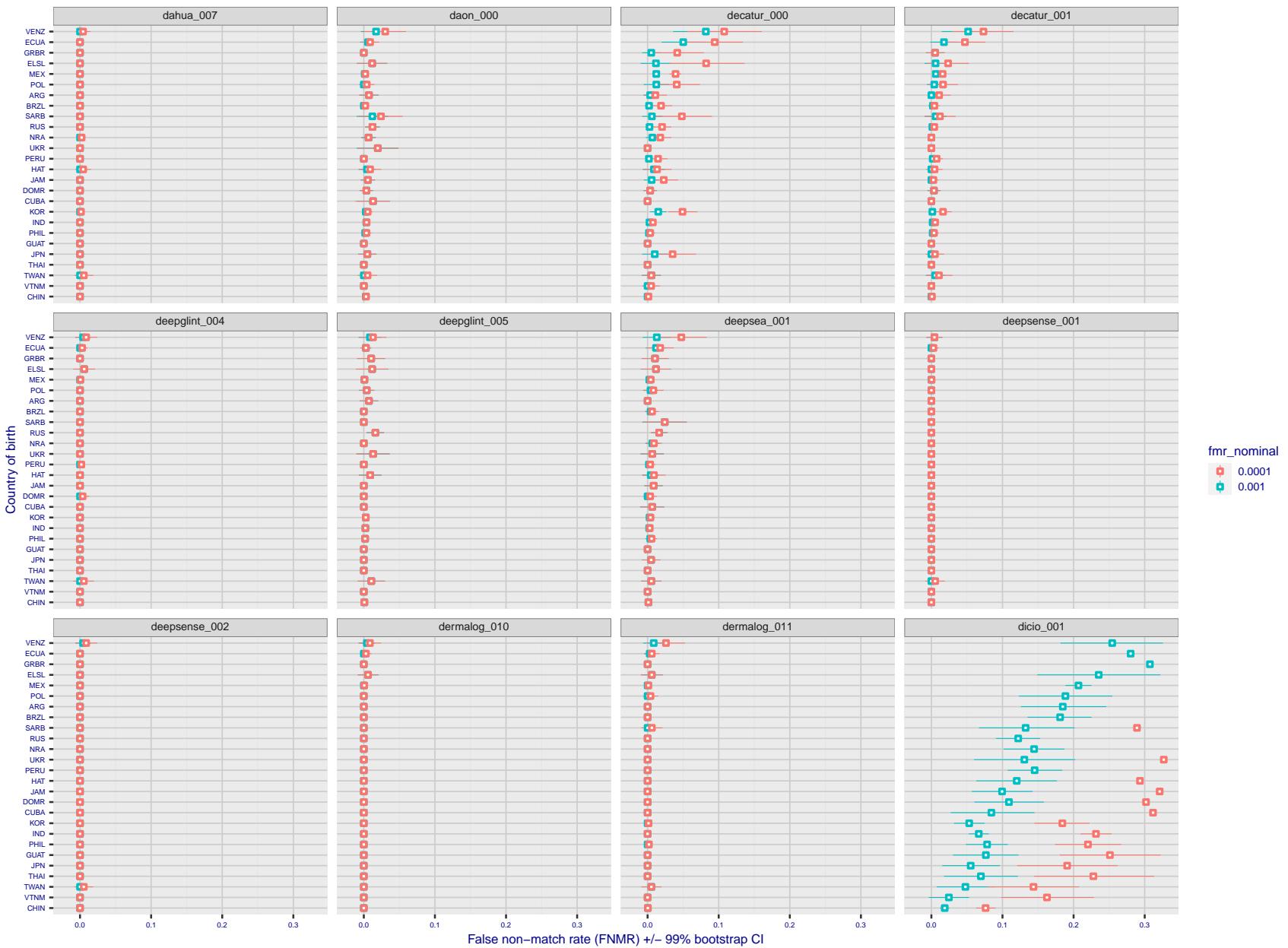


Figure 267: For the visa images, the dots show FNMR by country of birth for two globally set operating thresholds corresponding to $FMR = \{0.001, 0.0001\}$ computed over all on the order of 10^{10} impostor scores. The FMR in each bin will vary also - see subsequent impostor heatmaps in sec. 3.6.1. The figures shows an order of magnitude variation in FNMR across country of birth; these effects are likely due quality variations, then demographics like age and race. The error rates in some cases are zero, and in others the DET is flat so the error rates at the two thresholds are identical. The lines span 1% and 99% of bootstrap replicated FNMR estimates.

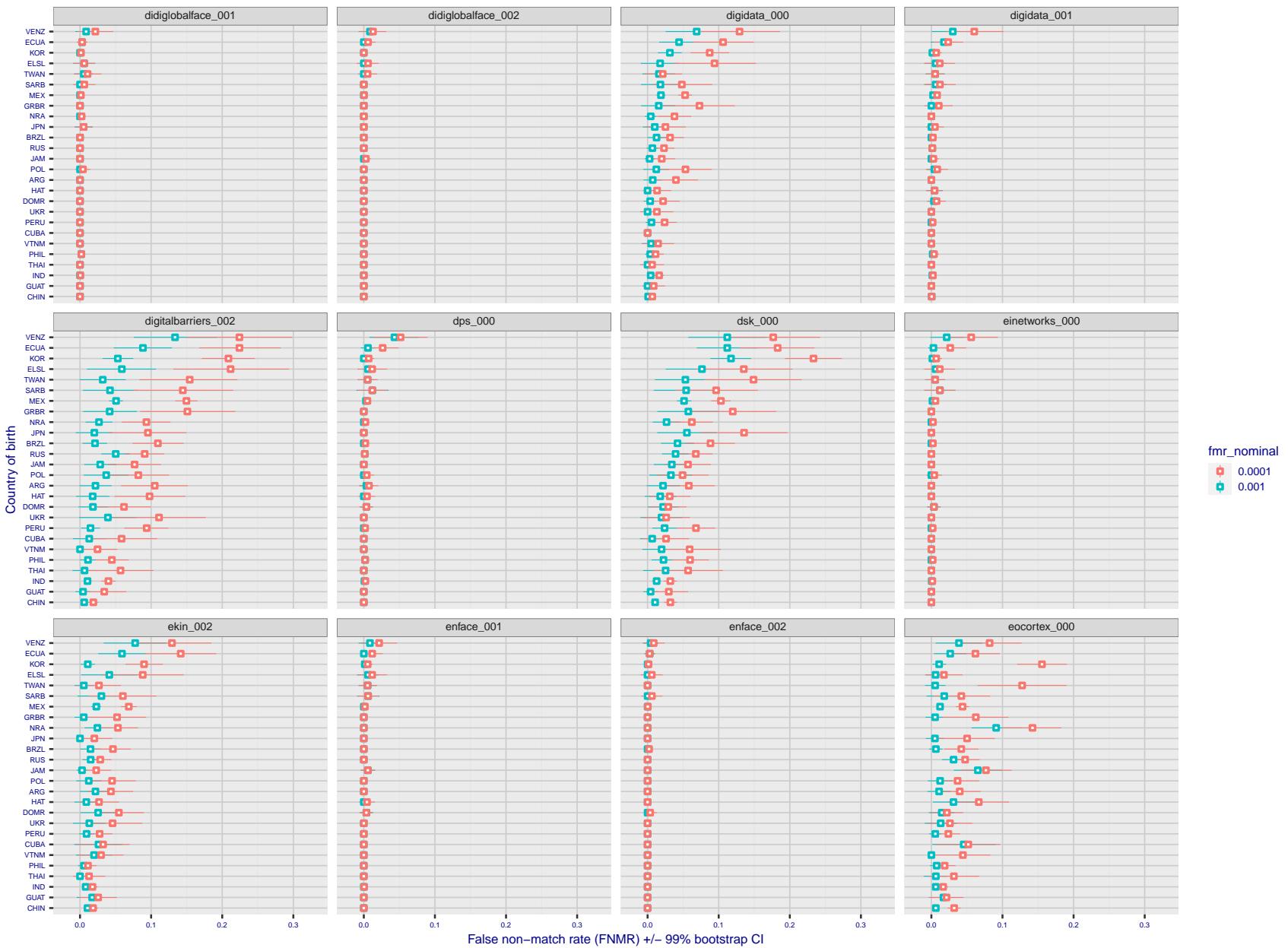


Figure 268: For the visa images, the dots show FNMR by country of birth for two globally set operating thresholds corresponding to $FMR = \{0.001, 0.0001\}$ computed over all on the order of 10^{10} impostor scores. The FMR in each bin will vary also - see subsequent impostor heatmaps in sec. 3.6.1. The figures shows an order of magnitude variation in FNMR across country of birth; these effects are likely due quality variations, then demographics like age and race. The error rates in some cases are zero, and in others the DET is flat so the error rates at the two thresholds are identical. The lines span 1% and 99% of bootstrap replicated FNMR estimates.

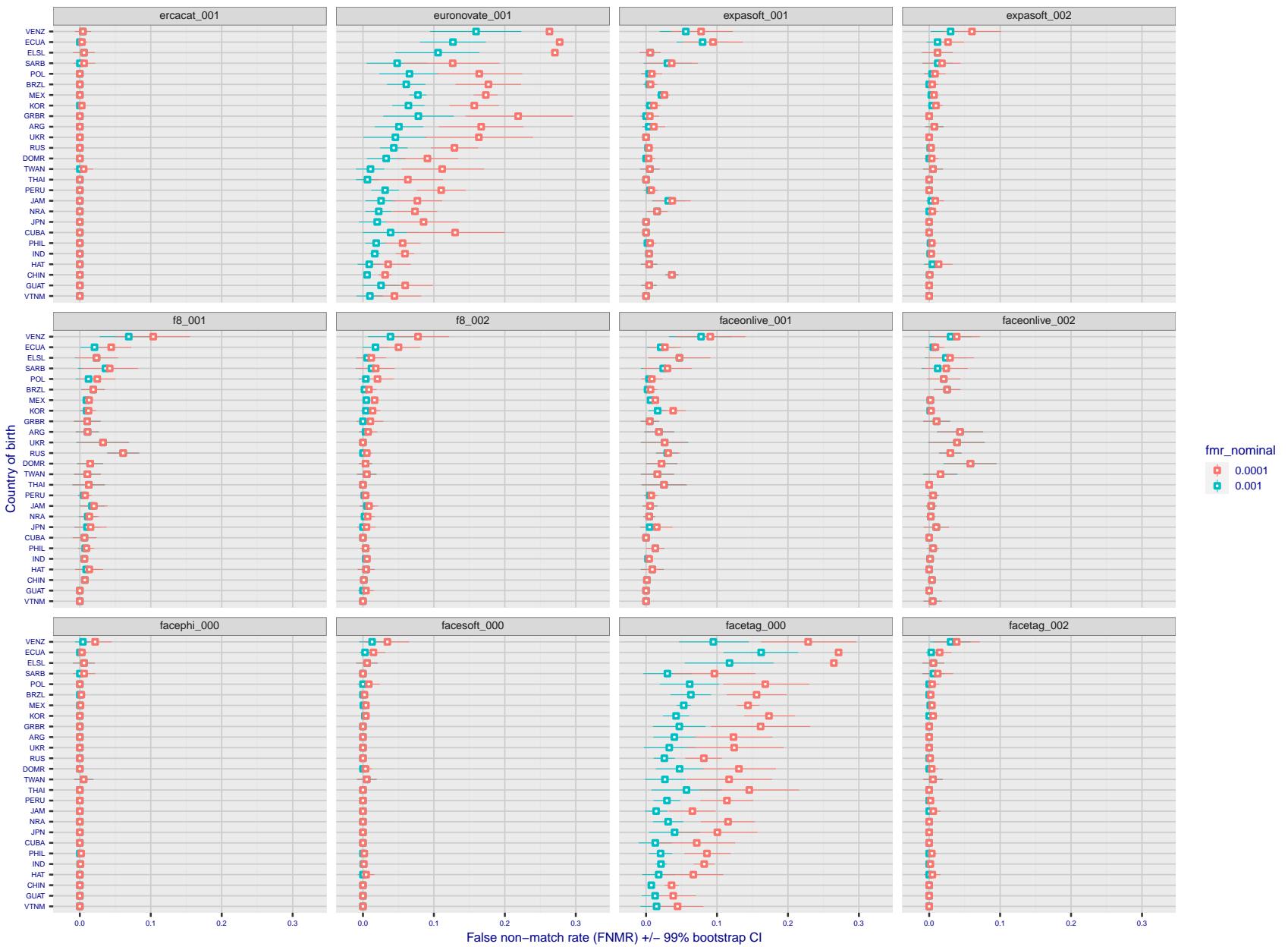


Figure 269: For the visa images, the dots show FNMR by country of birth for two globally set operating thresholds corresponding to $FMR = \{0.001, 0.0001\}$ computed over all on the order of 10^{10} impostor scores. The FMR in each bin will vary also - see subsequent impostor heatmaps in sec. 3.6.1. The figures shows an order of magnitude variation in FNMR across country of birth; these effects are likely due quality variations, then demographics like age and race. The error rates in some cases are zero, and in others the DET is flat so the error rates at the two thresholds are identical. The lines span 1% and 99% of bootstrap replicated FNMR estimates.

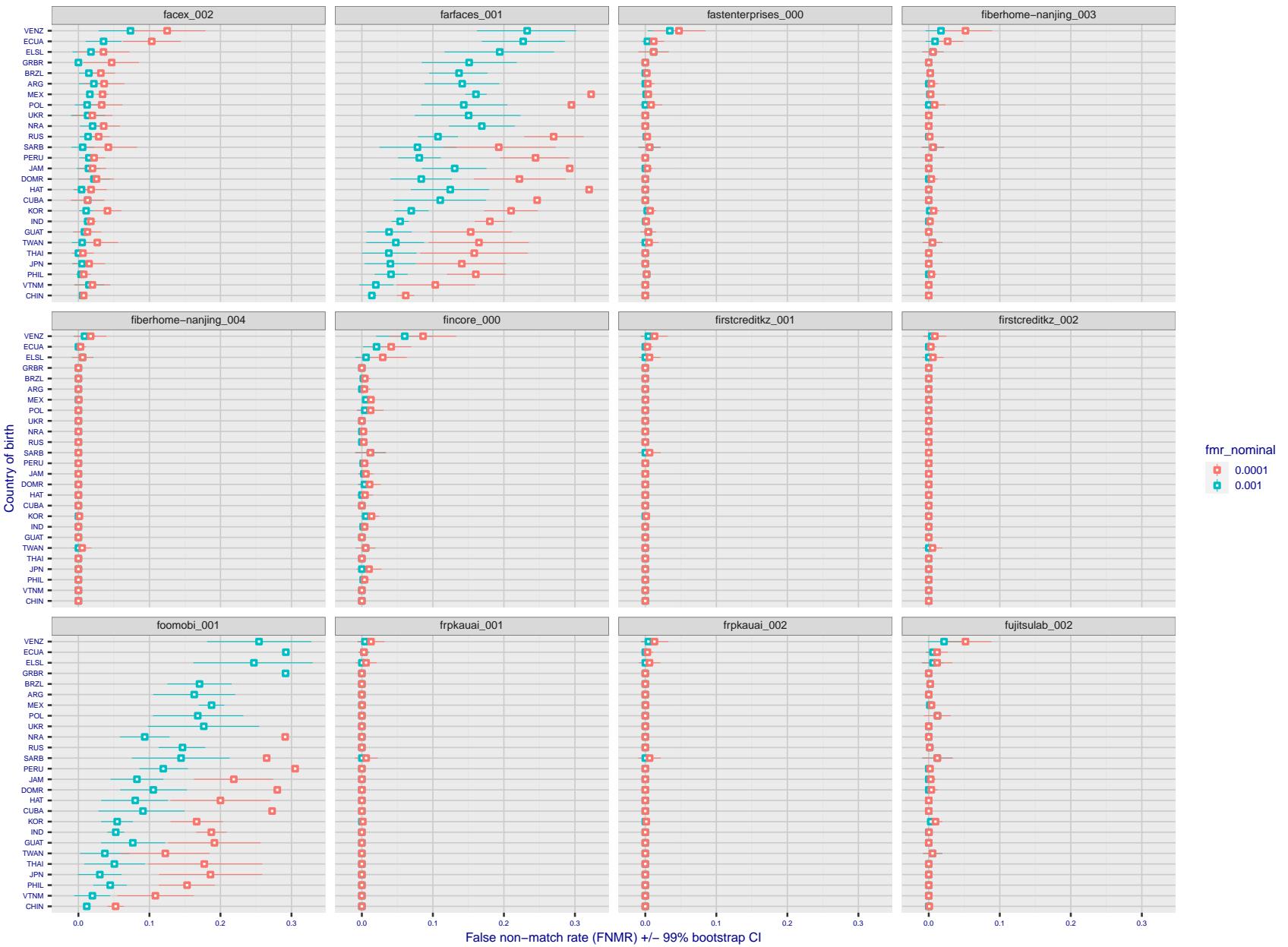


Figure 270: For the visa images, the dots show FNMR by country of birth for two globally set operating thresholds corresponding to $FMR = \{0.001, 0.0001\}$ computed over all on the order of 10^{10} impostor scores. The FMR in each bin will vary also - see subsequent impostor heatmaps in sec. 3.6.1. The figures shows an order of magnitude variation in FNMR across country of birth; these effects are likely due quality variations, then demographics like age and race. The error rates in some cases are zero, and in others the DET is flat so the error rates at the two thresholds are identical. The lines span 1% and 99% of bootstrap replicated FNMR estimates.

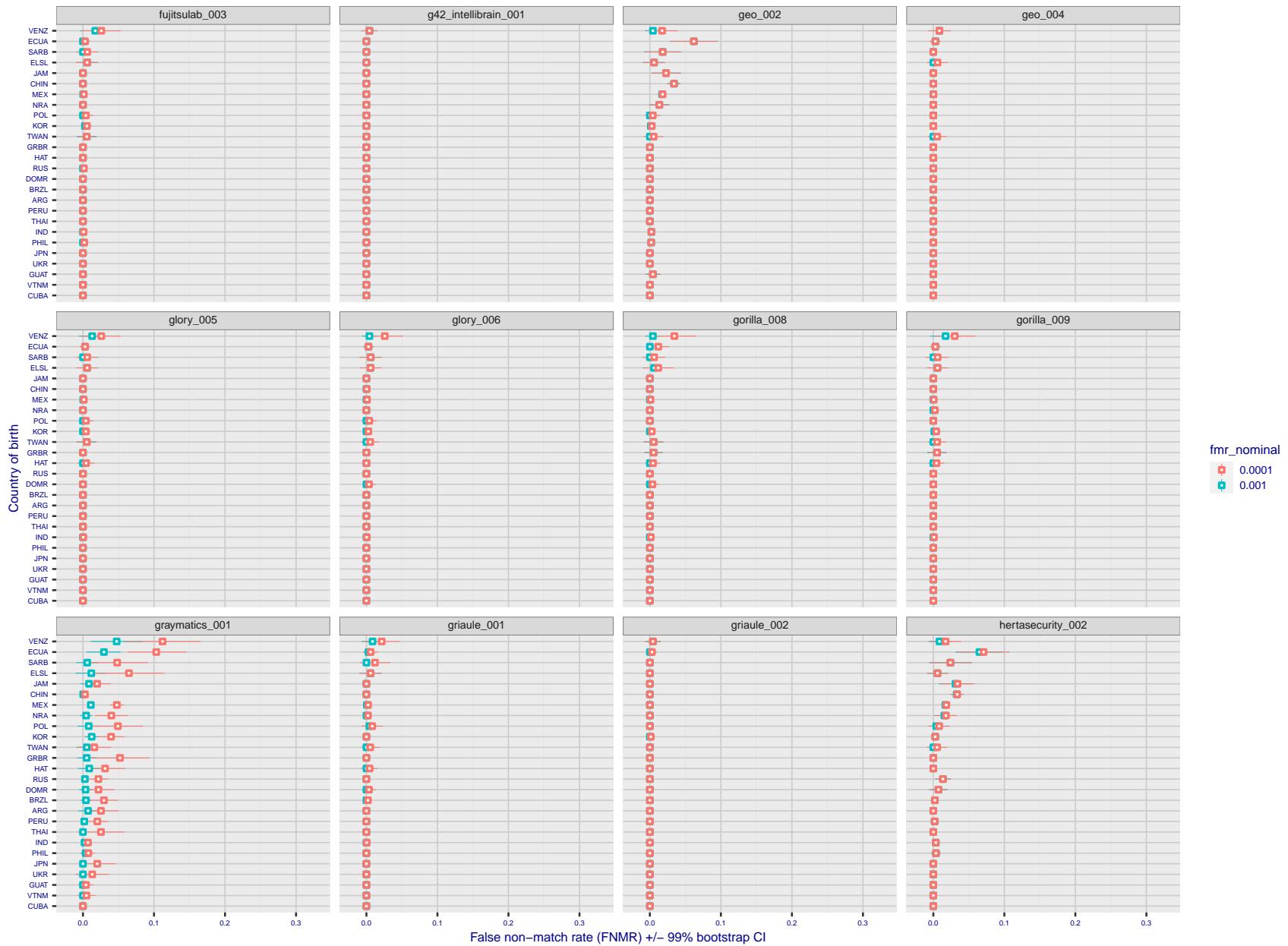


Figure 271: For the visa images, the dots show FNMR by country of birth for two globally set operating thresholds corresponding to $FMR = \{0.001, 0.0001\}$ computed over all on the order of 10^{10} impostor scores. The FMR in each bin will vary also - see subsequent impostor heatmaps in sec. 3.6.1. The figures shows an order of magnitude variation in FNMR across country of birth; these effects are likely due quality variations, then demographics like age and race. The error rates in some cases are zero, and in others the DET is flat so the error rates at the two thresholds are identical. The lines span 1% and 99% of bootstrap replicated FNMR estimates.

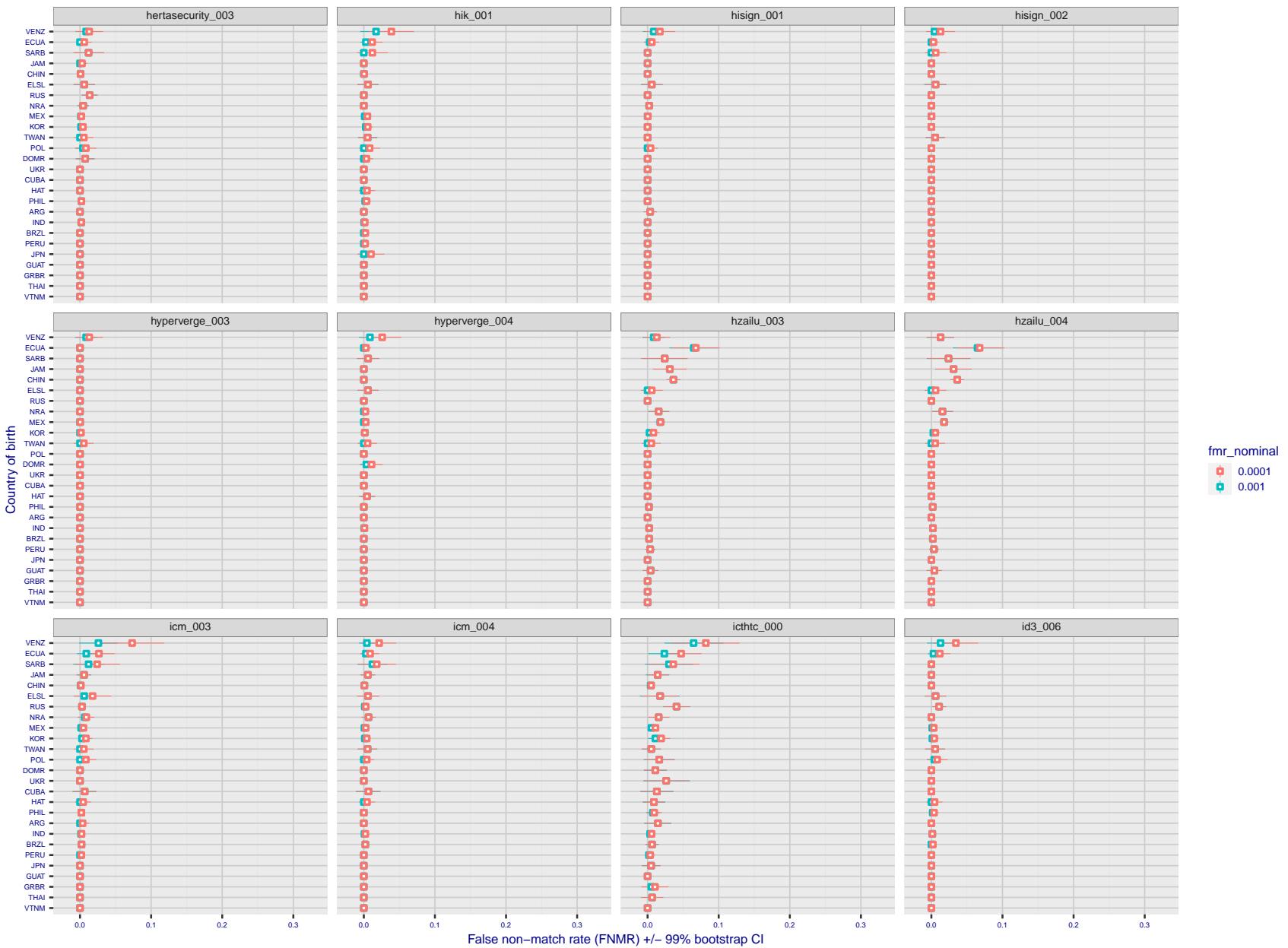


Figure 272: For the visa images, the dots show FNMR by country of birth for two globally set operating thresholds corresponding to $FMR = \{0.001, 0.0001\}$ computed over all on the order of 10^{10} impostor scores. The FMR in each bin will vary also - see subsequent impostor heatmaps in sec. 3.6.1. The figures shows an order of magnitude variation in FNMR across country of birth; these effects are likely due quality variations, then demographics like age and race. The error rates in some cases are zero, and in others the DET is flat so the error rates at the two thresholds are identical. The lines span 1% and 99% of bootstrap replicated FNMR estimates.

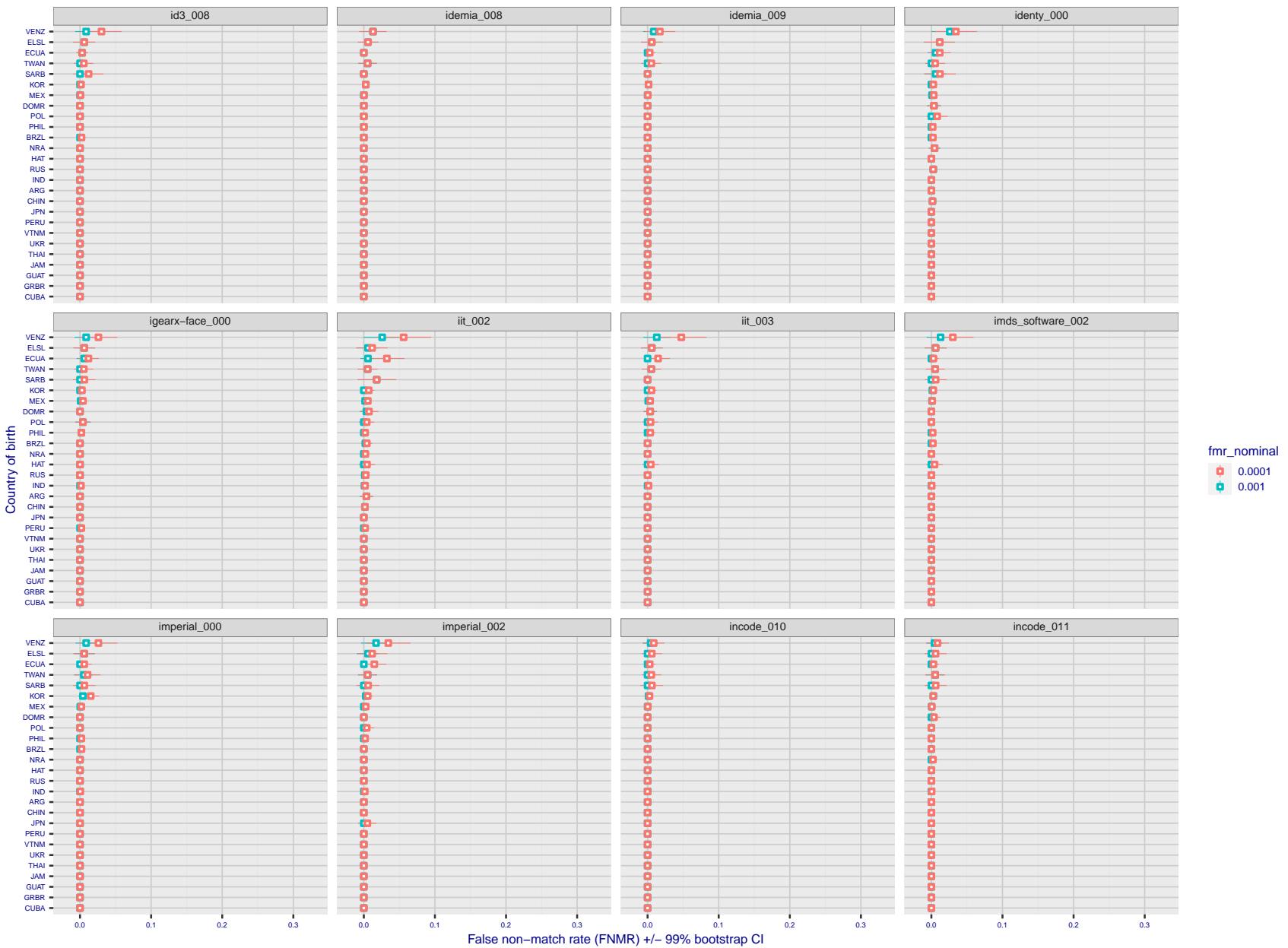


Figure 273: For the visa images, the dots show FNMR by country of birth for two globally set operating thresholds corresponding to $FMR = \{0.001, 0.0001\}$ computed over all on the order of 10^{10} impostor scores. The FMR in each bin will vary also - see subsequent impostor heatmaps in sec. 3.6.1. The figures shows an order of magnitude variation in FNMR across country of birth; these effects are likely due quality variations, then demographics like age and race. The error rates in some cases are zero, and in others the DET is flat so the error rates at the two thresholds are identical. The lines span 1% and 99% of bootstrap replicated FNMR estimates.

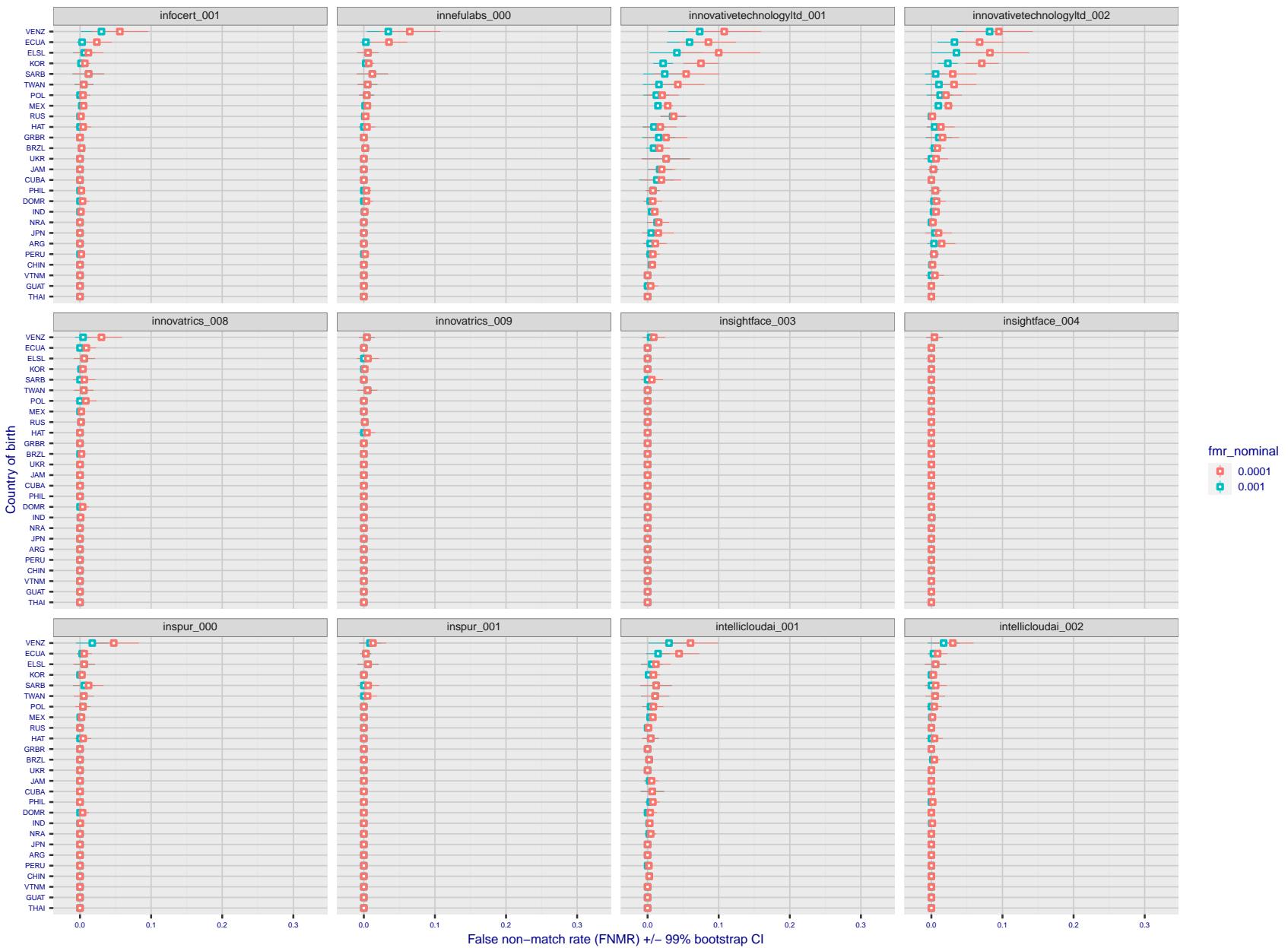


Figure 274: For the visa images, the dots show FNMR by country of birth for two globally set operating thresholds corresponding to $FMR = \{0.001, 0.0001\}$ computed over all on the order of 10^{10} impostor scores. The FMR in each bin will vary also - see subsequent impostor heatmaps in sec. 3.6.1. The figures shows an order of magnitude variation in FNMR across country of birth; these effects are likely due quality variations, then demographics like age and race. The error rates in some cases are zero, and in others the DET is flat so the error rates at the two thresholds are identical. The lines span 1% and 99% of bootstrap replicated FNMR estimates.

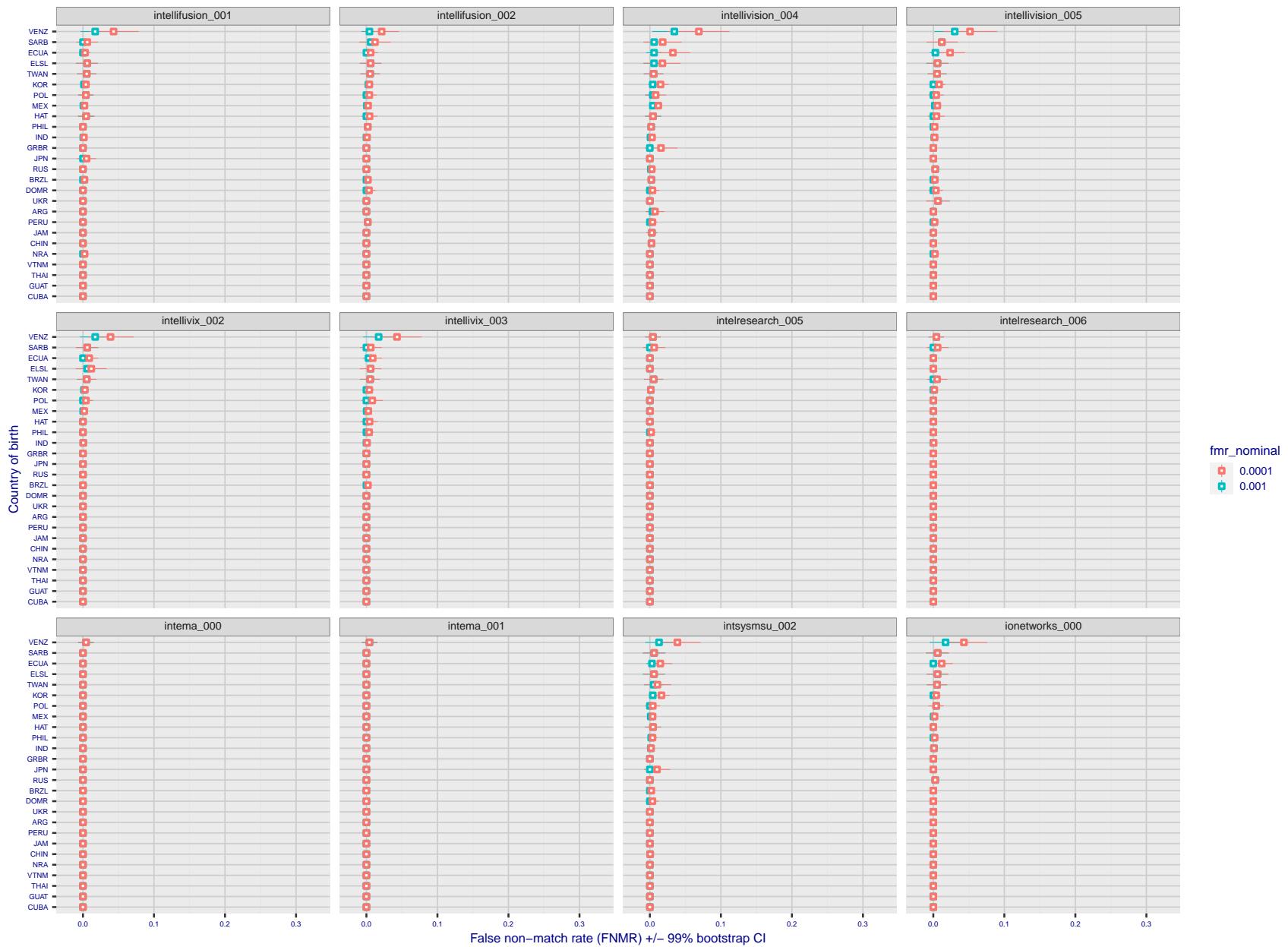


Figure 275: For the visa images, the dots show FNMR by country of birth for two globally set operating thresholds corresponding to $FMR = \{0.001, 0.0001\}$ computed over all on the order of 10^{10} impostor scores. The FMR in each bin will vary also - see subsequent impostor heatmaps in sec. 3.6.1. The figures shows an order of magnitude variation in FNMR across country of birth; these effects are likely due quality variations, then demographics like age and race. The error rates in some cases are zero, and in others the DET is flat so the error rates at the two thresholds are identical. The lines span 1% and 99% of bootstrap replicated FNMR estimates.

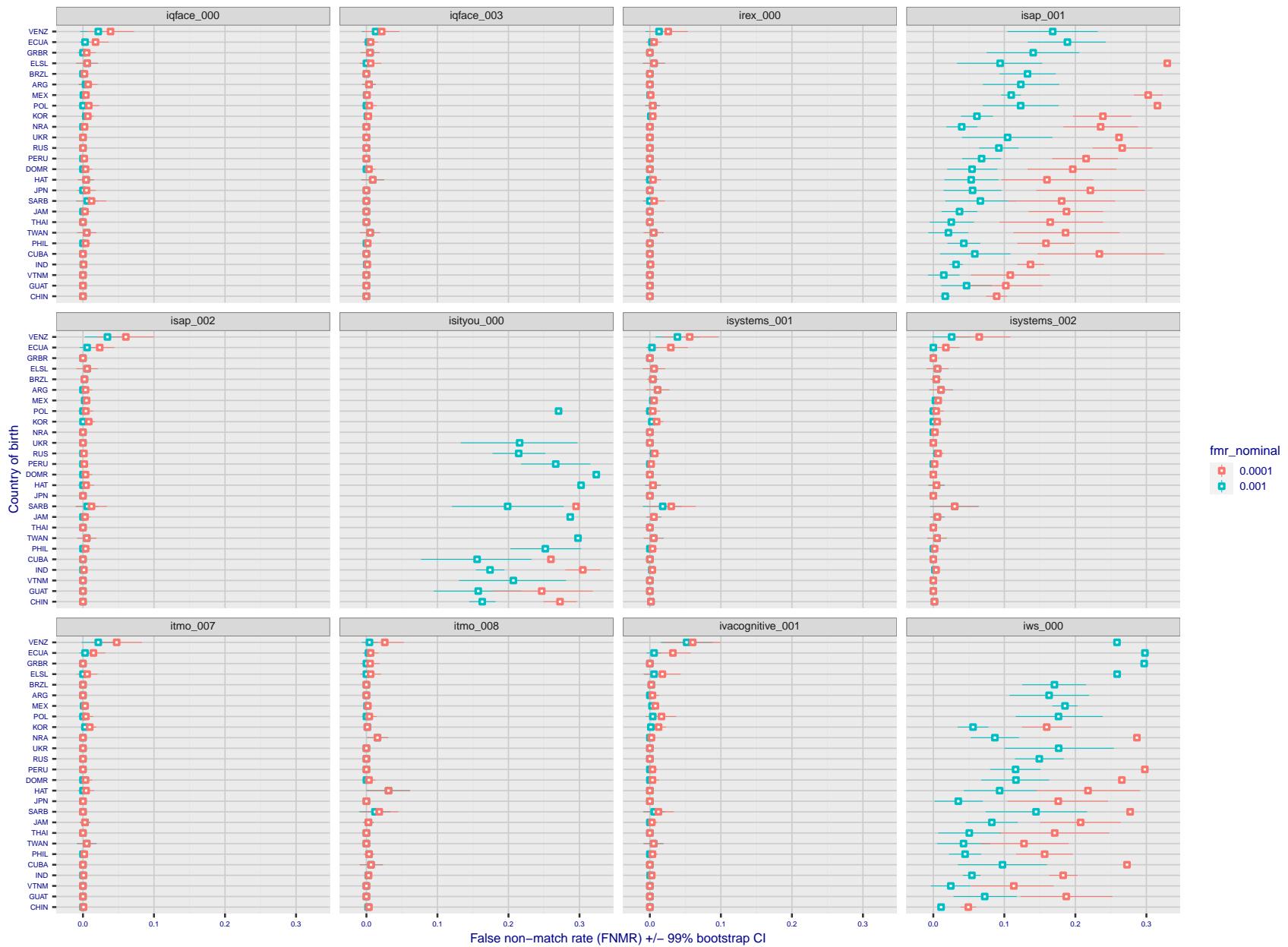


Figure 276: For the visa images, the dots show FNMR by country of birth for two globally set operating thresholds corresponding to $FMR = \{0.001, 0.0001\}$ computed over all on the order of 10^{10} impostor scores. The FMR in each bin will vary also - see subsequent impostor heatmaps in sec. 3.6.1. The figures shows an order of magnitude variation in FNMR across country of birth; these effects are likely due quality variations, then demographics like age and race. The error rates in some cases are zero, and in others the DET is flat so the error rates at the two thresholds are identical. The lines span 1% and 99% of bootstrap replicated FNMR estimates.

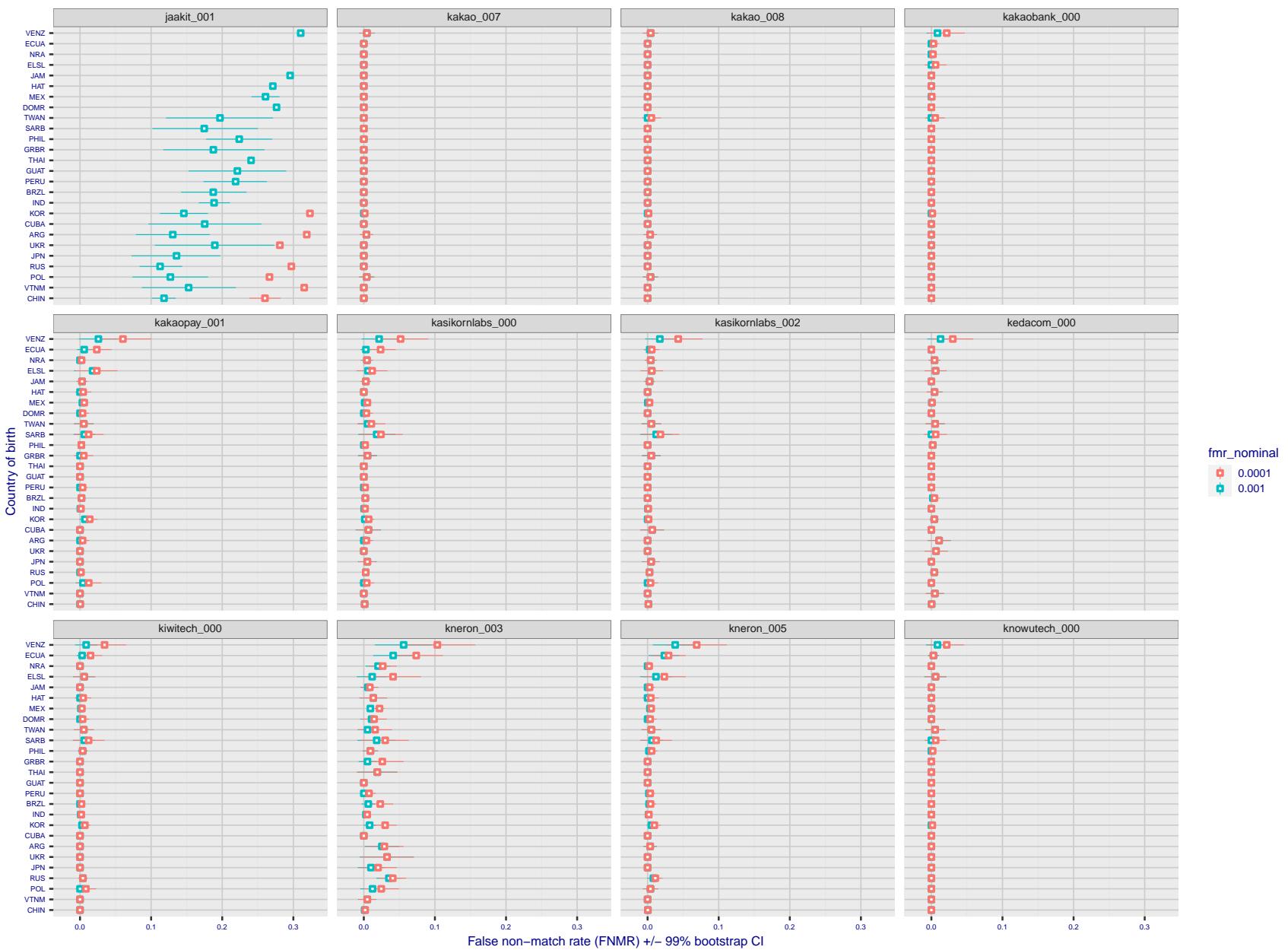


Figure 277: For the visa images, the dots show FNMR by country of birth for two globally set operating thresholds corresponding to $FMR = \{0.001, 0.0001\}$ computed over all on the order of 10^{10} impostor scores. The FMR in each bin will vary also - see subsequent impostor heatmaps in sec. 3.6.1. The figures shows an order of magnitude variation in FNMR across country of birth; these effects are likely due quality variations, then demographics like age and race. The error rates in some cases are zero, and in others the DET is flat so the error rates at the two thresholds are identical. The lines span 1% and 99% of bootstrap replicated FNMR estimates.

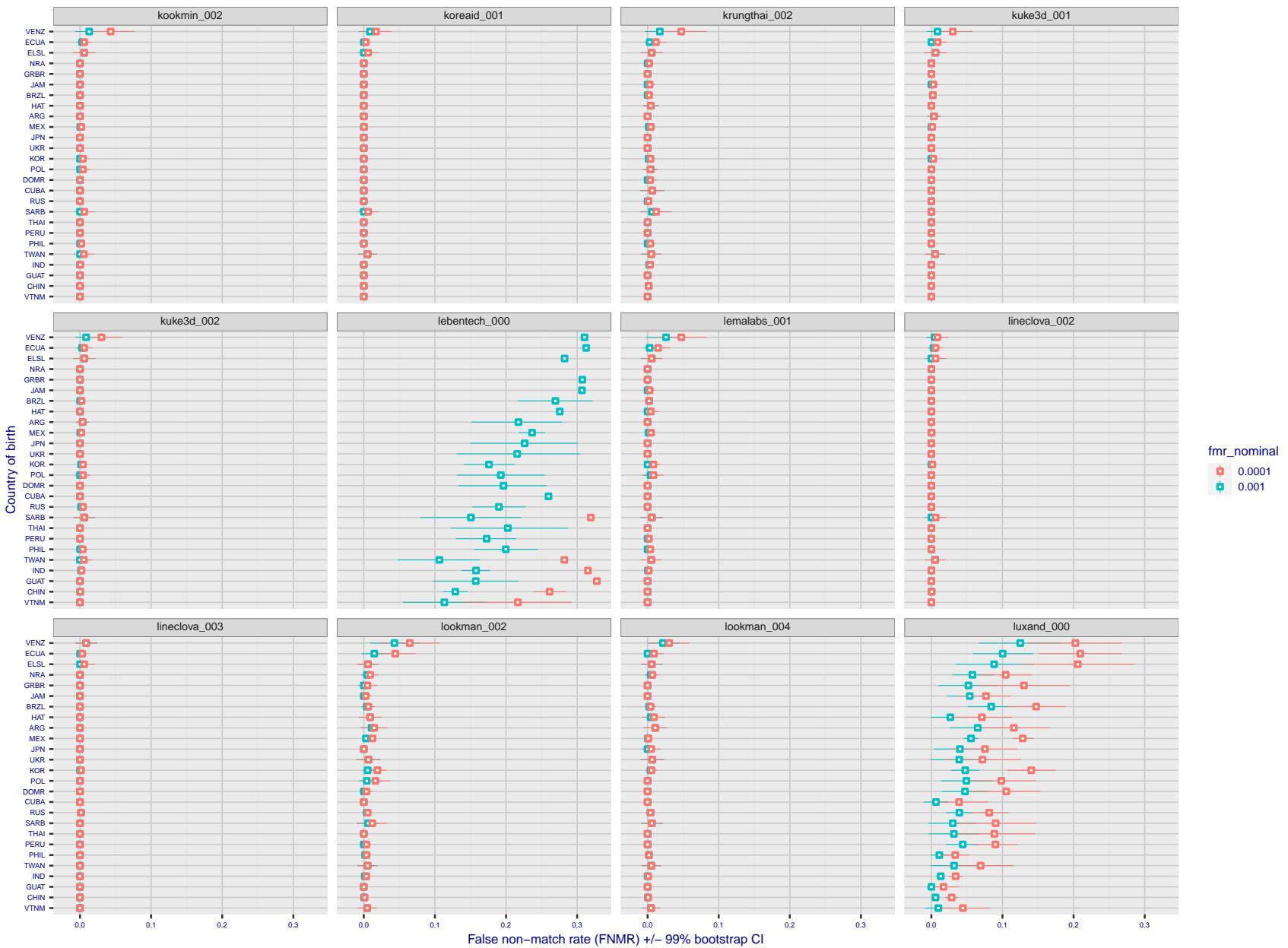


Figure 278: For the visa images, the dots show FNMR by country of birth for two globally set operating thresholds corresponding to $FMR = \{0.001, 0.0001\}$ computed over all on the order of 10^{10} impostor scores. The FMR in each bin will vary also - see subsequent impostor heatmaps in sec. 3.6.1. The figures shows an order of magnitude variation in FNMR across country of birth; these effects are likely due quality variations, then demographics like age and race. The error rates in some cases are zero, and in others the DET is flat so the error rates at the two thresholds are identical. The lines span 1% and 99% of bootstrap replicated FNMR estimates.

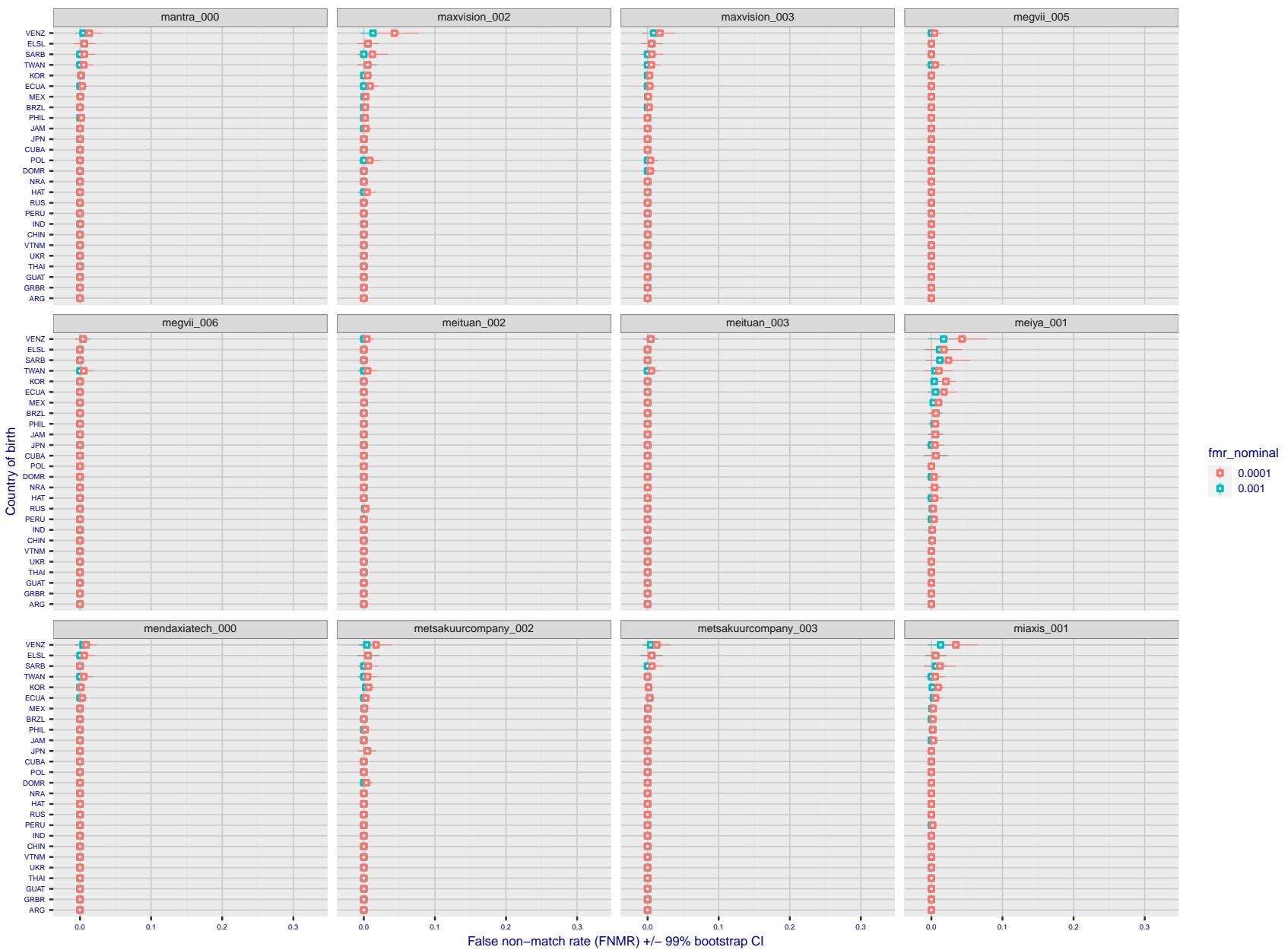


Figure 279: For the visa images, the dots show FNMR by country of birth for two globally set operating thresholds corresponding to $FMR = \{0.001, 0.0001\}$ computed over all on the order of 10^{10} impostor scores. The FMR in each bin will vary also - see subsequent impostor heatmaps in sec. 3.6.1. The figures shows an order of magnitude variation in FNMR across country of birth; these effects are likely due quality variations, then demographics like age and race. The error rates in some cases are zero, and in others the DET is flat so the error rates at the two thresholds are identical. The lines span 1% and 99% of bootstrap replicated FNMR estimates.

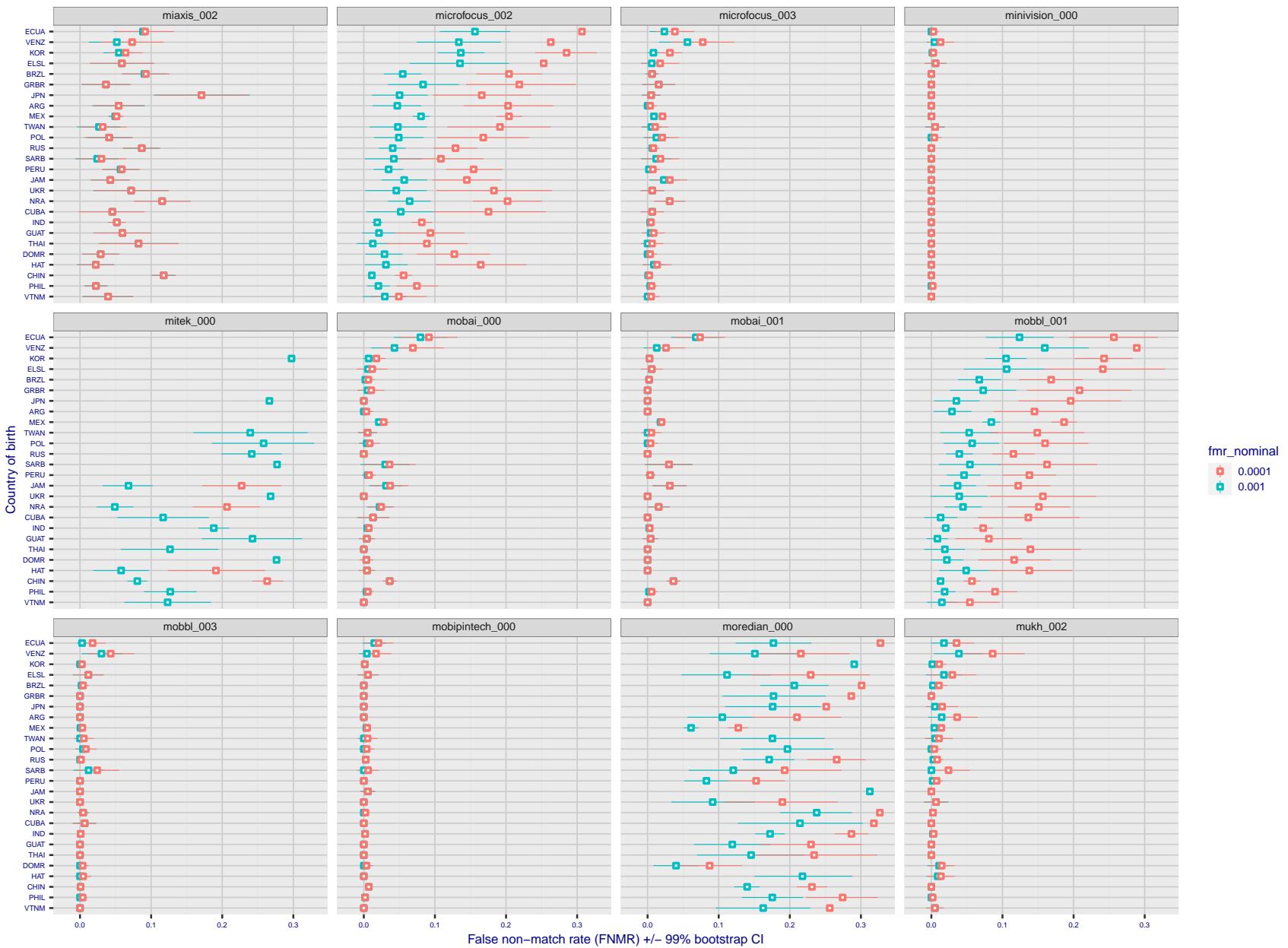


Figure 280: For the visa images, the dots show FNMR by country of birth for two globally set operating thresholds corresponding to $FMR = \{0.001, 0.0001\}$ computed over all on the order of 10^{10} impostor scores. The FMR in each bin will vary also - see subsequent impostor heatmaps in sec. 3.6.1. The figures shows an order of magnitude variation in FNMR across country of birth; these effects are likely due quality variations, then demographics like age and race. The error rates in some cases are zero, and in others the DET is flat so the error rates at the two thresholds are identical. The lines span 1% and 99% of bootstrap replicated FNMR estimates.

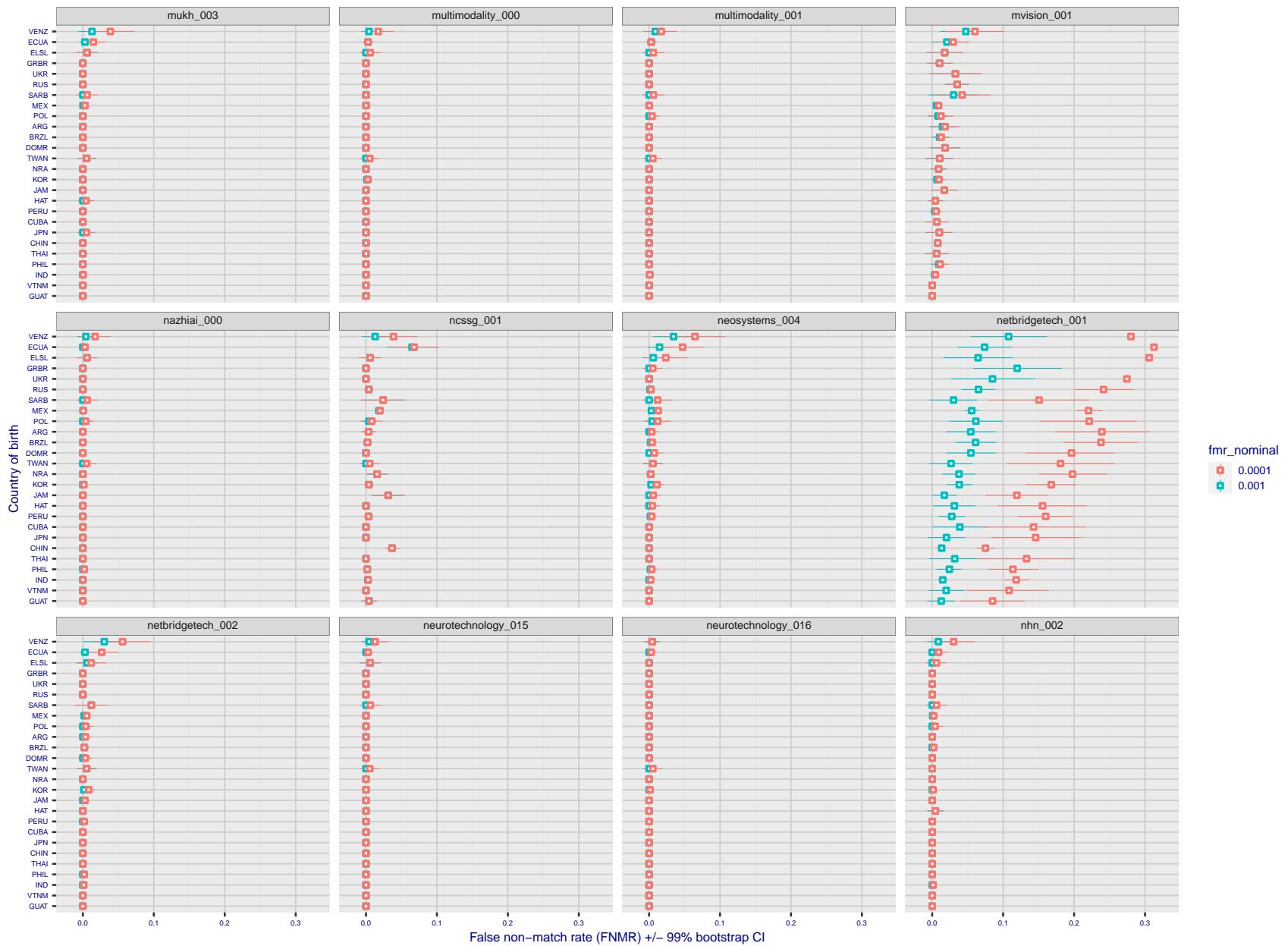


Figure 281: For the visa images, the dots show FNMR by country of birth for two globally set operating thresholds corresponding to $FMR = \{0.001, 0.0001\}$ computed over all on the order of 10^{10} impostor scores. The FMR in each bin will vary also - see subsequent impostor heatmaps in sec. 3.6.1. The figures shows an order of magnitude variation in FNMR across country of birth; these effects are likely due quality variations, then demographics like age and race. The error rates in some cases are zero, and in others the DET is flat so the error rates at the two thresholds are identical. The lines span 1% and 99% of bootstrap replicated FNMR estimates.

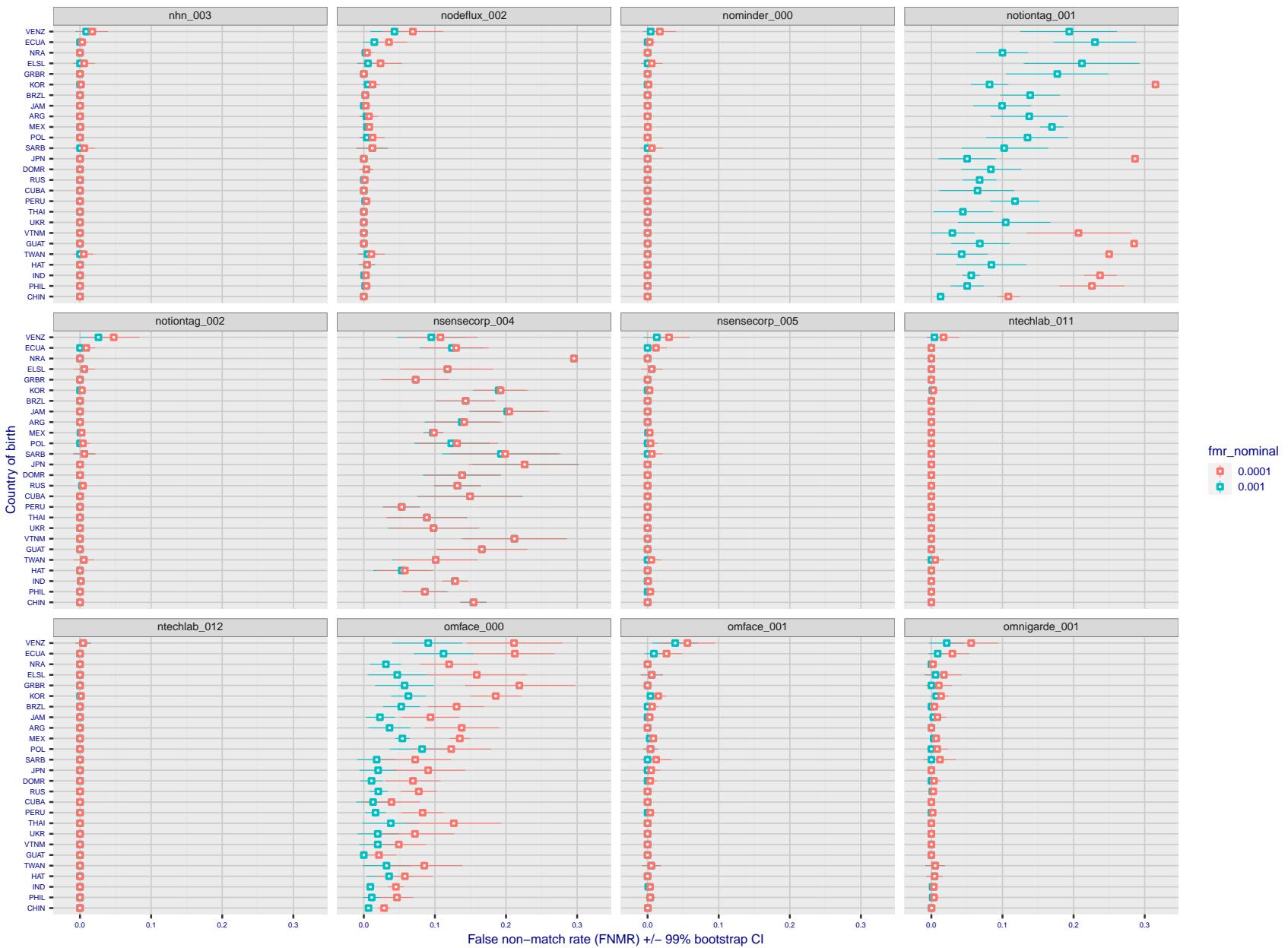


Figure 282: For the visa images, the dots show FNMR by country of birth for two globally set operating thresholds corresponding to $FMR = \{0.001, 0.0001\}$ computed over all on the order of 10^{10} impostor scores. The FMR in each bin will vary also - see subsequent impostor heatmaps in sec. 3.6.1. The figures shows an order of magnitude variation in FNMR across country of birth; these effects are likely due quality variations, then demographics like age and race. The error rates in some cases are zero, and in others the DET is flat so the error rates at the two thresholds are identical. The lines span 1% and 99% of bootstrap replicated FNMR estimates.

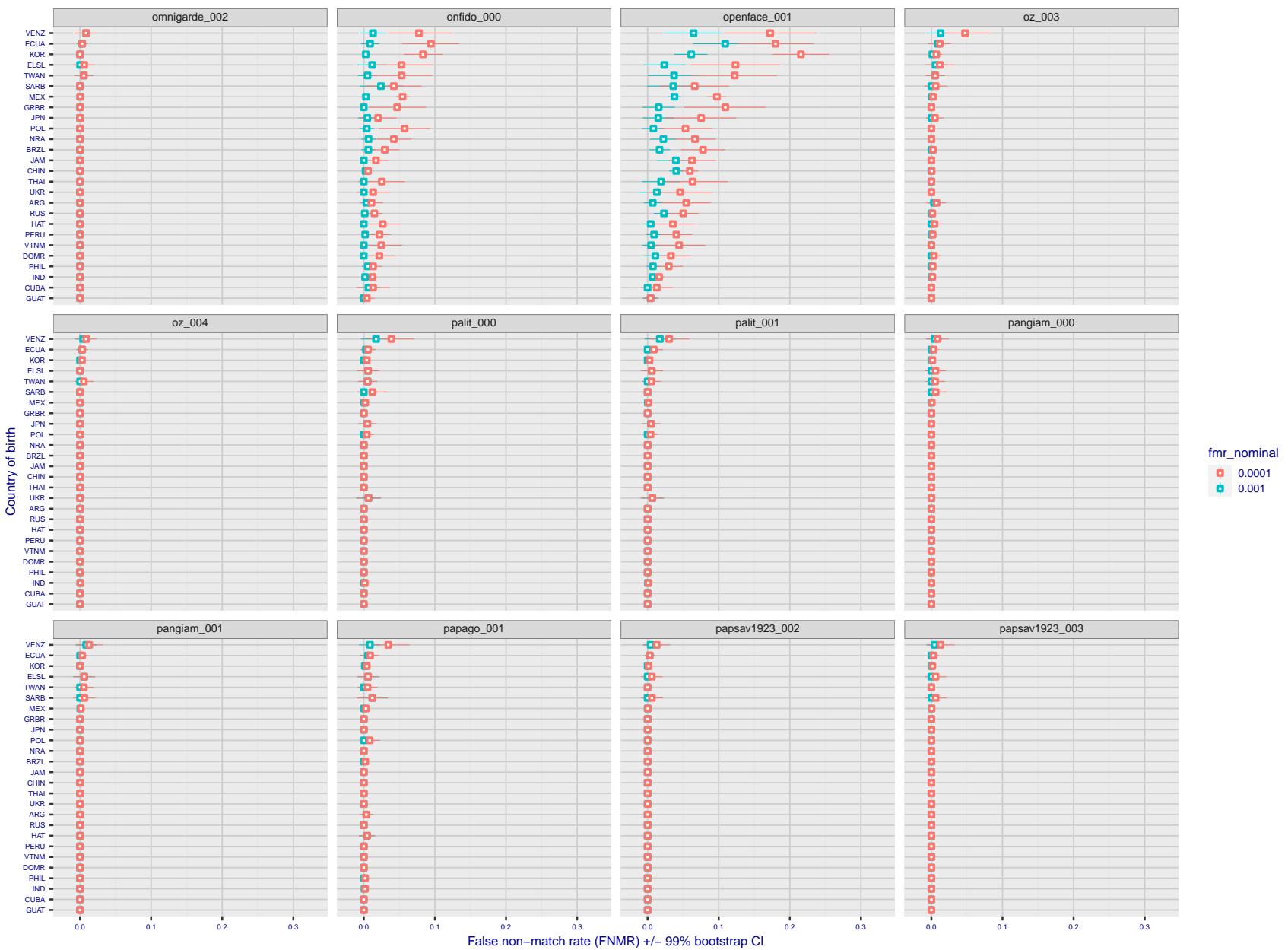


Figure 283: For the visa images, the dots show FNMR by country of birth for two globally set operating thresholds corresponding to $FMR = \{0.001, 0.0001\}$ computed over all on the order of 10^{10} impostor scores. The FMR in each bin will vary also - see subsequent impostor heatmaps in sec. 3.6.1. The figures shows an order of magnitude variation in FNMR across country of birth; these effects are likely due quality variations, then demographics like age and race. The error rates in some cases are zero, and in others the DET is flat so the error rates at the two thresholds are identical. The lines span 1% and 99% of bootstrap replicated FNMR estimates.

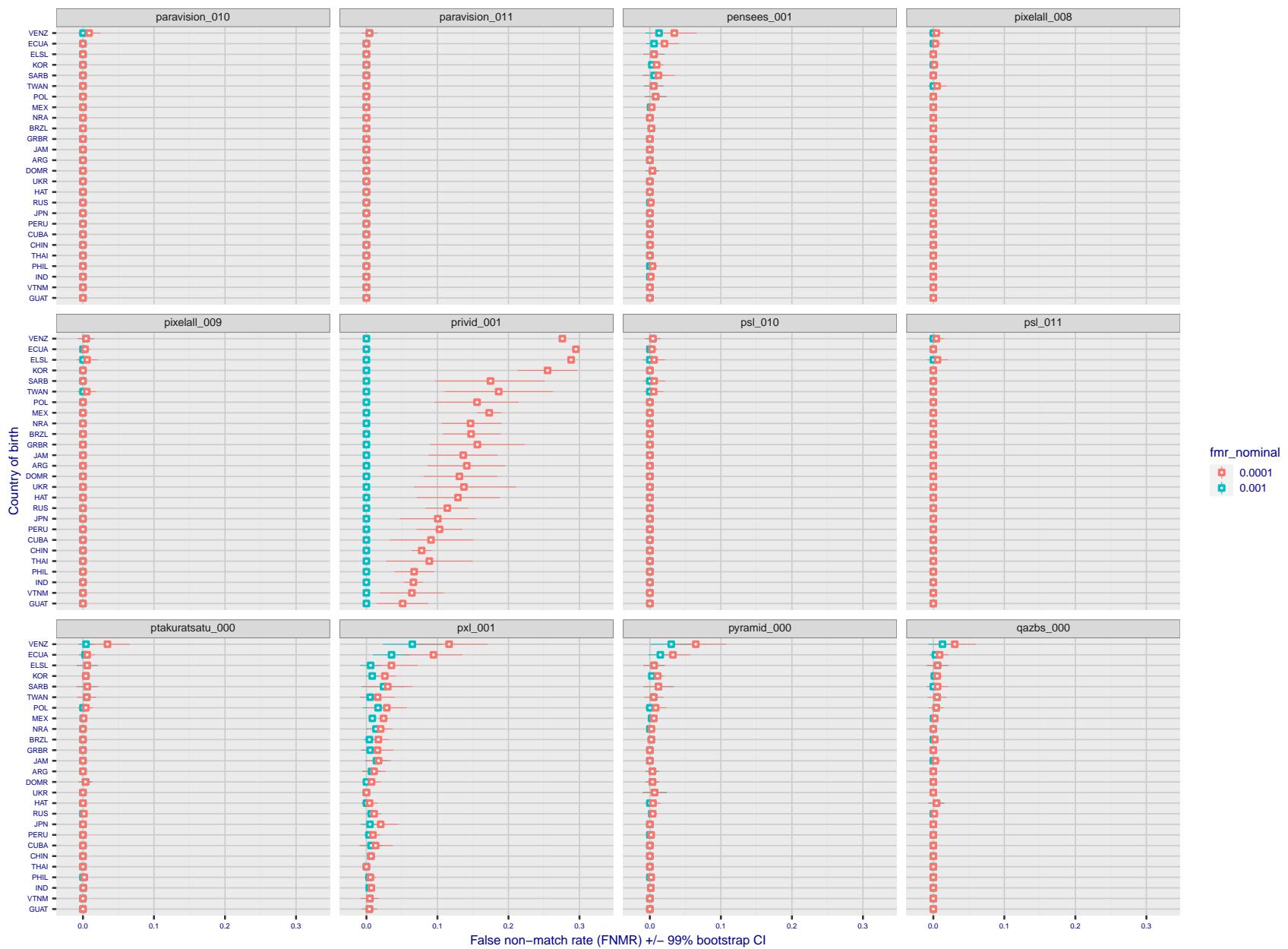


Figure 284: For the visa images, the dots show FNMR by country of birth for two globally set operating thresholds corresponding to $FMR = \{0.001, 0.0001\}$ computed over all on the order of 10^{10} impostor scores. The FMR in each bin will vary also - see subsequent impostor heatmaps in sec. 3.6.1. The figures shows an order of magnitude variation in FNMR across country of birth; these effects are likely due quality variations, then demographics like age and race. The error rates in some cases are zero, and in others the DET is flat so the error rates at the two thresholds are identical. The lines span 1% and 99% of bootstrap replicated FNMR estimates.

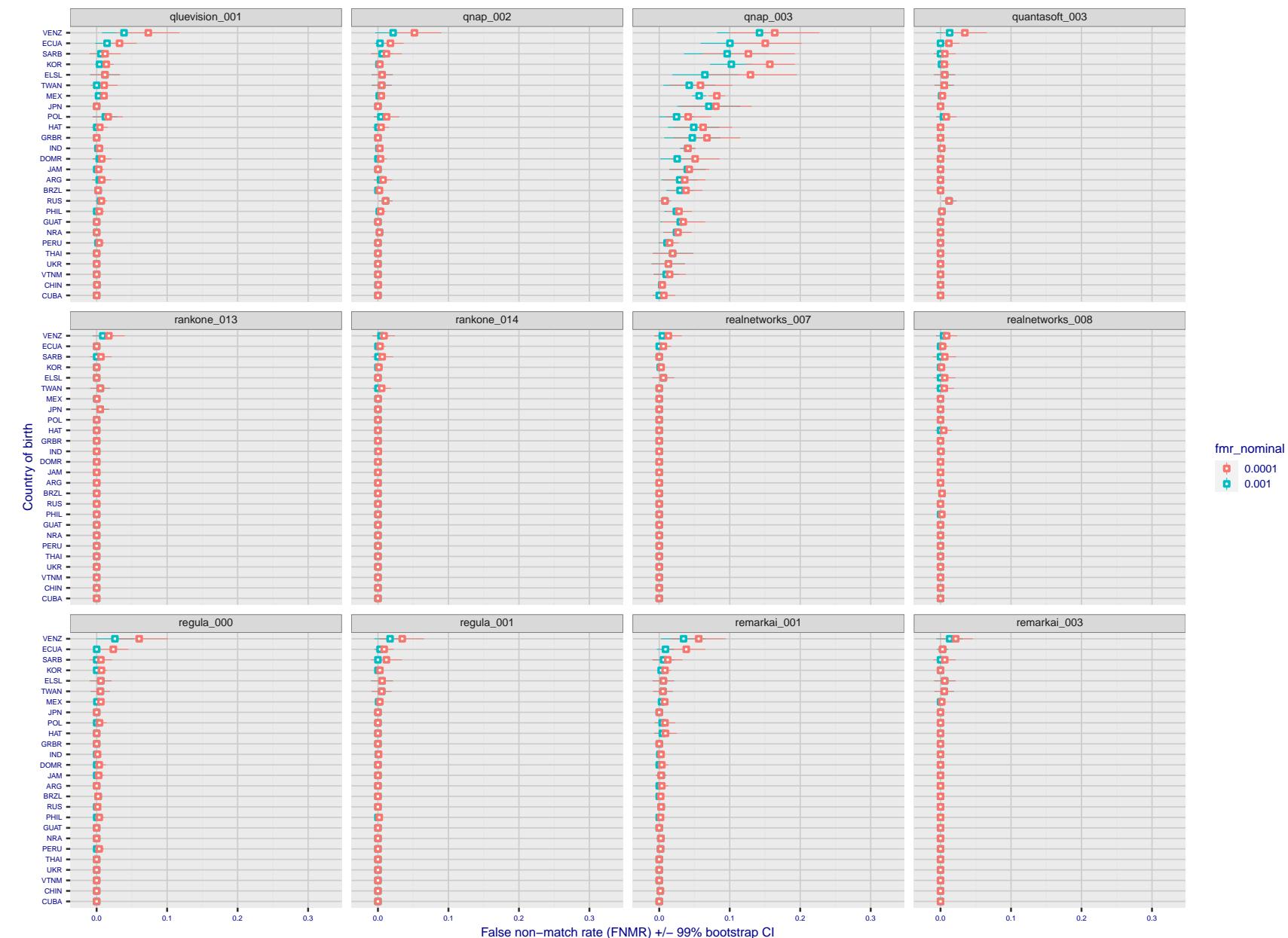


Figure 285: For the visa images, the dots show FNMR by country of birth for two globally set operating thresholds corresponding to $FMR = \{0.001, 0.0001\}$ computed over all on the order of 10^{10} impostor scores. The FMR in each bin will vary also - see subsequent impostor heatmaps in sec. 3.6.1. The figures shows an order of magnitude variation in FNMR across country of birth; these effects are likely due quality variations, then demographics like age and race. The error rates in some cases are zero, and in others the DET is flat so the error rates at the two thresholds are identical. The lines span 1% and 99% of bootstrap replicated FNMR estimates.

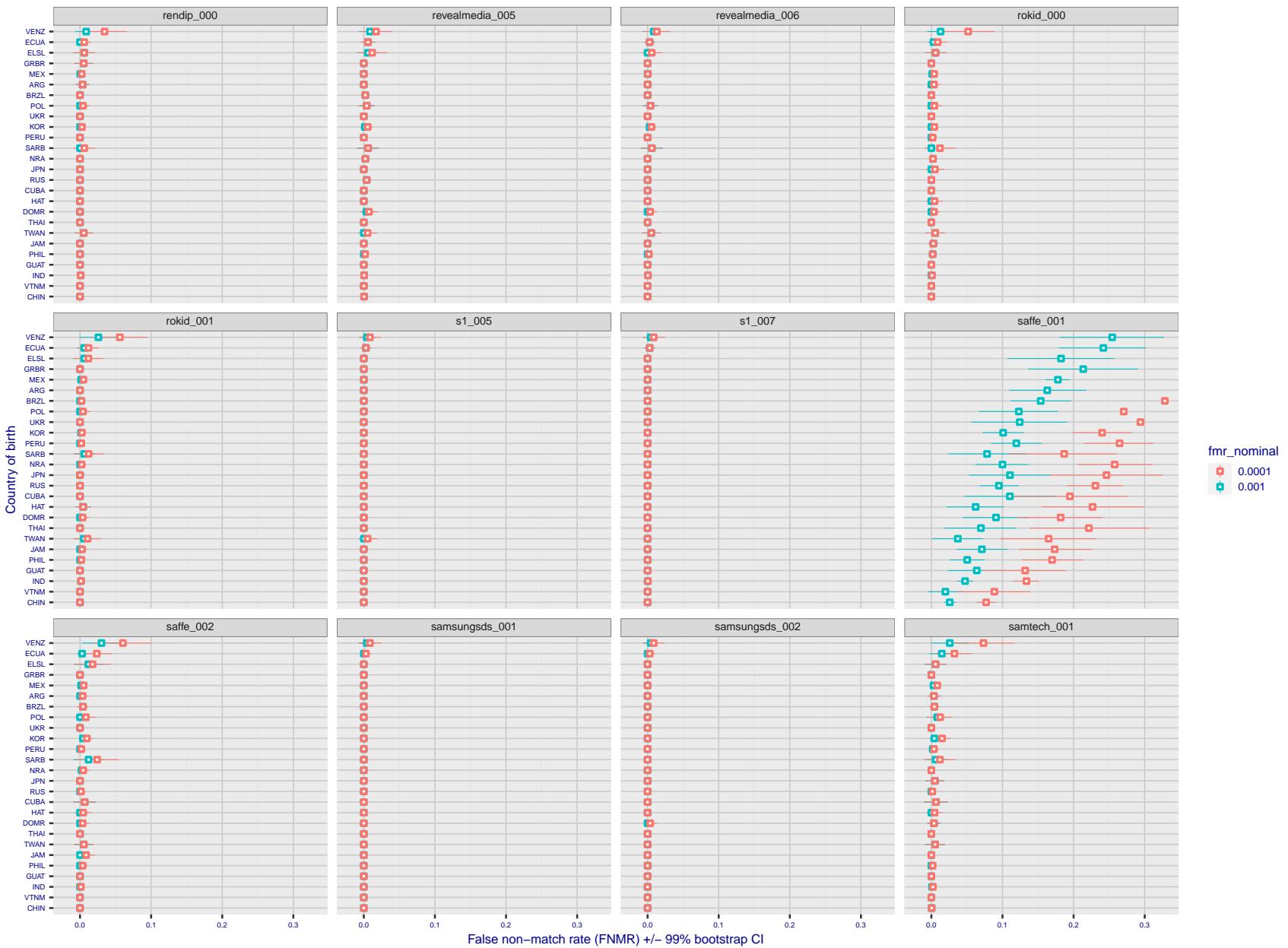


Figure 286: For the visa images, the dots show FNMR by country of birth for two globally set operating thresholds corresponding to $FMR = \{0.001, 0.0001\}$ computed over all on the order of 10^{10} impostor scores. The FMR in each bin will vary also - see subsequent impostor heatmaps in sec. 3.6.1. The figures shows an order of magnitude variation in FNMR across country of birth; these effects are likely due quality variations, then demographics like age and race. The error rates in some cases are zero, and in others the DET is flat so the error rates at the two thresholds are identical. The lines span 1% and 99% of bootstrap replicated FNMR estimates.

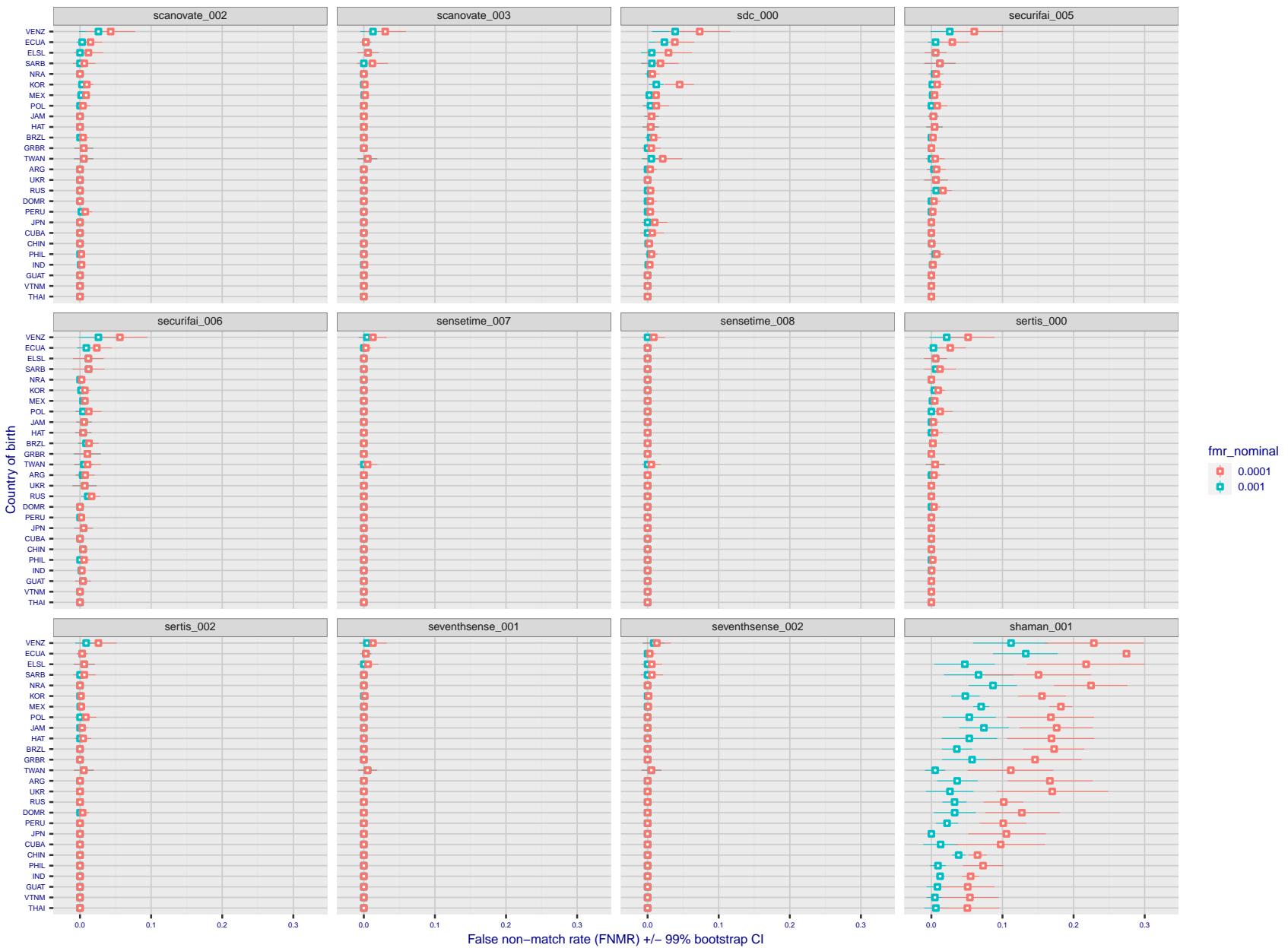


Figure 287: For the visa images, the dots show FNMR by country of birth for two globally set operating thresholds corresponding to $FMR = \{0.001, 0.0001\}$ computed over all on the order of 10^{10} impostor scores. The FMR in each bin will vary also - see subsequent impostor heatmaps in sec. 3.6.1. The figures shows an order of magnitude variation in FNMR across country of birth; these effects are likely due quality variations, then demographics like age and race. The error rates in some cases are zero, and in others the DET is flat so the error rates at the two thresholds are identical. The lines span 1% and 99% of bootstrap replicated FNMR estimates.

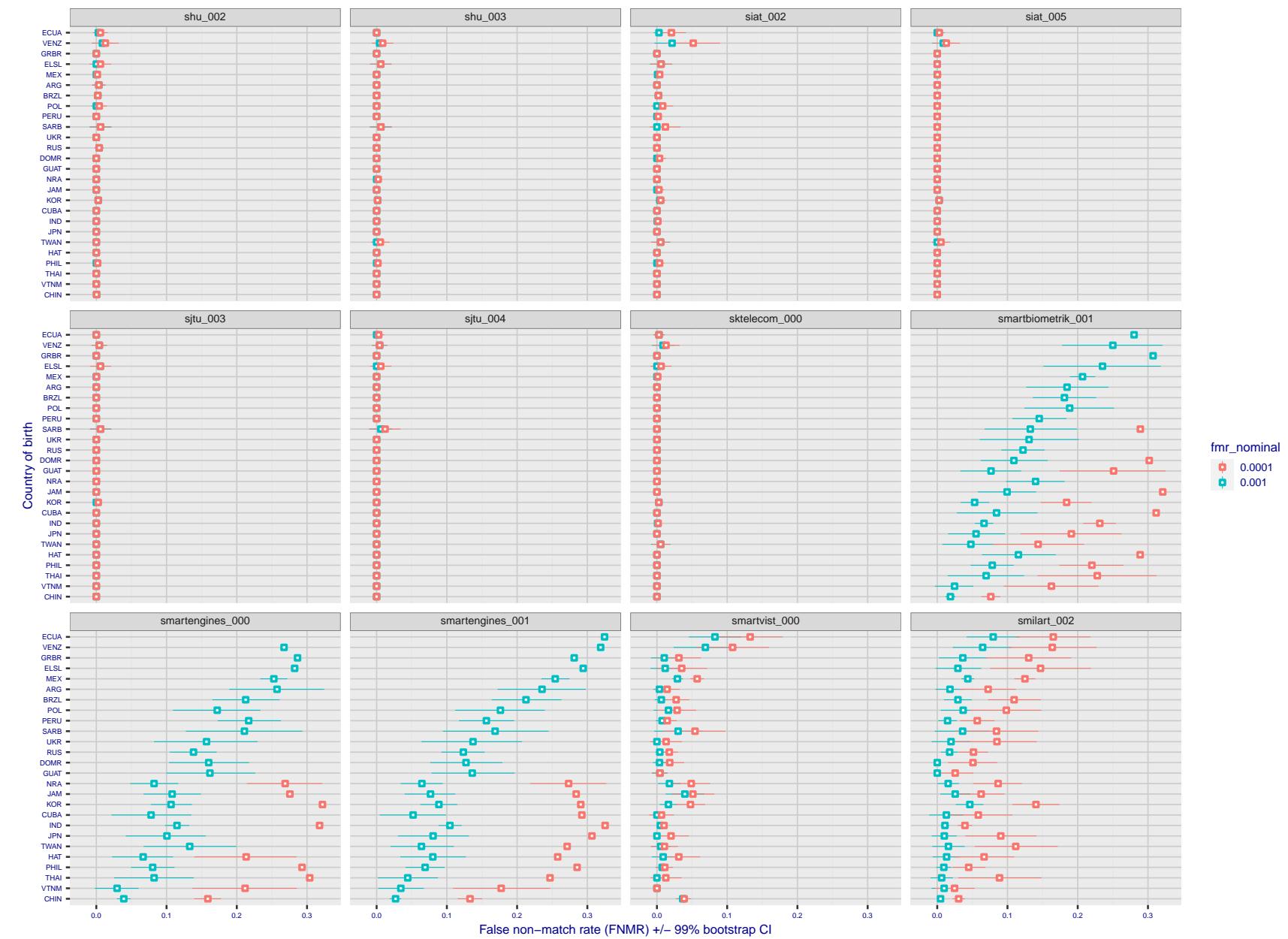


Figure 288: For the visa images, the dots show FNMR by country of birth for two globally set operating thresholds corresponding to $FMR = \{0.001, 0.0001\}$ computed over all on the order of 10^{10} impostor scores. The FMR in each bin will vary also - see subsequent impostor heatmaps in sec. 3.6.1. The figures shows an order of magnitude variation in FNMR across country of birth; these effects are likely due quality variations, then demographics like age and race. The error rates in some cases are zero, and in others the DET is flat so the error rates at the two thresholds are identical. The lines span 1% and 99% of bootstrap replicated FNMR estimates.

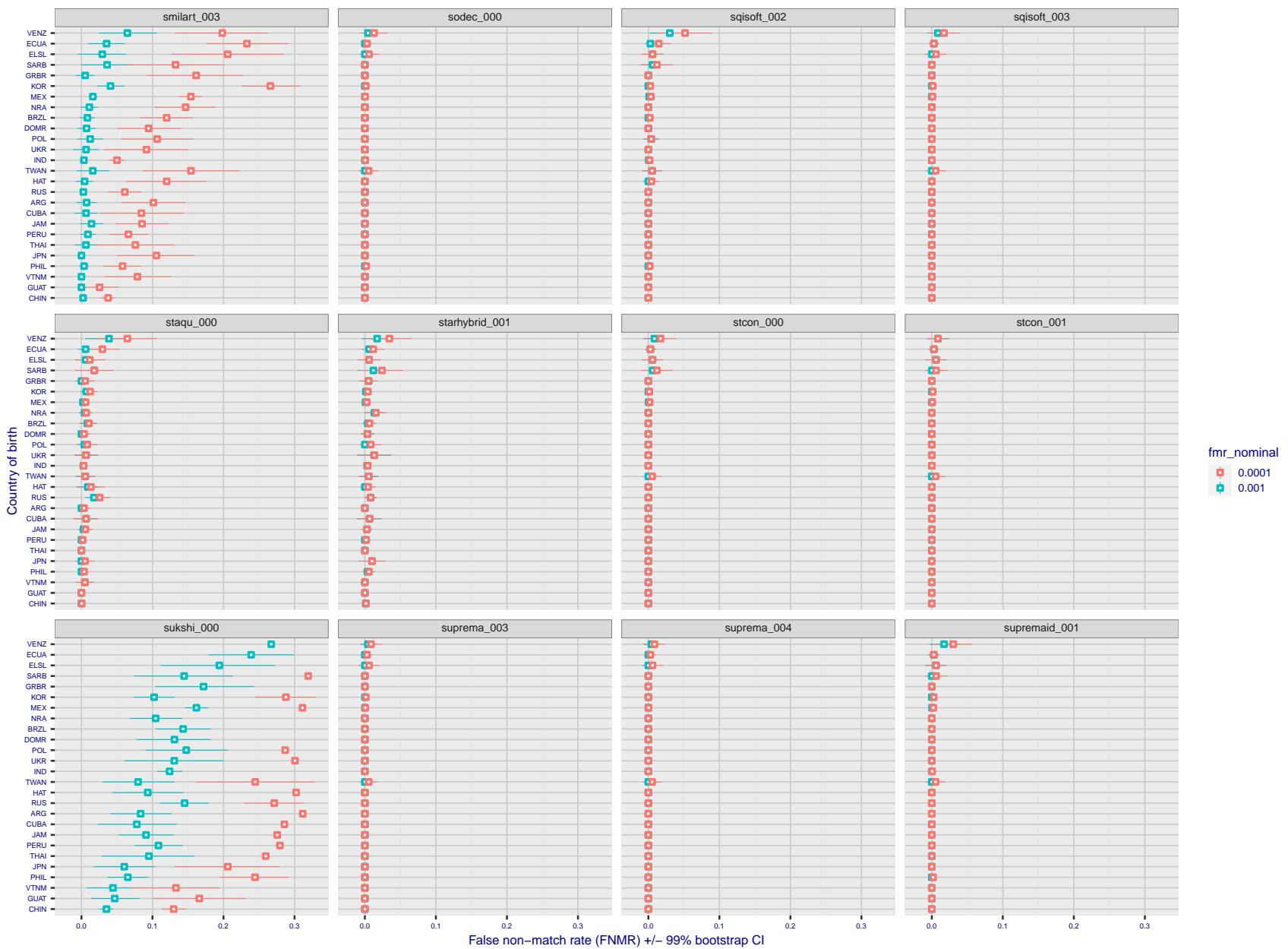


Figure 289: For the visa images, the dots show FNMR by country of birth for two globally set operating thresholds corresponding to $FMR = \{0.001, 0.0001\}$ computed over all on the order of 10^{10} impostor scores. The FMR in each bin will vary also - see subsequent impostor heatmaps in sec. 3.6.1. The figures shows an order of magnitude variation in FNMR across country of birth; these effects are likely due quality variations, then demographics like age and race. The error rates in some cases are zero, and in others the DET is flat so the error rates at the two thresholds are identical. The lines span 1% and 99% of bootstrap replicated FNMR estimates.

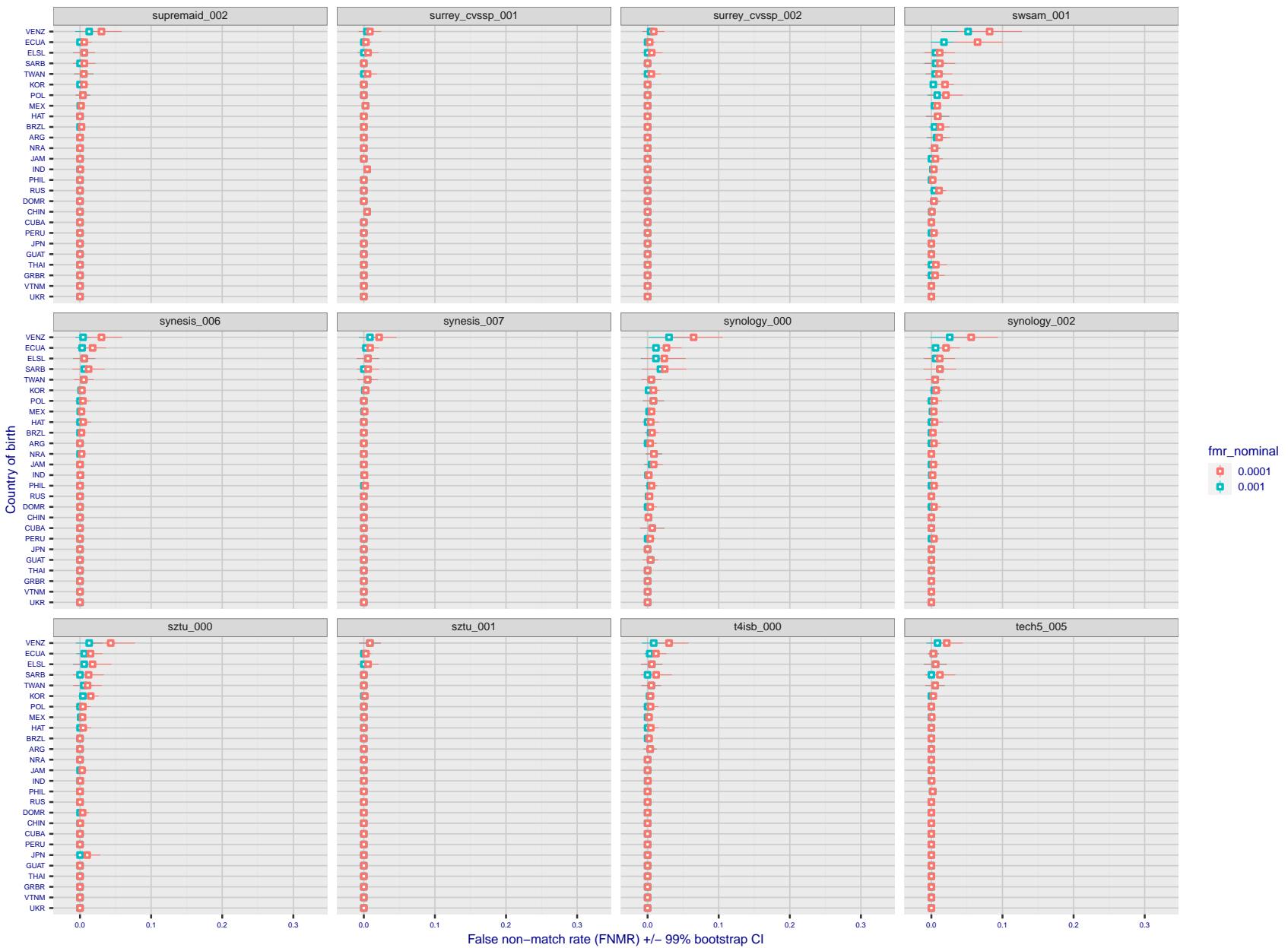


Figure 290: For the visa images, the dots show FNMR by country of birth for two globally set operating thresholds corresponding to $FMR = \{0.001, 0.0001\}$ computed over all on the order of 10^{10} impostor scores. The FMR in each bin will vary also - see subsequent impostor heatmaps in sec. 3.6.1. The figures shows an order of magnitude variation in FNMR across country of birth; these effects are likely due quality variations, then demographics like age and race. The error rates in some cases are zero, and in others the DET is flat so the error rates at the two thresholds are identical. The lines span 1% and 99% of bootstrap replicated FNMR estimates.

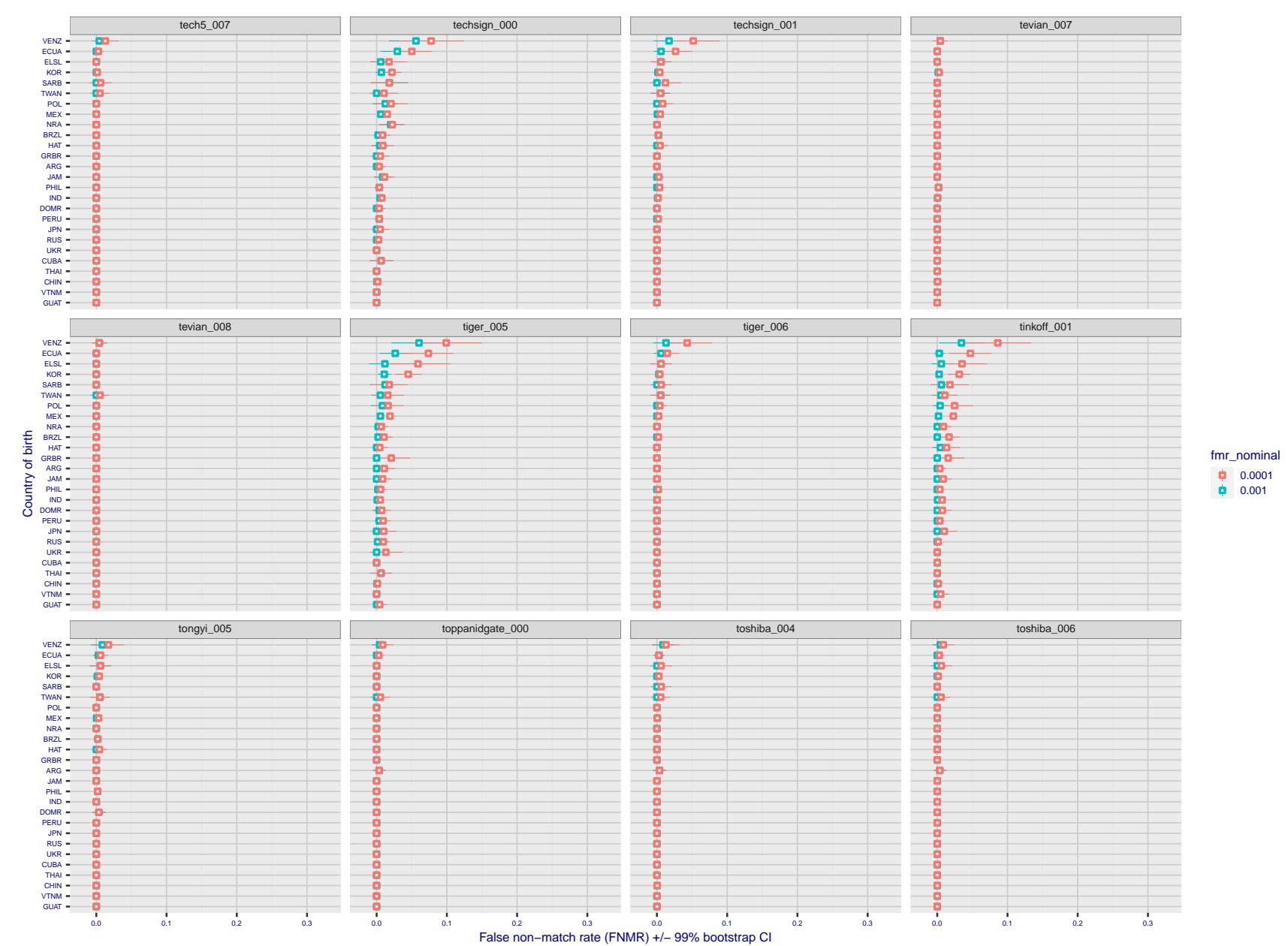


Figure 291: For the visa images, the dots show FNMR by country of birth for two globally set operating thresholds corresponding to $FMR = \{0.001, 0.0001\}$ computed over all on the order of 10^{10} impostor scores. The FMR in each bin will vary also - see subsequent impostor heatmaps in sec. 3.6.1. The figures shows an order of magnitude variation in FNMR across country of birth; these effects are likely due quality variations, then demographics like age and race. The error rates in some cases are zero, and in others the DET is flat so the error rates at the two thresholds are identical. The lines span 1% and 99% of bootstrap replicated FNMR estimates.

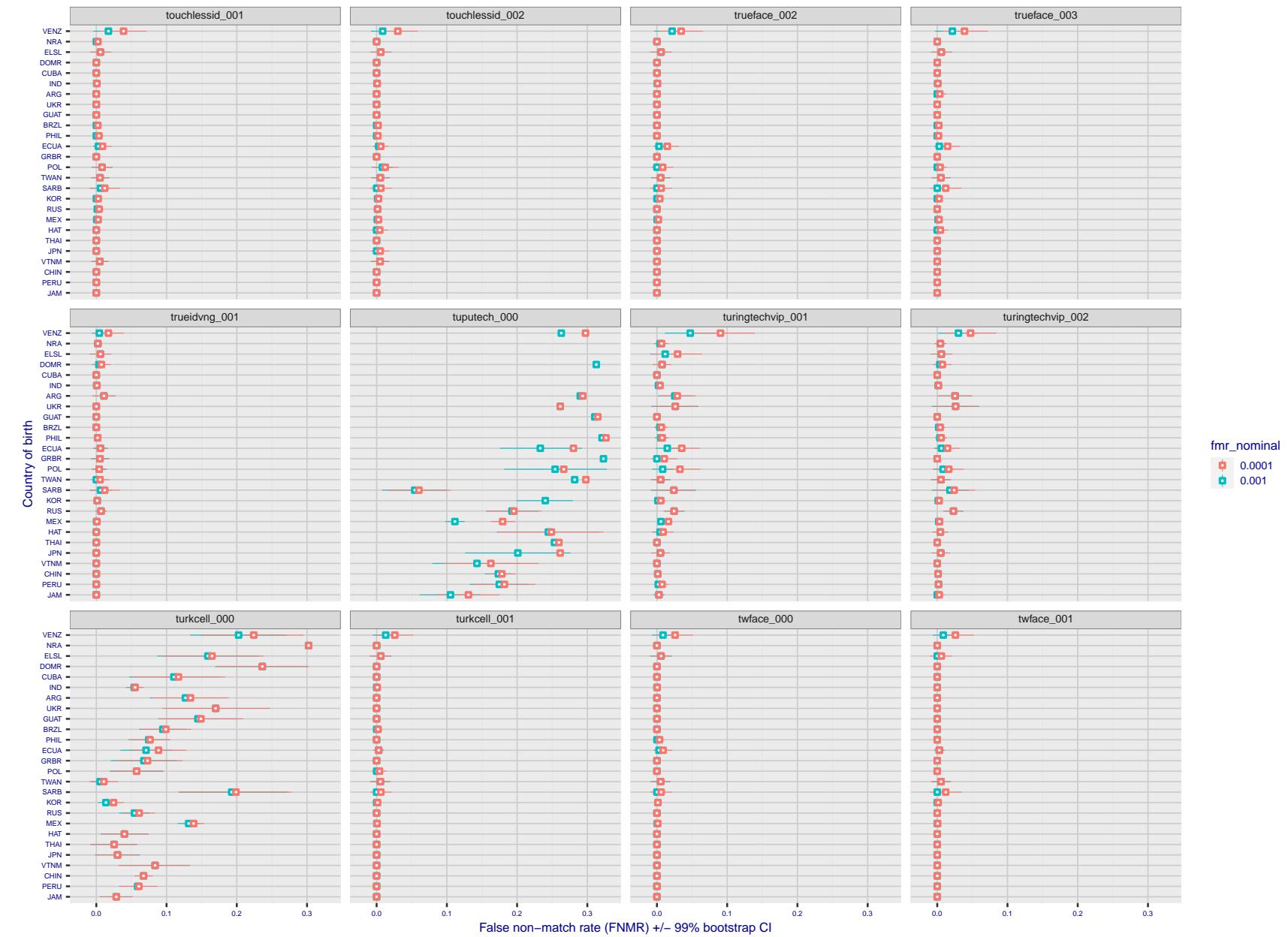


Figure 292: For the visa images, the dots show FNMR by country of birth for two globally set operating thresholds corresponding to $FMR = \{0.001, 0.0001\}$ computed over all on the order of 10^{10} impostor scores. The FMR in each bin will vary also - see subsequent impostor heatmaps in sec. 3.6.1. The figures shows an order of magnitude variation in FNMR across country of birth; these effects are likely due quality variations, then demographics like age and race. The error rates in some cases are zero, and in others the DET is flat so the error rates at the two thresholds are identical. The lines span 1% and 99% of bootstrap replicated FNMR estimates.

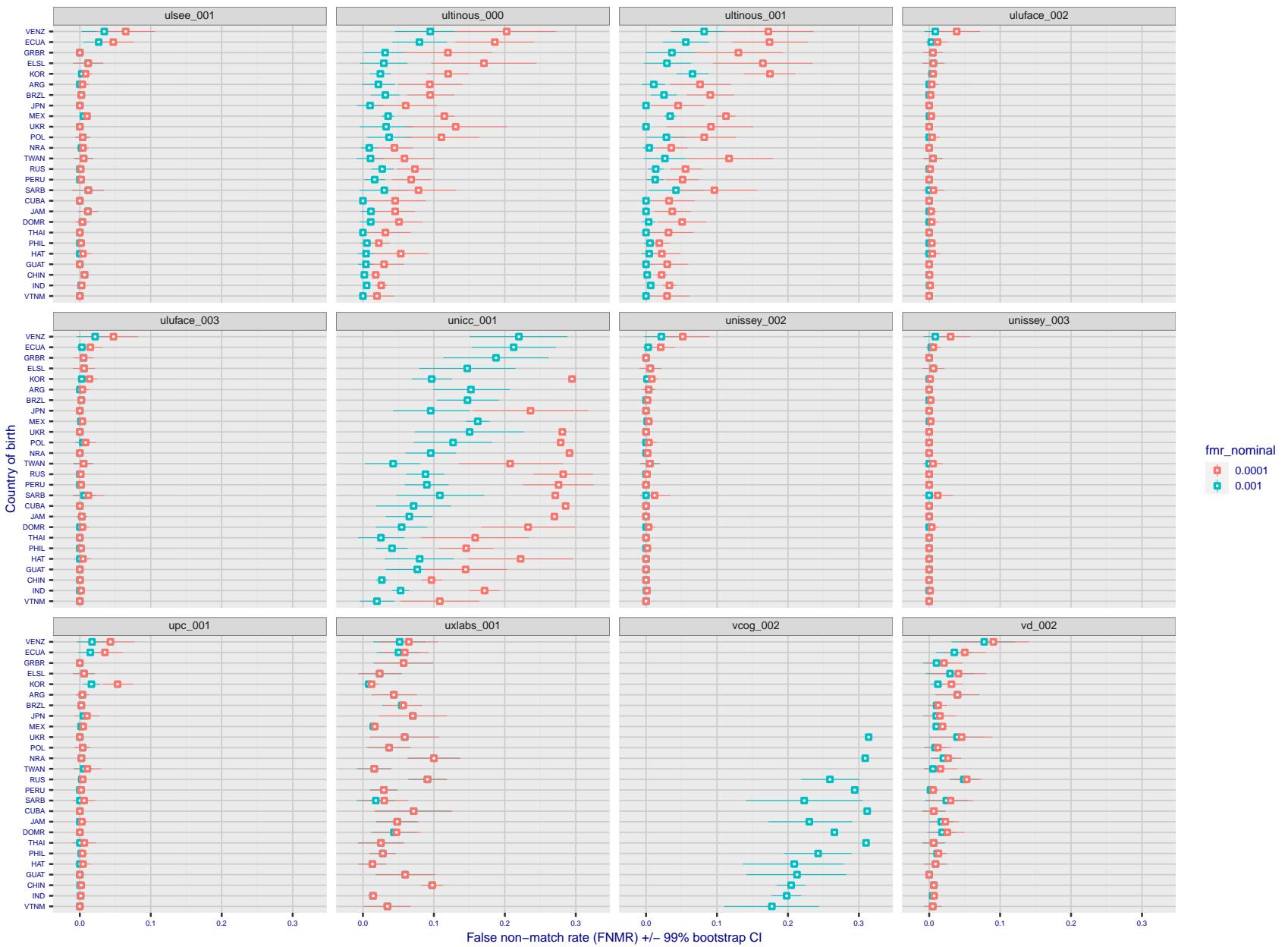


Figure 293: For the visa images, the dots show FNMR by country of birth for two globally set operating thresholds corresponding to $FMR = \{0.001, 0.0001\}$ computed over all on the order of 10^{10} impostor scores. The FMR in each bin will vary also - see subsequent impostor heatmaps in sec. 3.6.1. The figures shows an order of magnitude variation in FNMR across country of birth; these effects are likely due quality variations, then demographics like age and race. The error rates in some cases are zero, and in others the DET is flat so the error rates at the two thresholds are identical. The lines span 1% and 99% of bootstrap replicated FNMR estimates.

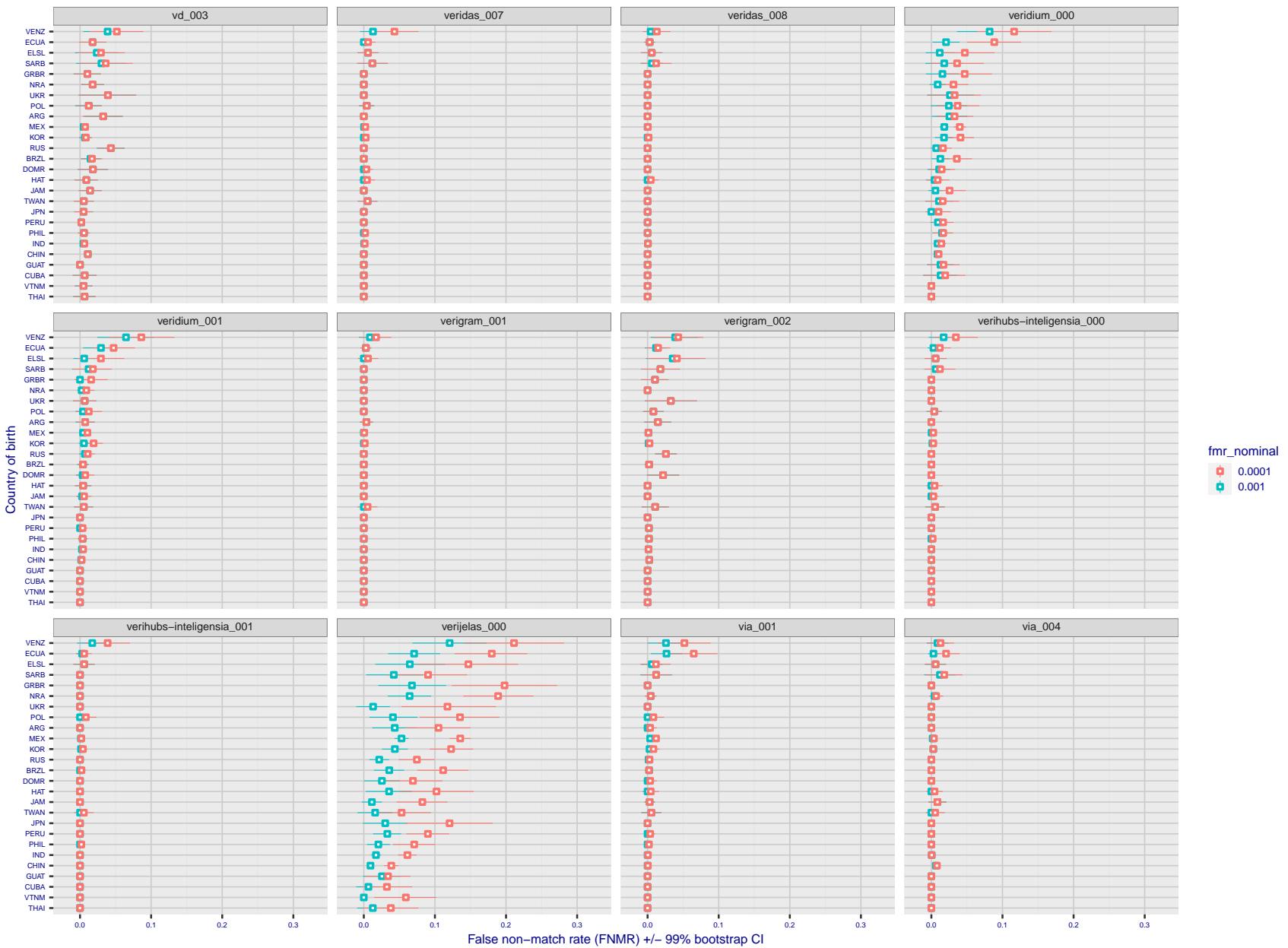


Figure 294: For the visa images, the dots show FNMR by country of birth for two globally set operating thresholds corresponding to $FMR = \{0.001, 0.0001\}$ computed over all on the order of 10^{10} impostor scores. The FMR in each bin will vary also - see subsequent impostor heatmaps in sec. 3.6.1. The figures shows an order of magnitude variation in FNMR across country of birth; these effects are likely due quality variations, then demographics like age and race. The error rates in some cases are zero, and in others the DET is flat so the error rates at the two thresholds are identical. The lines span 1% and 99% of bootstrap replicated FNMR estimates.

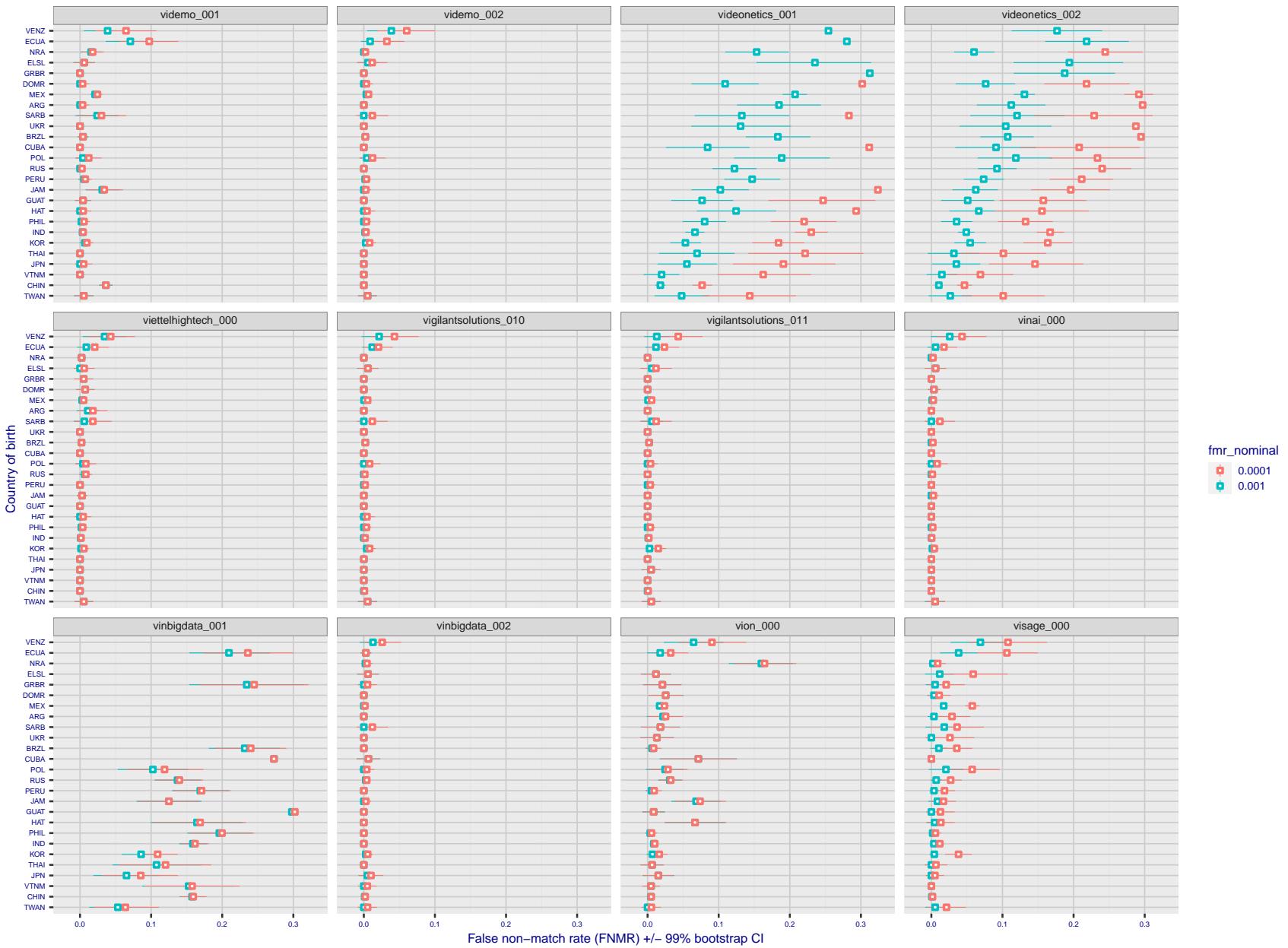


Figure 295: For the visa images, the dots show FNMR by country of birth for two globally set operating thresholds corresponding to $FMR = \{0.001, 0.0001\}$ computed over all on the order of 10^{10} impostor scores. The FMR in each bin will vary also - see subsequent impostor heatmaps in sec. 3.6.1. The figures shows an order of magnitude variation in FNMR across country of birth; these effects are likely due quality variations, then demographics like age and race. The error rates in some cases are zero, and in others the DET is flat so the error rates at the two thresholds are identical. The lines span 1% and 99% of bootstrap replicated FNMR estimates.

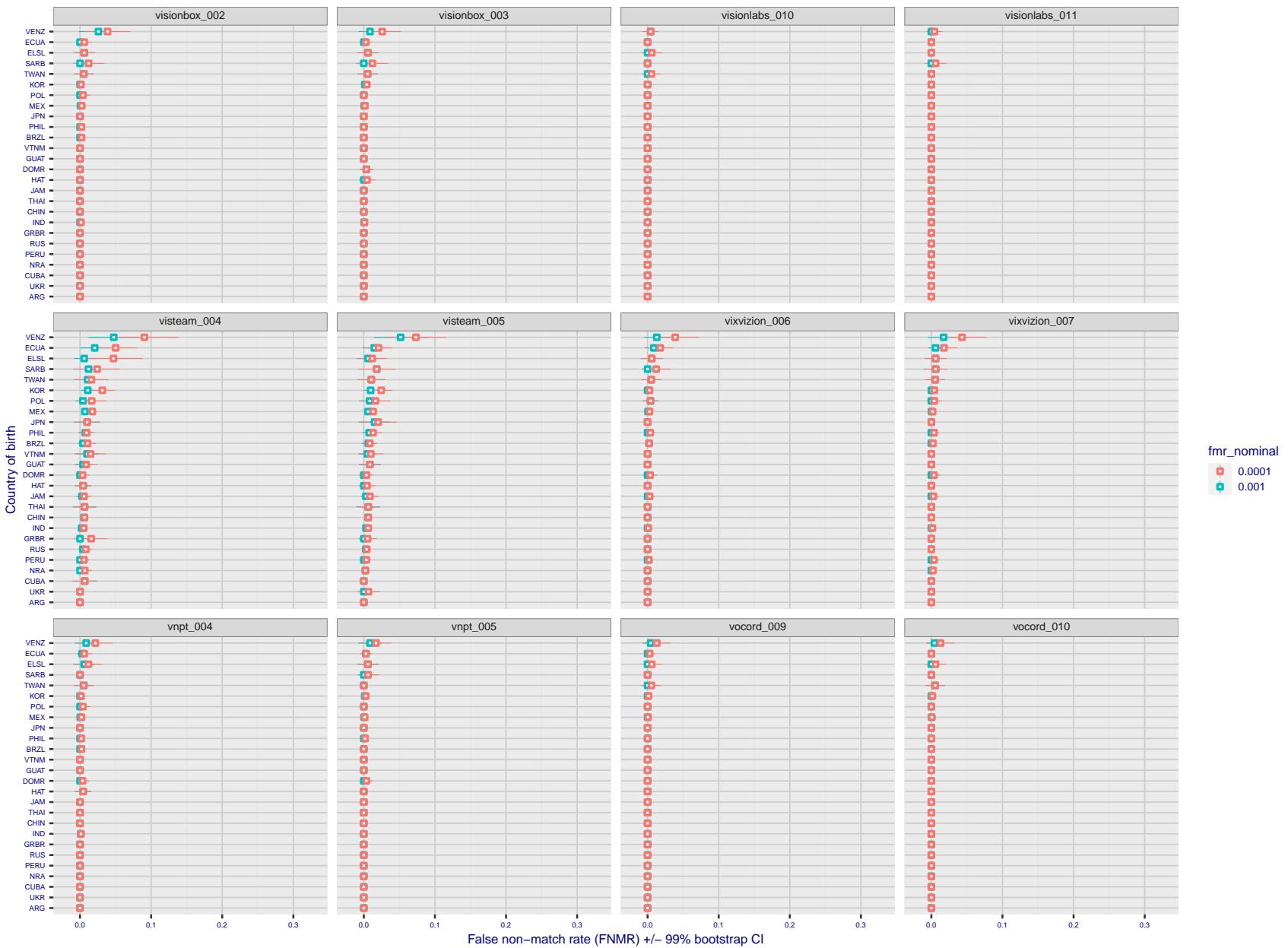


Figure 296: For the visa images, the dots show FNMR by country of birth for two globally set operating thresholds corresponding to $FMR = \{0.001, 0.0001\}$ computed over all on the order of 10^{10} impostor scores. The FMR in each bin will vary also - see subsequent impostor heatmaps in sec. 3.6.1. The figures shows an order of magnitude variation in FNMR across country of birth; these effects are likely due quality variations, then demographics like age and race. The error rates in some cases are zero, and in others the DET is flat so the error rates at the two thresholds are identical. The lines span 1% and 99% of bootstrap replicated FNMR estimates.

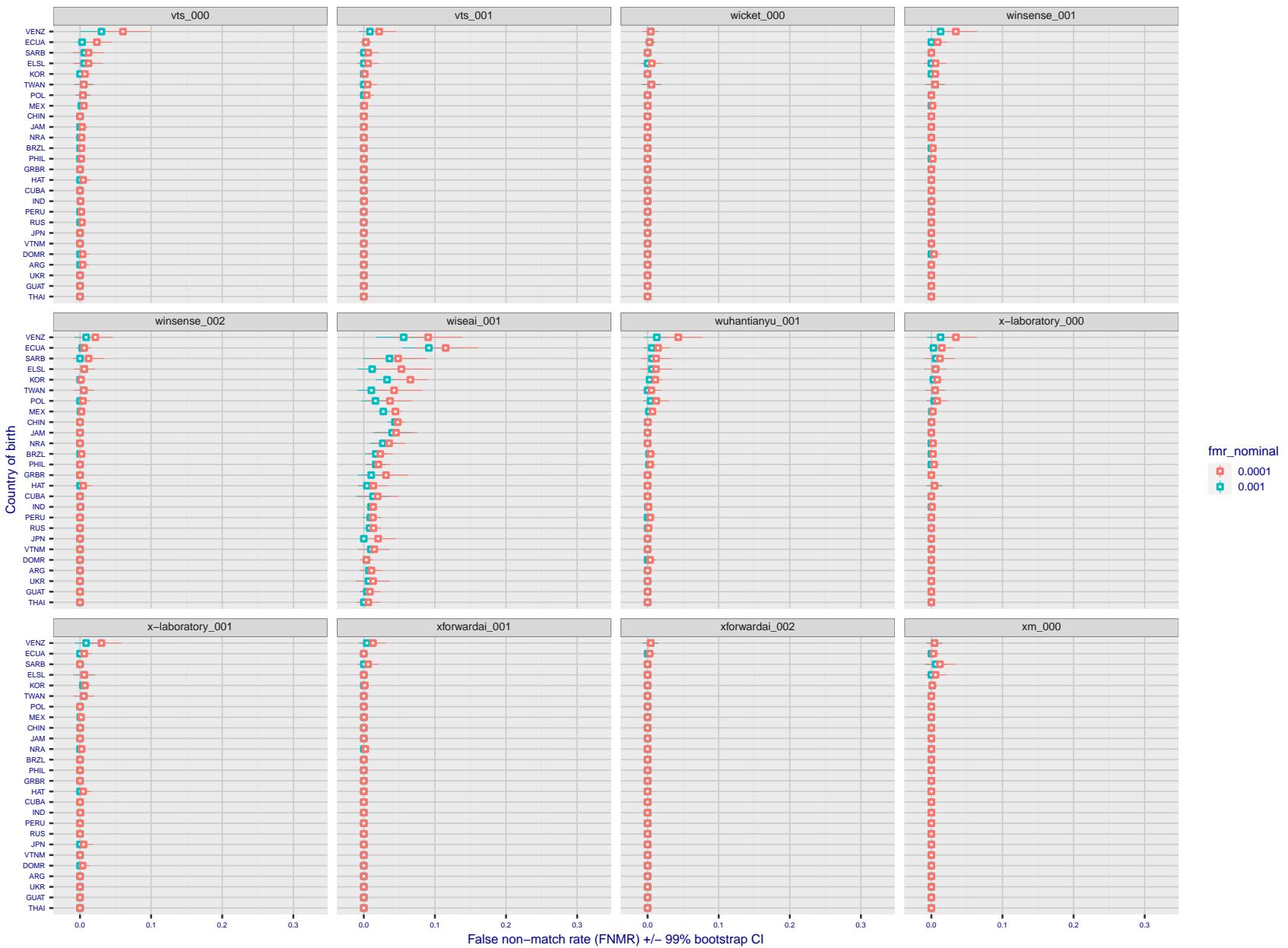


Figure 297: For the visa images, the dots show FNMR by country of birth for two globally set operating thresholds corresponding to $FMR = \{0.001, 0.0001\}$ computed over all on the order of 10^{10} impostor scores. The FMR in each bin will vary also - see subsequent impostor heatmaps in sec. 3.6.1. The figures shows an order of magnitude variation in FNMR across country of birth; these effects are likely due quality variations, then demographics like age and race. The error rates in some cases are zero, and in others the DET is flat so the error rates at the two thresholds are identical. The lines span 1% and 99% of bootstrap replicated FNMR estimates.



Figure 298: For the visa images, the dots show FNMR by country of birth for two globally set operating thresholds corresponding to $FMR = \{0.001, 0.0001\}$ computed over all on the order of 10^{10} impostor scores. The FMR in each bin will vary also - see subsequent impostor heatmaps in sec. 3.6.1. The figures shows an order of magnitude variation in FNMR across country of birth; these effects are likely due quality variations, then demographics like age and race. The error rates in some cases are zero, and in others the DET is flat so the error rates at the two thresholds are identical. The lines span 1% and 99% of bootstrap replicated FNMR estimates.

Caveats: The results may not relate to subject-specific properties. Instead they could reflect image-specific quality differences, which could occur due to collection protocol or software processing variations.

3.5.2 Effect of ageing

Background: Faces change appearance throughout life. This change gradually reduces similarity of a new image to an earlier image. Face recognition algorithms give reduced similarity scores and more frequent false rejections.

Goal: To quantify false non-match rates (FNMR) as a function of elapsed time in an adult population.

Methods: Using the mugshot images, a threshold is set to give FMR = 0.00001 over the entire impostor set. Then FNMR is measured over 1000 bootstrap replications of the genuine scores.

Results: For the visa images, Figure 329 shows how false non-match rates for genuine users, as a function of age group.

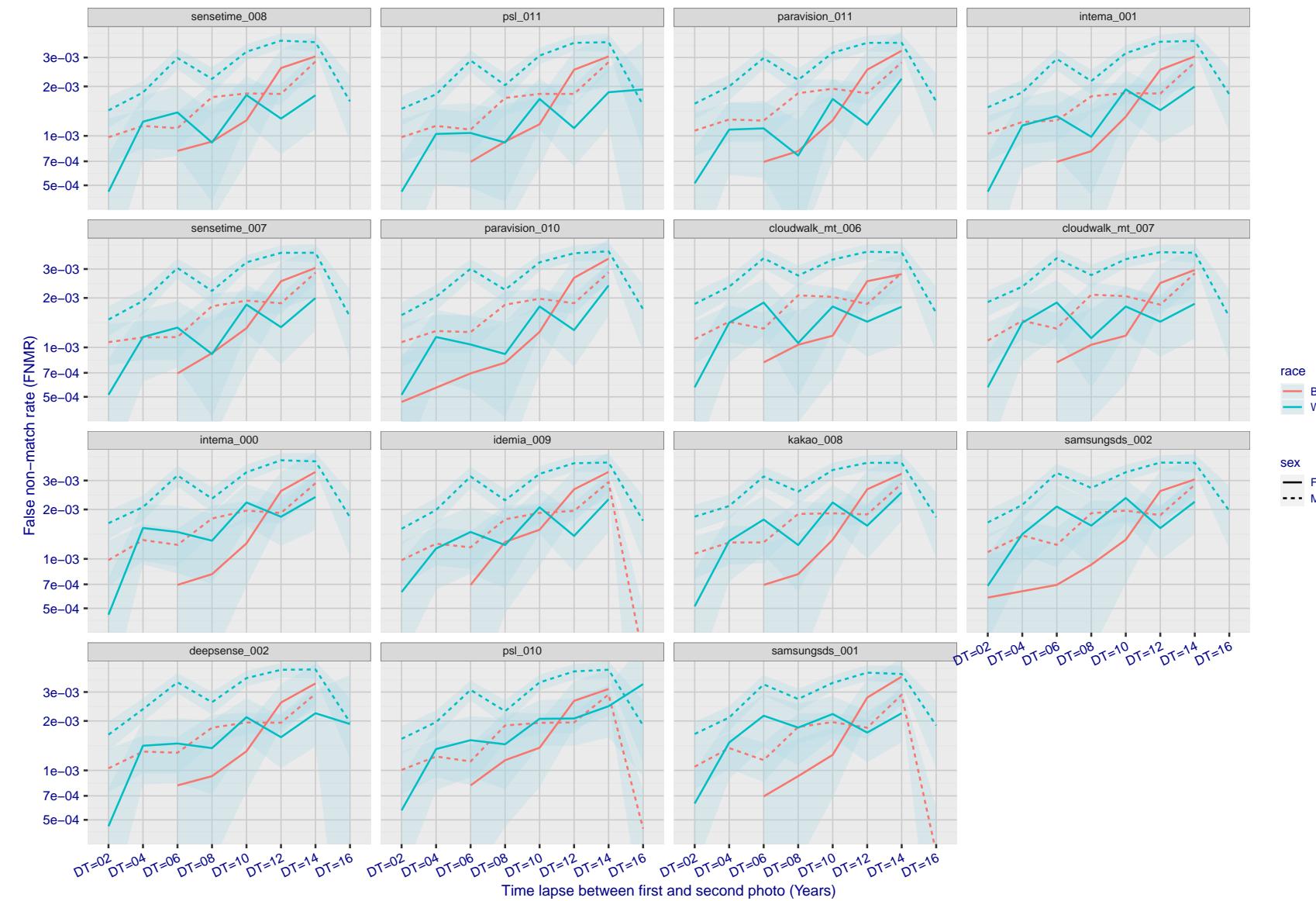


Figure 299: For the mugshot images, FNMR as a function of elapsed time between initial enrollment and second verification images. The panels appear most accurate first, and vertical scale changes on each page. The four traces correspond to images annotated with codes for black female, black male, white female, white male. The threshold is fixed for each algorithm to give FMR = 0.00001 over all (10^8) impostor comparisons. For short time-lapses, the most accurate algorithms give very few errors (FNMR < 0.001) so that the uncertainty estimates are high.

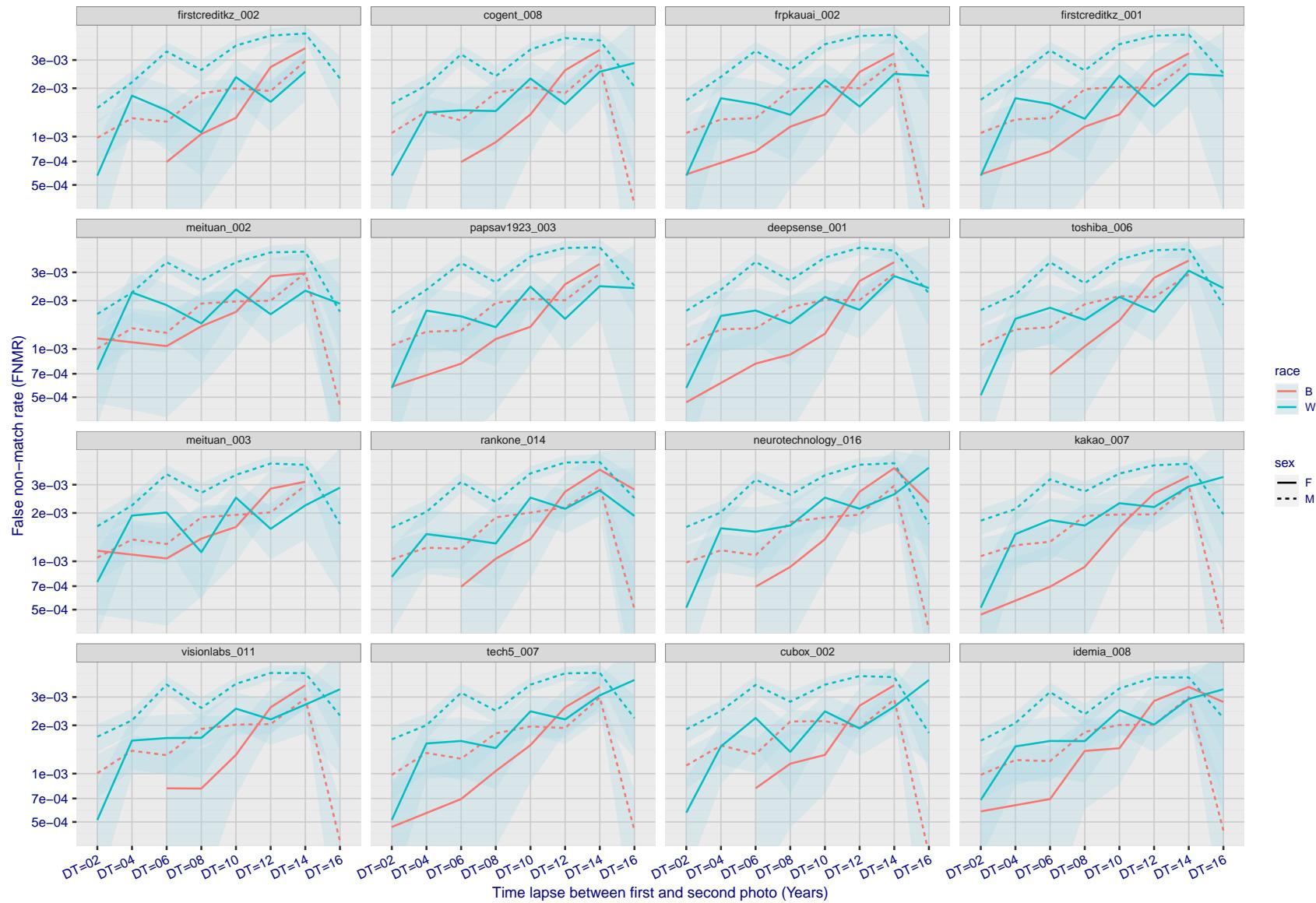


Figure 300: For the mugshot images, FNMR as a function of elapsed time between initial enrollment and second verification images. The panels appear most accurate first, and vertical scale changes on each page. The four traces correspond to images annotated with codes for black female, black male, white female, white male. The threshold is fixed for each algorithm to give $FMR = 0.00001$ over all (10^8) impostor comparisons. For short time-lapses, the most accurate algorithms give very few errors ($FNMR < 0.001$) so that the uncertainty estimates are high.

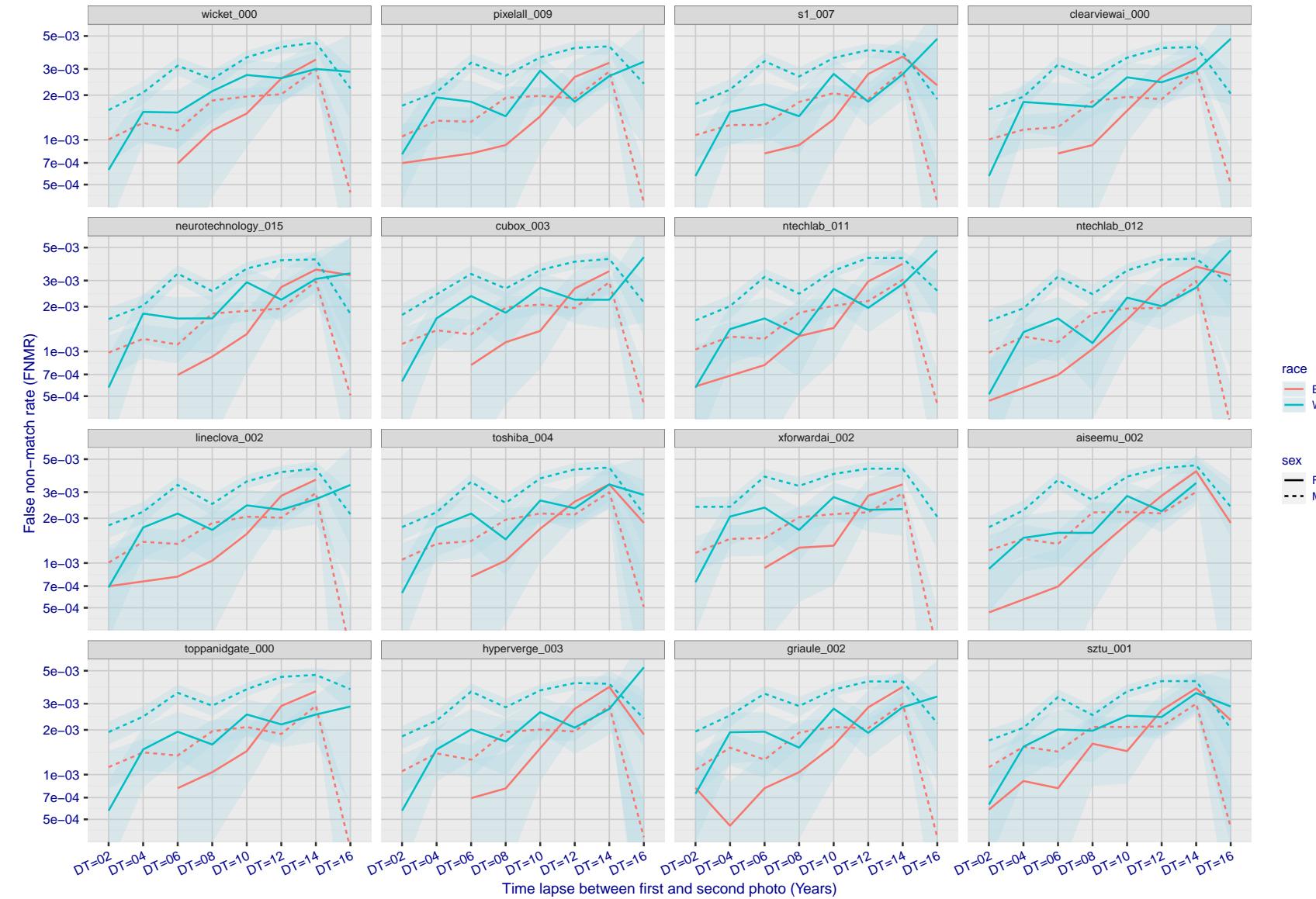


Figure 301: For the mugshot images, FNMR as a function of elapsed time between initial enrollment and second verification images. The panels appear most accurate first, and vertical scale changes on each page. The four traces correspond to images annotated with codes for black female, black male, white female, white male. The threshold is fixed for each algorithm to give FMR = 0.00001 over all (10^8) impostor comparisons. For short time-lapses, the most accurate algorithms give very few errors (FNMR < 0.001) so that the uncertainty estimates are high.

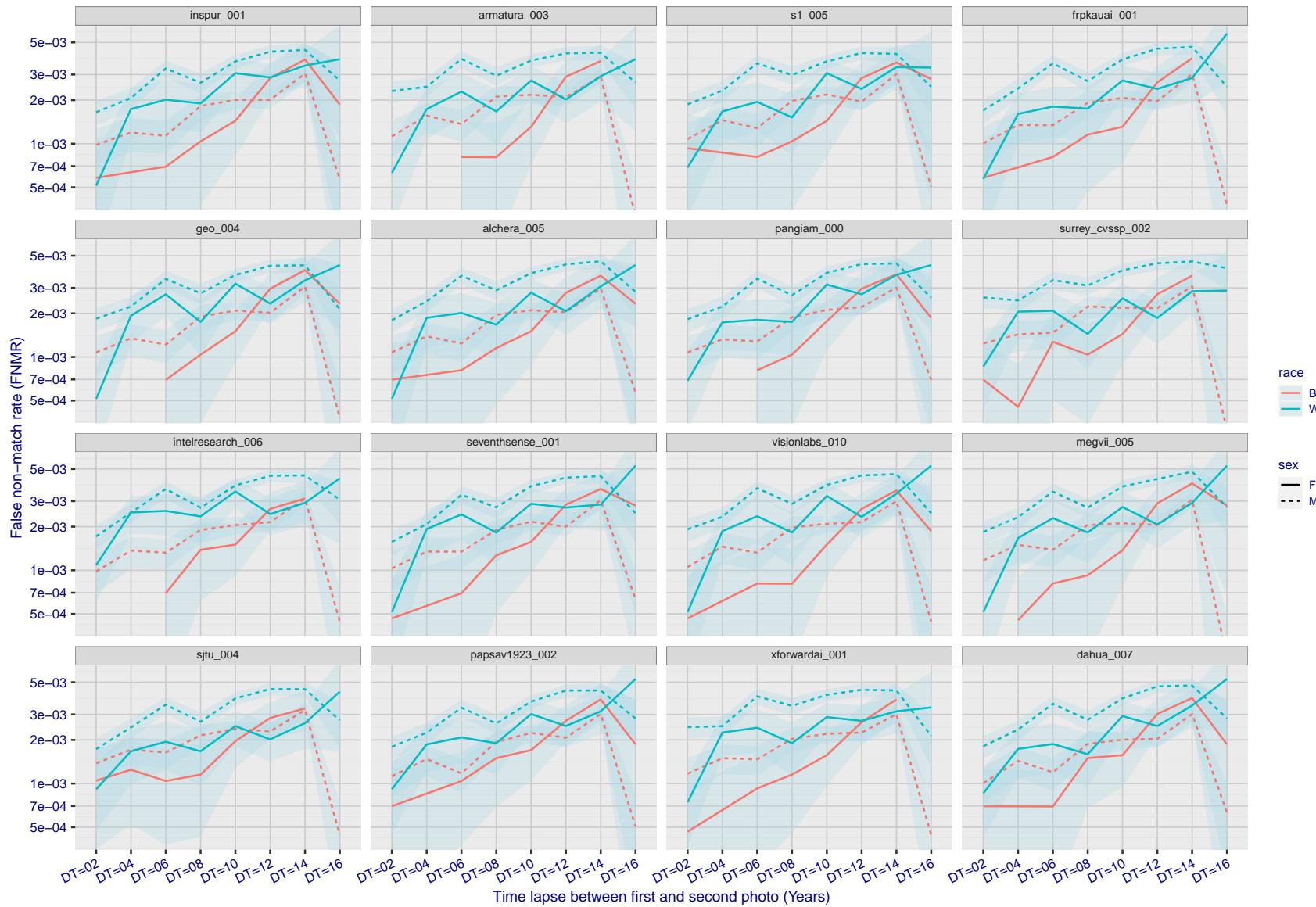


Figure 302: For the mugshot images, FNMR as a function of elapsed time between initial enrollment and second verification images. The panels appear most accurate first, and vertical scale changes on each page. The four traces correspond to images annotated with codes for black female, black male, white female, white male. The threshold is fixed for each algorithm to give FMR = 0.00001 over all (10^8) impostor comparisons. For short time-lapses, the most accurate algorithms give very few errors (FNMR < 0.001) so that the uncertainty estimates are high.

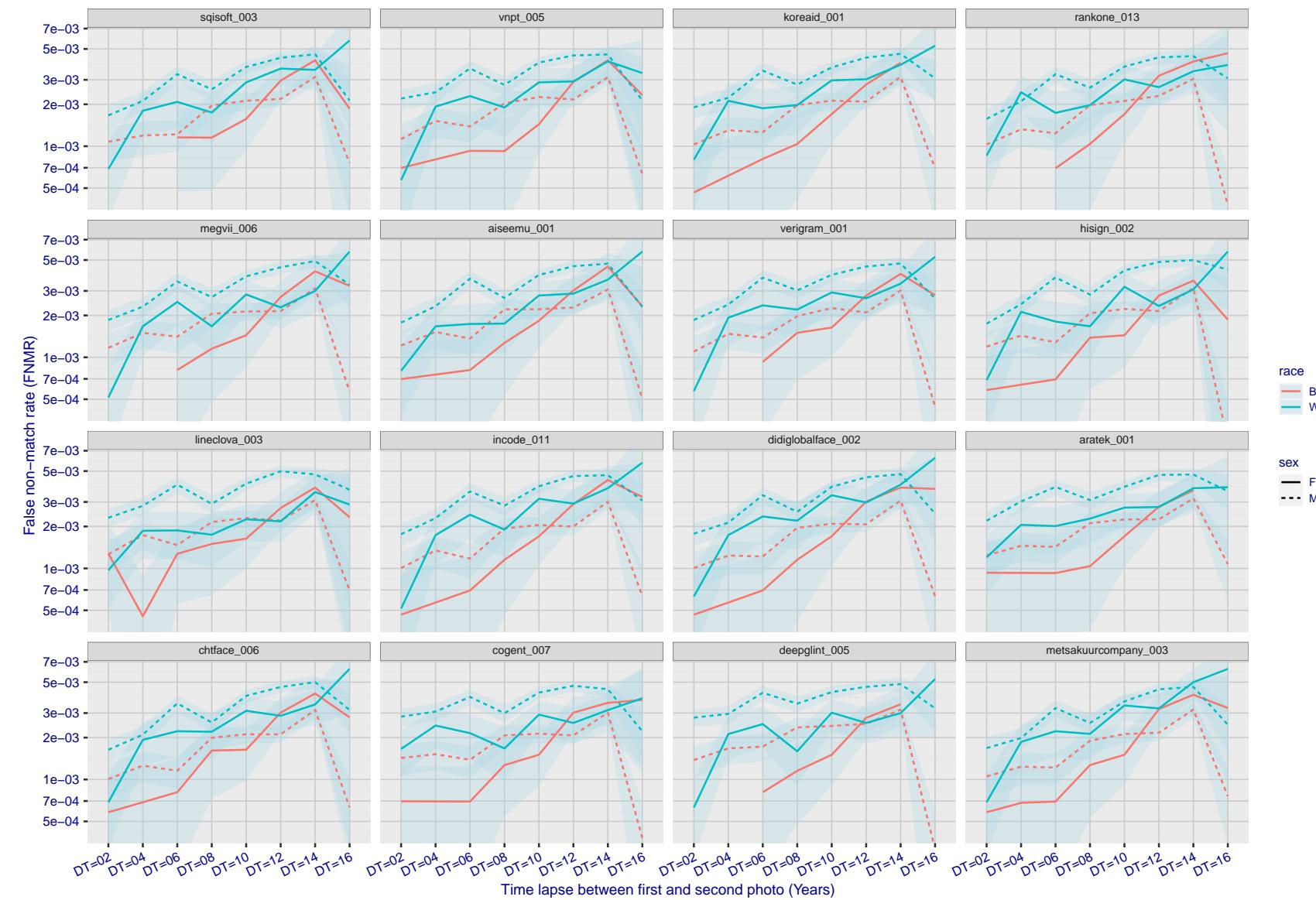


Figure 303: For the mugshot images, FNMR as a function of elapsed time between initial enrollment and second verification images. The panels appear most accurate first, and vertical scale changes on each page. The four traces correspond to images annotated with codes for black female, black male, white female, white male. The threshold is fixed for each algorithm to give $FMR = 0.00001$ over all (10^8) impostor comparisons. For short time-lapses, the most accurate algorithms give very few errors ($FNMR < 0.001$) so that the uncertainty estimates are high.

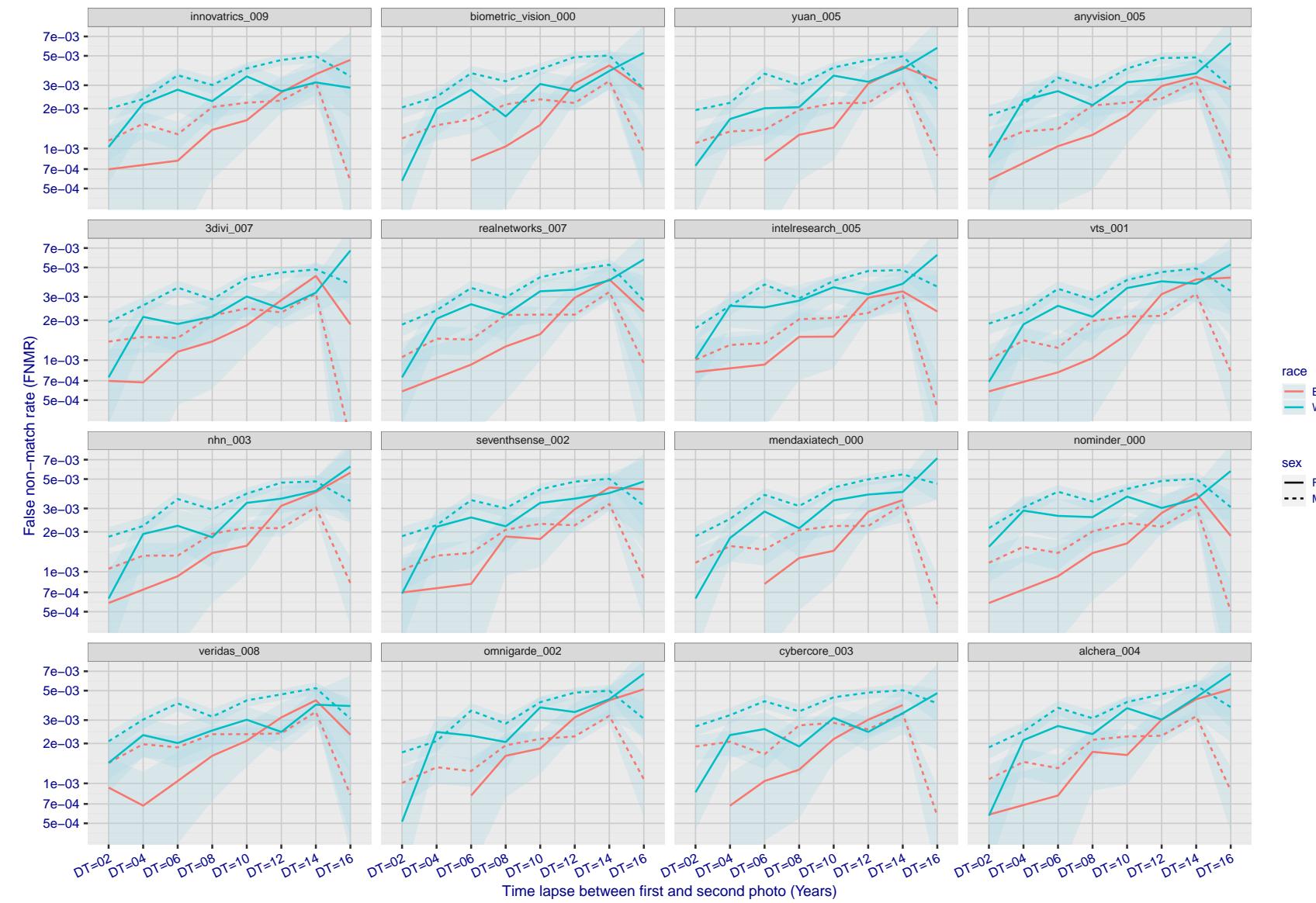


Figure 304: For the mugshot images, FNMR as a function of elapsed time between initial enrollment and second verification images. The panels appear most accurate first, and vertical scale changes on each page. The four traces correspond to images annotated with codes for black female, black male, white female, white male. The threshold is fixed for each algorithm to give $FMR = 0.00001$ over all (10^8) impostor comparisons. For short time-lapses, the most accurate algorithms give very few errors ($FNMR < 0.001$) so that the uncertainty estimates are high.

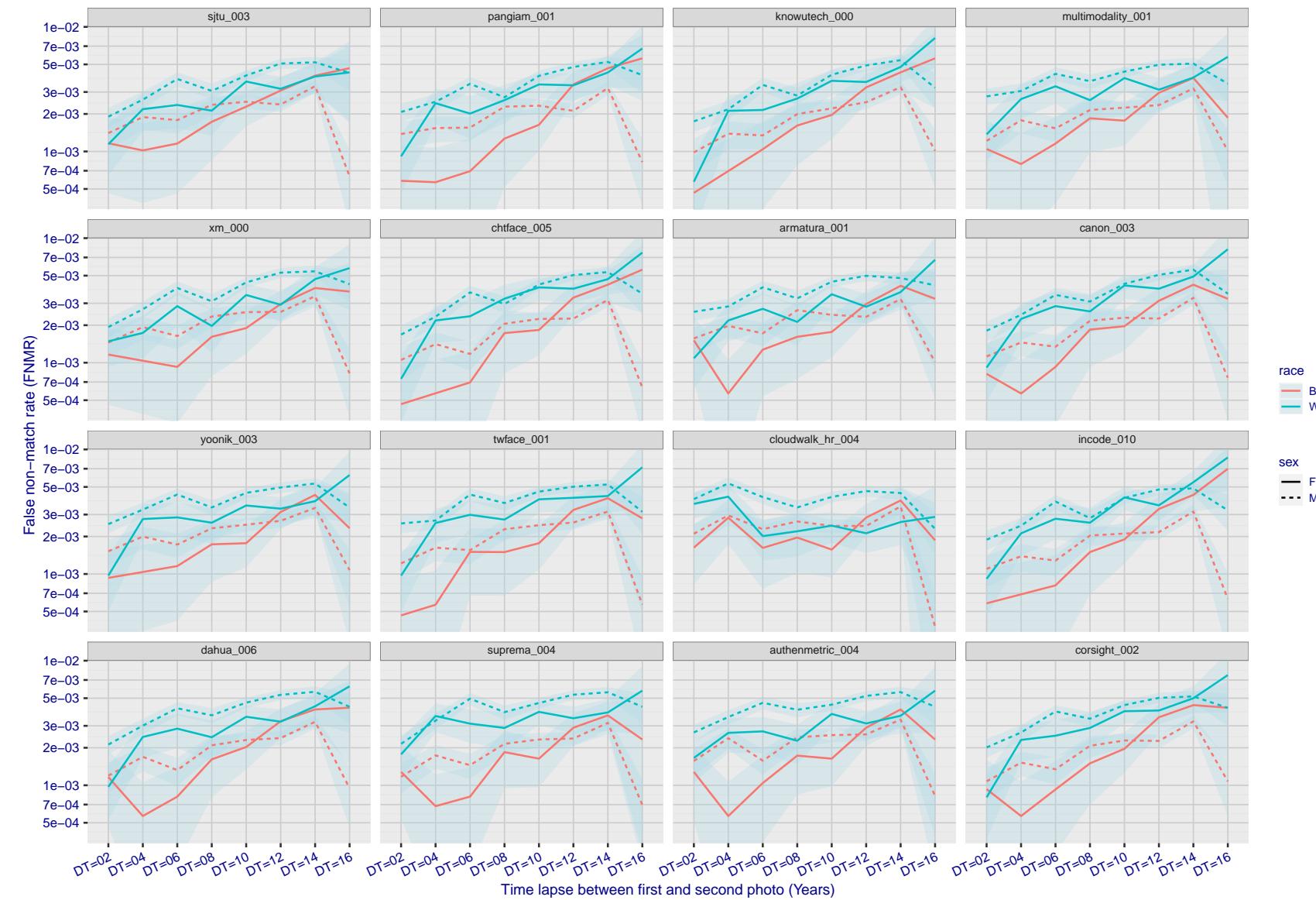


Figure 305: For the mugshot images, FNMR as a function of elapsed time between initial enrollment and second verification images. The panels appear most accurate first, and vertical scale changes on each page. The four traces correspond to images annotated with codes for black female, black male, white female, white male. The threshold is fixed for each algorithm to give $FMR = 0.00001$ over all (10^8) impostor comparisons. For short time-lapses, the most accurate algorithms give very few errors ($FNMR < 0.001$) so that the uncertainty estimates are high.

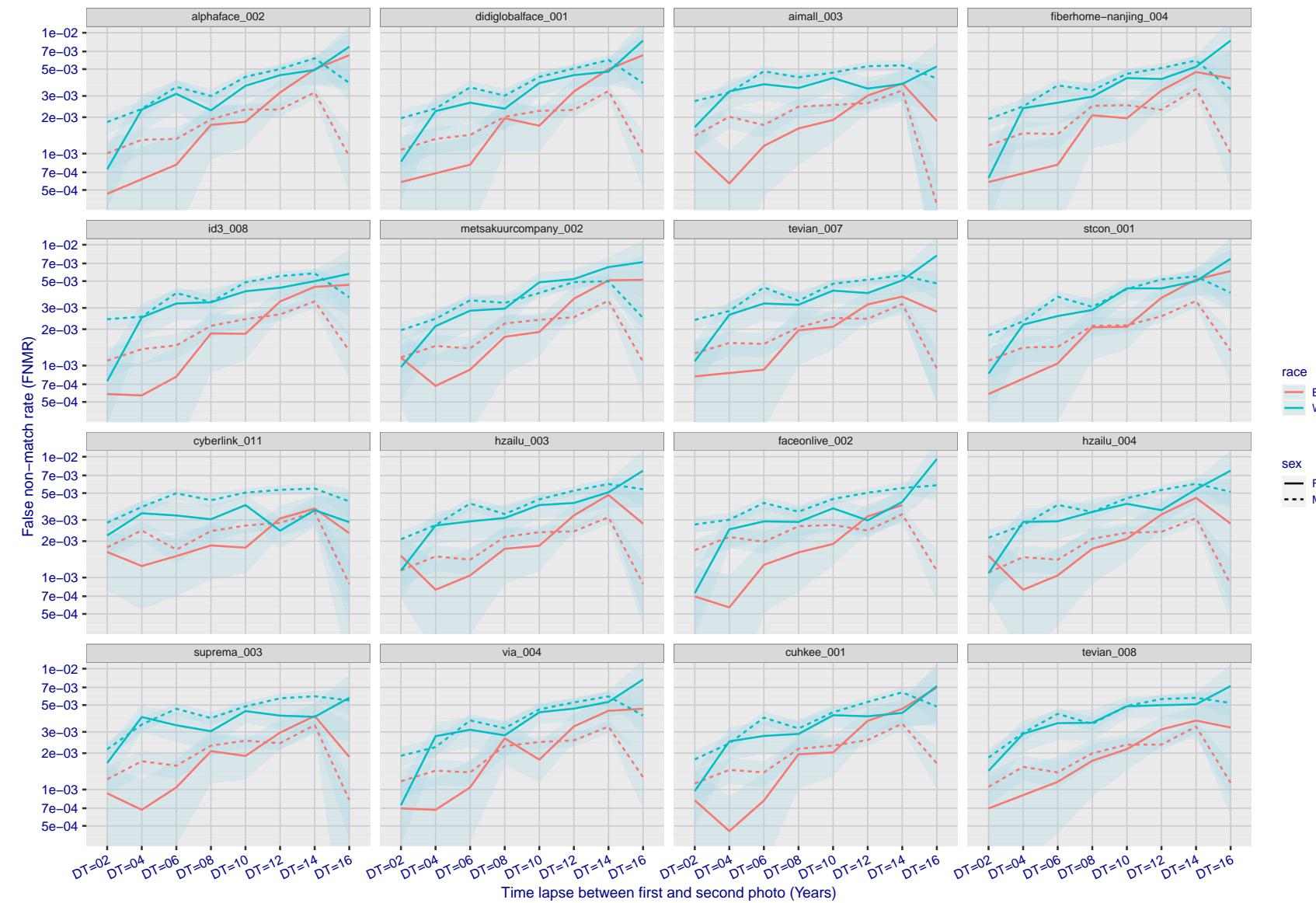


Figure 306: For the mugshot images, FNMR as a function of elapsed time between initial enrollment and second verification images. The panels appear most accurate first, and vertical scale changes on each page. The four traces correspond to images annotated with codes for black female, black male, white female, white male. The threshold is fixed for each algorithm to give $FMR = 0.00001$ over all (10^8) impostor comparisons. For short time-lapses, the most accurate algorithms give very few errors ($FNMR < 0.001$) so that the uncertainty estimates are high.

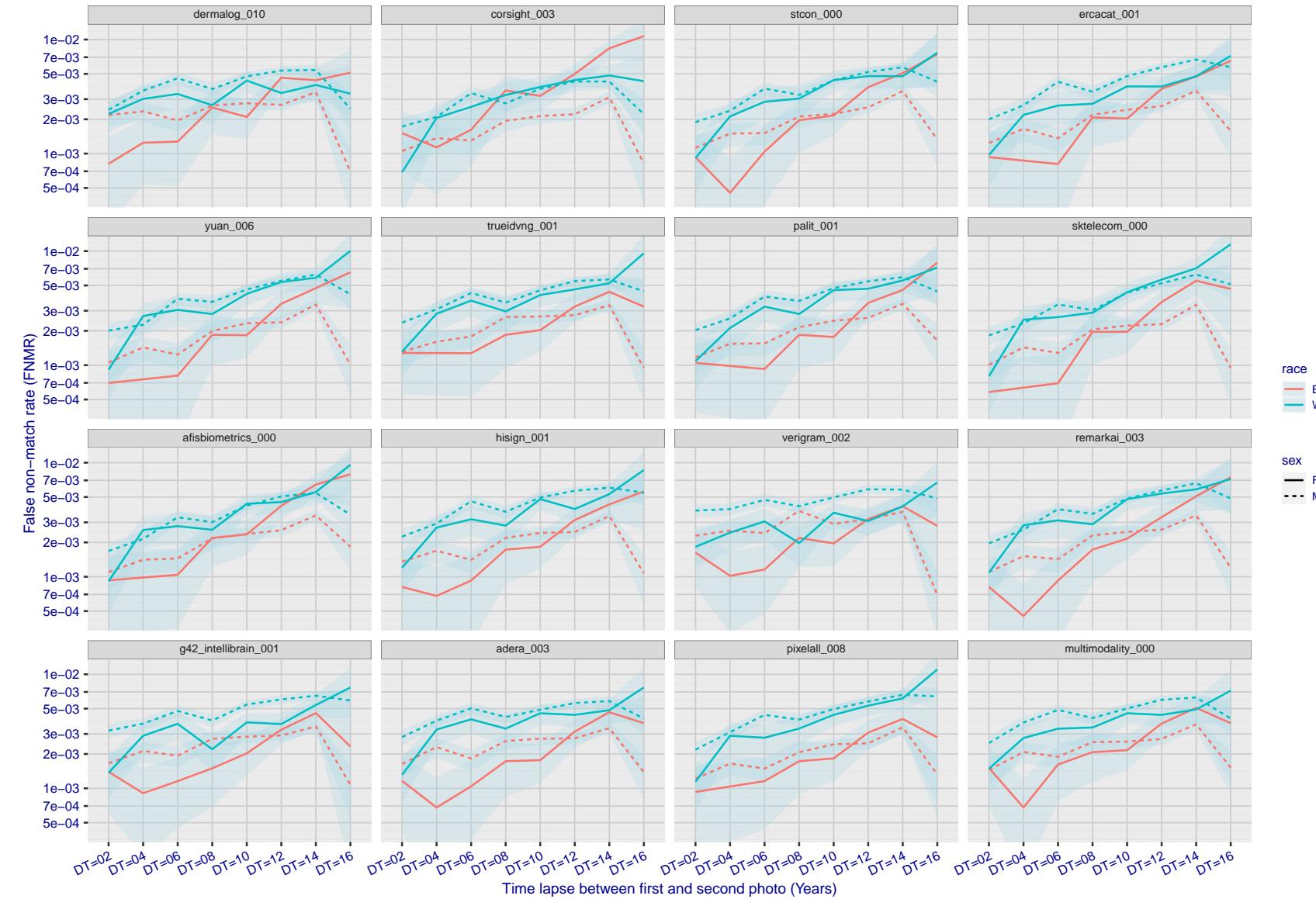


Figure 307: For the mugshot images, FNMR as a function of elapsed time between initial enrollment and second verification images. The panels appear most accurate first, and vertical scale changes on each page. The four traces correspond to images annotated with codes for black female, black male, white female, white male. The threshold is fixed for each algorithm to give $FMR = 0.00001$ over all (10^8) impostor comparisons. For short time-lapses, the most accurate algorithms give very few errors ($FNMR < 0.001$) so that the uncertainty estimates are high.

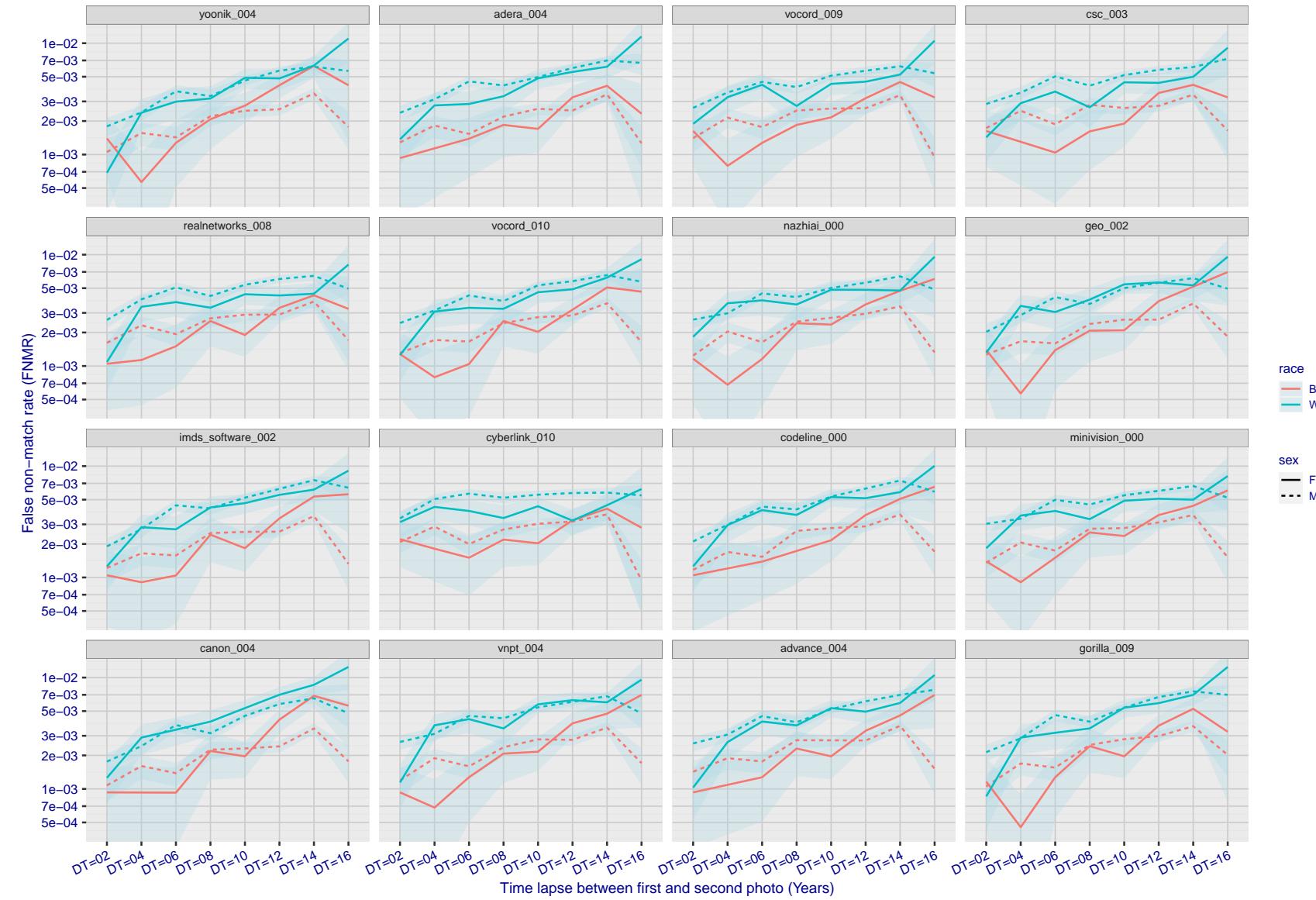


Figure 308: For the mugshot images, FNMR as a function of elapsed time between initial enrollment and second verification images. The panels appear most accurate first, and vertical scale changes on each page. The four traces correspond to images annotated with codes for black female, black male, white female, white male. The threshold is fixed for each algorithm to give $FMR = 0.00001$ over all (10^8) impostor comparisons. For short time-lapses, the most accurate algorithms give very few errors ($FNMR < 0.001$) so that the uncertainty estimates are high.

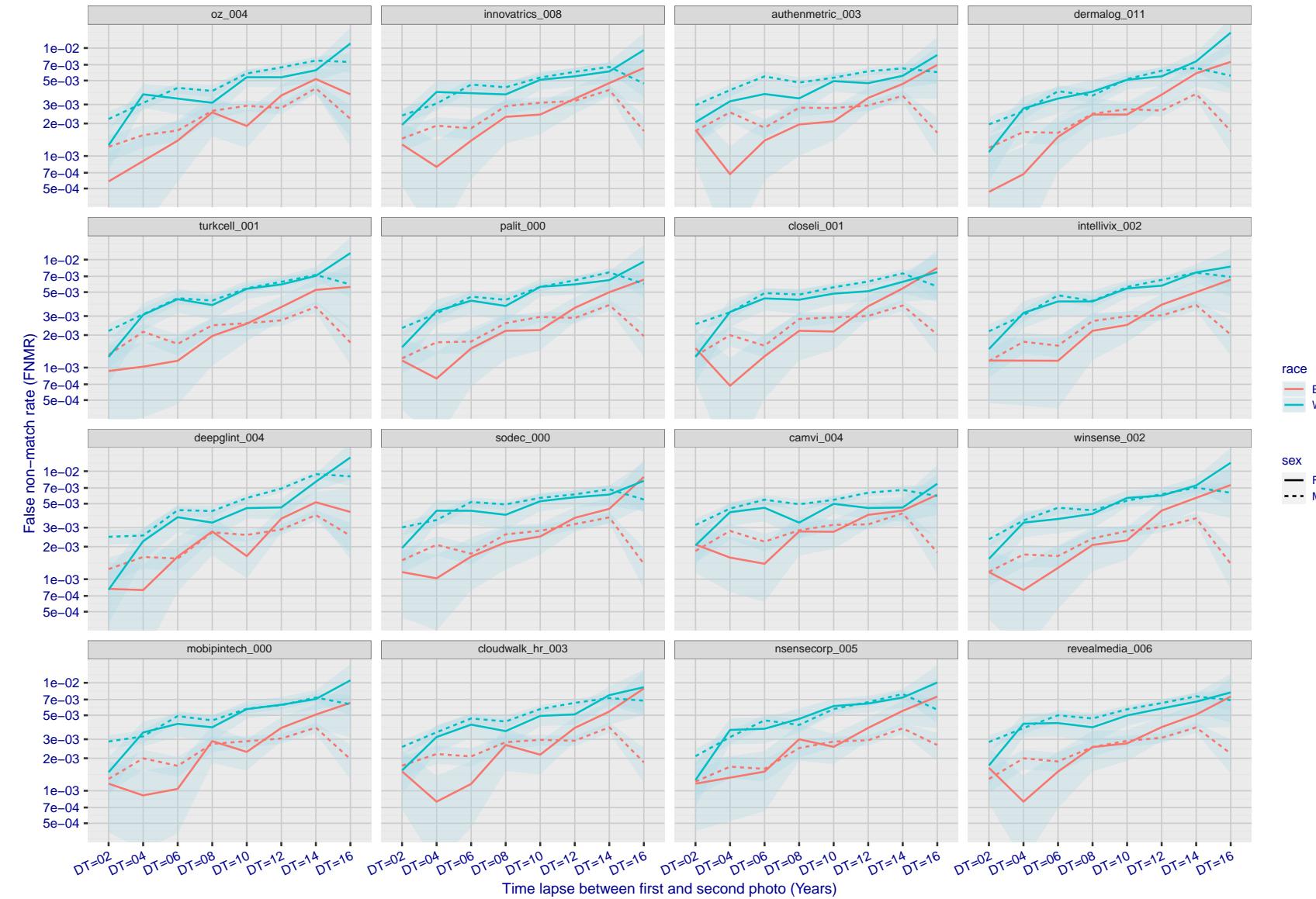


Figure 309: For the mugshot images, FNMR as a function of elapsed time between initial enrollment and second verification images. The panels appear most accurate first, and vertical scale changes on each page. The four traces correspond to images annotated with codes for black female, black male, white female, white male. The threshold is fixed for each algorithm to give $FMR = 0.00001$ over all (10^8) impostor comparisons. For short time-lapses, the most accurate algorithms give very few errors ($FNMR < 0.001$) so that the uncertainty estimates are high.

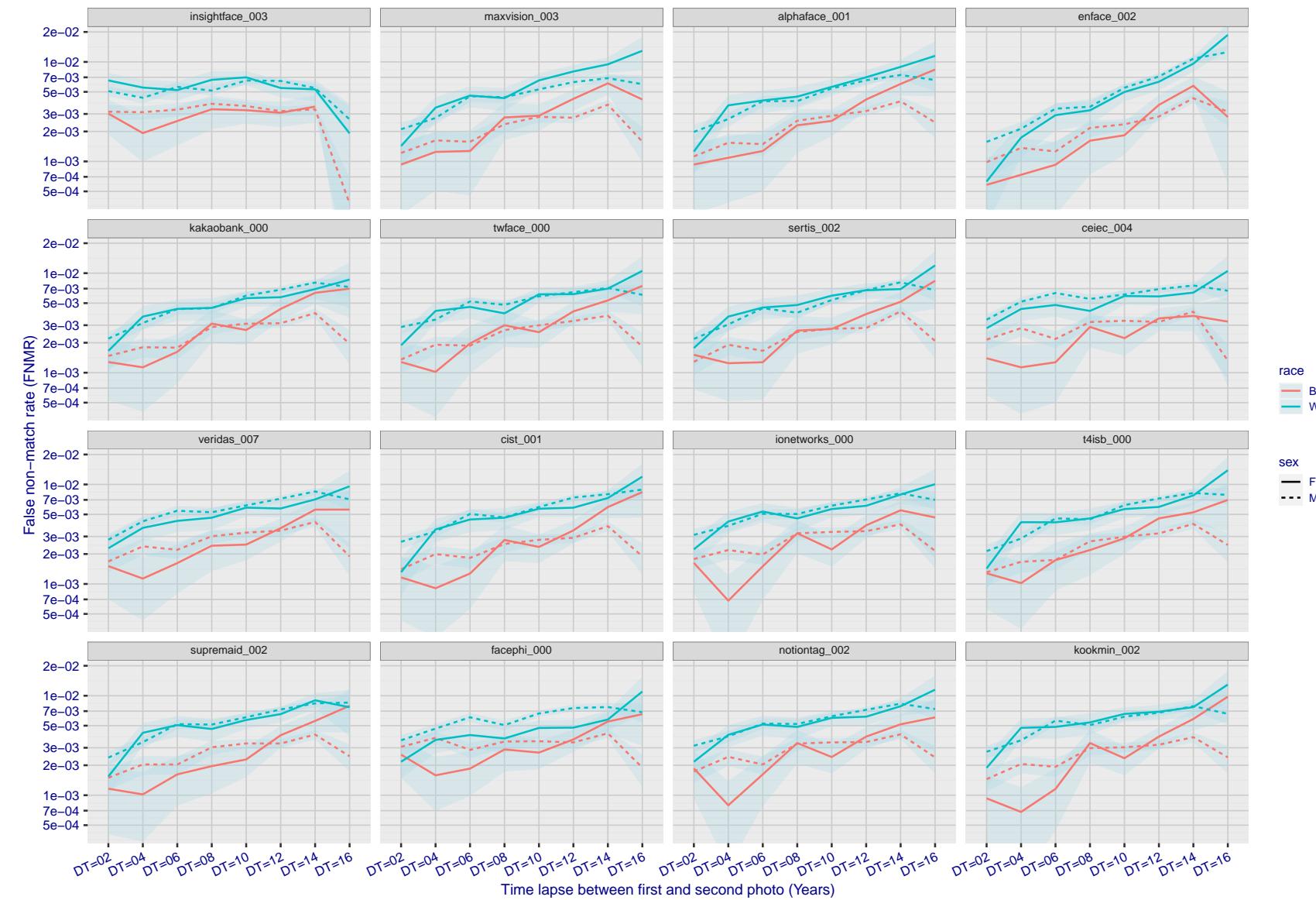


Figure 310: For the mugshot images, FNMR as a function of elapsed time between initial enrollment and second verification images. The panels appear most accurate first, and vertical scale changes on each page. The four traces correspond to images annotated with codes for black female, black male, white female, white male. The threshold is fixed for each algorithm to give $FMR = 0.00001$ over all (10^8) impostor comparisons. For short time-lapses, the most accurate algorithms give very few errors ($FNMR < 0.001$) so that the uncertainty estimates are high.

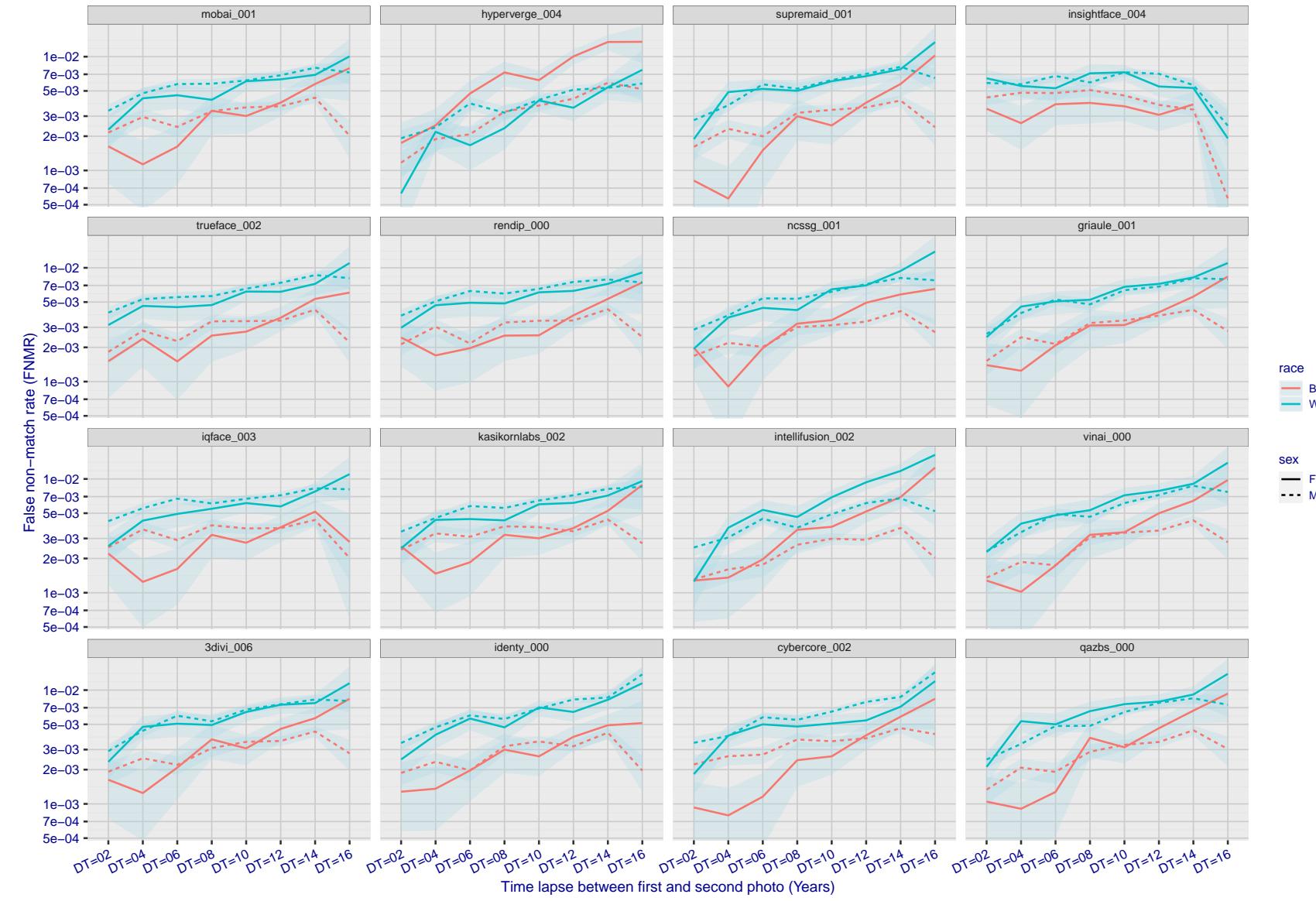


Figure 311: For the mugshot images, FNMR as a function of elapsed time between initial enrollment and second verification images. The panels appear most accurate first, and vertical scale changes on each page. The four traces correspond to images annotated with codes for black female, black male, white female, white male. The threshold is fixed for each algorithm to give $FMR = 0.00001$ over all (10^8) impostor comparisons. For short time-lapses, the most accurate algorithms give very few errors ($FNMR < 0.001$) so that the uncertainty estimates are high.

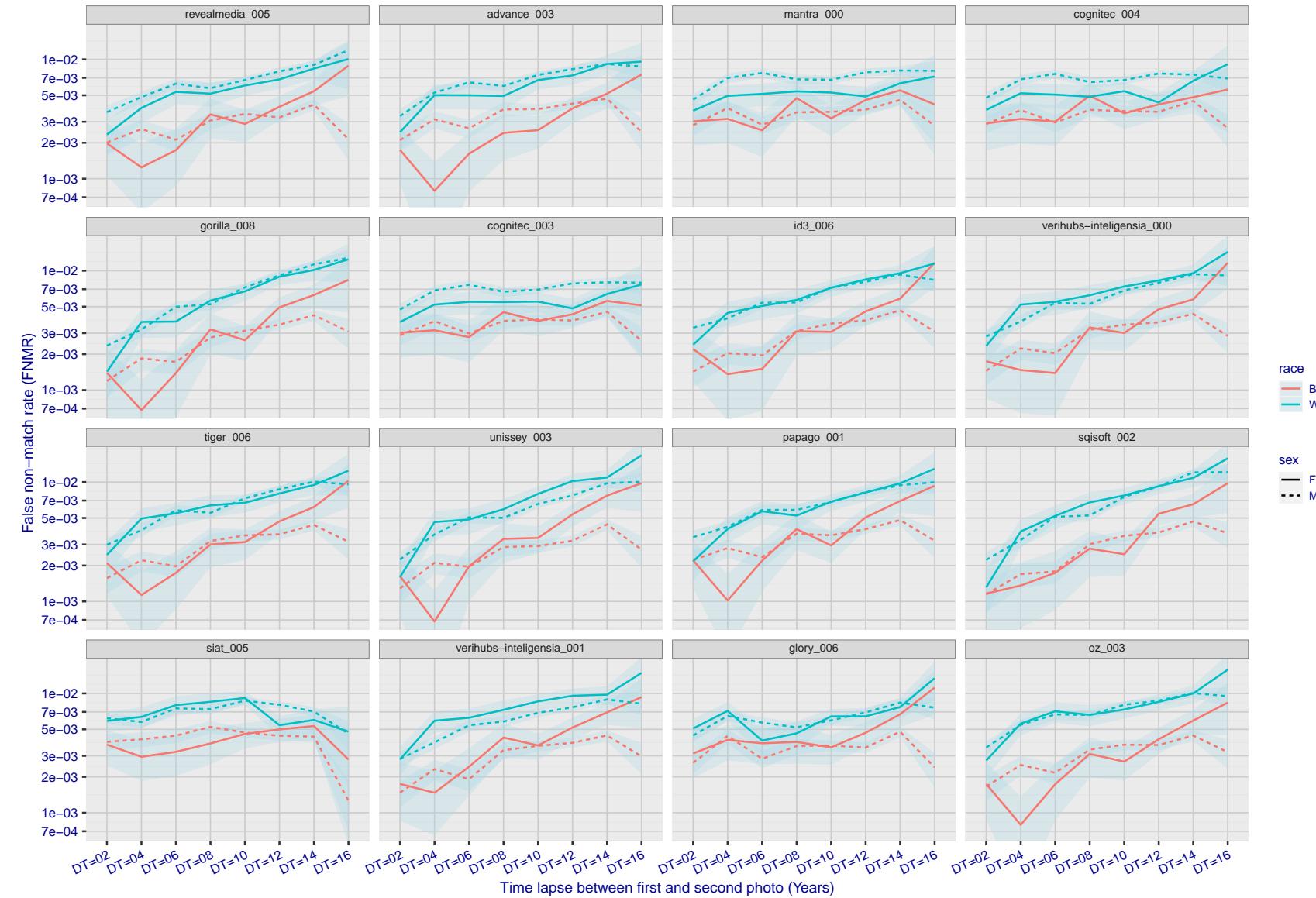


Figure 312: For the mugshot images, FNMR as a function of elapsed time between initial enrollment and second verification images. The panels appear most accurate first, and vertical scale changes on each page. The four traces correspond to images annotated with codes for black female, black male, white female, white male. The threshold is fixed for each algorithm to give $FMR = 0.00001$ over all (10^8) impostor comparisons. For short time-lapses, the most accurate algorithms give very few errors ($FNMR < 0.001$) so that the uncertainty estimates are high.

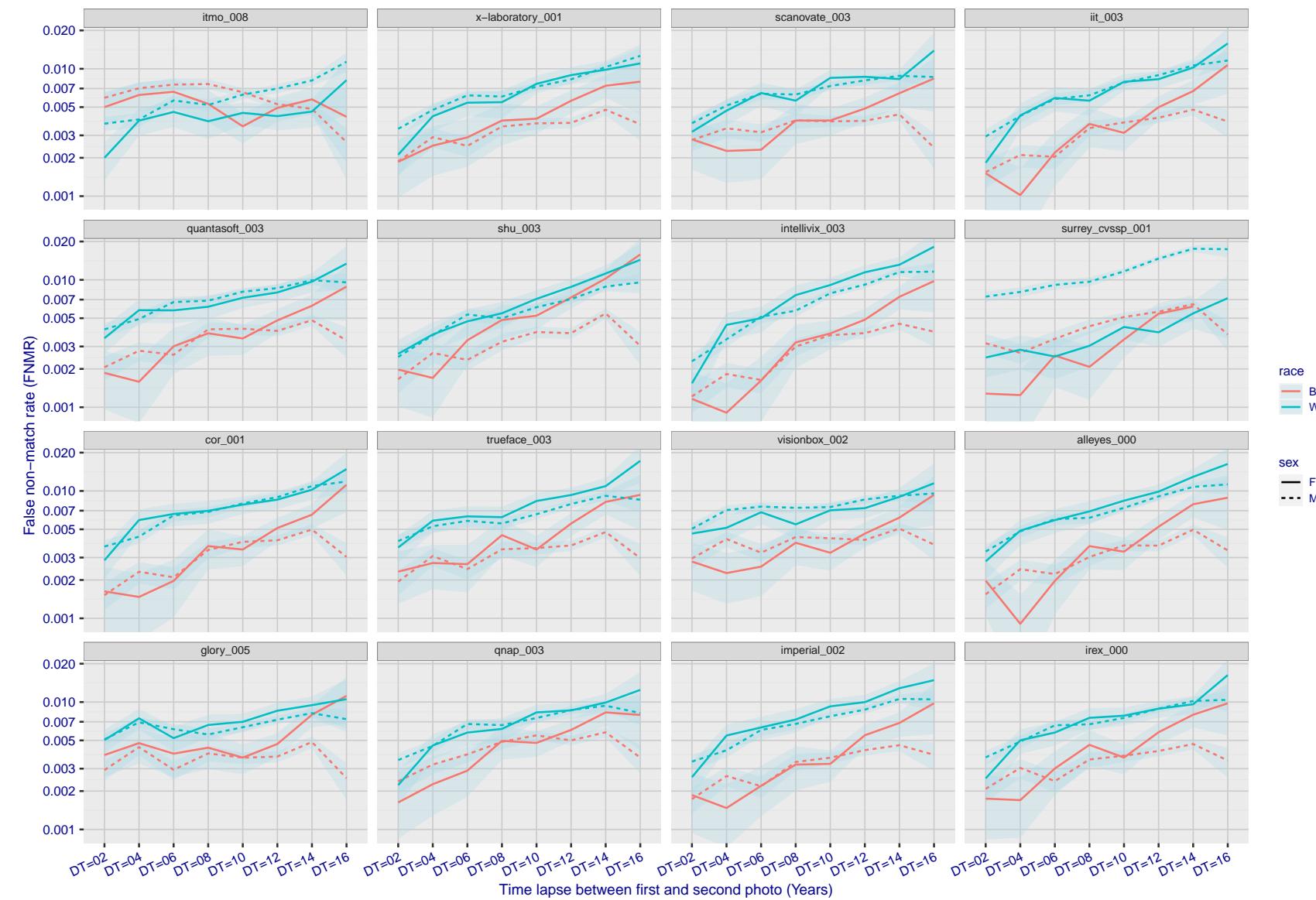


Figure 313: For the mugshot images, FNMR as a function of elapsed time between initial enrollment and second verification images. The panels appear most accurate first, and vertical scale changes on each page. The four traces correspond to images annotated with codes for black female, black male, white female, white male. The threshold is fixed for each algorithm to give $FMR = 0.00001$ over all (10^8) impostor comparisons. For short time-lapses, the most accurate algorithms give very few errors ($FNMR < 0.001$) so that the uncertainty estimates are high.

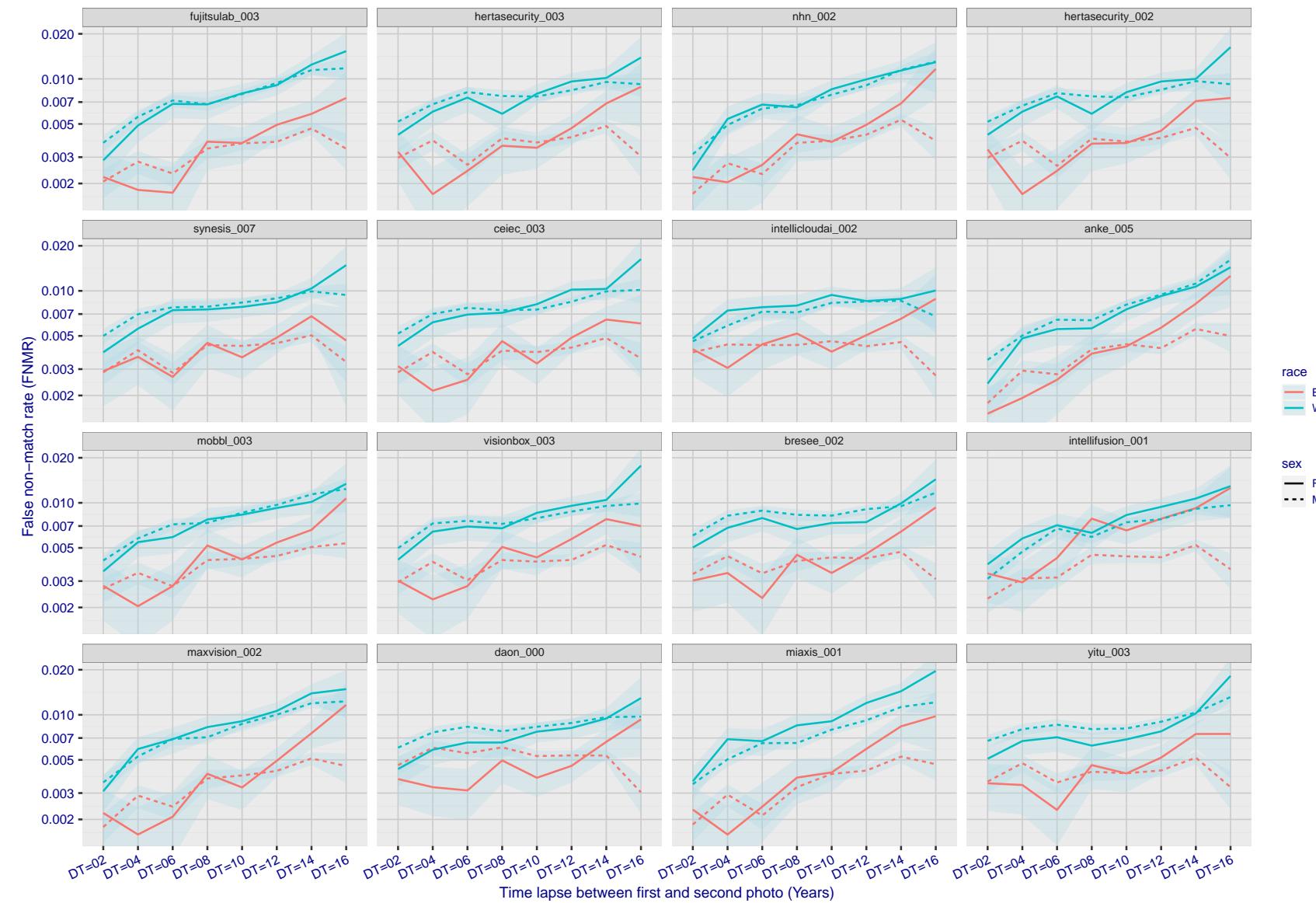


Figure 314: For the mugshot images, FNMR as a function of elapsed time between initial enrollment and second verification images. The panels appear most accurate first, and vertical scale changes on each page. The four traces correspond to images annotated with codes for black female, black male, white female, white male. The threshold is fixed for each algorithm to give FMR = 0.00001 over all (10^8) impostor comparisons. For short time-lapses, the most accurate algorithms give very few errors (FNMR < 0.001) so that the uncertainty estimates are high.

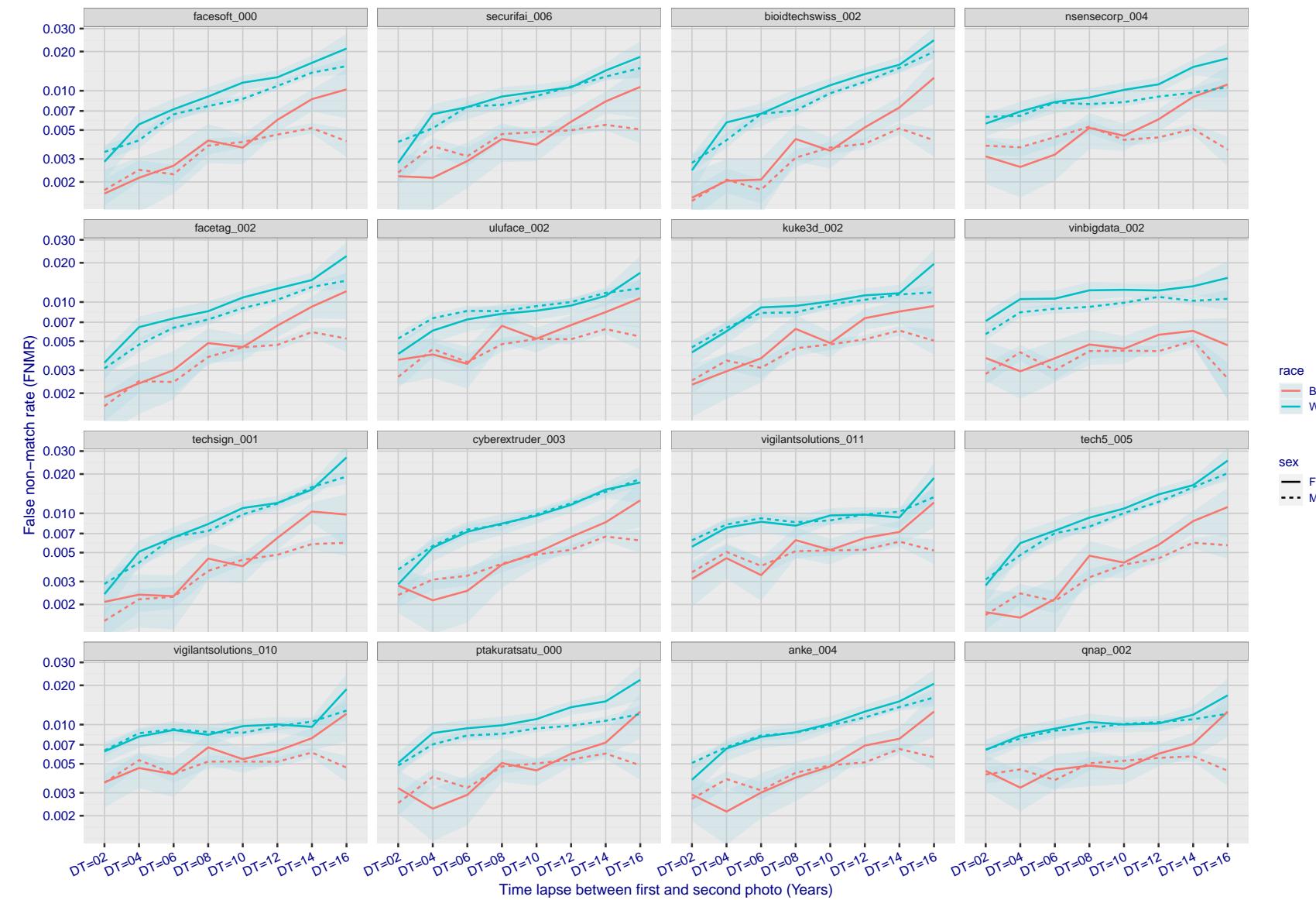


Figure 315: For the mugshot images, FNMR as a function of elapsed time between initial enrollment and second verification images. The panels appear most accurate first, and vertical scale changes on each page. The four traces correspond to images annotated with codes for black female, black male, white female, white male. The threshold is fixed for each algorithm to give FMR = 0.00001 over all (10^8) impostor comparisons. For short time-lapses, the most accurate algorithms give very few errors (FNMR < 0.001) so that the uncertainty estimates are high.

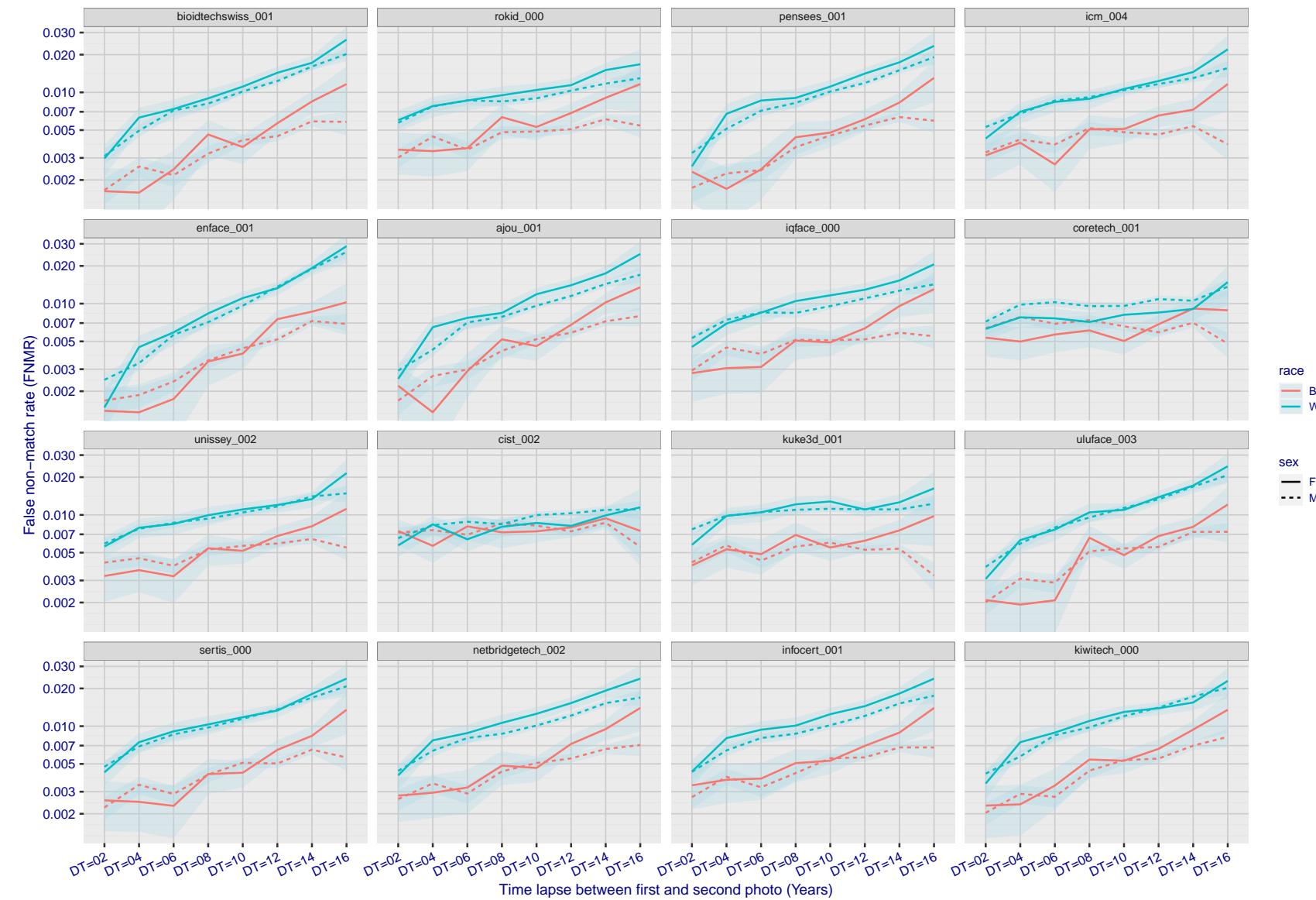


Figure 316: For the mugshot images, FNMR as a function of elapsed time between initial enrollment and second verification images. The panels appear most accurate first, and vertical scale changes on each page. The four traces correspond to images annotated with codes for black female, black male, white female, white male. The threshold is fixed for each algorithm to give FMR = 0.00001 over all (10^8) impostor comparisons. For short time-lapses, the most accurate algorithms give very few errors (FNMR < 0.001) so that the uncertainty estimates are high.

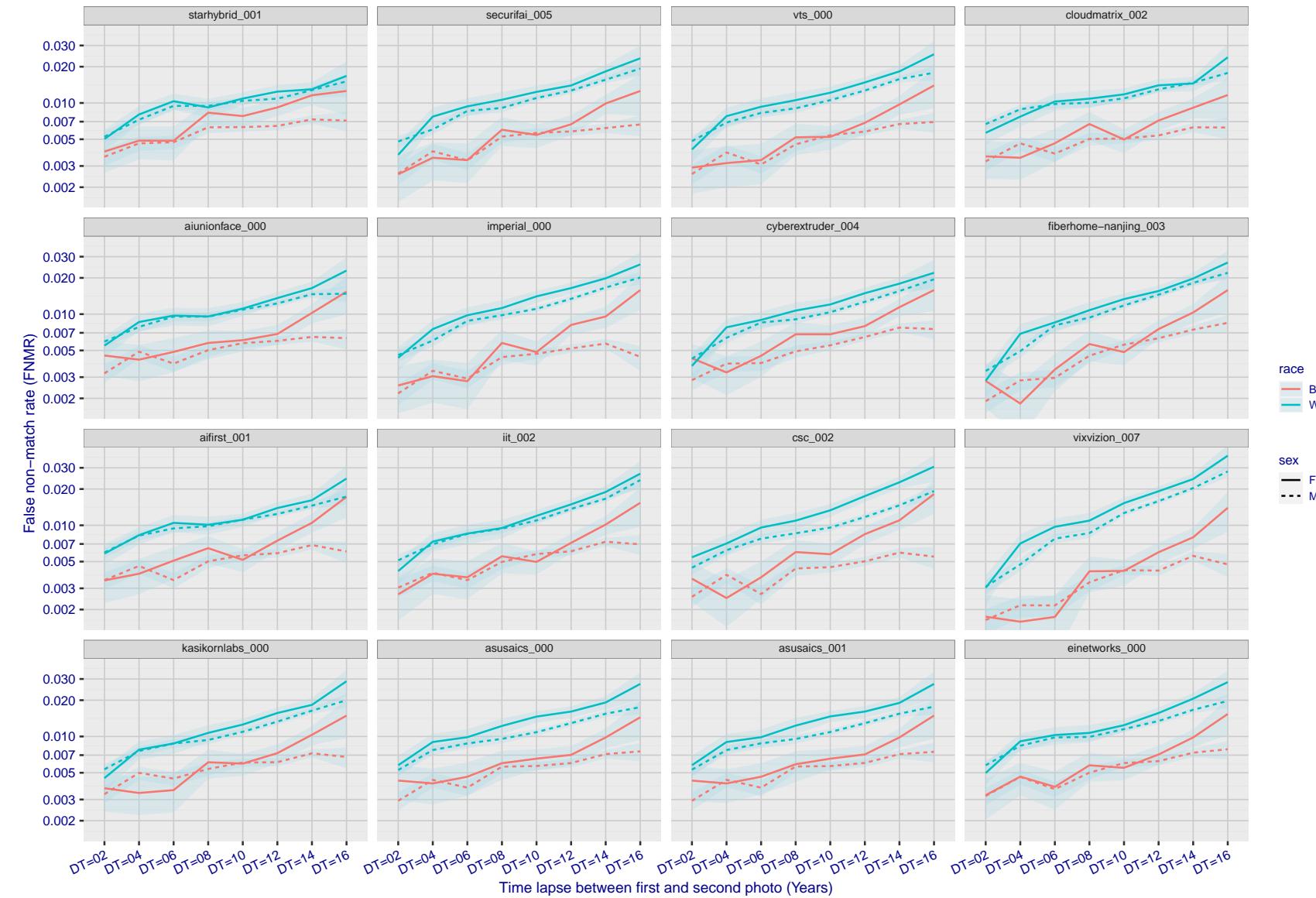


Figure 317: For the mugshot images, FNMR as a function of elapsed time between initial enrollment and second verification images. The panels appear most accurate first, and vertical scale changes on each page. The four traces correspond to images annotated with codes for black female, black male, white female, white male. The threshold is fixed for each algorithm to give FMR = 0.00001 over all (10^8) impostor comparisons. For short time-lapses, the most accurate algorithms give very few errors (FNMR < 0.001) so that the uncertainty estimates are high.

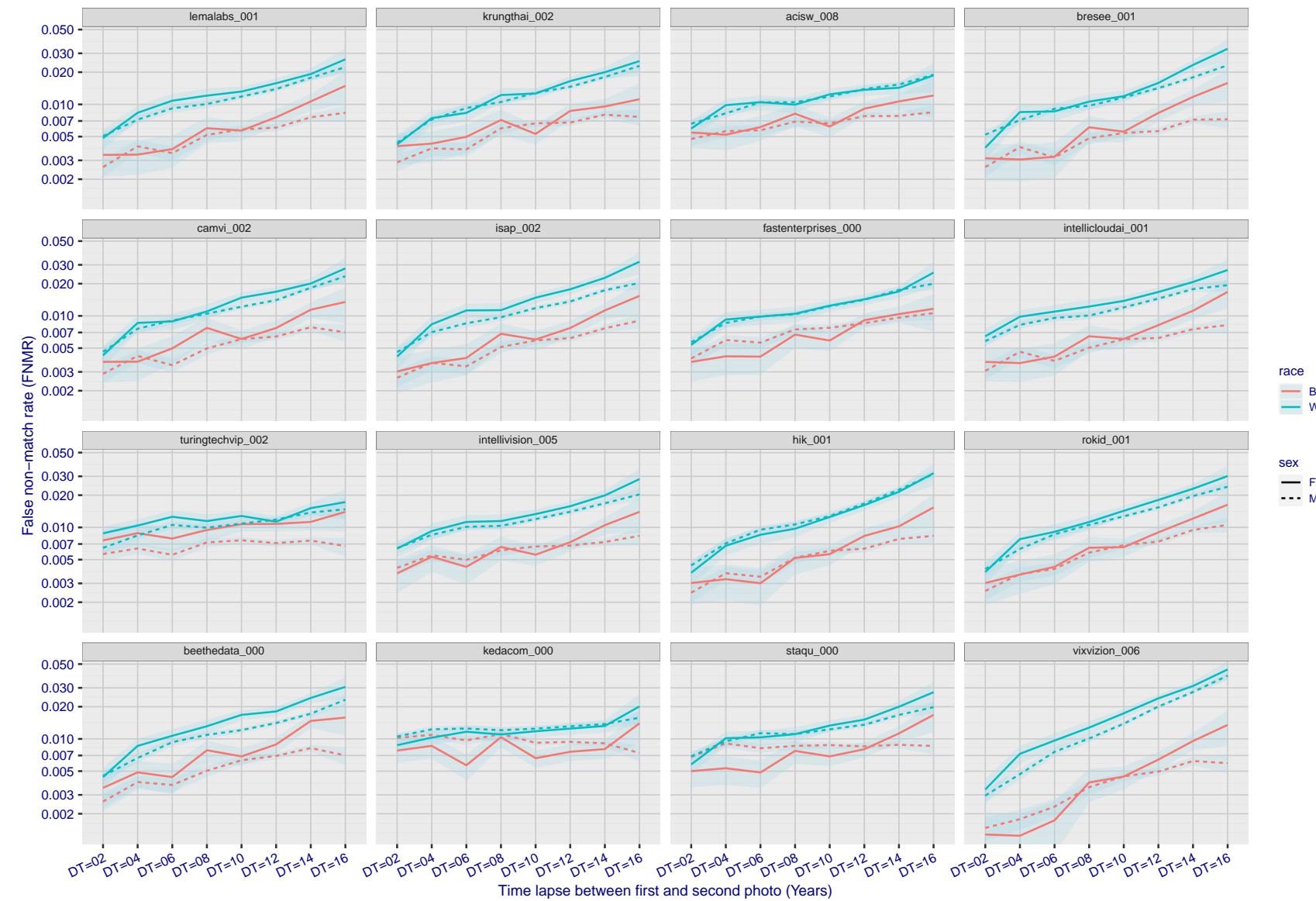


Figure 318: For the mugshot images, FNMR as a function of elapsed time between initial enrollment and second verification images. The panels appear most accurate first, and vertical scale changes on each page. The four traces correspond to images annotated with codes for black female, black male, white female, white male. The threshold is fixed for each algorithm to give FMR = 0.00001 over all (10^8) impostor comparisons. For short time-lapses, the most accurate algorithms give very few errors (FNMR < 0.001) so that the uncertainty estimates are high.

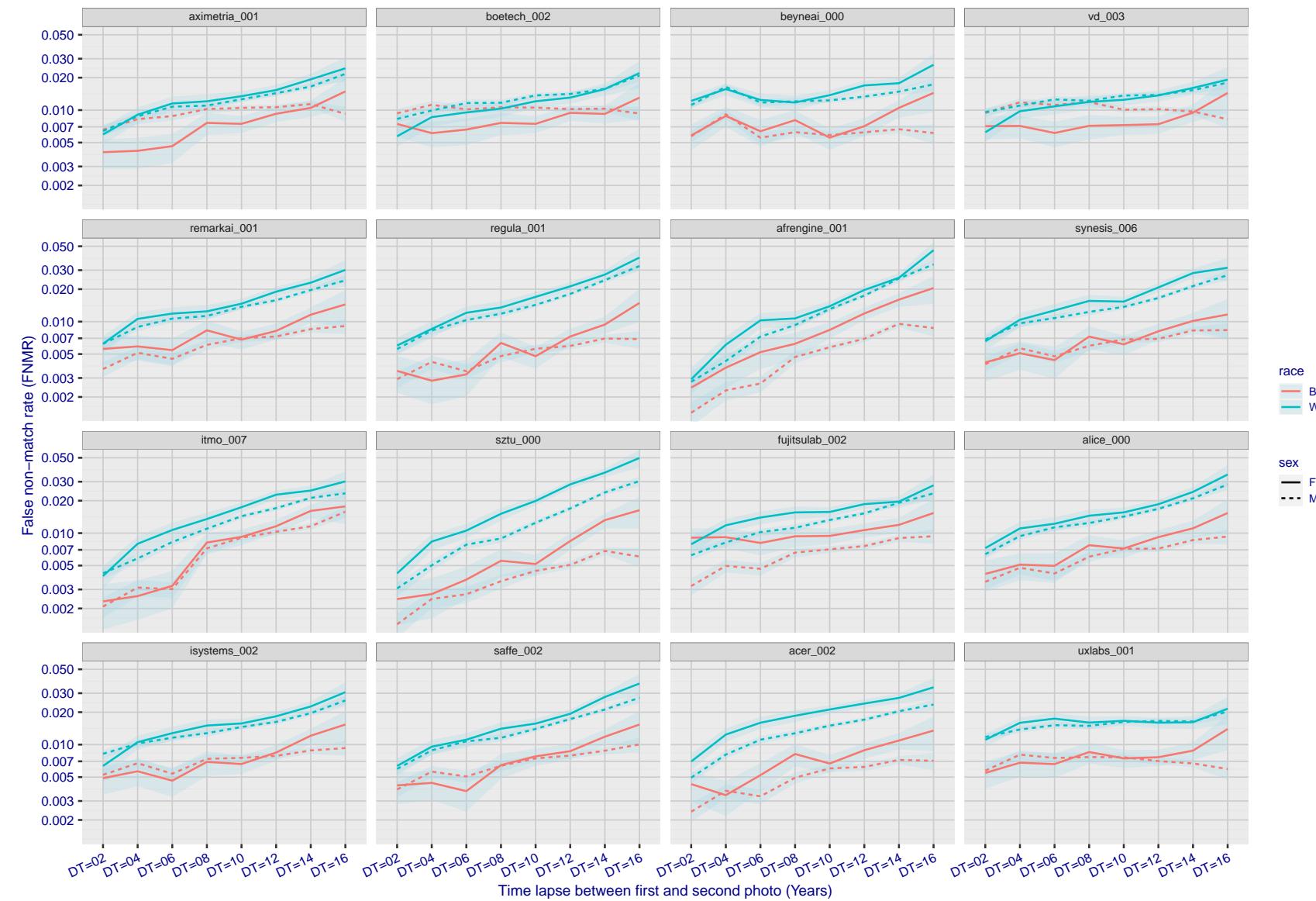


Figure 319: For the mugshot images, FNMR as a function of elapsed time between initial enrollment and second verification images. The panels appear most accurate first, and vertical scale changes on each page. The four traces correspond to images annotated with codes for black female, black male, white female, white male. The threshold is fixed for each algorithm to give $FMR = 0.00001$ over all (10^8) impostor comparisons. For short time-lapses, the most accurate algorithms give very few errors ($FNMR < 0.001$) so that the uncertainty estimates are high.

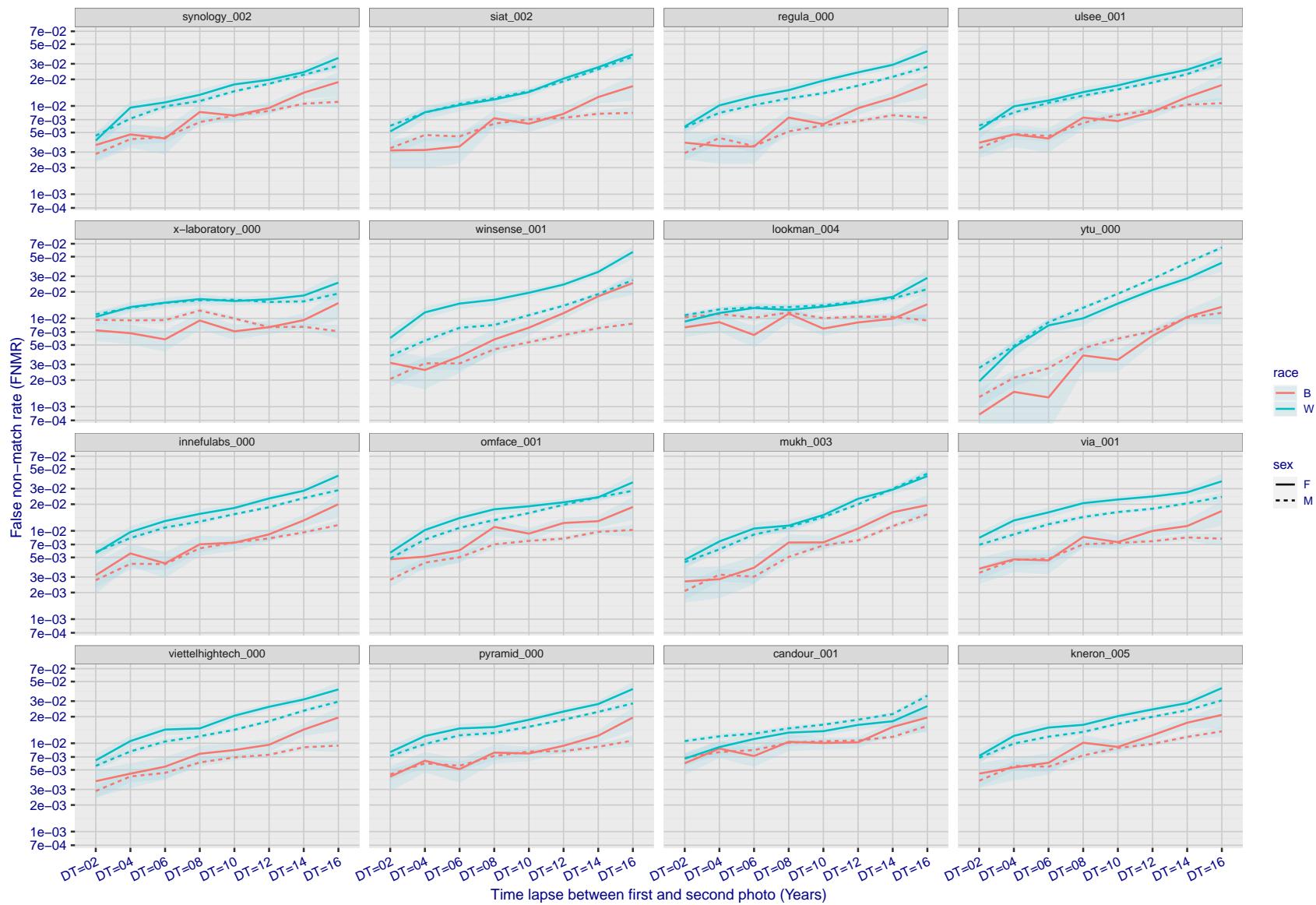


Figure 320: For the mugshot images, FNMR as a function of elapsed time between initial enrollment and second verification images. The panels appear most accurate first, and vertical scale changes on each page. The four traces correspond to images annotated with codes for black female, black male, white female, white male. The threshold is fixed for each algorithm to give $FMR = 0.00001$ over all (10^8) impostor comparisons. For short time-lapses, the most accurate algorithms give very few errors ($FNMR < 0.001$) so that the uncertainty estimates are high.

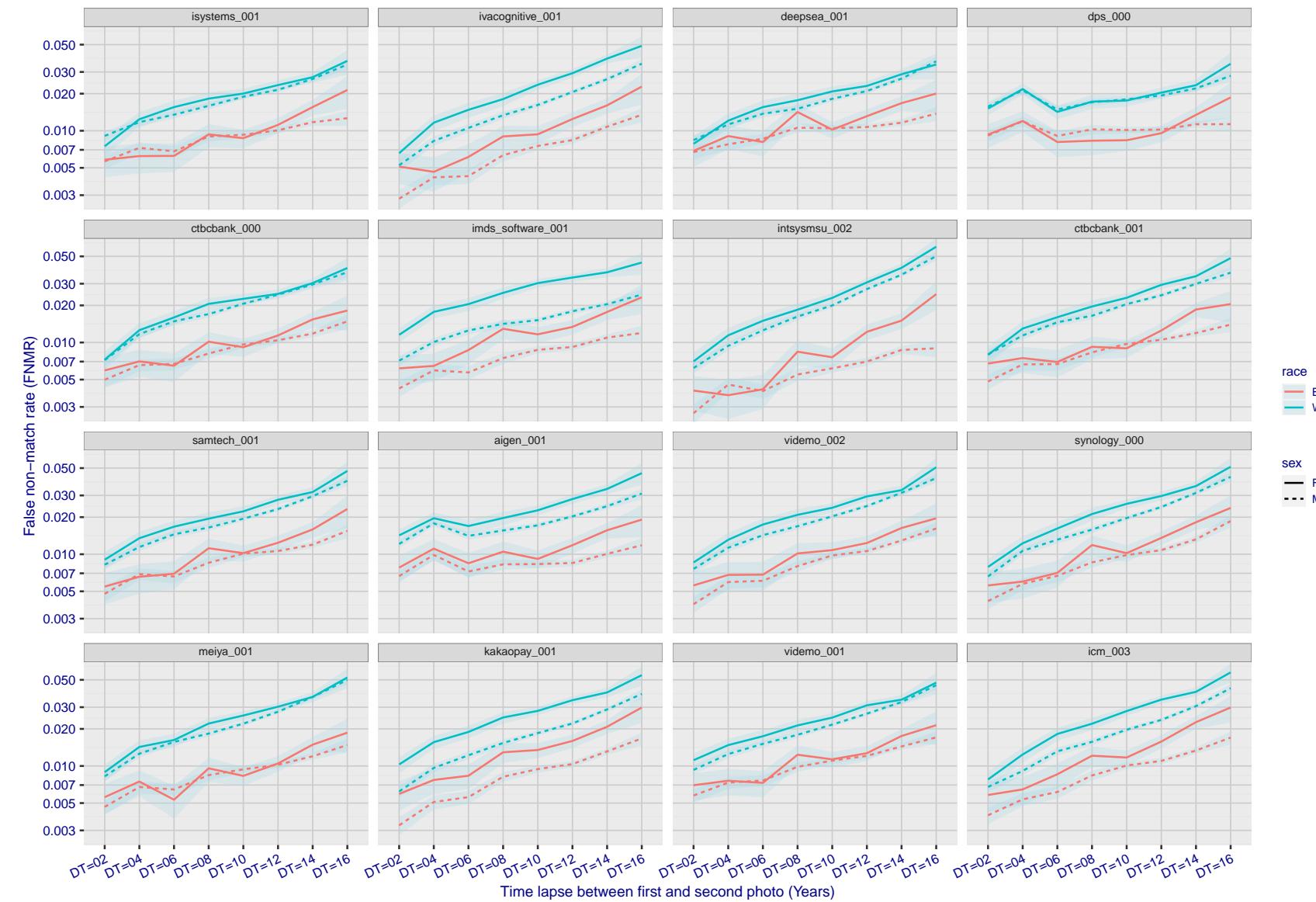


Figure 321: For the mugshot images, FNMR as a function of elapsed time between initial enrollment and second verification images. The panels appear most accurate first, and vertical scale changes on each page. The four traces correspond to images annotated with codes for black female, black male, white female, white male. The threshold is fixed for each algorithm to give FMR = 0.00001 over all (10^8) impostor comparisons. For short time-lapses, the most accurate algorithms give very few errors (FNMR < 0.001) so that the uncertainty estimates are high.

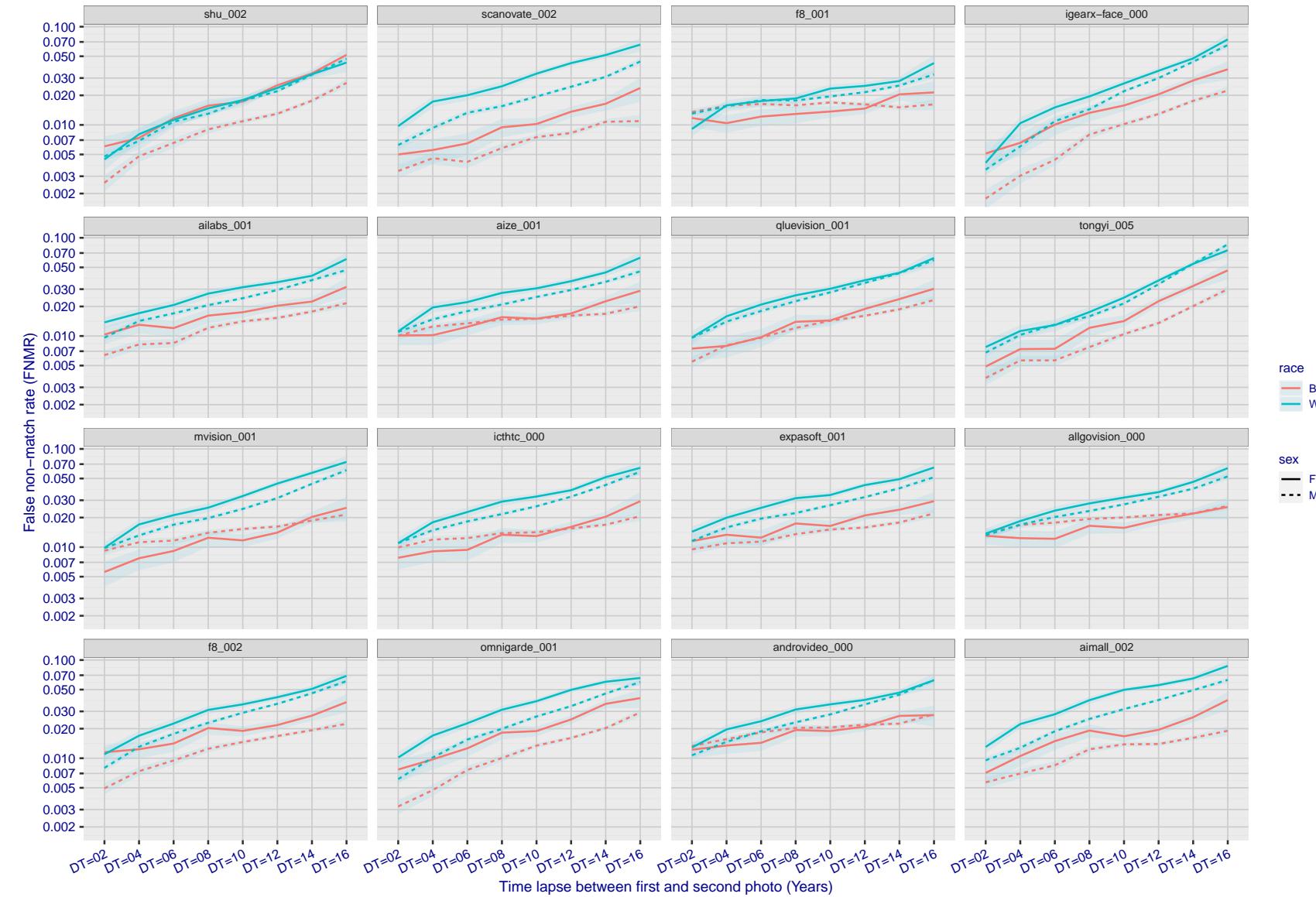


Figure 322: For the mugshot images, FNMR as a function of elapsed time between initial enrollment and second verification images. The panels appear most accurate first, and vertical scale changes on each page. The four traces correspond to images annotated with codes for black female, black male, white female, white male. The threshold is fixed for each algorithm to give FMR = 0.00001 over all (10^8) impostor comparisons. For short time-lapses, the most accurate algorithms give very few errors (FNMR < 0.001) so that the uncertainty estimates are high.

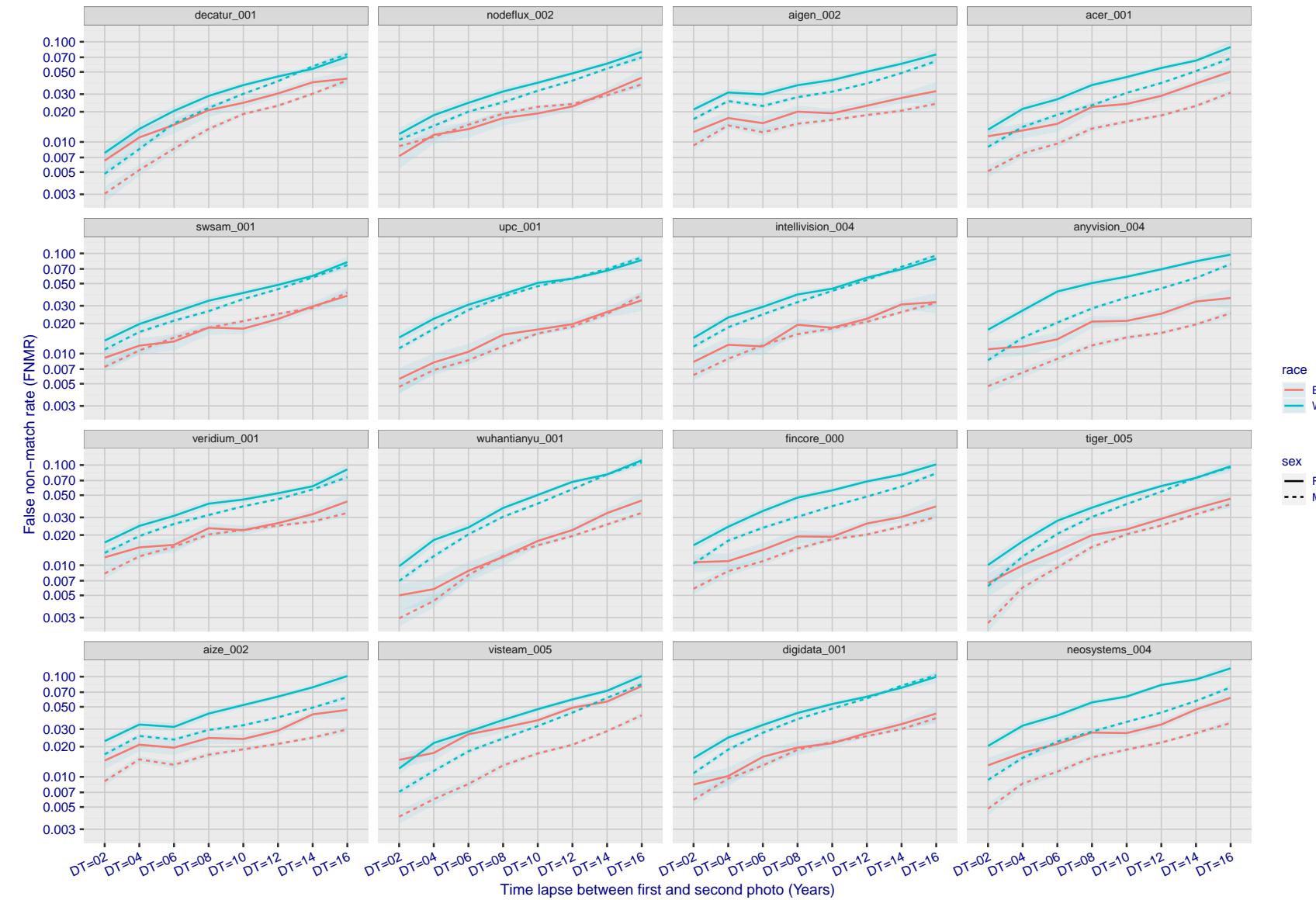


Figure 323: For the mugshot images, FNMR as a function of elapsed time between initial enrollment and second verification images. The panels appear most accurate first, and vertical scale changes on each page. The four traces correspond to images annotated with codes for black female, black male, white female, white male. The threshold is fixed for each algorithm to give $FMR = 0.00001$ over all (10^8) impostor comparisons. For short time-lapses, the most accurate algorithms give very few errors ($FNMR < 0.001$) so that the uncertainty estimates are high.

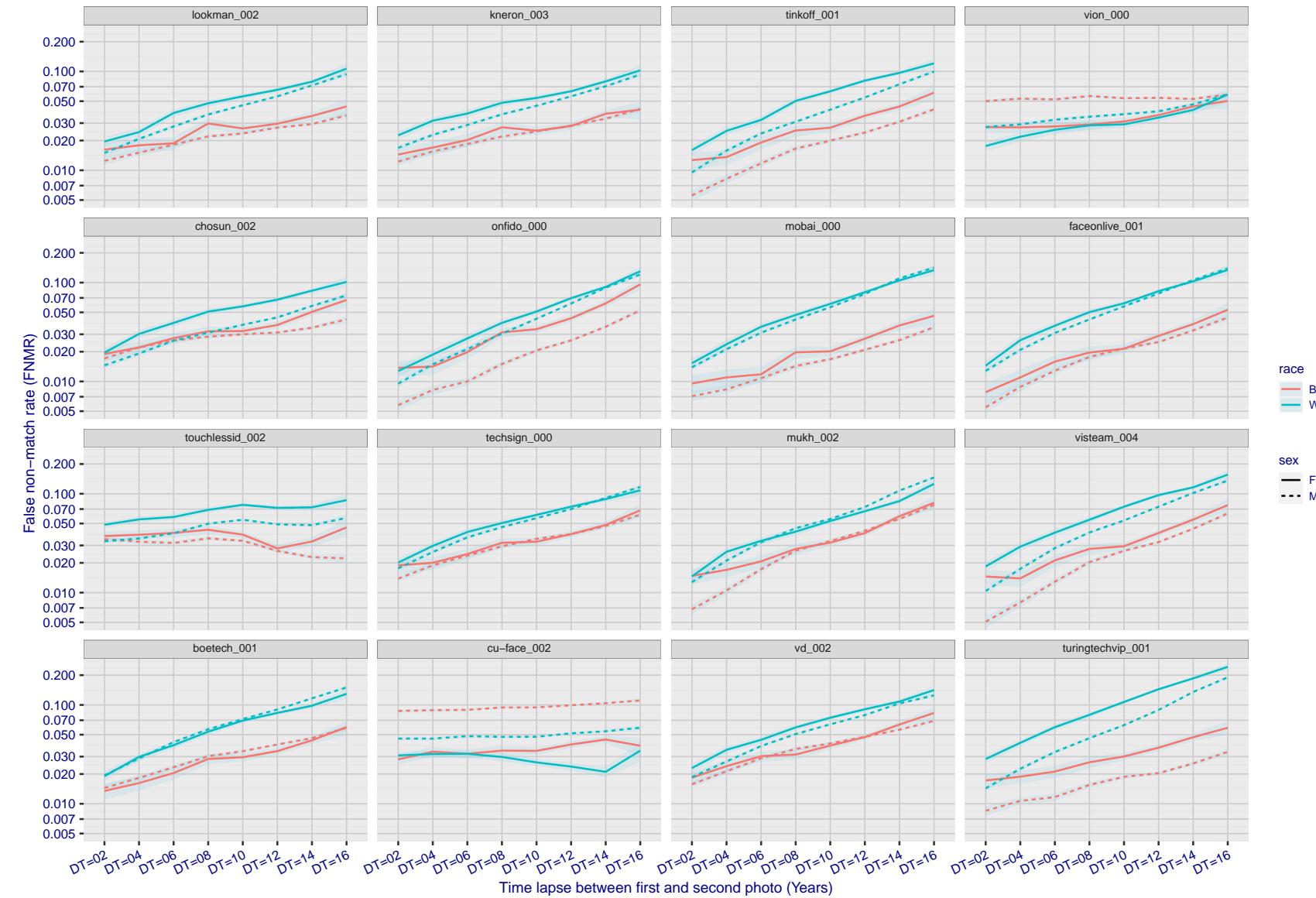


Figure 324: For the mugshot images, FNMR as a function of elapsed time between initial enrollment and second verification images. The panels appear most accurate first, and vertical scale changes on each page. The four traces correspond to images annotated with codes for black female, black male, white female, white male. The threshold is fixed for each algorithm to give FMR = 0.00001 over all (10^8) impostor comparisons. For short time-lapses, the most accurate algorithms give very few errors (FNMR < 0.001) so that the uncertainty estimates are high.

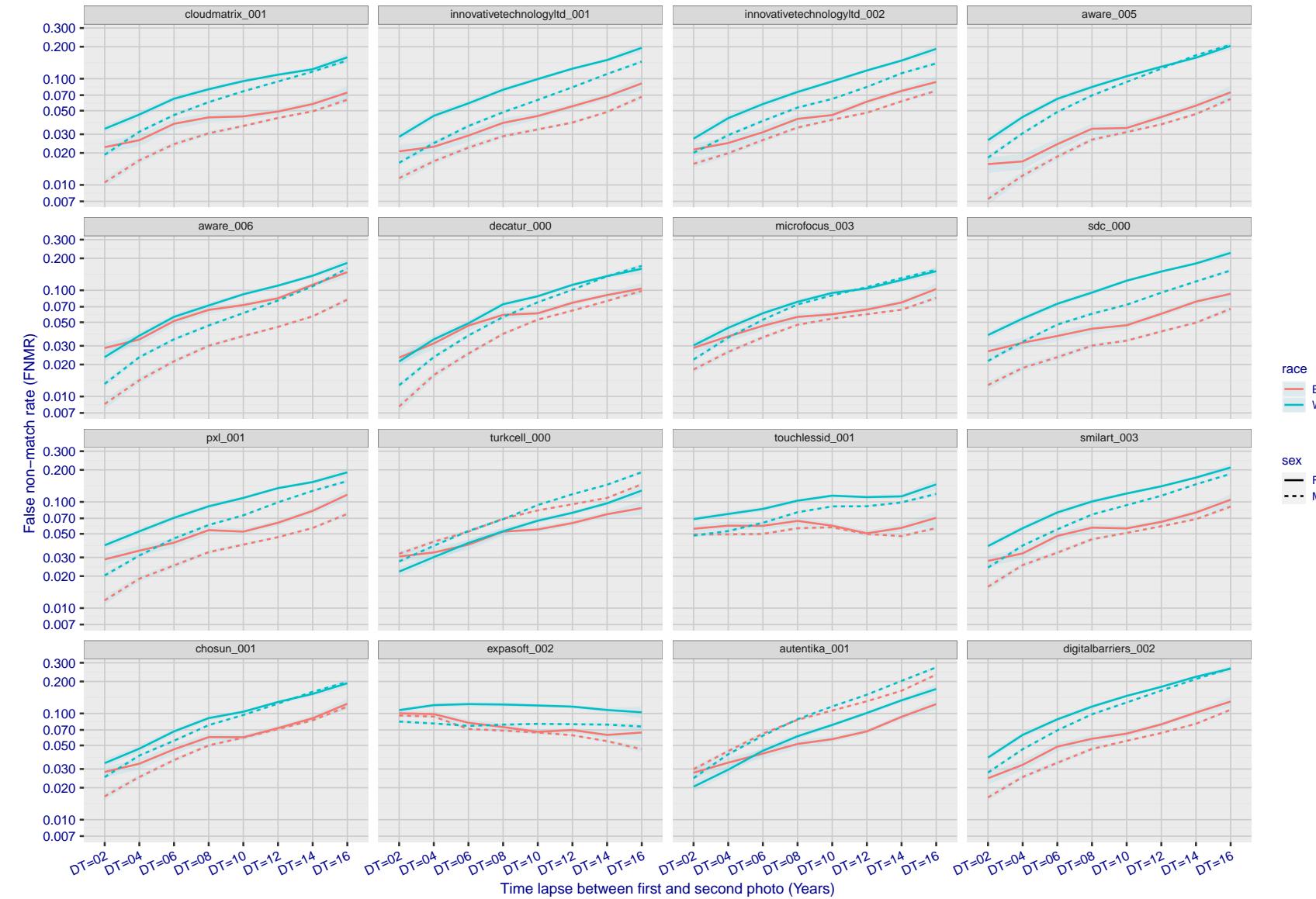


Figure 325: For the mugshot images, FNMR as a function of elapsed time between initial enrollment and second verification images. The panels appear most accurate first, and vertical scale changes on each page. The four traces correspond to images annotated with codes for black female, black male, white female, white male. The threshold is fixed for each algorithm to give FMR = 0.00001 over all (10^8) impostor comparisons. For short time-lapses, the most accurate algorithms give very few errors (FNMR < 0.001) so that the uncertainty estimates are high.

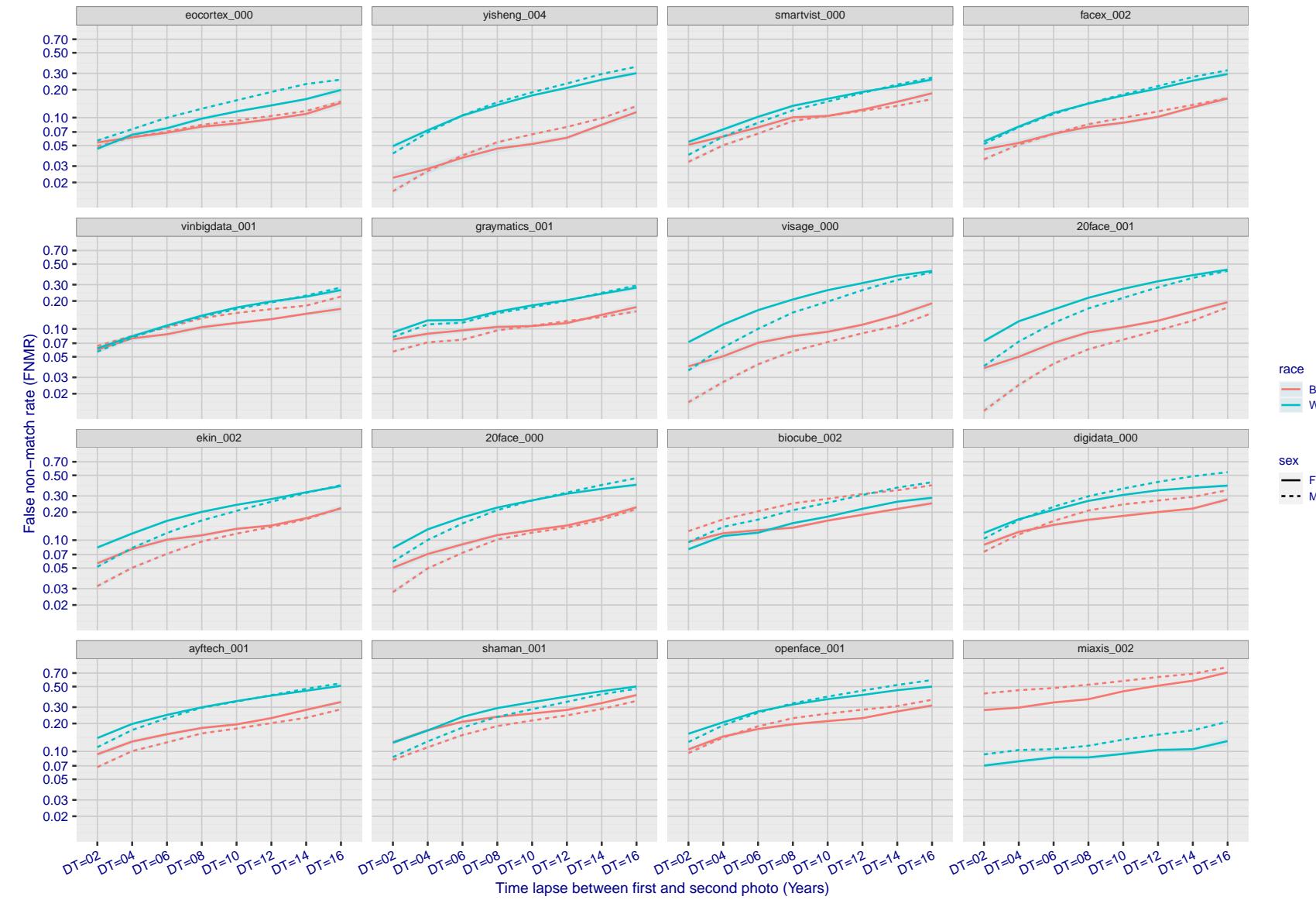


Figure 326: For the mugshot images, FNMR as a function of elapsed time between initial enrollment and second verification images. The panels appear most accurate first, and vertical scale changes on each page. The four traces correspond to images annotated with codes for black female, black male, white female, white male. The threshold is fixed for each algorithm to give $FMR = 0.00001$ over all (10^8) impostor comparisons. For short time-lapses, the most accurate algorithms give very few errors ($FNMR < 0.001$) so that the uncertainty estimates are high.

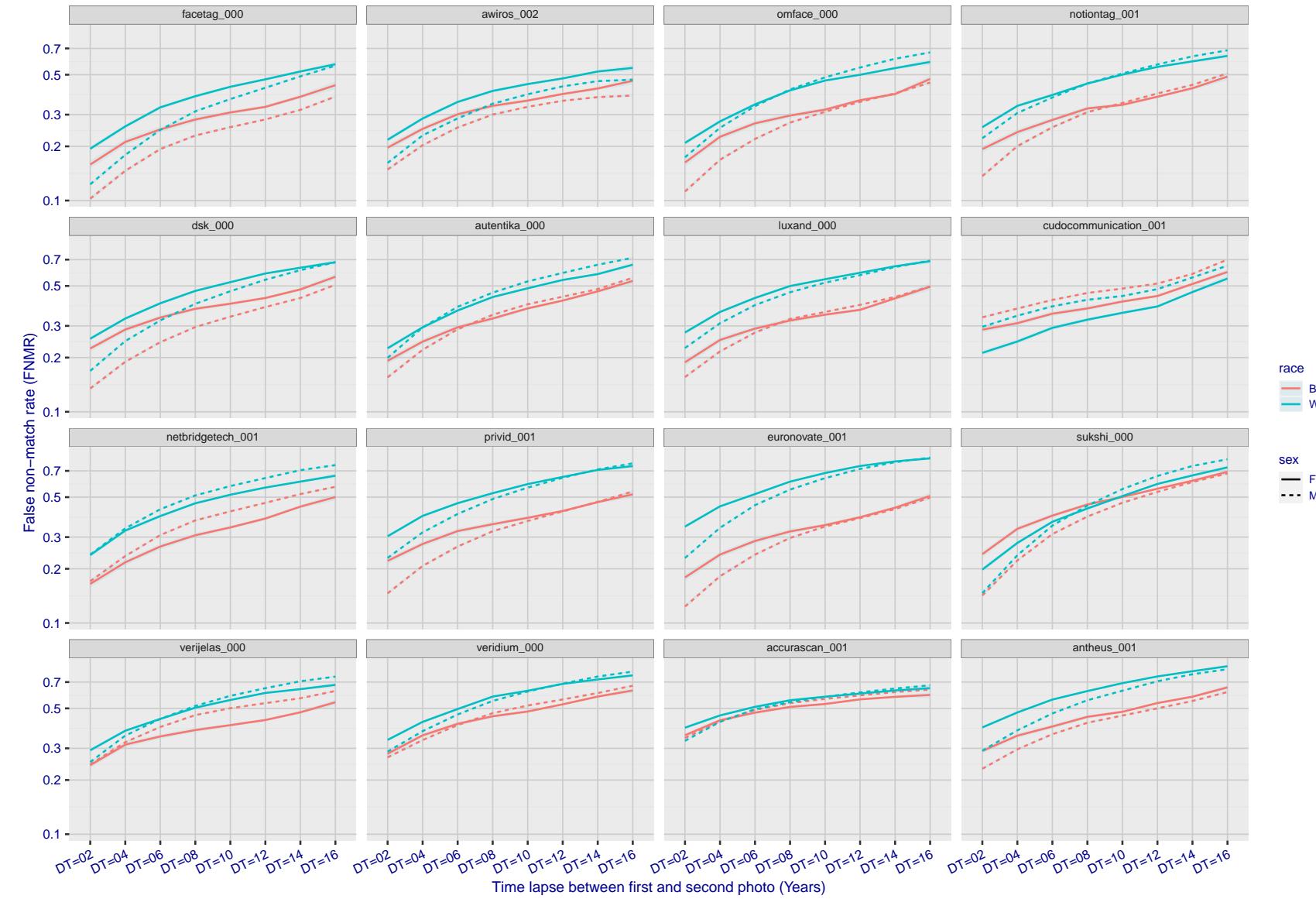


Figure 327: For the mugshot images, FNMR as a function of elapsed time between initial enrollment and second verification images. The panels appear most accurate first, and vertical scale changes on each page. The four traces correspond to images annotated with codes for black female, black male, white female, white male. The threshold is fixed for each algorithm to give $FMR = 0.00001$ over all (10^8) impostor comparisons. For short time-lapses, the most accurate algorithms give very few errors ($FNMR < 0.001$) so that the uncertainty estimates are high.

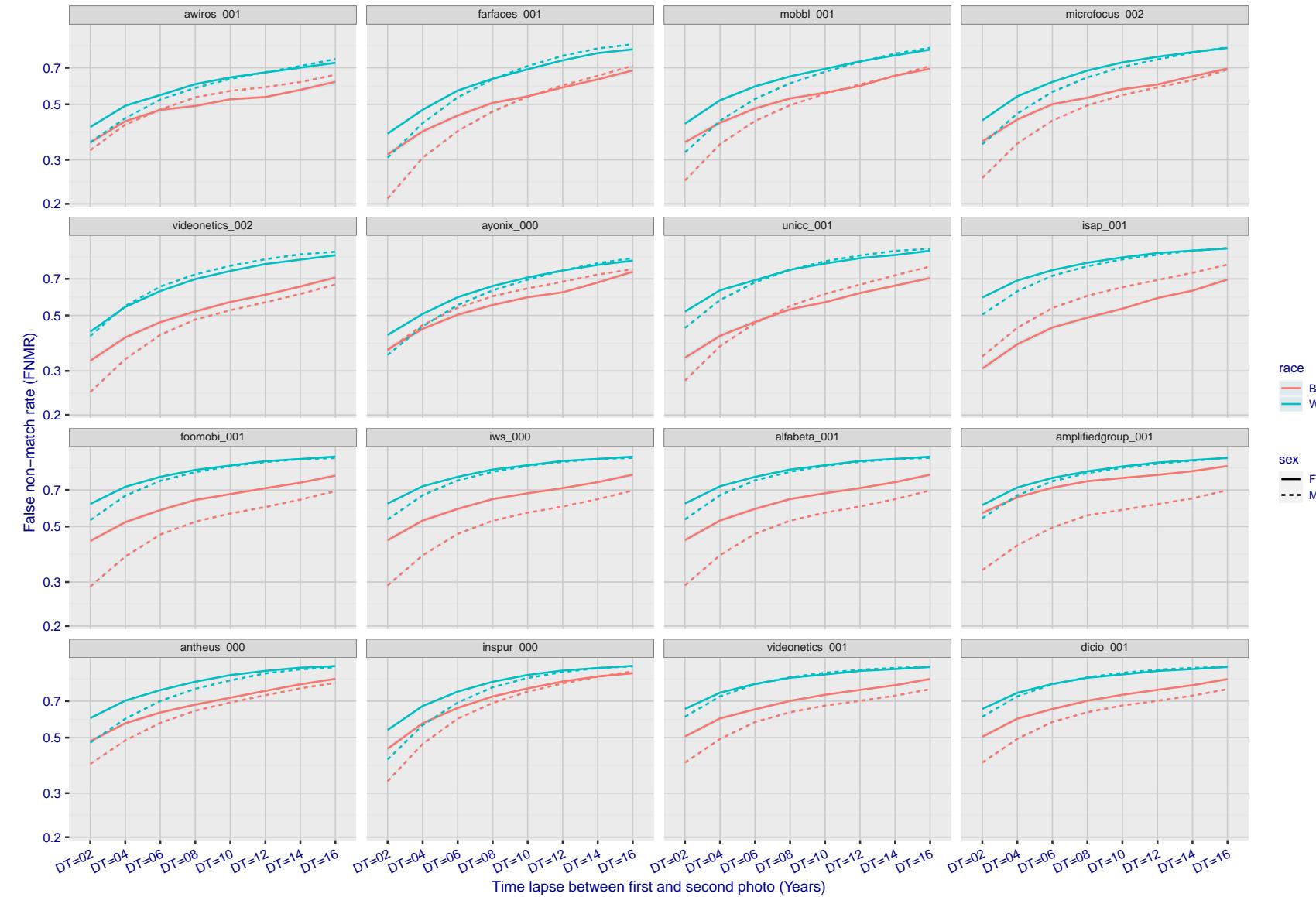


Figure 328: For the mugshot images, FNMR as a function of elapsed time between initial enrollment and second verification images. The panels appear most accurate first, and vertical scale changes on each page. The four traces correspond to images annotated with codes for black female, black male, white female, white male. The threshold is fixed for each algorithm to give FMR = 0.00001 over all (10^8) impostor comparisons. For short time-lapses, the most accurate algorithms give very few errors (FNMR < 0.001) so that the uncertainty estimates are high.

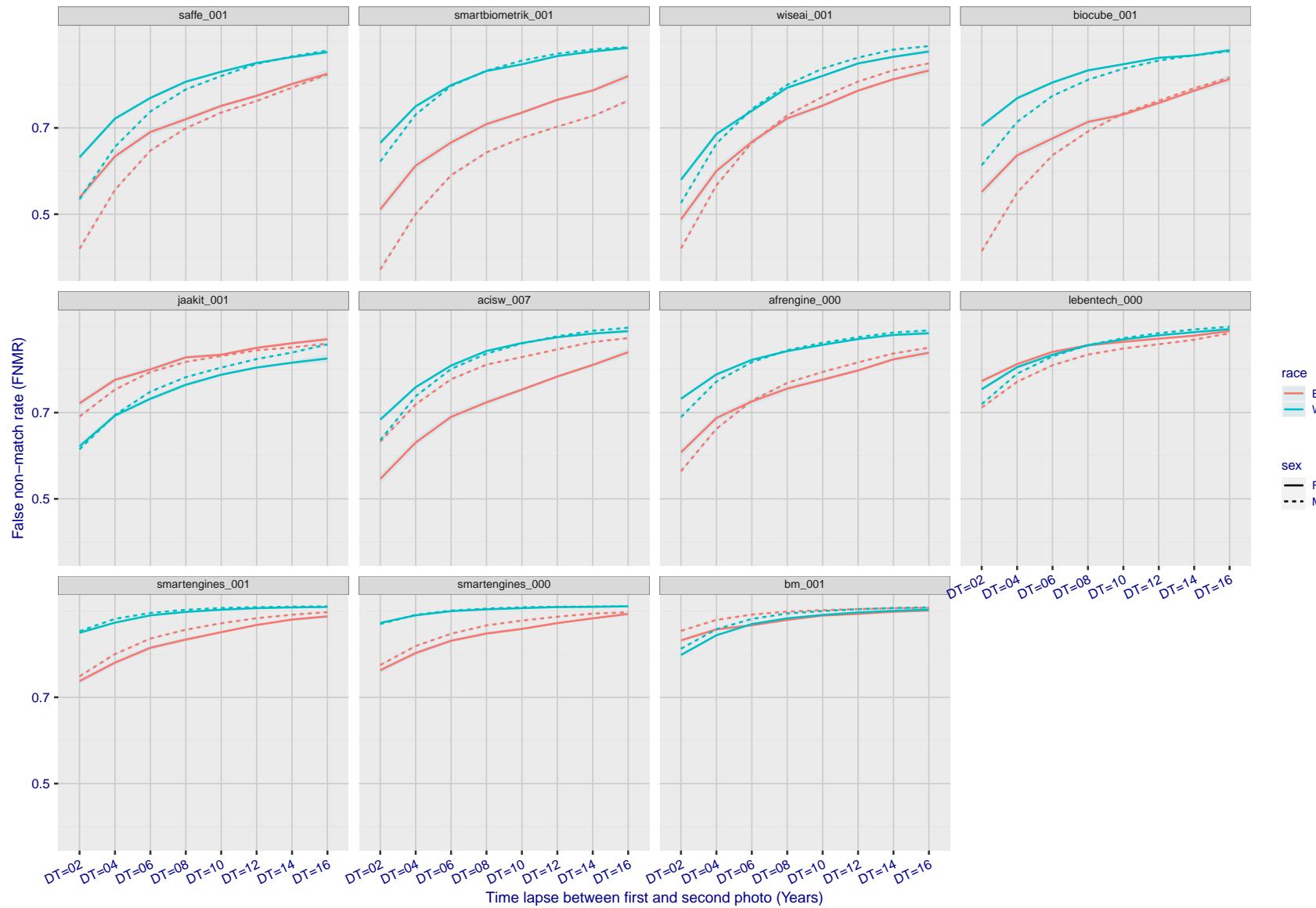


Figure 329: For the mugshot images, FNMR as a function of elapsed time between initial enrollment and second verification images. The panels appear most accurate first, and vertical scale changes on each page. The four traces correspond to images annotated with codes for black female, black male, white female, white male. The threshold is fixed for each algorithm to give FMR = 0.00001 over all (10^8) impostor comparisons. For short time-lapses, the most accurate algorithms give very few errors (FNMR < 0.001) so that the uncertainty estimates are high.

3.5.3 Effect of age on genuine subjects

Background: Faces change appearance throughout life. Face recognition algorithms have previously been reported to give better accuracy on older individuals (See NIST IR 8009).

Goal: To quantify false non-match rates (FNMR) as a function of age, without an ageing component.

Methods: Using the visa images, which span fewer than five years, thresholds are determined that give FMR = 0.001 and 0.0001 over the entire impostor set. Then FNMR is measured over 1000 bootstrap replications of the genuine scores.

Results: For the visa images, Figure 371 shows how false non-match rates for genuine users, as a function of age group.

The notable aspects are:

- ▷ Younger subjects give considerably higher FNMR. This is likely due to rapid growth and change in facial appearance.
- ▷ FNMR trends down throughout life. The last bin, AGE > 72, contains fewer than 140 mated pairs, and may be affected by small sample size.

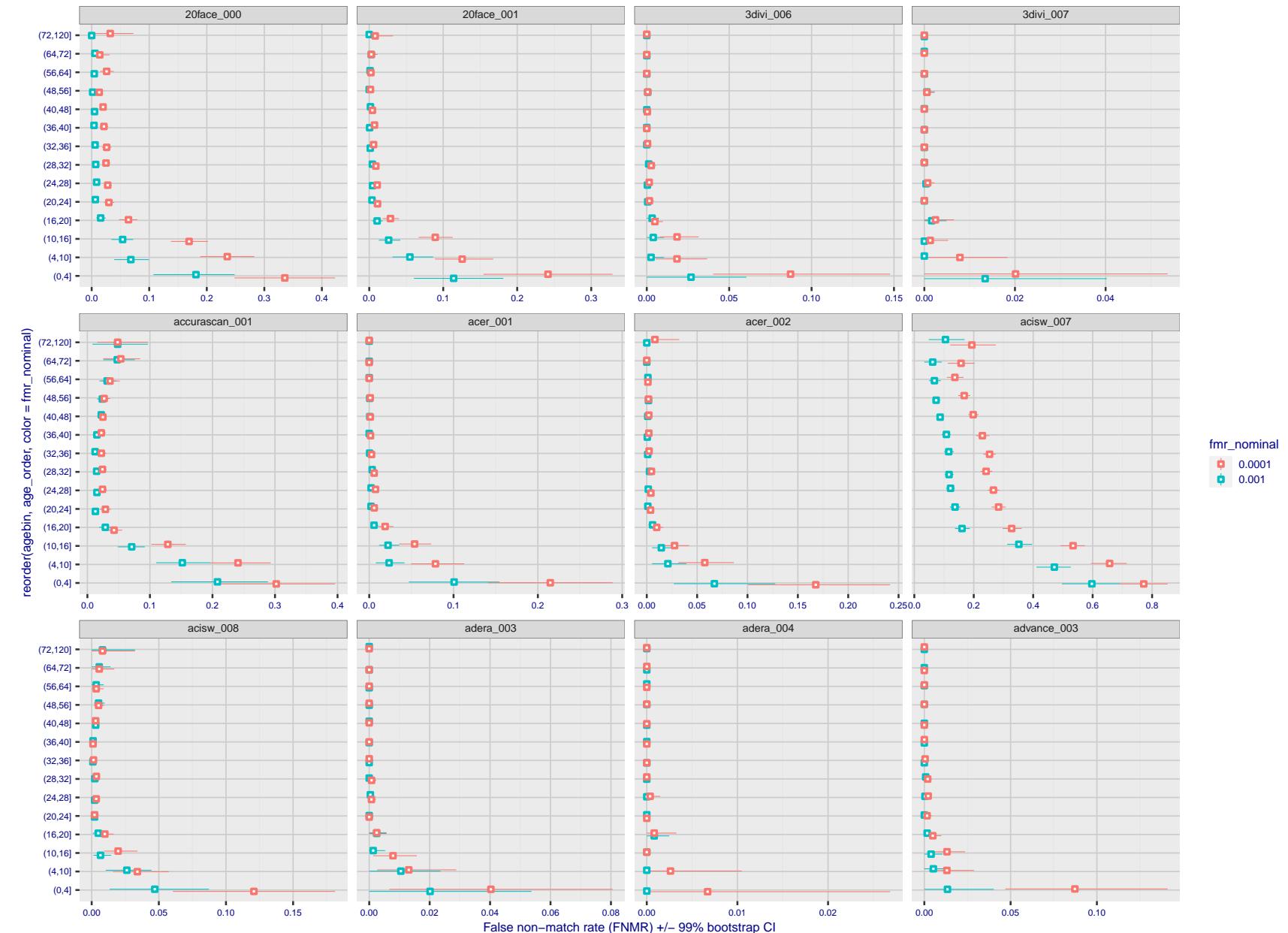


Figure 330: For the visa images, the dots show FNMR by age group for two operating thresholds corresponding to $FMR = \{0.001, 0.0001\}$ computed over all on the order of 10^{10} impostor scores. The FMR in each bin will vary also - see subsequent impostor heatmaps in sec. 3.6.2. Given a pair of face images taken at different times, we assign the comparison to the bin that is the arithmetic average of the subject's ages. This plot shows only the effect of age, not ageing. The number of comparisons in each bin is generally in the thousands, however the first and last bins are computed over 149 and 124 respectively. The error rates in some (adult) cases are zero, and in others the DET is flat so the error rates at the two thresholds are identical. The lines span 1% and 99% of bootstrap replicated FNMR estimates.

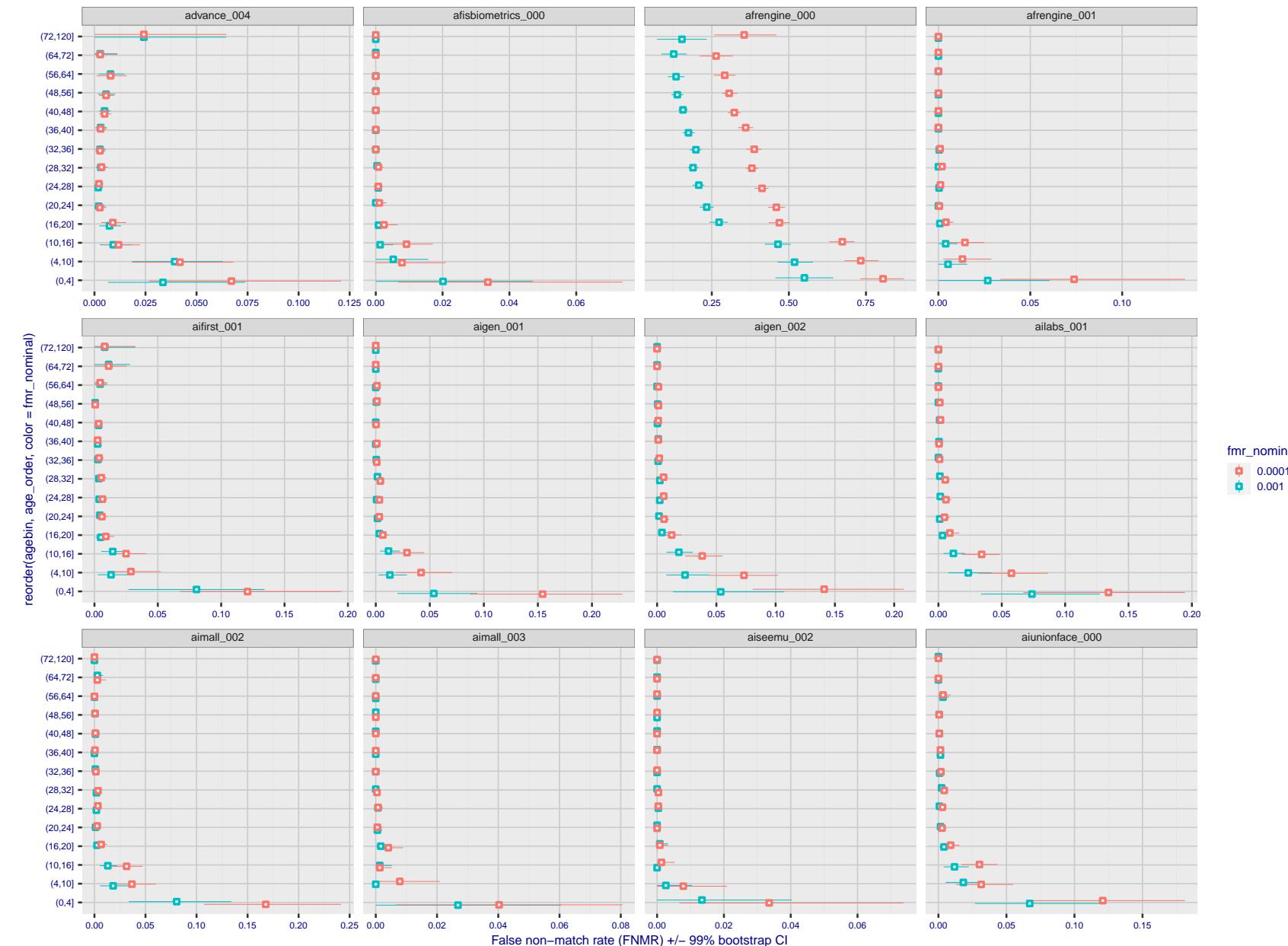


Figure 331: For the visa images, the dots show FNMR by age group for two operating thresholds corresponding to $FMR = \{0.001, 0.0001\}$ computed over all on the order of 10^{10} impostor scores. The FMR in each bin will vary also - see subsequent impostor heatmaps in sec. 3.6.2. Given a pair of face images taken at different times, we assign the comparison to the bin that is the arithmetic average of the subject's ages. This plot shows only the effect of age, not ageing. The number of comparisons in each bin is generally in the thousands, however the first and last bins are computed over 149 and 124 respectively. The error rates in some (adult) cases are zero, and in others the DET is flat so the error rates at the two thresholds are identical. The lines span 1% and 99% of bootstrap replicated FNMR estimates.

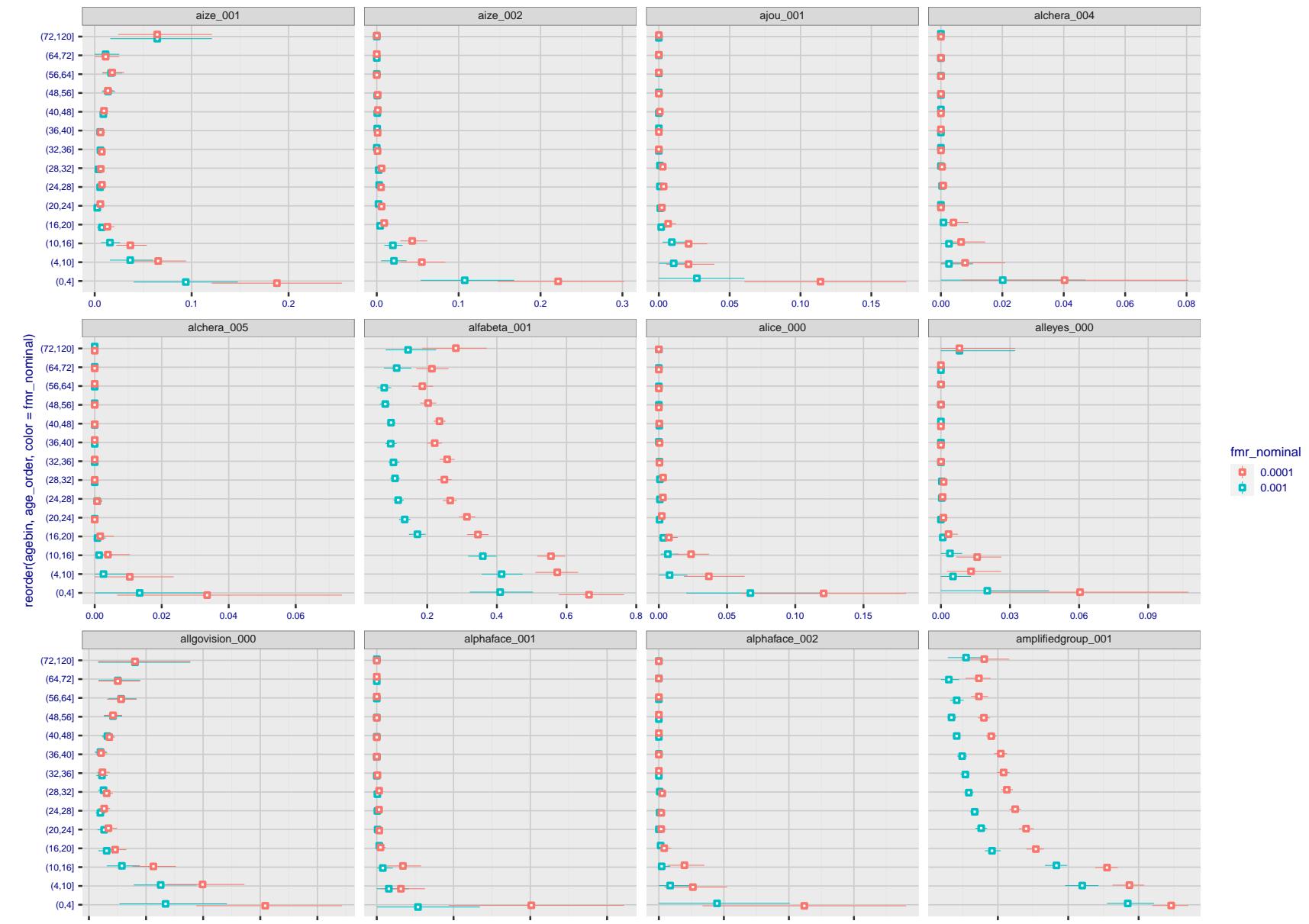


Figure 332: For the visa images, the dots show FNMR by age group for two operating thresholds corresponding to $FMR = \{0.001, 0.0001\}$ computed over all on the order of 10^{10} impostor scores. The FMR in each bin will vary also - see subsequent impostor heatmaps in sec. 3.6.2. Given a pair of face images taken at different times, we assign the comparison to the bin that is the arithmetic average of the subject's ages. This plot shows only the effect of age, not ageing. The number of comparisons in each bin is generally in the thousands, however the first and last bins are computed over 149 and 124 respectively. The error rates in some (adult) cases are zero, and in others the DET is flat so the error rates at the two thresholds are identical. The lines span 1% and 99% of bootstrap replicated FNMR estimates.

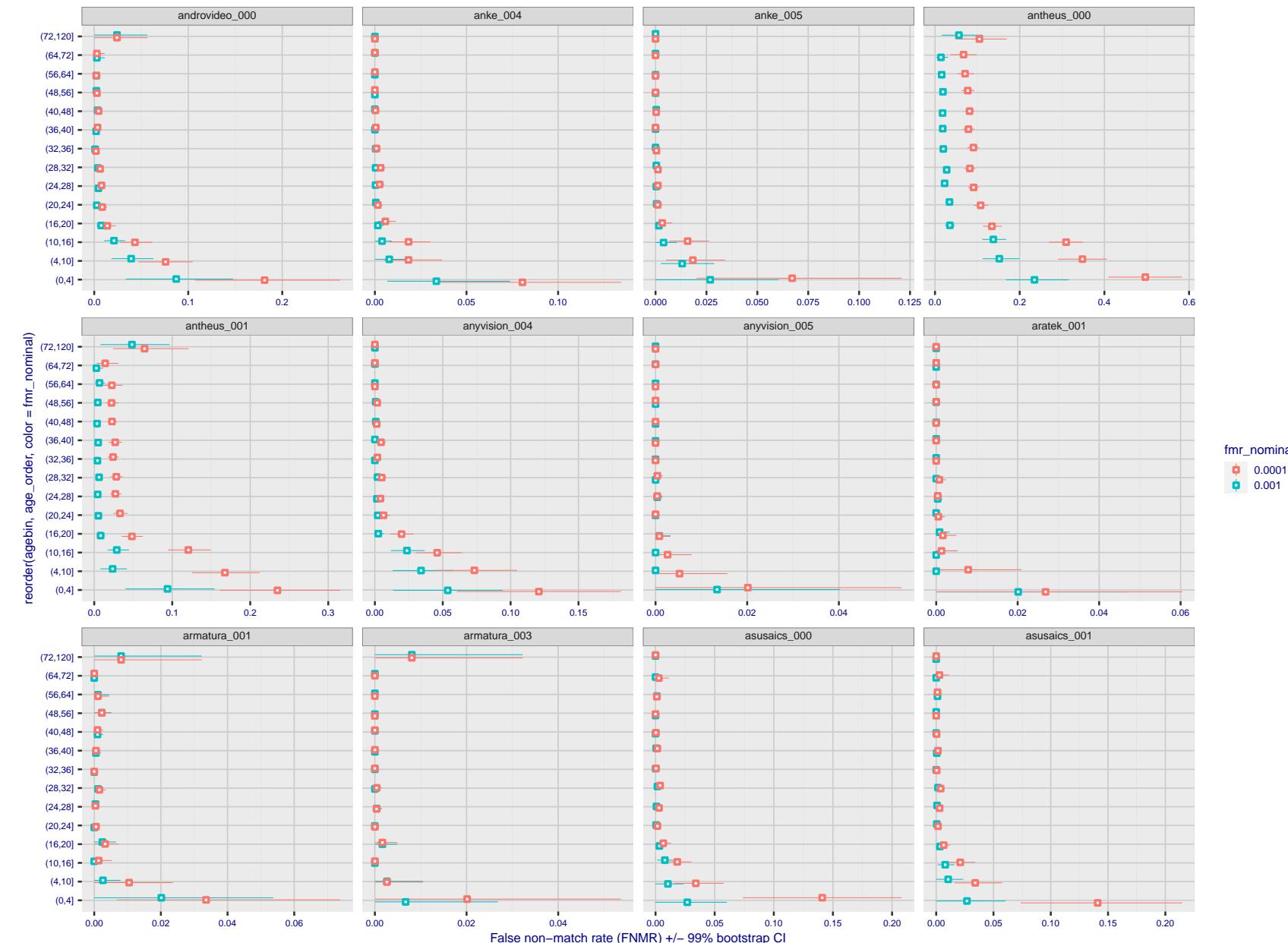


Figure 333: For the visa images, the dots show FNMR by age group for two operating thresholds corresponding to $FMR = \{0.001, 0.0001\}$ computed over all on the order of 10^{10} impostor scores. The FMR in each bin will vary also - see subsequent impostor heatmaps in sec. 3.6.2. Given a pair of face images taken at different times, we assign the comparison to the bin that is the arithmetic average of the subject's ages. This plot shows only the effect of age, not ageing. The number of comparisons in each bin is generally in the thousands, however the first and last bins are computed over 149 and 124 respectively. The error rates in some (adult) cases are zero, and in others the DET is flat so the error rates at the two thresholds are identical. The lines span 1% and 99% of bootstrap replicated FNMR estimates.



Figure 334: For the visa images, the dots show FNMR by age group for two operating thresholds corresponding to $FMR = \{0.001, 0.0001\}$ computed over all on the order of 10^{10} impostor scores. The FMR in each bin will vary also - see subsequent impostor heatmaps in sec. 3.6.2. Given a pair of face images taken at different times, we assign the comparison to the bin that is the arithmetic average of the subject's ages. This plot shows only the effect of age, not ageing. The number of comparisons in each bin is generally in the thousands, however the first and last bins are computed over 149 and 124 respectively. The error rates in some (adult) cases are zero, and in others the DET is flat so the error rates at the two thresholds are identical. The lines span 1% and 99% of bootstrap replicated FNMR estimates.

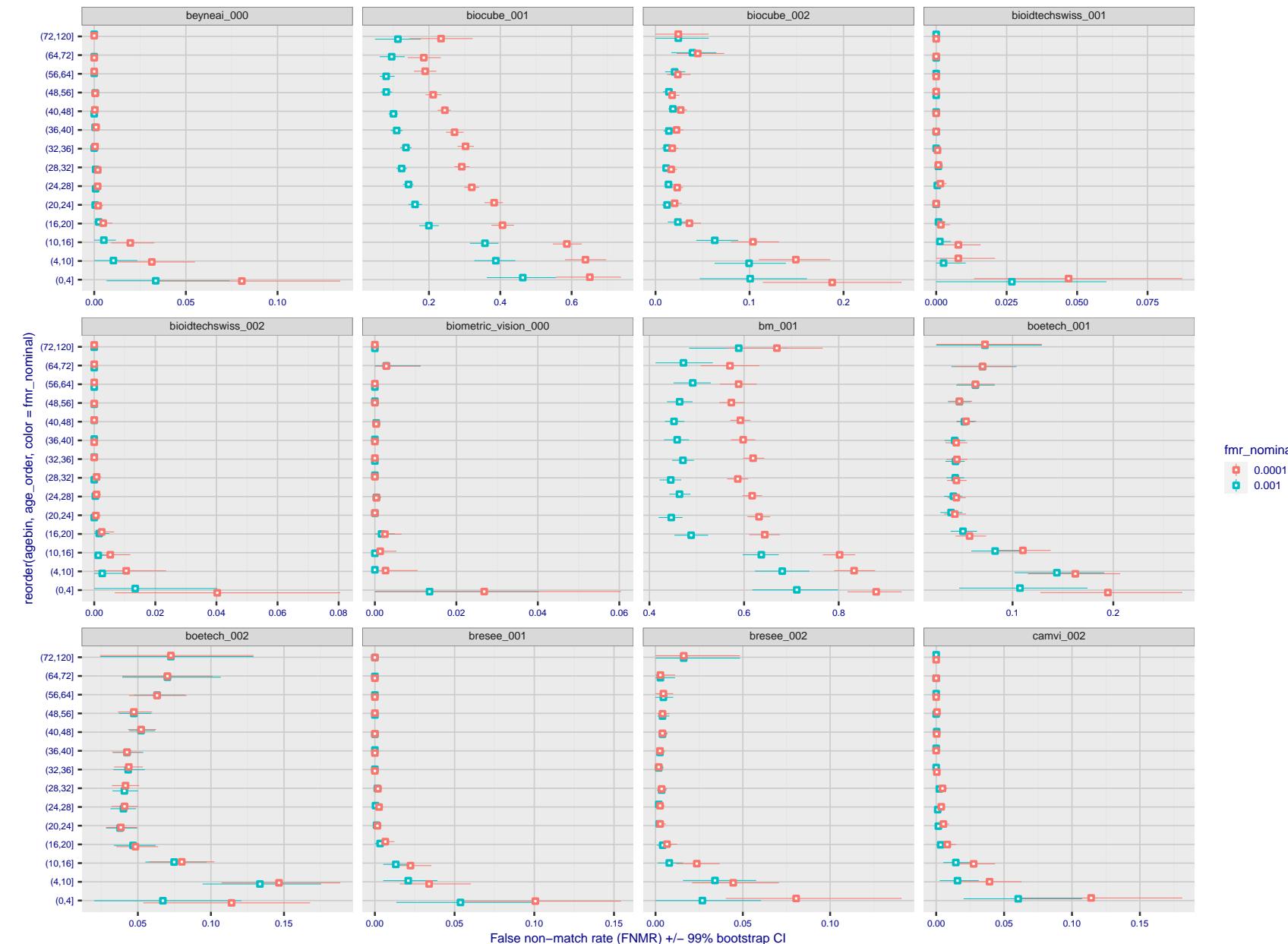


Figure 335: For the visa images, the dots show FNMR by age group for two operating thresholds corresponding to $FMR = \{0.001, 0.0001\}$ computed over all on the order of 10^{10} impostor scores. The FMR in each bin will vary also - see subsequent impostor heatmaps in sec. 3.6.2. Given a pair of face images taken at different times, we assign the comparison to the bin that is the arithmetic average of the subject's ages. This plot shows only the effect of age, not ageing. The number of comparisons in each bin is generally in the thousands, however the first and last bins are computed over 149 and 124 respectively. The error rates in some (adult) cases are zero, and in others the DET is flat so the error rates at the two thresholds are identical. The lines span 1% and 99% of bootstrap replicated FNMR estimates.

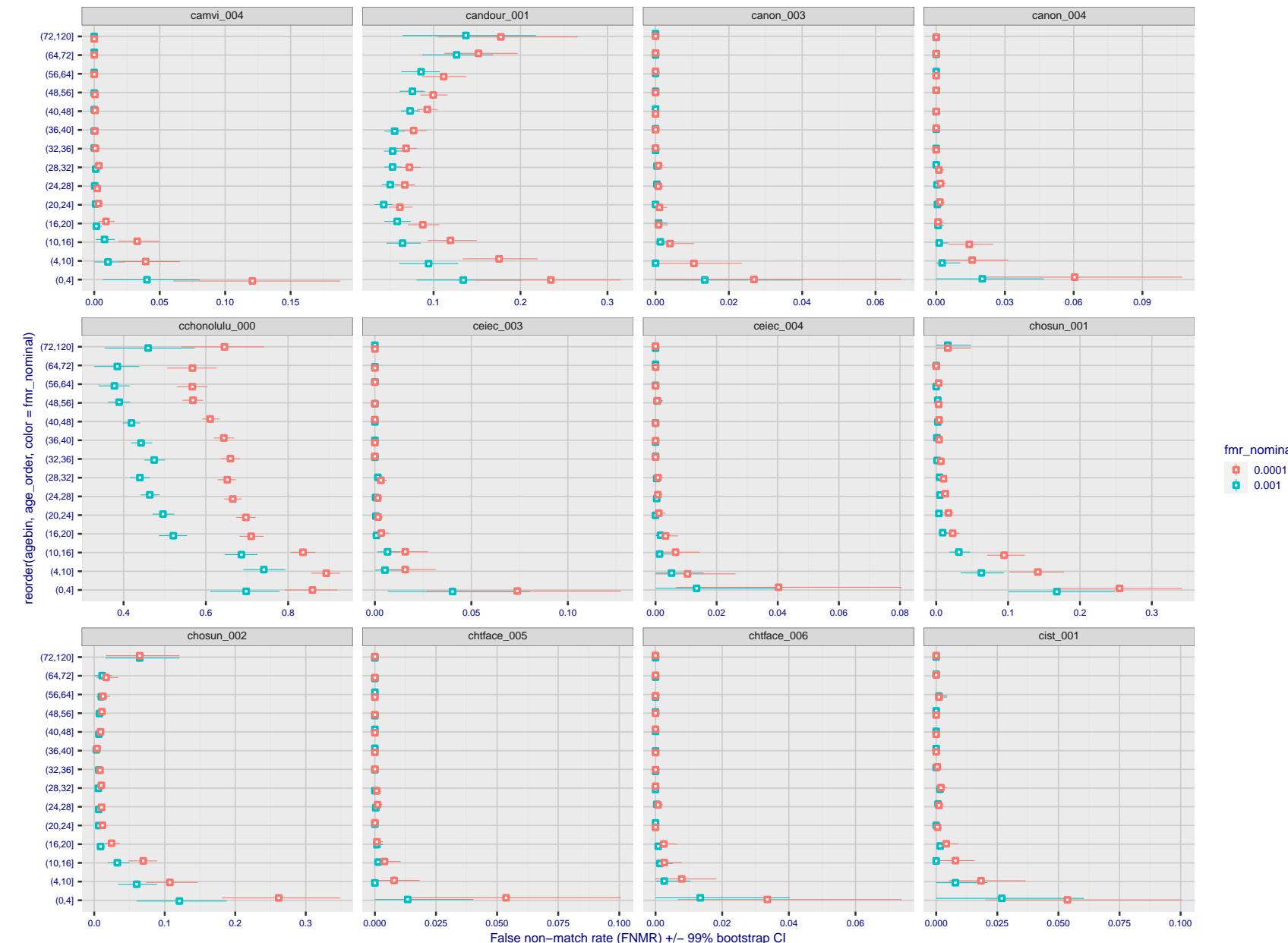


Figure 336: For the visa images, the dots show FNMR by age group for two operating thresholds corresponding to $FMR = \{0.001, 0.0001\}$ computed over all on the order of 10^{10} impostor scores. The FMR in each bin will vary also - see subsequent impostor heatmaps in sec. 3.6.2. Given a pair of face images taken at different times, we assign the comparison to the bin that is the arithmetic average of the subject's ages. This plot shows only the effect of age, not ageing. The number of comparisons in each bin is generally in the thousands, however the first and last bins are computed over 149 and 124 respectively. The error rates in some (adult) cases are zero, and in others the DET is flat so the error rates at the two thresholds are identical. The lines span 1% and 99% of bootstrap replicated FNMR estimates.



Figure 337: For the visa images, the dots show FNMR by age group for two operating thresholds corresponding to $FMR = \{0.001, 0.0001\}$ computed over all on the order of 10^{10} impostor scores. The FMR in each bin will vary also - see subsequent impostor heatmaps in sec. 3.6.2. Given a pair of face images taken at different times, we assign the comparison to the bin that is the arithmetic average of the subject's ages. This plot shows only the effect of age, not ageing. The number of comparisons in each bin is generally in the thousands, however the first and last bins are computed over 149 and 124 respectively. The error rates in some (adult) cases are zero, and in others the DET is flat so the error rates at the two thresholds are identical. The lines span 1% and 99% of bootstrap replicated FNMR estimates.

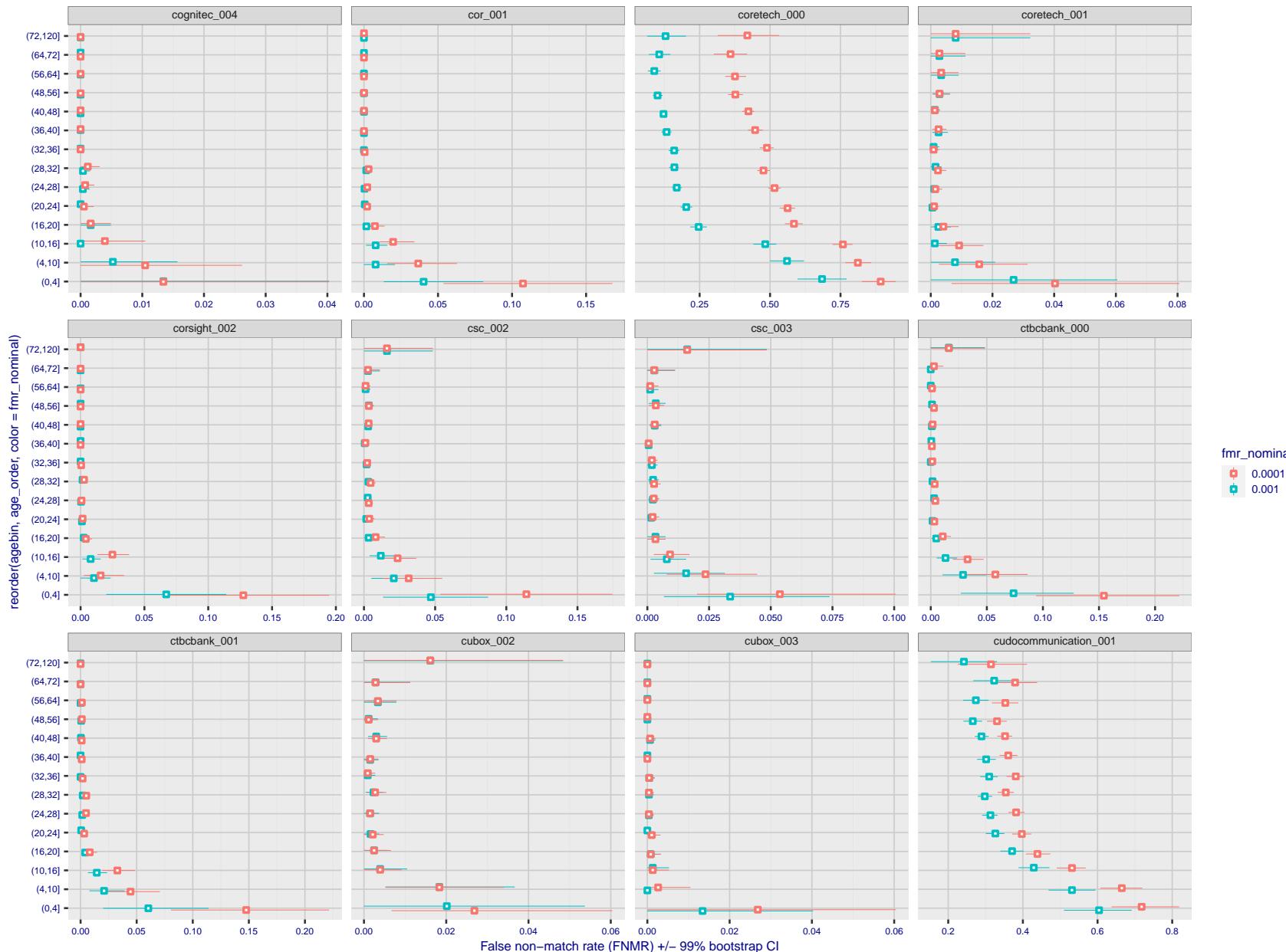


Figure 338: For the visa images, the dots show FNMR by age group for two operating thresholds corresponding to $FMR = \{0.001, 0.0001\}$ computed over all on the order of 10^{10} impostor scores. The FMR in each bin will vary also - see subsequent impostor heatmaps in sec. 3.6.2. Given a pair of face images taken at different times, we assign the comparison to the bin that is the arithmetic average of the subject's ages. This plot shows only the effect of age, not ageing. The number of comparisons in each bin is generally in the thousands, however the first and last bins are computed over 149 and 124 respectively. The error rates in some (adult) cases are zero, and in others the DET is flat so the error rates at the two thresholds are identical. The lines span 1% and 99% of bootstrap replicated FNMR estimates.



Figure 339: For the visa images, the dots show FNMR by age group for two operating thresholds corresponding to $FMR = \{0.001, 0.0001\}$ computed over all on the order of 10^{10} impostor scores. The FMR in each bin will vary also - see subsequent impostor heatmaps in sec. 3.6.2. Given a pair of face images taken at different times, we assign the comparison to the bin that is the arithmetic average of the subject's ages. This plot shows only the effect of age, not ageing. The number of comparisons in each bin is generally in the thousands, however the first and last bins are computed over 149 and 124 respectively. The error rates in some (adult) cases are zero, and in others the DET is flat so the error rates at the two thresholds are identical. The lines span 1% and 99% of bootstrap replicated FNMR estimates.



Figure 340: For the visa images, the dots show FNMR by age group for two operating thresholds corresponding to $FMR = \{0.001, 0.0001\}$ computed over all on the order of 10^{10} impostor scores. The FMR in each bin will vary also - see subsequent impostor heatmaps in sec. 3.6.2. Given a pair of face images taken at different times, we assign the comparison to the bin that is the arithmetic average of the subject's ages. This plot shows only the effect of age, not ageing. The number of comparisons in each bin is generally in the thousands, however the first and last bins are computed over 149 and 124 respectively. The error rates in some (adult) cases are zero, and in others the DET is flat so the error rates at the two thresholds are identical. The lines span 1% and 99% of bootstrap replicated FNMR estimates.

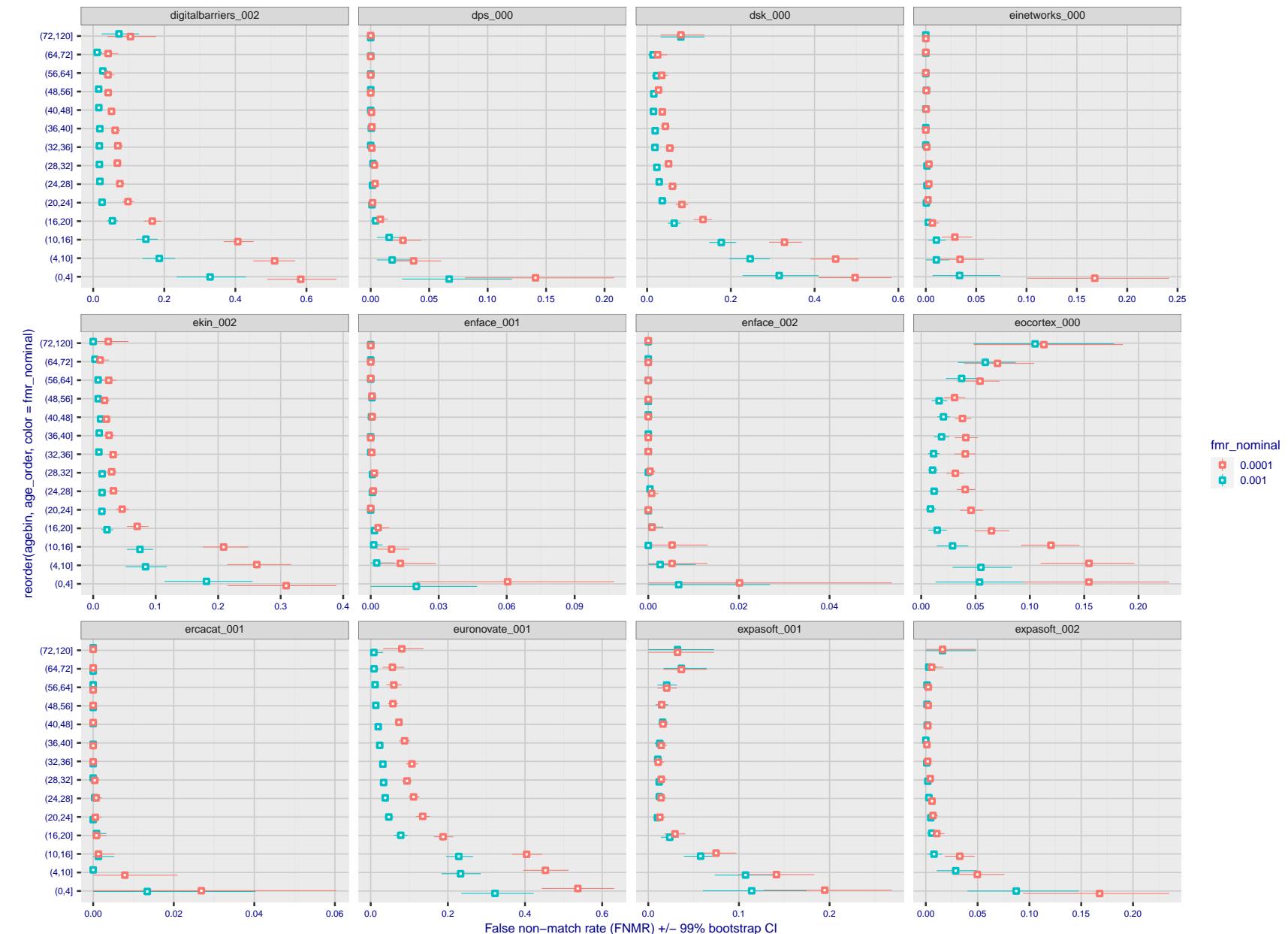


Figure 341: For the visa images, the dots show FNMR by age group for two operating thresholds corresponding to $FMR = \{0.001, 0.0001\}$ computed over all on the order of 10^{10} impostor scores. The FMR in each bin will vary also - see subsequent impostor heatmaps in sec. 3.6.2. Given a pair of face images taken at different times, we assign the comparison to the bin that is the arithmetic average of the subject's ages. This plot shows only the effect of age, not ageing. The number of comparisons in each bin is generally in the thousands, however the first and last bins are computed over 149 and 124 respectively. The error rates in some (adult) cases are zero, and in others the DET is flat so the error rates at the two thresholds are identical. The lines span 1% and 99% of bootstrap replicated FNMR estimates.

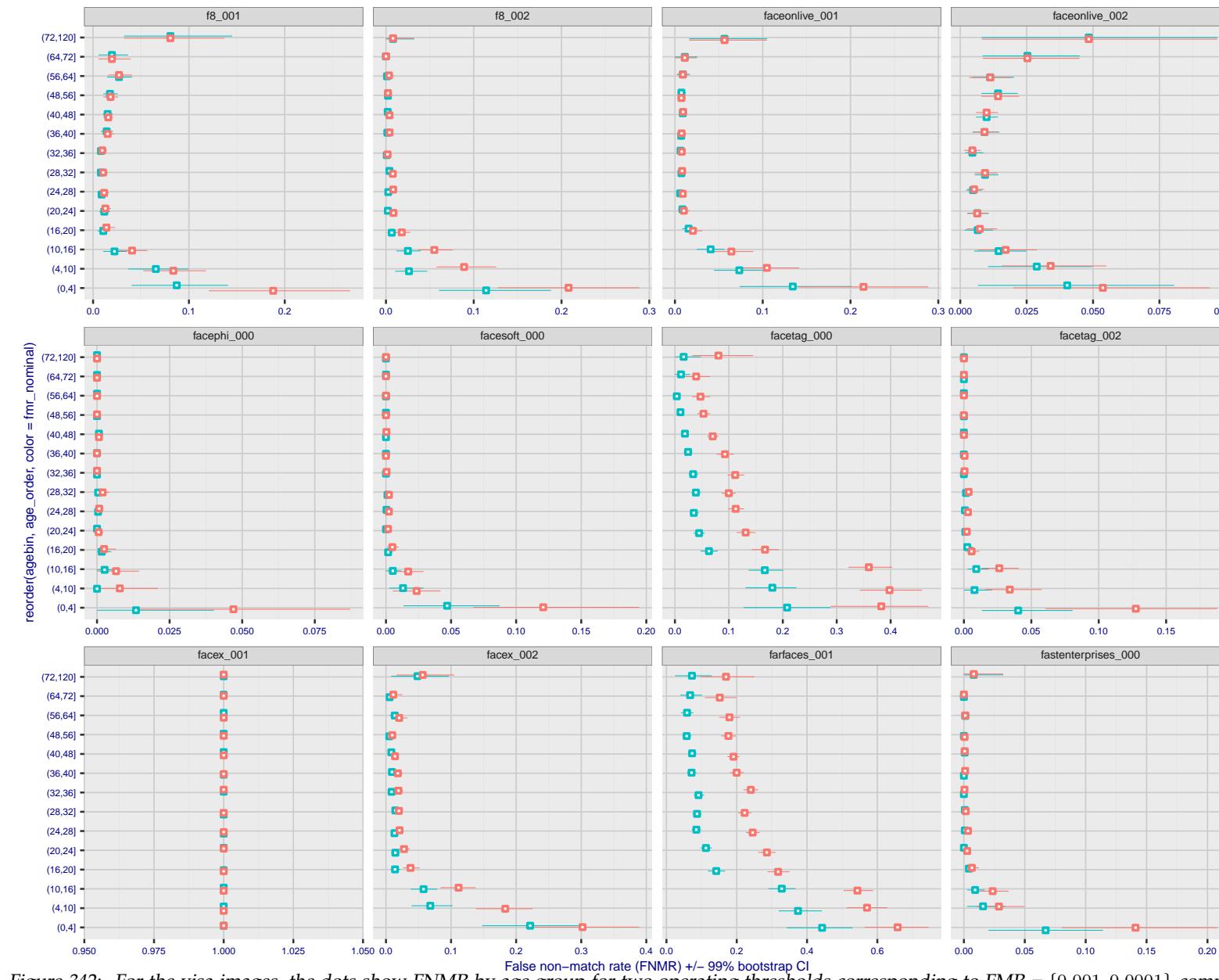


Figure 342: For the visa images, the dots show FNMR by age group for two operating thresholds corresponding to $FMR = \{0.001, 0.0001\}$ computed over all on the order of 10^{10} impostor scores. The FMR in each bin will vary also - see subsequent impostor heatmaps in sec. 3.6.2. Given a pair of face images taken at different times, we assign the comparison to the bin that is the arithmetic average of the subject's ages. This plot shows only the effect of age, not ageing. The number of comparisons in each bin is generally in the thousands, however the first and last bins are computed over 149 and 124 respectively. The error rates in some (adult) cases are zero, and in others the DET is flat so the error rates at the two thresholds are identical. The lines span 1% and 99% of bootstrap replicated FNMR estimates.

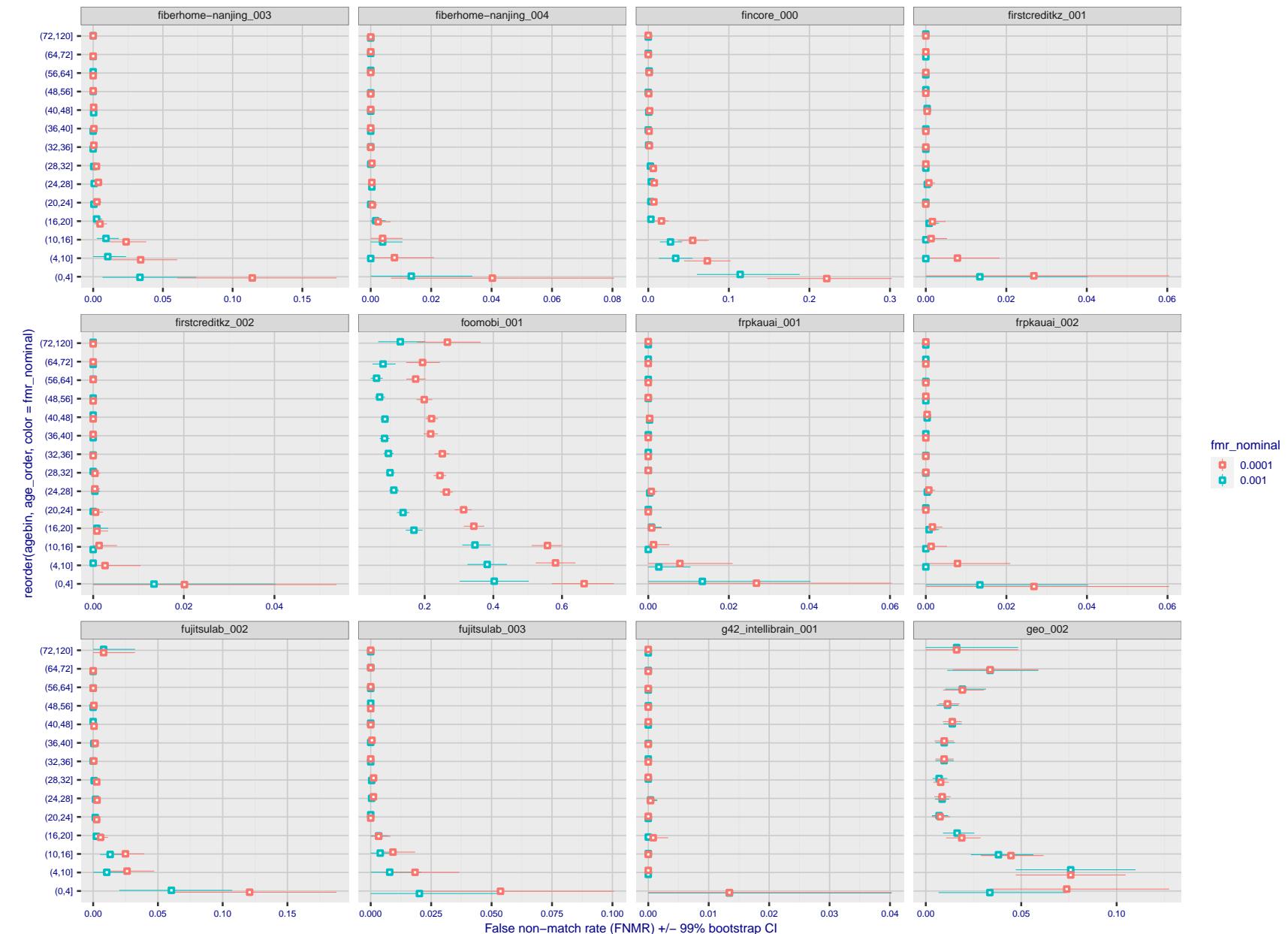


Figure 343: For the visa images, the dots show FNMR by age group for two operating thresholds corresponding to $FMR = \{0.001, 0.0001\}$ computed over all on the order of 10^{10} impostor scores. The FMR in each bin will vary also - see subsequent impostor heatmaps in sec. 3.6.2. Given a pair of face images taken at different times, we assign the comparison to the bin that is the arithmetic average of the subject's ages. This plot shows only the effect of age, not ageing. The number of comparisons in each bin is generally in the thousands, however the first and last bins are computed over 149 and 124 respectively. The error rates in some (adult) cases are zero, and in others the DET is flat so the error rates at the two thresholds are identical. The lines span 1% and 99% of bootstrap replicated FNMR estimates.



Figure 344: For the visa images, the dots show FNMR by age group for two operating thresholds corresponding to $FMR = \{0.001, 0.0001\}$ computed over all on the order of 10^{10} impostor scores. The FMR in each bin will vary also - see subsequent impostor heatmaps in sec. 3.6.2. Given a pair of face images taken at different times, we assign the comparison to the bin that is the arithmetic average of the subject's ages. This plot shows only the effect of age, not ageing. The number of comparisons in each bin is generally in the thousands, however the first and last bins are computed over 149 and 124 respectively. The error rates in some (adult) cases are zero, and in others the DET is flat so the error rates at the two thresholds are identical. The lines span 1% and 99% of bootstrap replicated FNMR estimates.



Figure 345: For the visa images, the dots show FNMR by age group for two operating thresholds corresponding to $FMR = \{0.001, 0.0001\}$ computed over all on the order of 10^{10} impostor scores. The FMR in each bin will vary also - see subsequent impostor heatmaps in sec. 3.6.2. Given a pair of face images taken at different times, we assign the comparison to the bin that is the arithmetic average of the subject's ages. This plot shows only the effect of age, not ageing. The number of comparisons in each bin is generally in the thousands, however the first and last bins are computed over 149 and 124 respectively. The error rates in some (adult) cases are zero, and in others the DET is flat so the error rates at the two thresholds are identical. The lines span 1% and 99% of bootstrap replicated FNMR estimates.



Figure 346: For the visa images, the dots show FNMR by age group for two operating thresholds corresponding to $FMR = \{0.001, 0.0001\}$ computed over all on the order of 10^{10} impostor scores. The FMR in each bin will vary also - see subsequent impostor heatmaps in sec. 3.6.2. Given a pair of face images taken at different times, we assign the comparison to the bin that is the arithmetic average of the subject's ages. This plot shows only the effect of age, not ageing. The number of comparisons in each bin is generally in the thousands, however the first and last bins are computed over 149 and 124 respectively. The error rates in some (adult) cases are zero, and in others the DET is flat so the error rates at the two thresholds are identical. The lines span 1% and 99% of bootstrap replicated FNMR estimates.



Figure 347: For the visa images, the dots show FNMR by age group for two operating thresholds corresponding to $FMR = \{0.001, 0.0001\}$ computed over all on the order of 10^{10} impostor scores. The FMR in each bin will vary also - see subsequent impostor heatmaps in sec. 3.6.2. Given a pair of face images taken at different times, we assign the comparison to the bin that is the arithmetic average of the subject's ages. This plot shows only the effect of age, not ageing. The number of comparisons in each bin is generally in the thousands, however the first and last bins are computed over 149 and 124 respectively. The error rates in some (adult) cases are zero, and in others the DET is flat so the error rates at the two thresholds are identical. The lines span 1% and 99% of bootstrap replicated FNMR estimates.



Figure 348: For the visa images, the dots show FNMR by age group for two operating thresholds corresponding to $FMR = \{0.001, 0.0001\}$ computed over all on the order of 10^{10} impostor scores. The FMR in each bin will vary also - see subsequent impostor heatmaps in sec. 3.6.2. Given a pair of face images taken at different times, we assign the comparison to the bin that is the arithmetic average of the subject's ages. This plot shows only the effect of age, not ageing. The number of comparisons in each bin is generally in the thousands, however the first and last bins are computed over 149 and 124 respectively. The error rates in some (adult) cases are zero, and in others the DET is flat so the error rates at the two thresholds are identical. The lines span 1% and 99% of bootstrap replicated FNMR estimates.

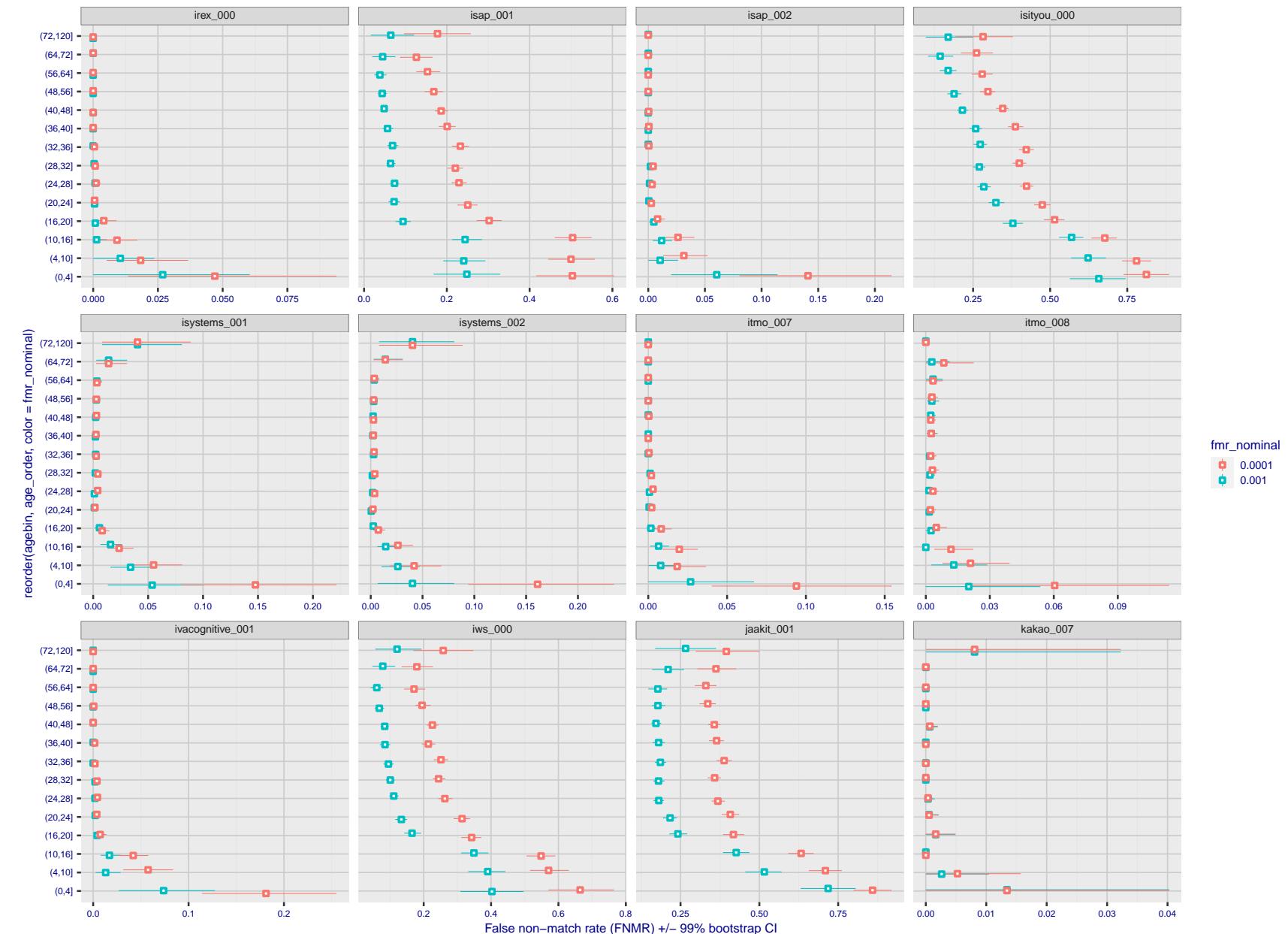


Figure 349: For the visa images, the dots show FNMR by age group for two operating thresholds corresponding to $FMR = \{0.001, 0.0001\}$ computed over all on the order of 10^{10} impostor scores. The FMR in each bin will vary also - see subsequent impostor heatmaps in sec. 3.6.2. Given a pair of face images taken at different times, we assign the comparison to the bin that is the arithmetic average of the subject's ages. This plot shows only the effect of age, not ageing. The number of comparisons in each bin is generally in the thousands, however the first and last bins are computed over 149 and 124 respectively. The error rates in some (adult) cases are zero, and in others the DET is flat so the error rates at the two thresholds are identical. The lines span 1% and 99% of bootstrap replicated FNMR estimates.

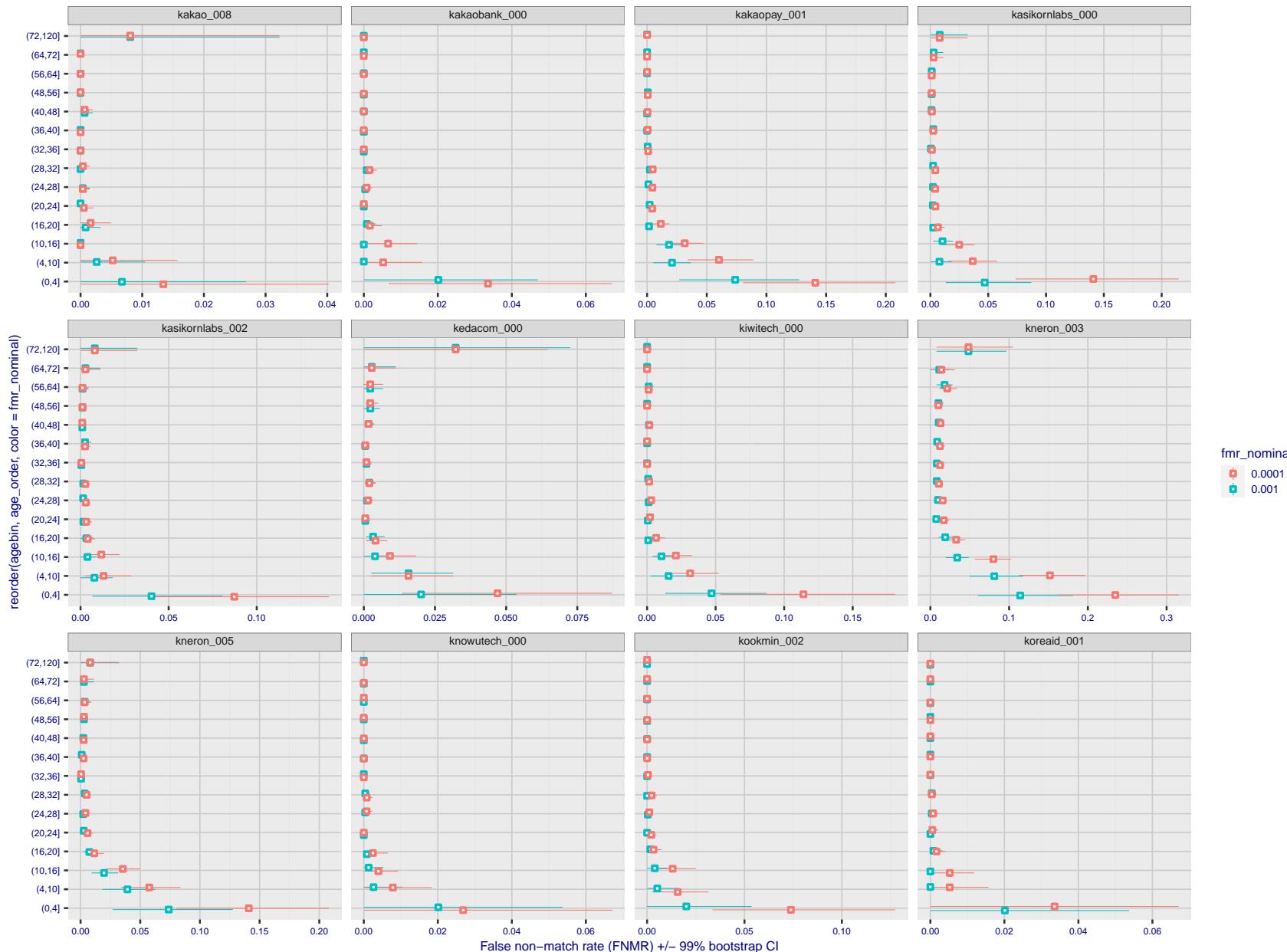


Figure 350: For the visa images, the dots show FNMR by age group for two operating thresholds corresponding to $FMR = \{0.001, 0.0001\}$ computed over all on the order of 10^{10} impostor scores. The FMR in each bin will vary also - see subsequent impostor heatmaps in sec. 3.6.2. Given a pair of face images taken at different times, we assign the comparison to the bin that is the arithmetic average of the subject's ages. This plot shows only the effect of age, not ageing. The number of comparisons in each bin is generally in the thousands, however the first and last bins are computed over 149 and 124 respectively. The error rates in some (adult) cases are zero, and in others the DET is flat so the error rates at the two thresholds are identical. The lines span 1% and 99% of bootstrap replicated FNMR estimates.



Figure 351: For the visa images, the dots show FNMR by age group for two operating thresholds corresponding to $FMR = \{0.001, 0.0001\}$ computed over all on the order of 10^{10} impostor scores. The FMR in each bin will vary also - see subsequent impostor heatmaps in sec. 3.6.2. Given a pair of face images taken at different times, we assign the comparison to the bin that is the arithmetic average of the subject's ages. This plot shows only the effect of age, not ageing. The number of comparisons in each bin is generally in the thousands, however the first and last bins are computed over 149 and 124 respectively. The error rates in some (adult) cases are zero, and in others the DET is flat so the error rates at the two thresholds are identical. The lines span 1% and 99% of bootstrap replicated FNMR estimates.

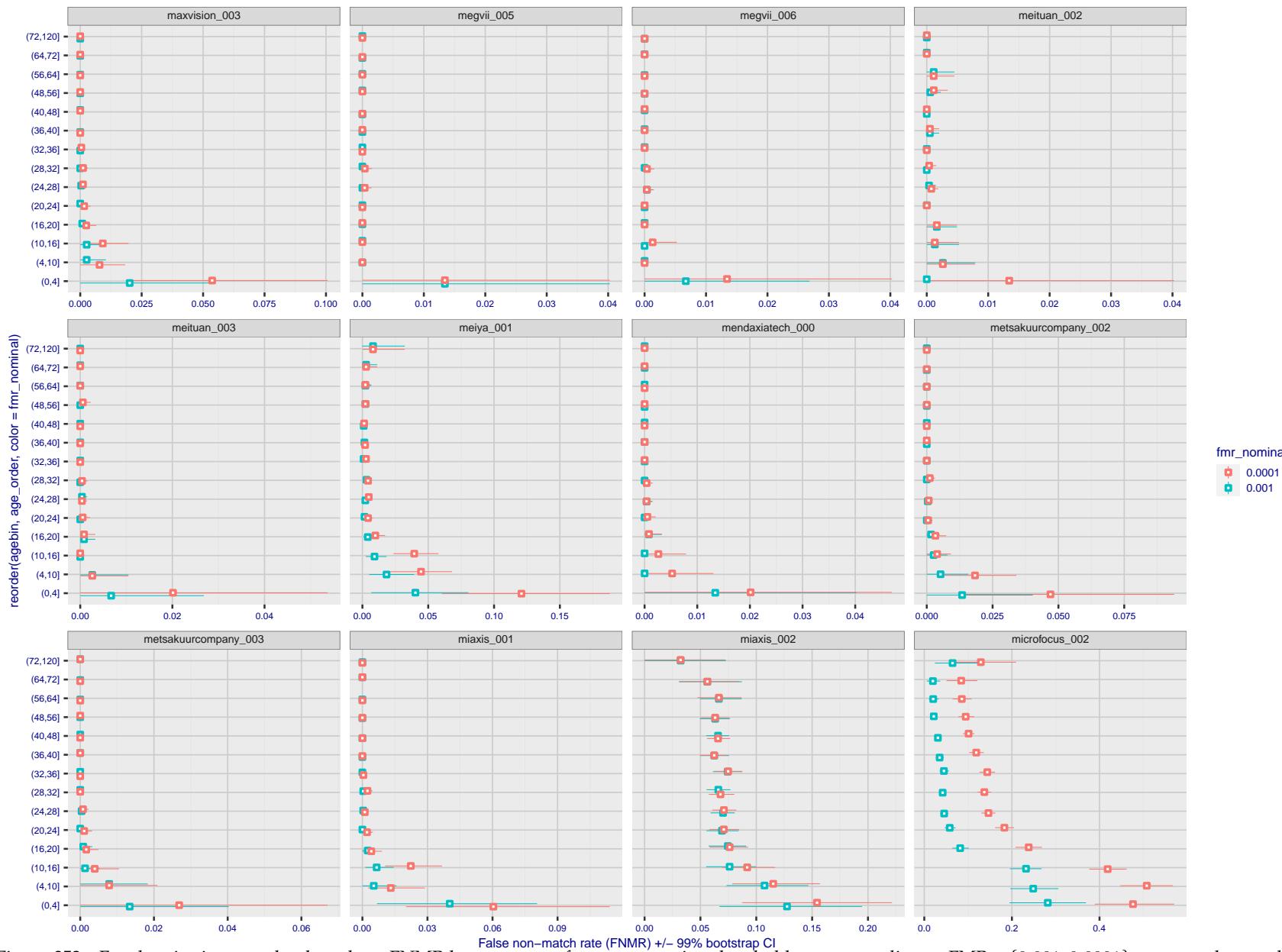


Figure 352: For the visa images, the dots show FNMR by age group for two operating thresholds corresponding to $FMR = \{0.001, 0.0001\}$ computed over all on the order of 10^{10} impostor scores. The FMR in each bin will vary also - see subsequent impostor heatmaps in sec. 3.6.2. Given a pair of face images taken at different times, we assign the comparison to the bin that is the arithmetic average of the subject's ages. This plot shows only the effect of age, not ageing. The number of comparisons in each bin is generally in the thousands, however the first and last bins are computed over 149 and 124 respectively. The error rates in some (adult) cases are zero, and in others the DET is flat so the error rates at the two thresholds are identical. The lines span 1% and 99% of bootstrap replicated FNMR estimates.

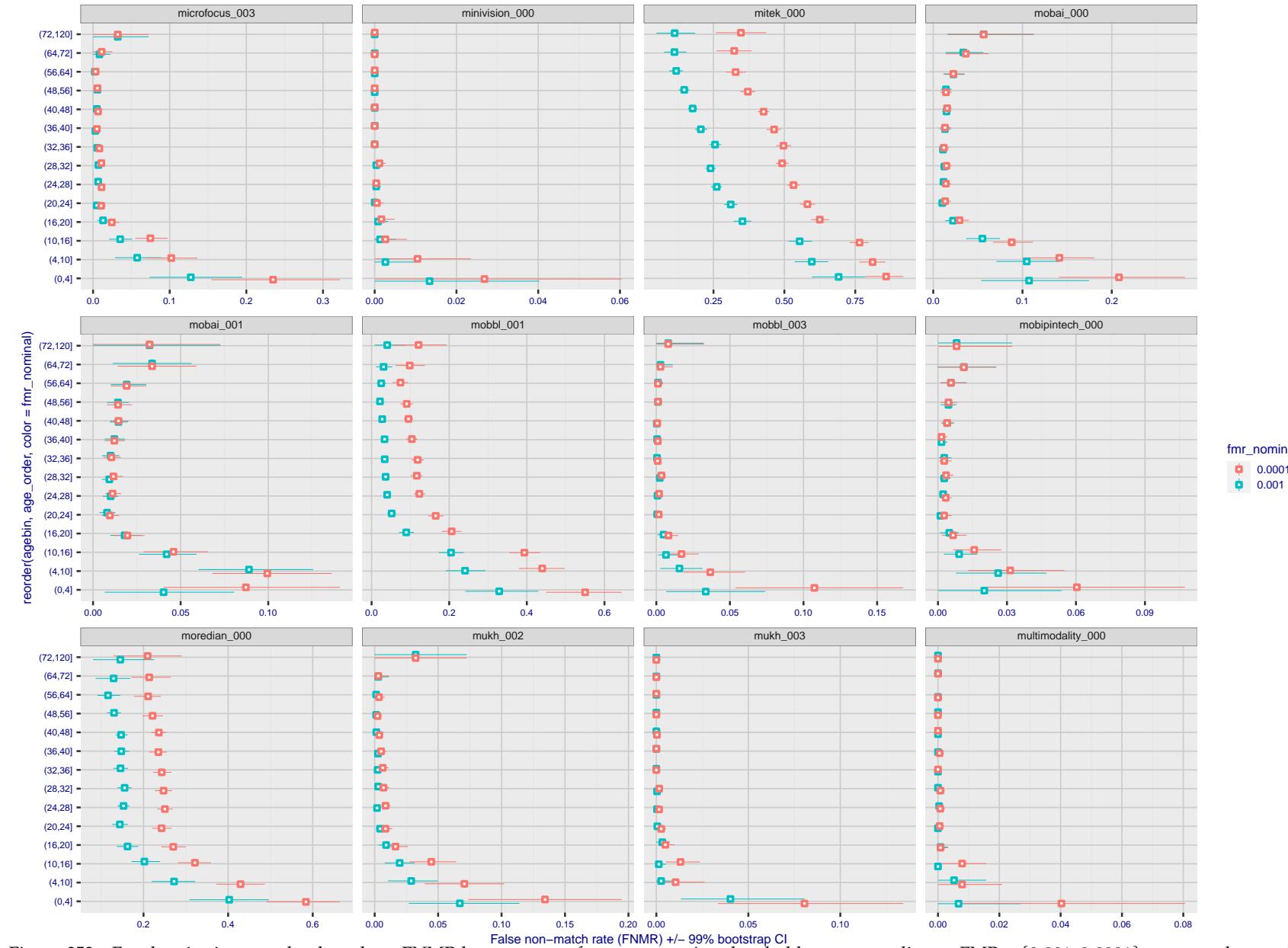


Figure 353: For the visa images, the dots show FNMR by age group for two operating thresholds corresponding to $FMR = \{0.001, 0.0001\}$ computed over all on the order of 10^{10} impostor scores. The FMR in each bin will vary also - see subsequent impostor heatmaps in sec. 3.6.2. Given a pair of face images taken at different times, we assign the comparison to the bin that is the arithmetic average of the subject's ages. This plot shows only the effect of age, not ageing. The number of comparisons in each bin is generally in the thousands, however the first and last bins are computed over 149 and 124 respectively. The error rates in some (adult) cases are zero, and in others the DET is flat so the error rates at the two thresholds are identical. The lines span 1% and 99% of bootstrap replicated FNMR estimates.



Figure 354: For the visa images, the dots show FNMR by age group for two operating thresholds corresponding to $FMR = \{0.001, 0.0001\}$ computed over all on the order of 10^{10} impostor scores. The FMR in each bin will vary also - see subsequent impostor heatmaps in sec. 3.6.2. Given a pair of face images taken at different times, we assign the comparison to the bin that is the arithmetic average of the subject's ages. This plot shows only the effect of age, not ageing. The number of comparisons in each bin is generally in the thousands, however the first and last bins are computed over 149 and 124 respectively. The error rates in some (adult) cases are zero, and in others the DET is flat so the error rates at the two thresholds are identical. The lines span 1% and 99% of bootstrap replicated FNMR estimates.

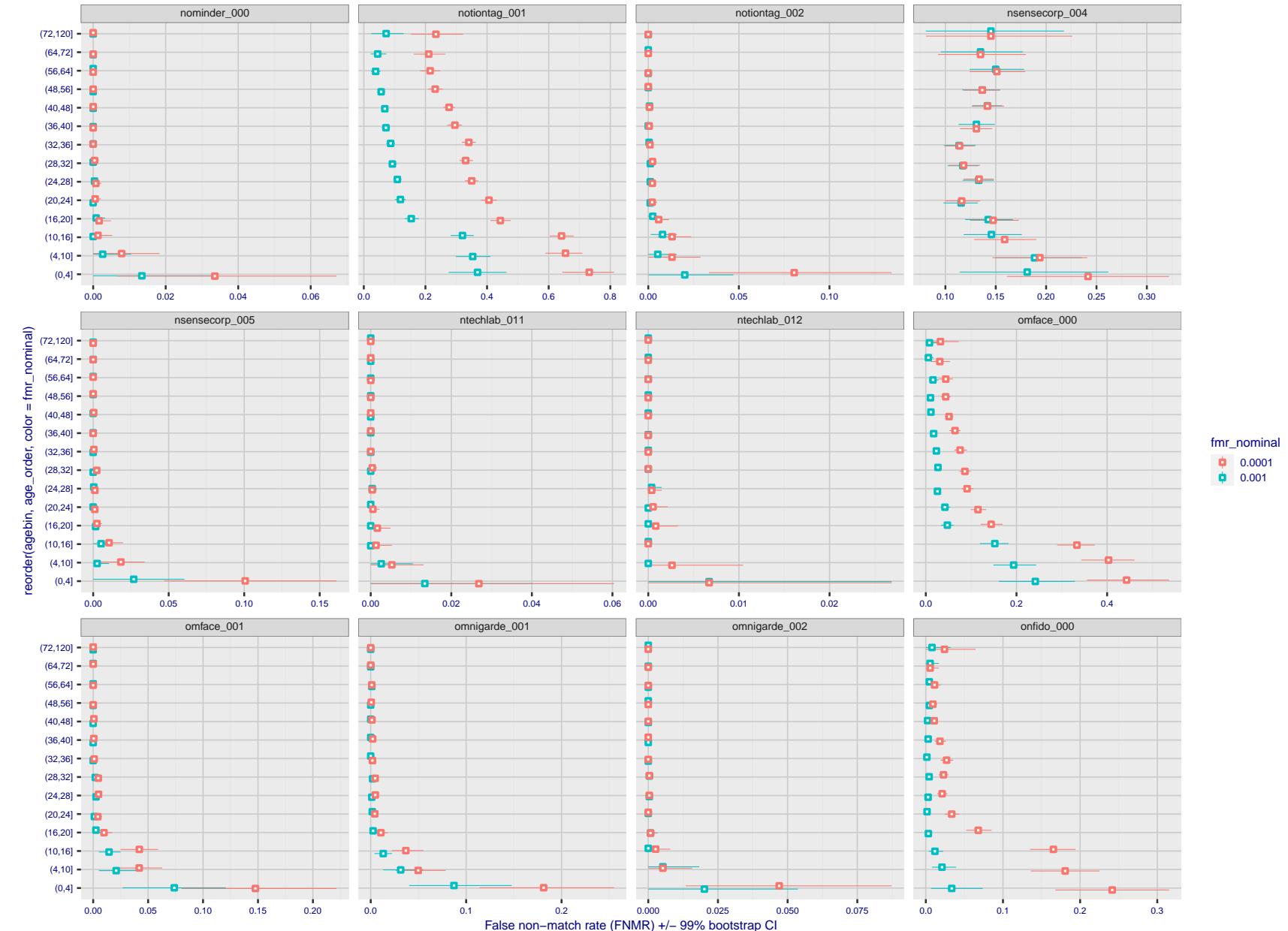


Figure 355: For the visa images, the dots show FNMR by age group for two operating thresholds corresponding to $FMR = \{0.001, 0.0001\}$ computed over all on the order of 10^{10} impostor scores. The FMR in each bin will vary also - see subsequent impostor heatmaps in sec. 3.6.2. Given a pair of face images taken at different times, we assign the comparison to the bin that is the arithmetic average of the subject's ages. This plot shows only the effect of age, not ageing. The number of comparisons in each bin is generally in the thousands, however the first and last bins are computed over 149 and 124 respectively. The error rates in some (adult) cases are zero, and in others the DET is flat so the error rates at the two thresholds are identical. The lines span 1% and 99% of bootstrap replicated FNMR estimates.

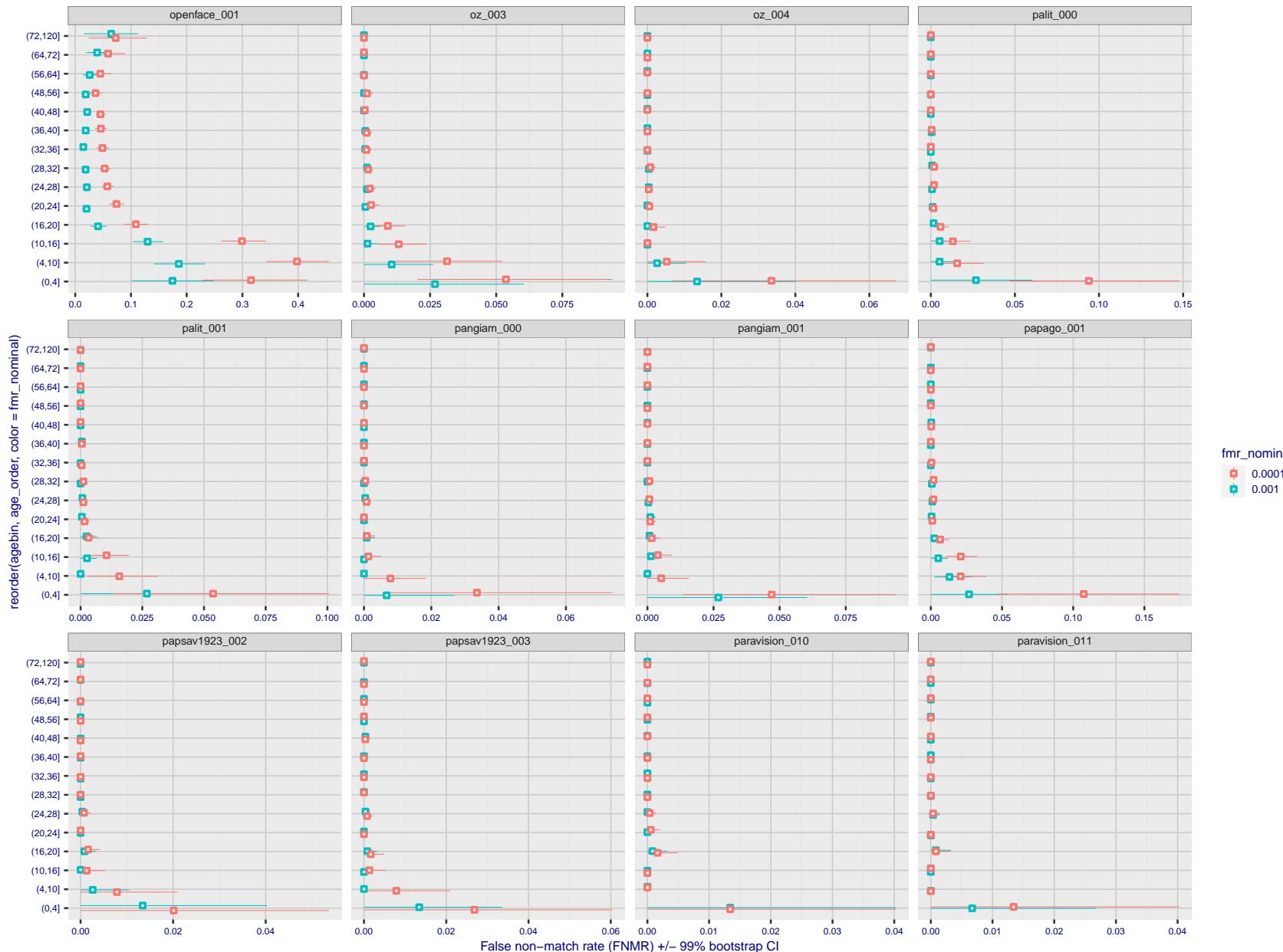


Figure 356: For the visa images, the dots show FNMR by age group for two operating thresholds corresponding to $FMR = \{0.001, 0.0001\}$ computed over all on the order of 10^{10} impostor scores. The FMR in each bin will vary also - see subsequent impostor heatmaps in sec. 3.6.2. Given a pair of face images taken at different times, we assign the comparison to the bin that is the arithmetic average of the subject's ages. This plot shows only the effect of age, not ageing. The number of comparisons in each bin is generally in the thousands, however the first and last bins are computed over 149 and 124 respectively. The error rates in some (adult) cases are zero, and in others the DET is flat so the error rates at the two thresholds are identical. The lines span 1% and 99% of bootstrap replicated FNMR estimates.



Figure 357: For the visa images, the dots show FNMR by age group for two operating thresholds corresponding to $FMR = \{0.001, 0.0001\}$ computed over all on the order of 10^{10} impostor scores. The FMR in each bin will vary also - see subsequent impostor heatmaps in sec. 3.6.2. Given a pair of face images taken at different times, we assign the comparison to the bin that is the arithmetic average of the subject's ages. This plot shows only the effect of age, not ageing. The number of comparisons in each bin is generally in the thousands, however the first and last bins are computed over 149 and 124 respectively. The error rates in some (adult) cases are zero, and in others the DET is flat so the error rates at the two thresholds are identical. The lines span 1% and 99% of bootstrap replicated FNMR estimates.

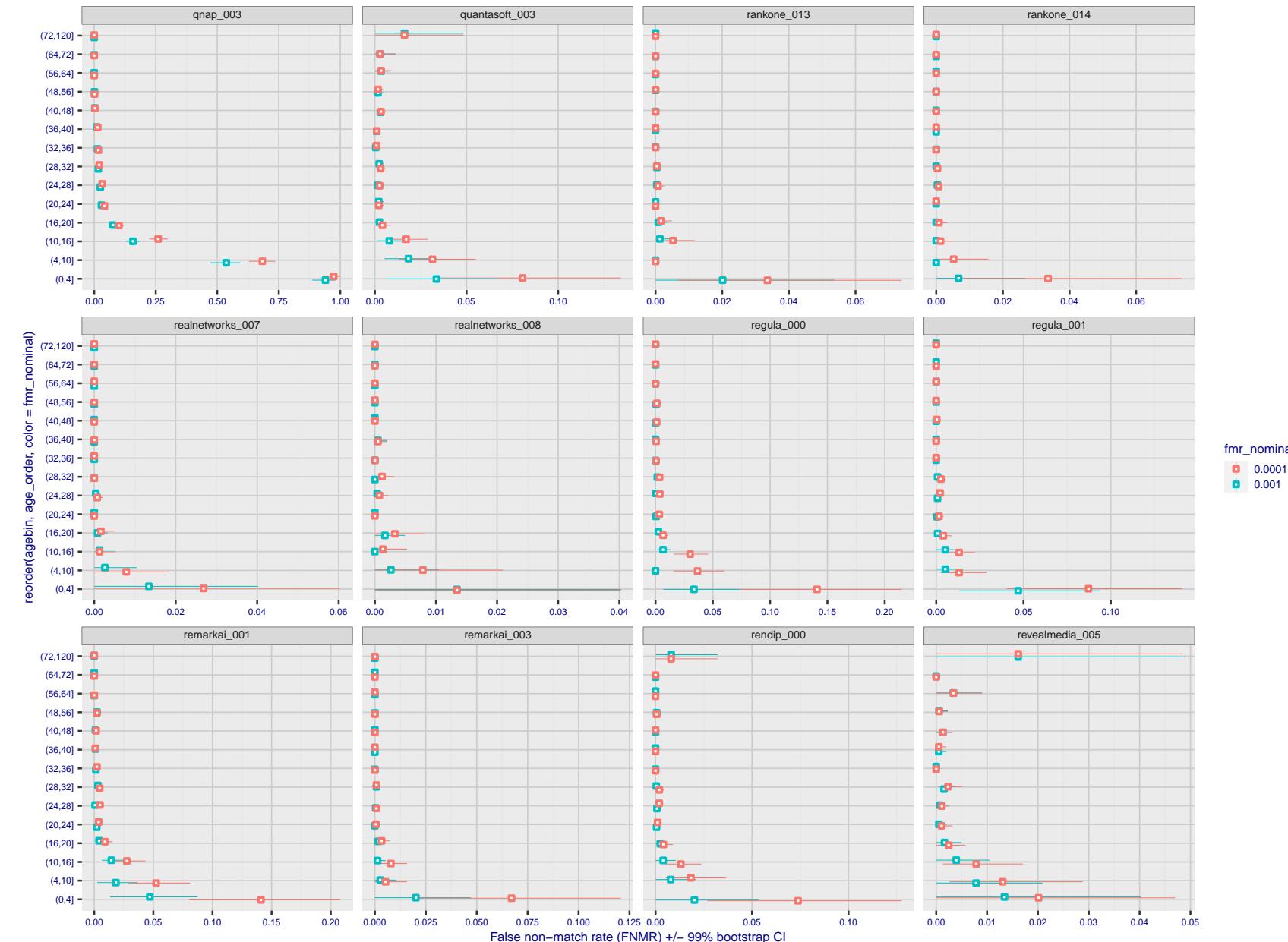


Figure 358: For the visa images, the dots show FNMR by age group for two operating thresholds corresponding to $FMR = \{0.001, 0.0001\}$ computed over all on the order of 10^{10} impostor scores. The FMR in each bin will vary also - see subsequent impostor heatmaps in sec. 3.6.2. Given a pair of face images taken at different times, we assign the comparison to the bin that is the arithmetic average of the subject's ages. This plot shows only the effect of age, not ageing. The number of comparisons in each bin is generally in the thousands, however the first and last bins are computed over 149 and 124 respectively. The error rates in some (adult) cases are zero, and in others the DET is flat so the error rates at the two thresholds are identical. The lines span 1% and 99% of bootstrap replicated FNMR estimates.

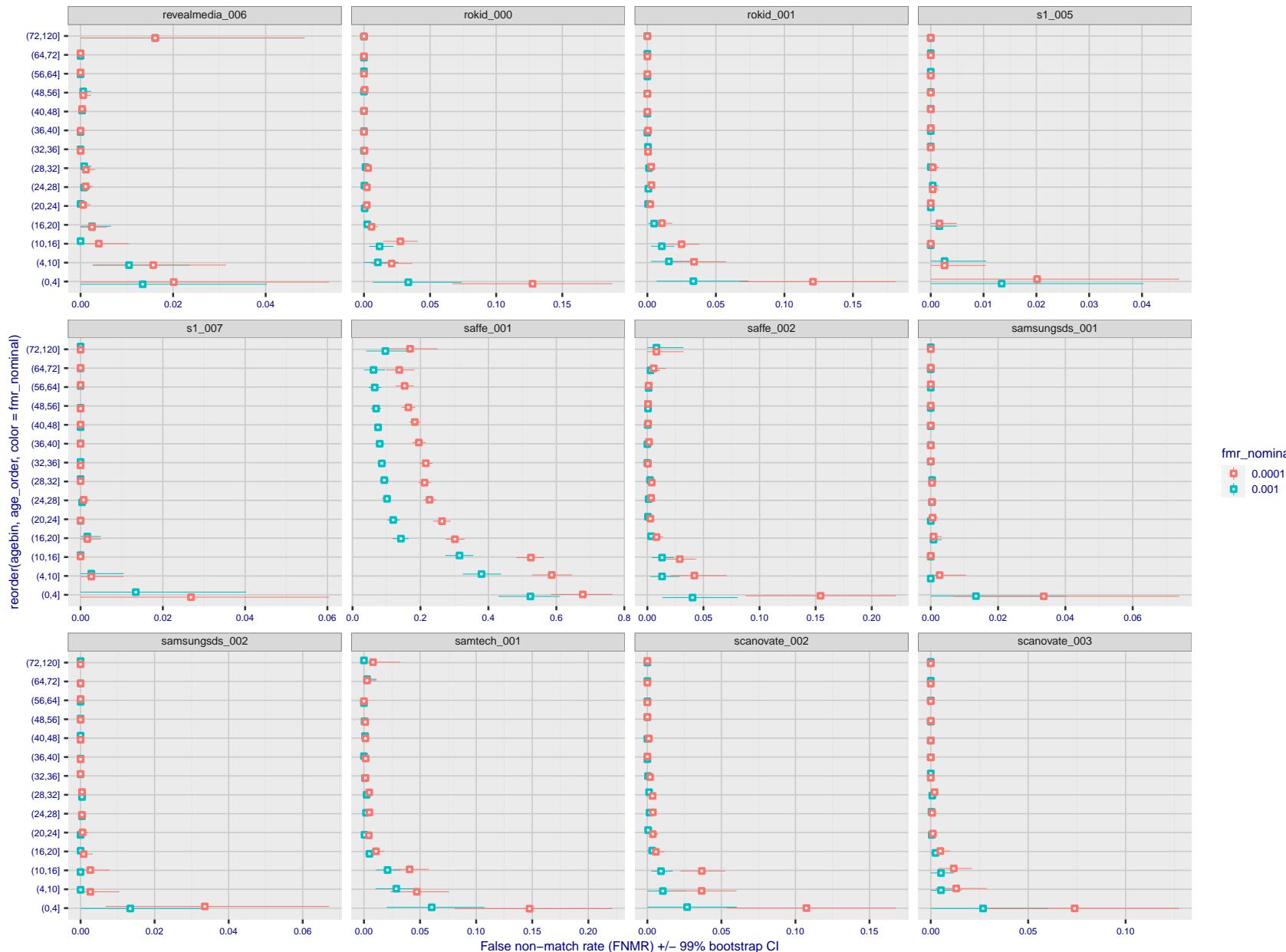


Figure 359: For the visa images, the dots show FNMR by age group for two operating thresholds corresponding to $FMR = \{0.001, 0.0001\}$ computed over all on the order of 10^{10} impostor scores. The FMR in each bin will vary also - see subsequent impostor heatmaps in sec. 3.6.2. Given a pair of face images taken at different times, we assign the comparison to the bin that is the arithmetic average of the subject's ages. This plot shows only the effect of age, not ageing. The number of comparisons in each bin is generally in the thousands, however the first and last bins are computed over 149 and 124 respectively. The error rates in some (adult) cases are zero, and in others the DET is flat so the error rates at the two thresholds are identical. The lines span 1% and 99% of bootstrap replicated FNMR estimates.

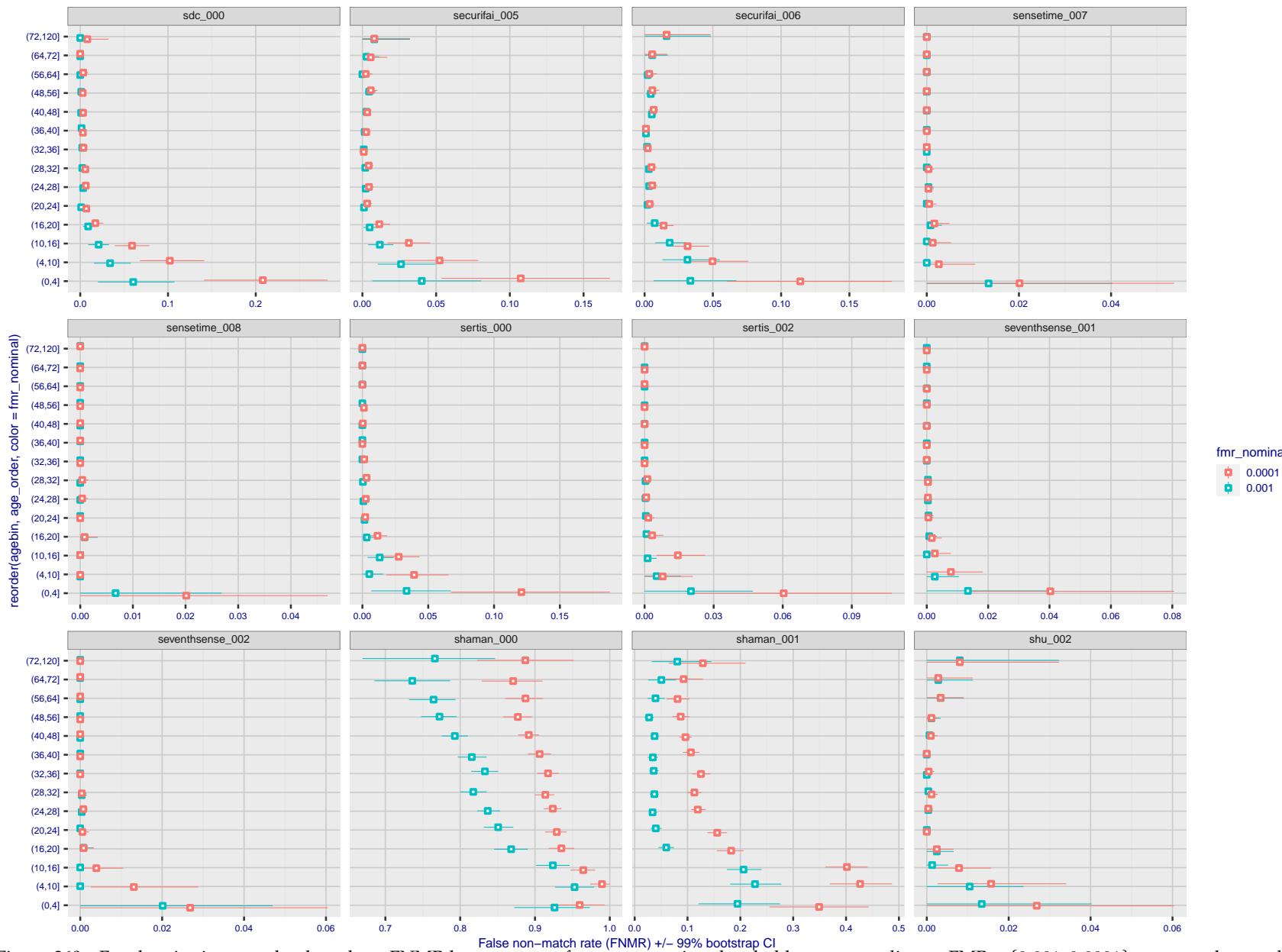


Figure 360: For the visa images, the dots show FNMR by age group for two operating thresholds corresponding to $FMR = \{0.001, 0.0001\}$ computed over all on the order of 10^{10} impostor scores. The FMR in each bin will vary also - see subsequent impostor heatmaps in sec. 3.6.2. Given a pair of face images taken at different times, we assign the comparison to the bin that is the arithmetic average of the subject's ages. This plot shows only the effect of age, not ageing. The number of comparisons in each bin is generally in the thousands, however the first and last bins are computed over 149 and 124 respectively. The error rates in some (adult) cases are zero, and in others the DET is flat so the error rates at the two thresholds are identical. The lines span 1% and 99% of bootstrap replicated FNMR estimates.

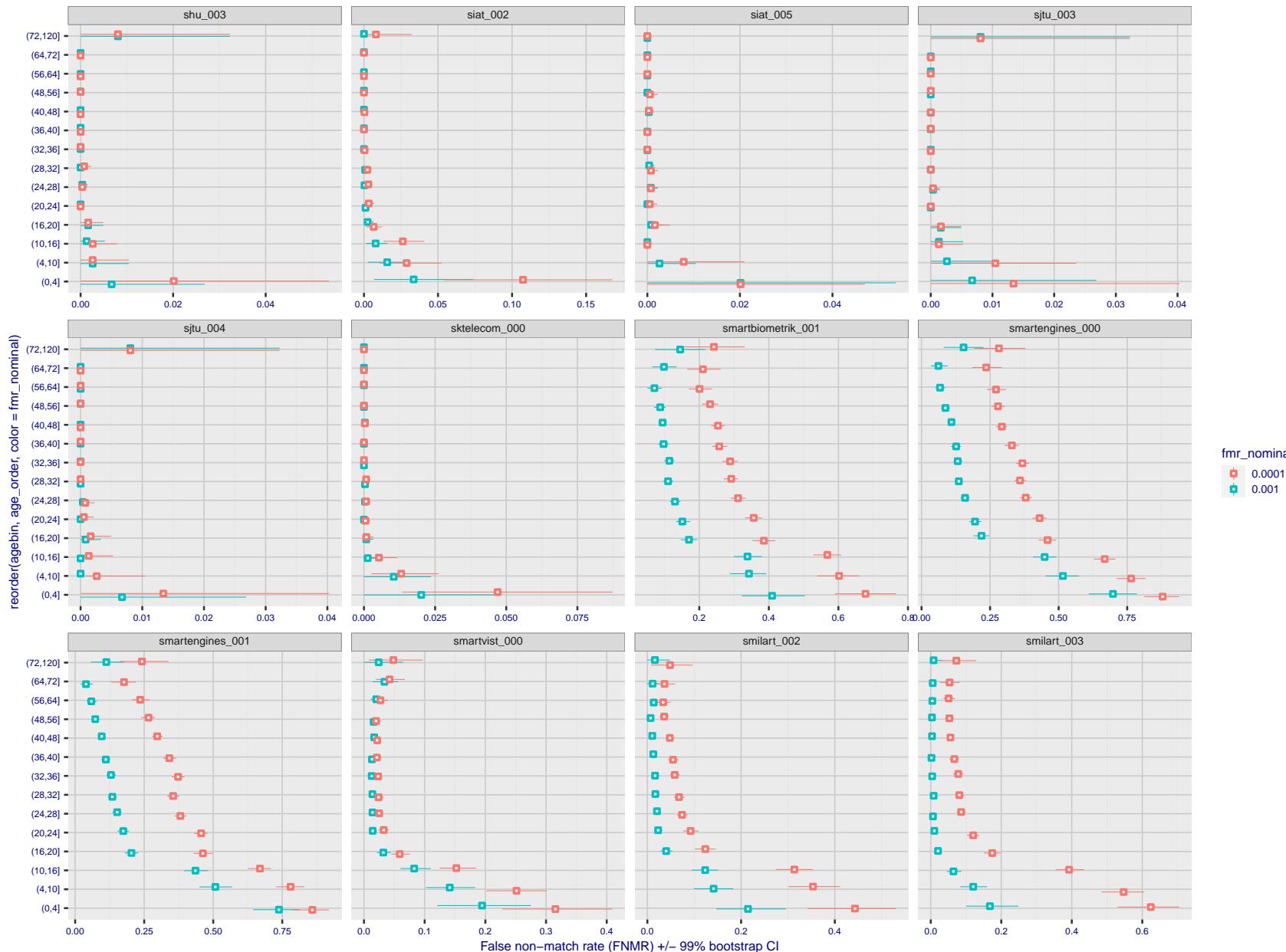


Figure 361: For the visa images, the dots show FNMR by age group for two operating thresholds corresponding to $FMR = \{0.001, 0.0001\}$ computed over all on the order of 10^{10} impostor scores. The FMR in each bin will vary also - see subsequent impostor heatmaps in sec. 3.6.2. Given a pair of face images taken at different times, we assign the comparison to the bin that is the arithmetic average of the subject's ages. This plot shows only the effect of age, not ageing. The number of comparisons in each bin is generally in the thousands, however the first and last bins are computed over 149 and 124 respectively. The error rates in some (adult) cases are zero, and in others the DET is flat so the error rates at the two thresholds are identical. The lines span 1% and 99% of bootstrap replicated FNMR estimates.



Figure 362: For the visa images, the dots show FNMR by age group for two operating thresholds corresponding to $FMR = \{0.001, 0.0001\}$ computed over all on the order of 10^{10} impostor scores. The FMR in each bin will vary also - see subsequent impostor heatmaps in sec. 3.6.2. Given a pair of face images taken at different times, we assign the comparison to the bin that is the arithmetic average of the subject's ages. This plot shows only the effect of age, not ageing. The number of comparisons in each bin is generally in the thousands, however the first and last bins are computed over 149 and 124 respectively. The error rates in some (adult) cases are zero, and in others the DET is flat so the error rates at the two thresholds are identical. The lines span 1% and 99% of bootstrap replicated FNMR estimates.



Figure 363: For the visa images, the dots show FNMR by age group for two operating thresholds corresponding to $FMR = \{0.001, 0.0001\}$ computed over all on the order of 10^{10} impostor scores. The FMR in each bin will vary also - see subsequent impostor heatmaps in sec. 3.6.2. Given a pair of face images taken at different times, we assign the comparison to the bin that is the arithmetic average of the subject's ages. This plot shows only the effect of age, not ageing. The number of comparisons in each bin is generally in the thousands, however the first and last bins are computed over 149 and 124 respectively. The error rates in some (adult) cases are zero, and in others the DET is flat so the error rates at the two thresholds are identical. The lines span 1% and 99% of bootstrap replicated FNMR estimates.

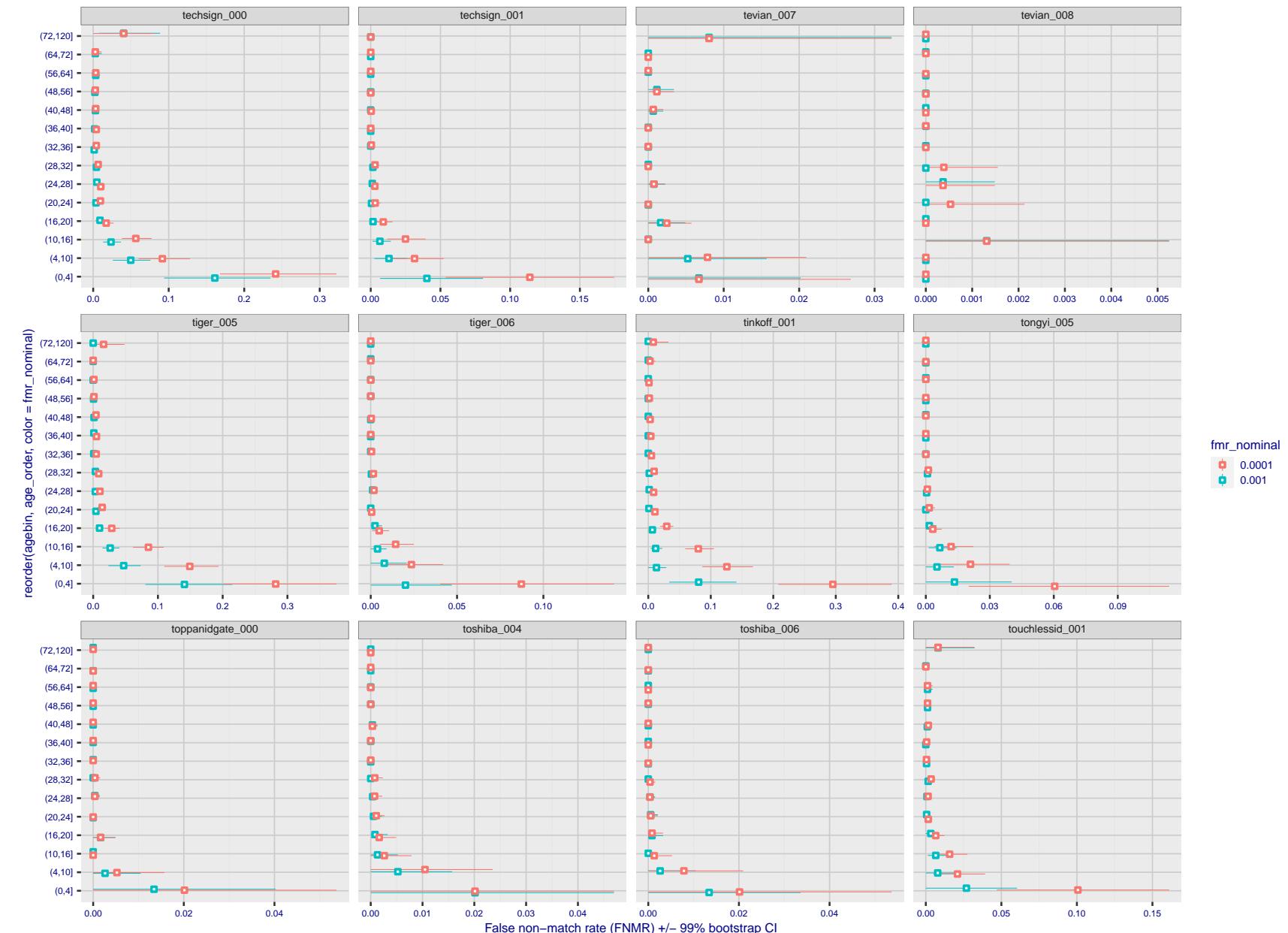


Figure 364: For the visa images, the dots show FNMR by age group for two operating thresholds corresponding to $FMR = \{0.001, 0.0001\}$ computed over all on the order of 10^{10} impostor scores. The FMR in each bin will vary also - see subsequent impostor heatmaps in sec. 3.6.2. Given a pair of face images taken at different times, we assign the comparison to the bin that is the arithmetic average of the subject's ages. This plot shows only the effect of age, not ageing. The number of comparisons in each bin is generally in the thousands, however the first and last bins are computed over 149 and 124 respectively. The error rates in some (adult) cases are zero, and in others the DET is flat so the error rates at the two thresholds are identical. The lines span 1% and 99% of bootstrap replicated FNMR estimates.



Figure 365: For the visa images, the dots show FNMR by age group for two operating thresholds corresponding to $FMR = \{0.001, 0.0001\}$ computed over all on the order of 10^{10} impostor scores. The FMR in each bin will vary also - see subsequent impostor heatmaps in sec. 3.6.2. Given a pair of face images taken at different times, we assign the comparison to the bin that is the arithmetic average of the subject's ages. This plot shows only the effect of age, not ageing. The number of comparisons in each bin is generally in the thousands, however the first and last bins are computed over 149 and 124 respectively. The error rates in some (adult) cases are zero, and in others the DET is flat so the error rates at the two thresholds are identical. The lines span 1% and 99% of bootstrap replicated FNMR estimates.

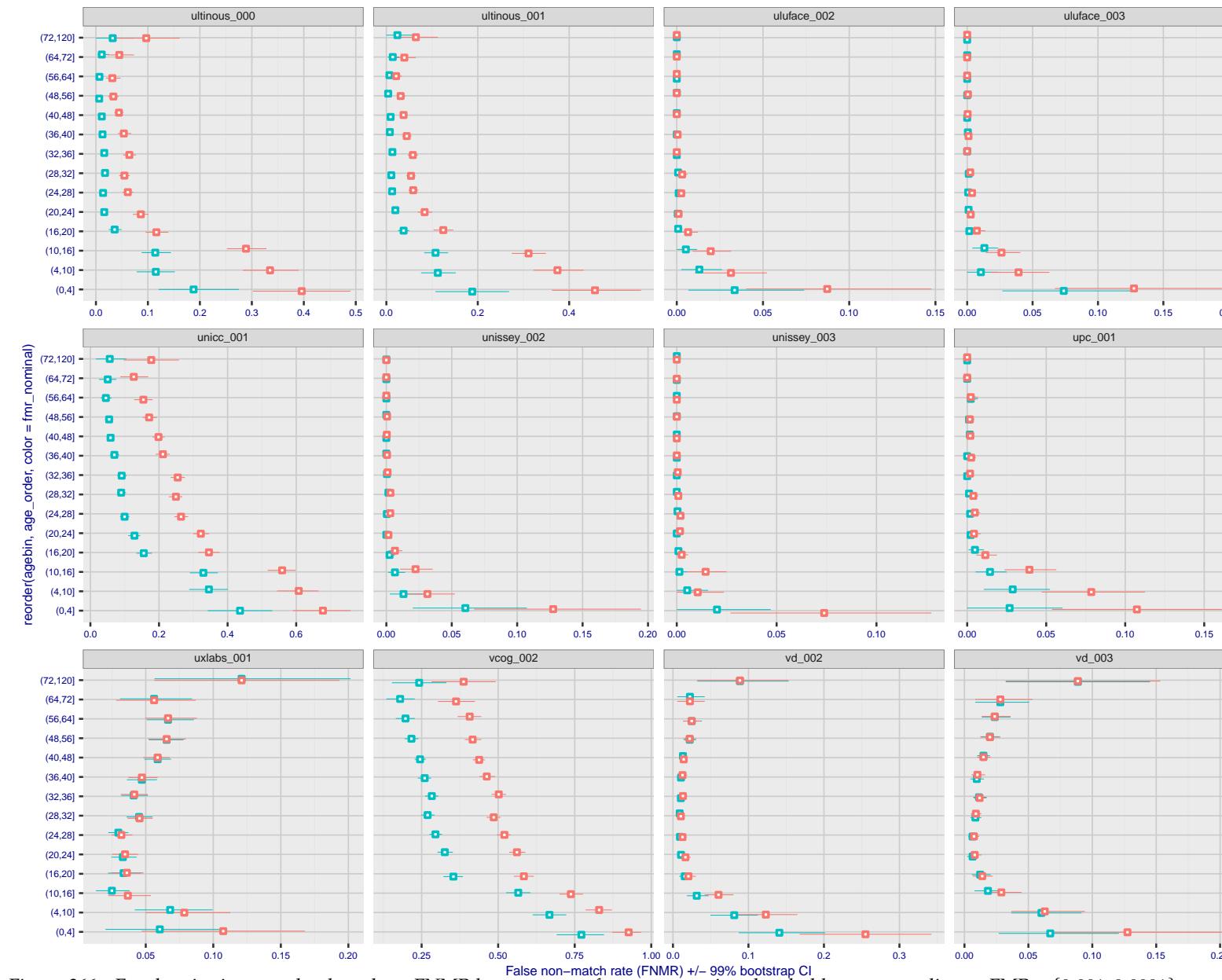


Figure 366: For the visa images, the dots show FNMR by age group for two operating thresholds corresponding to $FMR = \{0.001, 0.0001\}$ computed over all on the order of 10^{10} impostor scores. The FMR in each bin will vary also - see subsequent impostor heatmaps in sec. 3.6.2. Given a pair of face images taken at different times, we assign the comparison to the bin that is the arithmetic average of the subject's ages. This plot shows only the effect of age, not ageing. The number of comparisons in each bin is generally in the thousands, however the first and last bins are computed over 149 and 124 respectively. The error rates in some (adult) cases are zero, and in others the DET is flat so the error rates at the two thresholds are identical. The lines span 1% and 99% of bootstrap replicated FNMR estimates.

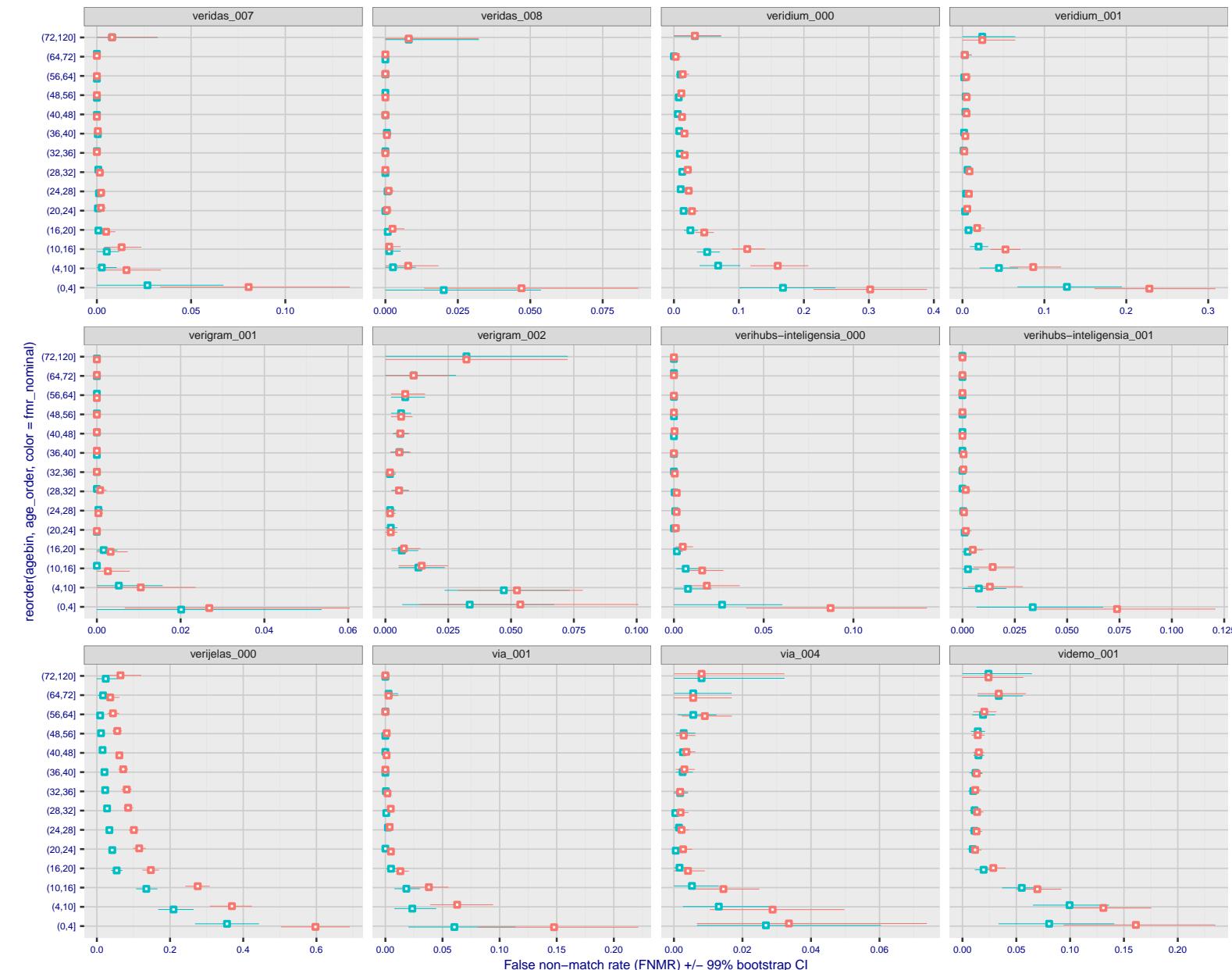
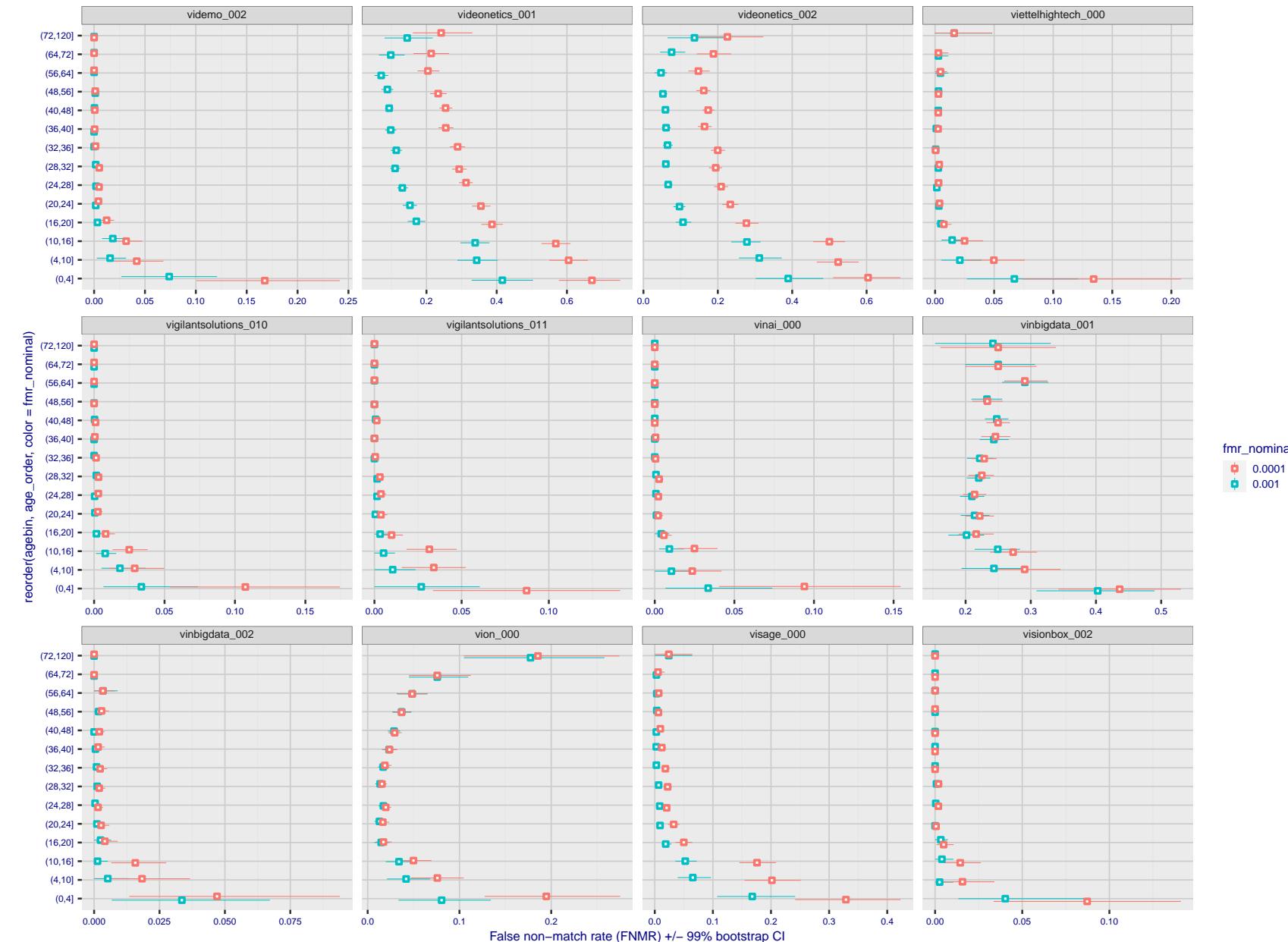


Figure 367: For the visa images, the dots show FNMR by age group for two operating thresholds corresponding to $FMR = \{0.001, 0.0001\}$ computed over all on the order of 10^{10} impostor scores. The FMR in each bin will vary also - see subsequent impostor heatmaps in sec. 3.6.2. Given a pair of face images taken at different times, we assign the comparison to the bin that is the arithmetic average of the subject's ages. This plot shows only the effect of age, not ageing. The number of comparisons in each bin is generally in the thousands, however the first and last bins are computed over 149 and 124 respectively. The error rates in some (adult) cases are zero, and in others the DET is flat so the error rates at the two thresholds are identical. The lines span 1% and 99% of bootstrap replicated FNMR estimates.



fmr_nominal
0.0001
0.001

Figure 368: For the visa images, the dots show FNMR by age group for two operating thresholds corresponding to $FMR = \{0.0001, 0.0001\}$ computed over all on the order of 10^{10} impostor scores. The FMR in each bin will vary also - see subsequent impostor heatmaps in sec. 3.6.2. Given a pair of face images taken at different times, we assign the comparison to the bin that is the arithmetic average of the subject's ages. This plot shows only the effect of age, not ageing. The number of comparisons in each bin is generally in the thousands, however the first and last bins are computed over 149 and 124 respectively. The error rates in some (adult) cases are zero, and in others the DET is flat so the error rates at the two thresholds are identical. The lines span 1% and 99% of bootstrap replicated FNMR estimates.

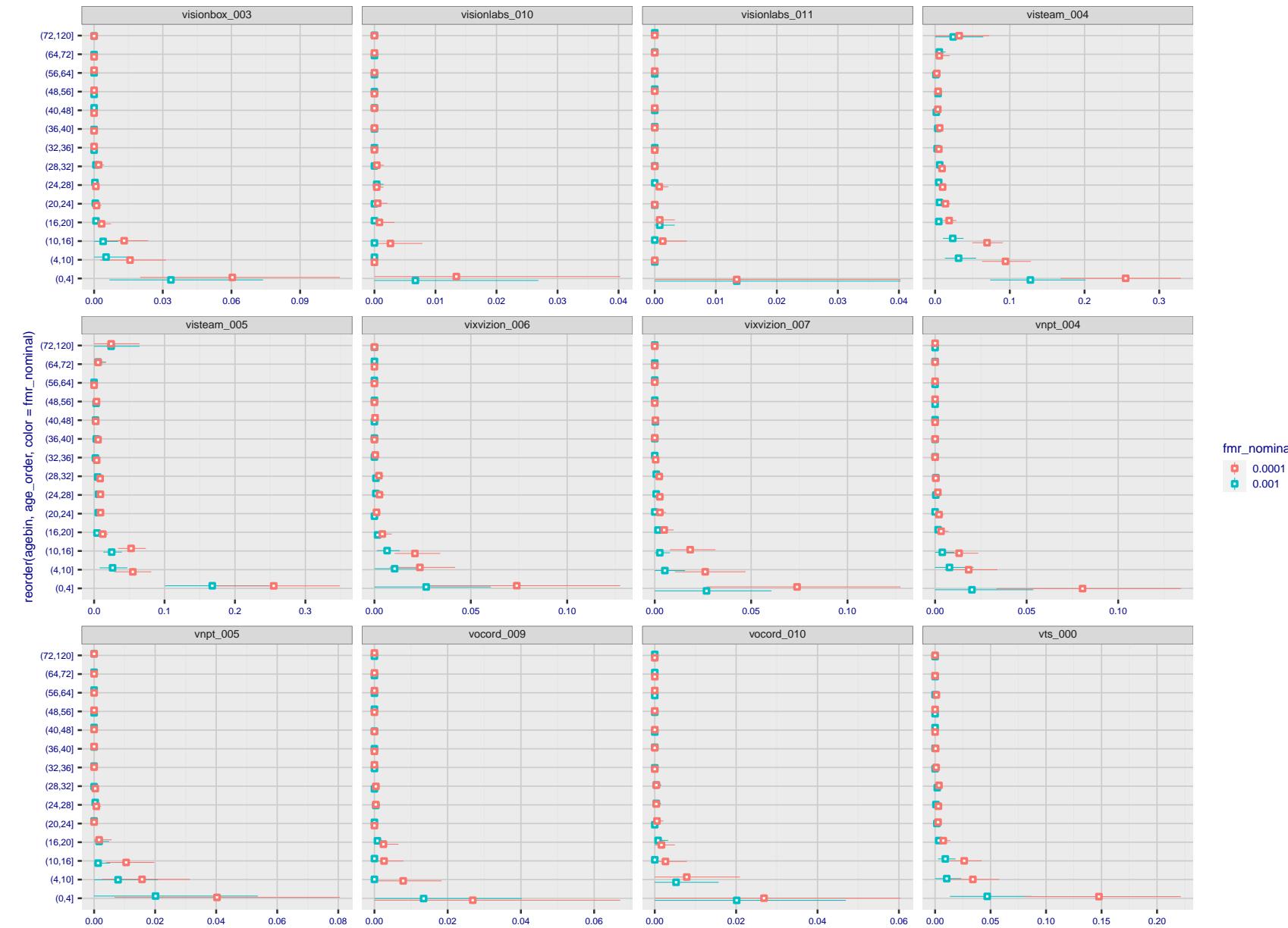
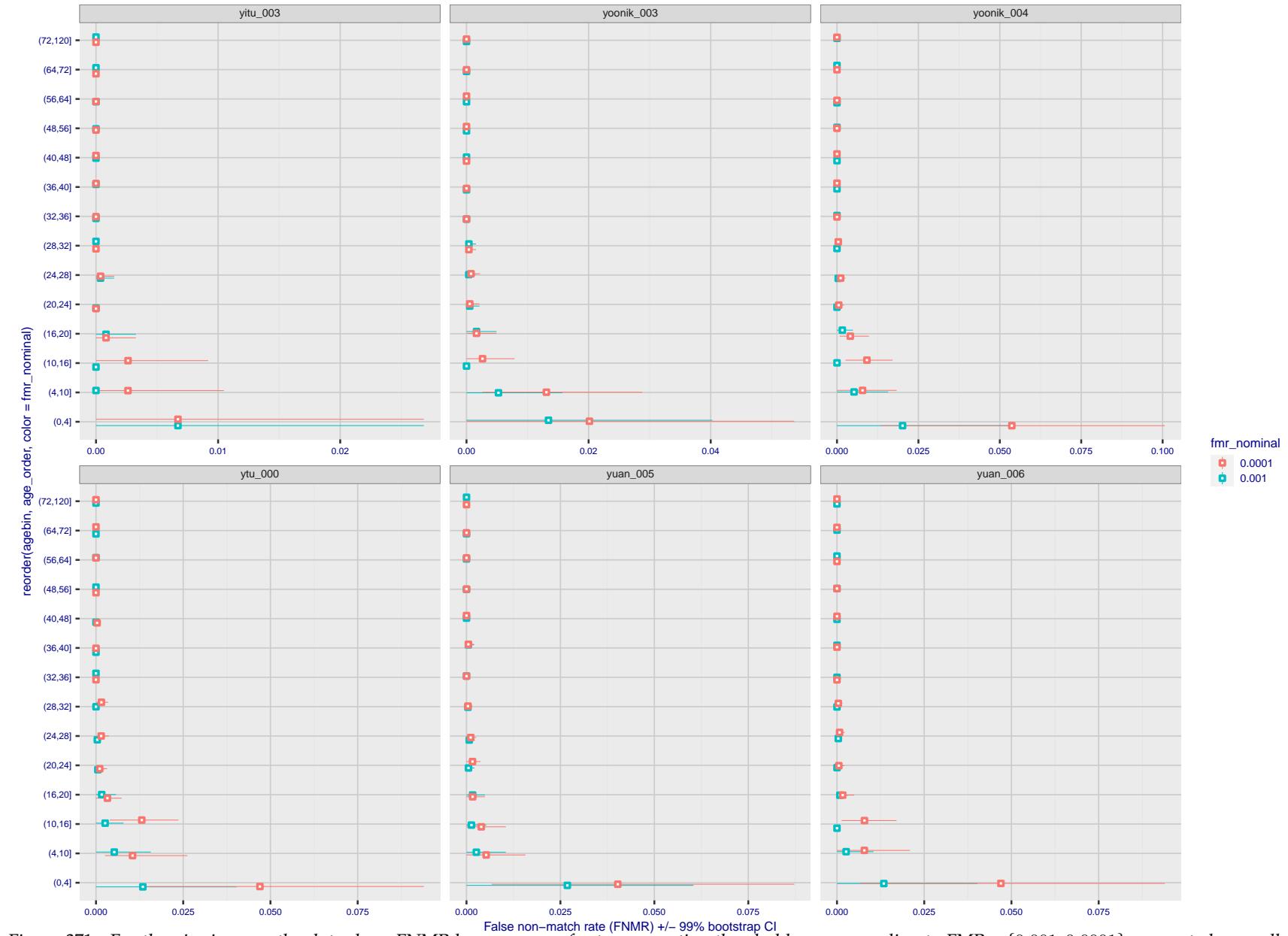


Figure 369: For the visa images, the dots show FNMR by age group for two operating thresholds corresponding to $FMR = \{0.001, 0.0001\}$ computed over all on the order of 10^{10} impostor scores. The FMR in each bin will vary also - see subsequent impostor heatmaps in sec. 3.6.2. Given a pair of face images taken at different times, we assign the comparison to the bin that is the arithmetic average of the subject's ages. This plot shows only the effect of age, not ageing. The number of comparisons in each bin is generally in the thousands, however the first and last bins are computed over 149 and 124 respectively. The error rates in some (adult) cases are zero, and in others the DET is flat so the error rates at the two thresholds are identical. The lines span 1% and 99% of bootstrap replicated FNMR estimates.



Figure 370: For the visa images, the dots show FNMR by age group for two operating thresholds corresponding to $FMR = \{0.001, 0.0001\}$ computed over all on the order of 10^{10} impostor scores. The FMR in each bin will vary also - see subsequent impostor heatmaps in sec. 3.6.2. Given a pair of face images taken at different times, we assign the comparison to the bin that is the arithmetic average of the subject's ages. This plot shows only the effect of age, not ageing. The number of comparisons in each bin is generally in the thousands, however the first and last bins are computed over 149 and 124 respectively. The error rates in some (adult) cases are zero, and in others the DET is flat so the error rates at the two thresholds are identical. The lines span 1% and 99% of bootstrap replicated FNMR estimates.



Caveats: None.

3.6 Impostor distribution stability

3.6.1 Effect of birth place on the impostor distribution

Background: Facial appearance varies geographically, both in terms of skin tone, cranio-facial structure and size. This section addresses whether false match rates vary intra- and inter-regionally.

Goals:

- ▷ To show the effect of birth region of the impostor and enrollee on false match rates.
- ▷ To determine whether some algorithms give better impostor distribution stability.

Methods:

- ▷ For the visa images, NIST defined 10 regions: Sub-Saharan Africa, South Asia, Polynesia, North Africa, Middle East, Europe, East Asia, Central and South America, Central Asia, and the Caribbean.
- ▷ For the visa images, NIST mapped each country of birth to a region. There is some arbitrariness to this. For example, Egypt could reasonably be assigned to the Middle East instead of North Africa. An alternative methodology could, for example, assign the Philippines to *both* Polynesia and East Asia.
- ▷ FMR is computed for cases where all face images of impostors born in region r_2 are compared with enrolled face images of persons born in region r_1 .

$$\text{FMR}(r_1, r_2, T) = \frac{\sum_{i=1}^{N_{r_1, r_2}} H(s_i - T)}{N_{r_1, r_2}} \quad (5)$$

where the same threshold, T , is used in all cells, and H is the unit step function. The threshold is set to give $\text{FMR}(T) = 0.001$ over the entire set of visa image impostor comparisons.

- ▷ This analysis is then repeated by country-pair, but only for those country pairs where both have at least 1000 images available. The countries¹ appear in the axes of graphs that follow.
- ▷ The mean number of impostor scores in any cross-region bin is 33 million. The smallest number of impostor scores in any bin is 135000, for Central Asia - North Africa. While these counts are large enough to support reasonable significance, the number of individual faces is much smaller, on the order of $N^{0.5}$.
- ▷ The numbers of impostor scores in any cross-country bin is shown in Figure 372.

Results: Subsequent figures show heatmaps that use color to represent the base-10 logarithm of the false match rate. Red colors indicate high (bad) false match rates. Dark colors indicate benign false match rates. There are two series of graphs corresponding to aggregated geographical regions, and to countries. The notable observations are:

- ▷ The on-diagonal elements correspond to within-region impostors. FMR is generally above the nominal value of $\text{FMR} = 0.001$. Particularly there is usually higher FMR in, Sub-Saharan Africa, South Asia, and the Caribbean. Europe and Central Asia, on the other hand, usually give FMR closer to the nominal value.
- ▷ The off-diagonal elements correspond to across-region impostors. The highest FMR is produced between the Caribbean and Sub-Saharan Africa.
- ▷ Algorithms vary.

¹These are Argentina, Australia, Brazil, Chile, China, Costa Rica, Cuba, Czech Republic, Dominican Republic, Ecuador, Egypt, El Salvador, Germany, Ghana, Great Britain, Greece, Guatemala, Haiti, Hong Kong, Honduras, Indonesia, India, Israel, Jamaica, Japan, Kenya, Korea, Lebanon, Mexico, Malaysia, Nepal, Nigeria, Peru, Philippines, Pakistan, Poland, Romania, Russia, South Africa, Saudi Arabia, Thailand, Trinidad, Turkey, Taiwan, Ukraine, Venezuela, and Vietnam.

- ▷ We computed the same quantities for a global FMR = 0.0001. The effects are similar.

Caveats:

- ▷ The effects of variable impostor rates on one-to-many identification systems may well differ from what's implied by these one-to-one verification results. Two reasons for this are a) the enrollment galleries are usually imbalanced across countries of birth, age and sex; b) one-to-many identification algorithms often implement techniques aimed at stabilizing the impostor distribution. Further research is necessary.
- ▷ In principle, the effects seen in this subsection could be due to differences in the image capture process. We consider this unlikely since the effects are maintained across geography - e.g. Caribbean vs. Africa, or Japan vs. China.

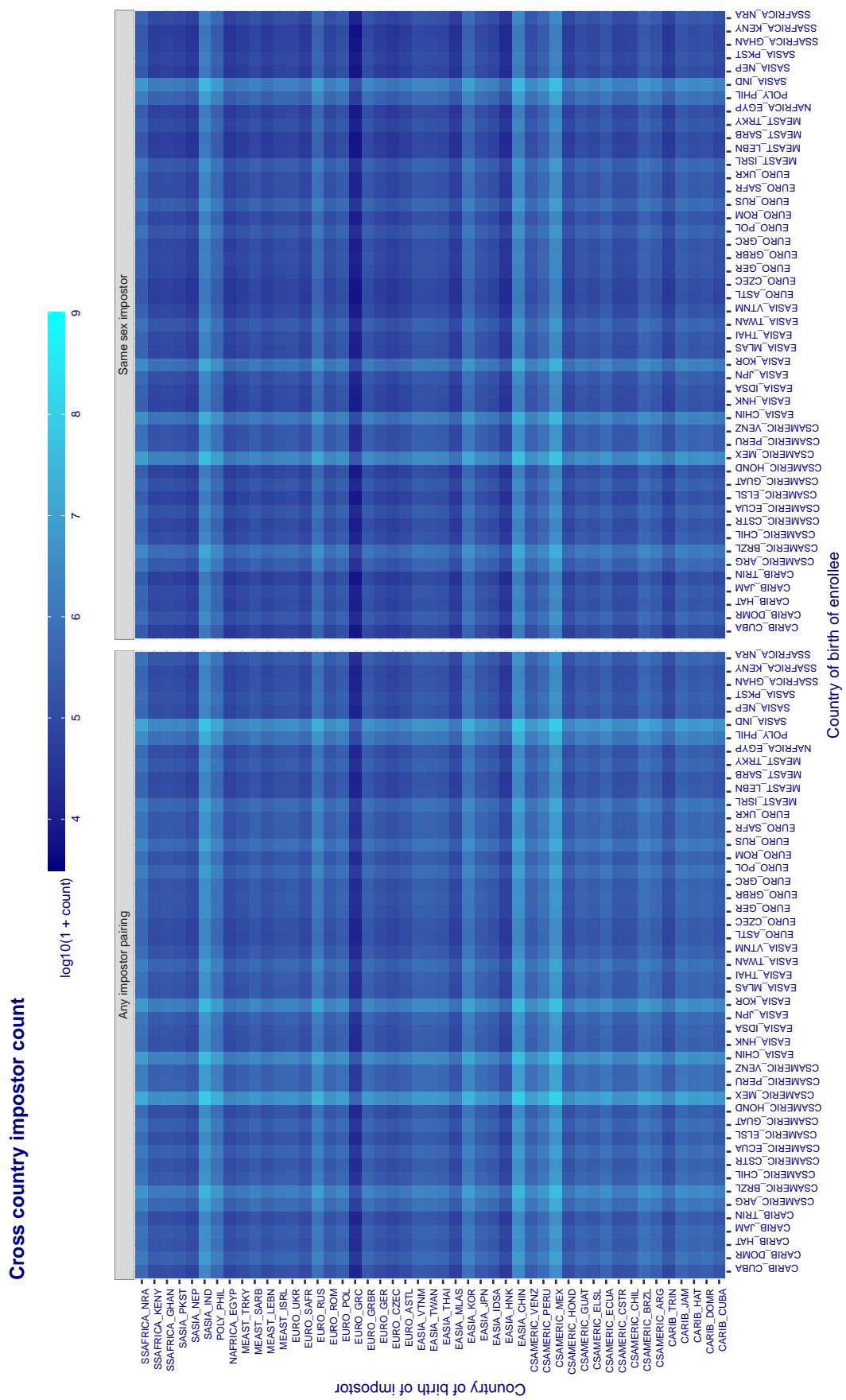


Figure 372: For visa images, the heatmap shows the count of impostor comparisons of faces from different individuals who were born in the given country pair. The FMR heatmaps themselves appear in the 1:1 report cards, for example, [this one](#).

3.6.2 Effect of age on impostors

Background: This section shows the effect of age on the impostor distribution. The ideal behaviour is that the age of the enrollee and the impostor would not affect impostor scores. This would support FMR stability over sub-populations.

Goals:

- ▷ To show the effect of relative ages of the impostor and enrollee on false match rates.
- ▷ To determine whether some algorithms have better impostor distribution stability.

Methods:

- ▷ Define 14 age group bins, spanning 0 to over 100 years old.
- ▷ Compute FMR over all impostor comparisons for which the subjects in the enrollee and impostor images have ages in two bins.
- ▷ Compute FMR over all impostor comparisons for which the subjects are additionally of the same sex, and born in the same geographic region.

Results:

The notable aspects are:

- ▷ Diagonal dominance: Impostors are more likely to be matched against their same age group.
- ▷ Same sex and same region impostors are more successful. On the diagonal, an impostor is more likely to succeed by posing as someone of the same sex. If $\Delta \log_{10} \text{FMR} = 0.2$, then same-sex same-region FMR exceeds the all-pairs FMR by factor of $10^{0.2} = 1.6$.
- ▷ Young children impostors give elevated FMR against young children. Older adult impostor give elevated FMR against older adults. These effects are quite large, for example if $\Delta \log_{10} \text{FMR} = 1.0$ larger than a 32 year old, then these groups have higher FMR by a factor of $10^1 = 10$. This would imply an FMR above 0.01 for a nominal (global) FMR = 0.001.
- ▷ Algorithms vary.
- ▷ We computed the same quantities for a global FMR = 0.0001. The effects are similar.

Note the calculations in this section include impostors paired across all countries of birth.

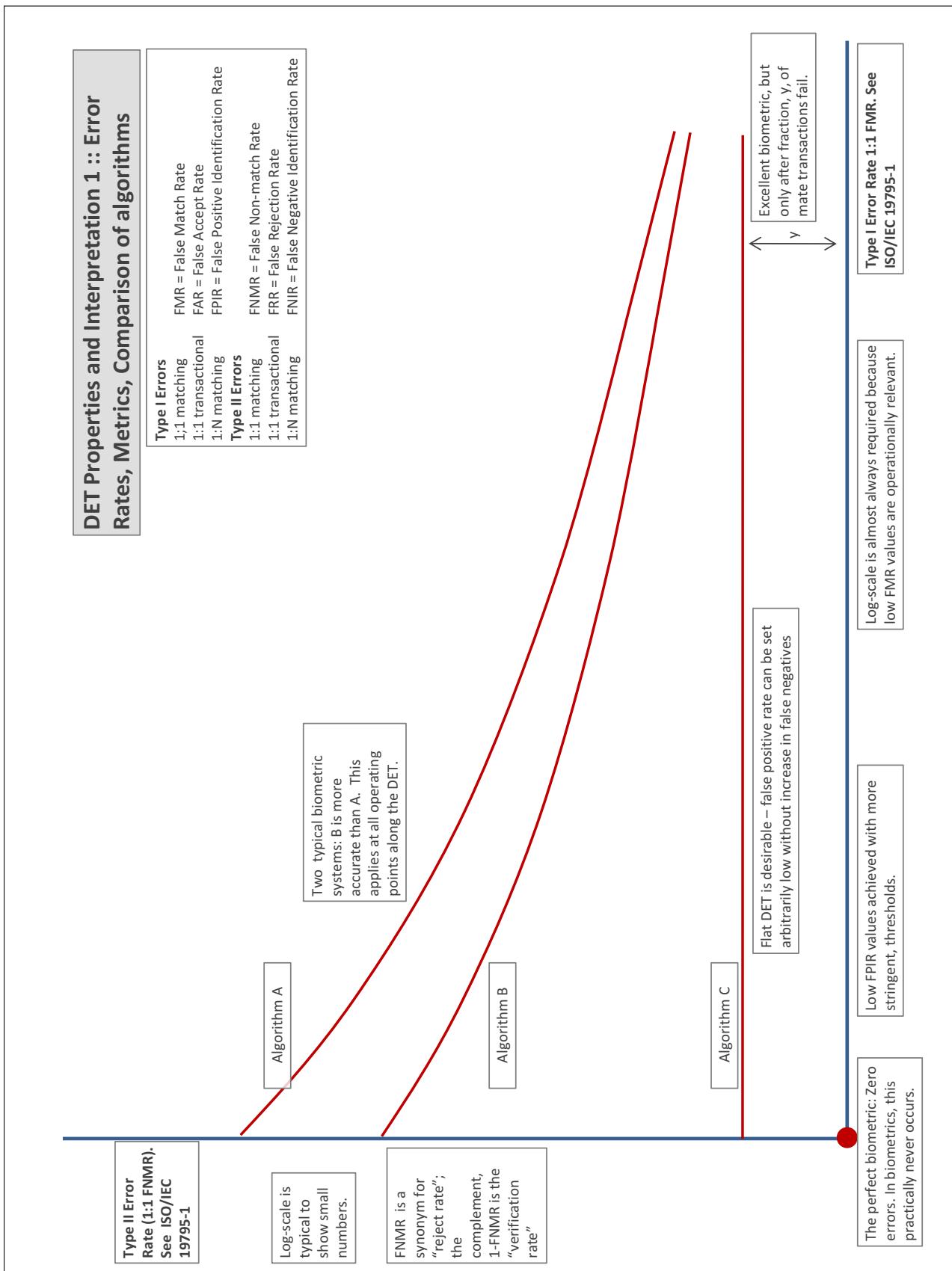
Accuracy Terms + Definitions

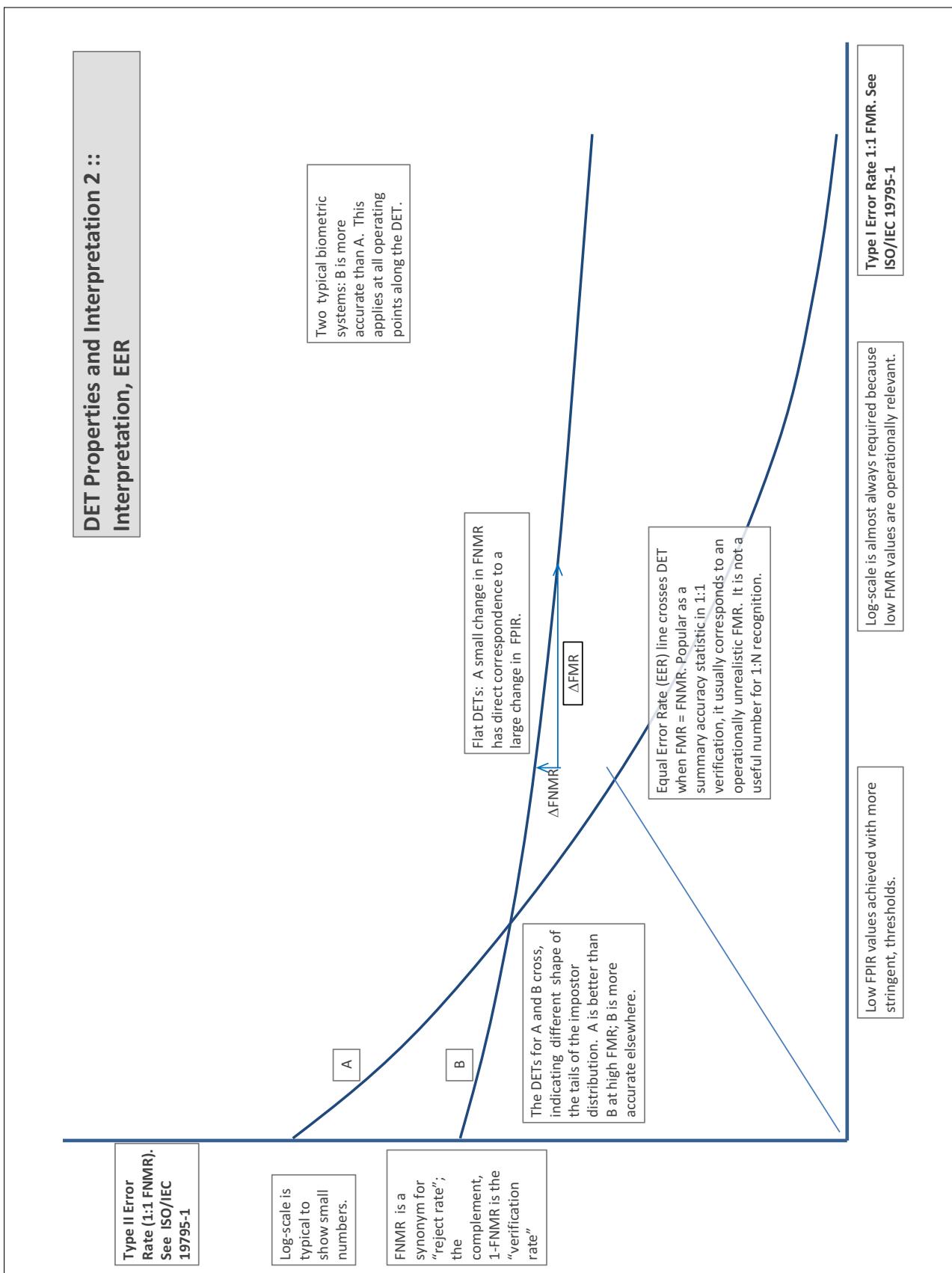
In biometrics, Type II errors occur when two samples of one person do not match – this is called a **false negative**. Correspondingly, Type I errors occur when samples from two persons do match – this is called a **false positive**. Matches are declared by a biometric system when the native comparison score from the recognition algorithm meets some **threshold**. Comparison scores can be either **similarity scores**, in which case higher values indicate that the samples are more likely to come from the same person, or **dissimilarity scores**, in which case higher values indicate different people. Similarity scores are traditionally computed by **fingerprint** and **face** recognition algorithms, while dissimilarities are used in **iris recognition**. In some cases, the dissimilarity score is a distance; this applies only when **metric** properties are obeyed. In any case, scores can be either **mate** scores, coming from a comparison of one person's samples, or **nonmate** scores, coming from comparison of different persons' samples. The words **genuine** or **authentic** are synonyms for mate, and the word **impostor** is used as a synonym for nonmatch. The words mate and nonmatch are traditionally used in identification applications (such as law enforcement search, or background checks) while genuine and impostor are used in verification applications (such as access control).

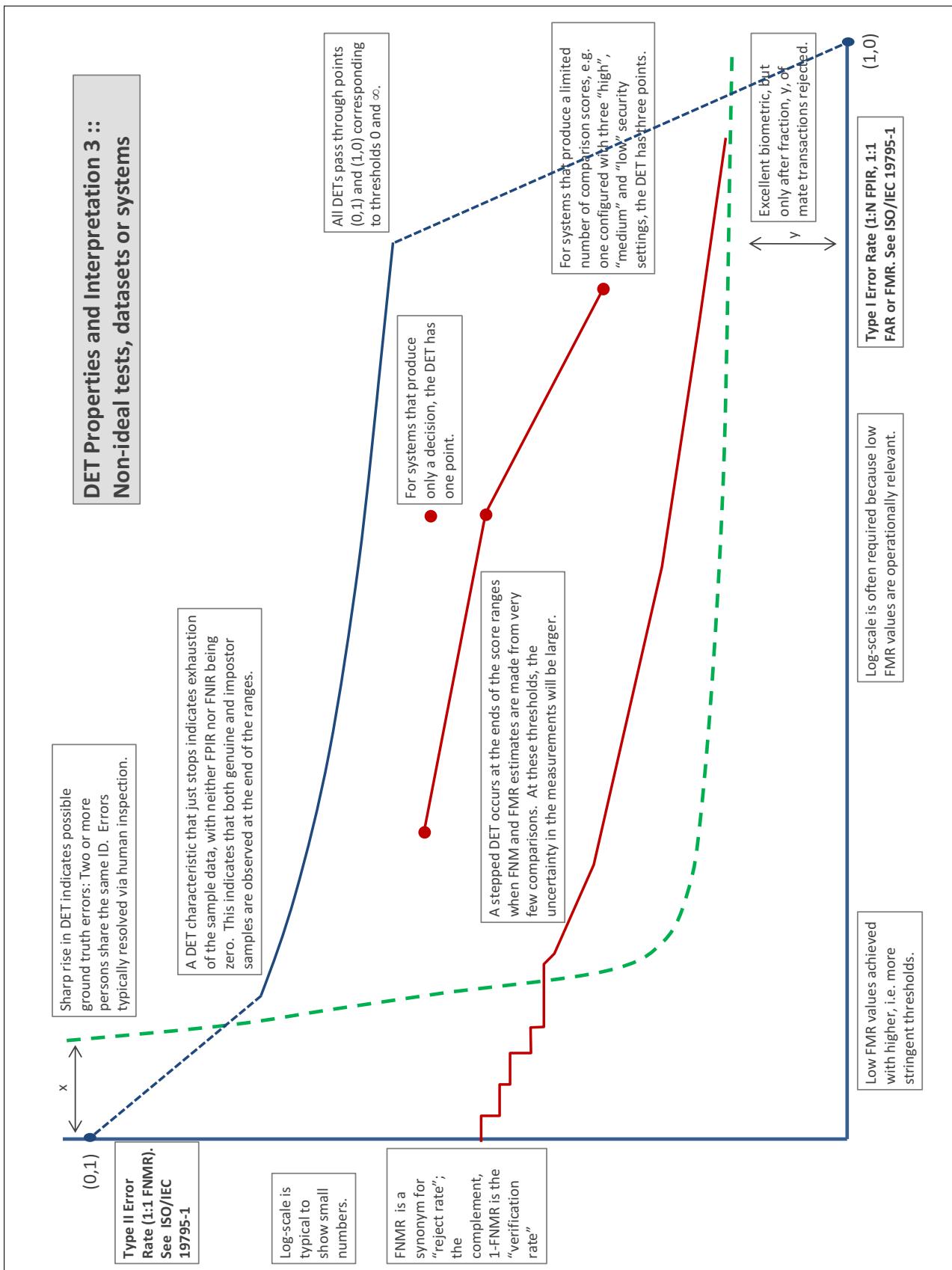
A **error tradeoff** characteristic represents the tradeoff between Type II and Type I classification errors. For verification this plots false non-match rate (FNMR) vs. false match rate (FMR) parametrically with T.

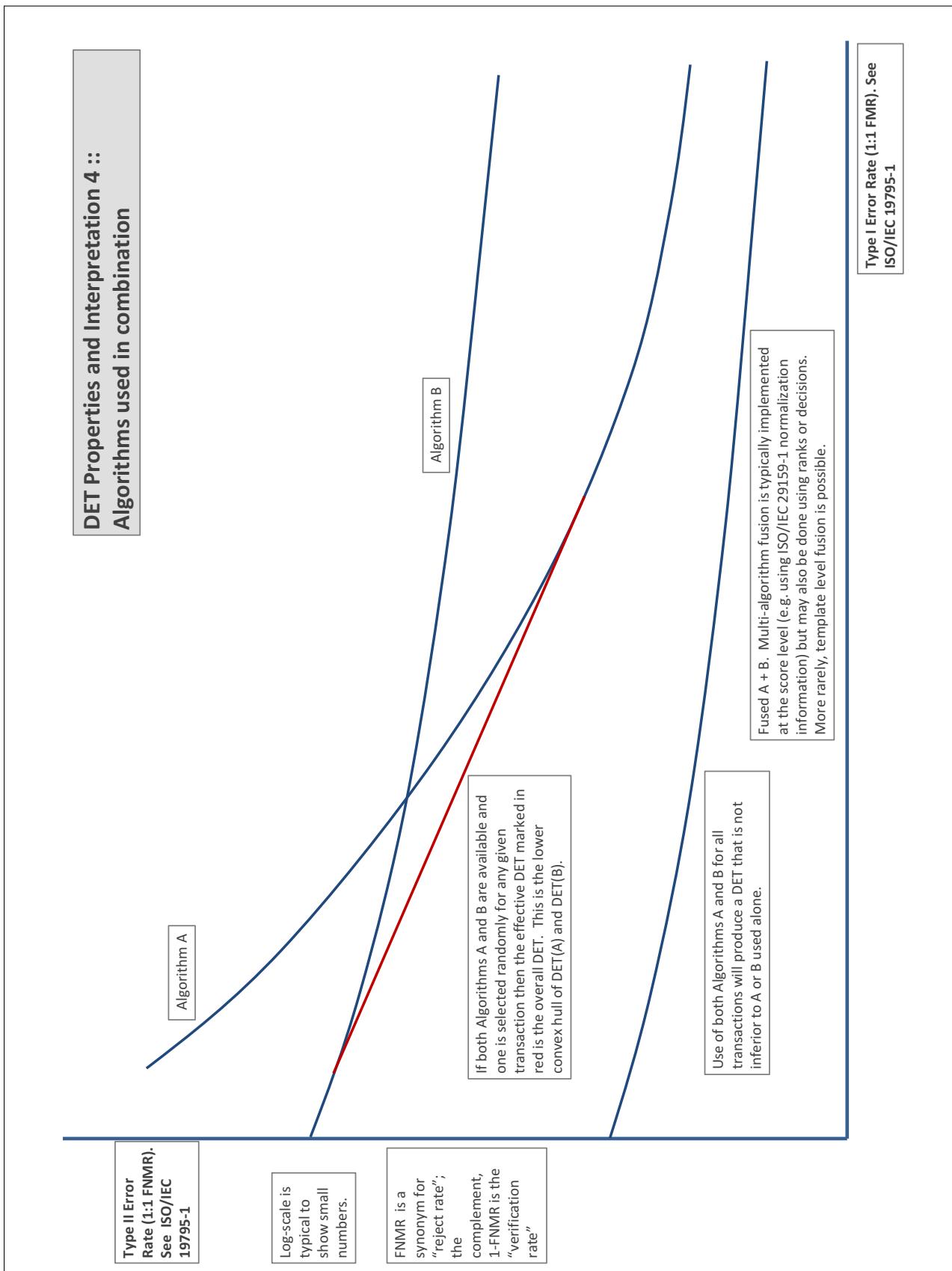
The error tradeoff plots are often called **detection error tradeoff (DET)** characteristics or **receiver operating characteristic (ROC)**. These serve the same function but differ, for example, in plotting the complement of an error rate (e.g., $TMR = 1 - FNMR$) and in transforming the axes most commonly using logarithms, to show multiple decades of FMR. More rarely, the function might be the inverse Gaussian function.

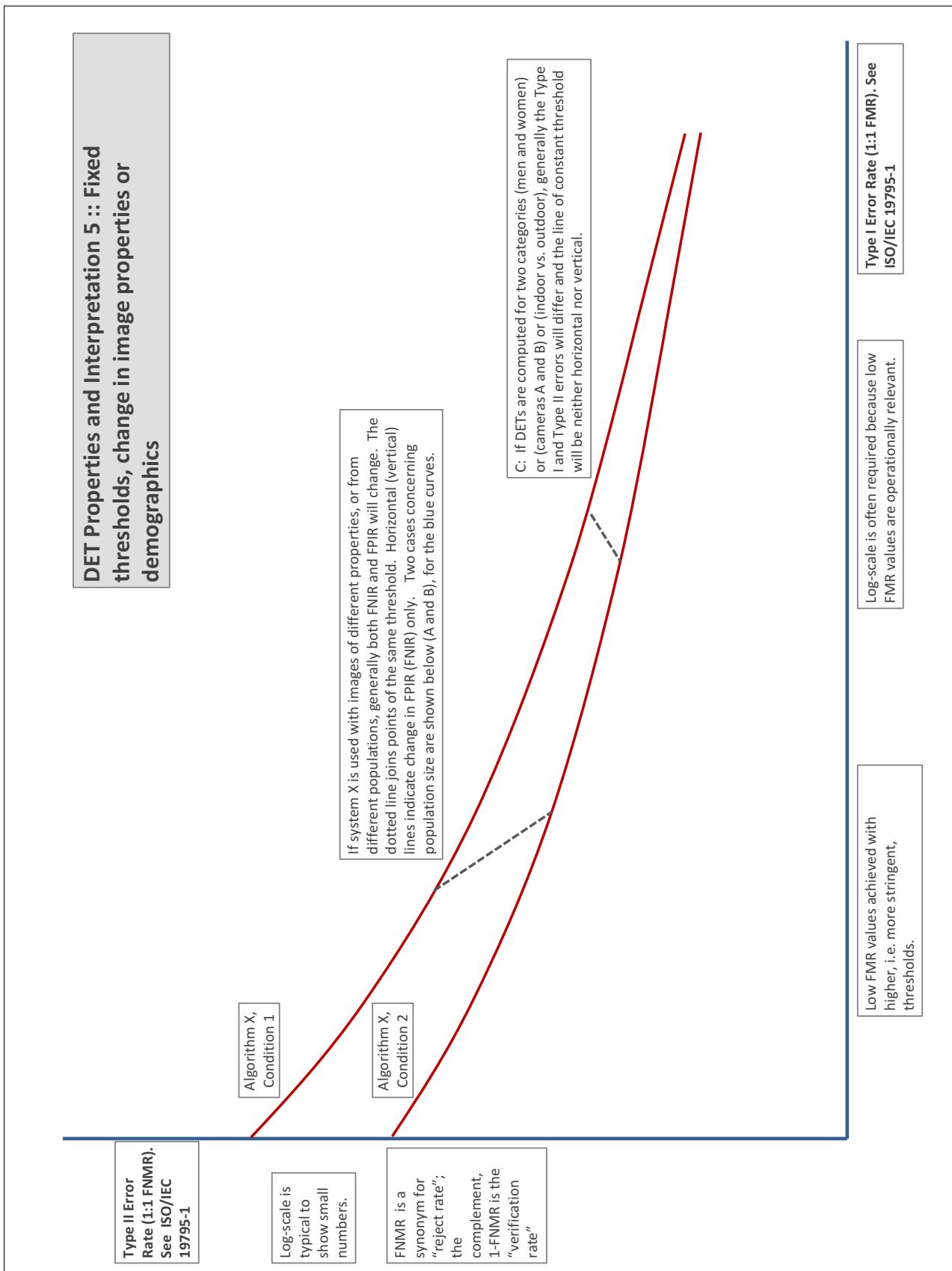
More detail and generality is provided in formal biometrics testing standards, see the various parts of [ISO/IEC 19795 Biometrics Testing and Reporting](#). More terms, including and beyond those to do with accuracy, see [ISO/IEC 2382-37 Information technology -- Vocabulary -- Part 37: Harmonized biometric vocabulary](#)











References

- [1] P. Jonathon Phillips, Amy N. Yates, Ying Hu, Carina A. Hahn, Eilidh Noyes, Kelsey Jackson, Jacqueline G. Cavazos, Géraldine Jeckeln, Rajeev Ranjan, Swami Sankaranarayanan, Jun-Cheng Chen, Carlos D. Castillo, Rama Chellappa, David White, and Alice J. O'Toole. Face recognition accuracy of forensic examiners, superrecognizers, and face recognition algorithms. *Proceedings of the National Academy of Sciences*, 115(24):6171–6176, 2018.